

The Eurasia Proceedings of Science, Technology, Engineering & Mathematics

EPSTEM

VOLUME 23 ICRETS CONFERENCE

ISSN: 2602-3199

ISBN: 978-625-6959-08-8

**ICRETS 2023: International Conference on Research in Engineering,
Technology and Science (ICRETS)**

July 06 - 09, 2023

Budapest, Hungary

Edited by: Mehmet Ozaslan (Chair), Gaziantep University, Turkey

ICRETS 2023

Volume 23, Pages 1-572 (September 2023)

The Eurasia Proceedings of Science, Technology, Engineering & Mathematics
(EPSTEM)

e-ISSN: 2602-3199

©2023 Published by the ISRES Publishing

Address: Istanbul C. Cengaver S. No 2 Karatay/Konya/TURKEY

Website: www.isres.org

Contact: isrespublishing@gmail.com

Conference: ICRETS2023: International Conference on Research in Engineering,
Technology and Science

Conference website: <https://www.2023.icrets.net>

Dates: July 06 – 09, 2023

Location: Budapest, Hungary

Edited by: Mehmet Ozaslan

About Editor(s)

Prof Dr. Mehmet Ozaslan

Department of Biology, Gaziantep University, Turkey

Website: mehmetozaslan.com

E-mail: ozaslanmd@gantep.edu.tr

Language Editor(s)

Assoc. Prof. Dr. Kagan Buyukkarci

Department of English Language Education, Suleyman Demirel University, Turkey

E-mail: kaganbuyukkarci@sdu.edu.tr

CONFERENCE PRESIDENT

Prof. Dr. Mehmet Özasan - Gaziantep University, Turkey

SCIENTIFIC BOARD

Ágnes Csiszárík-Kocsir, Óbuda University, Hungary

Bálint Blaskovics, Corvinus University, Hungary

Besnik Hajdari - University "Isa Boletini" Mitrovica, Kosovo

Bogdan Patrut - Alexandru Ioan Cuza Üniversitesi, Romania

Chalavadi Sulochana - Gulbarga University, India

Csaba Antonya - Transilvania University of Brasov, Romania

Dariusz Jacek Jakóbczak - Technical University of Koszalin, Poland

Dehini Rachid - University of Bechar, Algeria

Eleonora Guseinoviene - Klaipeda University, Lithuania

Elena Krelja Kurelovic - Polytechnic of Rijeka, Croatia
Eva Trnova - Masaryk University, Czech Republic
Farhad Balash - Kharazmi University, Iran
Fundime Miri - University of Tirana, Albania
Gabriel Delgado-Toral - Universidad Nacional Autónoma de México, Mexico
Gordana Savic - University of Belgrade, Serbia
Hasan Mlinaku, VUZF, Sofia in Bulgaria
Irina Andreeva - Peter The Great St. Petersburg Polytechnic University, Russia
Isti Hidayah - Semarang State University, Indonesia
János Varga, Óbuda University, Hungary
Jose Manuel Lopez Guede - University of Basque Country, Spain
Kamil Yurtkan - Cyprus International University, Cyprus
Katsina Christopher Bala - Federal University of Technology, Minna, Nigeria
Khitam Shraim - Palestine Technical University, Palestine
Marija Stanić - University of Kragujevac, Serbia
M. Hanefi Calp - Karadeniz Technical University, Turkey
Mohamed Ahmed - Mansoura University, Egypt
Mousa Attom- American University of Sharjah, U.A.E.
Nicu Bizon - Pitesti University, Romania
Pandian Vasant - Teknology Petronas University, Romania
Rajnalkar Laxman - Gulbarga University, India
Richárd Horváth, Óbuda University, Hungary
Sanaa Al-Delaimy - Mosul University, Iraq
Shadi Aljawarneh - Jordan University of Science and Technology, Jordan
Shynar Baimaganbetova - Nazarbayev University, Kazakhstan
Svetlana Khan - Almaty University of Power Engineering and Telecommunications, Kazakhstan
Yiyang Chen - Soochow University (CN), China
Zipporah Pawat Duguryil - Federal College of Education, Nigeria
Zoltán Rajnai, Óbuda University, Hungary

ORGANIZING COMMITTEE

Ágnes Csiszárík-Kocsir, Óbuda University, Hungary
Aynur Aliyeva - Institute of Dendrology of Anas, Azerbaijan
Besnik Hajdari - University "isa Boletini" Mitrovica, Kosovo
Cemil Aydogdu - Hacettepe University, Turkey
Csilla Mizser, Óbuda University, Hungary
Danielle Gonçalves de Oliveira Prado-Federal Technological University of Paraná, Brazil
Dariusz Jacek Jakóbczak - Technical University of Koszalin, Poland
Elman Iskender - Central Botanical Garden of Anas, Azerbaijan
Halil Snopce - South East European University, Macedonia
Hasan Mlinaku, VUZF, Sofia in Bulgaria
Ishtar Imad - Uruk University, Iraq
Jaya Bishnu Pradhan-Tribhuvan University, Mahendra Ratna Campus, Nepal
János Varga, Óbuda University, Hungary
Mónika Garai-Fodor, Óbuda University, Hungary
Mohammad Sarwar - Scialert, Dubai, United Arab Emirates
Murat Beytur - Kafkas University, Turkey

Réka Saáry, Óbuda University, Hungary
S.Ahmet Kiray - Necmettin Erbakan University, Turkey
Samire Bagirova - Institute of Dendrology of Anas, Azerbaijan
Shafag Bagirova - Baku State University, Azerbaijan
Suhail Bayati - Hadi University College, Iraq
Zsolt Téglá, Óbuda University, Hungary

Editorial Policies

ISRES Publishing follows the steps below in the proceedings book publishing process.

In the first stage, the papers sent to the conferences organized by ISRES are subject to editorial oversight. In the second stage, the papers that pass the first step are reviewed by at least two international field experts in the conference committee in terms of suitability for the content and subject area. In the third stage, it is reviewed by at least one member of the organizing committee for the suitability of references. In the fourth step, the language editor reviews the language for clarity.

Review Process

Abstracts and full-text reports uploaded to the conference system undergo a review procedure. Authors will be notified of the application results in three weeks. Submitted abstracts will be evaluated on the basis of abstracts/proposals. The conference system allows you to submit the full text if your abstract is accepted. Please upload the abstract of your article to the conference system and wait for the results of the evaluation. If your abstract is accepted, you can upload your full text. Your full text will then be sent to at least two reviewers for review. **The conference has a double-blind peer-review process.** Any paper submitted for the conference is reviewed by at least two international reviewers with expertise in the relevant subject area. Based on the reviewers' comments, papers are accepted, rejected or accepted with revision. If the comments are not addressed well in the improved paper, then the paper is sent back to the authors to make further revisions. The accepted papers are formatted by the conference for publication in the proceedings.

Aims & Scope

Engineering, technology and basic sciences are closely related fields. Developments and innovations in one of them affect the others. Therefore, **the focus of the conference** is on studies related to these three fields. Studies in the fields of engineering, technology and basic science are accepted to the conference even if they are not associated with other fields. The conference committee thinks that a study in only one field (for example, mathematics, physics, etc.) will contribute to other fields (for example, engineering, technology, etc.) in future studies, even if it is not associated with the presentation at the conference. In line with this perspective, studies in the following fields are accepted to the conference: *Biology, Chemistry, Engineering, Mathematics, Physics and Technology*. The aim of the conference is to bring together researchers and administrators from different countries, and to discuss theoretical and practical issues in all fields of Engineering, Technology and Basic Sciences.

Articles: 1-62

CONTENTS

Experimental Analysis on a Set of Four CFT Subjected to Monotonic and Cyclic Loading / Pages: 1-10
Donato ALIBERTI, Elide NASTRI, Vincenzo PILUSO, Paolo TODISCO, Rosario MONTUORI

Perception of Public Transport Megaprojects through a User Perspective / Pages: 11-18
Agnes CSÍSZARÍK-KOCSÍR, Janos VARGA

Biodiesel Production Using Supercritical Methanol in Bench-Scale Reactor / Pages: 19-25
Filiz ALSHANABLEH, Mahmut A. SAVAS

Data Cleaning in Medical Procurement Database: Performance Comparison of Data Mining Classification Algorithms for Tackling Missing Value / Pages: 26-33
Amarawan PENTRAKAN, Arbee L. P. CHEN

Optimal Position of Two Fans Cooling a Large PV Panel / Pages: 34-41
Rezki NEBBALI, Idir KECILI

Possibilities to Construct Combined Mine Waste Dump Facility with Better Operational Sequence / Pages: 42-49
Ljupcho DIMITROV, Irena GRIGOROVA, Teodora YANKOVA

Stochastic Longitudinal Autopilot Tuning for Best Autonomous Flight Performance of a Morphing Decacopter / Pages: 50-58
Tugrul OKTAY, Firat SAL, Oguz KOSE, Enes OZEN

A Quantitative Blockchain-Based Model for Construction Supply Chain Risk Management / Pages: 59-68
Clarissa AMICO, Roberto CIGOLINI

Comparative Experimental and Theoretical Study on the Structure of Potassium 2,4-Hexadienoate: Structure-Activity Relationship / Pages: 69-84
Manel TAFERGUENNIT, Noura KICHOU, Zakia HANK

Alternative Aviation Fuel Types Used in Aircraft Engine / Pages: 85-92
Ayhan UYAROĞLU, Mahmut UNALDI

On the Development of the Fluorescence Excitation-Emission Etalon Matrix Algorithm of Wine / Pages: 93-99
Miranda KHAJISHVILI, Jaba SHAINIDZE, Kakha MAKHARADZE, Nugzar GOMIDZE

Green Hydrogen from PV-Supplied Sono-Electrolysis: Modelling and Experimental Investigations of the Mechanism and Performance / Pages: 100-105
Nour Hane MERABET, Kaouther KERBOUA

SaaS Model Assessment- A DEA Approach / Pages: 106-116
Thi Minh Nhut VO, Chia-nan WANG, Fu-chiang YANG, Van Thanh Tien NGUYEN

Microstructure and Mechanical Properties Analysis of Al-6061/B4C Composites Fabricated by Conventional and Bobbin Tool Friction Stir Processing / Pages: 117-123
Dhaivat DIVEKAR, Kishan FUSE, Vishvesh BADHEKA

An App for the Registration of Traffic Injuries / Pages: 124-130

Daniel SUAREZ, Javier URIOS, Jesus TOMAS, Sandra SENDRA, Jaime LLORET, Sandra VICIANO

A Proposed Conceptual Design for a Computer-Based Ambulance System in Libya Using IoT / Pages: 131-142

Arwa F. ALBILLALI, Ehab A. Omar ELFALLAH, Bilal A. ALJABOUR, Tawfiq TAWILL

Non-linear Viscoelastic Beams Under Periodic Strains: An Approach for Analyzing of Longitudinal Fracture / Pages: 143-150

Victor RIZOV

Research on Media Presentation and Public Reaction to the First Health Digital Assistant in Croatia / Pages: 151-164

Stjepan PETRICEVICA, Daria MUSTIC

Computer-Aided Planning of Radial and Diameter Routes in Local Public Transport Networks / Pages: 165-172

Agoston WINKLER

Effect of Urea Usage Rate on Thixotropic Behavior of Cementitious Systems / Pages: 173-178

Neslihan CAPAROGLU, Ozgur BIRICIK, Ali MARDANI

Estimation of Red Meat Production in Turkey according to the Grey-Markov Chain Model / Pages: 179-188

Halil SEN

Properties Experimental Analysis Bio-Monograde Engine Oil: Blended Mono-Grade Engine Oil SAE 40 with Fresh Coconut Oil / Pages: 189-201

Othman INAYATULLAH, Mohamad Faizi ZAINULABIDIN, Nor Asrina RAMLEE

Blockchain Security-Efficiency Analysis based on DEA-SBM Model / Pages: 202-208

Thi Minh Nhut VO, Chia-nan WANG, Fu-chiang YANG, Van Thanh Tien NGUYEN

Bi-Directional LSTM-Based COVID-19 Detection Using Clinical Reports / Pages: 209-219

Salah BOUKTIF, Akib Mohi Ud Din KHANDAY, Ali OUNI

The Effectiveness of the Implementation of Speech Command Recognition Algorithms in Embedded Systems / Pages: 220-224

Kamoliddin SHUKUROV, Umidjon KHASANOV, Boburkhan TURAEV, A'lokhan KAKHKHAROV

Improved Tailings Consolidation Using Dewatering Agents: A Step towards Safer and Sustainable Mining Waste Management / Pages: 225-231

Ljupcho DIMITROV, Irena GRIGOROVA

Evaluation of the Spread of Respiratory Diseases in the City of Batna Cover a Period of Five Years (2018-2023) / Pages: 232-240

Sahraoui NABIL, Laidoune ABDELBAKI

From Human to Robot Interaction towards Human to Robot Communication in Assembly Systems /
Pages: 241-252

Ikrom KAMBAROV, Matthias BROSSOG, Jorg FRANKE, David KUNZ, Jamshid INOYATKHODJAEV

Embracing Green Choices: Sentiment Analysis of Sustainable Consumption / Pages: 253-261

Ceren CUBUKCU-CERASÍ, Yavuz Selim BALCIOGLU, Asli KILIC, Farid HUSEYNOV

Enhancing Cybersecurity with Trust-Based Machine Learning: A Defense against DDoS and Packet
Suppression Attacks / Pages: 262-268

Adnan AHMED, Muhammad AWAIS, Mohammad SIRAJ, Muhammad UMAR

Some Engineering Properties of Pineapple Fruit / Pages: 269-281

*Rosnah SHAMSUDIN, Hasfalina CHE-MAN, Siti Hajar ARIFFIN, Siti Nor Afiekah MOHD-GHANI, Nazatul
Shima AZMI*

Synthesis, Biological Evaluation and Theoretical Studies of Hydrazone Derivatives / Pages: 282-291

Noura KICHOU, Nabila GUECHTOULI, Karima IGHILAHRIZ, Manal TEFERGHENIT, Zakia HANK

Applicability of a Gage R&R Study on a Home Blood Glucose Meter / Pages: 292-299

Zoltan VARADI, Gyozo Attila SZILAGYI

A Comparative Study on Microwave Assisted Dyeing Properties of Conventional and Recycled
Polyester Fabrics / Pages: 300-306

Yasemin DÜLEK, Ipek YILDIRAN, Bugce SEVİNC, Esra MERT, Burcu YILMAZ, Dilek KUT

Benefits of Circular Design Adoption in the Nigerian Building Industry / Pages: 307-315

Taofeek SULEMAN, Isidore EZEMA, Peter ADERONMU

Improvement of Solution Using Local Search Operators on the Multi-Trip Electric Vehicle Routing
Problem Backhaul with Time Window / Pages: 316-331

Zelania In HARYANTO, Niniet Indah ARVITRIDA

A Comparative Analysis of Uncertainty Assessment for Annual Yield Prediction of Citrus Growth Using
FIS and ANFIS Models / Pages: 332-337

Filiz ALSHANABLEH

Single Objective Optimization of Cutting Parameters for Surface Roughness in Turning of Inconel 718
Using Taguchi Approach / Pages: 338-348

Fatlume ZHUJANI, Georgi TODOROV, Konstantin KAMBEROV

Technological Trend Analysis for Surgical Operation Duration Estimation / Pages: 349-360

Ziya KARAKAYA, Bahadır TATAR

Determination of the Shear Force in RC Interior Beam-Column Connections / Pages: 361-371

Albena DOICHEVA

Development of Inventory Model for Perishable Product with Dynamic Pricing / Pages: 372-380

Teodosius Raditya ANANTO, Nurhadi SISWANTO

Investigation of Magnetorheological Shock Absorber Used in Semi-Active Suspension/ Pages: 381-387
Ramazan FERIK, Murat YAZICI, Orhan KURTULUS

Internet of Things (IoT): Wireless Communications for Unmanned Aircraft System / Pages: 388-399
Thi Minh Nhut VO, Chia-nan WANG, Fu-chiang YANG, Van Thanh Tien NGUYEN, Mandeep SINGH

Comprehensive Modeling Study of the Electrical Performance of a Sono-Electrolyzer under a Voltage and Current Sources Supply: From Grey to Green Hydrogen / Pages: 400-405
Nour Hane MERABET, Kaouther KERBOUA

Analysis of Temperature Change Effect on Dissipation of Energy in Functionally Graded Beams / Pages: 406-412
Victor RIZOV

Stochastic Longitudinal Autopilot Tuning for Best Autonomous Flight Performance of a Morphing VTOL Drone / Pages: 413-419
Tugrul OKTAY, Firat SAL, Oguz KOSE, Abdullah KOCAMER

Route Choice Preferences of Public Transport Passengers in Different Cities / Pages: 420-428
Agoston WINKLER

Impact of Deepfake Technology on Social Media: Detection, Misinformation and Societal Implications/ Pages: 429-441
Samer Hussain AL-KHAZRAJI, Hassan Hadi SALEH, Adil Ibrahim KHALID, Israa Adnan MISHKHAL

Probabilistic Piecewise-Objective Optimization Model for Integrated Supplier Selection and Production Planning Problems Involving Discounts and Probabilistic Parameters: Single Period Case / Pages: 442-451
Sutrisino SUTRISNO, Widowati WIDOWATI, Robertus Heri Soelistyo UTOMO

Integrated Model of Lean and Risk Mitigation for Sustainability Performance Measurement in the Lubricants Manufacturing Industry / Pages: 452-463
Fara Kamila HUDY, Nidaru Ainul FIKRI, Udisubakti CIPTOMULYONO

User Evaluation of Innovative Megaprojects Induced by Environmental Change Using Primary Data / Pages: 464-470
Janos VARGA, Agnes CSISZARIK-KOCSIR

Improving the Supply Chain - Marketing Interface, Translating the Voice of the Customer into Processes / Pages: 471-484
Simone FRANCESCHETTO, Roberto CIGOLINI, Lucio LAMBERTI

ETF Markets' Prediction & Assets Management Platform Using Probabilistic Autoregressive Recurrent Networks / Pages: 485-494
Waleed Mahmoud SOLIMAN, Zhiyuan CHEN, Colin JOHNSON, Sabrina WONG

Direct Labor Market Effects of Artificial Intelligence Assisted Applications Based on the Opinions of Illustrators and Company Managers: Hungarian Case Study / Pages: 495-504
Szilard BERKE

The Role of Public Transport in Transport Safety and Public Safety / Pages: 505-512

Diana HENEZI, Agoston WINKLER

Investigating the Effect of Information Systems and Decision Quality on Organizational Performance in Business Firms / Pages: 513-520

Ahmad NABOT

Desk Analysis of Crisis Communication by Public Authorities During Health Crises / Pages: 521-530

Stjepan PETRICEVIC

Estimation of Poultry Meat Production in Turkey Using GM (1,1) with Second Parameter Fitting-Markov Model / Pages: 531-538

Halil SEN

The Effect of Clay Type, Fineness and Methylene Blue Value on Mini-Slump Performance of Cementitious Systems / Pages: 539-547

Fatmanur SAHIN, Ozgur BIRICIK, Ali MARDANI

DFT Study of a Schiff Base Ligand and Its Nickel and Copper Complexes: Structure, Vibration, Chemical Reactivity and in Silico Biological / Pages: 548-555

Nabila GUECHTOULI, Noura KICHOU, Amal BOUZAHEUR, Celia ADJAL

Renewal Energy Efficiency Assessment / Pages: 556-563

Thi Minh Nhut VO, Chia-nan WANG, Fu-chiang YANG, Van Thanh Tien NGUYEN

Activation Condition of a Fan that Cools a PV Panel by Blowing Ambient Air on Its Rear Face / Pages: 564-572

Djamila ZEMBRI-NEBBALI, Idir KECILI, Sonia AIT SAADA, Rezki NEBBALI

The Eurasia Proceedings of Science, Technology, Engineering & Mathematics (EPSTEM), 2023

Volume 23, Pages 1-10

ICRETS 2023: International Conference on Research in Engineering, Technology and Science

Experimental Analysis on a Set of Four CFT Subjected to Monotonic and Cyclic Loading

Donato Aliberti

University of Salerno

Elide Natri

University of Salerno

Vincenzo Piluso

University of Salerno

Paolo Todisco

University of Salerno

Rosario Montuori

University of Salerno

Abstract: The main purpose of this work is the evaluation of the ultimate behaviour of Concrete Filled Tubes (CFT) subjected non uniform bending. The novelty point of this paper regards the use of big steel tubes whose material behaves like a high strength steel. Four experimental tests have been performed at the STRENGTH Laboratory of the of the University of Salerno under both monotonic and cyclic loading conditions. In particular, both constant and variable amplitude tests are considered. The three-point bending scheme is adopted for testing specimens, where a hydraulic actuator is used for the transmission of the transverse load at midspan under displacement control and an LVDT is used to measure the corresponding maximum transverse displacement.

Keywords: Concrete filled tubes, Ultimate behaviour, Cyclic tests, FEM

Introduction

Research on composite structures has attracted increasing interest, for their ability to provide excellent performance in terms of stiffness, strength and ductility, provided that adequate design and detail rules are applied (Romero et al., 2020; Lapuebla-Ferri et al., 2021). Therefore, researchers are increasingly focusing their attention on design issues concerning the behaviour of this structural typology not only with reference to building structures, but also in the case of bridges (Figure 1). CFT elements, in fact, can be effectively adopted as bridge stacks, exploiting their high ductility and energy dissipation capacity. They can also be adopted for the construction of columns, obtaining considerable advantages when large cross-sections are required.

In China, concrete-filled steel tubes have been used for over 50 years, mainly exploiting their compressive strength. Since the 80s, they have been used in buildings to avoid having very large columns, connected mainly to additional steel elements. An example is represented by the Canton Tower in Guangzhou (Figure 2), a tower about 454 meters high and reaching 600 meters at the pinnacle. Twenty-four inclined circular tubular steel elements, filled with concrete, were used for its construction, with a maximum diameter of each element equal to 2000 mm and a maximum thickness of 50 mm.

- This is an Open Access article distributed under the terms of the Creative Commons Attribution-Noncommercial 4.0 Unported License, permitting all non-commercial use, distribution, and reproduction in any medium, provided the original work is properly cited.

- Selection and peer-review under responsibility of the Organizing Committee of the Conference

Extensive research has been devoted to the study of concrete-filled tubes (CFTs), with particular emphasis on their structural behaviour under various loading conditions. Experimental tests play a crucial role in understanding the mechanical properties and performance characteristics of CFTs. In this study, a comprehensive series of experimental tests was conducted on four CFT specimens labeled S5-S8. These specimens were subjected to both monotonic and cyclic loading in bending, with consideration given to both constant and variable amplitude loading conditions. The primary objective of the experimental tests was to investigate the flexural behaviour of the CFTs.



Figure 1. CFTs in bridges - Juscelino Kubitschek Bridge.



Figure 2. Canton tower.

The tests involved measuring and recording the load-deformation responses, observing the failure modes, and determining the ultimate strength of the specimens. The experimental results provide valuable data for analyzing the structural response, understanding the deformation patterns, and assessing the overall performance of CFT members under different loading scenarios.

In addition to the experimental investigations, Finite Element (FE) modelling was utilized using ABAQUS software to further analyze the behaviour of the tested concrete-filled tubes. A sophisticated FE model was developed, taking into account the material properties of steel and concrete and capturing their non-linear behaviour. The FE simulations enabled a thorough examination of stress distribution, load transfer mechanisms, and deformation patterns within the CFT specimens. This comprehensive analysis provided valuable insights into the structural response and performance of the concrete-filled tubes under different loading conditions.

Mechanical Behaviour of Concrete-Filled Tubes

Concrete-filled tubes (CFTs) exhibit remarkable structural behavior and offer several mechanical advantages due to the interaction between steel and concrete, confinement effects, and their ability to mitigate buckling. Understanding these characteristics is crucial for comprehending the performance and benefits of CFT structures (Iannone et al., 2009).

Introduction and Main Advantages

It is known that the compressive strength of concrete is much higher than its tensile strength. For structural steel the tensile strength is high while the shape can locally bend under compression actions. In tubular steel elements filled with concrete, these two elements are used in such a way as to exploit their natural and most significant characteristics.

CFTs do not require other reinforcements as it is the pipe itself that acts as a longitudinal and lateral reinforcement for the concrete core. As regards the placement of steel in the longitudinal direction with respect to the perimeter of the section, this is the most efficient use of steel as it provides the best contribution to the moment of inertia and to the flexural strength of the section. In addition, the continuous confinement provided to the concrete core (Montuori et al., 2012; Montuori et al., 2013) by the steel pipe improves the strength and ductility of the core and prevents chipping of the concrete. The concrete core makes a great contribution to the load-bearing capacity under axial loads and delays the local instability of the steel pipe preventing inward instability (Han et al., 2005; Shams et al., 1999).

The local instability of a hollow steel tube, in fact, is characterized by the combination of inward and outward deformations of the plates while in the case of SHS (square hollow sections) and RHS (rectangular hollow sections) elements these deformations interact through rotations at the edges for compatibility needs. In contrast, only outward deformations of the plate elements that make up the steel tube are allowed in CHS elements. The local instability of a hollow steel tube, in fact, is characterized by the combination of inward and outward deformations of the plates while in the case of SHS (square hollow sections) and RHS (rectangular hollow sections) elements these deformations interact through rotations at the edges for compatibility needs. In contrast, only outward deformations of the plate elements that make up the steel tube are allowed in CHS elements (Susantha et al., 2002; Gourley et al., 2001; NASTRI et al., 2022).

Fire Behaviour of CFTs

Among the non-negligible advantages should be considered the high fire resistance offered by this type of pillars thanks to the dissipating effect provided by concrete, which delays the increase in temperature in composite sections compared to bare steel sections. The literature suggests that the typical behavior of a CFT column subjected to standard fire testing can be divided into four phases (Lapuebla Ferri et al., 2021). At the beginning of the test, in fact, the steel pipe heats up more quickly and expands faster than the concrete core (phase 1), being directly exposed to the heat source. The increased thermal conductivity of steel accelerates the heating of the outer tube and thus its thermal expansion. Due to this faster axial elongation of the steel pipe and the occurrence of sliding at the steel-concrete interface, the concrete core loses contact with the plate and the axial load ratio of the steel increases progressively until the entire applied load is supported by the steel pipe alone. The outer tube remains at full load for a significant time until the critical temperature of the steel is

reached. At this point the local failure of the steel pipe occurs and begins to shorten (phase 2), allowing the plate to meet the concrete core again. As the column gets shorter, the steel pipe progressively transfers the load to the concrete (phase 3) and a reversal of the axial force ratio occurs, so that it is the concrete core that becomes the main resistant element of the column, since the pipe has lost its bearing capacity. Thanks to its low thermal conductivity, the concrete core degrades slowly with advancing temperature, until the total loss of its strength and rigidity and, therefore, to failure. This, however, guarantees high fire resistance and longer times before complete collapse.

Experimental Tests

According to the pre-planned experimental procedure, four Concrete-Filled Steel Tube (CFT) columns were tested (Figure 3).



Figure 3. C5-C8 CFT specimens.

Description of the Experimental Tests

Four steel concrete filled columns were analysed, on which a series of cyclic tests have been carried out through a hydraulic actuator. The main difference between the tested specimens is the width-to-thickness ratio D/t . The steel used is S355 grade, but it behaves more like a high strength steel. As regards concrete, class C30/35 has been adopted (Roesler et al., 2007; Guo, 2014). Each model has been made from a rolled steel sheet, welded along a longitudinal side. The tubes tubes have an outer diameter (D) ranging from 249.2 to 260.4 mm, a height (h) of 2400 mm, and a wall thickness (t) varying between 6.1 and 10.6 mm. Both ends of these tubes were welded with 20 mm thick plates. The geometry is summarized in Table 1.

Table 1. Geometry of the CFT specimens.

Label	h [mm]	D [mm]	t [mm]	D/t [-]
C5	2400	249.2	6.1	40.85
C6	2400	260.4	10.4	25.04
C7	2400	249.4	6.2	40.23
C8	2400	255.2	10.6	24.08

To achieve composite action, the steel tubes were filled with the C30/35 concrete mix using a truck-mounted pump. Subsequently, internal consolidation of the concrete was accomplished using a vibrating poker. Finally, the specimens were carefully stored for an appropriate duration to ensure proper curing.

Experimental Setup

Four steel concrete filled columns were analysed, on which a series of cyclic tests have been carried out through a hydraulic actuator. Regarding the CFT elements under examination, three-point bending tests were performed under both cyclic load conditions. In particular, the specimens called C5-CA and C7-CA were subjected to cyclic testing at constant amplitude (0-140 mm) and speed, while the C6-VA and C8-VA specimens were subjected to cyclic testing at increasing amplitude and speed (Table 2).

Table 2. Displacement history of the cyclic test (C6, C8).

n.cycles	Drift angle [rad]	Displacement [mm]
6	0.00375	5.64375
6	0.005	7.525
6	0.0075	11.2875
4	0.01	15.05
2	0.015	22.575
2	0.02	30.1
2	0.03	45.15
2	0.04	60.2
2	0.05	75.25
2	0.06	90.3
2	0.07	105.35
2	0.08	120.4
Until rupture	0.08	120.4

No axial load was applied to the specimens. Consequently the response of these structural elements has been strongly governed by flexural behaviour (Montuori et al., 2015). Figure 4 depicts a schematic view of the test setup used in the experimental investigation. The setup involved the arrangement of two articulated pins at the ends of the beam, with the two plates being fixed to the pins using 16 bolts of M20 type on each plate. The articulated supports were securely fixed to the testing machine's plane using 8 M22 pins. This setup allowed for free rotation of the specimen's ends within the plane, enabling a simply supported configuration.

The flexural load was applied to the specimen at its center using a hydraulic actuator. To connect the specimen with the actuator, a hollow semi-cylindrical element was placed at the center of the specimen and secured with 3 bolts on each side to ensure a conforming connection.

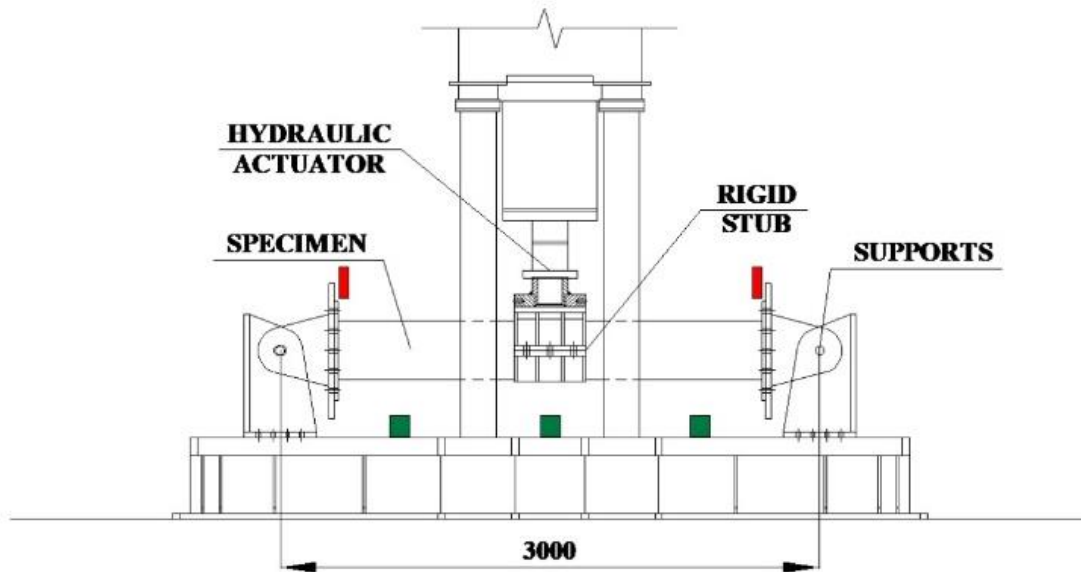


Figure 4. Experimental setup scheme.

The C5-CA specimen was subjected to a cyclic test at a constant amplitude of 0-140 mm, with a constant speed of 0.25 mm/s. The specimen developed two bulges and cracks near the attachment to the load cell and reached rupture after 21 cycles. (Figure 5).

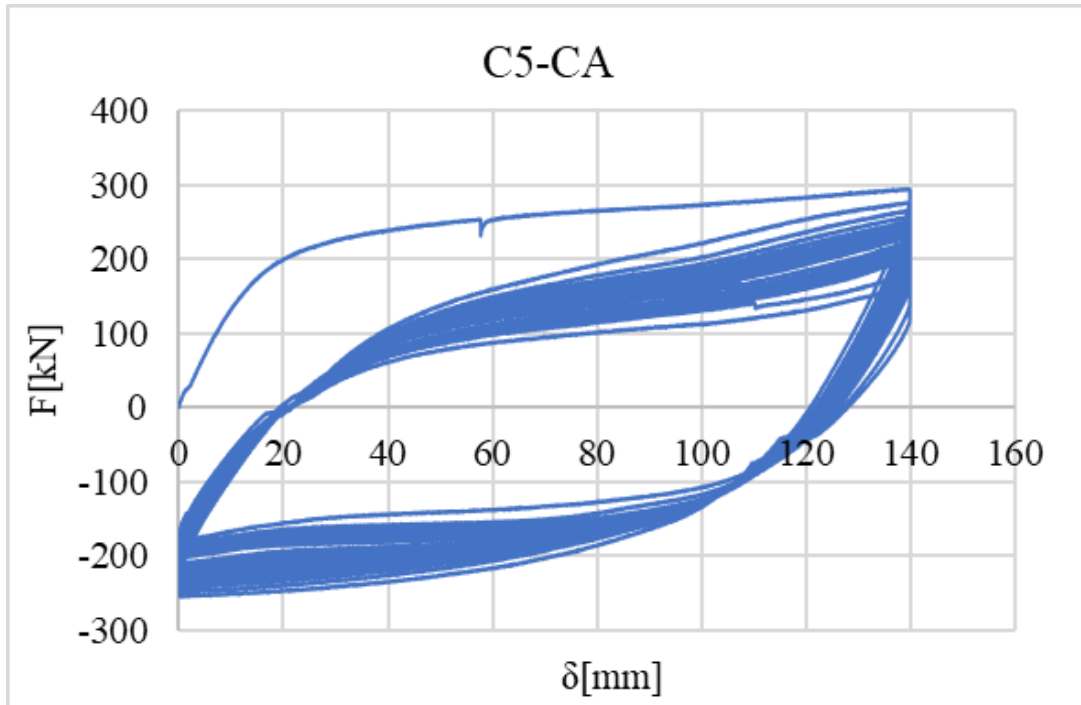


Figure 5. C5 Experimental curve.

The **C6-VA** specimen underwent a cyclic test with a variable and increasing amplitude following the AISC protocol. The initial amplitude was set at 0.1 mm, and the test started with an initial speed of 4.425 mm/s. It reached rupture after 28 cycles, occurring near the hinge side due to a welding defect

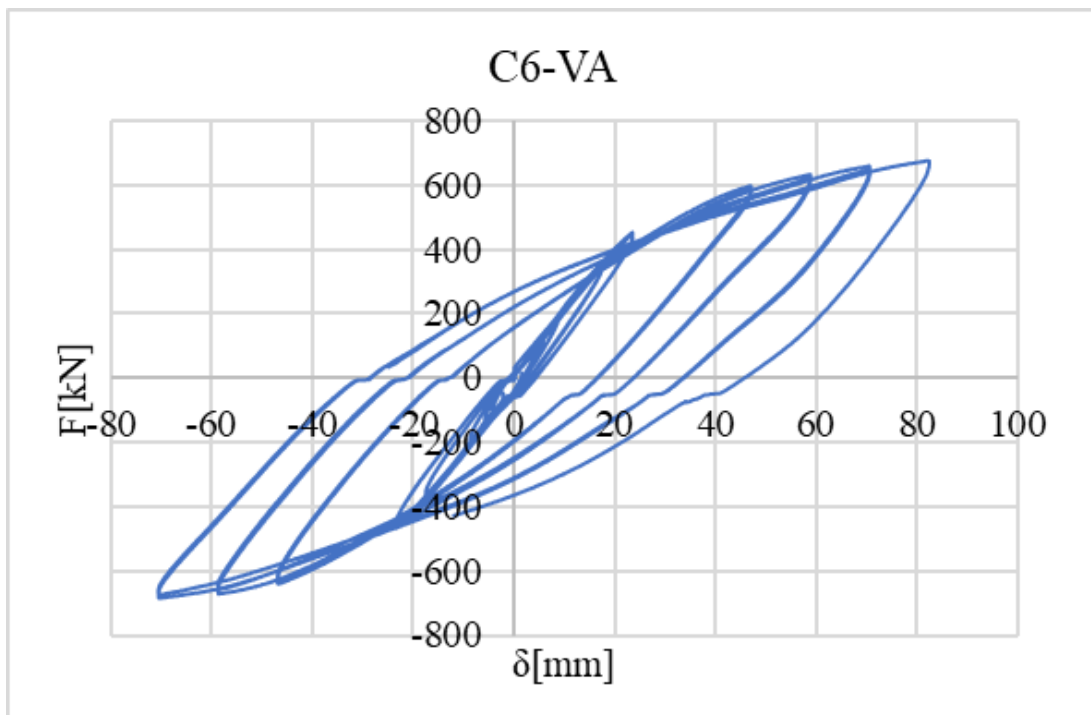


Figure 6. C6 Experimental curve.

The **C7-CA** specimen also underwent a cyclic test at a constant amplitude of 0-140 mm, with a constant speed of 1 mm/s.. Similar to the C5-CA specimen, it developed two bulges and cracks near the attachment to the load cell and reached rupture after 24 cycles. (Figure 6).

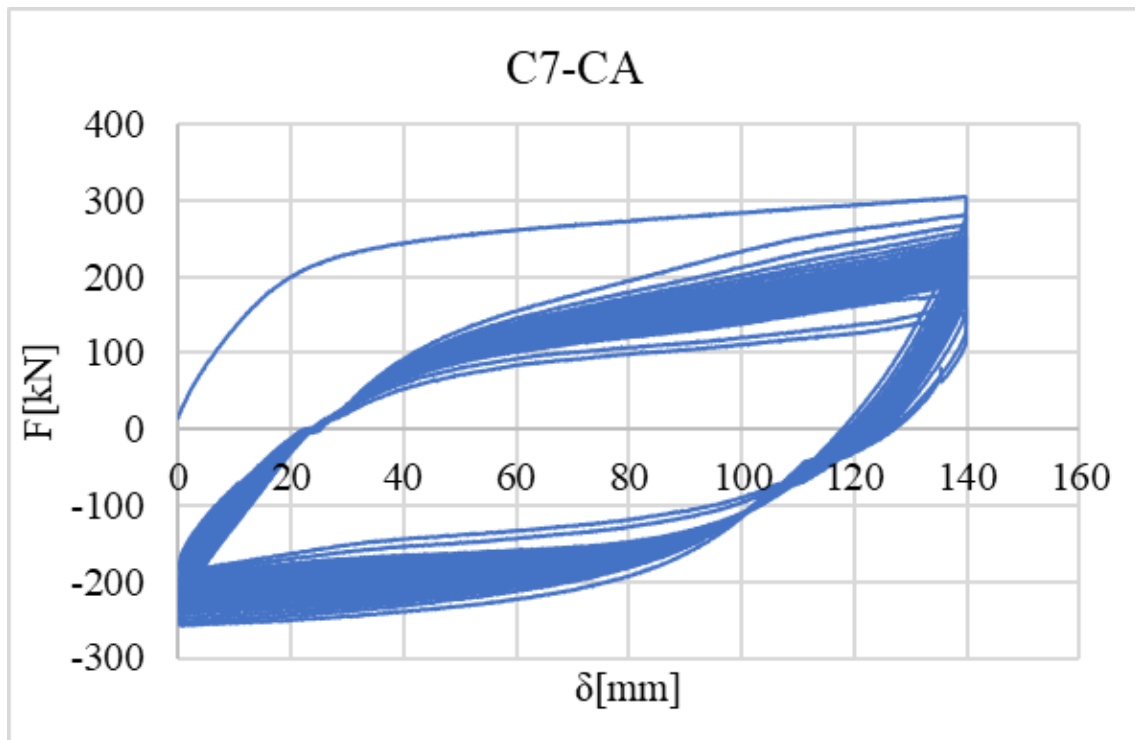


Figure 6. C7 Experimental curve.

The **C8-VA** specimen was subjected cyclic test with a variable and increasing amplitude following the AISC protocol. The initial amplitude was set at 0.1 mm, and the test started with an initial speed of 4.425 mm/s. It reached rupture after 48 cycles, occurring near the rigid stub (Figure 7).

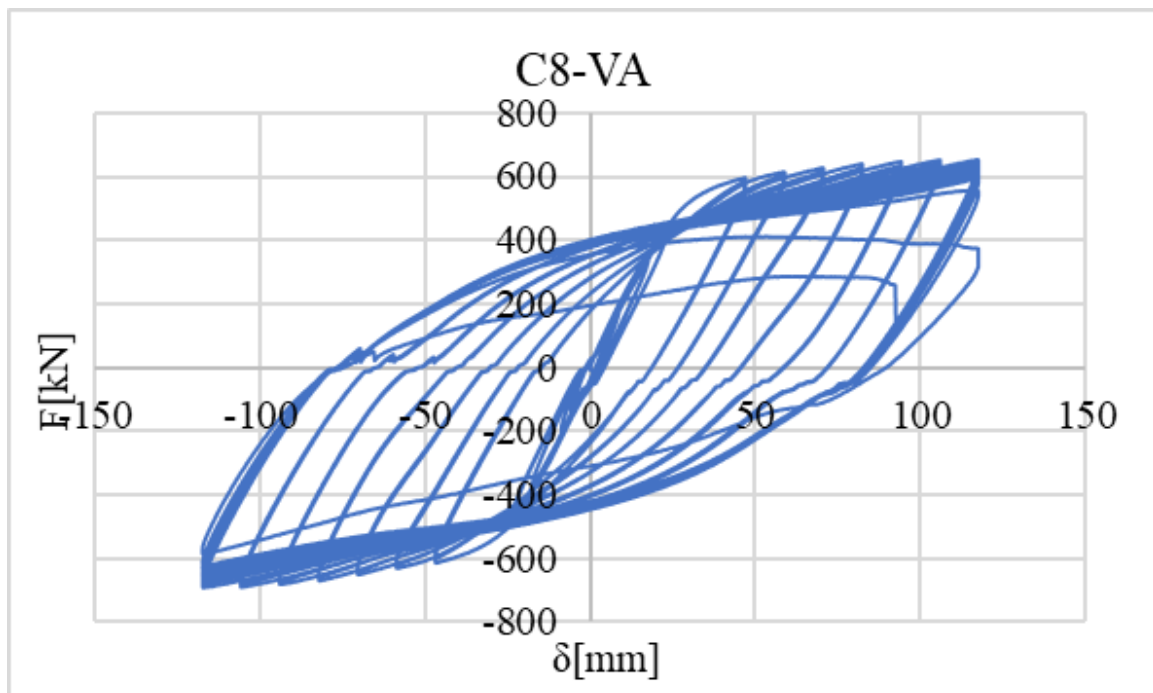


Figure 7. C8 Experimental curve.

Finite Elements Simulation

The finite element modeling in this study was performed using Abaqus software. The "Concrete Damaged Plasticity" failure criterion was utilized to model the plastic behavior and damage of the concrete core. This

criterion requires input parameters such as uniaxial tension and compression curves, along with associated damage, calibrated based on average failure load values obtained from tests conducted on cubic specimens of concrete. The calibration parameters were determined based on (Nastri et al., 2022; Guo, 2014; Nastri et al., 2023).

For modeling the plastic behavior of the steel, a combined hardening model was employed. This model was calibrated using experimental data obtained from dog bone specimens extracted from the concrete-filled tubes. The Johnson-Cook model was applied to capture the damage evolution, which requires the definition of damage initiation and displacement at failure. Interface contact was modeled with a tangential frictional coefficient of 0.6 and a hard normal contact (Montuori et al., 2015; Han et al., 2014).

To assess the accuracy of the simulations, a comparison was made between the experimental reaction force-displacement curve and the corresponding curve obtained from the finite element model for the constant amplitude specimens (C7) (Figure 8a). Furthermore, the skeleton curve, representing the locus of peaks resulting from the cycles, was used to compare the experimental and FE results for the variable amplitude tests. An example of this comparison is shown for specimen C8 (Figure 8b).

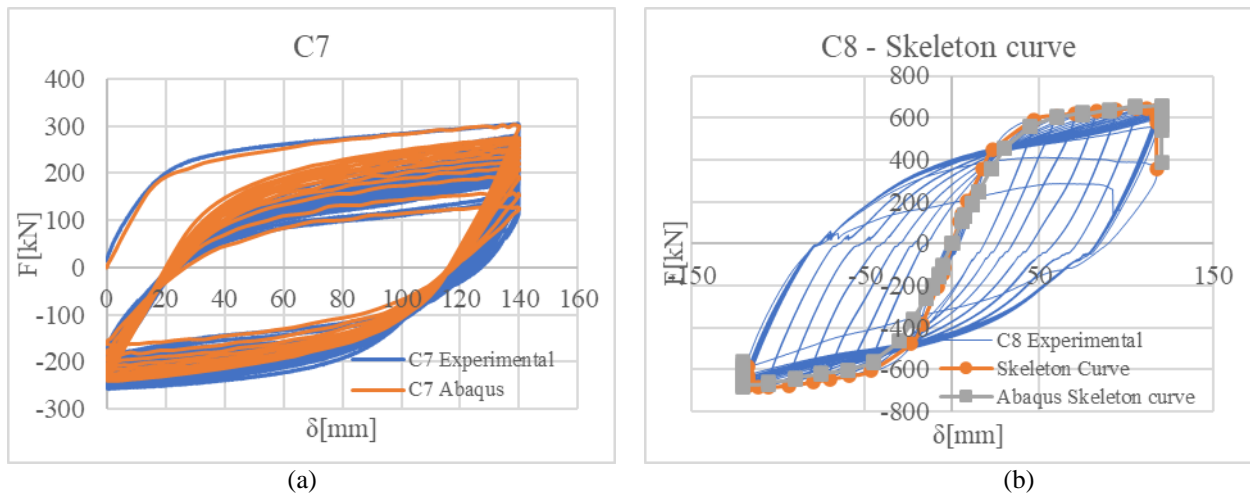


Figure 8. C7-C8 Experimental vs Abaqus.

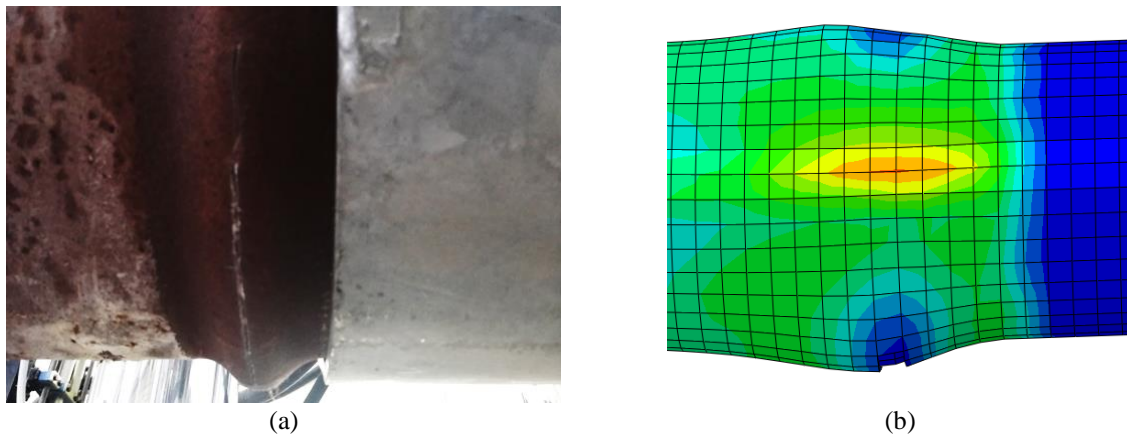


Figure 9. Damage occurred near the rigid stub.

The agreement between the simulated and experimental results was evaluated by analyzing the area under the curves, which represents the energy dissipated during cyclic bending. The error in estimating this value ranged from 1% to 5% across all tests, indicating a satisfactory level of accuracy. The simulations accurately captured the plastic deformations that occurred under the tensional state.

A further aspect of comparison involves visualizing the damage formation in the steel material. Figure 9 illustrates the comparison between the observed damage during the experimental test (a) and the damage obtained by removing the mesh elements that reached the maximum damage level in the Abaqus simulation (b).

Conclusions

This study aims to contribute to the existing knowledge on concrete-filled tubes, providing valuable insights for engineers and researchers involved in the design and analysis of composite structures. The combined experimental and FE modeling approach offers a comprehensive evaluation of the structural behavior of CFTs under various loading conditions. The results obtained from the experimental tests and the corresponding FE simulations can provide guidance for future design improvements, optimization strategies, and practical applications of concrete-filled tubes.

The analysis of the results of the experimental tests carried out confirmed the high ductility and energy dissipation capacity of CFTs. The CFT profiles have shown failure in the expected area, except for a specimen evidently affected by a construction defect; Most profiles have collapsed by simple bending resulting in cracking and breaking of the steel profile; The combination of concrete and steel affects the strength of the profile increasing its performance.

Comprehensive information regarding the geometry of the specimens and the test procedures was provided for the experimental tests, serving as a valuable reference for future experiments. These details are also essential for developing a precise finite element (FE) model. In the FE simulation, failure criteria and damage models were implemented for both the steel and concrete materials, considering their interaction. The comparison between the experimental and simulated results, specifically in terms of energy dissipation, revealed errors ranging from 1% to 5%. Furthermore, a graphical comparison of the formation of lesions was presented. In this aspect as well, the simulated model exhibited good agreement as the removal of mesh elements that reached the maximum damage level occurred near the bulging regions, similar to the observed behavior in the experimental tests.

Scientific Ethics Declaration

The authors declare that the scientific ethical and legal responsibility of this article published in EPSTEM journal belongs to the authors.

Notes

* This article was presented as an oral presentation at the International Conference on Research in Engineering, Technology and Science (www.icrets.net) held in Budapest/Hungary on July 06-09, 2023.

References

- Angeli, E., Wagner, J., Lawrick, E., Moore, K., Anderson, M., Soderland, L., & Brizee, A. (2010, May 5). General format. <http://owl.english.purdue.edu/owl/resource/560/01/>
- Gourley, B.C., Tort, C. Hajjar, J.F., & Schiller, P.H. (2001). *Asynopsis of studies of the monotonic and cyclic behavior of concrete-filled steel tube beam – columns*. Structural Engineering Report N.ST2001:01–4.
- Guo, Z. (2014). *Principles of reinforced concrete*. Tsinghua university press. 30 – 44.
- Han, L.H., & Yang, Y.F. (2005). Cyclic performance of concrete-filled steel CHS columns under flexural loading. *Journal of Constructional Steel Research*, 61, 423–52.
- Han, L.H., Li, W., & Bjorhovde, R. (2014). Developments and advanced applications of concrete-filled steel tubular (CFST) structures: Members. *Journal of Constructional Steel Research*, 100, 211–228.
- Iannone, F., Mastrandrea, L., Montuori, R., & Piluso, V. (2009). Experimental analysis of the cyclic response of CFT-SHS members. In: *Proc. of Stessa2009, sixth international conference on behaviour of steel structures in seismic areas.*, 16–20 August, Philadelphia, U.S.A.
- Lapuebla-Ferri, A., Pons, D., & Romero, M.L (2021). Load and temperature influence on the post-fire mechanical properties of steel reinforcements. *Journal of Constructional Steel Research*, 185, art. no. 106866.
- Montuori, R., Piluso, V., & Tisi, A. (2012). Comparative analysis and critical issues of the main constitutive laws for concrete elements confined with FRP. *Composites Part B: Engineering*, 43(8), 3219-3230.
- Montuori, R., Piluso, V., & Tisi, A. (2013). Ultimate behaviour of FRP wrapped sections under axial force and bending: Influence of stress-strain confinement model. *Composites Part B: Engineering*, 54(1), 85-96.
- Montuori, R., & Piluso, V. (2015). Analysis and modelling of CFT members: Moment curvature analysis. *Thin-Walled Structures*, 86, 157–166.

- Nastri E., Tenore M., & Todisco P. (2023). Calibration of concrete damaged plasticity materials parameters for tuff masonry types of the Campania area. *Engineering Structures*, 283, art. no. 115927.
- Nastri, E., & Todisco, P. (2022) Macromechanical failure criteria: Elasticity, plasticity and numerical applications for the non-linear masonry. *Buildings*, 12, 1245. <https://doi.org/10.3390/>
- Romero, M.L., Espinós, A., Lapuebla-Ferri, A., Albero, V., & Hospitaler, A. (2020). Recent developments and fire design provisions for CFST columns and slim-floor beams. *Journal of Constructional Steel Research*, 172, art. no. 106159.
- Roesler, J., Harders, H., & Baeker, M. (2007). *Mechanical behaviour of engineering material*, Springer, Pag 175-178.
- Shams, M., & Saadeghvaziri, M.A. (1999). Nonlinear response of concrete filled steel tubular columns under axial loading. *ACI Struct J.*, 96(6),1009–19.
- Susantha, K.A.S., Ge, H., & Usami, T. (2002) Cyclic analysis and capacity prediction of concrete-filled steel box columns. *Earthquake Engineering and Structural Dynamics*, 31, 195–216.

Author Information

Donato Aliberti

University of Salerno
Via Giovanni Paolo II, 132, 84084 Fisciano SA, Italy

Elide Nastri

University of Salerno
Via Giovanni Paolo II, 132, 84084 Fisciano SA, Italy

Vincenzo Piluso

University of Salerno
Via Giovanni Paolo II, 132, 84084 Fisciano SA, Italy

Paolo Todisco

University of Salerno
Via Giovanni Paolo II, 132, 84084 Fisciano SA, Italy

Rosario Montuori

University of Salerno
Via Giovanni Paolo II, 132, 84084 Fisciano SA, Italy
Contact e-mail: r.montuori@unisa.it

To cite this article:

Aliberti, D., Nastri, E., Piluso, V., Todisco, P. & Montuori, R. (2023). Experimental analysis on a set of four CFT subjected to monotonic and cyclic loading. *The Eurasia Proceedings of Science, Technology, Engineering & Mathematics (EPSTEM)*, 23, 1-10.

The Eurasia Proceedings of Science, Technology, Engineering & Mathematics (EPSTEM), 2023

Volume 23, Pages 11-18

ICRETS 2023: International Conference on Research in Engineering, Technology and Science

Perception of Public Transport Megaprojects through a User Perspective

Agnes Csiszarik-Kocsir
Obuda University

Janos Varga
Obuda University

Abstract: One of the biggest challenges of the 21st century is to manage population growth and the resulting impacts. Population numbers that exceed the earth's carrying capacity are placing huge environmental pressures on the environment. This is not only reflected in waste management, energy consumption and the use of fossil fuels, but also in a deteriorating quality of life. The millions of people living in metropolises around the world, with their given road networks, create huge transport anomalies that need to be addressed at national and international level. Road congestion, drastic increases in journey times and the rising cost of travel have highlighted the importance of improving public transport. However, for public transport to be attractive, it is essential that the transport alternative itself is fast, comfortable and modern. In the present study, two metro construction projects in cities with high populations (Mumba, Ryadh) are examined, with particular attention to the scale of the project and its usability. The study aims to highlight the visible objectives expressed by the end-users and their reflection in the project based on the results of a primary survey in 2022 and a primary survey in 2023. We will focus on the different phases of project management that lead to the success of the project.

Keywords: Transport, Sustainability, Project, Project scope

Introduction

Defining sustainability is not an easy thing. Many people define its concept in the most different ways, while there are also many people who are not fully aware of the meaning of the concept. Nowadays we say that many things are sustainable and many people consider themselves to be sustainable, but is this really true? Are we aware of what it means to be sustainable? Sustainability has become a popular term today. If you search the internet for sustainability, you will get 2.2 billion results in 0.55 seconds. This shows that sustainability is a much sought-after and popular topic for many people, but it is not the only reason why we need to address it. Indeed, the planet has undergone a major transformation and the last decades have seen an unprecedented explosion in many ways. The world's GDP or the volume of world trade has risen at an unprecedented rate since 1960, as has been seen in the change in population numbers, among other things. In a very short space of time, we have witnessed large-scale increases that have shed new light on the finite capacities of our planet. We have finite resources and opportunities in the face of infinite growth, so it is only a matter of time before the two are finally separated. Sustainability has become not only a fashionable term, but also a concept that increasingly affects our lives. It indicates a major problem, behind which we can assume that something is not working very well and that major change is needed. Meanwhile, globalisation and increasingly intense change are placing new challenges on the shoulders of humanity. Globalisation and digitalisation have significantly changed market and consumer expectations, generating new needs, new services, new strategic solutions and new consumer competences (Garai-Fodor, et al., 2023; Garai-Fodor 2022; 2023). The question rightly arises: in what ways can we sustainably maintain or improve our quality of life? Today, our lives are hampered by many problems. Rising energy prices, population growth and dwindling resources are all pushing us to look at sustainability in a new light. We also need to be clear that sustainability is no longer just about our consumption, but also about

- This is an Open Access article distributed under the terms of the Creative Commons Attribution-NonCommercial 4.0 Unported License, permitting all non-commercial use, distribution, and reproduction in any medium, provided the original work is properly cited.

- Selection and peer-review under responsibility of the Organizing Committee of the Conference

© 2023 Published by ISRES Publishing: www.isres.org

being sustainable in areas such as public transport, which is used by many people. In the case of public transport, too, the increasing number of passengers, the drastic rise in energy prices or the shortage of raw materials and commodities that are important for transport can cause problems on a daily basis. From this perspective, sustainability must also be interpreted and even examined in relation to public transport, given that we are talking about a system that offers a significant proportion of humanity a choice of alternatives and services. However, while we are striving for sustainability in transport, we must not lose sight of the fact that we must at the same time be able to provide a service that is of the right quality, up-to-date and that offers maximum passenger satisfaction. We must provide a sustainable, economical, efficient and high-quality service, which is often not easy, but the challenges of the 21st century have made such demands on transport.

Literature Review

The issue of lifestyle is closely related to sustainability. Sustainable living defines important conditions for everyday people. We really need to think differently about life, we need to change our perception of life, our relationship with nature and our role on the planet. Sustainability is most often associated with consumption (Tseng et al, 2016; Csutora et al., 2022), where it is often thought that all that is needed to have a sustainable world is to consume more consciously or less (Harjato et al, 2021; Wang et al, 2019). If we want to understand sustainability in this dimension for transport, we could say that sustainable transport means travelling less. Most definitions associate sustainability with the finite resources and potential of our planet, but again this implies a consumption-centred approach (Dolan, 2002; Pogutz & Micale, 2011). However, sustainability cannot be linked to consumption alone, as the pursuit of sustainability has a well-defined purpose. Namely, to protect the condition and quality of our environment so that we can live in an environment that provides a suitable living space for all. Defining sustainability is still a challenge today, as many things can be sustainable. Sustainable systems, sustainable cities, sustainable budgets, sustainable tax systems, sustainable entrepreneurship (Győri - Ócsai, 2013), sustainable business environments, sustainable finance and banking (Győri et al., 2021) sustainable tourism (Borzán & Szekeres, 2019; Borzán & Szekeres, 2021), sustainable education (Borzán et al, 2022) and so on. Sustainability could be an important issue in project management as well (Blaskovics, 2016; 2018; Blaskovics et al., 2023). We also hear a lot about sustainable transport or transport systems. It is safe to say that sustainability has a slightly different meaning everywhere, as it means something different in economic, ecological or even transport terms (Morelli, 2011). It was mentioned earlier that sustainability actually requires a complete change of consciousness and lifestyle from humanity. Despite this, we often associate the issue of sustainability only with consumption. However, sustainability covers more than that, it can really require a change of lifestyle. Sustainable life refers to a lifestyle and way of living that meets the needs of the present generation without compromising the ability of future generations to meet their own needs. It involves making conscious choices and adopting practices that minimize negative impacts on the environment, society, and economy. A sustainable life prioritizes resource conservation, social equity, and economic viability, aiming to create a balanced and harmonious relationship between human activities and the natural world. This encompasses actions such as reducing waste and consumption, promoting renewable energy sources, supporting local communities, practicing eco-friendly habits, and fostering a deeper connection with nature. Sustainable living is the practice of adopting habits and behaviors that promote long-term environmental, social, and economic well-being (Livermore, 2012). It involves conscious efforts to reduce one's ecological footprint by making choices that are less resource-intensive and environmentally damaging. Sustainable living encompasses various aspects of daily life, including housing, transportation, food choices, energy consumption, waste management, and consumer behavior. It emphasizes the use of renewable resources, responsible consumption, recycling, reusing, and supporting ethical and eco-friendly products and services. Sustainable living encourages individuals and communities to take active roles in preserving the Earth's ecosystems, biodiversity, and natural resources for future generations (Butters, 2021). A sustainable lifestyle is a way of living that incorporates sustainable practices and values into all aspects of life. It involves making deliberate choices aligned with environmental and social consciousness to reduce one's impact on the planet. A sustainable lifestyle embraces simplicity, mindfulness, and a sense of interconnectedness with nature and fellow human beings (Dimitrova et al, 2021). Key elements of a sustainable lifestyle include reducing waste, conserving energy, opting for sustainable transportation, supporting local and organic products, engaging in environmental activism and advocacy, and promoting social equity and justice. By adopting a sustainable lifestyle, individuals strive to be responsible global citizens, actively contributing to the preservation and regeneration of the Earth's ecosystems and fostering a more equitable and thriving world (Böhme, 2022). However, all definitions of sustainability have something in common. Wherever sustainability is pursued, it is always aimed at having a positive impact on the environment. We want to strive for sustainability in order to make a positive change and a positive impact on our environment. The definition of transport and sustainable transport, which is the subject of this study, is a perfect example of this. The OECD links sustainability and transport. It mentions that transport faces

the same challenges of resource scarcity or increasing demand for services as other productive or service sectors. Moreover, public transport is often under an even greater burden, often having to provide a sustainable service to millions of people on a daily basis. Sustainable transport, according to the OECD, is transport that does not endanger public health and the ecosystem, but provides a service that meets transport needs at the right quality (OECD, 2022). Sustainable transport is expected to use renewable resources at a slower rate than the time it would take to recycle them. And resources that cannot be renewed are used much more slowly than renewable resources. All this points to the need for sustainable transport in this sense to have a positive impact on people's environment, but also to ensure an adequate level of service. The significant positive and negative impacts of transport systems on both the sustainability of cities and people's lives have been demonstrated in several cases. In order to promote sustainability, a number of transport improvement projects are being launched, often with technical or financial constraints. This makes it difficult to implement such projects (Mahmoudi et al, 2021). Creating sustainable transport can be important not only at regional, state or city level. The European Union itself has set significant climate targets, one of the most important of which is the decarbonisation of the transport sector. The EU has pledged to reduce emissions to 0% by 2050 and achieve a form of climate neutrality. This requires a significant reduction in greenhouse gas emissions, but still providing services and solutions that are affordable for citizens (EC, 2022). Among these initiatives, we can assume a significant transformation, with a large number of investments and projects (Varga – Csiszárík-Kocsir, 2019; Dobos et al, 2022). Achieving zero emissions in the transport sector will require replacing, upgrading or adapting many of the technologies or devices that have been in place in the past. But transport cannot be left out of the continuous improvement and regular investment. Public transport is seen as a key element in building sustainable cities and should therefore be central to the sustainability of cities and regions (Miller et al., 2016; Kovács et al., 2020). Sustainable transport is not just about the environmental quality of the means of transport themselves. It means at the same time environmentally sustainable transport, sustainable transport system and sustainability of transport processes (Cheba & Saniuk, 2016). A sustainable transport system should enable mobility for all inhabitants, but in a way that is safe and environmentally friendly. This is not an easy task, as the needs and demands of people from different income groups are different, and it is not always possible to provide this at the same level (Mohan & Tiwari, 2000). However, transport sustainability in this interpretation is also strongly linked to its impact on the immediate environment. The positive relationship between transport sustainability and quality of life has also been clearly confirmed (Steg & Gifford, 2005). Sustainable transport also seeks to maintain a balance. This balance should not only be between transport and quality of life, but should also focus on environmental, economic and social aspects. Sustainable transport must therefore be able to provide environmental, economic and social benefits at the same time (Gilbert & Tanguay, 2000). The relationship between transport and the environment is very closely linked, and this includes the development of transport infrastructure or the modernisation of transport facilities in such a way that transport itself becomes more environmentally friendly and environmentally aware. Challenges in implementing sustainable transport programmes and projects include the complexity of transport problems in the urban environment, conflicts of interest or lack of adequate resources (Fernandez-Sanchez et al, 2020). There is also a strong link between sustainable transport development and project management. While it has become essential to apply sustainability criteria to public transport, economic aspects cannot be ignored. Development projects often have significant cost and time requirements, in addition to the scarcity of other resources in the transport sector. In most cases, development takes the form of major projects or programmes, all with a single objective: to achieve a positive impact that safeguards environmental assets without depriving citizens of transport services. In this way, public transport projects try to achieve the desired impact by maximising resource constraints and, while at the same time being cost and time-constrained, by trying to produce an outcome that meets citizens' expectations while at the same time having a positive impact on their quality of life and the environment.

Material and Methods

The megaprojects presented in this study are included in the top 50 projects list published by the Project Management Institute (PMI, 2021), an organisation that develops project management standards and selects each year the most inspiring and exemplary projects of the year to be used as a model for future similar initiatives. In this study, we would like to present two projects that aim to improve public transport, educate people about the use of cars and reduce the time and safety of transport. The modernisation of public transport will encourage more people to choose surface or underground solutions rather than driving and generating congestion. The two projects presented are metro projects in cities with very high populations (Ryad and Mumbai). The two projects under study are analysed from a user perspective, so no filtering criteria were applied in the selection of the sample of respondents, i.e. educational qualifications, previous project management knowledge were not criteria, i.e. anyone could fill in the questionnaire as a basis for the evaluation. Respondents were asked to rate the selected projects on the basis of some factors related to the scope of the

project. Respondents rated the factors on a scale of 1 to 4, with a score of 1 indicating a very weak factor and a score of 4 indicating a very strong factor. The characterisation of project scope is presented using a word cloud. 39.5% of the sampled respondents have a tertiary education, while 60.5% have a secondary education. 12.2% of respondents are Generation Y, 23.3% are Generation X and 64.5% are Generation Z. The survey was conducted in April and May 2022.

Results and Discussion

The Mumbai-Metro Project

Mumbai is one of the world's most populous cities. The city's rail system moves more than 7 million people commuting daily, which means that situations that endanger passengers are very common. Due to the large crowds, passengers often fall in front of trains or get injured in the crowd. This is why the city authorities decided to modernise the public transport network. The construction of metro line 3 was a huge challenge for the contractors. The first step was to create one of the longest tunnel systems in the world, 33.5 km of underground tunnels with 27 stations. This was a huge challenge, as the line ran through highly populated parts of the city, passing under many tall and listed buildings, and was complicated by overpasses, metro viaducts and railway lines. Getting the tunnel boring machine to the starting point was also a major challenge. During the construction, 8,000 workers and 17 drilling machines worked 24 hours a day to ensure that the plans could be kept on schedule. (PMI, 2021). However, an outbreak of the coronavirus made it very difficult to complete the work on time. Every time a worker fell ill, a team was quarantined, resulting in huge delays to the project. In addition, the works were scheduled during the monsoon season, which meant that flooding also posed a risk to the people working in the tunnel. This project was also specifically designed with the environment in mind. The basic mission of the project is also to reduce the city's carbon dioxide emissions, both by reducing the number of vehicles and by the forest development associated with the project. When respondents were asked to characterise the project scope along the given characteristics, it was seen that it was rated as being of public interest, useful and usable with a much higher ratio compared to the previous project, as the average score for these three characteristics was above 3.6 in all cases. This was followed by a markedly lower average score (around 3.2) for relevance, future focus and feasibility. Respondents ranked the project scope as the least cost-efficient and innovative, with the uniqueness and uniqueness of the project ranking third.

Table 1. The ranking of the scope elements of the Mumbai-Metro project

	Mean	Std. Deviation
novelty	2,517	0,834
usefulness	3,669	0,530
interesting	2,616	0,926
future focus	3,227	0,795
sustainability	3,023	0,823
relevance	3,273	0,742
feasibility	3,221	0,699
usability	3,610	0,653
public interest	3,721	0,544
profit orientation	2,523	0,927
uniqueness	2,523	1,011
cost-effectiveness	2,448	0,887
environmental awareness	3,006	0,921

Source: own research, 2022, N = 172

The research also assessed the average evaluation of the project from the users' perspective. It can be seen that more than 75% of the respondents rated it as good or better, which is definitely a sign of user acceptance.

Table 2. The overall evaluation of the Mumbai-Metro project

	Percent
satisfactory	4,070
medium	19,767
good	50,581
excellent	25,581

Source: own research, 2022, N = 172

We also wanted to investigate the impact of the overall project evaluation on the rating of each element of the project scope. To do this, we carried out an analysis of variance and considered the relationship to be significant where the significance value was below 5%. The results in the table below show that virtually all elements are influenced by the average project perception, which implies that winning the end-user in the first round is a very important factor.

Table 3. Correlation between the Mumbai-Metro project scope perception and average project rating

	F	Sig.
novelty	1,932	0,126
usefulness	5,546	0,001
interesting	4,049	0,008
future focus	7,747	0,000
sustainability	6,791	0,000
relevance	6,064	0,001
feasibility	3,658	0,014
usability	5,296	0,002
public interest	9,897	0,000
profit orientation	4,943	0,003
uniqueness	6,010	0,001
cost-effectiveness	12,321	0,000
environmental awareness	18,592	0,000

Source: own research, 2022, N = 172 (One-way ANOVA, sig = 0,05)

The Riyadh-Metro Project

Saudi Arabia's largest city, Riyadh, previously had no culture of public transport use. With a population of 8.3 million expected by the end of the decade, the vast majority of people in the city will be travelling by car, causing huge environmental damage, congestion and air pollution, and degrading the quality of life of the people living there. The metro project to be unveiled consists of six autonomous lines totalling 176 km, making it the largest public transport project in the world. This is complemented by an extensive network of bus lines, which will cover a further 1150 km (PMI, 2021). The project had a budget of USD 23 billion and was planned to be completed in seven years. The project has a constant focus on a greener approach to a more sustainable future. The design has also taken care of cooling and shading the surrounding areas, using innovative solutions (irrigation channels, canopy, internal and external vegetation). Respondents were then asked to rate one characteristic of project scope on a four-point scale. Here, the highest average scores were given for usefulness, public interest, usability and future focus. The four attributes were all rated above 3.5. In addition, a very high proportion considered the project to be environmentally friendly, sustainable, relevant and feasible, as indicated by average scores above 3.0. The project was considered least profit-oriented, as it received the lowest average rating. Similarly, cost-effectiveness was also rated low, with the uniqueness and uniqueness of the project ranking third from the bottom. The latter is not surprising as the public transport infrastructure is not particularly unique in itself, but the technology used, the architectural solutions and the solutions to protect the environment fall into this category. However, this is not something that the survey respondents have seen from the outside at this stage of the project.

Table 4. Evaluation of the scope of the Riyadh-Metro project

	Mean	Std. Deviation
novelty	2,866	0,851
usefulness	3,576	0,649
interesting	2,860	0,926
future focus	3,500	0,697
sustainability	3,297	0,725
relevance	3,180	0,618
feasibility	3,017	0,761
usability	3,529	0,644
public interest	3,547	0,678
profit orientation	2,401	0,934
uniqueness	2,657	0,951
cost-effectiveness	2,610	0,921
environmental awareness	3,442	0,751

Source: own research, 2022, N = 172

In this case, we also assessed the average evaluation of the project from the users' perspective. It can be seen that more than 75% of the respondents rated it as good or better, which is definitely a sign of user acceptance. However, this also includes potential end-users who rated the project as unsatisfactory and expressed their displeasure.

	Percent
unsatisfactory	2,326
satisfactory	5,233
medium	13,372
good	50,581
excellent	28,488

Source: own research, 2022, N = 172

We were also interested to see to what extent the average rating of the project influenced the perception of each element of the project scope. The data show that the rating of the vast majority of the factors is not affected by the overall rating of the users. The only factors that influenced were future focus, relevance, public interest and profit orientation. This is surprising because in the previous case almost all factors were influenced by the average rating. It should be noted, however, that in this case the rejection of the project has already appeared, as indicated by the average rating.

Table 6. Correlation between the Ryadh-Metro project scope perception and average project rating

	F	Sig.
novelty	2,622	0,052
usefulness	1,843	0,141
interesting	2,440	0,066
future focus	3,383	0,020
sustainability	1,215	0,306
relevance	10,408	0,000
feasibility	0,892	0,447
usability	1,013	0,388
public interest	6,106	0,001
profit orientation	4,313	0,006
uniqueness	1,829	0,144
cost-effectiveness	2,441	0,066
environmental awareness	1,352	0,259

Source: own research, 2022, N = 172 (One-way ANOVA, sig = 0,05)

Conclusion

If we evaluate the two projects as a whole, it can be said that the social utility of each of them is outstanding. Many cities, including Riyadh and Mumbai, have realised that while car transport is more convenient and practical in many cases than public transport, it still places a huge burden on cities and therefore the planet. Public transport offers an alternative to environmentally damaging car travel, by providing an efficient way to get large numbers of people where they need to go. By reducing air pollution, congestion and the negative impact on the environment. The evaluation of the projects shows that they were very positively received by the respondents, even though they may not be direct users. The message value of the projects was that they were perceived as being of most public interest, useful and usable, as these three main characteristics dominated the top three places in the respondents' opinion. In terms of cost-effectiveness, however, respondents had doubts. Obviously this is not a coincidence, as a project to improve public transport is implemented with a huge budget, the benefits of which will only be felt after several years or even decades. Adequate quality public transport and education can certainly be a solution to the environmental problems of our time. The two projects presented in this case and their evaluation by users are certainly a message for future developments, which can help to determine the purpose and direction of similar projects.

Scientific Ethics Declaration

The authors declare that the scientific ethical and legal responsibility of this article published in EPSTEM journal belongs to the authors.

Acknowledgements or Notes

This article was presented as a poster presentation at the International Conference on Research in Engineering, Technology and Science (www.icrets.net) held in Budapest/Hungary on July 06-09, 2023.

References

- Blaskovics, B. (2016). Differences between managing projects in an SME and in a large company. In 4th *International Conference on Management and Organization Brdo* (pp. 159-176).
- Blaskovics, B. (2018). Aspects of digital project management. *Dynamic Relationship Management Journal*, 7(2), 25-37.
- Blaskovics, B., Maró, Z.M., Klimkó, G., Papp-Horváth, V., & Csiszárík-Kocsir, Á. (2023). Differences between public-sector and private-sector project management Practices in Hungary from a competency point of view. *Sustainability*, 15(14), 11236.
- Borzán, A., & Szekeres, B. (2019). Accounting tourism development grants in Hungary. *Polgári Szemle*, 15, Special Issue, (pp. 334-349).
- Borzán, A., & Szekeres, B. (2021). A hazai turizmus támogatási formái. *Polgári Szemle*, 17. évf. 1-3. sz. (pp. 78-94).
- Borzán, A., Szekeres, B., & Szigeti, C. (2022). *Digitalizáció és fenntarthatóság a számvitel és a gazdasági szakismeretek tárgyak oktatásában. A számvitel és a controlling elmélete és gyakorlata: Tanulmányok Bíró Tibor és Sztanó Imre tiszteletére*. Budapesti Gazdasági Egyetem (pp.175-188).
- Böhme, J., Walsh, Z., & Wamsler, C. (2022). Sustainable lifestyles: towards a relational approach. *Sustainability Science*, 17, 2063–2076
- Butters, C. (2021). Myths and issues about sustainable living. *Sustainability*, 13, 7521.
- Cheba, K., & Saniuk, S. (2016). Sustainable urban transport - The Concept of measurement in the field of city logistics. *Transportation Research Procedia*, 16, 35-45.
- Csutora, M., Harangozo, G., & Szigeti, C. (2022). Factors behind the consumer acceptance of sustainable business models in pandemic times. *Sustainability*, 14(15), 9450.
- Deakin, E (2003). *Sustainable development and sustainable transportation: strategies for economic prosperity, environmental quality and equity*. Working Paper 2001-03. University of California at Berkeley Institute of Urban and Regional Development. <https://escholarship.org/content/qt0m1047xc/qt0m1047xc.pdf>
- Dimitrova, A., Vaishar, A., & Šťastná, M. (2021). Preparedness of young people for a sustainable lifestyle: Awareness and willingness. *Sustainability*, 13, 7204.
- Dobos, O., Tóth, I.M., Csiszárík-Kocsir, Á., Garai-Fodor, M., & Kremmer, L. (2022) How generation Z managers think about the agility in a world of digitalization. In: Szakál, Anikó (ed.) *IEEE 20th Jubilee World Symposium on Applied Machine Intelligence and Informatics SAMI (2022) : Proceedings, Poprad, Slovakia* (pp. 207-212).
- Dolan, P. (2002). The sustainability of sustainable consumption. *Journal of Macromarketing*, 22(2), 170-181.
- Fernandez-Sanchez, G, Terrón, J.A., & Fernandez-Heredia, Á. (2020). Evolution towards a sustainable public transport in the city of Madrid. In B. Llamas, M.F.O. Romero & E. Sillero (Eds), *Sustainable Mobility* April 22nd, 2020. <https://www.intechopen.com/chapters/70092>
- Garai-Fodor, M., Vasa, L., & Jäckel, K. (2023). Characteristics of segments according to the preference system for job selection, opportunities for effective incentives in each employee group. *Decision Making: Applications in Management and Engineering*, 6(2), 557-580.
- Garai-Fodor, M. (2022). The impact of the coronavirus on competence, from a generation-specific perspective. *Acta Polytechnica Hungarica*, 19(8), 111-125.
- Garai-Fodor, M. (2023). Digitalisation trends based on consumer research. *IEEE 17th International Symposium on Applied Computational Intelligence and Informatics SACI 2023*. Proceedings, IEEE Hungary Section, 349-352.
- Gilbert, R., & Tanguay, H. (2000). *Sustainable transportation performance indicators project. Brief review of some relevant worldwide activity and development of an initial long list of indicators*. The Centre for Sustainable Transportation, Toronto, Ontario, Canada
- Györi, Zs., & Ócsai, A. (2013). Ecologically-oriented enterprises in Hungary. *World Review of Entrepreneurship, Management and Sustainable Development*, 10(1), 52-65.
- Györi, Zs., Kahn, Y., & Szegedi, K. (2021). Business model and principles of a values-based bank—Case study of MagNet Hungarian Community Bank. *Sustainability*, 13(16), 9239,
- Harjoto, M.A., Kownatzki, C., Alderman, J., & Lee, R. (2021). Sustainable consumption and production, climate change and firm performance. *Journal of Impact and ESG Investing*, 2(2), 8-34.

- Kovács, Z., Farkas, J.Zs., Szigeti, C., & Harangozó, G. (2022). Assessing the sustainability of urbanization at the sub-national level: The ecological footprint and biocapacity accounts of the Budapest Metropolitan Region, Hungary, *Sustainable Cities and Society*, 84, 104022.
- Livermore, J. (2012). *Simple, sustainable living: An illustrated journal*. Independent Study Project (ISP) Collection. 1462. Retrieved from https://digitalcollections.sit.edu/isp_collection/1462 (downloaded: 17.07.2023)
- Mahmoudi, R., Shetab-Boushehri, S.N., & Emrouznejad, A. (2021). Sustainability in the evaluation of bus rapid transportation projects considering both managers and passengers perspectives: A triple-level efficiency evaluation approach. *International Journal of Sustainable Transportation*, 16(12). 2022.
- Miller, P., De Barros, A., Kattan, L., & Wirasinghe, S.C. (2016). Public transportation and sustainability: A review. *KSCE Journal of Civil Engineering*, 20(3), 1076-1083
- Mohan, D., & Tiwari, G (2000). *Sustainable transport systems: linkages between environmental issues, public transport, non-motorised transport and safety*. Transportation Research and Injury Prevention Programme. Indian Institute of Technology
- Morell, J. (2011). Environmental sustainability: a definition for environmental professionals. *Journal of Environmental Sustainability*, 1(1). Article 2.
- Project Management Institute (2021). *Most influential projects*. <https://www.pmi.org/most-influential-projects-2021> (downloaded: 19/03/2022)
- Pogutz, S., & Micale, V. (2011). Sustainable consumption and production. *Society and Economy*. 33(1), 29-50.
- Steg, L., & Gifford, R. (2005). Sustainable transportation and quality of life. *Journal of Transport Geography*, 13, 59-69
- Tseng, M.L., Tan, K.H., Geng, Y., & Govindan, K. (2016). Sustainable consumption and production in emerging markets. *International Journal of Production Economics*, 181, 257-261
- Varga, J., & Csiszárík-Kocsir, Á. (2019). Redefining the role of project leader for achieving a better project result. *PM World Journal*, 8(8), 1-18.
- Wang, C., Ghadimi, P., Lim, M., & Tseng, M.L. (2019). A literature review of sustainable consumption and production: A comparative analysis in developed and developing economies. *Journal of Cleaner Production*, 206, 741-754.

Author Information

Ágnes Csiszárík-Kocsir

Óbuda University, Keleti Károly Faculty of Business and Management, 1084 Budapest, Tavaszmező 15-17, Hungary
Contact e-mail: kocsir.agnes@uni-obuda.hu

János Varga

Óbuda University, Keleti Károly Faculty of Business and Management, 1084 Budapest, Tavaszmező 15-17, Hungary

To cite this article:

Csiszárík-Kocsir, A., & Varga, J. (2023). Perception of public transport megaprojects through a user perspective. *The Eurasia Proceedings of Science, Technology, Engineering & Mathematics (EPSTEM)*, 23, 11-18.

The Eurasia Proceedings of Science, Technology, Engineering & Mathematics (EPSTEM), 2023

Volume 23, Pages 19-25

ICRETS 2023: International Conference on Research in Engineering, Technology and Science

Biodiesel Production Using Supercritical Methanol in Bench-Scale Reactor

Filiz Alshanableh

Near East University

Mahmut A. Savas

Near East University

Abstract: Biodiesel is preferred as an alternative fuel due to its sustainability and easy availability of raw materials. Studies to improve biodiesel production time and costs are gaining importance in terms of being used in higher portions as a fuel. Traditional catalytic biodiesel production is time- energy-consuming due to feedstock preprocessing, product separation, and purification steps. Non-catalytic biodiesel production using supercritical alcohol may shorten and eliminate the pre- and post-production stages in terms of time and cost compared to traditional methods. In this study, canola oil was converted to biodiesel using supercritical methanol. Biodiesel production was carried out in the bench-size supercritical reactor that was fabricated as part of this study. The higher yield was obtained from biodiesel produced using canola oil and supercritical methanol compared to the traditional catalytic methods. 98.8 % yield was obtained at 240°C and 8.3 MPa which were just above the critical temperature and pressure of methanol. Including reaction and separation, the complete process via supercritical transesterification took 180 minutes, while the whole traditional base-catalyzed transesterification process takes approximately one day.

Keywords: Biodiesel, Supercritical methanol, Transesterification

Introduction

Catalytic biodiesel (BD) production is a time and energy-consuming process that involves various preprocessing, separation, and purification steps. In contrast, non-catalytic BD production using supercritical alcohol offers the potential to simplify these stages (Saka & Kusdiana, 2001; Demirbas, 2006). Supercritical alcohol can create a homogeneous phase with triglycerides at high pressures and temperatures, allowing reactions to occur without needing a catalyst. The separation of BD from glycerol is also easier in the supercritical method than in conventional technologies requiring additional purification steps. While the supercritical method requires high temperatures and pressures, it presents advantages over traditional methods.

Supercritical methanol (SCM) refers to methanol in a state above its critical point as shown Figure 1, where the phase boundary between liquid and vapor disappears. At these conditions, methanol exhibits a liquid-like density and gas-like transport properties such as diffusivity and viscosity. The single-phase characteristics of SCM make it an excellent solvent for biodiesel production.

Although base catalyzed transesterification has been used for BD production for decades, the feedstock used has certain limitations, including their free fatty acid (FFA) and water content, the length of time required for the purification of reaction products, and the large amount of waste water that is generated (Meher et al., 2006; Sharma & Singh, 2007). As a solution to these problems, in 1998 Diasakou et al. developed the non-catalytic transesterification method using a subcritical temperature of methanol (240°C, 220°C, 235°C). Previous studies have investigated supercritical transesterification using methanol as a supercritical fluid. Researchers have explored various temperatures, pressures, reactor sizes, and oil types to achieve high conversion rates within

- This is an Open Access article distributed under the terms of the Creative Commons Attribution-Noncommercial 4.0 Unported License, permitting all non-commercial use, distribution, and reproduction in any medium, provided the original work is properly cited.

- Selection and peer-review under responsibility of the Organizing Committee of the Conference

© 2023 Published by ISRES Publishing: www.isres.org

short reaction times. For instance, Saka and Kusdiana (2001) successfully produced BD from rapeseed oil using SCM in a 5 mL Inconel 625 batch reactor, achieving over 95% conversion in 5 minutes. Table 1 summarizes some of the notable studies on SCM transesterification with different oils and reaction conditions.

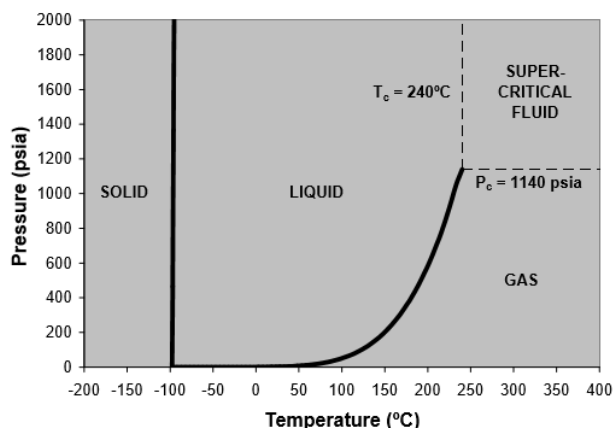


Figure 1. Phase diagram of methanol (Ebert, 2008)

Table 1. Some SCM transesterification of various vegetable oils (Silva & Oliveria, 2014).

Temperature Pressure	Oil type	Oil :Alcohol (molar ratio)	Reaction time	Reactor type	Conversion of methylester	Reference
350°C, 450 bar	rapeseed	1:42	4 min	5 mL, BR Inconel	>95 %	Saka and Kushidiana, 2001
350°C, Not recorded	hazelnut	1:41	5 min	100 mL, BR, SS	95 %	Demirbaş, 2002
350°C, 200 bar	sunflower	1:40	40 min	8 mL, BR, SS	96 %	Madras et al., 2004
350°C, 180 bar	coconut	1:42	7 min	TR, SS	95 %	Bunyakiat et al., 2006
280°C, 250 bar	soybean	1:42	30 min	200 mL BR	90 %	He et al., 2007
300°C, 150 bar	soybean	1:40	20 min	BR	70 %	Wang et al., 2008
350°C, Not recorded	palm oil	1:40	20 min	BR	80 %	Tan et al., 2010
350°C, 350 bar	palm olein	1:40	~15min	TR	85 %	Choi et al., 2011
270°C, 100 bar	waste canola	1:1 (mass ratio)	45 min	BR	96.4 %	Lee et al., 2012

BR: batch reactor; TR: tubular reactor; SS: stainless steel

While maximum operating pressures, operating temperatures, and reactor sizes were reported in previous studies to be 450 bars (Saka & Kushidiana, 2001), 350°C and 200 mL (He et al., 2007), their minimum values were 100 bar, 270°C (Lee et al., 2012) and 5 mL (Saka & Kushidiana, 2001), respectively.

It was necessary to design and manufacture a bench-scale batch reactor in order to meet the extreme process conditions of high pressure and temperature required to manufacture BD using the supercritical fluid method (Al-Shanableh, 2017; Al-Shanableh & Savas, 2022). By using the designed supercritical reactor, canola oil was transformed into BD. This study focuses on the production of BD using supercritical methanol (SCM) in a bench-scale reactor.

Method

Materials

Refined canola oil (RCO) and anhydrous methanol (MeOH) were used as the feedstock for BD production. The canola oil was purchased from a local supermarket, while the methanol (99.8 % purity) was obtained from Merck. Fatty acid compositions of RCO was determined following the EN ISO 5508 in the TRNC- Ministry of Health-Directorate State Laboratory-Nicosia using Gas Chromatography (GC). Fatty acid content of RCO was

found as 0.08 wt % of lauric acid (C12:0), 5.63 wt % of palmitic acid (C16:0), 1.57 wt % of stearic acid (C18:0), 62.97 wt % of oleic acid (C18:1), 21.34 wt % of linoleic acid (C18:2), 6.99 wt % of linolenic acid (C18:3), 0.46 wt % of arachidic acid (C20:0) and 1.04 wt % of gondoic acid (C20:1). Trace amounts of other FA constituents like 0.001 wt % of erucic acid (C22:1) in RCO were not taken into consideration.

Experimental Setup for Biodiesel Production by SCM

The experimental setup involved a bench-size, batch-type reactor designed to handle the extreme process conditions of high temperature and pressure as shown in Figure 2 (Al-Shanableh, 2017).



Figure 2. Photograph of designed and manufactured supercritical reactor.

The experimental setup for one-step supercritical methanol transesterification was designed to operate under high temperatures and pressures. Nitrogen gas was used as an inert medium to provide pressure, and a flexible high-pressure hose connected the supercritical reactor. The reactor was equipped with an external heater, insulating mantle, electromagnetic stirrer, safety valve, pressure gauge, and thermocouple for temperature measurement. A laboratory type double pipe heat exchanger served as the condenser. The experimental setup used is illustrated in Figure 3.

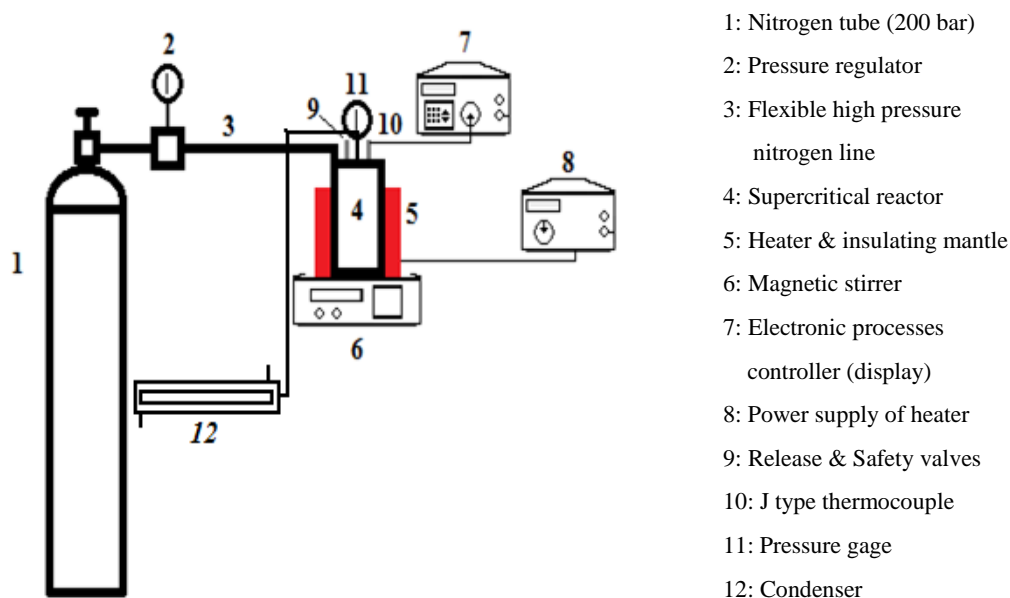


Figure 3. Schematic diagram of supercritical BD production set-up

Experimental procedure for Biodiesel Production by SCM

The supercritical methanol transesterification of canola oil was carried out using the experimental setup described above and following the steps in the flowchart as shown in Figure 4.

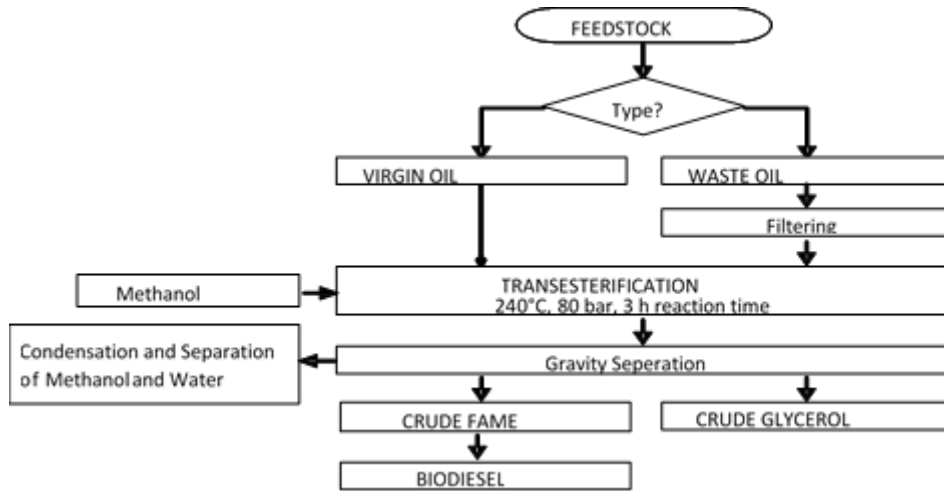


Figure 4. Flowchart for the experimental procedure of the SCM biodiesel production

The procedure involved charging a mixture of RCO and methanol into the supercritical reactor, mixing them to obtain a homogeneous mixture, closing the reactor, and adjusting the temperature and pressure to reach the supercritical fluid region. The reaction time varied from 1 to 3 hours, and after the specified reaction time, the reaction vessel was removed from the heating jacket, and the cooling process took place. The excess methanol was transferred to the condenser, and the product mixture was poured into a separation funnel to separate the fatty acid methyl esters (FAME) and glycerol phases. The FAME was further heated to remove any remaining water or methanol, and its weight was measured to determine the transesterification yield. After production was completed to ensure the quality of produced biodiesel, its properties such as viscosity, cloud point, and pour point were measured following corresponding ASTM and EN-ISO standards.

Results and Discussion

Biodiesel Yield by SCM Transesterification

SCM transesterification experiments were conducted as five batches at constant temperature and pressure of 240°C and 8.3 Mpa, respectively which were just above the critical temperature and pressure of methanol. These minimum operating temperature and pressure were preferred to ensure safety, even though it would result in longer reaction times. The reaction time started from 1 hour for the first batch, then, increased by half an hour for the next batch and so on. The percent conversion of canola oil to biodiesel was determined using the equation below (Phan and Phan, 2008).

$$\% \text{ Yield} = \frac{m_{\text{ester}}}{3 \times \frac{m_{\text{oil}}}{MW_{\text{oil}}} \times MW_{\text{ester}}}$$

where MW_{oil} and MW_{ester} are the averaged molecular weight of feedstock oil (RCO) and FAME (RCOME) produced, respectively.

Table 2. % Yield of RCO to RCOME by supercritical transesterification

Batch No. (reaction time)	% Conversion of FAME produced
Batch 1 (60 min)	86.4
Batch 2 (90 min)	89.0
Batch 3 (120 min)	97.9
Batch 4 (150 min)	98.2
Batch 5 (180 min)	98.8

The results showed that longer reaction times resulted in higher conversions, as shown in Table 2. The percent yield increased from 86.4% to 98.8% as the reaction time increased from 1 to 3 hours. The obtained conversions met the minimum ester content requirement of 96.5% specified by the EN 14214 standard. The results were compared with previous studies which are used similar conditions, for example, Lee et al. working with little

higher temperature at 270 °C obtained a 96.4 % yield in 45 minutes (Lee et al., 2012). The comparison indicates that higher pressure and temperature can significantly reduce the reaction time required for biodiesel production

Characterization of Produced Biodiesel

The produced biodiesel samples for each batch were tested for their viscosity, cloud point, and pour point following either ASTM D6751 or EN 14214 standards. The viscosity values fell within the acceptable range specified by ASTM D446. The kinematic viscosities of the biodiesel produced via base-catalyzed transesterification (Al-Shanableh et al., 2023) and supercritical methanol transesterification were comparable. However, the supercritical method required significantly less time to complete the production process, including device preparation, reaction, and separation. The results of the viscosity, cloud point, and pour point tests are presented in Table 3. As the percent conversion of RCO to RCOME increased, its kinematic viscosity decreased.

Table 3. Viscosity, CP and PP test result for RCOME

	Kinematic Viscosity (mm ² /s)	Cloud Point (°C)	Pour Point (°C)
Base Catalyzed Transesterification *	4.582	-3.5	-10
Batch 1	5.966	4.3	-5.5
Batch 2	5.230	4.0	-6.0
Batch 3	4.760	-2.0	-8.8
Batch 4	4.592	-3.0	-9.0
Batch 5	4.580	-3.0	-9.0

*Al-Shanableh et al., 2023

The fuel properties of the biodiesel produced by the traditional method with the same feedstock-RCO were compared to Batch 5 biodiesel that was produced by in this study as shown in Table 4.

Table 4. The fuel properties of of base-catalyzed and SCM BD

	Method	Limits	RCOME by Base-catalyzed	RCOME by SCM-Batch #5
Kinematic viscosity at 40 °C	ASTM D 445	1.9-6.0	4.582	4.580
Higher heating value	ASTM D 4809	35.0	39.23	39.18
Free glycerin (wt %, max.)	EN 14105	0.02	0.003	0.003
Total glycerin (wt %, max.)	EN 14105	0.25	0.196	0.192
Mono glyceride (wt %, max.)	EN 14105	0.80	0.64	0.61
Diglyceride (wt %, max.)	EN 14105	0.20	0.20	0.20
Triglyceride (wt %, max.)	EN 14105	0.20	0.1	0.1
Ester contents (wt %, max.)	EN 14103	96.5	97.0	98.8
Linoleic acid methyl esters	EN 14103	12.0	6.8	4.5
Iodine value (g I ₂ / 100 g,	EN 14111	120	66	66
Cloud point (°C)	D 2500		-3.5	-3
Pour point (°C)	D 97		-10	-9
Cold filter plugging point	D 6371		-7.5	-7

Table 5. A comparison of base-catalyzed and SCM transesterification methods

	Base-Catalyzed Transesterification	SCM Transesterification
Reaction time (min)	60	180
Reaction temperature(°C)	60	240
Reaction pressure (bar)	Atmospheric pressure	83
Separation from glycerol	Need min 8 hours	10 min
FFAs in feedstock	Need to be determined	No need to determine
Water in feedstock	Need minimum 2 hours for removal	No influence
Yield of FAME (%)	97.0	98.8
Purification of FAME	Difficult –Require water washing and drying min. 6 hours	none

Compared to base-catalyzed transesterification, the major disadvantage of SCM seems to be only high temperature and pressure as seen in Table 5. Once the system is built, production can be performed at higher

temperatures and pressures, resulting in a higher BD conversion and a shorter reaction time. The short reaction time of SCM makes it more suitable for continuous production.

Conclusion

The study successfully demonstrated the production of biodiesel using supercritical methanol in a bench-scale reactor. The supercritical fluid method showed promising results in terms of efficiency and reduced production time compared to base-catalyzed transesterification. The one-step process using a bench-scale reactor yielded high conversion rates within a relatively short time. 98.8 % yield was obtained at 240°C and 8.3 MPa, just above the critical temperature and pressure of methanol. Including reaction and separation, the complete process via supercritical transesterification took 180 minutes. The results indicate that the supercritical method has the potential for large-scale biodiesel production, particularly due to its shorter reaction time. Further research and optimization of the process parameters can lead to even higher conversions and improved overall efficiency in biodiesel production using supercritical methanol.

Scientific Ethics Declaration

The authors declare that the scientific ethical and legal responsibility of this article published in EPSTEM journal belongs to the authors.

Acknowledgements

* This article was presented as an oral presentation at the International Conference on Research in Engineering, Technology and Science (www.icrets.net) held in Budapest/Hungary on July 06-09, 2023.

* The authors would like to express their sincere thanks to Assoc. Prof. Dr. Ali Evcil for his contributions during the reactor design and biodiesel production phase.

* The authors would also like to acknowledge to Eng. Birgul Kaya, and Eng. Muzaffer Kaya for their endless financial and moral support during the manufacturing and testing of the reactor.

* This work was supported by the Near East University Research Fund under project no. YDU/2010-2-21.

References

- Al-Shanableh, F. (2017). *Characterization of cold flow properties of biodiesel transesterified from waste frying oil*. Ph. D. Thesis in Mechanical Engineering. Retrieved from <http://docs.neu.edu.tr/library/6533447758.pdf>.
- Al-Shanableh, F., Bilin, M., Evcil, A., & Savas, M. A. (2023). Estimation of cold flow properties of biodiesel using ANFIS-based models. *Energy Sources, Part A: Recovery, Utilization, and Environmental Effects*, 45(2), 5440-5457.
- Al-Shanableh, F. & Savas, M. A. (2022). Material selection of batch type supercritical reactor for biodiesel production. *The Eurasia Proceedings of Science Technology Engineering and Mathematics*, 21, 477-483.
- Demirbas, A. (2006). Biodiesel production via non-catalytic SCF method and biodiesel fuel characteristics. *Energy Conversion Management*, 47, 2271–82.
- Diasakou, M., Louloudi, A., & Papayannakos, N. (1998). Kinetics of the non-catalytic transesterification of soybean oil. *Fuel*, 77, 1297-1302.
- Ebert, J. (2008). Supercritical methanol for biodiesel production. *Biodiesel Magazine*, April, 80-85.
- He, H., Sun, S., & Wang, T. (2007). Transesterification kinetics of soybean oil for production of biodiesel in supercritical methanol. *The Journal of the American Oil Chemists' Society*, 84, 399.
- Lee, Y., Park, S.H., Lim, I.T., Han, K., & Lee, S.Y. (2000). Preparation of alkyl (R)-(2)-3-hydroxybutyrate by acidic alcoholysis of poly-(R)-(2)-3-hydroxybutyrate. *Enzyme Microbial Technology*, 27, 33–6.
- Meher, L.C., Kulkarni, M.G., Dalai, A.K., & Naik, S.N. (2006). Transesterification of karanja (Pongamia pinnata) oil by solid basic catalysts. *European Journal of Lipid Science and Technology*, 108, 389–97.
- Phan, A.N., & Phan, T.M. (2008). Biodiesel production from waste cooking oils. *Fuel*, 87, 3490-3496.
- Saka, S., & Kusdiana, D. (2001). Biodiesel fuel from rapeseed oil as prepared in supercritical methanol. *Fuel*, 80, 225–31.

Sharma, Y.C., Singh, Y.C., & Upadhyay, S.N. (2007). Advancements in development and characterization of biodiesel: A Review. *Fuel*, 87, 2355-2373.

Silva, C., & Oliveria, V. (2014). Biodiesel production through non-catalytic supercritical transesterification: current state and perspectives. *Brazilian Journal of Chemical Engineering*, 31, 271 – 285.

Author Information

Filiz Al-Shanableh

Near East University

Nicosia, Mersin 10, Turkey

Contact e-mail: filiz.shanableh@neu.edu.tr

Mahmut A. Savas

Near East University

Nicosia, Mersin 10, Turkey

To cite this article:

Al-Shanableh, F. & Savas, M. A. (2023). Biodiesel production using supercritical methanol in bench-scale reactor. *The Eurasia Proceedings of Science, Technology, Engineering & Mathematics (EPSTEM)*, 23, 19-25.

The Eurasia Proceedings of Science, Technology, Engineering & Mathematics (EPSTEM), 2023

Volume 23, Pages 26-33

ICRETS 2023: International Conference on Research in Engineering, Technology and Science

Data Cleaning in Medical Procurement Database: Performance Comparison of Data Mining Classification Algorithms for Tackling Missing Value

Amarawan Pentrakan
Prince of Songkla University

Arbee L. P. Chen
Asia University

Abstract: Data cleaning is an important process for improving the quality of decision-making information. One of today's popular cleaning tools is data mining techniques. In this paper, we focused on using data mining classification algorithms to resolve missing values in medical purchasing databases. To serve this purpose, the predictive performance of four different classifiers: Decision Tree, Naïve Bayes, K-Nearest Neighbor, and Support Vector Machine (SVM) were compared in this study. We used 2,311 medical data records from procurement database in Thailand between July 2019 and December 2019 in the experimental process. We also discussed the function of feature selection and test options that support analysis to improve model performance. The results showed that the SVM algorithm outperforms with a maximum accuracy of 89.61%. Additionally, we discussed the strengths and weaknesses of these data mining techniques for data cleaning and future research.

Keywords: Data mining techniques, Classification algorithms, Medical procurement database, Missing values

Introduction

The use of medical procurement data in clinical research and management has increased dramatically, but the missing value resources pose data cleaning challenges (Sakly et al., 2022). Although nowadays there are many popular data cleaning tools in various domains, they often process all variables uniformly (Shi et al., 2021), meaning that they might not serve well for medical procurement database because there is specific information to the variables that must be considered. Thus, in this paper, our study proposes a data cleaning tools to correct missing values in the data variables of medical procurement with data mining knowledge widely-used techniques taken into consideration.

Medical procurement data may include a wide range of data, including purchasing products, suppliers, related services, payment information, and the purchase conditions of health facilities (Pentrakan et al., 2023). In the case of medication, it may occur after the product has been selected for inclusion on the health facility list and/or the national reimbursement list. The data collected from real practice is frequently incomplete (Wang et al., 2021), including lots of typos, errors, and missing values. Therefore, the abundance of data resources often raises the challenge of data cleaning. This results in large amounts of time and budget for many analyses.

Data cleaning is a fundamental step of data analysis with the goal of cleaning up raw data (Xu et al., 2015). This is a very important process because all analyses require quality data to find the reliable results. The cleaning process can begin with identifying information that is incomplete or unreasonable, and then improves quality by correcting detected errors and omissions. In practice, it is generally found that data cleaning and preparation take up about 80% of the total data engineering effort (Zhang et al., 2003). This is a crucial research problem for

- This is an Open Access article distributed under the terms of the Creative Commons Attribution-Noncommercial 4.0 Unported License, permitting all non-commercial use, distribution, and reproduction in any medium, provided the original work is properly cited.

- Selection and peer-review under responsibility of the Organizing Committee of the Conference

many analysts and organizations. Consequently, a powerful tool for medical procurement systems that cleans data more accurately and faster, can save time and increase efficiency in data analysis.

With the need for effective cleaning of medical data, many studies have been conducted on the general framework to only intend to assess the quality of the data, but there are no data cleaning procedures (Shi et al., 2021). While other domains have been extensively investigated in data cleaning, one interesting thing is that the problem of estimating missing values can be processed by using data mining techniques. Data mining is used to extract knowledge from existing data. It can be used to discover things that were previously unknown and retrieve interesting patterns and related relationships in a given dataset, including classification rules or trees, sequence modeling, clustering, regression, dependency, and so forth. This knowledge can be utilized in calculating the estimates for missing values. However, each data mining algorithm may have its own specific performance for each task, and no one can be effective for all data (Mandal & Jana, 2019). The chosen algorithm used for each domain depends on the unique variables in each field and its constraints.

Our study aims to examine the performance of data mining techniques for handling missing values by comparing the performance of four different classification algorithms: Decision Tree, Naïve Bayes, K-Nearest Neighbor, and Support Vector Machine. The study is evaluated in terms of accuracy, error distribution, and the time spent building and testing the model. We also discuss the function of feature selection and the testing options that underpin the analysis in this experimental process. The results show both the pros and cons of those algorithms. The expected outcome is to assist users and decision-makers in selecting the best techniques to resolve missing values in medical procurement databases.

Description of Algorithms and Tools

Several open-source data mining software are available for free on the Web. In this experimental study, we applied the Waikato Environment for Knowledge Analysis (WEKA) tool version 3.9.3 for processing classification models. WEKA has become widely used as a toolkit for data mining tasks and was originally established by the University of Waikato (New Zealand). This software contains a large function of data mining techniques and can be accessed through standard terminal applications. It contains several techniques for pre-processing, classification, clustering, association rules, visualization, and regression (Holmes et al., 1994). It also supported versions for Windows, Linux, and MAC operating systems. WEKA, therefore, is currently popular with academics and widely applied for teaching, research, and industrial applications (Hussain et al., 2018). Additionally, we also use Tableau software for data visualization (Chabot et al., 2003). This tool can provide an accessible way to understand patterns and results (Batt et al., 2020).

In this article, we determine four classifier learning algorithms that are implemented in WEKA (Sahoo & Kumar, 2012). Three algorithms consist of Decision Tree (DT), Naïve Bayes (NB), and Support Vector Machine (SVM) techniques, which are parametric classifiers based on statistical probability distributions. The other one, the K-Nearest Neighbor (KNN), is a nonparametric classifier based on the probability density function. A brief description of each algorithm and how it works in WEKA is detailed as follows: (1) DT is one of the data mining techniques that classifies recursive training data instances by deep-first or broad-first greedy methods until all data instances belong to a specific class. Of them, there are many advanced DT algorithms such as, CART, ID3, C4.5, C5.0, etc. This paper uses the C4.5 algorithm developed by Ross Quinlan, which is called J48 in WEKA. It can handle both categorical and numerical entries, and can generate thresholds to use for continuous-label classification (Patil et al., 2009); (2) NB works in conjunction with Bayes theorem-based statistical methods (Bouckaert, 2008). The probabilities for each class are calculated from the given data and are considered independent of each other. This may be called conditionally independent. With this classification, it is possible to predict the probability of group membership and can remove irrelevant data; and (3) KNN is an instance learning method also known as lazy learning. It stores all available data and classifies the new data points based on their similarity (Steinbach & Tan, 2009). This means that when new information appears, the dataset can be easily classified into categories. Therefore, it runs very quickly during training, but it takes more computational time to classify new instances that come into the model (Zhang, 2010). Additionally, it is susceptible to noise in the dataset and memory limitations; and (4) the SVM technique is a classifier method that performs classification tasks by constructing hyperplanes. It was generally developed for binary classification problems, but now extensions to this technique have been made to support multi-class classification (Rajvanshi & Chowdhary, 2017). In WEKA, this technique can be selected at the SMO function, which stands for Sequential Minimal Optimization. It is the specific efficient optimization algorithm used inside the SVM implementation and works by finding a line that best separates the data into the two groups. This is done by an optimization process that considers only those data instances in the training data set that are closest to the line

that best separates the classes (Pentrahan, 2021). These instances are known as support vectors. This calculates the maximal margin that can reduce the generalization error.

In addition, this study also examines two test option techniques to test whether there is an improvement in the accuracy measure when using suitable test options. First is the Cross-Validation (k-fold) option (Browne, 2000). The performance measure designed by k-fold cross-validation is the average of the values computed in the loop. The training set is split into k smaller groups, and then using k-1 of the folds trained model as training data. Then, the resulting model is validated in the remaining part of the data. This is used as a test set to estimate a performance measure, such as accuracy. The second is the Percentage Split option. The dataset is randomly split into two disjoint sets (Kabakchieva, 2013). The first set is called the training set that works as knowledge form. This extracted knowledge is used to test against the second set which is called the test set.

Method

Dataset and Process

The study dataset contains medical procurement data in Thailand from July 2019 to December 2019. We have listed all relevant features in Table 1. A total of 2,749 transaction records were associated with 2,311 complete records and 438 incomplete records. If the analyst excludes those records from the analysis, they may lose important values and cause significant errors in calculating the average price of each medical product. Therefore, in this study, we aimed to investigate the effectiveness of data mining techniques for handling missing values of the units per pack (SIZE feature) for this sample dataset.

To serve this purpose, we used 2,311 complete records without missing values to examine the model of each classifier. We hypothesized that six features that exhibit in this dataset (the segmented purchasers, the group of generic product and trade product names, procurement methods, suppliers, and total purchase budgets) could be used in developing the model to estimate the missing values of pack sizes for medical products effectively.

Table 1. Features and the definitions of a dataset

Features	Definition	Distinct values	Total records	Missing values (%)
DEPT	Departments who purchase the medical product	394	2,747	2 (0.07%)
GEN	Generic product name (e.g., Parecoxib 40 mg injection)	4	2,746	3 (0.11%)
TRAD	Trade product name or brand (e.g., DYNASTAT [®])	36	2,746	3 (0.11%)
METH	Procurement method (e.g., bidding method)	2	2,749	0 (0%)
COM	Company or supplier who sells the medical product	38	2,749	0 (0%)
PRICE	The purchasing price per pack (Thai Baht)	572	2,749	0 (0%)
SIZE*	The number of units per pack (e.g., 30 tablets per box)	12	2,319	430(15.6%)

*Output variable corresponding to the class labels of pack size for medical products.

We used six purchasing properties as input features: DEPT, GEN, TRAD, METH, COM, and PRICE according to the different descriptions and values shown in Table 1: DEPT is the name of 394 purchasing departments that make the decision to buy medical products for hospitals; GEN is the name of a generic product with four different names according to the anatomical chemotherapy (ATC) classification code; and TRAD is the name of a trade product with 36 different names. METH is the procurement method that includes two approaches used in the procurement system; COM is the winning company or supplier associated with 38 different companies that is recorded to sell medical products to hospitals; and PRICE is the total purchase budget consisting of 572 various labels. These six features were used to develop a model to estimate the missing value of package sizes (SIZE) for medical products.

In the pre-processing step, we have discretized the continuous values of the SIZE feature into the class label of nominal values. The price values of PRICE feature were also discretized into class labels of price ranges for medical products. To remove irrelevant and redundant features, all features were examined using the feature selection method. This was intended to maximize classification accuracy. To do this process, we used the function of wrapper subset evaluator (Karegowda et al., 2010) implemented in the WEKA. The features selected depend on the classifier that builds the model. It worked to find the smallest subset of the attribute by selecting important features for the underlying clusters based on the criteria of the algorithm. Then, in this step, we examined two test options (cross-validation and the percentage split) to determine the best options for classification algorithms.

Model Evaluation Metrics

After the model was developed and validated by test options, we can obtain feedback from metrics that can explain the performance of the model. Generally, the performance comparison of the four different algorithms was measured in terms of measuring accuracy and error distribution (Galdi & Tagliaferri, 2018). Accordingly, this study used several relevant metrics, including accuracy rate, F-measure, precision, recall (sensitivity), mean absolute error (MAE), and root mean squared error (RMSE). We also used the kappa statistic (McHugh, 2012) and an area under the receiver operating characteristic curve (Hamel, 2009). In addition, the time spent building and testing the model were represented in the results of our study.

Results and Discussion

In this section, we discuss the empirical analysis of the study. First, we represent the descriptive statistics of variables to give information about relevant variables. Then, we discuss the results of the feature and test option analyses followed by the performance analysis.

Descriptive Statistics

In our analysis, we used the complete input data of 2,311 records to develop the model. The sample dataset consisted of four generic products frequently purchased from July 2019 to December 2019. All medical products listed in the purchasing dataset were defined according to the lowest level of the Anatomical Chemotherapy (ATC) classification system (Skrbo, 2004), as shown in Table 2.

Table 2. Descriptive statistics of medicine used in this study

ATC code of medical products	Package size	Number of records	Number of trade products	Number of purchasing departments	Number of selling companies	Range of purchasing budgets
M01AH04	1 unit/box	258	2	47	4	1,939 – 5,816,400
	5 units/box	416	2	79	12	969 – 930,643
	10 units/box	9	2	5	3	969 – 963,942
	50 units/box	5	2	1	1	19,388 – 198,388
	100 units/box	3	1	1	1	19,388 – 19,388
A02BA02	1 unit/box	335	17	107	9	200 – 97,200
	10 units/box	9	4	9	4	2,000 – 20,000
	50 units/box	8	7	1	6	792 – 40,000
	100 units/box	348	16	125	10	190 – 126,720
	250 units/box	6	4	4	5	160 – 10,000
	500 units/box	145	3	86	3	400 – 99,000
C10AA07	1000 units/box	30	3	18	4	600 – 478,932
	1 unit/box	129	6	23	6	6,420 – 832,032
	28 units/box	328	7	49	11	706 – 499,647
	30 units/box	32	1	9	3	9,540 – 256,800
	56 units/box	7	3	6	3	23,946 – 360,323
C10AA01	84 units/box	4	1	2	1	12,947 – 25,894
	1 unit/box	53	7	29	5	4,000 – 1,144,044
	100 units/box	81	4	36	2	2,000 – 500,000
	250 units/box	6	5	5	3	12,000 – 497,250
	500 units/box	2	2	2	2	7,200 – 25,145
	1000 units/box	97	4	47	3	4,200 – 288,000

Feature Analysis

The alternative of selecting features depends on both the algorithm used and the type of data given. In this study, we used the wrapper subset estimator to select relevant features based on the algorithm applied in the model. As shown in Table 3, the results show that the features of generic products (GEN) and the purchase budgets (PRICE) were selected for all algorithms. The feature of company supplier (COM) was further selected in the Decision Tree and Support Vector Machine applications. Two additional features, the departmental group

(DEPT) and trade product (TRAD), showed important contributions to the Naïve Bayes algorithms while the feature of the procurement method (METH) was not selected for the entire algorithm's operation.

Table 3. Relevant features selected for four different algorithms

Algorithms	Selected features	Number of features
Naïve Bayes (NB)	GEN, COM, PRICE, DEPT, TRAD	5
Decision Tree (DT)	GEN, COM, PRICE	3
Support Vector Machine (SVM)	GEN, COM, PRICE	3
K-Nearest Neighbor (KNN)	GEN, PRICE	2

The optimum split of the test, validation, and train set depends upon the features, algorithms, and dimension of the given data. Therefore, after selecting the relevant features, we then examined two widely-used test option techniques: cross-validation (k-fold) and percentage split options for algorithms.

As shown in Figure 1, the results showed different trend patterns between those two options. First, when performing cross-validation, we tried different number of folds settings. The results presented differences in performance. The increased number of folds smoothly increased accuracy, while SVMs with 10 folds (k=10) provided excellent performance. Second, increasing the percent splitting of the data for training greatly improves accuracy. We found that SVMs with 90% splitting for training provided the highest accuracy and were more accurate than those using cross-validation techniques. That means, if we used 10% data for testing and the remaining 90% data for training in this research, the SVM technique could have approximately 89.61% of the best properly classified instances, followed by KNN, DT, and NB with 88.74%, 86.15%, and 80.09, respectively.

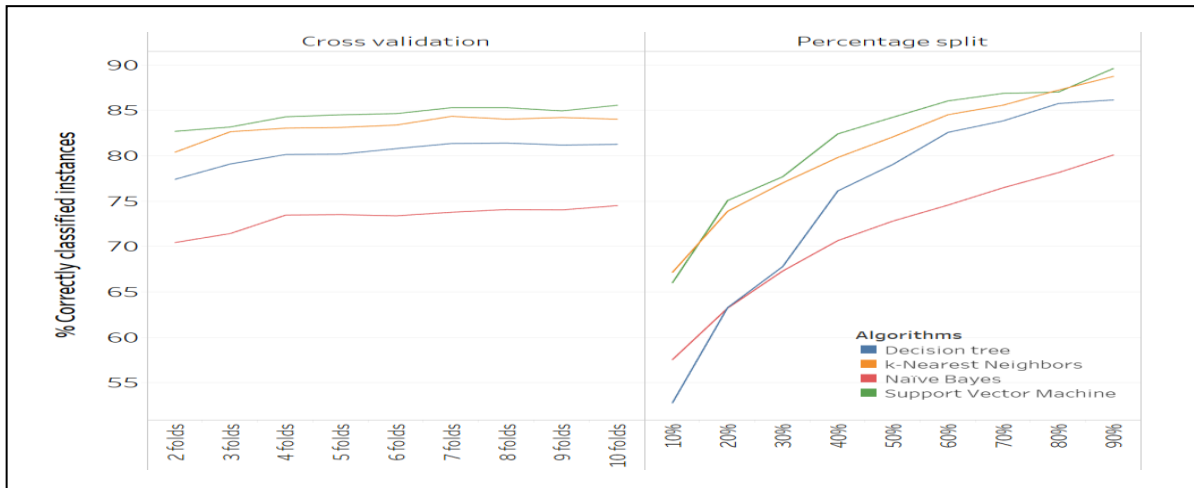


Figure 1. Comparing the percentage of correctly classified instances between two different test options

Performance Evaluation

After analyzing the features, those features selected for each algorithm were used to develop a model for classifying the package size of medical product corresponding to the twelve class labels, described in Table 1. The results of model testing show that all algorithms provide good model performance in our metrics. The evaluation results obtained after testing four algorithms using the 90 percent split test were shown in Figure 1. The proposed model from SVM outperformed the prediction accuracy and has significant agreement for the kappa statistical coefficient. In addition, the model had great precision, sensitivity (recall), and F-measurement. However, after we calculated the time spent building and testing the model, the SVM took much longer than other algorithms while NB and KNN provided very high speeds in less than 0.01 seconds in modeling.

In our study, there was a limitation in our proposed model. The results of model performance were based on the specific characteristics of medical products procured in the given time period. Different types of products and study periods could yield different findings. Therefore, future studies may use more types of products to further examine these classification algorithms.

Table 4. Results of the accuracy measures tested in four classification algorithms

Parameters	DT	NB	KNN	SVM
Accuracy	0.862	0.801	0.887	0.896
Kappa statistic	0.814	0.727	0.849	0.861
Precision	0.907	0.876	0.952	0.952
Recall	0.951	0.961	0.971	0.971
F-Measure	0.929	0.917	0.962	0.962
ROC area	0.945	0.972	0.995	0.981
MAE	0.012	0.015	0.009	0.048
RMSE	0.080	0.088	0.068	0.153
Time to build model (seconds)	0.10	<0.01	<0.01	14.65
Time to test model (seconds)	0.01	0.02	0.02	0.88

Conclusion

Tackling missing data in medical procurement databases is very important because it can often bias analyzes (Groenwold & Dekkers, 2020). Medical purchase data also needs a powerful tool to solve this problem in order to improve analytics and results. As an example of drug procurement data available in the Thai government's procurement system, we found many missing values for package sizes that cause big problems for analysts. In this paper, we therefore examined four models developed from data mining classification techniques to predict missing values for these package sizes. To do so, we used the complete medical data samples as inputs for model training and used six relevant purchasing features as input features (Pentraikan et al., 2022). We also tried to improve the prediction accuracy of model by using these algorithms with the wrapper feature selection function. The results in Table 4 show that the data mining classification algorithm can provide good performance in predicting the missing values of a given data set. As summarized in Figure 2, our study supports that Support Vector Machine (SVM) with 90% splitting of data for training can stand out for being more accurate than the others (Mustaqeem et al., 2018), although this algorithm takes more time for modeling.

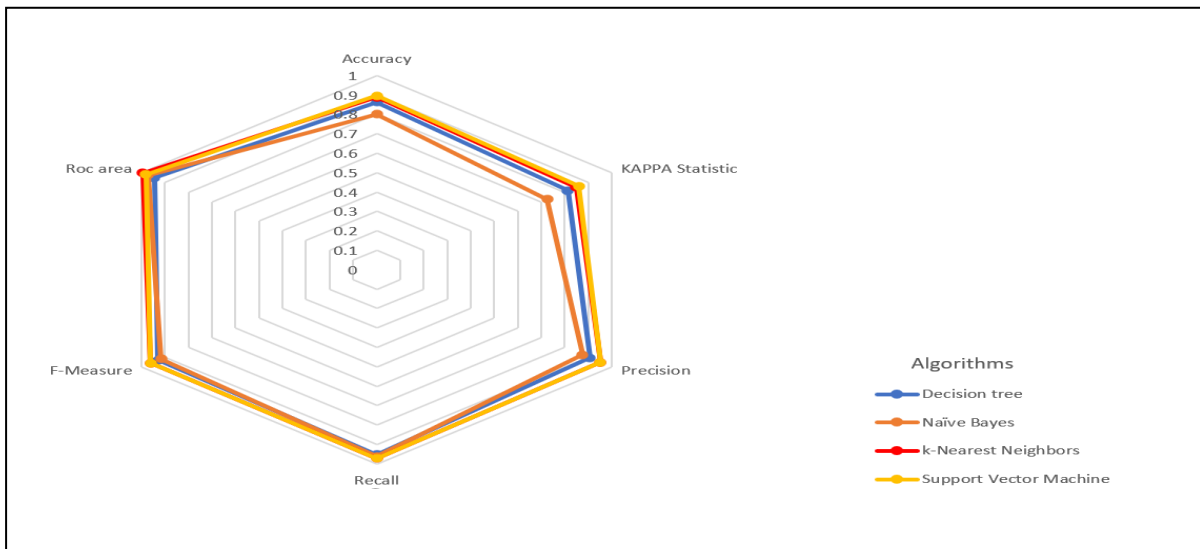


Figure 2. Comparing the accuracy measures of four classification algorithms

Our study application allows medical analysts to resolve the problem of missing values and perform better analyses. This can save a lot of time cleaning up and make their data more reliable. Although some methods have been developed to estimate missing values in many sectors, there is limited evidence and application for the medical procurement system. Therefore, the findings of our study might be useful in applying them to this system and other countries that are facing the challenge of missing medical supply information.

Scientific Ethics Declaration

The authors declare that the scientific ethical and legal responsibility of this article published in EPSTEM journal belongs to the authors.

Acknowledgements or Notes

* This article was presented as a poster presentation at the International Conference on Research in Engineering, Technology and Science (www.icrets.net) held in Budapest/Hungary on July 06-09, 2023.

*We also thank the Comptroller General's Department of Thailand for providing access to the procurement data in pharmaceuticals. We thank the Thai Health Information Standards Development Center (THIS) in Thailand for providing the updated data of Thai Medicine Terminology (TMT).

References

- Batt, S., Grealis, T., Harmon, O., & Tomolonis, P. (2020). Learning Tableau: A data visualization tool. *The Journal of Economic Education*, 51(3-4), 317-328.
- Bouckaert, R. R. (2008). Bayesian network classifiers in weka for version 3-5-7. *Artificial Intelligence Tools*, 11(3), 369-387.
- Browne, M. W. (2000). Cross-validation methods. *Journal of Mathematical Psychology*, 44(1), 108-132.
- Chabot, C., Stolte, C., & Hanrahan, P. (2003). Tableau software. *Tableau Software*, 6.
- Galdi, P., & Tagliaferri, R. (2018). Data mining: accuracy and error measures for classification and prediction. *Encyclopedia of Bioinformatics and Computational Biology*, 1, 431-436.
- Hamel, L. (2009). Model assessment with ROC curves. In *Encyclopedia of Data Warehousing and Mining, Second Edition* (pp. 1316-1323). IGI Global.
- Holmes, G., Donkin, A., & Witten, I. H. (1994, 29 Nov.-2 Dec. 1994). WEKA: a machine learning workbench. *Proceedings of ANZIS '94 - Australian New Zealand Intelligent Information Systems Conference*.
- Hussain, S., Dahan, N. A., Ba-Alwib, F. M., & Ribata, N. (2018). Educational data mining and analysis of students' academic performance using WEKA. *Indonesian Journal of Electrical Engineering and Computer Science*, 9(2), 447-459.
- Kabakchieva, D. (2013). Predicting student performance by using data mining methods for classification. *Cybernetics and Information Technologies*, 13(1), 61-72.
- Karegowda, A. G., Jayaram, M., & Manjunath, A. (2010). Feature subset selection problem using wrapper approach in supervised learning. *International Journal of Computer Applications*, 1(7), 13-17.
- Mandal, L., & Jana, N. D. (2019, 13-15 Dec. 2019). A comparative study of naive bayes and k-NN algorithm for multi-class drug molecule classification. *2019 IEEE 16th India Council International Conference*.
- McHugh, M. L. (2012). Interrater reliability: the kappa statistic. *Biochemia Medica*, 22(3), 276-282.
- Mustaqeem, A., Anwar, S. M., & Majid, M. (2018). Multiclass classification of cardiac arrhythmia using improved feature selection and SVM invariants. *Computational and Mathematical Methods in Medicine*. Article ID 7310496. <https://doi.org/10.1155/2018/7310496>.
- Patil, B. M., Toshniwal, D., & Joshi, R. C. (2009, 6-7 March 2009). Predicting burn patient survivability using decision tree in WEKA environment. *2009 IEEE International Advance Computing Conference*.
- Pentrahan, A., Lin, K. H., Sriphon, T., Wang, J. Y., & Wong, W. K. (2022). The impact of pharmaceutical electronic bidding procurement on prices of medicines: A systematic review. *Indian Journal of Pharmaceutical Sciences*, 86-98.
- Pentrahan, A., Wang, J.-Y., & Wong, W.-K. (2023). The impact of centralized electronic bidding system on procurement prices for generic medicines: A case study from Thailand. *Songklanakarin Journal of Science and Technology*, 44, 1532-1538.
- Pentrahan, A., Yang, C.-C., & Wong, W.-K. (2021). How well does a sequential minimal optimization model perform in predicting medicine prices for procurement system? *International Journal of Environmental Research and Public Health*, 18(11), 5523.
- Rajvanshi, N., & Chowdhary, K. (2017). Comparison of SVM and naïve Bayes text classification algorithms using WEKA. *International Journal of Engineering Research and*, 6(09), 141-143.
- Sakly, H., Said, M., Seekins, J., & Tagina, M. (2022). Big data and artificial intelligence for e-health. In N. Rezaei (Ed.), *Multidisciplinarity and interdisciplinarity in health* (pp. 525-544). Springer International Publishing.
- Shi, X., Prins, C., Van Pottelbergh, G., Mamouris, P., Vaes, B., & De Moor, B. (2021). An automated data cleaning method for electronic health records by incorporating clinical knowledge. *BMC Medical Informatics and Decision Making*, 21(1), 267.

- Skrbo, A., Begović, B., & Skrbo, S. (2004). Classification of drugs using the ATC system (Anatomic, Therapeutic, Chemical Classification) and the latest changes. *Medicinski Arhiv*, 58(1 Suppl 2), 138-141.
- Steinbach, M., & Tan, P.-N. (2009). kNN: k-nearest neighbors. In *The top ten algorithms in data mining* (pp. 165-176). Chapman and Hall/CRC.
- Wang, J., Yang, Y., Xu, L., Shen, Y., Wen, X., Mao, L., Wang, Q., Cui, D., & Mao, Z. (2021). The impact of national centralized drug procurement policy on the use of policy-related original and generic drugs in public medical institutions in China: A difference-in-difference analysis based on national database. *MedRxiv*, 2021-06.
- Xu, S., Lu, B., Baldea, M., Edgar, T. F., Wojsznis, W., Blevins, T., & Nixon, M. (2015). Data cleaning in the process industries. *Reviews in Chemical Engineering*, 31(5), 453-490.
- Zhang, M.-L. (2010). A k-nearest neighbor based multi-instance multi-label learning algorithm. *22nd IEEE international conference on tools with artificial intelligence*.
- Zhang, S., Zhang, C., & Yang, Q. (2003). Data preparation for data mining. *Applied Artificial Intelligence*, 17(5-6), 375-381.

Author Information

Amarawan Pentrakan

Prince of Songkla University, Thailand
15 Karnjanavanich Rd., Hat Yai, Songkhla City,
Thailand 90110, Thailand
Contact e-mail: amarawan.p@psu.ac.th

Arbee L.P. Chen

Asia University, Taiwan
No. 500, Liufeng Rd, Wufeng District, Taichung City,
Taiwan 413, Taiwan

To cite this article:

Pentrakan, A. & Chen, A.L.P. (2023). Data cleaning in medical procurement database: Performance comparison of data mining classification algorithms for tackling missing value. *The Eurasia Proceedings of Science, Technology, Engineering & Mathematics (EPSTEM)*, 23, 26-33.

The Eurasia Proceedings of Science, Technology, Engineering & Mathematics (EPSTEM), 2023

Volume 23, Pages 34-41

ICRETS 2023: International Conference on Research in Engineering, Technology and Science

Optimal Position of Two Fans Cooling a Large PV Panel

Rezki Nebbali

Université Mouloud Mammeri de Tizi-Ouzou

Idir Kecili

Université Mouloud Mammeri de Tizi-Ouzou

Abstract: To overcome the negative effect of the rise in temperature of photovoltaic (PV) panel on its performance, cooling is used. However, this cooling must be as homogeneous as possible. Indeed, the uniform cooling of a photovoltaic (PV) panel is important to maintain its conversion efficiency at a high level. In this work, a cooling system is proposed using two fans that blow ambient air onto the backside of the PV panel. Several configurations of fans positions (air inlets) and air outlets are studied by simulations in order to optimize the cooling system and to achieve a uniform temperature distribution on the PV panel. On a typical summer day with an optimal air flow rate of 200g/s, the optimized cooling system reduces the temperature of the PV panel by 21.66°C and improves its conversion efficiency by about 8.85%. In the absence or at low wind speeds, these values can reach 35.84°C and 16.5%.

Keywords: Cooling, efficiency, Fan, Homogenization, Temperature field, Photovoltaic panel.

Introduction

Air cooling of solar PV panels has been widely investigated (Shukla et al., 2017; Hasanuzzaman et al., 2016). Most of them were only interested in improving the efficiency of the cooled PV panel without taking into account the homogeneity of the temperature field distribution on the PV panel. Indeed, significant temperature gradients on the PV panel can generate thermal stresses which can contribute to its premature degradation (Røyne, 2005).

Muneeshwaran et al. (2020) proposed to use the air supplied by an air conditioning unit to cool a PV panel. The cold air then circulates through a channel of uniform section. Thus, the maximum temperature gradient reached 7°C. By using a converging cross-section channel, the temperature gradient was reduced to only 2.5°C. This resulted in a 20-25% efficiency improvement. Another cooling system that consists on fans that blow ambient air on the rear face of a PV panel was investigated by Bayrak (2022). He studied the influence of the number of fans that cool a medium-sized (0.665m²) PV panel. He improved the electrical efficiency of the PV panel by only 2.69% by using four fans.

Syafiqah et al. (2017) investigated the cooling of a medium-sized (0.648m²) PV panel using two fans. They improved the electrical efficiency of the PV panel by 3% by lowering the average PV panel temperature from 66.2°C to 53.6°C. However, the temperature distribution was not uniform. It showed a maximum temperature difference between the cold and hot zones of about 14°C. Using a single fan on a small PV panel (0.064 m²), Nebbali et al. (2020) obtained 29% of the efficiency improvement of the cooled PV panel but with a significant heterogeneity of the temperature field. Bevilacqua et al. (2020) confirmed this observation on a large PV panel (1.66m²) cooled by a single fan.

The objective of this work is to investigate the cooling provided by two fans placed at the backside of a standard size (1.28m²) PV panel. Through 3D numerical simulations, the effect of different positions of these fans, associated with two air outlets configurations were studied to determine the optimal configuration. In addition, the thermal and electrical responses of the PV panel during a typical day were also studied.

Problem Position

The device consists of a standard size (158x80.8cm) PV panel that is cooled from its rear face by the ambient air which is blowing by two fans. The optimal case that corresponds to the judicious positions of the two fans and the air outlets (Fig. 1) which allow better ventilation was determined in order to ensure well cooling of the PV panel with homogeneous temperature field. For this purpose, six scenarios were considered (Fig. 1, Table 1).

Simulations were carried out under extreme climatic conditions characterized by a situation of no wind, 1000W/m² of solar radiation and 50°C of air temperature. Thus, the total air flow rate supplied by the two fans was considered equal to 400 g/s. Finally, using the optimal case, we studied the effect of climatic conditions of a typical summer day on the performance of the cooled PV panel.

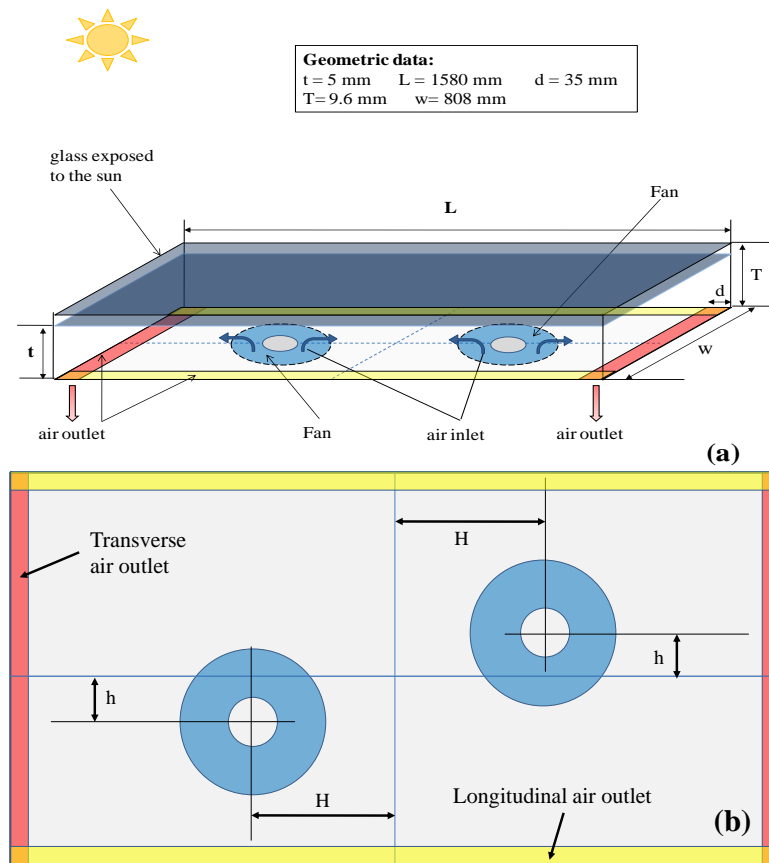


Figure 1. (a) Sketch of the PV panel with the cooling system; (b) Bottom view of the cooled PV panel with different configurations.

Table 1. Positions of the fans and of the air outlets.

	H(cm)	h(cm)	Diameter of two fans (cm)	Air Outlet
Case (a)	39.5	0	30	Transverse air Outlet
Case (b)	39.5	0	30	Longitudinal air outlet
Case (c)	0	20.2	20	Transverse air Outlet
Case (d)	0	20.2	20	Longitudinal air outlet
Case (e)	29.5	10	30	Transverse air outlet
Case (f)	29.5	10	30	Longitudinal air outlet

Calculation Domain, Mesh and Boundary Conditions

The six calculations domains were constructed in 3D. Each of them, included the airflow cavity, the air inlets occurred by fans, air outlets and the different layers that make up the PV panel (Table. 2).

Table 2. Characteristics of the different layers that make up the photovoltaic module(Armstrong and Hurley, 2010).

Layer	Thickness “e” (mm)	λ (W/m/k)	ρ (kg/m ³)	C_p (J/kg/°C)
Glass	3.2	1.8	3000	500
Silicon	0.3	148	2330	677
EVA	0.5	0.35	960	2090
Tedlar	0.1	0.2	1200	1250

For good mesh resolution, the bottom plane of the PV panel, where the air inlets and outlets were grafted, was first meshed in 2D. Then, by extrusion, a 3D mesh was generated. For the 5mm high air cavity a 1mm deep mesh was used, while for Tedlar, EVA, Silicone and Glass the depth equal to the thickness of each layer.

The air inlets, which represent the cross-sections of the fans, were equated to the "MASSFLOW-INLET" type condition which allowed define the air mass flow rate as well as the air temperature blowing by the two fans. The air outlet sections were "OUTFLOW" type. This ensured the conservation of flows between the air inlets and outlets. The glass and the silicon media were the seat of heat sources produced by the heat exchanged between the PV panel and its surrounding.

Associate Equations

Heat Equation

The heat equation associated to each solid layer of the PV panel corresponds to the Poisson equation in steady state. It is expressed by the equations (1) and (2), respectively, for the glass (g) and silicon (si):

$$\Delta T + \frac{\alpha_g R_G - \varepsilon \sigma (T_g^4 - T_V^4)}{e_g \lambda_g} = 0 \quad (1)$$

$$\Delta T + \frac{\alpha_{si} \tau_g R_G}{e_{si} \lambda_{si}} = 0 \quad (2)$$

where “ Δ ” is the Laplacian operator, T is the temperature, α is the absorption coefficient, ε is the emissivity of the surface of the PV, σ is the Boltzmann constant, e is the thickness and τ_g is the transmissivity of the glass. T_V is the sky temperature correlated by the following relation (Kaplani and Kaplanis, 2014):

$$T_V = 0.0552 T_{air}^{1.5} \quad (3)$$

Furthermore, the EVA is considered transparent while the silicon is opaque.

In addition, the PV panel is the seat of convective heat exchange between each face and the ambient air. Thus, for a PV panel inclined at $\theta < 60^\circ$ with respect to the vertical, the Nusselt number of the front face in natural convection is expressed by (Fujii and Imura (1972), Kaplani and Kaplanis (2014)):

$$N_{un} = \begin{cases} f \{ 0.16 [R_a^{0.33} - (G_{rc} P_r)^{0.33}] \} + 0.56 (G_{rc} P_r \cos \cos(\theta))^{0.25}, & R_a < 5 \cdot 10^8 \\ f \{ 0.13 [R_a^{0.33} - (G_{rc} P_r)^{0.33}] \} + 0.56 (G_{rc} P_r \cos \cos(\theta))^{0.25}, & R_a \geq 5 \cdot 10^8 \end{cases} \quad (4)$$

$$G_{rc} = 1.327 \cdot 10^{10} e^{(-3.708(\frac{\pi}{180}\theta))}$$

$$f = 0 \text{ si } R_a < G_{rc} P_r$$

$$f = 1 \text{ si } R_a > G_{rc} P_r$$

While for the rear side of the uncooled PV panel, the Nusselt number corresponds to (Bergman et al. 2011):

$$N_{un} = \begin{cases} 0.68 + \frac{0.67 R_a^{0.25}}{\left(1 + \left(\frac{0.492}{Pr}\right)^{\frac{9}{16}}\right)^{\frac{4}{9}}}, & R_a \leq 10^9 \\ \left(0.825 + \frac{0.387 R_a^{\frac{1}{4}}}{\left(1 + \left(\frac{0.492}{Pr}\right)^{\frac{9}{16}}\right)^{\frac{2}{7}}}\right)^2, & R_a > 10^9 \end{cases} \quad (5)$$

In other convections situations occurred by the wind, the following relationships are adopted (Armstrong and Hurley (2010); Kaplani and Kaplanis(2014)):

$$h_{conv} = \begin{cases} h_n = \frac{N_{un} \lambda_{air}}{L_c}, & \frac{Gr}{Re^2} > 100 \\ h_f = 2.56 V + 8.55, & \frac{Gr}{Re^2} < 0.01 \\ h_{mixt} = \sqrt[3]{h_n^3 + h_f^3}, & 0.01 \leq \frac{Gr}{Re^2} \leq 100 \end{cases} \quad (6)$$

Where Ra is the Rayleigh number which is a function of the Grashof and Prandtl. L_c is the characteristic dimension of the plate expressed as the ratio of the area of the plate to its perimeter. For the cooled PV panel, the heat exchange between the rear face and the ambient air is determined by solving the coupled equations of continuity, momentum and energy. To do this, we used CFD-Fluent code (Fluent Inc., 2001).

Fan Power

Nominal values of the fan are given by the manufacturer, as well as: Power fan ($P_{fan}^n=80W$), air flowrate ($Q^n=980g/s$), Diameter ($D^n=30.5cm$) and rotation speed ($N^n=2250rpm$). In other operating conditions, the electrical power P_{fan} consumed by the fan of diameter D, that blow an airflow Q at rotation speed of N , can be evaluated by the following expressions (He et al. 2014, Zhang et al. 2022):

$$\frac{Q}{Q^n} = \left(\frac{D}{D^n}\right)^3 \frac{N}{N^n} \quad (7)$$

$$\frac{P_{fan}}{P_{fan}^n} = \left(\frac{D}{D^n}\right)^5 \left(\frac{N}{N^n}\right)^3 \quad (8)$$

PV Panel Efficiency

The electrical efficiency of a PV panel is defined by (Skoplaki and Palyvos, 2009):

$$\eta = \eta_{ref}(1 - \mu(T_{si} - 25)).100 \quad (9)$$

Where $\eta_{ref}=15.74\%$ is the efficiency of the PV panel at standard conditions. μ is the power temperature coefficient equal to $0.37\%/^{\circ}C$ and T_{si} is the equilibrium temperature of the uncooled PV panel. In the case of the cooled PV panel, which equilibrium temperature is T_{si}^* , the electrical power P_{fan} consumed by the two fans supplied by the PV panel must be taken into account, so the efficiency (η^*) of the cooled PV panel that area is S, becomes:

$$\eta^* = 100 \left(\eta_{ref}(1 - \mu(T_{si}^* - 25)) - \frac{P_{fan}}{R_{GS}} \right) \quad (10)$$

The improvement electrical efficiency of the cooled PV panel compared to the uncooled one is then quantified by:

$$\eta_r = 100. \frac{\eta^* - \eta}{\eta} \quad (11)$$

Results and Discussion

Temperature Field

Optimal Configuration

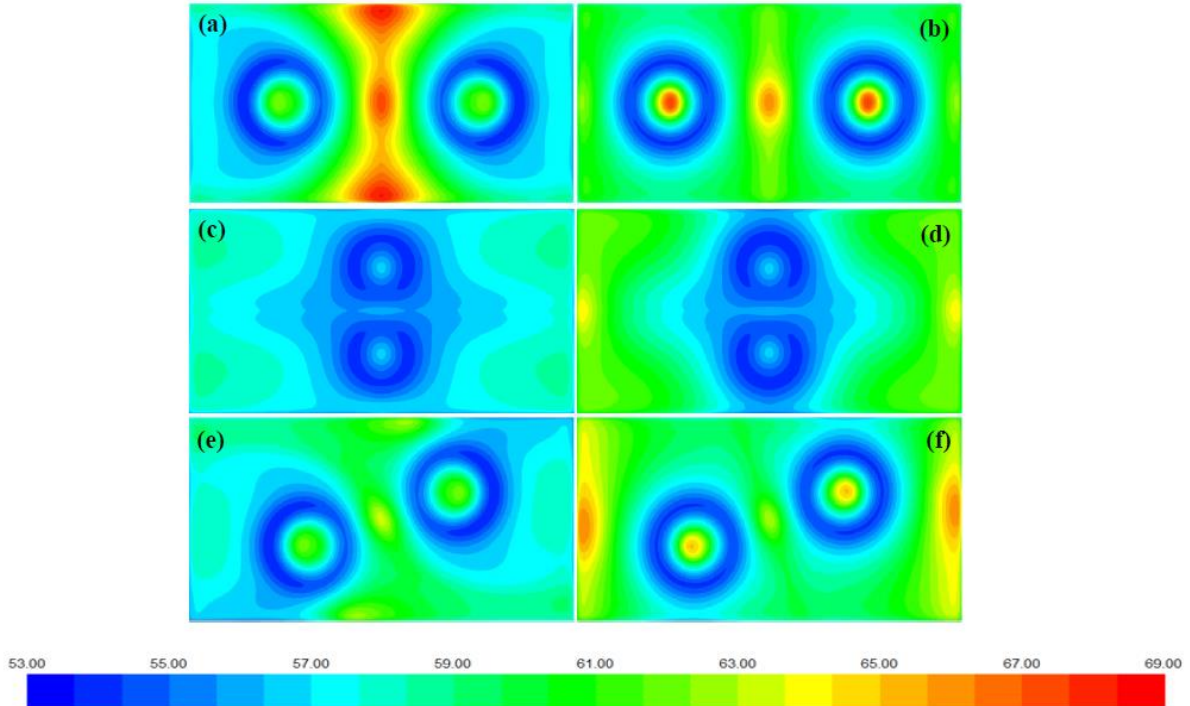


Figure 2. Temperature field ($^{\circ}\text{C}$) on the cooled PV panel for the six configurations at $T_{\text{air}} = 50^{\circ}\text{C}$, $R_G = 1000\text{W/m}^2$ and $Q = 400\text{g/s}$.

Fig. 2 shows the temperature distribution on the cooled PV panel with different fans configurations as shown in Table 1. It appears that the case (c) is the optimum configuration. Indeed, it allows good circulation of air through the cavity and ensures better cooling with lowest average silicon temperature of 56.74°C and well homogeneity of the temperature field ($\delta T_{\text{max}} = 4.5^{\circ}\text{C}$).

Effect of Real Climatic Conditions

By using the optimal configuration (Case C), we studied the effect of the climatic conditions varying during a typical summer day of 30 July prevailing at Tizi-Ouzou, north of Algeria (36.7N , 4.05E). Thus, The PV panel was oriented facing south and tilted by 32° (Kecili et al., 2022). Moreover, the PV panel was cooled by two fans that blow a total mass flow rates varying from 100 to 250g/s. Using the PVGIS database for the year 2020, we obtained the daily evolution of the global incident solar radiation (R_G), the ambient air temperature (T_{air}) and the wind speed (Fig. 3-a).

The simulations led then to the daily evolution of the PV panel temperature in cooled and uncooled situations (Fig. 3-b). The maximum temperature of the uncooled PV panel reaches 69°C at the culmination time (midday) while the temperature of the cooled PV panel drops significantly.

In addition, Table 3 gives the temperature difference (δT) between the minimum and maximum values reached by the cooled PV panel for each airflow. This allowed to assess the homogeneity of the temperature field on the PV panel. It appears that the increase in the air flow attenuates the heterogeneity of the temperature field. The maximum temperature difference between the hot and cold zones reaches 9.47°C with 100 g/s of airflow to settle at only 5.46°C with 250 g/s. Moreover, the lowering temperature (σT) generated by the cooling of the PV panel rises when the airflow increases. Indeed, σT reaches 17.06°C at 100g/s airflow and 22.34°C at 250g/s.

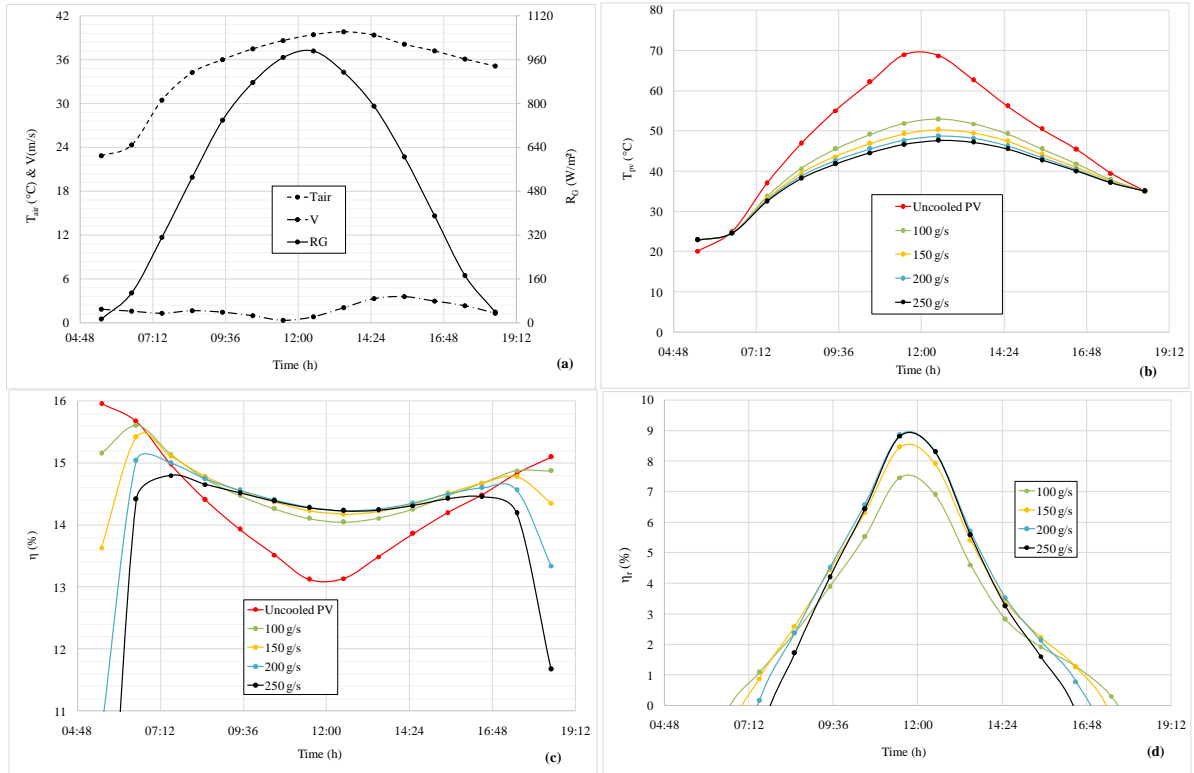


Figure 3. Evolution of: (a) temperature ambient, solar radiation and wind velocity on 30 July, (b) PV panel temperature, (c) PV efficiency and (d) efficiency improvement of the cooled PV with respect of the uncooled one for different airflow rates.

Table 3. Minimum (T_{min}), maximum (T_{max}) and average temperatures of the cooled and uncooled PV panel at midday.

Airflow rate	Cooled PV panel			Uncooled PV panel		$\sigma T = T_{PV}^{uncooled} - T_{PV}^{cooled}$
	T _{min}	T _{max}	$\Delta T = T_{max} - T_{min}$	T _{PV} ^{cooled} (°C)	T _{PV} ^{uncooled} (°C)	
100 g/s	45.16	54.63	9.47	51.86		17.06
150 g/s	44.02	51.57	7.55	49.25	68.92	19.67
200 g/s	43.35	49.68	6.33	47.66		21.26
250 g/s	42.92	48.38	5.46	46.58		22.34

Efficiency Improvement

The efficiencies of the PV panel are shown in Fig. 3-c, the effect of cooling is clearly seen during the period between two hours after sunrise and two hours before sunset. Thus, higher is the airflow, better is the efficiency. Outside this period, the efficiency of the cooled PV panel is significantly lower than that of the uncooled one, as the fans consume more energy than the gain generated by the cooled PV panel. The efficiency improvement of the cooled PV panel compared to the uncooled one is given by the figure (3-d). We can observe that the maximum improvement of 8.85% is reached at only 200g/s of airflow.

Conclusion

The homogenization of the temperature field in a PV panel is an important parameter that should not be neglected in a study of a cooling system. For this purpose, numerical simulations were carried out to propose an optimal cooling device that allows homogenize this temperature distribution. Using two axial fans that blow air onto the backside of a large standard commercial PV panel, the effect of their positions and those of the air outlet sections on the cooling provided were studied. First, the simulations were carried out under extreme climatic conditions (No wind situation, R_G=1000W/m² and T_{air}= 50°C). Then, the configuration favoring the

consequent cooling of the PV panel with a homogeneous temperature distribution was selected as the optimal configuration. Then, we studied the effect of the climatic conditions varying during a typical summer day of 30 July prevailing at Tizi-Ouzou, north of Algeria (36.7N, 4.05E). It was shown that at noon, from an air flow of 200g/s, the improvement in the efficiency of the cooled PV panel was settled 8.85% while the lowering of temperature was 21.26°C.

Scientific Ethics Declaration

The authors declare that the scientific ethical and legal responsibility of this article published in EPSTEM journal belongs to the authors.

Acknowledgements or Notes

This article was presented as an oral presentation at the International Conference on Research in Engineering, Technology and Science (www.icrets.net) held in Budapest/Hungary on July 06-09, 2023.

References

- Armstrong, S., & Hurley, W.G. (2010). A thermal model for photovoltaic panels under varying atmospheric conditions. *Applied Thermal Engineering*, 30, 1488–1495.
- Bayrak, F. (2022). Energy, exergy and sustainability indicators of photovoltaic panel cooling under forced convection. *Erzincan Üniversitesi Fen Bilimleri Enstitüsü Dergisi* 15, 340–359.
- Bergman, T.L., Lavine, A.S., Incropera, F.P., & Dewitt, D.P. (2011). *Fundamentals of heat and mass transfer*, 7th ed. ed. Wiley, Hoboken, NJ.
- Bevilacqua, P., Bruno, R., & Arcuri, N. (2020). Comparing the performances of different cooling strategies to increase photovoltaic electric performance in different meteorological conditions. *Energy*, 195, 116950
- European Commission EU Science Hub (2017), Photovoltaic Geographical Information System (PVGIS 5). https://re.jrc.ec.europa.eu/pvg_tools/en/tools.html.
- Fluent Inc. (2001). *Fluent v.6.1 user's guide*. Fluent Inc. Centerra Resource Park, Lebanon.
- Fujii, T., & Imura, H. (1972). Natural-convection heat transfer from a plate with arbitrary inclination. *International Journal of Heat and Mass Transfer*, 15, 755–767.
- Hasanuzzaman, M., Malek, A.B.M.A., Islam, M.M., Pandey, A.K., & Rahim, N.A. (2016). Global advancement of cooling technologies for PV systems: A review. *Solar Energy* 137, 25–45.
- He, W., Dai, Y., Han, D., Yue, C., & Pu, W. (2014). Influence from the rotating speed of the windward axial fans on the performance of an air-cooled power plant. *Applied Thermal Engineering*, 65, 14–23.
- Kaplani, E., & Kaplanis, S. (2014). Thermal modelling and experimental assessment of the dependence of PV module temperature on wind velocity and direction, module orientation and inclination. *Solar Energy* 107, 443–460.
- Kecili, I., Nebbali, R., & Ait Saada, S. (2022). Optimal tilt angle of a solar panel for a wide range of latitudes. Comparison between tilted and horizontal configurations. *International Journal of Ambient Energy* 43, 8697–8709.
- Muneeshwaran, M., Sajjad, U., Ahmed, T., Amer, M., Ali, H.M., & Wang, C.-C. (2020). Performance improvement of photovoltaic modules via temperature homogeneity improvement. *Energy*, 203, 117816.
- Nebbali, D., Nebbali, R., & Ouibrahim, A. (2020). Improving photovoltaic panel performance via an autonomous air cooling system – experimental and numerical simulations. *International Journal of Ambient Energy* 41, 1387–1403.
- RØYNE, A. (2005). *Cooling devices for densely packed, high concentration Pv arrays*. University of Sydney for the degree of Master Of Science.
- Shukla, A., Kant, K., Sharma, A., & Biwole, P.H. (2017). Cooling methodologies of photovoltaic module for enhancing electrical efficiency: A review. *Solar Energy Materials and Solar Cells* 160, 275–286.
- Skoplaki, E., & Palyvos, J.A. (2009). On the temperature dependence of photovoltaic module electrical performance: A review of efficiency/power correlations. *Solar Energy* 83, 614–624.
- Syafiqah, Z., Irwan, Y.M., Amin, N.A.M., Irwanto, M., Leow, W.Z., & Amelia, A.R. (2017). Thermal and electrical study for PV panel with Cooling. *IJEECS* 7, 492.
- Zhang, W., Wang, D., Zhang, S., Yang, Z., & Lin, Z. (2022). Research on models for estimating aerodynamic

and energy consumption performance of fan filter units (FFUs). *Building and Environment* 207.

Author Information

Rezki Nebbali

Laboratory of Energy, Mechanics and Materials (LEMM).
Mouloud Mammeri University of Tizi-Ouzou. BP RP17,
15000 , Tizi-Ouzou. Algeria
Contact e-mail: rezki.nebbali@ummto.dz

Idir Kecili

Laboratory of Energy, Mechanics and Materials (LEMM).
Mouloud Mammeri University of Tizi-Ouzou. BP RP17,
15000 , Tizi-Ouzou. Algeria

To cite this article:

Nebbali, R. & Kecili, I. (2023). Optimal position of two fans cooling a large PV panel. *The Eurasia Proceedings of Science, Technology, Engineering & Mathematics (EPSTEM)*, 23, 34-41.

The Eurasia Proceedings of Science, Technology, Engineering & Mathematics (EPSTEM), 2023

Volume 23, Pages 42-49

ICRETS 2022: International Conference on Research in Engineering, Technology and Science

Possibilities to Construct Combined Mine Waste Dump Facility with Better Operational Sequence

Ljupcho Dimitrov

University of Mining and Geology

Irena Grigorova

University of Mining and Geology

Teodora Yankova

University of Mining and Geology

Abstract: An integrated mine waste facility is designed for the Khan Krum deposit in Bulgaria (Eldridge, Wickland, Goldstone, & Kissiova, 2011). A substantial environmental benefit was achieved by designing such a facility because constructing a conventional tailings storage facility (TSF) would've needed much more surface area. However, the paper from (Eldridge, Wickland, Goldstone, & Kissiova, 2011), is mentioned that achieving a good operational sequence for constructing the facility would be a challenge. This paper evaluates how choosing the proper form for the combined mine waste dump facility (CMWDF) can help in having better control over the operational sequence. For comparison, two designs of CMWDF were designed. Each can accumulate the predicted amount of tailings the processing plant will produce. The first design has a broader construction body, and the other is narrower. It was decided like so because the broader body ensures more cells which means a better operational sequence can be achieved. Also, a conventional tailings facility was designed to compare the surface area and volume of waste rock needed for construction. All the designed Tailings Storage Facilities (TFS) require different surface areas and waste rock to be built.

Keywords: Tailings storage facility, Tailings deposition, Operational sequence

Introduction

The storage of tailings was always one of the major challenges. There are many ways to store tailings, such as in lakes or in artificial structures such as tailings storage facilities. Tailings storage facilities are challenging to construct and operate. There are approximately 3500 TSF in the world, from which about 3 of them fail in a year (Lyu et al., 2019).

Besides the risk of failure, TSF needs a wide surface to construct, which means cutting local forests and, in some cases removing local fauna. To decrease the environmental impact and increase the factor of safety, Eldridge, Wickland, Goldstone and Kissiova, (2011) designed an Integrated Mine waste dump facility for the Khan Krum deposit in Bulgaria. In the previous paper the authors also said that the IMWF needs only 41 hectares of surface area compared to the 96 hectares required for conventional TSF and waste dump. With that also the need for tailings dam and post-closure of unconsolidated tailings deposit is eliminated (Eldridge et al., 2011).

Combined Mine Waste Dump Facility (CMWDF)

- This is an Open Access article distributed under the terms of the Creative Commons Attribution-Noncommercial 4.0 Unported License, permitting all non-commercial use, distribution, and reproduction in any medium, provided the original work is properly cited.

- Selection and peer-review under responsibility of the Organizing Committee of the Conference

© 2023 Published by ISRES Publishing: www.isres.org

The new facility for storing tailings and waste rock is based on a combined deposition method of waste mine materials (tailings and waste rock). This design has few significant advantages compared to conventional tailings storage methods. The benefits are that less surface area is required, a more significant factor of safety is achieved, the risk of pollution is minimized, lower costs for monitoring, etc. (Eldridge et al., 2011). Dewatered tailings is recommended to be stored. Thus, water from the dewatering process can be used, reducing the need for additional fresh water (Eldridge et al., 2013).

The combined mine waste dump facility is composed of waste rock and tailings. The tailings are stored in cells built from compacted waste rock. The facility in the Krumovgrad Gold project is built bench by bench, as the front wall of the bench is whole and well compacted with an intervening slope constructed at 2.5 horizontal to 1 vertical (Eldridge et al., 2011). The facility is designed with an underlying drainage system that's meant to drain the water from the tailings consolidation and the atmospheric water. A geomembrane layer is placed under the drainage system to prevent mixing the drainage water with the underground water. Cells are lined with heavy non-woven geotextile and a layer of sand, which will prevent mixing the tailings with the waste rock (Eldridge et al., 2011).

The above-described constructive parameters are from the Krumovgrad gold project Bulgaria for the integrated mine waste facility (IMWF), which is currently under construction by Dundee Precious Metals Krumovgrad EAD (Grigorova, 2011). The facility is constructed with an upstream design method (Eldridge et al., 2011). The tailings from the "Ada Tepe" mine are stored in the facility.

The main disadvantage is that while constructing the facility, an excellent operational sequence is needed, and if this is not the case, it can lead to interruption of the workflow or stop the work of the processing plant. For this not to happen in the Krumovgrad gold project in Bulgaria, Contingency storages are built so that the tailings will temporarily be stored in them when a cell is not ready to be filled (Eldridge et al., 2013). Other disadvantages are the high construction costs and the unavailability or difficulty to later extract the metal that was contained in the waste rock.

Comparison between Different Designs of CMWDF

For comparison, 2 CMWDF are designed. The goal is to store 5.9 million m³ of tailings, and the volume of waste rock varies.

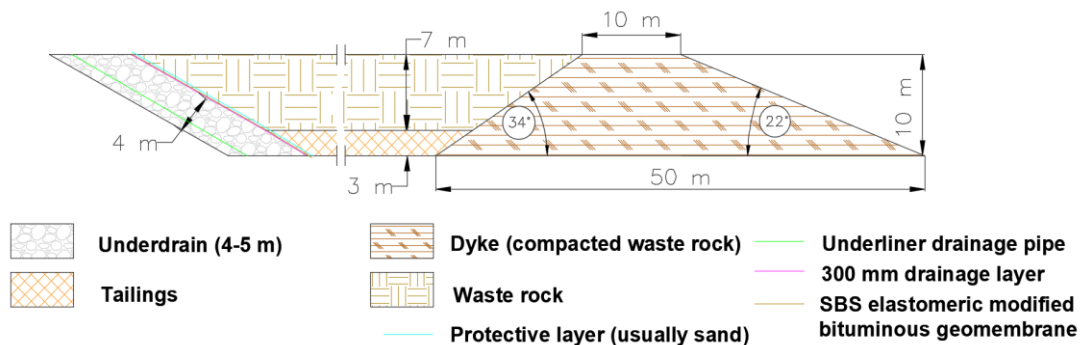


Figure 1. Profile of a single bench with its construction elements (Dimitrov, 2021)

Design 1

Design 1 is started lower in the valley, and its finishing form ends in both ravines (Figure 2). To store 5.9 million m³ of tailings, 23 million m³ of waste rock must be used. The height of the tailings is chosen to be 3 m (30% of the bench height). The rest was calculated as waste rock. The total surface area needed for the facility to be built in this way was 628 daa. The area that can be reclaimed and used for different purposes is about 340 daa, 54 % of the land used for building the facility.

The broader body of the facility means that the benches will be wider. Hence the flexibility for building the cells will be more significant, and more cells can be built. The operational sequence can be greatly improved with a greater number of cells. Another advantage for the wider construction is that for constructing a cell with minimal capacity is needed 2-3 times less waste rock in comparison with design 2. That means tailings deposition can start with less initial capital and operational costs.

Building a wider CMWDF allows the construction of more cells, which means that the possibilities for constructing a cell before the previous one is filled will be greater. Hence the need for contingency storage throughout the construction period will be decreased or eliminated. If there is a need for contingency storage, it can be built in the area planned for the facility. Thus using more forest space will not be necessary. A need for contingency storage will emerge if the next cell is not finished and if cells that are built are not capable of accumulating the whole pulp in the processing plant during a need of emergency shut down. There is also a possibility that starting with a broader starter platform can ensure a more stable starting platform for the facility. The other positive thing with a wider design is that the last bench ends with a wide surface. That will leave the opportunity to restart the mining activities if the conditions change (this is only in some cases) or to use it for other purposes such as agriculture or tourism. The negative side of a wider CMWDF could be that more surface area will sometimes be needed to build such a facility.

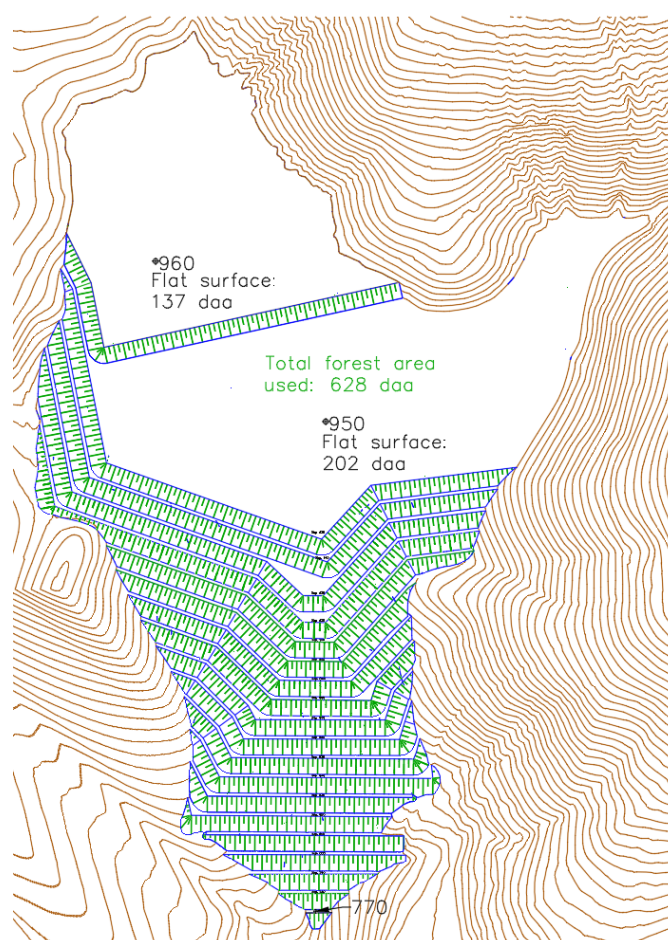


Figure 2. Combined mine waste dump facility with wider construction body (Design 1)

Design 2

Design 2 is designed in the ravines with starting elevation of 825 (Figure 3). The volume of deposited tailings for east and south CMWDF is different, but the overall volume is equal to design 1. However, the volume of waste rock is 29.5 million m^3 , which is 6.5 million m^3 more. The surface area needed for both to be built is 783 daa. As mentioned in the description for design 1, for building cells with the volume equal to the volume of tailings produced for the period of consolidation, twice as much waste rock will be needed for this design. This is because the narrow terrain limits the width of the benches, so the starting platform consists of more benches to gain elevation and reach a favorable width of the terrain.

The operational sequence at the beginning of the construction can be challenging as the number of cells is limited even with both ravines being constructed at the same time. Therefore, contingency storage is recommended at the beginning. If possible, contingency storage is recommended to be built in the area planned for construction. Two cases were discussed for constructing design 2.

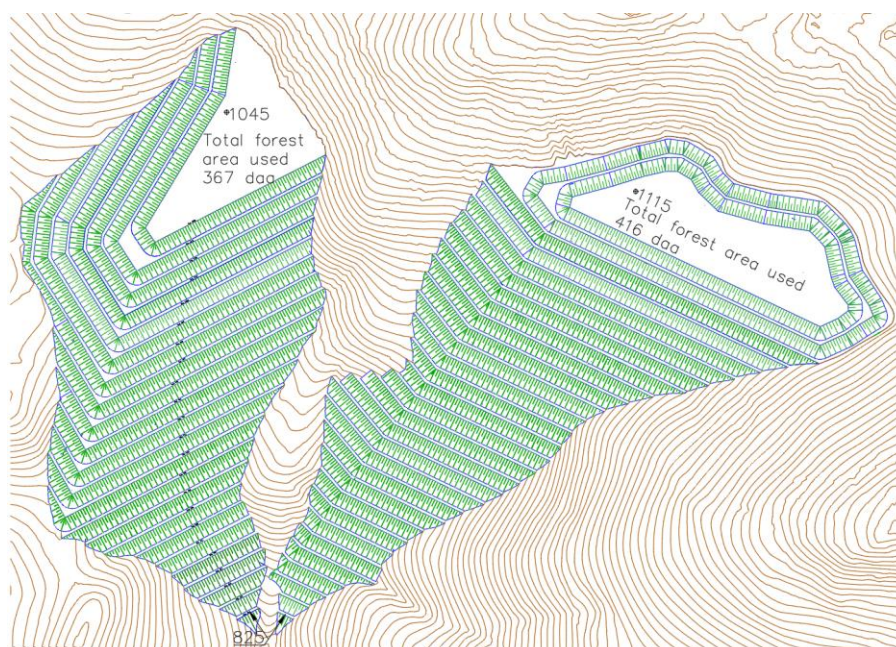


Figure 3. Combined mine waste dump facility built in the ravines (Design 2)

Case 1. To start and continue to build one of the CMWDF. For example, to start with the east one and build contingency storage in the west ravine with a capacity of at least twice the volume of tailings produced for the time needed for a 3 m thick layer of tailings to consolidate. And then leave cells capable of accumulating the same volume of tailings at the top of the CMWDF in the east ravine, which will serve as contingency storage and start constructing the CMWDF in the west ravine.

Case 2. To start with, the construction in both ravines at the same time. This case will need a greater volume of waste rock at the beginning. The construction of both CMWDF will continue until there are enough cells to be used as contingency storage in one of the CMWDF. After that, only one CMWDF can continue with construction. When the construction of one is almost finished, the deposition of tailings can continue in the other one. Before starting to deposit in the other one, it is best to leave 1÷3 cells at this CMWDF serving as contingency storage, ensuring the operational sequence. This case is better and that is why it will be used as an example when discussing "Operational sequence."

Results

Operational Sequence

As mentioned in the papers and reports from (Eldridge, Wickland, Goldstone, & Kissiova, 2011), the operational sequence is critical for the successful and proper construction of the facility. In the paper from (Aleksandrova et al. 2021), the critical path method (CPM) is recommended for managing the operational sequence. The CPM can be used to estimate which operation can be prolonged or for how long it can be delayed (Zlatanov, 2010). Considering the processes that are involved in the construction of the CMWDF few rules are recommended:

1. The time needed for the construction of one cell is less than the time necessary for one cell to be filled with tailings.
2. The minimal volume of a cell for tailings storage is recommended to equal the quantity of tailings produced in the time needed for the tailings to consolidate. However, the cell's maximal volume is also recommended to be limited as it affects the factor of safety. The maximal volume of the cell should be determined according to the rock properties.
3. Operations and construction need to be planned so that the first cell is filled with tailings and waste rock before starting to fill the last cell with tailings (Figures 4 and 5). That will ensure that a cell on the subsequent elevation can be started and finished before the last cell in the previous bench is filled with tailings.

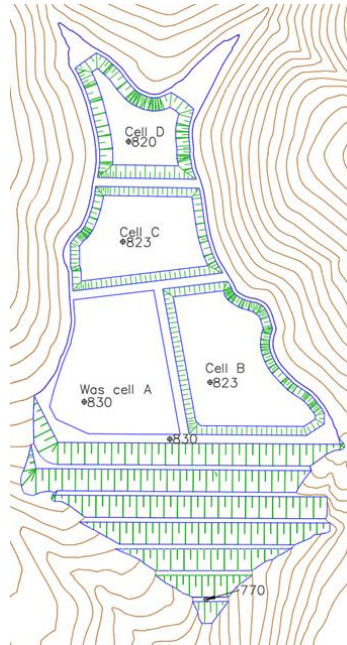


Figure 4. Different stages of cell construction and tailings deposition for design 1

Figures 4 and 5 show the different stages of filling the cells with tailings. Both designs are shown in the stages with the same tailings capacity. Four cells in design 1 are equal in volume to the four cells from both CMWDF in design 2. The cells are shown in different stages of construction. Cell "A" is already filled with tailings and waste rock for both designs. Cell "B" is filled with tailings, and the consolidating process has finished, so it is ready to be filled with waste rock. Tailings deposition in Cell "C" is finished and will start consolidating. Cell "D" is constructed and prepared to be filled with tailings. As shown in both figures (Figures 4 and 5), more cells ensure a better operational sequence.

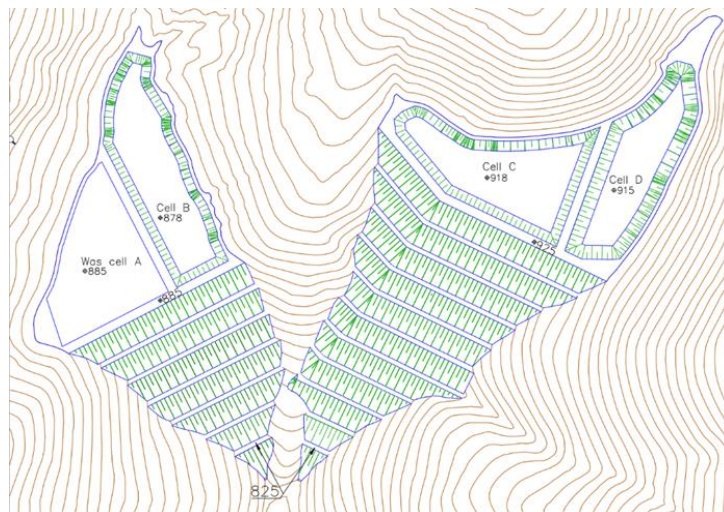


Figure 5. Different stages of cell construction and tailings deposition for design 2, case 2

Comparison between Stored Tailings Used Surface Area and Waste Material (Overburden)

Comparing the line charts from figure 6 to 9, a difference can be noticed between both designs. One is the different volumes of waste material (over burden) needed to store 5,9 million m³ of tailings for different surface areas. The chart from figure 6 shows that design 1 needs 200 daa of surface area and 2 707 400 m³ overburden to hold 725 000 m³ of tailings. In order to hold this volume of material, the facility will rise to an elevation of 850 a.s.l. The ratio between overburden and tailings stored will be 3,7. After that, it rises. The ratio from 860÷900 a.s.l is 4,4, and from 910÷960 a.s.l is 4,1.

If both KWDF are built together in design 2 on a 200 daa surface area, 2 528 000 m³ waste material and 529 150 m³ tailings can be stored. This can be achieved when both facilities reach 905 a.s.l, and the overburden to tailings will be 4,77. The ratio from 915÷995 a.s.l is 4,67, and from 1005÷1115 a.s.l is 4,97. The higher the ratio, the more waste rock is needed to store the tailings. That increases construction costs.

Kaykov and Koprev (2020) investigated a similar problem regarding an overburden waste dump's optimal shape and location. They considered the waste volume to surface area ratio to be a variable that depends on the terrain features, the design features of the waste dump, and the sequence of its construction. Although their research is limited to overburden allocation, a similar approach can be utilized for combined waste dump mine facilities, including tailings and overburden volumes.

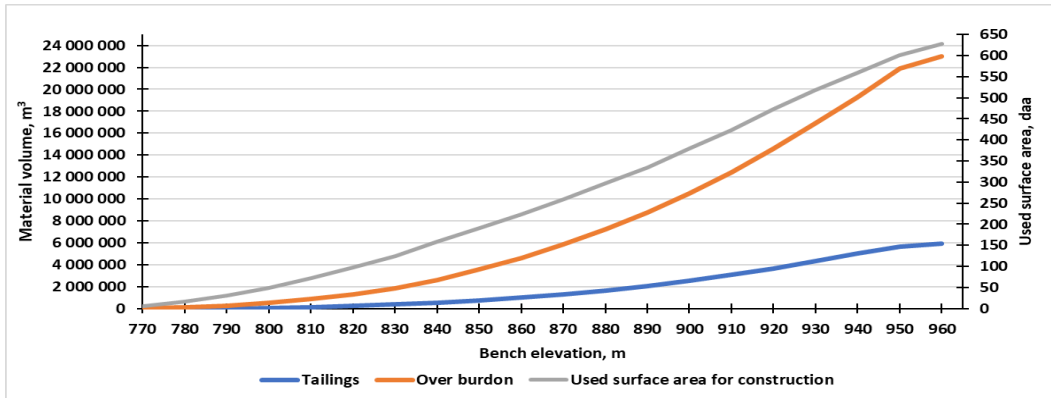


Figure 6. Used surface area and overburden to store 5,9 million m³ of tailings for design 1

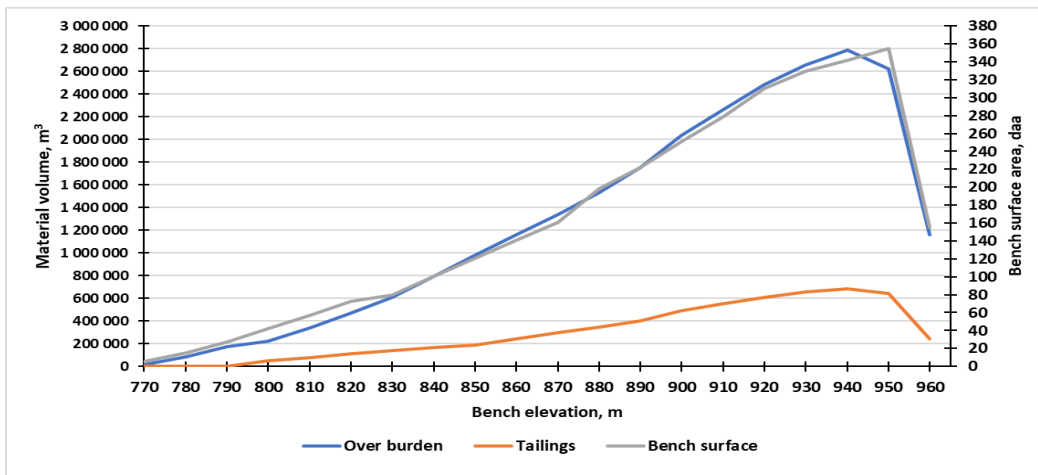


Figure 7. Used surface area and overburden for every bench to store tailings for design 1

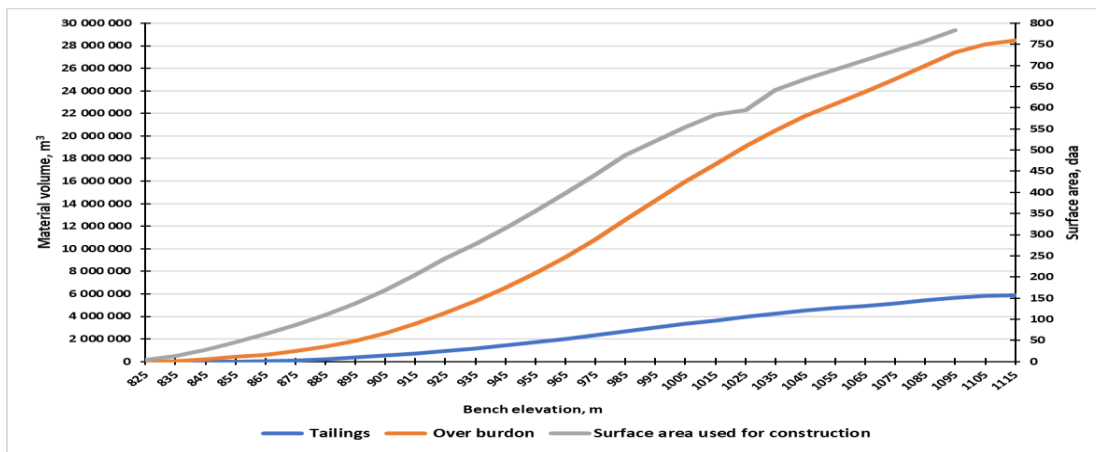


Figure 7. Used surface area and overburden to store 5,9 million m³ of tailings for design 2

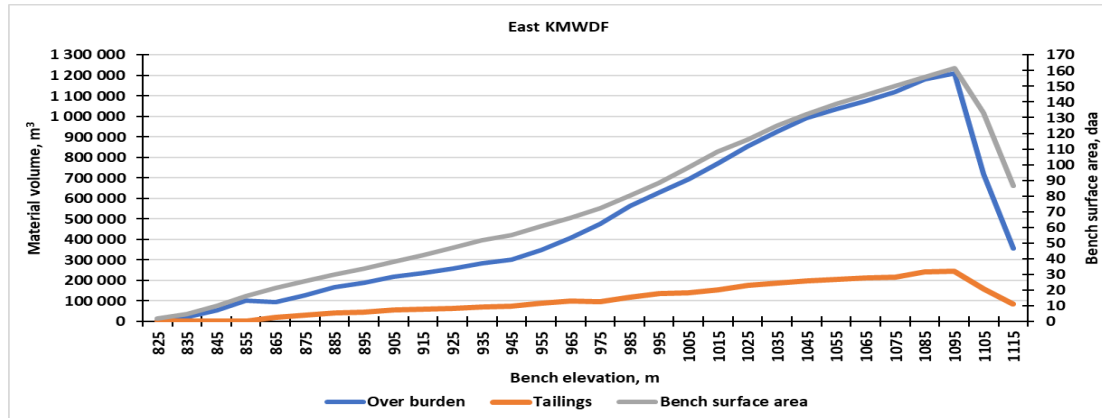


Figure 8. Used surface area and over burden for every bench to store tailings for design 2

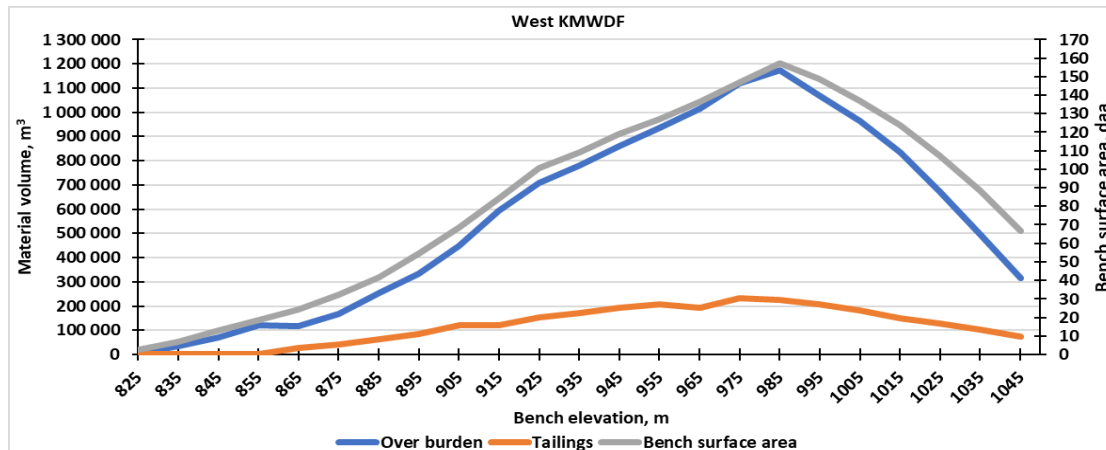


Figure 9. Used surface area and overburden for every bench to store tailings for design 2

Conclusion

With choosing to build a wider construction, a greater number of cells can be fitted in one bench. Thus, a better operational sequence will be achieved because the construction of the cell will not lay on the critical path. With constructing wider CMWDF, the need for contingency storage throughout the lifetime of the mine will be eliminated because of the capability to have a greater number of cells from the early stage of construction. The wider design would end with a wide flat bench leaving the possibility to restart mining activities if there were reserves left behind that were not economically extractable at the time.

To achieve a good operational sequence, a minimum of 3 cells in different stages is recommended at all times. One that the consolidation of tailings is over, and it can be filled with waste rock, one that the deposition of tailings is over, and one that is constructed and ready to be filled with tailings. The minimal volume of a cell is recommended to be designed so that the volume of tailings produced in the period needed for consolidation of the tailings can be accumulated in the predicted volume of the cell.

Steep and narrow terrain can limit the space for cell construction. That can be noticed in the case of CMWDF from design 2. As the facility rises in height and the benches get wider, cells with better form can be constructed, so the volume ratio between tailings and the cell volume increases. The volume of tailings accumulated in the cell when the bench is narrower is 24 %, and it rises as the bench gets wider.

Scientific Ethics Declaration

The authors declare that the scientific ethical and legal responsibility of this article published in EPSTEM journal belongs to the authors.

Acknowledgements or Notes

*This article was presented as an oral presentation at the International Conference on Research in Engineering, Technology and Science (www.icrets.net) held in Budapest/Hungary on July 06-09, 2023.

* This research is supported by the Bulgarian Ministry of Education and Science under the National Program "Young Scientists and Postdoctoral Students – 2".

References

- Aleksandrova, E., Dimitrov, L., & Kaykov, D. (2021). Operational sequence for constructing an combined mine waste facility. *XVI International Conference of the Open and Underwater Mining of Minerals*, (pp. 7-13). Varna.
- Dimitrov, L. (2021, 9-10). Types of tailings facilities in the processing of mineral raw materials - advantages and disadvantages. *Geology and Mineral Resources* (pp. 5-11).
- Eldridge, T., Kissiova, M., Wickland, B., Ahmed, I. B., & Laurin, J.-F. (2013). Integrated mine waste storage facility, Krumovgrad gold project, Bulgaria. *XV Balkan Mineral Processing Congress*. Sozopol.
- Eldridge, T., Wickland, B., Goldstone, A., & Kissiova, M. (2011). Integrated mine waste storage concept, Krumovgrad gold project, Bulgaria. *Tailings and Mine Waste*. Vancouver.
- Grigorova, I. (2011). *Gravitational technologies in mining waste management*. Sofia: RITT.
- Kaykov, D., & Koprev, I. (2020). Rationalizing the location and design of the waste dump in the case of open pit mining. *Sustainable Extraction and Processing of Raw Materials*, 42-46.
- Lyu, Z., Chai, J., Xu, Z., Qin, Y., & Cao, J. (2019). A comprehensive review on reasons for tailings dam failiures based on case history. *Advances in Civil Engineering*, 1-18. Article ID 4159306 <https://doi.org/10.1155/2019/4159306>
- Zlatanov, P. (2010). *Modeling and management of technological processes in open pit mines*. Sofia: Avangard Prima.

Author Information

Ljupcho Dimitrov

UMG "St. Ivan Rilski"
st. prof. Boyan Kamenov, Sofia, Bulgaria
Contact e-mail: ljupcho.dimitrov@mgu.bg

Irena Grigorova

UMG "St. Ivan Rilski"
st. prof. Boyan Kamenov, Sofia, Bulgaria

Teodora Yankova

UMG "St. Ivan Rilski"
st. prof. Boyan Kamenov, Sofia, Bulgaria

To cite this article:

Dimitrov, L. Grigorova, I. & Yankova, T. (2023). Possibilities to construct combined mine waste dump facility with better operational sequence. *The Eurasia Proceedings of Science, Technology, Engineering & Mathematics (EPSTEM)*, 23, 42-49.

The Eurasia Proceedings of Science, Technology, Engineering & Mathematics (EPSTEM), 2023

Volume 23, Pages 50-58

ICRETS 2023: International Conference on Research in Engineering, Technology and Science

Stochastic Longitudinal Autopilot Tuning for Best Autonomous Flight Performance of a Morphing Decacopter

Tugrul Oktay
Erciyes University

Firat Sal
Iskenderun Technical University

Oguz Kose
Erzincan Binali Yildirim University

Enes Ozen
Erciyes University and Hasan Kalyoncu University

Abstract: In this conference paper autonomous flight performance maximization of a morphing decacopter is considered by using stochastic optimization approach. For flight controller a PID based hierarchical control system is chosen. In this paper PID controller which is used for pitch angle is considered. In this application only longitudinal flight and longitudinal autopilot is considered where the pitch motion is in primary interest and the used controller is the pitch control. For optimization technique simultaneous perturbation stochastic approximation (i.e., SPSA) is selected. It is fast and safe in stochastic optimization problems when it is not possible to evaluate gradient analytically. At the end a cost function consisting terms that settling time, rise time and overshoot is minimized. A detailed graphical analysis is done in order to better present effect of morphing on longitudinal flight of decacopter flight. Moreover, the cost function consist of rise time, settling time, and overshoot during trajectory tracking.

Keywords: Decacopter, Stochastic optimization, Morphing, Autonomous flight performance.

Introduction

UAVs can be divided into two groups; fixed blades and rotary blades. The fixed-wing vehicle has a long range and a high flight time. On the other hand, rotary wing systems have good maneuverability; they can hover, land and take off vertically (Austin, 2011). Rotary-wing aircraft are named according to the number of rotors they have. Single rotor aircraft are called helicopters. It is the aircraft with the highest payload capacity. It has a swash plate mechanism to move the angle of attack in three-dimensional space. It also has a tail rotor. That's why it has so many mechanical connections. It is disadvantageous in terms of maintenance and manufacturability. Multi-rotor aircraft can control thrust and torque by simply varying the rotational speed of the propellers. It is easy to maintain, but has a lower payload and flight time compared to other types of aircraft. Their propellers are smaller than equivalent helicopter propellers. They can fly in harsh environments with lower risk (Abdelhay et al., 2019).

The main components of a multi-rotor aircraft are the frame, engines and propellers. Frame; carries the controller, sensor, power supply and communication means, carries the motor and propeller, which are located at the end of the frame arm. In a multi-rotor aircraft, the fixed rotors generate thrust vectoring from the ground up. When the multi-rotor aircraft increases the rotational speed of the propellers by the same amount, the vehicle

- This is an Open Access article distributed under the terms of the Creative Commons Attribution-Noncommercial 4.0 Unported License, permitting all non-commercial use, distribution, and reproduction in any medium, provided the original work is properly cited.

- Selection and peer-review under responsibility of the Organizing Committee of the Conference

© 2023 Published by ISRES Publishing: www.isres.org

lifts. If the thrust vector is equal to the vehicle weight, it maintains its own height. Attitude behavior of the system; controlled by roll, pitch and yaw moments. A positive roll angle is obtained by increasing the speed of the left-hand propellers and decreasing the speed of the right-hand propellers. This causes the rolling moment. It allows the system to rotate around the X-axis. A roll angle is created by the speed differences. The pitching moment between the front and rear propellers is obtained in the same way. In a multi-rotor aircraft, each successive propeller rotates in the opposite direction to balance the drag moments and zero the torque with respect to the total z-axis. A multi-rotor aircraft can create an imbalance by varying the rotational speed of the propellers to achieve a yaw angle, with the total torque reaching a plus or minus value other than 0, yaw occurs (Prisacariu et al., 2016). The system is a system with missing actuators, referring to the fact that the number of inputs is small. The degrees of freedom are greater than the inputs of the system. The multi-rotor aircraft has six degrees of freedom (DOF), but only four inlets. Therefore, the two degrees of freedom depend on the others. When the tilt angles (roll and pitch angle) are changed, a horizontal component of the thrust vector is obtained, which moves the system in the X - Y plane (Alanezi et al., 2022).

In this study, the distance between the rotors of the ten rotor aircraft and the fuselage center of gravity may vary. While this allows the vehicle to expand in atmospheric disturbances and fly more stable, it has an active morphing feature that allows it to narrow and make aggressive maneuvers and avoid obstacles (Desbiez et al., 2017). In this study, by using the simultaneous perturbation stochastic approximation (SPSA) optimization algorithm, the values that stabilize the lateral and longitudinal flight of the ten rotor aircraft, in which the morphing amount and the best Proportional-Integral-Derivative (PID) coefficients are determined, are obtained (Kose et al., 2022). Decacopter is a rotary-wing aircraft that generates thrust thanks to its 10 propellers and the rotor that drives them. An algorithm and PID controller are being developed to obtain position and attitude control of the active deformable aircraft during flight. As a result, the performance of the ten rotor aircraft was improved and controlled by the SPSA optimization method of metamorphism parameters, PID gain parameters.

Method

Decacopter Design and Proposed Model

A decacopter consists of 10 rotors positioned equidistant from the center of mass. As in quadrotor, hexarotor and octocopter type UAVs, the speed of each rotor is controlled independently to perform decacopter movements. Decacopter has six degrees of freedom (6DOF). 6DOF defines the number of axes that a solid object can move in three-dimensional space. At the same time, 6DOF defines the configuration of a mechanical system with independent parameters. The decacopter also has four control inputs. Control inputs are used to define the movements on the axes. The control inputs are used for hover, longitudinal, lateral and yaw movements. Figure 1 shows the decacopter and its axes.

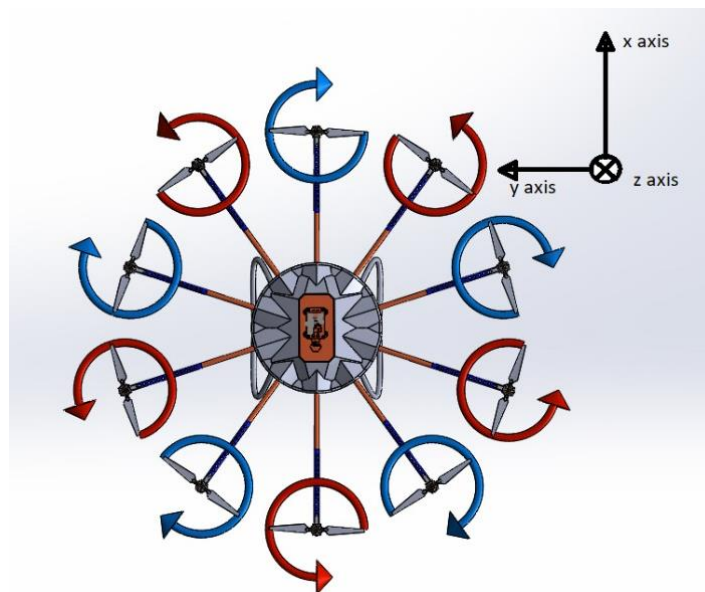


Figure 1. The decacopter and its axes

In Figure 1, there are two axes of the decacopter. These are earth and body frame. The decacopter performs its longitudinal movement on the y axis and this movement is indicated by θ . Longitudinal movement is used for the decacopter to perform forward and backward movement. In addition, in order to perform this movement, the decacopter must increase the speed of the x and y motors and decreases the speed of the k and l rotors according to the rotor sequences shown in Figure 1.

As with quadrotor, hexarotor and octorotor type UAVs, a mathematical model must be obtained for the decacopter type UAV. Newton's laws of motion and Euler's laws are used for the mathematical model of such UAVs (Mustapa, 2015). Accordingly, the mathematical position vectors (x, y and z) of the decacopter are shown in equations 1, 2 and 3 and the Euler angles (θ) are shown in equations 4, 5 and 6.

$$m\ddot{x} = -(T + w_x) \sin \theta \quad (1)$$

$$m\ddot{y} = (T + w_y) \cos \theta \sin \phi \quad (2)$$

$$m\ddot{z} = (T + w_z) \cos \theta \cos \phi - mg \quad (3)$$

$$I_x \ddot{\theta} = \tau_x + w_\theta \quad (4)$$

$$I_y \ddot{\phi} = \tau_y + w_\phi \quad (5)$$

$$I_z \ddot{\psi} = \tau_z + w_\psi \quad (6)$$

Equations 1-6 are nonlinearly expressed equations. In order to facilitate simulations and successful implementation of control algorithms, they are converted into linear form by various approaches. Accordingly, the linear equations of motion of the decacopter can be expressed as follows.

$$\ddot{x} = g\theta \quad (7)$$

$$\ddot{y} = -g\phi \quad (8)$$

$$\ddot{z} = -g + \frac{T}{m} \quad (9)$$

$$\ddot{\phi} = \frac{\tau_x}{I_x} \quad (10)$$

$$\ddot{\theta} = \frac{\tau_y}{I_y} \quad (11)$$

$$\ddot{\psi} = \frac{\tau_z}{I_z} \quad (12)$$

T is the total thrust generated by the 10 rotors. τ_x , τ_y and τ_z are the roll, pitch and yaw torques respectively. These torques and total thrust are the inputs required to control the desired motion of the decacopter. I_x , I_y and I_z are the moments of inertia of the decacopter.

The decacopter performs morphing by changing the arm lengths during its flight. Morphing is a developmental feature that has recently started to be applied in UAVs. Morphing is a change in the geometry of the UAV before or during flight (Oktay and Kose, 2020). If the UAV changes its geometry before flight, such as changing the length of the arm or changing another geometric feature, this is characterized as passive morphing (Oktay and Coban, 2017). If the UAV performs this while in the air during flight, this is called active morphing (Kose

and Oktay, 2021). In this study, the decacopter performed morphing by simultaneously lengthening and shortening the arm lengths during flight. With morphing, the arm length of the decacopter can be shortened by a minimum of 65 cm and lengthened by a maximum of 80 cm. Examples of the morphing situation are shown in Figure 2.

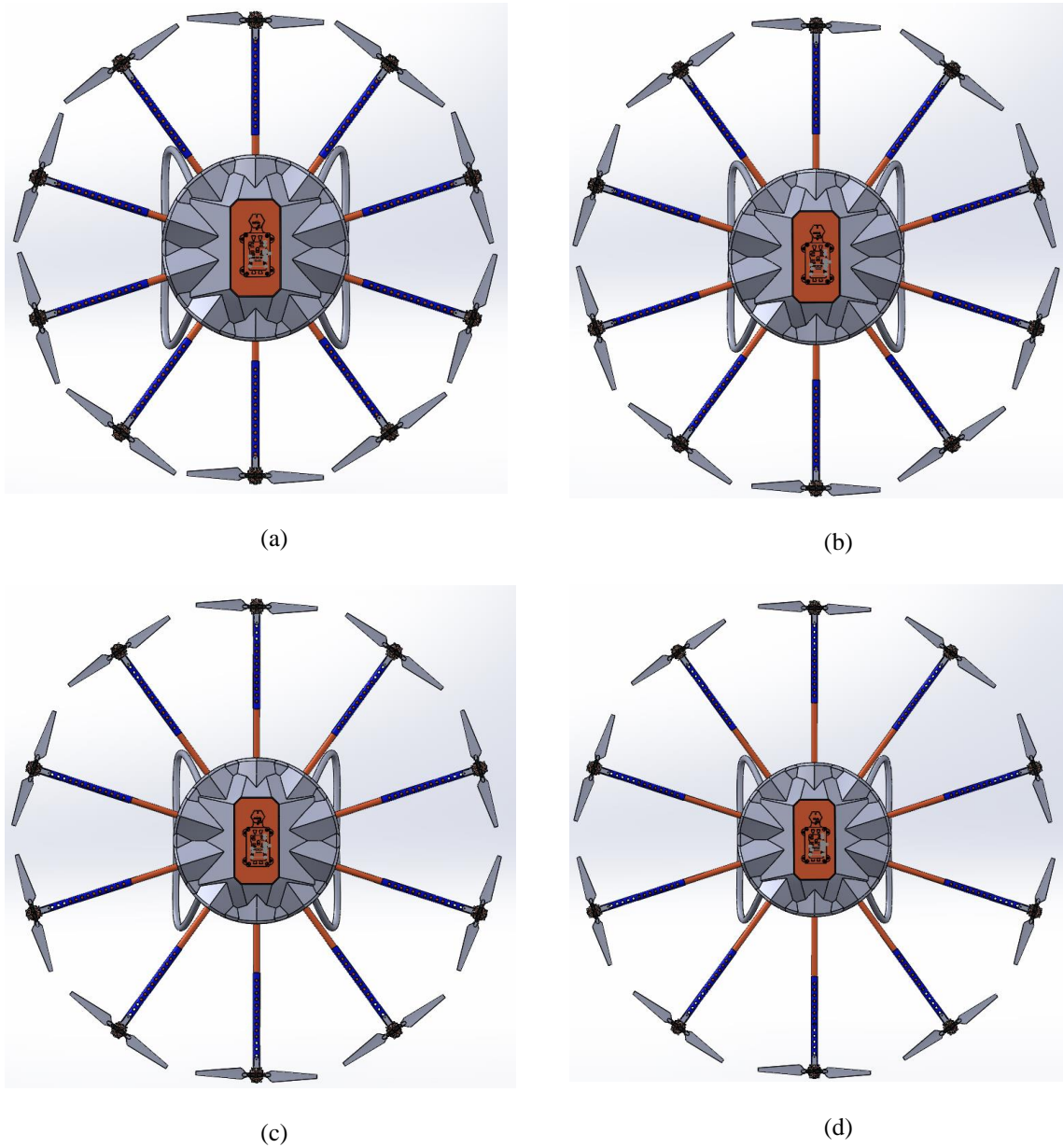


Figure 2. (a) 65 cm arm length, (b) 70 cm arm length, (c) 75 cm arm length, (d) 80 cm arm length

With morphing, the distances of the arms to the axes of rotation will change. However, there will also be changes in the values of the moments of inertia. Since moments of inertia are divisors in equations 10, 11 and e12, they will have an effect on the equations of motion and therefore on longitudinal flight. The new moment of inertia calculation for each morphing condition is shown below:

$$I_x = \frac{1}{3} * \frac{m}{10} * 4 * (L * \sin(\alpha_1))^2 + \frac{1}{3} * \frac{m}{10} * 4 * (L * \sin(\alpha_2))^2 \quad (13)$$

$$I_y = \frac{1}{3} * \frac{m}{10} * 4 * (L * \sin(\alpha_1))^2 + \frac{1}{3} * \frac{m}{10} * 4 * (L * \sin(\alpha_2))^2 + \frac{1}{3} * \frac{m}{10} * 2 * L^2 \quad (14)$$

$$I_z = \frac{1}{3} * m * L^2 \tag{15}$$

SPSA and Control Algorithm

There are several unknown parameters in decacopter control. These parameters are control algorithm coefficients and morphing ratio. The unknown parameters need to be obtained quickly and reliably (Spall, 1998). For this purpose, SPSA algorithm is preferred. SPSA algorithm is an algorithmic method used to optimise systems with multiple unknown parameters (Maryak et al., 2001). SPSA is a global minimisation search method. No matter how large the size of the optimization problem is, SPSA makes only two predictions in each iteration (Ko et al., 2008). This feature distinguishes it from similar algorithms.

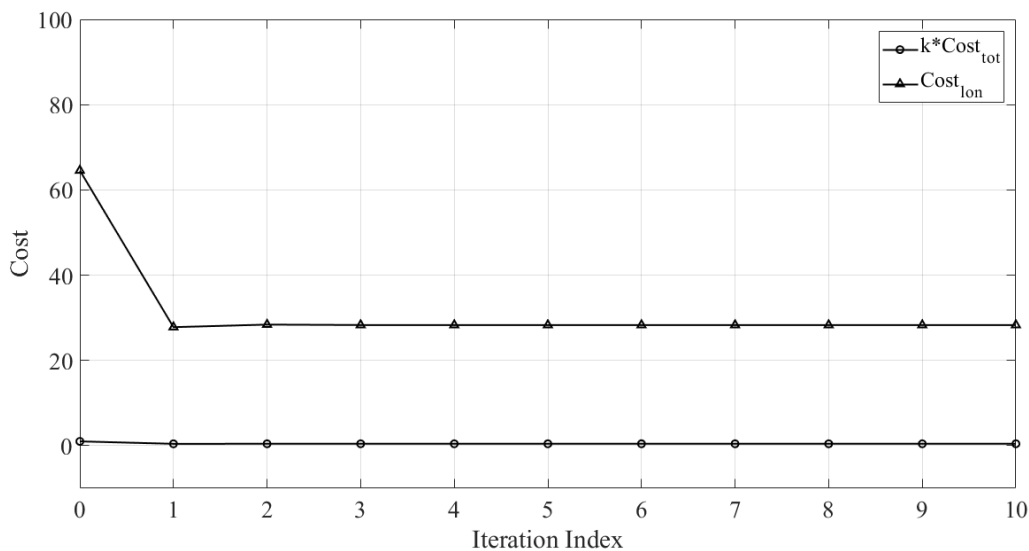
Since there is a complex relationship between the decacopter control algorithm parameters and morphing, it is difficult to calculate or obtain these values. For this purpose, the following cost function is generated simultaneously for the decacopter longitudinal flight.

$$J_{long} = T_{rt_{long}} + T_{st_{long}} + OS_{long} \tag{16}$$

The cost function is a function of decacopter rise time, settling time and overshoots values. The control algorithm coefficients estimated by SPSA are effective in longitudinal control of the decacopter. PID control algorithm is used for longitudinal control of the decacopter. PID is a feedback control loop mechanism widely used in industrial systems (Haddadi et al., 2015). The PID control algorithm continuously calculates an error value. The error value consists of the difference between the set point of the system and the feedback value. The error value is multiplied by K_p proportional, K_i integral and K_d derivative terms and transferred to the system output. In this study, the SPSA algorithm estimated the K_p , K_i ve K_d values required for the control algorithm.

Conclusion

In this study, the longitudinal flight control of a decacopter type UAV with morphing is implemented using SPSA and PID control algorithms. The full model of the decacopter was drawn in Solidworks and the mass and arm length information of the decacopter were obtained. The mathematical model of the decacopter was created using the Newton-Euler approach. Linear equations of motion were used for the state space model approach. Determination of the decacopter morphing rate and control algorithm coefficients were used for longitudinal flight. Here, the SPSA optimization method was used to estimate the parameters. As shown in Figure 3, the cost index and total cost index were minimized by SPSA.



(a)

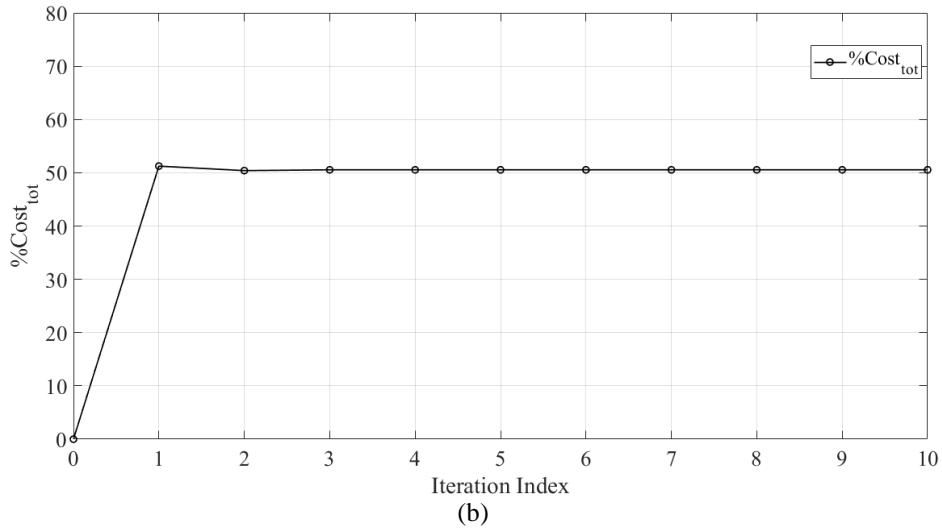


Figure 3. (a) Cost index, (b) Total Cost index

As can be seen in Figure 3, the cost index was improved by 50% and the total cost index was improved by 50%. The arm length values predicted by the SPSA optimization method in each iteration, which was run for 11 iterations in total, are shown in Figure 4.

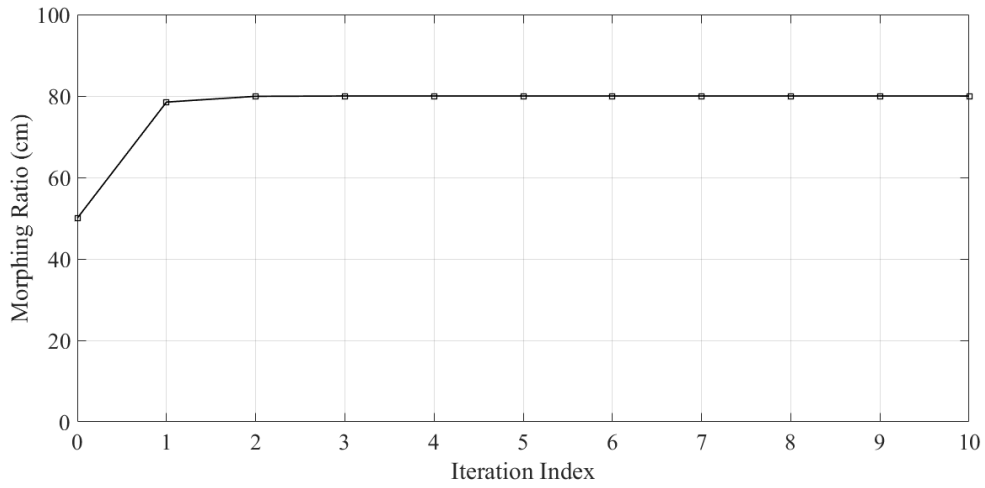


Figure 4. Morphing rate at each iteration

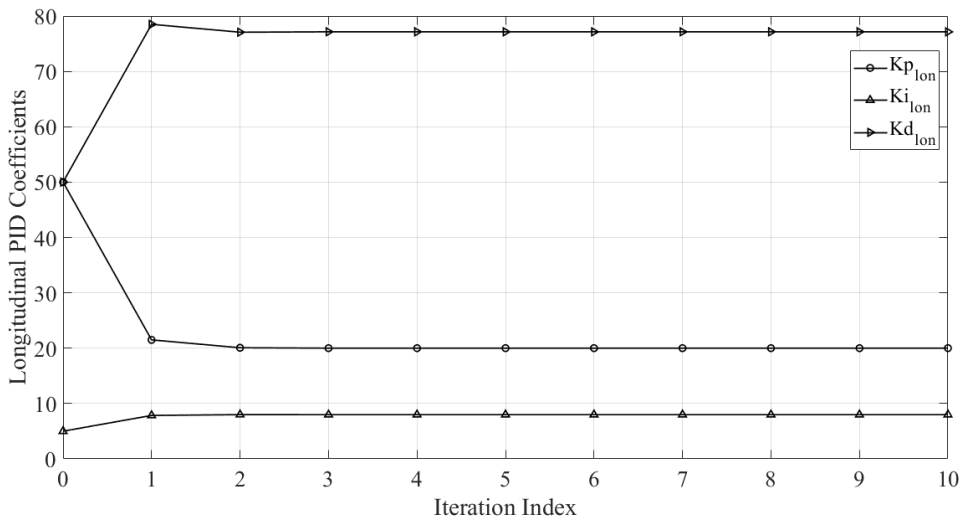


Figure 5. PID coefficients

The PID coefficients obtained in 11 iterations are shown in Figure 5. The rise time, settling time and overshoot values, which are the design performance criteria in the simulations performed at each iteration, are shown in Figure 6.

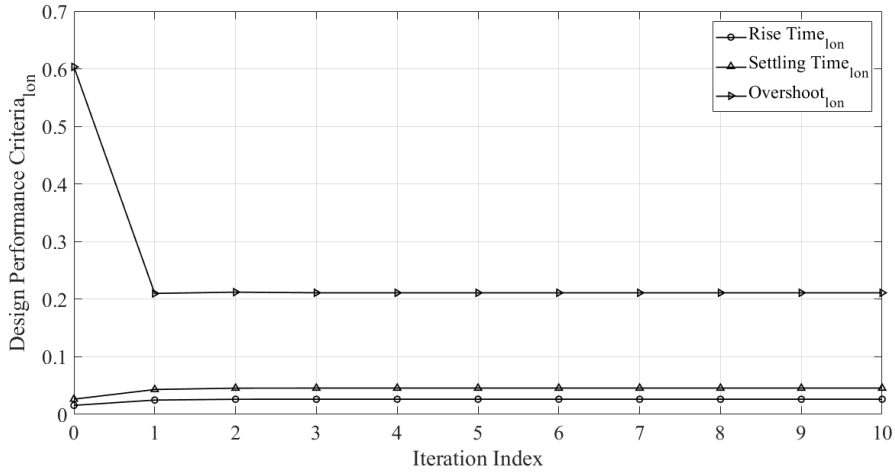
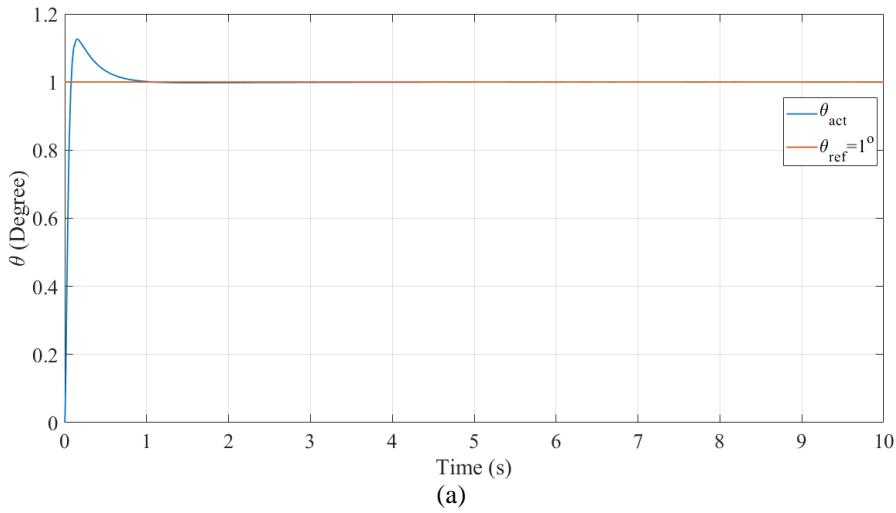
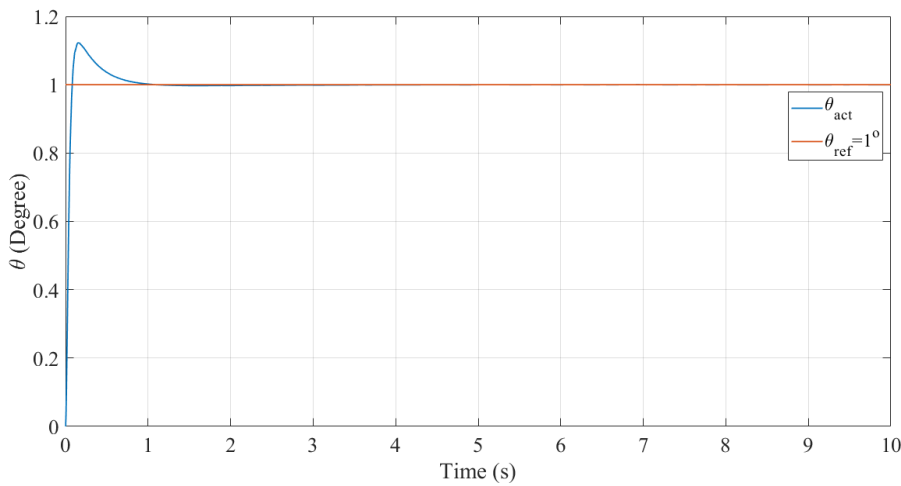


Figure 6. Design performance criteria

The second and fifth iteration simulations were performed with all the data obtained. In the simulation, the decacopter was asked to follow a 1° trajectory for longitudinal flight. Figure 7 shows the simulation outputs.



(a)



(b)

Figure 7. (a) Simulation 2, (b) Simulation 5

The decacopter successfully followed the given trajectory. However, when the design performance criteria were examined, it was found that there was no excessive behavior in the settling and rise time values while there was a serious decrease in the ascent value. This showed that longitudinal flight with morphing was successfully implemented in the decacopter.

Scientific Ethics Declaration

The authors declare that the scientific ethical and legal responsibility of this article published in EPSTEM journal belongs to the authors.

Acknowledgements or Notes

*This article was presented as an oral presentation at the International Conference on Research in Engineering, Technology and Science (www.icrets.net) held in Budapest/Hungary on July 06-09, 2023.

*This work has been supported by Erciyes University Scientific Research Projects Coordination Unit under grant number FBA-2022-12375.

References

- Abdelhay, S., & Zakriti, A. (2019). Modeling of a quadcopter trajectory tracking system using PID controller. *Procedia Manufacturing*, 32, 564–571.
- Alanezi, M. A., Haruna, Z., Sha'aban, Y. A., Bouchekara, H. R. E. H., Nahas, M., & Shahriar, M. S. (2022). Obstacle avoidance-based autonomous navigation of a quadrotor system. *Drones*, 6(10), 1–19.
- Austin, R. (2011). *Unmanned aircraft systems: UAVS design, development and deployment*, 54. John Wiley & Sons.
- Desbiez, A., Expert, F., Boyron, M., Diperi, J., Viollet, S., Ruffier, F., Desbiez, A., Expert, F., Boyron, M., Diperi, J., Viollet, S., Desbiez, A., Expert, F., Boyron, M., Diperi, J., Viollet, S., & Ruffier, F. (2017). *X-Morf: a crash-separable quadrotor that morfs its X-geometry in flight To cite this version : HAL Id : hal-01644528*.
- Haddadi, S. J., Emamaghali, O., Javidi, F., & Fakharian, A. (2015). Attitude control and trajectory tracking of an autonomous miniature aerial vehicle. *2015 AI and Robotics, IRANOPEN 2015 - 5th Conference on Artificial Intelligence and Robotics*.
- Ko, H.-S., Lee, K. Y., & Kim, H.-C. (2008). A simultaneous perturbation stochastic approximation (SPSA)-based model approximation and its application for power system stabilizers. *International Journal of Control, Automation, and Systems*, 6(4), 506–514.
- Kose, O., & Oktay, T. (2021). *Combined quadrotor autopilot system and differential morphing system design. Journal of Aviation*, 5(2), 64–71.
- Kose, O., & Oktay, T. (2022). Hexarotor yaw flight control with SPSA , PID algorithm and morphing. *International Journal of Intelligent Systems and Applications in Engineering*, 10(2), 216–221.
- Maryak, J. L., & Daniel, C. C. (2001). *Global random optimization by simultaneous perturbation stochastic approximation*. In *Proceedings of the 2001 American control conference*.(Cat. No. 01CH37148) (Vol. 2, pp. 756-762). IEEE.
- Mustapa, M. Z. (2015). Altitude controller design for quadcopter UAV. *Jurnal Teknologi*, 74(1), 187–194.
- Oktay, T., & Coban, S. (2017). Simultaneous longitudinal and lateral flight control systems design for both passive and active morphing TUAVs. *Elektronika Ir Elektrotehnika*, 23(5), 15–20.
- Prisacariu, V., Air, R., & Academy, F. (2016). *Introduction morphing technology in unmanned aircraft vehicles In International Conference of Scientific Paper, AFASES*.
- Spall, J. C. (1998). An overview of the simultaneous perturbation method for efficient optimization, *Johns Hopkins Apl Technical Digest*, 19(4), 482-492.
- Oktay T. & Kose. O. (2020). Simultaneous quadrotor autopilot system and collective morphing system design. *Aircraft Engineering and Aerospace Technology*, 92(7), 1093–1100.

Author Information

Tuğrul Oktay

Erciyes University
Kayseri, Turkey

Contact e-mail: tugruloktay52@gmail.com

Fırat Şal

Iskenderun Technical University
Iskenderun, Turkey

Oğuz Köse

Erzincan Binali Yıldırım University
Merkez / Erzincan, Turkey-

Enes Özen

Erciyes University and Hasan Kalyoncu University
Kayseri, Turkey and Gaziantep, Turkey

To cite this article:

Oktay, T. Sal, F. Kose, O. & Ozen, E. (2023). Stochastic longitudinal autopilot tuning for best autonomous flight performance of a morphing decacopter. *The Eurasia Proceedings of Science, Technology, Engineering & Mathematics (EPSTEM)*, 23, 50-58.

The Eurasia Proceedings of Science, Technology, Engineering & Mathematics (EPSTEM), 2023

Volume 23, Pages 59-68

ICRETS 2023: International Conference on Research in Engineering, Technology and Science

A Quantitative Blockchain-Based Model for Construction Supply Chain Risk Management

Clarissa Amico
Politecnico di Milano

Roberto Cigolini
Politecnico di Milano

Abstract: Although the use of Blockchain Technology in construction industry has been limited, nowadays several cases of adoption of this technology in construction sector can be identified. Such examples consist of maintaining digital asset records, timestamps for contracts or transactions, multiple signature transactions, smart contracts, and the repository of real information. This paper proposes a methodology consisting of a Electre Tri multi-criteria analysis method where a list of indicators and a questionnaire are used to fill a model that can be applied to evaluate the suitability of blockchain technology as a tool to mitigate supply chain risks that small and medium enterprises face in the construction industry. The model has been applied to two companies operating in the construction industry. This study contributes to the existing literature by quantitatively assessing the adoption of blockchain technology on two real case studies – company Alpha and company Beta – to limit supply chain risk in the construction sector. The dimensions considered in the analysis are company data, payments, materials, supply chain structure and information and document flow. According to the findings, the model suggests that for company Alpha blockchain technology is recommended but not useful to mitigate risks and so improving supply chain performance. On the contrary, results show that for company Beta the implementation of blockchain technology is useful.

Keywords: Supply chain management, Blockchain technology, Construction industry

Introduction

Nowadays, in the construction industry, risks cause a net decrease in productivity and a slowdown in the project process (Al-Werikat, 2017). The analysis of the Italian construction sector has reserved important attention because it is considered of strategic importance (Kim et al., 2020; Cigolini et al., 2022), since deals with the structures and infrastructures, which can be used by all other sectors (Cannas et al., 2020; Rossi et al., 2020) involved in the European economy and society (Harouache et al., 2021).

Small and medium enterprises in Europe and Italy are characterized by low Supply Chain (SC) performance level (Mafundu & Mafini 2019; Cigolini et al., 2022). The recent Covid-19 pandemic has caused a chain reaction in all economic sectors around the world, exacerbating this situation. Although signs of recovery are weak, Italian small and medium-sized companies seem not to have recovered from the 2008 financial crisis and have long been plagued by low productivity (Ferreira de Araújo Lima et al., 2021).

In this context, Supply Chain Management plays pivotal role especially because today, due to increasing globalization, SCs are more fragile than they used to be (Layaq et al., 2019; Pero et al., 2016; Amico et al., 2022; Franceschetto et al., 2022). Because of cheap labour abroad, many companies manufacture or source products internationally. This creates many types of risks in the SC appropriately managed with the risk management process (Shemov et al., 2020) where risks are dealt with suitable risk reduction techniques.

- This is an Open Access article distributed under the terms of the Creative Commons Attribution-Noncommercial 4.0 Unported License, permitting all non-commercial use, distribution, and reproduction in any medium, provided the original work is properly cited.

- Selection and peer-review under responsibility of the Organizing Committee of the Conference

Blockchain technology can be indeed a tool for reducing risks due to its tamper-proof record (Xu et al., 2020; Difrancesco et al., 2022; Amico & Cigolini 2023). Blockchain technology is used to trace the origin of the materials or components used in the manufacture of products (Xu et al., 2020). Small and medium enterprises, to compete with the other global players, should develop new innovation-based business strategies that ensure efficiency, flexibility, and high-quality processes (Pozzi et al., 2019; Franceschetto et al., 2023). Digitizing processes means moving away from paper and toward online and real-time information sharing to ensure transparency and collaboration between the actors involved in the process. One reason for the industry's low productivity is that it still relies primarily on paper to manage its processes (Difrancesco et al., 2022; Amico & Cigolini 2023), and deliverables, such as blueprints, project drawings, purchase orders and supply chains, equipment records, and daily progress reports (Kim et al., 2020).

Literature related on the classification of risks in the SCs of small and medium enterprises in the construction industry, as well as the definition of specific indicators to evaluate blockchain suitability as risk mitigator, is scant. Thus, this paper aims to fill this gap by understanding, through a model based on *Electre Tri* methodology (élimination et choix traduisant la réalité, French for elimination and choice expressing reality, see Del Rosso Calache et al., 2018) whether small and medium enterprises can adopt blockchain technology as a risk mitigator tool to improve companies SC performance. Moreover, this study allows small and medium enterprises to understand if blockchain could be the right solution for the specific context of their organization. In fact, this paper can help to catalogue and study various aspects and the related risks of the SC by providing a clear outcome in terms of adaptability of blockchain technology to a fragmented and heterogeneous context such as that of small and medium enterprises in the construction industry.

The paper is structured as follows: section 2 is devoted to the description of the research background to define the SC of the construction industry and the related risks as well as the main characteristics of blockchain technology. Section 3 describes the methodology adopted while section 4 illustrates the model. Section 5 shows the main findings. Finally, section 6 draws some conclusions and suggests future research paths.

Background

Construction SCs are complex systems especially when a variety of site materials and parties (like suppliers and sub-contractors) are involved in a construction project (Papadopoulos et al., 2016). The more people are engaged (e.g., first tier, second tier suppliers and other tiers of sub-contractors, see Rossi et al., 2017, Pero et al., 2020, Afraz et al., 2021), the more complex is the project. Furthermore, construction industry deals with complex SCs because more worker, parties and materials are required to a specific project. A construction project necessitates collaboration and cooperation among SC actors to define the best planning and organization for the project (Gosling et al., 2016).

According to Koskela et al. (2020), the construction SC can be differentiated as a converging SC since all materials are directed to the construction site where the object is assembled from incoming materials. Moreover, construction SC is fragmented since construction contractors, suppliers and other participants are active in different stages of the project, and the distribution of responsibility and authority could change over time. Finally, construction SC is temporary because when a construction project is completed, all participants and companies involved are usually dismissed as soon as all the actors participating in the project complete their duties.

Furthermore, the construction SC is composed by the following three elements. (i) The primary SC that is the stream that delivers the materials used in the final stage of the construction process. (ii) The support chain is in charge for providing expertise and equipment that facilitate the realization of construction project (e.g., scaffolding and excavation supports). (iii) The human resource SC that includes the supervisory staff and labour useful for the construction process. Hence, the construction SC consists of the human resource SC, the support chain, the primary chain, and it is also characterised to be temporary, make to order, complex and converging (Al-Werikat, 2017). According to Papadopoulos et al. (2016) most of the issues in the construction industry arises at the interfaces between the various activities or roles and are due to the complex nature of the construction environment. The main issues concern the so-called design interface phase between the client and field contractor that embraces several difficulties in defining and then realizing client's wishes.

Moreover, within the engineering phase between the field design contractor and the engineering contractor – the so-called engineering interface – some documents may prove to be incorrect the design can change and –

consequently – the approval of the design changes can be very long. Within the procurement phase between the engineering contractor and the procurement actors there is the so-called vendors interface, and some drawings may show inaccurate data, or they are not usable by vendors. Within the construction phase, some issues can occur between vendors and suppliers: for example lack of coordination, collaboration and commitment between suppliers, poor quality of materials and components. In the completion of the project between the site and the commissioning contractor – the so-called commissioning interfaces – some issues could be related to safety issues and difficulties with local communities. Finally, after commissioning there is the so-called operation interface: there can be problems due to unresolved quality and technical issues, delayed operational time due to late completion (Nanayakkara et al., 2021).

All the previous mentioned issues are related to the concept of risk. SC risk is an adverse event since it negatively influences the desired performance of an industry (Layaq et al., 2019). In the construction industry, examples of risks are related to demand (e.g., order fulfilment errors, inaccurate forecasts due to longer lead times, product variety) and inventory (e.g., costs of holding inventories, rate of product obsolescence and supplier fulfilment, see Pero et al., 2020; Ferreira de Araújo Lima et al., 2021).

The risk management process is a useful method to limit these SC risks and it is defined by five phases: risk identification, risk measurement, risk assessment, risk evaluation and risk control and monitoring. Such process allows to mitigate all the challenges that small and medium enterprises must face. To compete with the other global players, small and medium enterprises should develop new innovation-based business strategies that ensure efficiency, flexibility, and high-quality processes (Pournader et al., 2020).

Digitizing processes means moving away from paper and toward online and real-time information sharing to ensure transparency and collaboration, timely progress and risk assessment, quality control, and ultimately, better and more reliable results (Difrancesco et al., 2022; Amico et al., 2022). Blockchain technology offers to small and medium enterprises the opportunity to increase productivity. Blockchain technology can record data, transferred though all the actor involved in the SC, in a decentralized manner. This provides transparency between members and the ability to follow the record of the entire flow of information. This information is verifiable and allows the origin to be traced and completed (Pournader et al., 2020).

One of the main benefits of adopting a blockchain technology is that it is highly effective and transparent to all parties involved. Blockchain is typically adopted for capital construction projects and complex contracts. Throughout the project lifecycle, blockchain technology ensure that all parties under contract are collaborating at all levels. Blockchain technology can ensure that all operations are always performed in accordance with the agreed-upon terms and conditions (Pournader et al., 2020; Amico et al., 2023). Finally, blockchain technology eliminates mutual dependence on the central authority. Its decentralization increases the importance of network effects (Kim et al., 2020).

Methodology

This section introduces the methodology used to outline the indicators to evaluate blockchain suitability for the small and medium enterprises construction SCs. Fifteen indicators (three for each category) are the input of the model designed to assess the level of suitability of blockchain as risk mitigator. Considering that the subset of indicators refers to different issues, the decision aiding methodology to define a model that assesses the level of blockchain suitability is a multicriteria procedure known as Electre (Norese & Carbone, 2014).

According to the research background discussed in the previous section, the main risks identified in the construction industry are the following ones. (i) Inefficient communication between the actors involved. (ii) Delay in the project due to SC structure inefficiency. (iii) Delays and lack payments. (iv) Loss of material traceability. Starting from these risks the dimensions in which the indicators can be grouped are defined. Company Data refer to the number of employees, company's turnover, and level of digitization. Payments are described by their reliability, the delay in receiving payments and the methods of payments. Materials are assessed in terms of quality, delivery time and traceability. SC Structure is defined by the number and localization of suppliers and the types of contracts. Finally, the information and document flow is referred to the channels employed to gather documents, archiving system and sources of documents.

These dimensions have the purpose to take into consideration all the worthy elements to evaluate blockchain suitability to mitigate risks. The importance of each dimension and then of each indicator with respect to the

others is expressed using a procedure to define weights. The procedure is the Analytic Hierarchy Process (AHP, see Saaty, 2008) and it is based on pairwise comparisons. The first step of AHP procedure is to define a scale of preference from 1 to 5 where 1 means equality and 5 means maximum preference. 1 = Equality, 2 = Minimum preference, 3 = Medium preference, 4 = Great preference, 5 =Maximum preference.

The second step is to perform the comparison matrix ($m \times n$) with row $i = (1, \dots, m)$ and column $j = (1, \dots, n)$. Such comparison matrix is defined from the pairwise comparison. The comparison matrix has always 1 on the diagonal and it is positive, reciprocal, and consistent. Positive means that $a_{ij} > 0$. Reciprocal means that $a_{ij} = 1/a_{ji}$. Consistent means that $a_{ij} = a_{ik}/a_{jk}$.

Once the comparison matrix is calculated, the third step consist of defining the priority vector that can be described as the normalized eigenvector of the matrix. The procedure chosen to define the priority vector is the so-called eigenvector method where power iterations (Saaty, 2008) are required in order that the algorithm produces a nonzero vector considered a good approximation of the eigenvector corresponding to the greatest eigenvalue of the matrix λ_{max} , called principal eigenvalue. In this way, in the comparison matrix the inconsistency will be distributed among all the elements of the matrix and the columns will be gradually close to proportionality.

When the consistency ratio is close to zero, the priority vector can be declared as the best expression of the weight system that will be used in the Electre Tri method. To evaluate the consistency ratio, the consistency level of the comparison matrix through the computation of the principal eigenvalue must be evaluated. The principal eigenvalue is obtained from the sum of the products between each element of the priority vector and the sum of the columns of the comparison matrix.

According to Saaty (2008), in a consistent reciprocal matrix, the largest eigenvalue is equal to the size of the comparison matrix. Meanwhile, if some inconsistencies are taken into consideration, it is required a measure of consistency using consistency index (CI), where $CI = (\lambda_{max} - n)/(n-1)$ that measures the level of consistency as a deviation from the size of the comparison matrix. The consistency index needs to be compared with the random index that is defined as the result of the average value obtained from 50,000 computation of the consistency ratio of a matrix with the entries above the main diagonal at random from the 17 values $\{1/9, 1/8, \dots, 1, 2, \dots, 8, 9\}$ and the entries below the diagonal by taking reciprocals (Saaty, 2008). In Table 3 the values obtained from one set of simulations for matrices of size 1, 2, ...,15 is illustrated. The result of this comparison is the consistency ratio (CR), where $CR = CI/RI$.

The analysis deals with a 5x5 matrix regarding dimensions while 3x3 concerning indicators, so the Random Index (RI) is 1.11 and 0.52, respectively (see Table 1).

Table 1. Random Index.

	Random Index Values				
Matrix Order	1	2	3	4	5
RI	0.00	0.00	0.52	0.89	1.11
Matrix Order	6	7	8	9	10
RI	1.25	1.35	1.40	1.45	1.49
Matrix Order	11	12	13	14	15
RI	1.52	1.54	1.56	1.58	1.59

When the consistency ratio is lower or equal to 10 percent the inconsistency can be considered acceptable and consequently the priority vector a good approximation of the weight system (Saaty, 2008). This process is employed to define the weight system of dimensions and indicators. In a primary analysis, the indicators' weights were deduced considering that, within the same dimension, they have equal weight one respect to the other. Then, it has been realized that there are some indicators with more importance that the others belonging to the same dimensions and so the AHP process has been performed to define indicators weights.

Model

This section outlines the model and provide the main results obtained from the priority vector of the considered dimensions (company data, payments, materials, SC structure, information, and document flow, see Table 2) as well as the indexes used to evaluate the consistency of the matrix (see Table 3).

Table 2. Priority vector.

Dimensions	Priority Vector	Category Weights
Company Data	0.0665	6.65
Payments	0.1820	18.20
Materials	0.1718	17.18
SC Structure	0.3296	32.96
Information and Document flow	0.2501	25.01

Table 3. Consistency indexes.

Categories	Values
λ_{max}	5.4
N	5
CI	0.1016
RI	1.11
CR	9.15%

The value of the consistency ratio (CR) is lower than 10% and so the priority vector can be considered a good approximation of the weight system (Saaty, 2008). Regarding the dimension’s weight system, it can be observed that “SC structure” is considered the main dimension according to the pairwise comparison executed, so the scores obtain within this dimension are relevant in determining the final category. Meanwhile, “Company data” is considered less important when compared to others. The other three dimensions (Payments, Materials, and Information and Document flow) are almost at the same level of importance in fact none of them is so relevant in the final category definition when compared to the others.

Considering “SC structure” dimension, Table 4 shows the results obtained from the indicators’ priority vector. The indexes used to evaluate the consistency of the matrix are: λ_{max} that is equal to 3.0735, the number of indicators equal to 3, the consistency index equal to 0.03668, the random index equal to 0.52 and the consistency ratio equal to 7.07%. Also in this case, the value of the consistency ratio is lower than 10% for each group of indicators and so the priority vector obtained can be considered a good approximation of the weight system (Saaty, 2008).

Table 4. Priority vector of indicators of the SC Structure dimension.

	Priority Vector	Category Weights
Number of suppliers	0.6144	61.44
Suppliers’ localization	0.1172	11.72
Typologies of contracts stipulated	0.2684	26.84

Regarding the indicators’ weight system, it can be observed that in “SC structure” dimension the prevailing indicator is “Number of suppliers” because blockchain technology is useful with complex SCs. To explain the importance of each category and of each indicator, in relation to the others, the weight system defined according to procedure described has been directly implemented in the Electre Tri model.

Then, to fill the model, a questionnaire is formulated considering the three indicators related to “SC structure” dimension (number of suppliers, suppliers’ localization, and typologies of contracts stipulated). For each indicator a specific question is formulated. Then, all the possible answers (four for each indicator) are quantified with a score from one to four where one corresponds to the situation in which blockchain technology cannot provide an improvement in company’s performance; while four represents the case in which blockchain is useful to mitigate risks and so increase the SC performance. Consequently, each answer considers a one to three value obtaining an overall scale from one to twelve that represents the scoring of the model. For each question, answer (i) gives a score from 1 to 3; answer (ii) from 4 to 6; answer (iii) from 7 to 9 while answer (iv) from 10 to 12.

According to the first indicator – the number of suppliers – the following question is formulated.

How many suppliers are involved in your company's SC?

The possible answers are: (i) less than 10 suppliers. (ii) Between 10 and 30 suppliers. (iii) Between 30 and 50 suppliers. (iv) more than 50 suppliers.

For the second indicator – suppliers’ localization – the question formulated is as follows.

Where are located your company suppliers in relation to your company?

The possible answers are: (i) less than 20 km; (ii) Between 20 and 100 km; (iii) Between 100 and 200 km; (iv) more than 200 km.

Finally, for the third indicator – typologies of contracts stipulated – the related question is the following one.

How often your company use long term contract with your suppliers?

The possible answers are: (i) never; (ii) a small percentage; (iii) the vast majority; (iv) always.

After formulating the questionnaire, in the Electre Tri method, to perform a rating, specific categories must be defined and, consequently, the definition of their profile is needed (Saaty 2008). Four different categories have been settled with their three relative profiles (see Table 5).

Table 5. Profile values.

Profiles	Value
D – C	3.5
C – B	6.5
B – A	9.5

Category A means that blockchain technology is completely useful for small and medium enterprises and is reached when most indicators’ scores suggest a situation that can take great advantages by the implementation of blockchain technology as a risk mitigator. Category B means that blockchain is useful and it indicates that there are several features that can be improved thanks blockchain technology, but it is not guaranteed that the overall process can take advantage from this implementation. In Category C the implementation of blockchain is suggested for small and medium enterprises but is not useful. In fact, this category includes firms for which blockchain can provide some occasional improvements and so it is suggested but considered not suitable to mitigate risks and so improving the SC performance. Finally, Category D means that blockchain is completely useless, thus firms do not benefit by the implementation of this technology.

Results

In this section, two model applications are provided to evaluate the process implemented in two real companies operating in the construction sector and differently categorized. The former (Alpha) can be considered a small enterprise while the latter one (Beta) is medium-sized company. The two companies are both located in the same area and so their SCs are facing similar issues.

Company Alpha can be classified as a small enterprise since the number of employees is higher than 10 and the turnover is slightly higher than 2 million. Moreover, the level of digitalisation of the company does not put in place significative initiatives thus, Alpha cannot be considered a digitized firm. Payments are received often on time while the materials flow in some cases is not completely transparent. The SC structure is characterized by several suppliers higher than fifty and almost all the contracts are based on long term relations. The suppliers are all located within 100 km with respect to the firm. Finally, the documents and information sources are received both in paper and in digital form, thus the archiving system is quite well organized.

Table 6 shows the model results for company Alpha. According to the model proposed in this study, the final category obtained is C: “Blockchain suggested but not useful”. The overall result is highly influenced by the “Company data”, “Payments” and “Information and Documents flow” dimensions.

Company Beta is a medium enterprise since the number of employees is greater than 50 and the turnover is more than 10 million. Until now, the level of digitization is quite low. The payments are usually reliable but when the company operates as a subcontractor there some cases in which the payment is not guaranteed. However, the payments are almost never received on time.

Table 6. Company Alpha model results.

Dimensions	Indicators	Weights		λ -cutting level	Category profile
		Dimensions	Indicator		
Company data	Number of employees	6.65	0.95	3.99	C
	Turnover		1.9		
	Level of digitalization		3.8		
Payment	Reliability	18.2	2.97	10.92	C
	Delay in receiving payments		9.82		
	Methods of payments		5.4		
Materials	Quality	32.95	2.01	10.3	A
	Delivery time		4.60		
	Traceability		10.55		
SC structure	Number of suppliers	17.17	20.24	19.77	A
	Suppliers' localization		3.86		
	Typologies of contracts stipulated		8.84		
Information and document flow	Channels used to gather documents	25.01	3.49	15.01	C
	Archiving system		13.20		
	Sources of documents		8.31		

Regarding materials, they are received often according to project requirements and ISO standard. Meanwhile, sometimes materials arrive later with respect to the project timing. Regarding the SC structure, the number of suppliers is around 50 and most contracts are established on long term dealings. Usually, suppliers are located 250 km from company Beta. Finally, regarding information and documents flow, the archiving system need improvement since the number of documents are huge. Table 7 shows the model results for company Beta and the final category registered is Category B "Blockchain useful". The overall result is influenced by the fact that the dimensions with the highest weight scores B.

The results obtained leave room to several insights. If companies obtain as a result for which the blockchain technology is not recommended or useless, there is the possibility to perform a deep dive analysis by understanding what the areas are where the implementation of this technology is not suggested. In fact, results show if there is a particular area where the implementation can provide an increase in SC performance

In the case of company Alpha, despite its final category is C, "materials" and "SC structure" dimensions reached category A showing that for these two dimensions blockchain technology is completely useful. It means that blockchain technology could improve materials traceability, quality, and the delivery time with respect to the company requirements. Moreover, blockchain technology can be useful since it can improve the optimum number and localisation of suppliers as well as the typology of contracts stipulated with them. The other three dimensions (company data, payment and information and document flow) have reached as final category C showing that blockchain technology is suggested but not useful for the company.

In the case of company Beta, "company data" and "information and document flow" dimensions reached category C. Also in this case, blockchain technology can be suggested but not useful for the company, especially in evaluating the sources and the channels to gathering documents and information as well as the quantities of documents and information shared. On the contrary, "payment", "materials" and "SC structure" dimensions show that blockchain is useful specifically by evaluating the reliability of the different payments methods and if payments are subject to delays. Finally, blockchain technology can be useful in improving SC indicators as well as quality, traceability, and delivery time of materials.

Table 7. Company beta model results

Dimensions	Indicators	Weights		λ -cutting level	Category profile
		Dimensions	Indicator		
Company data	Number of employees		0.95		
	Turnover	6.65	1.9	3.99	C
	Level of digitalization		3.8		
Payment	Reliability		2.97		
	Delay in receiving payments	18.2	9.82	10.92	B
	Methods of payments		5.41		
Materials	Quality		2.01		
	Delivery time	32.95	4.61	10.3	B
	Traceability		10.55		
SC structure	Number of suppliers		20.24		
	Suppliers' localization	17.17	3.86	19.77	B
	Typologies of contracts stipulated		8.84		
Information and document flow	Channels used to gather documents		3.49		
	Archiving system	25.01	13.2	15.01	C
	Sources of documents		8.31		

Conclusions and Future Research Paths

This paper focused on the definition of the main issues related to construction supply chain by investigating the main risks that small and medium enterprises have to face at supply chain level. Moreover, this paper explored the implementation of blockchain technology as risk mitigator for small and medium enterprises' supply chains in the construction industry.

The methodology adopted consists of a literature review and a quantitative model based on Electre Tri multicriteria analysis method. The main outcomes of the literature review showed that construction supply chain faces several issues generated at the interfaces between the various activities, for example design, engineering vendor's interfaces, as well as commissioning and operation interfaces.

The model performed in this paper aimed to assess the blockchain suitability as risk mitigator. This model was applied to two real companies, namely Alpha and Beta. Company Alpha is a small firm while company Beta a medium one. The model is based on a questionnaire – and then the related answers – built on a list of indicators (number of employees, turnover, level of digitalization, payments' reliability, delay in receiving payments, payments methods, quality, delivery time and traceability of materials, number and localization of suppliers, typologies of contracts stipulated with suppliers, channels used to gather documents and information, archiving system document and sources). Moreover, the model is built on a system of weights that represents the importance of each dimension (company data, payments, materials, supply chain structure, information and document flow). Then, a rating procedure was assessed where four categories has been defined: category A means that blockchain technology is completely useful; category B that blockchain is useful; category C that the technology is recommended but not useful and finally category D where blockchain technology is considered completely useless.

Findings show that for company Alpha blockchain technology is suggested but not useful because company data, payment and information and documentation flow dimensions obtained weights associated with profile category “C”. Regarding company Beta, the final category obtained is “B”, thus blockchain technology is considered useful for the company.

The model adopted in this study is an effective tool that allows small and medium enterprises to evaluate if the blockchain technology could act as risk mitigator and so improve firms’ supply chain performance. As future research paths, other studies could enhance the number of indicators considered in the model. Moreover, other research could consider different industries in which blockchain technology can be implemented, for example the apparel or transport sectors.

References

- Afraz, M. F., Bhatti, S. H., Ferraris, A., & Couturier, J. (2021). The impact of supply chain innovation on competitive advantage in the construction industry: Evidence from a moderated multi-mediation model. *Technological Forecasting and Social Change*, 162, 120370.
- Al-Werikat, G. (2017). Supply chain management in construction. *International Journal of Scientific and Technological Research*, 6(3), 106-110.
- Amico C., Cigolini R., & Franceschetto S. (2022a). Supply chain resilience in the European football industry: the impact of Covid-19. *Proceedings of the Summer School Francesco Turco*.
- Amico, C., Cigolini, R., & Franceschetto S. (2022b). Using blockchain to mitigate supply chain risks in the construction industry. *Proceedings of the Summer School Francesco Turco*.
- Amico, C., & Cigolini, R. (2023). Improving port supply chain through blockchain-based bills of lading: a quantitative approach and a case study. *Maritime Economics and Logistics*, <https://doi.org/10.1057/s41278-023-00256-y>
- Cannas, V., Ciccullo, F., Cigolini, R., & Pero, M. (2020). Sustainable innovation in the dairy supply chain: enabling factors for intermodal transportation. *International Journal of Production Research*, 58(24), 7314-7333.
- Cigolini, R., Gosling, J., Iyer, A., & Senicheva, O. (2022a). Supply chain management in construction and engineer-to-order industries. *Production Planning and Control*, 33(9-10), 803-810.
- Cigolini, R., Franceschetto, S., & Sianesi A. (2022b). Shop floor control in the VLSI circuit manufacturing: a simulation approach and a case study. *International Journal of Production Research*, 60(18), 5450–5467.
- Del Rosso Calache, L. D., Galo, N. R., & Ribeiro Carpinetti, L. C. (2018). A group decision approach for supplier categorization based on hesitant fuzzy and Electre Tri. *International Journal of Production Economics*, 202,182-196.
- Difrancesco, R. M., Meena, P., & Kumar, G. (2022). How blockchain technology improves sustainable supply chain processes: a practical guide. *Operations Management Research*, 1-22.
- Ferreira de Araújo Lima, P., Marcelino-Sadaba, S., & Verbano, C. (2021). Successful implementation of project risk management in small and medium enterprises: a cross-case analysis. *International Journal of Managing Projects in Business*, 14(4), 1023-1045.
- Franceschetto S., Amico C., Cigolini R. (2022). The ‘new normal’ in the automotive supply chain after Covid”. *Proceedings of the Summer School Francesco Turco*.
- Franceschetto, S., Amico, C., Brambilla, M., & Cigolini R. (2023). Improving supply chain in the automotive industry with the right bill of material configuration. *IEEE Engineering Management Review*.
- Gosling, J., Pero, M., Schoenwitz, M., Towill, D., & Cigolini, R. (2016). Defining and categorizing modules in building projects: an international perspective. *Journal of Construction Engineering and Management*, 142(11).
- Harouache, A., Chen, G. K., Sarpin, N. B., Hamawandy, N. M., Jaf, R. A., Qader, K. S., & Azzat, R. S. (2021). Importance of green supply chain management in Algerian construction industry towards sustainable. *Journal of Contemporary Issues in Business and Government*, 27(1), 1055-1070.
- Kim, K., Lee, G., & Kim, S. (2020). A study on the application of blockchain technology in the construction industry. *KSCE Journal of Civil Engineering*, 24 (9), 2561-2571.
- Koskela, L., Vrijhoef, R., & Dana Broft, R. (2020). Construction supply chain management through a lean lens. *Successful Construction Supply Chain Management: Concepts and Case Studies*, 109-125.
- Layaq, M. W., Goudz, A., Noche, B., & Atif, M. (2019). Blockchain technology as a risk mitigation tool in supply chain. *International Journal of Transportation Engineering and Technology*, 5(3), 50-59.

- Mafundu, R. H., & Mafini, C. (2019). Internal constraints to business performance in black-owned small to medium enterprises in the construction industry. *The Southern African Journal of Entrepreneurship and Small Business Management*, 11(1), 1-10.
- Nanayakkara, S., Perera, S., Senaratne, S., Weerasuriya, G. T., & Bandara, H. M. N. D. (2021). Blockchain and smart contracts: A solution for payment issues in construction supply chains. *In Informatics*, 8(2), 36.
- Norese, M. F., & Carbone, V. (2014). An application of Electre Tri to support innovation. *Journal of Multi-Criteria Decision Analysis*, 21 (1-2), 77-93.
- Papadopoulos, G. A., Zamer, N., Gayalis, S. P., & Tatsiopoulou, I. P. (2016). Supply chain improvement in construction industry. *Universal Journal of Management*, 4(10), 528-534.
- Pero, M., Rossi, M., Xu, J., & Cigolini, R. (2020). Designing supplier networks in global product development. *International Journal of Product Lifecycle Management*, 13(2), 115-139.
- Pero, M., Sianesi, A., & Cigolini, R. (2016). Reinforcing supply chain security through organizational and cultural tools within the intermodal rail and road industry. *International Journal of Logistics Management*, 27(3), 816-836.
- Pournader, M., Kach, A., & Talluri, S. (2020). A review of the existing and emerging topics in the supply chain risk management literature. *Decision Sciences*, 51(4), 867-919.
- Pozzi, R., Pero, M., Cigolini, R., Zaglio, F., & Rossi, T. (2019). Using simulation to reshape the maintenance systems of caster segments. *International Journal of Industrial and Systems Engineering*, 33(1), 75-96.
- Rossi, T., Pozzi, R., Pero, M., & Cigolini, R. (2017). Improving production planning through finite-capacity MRP. *International Journal of Production Research*, 55(2), 377-391.
- Rossi, T., Pozzi, R., Pirovano, G., Cigolini, R., & Pero, M. (2020). A new logistics model for increasing economic sustainability of perishable food supply chains through intermodal transportation. *International Journal of Logistics Research and Applications*, 24(4), 346-363.
- Saaty, T.L. (2008). Decision making with the analytic hierarchy process. *International Journal Services Sciences*, 1(1), 83-98.
- Shemov, G., Garcia de Soto, B., & Alkhzaimi, H. (2020). Blockchain applied to the construction supply chain: A case study with threat model. *Frontiers of Engineering Management*, 7(4), 564-577.
- Xu, J., Abdelkafi, N., & Pero, M. (2020). On the impact of blockchain technology on business models and supply chain management. *Proceedings of the Summer School Francesco Turco*.

Author Information

Clarissa Amico

Politecnico di Milano
Department of Management, Economics, and Industrial
Engineering, Politecnico di Milano
Via Lambruschini, 4/B, 20156 Milano – Italy
Contact e-mail: clarissavaleria.amico@polimi.it

Roberto Cigolini

Politecnico di Milano
Department of Management, Economics, and Industrial
Engineering, Politecnico di Milano
Via Lambruschini, 4/B, 20156 Milano – Italy

To cite this article:

Amico, C. & Cigolini, R. (2023). A quantitative blockchain-based model for construction supply chain risk management. *The Eurasia Proceedings of Science, Technology, Engineering & Mathematics (EPSTEM)*, 23, 59-68.

The Eurasia Proceedings of Science, Technology, Engineering & Mathematics (EPSTEM), 2023

Volume 23, Pages 69-84

ICRETS2023: International Conference on Research in Engineering, Technology and Science

Comparative Experimental and Theoretical Study on the Structure of Potassium 2,4-Hexadienoate: Structure-Activity Relationship

Manel Taferguennit

University of Sciences and Technology Houari Boumediene

Noura Kichou

University of Mouloud Mammeri of Tizi-Ouzou

Zakia Hank

University of Sciences and Technology Houari Boumediene

Abstract: For the first time, a density functional theory (DFT) study was conducted on the structure of a well-known antibacterial agent namely potassium 2,4-Hexadienoate, in order to elucidate its vibrational, electronic and reactivity proprieties. Structure optimization was performed using three common hybrid functionals (DFT/B3LYP-D3; DFT/M05-2X and DFT/M06-2X) to identify the suitable functional. Geometric parameters, IR and UV-vis spectra were well reproduced when using DFT/M06-2X with 6-311(d)G+ basis set ($R^2 = 0.99913$). The assimilation of IR frequencies has been achieved using potential energy distribution (PED) analysis at M06-2X/6-311(d) G + level. Time-dependent density functional theory (TD-DFT) and natural bond orbital (NBO) analysis were realized to identify the excited states of 2,4-Hexadienoate anion in the liquid phase, using the solute electron density solvation model (SMD). Moreover, reactive sites in the molecule were localized by molecular electrostatic potential (MEP) analysis. Highest Occupied Molecular Orbitals (HOMO), lowest Unoccupied Molecular Orbitals (LUMO) and energy gap (HOMO-LUMO gap), were used to calculate global reactivity descriptors (GRDs), according to the frontier molecular orbitals (FMO) theory, the resulting values were analyzed to explore the chemical reactivity of the molecule and elucidate the structure-activity relationship.

Keywords: Sorbate, DFT, HOMO-LUMO gap, NBO, Antimicrobial activity.

Introduction

Organic molecules are becoming widespread for practical applications in pharmaceutical fields (Salami & Shokri, 2021). Those molecules exist in the environment in the form of low molecular weight, small chain molecules, containing both carbon and hydrogen, and often other elements like oxygen, such as in organic acids (Strathmann & Myneni, 2004), (Reichle, 2020). Initially, organic acids are compounds that occur naturally from animal and plants sources. They are classified according to four characteristics: (1) carbon chain nature (cyclic, acyclic, alicyclic, and heterocyclic); (2) saturated or unsaturated chain; (3) the existence or inexistence of substituents; and (4) the number of carboxyl moiety (mono, di- or tri-carboxylic) (Chahardoli et al., 2020).

Previous research revealed the impressive effectiveness of organic acids such as benzoic acids, parabens, sorbic acid and their salts (i.e., sorbates, benzoates, propionates) against many microbial species including bacterial strains, yeast and molds (Baldevraj & Jagadish, 2011). Nowadays, sorbates are the 3rd most important group of antimicrobial food and pharmaceutical preservatives, after parabens and benzoates, whose safety has been discussed by recent publications (Mackowiak-Dryka et al., 2015; Piper, 2018). Although the antibacterial mechanism of sorbate is fully defined, its biological activity is often associated with its chemical structure

- This is an Open Access article distributed under the terms of the Creative Commons Attribution-Noncommercial 4.0 Unported License, permitting all non-commercial use, distribution, and reproduction in any medium, provided the original work is properly cited.

- Selection and peer-review under responsibility of the Organizing Committee of the Conference

© 2023 Published by ISRES Publishing: www.isres.org

(Davidson, 2005). The carboxyl group and the conjugated double bonds in this molecule are highly reactive (Davidson, 2005). In *Escherichia coli*, the mechanism of action of potassium sorbate consists of binding to enzymes related to the glycolysis metabolism, the Krebs cycle, and electron active transport (Santesteban-López et al., 2009) such as Enolase, Aspartase, Catalase, and Malate Dehydrogenase., by blocking their active sites, the assimilation of important substrates is thus decreased, causing the inhibition of *Escherichia coli* growth and its death (Santesteban-López et al., 2009). Computational approaches have received great attention in understanding the relationship between chemical structure and biological activity of studied compounds, commonly called Structure-Activity Relationship (SAR) (Guerrero-Perilla et al., 2015), (Kalhotra et al., 2018).

SAR analysis can be employed to develop more effective and targeted bioactive molecules by improving them and analyzing the various ways in which they binds to a receptor (James, 2022). There are numerous computational techniques that can identify the SAR, including physicochemical properties determination and drug-receptor interaction analysis using molecular docking. The physicochemical properties are computed to investigate one of the most common biological property i.e., “the bioavailability” in order to understand the Structure-Activity Relationship (SAR) (James, 2022), (D’Souza et al., 2009). In another hand, molecular docking predicts the position of a ligand, as an inhibitor of the target protein in its binding site, as well as the accurate estimation of the binding strength and the number and the nature of the involved interactions. It worth mentioning docking results accuracy is highly dependent to preparation conditions such as optimization of the structure of both of the ligand and the protein (Zaater et al., 2016). Based on the literature survey, no study was carried out applying computational methods to explain the antibacterial activity of sorbates.

Therefore, the current study is focused on the use of computational calculations to elucidate the structure-activity relationship in the case of potassium sorbate. Theoretical calculations, by means of DFT/B3LYP approach, were initially carried out in order to prepare the structure to molecular docking. Three common density theory functionals i.e., *B3LYP-D3*, *M05-2X* and *M06-2X* were tested, the calculated data were compared to the experimental data, the optimized structure with the appropriate functional was chosen to provide further structural characteristics such as molecular descriptors, highest occupied molecular orbital, molecular electrostatic potential mapping and chemical reactivity. The optimized structure of potassium sorbate was docked in the binding site of glycolytic metalloenzyme “Enolase” from *E. coli* (PDB: 6BFZ (Bank, 1971.)), all the involved interactions with the target protein residues were visualized. Furthermore, In here, physicochemical properties are predicted in silico using SwissADME server (Daina et al., 2017).

Method

For the purpose of the analysis, a Jasco FTIR 6000 Series Spectrometer recorded FT-IR spectra ($4000-400\text{ cm}^{-1}$) using potassium bromide pallet. A Jasco V-700 Series UV-VIS/NIR Spectrophotometer measured the electronic spectra from 200 to 800nm. Theoretical calculations of the structure of the sorbate molecule were realized using *Gaussian 09* program package (Liang et al, 2009), by the employment of three common density theory functionals: *B3LYP-D3* (Grimme et al., 2011), *M05-2X* (Dimić et al., 2018) and *M06-2X* (Zhao & Truhlar, 2008). The GaussView program v5.0.8 was employed to display the input files. After the verification of the absence of imaginary frequencies, the optimized structure of sorbate with the appropriate functional is ready to be docked into the target protein. Enolase metalloenzyme was chosen as a target protein. Its crystal structure of into the active site of glycolytic metalloenzyme “Enolase” from *E. coli* (PDB: 6BFZ (Bank, 1971)) was retrieved from protein data bank (PDB) (Kleeb, 2015).

Molecular docking was done using Molecular Operating Environment (MOE) 2015.10 software (Chemical Computing Group, Montreal, Canada, 2015). The structure of the Enolase was prepared with MOE QuikPrep tool at default parameters, where the co-crystallized ligand and all water molecules that are farther than 4.5 \AA from the enzyme were removed, except the co-factor Mg(II), all necessary hydrogen atoms were added to the structure, followed by its energy optimization. The prepared Enolase enzyme structure and the optimized sorbate were subject to a number of docking runs. The best binding conformation was selected based by following to “standard” docking solutions considered as typical in docking analysis i.e., (1) the minimal binding energy, that reflects the best docking pose, (2) the lowest with lowest root mean square deviation (RMSD) value that validate the docking process (Angelova et al., 2017), (Alomari, 2018).

A protein-ligand interactions diagram was constructed based on the best binding pose, using Ligand interactions entry in MOE software. The interactions were detected in the maximum distance of 4.5 \AA ; between heavy atoms of the ligand and the receptor residues (Angelova et al., 2017), and their nature was identified according to the diagram legend given in Ligand interactions entry. The ability of molecules to produce biological effect is

dependent on the impact of various physicochemical properties of the bioactive molecule on the protein with which it interacts (ALGHAMDI et al., 2020). In here, physicochemical properties are predicted in silico using SwissADME server (Daina et al., 2017).

Results and Discussion

Optimization of the Molecular Structure

In order to define the most appropriate functional for the optimization, different density functional theory hybrids were used, including *DFT/B3LYP-D3* (Grimme et al., 2011), *DFT/M05-2X* (Dimić et al., 2018) and *DFT/M06-2X* (Zhao & Truhlar, 2008) with *6-311+G(d)* basis set (Grimme et al., 2011). Analogous association has been used to provide a good description of similar molecular systems and to reproduce their spectra (Mehandzhyski et al., 2015), (Sert et al., 2015). Before optimization, the BSEE counterpoise correction method was used to adjust the interaction energies between the potassium cation and the sorbate anion (Mehta & Goerigk, 2021). The structure of the compound was optimized without any structural constraints and the inexistence of negative frequencies values proved that the obtained structure was in the minima energy state.

Optimized structure parameters (bond lengths, bond and dihedral angles) were compared with the experimental corresponding values and illustrated in Table 1. Due to unavailability of experimental data, the main structural parameters of the present compound have been compared to similar systems with solved crystal structures. (Schlitter & Beck, 1996). The structure and the atom numbering of potassium sorbate is reported in Figure 1.

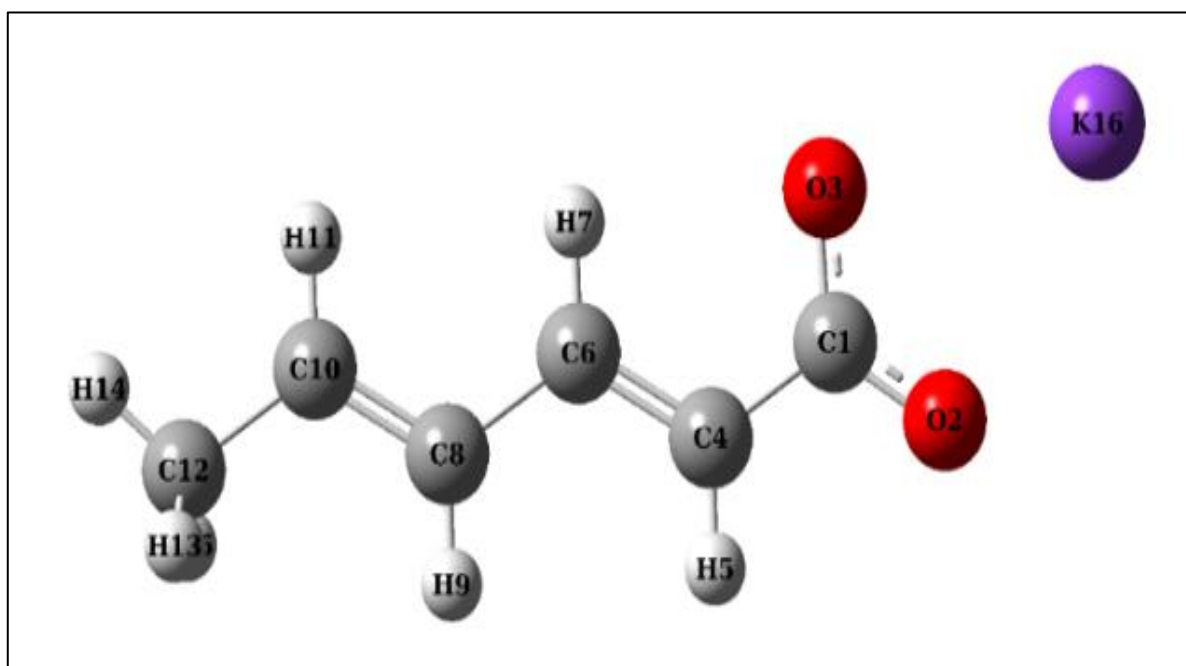


Figure 1. Molecular structure of potassium sorbate.

As the optimization was done in the gas phase, the optimized structure parameters calculated by the three functionals are shown to be either slightly longer or shorter than the experimental values obtained in solid phase (Sert, Singer, et al., 2014). From Table 1, it can be seen that the C-C bond lengths of C4-C6 and C8-C10 calculated with *B3LYP-D3*, *M05-2X* and *M06-2X* levels, were restricted in the range 1.335-1.342 Å, characterizing the C-C double bond lengths, which was found around 1.318 Å experimentally. In the carboxylate group of the title molecule, the calculated C1-O3 and C1-O2 bond lengths were found at 1.270 Å (*B3LYP-D3*), 1.263 Å (*M05-2X*) and 1.262 Å (*M06-2X*), these bond lengths were experimentally found to be 1.261 Å as to O2-C1-O3 bond angle was computed at 124.01° (*B3LYP-D3*), 124.22° (*M05-2X*) and 124.35° (*M06-2X*). These bond angles were experimentally found to be 123.3°. Although, the calculated C-H bond lengths of CH₃ group, ranging from 1.088 to 1.097 Å, are slightly far from the experimental values, H-C-H bond angle computed values are quietly close to experimental values.

Table1. Computed structural parameters for potassium sorbate

	B3LYP-D3/ 6-311(d) G+	M05-2X/ 6-311(d) G+	M06-2X/ 6-311(d) G+	*Experimental
Bond lengths (Å)				
C1-O2	1.270	1.263	1.262	1.261
C1-O3	1.271	1.263	1.262	1.267
C1-C4	1.494	1.493	1.498	1.480
C4-C6	1.342	1.335	1.336	1.318
C4-H5	1.087	1.083	1.086	0.96
C6-H7	1.088	1.084	1.088	1.00
C6-C8	1.449	1.454	1.455	1.436
C8-H9	1.090	1.086	1.089	0.93
C8-C10	1.342	1.335	1.336	1.302
C10-H11	1.090	1.086	1.089	0.90
C10-C12	1.498	1.495	1.496	1.486
C12-H13	1.094	1.088	1.094	0.90
C12-H14	1.097	1.091	1.094	1.01
C12-H15	1.097	1.091	1.091	1.00
Bond angles (°)				
O2-C1-O3	124.01	124.22	124.35	123.3
C1 -C4-C6	123.19	122.24	122.33	124.3
C4-C6-C8	124.36	124.02	124.24	126.2
C6-C8-C10	124.04	123.47	123.72	126.7
C8-C10-C12	124.90	124.75	124.95	127.7
C1-C4-H5	115.84	115.98	115.99	110.3
C4-C6-H7	117.75	117.87	117.77	117.3
C6-C8-H9	116.95	117.05	123.72	114
C8-C10-H11	118.38	118.41	118.34	118
H11-C10-C12	116.71	116.83	116.69	114
C10-C12-H14	111.27	111.00	111.09	110
H14-C12-H13	108.12	108.27	106.73	108
H14-C12-H15	106.46	106.86	108.18	113
H15-C12-H13	108.12	108.28	108.18	108
Dihedral angle (°)				
O3-C1-C4-C6	179.99	179.99	179.99	168.6
O3-C1-C4-H5	0	0	0	10.9
O2-C1-C4-H5	179.99	179.99	180.00	169.1
O2-C1-C4-C6	0	0	0	11.4
C1-C4-C6-H7	0	0	0	2
H5-C4-C6-H7	179.99	179.99	179.99	178
H5-C4-C6-C8	0	0	0	0
C1-C4-C6-C8	179.99	179.99	179.99	179.0
C4-C6-C8-H9	0	0	0	3
C4-C6-C8-C10	179.99	179.99	179.99	175.8
C6-C8-C10-H11	0	0	0	4
H7-C6-C8-H9	180.0	179.99	180.00	179
H7-C6-C8-C10	0	0	0	2
C6-C8-C10-C12	179.99	179.99	179.99	179.6

*Lithium sorbate data given in ref (Schlitter & Beck, 1996)

Vibrational Spectral Analysis

The IR data of fundamentals modes in the potassium sorbate molecule were computed at *B3LYP-D3*, *M05-2X* and *M06-2X* levels and listed in Table 2. All the vibrational assignments have been made using the *VEDA* software package, which uses potential energy distribution (PED) analysis for the estimation of normal modes percentage in each frequency (Dimić et al., 2018). The calculated vibrational frequencies have been scaled and all the calculations (vibrational wavenumbers, optimized geometric) were compared with the experimental corresponding results, in order to identify the most suitable functional has been identified.

Table 2. Experimental and computed IR frequencies of potassium sorbate.

Vib. no	Assignment (PED [*] %)	Calc.freq			Exp.freq
		B3LYP-D3 6-311(d)G+ 0.966 (CCCBDB Listing of Precalculated Vibrational Scaling Factors, 2022)	M05-2X 6-311 (d) G+ 0.9483(Sut ton et al., 2015)	M06-2X 6-311 (d)G+ 0.9567 (Ünal et al., 2021)	
v ₁	v CH (80%) in C10-H11 + v CH (15%) in C8-H9	3017 m	3028 m	3026 m	3014 m
v ₂	v _{asym} CH(100%) in CH3	2933 w	2954 w	2963 w	2919 w
v ₃	v _{sym} CH (83%) in CH3	2897 w	2911 w	2911 w	2850 w
v ₄	v _{sym} C=C (56%) in C8-C10 + v _{asym} CC (10%) in C6-C4	1653 m	1670 m	1679 m	1648 m
v ₅	v _{asym} C=C (64%) in C6-C4 + v _{sym} CC (10%) in C8-C10	1616 m	1628 m	1638 m	1618 s
v ₆	v _{asym} (85%) in O3-C1-O2	1505 s	1534 s	1562 s	1555 s
v ₇	β _{asym} HCH (90%) in CH3	1445 m	1438m	1435 m	1435 m
v ₈	v _{sym} (72%) in O3-C1-O2	1354 s	1387 s	1398 s	1387 s
v ₉	β _{asym} HCC (46%) in H5-C4-C1 + β CCC(18%) in C6-C8-C10	1269 m	1259 m	1259 m	1277 m
v ₁₀	β _{asym} HCC (79%) in H5-C4-C1	1237 w	1244 w	1233 w	1208 w
v ₁₁	v C-C (51%) in C6-C8 + β CCC (13%) in C6-C8-C10+β _{asym} HCC (10%) in H5-C4-C1	1181 w	1192 w	1186 w	1148 w
v ₁₂	τ HCCO (86%) in H5-C4-C1-O2	1039 s	1056 s	1052 s	1006 s
v ₁₃	β _{asym} HCC (12%) in H5-C4-C1 + v CC (53%) in C1-C4 + τ HCCC (10%) in H14-C12-C10-C8	978 m	1000 m	997 m	962 m
v ₁₄	v CC (28%) in C10-C12 +τ HCCC (26%) in H14-C12-C10-C8 + v CC (16%) in C4-C1	938 vw	948 w	941 w	952 w
v ₁₅	τ HCCO (60%) in H5-C4-C1-C2 + γ COOC (16%) in C4-O2-O3-C1	919 vw	940 m	937m	884 m
v ₁₆	τ HCCC (54%) in H11-C10-C8-C6 + τ HCCC (11%) in H13-C12-C10-C8 + γ COOC (22%) in C4-O2-O3-C1	831 vw	849 w	845 w	808 w
v ₁₇	τ HCCC (17%) in H11-C10-C8-C6 + τ CCCC (10%) in C1-C4-C6-C8	734 w	748 w	745 w	734 w
v ₁₈	β OCO (71%) in O2-C1-O3 + γ COOC (48%) in C4-O2-O3-C1	733 m	752 m	751 m	708 m
v ₁₉	β CCO (68%) in C4-C1-O3	588 m	594 m	592 m	577 m

v: stretching; β: in-plane bending; γ: out-of-plane bending; τ : torsion; as—asymmetric, sym—symmetric s: strong; m:medium; w: weak; vw: very weak, *Potential energy distribution (PED), less than 10%are not shown.

Since, the vibrational frequencies were calculated in the gas phase and the experimental values were obtained in solid phase, a difference was noticed between the theoretical and experimental frequencies, more precisely at high frequencies (above 1500 cm⁻¹). The high theoretical frequencies were therefore multiplied by a scaling factor to better fit the experimental results, this method has been frequently used by several researchers namely Jamrózet *al*(Jamróz & Dobrowolski, 2001), Kose(Kose, 2016)and Sert et *al*(Sert et al., 2015),(Sert, Singer, et al., 2014). The experimental FT-IR spectrum of the potassium sorbate was compared to the theoretical spectra and represented in Figure 2, Figure 3 and Figure 4 as well as the correlation graph that describes the agreement between the computed and experimental wavenumbers.

The resulting calculated and experimental wavenumber relationships are linearly related, the relationships are expressed by the following equation:

$$v_{\text{Cal}} = 1.00043 v_{\text{exp}} - 8.59377 \text{ for } B3LYP-D3 \text{ method}$$

$$v_{\text{Cal}} = 0.83242 v_{\text{exp}} - 211.1698 \text{ for } M05-2X \text{ method}$$

$$v_{\text{Cal}} = 1.00409 v_{\text{exp}} - 18.7901 \text{ for } M06-2X \text{ method}$$

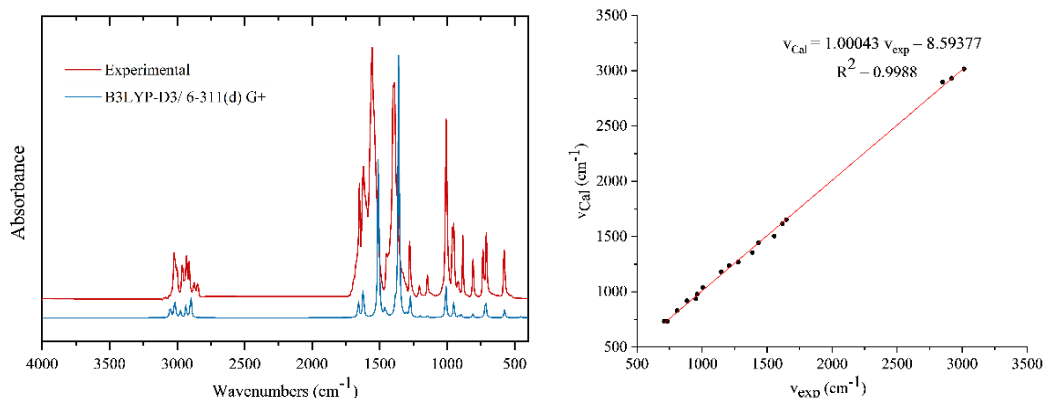


Figure 1. Comparison between experimental and computed vibrations with B3LYP-D3/6-311(d)G+

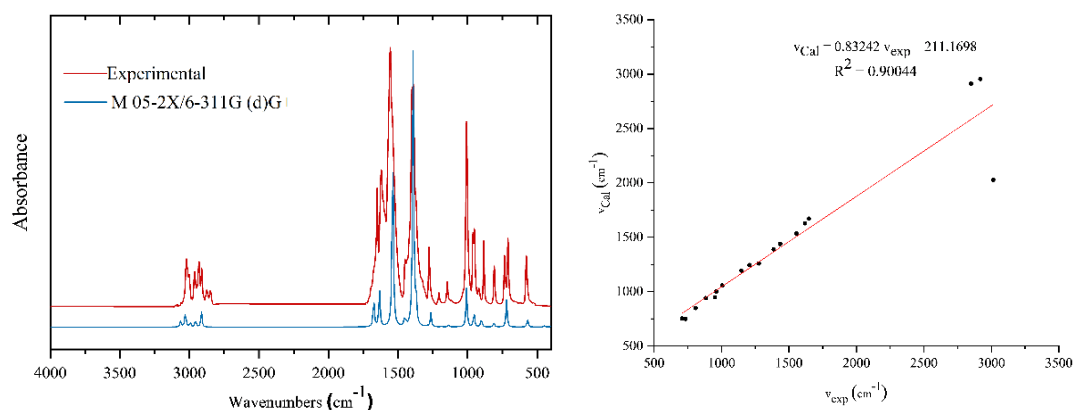


Figure 3. Comparison between experimental and computed vibrations with M05-2X/6-311(d)G+

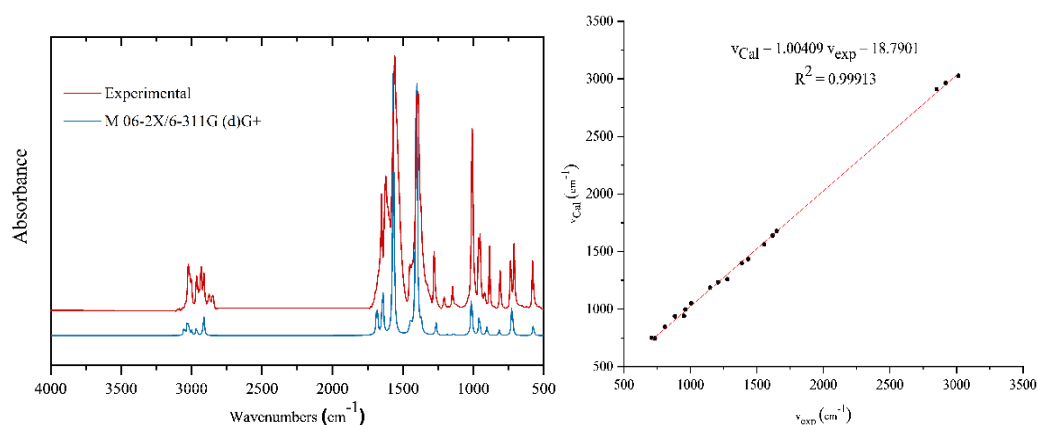


Figure 4. Comparison between experimental and computed vibrations with M06-2X/6-311(d)G+

The coefficient of correlation R^2 values ($R^2 = 0.9988$ for *B3LYP-D3*), ($R^2 = 0.90044$ for *M05-2X*) and ($R^2 = 0.99913$ for *M06-2X*) between the computed and experimental wavenumbers values. As it can be clearly seen, the calculated data describe an excellent correlation with the corresponding experimental data when using *M06-2X* functional.

UV-vis Spectral Analysis

The electronic spectrum of potassium sorbate in water shows a strong peak at 254 nm, corresponding to one transition from the ground state of the sorbate molecule to an excited state. The time-dependent density functional theory (TD-DFT (Hamrani et al., 2021)) calculations were conducted at *M06-2X/6-311(d) G + level*, in order to identify the number and contributions of the molecular orbitals involved in the electronic transitions, the theoretical data were extracted using the Gauss-Sum 2.2 program (Halim & Ibrahim, 2021a) and tabulated in Table 3. It worth noting that the solute electron density solvation model (SMD (Sutton et al., 2015)) was applied in the calculations considering possible interactions between the solvent molecules and the sorbate anion, that affect the electronic spectrum.

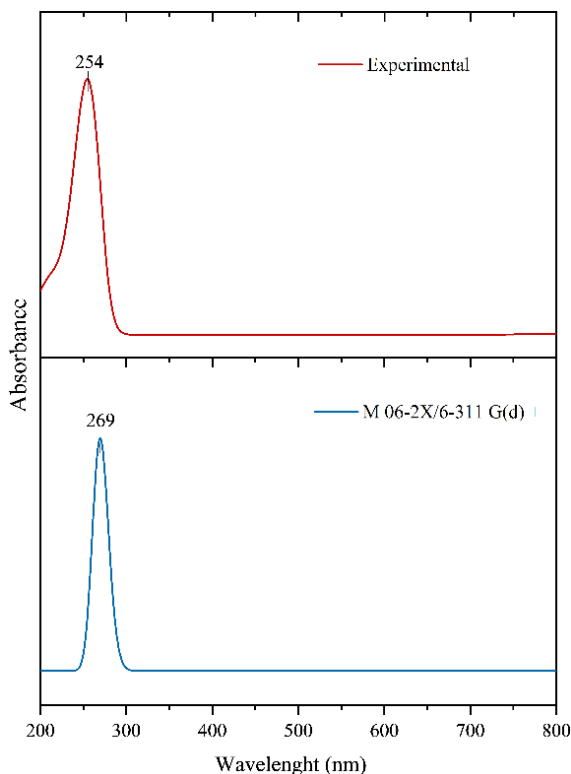


Figure 5. Comparison between experimental and calculated UV-Vis spectra

Table3. Experimental and computed spectroscopic parameter of sorbate anion.

Observed Transition	Observed λ_{\max} (nm)	Calculated λ_{\max} (nm)	Oscillatory Strength f (a.u)	No.OM	Contributing Molecular orbital (%)
1	254	269	0.9319	30,31	HOMO \rightarrow LUMO (97%)
2	--	271	0.0001	28,31	HOMO - 2 \rightarrow LUMO (98%)
3	--	302	0.0	29,31	HOMO - 1 \rightarrow LUMO (97%)

The TD-DFT calculations are in a good agreement with the experimental data, by anticipating an intense electronic transition at 269 nm with an oscillator strength $f = 0.9319$ nearly equal to 1. Two more transitions were predicted, with oscillator strength values close to zero indicating low intensities, which explains their non-appearances in the electronic spectrum.

The molecular orbitals contributing in the electronic transitions (HOMO) and (LUMO), as well as (HOMO - 1) and (HOMO - 2) along with their calculated energies were representing in Figure 6, where the positive zone is red and the negative zone is green (Halim & Ibrahim, 2021a).

From Figure 6, it can be seen that the HOMO which represents the highest occupied molecular orbital, was mainly situated on the π -bonding of the two oxygens contained in the carboxyl moiety, as well as on the π -bonding of the double bound carbons. Whereas, the LUMO which represents the highest excited state has an electron density mainly localized on the two oxygens of the carboxyl group, identified by π^* -antibonding of C1-O3, C1-O2 bonds. This brief analysis suggests that the observed transition on the UV-Vis spectrum may corresponds to the transition from the π -bonding of the HOMO to the π^* -anti-bonding of the LUMO, an NBO analysis must be done to confirm that.

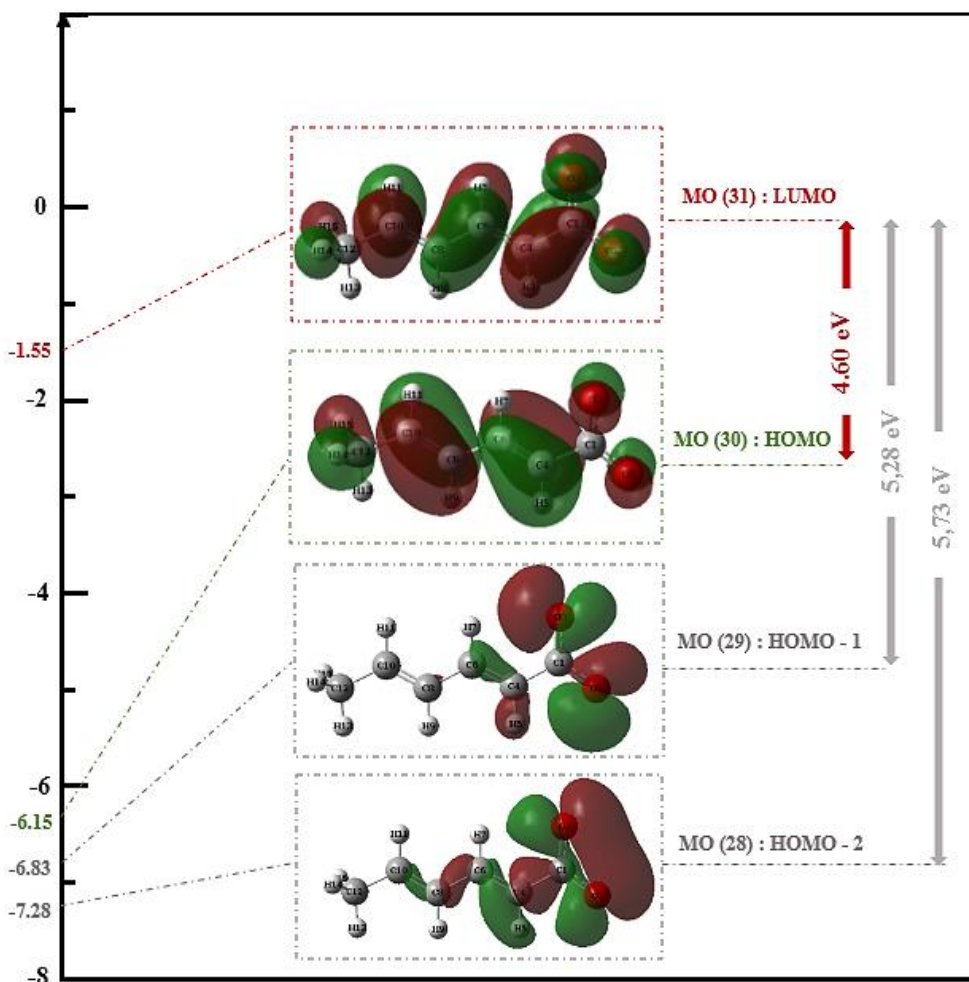


Figure 6. 3D plot molecular orbitals and their energies of transition

Natural Bond Orbital (NBO) Analysis

NBO analysis was conducted at *M06-2X/6-311(d) G+* in order to confirm the nature of observed transitions in the theoretical UV-Vis Spectrum. NBO analysis is based on the electron density delocalization from the occupied Lewis-type (donor) natural bond orbitals to unoccupied non-Lewis-type (acceptor) natural bond orbitals. According to the second order Fock matrix in NBO analysis (Devi et al., 2018), the correlation between donor (i), acceptor (j) level bonds and stabilization energy $E(2)$ [donor (i) \rightarrow acceptor (j)] is expressed as follows (Devi et al., 2018):

$$E(2) = \Delta E_{ij} = q_i \frac{(F_{ij})^2}{(E_j - E_i)} \dots (1) \text{ (Devi et al., 2018)}$$

Where, q_i : occupancy of donor orbital; E_i and E_j : diagonal elements; F_{ij} : off diagonal NBO Fock matrix element. In here, several donor/acceptor interactions were identified for the sorbate anion. The major intramolecular transitions and their stabilization energies $E(2)$ are tabulated in descending order in Table 4.

According to the literature, the higher stabilization energy $E(2)$ value, more intense is the interaction between electron donors and acceptors (Devi et al., 2018; Kerru et al., 2019). The highest stabilization energy for sorbate anion was noticed for the intramolecular transition the π (C4 – C6) bond to the π^* (C8 – C10) anti-bonds with stabilization energy $19.80 \text{ Kcal mol}^{-1}$, which indicate the probable intramolecular interaction in HOMO-LUMO transition. Thus, the suggestion proposed using UV-Vis analysis were successfully confirmed.

Other intramolecular charge transfers happen from A charge transfer is also seen from π (C8 - C10) to π^* (C4 – C6) and with stabilization energy $12.85 \text{ Kcal mol}^{-1}$. It worth noting that lower stabilization energies were observed with 5.59, 5.29 and 5.27 Kcal/mol, corresponding to transitions from σ (C10 – H11), σ (C8 - H9) and σ (C6 - H7) bonds to σ^* (C8 - H9), σ^* (C10 - H11) and σ^* (C4 - H5) bonds, respectively.

Table 4. Experimental and computed spectroscopic parameter values of sorbate anion.

Donor (i)	Type	Acceptor (j)	Type	E (2)(Kcal/mol)	E(j) - E(i) (a.u)	F(i,j) (a.u)
C 4 – C 6	π	C 8 - C 10	π^*	19.80	0.28	0.066
O2	n	C 1 - O3	π^*	19.77	0.71	0.107
O3	n	C1 - C 4	π^*	15.60	0.60	0.087
O2	n	C 1 – C4	π^*	13.85	0.61	0.082
C 4 - C 6	π	C 1 - O 2	π^*	13.00	0.29	0.060
C 8 - C 10	π	C4-C6	π^*	12.85	0.34	0.059
C 1 - O 2	π	C4-C6	π^*	6.80	0.33	0.043
C 10 – H 11	σ	C 8 - H 9	σ^*	5.59	0.93	0.064
C 8 - H 9	σ	C 10 - H 11	σ^*	5.29	0.92	0.062
C 6 - H 7	σ	C 4 - H 5	σ^*	5.27	0.93	0.063
C 1 - C 4	σ	C 6 - C 8	σ^*	4.68	1.09	0.064
C 6 - H 7	σ	C 8 - H 9	σ^*	3.92	0.89	0.053
C 6 - C 8	σ	C 10 - C 12	σ^*	3.84	1.05	0.057
C 12 - H 13	σ	C 10 - H 11	σ^*	3.77	0.93	0.053
C 10 - C 12	σ	C 6 - C 8	σ^*	3.63	1.16	0.058

n : lone pair or nonbonding orbital ; π : pi-bonding orbital ; σ : sigma- bonding orbital ; π^* : pi-antibonding orbital ; σ^* : sigma-antibonding orbital

Molecular Electrostatic Potential (MEP) Analysis

One of the most interesting characteristics of quantum chemistry is the capacity to anticipate the reactive sites in the molecule using the MEP surface (Devi et al., 2018), which plot the charge distribution of the molecules in three dimensions (Devi et al., 2018), this charge can be used to determine electrophilic, nucleophilic sites (Devi et al., 2018). In the MEP map, the potential varies between -0.256 a.u and 0.256 a.u and enhance in the order of red < orange < yellow < green < blue (Devi et al., 2018), (Halim & Ibrahim, 2021b), where blue indicates the most attractive sites and red the most repulsive sites (Halim & Ibrahim, 2021b). In another words, the red region (negative electrostatic potential) represents the electrophilic attack, while the blue region (positive electrostatic potential) represents the nucleophilic attack (Halim & Ibrahim, 2021b). For the sorbate anion, molecular electrostatic potential (MEP) 3D surfaces were obtained at *M06-2X/6-311 (d) G+* level and represented in Figure 7.

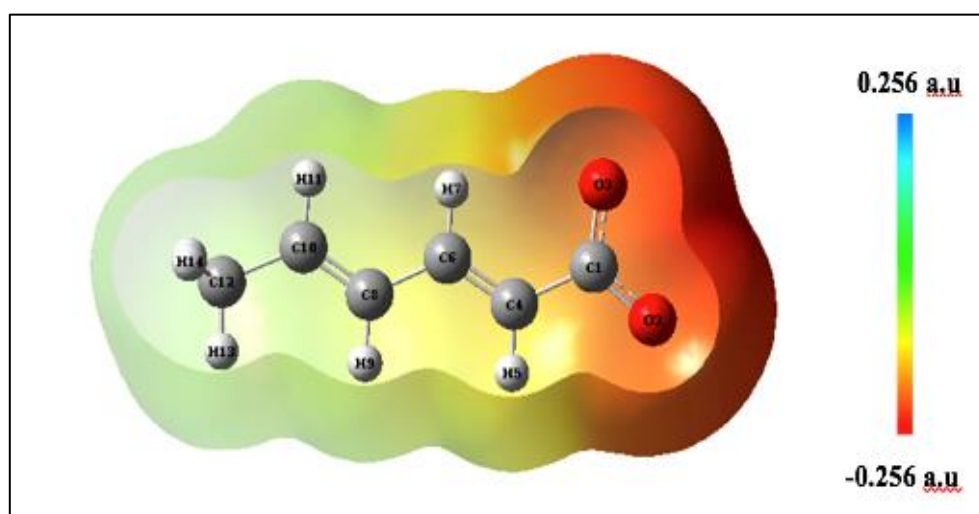


Figure 7. MEP map of the optimized structure of sorbate anion

The red region located on the oxygen atoms O2 and O3 represents the most negative electrostatic potential region with the following values -0.216 to -0.23 a.u. Thus, the oxygens O2 and O3 having the strongest repulsion and are the most expected sites to be attacked. Additionally, the negative orange and yellow regions (C 8 - C 10) and (C 4 – C 6) are related to electrophilic reactivity (Halim & Ibrahim, 2021b). These investigations are useful to provide information about the reactivity of the molecule for further studies.

Global Reactivity Descriptors (GRDs)

GRDs such as ionization potential (IP), electron affinity (EA), electronegativity (χ), chemical potential (μ), chemical hardness (η) and the electrophilicity index (ω) (Saravanamoorthy et al., 2021), are important for the reactivity investigation of molecular systems (Zaater et al., 2016). These parameters can be calculated from the HOMO- LUMO orbitals values according to Parr and Pearson (Parr & Pearson, 1983) and employing the following equations (1-6) given in ref (Devi et al., 2018), (Pearson, 1986), (Yang & Parr, 1985). The global reactivity descriptors of potassium sorbate were calculated, and their values were summarized in Table 5.

$$IP = -E_{HOMO} \dots (1)$$

$$EA = -E_{LUMO} \dots (2)$$

$$\chi = -\frac{1}{2}(E_{LUMO} + E_{HOMO}) \dots (3)$$

$$\mu = -\chi = \frac{1}{2}(E_{LUMO} + E_{HOMO}) \dots (4)$$

$$\eta = \frac{1}{2}(E_{LUMO} - E_{HOMO}) \dots (5)$$

$$s = \frac{1}{2\eta} \dots (6)$$

$$\omega = \frac{\mu^2}{2\eta} \dots (7)$$

Table 5 .Global reactivity descriptors of the optimized structure of potassium sorbate

Global reactivity descriptors	Values (eV)
HOMO–LUMO band gap (E gap)	4.60
HOMO energy (E_{HOMO})	-6.15
LUMO energy (E_{LUMO})	-1.55
Ionization potential (IP)	6.15
Electron affinity (EA)	1.55
Electronegativity (χ)	2.3
Chemical potential (μ)	-2.3
Chemical hardness (η)	2.3
Chemical softness (s)	0.23
Electrophilicity index (ω)	1.15

As mentioned in Figure 6, the HOMO and LUMO are predicted to be equal to -6.15 eV and -1.55 eV, respectively. The difference HOMO-LUMO energy gap (E_{gap}) is equal to 4.60 eV directly related to the chemical reactivity of the molecule (Sert, Balakit, et al., 2014); It reflects the capacity for charge transfer interactions to occur within the molecule (Nemes et al., 2020). In the literature, a low band gap energy (< 5 eV) suggests a high chemical reactivity (Saravanamoorthy et al., 2021), which is often responsible of the bioactivity of molecules, since it facilitated the charge transfers between the molecules and the proteins (Zaater et al., 2016).

The ionization energy value implies that an energy value of 6.15 eV is needed to withdraw an electron from the HOMO (Fathima Rizwana et al., 2019). In another hand, the lower value of electron affinity (1.55 eV) displays that the molecule can easily accept electrons, these values are also reflecting the biological activity of the title compound (Ait Ramdane et al., 2021).

Structure–Activity Relationship

Molecular Docking

Enolase is a glycolytic metalloenzyme implicated in carbon metabolism. The interest in targeting enolase is in its essential role in a number of biological processes, such as cell wall formation and RNA synthesis, as well as its role as a plasma cell receptor. Validating the antibacterial potential of candidate molecule is done by examining carefully the position and character of chelating moieties for stronger interaction with metal ions and enolase active site residues (Krucinska et al., 2019).

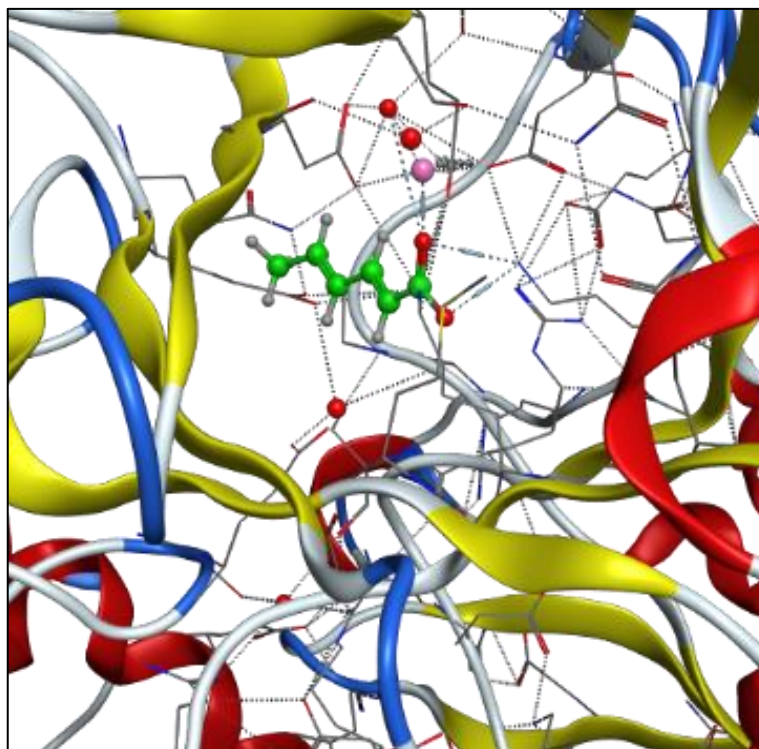


Figure 8. 3D representation of the best binding pose

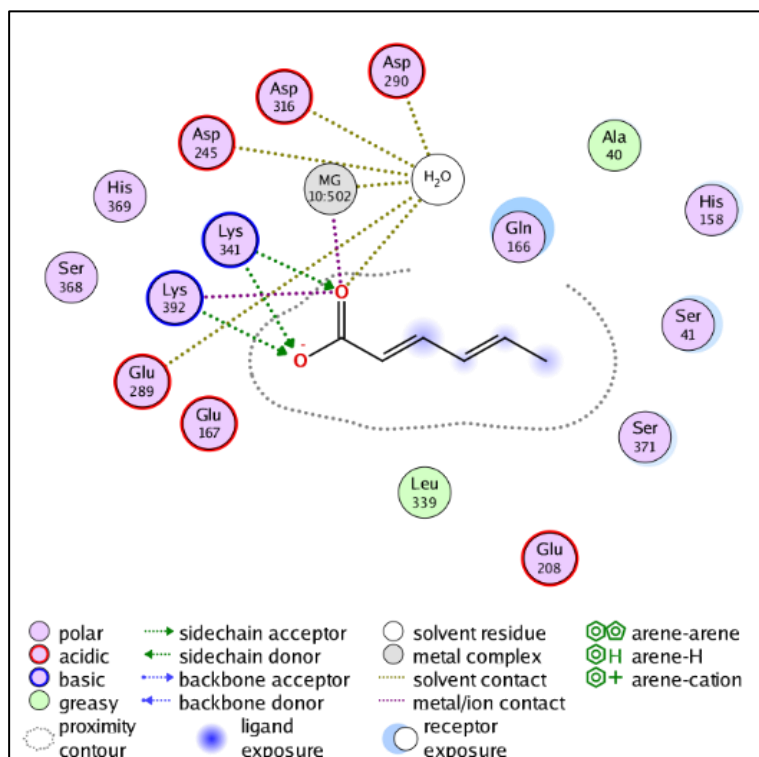


Figure 9. 2D representation of the best binding pose

The docking of sorbate anion in the active site of enolase (Figure 8 and 9) shows that the molecule interacts with Mg(II) cation through an electrostatic interaction. It also interacts with the residues Lys341 and Lys391, and with Asp245, Asp316 and Asp 290 through H₂O. These numerous interactions explained the quite high value of the binding energy (6.3 Kcal/mol). The results displayed clearly that the carboxylate group in the sorbate anion molecule is the one that interacts in the binding site of enolase, as supported by previous theoretical calculations this group is the more chemically reactive, and molecular docking analysis proved in here that this group is responsible for the biological activity of sorbate.

In Silico ADME Analysis

The most popular method used for defining the drug-likeness is the prediction of six physicochemical properties like lipophilicity, size, hydrogen-bonding etc. In here, those parameters were conducted using SwissADME server and summarized in Table 6.

Table 6. Physicochemical descriptors predicted by SwissADME server

Physicochemical property	Physicochemical descriptors	Sorbate anion
Lipophilicity	Log P	0.86
	H-bond donors	0
Hydrogen bonds	H-bond acceptors	2
Molecular weight	MW (g.mol ⁻¹)	111.12
Flexibility	Rotatable bonds	2
Polarity	TPSA (Å ²)	40.13
Solubility	Log S	-1.23
Saturation	Fraction of C sp ³	0.17

According to Lipinski's rule of five, the compounds with a logP (octanol–water partition coefficient) ≤ 5 possesses a good lipophilicity, which induce a significant permeability in the cellular plasma membrane (Turner & Agatonovic-Kustrin, 2007), (Winiwarter et al., 2007). In here sorbate anion has a low lipophilicity, as seen from Table 6, attesting of a good cell permeability favoring the permeation through the lipid layers of the bacterial membranes (Riswan Ahamed et al., 2014).

The existence of many hydrogen bonds can increase diffusion of a drug across cell membranes, and further, the ability to establish important interactions with the protein targets (Coimbra et al., 2020), In the other hand, too many hydrogen bond donors/acceptors can cause a decrease of the affinity toward the lipid membrane (Coimbra et al., 2020), In that regard, the rule of five attests that a number of hydrogen bond donor lower than five and hydrogen bond acceptors (N and O atoms) lower than 10 are favorable for a good bioavailable molecule (Winiwarter et al., 2007), which is the case of the sorbate anion.

Molecular weight is widely applied to separate molecules with important bioavailability from those with less. In fact, compounds with molecular weight greater than 500 g.mol⁻¹ are considered as poor bioavailable. However, there are recent reports suggesting that compounds with a molecular weight higher than 500 g.mol⁻¹ and meet the two criteria of : (1) ten or fewer rotatable bonds (flexibility) and (2) topologic polar surface area (TPSA) equal to or less than 140 (Å²) will have a high probability of good bioavailability (Df et al., 2002), In our case, it is clear that the sorbate anion tends to fulfil those two criteria, despite its low molecular weight (111.12 g.mol⁻¹).

Sufficient aqueous solubility is an essential requirement for small molecule to interfere the bacterial cell , and improving the aqueous solubility of bioactive compounds is often a major problem for medicinal chemists (Ishikawa, 2022). Fortunately, the sorbate anion possesses a high solubility ($-6 \leq \text{Log S}$ (Daina et al., 2017)). Figure 9 represents the bioavailability radar generated by SwissADME, it can be clearly seen that the sorbate anion is in the optimum range of bioavailable molecule (red area).

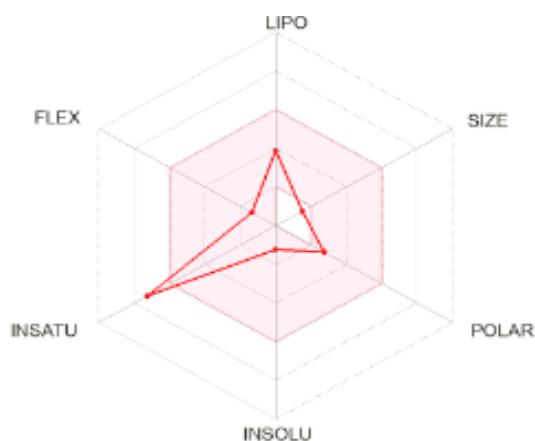


Figure 9. Bioavailability radar of sorbate provided by SwissADME

Conclusion

In this investigation, the geometry of the potassium sorbate was optimized with three functionals: *B3LYP-D3*, *M05-2X* and *M06-2X* using 6-311 (d) G+ basis set. The theoretical results were compared to the corresponding experimental results and a considerable level of correlation has been noticed when using DFT/M06-2X with 6-311+G(d) basis set ($R^2 = 0.99913$). TD-DFT approach was conducted on the optimized structure of the sorbate anion, in order to explore its probable electronic transitions, UV-vis spectrum showed one transition at 269 nm, which matched perfectly with the experimental spectrum and corresponded to the transition of electrons from HOMO to LUMO orbitals. According NBO analysis, the π -orbitals and π^* - orbitals contained in HOMO and LUMO molecular orbitals are in the origin of the transition observed in UV-Vis spectrum. Molecular electrostatic potential (MEP) revealed that electrophilic sites are found around the oxygen atoms of the carboxylate moiety in the sorbate anion. The HOMO, LUMO and HOMO-LUMO gap values were -6.15 eV, -1.55 eV and 4.60 eV, respectively, and the global reactivity descriptors (GRDs) demonstrated that the charge is transferred easily within the sorbate molecule, which confirmed again its high reactivity. Molecular docking of sorbate anion supports the fact that the expected reactive group i.e., carboxylate group is responsible of the biological activity of sorbate, by interacting with Mg(II) and amino- acids residues of Enolase enzyme. The computational ADME properties were predicted and summarized via the SwissADME computational tool and the results were supporting the structure-activity relationship of the sorbate anion for the aspect of antibacterial activity.

Recommendations

The findings of this study revealed the structure-activity relationship between the structure of sorbate anion and its biological activity, and will greatly help for further investigation on the sorbate molecule.

Scientific Ethics Declaration

The authors declare that the scientific ethical and legal responsibility of this article published in EPSTEM journal belongs to the authors.

Acknowledgements or Notes

*This article was presented as a poster presentation at the International Conference on Research in Engineering, Technology and Science (www.icrets.net) held in Budapest/Hungary on July 06-09, 2023.

References

- Ait Ramdane, K., Terbouche, A., Ait Ramdane-Terbouche, C., Lakhdari, H., Bachari, K., Merazig, H., Roisnel, T., Hauchard, D., & Mezaoui, D. (2021). Crystal structure, characterization and chemical reactivity of novel piperazine derivative ligand for electrochemical recognition of nitrite anion. *Journal of Chemical Sciences*, 133(1), 18.
- Alghamdi, A. A., Alam, M. M., & Nazreen, S. (2020). In silico ADME predictions and in vitro antibacterial evaluation of 2-hydroxy benzothiazole-based 1,3,4-oxadiazole derivatives. *Turkish Journal of Chemistry*, 44(4), 1068–1084.
- Alomari, A. (2018). *Biophysical and kinetic analysis of escherichia coli DNA ligase activity and inhibition*. (Doctoral dissertation, University of Portsmouth).
- Angelova, V. T., Valcheva, V., Pencheva, T., Voynikov, Y., Vassilev, N., Mihaylova, R., Momekov, G., & Shivachev, B. (2017). Synthesis, antimycobacterial activity and docking study of 2-aryl-[1]benzopyrano[4,3-c]pyrazol-4(1H)-one derivatives and related hydrazide-hydrazones. *Bioorganic & Medicinal Chemistry Letters*, 27(13), 2996–3002.
- Baldevraj, R. S. M., & Jagadish, R. S. (2011). 14—Incorporation of chemical antimicrobial agents into polymeric films for food packaging. In J.-M. Lagarón (Ed.), *Multifunctional and Nanoreinforced Polymers for Food Packaging* (pp. 368–420). Woodhead Publishing.
- Bank, R. P. D. (1971). *RCSB PDB - 6BFZ: Crystal structure of enolase from E. coli with a mixture of apo form, substrate, and product form*. Retrieved June 29, 2023, from <https://www.rcsb.org/structure/6BFZ>

- CCCBDB listing of precalculated vibrational scaling factors. (2022). Retrieved October 10, 2021, from <https://cccbdb.nist.gov/vibscalejust.asp>
- Chahardoli, A., Jalilian, F., Memariani, Z., Farzaei, M. H., & Shokoohinia, Y. (2020). Chapter 26—Analysis of organic acids. In A. Sanches Silva, S. F. Nabavi, M. Saeedi, & S. M. Nabavi (Eds.), *Recent Advances in Natural Products Analysis* (pp. 767–823). Elsevier.
- Chemical Computing Group, Montreal, Canada. (2015). *Molecular Operating Environment (MOE)*. <http://www.chemcomp.com>
- Coimbra, J. T. S., Feghali, R., Ribeiro, R. P., Ramos, M. J., & Fernandes, P. A. (2020). The importance of intramolecular hydrogen bonds on the translocation of the small drug piracetam through a lipid bilayer. *RSC Advances*, 11(2), 899–908.
- Daina, A., Michielin, O., & Zoete, V. (2017). SwissADME: A free web tool to evaluate pharmacokinetics, drug-likeness and medicinal chemistry friendliness of small molecules. *Scientific Reports*, 7(1), Article 1.
- Davidson, P. M. (2005). *Antimicrobials in food* (3rd ed.). Taylor & Francis Group.
- Devi, P., Fatma, S., Bishnoi, A., Srivastava, K., Shukla, S., & Kumar, R. (2018). Synthesis, spectroscopic and DFT studies of novel 4-(morpholinomethyl)-5-oxo-1-phenylpyrrolidine-3-carboxylic acid. *Journal of Molecular Structure*, 1157, 551–559.
- Df, V., Sr, J., Hy, C., Br, S., Kw, W., & Kd, K. (2002). Molecular properties that influence the oral bioavailability of drug candidates. *Journal of Medicinal Chemistry*, 45(12).
- Dimić, D., Milenković, D., Ilić, J., Šmit, B., Amić, A., Marković, Z., & Dimitrić Marković, J. (2018). Experimental and theoretical elucidation of structural and antioxidant properties of vanillylmandelic acid and its carboxylate anion. *Spectrochimica Acta Part A: Molecular and Biomolecular Spectroscopy*, 198, 61–70.
- D'Souza, M. J., Koyoshi, F., & Everett, L. M. (2009). Structure activity relationships (SARs) using a structurally diverse drug database: Validating success of predictor tools. *Pharmaceutical Reviews*, 7(5), <https://web.archive.org/web/20100125114948/http://www.pharmainfo.net/reviews/structure-activity-relationships-sars-using-structurally-diverse-drug-database-validating-su>.
- Fathima Rizwana, B., Christian Prasana, J., Muthu, S., & Susan Abraham, C. (2019). Spectroscopic (FT-IR, FT-Raman, NMR) investigation on 2-[(2-amino-6-oxo-6,9-dihydro-3H-purin-9-yl)methoxy]ethyl(2S)-2-amino-3-methylbutanoate by density functional theory. *Materials Today: Proceedings*, 18, 1770–1782.
- Grimme, S., Ehrlich, S., & Goerigk, L. (2011). Effect of the damping function in dispersion corrected density functional theory. *Journal of Computational Chemistry*, 32(7), 1456–1465.
- Guerrero-Perilla, C., Bernal, F. A., & Coy-Barrera, E. D. (2015). Molecular docking study of naturally occurring compounds as inhibitors of N-myristoyl transferase towards antifungal agents discovery. *Revista Colombiana de Ciencias Químico Farmacéuticas*, 44(2), 162–178.
- Halim, S. A., & Ibrahim, M. A. (2021a). Synthesis, FT-IR, structural, thermochemical, electronic absorption spectral, and NLO analysis of the novel 10-methoxy-10 H -furo[3,2- g]chromeno[2,3- b][1,3]thiazolo[5,4- e]pyridine-2,10(3 H)-dione (MFCTP): A DFT/TD-DFT study. *RSC Advances*, 11(51), 32047–32066.
- Halim, S. A., & Ibrahim, M. A. (2021b). Synthesis, FT-IR, structural, thermochemical, electronic absorption spectral, and NLO analysis of the novel 10-methoxy-10 H -furo[3,2- g]chromeno[2,3- b][1,3]thiazolo[5,4- e]pyridine-2,10(3 H)-dione (MFCTP): A DFT/TD-DFT study. *RSC Advances*, 11(51), 32047–32066.
- Hamrani, O., Amina, Z., Boutamine, S., Taïri-Kellou, S., & Hank, Z. (2021). Structure-properties relationship of Cu (II) – paracetamol based complex. density functional theory and spectroscopic studies. *Novel Approaches in Drug Designing & Development*, 5(4), 555667.
- Ishikawa, M. (2022). [Improvement in aqueous solubility of bioactive molecules by decreasing intermolecular interaction]. *Yakugaku Zasshi: Journal of the Pharmaceutical Society of Japan*, 142(4), 365–379.
- James, H. (2022). Structural activity relationship of drugs and its applications. *Journal of Pharmacological Reports*, 6(2), 1–1.
- Jamróz, M. H., & Dobrowolski, J. Cz. (2001). Potential energy distribution (PED) analysis of DFT calculated IR spectra of the most stable Li, Na, and Cu(I) diformate molecules. *Journal of Molecular Structure*, 565–566, 475–480.
- Kalhotra, P., Chitpepu, V. C. S. R., Osorio-Revilla, G., & Gallardo-Velázquez, T. (2018). Structure–activity relationship and molecular docking of natural product library reveal chrysin as a novel dipeptidyl peptidase-4 (dpp-4) inhibitor: An integrated in silico and in vitro study. *Molecules*, 23(6), Article 6.
- Kerru, N., Gummidi, L., Bhaskaruni, S. V. H. S., Maddila, S. N., Singh, P., & Jonnalagadda, S. B. (2019). A comparison between observed and DFT calculations on structure of 5-(4-chlorophenyl)-2-amino-1,3,4-thiadiazole. *Scientific Reports*, 9(1), 19280.
- Kleeb, S. (2015). *Crystal structure of FimH in complex with 3'-Chloro-4'-(alpha-D-mannopyranosyloxy)-biphenyl-4-carbonitrile*. Retrieved September 20, 2022, from <https://www.rcsb.org/structure/4CST>

- Kose, E. (2016). The spectroscopic analysis of 2,4'-dibromoacetophenone molecule by using quantum chemical calculations. *Anadolu University Journal of Science and Technology A - Applied Sciences and Engineering*, 17(AFG5 SPECIAL ISSUE), 677–677.
- Krucinska, J., Falcone, E., Erlandsen, H., Hazeen, A., Lombardo, M. N., Estrada, A., Robinson, V. L., Anderson, A. C., & Wright, D. L. (2019). Structural and functional studies of bacterial enolase, a potential target against gram-negative pathogens. *Biochemistry*, 58(9), 1188–1197.
- Liang, M., Hada, M., Ehara, K., Toyota, R., Fukuda, J., Hasegawa, M., Ishida, T., Nakajima, Y., Honda, O., Kitao, H., Nakai, T., Vreven, K., Throssell, J. A., Montgomery, Jr., J. E., Peralta, F., Ogliaro, M., Bearpark, J. J., Heyd, E., Brothers, K. N., Kudin, V. N., Staroverov, T., Keith, R., Kobayashi, J., Normand, K., Raghavachari, A., Rendell, J. C., Burant, S. S., Iyengar, J., Tomasi, M., Cossi, J. M., Millam, M., Klene, C., Adamo, R., Cammi, J. W., Ochterski, R. L., Martin, K., Morokuma, O., Farkas, J. B., Foresman, D. J., & Wallingford CT. (2009). *Gaussian 09* (Revision A.02) Gaussian, Inc., [Computer software].
- Mackowiak-Dryka, M., Paszkiewicz, W., & Drozd, L. (2015). Parabens: Food preservatives and consumer safety. *Medycyna Weterynaryjna*, 71, 553–556.
- Mehandzhiyski, A. Y., Riccardi, E., van Erp, T. S., Koch, H., Åstrand, P.-O., Trinh, T. T., & Grimes, B. A. (2015). Density functional theory study on the interactions of metal ions with long chain deprotonated carboxylic acids. *The Journal of Physical Chemistry A*, 119(40), 10195–10203.
- Mehta, N., & Goerigk, L. (2021). Assessing the applicability of the geometric counterpoise correction in B2PLYP/Double- ζ calculations for thermochemistry, kinetics, and noncovalent interactions*. *Australian Journal of Chemistry*.
- Nemes, D., Kovács, R., Nagy, F., Tóth, Z., Herczegh, P., Borbás, A., Kelemen, V., Pfliegler, W. P., Rebenku, I., Hajdu, P. B., Fehér, P., Ujhelyi, Z., Fenyvesi, F., Váradi, J., Vecsernyés, M., & Bácskay, I. (2020). Comparative biocompatibility and antimicrobial studies of sorbic acid derivatives. *European Journal of Pharmaceutical Sciences*, 143, 105162.
- Parr, R. G., & Pearson, R. G. (1983). Absolute hardness: Companion parameter to absolute electronegativity. *Journal of the American Chemical Society*, 105(26), 7512–7516.
- Pearson, R. G. (1986). Absolute electronegativity and hardness correlated with molecular orbital theory. *Proceedings of the National Academy of Sciences*, 83(22), 8440–8441.
- Piper, P. W. (2018). Potential Safety Issues Surrounding the Use of Benzoate Preservatives. *Beverages*, 4(2).
- Reichle, D. E. (2020). Chapter 2—The physical and chemical bases of energy. In D. E. Reichle (Ed.), *The Global Carbon Cycle and Climate Change* (pp. 5–14). Elsevier.
- Riswan Ahamed, M. A., Azarudeen, R. S., & Kani, N. M. (2014). Antimicrobial applications of transition metal complexes of benzothiazole based terpolymer: Synthesis, characterization, and effect on bacterial and fungal strains. *Bioinorganic Chemistry and Applications*, 2014, 1–16.
- Salami, N., & Shokri, A. (2021). Chapter 5—Electronic structure of solids and molecules. In M. Ghaedi (Ed.), *Interface Science and Technology*, 32, 325–373. Elsevier.
- Santiesteban-López, N. A., Rosales, M., Palou, E., & López-Malo, A. (2009). Growth response of *Escherichia coli* ATCC 35218 adapted to several concentrations of sodium benzoate and potassium sorbate. *Journal of Food Protection*, 72(11), 2301–2307.
- Saravanamoorthy, S. N., Vasanthi, B., & Poornima, R. (2021). *Molecular geometry, vibrational spectroscopic, molecular orbital and Mulliken charge analysis of 4-(carboxyamino)-benzoic acid: Molecular docking and DFT calculations*. file:///C:/Users/pc/Downloads/preprints202107.0215.v1.pdf
- Savjani, K. T., Gajjar, A. K., & Savjani, J. K. (2012). Drug solubility: Importance and enhancement techniques. *ISRN Pharmaceutics*, 2012, 195727.
- Schlitter, S. M., & Beck, H. P. (1996). Crystal structure, solid-state polymerization, and ionic conductivity of alkali salts of unsaturated carboxylic acids, 4. investigations on lithium sorbate. *Chemische Berichte*, 129(12), 1561–1564.
- Sert, Y., Balakit, A. A., Öztürk, N., Uçun, F., & El-Hiti, G. A. (2014). Experimental (FT-IR, NMR and UV) and theoretical (M06-2X and DFT) investigation, and frequency estimation analyses on (E)-3-(4-bromo-5-methylthiophen-2-yl)acrylonitrile. *Spectrochimica Acta Part A: Molecular and Biomolecular Spectroscopy*, 131, 502–511.
- Sert, Y., Puttaraju, K. B., Keskinoglu, S., Shivashankar, K., & Uçun, F. (2015). FT-IR and Raman vibrational analysis, B3LYP and M06-2X simulations of 4-bromomethyl-6-tert-butyl-2H-chromen-2-one. *Journal of Molecular Structure*, 1079, 194–202.
- Sert, Y., Singer, L. M., Findlater, M., Doğan, H., & Çırak, Ç. (2014). Vibrational frequency analysis, FT-IR, DFT and M06-2X studies on tert-Butyl N-(thiophen-2-yl)carbamate. *Spectrochimica Acta Part A: Molecular and Biomolecular Spectroscopy*, 128, 46–53.

- Strathmann, T. J., & Myneni, S. C. B. (2004). Speciation of aqueous Ni(II)-carboxylate and Ni(II)-fulvic acid solutions: Combined ATR-FTIR and XAFS analysis. *Geochimica et Cosmochimica Acta*, 68, 3441–3458.
- Sutton, C. C. R., Franks, G. V., & da Silva, G. (2015). Modeling the antisymmetric and symmetric stretching vibrational modes of aqueous carboxylate anions. *Spectrochimica Acta Part A: Molecular and Biomolecular Spectroscopy*, 134, 535–542.
- Turner, J. V., & Agatonovic-Kustrin, S. (2007). 5.29—In silico prediction of oral bioavailability. In J. B. Taylor & D. J. Triggle (Eds.), *Comprehensive Medicinal Chemistry II* (pp. 699–724). Elsevier.
- Ünal, Y., Nassif, W., Özeydin, B. C., & Sayin, K. (2021). Scale factor database for the vibration frequencies calculated in M06-2X, one of the DFT methods. *Vibrational Spectroscopy*, 112, 103189.
- Winiwarter, S., Ridderström, M., Ungell, A.-L., Andersson, T. B., & Zamora, I. (2007). Use of molecular descriptors for absorption, distribution, metabolism, and excretion predictions. In J. B. Taylor & D. J. Triggle (Eds.), *Comprehensive Medicinal Chemistry II* (pp. 531–554). Elsevier.
- Yang, W., & Parr, R. G. (1985). Hardness, softness, and the Fukui function in the electronic theory of metals and catalysis. *Proceedings of the National Academy of Sciences*, 82(20), 6723–6726.
- Zaater, S., Bouchoucha, A., Djebbar, S., & Brahimi, M. (2016). Structure, vibrational analysis, electronic properties and chemical reactivity of two benzoxazole derivatives: Functional density theory study. *Journal of Molecular Structure*, 1123, 344–354.
- Zhao, Y., & Truhlar, D. G. (2008). The M06 suite of density functionals for main group thermochemistry, thermochemical kinetics, noncovalent interactions, excited states, and transition elements: Two new functionals and systematic testing of four M06-class functionals and 12 other functionals. *Theoretical Chemistry Accounts*, 120(1), 215–241.

Author Information

Manel Taferguennit

University of Sciences and Technology Houari Boumediene
BP 32, 16111 Algiers, Algeria.
Contact e-mail: mtaferguennit@usthb.dz

Noura Kichou

University of Mouloud Mammeri of Tizi-Ouzou,
Tizi-Ouzou, Algeria.

Zakia Hank

University of Sciences and Technology Houari Boumediene
BP 32, 16111 Algiers, Algeria.

To cite this article:

Taferguennit, M., Kichou, N., & Hank, Z. (2023). Comparative experimental and theoretical study on the structure of potassium 2,4-hexadienoate: structure-activity relationship. *The Eurasia Proceedings of Science, Technology, Engineering & Mathematics (EPSTEM)*, 23, 69-84.

The Eurasia Proceedings of Science, Technology, Engineering & Mathematics (EPSTEM), 2023

Volume 23, Pages 85-92

ICRETS 2023: International Conference on Research in Engineering, Technology and Science

Alternative Aviation Fuel Types Used in Aircraft Engine

Ayhan Uyaroglu
Selçuk University

Mahmut Unaldi
Selçuk University

Abstract: Air transportation is a preferred mode of transportation due to the fastest of methods transport. In this respect, air transport in terms of passengers and freight has been increasing continuously since the 1970s. Due to the increasing number of aircraft and flights, the demand for aviation fuel also increases. Jet engines and auxiliary power unit (APU) are the two main sources of aircraft emissions as they use fuel. Aircraft engine emissions have not received as much attention as emissions from other energy sources until recent years. However, the International Civil Aviation Organization (ICAO) has set limits for commercial jet engines in respect to nitrogen oxides, unburned hydrocarbons, carbon monoxide and smoke emissions. These limitations were determined for a specified landing and take-off cycle (LTO) to limit emissions near ground level as well as indirectly limit emissions at altitude. The world's carbon dioxide emissions of 2%, originate from air transportation. In order to reduce greenhouse gas (GHG) emissions, especially carbon dioxide emissions, the use of alternative fuels instead of fossil fuels is increasing in aviation transportation. In this study, it is aimed to examine the use of alternative aviation fuel types produced by different methods in aircraft engines.

Keywords: Aircrafts, Kerosene, Vegetable oil, Sustainable aviation fuels, Emissions

Introduction

The jet fuel used in aircraft engines to obtain propulsion as a result of combustion is of petroleum origin. According to United States (US) Energy Information Administration (EIA), approximately 3-4 gallons of jet fuel are obtained from a 42-gallon barrel of crude oil (Refining crude oil - U.S. Energy Information Administration (EIA), 2023) and fuel costs of airlines are approximately 30% of their operating costs (Chiaramonti et al., 2014). Air transport produced 781 million tons of CO₂, which corresponds to 2% of greenhouse gas, by consuming 177 billion liters of kerosene from 25000 aircraft to carry 6 billion passengers in 2015 (Baumi et al., 2020). The percentages of carbon dioxide by sectors between the years 2019-2022 are shown in the Figure 1 (Global CO₂ emissions by sector, 2019-2022 – Charts – Data & Statistics, 2023), carbon dioxide emissions are in the order of highest to lowest in power, industry, transportation and buildings. Global carbon dioxide emissions fluctuated during this three-year period. The distribution of carbon dioxide emissions in transport sector is shown Figure 2 (Global transport CO₂ emissions breakdown 2021, 2023).

When we look at the CO₂ emissions of transportation vehicles in particular, it can be seen from the Fig. 2 that the aviation sector is 9%. Due to the fact that the number of passenger vehicles is higher than other vehicle types the highest percentage was realized in passenger cars with 39%.

In addition to carbon dioxide emissions that cause global warming, The ICAO has get limitations for nitrogen oxides, unburned hydrocarbons, carbon monoxide and smoke emissions from commercial jet engines according to landing and take-off cycle (LTO). Figure 3 (ICAO Standards and Recommended Practices: Annex 16, Volume II, 2023), depicted to ICAO engine emission certification LTO cycle.

- This is an Open Access article distributed under the terms of the Creative Commons Attribution-Noncommercial 4.0 Unported License, permitting all non-commercial use, distribution, and reproduction in any medium, provided the original work is properly cited.

- Selection and peer-review under responsibility of the Organizing Committee of the Conference

© 2023 Published by ISRES Publishing: www.isres.org

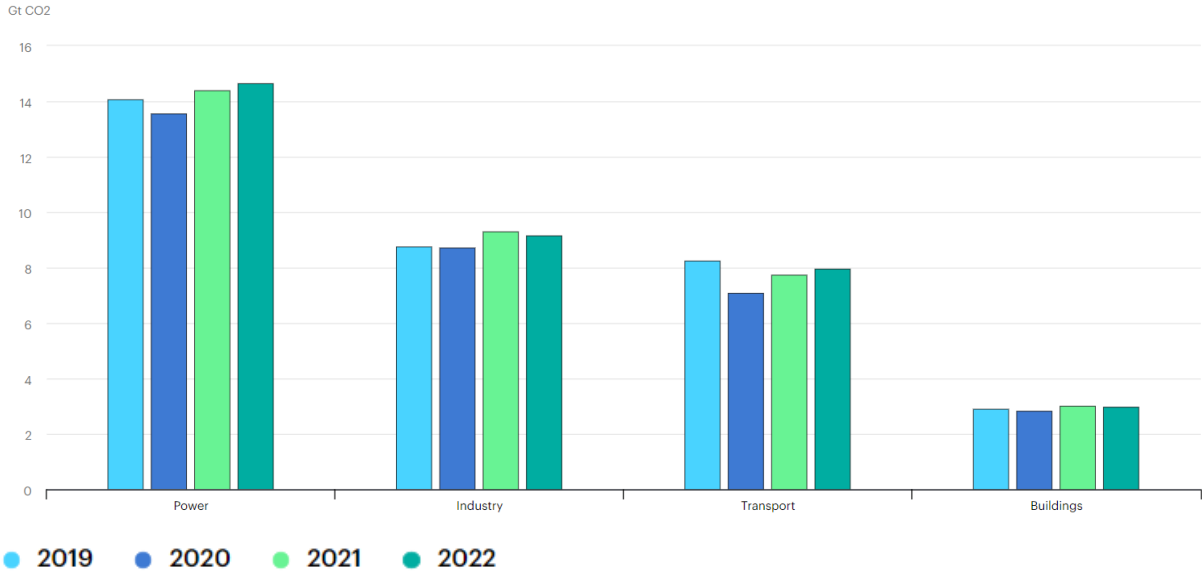


Figure 1. Global CO₂ emissions by sector, 2019-2022 (Global CO₂ emissions by sector, 2019-2022 – Charts – Data & Statistics, 2023)

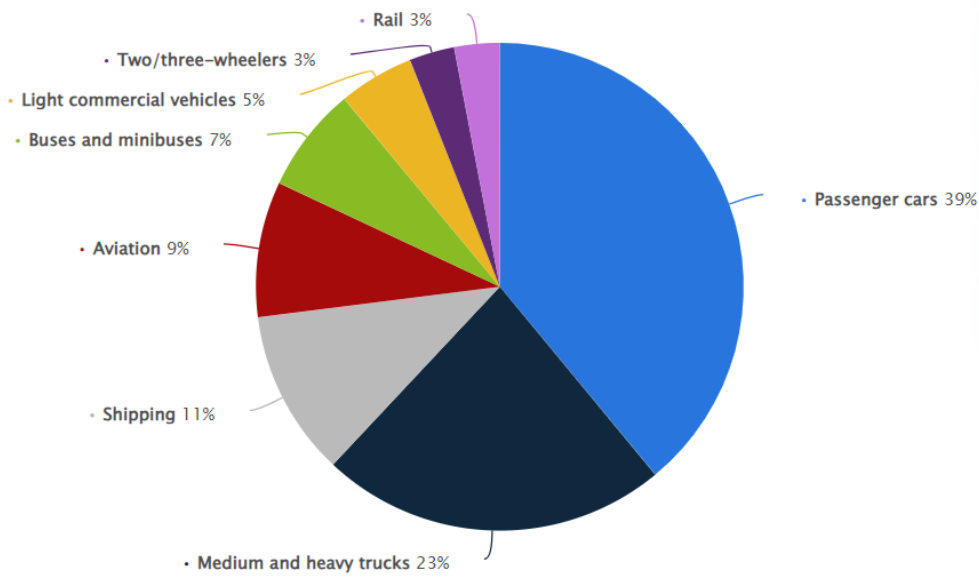


Figure 2. CO₂ emissions from mode of transports worldwide in 2021 (Global transport CO₂ emissions breakdown 2021, 2023)

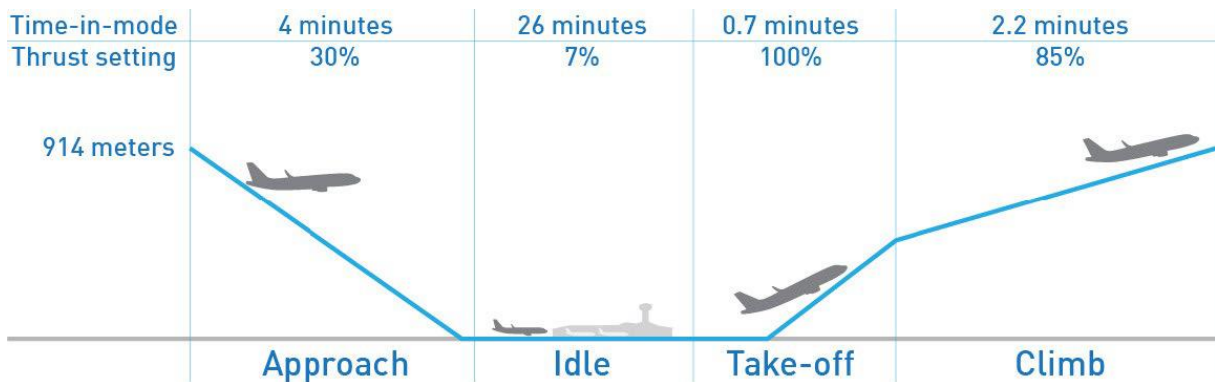


Figure 3. ICAO engine emission certification landing and take-off (LTO) cycle (ICAO Standards and Recommended Practices: Annex 16, Volume II, 2023)

Figure 4 (Tokuşlu, 2021), indicates the NOx, CO and HC emissions for LTO modes. The highest NOx was in the climb mode, CO in taxi mode and HC in taxi mode. Table 1 (Tokuşlu, 2021), shows the emission factors of a number of aircrafts that from the ICAO Engine Exhaust Emission Databank.

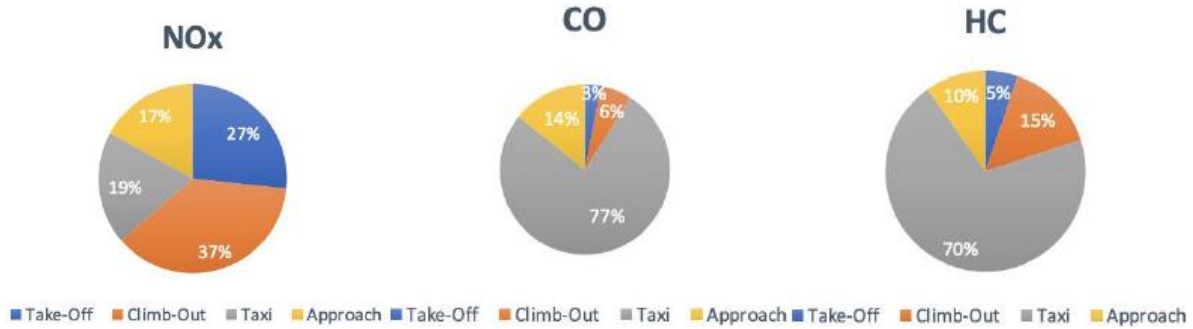


Figure 4. The distribution of aircraft emissions (NOx, CO, HC) for LTO modes (Tokuşlu, 2021)

Liu et al., (2020) in their study on alcohol/kerosene mixtures; short-chain alcohols such as ethanol, n-propanol and n-butanol were blended with aviation kerosene (RP-3) at 30%, 50% and 70% by volume, respectively. They found that the brake thermal efficiency (BTE) (alcohol content $\geq 50\%$) of alcohol/kerosene mixtures is higher than gasoline. The brake thermal efficiency of E70, P70 and B70 was improved 2.15%, 3.52% and 6.51%, respectively. In terms of carbon monoxide (CO) and nitrogen oxides (NOx), lower values were obtained in the blended fuels. The CO emissions of E70, P70 and B70 fuels reduced by 39.8%, 38.5% and 49%, respectively, and also decreased in HC, CO and soot emissions as the alcohol content in the mixture increased. Among the experimental fuels, n-butanol/kerosene blends had better combustion and lower emissions, with higher efficiency and reduced HC, CO and soot emissions (Liu et al., 2020).

Table 1. Emission factors (Tokuşlu, 2021)

Aircraft	CO (kg/LTO)	NO _x (kg/LTO)	HC (kg/LTO)
Boeing 737	16.9	9.0	4.1
Boeing 727, 757	25.4	13.4	6.1
Boeing 747	65.8	47.7	19.6
Boeing 767, 707	119.1	11.6	99.0
Airbus A300, 310	119.1	11.6	99.0
Airbus A319	6.35	8.73	0.59
Airbus A320	24.6	9.7	5.9
Tupolev 154	25.4	13.4	6.1
Tupolev 134	24.6	9.7	5.9
Saab 340	22.1	0.3	14.1
DC9	16.9	9.0	4.1
CRJ2	4.14	4.41	0.04
Tupolev 154	25.4	13.4	6.1
Tupolev 134	24.6	9.7	5.9
Fokker F27	22.1	0.3	14.1
Fokker F28, 50, 100	64.1	8.2	47.1
Concorde	384	41	112

SAF, which is used to propel the aircraft engine, is a biofuel with similar properties to conventional jet fuel, but with lower carbon footprint. Thanks to the technology and raw materials used to obtain SAF can significantly reduce greenhouse gas emissions compared to conventional jet fuel (Sustainable Aviation Fuels, 2023). Governments assent to the usage of SAF and its amendment effect on the decarbonization, which was held in October 2022 of 41st Assembly of the ICAO for Long Term Aspirational Goal (LTAG) about climate (IATA, 2023).

Thanks to SAFs, which can be obtained from waste oils and fats, green and municipal wastes and non-food products and used in aviation today, CO₂ emissions are reduced by up to 80% (Net zero 2050: sustainable aviation fuels, 2023). With the use of SAFs, it aims to achieve net zero carbon emissions through the impact of innovative propulsion technologies and other efficiency developments to ensure maximum reduction in emissions in the aviation industry. Figure 5 (Developing Sustainable Aviation Fuel (SAF), 2023), shows the projection for net zero carbon attain in 2050. To achieve this purpose, SAF production is increasing rapidly. Table 2 (IATA, 2023), proves this increment.

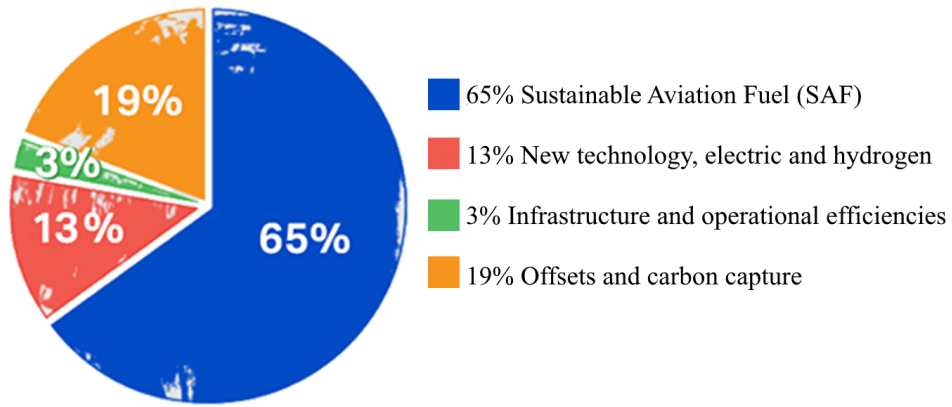


Figure 5. Projection for net zero carbon attain in 2050 (Developing Sustainable Aviation Fuel (SAF), 2023)

Table 2. SAF production (IATA, 2023)

Year	2019	2020	2021	2022E
Estimated SAF output (Million liters)	25	62.5	100	300-450

There are technical impediments to the changeover to electric or hydrogen powered aircraft and it is anticipated that liquid fuels will continue until 2050. This is especially true for medium and long distance flights, which account for two-thirds of aviation emissions. Sustainable aviation fuels (SAF) will be important for the goal of reducing greenhouse gas (GHG) emissions by 50% by 2050. It is stated that the carbon intensity of petroleum-derived jet fuel is between 85 and 95 grams of carbon dioxide equivalent per megajoule of fuel (g CO₂e/MJ) of which approximately 73 g CO₂e/MJ is due to the combustion of the fuel and the rest is due to the extraction, refining process and transportation of this fuel (Pavlenko & Searle, 2021). Although synthetic jet fuels have advantages such as without sulfur, low viscosity at low temperatures, high thermal stability and reduced particulate emission, they also have the disadvantages of poor lubricating properties, low volumetric thermal content, prone to fuel system elastomer leakage and increased CO₂ emissions through the production process (Daggett et al., 2006).

Sustainable Aviation Fuel Pathways

Figure 6 (Cabrera & de Sousa, 2022), demonstrates the sustainable aviation fuel pathways today. These pathways will be explained below.

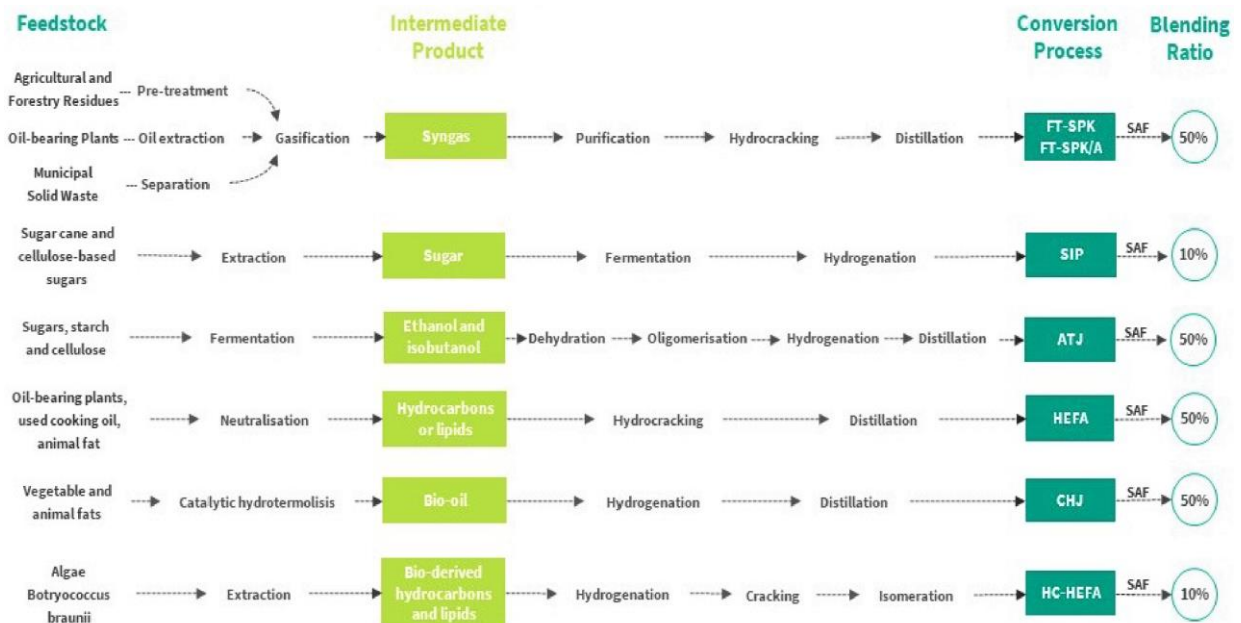


Figure 6. Approved SAF produce methods for D7566 (Cabrera & de Sousa, 2022)

Fischer Tropsch Synthesized Isoparaffinic Kerosene (FT-SPK)

Franz Fischer and Hans Tropsch discovered the method of producing liquid hydrocarbons from coal in the 1920s. Fischer Tropsch-synthesized isoparaffinic kerosene (FT-SPK) FT-SPK was certified by ASTM for inclusion in ASTM D7566 in September 2009. In the FTSPK process, feedstocks such as coal (coal-to-liquid-CtL), natural gas (GtL) or biomass (BtL) are first pre-treated to achieve a homogeneous consistency, followed by a partial oxidation process called gasification to produce synthesis gas or syngas. This syngas consists mainly of a mixture of CO and H₂, with smaller amounts of other gases such as CO₂ and CH₄. It is then cleaned, conditioned and purified. From this syngas is obtained the desired final product such as liquid hydrocarbon fuel (synthetic kerosene and diesel) by means of the catalytic conversion in that using cobalt and iron as catalyst in the FT reactor. FT-SPK/A is a variant of the FT process containing alkylation of light aromatics, mainly benzene in which a fully synthetic alternative aviation fuel is produced, and was approved for inclusion in ASTM D7566 in November 2015.

Fischer Tropsch fuels are characterized by non-toxic, low sulfur, and contain very few aromatics compared to diesel and gasoline, which results in lower emissions such as particulate matter, carbon dioxide and hydrocarbon emissions. Thanks to the higher hydrogen-to-carbon ratio (H/C-ratio) decreased particulate emission may result. Due to the high thermal stability of FT fuels, it is possible to use them at high engine fuel temperatures. In this way, engine fuel efficiency can be increased. On the other hand, the low viscosity of FT fuels at low temperatures improves the operability of aircraft at high altitudes and low temperatures. In addition, thanks to the capability of decrease the temperature of the cooling air of turbine blades and lowering the engine oil temperature increase the durability of the engine. In accordance with the ASTM D7566 standard for SPK and SIP fuels, the aromatic amount should not exceed 0.5% by volume; hereby, the low amount of aromatic should not lead to a notable problem. However, the absence of aromatics can result in lower lubricity properties and seal swelling. The lubricating properties of FT fuels are low, just like HEFA, due to the lack of sulfur (Cabrera & de Sousa, 2022; Fact Sheet 2 – IATA, 2023; Pavlenko & Searle, 2021; Kaltschmitt & Neuling, 2017; Detsios et al., 2023; Marszałek & Lis, 2022; Daggett et al., 2006).

Synthesized Iso-Paraffins (SIP)

Synthesized iso-paraffins (SIP) was also entitled to as direct sugar to hydrocarbon process (DHSC). Synthesized iso-paraffins (SIP) process was approved into ASTM D7566 in July, 2014 by ASTM. From feedstocks such as cellulosic sugars, halophytes, sugar beets, sugar cane and sweet sorghum, with biochemical conversion technology, sugar is converted into hydrocarbon fuel by fermentation. The DHSC process consists of hydrolysis of the biomass, carbohydrate fermentation, purification and hydroprocessing. The sugars are converted into C15 alkene with four double bonded hydrocarbons, called farnesene (C₁₅H₂₄) by fermentation which has a higher energy density and longer carbon chain than ethanol or isobutanol. Farnesene is converted into alkane hydrocarbons, called farnesane (C₁₄H₃₂), which is afterwards distilled to obtain at 10% blend levels in jet aviation fuel. The DSHC method is the most expensive alternative fuel conversion method, as the complexity and low efficiency of the steps in transforming lignocellulosic sugars into fuels via DSHC lead to high raw material cost and higher energy consumption. Although DSHC-SIP fuel is successful in test flights with a mixing ratio of 20%, it should be used in mixtures with a mixing ratio not exceeding 10%, since there is no synthesized paraffinic kerosene such as FT and HEFA (Fact Sheet 2 – IATA, 2023; Pavlenko & Searle, 2021; Cabrera & de Sousa, 2022; Detsios et al., 2023; Marszałek & Lis, 2022).

HH-SPK (Hydroprocessed Hydrocarbons- Synthesized Isoparaffinic Kerosene) or HC-HEFA

HH-SPK (Isoparaffinic kerosene synthesized with Hydroprocessed Hydrocarbons) denominated as HC-HEFA was certified to ASTM D7566 in May 2020. The feature that distinguishes HC-HEFA from HEFA is that algae called *Botryococcus braunii* are used as raw materials in HC-HEFA, and HC-HEFA blending ratio up to the 10% (Fact Sheet 2 – IATA, 2023; Cabrera & de Sousa, 2022; Detsios et al., 2023).

Hydroprocessed Fatty Acid Esters and Fatty Acids (HEFA)

Hydroprocessed Esters and Fatty Acids Synthetic Paraffinic Kerosene (HEFA-SPK): HEFA is obtained from *Jatropha*, algae, camelina, and yellow grease and so on by deoxygenation followed by hydrotreating, hydroisomerization, or hydro-cracking. HEFA was certificated by ASTM for ASTM D7566 in June, 2011.

Priorly 2011, the expression of Hydroprocessed Esters and Fatty Acids was often termed to as hydrotreated vegetable oils (HVO), but a new abbreviation, HRJ, stands for hydroprocessed renewable jet, was emerged to cover all possible types of raw materials. The type of catalyst used influences the efficiency of the hydrotreating of triglycerides and the composition of products. These products have different carbon number such as green diesel (C14-C20), green jet fuel (C11-C13), green naphtha (C5-C10), and and even green liquid petroleum gas (LPG). HEFA fuels have similar properties to petroleum-based fuels, as well as advantages such as high cetane number, low aromatic content, low sulfur and low greenhouse gases (Sotelo-Boyás et al., 2012; Fact Sheet 2 – IATA, 2023; Tao et al., 2017; Pavlenko & Searle, 2021; Cabrera & de Sousa, 2022).

Alcohol to Jet (ATJ)

Alcohol to jet (ATJ) endorsement for ASTM D7566 is taken place in April 2016 for isobutanol with a blend limit of 50% and for ethanol at blend limit 50% in April 2018. For an alcoholic fermentation can use sugary, starchy and lignocellulosic biomass such as sugar cane, sugar beet, switchgrass, maize and wheat. Producing ATJ fuels as a pure hydrocarbon can be done through biochemical or thermochemical conversion involved dehydration (water elimination), oligomerization (creation of more complex molecules), and hydro processing (addition of hydrogen). The blend ratio of 50% is allowed. If ever there was the aircraft fully Ethanol-powered: Since the ethanol fuel needs approximately 64% more storage volume to meet the energy amount of kerosene, the increase in storage volume causes the aircraft wing to be made 25% larger, resulting in an increase in the empty weight of the aircraft by 20% (Fact Sheet 2 – IATA, 2023; Pavlenko & Searle, 2021; Kaltschmitt & Neuling, 2017; Cabrera & de Sousa, 2022; Detsios et al., 2023; Daggett et al., 2006; Yao et al., 2017).

Catalytic Hydrothermolysis Jet Fuel (CHJ)

The catalytic hydrothermolysis jet (CHJ) process (also denominated hydrothermal liquefaction) similar to those of the HEFA was receive certification in 2020 with a maximum blending ratio of 50%. The reaction steps are cracking, hydrolysis, decarboxylation, isomerization and cyclization that progress at presence of supercritical water (SCW) and with/without a catalyst under high temperature and pressure conditions. FFAs from fats, oils, and greases (FOGs) convert into paraffin, isoparaffin, cycloparaffin, and aromatic compounds (Fact Sheet 2 – IATA, 2023; Pavlenko & Searle, 2021; Cabrera & de Sousa, 2022; Detsios et al., 2023; Marszałek & Lis, 2022).

Co-processing

Co-processing has been approved to ASTM D-1655 in April 2018. Fats, oils and greases are mixed up to 5% by volume with fossil crude for supplying the refining process in conventional petroleum refinery. This method may be cheaper as it can use the existing oil refining infrastructure and save the burden of building a dedicated biorefinery (Prussi et al., 2019; Marszałek & Lis, 2022; Cabrera & de Sousa, 2022; Pavlenko & Searle, 2021).

Conclusion

While studies on reducing the environmental impact of Greenhouse gas (GHG) emissions have been going on in road transport for decades, these studies within the aviation sector have become official since 2009 that FT-SPK as Sustainable Aviation Fuel (SAF) was the first approved (SAF) by ASTM. In order to reduce the carbon footprint, on the one hand, studies on various types of Sustainable aviation fuels have been and continue to be made, and on the other hand, the production and use of SAF fuel is increasing. As a result, International Air Transport Association (IATA) is aimed to attain for net zero carbon in 2050.

Scientific Ethics Declaration

The authors declare that the scientific ethical and legal responsibility of this article published in EPSTEM journal belongs to the authors.

Acknowledgements or Notes

* This article was presented as an oral presentation at the International Conference on Research in Engineering, Technology and Science (www.icrets.net) held in Budapest/Hungary on July 06-09, 2023.

References

- Baumi, J., Bertosse, C. M., & Guedes, C. L. B. (2020). Aviation fuels and biofuels. In *Renewable Energy-Resources, Challenges and Applications*. IntechOpen.
- Cabrera, E., & de Sousa, J. M. M. (2022). Use of sustainable fuels in aviation—A review. *Energies*, *15*(7), 2440.
- Chiaramonti, D., Prussi, M., Buffi, M., & Tacconi, D. (2014). Sustainable bio kerosene: Process routes and industrial demonstration activities in aviation biofuels. *Applied Energy*, *136*, 767-774.
- Daggett, D., Hendricks, R., & Walther, R. (2006, October). Alternative fuels and their potential impact on aviation. In *25th Congress of the International Council of the Aeronautical Sciences (ICAS 2006)* (No. E-15568).
- Detsios, N., Theodoraki, S., Maragoudaki, L., Atsonios, K., Grammelis, P., & Orfanoudakis, N. G. (2023). Recent advances on alternative aviation fuels/pathways: A critical review. *Energies*, *16*(4), 1904. from <https://www.iata.org/en/pressroom/2022-releases/2022-12-07-01/>.
- Energy.gov (2023). Sustainable Aviation Fuels. Retrieved June 29, 2023, from <https://www.energy.gov/eere/bioenergy/sustainable-aviationfuels#:~:text=SAF%20is%20a%20biofuel%20used,compared%20to%20conventional%20jet%20fuel>.
- IATA (2023). 2022 SAF Production Increases 200% - More Incentives Needed to Reach Net Zero. Retrieved June 29, 2023, <https://www.iata.org/en/pressroom/2022-releases/2022-12-07-01/>.
- IATA (2023). *Developing Sustainable Aviation Fuel (SAF)*. Retrieved June 29, 2023, from <https://www.iata.org/en/programs/environment/sustainable-aviation-fuels/>.
- IATA (2023). Fact Sheet 2 – IATA. Retrieved June 29, 2023, from <https://www.iata.org/contentassets/d13875e9ed784f75bac90f000760e998/saf-technical-certifications.pdf>.
- IATA (2023). *Net zero 2050: sustainable aviation fuels*. Retrieved June 29, 2023, from <https://www.iata.org/en/iata-repository/pressroom/fact-sheets/fact-sheet---alternative-fuels/>.
- ICAO Standards and Recommended Practices: Annex 16, Volume II. Retrieved June 29, 2023, from https://www.icao.int/environmental-protection/Documents/EnvironmentalReports/2022/ENVReport2022_Art17.pdf.
- IEA (2023). *Global CO2 emissions by sector, 2019-2022 – Charts – Data & Statistics*. Retrieved June 29, 2023, from <https://www.iea.org/data-and-statistics/charts/global-co2-emissions-by-sector-2019-2022>.
- Kaltschmitt, M., & Neuling, U. (Eds.). (2017). *Biokerosene: Status and prospects*. Springer. (pp. 444-469).
- Liu, G., Ruan, C., Li, Z., Huang, G., Zhou, Q., Qian, Y., & Lu, X. (2020). Investigation of engine performance for alcohol/kerosene blends as in spark-ignition aviation piston engine. *Applied Energy*, *268*, 114959.
- Marszałek, N., & Lis, T. (2022). The future of sustainable aviation fuels. *Combustion Engines*, *61*.
- Pavlenko, N., & Searle, S. (2021). *Assessing the sustainability implications of alternative aviation fuels*. The International Council on Clean Transportation.
- Prussi, M., O'connell, A., & Lonza, L. (2019). Analysis of current aviation biofuel technical production potential in EU28. *Biomass and Bioenergy*, *130*, 105371.
- Refining crude oil - U.S. Energy Information Administration (EIA). Retrieved June 29, 2023, from <https://www.eia.gov/energyexplained/oil-and-petroleum-products/refining-crude-oil.php>.
- Sotelo-Boyás, R., Trejo-Zarraga, F., & de Jesús Hernández-Loyo, F. (2012). Hydroconversion of triglycerides into green liquid fuels. Chapter 8. *by I. Karamé InTech, Rijeka*. (pp. 187-216).
- Statista (2023). Global transport CO2 emissions breakdown 2021. Retrieved 2023, from <https://www.statista.com/statistics/1185535/transport-carbon-dioxide-emissions-breakdown/#:~:text=The%20global%20transportation%20sector%20is,percent%20of%20global%20transportation%20emissions>.
- Tao, L., Milbrandt, A., Zhang, Y., & Wang, W. C. (2017). Techno-economic and resource analysis of hydroprocessed renewable jet fuel. *Biotechnology for Biofuels*, *10*, 1-16.
- Tokuşlu, A. (2021). Calculation of aircraft emissions during landing and take-off (LTO) cycles at Batumi International Airport, Georgia. *International Journal of Environment and Geoinformatics*, *8*(2), 186-192.
- Yao, G., Staples, M. D., Malina, R., & Tyner, W. E. (2017). Stochastic techno-economic analysis of alcohol-to-jet fuel production. *Biotechnology for Biofuels*, *10*(1), 1-13.

Author Information

Ayhan Uyaroglu

Selcuk University Cihanbeyli High Vocational School,
Konya, Turkey

Contact e-mail: ayhan.uyaroglu@selcuk.edu.tr

Mahmut Unaldi

Selcuk University Cihanbeyli High Vocational School,
Konya, Turkey

To cite this article:

Uyaroglu, A. & Unaldi, M. (2023). Alternative aviation fuel types used in aircraft engine. *The Eurasia Proceedings of Science, Technology, Engineering & Mathematics (EPSTEM)*, 23, 85-92.

The Eurasia Proceedings of Science, Technology, Engineering & Mathematics (EPSTEM), 2023

Volume 23, Pages 93-99

ICRETS 2023: International Conference on Research in Engineering, Technology and Science

On the Development of the Fluorescence Excitation-Emission Etalon Matrix Algorithm of Wine

Miranda Khajishvili

Batumi Shota Rustaveli State University

Jaba Shainidze

Batumi Shota Rustaveli State University

Kakha Makharadze

Batumi Shota Rustaveli State University

Nugzar Gomidze

Batumi Shota Rustaveli State University

Abstract: Our research provides for the analysis of different types of Georgian wine based on 3D fluorescence spectroscopy (3DF) using the Black Comet (200-950 nm) spectrometer manufactured by StellarNet. In this method, the 3D fluorescence signal is divided into a fixed number of statistical components. For each type of wine, a 3D database is strictly defined, which we conventionally call references. The etalon describe the excitation/emission spectra in detail. The advantage of the 3DF method compared to other statistical methods, such as peak component analysis (PCA), lies in the uniqueness of the unfolding of the spectra. The fluorescence spectra of the wine will be further analyzed by peak component analysis (PCA). After performing the PCA analysis, in order to reduce the number of tolerant etalon, we used the tolerant etalon sample (TES) comparison analysis, thus determining how tolerant the researched wine sample is to this or that specific etalon.

Keywords: 3D fluorescence spectroscopy, Peak component analysis, Wine analysis, Georgian wine, Tolerant etalon sample

Introduction

The combination of 3D fluorescence spectroscopy (3DF) and peak component analysis (PCA) has been used in various fields, including chemistry, biology, environmental science, and food analysis. The combination of 3D fluorescence spectroscopy (3DF) and peak component analysis (PCA) presents a powerful tool for quality control and authentication in the wine industry, particularly for Georgian wine. Here are some key points to highlight about how this combination can be beneficial:

- 3DF is known for its high sensitivity, allowing it to detect even subtle differences in fluorescence patterns. By employing PCA, which helps in identifying specific spectral features, the method becomes even more discriminative. This means that even small variations in the fluorescence spectra of different wine samples can be distinguished and analyzed effectively.
- The unique fluorescence patterns obtained through 3DF can reveal a wealth of information about the chemical composition and structural properties of the wine. PCA further enhances this characterization

- This is an Open Access article distributed under the terms of the Creative Commons Attribution-Noncommercial 4.0 Unported License, permitting all non-commercial use, distribution, and reproduction in any medium, provided the original work is properly cited.

- Selection and peer-review under responsibility of the Organizing Committee of the Conference

© 2023 Published by ISRES Publishing: www.isres.org

by extracting the most significant spectral components. As a result, a comprehensive and detailed picture of each wine type's fluorescence profile is obtained.

- The use of well-defined references (etalons) for each type of Georgian wine enables the establishment of a reliable database. This database acts as a benchmark against which new wine samples can be compared. Any deviation from the known fluorescence profiles can raise a flag for further investigation, helping to identify potential adulteration or counterfeit products.
- With a robust database of fluorescence spectra for various Georgian wines, it becomes easier to trace the origin of a specific wine sample. This is especially valuable for safeguarding wines with geographical indications, as it helps verify whether a wine truly originates from the claimed region.
- One significant advantage of 3DF and PCA is that they are non-destructive techniques. This means that the wine samples do not undergo any chemical alteration during analysis, making it possible to preserve the integrity of the samples for further studies or sensory evaluations.
- Once the reference database is established, the analysis of new wine samples becomes more efficient in terms of time and cost. The comparison with etalons can quickly provide information about the wine's authenticity and potential quality.
- The combination of 3DF and PCA not only benefits wine producers and regulators but also contributes to scientific research. It offers insights into the variability of wine compositions and how different factors, such as grape variety, terroir, and winemaking techniques, influence the fluorescence patterns.

Literature Review

The algorithm for processing the fluorescence excitation-emission matrix for the classification of Argentine white wine is presented in (Azcarate et al., 2015). The effectiveness of using the TES method in wine classification lies in the fact (Wold, 1976) that the types of molecules (such as polyphenols, vitamins, amino acids) and the amount depend on the specific type and maturity of the wine, as well as the wine technology (Urbano et al., 2006; Airado-Rodriguez et al., 2011).

The study includes fluorescence spectroscopy excitation/emission matrix (AEM) analysis, peak component analysis (PCA) and tolerance etalon sample (TES) comparison analysis method development and modeling according to wine product variety and origin. About 100 samples of four types of white Georgian wine were taken. The methodology chosen by us is based on the one hand on the hardware complex, which was gradually modernized by our group (Gomidze et al., 2012; Gomidze et al., 2014; Gomidze et al., 2016; Gomidze et al., 2018), on the other hand on the development of new analytical approaches (Khajisvili et al., 2021) that are quite acceptable to be used in typical laboratory control of food products and beverages. For analyses 3D spectra it is known techniques that are specifically designed for spectroscopic data analysis, such as Multivariate Curve Resolution (MCR), Parallel Factor Analysis (PARAFAC), or Multivariate Analysis of Variance (MANOVA).

Description of the Experiment

Fluorescence spectra were recorded using a Black Comet (200-950 nm) spectrometer manufactured by StellarNet. LED lamps of different frequencies were used as light sources. A wine sample of 100 μ l is placed in a quartz cuvette and the spectra are recorded at room temperature. The number of scans is determined from the same experimental measurement to exclude drift effects on the sample. At the beginning of each experiment, the standard is calibrated. The excitation wavelength range is between 250-500 nm, and the emission wavelength is between 275-600 nm. Measurements are performed at different excitation wavelengths with a 5 nm bias. The total time to scan a sample is approximately 10 minutes. Measurements were performed over a short period of time (10-15 days), thereby minimizing the influence of atmospheric effects and instrumental fluctuations (eg. lamp intensity fluctuations). PCA was performed for descriptive analysis of spectral features and TES modeling of analog classes will be used to classify these data. SpectraWiz and LAbView software were used for graphical visualization of the spectra. Data recording and processing were performed in MS Excel and MySQL.

Description of the Theory and Method

Given a dataset with n observations (data points) and 'm' features (variables), we first preprocess the data by centering the variables. Let's assume the centered dataset as x_C . The covariance matrix (C) of the centered data

x_C is a square $m \times m$ matrix where each element $C(i, j)$ represents the covariance between the i -th and j -th variables. The formula for the covariance between two variables x_i and x_j is given as:

$$C(x_i, x_j) = \sum_{n=1}^N \frac{(x_i - \bar{x}_i)(x_j - \bar{x}_j)}{n - 1}$$

Next, we perform eigendecomposition on the covariance matrix C to find its eigenvalues (λ) and corresponding eigenvectors (v). The eigendecomposition equation is:

$$C v = \lambda v$$

Where v is the eigenvector, and λ is the corresponding eigenvalue. The eigenvectors are sorted in descending order based on their corresponding eigenvalues (in decreasing order of importance). This sorting will help us select the most significant principal components. After sorting the eigenvectors, we select the k eigenvectors with the highest corresponding eigenvalues to form the principal components. k is the number of dimensions we want to reduce the data to, and it is typically chosen based on a desired level of explained variance or the number of significant components required for analysis.

We create a matrix W by stacking the k selected eigenvectors as columns. The matrix W will have dimensions $m \times k$. We then transform the original centered data x_C into a reduced-dimensional space by multiplying it with W . This transformation gives us the reduced dataset x_{PCA} :

$$x_{PCA} = x_C \times W$$

The resulting dataset x_{PCA} contains the principal components, which are the linear combinations of the original features. Each principal component captures a different direction of maximum variance in the data. The first principal component has the highest variance, and subsequent components capture progressively less variance. The principal components can be used for data visualization, feature selection, or as input for other machine learning algorithms. They represent new axes in the reduced-dimensional space that provide a more concise representation of the original data while preserving most of the variance.

PARAFAC (Parallel Factor Analysis), also known as CANDECOMP or PARAFAC (Canonical Decomposition), is a multivariate statistical method used for analyzing multi-way arrays or tensors. It is a powerful technique for decomposing higher-order data structures into a set of component matrices and capturing the underlying latent factors that explain the observed data. PARAFAC deals with multi-way data arrays (tensors) rather than simple matrices. A tensor is a generalization of a matrix and can be thought of as an n -dimensional array. For example, a matrix is a 2-way tensor (rows and columns), and a 3-way tensor has three modes. PARAFAC aims to approximate the original tensor X with a lower-rank approximation, represented by three component matrices (A, B , and C). The rank of the PARAFAC model is the number of components used to approximate the original tensor.

For a 3-way tensor X with dimensions $I \times J \times K$, the PARAFAC model can be represented as:

$$X = \sum_{i=1}^N \sum_{j=1}^N \sum_{k=1}^N A_i B_j C_k$$

Here, A is a matrix of dimension $I \times \text{rank}$, B is a matrix of dimension $J \times \text{rank}$, and C is a matrix of dimension $K \times \text{rank}$.

The goal is to find the factor matrices A, B , and C such that their product approximates the original tensor X as closely as possible. This can be achieved through methods like alternating least squares (ALS) or non-linear optimization techniques. Once the factor matrices A, B , and C are obtained, they provide insights into the underlying latent factors that explain the structure of the original tensor. Each row of A, B , and C represents a specific "mode" or factor of the data. These factors are often interpreted based on the context of the problem.

One common problem with PARAFAC is determining the appropriate rank (number of components) for the model. Choosing the right rank is essential because too low a rank may lead to an oversimplified representation of the data, while too high a rank may lead to overfitting and capturing noise.

Problem Statement: Given a multi-way tensor dataset, we want to apply the PARAFAC method to extract underlying latent factors. However, we are unsure about the appropriate rank for the model. How can we determine the best rank that adequately represents the data without overfitting or underfitting?

In order to model excitation-emission data, the excitation/emission wavelengths of N samples must be placed in a three-dimensional array of size $i \times j \times k$, where i is the number of samples, j is the number of emission wavelengths, k is the number of excitation wavelengths:

$$x_{ijk} = \sum_{n=1}^N a_{in} b_{jn} c_{kn} + e_{ijk}$$

where N is the number of samples. Matrix A with elements a_{in} in is conventionally called stroboscopic, and matrices B and C with elements b_{jn} and c_{kn} respectively are called emission and excitation loads. The e_{ijk} elements represent the deviation from the statistical mean for each sample. x_{ijk} - practically represents the sum of signals received from fluorophores.

Within this model, the elements of the matrix a_{in} can be interpreted as the concentration of fluorophores n in sample i . The load matrix elements b_{jn} are the basis for the scaled spectrum estimation of the n -th fluorophore at the j -frequency, while the c_{kn} matrix element is proportional to the absorption coefficient of the fluorophore at the k -th frequency (Andersen C. M. & Bro, R., 2003). Excitation/emission array (AEM) coefficients cannot be negative.

Standardization is done by grouping the data for each variety of grapes and their geographical origin, for example West Georgia or East Georgia. In order to perform the analysis of the fluorescence signals of the main components at a fixed - specific k -frequency of excitation, it is necessary to form a two-dimensional matrix $i \times j$ from the main initial array x_{ij} . The goal of PCA analysis is to reduce the rank of the matrix by eliminating redundant members from the data array. For this, we need to find an array of new elements of the matrix in the j -dimensional frequency domain (space) and project the data onto it. The axes of the matrix should be selected so that the data

$$x_{ij} = \sum_{r=1}^R t_{ir} p_{jr} + e_{ij}$$

have maximum variance. It turns out that the unit vectors of this new array are precisely the eigenvectors of the xx^T matrix.

Results

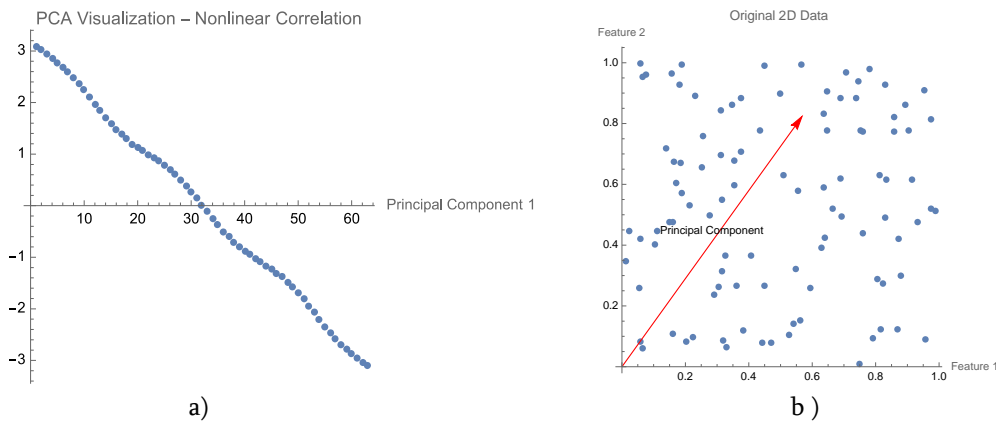


Figure 1. a) 2D data with non-linear correlation and the execution of PCA to reduce the dimensionality to 1D, b) 2D plot that visualizes the original 2D data and the first principal component vector obtained from PCA

With PCA analysis, we will build tables and graphs for the sample of a specific group. Figure 1a shows the generation of 2D data with non-linear correlation and the execution of PCA to reduce the dimensionality to 1D. We visualize data points in a reduced one-dimensional space. Figure 1b shows a 2D plot that visualizes the original 2D data and the first principal component vector obtained from PCA. In Figure 1b visualized the original 2D data as scattered points and plot the first principal component vector obtained from PCA as a red arrow. The arrow represents the direction of maximum variance in the data, which corresponds to the first principal component. The plot also includes a label indicating that it represents the principal component.

In Figure 2 given 3D plot to visualize the original 3D data, the principal component vectors obtained from PCA, and the data points projected onto the principal component subspace. In this 3D plot, we visualize the original 3D data as scattered points, plot the first two principal component vectors obtained from PCA. The data points projected onto the principal component subspace as green points.

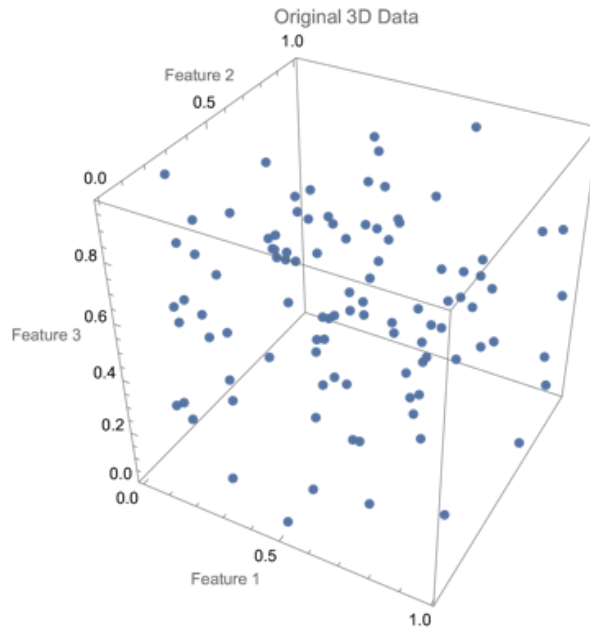


Figure 2. 3D plot to visualize the original 3D data, the principal component vectors obtained from PCA

Figure 3 shows emission spectra of Georgian white wine for Tsolikauri (blue) and Rkatsiteli (red). Three-dimensional graphs account for excitation/emission wavelengths.

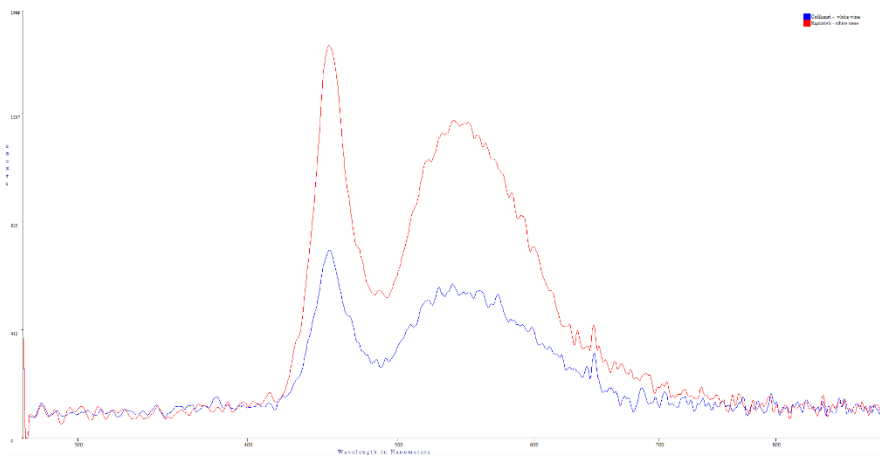


Figure 3. Emission spectra of Georgian white wine: Tsolikauri (blue), Rkatsiteli (red)

Thus, in order to classify wine by type, it is necessary to select a database of a subgroup, which can be called a study group, which in the case of a known type of wine includes many (several dozen) samples. PCA analysis is performed independently on a subset of each known species. This data gives us a spatial picture with the main components. Obviously, the surface of this spatial image is very sensitive to the data of the selected subgroup, so the next step is to analyze and exclude the components with high dispersion from the statistical average.

which is carried out by comparing the selected group and the main components. More precisely by determining the distance between the peaks. If the distance is smaller than some critical value s_0 , then the research sample belongs to the class used for comparison. Once such a procedure is completed, a model will be created for each variety of wine, which can be used as a etalons.

Conclusion

The combination of 3DF and PCA allows for a detailed assessment of the unique fluorescence patterns present in different types of Georgian wine. This can be used as a reliable method for quality control and authentication, helping to identify any adulteration or counterfeit products in the market. By comparing the fluorescence spectra of a given wine sample with the well-defined references (etalons), we can verify its authenticity and origin. The fluorescence spectra of wine can be influenced by factors such as grape variety, soil composition, and climate conditions. The 3DF method, combined with PCA and etalon references, can potentially be used to establish a link between the fluorescence patterns and the geographical origin of the wine. This could be valuable for wine producers aiming to protect and promote wines with specific geographical indications. Different vintages of the same wine type can exhibit variations in their fluorescence properties due to varying environmental conditions and winemaking processes. The 3DF analysis, along with PCA and etalon references, might help discern these subtle differences and aid in distinguishing between wines from different years. Some wines are known for their unique characteristics and premium quality, which are often reflected in their distinct fluorescence profiles. Utilizing the 3DF method with PCA analysis can help classify wines into different quality grades based on their fluorescence patterns. This information can be valuable for consumers, sommeliers, and wine enthusiasts when making purchasing decisions. Understanding the fluorescence properties of different wines can provide insights into the chemical composition and structural changes during the winemaking process. This knowledge may assist winemakers in optimizing their production techniques and ensuring consistent quality in the final product.

The 3DF technique can provide a wealth of data on the complex chemical composition of wines. Researchers can use this information to study the presence of various compounds and their interactions, contributing to a deeper understanding of wine chemistry and its influence on wine characteristics. Overall, the combination of 3DF, PCA, and etalon references in the analysis of Georgian wine offers a powerful and sophisticated approach to gain valuable insights into the unique fluorescence properties of different wine types. As this technology evolves and becomes more established, it has the potential to revolutionize the field of wine analysis and enhance various aspects of the wine industry.

Scientific Ethics Declaration

The authors declare that the scientific ethical and legal responsibility of this article published in EPSTEM journal belongs to the authors.

Acknowledgements or Notes

* This article was presented as an oral presentation at the International Conference on Research in Engineering, Technology and Science (www.icrets.net) held in Budapest/Hungary on July 06-09, 2023.

* This work was supported by the 2023 Competition for Targeted Scientific Research Projects titled “On the Development of the Fluorescence Excitation-Emission Etalon Matrix Algorithm of Wine” by Batumi Shota Rustaveli State University. The project manager of this project is Dr. Miranda Khajishvili.

References

- Airado-Rodríguez D., Durán-Merás, I., Galeano-Díaz, T. & Wold, J. P. (2011). Front-face fluorescence spectroscopy: A new tool for control in the wine industry. *J. Food Compos. Anal.*, 24(2), 257–264.
- Andersen C. M. & Bro, R. (2003). Practical aspects of PARAFAC modeling of fluorescence excitation – emission data. *J. Chemometer*, 17, 200–215.

- Azcarate S. M. et al. (2015). Modeling excitation–emission fluorescence matrices with pattern recognition algorithms for classification of Argentine white wines according grape variety. *Food Chem*, 184, 214–219.
- Gomidze N., Jabnidze I., Makharadze K., Khajishvili M., Shashikadze Z., Surmanidze Z., Surmanidze I. (2012). Numerical analyses of fluorescence characteristics of watery media via laser spectroscopy *Method. Journal of Advanced Materials Research*, 590, 206-211.
- Gomidze N.K., Makharadze K.A., Khajishvili M.R., Jabnidze I.N., & Shashikadze Z.K. (2014). Some issues of fluorescence characteristics aqueous media via diagnosis of laser spectroscopy method. *International Journal of Engineering, Science and Innovative Technology*, 3(3), 142-152.
- Gomidze N.K., Jabnidze I.N., & Surmanidze Z.J. (2016). Stroboscopic method of fluorescence analyses of optically solid media. *IEEE 7th International Conference on Advanced Optoelectronics and Lasers (CAOL)*. September 12-15, Odessa, Ukraine, (pp. 34-36).
- Gomidze N., Shainidze J., Shengelia G., & Turmanidze R. (2018). To the problems of fluorescence excitation spectrums. *Machines. Technologies. Materials.*, 12(7), 279-282.
- Khajishvili M.R., Gomidze N.K., & Shainidze J.J. (2021). 3D fluorescence spectroscopy of liquid media via internal reference method. In *International Conference on Global Research and Education* (pp. 59-71). Singapore: Springer Singapore.
- Urbano M., Luque de Castro, M. D., Pérez, P. M., García – Olmo, J. & Gómez – Nieyo, M. A. (2006). Ultraviolet – visible spectroscopy and pattern recognition methods for differentiation and classification of wines. *Food Chem*, 97(1), 166–175.
- Wold S. (1976). Pattern recognition by means of disjoint principal components models. *Pattern Recognit*, 8, 127–139.

Author Information

Miranda Khajishvili

Batumi Shota Rustaveli State University
35/32, Ninoshvili/Rustaveli str., Batumi,
Georgia Contact e-mail: mirandukht@gmail.com

Jaba Shainidze

Batumi Shota Rustaveli State University
35/32, Ninoshvili/Rustaveli str., Batumi, Georgia

Kakha Makharadze

Batumi Shota Rustaveli State University
35/32, Ninoshvili/Rustaveli str., Batumi, Georgia

Nugzar Gomidze

Batumi Shota Rustaveli State University
35/32, Ninoshvili/Rustaveli str., Batumi, Georgia

To cite this article:

Khajishvili, M., Shainidze, J., Makharadze, K. & Gomidze, N. (2023). On the development of the fluorescence excitation-emission etalon matrix algorithm of wine. *The Eurasia Proceedings of Science, Technology, Engineering & Mathematics (EPSTEM)*, 23, 93-99.

The Eurasia Proceedings of Science, Technology, Engineering & Mathematics (EPSTEM), 2023

Volume 23, Pages 100-105

ICRETS 2023: International Conference on Research in Engineering, Technology and Science

Green Hydrogen from PV-Supplied Sono-Electrolysis: Modelling and Experimental Investigations of the Mechanism and Performance

Nour Hane Merabet

Karlsruhe University of Applied Sciences

Kaouther Kerboua

National Higher School of Technology and Engineering

Abstract: Water and energy are the two most essential assets for a sustainable global human society. However, the high carbon footprint and global warming effects caused by non-renewable sources have made energy transition a key element to ensure sustainable development. Currently, hydrogen produced from water supplied by renewable energy is considered an ideal and sustainable energy carrier for the future. Herein, we investigate experimentally and theoretically using MatLab modeling the production of hydrogen via PV supplied alkaline electrolysis of water coupled to 40 kHz ultrasonic bath. Nickel plates and nickel foam were used as electrode's material immersed in 25% of KOH electrolyte while a 12V solar panel was used as a green source of power supply. The experimental and the modeling results related to the ultrasounds effect on hydrogen production efficiency showed a high agreement. The integration of ultrasound showed a reduction in electrode coverage by bubbles of approximately 54.8%, which was equivalent to 9.32% of the reduction in cell voltage according to the experiments.

Keywords: Sonoelectrolysis, Green hydrogen, Solar hydrogen, Ultrasound, Electrode coverage, Resistance.

Introduction

As the intergovernmental panel climate change's IPCC's latest report makes clear, while the temperature continues to rise, the risk of catastrophic events increases. Therefore, the transition to cleaner sources of energy is seen as an imperative step in order to reduce the carbon footprint of fossil fuels and conventional sources of energy (Hofrichter et al., 2022). Strategies for producing hydrogen that rely on renewable energy sources have been developed and implemented. Where the dispersion of ozone-depleting substances is also prohibited in these strategies (Gopinath & Marimuthu, 2022). In previous studies, the modelling and dimensioning of plants with hydrogen production from renewable energy sources such as PV have been investigated (Maurer et al., 2022).

The various established methods of solar hydrogen production use water as the critical reactant, as water separation produces oxygen and hydrogen (Burton et al., 2020). In addition, hydrogen production from water electrolysis is seen as a promising technology to produce hydrogen with high purity of 99.99% (Kerboua & Merabet, 2023).. Membrane free electrolyzers, with potential advantages in durability and manufacturability made possible by eliminating membranes or diaphragms from the device architecture, offer an attractive approach to reducing the cost of hydrogen (H₂) production from water electrolysis (Pang et al., 2020). With easier device designs that can be made from fewer components, membraneless electrolyzers have the potential to reduce material and assembly costs (Esposito, 2017). However, the increase of the ohmic resistance in the electrolyte remains a challenge for the electrolytic technique, as bubble formation limits the operating current density in alkaline water electrolysis, increases electrolyte resistance and reduces electrode active area (Marini et al., 2012).

- This is an Open Access article distributed under the terms of the Creative Commons Attribution-Noncommercial 4.0 Unported License, permitting all non-commercial use, distribution, and reproduction in any medium, provided the original work is properly cited.

- Selection and peer-review under responsibility of the Organizing Committee of the Conference

© 2023 Published by ISRES Publishing: www.isres.org

It has been reported in literature that the integration of ultrasonic power has an improvement effect on mass transport enhancement due to the combined effect of microjets and microstreaming (Islam et al., 2020) and the efficient bubble removal from the electrode's surface (Li et al., 2009; Walton et al., 1996; Zadeh, 2014). In this context, it has been demonstrated very recently using modeling that the ohmic resistance and bubble coverage may be reduced due to the shockwave and microjets phenomena related to the ultrasound propagation in the electrolyte medium (Kerboua & Merabet, 2023).

The aim of the present study is to investigate experimentally and numerically the effect of ultrasound on the removal of bubbles from the electrode surface and to quantify the ultrasound effect on the fraction of the electrodes' area covered by bubbles, and hence the bubble and ohmic resistances, under a source of current, namely a PV solar panel as a source supplying a membraneless KOH electrolyzer.

Material and methods

Membraneless Sono-Electrolyzer

An H-cell electrolyzer of 300 mL of total capacity was filled with 25% of KOH aqueous solution. The electrolyzer counts nickel plates or nickel foam electrode's material of 13.5 cm² of working area. As a source of indirect continuous sonication, an ultrasound bath of 40 kHz and 60W_e has been employed.

Pv Solar Supply

The power supply consists of a 30 W monocrystalline solar photovoltaic panel (ET Solar-ET- M53640) connected to a Maximum Power Point Tracking regulator MPPT.

MatLab Modeling

The MatLab code is first based on the mathematical modeling of the PV supply, delivering a current I according to Eq.1 (Rahim et al., 2015; Villalva et al., 2009)

$$I = I_{pv} - I_d - I_{sh} \quad (1)$$

$$I_{pv} = \frac{(I_{pv0} + K\Delta T) G}{G_0} \quad (2)$$

$$I_d = I_0 \left(e^{\left(\frac{R_s I + V}{V_t a} \right)} - 1 \right) \quad (3)$$

$$I_{sh} = \frac{V + R_s I}{R_p} \quad (4)$$

Where I_{pv} is the light-generated current of the PV cell is directly dependent on the solar irradiation G. As a next step, the produced current is injected to the electrolyser's mathematical model, accounting for Eqs.5 to 9 (Abul Kalam Azad & Khan, n.d.; Mohamed et al., 2016; Tijani et al., 2018).

$$U_{cell} = E_{rev} + U_{act} + U_{ohm} + U_{conc} \quad (5)$$

$$E_{rev}(T, P) = E_{rev}(T) + \frac{RT}{ZF} \ln \left(\frac{P_v^*(P - P_v)^{1.5}}{P_v} \right) \quad (6)$$

$$U_{act} = \frac{2.3026 RT}{ZF a_a} \log \left(\frac{I_a}{I_{0a}} \right) + \frac{2.3026 RT}{ZF a_c} \log \left(\frac{I_c}{I_{0c}} \right) \quad (7)$$

$$U_{ohm} = I(R_{cell} + R_{electrodes} + R_{electrolyte} + R_{electrical}) \quad (8)$$

$$U_{conc} = \frac{RT}{ZF} \left(\ln \left(1 - \left(\frac{I}{I_{lim}} \right) \right) \right) \quad (9)$$

Where E_{rev} is the reversible voltage, U_{act} is the activation voltage, U_{ohm} is the ohmic voltage and U_{conc} is the concentration voltage.

The effect of sonication was evaluated according to the electrode coverage by bubbles that govern the ohmic resistance as shown in Eqs.10 to 12 (Gambou et al., 2022).

$$R_{electrolyte} = R_{bf} + R_b \quad (10)$$

$$R_{bf} = \frac{1}{\sigma_{bf}} \left(\frac{d_a}{S_a} + \frac{d_c}{S_c} \right) \quad (11)$$

$$R_b = R_{bf} \left(\frac{1}{\left(1 - \frac{2}{3}e \right)^{1.5}} - 1 \right) \quad (12)$$

S_a and S_c are anode and cathode cross sections respectively, d_a and d_c are distances from anode and cathode to membrane, σ_{bf} is the bubble-free electrolyte conductivity.

Results and Discussion

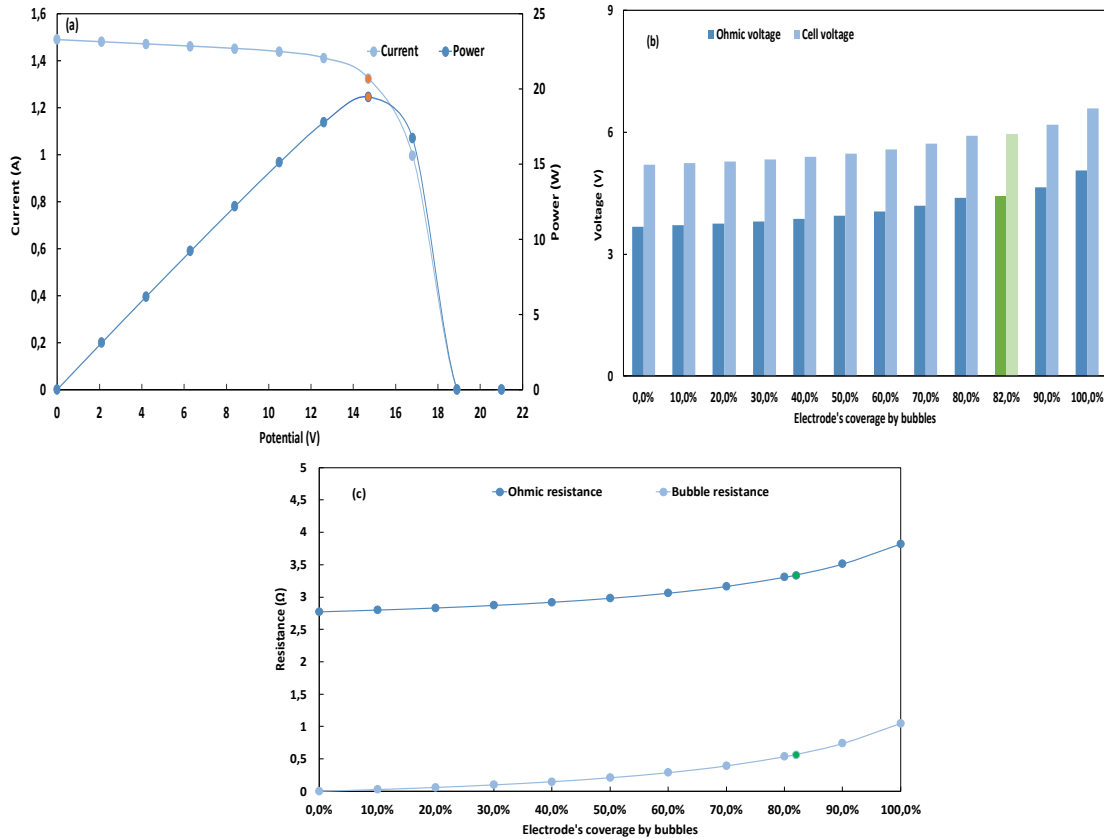


Figure 1. Simulated I-V and P-V characteristics of the solar panel feeding the electrolyzer under real solar radiation (a) and the effect of the electrodes' coverage by bubbles on the ohmic and cell voltage (b) and ohmic and bubble resistance (c) in silent conditions

Figure.1 presents the results of simulation under silent conditions and a solar irradiation of 827 W/m^2 . Based on the polarization curve of the panel controlled by an MPPT controller, the performance of the PV panel is first described in Fig.1 (a) where the numerically obtained current-voltage I-V and power-potential P-V curves are described both with the maximum power point and its equivalent current and potential. Maximum power delivered corresponds to $19,481 \text{ W}$, corresponding to a voltage of $14,7 \text{ V}$ and a current of $1,325 \text{ A}$. Use of MPPTs allows to maintain input current at a steady value during electrolysis, avoiding any effect of intermittent photovoltaic power.

Both the obtained ohmic overpotential and the electrolysis potential depend on the percentage of electrode coverage, as shown in Fig.1 (b), it can be observed that, when the percentage of electrode coverage varies between 0 and 100%, the electrolysis cell studied develops a total potential ranging from 5.2386 to 6.5946 V (with an increase of 25.88%). The ohmic overpotential rises as well, with the above-mentioned variation of the e factor, from 3.6728 to 5.0650 V , which corresponds to 68.93% to 76.81% of the value of the total potential. According to the experimental resulting voltage that consist of cell potential of 5.9571 V , To meet the corresponding electrode coverage equals 81.98% and is represented in green color in Fig.1 (b). Accordingly, the ohmic overpotential characterizing the studied configuration is 4.4275 V .

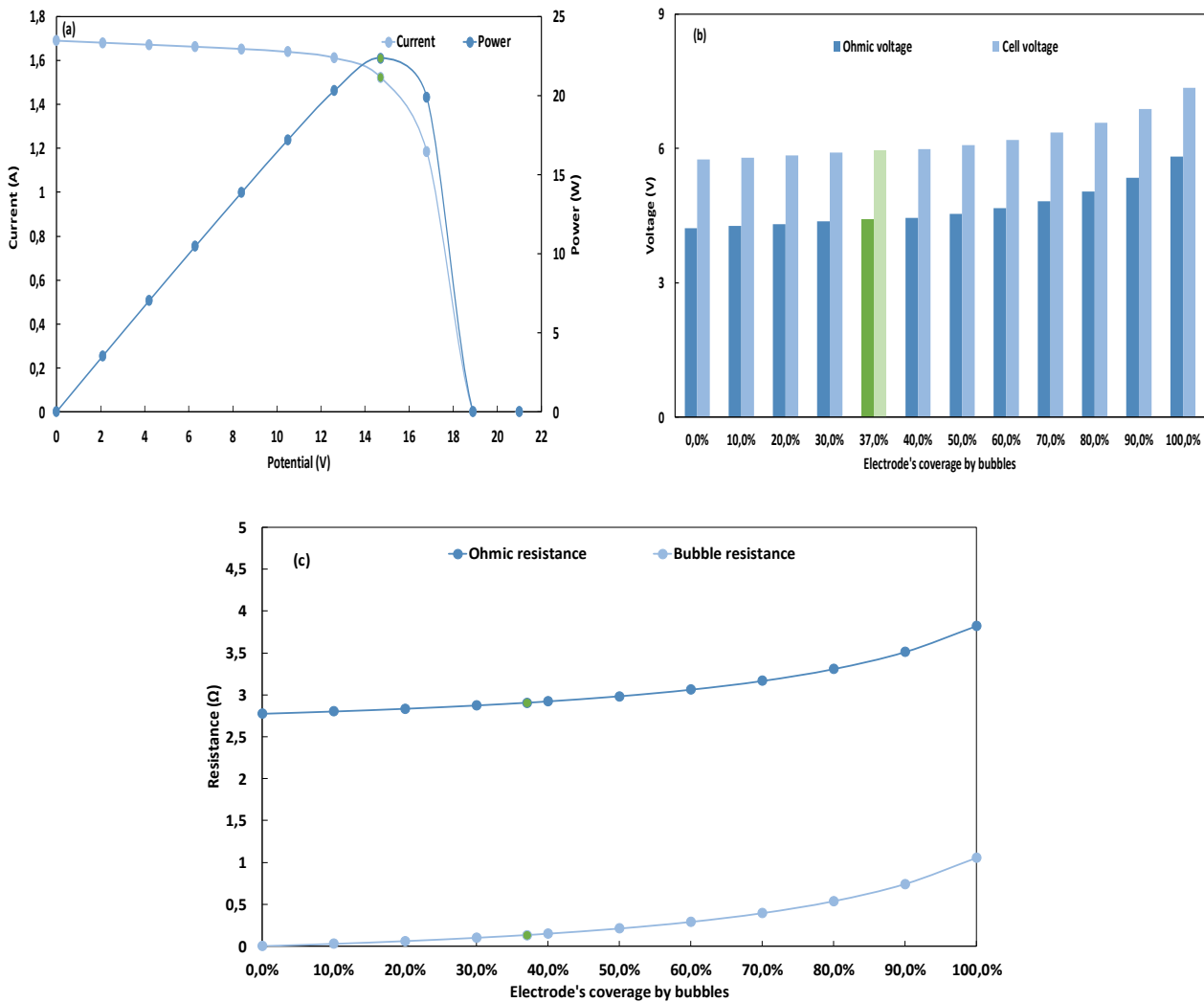


Figure 2. Simulated I-V and P-V characteristics of the solar panel feeding the electrolyzer under real solar radiation (a) and the effect of the electrodes' coverage by bubbles on the ohmic and cell voltage (b) and ohmic and bubble resistance (c) under ultrasonic power

The variation of the ohmic and bubble resistances in function of the electrode's bubble coverage is elucidated more specifically in Fig.1 (c), the variation of the e factor from 0 to 100% increases the Ohmic resistance from its lowest value of 2.7714Ω to 3.822Ω . In addition, the bubble resistance that constitutes 27.49% of the Ohmic resistance reaches its maximum value of 1.0505Ω at a 100% of coverage consequence, the same cell potential as that retrieved experimentally with the silent configuration under a lower incident radiation and a higher

current were recorded. From Fig.2(a), it is clear that the maximum power equals 22.39 W and is achieved at a panel current of 1.523 A and a deliverable potential of 14.7 V. Thus, with the MPPT regulation, the electrolyzer is supplied with a direct current of 1.523 A.

Fig.2(b) presents the evolutions of the overall cell voltage and the Ohmic overpotential as a function of the electrodes' coverage percentage under the continuous ultrasound conditions. When the e factor is increased from 0 to 100%, the cell potential increases from 5.7558V to 7.3559V. The ohmic overpotential constitutes the major part of the cell potential, with a proportion ranging between 73.34% and 79.14%. while Experimental cell potentials measured under continuous sonication conditions were obtained for an electrode coverage of 30 to 40 %.

The simulation with a linear step on the value of e allowed the determination of the percentage of electrode coverage corresponding to the measured cell potential, i.e. 5.9577 V. This value corresponds to 37%, its associated ohmic overpotential is 4.4232 V, which corresponds to 2.904 Ω . In this case, as shown in Fig.7 (b), the bubble resistance is limited to 132.54m Ω , whereas it reaches 1.0505m Ω with 100% electrode coverage.

Conclusion

The effect of sonication on the bubble resistance and hence the ohmic resistance in a membraneless H-cell alkaline electrolyzer fed by PV has been studied experimentally and numerically in the present study. The combined experimental and fundamental modelling approach was based on the variation of the ohmic resistance parameters as a function of the coverage of the electrodes by bubbles, which was assumed to be reduced in the presence of sonication due to streaming, microjets and shockwaves.

The lowest electrode coverage was achieved with indirect continuous sonoelectrolysis, with a value of 37%, compared to 82% under silent conditions which corresponds to a reduction of approximately 54.8%. The resulting bubble resistance ranged from 569.81 m Ω in the absence of ultrasound to 132.54 m Ω with integrated continuous sonication. In fact, it is assumed that ultrasound results in a stirring effect in the bulk electrolyte and near the surface of the electrode, promoting the desorption of gas bubbles from the electrode.

Scientific Ethics Declaration

The authors declare that the scientific ethical and legal responsibility of this article published in EPSTEM journal belongs to the authors.

Acknowledgements or Notes

This article was presented as an oral presentation at the International Conference on Research, Engineering and Technology (www.icrets.net) held in Budapest/Hungary on July 06-09 2023.

References

- Azad, A. K., & Khan, M. M. K. (Eds.). (2021). *Bioenergy Resources and Technologies*. Academic Press.
- Burton, N. A., Padilla, R. V, Rose, A., & Habibullah, H. (2020). Increasing the efficiency of hydrogen production from solar powered water electrolysis. *Renewable and Sustainable Energy Reviews*, 135(08), 110255.
- Esposito, D. V. (2017). Membraneless electrolyzers for low-cost hydrogen production in a renewable energy future. *Joule*, 1(4), 651–658.
- Gambou, F., Guilbert, D., Zasadzinski, M., Rafaralahy, H., Gambou, F., Guilbert, D., Zasadzinski, M., Rafaralahy, H., Gambou, F., Guilbert, D., Zasadzinski, M., & Rafaralahy, H. (2022). A comprehensive survey of alkaline electrolyzer modeling: electrical domain and specific electrolyte conductivity. *Energies*, 15(9), 3452.
- Gopinath, M., & Marimuthu, R. (2022). A review on solar energy-based indirect water-splitting methods for hydrogen generation. *International Journal of Hydrogen Energy*, 47(09), 37742–37759.
- Hofrichter, A., Rank, D., Heberl, M., & Sterner, M. (2022). Determination of the optimal power ratio between

- electrolysis and renewable energy to investigate the effects on the hydrogen production costs. *International Journal of Hydrogen Energy*, 48(5), 1651-1663.
- Islam, M. H., Lamb, J. J., Burheim, O. S., & Pollet, B. G. (2020). Ultrasound-assisted electrolytic hydrogen production. In *Micro-Optics and Energy: Sensors for Energy Devices* (pp. 73–84), Springer Nature
- Kerboua, K., & Merabet, N. H. (2023). Sono-electrolysis performance based on indirect continuous sonication and membraneless alkaline electrolysis: Experiment, modelling and analysis. *Ultrasonics Sonochemistry*, 96(2), 106429.
- Li, S. De, Wang, C. C., & Chen, C. Y. (2009). Water electrolysis in the presence of an ultrasonic field. *Electrochimica Acta*, 54(15), 3877–3883.
- Marini, S., Salvi, P., Nelli, P., Pesenti, R., Villa, M., Berrettoni, M., Zangari, G., & Kiros, Y. (2012). Advanced alkaline water electrolysis. *Electrochimica Acta*, 82(05), 384–391.
- Maurer, W., Rechberger, P., Justl, M., & Keuschnigg, R. (2022). Parameter study for dimensioning of a PV optimized hydrogen supply plant. *International Journal of Hydrogen Energy*, 47(10), 40815–40825.
- Mohamed, B., Ali, B., Ahmed, B., Ahmed, B., Salah, L., & Rachid, D. (2016). Study of hydrogen production by solar energy as tool of storing and utilization renewable energy for the desert areas. *International Journal of Hydrogen Energy*, 41(45), 20788–20806.
- Merabet, N. M., & Kaouther Kerboua, O. H. (2023). Converting PV solar energy to green hydrogen. In *Reference Module in Earth Systems and Environmental Sciences* (pp. 1–10). Elsevier
- Pang, X., Davis, J. T., & Esposito, D. V. (2020). Framework for evaluating the performance limits of membraneless electrolyzers. *Energy and Environmental Science*, 13, 3663–3678.
- Rahim, A. H. A., Salami, A., Fadhlullah, M., Hanapi, S., & Sainan, K. I. (2015). Optimization of direct coupling solar PV panel and advanced alkaline electrolyzer system. *Energy Procedia*, 79, 204–211.
- Tijani, A. S., Afiqah, N., & Kamarudin, B. (2018). Investigation of the effect of charge transfer coefficient (CTC) on the operating voltage of polymer electrolyte membrane (PEM) electrolyzer. *International Journal of Hydrogen Energy*, 43(19), 9119-9132.
- Villalva, M. G., Gazoli, J. R., & Filho, E. R. (2009). Comprehensive approach to modeling and simulation of photovoltaic arrays. *IEEE Transactions On Power Electronics*, 24(5), 1198–1208.
- Walton, D. J., Burket, L. D., & Murphy, M. M. (1996). Sono-electrochemistry :Chlorine, hydrogen and oxygen evolution at platinised platinum. *Electrochimica Acta*, 41(17), 2747–2751.
- Zadeh, S. H. (2014). Hydrogen production via ultrasound-aided alkaline water electrolysis. *Automation and Control Engineering*, 2(1), 103-109

Author Information

Nour Hane Merabet

Center of Applied Research, Karlsruhe University of Applied Sciences, Moltkestr, 30, 76133 Karlsruhe, Germany

National Higher School of Technology and Engineering, 23005 Annaba, Algeria
Laboratory of Technologies of Energetic Systems
E3360100, 23005 Annaba, Algeria
Contact e-mail:n.merabet@esti-annaba.dz

Kaouther Kerboua

National Higher School of Technology and Engineering, 23005 Annaba, Algeria

To cite this article:

Merabet N. H. & Kerboua K. (2023), Green hydrogen from PV-supplied sono-electrolysis: Modelling and experimental investigations of the mechanism and performance. *The Eurasia Proceedings of Science, Technology, Engineering & Mathematics (EPSTEM)*, 23, 100-105.

The Eurasia Proceedings of Science, Technology, Engineering & Mathematics (EPSTEM), 2023

Volume 23, Pages 106-116

ICRETS 2023: International Conference on Research in Engineering, Technology and Science

SaaS Model Assessment- A DEA Approach

Thi Minh Nhut Vo

National Kaohsiung University of Science and Technology

Chia-Nan Wang

National Kaohsiung University of Science and Technology

Fu-Chiang Yang

National Kaohsiung University of Science and Technology

Van Thanh Tien Nguyen

Industrial University of Ho Chi Minh City

Abstract: The Software as a Service (SaaS) industry is expected to experience growth in the coming years for these reasons. These include the rising demand for affordable and adaptable software solutions, the popularity of cloud computing, and the increasing trend of work. In a study comparing the 11 SaaS providers using DEA SBM analysis Aspen Technology Inc, HubSpot Inc, Rapid 7 Inc, and Ring Central emerged as the most efficient company. These research findings offer a framework to assess the efficiency of leading SaaS providers. By adopting this approach, businesses across sectors can gain insights into market trends, identify opportunities that drive digital transformation efforts, and foster creativity. Individuals interested in this field can leverage this methodology to evaluate the success of leading SaaS companies.

Keywords: SaaS model Assessment, Software as a Service industry, A DEA Approach, DEA SBM analysis.

Introduction

Thanks to the increasing need for affordable, scalable, and flexible software solutions, the Software as a Service (SaaS) sector has progressed. As cloud computing becomes remote work gains momentum, businesses of all sizes rely on SaaS offerings to access advanced technologies without the burden of heavy infrastructure investments. In this SaaS landscape, it is crucial to evaluate the efficiency and performance of SaaS providers to identify key players and drive innovation in the industry. Therefore, this study aims to assess the efficiency of 11 SaaS companies using the Slack Based Measure (SBM) methodology. The growth trajectory of the SaaS industry has been remarkable over the decade. It shows no signs of slowing down. Several factors have contributed to this expansion and reshaped how businesses operate. Firstly, there is a growing demand for cost-adaptable software solutions that offer flexibility, seamless updates, and easy accessibility through cloud-based applications.

The shift towards SaaS offerings of software models has been beneficial for businesses in terms of reducing IT infrastructure costs and providing scalability and user-friendly interfaces. Cloud computing has revolutionized how businesses function by enabling data storage and access from an internet connection. This transformation has made SaaS a choice for companies aiming to streamline operations and thrive in today's dynamic business landscape. The rise in work has dramatically impacted on the SaaS market. With more employees working from home or remote locations, cloud-based collaboration, and productivity tools are demanded. SaaS applications

- This is an Open Access article distributed under the terms of the Creative Commons Attribution-Noncommercial 4.0 Unported License, permitting all non-commercial use, distribution, and reproduction in any medium, provided the original work is properly cited.

- Selection and peer-review under responsibility of the Organizing Committee of the Conference

© 2023 Published by ISRES Publishing: www.isres.org

like project management, communication, and file-sharing platforms have become essential for seamless team collaboration. They are maintaining productivity across dispersed teams.

Assessing the efficiency of SaaS providers is crucial as the industry continues to expand, with providers competing for market share. Businesses need to understand the efficiency of these providers to make informed decisions when selecting software solutions that align with their needs, budget, and growth plans. SaaS providers that operate efficiently can provide value for the price, exceptional customer support, and seamless integration with existing business processes. Furthermore, investors and industry analysts find these evaluations valuable as they understand SaaS companies' stability and growth potential. Identifying SaaS providers enables investors to make informed investment choices while industry analysts can predict trends and foresee changes in the market.

The primary objective of this study is to evaluate the efficiency of 11 prominent SaaS providers using the Slack Based Measure (SBM) methodology. The SBM approach, specifically DEA with the BCC model, allows for a comprehensive assessment by considering multiple inputs and outputs, thus providing a holistic view of each company's efficiency. Through this analysis, we aim to identify the most efficient SaaS provider, uncover the key factors contributing to their efficiency, and understand potential areas of improvement for other providers. The findings of this study will offer businesses across sectors a framework to assess leading SaaS providers, empowering them to make data-driven decisions while selecting software solutions. Furthermore, individuals interested in the SaaS industry can leverage this methodology to evaluate the success and efficiency of various SaaS companies in their pursuit of digital transformation and innovation.

Literature Review

In this paper, we aim to explore the various studies that have applied DEA-SBM to assess the efficiency of SaaS providers. By examining the methodologies, data sources, and findings of these studies, we seek to uncover the factors contributing to the efficiency of successful SaaS companies and understand the implications of inefficiency in others.

Kalantary et. al., 2019 Introduce a network dynamic DEA model to assess the sustainability of supply chains in multiple periods (Kalantary, Saen, & Engineering, 2019). While several prominent network DEA models have been proposed in the literature in multiplier and envelopment forms, it is still doubtful or unclear whether and how the exact primal-dual correspondence can be retained between the two types of network DEA models as in the standard DEA. To address this issue Lim et. al., 2019 develop an axiomatic derivation of some two-stage network DEA models focusing on the basic two-stage serial process structure(Lim & Zhu, 2019). Wang et. al., 2019 proposes a hybrid super-efficiency DEA model which combines hybrid DEA with super-efficiency DEA, separating the input and undesirable output variables into radial and non-radial parts using variable correlations Geng et. al., 2019 focus on energy efficiency evaluation and energy saving based on dea integrated affinity propagation clustering: a case study of complex petrochemical industries(Geng, Zeng, Han, Zhong, & Fu, 2019). A novel DEA model is proposed based on the affinity propagation (AP) clustering algorithm (AP-DEA). Kaffash et. al., 2020 analyze 132 DEA application studies in the insurance industry published from 1993 through July 2018, covering both applications and methodologies(Kaffash, Azizi, Huang, & Zhu, 2020). Mahmoudi et. al., 2020 present a literature review and classification of the applications of DEA in transportation systems (TSs)(Mahmoudi, Emrouznejad, Shetab-Boushehri, & Hejazi, 2020). (hu, 2020 propose that data envelopment analysis (DEA) should be viewed as a method (or tool) for data-oriented analytics in performance evaluation and benchmarking(Zhu, 2022). Youn et. al., 2020 review four popular subjects for applying DEA: soft robot hand, locomotion robots, wearable devices, and tunable optical components(Youn et al., 2020). Arana-Jiménez et. al., 2020 deal with the problem of efficiency assessment using Data Envelopment Analysis (DEA) when the input and output data are given as fuzzy sets(Arana-Jiménez, Sánchez-Gil, Lozano, & Mathematics, 2022). The purpose of Fathi et. al., 2021 is to examine the energy, environmental, and economic (E3) efficiency in fossil fuel exporting countries during 2015-2017, using traditional Data Envelopment Analysis (DEA) and a bargaining game cross-efficiency DEA approach(Fathi, Ashena, Bahari, & Consumption, 2021).

By synthesizing and analyzing the existing literature on the use of DEA-SBM in assessing SaaS providers, we aim to provide a comprehensive understanding of the benefits and limitations of this approach. Furthermore, it will pave the way for our empirical study, which applies DEA-SBM to evaluate the efficiency of 11 leading SaaS companies, contributing to the body of knowledge in both DEA methodology and the SaaS industry.

Methodology

Data Collection and Selection of SaaS Providers

To begin the efficiency assessment of SaaS providers using Data Envelopment Analysis (DEA) with the Slack Based Measure (SBM) approach we must first. Choose data carefully. In this analysis our focus is, on evaluating the efficiency of 10 known SaaS companies, from the Decision Making Unit (DMU) mentioned in table 1.

Table 1. List of 10 selected SaaS Companies

DMU	Company name
S1	Aspen Technology Inc
S2	BigCommerce Holdings Inc
S3	Cloudflare Inc Net
S4	Crowdstrike Holdings
S5	Fiverr International Ltd
S6	Futu Holdings Ltd
S7	Hubspot Inc
S8	Jamf Holding Corp
S9	Rapid 7 Inc
S10	Ring Central

The application of DEA-SBM on this selected set of companies will provide valuable insights into their operational efficiency, potentially identifying best practices and areas for improvement within the SaaS market.

Explanation of the DEA SBM (Slack Based Measurement) Model

The SBM model, known as the Slacks Based Measure is a recognized approach used in efficiency analysis and performance evaluation. SBM model is one of the variations of the DEA technique—a non parametric method employed to assess the relative efficiency of decision making units (DMUs). The SBM model was introduced by Tone (2001) (see also Pastor et al. (1999)) (Tone & Sahoo, 2004) . It has three variations, i.e., input-, output- and non-oriented. The non-oriented model indicates both input- and output-oriented. The production possibility set is determined by utilizing the combinations of DMUs, in set J ensuring that all values are non negative.

$$P = \{(x, y) | x \geq \sum_{j=1}^n \beta_j x_j, 0 \leq y \leq \sum_{j=1}^n \beta_j y_j, \beta \geq 0\} \quad (1)$$

$\beta_j = (\beta_1, \beta_2, \dots, \beta_n)^T$ Is called the intensity vector

In order to convert the inequalities in equation (1) into equalities we can introduce slacks for the J in the manner;

$$x = \sum_{j=1}^n \beta_j x_j + s^-$$

$$y = \sum_{j=1}^n \beta_j y_j - s^+$$

$$s^- \geq 0, s^+ \geq 0,$$

The slacks that are denoted as Where $s^- = (s^-_1, s^-_2, \dots, s^-_m) \in R^m$ and $s^+ = (s^+_1, s^+_2, \dots, s^+_m) \in R^S$ respectively are referred to as input and output slacks.

Variables Considered in the Assessment

When evaluating a company's performance and effectiveness there are important factors to consider such as, Total Assets, Liabilities, Equity and Profit. These factors play a role in assessing the company's well being, stability and profitability. Lets explore each of these factors in detail;

Total Assets: Total Assets encompass all the resources owned by a company. These resources can be assets like buildings, equipment, inventory and cash well as intangible assets like patents, trademarks and goodwill. Total Assets provide a view of the company's operations size and extent. Investors, creditors and stakeholders need to understand the company's asset base and its potential to generate revenue.

Liabilities: Liabilities refer to a company's debts and financial obligations which include loans accounts payable and other forms of debt. Liabilities represent the claims that creditors have on the company's assets. Evaluating a company's liabilities is crucial for understanding its risk and its ability to meet commitments. It helps determine how dependent the company is, on financing and whether it can effectively manage its debt load.

Equity: Equity also referred to as Shareholders Equity or Owners Equity represents the remaining interest, in a company's assets after deducting its liabilities. It signifies the ownership stake that shareholders possess in the company. Equity reflects the worth of the company. Indicates the amount shareholders would receive if all assets were sold and all debts were settled. Positive equity signifies a position whereas negative equity raises concerns as it suggests that liabilities outweigh assets.

Profit: Profit refers to the gain attained by a company through its operations after subtracting all expenses including costs related to goods sold operational expenses, interest, taxes and other relevant costs(C.-N. Wang, Yang, Vo, & Nguyen, 2023). Profit serves as an indicator of a company's performance and its ability to generate returns for shareholders. It takes forms such as Gross Profit, Operating Profit and Net Profit (the figure after deducting all expenses). The sustainability of profits is vital for long term viability and growth of a company. These variables form the foundation of analysis. Play significant roles in various financial ratios and metrics. Some used financial ratios involving these variables include(Nguyen, Wang, Yang, & Vo, 2022).

Debt, to Assets Ratio;The debt, to equity ratio is a measure that shows the proportion of a company's assets financed by debt. It compares the liabilities of the company to its shareholders equity, which gives us an idea of the level of leverage. Another important metric is the return on assets (ROA) which tells us how effectively a company utilizes its assets to generate profit. Additionally we have the return on equity (ROE) which helps evaluate the profitability of a company to its shareholders equity. To sum it up when assessing a company's position, performance and overall stability it is crucial to analyze variables such as assets, liabilities, equity and profit as they provide valuable insights.

Table 2 provides data statistics, for both the input and output. These statistics encompass a range of measures that describe the characteristics and performance of the decision making units (DMUs) being evaluated. DMUs can take forms, such as companies organizations, departments or any other units that are being compared in terms of efficiency or performance.

Table 2. Statistics on Input/Output Data

	Total assets	Liabilities	Equity	Profit
Max	101538.51	80552.955	20985.559	5909.256
Min	555.46	417.172	-125.995	171.376
Average	11711.447	9133.0131	2578.4341	1096.0654
SD	29950.169	23813.377	6144.5616	1634.0856

In Table 3 you will find a matrix that shows the correlation coefficients, which helps us measure the relationship between pairs of variables in a dataset. Correlation tells us about the strength and direction of the connection between two variables revealing how they tend to change. This is a tool we use to determine how dependent or independent different variables are from each other, in a dataset.

Table 3. Correlation

	Total Assets	Liabilities	Equity	Profit
Total Assets	1	0.9999331	0.9989948	0.9848491
Liabilities	0.9999331	1	0.9984095	0.9847212
Equity	0.9989948	0.9984095	1	0.9840999
Profit	0.9848491	0.9847212	0.9840999	1

Results and Findings

Efficiency Scores of the 11 SaaS Providers under DEA SBM Analysis

The Efficiency scores of the 11 Software, as a Service (SaaS) providers in the DEA SBM analysis indicate how efficient they are compared to the performing SaaS provider or benchmark in the dataset. The DEA SBM analysis helps assess how well multiple decision making units (in this case SaaS providers) utilize inputs to generate outputs (Kler et al., 2022).

These Efficiency scores range from 0 to 1. A score of 1 means a SaaS provider is fully efficient operating at the level as the benchmark. On the hand a score of 0 indicates inefficiency. Scores between 0 and 1 show varying degrees of inefficiency relative to the benchmark with values to 1 representing efficiency. To calculate each SaaS providers efficiency score we compare its input output relationship with that of the benchmark. If a providers ratios match or exceed those of the benchmark it receives an efficiency score of 1. Conversely if its ratios are worse than the benchmark it receives a score below 1 indicating its level of inefficiency.

In Table 4 you can find the efficiency scores of 11 companies that offer Software, as a Service (SaaS). These scores were determined through a performance analysis technique, like Data Envelopment Analysis (DEA) or its variant the DEA SBM (Slacks Based Measure) model.

Table 4. Efficiency score of 11 SaaS Companies

No.	DMU	Score	Rank
1	DMU1	1	1
2	DMU2	0.62109	5
3	DMU3	0.43569	8
4	DMU4	0.47564	7
5	DMU5	0.54183	6
6	DMU6	0.11918	10
7	DMU7	1	1
8	DMU8	0.38912	9
9	DMU9	1	1
10	DMU10	1	1

DEA SBM analysis offers insights to both SaaS providers and decision-makers. It helps identify areas where inefficient providers can enhance their operations optimize resource utilization and improve performance to achieve levels of efficiency. Additionally it aids in establishing practices through benchmarking and fosters competition, within the SaaS industry(Peng, Wang, Xuan, Nguyen, & Management, 2022).

Comparison of efficiency scores and identification of the most efficient company

If all the companies, including Aspen Technology Inc, HubSpot Inc, Rapid7 Inc and RingCentral have an efficiency score of 1 it means that they are all operating at the level of efficiency, as the benchmark or the efficient company in the dataset. When a company has an efficiency score of 1 it indicates that they are utilizing their resources optimally and achieving their desired outputs without any inefficiencies.

In this scenario, four companies have an efficiency score of 1 indicating that they are equally efficient. Therefore there is no distinction among them in terms of efficiency. All companies are performing at the level. Have effectively utilized their resources to achieve their respective output levels.

When all companies achieve an efficiency score of 1 it signifies that they have reached performance with no room for improvement in their operations.

Aspen Technology Inc; Efficiency Score = 1

HubSpot Inc; Efficiency Score = 1

Rapid7 Inc; Efficiency Score = 1

RingCentral; Efficiency Score = 1

These companies serve as benchmarks for efficiency, within the dataset.

It's important to note that this situation is not very common, in real world scenarios since companies usually have varying levels of efficiency. In cases where all companies have an efficiency score of 1 it could mean that the dataset is small or homogeneous or the analysis fails to capture complexities that could impact efficiency evaluations.

Figure 2 acts as a depiction of the research results highlighting the importance of utilizing the DEA method to assess and compare the performance of SaaS providers. This ranking not helps identify players, in the industry but also provides essential insights for making strategic decisions optimizing resources and promoting innovation, within the SaaS sector.

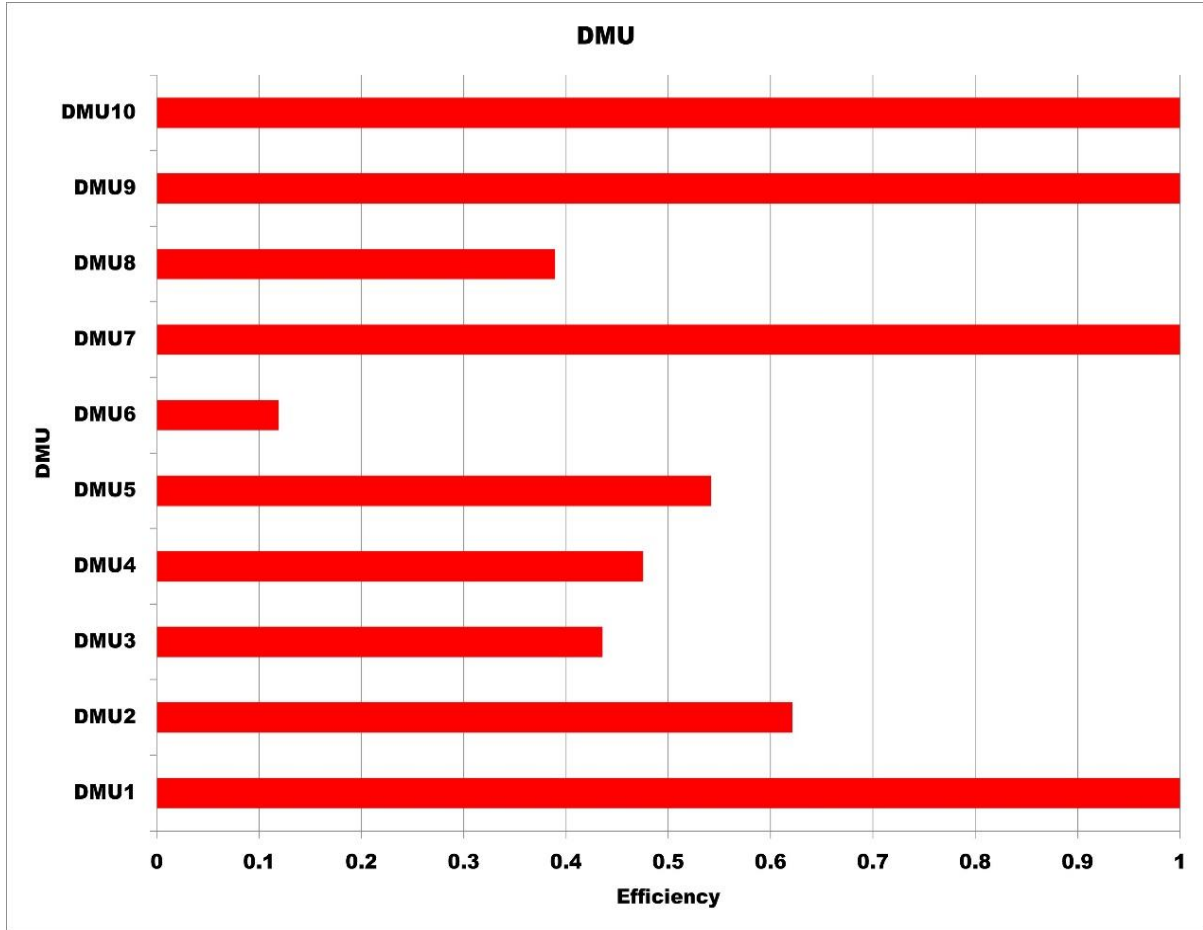


Figure 2. Final ranking of 11 SaaS Companies

To draw conclusions it's crucial to take into account the specific context, underlying assumptions and methodology used for calculating the efficiency scores. Additionally conducting analyses and comparing against industry standards can provide additional insights into how well these companies perform relative, to others in a broader context.

Implications of the Findings for the SaaS Industry

Identification of Best Practices; The analysis of efficiency helps us identify the SaaS companies in the dataset. These performing companies serve as benchmarks. Offer valuable insights into the strategies and practices that lead to higher efficiency. Other companies, in the industry can learn from these practices. Implement them to enhance their own efficiency.

Competition and Innovation; When efficiency scores are revealed it sparks a sense of competition among SaaS providers. Companies with efficiency scores may be motivated to improve their operations optimize resource allocation and innovate in order to catch up with efficient competitors. This drive for improvement fosters increased innovation within the industry as companies strive to gain an edge.

Resource Allocation and Investment Decisions; The findings can have an impact on resource allocation decisions made by investors and stakeholders. Companies with efficiency scores are often seen as investment options leading to increased funding and capital inflow. Conversely companies with efficiency scores may face challenges in attracting investments unless they can demonstrate a plan, for enhancing their efficiency.

Performance Management; Efficiency scores can serve as performance indicators for SaaS companies. Executives and managers can use these scores to evaluate their company's performance compared to competitors and industry benchmarks. It can be beneficial, in establishing performance goals and identifying areas that need improvement.

Market Reputation; SaaS companies with efficiency scores can utilize this information to enhance their market position and reputation. They can highlight their efficiency to attract clients and showcase their ability to provide effective value. Conversely companies with efficiency scores may encounter difficulties in building trust with customers.

Industry Regulation and Standards; The insights gained from analyzing efficiency levels can also grab the attention of bodies and policymakers. This may lead to discussions on industry standards and guidelines aimed at promoting efficiency and fostering competition within the SaaS sector.

Acquisitions; Companies looking to expand or boost their efficiency might consider merging or acquiring firms. Targeting and integrating these companies could help improve performance and market standing.

Customer Perception; The efficiency of SaaS companies has an impact on how customers perceive them and their level of satisfaction. Efficient companies are more likely to deliver services in a cost manner, which can result in customer satisfaction rates and improved customer retention. It can stimulate competition, innovation and advancements in effectiveness benefiting both companies operating within this sector well as their customers.

However it's crucial to incorporate efficiency scores in conjunction, with performance measurements and take into account the industry landscape in order to make informed choices and foster long term sustainable growth.

Discussion

The analysis conducted on Aspen Technology Inc, HubSpot Inc, Rapid7 Inc and RingCentral using the DEA SBM model has given us insights, into how efficient these SaaS providers are. The efficiency scores obtained for each company measure their ability to effectively convert inputs into outputs.

Interpretation of Results; All four SaaS companies (Aspen Technology Inc, HubSpot Inc Rapid7 Inc and RingCentral) have been found to be operating at efficiency with a score of 1. This means that all the companies are performing at the level as the benchmark and utilizing their resources optimally to achieve desired outcomes.

1. Significance; These results hold two implications. Firstly it demonstrates the level of efficiency within this specific subset of the SaaS industry. The fact that all four companies achieved a score of 1 indicates a well optimized sector. Secondly it highlights the potential for practices and operational excellence among these companies serving as an example, for other SaaS providers looking to improve their efficiency.

To gain an understanding of what contributes to the efficiency of Aspen Technology Inc, HubSpot Inc, Rapid7 Inc and RingCentral further analysis is necessary. We should explore factors that could be influencing their efficiency;

The efficiency of SaaS providers can be affected by the technology they use and the quality of their products or services. Companies that offer user friendly solutions tend to attract customers and generate higher output resulting in greater efficiency.

2. Infrastructure; In the SaaS industry it's crucial to have the ability to scale operations efficiently. Companies, with infrastructure and scalable systems can handle increased demand without increasing their inputs. This leads to efficiency.

3. Business Processes; Efficient and streamlined business processes have an impact, on a company's efficiency. When companies optimize their processes and workflows they can better utilize resources. Generate output more effectively.
4. Customer Base and Market Reach; The size and diversity of a company's customer base play a role in its efficiency. Companies that have a market reach and a diverse customer portfolio often enjoy stable revenue streams contributing to their overall efficiency.
5. Organizational Structure; Effective management practices and a organized company can significantly improve efficiency. Companies that have leadership and clear decision making processes are better able to allocate resources

While Aspen Technology Inc, HubSpot Inc, Rapid7 Inc and RingCentral were found to be fully efficient it's important to explore reasons for inefficiencies in other SaaS providers. Some factors that could contribute to these inefficiencies include;

1. Suboptimal Resource Allocation; Inefficient SaaS providers may struggle with allocating their resources. This could be due to planning, a misalignment of resources with business objectives or poor decision making.
2. Lack of Innovation; Companies that fail to keep up with advancements or innovate their products may experience inefficiencies compared to innovative competitors.
3. Market Niche and Competition; Companies operating in markets or specific niches may find it challenging to achieve efficiency due to pricing pressures and the constant need, for differentiation.
4. Poor Customer Retention; Inefficiencies can arise if a company experiences customer churn rates. It is generally more cost effective for companies to retain existing customers than constantly acquiring ones. Ineffective Marketing and Sales Strategies; Companies that have marketing and sales approaches might encounter challenges, in acquiring customers leading to inefficiency.

Regulatory and Compliance Issues; Difficulties in complying with regulations to the industry can result in inefficiencies if not effectively managed. Analyzing the efficiency scores of Aspen Technology Inc, HubSpot Inc Rapid7 Inc and RingCentral provides insights into their excellence. Understanding what factors contribute to their efficiency while also exploring reasons for inefficiencies among SaaS providers can help guide decision making and drive improvements, within the industry.

Limitations

There are challenges when it comes to collecting and analyzing data;

1. Availability of Data; To effectively analyze efficiency using DEA (Data Envelopment Analysis) we require data, on inputs and outputs for each decision making unit. However gathering data can be difficult for complex organizations. Incomplete or missing data can significantly impact the accuracy of the efficiency analysis.
2. Quality of Data; The accuracy and reliability of the data used in DEA analysis are crucial. If the data is inaccurate or unreliable it can lead to results and conclusions. Ensuring the accuracy and consistency of the data poses challenges particularly when dealing with information from sources or units.
3. Subjectivity and Bias; The process of collecting and analyzing data is prone to decisions and biases. Deciding which inputs and outputs should be considered, as selecting a benchmark for comparison may introduce subjectivity that could influence the final efficiency scores.
4. Time and Cost; Collecting and processing data for DEA analysis can be time consuming and expensive. Companies with resources may face challenges when attempting to conduct comprehensive efficiency analyses. One limitation of the DEA SBM (Slack Based Measure) approach is that it assumes no substitution, between inputs and outputs. However in reality companies often adjust their input output mix to enhance efficiency—a factor that this model fails to capture (C.-N. Wang et al., 2023; C.-n. WANG, YANG, VO, & Mathematics, 2022).

Another important point to consider is that the DEA SBM model assumes that all input and output data are predictable and does not take into account uncertainties or random variations. This oversimplification may not accurately reflect the complexities and uncertainties faced by businesses, in the world.

Additionally the DEA SBM model assumes that production technology follows a shape, known as convexity. However there are production technologies that exhibit non convexities which can limit our ability to capture efficiency patterns effectively.

It's worth mentioning that the DEA SBM model does not explicitly distinguish between inefficiency and scale inefficiency. It only attributes inefficiencies to factors while overlooking how scale inefficiency can impact efficiency scores.

Moreover the DEA SBM model can be sensitive to values or outliers in the data. These outliers have the potential to disproportionately influence efficiency scores. Lastly it's important to note that the DEA SBM model is based on a single period analysis and does not account for changes over time. This limitation prevents us from capturing any evolving trends or shifts in efficiencies across time periods.

In summary, while the DEA SBM model offers insights, for efficiency analysis it does have limitations concerning data collection assumptions made and its deterministic approach. Users should keep in mind these limitations. Consider them when interpreting the results and making business decisions based on the DEA analysis. It is also essential to validate the models findings using techniques and take into account the context of each analysis.

Conclusion

The current study emphasizes the role of using the Data Envelopment Analysis (DEA) method to evaluate the effectiveness and performance of Software, as a Service (SaaS) providers. By analyzing known companies like Aspen Technology Inc, HubSpot Inc, Rapid7 Inc and RingCentral the DEA approach reveals that all four entities operate at efficiency with a perfect score of 1. This evidence indicates their utilization of resources to achieve desired outcomes.

The DEA approach has become a tool for businesses, in industries as it offers decision support in assessing performance optimizing resources, benchmarking and making strategic decisions. By leveraging DEA analysis organizations can gain insights into areas that need improvement and identify practices. This enables them to set performance standards aligned with industry norms or top competitors.

Within the SaaS sector implementing the DEA approach brings benefits by promoting efficiency and driving innovation. It helps identify industry leaders and their strategies while fostering competition and streamlining decision making processes(Peng et al., 2022; C. N. Wang, Yang, Nguyen, & Vo, 2022). Notably efficient resource allocation facilitated by DEA analysis empowers SaaS companies to invest in research and development leading to innovation and product enhancement.

Looking ahead at research directions there are areas that deserve further exploration.

To begin with conducting an analysis of SaaS providers using a comprehensive dataset can offer valuable insights into efficiency trends, across the industry. This can help identify areas where improvements can be made. Additionally studying the efficiency of SaaS providers over time periods can reveal performance dynamics and long term changes.

Moreover it would be beneficial to focus research efforts on understanding how specific factors like customer retention strategies, marketing effectiveness or technological innovations impact the efficiency of SaaS companies. Gaining this knowledge would enable companies to optimize their performance and stay competitive. Furthermore future research should not measure efficiency. Also explore its relationship with other key performance indicators like customer satisfaction, revenue growth or market share. Such insights would contribute to an understanding of the factors that contribute to overall business success.

The use of the DEA approach is not essential for evaluating SaaS providers. Also serves as a valuable framework for decision making in the industry. The findings from this research emphasize the significance of

resource utilization and strategic planning in achieving success in today's SaaS landscape. Given the changing nature of the industry it is crucial to conduct research using analytical techniques, alongside the DEA approach. These efforts are sure to spark innovation improve performance and influence the direction of the changing SaaS industry.

Scientific Ethics Declaration

The authors declare that the scientific ethical and legal responsibility of this article published in EPSTEM journal belongs to the authors.

Acknowledgements or Notes

* The authors would like to thank Ministry of Science and Technology, Taiwan. We also would like to thank the National Kaohsiung University of Science and Technology, Industrial University of Ho Chi Minh City, and Thu Dau Mot University for their assistance. Additionally, we would like to thank the reviewers and editors for their constructive comments and suggestions to improve our work.

* This article was presented as an oral presentation at the International Conference on Research in Engineering, Technology and Science (www.icrets.net) held in Budapest/Hungary on July 06-09, 2023.

References

- Arana-Jiménez, M., Sánchez-Gil, M. C., Lozano, S. J. J. O. C (2022). A fuzzy DEA slacks-based approach. *Mathematics*, 404, 113180.
- Fathi, B., Ashena, M., Bahari, A. R. J. S. P. (2021). Energy, environmental, and economic efficiency in fossil fuel exporting countries: A modified data envelopment analysis approach. *Consumption*, 26, 588-596.
- Geng, Z., Zeng, R., Han, Y., Zhong, Y., & Fu, H. J. E. (2019). Energy efficiency evaluation and energy saving based on DEA integrated affinity propagation clustering: Case study of complex petrochemical industries. *Energy*, 179, 863-875.
- Kaffash, S., Azizi, R., Huang, Y., & Zhu, J. J. E. (2020). A survey of data envelopment analysis applications in the insurance industry 1993–2018. *European Journal of Operational Research*, 284(3), 801-813.
- Kalantary, M., & Saen, R. F. J. C. (2019). Assessing sustainability of supply chains: An inverse network dynamic DEA model. *Computers & Industrial Engineering*, 135, 1224-1238.
- Kler, R., Gangurde, R., Elmirzaev, S., Hossain, M. S., Vo, N. V. T., Nguyen, T. V. T., & Kumar, P. N. (2022). Optimization of meat and poultry farm inventory stock using data analytics for green supply chain network. *Discrete Dynamics in Nature and Society*, 2022. Article ID 8970549 <https://doi.org/10.1155/2022/8970549>
- Lim, S., & Zhu, J. J. O. (2019). Primal-dual correspondence and frontier projections in two-stage network DEA models. *Omega*, 83, 236-248.
- Mahmoudi, R., Emrouznejad, A., Shetab-Boushehri, S.-N., & Hejazi, S. R. J. S.-E. P. S. (2020). The origins, development and future directions of data envelopment analysis approach in transportation systems. *Socio-Economic Planning Sciences*, 69, 100672.
- Nguyen, V. T. T., Wang, C. N., Yang, F. C., & Vo, T. M. N. (2022). Efficiency evaluation of cyber security based on EBM-DEA Model. *The Eurasia Proceedings of Science, Technology, Engineering and Mathematics*, 17, 38-44. <https://doi.org/10.55549/epstem.1175908>
- Peng, F., Wang, Y., Xuan, H., Nguyen, T. V. T. (2022). Efficient road traffic anti-collision warning system based on fuzzy nonlinear programming. *International Journal of System Assurance Engineering and Management*, 13(1), 456-461.
- Tone, K., & Sahoo, B. K. J. E (2004). Degree of scale economies and congestion: A unified DEA approach. *European Journal of Operational Research*, 158(3), 755-772.
- Wang, C.-N., Yang, F.-C., Vo, N. T., & Nguyen, V. T. T. (2023). Enhancing Lithium-Ion Battery Manufacturing Efficiency: A Comparative Analysis Using DEA Malmquist and Epsilon-Based Measures. *Batteries*, 9(6), 317.
- Wang, C. N., Yang, F. C., Nguyen, V. T. T., & Vo, N. T. M. (2022). CFD analysis and optimum design for a centrifugal pump using an effectively artificial intelligent algorithm. *Micromachines*, 13(8).
- Youn, J.-H., Jeong, S. M., Hwang, G., Kim, H., Hyeon, K., Park, J., & Kyung, K.-U. J. A. S. (2020). Dielectric

elastomer actuator for soft robotics applications and challenges. *Applied Sciences*, 10(2), 640.
Zhu, J. (2022). DEA under big data: Data enabled analytics and network data envelopment analysis. *Annals of Operations Research*, 309(2), 761-783.

Author Information

Thi Minh Nhut Vo

National Kaohsiung University of Science and Technology, 415 Jiangong, Sanmin, Kaohsiung, Taiwan
Thu Dau Mot University, Vietnam

Chia-Nan Wang

National Kaohsiung University of Science and Technology, 415 Jiangong, Sanmin, Kaohsiung, Taiwan

Fu-Chiang Yang

National Kaohsiung University of Science and Technology, 415 Jiangong, Sanmin, Kaohsiung, Taiwan

Van Thanh Tien Nguyen

Industrial University of Ho Chi Minh City
12, Nguyen Van Bao, Go Vap, Ho Chi Minh City, Vietnam
Corresponding author's contact e-mail: thanhtienck@ieee.org

To cite this article:

Vo, T.M.N., Wang, C.N., Yang, F.C. & Nguyen, V.T.T. (2023). SaaS model assessment- A DEA approach. *The Eurasia Proceedings of Science, Technology, Engineering & Mathematics (EPSTEM)*, 23, 106-116.

The Eurasia Proceedings of Science, Technology, Engineering & Mathematics (EPSTEM), 2023

Volume 23, Pages 117-123

ICRETS 2023: International Conference on Research in Engineering, Technology and Science

Microstructure and Mechanical Properties Analysis of Al-6061/B₄C Composites Fabricated by Conventional and Bobbin Tool Friction Stir Processing

Dhaivat Divekar

Pandit Deendayal Energy University

Kishan Fuse

Pandit Deendayal Energy University

Vishvesh Badheka

Pandit Deendayal Energy University

Abstract: Friction stir processing (FSP) is one of the solid-state processing technique that has gained significant attention from researchers and engineers for fabricating composites. Bobbin tool friction stir processing (BTFSP) is a novel version of conventional FSP. In the present paper, 6 mm thick plates of Al-Mg-Si (6061Al –T6) were subjected to BTFSP and CFSP using B₄C reinforcement particles for comparison. The reinforcement particle distribution and mechanical properties were investigated in the fabricated composites. Agglomeration was observed in BTFSP composites. The crack formation in the BTFSP was due to the absence of forging action, which deposited the B₄C particles in the crack. CFSP composites obtained uniform distribution of the B₄C particles at the top surface. The tilt of the tool in CFSP helped in effective forging action by the shoulder at the trailing edge. Micro-hardness results indicated improved hardness at the top surface for both the processed composites.

Keywords: Friction stir processing, Bobbin tool, Composite, Tilt angle, Microhardness

Introduction

Space applications and automobile industries find aluminium the best choice. The light weight of the parts manufactured from aluminium gives the industries a technical and cost-effective solution (Patidar & Rana, 2017). It has outstanding strength and possesses excellent electrical and thermal properties. Composite materials are replacing conventional materials in industries because of their unmatched elastic modulus, high strength, incredible resistance to fatigue, creep, wear, corrosion, etc. (Jaiswal et al., 2022). Various processes can employ composite fabrication. Some popular techniques to enhance the surface finish are high-energy electron transfer (Kumar et al., 2020), Laser-based surface modification (Quazi et al., 2015), Mechanical alloying (Banhart, 2001), Powder metallurgy (Bains et al., 2016), etc. One such process gaining popularity is Friction Stir Processing (FSP). The fabrication of composite using FSP requires depositing reinforcement particles in the desired region. The rotating FSP tool stirs the metal matrix in the processing region and produces a localized composite structure. The FSP technique has emerged from the Friction Stir Welding (FSW) fundamentals. A unique feature of the FSP is its eco-friendly nature. This makes it the most suitable composite fabrication technique for industries (Teo et al., 2021). The fabrication of the composite using FSP is done significantly through plasisazing of the material, material stirring and mixing, and thermal exposure. Moreover, the FSP leads to homogenous distribution and improved density of the reinforced material in the processed region (Ma, 2008).

- This is an Open Access article distributed under the terms of the Creative Commons Attribution-Noncommercial 4.0 Unported License, permitting all non-commercial use, distribution, and reproduction in any medium, provided the original work is properly cited.

- Selection and peer-review under responsibility of the Organizing Committee of the Conference

© 2023 Published by ISRES Publishing: www.isres.org

Conventional FSP technique has been explored to a great extent in fabricating composites. The size of the grains escalated as there was an increment in the rotation of the tool speed between 300 to 700 rpm during FSP on Al 6063. With incrementing speed, the strength raised slowly and then became more than the BM. Eventually, strain results were all below than BM (Zhao et al., 2019). Hybrid FSP with simultaneous cooling approach enhanced superplastic behavior. Various cooling rates were achieved by introducing varied cooling mediums, such as water and gaseous mediums like compressed air and carbon dioxide, during FSP on AA 7075 alloy (Patel et al., 2019). Al6082 metal matrix was fabricated in composite by adding CaCO₃ particles using FSP to study friction and wear properties. Adding CaCO₃ doubled the wear properties of FSPed Al6082/CaCO₃ composite compared to the FSPed Al6082 (Sivanesh Prabhu et al., 2019).

The rotational speed did not affect much on the tensile strength of the metal. It was recommended that the multiple passes led to a deterioration in the strength of the metal. The feed rate has positive correlation to the UTS of the composite created. Dynamic recrystallization of the grains was seen with as the passes increased. (El-Rayes & El-Danaf, 2012). The Al 6061-T6 sheet fabricated using FSP with TiB₂ as the reinforcement material was subjected to a pin-on-disc wear resistance test at a higher temperature. The results showed that the increase in the reinforcement in the composite reduced strength (Rao & Mallikarjuna Rao, 2018). Al-6061 sheets which were 3 mm thick were examined using stationary-shoulder FSP (SFSP) and CFSP. All the process parameters were kept similar for both composites. For a defect-free composite, the CFSP composite showed a better tensile strength, and the SFSP had a tensile strength lower than 10% compared to the CFSP. However, the SFSP composite showed better elongation than the CFSP since the SFSP had fine microstructures at the fracture location (Chen et al., 2020). 3 mm deep composite surface was fabricated in aluminium 6061-T651 alloy plate by reinforcing with sub-micro-size Al₂O₃ and SiC particles. This processed composite showed a reduced friction and wear by 40% and 90% respectively compared to the base metal. Further enhancement was noted in the plate after post-FSP heat treatment. The incremented dislocation density in the composite surface is a possible reason for such enhanced properties in the metal composite (Qu et al., 2011). A aluminium sheet was prepared using WAAM, and post WAAM a, FSP was done on the plate. The FSP helped enhance the microstructure and contributed towards porosity reduction. For instance, a significant drop in the grain size was observed (it reduced from 128 µm to 5 µm). The decreased porosity and enhanced microstructure enable microhardness, yield strength, and ultimate tensile strength to increase by 31.5 %, 23.3 %, and 6.0 %, respectively (He et al., 2023). A variation in the FSPed composites was observed with the variation of the eccentricity of the tool's pin. The experimentation showed that the Pin Affected Zone (PAZ) enlarged, and size of the grain in the stir zone was reduced with an increment in the eccentricity of the tool pin. The composite produced with a pin without eccentricity showed higher hardness and yield strength than the one created with pin eccentricity. However, the FSPed composite with an eccentric pin showed an overall escalation in the tensile properties in FSP composite (Chen et al., 2019). A 12 mm thick aluminium alloy (Al-6061-T6) was subjected to general FSP. The experimentation revealed that there was a five times increment in the impact toughness and very good tensile property was exhibited. A detailed study revealed that, the second phase had even distribution of particles. Such enhancement in the properties are reasoned to homogenised deformation, evolved recrystallized microstructure, refined grains, and quality of SZ, moreover the homogeneous distribution of the precipitates adds to this property enhancement. When it comes to the processing of aluminium and B₄C via FSP, the main parameters that affect the results are the speed of the tool rotation, speed of traverse, and the tool tilt angle (Rathee et al., 2016).

Bobbin tool friction stir processing (BTFSP) is one of the novel variants of CFSP. BTFSP is based on a similar principle to CFSP. The BTFSP tool consists of a double shoulder arrangement compared to the CFSP tool (Cui et al., 2009). This modification in the tool delivers many advantages over CFSP, such as dual-side composite fabrication, easy set-up requirement, improved stirring, the requirement of the less rigid machine, etc. Although BTFSP has the potential to eliminate many limitations of FSW/FSP, it has been less explored by researchers (Fuse & Badheka, 2019). Aluminium sheet (Al-6061 T6) of 6 mm thickness was introduced to a bobbin tool FSP for dual-sided composite preparation with B₄C as the reinforcement. Very precise and uniform distribution of the B₄C particles was observed on the lower side of the composite. Experimentation results were enhanced when the number of passes was increased to three. The grain refinement and the even distribution of the reinforcement particles helped to achieve better microhardness as well as wear properties of the composite that was fabricated (Fuse et al., 2021). The comparative studies between BTFSP and CFSW have revealed that the BTFSP show equivalent or slightly higher strength values than the CFSW (Yang et al., 2018). Moreover, some studies even admitted that the process parameters' combined effect helped the BTFSP joints compared with CFSW and helped the BTFSPed joints gain higher strength (Esmaily et al., 2016). The authors of this paper compared the composites fabricated using conventional FSP and Bobbin tool FSP with B₄C reinforcement. This research has been carried out using B₄C (Boron Carbide) as the reinforcement material because the high hardness and low density of B₄C make it a perfect fit for defense applications (Patidar & Rana, 2017).

Experimental Methodology

The base plates for the CFSP and BTFSP were cut in the required dimension of 150 x 100 x 6 mm in aluminium 6061-T6 plate. The plates were then prepared for packing the B₄C powder by making a groove of 1.5 mm depth and 2 mm wide. A wire cut EDM machine was used to prepare the groove with high precision in both the aluminium plates. The B₄C reinforcement particles are mixed in an acetone solution. Further, the mixture was filled in the grooved composite. The plates were kept to dry and let the acetone evaporate, eventually filling the groove with B₄C powder.



Figure 1. Vertical milling machine used for experiments

The fabrication of composites was done on a vertically oriented semi-automatic milling machine, as shown in Figure 1. A pinless tool was used to cover the groove so that the B₄C powder does not escape due to vibration while processing. The bobbin tool used for the BTFSP had symmetric upper and lower shoulders connected via a pin with three flats. The tool's Shoulder diameter and the diameter and height of the pin were 22 mm, 8 mm, and 6 mm, respectively. The tool used for CFSP had a single shoulder of 22 mm diameter and a tapered pin. The tools used during experiments are presented in Figure 2. A rotational speed of 1500 rpm was maintained for both experiments. The machine's feed rate was set constant at 33 mm/min. The angle of tilt for the tool was 2° for CFSP and 0° for BTFSP processes. Three passes were made for BTFSP and CFSP. The fabricated composite composites were further grinded, polished, and then etched using Keller's reagent (NH₃: HCl: HF: H₂O = 2.5: 1.5: 1: 95 vol%) to reveal the grain structure of the processed region. The microstructural observations were carried out using Olympus upright metallurgical microscope with a range of 50X- 2000X. The hardness was measured at an interval of 1 mm along the longitudinal direction. The hardness measurement was carried out along the top and middle (2 mm and 4 mm from the upper surface, respectively) on the cross-section which was along the center line. During measurement the load was fixed at 300g for a time span of 10 seconds.

Results and Discussion

Microstructure Analysis of BFSP and CFSP

The optical micrograph of Al 6061-T6 alloy and SEM micrograph of B₄C reinforcement particle is shown in Figure 3. The figure revealed elongated grains of BM.

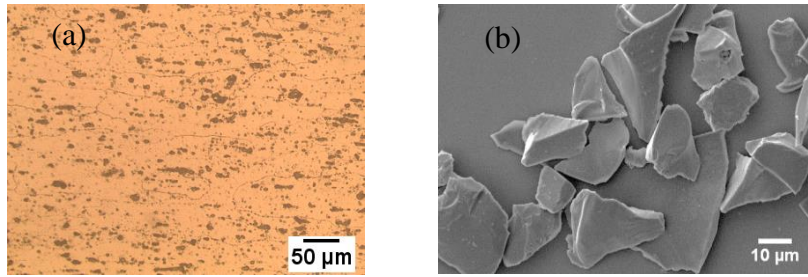


Figure 3. (a) Optical micrograph of Al 6061-T6 aluminium alloy (b) SEM micrograph of B₄C particles

Figure 4 (a) depicts the macrograph of the BTFSPed composite. It indicates the flash formation at the top and bottom of the composite. The both-side flash formation was due to the dual-side shoulder nature of the BTFSP tool, and it suggests the proper grabbing of the aluminium plate. A systematic pattern of alternate lines is visible at the advancing side (AS) of the BTFSPed composite (Figure 4 (b)). The alternate line formation is due to the stirring effect created by the three-face pin that connects the two shoulders of the BTFSP tool. These lines indicate the flow of material and B₄C particles at the AS from the top to the middle of the composite. The shining particles are the B₄C reinforcement particles. It is evident from Figure 4 (b) that the reinforcement material's proper distribution has occurred on the AS of the BTFSPed composite. The macroscopic view of region B in Figure 4 (a) revealed a crack. The magnified view of the crack is presented in Figure 4(c), indicating the agglomeration of the B₄C particles at that region. Figure 4(d) is a microscopic image of region C which is the bottom region of the composite. There is no evidence of any B₄C particle in this region. This is because the B₄C particles were deposited up to 1.5 mm depth only. Figure 4 (e) is a magnified view of region D in Figure 4(a). A similar trend of accumulation of the reinforcement particles is seen in this region. Figure 4(f) is a magnified image of region D' in Figure 4(e), which indicate well distributed B₄C particles in the crack. This observation highlights that even though the BTFSP tool had an extra shoulder at the bottom, this lower shoulder has not contributed to spreading B₄C particles.

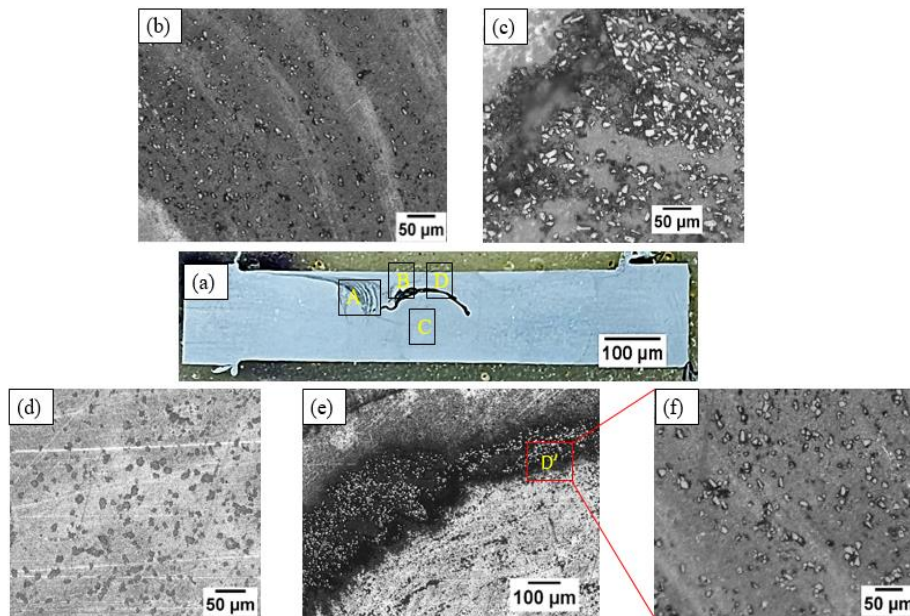


Figure 4. (a) macrostructure image of the BTFSP, (b) magnified image of the region marked as A in (a), (c) magnified image of the region marked as B in (a), (d) magnified image of the region marked as C in (a), (e) magnified image of the region marked as D in (a), (f) magnified image of the region marked as D' in (e).

Figure 5(a) shows the macroscopic view of the CFSPed composite, which appears to have a U-shaped profile in the SZ. A minor porosity at the top of the SZ on AS can be seen in the macroscopic image. This porosity could be a result of the improper intermixing of B₄C particles with plasticized BM. Additionally, It can be noted that the density of B₄C particles in the crack zone of the BTFSP composite was much higher than CFSP. The interface of BM and SZ can be easily observed in Figure 5 (b).

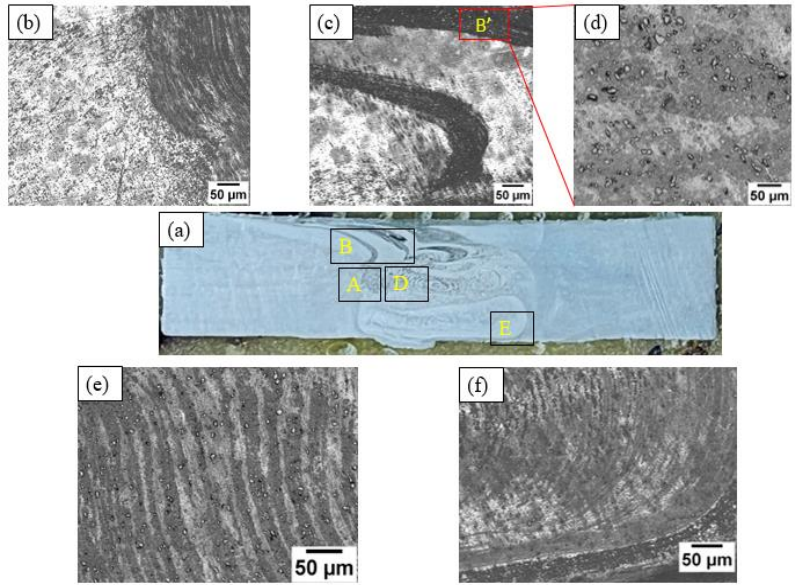


Figure 5. (a) macrostructure image of the CFSP, (b) magnified image of the region marked as A in (a), (c) magnified image of the region marked as B in (a), (d) magnified image of the region marked as B' in (c), (e) magnified image of the region marked as D in (a), (f) magnified image of the region marked as E in (e).

Figure 5(c) shows the magnified view of region B. It is interesting to observe an alternate pattern in the image. This may be due to the threaded pin used in CFSP. This pattern is similar to the BTFSPed composite. But, the distance between the dark strands in the CFSP composite is more significant as compared to the BTFSP. Figure 5 (d) shows the magnified image of region B'. This image reveals a proper and even distribution of the reinforcement particles in the upper region of the SZ. Figure 5(e) shows the microscopic structure of the D region. Flow lines are clearly evident in this zone, and moderate distribution of B₄C particles can also be observed. It is interesting to observe the reinforcement particles in this region, which is the bottom part of the composite. The presence of B₄C particles at the bottom can be due to threaded pin because threads tend to move material from top to bottom. Figure 5 (f) shows the bottom region E on the retreating side (RS). The downward marks in the figure revealed the flow of material from the middle to the bottom of the center of SZ on RS.

Microhardness Distribution

Figure 6 shows the graph of the microhardness recorded at different locations and regions of the BTFSP and CFSP composites. The highest recorded hardness value was 85.1 HV for the CFSPed composite in the SZ. It is interesting to observe that the highest value of hardness for BTFSPed was 83.1 HV.

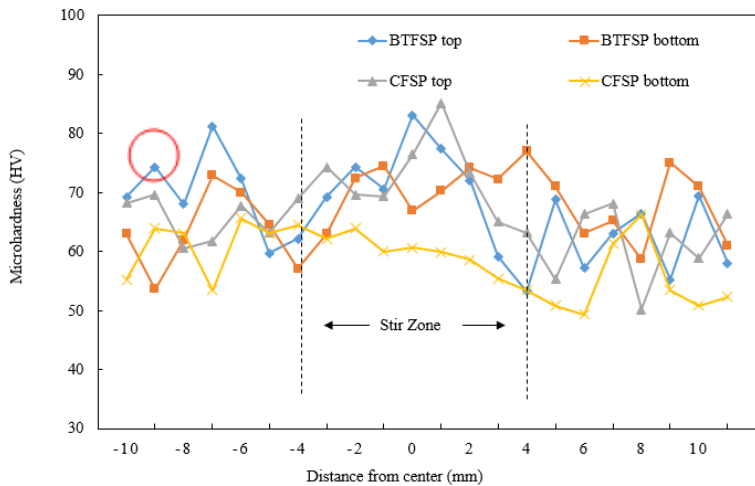


Figure 6. Microhardness distribution in CFSP and BTFSP

The difference in the hardness values of both composites is negligible but can be attributed to proper stirring in the CFSPed composite. It is observed that the average hardness at the top surface of CFSP and BTFSP composites is higher than the bottom surface of both composites. This is obviously due to the presence of B₄C particles at the top surface. The readings of the graph suggest that the average microhardness was 70 HV adjacent to the SZ. The lowest hardness was encountered at the interface of the TMAZ and the HAZ zone. There is an evident spike in the hardness at the top of the BTFSPed composite in the TMAZ with a hardness value of 81.2 HV, as shown by the red circle. This could be due to the striking of an indenter on a B₄C particle at a particular location.

Conclusion

The fabrication of composite of Al 6061/ B₄C was done at the top surface using conventional FSP and a novel bobbin tool technique. The microstructure and microhardness of the developed composites have been examined. The conclusion of the study can be summarized in the points mentioned below:

1. Microstructural study revealed the agglomerated distribution of the B₄C particles in the crack zone in both CFSP and BTFSP composite. However, CFSP composites obtained uniform distribution of the B₄C particles at the top surface.
2. The distance between the dark strands in the CFSP composite is more significant as compared to the BTFSP composite.
3. CFSPed composite exhibited presence of B₄C particles in the lower region of the composite due to the threaded pin. No trace of reinforcement particles was found at the bottom for the BTFSPed composite.
4. At the top CFSPed and BTFSPed composites reached maximum microhardness of 85.1 and 83.1 HV, respectively, indicating substantial hardness improvement.

Scientific Ethics Declaration

The authors declare that the scientific ethical and legal responsibility of this article published in EPSTEM journal belongs to the authors.

References

- Bains, P. S., Sidhu, S. S., & Payal, H. S. (2016). Fabrication and machining of metal matrix composites: A Review. *Materials and Manufacturing Processes*, 31(5), 553–573.
- Banhart, J. (2001). Manufacture, characterisation and application of cellular metals and metal foams. *Progress in Materials Science*, 46(6), 559–632.
- Chen, Y., Li, H., Wang, X., Ding, H., & Zhang, F. (2020). A comparative study on stationary-shoulder and conventional friction-stir-processed Al-6061 Alloy. *Journal of Materials Engineering and Performance*, 29(2), 1185–1193.
- Chen, Y., Wang, H., Ding, H., Zhao, J., Zhang, F., & Ren, Z. (2019). Effect of tool pin eccentricity on the microstructure and mechanical properties of friction stir processed Al-6061 Alloy. *Journal of Materials Engineering and Performance*, 28(5), 2845–2852.
- Cui, G. R., Ma, Z. Y., & Li, S. X. (2009). The origin of non-uniform microstructure and its effects on the mechanical properties of a friction stir processed Al–Mg alloy. *Acta Materialia*, 57(19), 5718–5729.
- El-Rayes, M. M., & El-Danaf, E. A. (2012). The influence of multi-pass friction stir processing on the microstructural and mechanical properties of Aluminum Alloy 6082. *Journal of Materials Processing Technology*, 212(5), 1157–1168.
- Esmaily, M., Mortazavi, N., Osikowicz, W., Hindsefelt, H., Svensson, J. E., Halvarsson, M., Martin, J., & Johansson, L. G. (2016). Bobbin and conventional friction stir welding of thick extruded AA6005-T6 profiles. *Materials & Design*, 108, 114–125.
- Fuse, K., & Badheka, V. (2019). Bobbin tool friction stir welding: A review. *Science and Technology of Welding and Joining*, 24(4), 277–304.
- Fuse, K., Badheka, V., Patel, V., & Andersson, J. (2021). Dual sided composite formation in Al 6061/B₄C using novel bobbin tool friction stir processing. *Journal of Materials Research and Technology*, 13, 1709–1721.

- He, P., Bai, X., & Zhang, H. (2023). Microstructure refinement and mechanical properties enhancement of wire and arc additively manufactured 6061 aluminum alloy using friction stir processing post-treatment. *Materials Letters*, 330, 133365.
- Jaiswal, R., Kumar, A., & Singh, R. (2022). Effect of process parameter on surface composite developed through friction stir processing: A review. In A. Dvivedi, A. Sachdeva, R. Sindhvani, & R. Sahu (Eds.), *Recent Trends in Industrial and Production Engineering* (pp. 1–22). Springer.
- Kumar, S., Singh, R., Jaiswal, R., & Kumar, A. (2020). Optimization of process parameters of electron beam welded Fe49Co2V Alloys. *International Journal of Engineering, Transactions B: Applications*, 33, 870–876.
- Ma, Z. Y. (2008). Friction stir processing technology: A review. *Metallurgical and Materials Transactions A*, 39(3), 642–658.
- Patel, V., Badheka, V., Li, W., & Akkireddy, S. (2019). Hybrid friction stir processing with active cooling approach to enhance superplastic behavior of AA7075 aluminum alloy. *Archives of Civil and Mechanical Engineering*, 19(4), 1368–1380.
- Patidar, D., & Rana, R. S. (2017). Effect of B4C particle reinforcement on the various properties of aluminium matrix composites: A survey paper. *Materials Today: Proceedings*, 4(2, Part A), 2981–2988.
- Qu, J., Xu, H., Feng, Z., Frederick, D. A., An, L., & Heinrich, H. (2011). Improving the tribological characteristics of aluminum 6061 alloy by surface compositing with sub-micro-size ceramic particles via friction stir processing. *Wear*, 271(9), 1940–1945.
- Quazi, M., M. A., F., Haseeb, A. S. M. A., Yusof, F., Masjuki, H. H., & Ahmed, A. (2015). Laser-based surface modifications of aluminum and its alloys. *Critical Reviews in Solid State and Materials Sciences*, 41, 1–26.
- Rao, Ch. M., & Mallikarjuna Rao, K. (2018). Abrasive wear behaviour of tib2 fabricated aluminum 6061. *Materials Today: Proceedings*, 5(1, Part 1), 268–275.
- Rathee, S., Maheshwari, S., Noor Siddiquee, A., Srivastava, M., & Kumar Sharma, S. (2016). Process parameters optimization for enhanced microhardness of AA 6061/ SiC surface composites fabricated via Friction Stir Processing (FSP). *Materials Today: Proceedings*, 3(10, Part B), 4151–4156.
- Sivanesh Prabhu, M., Elaya Perumal, A., Arulvel, S., & Franklin Issac, R. (2019). Friction and wear measurements of friction stir processed aluminium alloy 6082/CaCO3 composite. *Measurement*, 142, 10–20.
- Teo, G. S., Liew, K. W., & Kok, C. K. (2021). Enhancement of microhardness and tribological properties of recycled AA 6063 using energy-efficient and environment-friendly friction stir processing. *IOP Conference Series: Earth and Environmental Science*, 943(1), 012019. <https://doi.org/10.1088/1755-1315/943/1/012019>
- Yang, C., Ni, D. R., Xue, P., Xiao, B. L., Wang, W., Wang, K. S., & Ma, Z. Y. (2018). A comparative research on bobbin tool and conventional friction stir welding of Al-Mg-Si alloy plates. *Materials Characterization*, 145, 20–28.
- Zhao, H., Pan, Q., Qin, Q., Wu, Y., & Su, X. (2019). Effect of the processing parameters of friction stir processing on the microstructure and mechanical properties of 6063 aluminum alloy. *Materials Science and Engineering: A*, 751, 70–79.

Author Information

Dhaivat Divekar

Pandit Deendayal Energy University
Gandhinagar, Gujarat, India-382007
India

Kishan Fuse

Pandit Deendayal Energy University
Gandhinagar, Gujarat, India-382007
India
Contact e-mail: Kishan.fuse@sot.pdpu.ac.in

Vishvesh Badheka

Pandit Deendayal Energy University
Gandhinagar, Gujarat, India-382007
India

To cite this article:

Divekar D.N., Fuse K.A., & Badheka V.J. (2023). Microstructure and mechanical properties analysis of Al-6061/B4C composites fabricated by conventional and bobbin tool friction stir processing. *The Eurasia Proceedings of Science, Technology, Engineering & Mathematics (EPSTEM)*, 23, 117-123.

The Eurasia Proceedings of Science, Technology, Engineering & Mathematics (EPSTEM), 2023

Volume 23, Pages 124-130

ICRETS 2023: International Conference on Research in Engineering, Technology and Science

An App for the Registration of Traffic Injuries

Daniel Suarez

Fisabio Primary Care Orihuela Hospital (Alicante)

Javier Urios

Fisabio Primary Care Orihuela Hospital (Alicante)

Jesus Tomas

Valencia Politécnic University

Sandra Sendra

Valencia Politécnic University

Jaime Lloret

Valencia Politécnic University

Sandra Viciano

Valencia Politécnic University

Abstract: We present the development of an application as a mobile tool to carry out the assessment of bodily damage suffered by a traffic accident. The scale used to assess traffic accidents can be used for any other circumstance that produces injury or bodily sequelae. The software developed will allow the expert to be guided through all the cases to generate a report where the corresponding compensation is obtained, both for bodily harm and possible disabilities. In the event of death, it also makes it possible to determine compensation to relatives and relatives based on kinship and circumstances. Of course, the role of the expert does not disappear. In many cases, forks appear, and compensation must be argued. However, this application will allow it to be operated by a physician without much experience in this legislation. The application will ask you for the details of the accident and will indicate the compensation ranges that can be applied. On the other hand, the application allows you to collect all kinds of documents that can be attached to the final report. These include medical reports and all kinds of expenses caused as an accident (hospitalization, prosthesis, transportation, repatriation). A mobile application is proposed that allows automating this process, which can be used by personnel without previous experience and drastically reducing the time necessary to carry out the measurements. Another advantage is that the software runs on a mobile device using the mobile device's camera. This allows the system to be used in any location and with minimal economic cost. On the other hand, a complete patient registration system has been implemented, and the possibility of keeping a history of each one, to assess their evolution.

Keywords: Mobile tool, Body damage, Telemedicine

Introduction

From the beginning it was decided to develop a multiplatform application (Delia, et al., 2015) that could be used from both personal computers and mobile devices. Development platform: First, the use of the React Native tool was evaluated, as it is one of the most widely used today in the development of multiplatform applications. However, this option was discarded, the use of the Java Script programming language caused many errors at

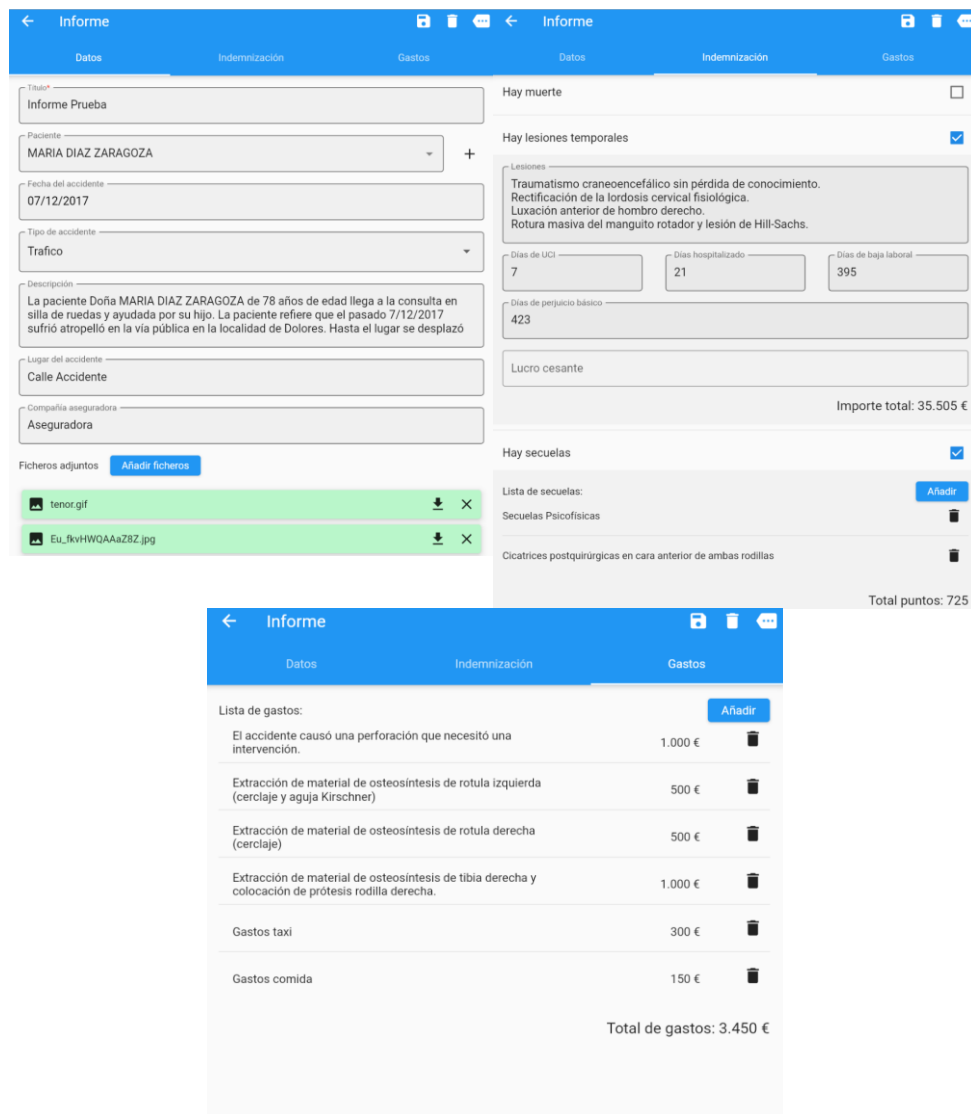
- This is an Open Access article distributed under the terms of the Creative Commons Attribution-Noncommercial 4.0 Unported License, permitting all non-commercial use, distribution, and reproduction in any medium, provided the original work is properly cited.

- Selection and peer-review under responsibility of the Organizing Committee of the Conference

© 2023 Published by ISRES Publishing: www.isres.org

runtime. Also, some of the libraries gave problems when switching platforms. Second, Google's Flutter tool was evaluated. It was decided to select this option, because it uses a more robust language, Dart, and because it causes much less problems with the libraries. Mobile Backend as a Services (MBaaS) (Costa et al., 2016): The development of modern applications has been boosted by the appearance of work tools in the cloud to enhance all kinds of functionalities with little effort for the developer. Solutions such as Amazon Web Services, Microsoft Azure or Google Services stand out. Firebase has been selected for this project because it has a series of advantages: Its cost is very low, it can even be zero until it reaches a significant volume of use. It is perfectly integrated with the development tool (Moroney, 2017). Last but not least, the development team has extensive experience in its use.

This application will allow it to be operated by a physician without much experience in this legislation. The application will ask you for the details of the accident and will indicate the compensation ranges that can be applied. The following screenshots show some phases of generating a report:



In this project, three types of cloud service will be mainly used: User authentication: A user must be able to identify themselves in a 100% secure way in the application, so that other users cannot impersonate their identity. However, it must be possible for the user to access from different places and devices and have access to all the information stored in the cloud. As authentication method, two have been selected: The use of the typical email and password and the possibility of using a previously created Google account. Databases in the cloud: It will allow saving the data of the patients and the different reports entered. The NO SQL type database, Firestore, is used (Sukmana & Rosmansyah, 2021). File storage in the cloud: Each report must attach a wide variety of documents: medical reports, invoices, etc. All this information must remain in the cloud, so that it can only be

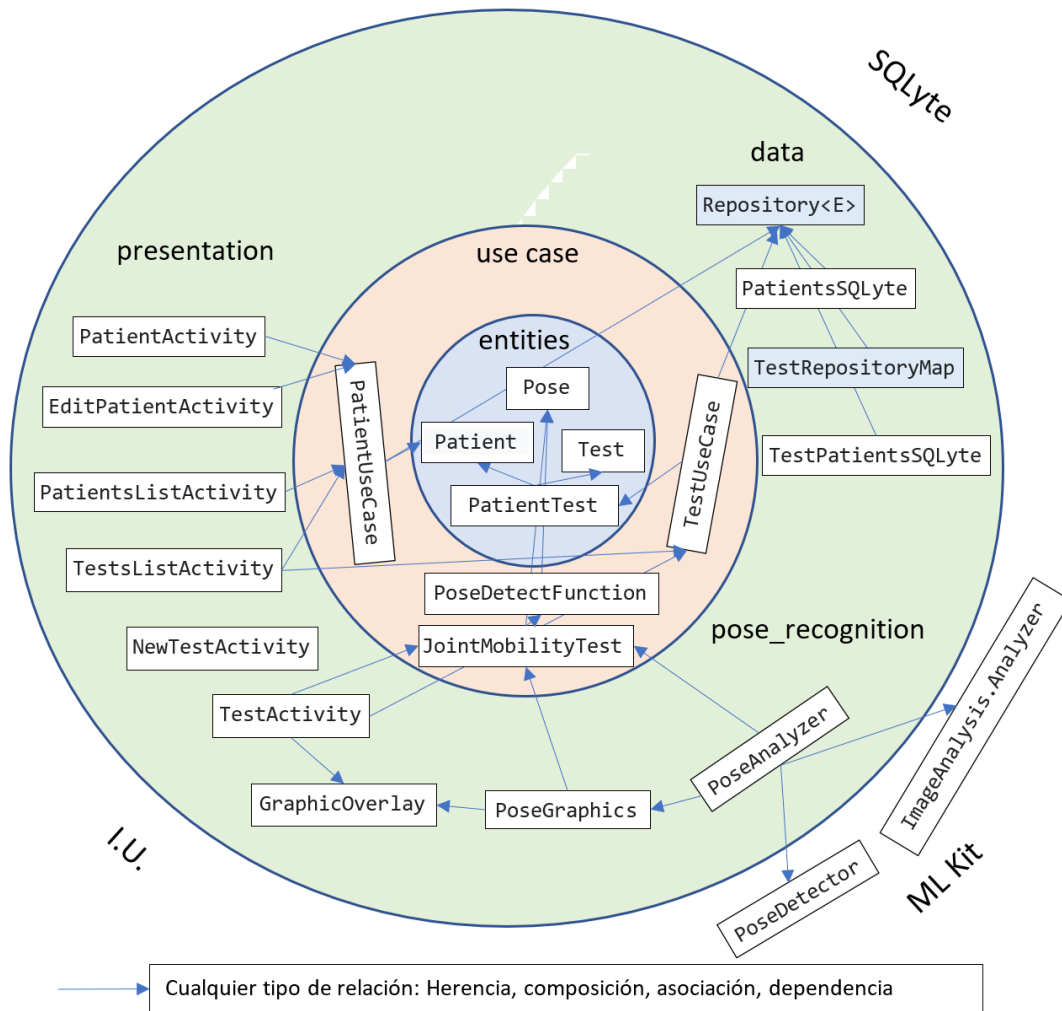
accessed by the user who created the report. This functionality is achieved thanks to Firebase cloud storage services.

It is planned that the software will be registered in the database of transferable results of the UPV. Furthermore, it is intended to publish a demo version on the Web and in mobile app stores. In a first phase, it has been planned to publish it on the Web, in a second in Google Play and in a third in the App Store. In this way, we intend to give visibility to the applications and thus be able to attract potential companies interested in their commercialization

Method

Development platform: The possibility of developing a multiplatform application was considered, which could be used from both personal computers and mobile devices and which stored the data in the cloud. This approach, which was ideal for the previous application, was not so suitable for an artificial vision application. These types of applications require the use of native programming, which must be carried out in a differentiated way in Android and iOS. It was decided to start with Android, leaving iOS development for the future. Android Studio was used as a development tool and Kotlin as a programming language (Oliveira et al., 2020).

Data storage: Continuing with the previous line, it was thought that local storage on the application user's device would be simpler and more effective. This would allow the use of the application without having access to the Internet, but it would have the drawback that the data could only be accessed from the doctor's device. Another advantage of local storage is that the application does not need user identification. We can assume that the only user who will have access to the mobile is its owner. It was decided to use SQLite to store the databases locally, since it is the platform integrated into Android (Bhargave et al., 2013).

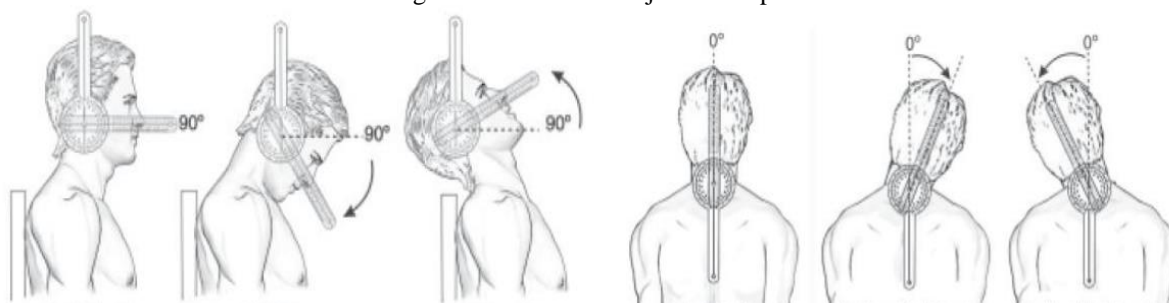


Posture detection: A posture detection software (pose detection, in English) allows you to detect a person's joints from an image. The development of Deep Learning techniques have led to the appearance of several deep neural networks that solve this problem. In this project we have evaluated some of them to try to integrate them into the system. The open source software OpenPose has given us good results⁷. But it had the drawback of being not very robust in the case of images where the person was not shown full-length. Finally, it was decided to use the free software ML Kit, as it gave much more robust results.

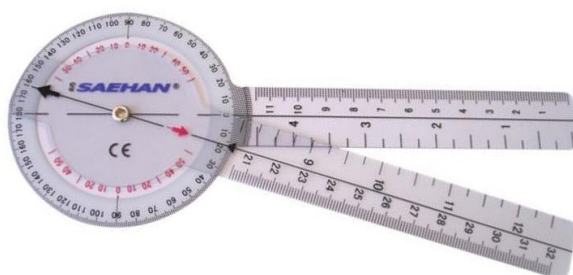
Software architecture: The development of the application has been guided by the use of the CLEAN architecture. The following diagram shows the relationship between the project classes and their location within the architecture. We can highlight three external layers to the development: ML Kit, for the detection of the different joints of a person from the images obtained by the camera. SQLyte, for data storage and the Android user interface system⁸. Then the outermost layers would come, such as the data layer, the presentation layer and the posture recognition layer. More internally we would have the use cases and in the center of the development, the entities.

Results and Discussion

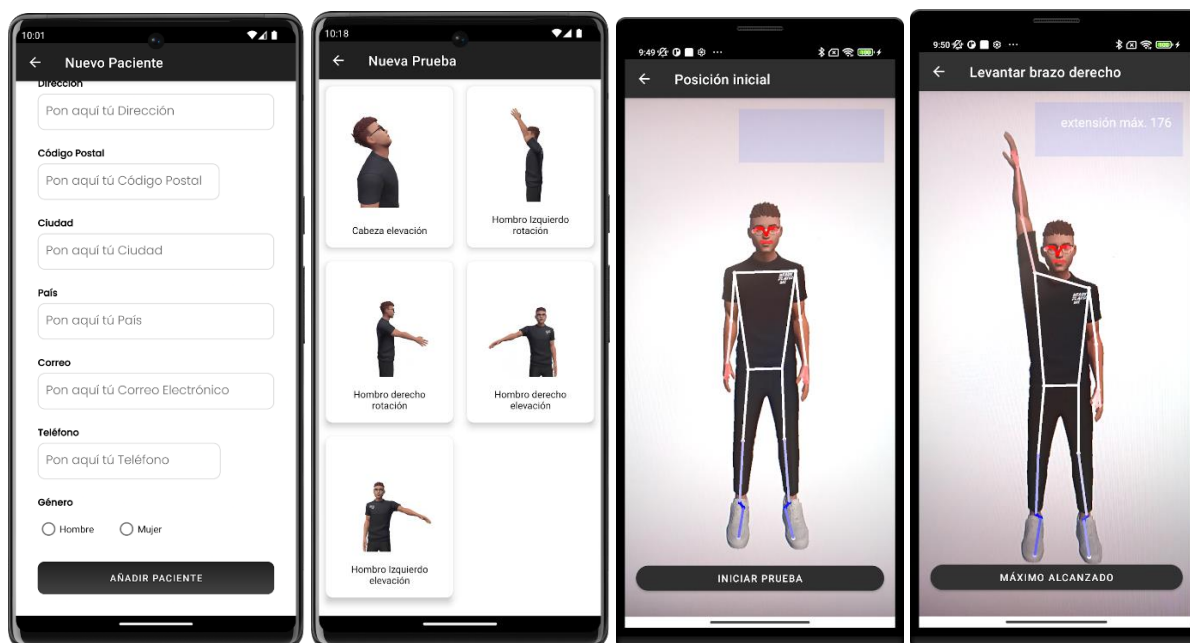
After a traffic accident, it is common for some joints, such as the neck and back, to be affected. Similar problems appear in the field of occupational accidents and handicaps. For this reason, having a fast and precise measurement system for the movement of the different joints could be of great help. Goniometry in clinical examinations is used to measure the angles that the different joints of a patient can reach.



Traditionally, the goniometer has been used to obtain these angles:



We propose a system, very easy to operate, that will allow the physician to automate the obtaining of goniometric measurements of different joints. We now describe the solution we propose. Below is a set of screenshots to illustrate this explanation. First, the practitioner installs the application on his mobile phone. This must have a front camera, and it is not necessary to be connected to the Internet. The first step will be to register the data of a new patient. This will appear in the patient list. After selecting a patient, all the tests performed will be displayed in chronological order. In this way, a record of the patient's evolution can be kept. Pressing the + button will start a new test. The doctor has to focused on the patient, so that the appropriate part of the body is displayed on the screen. Following the indications shown in an animation, the patient performs a certain movement in a joint. The app records the range of motion performed. In most cases, the maximum and minimum angle that the patient manages to reach in this joint is stored. The physician does not have to register any value, it is all done automatically by the application. You simply must hold the mobile and make sure that the patient performs the movements properly.



Conclusion

Carrying out an expert report for the assessment of bodily harm or determination of the degree of disability requires in-depth knowledge of the legislation. Thanks to the software that we present, these reports can be carried out by health personnel with little knowledge in this field. Another advantage that it offers is the saving of time in the generation of these reports. You just have to fill in the requested data, and the application is responsible for generating a report in pdf. On the other hand, a multiplatform application has been developed that will allow it to be used from a desktop computer or from a mobile device. In addition, all the information is stored in the cloud, so it is accessible from anywhere with Internet access.

Using a traditional goniometer to determine joint movement is a complex task that can only be performed by qualified personnel. A mobile application is proposed that allows automating this process, which can be used by personnel without previous experience and drastically reducing the time necessary to carry out the measurements. Another advantage is that the software runs on a mobile device using the mobile device's camera. This allows the system to be used in any location and with minimal economic cost. On the other hand, a complete patient registration system has been implemented, and the possibility of keeping a history of each one, in order to assess their evolution.

This tool will facilitate the calculation of the bodily damage of people who suffer an injury. It has several advantages over the conventional process; minimizes possible subjectivity and inter-observer variability. Significantly reduces the time required for the valuation, by not having to continually consult the legislation. It can be used by professionals with little experience in this field. The application guides the user, according to the information entered. The possibility of making mistakes is reduced, as it is carried out exhaustively. Traceability processes are improved. It is expected that the application will present great interest in insurance companies, medical expertise companies, labor mutuals, etc.

For easy diffusion, the Google Play app store will be used as a distribution channel. The exploitation model may be carried out following any of the models described below: Freemium. This type of model is one of the most successful. It is based on the duality between a free system and a premium one with higher quality services, agreements with institutions. Specific contracts are established with the mutual or insurance companies that want to use the application. These agreements may require the adaptation of the software according to the field or the specific needs of the company.

The economic impact: The payment of insurance and pensions associated with personal injury and disability in the world of work moves billions of euros annually in Spain. A tool that makes it possible to reduce errors in the assessment of these damages will have a great economic impact for both individuals and insurance companies. The Social Security Institute, through the handicap assessment teams, assigns handicap percentages that have

financial compensation determined by law. Our tool can be useful to reduce the financial cost of litigation by individuals with the administration or insurance companies. Foreseeable socio-sanitary impact our tool will mean greater transparency in the evaluation of the injured person and will allow their evaluation even remotely in the new times of telemedicine, resulting in a better quality of care for said people. In addition, the complexity of the application of the tables of the medical scales for the evaluation of bodily damage and handicaps will be reduced, facilitating the work of health personnel. Finally, it will favor a better traceability of the evaluation process that is documented in the process of measuring the angles of movement reduction. It is intended to be an easy-to-use tool that helps in a step-by-step guided process to determine and quantify the damage suffered by the patient or the percentage of disability. Applicability: Our application could also be useful in determining temporary or permanent work disabilities. In a future development of the same, its use could be useful to determine “partial”, “total” or “absolute” permanent disabilities. It would be necessary to include in the assessment of bodily harm the evaluation of the ergonomic aspects of the job that the worker performs and a comprehensive assessment of this from the labor point of view. Therefore, the tool to be developed can be very useful for: - Medical-legal expert reports. - Planning or evaluation of treatments. - Control of the evolution or progress of the patient. - Determination or measurement of residual disability after a rehabilitation process. - Analysis of biomechanics before joining the job.

Scientific Ethics Declaration

The authors declare that the scientific ethical and legal responsibility of this article published in EPSTEM journal belongs to the authors.

Acknowledgements or Notes

* This article was presented as a poster presentation at the International Conference on Research in Engineering, Technology and Science (www.icrets.net) held in Budapest/Hungary on July 06-09, 2023.

* We want to expressly thank the support of the legal medicine professor Dr. Aurelio Luna Maldonado. This work has been financed by the Fisabio Program and the Polytechnic University of Valencia (Polisabio).

References

- Bhargave, A., Jadhav, N., Joshi, A., Oke, P., & Lahane, S. R. (2013). Digital ordering system for restaurant using Android. *International Journal of Scientific and Research Publications*, 3(4), 1-7.
- Bhosale, S. T., Patil, T., & Patil, P. (2015). Sqlite: Light database system. *Int. J. Comput. Sci. Mob. Comput*, 44(4), 882-885.
- Costa, I., Araujo, J., Dantas, J., Campos, E., Silva, F. A., & Maciel, P. (2016). Availability evaluation and sensitivity analysis of a mobile backend-as-a-service platform. *Quality and Reliability Engineering International*, 32(7), 2191-2205.
- Delia, L., Galdamez, N., Thomas, P., Corbalan, L., & Pesado, P. (2015, May). Multi-platform mobile application development analysis. In *2015 IEEE 9th International Conference on Research Challenges in Information Science (RCIS)* (pp. 181-186). IEEE.
- Kim, W., Sung, J., Saakes, D., Huang, C., & Xiong, S. (2021). Ergonomic postural assessment using a new open-source human pose estimation technology (OpenPose). *International Journal of Industrial Ergonomics*, 84, 103164.
- Moroney, L., & Moroney, L. (2017). The firebase realtime database. *The Definitive Guide to Firebase: Build Android Apps on Google's Mobile Platform*, 51-71.
- Oliveira, V., Teixeira, L., & Ebert, F. (2020, February). On the adoption of kotlin on android development: A triangulation study. In *2020 IEEE 27th International Conference on Software Analysis, Evolution and Reengineering (SANER)* (pp. 206-216). IEEE.
- Sukmana, Y., & Rosmansyah, Y. (2021, December). The use of cloud firestore for handling real-time data updates: An empirical study of gamified online quiz. In *2021 2nd International Conference on Electronics, Communications and Information Technology (CECIT)* (pp. 1239-1244). IEEE.

Author Information

Daniel Suárez

Fisabio Primary Care
Orihuela Hospital (Alicante), Spain
Contact e-mail: suarezdan2001@yahoo.es

Javier Urios

Fisabio Primary Care
Orihuela Hospital (Alicante), Spain

Jesús Tomás

Valencia Politécniciva Valencia
Campus Gandia (Valencia), Spain

Sandra Sendra

Valencia Politécniciva Valencia
Campus Gandia (Valencia), Spain

Jaime Lloret

Valencia Politécniciva University
Campus Gandia (Valencia), Spain

Sandra Viciano

Valencia Politécniciva University
Campus Gandia (Valencia), Spain

To cite this article:

Suárez, D., Urios, J., Tomás J., Sendra, S., Lloret, J., & Viciano, S. (2023). An app for the registration of traffic injuries . *The Eurasia Proceedings of Science, Technology, Engineering & Mathematics (EPSTEM)*, 23, 124-130.

The Eurasia Proceedings of Science, Technology, Engineering & Mathematics (EPSTEM), 2023

Volume 23, Pages 131-142

ICRETS 2023: International Conference on Research in Engineering, Technology and Science

A Proposed Conceptual Design for a Computer-Based Ambulance System in Libya Using IoT

Arwa F. Albillali

Libyan International Medical University

Ehab A. Omar Elfallah

Libyan International Medical University

Bilal A. Aljabour

Libyan International Medical University

Tawfiq Tawill

Libyan International Medical University

Abstract: Due to the increase in the world's population which increased road congestion, the ambulances that carry patients have so many difficulties in getting to the hospital before the patient's condition gets worse. The problem of the delayed arrival of the patient to the hospital was found globally in most countries. Especially in Libya, the problem is more complex, the ambulance services are weak, patients face problems in getting fresh blood packages, and the health system lacks an electronic health record. In this paper, a descriptive comparison is conducted to evaluate, compare, and analyze different proposed solutions. Then, a new different solution is proposed. To check the feasibility of the newly proposed solution, a survey was conducted to review the audience's level of satisfaction with the traditional ambulance services, as well as the proposed solution, the results showed the people's lack of trust in the current ambulance services, and their reluctance to rely on the service. However, the results also revealed the people's acceptance of the proposed solution, and their willingness to rely on it.

Keywords: Ambulance system, Healthcare system, IoT.

Introduction

Using modern technology in healthcare is popular these days and using technology to ensure patient well-being is attainable (Salau et al., 2020). In today's systems, advanced healthcare applications are required. As the world's population and technologies increase at exponential rates, so do the number of accidents and medical issues. In the medical area, several sorts of smart technologies have become a requirement (Dumka & Sah, 2019). Technology automates and extends activities that formerly required human intervention, allowing medical staff to focus their time and energy elsewhere, while potentially lowering total healthcare costs (Scherman, 2019). Information technology IT has become more important in the healthcare industry to ensure that medical and administrative operations function efficiently. Whether it's for workplace automation or to reduce medical errors, IT can help (Bernstein et al., 2007). By integrating medical devices, automating financial transactions, and eliminating errors, advances in information communications technology have the potential to alter the traditional healthcare system and increase consumer confidence in the system. Furthermore, as the need for ambulance services rises, many hospitals are finding it difficult to achieve response time goals. Although ambulance services normally perform both emergency response and patient transfer on behalf of the health sector, their primary job is to provide emergency pre-hospital medical care. In recent years, it has become clear

- This is an Open Access article distributed under the terms of the Creative Commons Attribution-NonCommercial 4.0 Unported License, permitting all non-commercial use, distribution, and reproduction in any medium, provided the original work is properly cited.

- Selection and peer-review under responsibility of the Organizing Committee of the Conference

© 2023 Published by ISRES Publishing: www.isres.org

that expanding healthcare system challenges cannot be overcome solely by additional resources; they also require new service delivery methods and techniques. Ambulance services can impact the success of health initiatives by integrating them into health systems in general, and by employing modern technologies to increase efficiency.

As a result, one of the key difficulties causing severity for a patient is a delay in travel time. Because of the delay in getting to the hospital, the doctor will not be able to treat the patient right away, and the preparation for treatment will begin only after the doctor has assessed the patient's health situation. This delay may put patients in jeopardy and, in some cases, lead to death. This paper proposes a conceptual design of an integrated and upgraded ambulance management system for Libya, connected to the main hospital, automates the process of admission, and enables remote treatment by increasing the awareness of the patient's current state.

Literature Review

The proposed ambulance system shared goals with several of the initiatives that offered various solutions. Smart city applications, IoT, 5G, and smart health systems were among the general subjects investigated.

The Use of Modern Technologies in Improving Health Care Systems

Modern technologies can be used to develop these emergency medical systems. The argument that 5G wireless technology, together with related developing technologies (such as Internet of Things IoT, big data, artificial intelligence, and machine learning), will change global healthcare systems soon (Latif et al., 2017). It was found that with the (IoT) rapidly emerging as the next phase of the Internet's growth, it's becoming increasingly important to recognize the many potential fields for IoT applications (Albayood et al., 2020). Therefore, the Internet of Things is paving the way for new types of research to be conducted (Nath Saha, 2020).

A review of recent works, presented a comprehensive overview of network layer solutions for IoT-based 5G smart healthcare, including scheduling, routing, and congestion control, that covered both recent work and future research opportunities. Finally, the open issues and challenges for future 5G smart healthcare were briefly discussed (Ahad et al., 2019). Another paper identifies current trends, applications, and procedures in healthcare data analytics and health informatics with decision support systems so that healthcare specialists, researchers, and analysts can have a better knowledge of their clinical applications (Godbole & Agarwal, 2020). The design and execution of a smart health monitoring system of leveraging cutting-edge technology, such as the IOT have been demonstrated by Vippalapalli and Ananthula. A patient can be monitored utilizing a set of lightweight wearable sensor nodes that allow for real-time sensing and analysis of numerous vital indicators (Kalarthi, 2016; Vippalapalli & Ananthula, 2016).

A report published in 2020 advocated the construction of a smart healthcare system that would use artificial intelligence to solve difficulties in the healthcare business and optimize patient care plans. It claimed that the suggested architecture can deal with a wide range of complex healthcare issues and may be implemented in any modern hospital to save time and money. This paper also demonstrates the current growth of AI applications in healthcare, which might be applied in the architecture described (Kamruzzaman, 2020). A framework for e-Health and m-Health that uses smartphone sensors and body sensors to acquire, process, and transfer patient health data to the cloud for storage is proposed by (Ullah et al., 2016). The suggested architecture, dubbed k-Healthcare, is made up of four layers that work together to enable effective data storage, processing, and retrieval (A. Al-Tawaty & Omar Elfallah, 2019).

Upgrading the Ambulance Services by the Integration of Modern Technologies

I. S. Sherly and M. A. Sobitham Princy have proposed a solution based on the Internet of Things. They are connecting the ambulance to the IoT, which includes biomedical sensors such as heartbeat rate sensors, temperature sensors, and ECG sensors that will sense and detect the injured person's health conditions and send the information to the hospital server. This proposed device is being developed to avoid lateral hospital arrangements (Sherly & Sobitham Princy, 2019). Another research on 2019, comprises an ambulance outfitted with wireless body area network (WBAN) sensors that detect real-time patient data. IoT data aggregation is used to deliver aggregate real-time data to clinicians at remote hospitals, and these sensors communicate data to the

center node or sink node via the Message Queuing Telemetry Transport (MQTT) protocol (Dumka & Sah, 2019).

A smart ambulance management system in a smart city in Turkey implemented which if a patient requires an ambulance, the system instructs the operator to locate the closest ambulance and send it to the patient. The system dynamically tracks ambulance locations, and Google Maps is utilized to compute the quickest way to the victim as a third-party service. Following contact with the patient, the expert (doctor or nurse) evaluates the issue and, using the suggested approach, locates the best available hospital (Akca et al., 2020). Another smart system was created to warn other cars of the ambulance's approach by making the ambulance's position information available. The suggested approach involves just installing a smartphone-based special application on a dashboard to turn an ambulance into an IoT device (Kobayashi et al., 2019).

The Smart Ambulance Traffic Control System was proposed in (Krishnan et al., 2021). It is a traffic light control system that is incorporated for emergency ambulance service. When an emergency ambulance approaches, the traffic lights can be controlled in a timely and efficient manner. During traffic congestion, Radio-Frequency Identification (RFID) is used as a tool to communicate with traffic lights. The emergency ambulance driver must activate the RFID tag for RFID readers to be detected and for traffic light operation to be controlled at upcoming traffic light junctions. The traffic lights in the path of the ambulance are forced to be green to allow the emergency ambulance to pass through the junction with top priority. The control system will reset and return to normal operations as soon as the ambulance passes through the intersection.

Another paper from Malaysia described a useful 5G health use case for transmitting medical ultrasound video streams in the uplink direction between a moving ambulance and a hospital. This use case is critical because the patient is most vulnerable and requires immediate attention. Furthermore, using ultrasound video streaming as an example of a critical m-health application, this article explored the feasibility of implementing mobile small cell networks in an m-health context (Rehman et al., 2018). The issues that emergency service providers face on the road network are discussed in this (Pasha, 2016) master thesis. A prototype system based on GIS, GPS, and GSM was developed for ambulance routing on Hyderabad's road network (Ambulance management system (AMS)). Using real-time technologies (GPS/GSM), this prototype locates an accident on the road network and locates the closest ambulance to the incident site. GIS users assessed this ambulance management system, which was designed utilizing a software engineering model rapid prototyping technique (Pasha, 2016).

This review (U, N, Aithal, Shripad Bhat, & K (2019)) offered an application called HPVB (High Priority Vehicle Booking), in which the user may book an ambulance with a single touch and monitor it using GPS on his mobile. A microcontroller-based hardware module was also utilized to enable a smooth flow for the ambulance to reach the desired destination. This is accomplished using 3RFID technology, which automatically controls traffic lights along the ambulance's path, reducing the time it takes to get to its destination. In other hand, research published in 2020, an RFID-based traffic management system was presented. Using this technology, traffic lights at intersections can be controlled and regulated when emergency vehicles approach. As a result, emergency vehicles will be able to travel through traffic with ease. An experimental setup employing Arduino and LED displays is used to model the suggested framework, which replicates a real-time traffic scenario. The simulation results show the parameters of detection as well as giving passage for the emergency vehicle during peak hours to avoid delays. The research claims that with this technology, emergency vehicles are less congested and arrive at their destinations faster (Girish et al., 2020).

Fong et al. (2018) proposed a smart ambulance system that consists of a network of connected medical devices, sensors, and wearable assistive devices worn by paramedics, as well as consumer health devices worn by patients. An IoT platform acts as a link between paramedics and patients, as well as the hospital network, providing assistance ranging from patient medical history retrieval to receiving remote support for on-scene treatment. It mentioned that wearable sensors are critical components of an IoT ecosystem that allows for continuous monitoring of a patient's health, giving paramedics a far more complete image of the patient than standard emergency medical techniques can provide (Fong et al., 2018).

Live monitoring system based on the Internet of Things was proposed for patients in danger of heart attack and having an inconsistent body temperature. A live trafficking system was also created, which uses Google Maps to ensure that the ambulance arrives on time. The research goal was to create an intelligent smart health system using sensors and microcontrollers that can sense the body's state and communicate the information to a collaborative hospital's website (Saha et al., 2017). Besides, A. G. Karkar presented a smart ambulance system that considers highlighted emergency routes. The solution is a set of smart healthcare emergency apps aimed at improving ambulance infrastructure. Its goal is to keep drivers informed about the emergency routes that

ambulances use. The suggested system consists of three parts: a server program, a user emergency end-user application, and a paramedic end-user application. Paramedics determined that the suggested approach would improve patient transportation time to hospitals based on an initial assessment utilizing questionnaires (Karkar, 2019).

Another research published in 2015 presented an E-Ambulance system, which is a smart ambulance model that enables auto-reaction activities as well as monitoring to improve the chances of saving patients from life-threatening situations. To accomplish this purpose, biosensors, actuators, intelligent units, GPS, and other components and technologies were employed. The Data Distribution Service (DDS) model is utilized to link these disparate components of the system. As a result, they assessed the latency and throughput performance metrics of wireless communication between a set of nodes using various QoS profiles. DDS demonstrated great performance in general and met medical standards for transmitting monitoring data within defined limits (Almadani et al., 2015).

A traffic controlling/movement system was proposed in a study conducted in 2018. This system uses a density-based system to reduce traffic congestion and unwanted long-time delays during traffic light switchovers, especially when traffic is light, by analyzing the counting and controlling system using IR technology and an 89C52 microcontroller. The traffic lights are controlled automatically by an algorithm based on the RF switch/key pressed by the ambulance driver while in range. Every patient in the monitoring system is given an RFID TAG/smart card that contains all the patient's information, such as name, age, sex, major diseases suffered, medical history, and so on. When the RFID TAG/smart card is swiped on an RFID reader (installed in the ambulance), the information is transferred to the hospital department using GSM technology (Bhatia et al., 2018). The concept behind (Bharade et al., 2017) is that anytime an ambulance comes to a standstill due to traffic congestion on its approach to the hospital, the RFID reader located at the traffic light scans the RFID-tagged ambulance and communicates its data to the microcontroller.

The suggested system in this research (Bhajantri et al., 2019) offered a proposal for an emergency patient transportation monitoring system. During the critical hour of patient transportation, continuous monitoring of ambulance location and status helps to enhance medical treatment. As a result, a quick, cost-effective, and efficient traffic management system is required. It may show the position of the ambulance as well as the patient's heart rate and temperature. The proposed system also keeps track of a patient's past prescription history, which will aid in improved treatment. The data of the patient can be retrieved using a biometric device that will be available in ambulances (Fadel et al., 2020).

Corradini and Gheorghiasa (2015) proposed a video streaming solution that promotes conversations between ambulance paramedics and the doctor in the emergency car in another paper done in Denmark, by including a 4G camera with an assigned phone number as part of each ambulance's equipment. In this method, a doctor in an emergency vehicle may simply phone the number of the camera linked with the ambulance to which he or she was dispatched (Corradini & Gheorghiasa, 2015).

Comparative Analysis

Different approaches were discussed to reach the same purpose, which is to deliver the patient to the hospital as fast and safely as possible. Some writers suggested implementing a traffic management system, by using RFID in the traffic lights to switch the light to green when it detects an ambulance. Meanwhile using google maps to suggest the shortest path possible to the patient.

Other writers suggested monitoring the patients' conditions, treating them, and getting their information before they arrive at the hospital, by using sensors connected via 5G with the cloud server of the hospital, to detect the biomedical status of the patients and share them with the intended hospital. Others suggested using cameras to help the doctors in monitoring the patient's status while they are on their way to the hospital.

If a patient requires an ambulance, the system detects and dispatches the nearest ambulance. After speaking with the patient, the expert examines the situation and locates the best available hospital using the specified technique. However, another Malaysian initiative proposed a Smart Ambulance Traffic Regulation System, which is an integrated system of traffic light control for emergency ambulance services. Radio-Frequency Identification (RFID) is used to communicate with traffic lights during traffic congestion. For RFID readers to be recognized and traffic light operation to be regulated at approaching traffic signal intersections, the emergency ambulance driver must activate the RFID tag. Furthermore, in Saudi Arabia, a solution was built to

locate an accident on the road network and the nearest ambulance to the event location. It also calculates the quickest route from the closest ambulance to the accident scene, and then to the nearest hospital. The quickest path on both main and minor roads is built to avoid traffic congestion during peak hours. Research in India proposed an application that would allow users to request an ambulance with a single tap and monitor it using GPS on their smartphone. They also employed RFID technology to guarantee that the ambulance arrives on time. In another study conducted in India in 2020, Arduino Uno has been upgraded to Arduino Mega Board, as Mega has a flash memory of 256kb compared to 32kb on Uno, which is sufficient to save patient vital signs while detecting the status of traffic lights present in various paths. The patient's vital signs are also sent to the destination hospital so that the medical staff can deal with the situation. According to the researchers, emergency vehicles would be less crowded and will get to their destinations faster using this technology.

Traffic Controlling Approach

In a study published in 2008, an intelligent traffic control system was proposed. Each road junction has four lanes and four traffic lights. An RFID reader and a controller unit are included with each transmission. When an ambulance comes within range of the traffic signal's RFID reader, the RFID reader scans the ambulance's RFID tag, and the control unit automatically turns that light to green while all other signals in the circle remain red. Arduino, RFID Reader, LED(Light Emitting Diode), LCD(Liquid Crystal Display), and power supply were included in the proposed project. When the Arduino and RFID reader is powered, the Arduino and RFID reader delivers electricity to the LED and LCD. The three LED kinds utilized are RED, YELLOW, and GREEN. When an RFID reader detects an RFID tag connected to an ambulance, it communicates the data contained in the tag to Arduino, which then checks the priority of the vehicle before turning on the Green LED of the relevant lane for a certain period. Arduino resumes regular functionality when the set time has passed. When an RFID tag is scanned by an RFID reader, the procedure is repeated.

However, in 2016 another paper discussed an ambulance management system (AMS) architecture for traffic control, which is a solution that utilizes ArcGIS9.1, GPS, and GSM. A GPS receiver is mounted in each ambulance to establish its real-time position (x, y coordinates) based on the signal supplied by satellite, and this information is transferred to the emergency hospital via a GSM modem. Data like route maps, directions, and voice messages can be sent over the GSM network. Each ambulance is also equipped with a computer or a personal digital assistant (PDA) that displays the route calculated by the AMS in the emergency room. When a call comes from the accident site to the traffic control room, the controller informs this information to the nearest emergency hospital, police station, and fire station (if any fire occurs on the spot). Emergency hospitals will use an Ambulance management system (AMS) to find the accident site on the road network (nearest road segment and landmark) and find the nearest ambulance to the accident site and allocate that ambulance to the accident site. AMS tools are used to find the fastest path from the nearest ambulance location to the accident site; from the accident site to the nearest hospital; a route map and directions are sent to the ambulance driver. In addition, another article from 2021 suggested using an RFID Transmitter (Tx) in an ambulance to transmit a signal to an RFID receiver (Rx) at the next impending traffic lights junction. Once the signal is received at the traffic light junction, the Near Field Communication (NFC) module and microcontroller will do a fast check to determine the route of the approaching ambulance, and if the ambulance is in the red lane, they will stop the present flow of traffic. The traffic lights along the ambulance path will thereafter be turned green by traffic control. It distinguishes out for its offline capabilities and the fact that it does not require the use of a server. Because the proposed SATCS(satellite communication service) is based on RFID technology, it is less expensive to install than equivalent current systems. Another study, on the other hand, employed cloud computing to store both RFID and app data. It also provides access to the cloud whenever needed. The data from the RFID and app is also delivered to the microcontroller, which processes it and changes the signal accordingly. In addition, another research in 2019 recommended that an ambulance smartphone application be developed and utilized to relay ambulance position data to a cloud server. They created the acoustic interface between the ambulance and the smartphone that was mounted on the ambulance's dashboard. When a siren rings, the ambulance smartphone application sends the location of the ambulance to a cloud server. The cloud server application, on the other hand, distributes ambulance position information to other general vehicles while meeting the requirements that the ambulance travels on a major road, the distance between the general vehicle and the ambulance is less than 500 meters, and the general vehicle and ambulance are in proximity.

Registration Method

The methods for registering for this ambulance management and patient monitoring systems vary; some articles advised that users utilize a mobile application. A study from 2008 proposed the High Priority Vehicle Booking Application. When a user loads a page, a socket connection is formed between the user and the server for communication purposes. When the user needs an ambulance, he or she will request one by pressing the Get Ambulance button. This button sends the user's created ID as well as the user's current location to the server. The Google Maps API is used to extract the supplied location.

Other papers, on the other hand, used a different registration method. According to a report published in 2016, registration would begin when an accident site calls the traffic control center, and the controller informs the nearest emergency hospital of the information. Ambulance management systems (AMS) will be used by emergency hospitals to locate the accident location on the road network, locate the closest ambulance to the accident site, and assign that ambulance to the accident site. Other systems, for example, just regulate traffic without dispatching ambulances to patients. However, in certain situations, the patient's information is scanned automatically. According to research published in 2018, a patient's RFID TAG may be swiped on a scanner, which sends the patient's details, such as name, age, ailment, and so on, to the hospital department via GSM technology. Similarly, in another paper in 2019, the patient with critical situations such as cardiac stroke patients are being monitored via sensors to detect their situation, and whenever the patient's heartbeat rate changes badly, the Arduino which records all the patient's information uses GSM shield to send an SMS message containing this information, patient ID and the location of the patient which has been taken via GPS shield, to his doctor's mobile phone, who in turns sends an ambulance to the patient's location. and in certain cases, the patient's information is already saved in the country's health database, and all the information, including his name, ID, and medical history, can be accessed simply by scanning his fingerprint while they are rescuing him in the ambulance (If the patient had a car accident for example and didn't call the ambulance).

Biomedical Sensors

Other authors proposed using telemedicine to keep the patient's condition stable while transporting him to the hospital. In 2019, a paper proposed a similar approach in which the injured individual's body condition is fetched through a sensor, and this device is used to avoid lateral arrangements in the hospital for treatment until the ambulance arrives, as well as informing the doctor and the injured patient's family about the accident. It makes use of an Arduino Uno that is connected to a computer through USB. The heartbeat sensor is connected to the microcontroller to measure BPM (Beats per Minute rate), the ECG sensor collects the electrical signals generated by the heart, the temperature sensor is used to quantify the temperature in blood vessels and estimate the cardiac output, and the fingerprint scanner scans and retrieves a person's fingerprint for security purposes. The fingerprint is used to acquire the victim's personal information.

Another study in India used the method of monitoring and tracking not just the patient's vital signs, but also important activities, physical and mental status, and drugs. In this article, WBAN is used to track and access data from patients (a network of heterogeneous sensors connected to a hub). Each ambulance is a node in the wireless network, which is connected through the internet to a centralized hospital server situated at a specific hospital. Similarly, numerous ambulances from the same hospital relay patient data to the same hospital's server. In contrast, the DHT11 Sensor was employed to measure body temperature in a report published in 2020. The measured temperature is sent serially to the controller. The NSK TCRT1000 heart rate sensor is used to measure heart rate. Photoplethysmography is the basis for its operation. A light detector and a light source are arranged on the same side of the sensor for measuring purposes. The finger is then moved to the opposite side. Following that, the light source emits light that passes through the patient's finger, and the light reflected is detected by the light detector within the sensor. The quantity of light reflected by the finger changes with the amount of blood flow induced by the heart pounding. Another research published in 2017 recommended utilizing Arduino, Raspberry Pi, a pulse rate sensor, a temperature sensor, and jumper wires to create a smart band that would sense the patient's biological status. The temperature sensor and the pulse rate sensor are linked to Arduino's Analog pins (A0 and A1). Using a serial USB converter, Arduino is linked to the Raspberry Pi.

Video Streaming Feature

In a paper published in 2015, the hardware for the enabling video streaming technique consisted of the Raspberry Pi B, which is a credit-card-sized single-board computer based on the Broadcom BCM2835 system on a chip. It also includes an ARM1176JZF-S 700 MHz processor, Video Core IV GPU, with 512 MB, a 15-pin MIPI camera interface, HDMI, and RCA for video in, a 640x350 to 1920x1200 resolution for video out, and

digital HDMI for audio. They also relied on the 3G/4G network for connectivity since they were the latest technology back then when the paper was issued. However, in 2018 another paper suggested using a small cell base station (HeNB) instead of the 4G network, which is located inside the ambulance.

A transceiver should be installed on the roof of the ambulance to transmit/receive data to/from the backhaul microcell network. The HeNB installed inside the ambulance makes a wireless connection between the paramedics and the small cell access point (SAP). The SAP and the transceiver are connected through the wired network. But nowadays with the development of the 5G network, with its special characteristics of reliability and high frequency of transferring a large amount of data in a matter of milliseconds, the use of video streaming would be much more popular. In a paper conducted in 2021, a 5G-enabled smart ambulance system was proposed with its ability to establish a 5G communication network, remote video communication and telemedicine medical data exchange. The approach uses VR glasses, or video terminals, in real-time, to grasp the condition of patients in transit. Emergency and critical patients can immediately receive expert rescue guidance.

System Conceptual Design

The Proposed System Architecture

The proposed system mainly consists of five main elements, the mobile application that all citizens can use to register for this service, the hospital server in the cloud in which all the patient's data would be stored, the doctor's, and the receptionist's system in corporation with the emergency department, and lastly the ambulance IoT sensors that sends the patient's data in real-time to the hospital server. The hospital system shares and forward the data and information of the citizen to the doctors and paramedics via the 5G network. As shown in Figure 1.



Figure 1. Shows general system view

The Patient Registration Mobile Application

Since in Libya, there is no electronic health record, there is no way to retrieve the patient health history base on his ID or national number as known in most developed countries. In this case, a mobile application is used so the patient can register himself and his family members, the user taps on the register, and fill in the fields with the necessary information such as the person's national number, name, gender, birth date, location, phone number, profile picture, blood group, and a relative's name and phone number in case of emergency, past medical history for example if they suffer from allergy or any chronic disease, and family history in case they have any common disease in their family. All this information would be directly stored in the hospital server and can be used as a mini health record in case of an emergency. The mobile application can be used to register multiple patients, in case the father downloads the application he can register his kid's information.

In case the user needs to call an ambulance, he can open the application and tap on the call ambulance, then a list of the hospital subscribed to this service would be displayed, prioritized by their closeness to the patient's

address, he can choose the nearest hospital or the hospital they prefer. In case the patient needs to change his location manually he can change his location in the request before the submission is done, otherwise, his current location would be sent to the hospital by GPS, then he submits the request.

The Receptionist Ambulance Management System

On the other hand, with the emergency room system, when the receptionist at the institution receives the request, strictly at the targeted hospital, the system displays the patient's location and name. The receptionist clicks on send ambulance button beside the patient information. The system then displays the ambulances list with their IDs and driver's name and phone number.

The receptionist then can review the patient's information then request a doctor could be done, by doctors' names, specializations, and phone numbers would be displayed, the receptionist should choose a doctor and click on the request to assign this particular patient to this doctor, and the patient's information is then sent to this doctor's application. As shown in figure 4.10. Also, the receptionist would start the admission procedure, and allocate a room for this patient, from the allocated room, just after the doctor decides the patient's condition severity level if he needs ICU (intensive care unit) or CCU (cardiac care unit) or Word unit.

The Integrated Rescue System in the Ambulance

Meanwhile, in the ambulance, the patient location and phone number of this particular request or call would be displayed on the ambulance driver application, so the driver can use google maps to display the shortest route to this destination. When the ambulance arrives at the patient's address, and the patient is carried in the ambulance, the paramedics attach the wireless body sensors to his body so that they start to detect his biological conditions, heart rate, blood pressure, oxygen levels, etc. as shown in Figure 2, and the paramedics would start treating the patient. The monitor that is connected to the system in the ambulance would display the patient's information. In case, the patient has bled the paramedics can use the Bank of blood local service to request blood for this patient blood group since in Libya we have ashortage of blood packages in hospitals, and this mobile application service can be helpful.

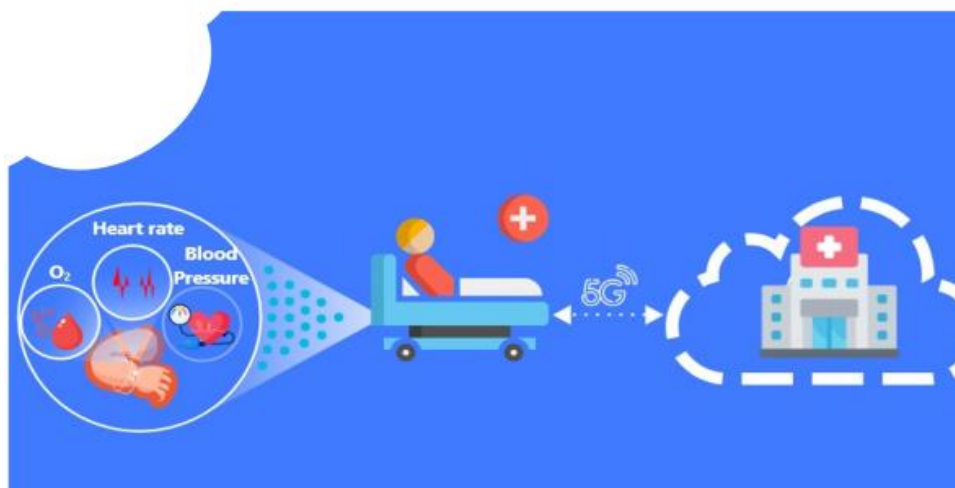


Figure 2. Body sensors sending real-time data to hospital via 5G

The Patient Monitoring and Tele-Diagnose System

On the doctor's side, the patient information would be displayed after the receptionist forwards the request and the information to this doctor. A real-time connection with the ambulance's system would be established, and the biological readings and vital signs of the patient would be displayed on the doctor's desktop or mobile application. The doctor can start diagnosing the patient and type the primitive diagnosis in the diagnosis text field, and then chooses from the list displayed choices if the patient needs to enter the ICU, CCU, or Word unit, depending on the patient's condition seriousness level. The receptionist receives what type of room the doctor has chosen and then allocates this room for the patient, and by that, the admission procedure is automatically

finished. The doctor can call the paramedics through the ambulance system attached to the ambulance equipped with a microphone, speakers, and a camera, in case video streaming is needed. This connection is done by the 5G technology for its reliability, and in case the 5G network is not available a connection established through SMS can be maintained as an alternative.

Survey Results and Analysis

Moreover, people's reactions and thoughts were collected about the proposed system through a survey. The survey's main purpose was to gather data about how local citizens feel about the traditional ambulance service in their country, and if they have ever used the service, as well as if the smart ambulance system was implemented in the real world would they change their mind and start using the system. The survey aims to gather data about the level of satisfaction of the population with the traditional and the proposed ambulance to measure the effectiveness of the proposed system.

The survey was open publicly to anyone; the responses are 224 responses in total, all Libyans. People from different specializations fill out the survey, including human medicine, information technology specialists, rescue services, and more. The method of data collection used was an electronic questionnaire powered by Google. The link to the questionnaire was shared publicly on different social media platforms, and a QR code was generated and shared with the medical and information technology students and teachers. More than half of the responses (59.2%) were from human medicine, 19.4% from information technology specialists, 2.2% from rescue services, and the rest are specialists in engineering, dentistry, economy, and public health.

The survey first asked the applicants if they have ever experienced an emergency case either by themselves or their family members and if they have ever called an ambulance when the situation occurred. Based on this answer they were two different sections one for the people who had called the ambulance, and the other for those who have never called the ambulance.

The first question related to the people's experience with the ambulance was, "have you or one of your family members ever entered the emergency department in the hospital", 69.5% answered yes, and 30.5% answered no. The percentage of people who have never used an ambulance is considerably high, which indicates a serious problem. The survey also asked why they didn't call the ambulance when they needed it, 38.9% said they don't trust the service responsiveness and the speed of the ambulance arrival. They chose "I don't trust the speed of the ambulance and their response", 38.4% chose "Nothing happened to me that required me to call an ambulance", and 18.2% said that they prefer to rescue their family members using their cars. The other 4.5% said the service was not available. The negative responses were much more than the positive responses, which indicates a problem. An investigation of this problem can be done after reviewing the data that the applicants submitted when answering about their trust in the current service.

The survey asked the audience if they trust the ambulance service in their countries, and why they trust or do not trust it. Around 153 responses out of 185 respondents said that they don't trust the ambulance services in their country, and 22 respondents answered that they do trust the service. The rest 10 answered that they don't know if there is an ambulance service in their country (Libya). The reason why they don't trust the ambulance services vary between the response time and the lack of technical support given to this section by the country, as well as the traffic on the road and the bad experiences they have seen or heard related to the service. Some others wrote that they use private rescue companies to request an ambulance, and a considerable number of applicants said that they don't even know the service number.

The Applicants' Experience with the Ambulance

This section had 6 questions and the first question asked whether the ambulance arrived at the right time. Most answered that they don't know or remember whether it arrived at the right time or not. The same answer appeared when asked about the patient's condition when he arrived at the hospital, whether he was transported safely, and if the ambulance got to the hospital at the right time. The other 2 questions were "Did you face the problem of the patient's blood type deficiency in the hospital?", and "Will you repeat your experience of calling an ambulance in case of another emergency?" When asked about blood deficiency, the answers were equal, 50% said yes, they had the problem of blood deficiency, and the other 50% said no they have not faced the problem.

People's Satisfaction with the Proposed System

The last section was about gathering the applicants' feedback on the proposed system. The survey contained a video describing the basic aspects of the system. Since the survey was open to the public, the video had only the most basic aspects with a non-technical description of the system. As shown in Figure 3, Several questions asked for the people's opinion on the system. Out of 224 applicants, 144 said excellent, 53 said very good, 24 answered good, 2 said poor, and 1 said very poorly. It can be concluded that the positive feedback was much higher than the negative feedback. Other questions were asked "Do you think this project can be implemented in your country?", and the result was 44.2% says maybe and 49.1 says yes were the rest disagreed with this question.

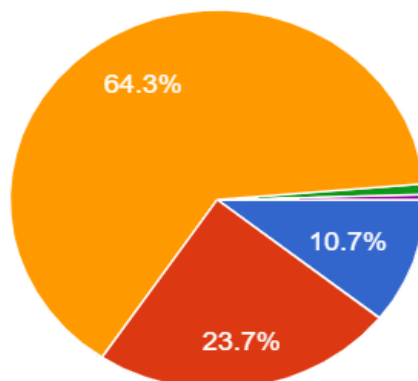


Figure 3. The percentage of the answers to the question "what is your opinion about the proposed system?"

Conclusion

The problem of the patient's delay to get treatment is a serious problem that may lead to the patient's severity or death. The literature of this paper overviews a set of proposed computer systems those help to provide solutions for such a problem. A conceptual design of the smart ambulance system was proposed, the design consisted of four parts, a patient registration mobile application in which patients can register their data and request an ambulance from the nearest hospital; the receptionist ambulance management system, which manages registered patients' data, stores their data as a mini health record, assigns each patient to a doctor, manages the ambulance requests, and sends the ambulance to the patient; the integrated rescue system in the ambulance, which consists of sensors that measure the patients' data and send it to the hospital in real-time by 5G technology; and the system requests blood from the Bank of blood by Almadar; and the patient monitoring and tele-diagnosing system in which doctors can monitor and diagnose the patient's condition.

A survey was conducted electronically to measure the people's satisfaction level with the current ambulance service, and the proposed system, and to gather their suggestions to improve the idea. An animated video that explains the system was created and involved in the survey, so people can understand the system clearly. The survey was opened to the public and shared through links on social media sites and for local university students to fill out.

The results of the survey have revealed the lack of trust in the current ambulance services, the people's independence in rescuing their patients, and the people's acceptance of the idea of solving the problem. The positive answers to the proposed solution have the majority of answers, most respondents liked and welcomed the idea, some had really good suggestions, and few people did not believe in the system's vision. According to the obtained results, it can be concluded that the proposed system would increase the population's trust in the ambulance services if applied, people's belief in the system's ability to solve common rescuing problems, and people's willingness to rely on such systems to rescue their loved ones.

Scientific Ethics Declaration

The authors declare that the scientific ethical and legal responsibility of this article published in EPSTEM journal belongs to the authors.

Acknowledgements or Notes

* This article was presented as an oral presentation at the International Conference on Research in Engineering, Technology and Science (www.icrets.net) held in Budapest/Hungary on July 06-09, 2023.

References

- A. Al-Tawaty, A., & Omar Elfallah, E. (2019). Health professional students' preparedness for E-Health. *Libyan International Medical University Journal*, 04(02), 74–81.
- Ahad, A., Tahir, M., & Yau, K. L. A. (2019). 5G-Based Smart Healthcare Network: Architecture, Taxonomy, Challenges and Future Research Directions. *IEEE Access*, 7, 100747–100762.
- Akca, T., Sahingoz, O. K., Kocyigit, E., & Tozal, M. (2020). Intelligent Ambulance Management System in Smart Cities. In *2020 International Conference on Electrical Engineering (ICEE)*. IEEE.
- Albayood, Z. S. A., Elfallah, E. A. O., & Elghriani, A. (2020). Measuring the awareness of health care providers at Benghazi medical center for health informatics. In *ACM International Conference Proceeding Series*.
- Almadani, B., Bin-Yahya, M., & Shakshuki, E. M. (2015). E-Ambulance: Real-time integration platform for heterogeneous medical telemetry system. *Procedia Computer Science*, 63, 400–407.
- Bernstein, M. L., McCreless, T., & Côté, M. J. (2007). Five constants of information technology adoption in healthcare. *Hospital Topics*, 85(1), 17–25. <https://doi.org/10.3200/htps.85.1.17-26>
- Bhajantri, R., Bhapkar, P., Chaugule, P., Patil, V., & Kotkar, M. (2019). Patient health care and ambulance tracking system. *Journal of Analysis and Computation*, 12(4), 1-10.
- Bharade, S., Botre, P., Nagane, S., & Shah, M. (2017). A novel approach for smart ambulance using intelligent traffic control system modern educational society 's college of engineering , Pune , 5(09), 1009–1010.
- Bhatia, N., Bedi, A., & Rajotiya, R. N. (2018). Smart ambulance movement and monitoring system using GSM and RFID technology. *International Research Journal of Engineering and Technology (IRJET) Volume*, 5, 1033–1036.
- Corradini, A., & Gheorghiasa, C. A. (2015). CAMbulance: A live video streaming system for ambulance services. In *2015 International Conference on Information and Communication Technology Research (ICTRC)*. IEEE.
- Dumka, A., & Sah, A. (2019). Smart ambulance system using concept of big data and internet of things. In *Healthcare Data Analytics and Management* (pp. 155–176). Elsevier.
- Fadel, M. A., Elfallah, E. A. O., & Elghriani, A. (2020). An evaluation of the attitudes of healthcare nurses towards new technologies. In *ACM International Conference Proceeding Series*.
- Fong, B., Fong, A. C. M., & Li, C. K. (2018). Internet of things in smart ambulance and emergency medicine. In *Internet of Things A to Z* (pp. 475–506). John Wiley & Sons, Inc.
- Girish, H. R., Kumar, J. V., Swamy, N. K., Kumar, M. S., & Sudhakara, H. M. (2020). A review: smart ambulance and traffic controlling system. *Int J Eng Res Technol (Ahmedabad)*, 9, 10-17577.
- Godbole, M., & Agarwal, A. (2020). Clinical data driven decision support in healthcare informatics. *International Journal of Engineering Research and Technology*, 13(1), 107.
- Kalarthi, Z. M. (2016). A Review paper on smart health care system using internet of things. *International Journal of Research in Engineering and Technology*, 05(03), 80–84.
- Kamruzzaman, M. M. (2020). Architecture of smart health care system using artificial intelligence. In *2020 IEEE International Conference on Multimedia & Expo Workshops (ICMEW)*. IEEE.
- Karkar, A. (2019). Smart ambulance system for highlighting emergency-routes. In *2019 Third World Conference on Smart Trends in Systems Security and Sustainability (WorldS4)*. IEEE.
- Kobayashi, T., Kimura, F., & Arai, K. (2019). Smart ambulance approach alarm system using smartphone. In *2019 IEEE International Conference on Consumer Electronics (ICCE)*. IEEE.
- Krishnan, S., Thangaveloo, R., Bin Abd Rahman, S.-E., & Sindramutty, S. R. (2021). Smart ambulance traffic control system. *Trends in Undergraduate Research*, 4(1), c28-34.
- Latif, S., Qadir, J., Farooq, S., & Imran, M. (2017). How 5G Wireless (and Concomitant Technologies) Will Revolutionize Healthcare? *Future Internet*, 9(4), 93.
- Nath Saha, H. (2020). Automatic ambulance system using IOT. *International Journal of Engineering and Science Invention*, 9(5), 1–3.
- Pasha, I. (2016). *Ambulance management system using GIS*. <https://www.diva-portal.org/smash/record.jsf?pid=diva2%3A22123&dsid=4837>
- Rehman, I. U., Nasralla, M. M., Ali, A., & Philip, N. (2018). Small cell-based ambulance scenario for medical video streaming: A 5G-health use case. In *2018 15th International Conference on Smart Cities: Improving Quality of Life Using ICT & IoT (HONET-ICT)*. IEEE.
- Saha, H. N., Raun, N. F., & Saha, M. (2017). Monitoring patient's health with smart ambulance system using

- Internet of things (IOTs). In *2017 8th Annual Industrial Automation and Electromechanical Engineering Conference (IEMECON)*. IEEE.
- Salau, S. A., Abifarin, F. P., Alhassan, J. A., & Udoudoh, S. J. (2020). Usability effectiveness of a federated search system for electronic theses and dissertations in Nigerian institutional repositories. *Performance Measurement and Metrics*, 22(1), 1–14.
- Scherman, J. (2019). 5 ways technology in healthcare is transforming the way we approach medical treatment Rasmussen University. <https://www.rasmussen.edu/degrees/health-sciences/blog/technology-in-healthcare-transformation/>
- Sherly, I. S., & Sobitham Princy, M. A. (2019). Smart ambulance rescue system with patient health monitoring using IoT. *International Journal of Advanced Research in Science, Engineering and Technology*, 6(2), 8222–8228.
- U, S., N, S., Aithal, S. R., , Shripad Bhat, S. & K, B. (2019). IoT based smart ambulance system. *International Research Journal of Engineering and Technology*, 6(7), 2328- 2332.
- Ullah, K., Shah, M. A., & Zhang, S. (2016). Effective ways to use internet of things in the field of medical and smart health care. In *2016 International Conference on Intelligent Systems Engineering (ICISE)*. IEEE.
- Vippalapalli, V., & Ananthula, S. (2016). Internet of things (IoT) based smart health care system. In *2016 International Conference on Signal Processing, Communication, Power and Embedded System (SCOPES)*. IEEE.

Author Information

Arwa F. Albillali

Libyan International Medical University
Benghazi -Libya

Ehab A. Omar Elfallah

Libyan International Medical University
Benghazi -Libya
Contact e-mail: ehab.elfallah@limu.edu.ly

Bilal A. Aljabour

Libyan International Medical University
Benghazi -Libya

Tawfiq Tawill

Libyan International Medical University
Benghazi -Libya

To cite this article:

Albillali, A.F. Elfallah, E. A. O. Aljabour, B. A. & Tawill, T. (2023). A proposed conceptual design for a computer-based ambulance system in Libya using IoT. *The Eurasia Proceedings of Science, Technology, Engineering & Mathematics (EPSTEM)*, 23, 131-142.

The Eurasia Proceedings of Science, Technology, Engineering & Mathematics (EPSTEM), 2023

Volume 23, Pages 143-150

ICRETS 2023: International Conference on Research in Engineering, Technology and Science

Non-linear Viscoelastic Beams Under Periodic Strains: An Approach for Analyzing of Longitudinal Fracture

Victor Rizov

University of Architecture, Civil Engineering and Geodesy

Abstract: This work describes a longitudinal fracture analysis of beam structure of circular cross-section under periodic strains. The material whose properties vary in radial direction has non-linear viscoelastic behaviour. The beam is loaded in torsion so that the twist angle represents a periodical function. Time-dependent behaviour under periodic strains is dealt with a model having a non-linear spring and a linear dashpot. The complementary strain energy in the beam is considered to determine the strain energy release rate. The balance of energy is examined to verify the strain energy release rate. The ascendancy of various parameters over strain energy release rate is assessed.

Keywords: Non-linear viscoelastic beam, Longitudinal fracture, Periodic strain

Introduction

One of the important tasks of up-to-date material science is the development and perfecting of continuously inhomogeneous structural materials. The properties of these materials are contingent on coordinates. In recent decades, the functionally graded materials have emerged as an advanced type of materials with continuous inhomogeneity (Fanani et al., 2021; Mahamood & Akinlabi, 2017; Nikbakht et al., 2019; Oza et al., 2021). The change of microstructure of functionally graded materials in a structural member or component is formed in a desired way during manufacturing (Dias et al., 2010; Gururaja Udupa et al., 2014; Gandra et al., 2011; Radhika et al., 2020).

In their life-time, many engineering structures made of continuously inhomogeneous materials undergo non-linear viscoelastic deformation under periodic loading that must be considered when analyzing fracture. On account of that, the aim of this work is to examine in analytical way the longitudinal fracture of a non-linear viscoelastic beam under periodic strains (prior papers in this field are focussed on linear viscoelastic beams (Narisawa, 1987; Rizov, 2022; Rizov, 2022)). The beam under examination has a circular section and is inhomogeneous in radial direction. The beam is under torsion. The strain energy release rate (SERR) is determined. The balance of energy (BE) is considered for control of the SERR solution.

Theoretical Analysis

In this paper, the non-linear viscoelastic mechanical model in Fig. 1 is used. The model consists of a non-linear spring with shear modulus, G_j , placed in parallel to a dashpot of linear behaviour (the viscosity coefficient is η). Shear strain, γ , in the model is a periodical function of time, t , as depicted in Fig. 2. The period of the shear strains is T . The maximum value of shear strains is γ_m . The period of shear strains is presented as $T = T_b + T_d$ where $T_b = pT$, $0 < p < 1$ (Fig. 2). Thus, $T_d = (1 - p)T$.

- This is an Open Access article distributed under the terms of the Creative Commons Attribution-Noncommercial 4.0 Unported License, permitting all non-commercial use, distribution, and reproduction in any medium, provided the original work is properly cited.

- Selection and peer-review under responsibility of the Organizing Committee of the Conference

© 2023 Published by ISRES Publishing: www.isres.org

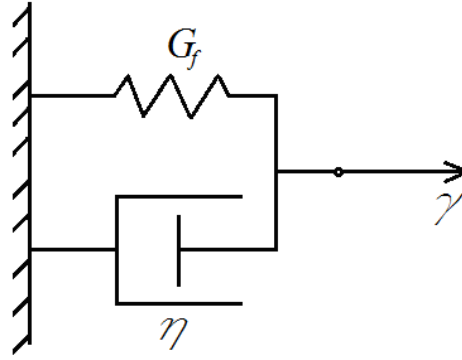


Figure 1. Non-linear viscoelastic model.

The shear strain is expanded in series of Fourier

$$\gamma(t) = q_0 + \sum_{j=1}^{\infty} q_j \cos(j\bar{\omega}t) + \sum_{j=1}^{\infty} r_j \sin(j\bar{\omega}t), \quad \bar{\omega} = \frac{2\pi}{T}. \quad (1)$$

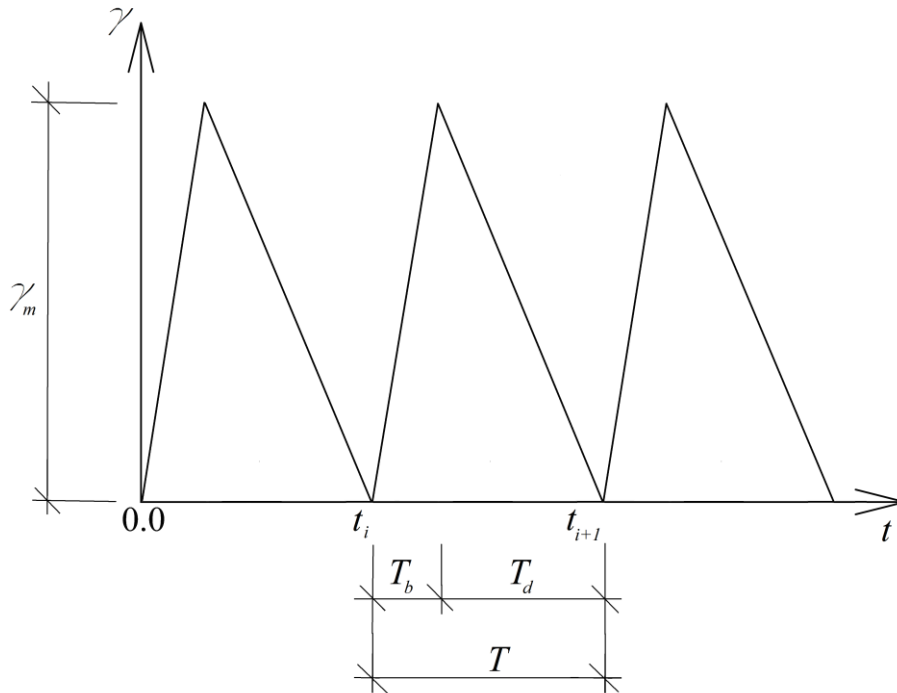


Figure 2. Periodic change of the shear strain.

by using the formulae

$$q_0 = \frac{1}{T} \int_0^T \gamma dt, \quad q_j = \frac{2}{T} \int_0^T \gamma \cos(j\bar{\omega}t) dt, \quad r_j = \frac{2}{T} \int_0^T \gamma \sin(j\bar{\omega}t) dt, \quad (2)$$

the coefficients in (1) are found as

$$q_0 = \frac{\gamma_m}{2}, \quad q_j = \frac{2\gamma_m}{T^2} \left\{ \frac{1}{pj^2\bar{\omega}^2} [j\bar{\omega}pT \sin(j\bar{\omega}pT) + \cos(j\bar{\omega}pT) - 1] + \right.$$

$$+ \frac{T}{(1-p)j\bar{\omega}} [\sin(j\bar{\omega}T) - \sin(j\bar{\omega}pT)] -$$

$$- \frac{1}{(1-p)j^2\bar{\omega}^2} [Tj\bar{\omega} \sin(j\bar{\omega}T) + \cos(j\bar{\omega}T) - pTj\bar{\omega} \sin(j\bar{\omega}pT) - \cos(j\bar{\omega}pT)] \Big\}, \quad (3)$$

$$r_j = \frac{2\gamma_m}{T^2} \left\{ \frac{1}{pj^2\bar{\omega}^2} [\sin(j\bar{\omega}pT) - j\bar{\omega}Tp \cos(j\bar{\omega}pT)] + \right.$$

$$\left. + \frac{T}{(1-p)j\bar{\omega}} \left\{ [\cos(j\bar{\omega}pT) - \cos(j\bar{\omega}T)] - \right. \right.$$

$$\left. \left. - \frac{1}{(1-p)j^2\bar{\omega}^2} [\sin(j\bar{\omega}T) - j\bar{\omega}T \cos(j\bar{\omega}T) - \sin(j\bar{\omega}pT) + j\bar{\omega}pT \cos(j\bar{\omega}pT)] \right\} \right\}. \quad (4)$$

The shear stress, τ_f , in the spring and the shear stress, τ_η , in the linear dashpot (Fig. 1) are expressed by the following laws:

$$\tau_f = G_f \gamma^n, \quad \tau_\eta = \eta \dot{\gamma}, \quad (5)$$

where n is a material property, η is the coefficient of viscosity.

The shear stress (refer to Fig. 1) is deduced as

$$\tau = \tau_f + \tau_\eta. \quad (6)$$

By using (1), (5) and (6), one derives

$$\tau = G_f \left[q_0 + \sum_{j=1}^{\infty} q_j \cos(j\bar{\omega}t) + \sum_{j=1}^{\infty} r_j \sin(j\bar{\omega}t) \right]^n +$$

$$+ \eta \left[\sum_{j=1}^{\infty} -q_j j\bar{\omega} \sin(j\bar{\omega}t) + \sum_{j=1}^{\infty} r_j j\bar{\omega} \cos(j\bar{\omega}t) \right]. \quad (7)$$

By combining of (5) and (7), one obtains

$$\tau = G_f \gamma^n + \eta \left[\sum_{j=1}^{\infty} -q_j j\bar{\omega} \sin(j\bar{\omega}t) + \sum_{j=1}^{\infty} r_j j\bar{\omega} \cos(j\bar{\omega}t) \right]. \quad (8)$$

Dependence (8) represents the non-linear stress-strain-time law of model (Fig. 2).

This law is used to model the mechanical behaviour of the clamped structure sketched in Fig. 3. The beam cross-section is a circle of radius, R_1 . The beam longitudinal size is l . We are focussed on a longitudinal crack in the form of cylindrical surface of radius, R_2 . The crack longitudinal size is a as depicted in Fig. 3. The beam is under torque so that the twist angle, φ , of external crack arm (the external crack arm section has internal and external radius, R_2 and R_1 , respectively) changes periodically with time (at $t_i \leq t \leq t_i + T_b$ the

angle of twist grows from 0 to φ_h ; at $t_i + T_b \leq t \leq t_i + T$ the angle decreases from φ_h to 0). The internal arm of crack is unstressed (the internal arm of crack has circular section with radius, R_2).

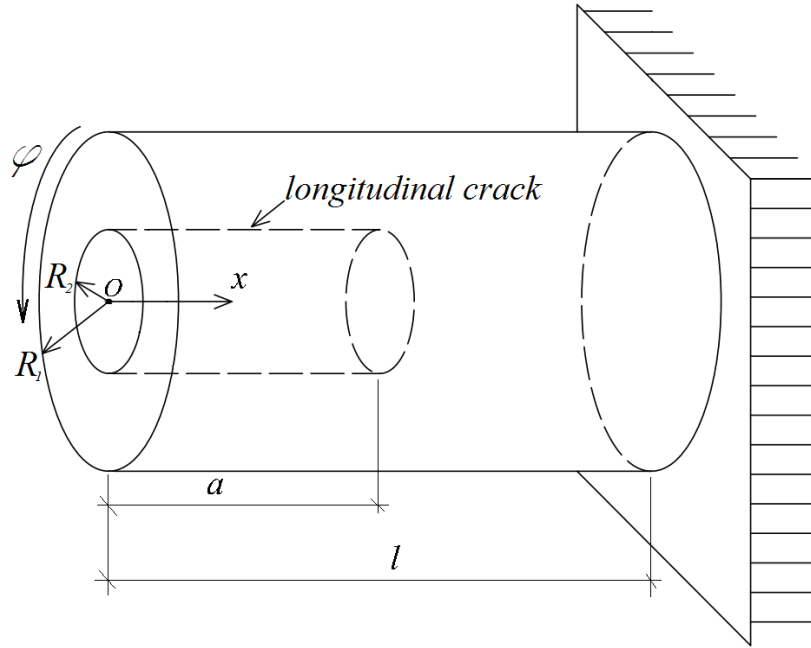


Figure 3. Static scheme of beam under examination.

The beam is inhomogenous in radial direction. Thus, material properties, G_f and η , change exponentially along section radius

$$G_f = G_{f0} e^{\frac{sR}{R_1}}, \quad \eta = \eta_0 e^{\frac{gR}{R_1}}. \quad (9)$$

Here, G_{f0} and η_0 are G_f and η magnitudes in the section centre, s and g are parameters.

The SERR, G , for the longitudinal crack (Fig. 3) is deduced as

$$G = \frac{dU^*}{2\pi R_2 da}, \quad (10)$$

where the complementary strain energy (CSE) in the beam is

$$U^* = U_1^* + U_2^* = a \int_{R_2}^{R_1} u_{01}^* 2\pi R dR + (l - a) \int_0^{R_1} u_{02}^* 2\pi R dR. \quad (11)$$

Here, u_{01}^* and u_{02}^* are CSE densities in the external arm of crack and in the intact portion of beam. u_{01}^* is calculated as

$$u_{01}^* = \tau\gamma - \int_0^\gamma \tau d\gamma. \quad (12)$$

The shear strain in section of the external arm of crack is

$$\gamma = \frac{\gamma_{ek}}{R_1} R. \quad (13)$$

In dependence (13), γ_{ek} is the strain magnitude at the surface.

The CSE density in the intact portion of beam is found by substituting $\tau = \tau_{un}$ and $\gamma = \gamma_{un}$ in formula (12) (τ_{un} and γ_{un} the shear stress and shear strain in the intact portion of beam). Distribution of γ_{un} in section of the intact portion of beam is obtained by substituting of $\gamma_{ek} = \gamma_{hw}$ in (13). Here, γ_{hw} is the strain magnitude at the surface of the intact portion of beam.

γ_{ek} and γ_{hw} are determined by applying the following approach. First, two equilibrium equations are formulated

$$T = \int_{R_2}^{R_1} \tau 2\pi R^2 dR, \quad T = \int_0^{R_1} \tau_{un} 2\pi R^2 dR. \quad (14)$$

where T is the torque in the external arm of crack.

Further, it follows from the Maxwell-Mohr integrals that

$$\varphi = \frac{\gamma_{ek}}{R_1} a + \frac{\gamma_{hw}}{R_1} (l - a). \quad (15)$$

γ_{ek} , γ_{hw} and T are determined from (14) and (15) by MatLab.

After combining of (10) and (11), one derives

$$G = \frac{1}{R_2} \left(\int_{R_2}^{R_1} u_{01}^* R dR - \int_0^{R_1} u_{02}^* R dR \right). \quad (16)$$

Integrals in (16) are treated by MatLab.

In order to verify (16), the SERR is determined as well by analyzing the BE. The result is

$$G = \frac{T}{2\pi R_2} \frac{\partial \varphi}{\partial a} - \frac{1}{2\pi R_2} \frac{\partial U}{\partial a}. \quad (17)$$

Here, the strain energy (SE), U , is reckoned by using (11) and (12). For this purpose, the CSE densities are replaced with the SE densities, u_{01} and u_{02} . The SE density in the external arm of crack is

$$u_{01} = \int_0^{\gamma} \tau d\gamma. \quad (18)$$

The SE density in the intact portion of beam is calculated by replacing of τ with τ_{un} in (18). By substituting of φ and U in (17), one obtains

$$G = \frac{T}{2\pi R_2} \left(\frac{\gamma_{ek}}{R_1} - \frac{\gamma_{hw}}{R_1} \right) - \frac{1}{R_2} \int_{R_2}^{R_1} u_{01} R dR + \frac{1}{R_2} \int_0^{R_1} u_{02} R dR. \quad (19)$$

Integrals in (19) are treated by MatLab. The SERR reckoned by (19) and (16) are match which is a verification of the present analysis.

Numerical Results

The SERR calculations are carried-out by using the following data: $R_1 = 0.008$ m, $l = 0.300$ m, $n = 0.6$, $p = 0.5$, $T = 80$ sec and $\varphi_h = 0.001$ rad.

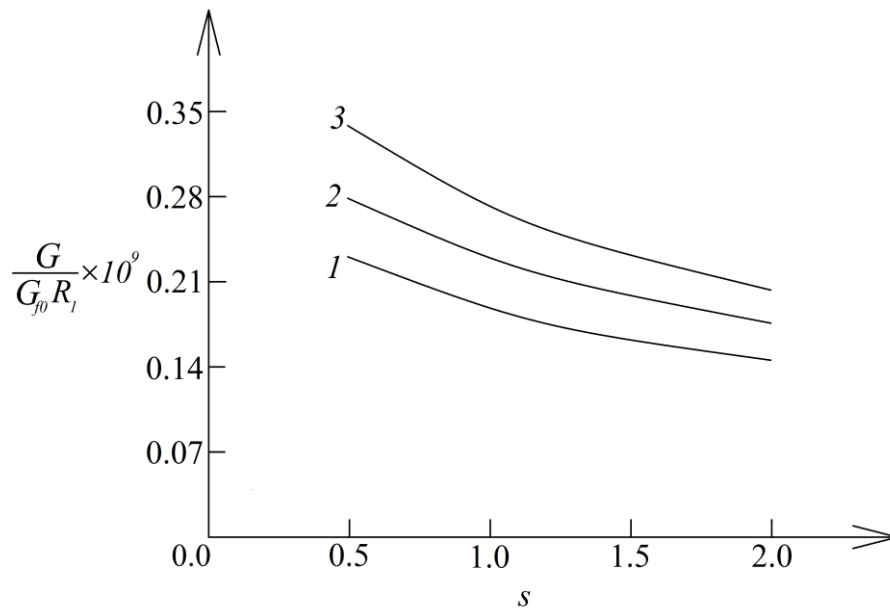


Figure 4. SERR - s curves (1 - at $R_2 / R_1 = 0.4$, 2 - at $R_2 / R_1 = 0.6$ and 3 - at $R_2 / R_1 = 0.8$).

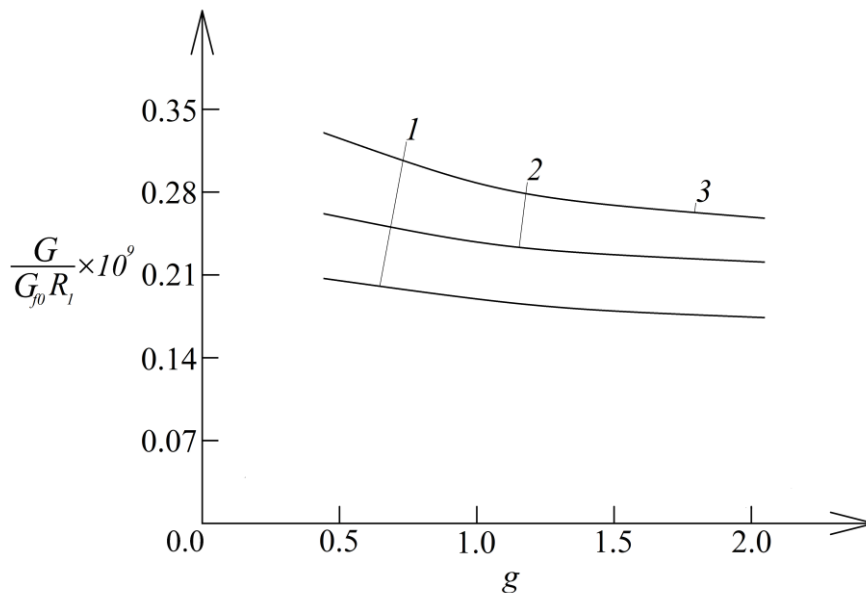


Figure 5. SERR - g curves (1 - at $\varphi_h = 0.0006$ rad, 2 - at $\varphi_h = 0.0008$ rad and 3 - at $\varphi_h = 0.001$ rad).

The SERR - s curves are presented at three R_2 / R_1 ratios in Fig. 4. The curves in Fig. 4 indicate that SERR reduces when s grows. However, growth of R_2 / R_1 ratio generates growth of SERR (Fig. 4). The influence of φ_h and g on SERR is assessed (Fig. 5). When the twist angle, φ_h , increases, SERR also increases. Increase of parameter, g , reduces SERR (Fig. 5).

Conclusion

An approach for analytical examination of the longitudinal fracture in non-linear viscoelastic inhomogeneous beam structure under periodically changing strains is presented. The beam is subjected to pure torsion. A model of non-linear spring placed in parallel to a linear dashpot is used for describing the beam mechanical behaviour. A solution of SERR that accounts for the beam non-linear viscoelastic deformation under periodic loading is derived. The influence of the periodic loading on SERR is assessed. Reckons of SERR are carried-out at different magnitudes of twist angle, φ_h . It is found that growth of φ_h generates growth of SERR. The SERR increases as well with growth of R_2 / R_1 ratio. The growth of parameters, s and g , induces reduction of SERR.

Recommendations

The approach presented in this paper can be developed further by analyzing the longitudinal fracture of beams subjected to torsion and bending under periodic strains.

Scientific Ethics Declaration

The author declares that the scientific ethical and legal responsibility of this article published in EPSTEM journal belongs to the author.

Acknowledgements or Notes

* This article was presented as a poster presentation at the International Conference on Research in Engineering, Technology and Science (www.icrets.net) held in Budapest/Hungary on July 06-09, 2023.

References

- Dias, C. M. R., Savastano, Jr. H., & John, V. M. (2010). Exploring the potential of functionally graded materials concept for the development of fiber cement. *Construction and Building Materials*, 24, 140-146.
- Fanani, E.W.A., Surojo, E., Prabowo, A. R., & Akbar, H. I. (2021). Recent progress in hybrid aluminum composite: Manufacturing and application. *Metals*, 11, 1919-1929.
- Gandra, J., Miranda, R., Vilaca, P., Velinho, A., & Teixeira, J.P. (2011). Functionally graded materials produced by friction stir processing. *Journal of Materials Processing Technology*, 211, 1659-1668.
- Gururaja U., Shrikantha Rao S., & Rao Gangadharan, K. (2014). Functionally graded composite materials: An overview. *Procedia Materials Science*, 5, 1291-1299.
- Mahamood, R. C., & Akinlabi, E. T. (2017). *Functionally graded materials*. Springer.
- Nikbakht, S., Kamarian, S., & Shakeri, M. (2019). A review on optimization of composite structures Part II: Functionally graded materials. *Composite Structures*, 214, 83-102.
- Narisawa, I. (1987). Strength of polymer materials. *Chemistry*, 400.
- Oza, M. J., Schell, K. G., Bucharsky, E. C., Laha, T., & Roy, S. (2021). Developing a hybrid Al-SiC-graphite functionally graded composite material for optimum composition and mechanical properties. *Materials Science and Engineering: A*, 805, 140625.
- Radhika, N., Sasikumar, J., Sylesh, J. L., & Kishore, R. (2020). Dry reciprocating wear and frictional behaviour of B4C reinforced functionally graded and homogenous aluminium matrix composites. *Journal of Materials Research and Technology*, 9, 1578-1592.

Rizov, V.I. (2022). Effects of periodic loading on longitudinal fracture in viscoelastic functionally graded beam structures. *J. Appl. Comput. Mech.*, 8, 370–378.

Rizov, V.I. (2022). Viscoelastic inhomogeneous beam subjected to mechanical loading and periodically varying temperature: a longitudinal fracture analysis. *Procedia Structural Integrity* 41, 103–114.

Author Information

Victor Rizov

University of Architecture, Civil Engineering and Geodesy

Sofia, Bulgaria

Contact e-mail: v_rizov_fhe@uacg.bg

To cite this article:

Rizov, V. (2023). Non-linear viscoelastic beams under periodic strains: An approach for analyzing of longitudinal fracture. *The Eurasia Proceedings of Science, Technology, Engineering & Mathematics (EPSTEM)*, 23, 143-150.

The Eurasia Proceedings of Science, Technology, Engineering & Mathematics (EPSTEM), 2023

Volume 23, Pages 151-164

ICRETS 2023: International Conference on Research in Engineering, Technology and Science

Research on Media Presentation and Public Reaction to the First Health Digital Assistant in Croatia

Stjepan Petricevic

Alma Mater Europaea Maribor

Daria Mustic

University of Zagreb

Abstract: This research paper investigates the perception, acceptance, and media presentation of the digital assistant *Andrija* in the healthcare sector during the COVID-19 pandemic. The research used combined methods that include analysis of the media presentation of the *Andrija* project and the public's reaction on Facebook, collection of public announcements on the Facebook social network, and their quantitative and qualitative analysis. The research sample consisted of 82 posts on Facebook that corresponded to the keywords "Andrija, digital assistant". The research results show that *Andrija* digital assistant played a key role in providing basic information about the COVID-19 pandemic and supporting the public in making informed decisions. The analysis of the media presentation of the *Andrija* project on Facebook revealed a diversity in the size of the posts, with an emphasis on image/video material and the presence of links to official websites. Also, *Andrija* chatbot was generally well received, with a high number of "Like" reactions and emotional connection expressed through "Love" reactions on analyzed Facebook posts. However, there are variations in user perception. Examination of the correlation between the size of the post (number of words) and reactions on Facebook posts did not show a statistically significant correlation between the size of the post and the total number of quick reactions, but a statistically significant positive correlation was found between the size of the post and the number of "Like" reactions.

Keywords: Health digital assistant, Andrija, Facebook, Media presentation, Crisis communication

Introduction

In the last few years, digital assistants and chatbots have become ubiquitous in our daily lives. Their application in various sectors, including healthcare, opens new opportunities for providing services and improving the user experience. Chatbots have the potential to revolutionize healthcare by providing patients with 24/7 access to information and support, assisting healthcare providers with administrative tasks, and improving patient engagement and outcomes (Božić, 2023).

Chatbots can also be used to triage patients who have certain symptoms, as well as provide additional consultative support after a clinical encounter. This functionality is particularly important in the context of the global shortage of health workers, which is estimated to be around 18 million by 2030 (Parmar et al., 2022). By using chatbots for triage, healthcare systems can reduce the burden on healthcare providers and prioritize patients most in need of emergency medical care.

A 2020 study identified 78 commercially available health bot applications in 33 countries and provided a comprehensive overview of these applications (Parmar et al., 2022). The results showed that most applications are focused on patients and on primary health care and mental health. According to a study by Amiri & Karahanna, which analyzed 61 chatbots used in more than 30 countries, chatbots provide complementary

- This is an Open Access article distributed under the terms of the Creative Commons Attribution-Noncommercial 4.0 Unported License, permitting all non-commercial use, distribution, and reproduction in any medium, provided the original work is properly cited.

- Selection and peer-review under responsibility of the Organizing Committee of the Conference

© 2023 Published by ISRES Publishing: www.isres.org

functionality that increases the activities of public health workers in responses related to public health; addressing capacity constraints, they go beyond the demands of social distancing and misinformation (Amiri & Karahanna, 2022).

The COVID-19 pandemic presented a global challenge that required the rapid dissemination of information, symptom monitoring, and mental health support for individuals around the world. In this context, chatbots have emerged as a useful tool for providing quick information and support to users. Organizations such as the Centers for Disease Control and Prevention (CDC) and the World Health Organization (WHO) have recognized the importance of new communication mechanisms in responding to citizen requests related to COVID-19. The implementation of chatbots by many countries as a means of monitoring symptoms, providing testing instructions, informing about safety measures, and providing general advice on disease prevention has proven extremely useful in situations of high demand for health services and limited resources. In the study by Amer et al. (2021), a proposed chatbot system was used that used a pre-trained Google BERT Language model along with a text classification and categorization technique based on word meaning. The results showed that such a system can effectively manage a large number of citizen requests during a pandemic, ensuring credible sources of information to prevent the spread of misinformation (Amer et al., 2021).

Chatbots must be effectively designed to prevent misinformation, and to help in symptom detection, encourage behaviors that reduce the risk of infection, and reduce the burden on the mental health of individuals facing the pandemic (Miner et al., 2020). Medical and public health professionals must also be involved in informing what chatbots are saying and how they are saying it. Translating medical information into public advice requires expertise and judgment to avoid unintended consequences. Reliability of evidence-based information, coordination with regional authorities and connecting users to reliable sources of information are also key aspects that chatbots should provide (Miner et al., 2020). Chin et al. (2023) investigated user communication with the chatbot SimSim on the basis of 19,782 chats in five culturally diverse countries and identified 18 new themes, which can be categorized into the following 5 overarching themes: "Questions about COVID-19 posed to the chatbot" (30.6%), "Preventive behavior" (25.3%), "The outbreak of COVID-19" (16.4%), "Physical and psychological impact of COVID-19" (16.0%) and "People and life in pandemic" (11.7%). A study found that users searched for health-related information and shared emotional messages with the chatbot, indicating the potential use of chatbots to provide accurate health information and emotional support during a global health crisis (Chin et al, 2023).

In the context of the COVID-19 pandemic, digital technology, including mobile apps and chatbots, has the potential to revolutionize mental health care. However, it is important that the implementation of these technologies is based on rigorous research and ethical principles to ensure safety, efficacy, and fairness for patients (Torous et al., 2021). In addition to the direct role and application in healthcare, chatbots can also have an indirect role in healthcare through the media. Maniou & Veglis (2020) investigated the use of chatbots on media platforms during crisis situations such as the COVID-19 pandemic, and at the same time highlights the advantages of implementing chatbots on news platforms during a crisis situation when the audience's needs for information grow rapidly.

This research aims to fill this knowledge gap and provide insight into the perception and acceptance of digital assistants in healthcare. By reviewing previous research, which investigates the perception and acceptance of chatbots for COVID-19 among different populations and contexts, the goal was to identify the key factors that influence the success of the implementation of such technologies. The aim of this research is to expand the previous research by Petričević and Mustić on the design and media presentation of the digital assistant *Andrija* through the analysis of the media presentation of the *Andrija* project and the public's reactions on Facebook during the COVID-19 pandemic. Also, paper analyzes the attitudes, perception, and acceptance of digital assistants in healthcare, identifies key aspects that influenced user acceptance or uncertainty, and provides guidelines for improving the design, media strategy and adoption of digital assistants in the healthcare sector. By studying the comments and reactions of users on *Andrija's* official Facebook page, the research will provide insight into the first impressions of the digital assistant, the main points of interest of users and their feedback.

Evaluation of Chatbots: Literature Overview

Evaluation of chatbots plays a key role in their successful application. An important factor in human-computer communication and interaction is design, which can significantly affect the reception of a message and the ways in which a person will act after receiving the message. Design refers to the aesthetic appearance, organization, and presentation of information, as well as the functionality of the interface between users and computer

systems. The way information is presented, as well as the user's experience interacting with the computer system, can shape the user's understanding and interpretation of the message. In the context of communication, design plays a key role in the successful transmission of messages. A good design should be intuitive and easy to use, allowing users to easily navigate through the computer system and perform the desired tasks. These include well-organized menus, logically arranged controls, and clear instructions. These basic guidelines of good design are also applicable to chatbots. Visual communication represents a complex and continuous communication process that takes place between the author (creator) as the sender of the message and the recipient of the message. The author creates visual communication with the goal of making the recipient believe that the message has a socially accepted meaning (Plenković & Mustić, 2020). However, in the modern digital age, chatbots have become ubiquitous in interacting with users, providing various services and information. This chapter analyzes several key aspects of the application and design of chatbots in the contemporary context.

Saeidnia et al. (2021) studied the HealthBuddy+ application developed by UNICEF ECARO and WHO/Europe. The app received positive ratings for system status visibility, system-to-real-world match, consistency and standards, and evidence-based content. However, vulnerabilities were identified in the areas of error prevention and flexibility. The authors suggest that heuristic assessment can be used for rapid assessment of mobile health applications, which is especially important during pandemics when a rapid response is required (Saeidnia et al. 2021).

A 2021 review (Höhn & Bongard-Blanchy, 2021) analyzed chatbots for COVID-19 and their compliance with design heuristics. The results showed that most chatbots scored well in terms of system status visibility, real-world match, consistency and standards, and aesthetic and minimalist design. However, chatbots scored poorly on user control and freedom, recognition instead of recall, flexibility, and efficiency of use, understanding of context, and ability to manage interactions.

Recent research has identified key factors influencing the adoption and engagement of chatbots for COVID-19. These factors include content, trust, digital capability, and acceptability. The study concludes that "there is a need for more comprehensive and routine reporting on factors influencing adoption and engagement" and highlights the potential of chatbots to disseminate high-quality information during a crisis, but also highlights the importance of understanding user experiences and preferences to ensure their effectiveness (White et al., 2022).

Espinoza et al. (2020) emphasize the importance of user-centered design and decision-making about goals, users, actions, and workflows in the development and implementation of chatbots for healthcare institutions. They recommend starting with user experience and process mapping for users and service providers who will interact with the chatbot. The authors also suggest institutions to clearly define what a chatbot can and cannot offer and identify the tools available to the chatbot to achieve the goal. In addition, they emphasize the importance of considering data governance, legal, and compliance issues, particularly when collecting protected health information/personal data (Espinoza et al., 2020).

The results of a study conducted on 371 participants, which aimed to understand people's reactions to COVID-19 screening chatbots, showed that if the perception of the capabilities of an agent, human or chatbot is the same, users do not view chatbots any differently or more positively than human agents. The primary factor driving the perception of capability was user trust. Therefore, it is important to proactively inform users about chatbot capabilities; that is, users should understand that chatbots use the same up-to-date knowledge base and follow the same set of validation protocols as human agents (Dennis et al., 2020).

Research which studied *Chasey*, a character-based COVID-19 chatbot, scored well in terms of usability and user experience. The chatbot provided users with various information about the disease COVID-19, such as tracking cases by country, giving advice, answering frequently asked questions, and checking symptoms. The chatbot had two characters (informal and formal) that the user could freely switch during the conversation, and the participants found that all the features of COVID-19 were useful. Most participants preferred the informal character over the formal character, but participants had mixed feelings about which character they trusted the most (El Hefny et al., 2021).

In an example of the effectiveness of chatbots in promoting compliance with social distancing guidelines during the COVID-19 pandemic, a study found that chatbots reminding individuals of their non-compliance with social distancing guidelines can induce guilt and increase adherence; and in this way, chatbots can be a cost-effective alternative to traditional approaches to encourage compliance. At the same time, the study says that the

effectiveness of this technique depends on the level of anthropomorphism of the chatbot, whereby human-like chatbots are more effective than machine-like ones (Kim & Ryoo, 2022).

In the context of the development of the chatbot itself, Bahja et al. (2020) talk about a user-friendly framework for designing and developing educational chatbots and emphasizes the importance of considering user needs and preferences in the design process. The pandemic prompted the development of a *Smart Ubiquitous Chatbot for COVID-19 Assistance* with a deep learning sentiment analysis model during and after quarantine. A chatbot was designed to collect information from users to understand their situation and provide actions accordingly. The study also included a sentiment analysis model based on an LSTM neural network to detect depression in user-supplied texts during an ongoing discussion (Ouerhani et al., 2020). Abdul-Kader & Woods (2015) concluded that creating a perfect chatbot is very difficult because it requires a very large database and it should give reasonable answers to all interactions.

A study conducted in Romania (Iancu & Iancu, 2023) investigated the perception of chatbots for COVID-19 among middle-aged and older adults. The results showed that perceived usefulness and subjective norms were the main predictors of behavioral intention to use chatbots, while age and gender did not significantly influence their perception. A further study conducted in Brazil (Chagas et al., 2023) evaluated user experience with a COVID-19 chatbot designed by a telehealth service. The results showed that the chatbot was generally well received by users, but opportunities for improvement were identified in terms of providing more practical guidance and updating information.

A study conducted in Southeast China during the Omicron wave of COVID-19 (Shan et al., 2022) investigated user experience and satisfaction with health chatbots among young people aged 17–35 years. The results showed a positive user experience and high satisfaction with healthcare chatbots, with personalized responses and convenience being key factors influencing their use. This study also developed a new user experience and satisfaction assessment model for research.

Media Presentation of Digital Assistants

Digitization of the media brings numerous changes in the way the media function, with a special emphasis on adaptation to technological innovations (Plenković & Mustić, 2011). Social media play a key role in communication during crisis situations such as a pandemic and can be a valuable tool for disseminating information and building public relations.

Media presentation of chatbots plays a key role in popularizing their use. In the modern digital age, where information is available in abundance, the media presentation of chatbots provides an opportunity to spread awareness of their presence and benefits among a wider range of users. Through adequate media presentation, chatbots can reach a larger number of people and create interest in their use. A strategic approach to the media presentation of chatbots can help break down prejudices and resistance to the use of such technology. Through objective and reliable media sources, it is possible to highlight the security, privacy, and reliability of chatbots. Informing users about how chatbots protect private data, use advanced technologies such as artificial intelligence and machine learning, and provide quality services can reduce reservations and increase user confidence in their use.

Research on the official Facebook pages of municipalities and emergency service agencies during three terrorist attacks in Berlin, London and Stockholm showed that the presence of a picture or video in a post significantly increases the number of reactions, and that the length of the text negatively affects the number of reactions (Ross et al., 2018.). During the COVID-19 pandemic, the use of social media has increased significantly, and platforms such as WhatsApp, Facebook, Instagram, and Twitter have become vital for disseminating information about the disease (Sathish et al., 2020). However, research has also shown that social media can be a source of false information and misinformation, which can cause anxiety and fear in people, especially when it comes to vaccines (Ennab et al., 2022; Gabarron et al., 2021, p 463). Malecki et al. (2021) emphasize the need for clinicians and public health professionals to be proactive in shaping messages and addressing sources of fear, anxiety, and misinformation; while MacKay et al. emphasize the importance of crisis communication messages on social media to be transparent, empathetic, consistent, accurate and timely.

Analyzing public comments on social media can help organizations understand public reactions and adjust their communication strategies (Coombs, W. T., & Holladay, S. J., 2014). It is also important to point out that the analysis of public online discourse can provide insight into different emotions, ideologies, and attitudes of

people in crisis situations. This can help decision makers better understand public expectations and concerns and develop more effective policies and responses (Khanum & Shahid, 2021). The importance of using Facebook in crisis management as well as interactions in social networks was investigated by the authors of the study Ki & Nekmat, (2014) and found a significant relationship between the organization's involvement in two-way communication and the overall positivity of the audience's tone in reaction to organizational crisis resolution (Ki & Nekmat, 2014). "Facebook continues to lead as a source of news compared to other social media,..." and in the Croatian sample, the very high position of Facebook as a source of news can also be confirmed (Vozab & Peruško, 2021).

In short, the digitization of media, the use of social media, chatbots and other digital technologies and the analysis of public discourse on social media play an important role during pandemics and crisis situations. However, it is important to manage these tools properly to ensure accurate and relevant information, and to protect the mental health and well-being of the public.

Analysis of the media presentation and public reaction to the Croatian version of the health digital chatbot can provide *Andrija* with guidelines for further improvement of the design, media strategy and adoption of digital assistants in healthcare. Discovering the key aspects that contributed to user acceptance or uncertainty can help develop strategies that will drive further adoption and integration of digital assistants into healthcare systems.

The public's reaction to digital assistants, such as *Andrija*, can reveal the attitudes, perception and acceptance of such technologies in society. Studying the comments and reactions of users on *Andrija*'s official Facebook page can give us an insight into how this digital assistant was received, what were the main points of interest of users and what was their feedback. Analysis of the media presentation, public reaction and user feedback provide us with valuable insights for the further development and adoption of such technologies in the health sector.

Method

This research aims to study the perception and acceptance of the digital assistant *Andrija* in the healthcare sector during the COVID-19 pandemic. Content-wise, the research is divided into two basic parts. The introductory part of the research summarizes the results of the previous research by Petričević, S., & Mustić, D. (2023) which is the basis for further research. The previous research, dealt with the design and media presentation of the digital assistant itself and has provide us with an introductory context and contributed to a better interpretation of the results of this research. The main part of the research includes an analysis of the media presentation of the *Andrija* project and reactions, as well as public comments on Facebook.

Sample

For data collection, public announcements on the Facebook social network were accessed. The keywords "Andrija, digital assistant" was entered into the search engine were used for the search on Facebook. All public announcements that corresponded to the keywords and research topic were observed. The collected data were analyzed using a research matrix that includes the following variables: publication date, publication size (number of words), type of image material, existence of a link to official pages, number and type of reactions, number of shares and analysis of comments according to sentiment (positive, negative, neutral). The unit of analysis was one Facebook post. In the research of posts on Facebook that corresponded to the keywords "Andrija, digital assistant", we analyzed a total of 82 posts published in the period from April 13, 2020. until 27.4.2022.

Procedures

A combination of qualitative and quantitative methods was applied for data analysis. All collected data were analyzed using the Microsoft Excel program. Qualitative content analysis was applied to selected examples of comments to better understand user opinions. The quantitative analysis included descriptive statistics, including frequencies and means, to describe the basic characteristics of the data. Inferential statistics were also applied to check for statistically significant differences or trends. To analyze associations between variables, we used multivariate analyzes to explore potential correlations. The combination of the above methods enabled a deeper understanding of the perception and acceptance of *Andrija*'s digital assistant in the health sector during the COVID-19 pandemic.

Ethics

Ethical guidelines were followed during the research. Special attention was paid to the protection of user privacy, and the authors adhered to ethical standards when collecting data on social media. For privacy protection purposes, personal names that are publicly available in the analyzed content were not used in the analysis.

Limitations of the Research

Limitations of this research include limited access to only public posts on Facebook and the possibility of bias in data collection due to the subjective choice of keywords. Also, it is important to note that the results of this research are based solely on the analysis of data from Facebook and do not include other platforms or communication channels.

Results and Discussion

The results of the first part of the research published by Petričević and Mustić (2023) provide an important context for the second part of the research. Those results indicate that *Andrija*, as a multipurpose chatbot, was focused on risk assessment and providing basic information about COVID-19. These results show that *Andrija* played a useful role in providing basic information about the pandemic and supporting the public in making informed decisions. Also, the research revealed that *Andrija* had limited functionality in disseminating information in a broader sense. The official presentation of the digital assistant *Andrija* was held on April 14th at the press conference of the Government of the Republic of Croatia, where the choice of the name *Andrija* was explained, but not the visual representation of the character of *Andrija*. In the presentation, it was stated that *Andrija* was named after Dr. *Andrija Štampar*, who established the fundamental principles of public health in Croatia that are applied throughout the world.

In the information dissemination category, the research identified seven subcategories, but *Andrija* supported only three of them, which indicates that his ability to disseminate information was not fully utilized (Table 1). This limitation may indicate potential flaws in the design or implementation of the chatbot. The most common combinations in multi-purpose chatbots were risk assessment and information dissemination, which was also demonstrated in *Andrija's* case.

Table 1. *Andrija* chatbot cases and usage definitions

Use-case category and associated use cases	Use-case description	Benefits
Risk assessment	Triage users based on their Covid- 19 symptoms and exposure risk and recommend a course of action.	Social distancing, capacity expansion, efficient capacity utilization, prevent virus transmission
Surveillance	/	/
Information dissemination	Virus and vaccine education Misinformation/disinformation debunking Proactive misinformation/disinformation debunking Nonpharmaceutical interventions (NPI) promotion Virus transmission data reporting Available public resources awareness Encouragement of activities (other than NPIs) to fight the pandemic	
Post-Covid-19 eligibility screening	/	/
Distributed coordination	/	
Vaccine scheduler	/	/

Andrija was a multipurpose chatbot that was available on the WhatsApp platform (Table 2). It did not ask for additional information about the user except for saving the number in the directory, and he was presented as a man (Figure 1). However, *Andrija* was not integrated into a high-traffic platform, which could have improved his visibility. The results suggest that *Andrija* was focused on risk assessment and providing basic information about COVID-19 but had limited functionality in disseminating information.

Table 2. Design characteristics of chatbot *Andrija*

	<i>Andrija</i>
Multipurpose versus single purpose	multipurpose
Chatbot platform	WhatsApp
Anonymity	does not enquire additional user identifying information
Anthropomorphism	male
Interface design	text-based
Follow-up and recurring conversation	no follow-up option



Figure 1. *Andrija* (available at: <https://vlada.gov.hr/vijesti/predstavljen-andrija-prvi-digitalni-asistent-u-borbi-protiv-koronavirusa/29226>)

The research also analyzed official government communication channels, including the websites of the Government of the Republic of Croatia and the Ministry of Health. Only a few pages were found that mentioned *Andrija* on those websites. Media sources were also analyzed and several publications and articles about *Andrija* were found. Only 3 pages were found on the official website of the Government, while only 1 page mentioning *Andrija* was found on the website of the Ministry of Health. The number of pages that refer to or mention *Andrija* is relatively low. On the official website of the Government, there were no further announcements on the subject of *Andrija*, digital assistant, while on the official website *andrija.ai* in the section "Andrija - How I am developing" - there were a total of eight announcements from April 14, 2020 to September 14, 2020. The section of the official website "Andrija in the Media" records thirty-three (33) publications in the media, i.e. a link in the media with publication dates from April 13, 2020 to May 4, 2020, which suggests that *Andrija* attracted media attention and was the subject of interest during that time. *Andrija's* media promotion was relatively modest. Although the chatbot attracted media attention for a certain period of time, the number of publications and articles related to *Andrija* was not large. These results serve as a starting point and provide an important context for the second part of the research, which will analyze media coverage on the Facebook social network and its impact on the perception of health chatbots among users and the general public.

In the main part of the research, we focused on the analysis of the media coverage of chatbot *Andrija* on the Facebook and its impact on the perception of users and the general public. The largest number of posts was recorded on 14/04/2020, which was the day of *Andrija's* official presentation, with as many as 44 posts. The next most represented date was April 15, 2020. with 22 posts. The other dates had a smaller number of posts, with most of them having only one or two posts (Table 3).

Petričević and Mustić (2023) state that *Andrija* attracted media attention during the period from April 13, 2020 to May 4, 2020 with a total of 33 media announcements, which suggests that he was the subject of media interest during that time and that there was significant reporting on it. Both of these pieces of information indicate that *Andrija* attracted attention both on social networks (through the number of posts on Facebook) and in the media (through publications in the media).

Next, the posts themselves were analyzed. The size of the posts was analyzed by number of words. The results showed a diversity in the size of posts on the social network. The average post size is 78 words, but with high

variability (Sd=164.33). The post size range is 1407 words. It is important to note that four of the posts do not have any words, which may indicate image or other types of posts that do not rely on textual content.

Table 3. Total number of publications by day

Date	Total number of posts on Facebook about Andrija
13.4.2020	2
14.4.2020	44
15.4.2020	22
16.4.2020	3
17.4.2020	1
18.4.2020	1
20.4.2020	1
28.4.2020	1
1.5.2020	1
24.6.2020	2
1.7.2020	1
14.7.2020	1
22.7.2020	1
27.4.2022	1

The type of image/video material contained in the post was also analyzed (Table 5). The results showed that in 8 posts there were no attached picture or video material, which means that these posts were exclusively textual in nature, while the most posts (60 post) showed a picture of the digital assistant *Andrija*. From these results, it can be concluded that images of *Andrija*'s digital assistant have a higher prevalence in posts compared to other types of image/video material.

Table 4. Type of image / video material

Type of image / video material	Number of image/video material
There is no image / video material	8
Other image/video material	3
Picture / video of people who used the digital assistant Andrija	1
Picture / video of a politician	3
Picture of digital assistant Andrija	60
Video through the Andrija application	7
Grand total	82

Table 5. Activities of announcements about Andrija

Date	Number of posts	Number of fast reactions	Number of comments	Number of shares
13.4.2020	2	67	37	15
14.4.2020	44	2376	379	357
15.4.2020	22	825	172	41
16.4.2020	3	542	25	24
17.4.2020	1	454	27	30
18.4.2020	1	31	0	2
20.4.2020	1	45	0	1
28.4.2020	1	6	0	0
1.5.2020	1	12	2	0
24.6.2020	2	10	1	6
1.7.2020	1	4	0	1
14.7.2020	1	20	20	1
22.7.2020	1	10	1	1
27.4.2022	1	55	0	0

55 posts had a link to official websites related to *Andrija*, such as government or ministerial websites. Compared to the number of pages related to *Andrija*, these results suggest a greater visibility and spread of posts on the social network. This indicates the importance of social networks as a channel for sharing information and

promoting *Andrija* as a digital assistant of the Ministry of Health. Integrating links and information from social networks to official pages can increase the availability and reach of information and research results can be useful for planning future marketing strategies on social networks. Furthermore, we quantitatively analyzed data on the activity of posts about *Andrija* on Facebook on different dates (Table 5).

This data set provides information on the activity of posts about *Andrija* on Facebook on specific dates, and user interaction with posts related to *Andrija*, such as likes, comments and shares. The results show how many posts were dedicated to *Andrija* on each of the listed dates. For example, 14/04/2020, which is also the day of the chatbot's official presentation to the public, was the day with the largest number of posts (44) quick reactions (2376), comments (379) and shares (357), while some dates had only one post. The total number of quick reactions shows how many quick reactions (like likes, smileys, hearts, etc.) have been received on *Andrija*'s posts. The number of comments reveals how actively users participated in discussions and conversations about *Andrija*. The total number of shares of the post indicates how many times posts about *Andrija* were shared by Facebook users. Higher number of quick reactions, higher number of quick reactions; of comments and shares may indicate a greater interest or engagement of users towards those posts. Based on these results, one can gain insight into user engagement, the popularity of posts about *Andrija* and the spread of information about that content on Facebook. It is also possible to monitor activity trends over time and identify dates with greater or lesser interest in posts about *Andrija*.

An analysis of 82 posts on Facebook related to *Andrija*, the digital assistant, recorded a total of 4461 quick reactions (Table 6). Quick Reactions include "Like", "Love", "Support", "Ha-ha", "Wow", "Sad" and "Angry" emoticons that allow users to express their opinions or emotions about posts. This high number of quick reactions indicates that the posts about *Andrija* caused interest and user engagement on Facebook, which suggests that *Andrija* has attracted the attention of the audience and caused emotional reactions from users. Also, these results indicate a positive response to posts about *Andrija*, which indicates that the digital assistant was well received.

Table 6. Quick reactions types

	Like	Love	Support	Ha-ha	Wow	Sad	Angry
M	46,01	3,05	0,01	4,56	0,26	0,17	0,34
SE	9,71	1,17	0,01	1,16	0,07	0,05	0,09
Md	13,5	0	0	0	0	0	0
Mo	10	0	0	0	0	0	0
SD	88,01	10,61	0,11	10,48	0,6	0,44	0,86
Var	7745,75	112,51	0,01	109,76	0,37	0,19	0,75
Sum	3773	250	1	374	21	14	28

Based on the reactions to Facebook posts about *Andrija*, the following can be concluded about the acceptance of the digital assistant:

- The reaction "Like" has a high mean value (46.01) and a significant sum (3773), which indicates a positive acceptance of *Andrija*. A high number of "Like" reactions implies that *Andrija* has attracted the attention and interest of users.
- The reaction "Love" also has a large sum (250) and a mean value (3.05), which indicates an emotional connection and a positive attitude towards *Andrija*.
- Other reactions like "Support," "Wow," "Sad," and "Angry" have low mean values and smaller totals. This indicates that these reactions are relatively rare and less relevant in the context of *Andrija*'s acceptance.
- The "Ha-ha" reaction also has a large sum (374) and a relatively high mean (4.56). However, the "Ha-ha" reaction can be interpreted in two ways: 1) as positive support, indicating the user's amusement or positive reaction to *Andrija*'s posts; and 2) as sarcasm, which may imply a reminder of a negative aspect or failure. Therefore, it is necessary to take into account the context and content of the posts in order to better understand the meaning and impact of "Ha-ha" reactions on *Andrija*'s acceptance.
- High values of standard deviation for reactions like "Like" (88.01) and "Ha-ha" (10.48) indicate great variability in users' perception and that users' opinions about *Andrija* are varied.

Positive reactions, such as "Like" and "Love", dominate user reactions. These reactions had a high mean value and a significant number, which indicates a positive acceptance of *Andrija*. On the other hand, negative or neutral reactions were less noticeable.

The results of the conducted research suggest that *Andrija*, as a digital assistant that provides information on the fight against Covid-19 and represents progress in technology, attracted attention and caused positive reactions from users on Facebook. However, it should be noted that these results assess only the quantitative aspect of reactions, while the qualitative aspects of acceptance could be better understood by analyzing the comments themselves.

Based on this, an analysis of the comments in the observed posts was carried out. All primary comments on the publication were analyzed and divided into three basic categories: comments with a positive connotation, comments with a negative connotation, and comments with a neutral connotation/comments unrelated to the topic of the publication (Table 7). The overall analysis of the results reveals that out of a total of 664 comments, 22.1% are positive comments, 32.2% are negative comments, and 45.7% are neutral comments or comments unrelated to the topic. In the context of positive/negative comments, we can conclude that in posts, negative comments are more frequent than positive ones.

Table 7. Data on comments

	Positive comments	Negative comments	Neutral comments /unrelated to the topic
Sum	147	214	303
Posts (N)	82	82	82

Analyzing the types of comments, we selected several examples from each type (Table 8).

Table 8. Examples of comments

Comment sentiment	Comment
Positive	"Andrija, ok. Modern."
	" Andrija, you are a great guy!"
	"Bravo! 👏🏆👍"
	"Bravo! Congratulations to the whole team! "
	" Wonderful. I'm looking forward. We need stories like this!"
Negative	"One of the biggest stupidities of our government "
	"... I don't want a guy...give me a woman... "
	"For people control... 🤖🤖🤖🤖 s****"
	"Quite primitive, I must admit, if compared to some other bots."
	" Thank you, but a computer epidemiologist cannot and should not replace a classical profession...."
Neutral / unrelated to the topic	" Andrija, I hit my finger with a hammer, are those pains symptoms of corona??"
	"...Andrija mine 🤖"
	" Andrija, what do you say about the new merge of cities and municipalities into 155 units?"
	" I am waiting for continued cooperation... Andrija 2.0 🤖"
	" How to win on a public tender? "

Analyzing the comments of users in the posts, some of which are shown in Table 8, one notices the mixed perception of chatbot *Andrija*. There are positive, negative and neutral comments that provide insight into users' attitudes and their reactions to using chatbots.

Positive comments emphasize the speed and efficiency of the chatbot compared to a phone call. Users express satisfaction and support for the chatbot, considering it an excellent tool. These positive comments provide confirmation that the chatbot has fulfilled its purpose in providing basic information about the pandemic and supporting users in making informed decisions.

Negative comments express the user's disappointment or dissatisfaction. Some users consider the chatbot frivolous, banal, or unintelligent, while others criticize the app's power or advertising. Also, criticisms is related to the design of the chatbot, the lack of a female name (character) or the perception of customer support. These negative comments point to the need to improve the chatbot to meet user expectations and respond to their needs. At the same time, given that our results showed that *Andrija's* image was the most represented in the posts, criticisms related to the design, or the perception of customer support can be useful guidelines for improving interaction and user experience.

Neutral comments refer to other topics or ask questions not directly related to the chatbot. They do not provide direct feedback about the chatbot or its shortcomings. Such comments can be useful for understanding other interests and needs of users, but do not provide concrete guidance for improving the chatbot.

It is important to note that the sample comments represent only a small sample of user opinions and do not reflect all possible perspectives. Comments are subjective and depend on the individual experience and expectations of the user. However, these comments can be useful for further improving the chatbot, including considering user suggestions, improving the design and efficiency of responses.

To assess the conformity of the dataset pertaining to the overall count of rapid reactions and post size to a normal distribution, the Kolmogorov-Smirnov (K-S) test was employed (Table 9). The outcomes of the K-S test revealed that the dataset does not adhere to a normal distribution. The K-S test statistic (D) obtained a value of .303, with a significance level of $p < .000$ for quick reactions and .317, with a significance level of $p < .000$ for post size (word count).

Table 9. Test statistics on count of quick reactions and post size (word count)

	Quick reactions	Post size (word count)
N	82	82
M	54.35	78.01
Md	16.5	40
Sd	101.61	164.33
Sk	3.06	6.83
Kt	9.39	54.03
D	.303	.317
p	< .000	< .000
r_s	.216	
p(2-tailed)	.051	

The quantity of quick reactions exhibited its highest peak during the initial phase of the observed period, coinciding with the media introduction of the chatbot, subsequently followed by a decline in reaction counts. In order to assess the relationship between the size of Facebook posts (measured by the number of words) and the total number of quick reactions, Spearman's rank correlation coefficient, a non-parametric test, was employed. The results of the Spearman's rank correlation test indicate that the correlation between the size of the post and the total number of quick reactions is not statistically significant ($r(80) = 0.22$, with a corresponding p-value of .05). This implies that the available statistical evidence does not support the presence of a meaningful relationship between these variables. However, there is a statistically significant correlation between the size of the post (number of words) and the number of "Like" reactions ($r(80) = .22$), with a corresponding p-value of .04. The result is significant at $p < .05$. We have to bear in mind that correlation does not imply causation. While a correlation between post length and the number of likes may exist, it does not necessarily mean that the length of posts directly causes the number of "Likes".

In short, based on these results, it can be concluded that the size of the post (number of words) is not correlated with the total number of quick reactions, but there is a statistically significant positive correlation between the size of the post (number of words) and the number of "Like" reactions. The relationship between post size and other quick reactions was not further examined due to a significantly smaller number of such reactions.

Conclusion

The research conducted on the chatbot *Andrija* has yielded several significant findings. The initial part of the study emphasizes the multifaceted role of *Andrija* as a chatbot important for disseminating basic information about the pandemic and assisting the public in making informed decisions. However, certain limitations were identified in the design and implementation of *Andrija*, particularly regarding information dissemination.

The subsequent phase of the research centres on the media coverage of chatbot *Andrija* on the Facebook and its impact on user perception and the general public. The results indicate a notable level of media attention during a specific timeframe. An examination of Facebook posts about *Andrija* revealed variation in post size, with a focus on visual media such as images/videos and links to official websites. Furthermore, the analysis of user reactions to *Andrija*'s posts demonstrated a largely positive reception, characterized by a high number of "Like"

reactions and a pronounced emotional connection reflected through "Love" reactions. Nevertheless, variations in user perception were observed.

Investigating the correlation between post size (word count) and reactions to Facebook posts indicated no statistically significant correlation between post size and the total number of quick reactions. However, a statistically significant positive correlation was identified between post size and the number of "Like" reactions.

Considering the research objective, it is concluded that the investigation of the chatbot *Andrija* has provided valuable insights into the perception and acceptance of digital assistants in the healthcare domain, particularly amidst the COVID-19 pandemic. An analysis of media presentation and the public's response to *Andrija* on the Facebook platform has underscored significant media and user interest, as well as extensive discourse surrounding the chatbot. The research findings offer guidance for enhancing the design, media strategy, and adoption of digital assistants in the healthcare sector.

Additionally, the study has identified key factors influencing user acceptance or uncertainty and unveiled the diversity of attitudes and perceptions among users regarding *Andrija*. Analysis of user comments and reactions on *Andrija*'s official Facebook page has yielded further insights into the reception of the chatbot, users' primary areas of interest, and feedback.

In summary, the research on chatbot *Andrija* contributes to our understanding of the role of digital assistants in communicating information about the pandemic and provides guidelines for the further development and application of such technologies in healthcare systems. The study has also shed light on deficiencies in the design and implementation of *Andrija*, emphasizing the importance of ongoing enhancements to its functionality. The research findings offer valuable guidance for improving design, refining media strategies, and facilitating the adoption of digital assistants within the healthcare sector. The identified factors influencing user acceptance or uncertainty provide crucial insights for the continued advancement of digital assistants.

Scientific Ethics Declaration

The authors declare that the scientific ethical and legal responsibility of this article published in EPSTEM journal belongs to the authors.

Acknowledgements or Notes

* This article was presented as an oral presentation at the International Conference on Research in Engineering, Technology and Science (www.icrets.net) held in Budapest/Hungary on July 06-09, 2023.

References

- Abdul-Kader, S. A., & Woods, J. C. (2015). Survey on chatbot design techniques in speech conversation systems. *International Journal of Advanced Computer Science and Applications*, 6(7). <https://doi.org/10.14569/IJACSA.2015.060712>
- Amer, E., Hazem, A., Farouk, O., Louca, A., Mohamed, Y., & Ashraf, M. (2021, May). A proposed chatbot framework for COVID-19. In *2021 International Mobile, Intelligent, and Ubiquitous Computing Conference (MIUCC) IEEE*, 263-268. <https://doi.org/10.1109/MIUCC52538.2021.9447652>
- Amiri, P., & Karahanna, E. (2022). Chatbot use cases in the Covid-19 public health response. *Journal of the American Medical Informatics Association*, 29(5), 1000-1010. <https://doi.org/10.1093/jamia/ocac014>
- Bahja, M., Hammad, R., & Butt, G. (2020). A user-centric framework for educational chatbots design and development. In *HCI International 2020-Late Breaking Papers: Multimodality and Intelligence: 22nd HCI International Conference, HCII 2020, Copenhagen, Denmark, July 19–24, 2020, Proceedings 22*, 32-43. Springer International Publishing. https://doi.org/10.1007/978-3-030-60117-1_3
- Božić, V. (2023). Chatbots in healthcare [Preprint]. <https://doi.org/10.13140/RG.2.2.13525.70887>
- Chagas, B. A., Pagano, A. S., Prates, R. O., Praes, E. C., Ferregueti, K., Vaz, H., Reis, Z. S. N., Ribeiro, L. B., Ribeiro, A. L. P., Pedroso, T. M., Beleigoli, A., Oliveira, C. R. A., & Marcolino, M. S. (2023). Evaluating user experience with a chatbot designed as a public health response to the COVID-19 pandemic in Brazil: Mixed methods study. *JMIR Human Factors*, 10, e43135. <https://doi.org/10.2196/43135>

- Chin, H., Lima, G., Shin, M., Zhunis, A., Cha, C., Choi, J., & Cha, M. (2023). User-chatbot conversations during the COVID-19 pandemic: study based on topic modeling and sentiment analysis. *Journal of Medical Internet Research*, 25, e40922. <https://doi.org/10.2196/40922>
- Coombs, W. T., & Holladay, S. J. (2014). How publics react to crisis communication efforts: Comparing crisis response reactions across sub-arenas. *Journal of Communication Management*, 18(1), 40-57. <https://doi.org/10.1108/JCOM-03-2013-0015>
- Dennis, A. R., Kim, A., Rahimi, M., & Ayabakan, S. (2020). User reactions to COVID-19 screening chatbots from reputable providers. *Journal of the American Medical Informatics Association*, 27(11), 1727-1731. <https://doi.org/10.1093/jamia/ocaa167>
- El Hefny, W., El Bolock, A., Herbert, C., & Abdennadher, S. (2021, August). Chase away the virus: a character-based chatbot for COVID-19. In *2021 IEEE 9th International Conference on Serious Games and Applications for Health (SeGAH)* (pp. 1-8). IEEE. <https://doi.org/10.1109/SEGAH52098.2021.9551895>
- Ennab, F., Babar, M. S., Khan, A. R., Mittal, R. J., Nawaz, F. A., Essar, M. Y., & Fazel, S. S. (2022). Implications of social media misinformation on COVID-19 vaccine confidence among pregnant women in Africa. *Clinical Epidemiology and Global Health*, 14, 100981. <https://doi.org/10.1016/j.cegh.2022.100981>
- Espinoza, J., Kaisler, M., & Lau, F. (2020). A framework for developing and implementing chatbots for health care organizations. *JMIR Public Health and Surveillance*, 6(2), e18808. <https://doi.org/10.2196/18808>
- Gabarron, E., Oyeyemi, S. O., & Wynn, R. (2021). COVID-19-related misinformation on social media: a systematic review. *Bulletin of the World Health Organization*, 99(6), 455-463A. <https://doi.org/10.2471/BLT.20.276782>
- Government of Croatia. (2020) Andrija – prvi digitalni asistent u borbi protiv koronavirusa u Hrvatskoj živi na WhatsAppu. <https://vlada.gov.hr/vijesti/andrija-prvi-digitalni-asistent-u-borbi-protiv-koronavirusa-u-hrvatskoj-zivi-na-whatsappu/29231> [Accessed 14th of February 2021]
- Höhn, S., & Bongard-Blanchy, K. (2021, February). Heuristic evaluation of COVID-19 chatbots. In *Chatbot Research and Design: 4th International Workshop, CONVERSATIONS 2020*, Virtual Event, November 23-24, 2020, Revised Selected Papers (pp. 131-144). Cham: Springer International Publishing.
- Iancu, I., & Iancu, B. (2023). Interacting with chatbots later in life: A technology acceptance perspective in COVID-19 pandemic situation. *Frontiers in Psychology*, 13, 1111003. <https://doi.org/10.3389/fpsyg.2022.1111003>
- Khanum, N., & Shahid, H. (2021). Crisis news and online public sphere: a discourse analysis of facebook comments on news stories about Aylan Kurdi. *PONTE International Journal of Science and Research*, 77(12), 84-95.
- Ki, E. J., & Nekmat, E. (2014). Situational crisis communication and interactivity: Usage and effectiveness of Facebook for crisis management by Fortune 500 companies. *Computers in Human Behavior*, 35, 140-147. <https://doi.org/10.1016/j.chb.2014.02.039>
- Kim, W., & Ryoo, Y. (2022). Hypocrisy Induction: Using chatbots to promote COVID-19 social distancing. *Cyberpsychology, Behavior and Social Networking*, 25(1), 27-36. <https://doi.org/10.1089/cyber.2021.0057>
- MacKay, M., Colangeli, T., Gillis, D., McWhirter, J., & Papadopoulos, A. (2021). Examining social media crisis communication during early COVID-19 from public health and news media for quality, content, and corresponding public sentiment. *International Journal of Environmental Research and Public Health*, 18(15), 7986. <https://doi.org/10.3390/ijerph18157986>
- Malecki, K. M. C., Keating, J. A., & Safdar, N. (2021). Crisis communication and public perception of COVID-19 risk in the era of social media. *Clinical Infectious Diseases*, 72(4), 697-702. <https://doi.org/10.1093/cid/ciaa758>
- Maniou, T. A., & Veglis, A. (2020). Employing a Chatbot for news dissemination during crisis: Design, implementation and evaluation. *Future Internet*, 12(7), 109. <https://doi.org/10.3390/fi12070109>
- Miner, A. S., Laranjo, L., Kocaballi, A. B., Chatzimichailidou, M. M., & de la Torre-Diez, I. (2020). Chatbots in the fight against the COVID-19 pandemic. *NPJ Digital Medicine*, 3(1), 1-4. <https://doi.org/10.1038/s41746-020-0280-0>
- Ministry of Health, Republic of Croatia. (2020a). Andrija (Ministarstvo zdravstva RH) – prvi digitalni asistent u borbi protiv koronavirusa u Hrvatskoj živi na WhatsAppu. Available from: <https://zdravlje.gov.hr/vijesti/andrija-ministarstvo-zdravstva-rh-prvi-digitalni-asistent-u-borbi-protiv-koronavirusa-u-hrvatskoj-zivi-na-whatsappu/5137> [Accessed 14th February 2021]
- Ouerhani, N., Maalel, A., Ben Gh'ezela, H., & Al-Jaroodi, J. (2020). Smart ubiquitous chatbot for COVID-19 assistance with deep learning sentiment analysis model during and after quarantine. arXiv preprint arXiv:2005.04243. <https://doi.org/10.21203/rs.3.rs-33343/v1>

- Parmar, P., Lee, J. S., & Kim, J. (2022). A systematic review of commercially available healthbots: NLP system design, geographic distribution, and evaluation criteria. *NPJ Digital Medicine*, 5(1), 21. <https://doi.org/10.1038/s41746-022-00560-6>
- Petričević, S., & Mustić, D., (2022). Communicating a global pandemic with WhatsApp and HealthBot in Croatia. In *11th International Symposium on Graphic Engineering and Design, GRID.*, 195-203. <https://doi.org/10.24867/GRID-2022-p20>
- Plenković, M., & Mustić, D. (2011). Graphic technologies and communicational behaviour in ecological crises. *Informatologia*, 44(4), 296-308.
- Plenković, M., & Mustić, D. (2020). Media communication and cultural hybridization of digital society. *Media, Culture and Public Relations*, 11(2), 151-160.
- Ross, B., Potthoff, T., Majchrzak, T. A., Chakraborty, N. R., Ben Lazreg, M., & Stieglitz, S. (2018). *The diffusion of crisis-related communication on social media: an empirical analysis of Facebook reactions.* <https://scholarspace.manoa.hawaii.edu/items/0aa4d12f-24a9-43d5-a0cf-d14bb39090e7>
- Saeidnia, H. R., Mohammadzadeh, Z., & Hassanzadeh, M. (2021). Evaluation of mobile phone healthcare applications during the COVID-19 pandemic. *Studies in Health Technology and Informatics*, 281, 1100–1101. <https://doi.org/10.3233/SHTI210363>
- Sathish, R., Manikandan, R., Priscila, S. S., Sara, B. V., & Mahaveerakannan, R. (2020, December). A report on the impact of information technology and social media on Covid–19. In 2020 3rd International Conference on Intelligent Sustainable Systems (ICISS) (pp. 224-230). IEEE.
- Shan, Y., Ji, M., Xie, W., Zhang, X., Qian, X., Li, R., & Hao, T. (2022). Use of health care chatbots among young people in china during the omicron wave of COVID-19: Evaluation of the user experience of and satisfaction with the technology. *JMIR Human Factors*, 9(2), e36831. <https://doi.org/10.2196/36831>
- Torous, J., Bucci, S., Bell, I. H., Kessing, L. V., Faurholt-Jepsen, M., Whelan, P., Carvalho, A. F., Keshavan, M., Linardon, J., & Firth, J. (2021). The growing field of digital psychiatry: current evidence and the future of apps, social media, chatbots, and virtual reality. *World Psychiatry : Official Journal of the World Psychiatric Association (WPA)*, 20(3), 318–335. <https://doi.org/10.1002/wps.20883>
- Vozab, D., & Peruško, Z. (2021). *Digitalne publike vijesti u Hrvatskoj 2017.-2021.* Zagreb: CIM - Centar za istraživanje medija i komunikacije, Fakultet političkih znanosti, Sveučilište u Zagrebu.
- White, B. K., Martin, A., & White, J. A. (2022). User experience of COVID-19 chatbots: Scoping review. *Journal of Medical Internet Research*, 24(12), e35903. <https://doi.org/10.2196/35903>

Author Information

Stjepan Petričević

Alma Mater Europaea Maribor
Slovenska 17, 2000 Maribor, Slovenia
Contact e-mail: stjepan.petricevic@almamater.si

Daria Mustić

University of Zagreb Faculty of Graphic Arts
Getaldićeva 2, 10000 Zagreb, Croatia

To cite this article:

Petričević, S. & Mustić, D. (2023). Research on media presentation and public reaction to the first health digital assistant in Croatia. *The Eurasia Proceedings of Science, Technology, Engineering & Mathematics (EPSTEM)*, 23, 151-164.

The Eurasia Proceedings of Science, Technology, Engineering & Mathematics (EPSTEM), 2023

Volume 23, Pages 165-172

ICRETS 2023: International Conference on Research in Engineering, Technology and Science

Computer-Aided Planning of Radial and Diameter Routes in Local Public Transport Networks

Ágoston Winkler
Széchenyi István University

Abstract: Local public transport network planning is a complex procedure affected by many aspects (e.g., city structure, travel needs, the budget for the service, vehicle types, service frequencies, timetable optimization of parallel routes etc.). Due to the high number of possible solutions, finding the optimum is usually a problem with NP computational complexity. Although an extensive toolkit is available for evaluating specific networks, the number of versions that can be realistically examined and compared is highly limited. This implies that the routine and creativity of the network planning specialists play an important role in the selection of the examined networks. However, in some special cases, the search space can be narrowed so that all network versions can be automatically generated and compared. This paper presents such a case: when applying radial and diameter routes only, the main question is which directions should be connected to each other as a diameter route, or left alone as a radial line. The algorithm is presented on the example of the city Győr.

Keywords: Public transport, Transport network, Radial routes, Diameter routes, Computer-aided planning

Introduction

A significant element of a city's infrastructure is the network and timetable of its public transport. These have a fundamental effect on the service quality, and consequently influence the people's choice of transport mode i.e., the modal split, and they have an indirect effect on the severity of congestions as well as air and noise pollution. As a result, network development and an optimized timetable are of vital importance, so that the requirements of the passengers are fulfilled, and also the services should be realistically financeable by the responsible authorities (typically by the local governments).

In network and timetable design, human creativity, intuition and experience is highly important still to this day due to the high number of potential combinations. During the design process people who possess these traits are the ones who are able to create solutions that can be examined and analyzed by the existing transport planning systems (e.g., PTV VISUM). These software solutions can also be helpful in the design process, but they do not replace the human factor, as it is still the most important asset. As a result, finding the optimal (or as close as possible) solution is highly dependent on the professional's capabilities.

Computer-aided network and timetable planning (due to the extent of search space) is not yet fully developed, however, there is ongoing research (Owais et al., 2014). The existing solutions usually apply a heuristic approach (Ciaffia et al., 2014) as well as processes that are based on randomization, and they often result in a good solution, but in less successful cases (when they exclude certain search areas by mistake) the optimal solution might be excluded, similarly to the human intuition-based design.

The baseline of this research is that in a few special cases the search space can be narrowed so that all network variants can be automatically generated and compared. This paper presents such a case: when applying radial and diameter routes only, the main question is which directions should be connected to each other as a diameter route, or left alone as a radial line.

- This is an Open Access article distributed under the terms of the Creative Commons Attribution-Noncommercial 4.0 Unported License, permitting all non-commercial use, distribution, and reproduction in any medium, provided the original work is properly cited.

- Selection and peer-review under responsibility of the Organizing Committee of the Conference

© 2023 Published by ISRES Publishing: www.isres.org

The structure of the paper is as follows. The next section specifies the problem and describes the theory behind it. The section after that discusses the implementation of the developed algorithm as well as the experiences gained throughout this process. This is followed by the presentation of the practical use by showing the properties of Győr's local bus network and the results of the software. The last section preceding the conclusion discusses the elements of the algorithm that still need improvement as well as the possible directions for further development.

The Specific Problem and Its Theoretical Background

As this research is at the early stages, the definition of the problem is limited in various aspects to ensure that the analysis can begin from the easiest perspective: this can naturally be extended later to best reflect reality. At this point we can specify the problem in this way: in a city, there are n line-ends starting in the city center and they can either operate as a radial line, or joined in pairs as a diameter route. (To simplify it, we will use one end in only one line.) In this case the number of the networks marked with N is given by (1) equation when n is an even number.

$$N_n = 1 + (n - 1)(n - 3) \dots \cdot 5 \cdot 3 + \binom{n}{2} (n - 3)(n - 5) \dots \cdot 5 \cdot 3 + \dots + \binom{n}{n-4} \cdot 3 + \binom{n}{n-2} \quad (1)$$

The number 1 refers to the case when we have all radial lines, while the second part defines the number of complete pairings (meaning all diameter lines): we can find $n-1$ pairs for the first free line-end, $n-3$ for the second, and so on. This is followed by the instances where we keep some line-ends as radial routes, and we examine the number of complete pairings for the rest of the line-ends.

$$\begin{aligned} N_{14} &= 1 + 13 \cdot 11 \cdot 9 \cdot 7 \cdot 5 \cdot 3 + \binom{14}{2} 11 \cdot 9 \cdot 7 \cdot 5 \cdot 3 + \binom{14}{4} 9 \cdot 7 \cdot 5 \cdot 3 + \\ &\binom{14}{6} 7 \cdot 5 \cdot 3 + \binom{14}{8} 5 \cdot 3 + \binom{14}{10} \cdot 3 + \binom{14}{12} = \\ &1 + 135135 + 91 \cdot 10395 + 1001 \cdot 945 + 3003 \cdot 105 + 3003 \cdot 15 + 1001 \cdot 3 + 91 = \\ &1 + 135135 + 945945 + 945945 + 315315 + 45045 + 3003 + 91 = 2390480 \end{aligned} \quad (2)$$

Based on the (2) calculations, the result for case $n=14$ (that will later appear in the example from Győr), is 2,390,480 network variants, which is a significantly big number for analysis.

In order to reduce the number of network variants to be examined, we need to implement one filter: those line-end pairs that are in a very similar direction from the city center (e.g., for simplicity, towards the same compass direction) cannot be considered useful diameter lines (and in fact, not even diameter lines at all, but rather "U" shaped), since circular or transversal links between the zones they serve may provide optimal access, so that these connections can be disregarded without risking the optimum result. Naturally, the number of disregarded network variants depends on the directional distribution of line-ends so we are not able to provide a definitive formula, but some sort of reduction is definitely expected.

Another important aspect of line-ends is the minimally offered service level, so the maximum time between departures (which is required to be provided for comfort, regardless of the number of passengers), and the recommended (or in some cases required) vehicle type: these can be used to determine the default service frequency for specific line combinations as well as vehicle type.

In the model used for this research, the service frequency is given in integer numbers (typically the divisors of 60) most commonly found in local timetables and easily remembered by passengers: 1, 2, 3, 4, 5, 7 (instead of $15 / 2 = 7.5$), 10, 12, 15, 20, 30, 40 and 60 minutes (but this can be changed, of course) and in the smaller and mid-sized cities mostly solo (75 passengers) and articulated buses (120 passengers) are used (Winkler, 2019). When generating line combinations, the algorithm assigns the higher frequency (i.e., less time between departures) of the two line-ends and the higher vehicle capacity to the diameter line. An exception could be in cases where a line-end must be operated by solo buses (most often due to physical restrictions such as a narrow curve where an articulated bus could not turn): in these cases, obviously only solo buses can operate on the

diameter line even if it means that the frequency should be significantly higher (although this is not necessarily a bad solution).

Naturally most networks do not only consist of radial and diameter lines (Fülöp et al., 2006) but other types as well (i.e., circular, partially circular, transversal, etc.), and there are potentially elements in the network that cannot be changed for various reasons (e.g., urban sections of regional bus lines used for local service as well), so in the applied model it should be possible to specify fixed lines, which should be considered for assignment and defining frequency in the same way as line variations created by combinations.

To sum up, the goal of the implemented algorithm is to create network variants based on the criteria above, and to assign the travel demand available in the form of an origin-destination matrix onto all network variants. During this, the frequencies will also be finalized: lines where the capacity was not sufficient upon the initial assignment will be iteratively increased in frequency. From these network variants, the main operational indicators (e.g., vehicle km, capacity km) and passenger-side characteristics (e.g., number of transfers, total travel times) are calculated and stored.

Implementing the Algorithm

The implementation of the algorithm specified in the previous section was carried out in Microsoft Windows 10, GNU environment in C++. The software, called „LiMa” (=Line Matcher) consists of two parts. The first program generates all possible network variants based on line-end description, and writes their description in an output file. The output file is in a simple format, so it is easy to check and it is easy to structure (for parallel processing). The second program, after reading the detailed description of the zones, the destination matrix, the (optional) inter-zone walking times, the fixed lines and the combinable line-ends, evaluates the networks read from the output of the first program, as described in the previous section.

The assignment and the search for the required shortest paths (Winkler, 2013) is carried out in a simplified way in the current version of the program. As the origin-destination matrix describes travel demands with zone accuracy, detailed line data (route, distance, journey time) and shortest paths are not entered at stop level but at zone level to speed up the operation of the program. The assignment process is frequency-based, so when boarding or transferring to a public service, the waiting time is calculated as a function of the frequency, and is "one-way, one-step", so it assigns all passengers on the most favorable single path, and does not take into account congestion (but increases frequency if necessary).

Partly due to the above simplifications and partly due to the closed operation of the program, the running speed was favorable and suitable for practical use. Previously there were discussion that the newly developed software would only create the network variants, and the assignment itself would be done by an already existing external professional program (e.g., PTV VISUM), through inter-software communication. However, these ideas were discarded as tests showed that the simplified analysis that the self-developed software created was about 2800 times faster than using the detailed calculations of PTV VISUM that would have increased running time to an unacceptable level. In case of the Győr model that contains approximately 300,000 network variants, the running time of „LiMa” was 45 minutes (properties of the computer: ACPI x64-based PC, Intel Pentium CPU G3420 @ 3.20 GHz processor, 4 GB DDR3 memory), on the other hand, using an external program, the test could have taken several months on the same computer.

The Results of the Experiment with Győr’s Example

In parallel with planning and developing the necessary software, a simplified model of public transport in Győr was developed to test the algorithm in practice. Although there are more than 60 local bus lines in Győr, it is important to note that about two thirds of these are intermittent or destination bus lines, and the core network consists of only 20 lines. Győr also has a large agglomeration (Jóna et al., 2021) which may be the topic of future research. The aim of this paper is to examine the 20 core lines in Győr and the possibilities for their reorganization, for which different solutions have been proposed in various conceptions over the years. The rest of the network can be considered unchanged. As certain areas (mainly industrial areas) are served by intermittent or destination lines only, these areas have been excluded from the analysis. Although some minor reorganizations of the network took place in April 2022, this paper starts from the service in operation at the beginning of 2022, for which complete data were available.

Table 1 shows the properties of the line-ends from (and back to) the city center (i.e., the town hall), derived from the radial and diameter lines of Győr, and Figure 1 shows their map.

Table 1. Properties of the possible line-ends in Győr

Sign	Route	Compass direction	Recommended vehicle type	Minimal service frequency
UN	Kossuth Lajos utca – Újváros, Nép utca	West	solo	30 minutes
RL	Radnóti Miklós utca – Liget utca, Nyár utca	West	articulated	30 minutes
PI	Pinnyéd	West	solo	60 minutes
SA	Városrét – Sárás	North	mandatory solo	60 minutes
BA	Bácsa, Ergényi lakótelep	North	articulated	30 minutes
LK	Likócs	East	mandatory solo	60 minutes
GS	Győrszentiván (loop)	East	articulated	60 minutes
ZZ	Zrínyi utca – Zöld utca, Szőnyi Márton utca	South	articulated	30 minutes
JK	Jereváni út – Kismegyer	South	solo	60 minutes
SK	Szabadhegy, vasútállomás – Kismegyer	South	solo	60 minutes
NM	Nagy Imre út – Marcalváros – Ménfőcsanak	South	articulated	30 minutes
KG	Kálvária utca – Marcalváros – Gyirmót	South	solo	60 minutes
TM	Adyváros (Tihanyi Árpád út) – Marcalváros	South	articulated	30 minutes
GM	Gyárváros – Adyváros – Marcalváros	South	articulated	30 minutes

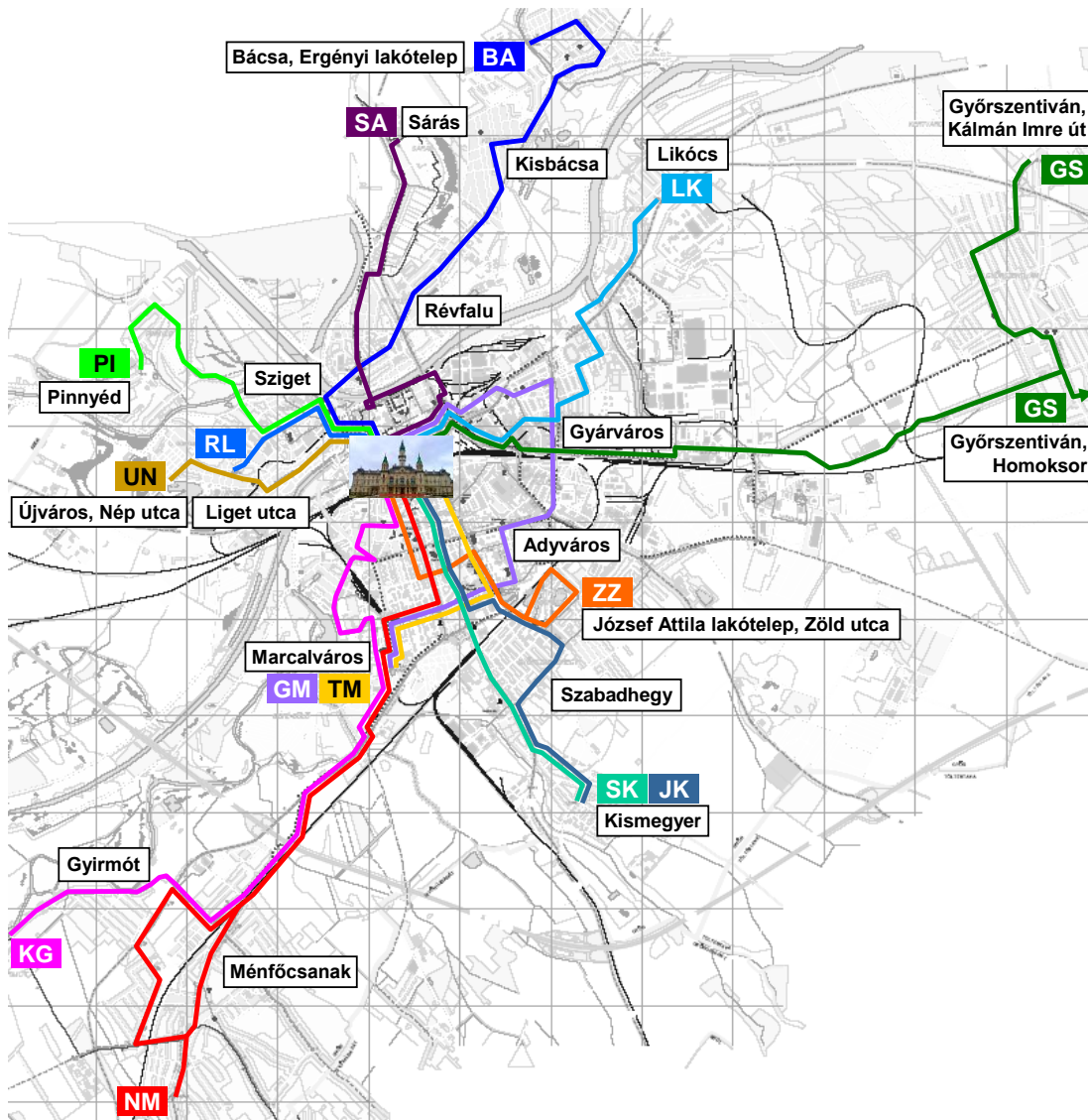


Figure 1. Map of the possible line-ends in Győr

The circular and regional lines shown in Table 2 were defined as fixed lines.

Table 2. Properties of the fixed lines in Győr

Sign	Route	General vehicle type	Average service frequency
7	Révai Miklós utca – Szabadhegy – Adyváros – Virágpiac	solo	25 minutes
9	Egyetem – Belváros – Adyváros – Révai Miklós utca	solo	26 minutes
10	Autóbusz-állomás – Víziváros – Bácsa	solo	100 minutes
17-17B	Virágpiac – Adyváros – Szabadhegy – Révai Miklós utca	solo	25 minutes
19	Révai Miklós utca – Adyváros – Belváros – Egyetem	solo	26 minutes
32	Autóbusz-állomás – Ménfőcsanak, Hegyalja utca	solo	64 minutes
34-36	Autóbusz-állomás – Ménfőcsanak, Győri út [- ...]	solo	54 minutes
CITY	Egyetem – Városrét – Belváros – Városrét – Egyetem	solo	15 minutes

It should be noted that although the present study is based on a regular school and work day, with a different timetable (frequency) for most lines at different times of the day, since the available destination matrix is all-day, for simplicity, average service frequencies are defined and used throughout the day. Using the directional filtering mentioned above, the nearly 2.4 million network variants identified by (2) could be narrowed down to 301,918 variants, so this filtering method proved to be very effective. The results of the evaluation program, which was run on about 300 thousand network variants, are shown in Table 3, which shows the indicators for some special network variants.

Table 3. Indicators for some special network variants

Position (by mean cost)	Specialty of the network	Vehicle km	Capacity km	Sum of gener. journey times	Transfers	Rel. capacity km	Rel. sum of gener. journey times	Mean of rel. costs
1	Best ranking	10,477	945,736	2,468,291	9,960	72.114	91.007	81.561
12	Best with no radial line	10,561	967,201	2,435,504	9,068	73.750	89.799	81.775
2,707	Least capacity km	10,277	914,227	2,617,100	11,388	69.711	96.494	83.103
41,530	Least vehicle km	9,552	932,965	2,651,669	9,224	71.140	97.769	84.454
57,553	Most similar to the current network	10,219	964,177	2,600,551	10,091	73.520	95.884	84.702
146,286	Least transfers	11,320	1,091,887	2,396,176	8,096	83.258	88.349	85.803
190,013	All lines are radial	10,041	955,996	2,712,186	13,121	72.896	100.000	86.448
297,164	Least generalized journey times	15,237	1,311,451	2,148,229	10,242	100.000	79.207	89.603
300,635	Worst with no radial line	14,000	1,273,442	2,259,471	8,828	97.102	83.308	90.205
301,918	Worst ranking	13,912	1,250,141	2,370,907	11,903	95.325	87.417	91.371

In this context, it is important to note that the suitability of network variants (and thus the ranking of all versions) was determined using the sum of the capacity km in terms of operating costs and the so-called generalized journey times which are good indicators of passenger preferences. The generalized journey time is based on the physical journey time, however a weighting is also used (waiting time: 1.6 multiplier, walking time: 1.7 multiplier), and the 11.7 minute "penalty" for transfers also expresses the inconvenience to passengers, thus reflecting their satisfaction with the service more accurately than the raw journey time (Winkler, 2013). As the dimension and magnitude of the operator and passenger metrics differ, relative values of both were determined and averaged over 50-50% to arrive at a mean indicator reflecting the perspective of both parties.

On the other hand, Figure 2 shows the main operator and passenger-side indicators for all the 301,918 network variants in the form of value pairs. From the point set, a linear relationship between the number of capacity kilometers issued and the generalized journey time of passengers can be clearly seen: to reduce generalized journey times, meaning to increase passenger satisfaction, it is generally necessary to increase the volume of service. It may be possible to achieve the same level of satisfaction with a smaller or a larger volume (i.e., less "smartly" designed) network (hence the "thickness" of the shape in Figure 2) but the general trend is the (logical) relationship above.

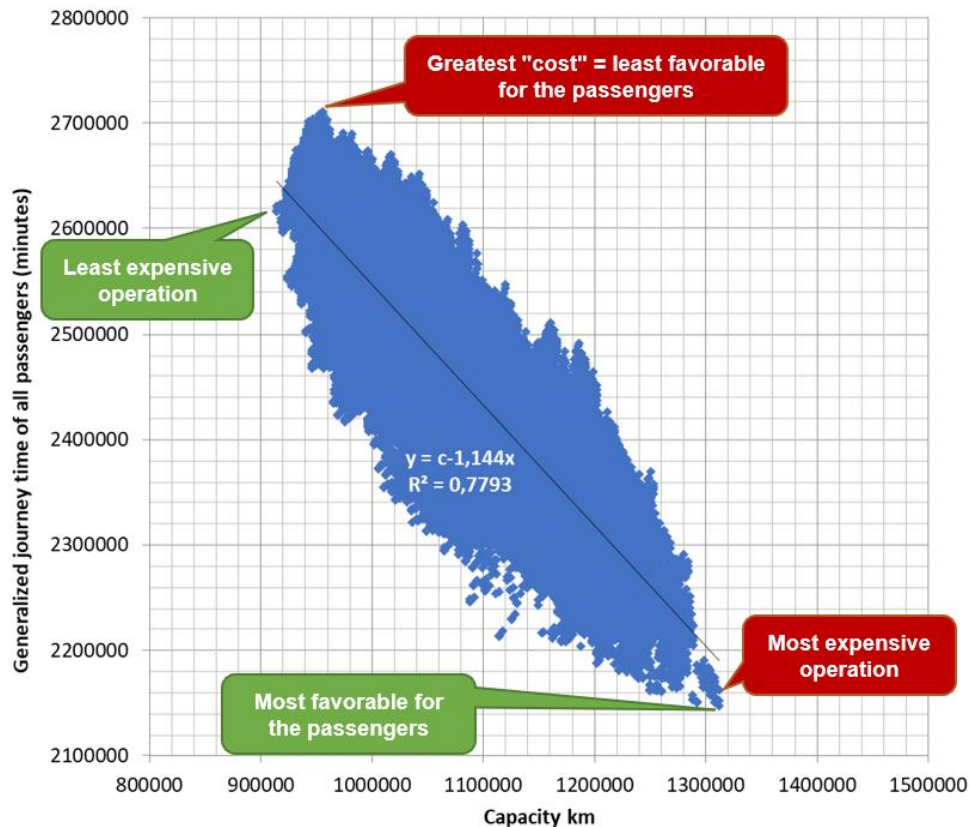


Figure 2. Map of the possible line-ends in Győr

A few important observations from the results:

- the most favorable network variant consists of 6 diameter lines and 2 radial lines, while the network operating in reality contained the same line-ends in the form of 5 diameter lines and 4 radial lines
- the best of the all-diameter networks ranked 12th in the order of suitability of all variants (true, the worst ranking of this type of network is 300,635, so you can design a very bad network with all-diameter lines, too!)
- in contrast, the network variant with only radial lines is ranked 190,013, well in the bottom half of the field
- the network variant operating in reality is ranked 57,553, thus in the top 20%.

Based on the observations above, it can be concluded that in the case of Győr, the structure of travel demands does indeed justify a high ratio of diameter lines, even more than what is available today, if the necessary infrastructure improvements could be implemented.

Table 4 shows the lines of the network version that came first in the suitability contest. As mentioned above, the majority of the lines are diameter, with only Győrszentiván and Gyirmót having a terminus in the city center. It should be noted, however, that this network would not be operational at present (or only with significant overheads), as there are no social facilities for bus drivers at the terminals of several suggested lines. The latter development would be appropriate for Kismegyér (new lines 1 and 3), Liget utca (new line 2) and Likócs (new line 6). (Of course, network variants that could not be operated with the current infrastructure could have been excluded in the pre-screening, but they were deliberately not filtered out, as the analysis method could also be used to identify the necessary location for such infrastructure improvements.)

Table 4. Lines of the network with the best ranking

Line (line-ends)	Route	General vehicle type	Average service frequency
1 UN-SK	Újváros, Nép utca – Kossuth Lajos utca – <i>City center</i> – Szabadhegy, vasútállomás – Kismegyer	solo	30 minutes
2 RL-NM	Liget utca, Nyár utca – Radnóti Miklós utca – <i>City center</i> – Nagy Imre út – Marcalváros – Ménfőcsanak, Győri út	articulated	15 minutes
3 PL-JK	Pinnyéd – <i>City center</i> – Jereváni út – Kismegyer	solo	60 minutes
4 SA-GM	Sárás – Városrét – <i>City center</i> – Gyárváros – Adyváros – Marcalváros	solo	30 minutes
5 BA-TM	Bácsa, Ergényi lakótelep – <i>City center</i> – Adyváros – Marcalváros	articulated	30 minutes
6 LK-ZZ	Likócs – <i>City center</i> – Zrínyi utca – Zöld utca, Szőnyi Márton utca	solo	30 minutes
7 GS	<i>City center</i> – Győrszentiván	articulated	40 minutes
8 KG	<i>City center</i> – Kálvária utca – Marcalváros – Gyirmót	solo	60 minutes

It is interesting to note that the new line 5 is practically identical to the current line 11, which has evolved in several stages to reach its current form, which is well established in practice and confirmed by this study. Another point in common with today's actual network is the radial (or more precisely Y-ended) nature of the Győrszentiván line group.

Possible Improvements

As already mentioned in previous sections of this paper, the research and development of the "LiMa" software is still in its early phase, so there are many opportunities for further development. The model is not yet able to deal with common line segments very well, e.g., where one line-end could be connected to several others (currently only one is possible). Of course, if this is achieved, work also needs to be done on the synchronization of the frequency of the lines containing the common segment.

In its current form, the algorithm is only usable in small or certain medium-sized single-center cities. For wider use, the model should also allow the possibility to compose lines of not just two, but more sections. In the Győr example, it would also have been possible to split the "NM" and "KG" line-ends in Marcalváros, thus allowing more combinations to be tested, but this would understandably have increased the running time of the program.

Additional solutions should also be considered when setting up frequency, as currently the aim is only to prevent passengers not being able to get on the buses, so frequencies are only increasing, but unused lines are not being decreased in frequency, so there could be significant unnecessary excess capacity. Of course, in designing the solution, attention should be paid in order to avoid creating an endless cycle of repeated decreasing and increasing in the algorithm. As another way to reduce unnecessary excess capacity, it would be important to manage shortened services. The first two improvements mentioned above, the management of common sections and the composing of more than two sections, would automatically enable this.

The assignment could be implemented by using stop-level journey planning, as well as a "multi-way" and/or "multi-step" assignment technique. Of course, the options mentioned above should be treated with caution, since even a small extension (e.g., 16 line-ends instead of 14) increases the number of possible networks by a factor of 20, and consequently the running time of the program.

However, a minor improvement in the assignment process is not expected to cause any major problems, since a slight increase in runtime would still mean a system that is practically usable, especially in light of the fact that the evaluation of network variants can be perfectly distributed and parallelized, i.e., the operation can be performed on several processors, possibly on several computers at the same time, and the results can easily be collected.

Conclusion

The paper presented the concept and theoretical background of an IT solution for the planning of radial-diameter local public transport networks, the applicable algorithms, and the experiences of the first implementation on the

example of local bus transport in the city of Győr. It is important to note that the presented results (network lines and frequencies) at this stage of the research, should not be regarded as solutions to be implemented immediately in practice in an unchanged form, since, as explained in the previous section, the model and software can still be further developed and improved in a number of areas. The presented network illustrates how the method works in a specific city, but if the method is further developed, the results will of course vary to a greater or lesser extent. However, the initial experiments are encouraging, as the program developed gives acceptable solutions to real-world problems, in a reasonable runtime, by exploring all reasonable possibilities.

Scientific Ethics Declaration

The author declares that the scientific ethical and legal responsibility of this article published in EPSTEM journal belongs to the author.

Notes

This article was presented as an oral presentation at the International Conference on Research in Engineering, Technology and Science (www.icrets.net) held in Budapest/Hungary on July 06-09, 2023.

References

- Ciaffia, F., Cipriana, E., Petrellia, M. & Ušpalyte-Vitkuniene, R. (2014, May 22-23). A new methodology for the public transport network design. *The 9th International Conference "Environmental Engineering"*, Vilnius Gediminas Technical University, Vilnius, Lithuania.
- Fülöp, G., Horváth, B., Prileszky, I. & Szabó, L. (2006). *Közforgalmú közlekedés I.* Széchenyi István Egyetem, Győr, Hungary.
- Jóna, L., Henézi, D. S., Döbrentei, B., & Gaál, B. (2021, June 10-11). A Szigetköz közlekedési kihívásai. *XI. Nemzetközi Közlekedéstudományi Konferencia: „Közlekedés a Járvány után: folytatás vagy újrakezdés”*, Széchenyi István University, Győr, Hungary.
- Owais, M., Moussa, G., Abbas, Y. & El-Shabrawy, M. (2014). Simple and effective solution methodology for transit network design problem. *International Journal of Computer Applications*, 89(14), 32-40.
- Winkler, Á. (2013). Utazói döntések modellezése a városi közforgalmú közlekedésben. (Doctoral dissertation). Retrieved from <https://mmti.sze.hu/winkler-agoston-2013->
- Winkler, Á. (2019, March 21-22). Sugaras-átmérős helyi közforgalmú közlekedési vonalhálózat tervezésének informatikai támogatása. *Közlekedéstudományi konferencia Győr 2019*, Széchenyi István University, Győr, Hungary.

Author Information

Ágoston Winkler

Széchenyi István University
H-9026 Győr, Egyetem tér 1. Hungary
Phone: +36 96 503400 / 3126
Fax: +36 96 613561
Contact e-mail: awinkler@sze.hu

To cite this article:

Winkler, A. (2023). Computer-aided planning of radial and diameter routes in local public transport networks. *The Eurasia Proceedings of Science, Technology, Engineering & Mathematics (EPSTEM)*, 23, 165-172.

The Eurasia Proceedings of Science, Technology, Engineering & Mathematics (EPSTEM), 2023

Volume 23, Pages 173-178

ICRETS 2023: International Conference on Research in Engineering, Technology and Science

Effect of Urea Usage Rate on Thixotropic Behavior of Cementitious Systems

Neslihan Caparoglu
Bursa Uludag University

Oznur Biricik
Bursa Uludag University

Ali Mardani
Bursa Uludag University

Abstract: It was understood that studies investigating the use of alternative materials have increased in order to develop concrete technology, to expand sustainability and to improve the fresh and hardened state properties of cementitious systems. It was reported that one of these alternative materials is urea, which can increase both the flow performance of the mixture and the freeze-thaw resistance. In this study, the effect of the use of urea on the thixotropic behavior of Portland cement systems was investigated. In addition to the urea-free control mix, 4 different batches of paste mixes were prepared by replacing the cement with urea at a rate of 2.5%, 5% and 10% by weight. The thixotropic behavior of the mixtures was evaluated by comparing the hysteresis area values obtained from the viscosity-shear rate graphs. It was determined that the structural recovery area measured at the initial and the structural breakdown area measured at the end of the 180 second rest period decreased with the use of urea. It was determined that the optimum urea utilization rate was 2.5% in terms of the thixotropic area value of the mixtures.

Keywords: Urea, Viscosity, Hysteresis area, Loop test, Thixotropy

Introduction

It is known that one of the most important factors affecting the durability of concrete negatively is the freeze-thaw event that occurs in cold weather conditions. It was emphasized that a 9% volume expansion occurs as a result of the water in the capillary spaces of the hardened concrete turning into ice with the decrease in temperature (Mardani Aghabaglou et al., 2019). Thus, it was reported that cracks occur in concrete samples as a result of the formation of internal tensile stresses (Erdogan, 2015).

It was declared that the water in the cavities of the concrete usually freezes at a temperature lower than 0°C due to the various salts it contains (Koefod, 2008). It was understood that the diameter of the cavity where the water is located affects the freezing temperature significantly (Berberoglu, 2011). It was reported that water freezes at 0°C in large capillary spaces, at temperatures between -15 and -20°C in very small capillary spaces, and at -78°C in gel spaces (Sahin, 2003). It was emphasized that the freezing of water in concrete occurs gradually, depending on the rate of heat transfer and the size of the void at the freezing point (Powers, 1965). It was declared that freezing starts from the water in large spaces and spreads towards small spaces (Postacioglu, 1987). It was reported that the resulting damage starts from the spills on the surface and progresses into the concrete by fragmentation into layers (Neville, 1995).

- This is an Open Access article distributed under the terms of the Creative Commons Attribution-Noncommercial 4.0 Unported License, permitting all non-commercial use, distribution, and reproduction in any medium, provided the original work is properly cited.

- Selection and peer-review under responsibility of the Organizing Committee of the Conference

It was understood that the degree of saturation of concrete and its porous structure are the most important parameters affecting the freeze-thaw resistance (Baradan, 2022). In order to increase the freeze-thaw resistance of concrete, an air-entraining admixture that will create permanent air spaces is added to the mixture (Sahin, 2003). However, it was reported that the compressive strength of concrete decreases with the addition of air-entraining admixture (Guleryuz, 2020). Numerous studies were carried out to improve both the freeze-thaw resistance and the fresh state and mechanical properties of concrete (Erdem & Ozturk, 2012). In this direction, it was understood that industrial urea has been examined in various studies (Shirayama et al., 2018).

Urea was discovered by the French scientist Hillaire Rouelle (1773) but began to be synthesized in 1828. Urea, known as carbamide, is an organic compound with the chemical formula $(\text{CO}(\text{NH}_2)_2)$ (Sant Ana Filho, 2012). As a bead-shaped solid product, urea has two $-\text{NH}_2$ groups joined by a carbonyl ($\text{C}=\text{O}$) functional group. The compound is commercially synthesized by a reaction of ammonia (NH_3) and carbon dioxide (CO_2) under conditions dependent on the technology used in the industrial plant (Sant Ana Filho et al., 2012). It is a colorless, odorless, easily soluble substance in water and alcohol (Kim, 2017).

In the literature, it was reported that urea improves the freeze-thaw resistance of cementitious systems (Demirboga, 2014), workability (Mwaiuwina, 1997; Demirboga, 2014), carbonation (Sadegzadeh, 1993) and drying-shrinkage (Sato, 2020) performance. It was declared that the use of urea, especially in mass concrete structures and in hot climate regions, provides a great advantage due to its lowering effect on the heat of hydration (Kim, 2021). Some research results on the subject are summarized here:

The effects of the use of rice husk ash (20%) and urea (0%, 5%, 10%, 20%) on the flow performance, compressive strength and heat of hydration properties of self-compacting concrete mixtures were investigated by Makul and Sua-iam (2017). It was reported that with the addition of urea, the heat of hydration and strength of the mixtures decrease, while the flow and strength performances increase. It was emphasized that this behavior was more evident with the increase in the urea utilization rate.

Wang et al. (2020), the effect of using urea at different rates (5%, 10% and 15%) on the hydration process and microstructure of the concrete mixture was investigated. They reported that the use of urea reduces the heat of hydration of the concrete mixture and has a retarding effect. It was emphasized that this behavior was more evident with the increase in the urea utilization rate.

It is known that chemical and mineral additives added to cementitious systems affect their rheological and thixotropic properties. It was understood that its thixotropic properties were evaluated with different approaches (Ma et al., 2018). In this context, it was emphasized that the thixotropic behavior of cementitious systems is generally investigated through hysteresis areas (Ma et al., 2018; Ferron et al., 2007). Zhang et al. (2021) the effects of different water-cement ratio and shear stress rate on the rheological and thixotropic properties of paste mixtures were investigated. When the constant shear stress was applied, it was measured that the hysteresis loop area and the destruction energy of the agglomeration structure decreased with the increase of the water-cement ratio. In the case of constant water-cement ratio, it was emphasized that with the decrease of the shear stress rate, the destruction energy and the degree of destruction of the agglomeration structure decrease. It was emphasized that with the increase of the shear stress rate, the agglomeration structure would increase the destruction energy.

As understood from the literature, it was emphasized by various researchers that urea has a significant positive effect on mechanical and durability properties (Mwaiuwina et al., 1997). However, no study was found on the effect of urea use on the rheological and thixotropic properties of cementitious systems. For this purpose, the effect of using different ratios of urea instead of cement on the thixotropic behavior of paste mixtures was investigated.

Material and Method

Materials

Cement

Within the scope of the study, CEM I 42.5R type cement (PC) produced by Bursa Cement was used. The chemical component, physical and mechanical properties of the cement supplied by the manufacturer are shown in Table 1. Some characteristics of the urea supplied by its manufacturer are presented in Table 2.

Table 1. Chemical composition, physical properties of cement.

Oxide	(%)	Mechanical and physical properties		
SiO ₂	18.74	Compressive strength (MPa)	1-Day	2.43
Al ₂ O ₃	5.37		28-Day	39.3
Fe ₂ O ₃	3.04	Setting Time (min)	Initial	201
CaO	64.11		Final	321
MgO	1.21	Fineness	Blaine specific surface (cm ² /g)	3600
Na ₂ O	0.34		Residual on 0.090 mm sieve (%)	0.4
K ₂ O	0.62		Residual on 0.045 mm sieve (%)	7.4
SO ₃	2.68		specific gravity	3.15
Cl ⁻	0.038	Volume expansion (mm)		<1

Table 2. Some properties of urea and air-entraining admixture

Admixture	Density (g/cm ³)	pH	Colour	Physical Condition	Melting point (°C)	Solids Ratio (%)
(CO(NH ₂) ₂)	1.32	9	White	Solid	133	-

Mixture Proportion

Within the scope of the study, a total of 4 different paste mixtures were produced by substituting urea at the rate of 2.5%, 5%, 10% of the cement weight into the control mixture that does not contain urea. In all mixtures, the water/cement ratio was kept constant as 0.35. The preparation of the mixtures was carried out in a room whose temperature was kept constant at 20±2°C. The denotation of the mixtures was made according to the urea usage rate. For example, the paste mixture prepared by replacing 2.5% of the cement weight with urea is called Urea_2.5%. In the preparation of the mixtures, firstly, urea and water were mixed at 62 rpm for 30 seconds, then cement was added and mixed at the same speed for another 30 seconds. Then, rheological measurements were carried out by mixing at 125 rpm for 120 seconds.

Test Methods

The thixotropic behavior of the paste mixtures prepared within the scope of the study was investigated by means of viscosity-shear stress graphs. The graphs in question were drawn through the data obtained from the Herschel Bulkley model analysis shown in Equation 1. In rheological measurements, hysteresis areas were created by increasing the shear rate from 0 s⁻¹ to 60 s⁻¹ and then decreasing it back to 0s⁻¹ (Figure 1). The hysteresis areas are calculated using Equations 2 and 3.

$$\tau = \tau_o + b \cdot \dot{\gamma}^P \tag{1}$$

- τ_o: dynamic yield stress
- b: Herschel-Bulkley coefficient,
- $\dot{\gamma}$: shear rate
- P: Herschel-Bulkley index

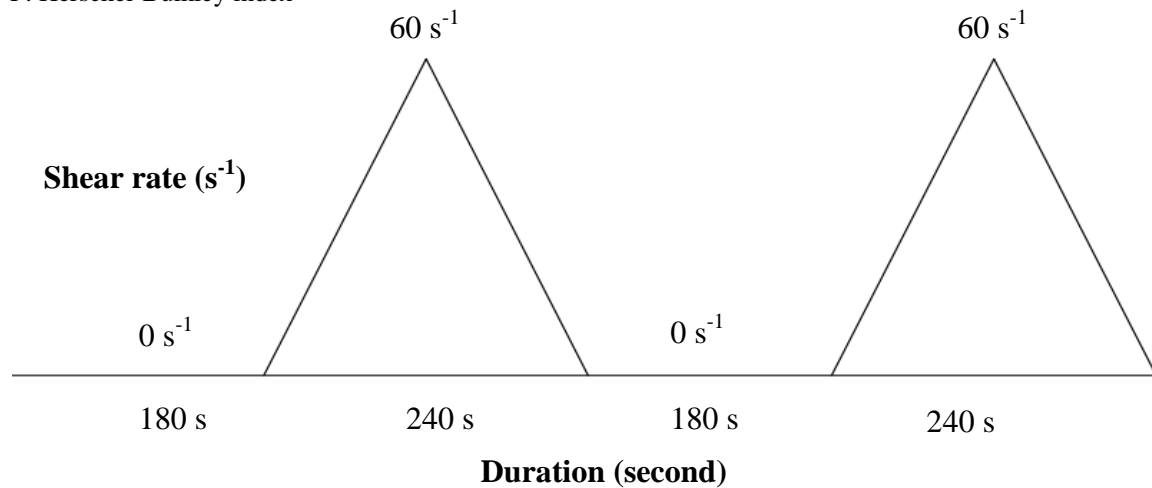


Figure 1. Rheological measurement process

$$A_{\text{viscosity}} = \left[\sum_{i=1}^{n-1} A_{i,\text{viscosity_up}} \right] - \left[\sum_{i=1}^{n-1} A_{i,\text{viscosity_down}} \right] \quad (2)$$

$$A_i = \frac{1}{2} \left[(\dot{\gamma}_i - \dot{\gamma}_{i+1}) \cdot (\eta_i + \eta_{i+1}) \right] \quad (3)$$

n: number of data

$\dot{\gamma}_i$: shear rate (s^{-1})

$A_{\text{viscosity}}$: hysteresis area (Pa) formed in the viscosity-shear rate graph.

$A_{i,\text{viscosity_up}}$: area under the up curve

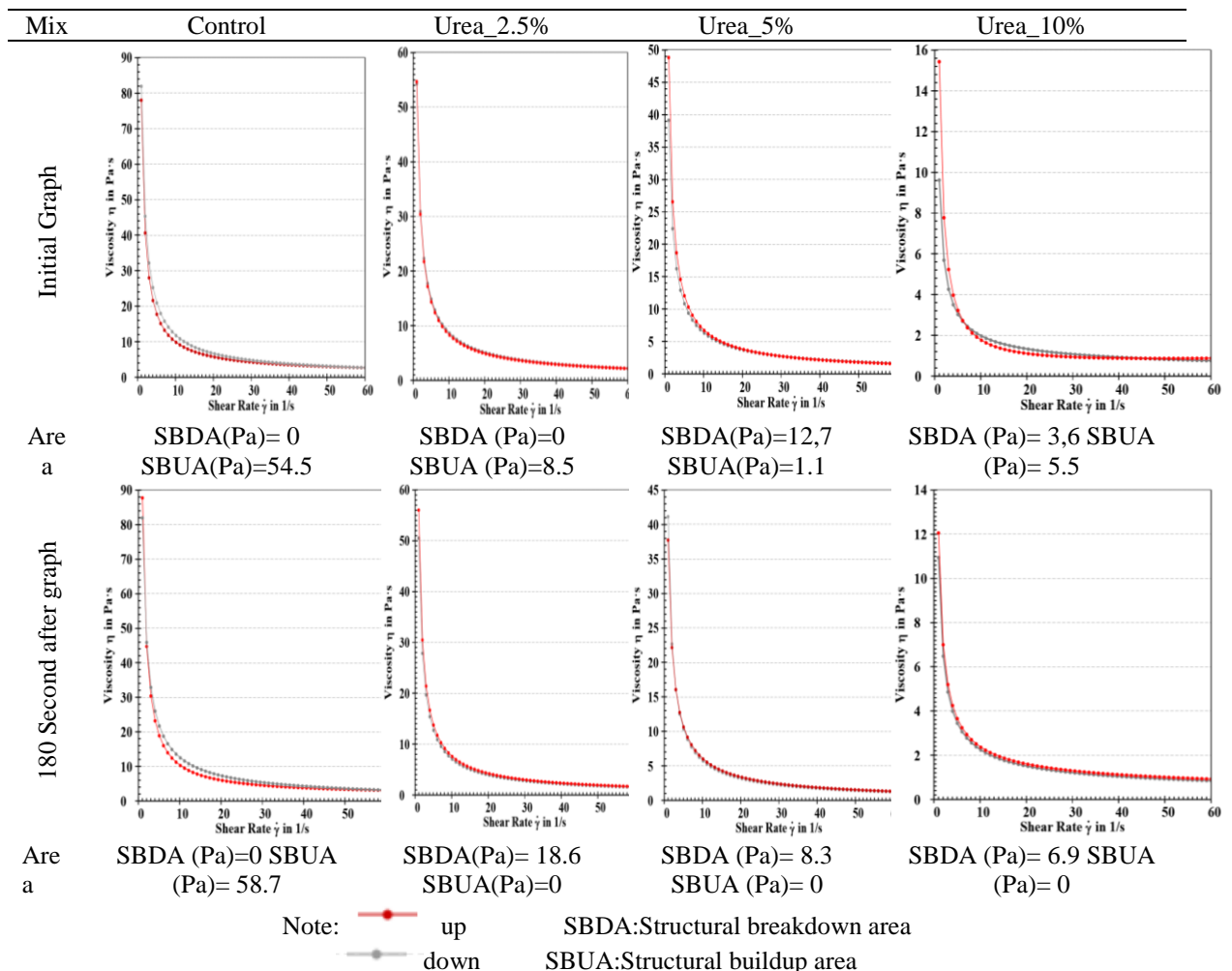
$A_{i,\text{viscosity_down}}$: area under the down curve (Pa)

η : apparent viscosity (Pa.s)

Discussion and Conclusion

The viscosity-shear rate graph of the mixtures and the 'structural breakdown area' (SBDA) and 'structural buildup area' (SBUA) values obtained from this graph are given in Figure 3.

Table 2. Viscosity-shear rate graphs of mixtures



With the addition of 2.5% and 5% urea to the control mixture, it was understood that the SBDA value decreased by 84% and 98%, respectively. However, it was measured that the SBUA value increased 5 times with an increase in the urea utilization rate from 5% to 10%. Despite the mentioned increase, it was understood that the mixture containing 10% urea had 90% and 35% lower SBUA values compared to the control and mixtures containing 2.5% urea. Thus, it was understood that the SBUA values generally decreased with the use of urea,

but after a certain value (10% for this study), this decreasing trend changed to an increasing trend. While the SBDA value was measured as 0 for the control and Urea_2.5% mixtures, the said value was measured as 12.7 Pa and 3.6 Pa for the Urea_5% and Urea_10% mixtures, respectively. Thus, it was understood that the Urea_5% mixture had the highest SBDA (thixotropic area) value and the said value started to decrease with 10% urea usage rate.

As can be seen from Table 4, an 8% increase in the SBUA value of the control mixture was detected after resting for 180 seconds. In the mixtures containing urea, the SBUA values were measured as 0. When the measurements at the end of 180 seconds were evaluated among themselves, the SBDA values decreased with the increase in the use of urea. The highest and lowest SBDA values were observed in Urea_2.5% and Urea_10% mixtures, respectively. Thus, it was understood that the optimum urea usage rate for portland cement mixtures is 2.5% in terms of thixotropic area value.

Conclusion

The results obtained in accordance with the materials and methods used in the study are presented below.

- Compared to initial, the SBUA value measured after the 180 second rest period increased in the control mixture and decreased in the mixtures containing urea.
- SBUA values measured at the initial generally decreased with the use of urea, and were measured as 0 after a rest period of 180 seconds.
- It was understood that the SBDA values measured after the 180 second rest period decreased with the use of urea.
- In terms of thixotropic area value, it was determined that the optimum urea usage rate for portland cement mixtures is 2.5%.

Conflicts of Interest/Competing Interests

The authors declare that they have no known competing financial interests or personal relationships that could have appeared to influence the work reported in this paper.

Scientific Ethics Declaration

The authors declare that the scientific ethical and legal responsibility of this article published in EPSTEM journal belongs to the authors.

Acknowledgements or Notes

* This article was presented as an oral presentation at the International Conference on Research in Engineering, Technology and Science (www.icrets.net) held in Budapest/Hungary on July 06-09, 2023.

* The authors appreciate contributions of the Bursa Uludağ University Science and Technology Centre (BAP) under grant numbers FHIZ- 2022-1165. In addition, the authors would like to acknowledge, Bursa Cement Factory for their kind assistance in providing the cements as well as determining the technical properties of these products.

* This research did not receive any specific grant from funding agencies in the public, commercial, or not-for-profit sectors.

* All data, models, and code generated or used during the study appear in the submitted article.

References

Baradan, B., Turkel, S., Yazıcı, H., Un, H., Yigiter, H., Felekoglu, B., Tosun, K., Aydın, S., Yardımcı, Y., M., Topal, A. & Ozturk, A. U. (2022). *Concrete*. (334). Dokuz Eylul University Faculty of Engineering Publications: İzmir.

- Berberoglu, S.(2011). *Beton yollarda buz cozucu tuz etkisine su-cimento oraninin etkileri*.(Master's thesis). Institute of Science, Sakarya University, Sakarya.
- Demirboga, R., Karagol, F., Polat, R., & Kaygusuz, M.A. (2014), The effects of urea on strength gaining of fresh concrete under the cold weather conditions, *Construction and Building Materials*, 64,114-120
- Erdem, R.T.,Ozturk A.U. (2012). Effect of marble powder additive on freezing-thawing properties of cement mortar. *BEU Journal of Science*, 1(2), 85-91.
- Erdogan. T.Y., (2016), *Beton*. ODTU Gelistirme Vakfi Yayıncılık.
- Guleryuz, E., Ozen, S., & Mardani Aghabaglou, A.(2020). Effect of utilization of mineral admixture on the fresh and hardened properties of air-entrained cement mortars, *Pamukkale University Journal of Engineering Sciences*, 26(6), 1053-1061.
- Kim, H.Y. (2017), Urea additives for reduction of hydration heat in cement composites, *Construction and Building Materials* 156 790–798.
- Kim, H.Y. (2021), On the feasibility of using industrial urea to mitigate thermal and shrinkage cracking in concrete, *Applied Science*. 11(6), 2483.
- Koefod, S., (2008), *Eutectic depressants. Surface transportation weather and snow removal and ice control technology*,. <https://onlinepubs.trb.org/Onlinepubs/circulars/ec126.pdf>
- Ma X., Yuan q., Liu. J., & Shi. C. (2018), Effect of water absorption of sap on the rheological properties of cement-based materials with ultra-low w/b ratio. *Construction and Building Materials*, 95, 66-74.
- Makul, N., & Sua-iam, G., (2018), Effect of granular urea on the properties of self-consolidating concrete incorporating untreated rice husk ash: Flowability, compressive strength and temperature rise, *Construction and Building Materials*, 162, 489–502.
- Mwaiuwinga, S., Ayona. T. & Sakata, K. (1997). Influence of urea in concrete. *Cement and Concrete Research*, 27(5), 733-745.
- Neville, A.M., (1995). *Properties of concrete* (4th ed.). Longman Scientific and Technical.
- Postacıoğlu, B., (1987), *Beton: Agregalar, Beton* (2th ed.). Matbaa Teknisyenleri :İstanbul
- Powers, T.C. (1965). *The mechanism of frost action in concrete*. <https://trid.trb.org/view/98537>
- Raissa, P., Ferron, R.P., Gregori, A., Sun, Z., & Shah, S.P.(2007). Rheological method to evaluate structural buildup in self-consolidating concrete cement pastes, *Acı Materials Journal Technical Paper*. 104.
- Sadegzadeh, M., Page. C.L. & Vassie, P.R.W. (1993). Effects of urea on durability of reinforced concrete. *Magazine of Concrete Research*, 45(164), 179-186.
- Sahin, R., (2003), *Normal portland cimentolu betonların don direncinin Taguchi yontemi ile optimizasyonu ve hasar analizi*. (Doctoral dissertation). Institute of Science, Atatürk University, Erzurum.
- Sant Ana Filho, C.R., Rossete, A.L.R.M.,Tavares, C.R.O.,Prestes C.V., & Bendassolli, J.A. (2012). Synthesis of 15N-enriched urea (CO(15NHNH₂)₂) from 15NH₃, CO, and S in a discontinuous process, *Brazilian Journal of Chemical Engineering*, 29(4), 795 – 806.
- Shirayama, K., Fujiwara H., Maruoka, M., & Lingling, L. (2018). Development of a new method to reduce drying shrinkage of concrete by applying urea. *International Conference on Durability of Concrete Structures University of Leeds*. United Kingdom, UK.
- Wang, L., Ju. S., Chu. H.,Liu Z., Yang. Z. & Wang, F. (2020). Hydration process and microstructure evolution of low exothermic concrete produced with urea. *Construction and Building Materials*, 248. 118640.
- Zhang, Y., Zuo, Y., Li C., Sun, H., Ye, G., (2021). Study on microstructure characteristics of fresh cement paste. *Journal of Physics: Conference Series*, 2044.

Author Information

Neslihan Caparoğlu
Bursa Uludag University
Bursa, Turkiye

Oznur Biricik
Bursa Uludag University
Bursa, Turkiye

Ali Mardani
Bursa Uludag University
Bursa, Turkiye
Contact e-mail: alimardani@uludag.edu.tr

To cite this article:

Caparoglu, N., Biricik, O. & Mardani, A.(2023). Effect of urea usage rate on thixotropic behavior of cementitious systems. *The Eurasia Proceedings of Science, Technology, Engineering & Mathematics (EPSTEM)*, 23, 173-178.

The Eurasia Proceedings of Science, Technology, Engineering & Mathematics (EPSTEM), 2023

Volume 23, Pages 179-188

ICRETS 2023: International Conference on Research in Engineering, Technology and Science

Estimation of Red Meat Production in Turkey according to the Grey-Markov Chain Model

Halil Sen

Burdur Mehmet Akif Ersoy University

Abstract: Today, due to the place and importance of red meat in terms of nutrition and public health, meeting the reliable supply of red meat to meet the demand has become one of the most important issues. The production source of red meat in Turkey is cattle, sheep, goat and buffalo. Although Turkey is a rich country in terms of different species and breeds and animal potential, the yield per unit animal is low. Most of the meat is consumed fresh in Turkey. With the increasing importance of meeting the reliable red meat supply, the necessity of following the sector has emerged. Accurate estimation of red meat production in Turkey is important for establishing short, medium and long-term policies that will balance supply and demand. In this study, Grey-Markov chain model, which is a combination of Markov chains method and Grey estimation model, which can be used to predict future data with very limited data and information, was used in the estimation of red meat production. The obtained results show that the Grey-Markov chain model used has high predictive precision and applicability.

Keywords: Grey estimation model, Markov chain, Meat production

Introduction

The livestock sector has a strategic importance in Turkey in terms of economic and social aspects such as adequate and balanced nutrition of the population, realization of rural development, and prevention of rural-urban migration by reducing agricultural unemployment (Saygın & Demirbas, 2017). The red meat sector is also important for the national economy, as it creates both consumption and a large production area within the livestock sector in Turkey. The continuation of livestock and red meat imports in Turkey reveals the necessity of policies that will bring structural solutions. In addition, it is stated that Turkey's geographical features are suitable for cattle and small cattle breeding, and red meat has a special importance for Turkey due to its cultural structure.

As of 2020, approximately 337 million tons of meat was produced in the world. Meat production sources in the world are diverse and abundant. Chicken meat accounts for 35% of meat production, pork 33% and cattle 20%. Approximately 134 million tons (40%) of the world's meat production is white meat, mainly chicken meat, while 60% (203 million tons) is red meat. Of the red meat, 54% is pork and more than 33% is cattle. Sheep meat accounts for 5% of red meat, goat meat only 3% and buffalo meat 2% (Ertas, 2023).

When examining the temporal change in the amount of red meat production in the world, it would be more accurate to examine it together with the world population in order to observe the amount per capita. If we examine the population growth in ten-year periods; the world population, which was around 3 billion in 1961, increased by 20% in 1970, 20% in 1980 and approached 4.5 billion, followed by 19% in 1990, 15% in 2000, 13% in 2010 and 11% in 2020. When the amount of red meat production is analyzed in ten-year periods; while it was around 60 million tons in 1961, it reached over 82 million tons in 1970 with an increase rate of 38%. In 1980, it increased by 30% and reached 108 million tons and increased by 26% in 1990, 19% in 2000, 18% in 2010 and 5% in 2020. As a result, it shows that the amount of meat per capita has increased since 1961. As a

- This is an Open Access article distributed under the terms of the Creative Commons Attribution-Noncommercial 4.0 Unported License, permitting all non-commercial use, distribution, and reproduction in any medium, provided the original work is properly cited.

- Selection and peer-review under responsibility of the Organizing Committee of the Conference

© 2023 Published by ISRES Publishing: www.isres.org

matter of fact, according to the calculation made by taking FAO data into account (total meat production / total population), while the amount of meat per capita was 19 kg in 1961, this value is approximately 26 kg today (Ertas, 2023).

For Turkey, in 1961, the population of Turkey was around 28 million. By 1970, the population had increased by 24% to 35 million, and by 1980 it had increased by 26% to around 44 million. By 2020, it had increased by 16% compared to 2010. While the rate of increase increased until 1980, it tends to decrease in the following periods. In red meat production, there was an increase of 14% from 1961 to 1970 and then a change of -6% in 1980. The 461 thousand tons of red meat produced in 1970 declined to 433 thousand tons in 1980. By 1990, it had increased by 71% to 743 thousand tons, but by 2000, this production had decreased by -34% to 491 thousand tons. This production amount increased by 59% in 2010 and 37% in 2020, reaching over 1 million tons (FAO,2023). Therefore, according to the rough calculation mentioned above, while the amount of red meat per capita in Turkey was 14 kg in 1961, it decreased to 13 kg in 1970 and 10 kg in 1980. While it was 14 kg in 1990, it decreased to 8 kg in 2000 (Ertas, 2023). As of 2020, the total amount of red meat per capita is approximately 26 kg per year, considering the red meat production of nearly 200 million tons and the world population of the same year. The amount of red meat per capita in Turkey is 18.5 kg/year. Therefore, Turkey is far behind both the world average and developed countries. Red meat production and change rates in Turkey are shown in Table 1 below. These data will be used to estimate the production in the following years.

Table 1. Production of red meat (tonnes) and change ratios, 2001-2021

Year	Cattle	Buffalo	Sheep	Goat	Total	Change ratios according to the previous year (%)
2001	493 763	6 486	225 555	57 537	783 341	-
2002	496 198	5 728	219 311	57 707	778 945	-0,6
2003	489 377	5 242	204 441	56 820	755 880	-3,0
2004	488 556	4 952	190 105	52 460	736 074	-2,6
2005	491 560	4 629	190 539	50 492	737 220	0,2
2006	514 042	4 442	187 236	48 906	754 625	2,4
2007	549 513	4 347	191 428	50 712	796 000	5,5
2008	581 497	4 128	192 647	50 254	828 527	4,1
2009	608 183	4 019	188 496	46 240	846 939	2,2
2010	647 067	3 785	186 121	42 846	879 819	3,9
2011	710 652	3 780	210 171	44 840	969 443	10,2
2012	790 034	4 027	220 359	53 133	1 067 553	10,1
2013	798 784	4 580	236 186	59 532	1 099 081	3,0
2014	815 674	5 004	238 670	63 711	1 123 059	2,2
2015	862 098	5 300	249 863	69 757	1 187 018	5,7
2016	956 180	5 470	266 675	75 322	1 303 648	9,8
2017	1 093 841	5 868	262 825	77 794	1 440 327	10,5
2018	1 281 234	6 515	291 179	82 839	1 661 767	15,4
2019	1 330 169	7 150	316 170	87 126	1 740 616	4,7
2020	1 341 446	8 424	345 639	90 443	1 785 952	2,6
2021	1 460 719	10 831	385 933	94 555	1 952 038	9,3

Source: TURKSTAT, Red Meat Production Statistics, 2001, 2021

Method

In this study, the situation of red meat production in Turkey in the following years was tried to be estimated by using the Grey-Markov Chain Model.

Grey System Theory and Grey-Markov Chain Model

The grey system theory developed by Ju Long Deng in 1982; In research in the field of condition analysis, forecasting and decision making, it focuses on uncertainty and lack of information to analyse and understand systems (Ju-Long, 1982). Grey system theory, which is an interdisciplinary approach, is an alternative method for quantifying uncertainty. The basic idea in its emergence is to predict the behaviour of uncertain systems, which cannot be overcome by stochastic or fuzzy methods, with the help of a limited number of data.

The main feature that distinguishes the grey prediction method, which is one of the main fields of work of grey system theory, from traditional prediction methods is that it needs a limited number of data to predict the behaviour of uncertain systems. Unlike traditional prediction methods, the main feature of the grey prediction method is that it does not need strict assumptions about the data set and can be successfully applied in the analysis of systems with limited data. The grey prediction method has been developed to make predictions about the future with the help of the grey model GM(1,1) using the available data. GM(1,1) is a time series forecasting model that contains a set of differentiable equations. The GM(1,1) notation is used to express the grey model with first-order differentiable equations with a single variable. The grey prediction method consists of the basic steps described in detail below (Liu & Lin, 2006).

Step-1: Let $X^{(0)}$ be the raw time series sequence with a single variable valence n magnitude that forms the time series.

$$X^{(0)} = (x^{(0)}(1), x^{(0)}(2), x^{(0)}(3), \dots, x^{(0)}(n)) ; n \geq 4 \tag{1}$$

$X^{(1)}$ is constructed using the first-order aggregate production operator.

$$x^{(1)}(k) = \sum_{i=1}^k x^{(0)}(i), (i = 1, 2, 3, \dots, n) \tag{2}$$

$$X^{(1)} = (x^{(1)}(1), x^{(1)}(2), x^{(1)}(3), \dots, x^{(1)}(n)) ; n \geq 4 \tag{3}$$

Step-2: Determination of Coefficients: $x^{(0)}(k) + ax^{(1)}(k) = b$ represents the original form of the model G(1,1). k is the time points; a is the coefficient of improvement; b represents the driver coefficient. $Z^{(1)}$ is generated using the first-order mean value generation operator.

$$z^{(1)}(k) = 0,5x^{(1)}(k) + 0,5x^{(1)}(k-1) \tag{4}$$

$$Z^{(1)} = (z^{(1)}(1), z^{(1)}(2), z^{(1)}(3), \dots, z^{(1)}(n)) \tag{5}$$

The basic form of the G(1,1) model is written as $x^{(0)}(k) + az^{(1)}(k) = b$ in which the $Z^{(1)}$ series is used. The least squares method is used in estimating the a and b parameters. If the equation is written in matrix form, $Y = B\tilde{a}$ equality can be obtained. Here, Y , B and \tilde{a} represent the matrices.

$$B = \begin{bmatrix} -z^{(1)}(2) & \dots & 1 \\ \vdots & \ddots & \vdots \\ -z^{(1)}(n) & \dots & 1 \end{bmatrix} \tag{6}$$

$$Y = \begin{bmatrix} x^{(0)}(2) \\ \vdots \\ x^{(0)}(n) \end{bmatrix} \tag{7}$$

$$\tilde{a} = \begin{bmatrix} a \\ b \end{bmatrix} \tag{8}$$

In order to obtain the vector \tilde{a} , the following operations must be performed in order.

$$Y = B\tilde{a} \tag{9}$$

$$B^T Y = B^T B \tilde{a} \tag{10}$$

$$\tilde{a} = (B^T B)^{-1} B^T Y \tag{11}$$

Step-3: Obtaining the GE equation. The prediction model is obtained by solving the differential equation 12.

$$\frac{dx^{(1)}(k)}{dk} + ax^{(1)}(k) = b \tag{12}$$

$$\hat{x}^{(1)}(k + 1) = \left[x^{(1)}(0) - \frac{b}{a} \right] e^{-ak} + \frac{b}{a} \tag{13}$$

Since the original data is made into a cumulative series for the GM (1,1) model to work, in order to obtain the forecast results, a backward cumulative series should be created using equation 14.

$$\hat{x}^{(0)}(k + 1) = \hat{x}^{(1)}(k + 1) - \hat{x}^{(1)}(k) \tag{14}$$

Step-4: In forecasting time series, the high volatility of the series usually reduces the forecasting performance. This can be overcome by modifying the results or combining different techniques. In this study, the GM (1,1) model is combined with a Markov chain (He & Huang, 2005).

$$\mathcal{E}^{(0)}(k) = (x^{(0)}(k) - \hat{x}^{(0)}(k))/x^{(0)}(k), k=1,2,3,4,\dots,n ;$$

obtained from the GM (1,1) model. Let the sequence of errors be expressed as $(\mathcal{E}^{(0)} = (\mathcal{E}^{(0)}(1), \mathcal{E}^{(0)}(2), \mathcal{E}^{(0)}(3), \dots, \dots, \mathcal{E}^{(0)}(k))$. In this case, we can divide the errors from the prediction model into S different states, and this new process is a Markov process. The intervals for the states are determined by considering the relative error values.

$$S_{i-} = A_i, \quad S_{i+} = B_i, \tag{15}$$

Here, when it is expressed as S_{1i} and S_{2i} , any s state within these states can be expressed as $S_i = [S_{1i}, S_{2i}]$. In obtaining the transition probabilities matrix $P_{ij}(a)$, a indicates the number of steps, G_{ij} is probability of transition from state S_i to state S_j ; and G_i is the number of observations in the S_i state.

$$p_{ij}(a) = \frac{G_{ij}(a)}{G_i} \quad (i, j = 1, \dots, s) \tag{16}$$

a-step transition probability matrix is;

$$P_{ij}(a) = \begin{pmatrix} p_{11}(a) & \cdots & p_{1j}(a) \\ \vdots & \ddots & \vdots \\ p_{i1}(a) & \cdots & p_{ij}(a) \end{pmatrix} \quad (i, j = 1, \dots, s) \quad \sum_{i=1}^s p_{ij}(a) = 1 \tag{17}$$

The transition probabilities matrix is used to predict the state of the next observation. Suppose that the Markov chain under consideration is currently in state S_i . Then when the line i elements in matrix $P_{ij}(1)$ are examined, $\max_j (p_{ij}(1)) = p_{i3}(1)$ the equality is satisfied, the Markov chain is predicted to transition to state S_3 in the next step. Finally, the modified forecasting data can be calculated:

$$\hat{x}^{(0)}(k) = \hat{x}^{(0)}(k)[1 + 0.5(A_i + B_i)] \tag{18}$$

It is observed that the grey Markov chain model is frequently used in all fields in the literature. The grey Markov chain model has been used to forecast annual maximum water levels at hydrological stations (Dong et al., 2012), to forecast fire accidents (Mao & Sun, 2011), to forecast financial crises for an enterprise (Chen & Guo, 2011) and to forecast the need for electrical energy in China (He & Huang, 2005). Duan et al., (2017), used a grey Markov chain model enhanced with Taylor approximation for forecasting urban medical services demand in China. In their study, Hu et al. (2017), presented a novel grey prediction model combining Markov chain with functional-link net and applied it to foreign tourist forecasting. Wang et al. (2018), put forward a grey Markov forecasting model to predict mine gas emissions by combining grey system theory and Markov chain theory. Ye et al., (2018), presented a grey Markov prediction model based on background value optimization and a central point triangular whitenization weight function.

Jabeen et al. (2019) used grey Markov chain model (G-MCM) and showed the effectiveness of model in handling dynamic software reliability data. Musa’s failure datasets from various projects used to evaluate the prediction capability of G-MCM and compared with GM (1, 1) and modified Jelinski-Moranda reliability prediction model. The comparison showed that the G-MCM has better prediction results than other models and has adequate applicability in software reliability prediction.

Urrutia et al. (2019) developed a prediction model of energy demand of the Philippines by using a markov chain grey model (MCGM). Data were gathered and obtained from the Department of Energy that covers a total of 17 years starting from year 2000 to 2016. Three time series models, namely, grey Markov model, grey model with rolling mechanism, and singular spectrum analysis (SSA) was used by Kumar and Jain (2010) to forecast

the consumption of conventional energy in India. Grey-Markov model employed to forecast crude-petroleum consumption while grey model with rolling mechanism to forecast coal, electricity (in utilities) consumption and SSA to predict natural gas consumption.

Yu et al. (2015) and Zhang and Chen (2021) used the grey Markov chain model in tax forecasting. Jia et al. (2020), presented a study based on the grey Markov chain model for forecasting coal consumption in Gansu Province. Song et al. (2020), used grey model theory to perform load forecasting of medium and long term power system and the accuracy of the model in load forecasting is tested using the posterior difference method. Liu (2022), conducted an empirical analysis of the relationship between renewable energy consumption and economic growth based on the grey Markov model.

Results and Discussion

In this study, the Grey-Markov chain model is used to forecast the red meat production in Turkey in the coming years. The annual data from Turkstat in Table 1 will constitute the data set of the study. Data on cattle, buffalo, sheep and goat meat will be evaluated.

Table 2. Cattle Meat Production in Turkey Actual and Estimated Values

Year	Actual Values (Tons)	Estimated Values with G(1,1) Model (Tons)	Estimated Values with Grey-Markov Chain Model (Tons)
2012	790034,434	790034,43	788.973,2290
2013	798783,896	777186,04	795.240,1716
2014	815673,775	843843,38	821.973,8220
2015	862098,119	916217,77	869.957,9481
2016	956180,377	994799,53	944.572,1167
2017	1093840,645	1080121,06	1.105.212,4141
2018	1281234,266	1172760,40	1.257.641,1421
2019	1330169,278	1273345,20	1.334.215,5646
2020	1341445,521	1382556,91	1.346.725,7143
2021	1460719,267	1501135,43	1.462.231,0899
2022		1629884,16	1.547.591,3277
2023		1769675,34	1.723.811,3491
2024		1921456,07	1.824.441,7813
2025		2086254,67	2.032.186,0120
2026		2265187,63	2.206.481,6433
2027		2459467,24	2.395.726,1852

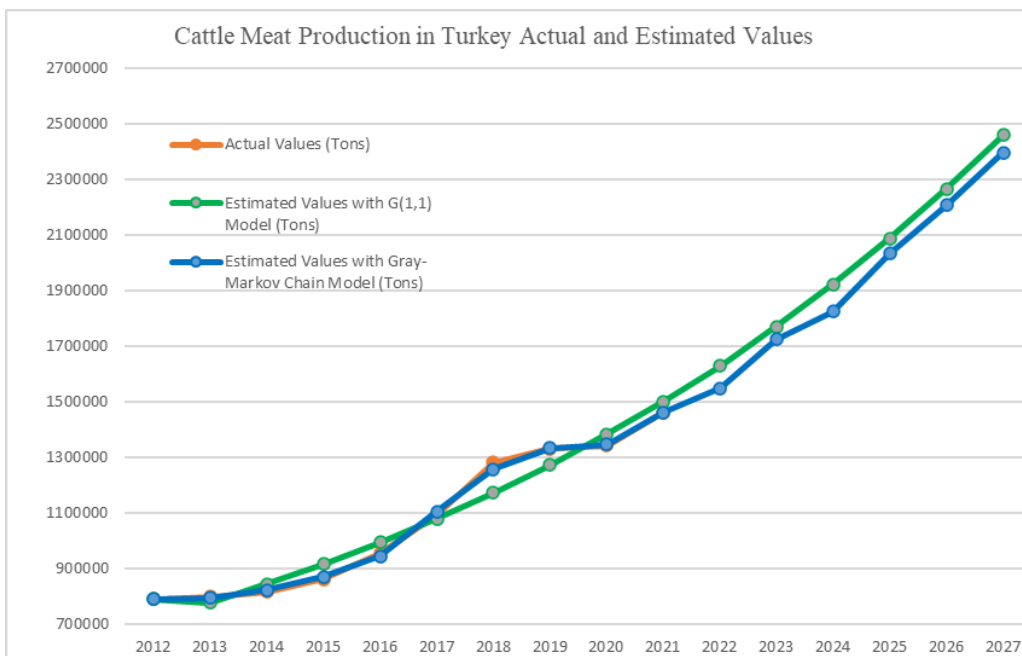


Figure 1. Cattle meat production in Turkey actual and estimated values graph

In this study, firstly, the data on cattle meat production was analyzed. The production levels for the coming years were first tried to be forecasted using the G(1,1) Model. Then, Grey-Markov chain model was used to improve the forecasting performance. Table 2 shows the results obtained for cattle meat production. Compared to the real data, the Grey-Markov chain model produced more realistic results. As can be seen in the graph in Figure 1, it is also seen visually that the prediction performance increases with the Grey-Markov model.

Secondly, data on buffalo meat production were analyzed. Production levels for the coming years are first tried to be forecasted using the G(1,1) Model. Then, the Grey-Markov chain model was used to improve the forecasting performance. Table 3 shows the results obtained for buffalo meat production. Compared to real data, the Grey-Markov chain model produced more realistic results. As can be seen in the graph in Figure 2, it can be seen visually that the forecasting performance improves with the Grey-Markov model for buffalo meat production forecasts.

Table 3. Buffalo Meat Production in Turkey Actual and Estimated Values

Year	Actual Values (Tons)	Estimated Values with G(1,1) Model (Tons)	Estimated Values with Grey-Markov Chain Model (Tons)
2012	4027,064	4027,06	4.019,0490
2013	4579,612	4030,23	4.443,4938
2014	5003,645	4497,88	4.959,0926
2015	5300,426	5019,79	5.359,6117
2016	5469,899	5602,26	5.395,9054
2017	5867,990	6252,31	5.804,1645
2018	6514,878	6977,80	6.477,6481
2019	7150,372	7787,46	7.229,2790
2020	8424,169	8691,08	8.370,9525
2021	10831,158	9699,54	10.694,1353
2022		10825,02	10.049,1169
2023		12081,10	11.215,1616
2024		13482,93	12.516,5077
2025		15047,41	13.968,8550
2026		16793,43	15.589,7247
2027		18742,05	17.398,6713

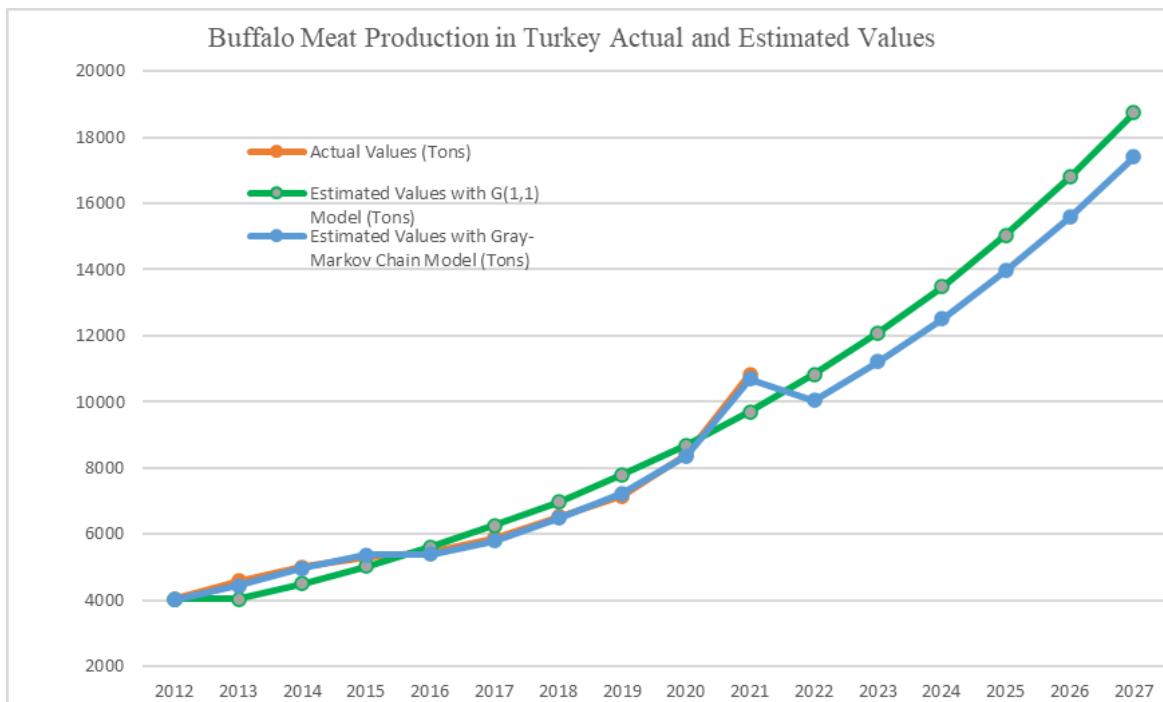


Figure 2. Buffalo meat production in Turkey actual and estimated values graph

Third, data on sheep meat production were analyzed. The production levels for future years were first studied with the G(1,1) Model and then the grey-Markov chain Model was used to improve the forecasting

performance. Table 4 shows the results obtained for sheep meat production. Compared to real data, the grey-Markov chain model produced more realistic results. As can be seen in the graph in Figure 3, it can be seen visually that the forecasting performance is improved with the grey-Markov chain model in the forecasts of sheep meat production.

Table 4. Sheep meat production in Turkey actual and estimated values

Year	Actual Values (Tons)	Estimated Values with G(1,1) Model (Tons)	Estimated Values with Grey-Markov Chain Model (Tons)
2012	220358,832	220358,83	222.474,8583
2013	236186,057	218926,73	232.145,6643
2014	238670,388	233572,72	235.815,6376
2015	249863,219	249198,52	251.591,4832
2016	266675,325	265869,67	268.422,7181
2017	262824,900	283656,10	264.774,7150
2018	291178,532	302632,43	290.171,4296
2019	316169,822	322878,25	317.781,1819
2020	345639,434	344478,51	347.786,4096
2021	385932,671	367523,80	389.715,1164
2022		392110,79	395.876,0934
2023		418342,64	422.359,8337
2024		446329,37	450.615,3115
2025		476188,39	480.761,0543
2026		508044,95	512.923,5191
2027		542032,68	547.237,6228

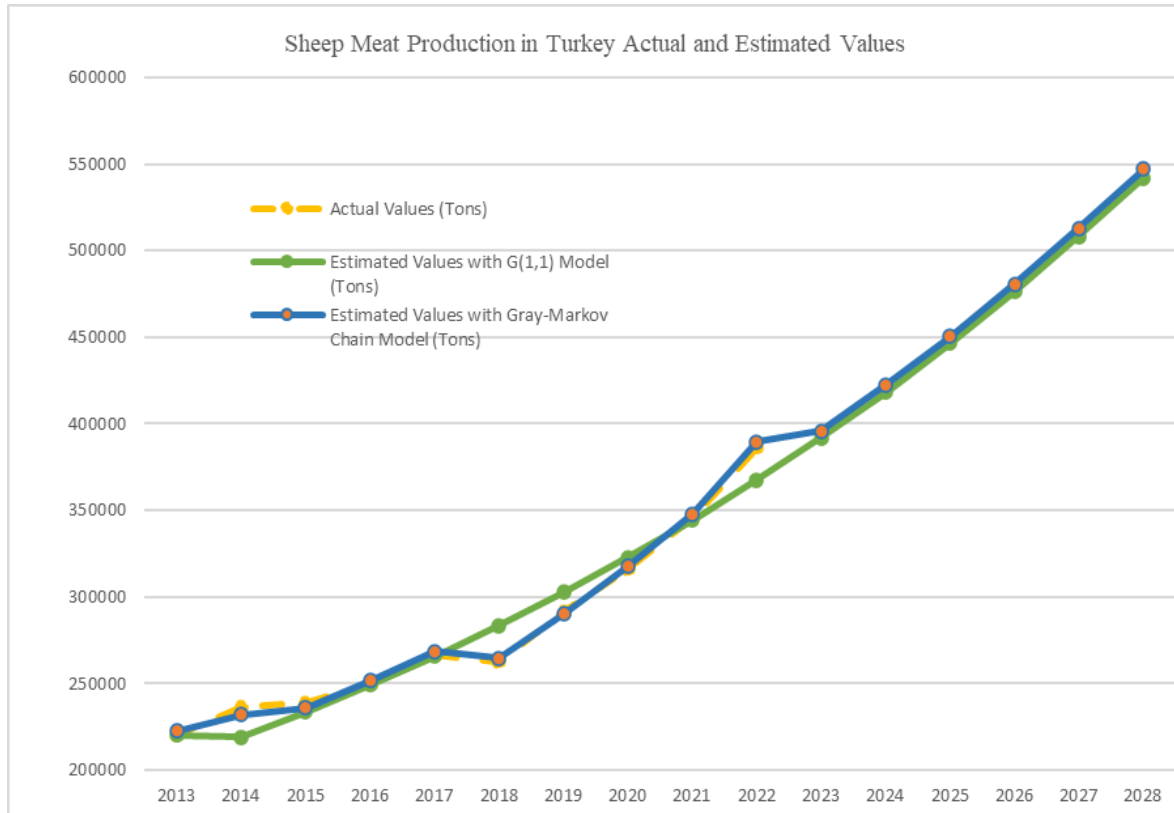


Figure 3. Sheep meat production in Turkey actual and estimated values graph

Finally, data on goat meat production were analyzed. The production levels for future years were first studied with the G(1,1) model and then the grey-Markov chain model was used to improve the forecasting performance. Looking at the actual production data, it is seen that there is not much fluctuation. For this reason, the data of the two methods are close to each other. Table 5 shows the results obtained for mutton production. In Figure 4, the data obtained are visually compared.

Table 5. Goat meat production in Turkey actual and estimated values

Year	Actual Values (Tons)	Estimated Values with G(1,1) Model (Tons)	Estimated Values with Grey-Markov Chain Model (Tons)
2012	53132,748	53132,75	53.285,9220
2013	59531,873	61750,86	59.803,4080
2014	63710,851	65276,85	63.967,1423
2015	69756,534	69004,17	69.994,8140
2016	75321,964	72944,33	74.828,4518
2017	77793,729	77109,47	78.216,4673
2018	82838,831	81512,43	82.682,6454
2019	87126,301	86166,81	87.403,8432
2020	90443,176	91086,96	90.304,4721
2021	94555,223	96288,04	94.356,1287
2022		101786,11	103.247,3773
2023		107598,12	109.142,8261
2024		113742,00	115.374,9063
2025		120236,69	121.962,8397
2026		127102,24	128.926,9457
2027		134359,80	136.288,7036

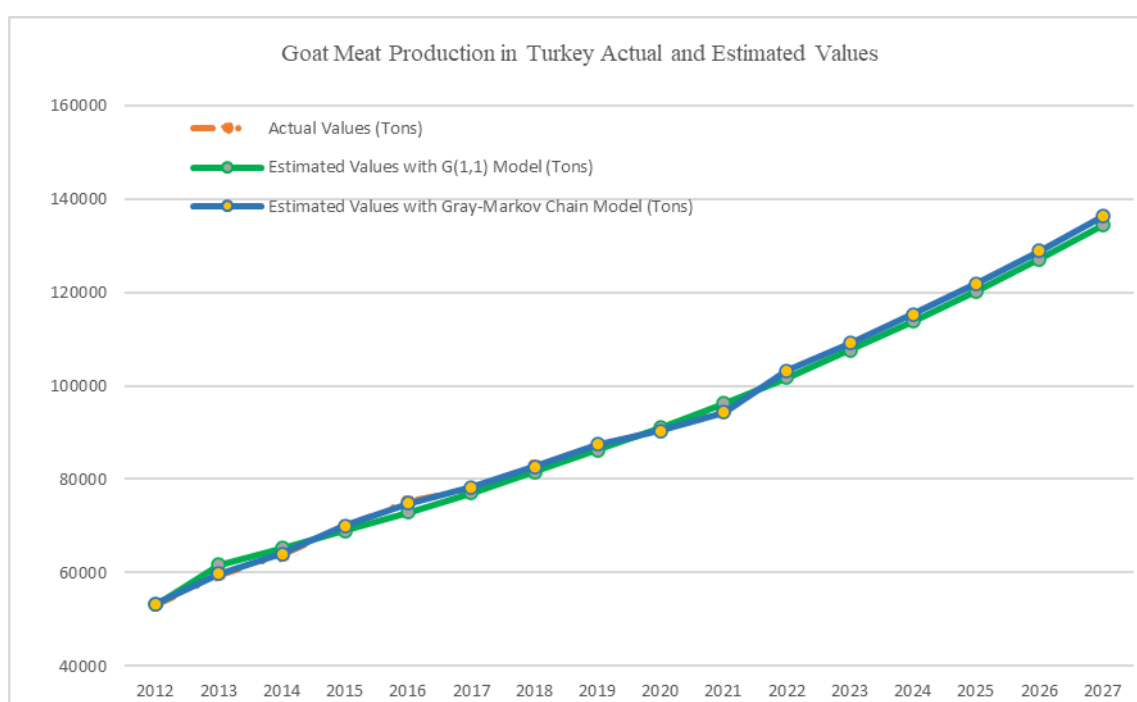


Figure 4. Goat meat production in Turkey actual and estimated values graph

Conclusion

Forecasting inherently involves error, which can be minimized. To do this, the data system needs to be properly analyzed and the appropriate method selected. In order to improve the prediction performance, methods can be combined with various methods. In this study, grey forecasting model and Markov chain model are combined to improve forecasting performance.

The continued import of livestock and red meat in Turkey reveals the necessity of policies that will bring structural solutions. In order to formulate policies, reliable forecasting data are needed. Therefore, this study may enable the formulation of such policies. In this study, data on cattle, buffalo, sheep and goat meat are evaluated and production amounts until 2027 are estimated. It is clear from the graphs that the grey-Markov chain method brings the forecasts closer to the real data and tries to mimic the system. According to the results, cattle meat production in the bovine group will increase from 1.460.719 tons to 2.395.726 tons; buffalo meat production will increase from 10.831 tons to 17.398 tons. In the ovine group, sheep meat production will

increase from 385.932 tons to 547.237 tons and goat meat production will increase from 94.555 tons to 136.288 tons.

Estimates show that production will increase in all four groups, and in future studies, this increase can be compared with the population and the amount of red meat production per capita can be calculated. The fact that the amount per capita is increasing is welcomed as positive. Implementation of policies that both increase the amount of production and reduce production costs will help to increase red meat production to the level of developed countries.

Scientific Ethics Declaration

The author declares that the scientific ethical and legal responsibility of this article published in EPSTEM journal belongs to the author.

Acknowledgements or Notes

* This article was presented as an oral presentation at the International Conference on Research in Engineering, Technology and Science (www.icrets.net) held in Budapest/Hungary on July 06-09, 2023.

References

- Chen, L. H., & Guo, T. Y. (2011). Forecasting financial crises for an enterprise by using the Grey Markov forecasting model. *Quality and Quantity*, 45(4), 911–922.
- Dong, S., Chi, K., Zhang, Q., & Zhang, X. (2012). The application of a Grey Markov model to forecasting annual maximum water levels at hydrological stations. *Journal of Ocean University of China*, 11(1), 13–17.
- Duan, J., Jiao, F., Zhang, Q., & Lin, Z. (2017). Predicting urban medical services demand in China: an improved Grey Markov Chain model by Taylor approximation. *International Journal of Environmental Research and Public Health*, 14(8), 883.
- Ertas, N. (2023). Uretim, tüketim ve pazarlama yonleriyle gecmisten gunumuze dunya kirmizi et piyasasında Turkiye'nin yeri. *Academic Social Resources Journal*, 8(46), 2191–2214.
- FAO. (2023, July 29). *FAOSTAT*. <https://www.fao.org/faostat/en/#data/QCL>
- He, Y., & Huang, M. (2005). A Grey-Markov forecasting model for the electric power requirement in China. *Lecture Notes in Computer Science (Including Subseries Lecture Notes in Artificial Intelligence and Lecture Notes in Bioinformatics)*, 3789, 574–582.
- Hu, Y. C., Jiang, P., Chiu, Y. J., & Tsai, J. F. (2017). A novel grey prediction model combining Markov Chain with functional-link net and its application to foreign tourist forecasting. *Information*, 8(4), 126. <https://doi.org/10.3390/info8040126>
- Jabeen, G., Yang, X., Luo, P., & Rahim, S. (2019). Application of Grey-Markov Chain model in software reliability prediction. *Journal of Computers*, 30(3), 14–27.
- Jia, Z. qian, Zhou, Z. fang, Zhang, H. jie, Li, B., & Zhang, Y. X. (2020). Forecast of coal consumption in Gansu Province based on Grey-Markov Chain model. *Energy*, 199, 117444.
- Ju-Long, D. (1982). Control problems of Grey systems. *Systems and Control Letters*, 1(5), 288–294.
- Kumar, U., & Jain, V. K. (2010). Time series models (Grey-Markov, Grey model with rolling mechanism and singular spectrum analysis) to forecast energy consumption in India. *Energy*, 35(4), 1709–1716.
- Liu, C. (2022). Empirical analysis of the relationship between renewable energy consumption and economic growth based on the Grey Markov model. *Journal of Mathematics*. Article ID 5679696 <https://doi.org/10.1155/2022/5679696>
- Liu, S., & Lin, Y. (2006). *Grey information: Theory and practical applications*. Springer: London.
- Mao, Z. L., & Sun, J. H. (2011). Application of Grey-Markov Model in forecasting fire accidents. *Procedia Engineering*, 11, 314–318.
- Saygın, O., & Demirbas, N. (2017). Turkiye'de kirmizi et sektorunun mevcut durumu ve cozum onerileri. *Hayvansal Uretim*, 58(1), 74–80.
- Song, F., Liu, J., Zhang, T., Guo, J., Tian, S., & Xiong, D. (2020). The Grey Forecasting Model for the medium- and long-term load forecasting. *Journal of Physics: Conference Series*, 1654(1).
- TURKSTAT. (2023, July 29). Red meat production statistics, 2020-2021. <https://data.tuik.gov.tr/Bulten/Index?p=Red-Meat-Production-Statistics-2020-2021-45671&dil=2>

- Urrutia, J. D., Antonil, F. E., Urrutia, J. D., & Antonil, F. E. (2019). A Markov Chain Grey model: a forecasting of the Philippines electric energy demand. *AIPC*, 2192(1). <https://doi.org/10.1063/1.5139183>
- Wang, Y., Yao, D., Lu, H., Wang, Y., Yao, D., & Lu, H. (2018). Mine gas emission prediction based on Grey Markov Prediction model. *Open Journal of Geology*, 8(10), 939–946.
- Ye, J., Dang, Y., & Li, B. (2018). Grey-Markov Prediction model based on background value optimization and central-point triangular whitenization weight function. *Communications in Nonlinear Science and Numerical Simulation*, 54, 320–330.
- Yu, Z., Yang, C., Zhang, Z., & Jiao, J. (2015). Error correction method based on data transformational GM(1,1) and application on tax forecasting. *Applied Soft Computing Journal*, 37, 554–560.
- Zhang, H., & Chen, Y. (2021). Analysis and application of Grey-Markov Chain model in tax forecasting. *Journal of Mathematics*, Article ID 9918411, <https://doi.org/10.1155/2021/9918411>

Author Information

Halil Sen

Burdur Mehmet Akif Ersoy University,

Burdur, Turkey

Contact e-mail: halilsen@mehmetakif.edu.tr

To cite this article:

Sen, H. (2023). Estimation of red meat production in Turkey according to the Grey-Markov Chain model. *The Eurasia Proceedings of Science, Technology, Engineering & Mathematics (EPSTEM)*, 23, 179-188.

The Eurasia Proceedings of Science, Technology, Engineering & Mathematics (EPSTEM), 2023

Volume 23, Pages 189-201

ICRETS 2023: International Conference on Research in Engineering, Technology and Science

Properties Experimental Analysis Bio-Monograde Engine Oil: Blended Mono-Grade Engine Oil SAE 40 with Fresh Coconut Oil

Othman Inayatullah

University of Technology Sarawak

Mohamad Faizi Zainulabidin

University of Technology Sarawak

Nor Asrina Ramlee

University of Technology Sarawak

Abstract: Mono-grade engine oil is the engine oil on the market and this engine oil has the lowest properties compared to multi-grade and synthetic engine oil. Mono-grade engine oil does not have viscosity index improving (VII) properties because it cannot be added polymer additive. Coconut oil is a vegetable oil produced from coconut milk that contains high fatty acids. The main objective of this study is to determine the effectiveness of fresh coconut oil being added to SAE 40 mono-grade engine oil by a different mixture composition. In this study, density, viscosity, kinematic viscosity, and viscosity index (VI) number is a measurement by using SVM 3000/G2 equipment. The engine oil used in this study is Petronas Mach 5 SAE 40 API SF mono-grade engine oil and fresh coconut oil is homemade manufactured. The results of the study show that the density and VI of the bland mono-grade engine oil increase but decrease in dynamic viscosity and kinematic viscosity concerning the percentage of fresh coconut oil mixture.

Keywords: Engine oil, Coconut oil, Mono-grade engine oil, Viscosity index, Percentage of fresh coconut oil

Introduction

Engine lubrication oil is a substance involving base oils upgraded with different added substances, especially anti-wear additives in addition to detergents, dispersants, and, multi-grades oils, and viscosity index improvers. It is utilized as the lubricant of an internal combustion engine. The fundamental function of engine lubrication oil is to reduce grating and wear on moving parts. It also neutralizes acids that start from the oxidation of the oil, improves the fixing of cylinder rings, and cools the engine by diverting heat from power strokes and moving parts. The classification of engine lubricating oils is done by the Society of Automotive Engineers (SAE). According to SAE, the engine lubricating oils can be divided into the multi-grade and the single-grade or known as mono-grade. Mono-grade engine oil does not have viscosity index improving (VII) properties because it cannot be added polymer additive. SAE J300 has established eleven viscosity grades, of which six are considered Winter-grades and given a W designation. The 11 viscosity grades are 0W, 5W, 10W, 15W, 20W, 25W, 20, 30, 40, 50, and 60 (Guan et al., 2008).

The quality of the engine oil is normally based on the viscosity of the grades of the engine oil other than a total base number (TBN) or total acid number (TAN). The quality of the engine oil is normally used to determine the life span of that engine oil. This was shown in the study done by Nordin Jamaludin et al. (2011) under the title relationship between engine oil viscosity with age and temperature and the study done by Othman Inayatullah et al. (2010) under the title development of acoustic emission viscosity model for measuring engine oil viscosity relationship with engine oil in-service age. Table 1 lists the limit for each grade of engine oil.

- This is an Open Access article distributed under the terms of the Creative Commons Attribution-Noncommercial 4.0 Unported License, permitting all non-commercial use, distribution, and reproduction in any medium, provided the original work is properly cited.

- Selection and peer-review under responsibility of the Organizing Committee of the Conference

© 2023 Published by ISRES Publishing: www.isres.org

Table 1. SAE J300 Viscosity table (2015)

Grade	Cold cranking CCS	Cold pumping MRV	Kinematic Viscosity @ 100°C		High-Temperature High Shear HTHS @150°C
Unit	cP @ T °C	cP @ T °C	cSt	cSt	cP
	Maximum	Minimum	Minimum	Maximum	Minimum
0W	6,200 @ -35	60,000 @ -40	3.8		
5W	6,600 @ -30	60,000 @ -35	3.8		
10W	7,000 @ -25	60,000 @ -30	4.1		
15W	7,000 @ -20	60,000 @ -25	5.6		
20W	9,500 @ -15	60,000 @ -20	5.6		
25W	13,000 @ -10	60,000 @ -15	9.3		
8			4.0	<6.1	1.7
12			5.0	<7.1	2.0
16			6.1	<8.2	2.3
20			5.6	<9.3	2.6
30			9.3	<12.5	2.9
40			12.5	<16.3	2.9 ^[1]
40			12.5	<16.3	3.7 ^[2]
50			16.3	<21.9	3.7
60			21.9	<26.1	3.7

Note: [1] 0W-40, 5W-40, and 10W-40. (For 0W, 5W, and 10W, the HTHS limit is 2.9 cSt.)
 [2] 15W-40, 20W-40, 25W-40 and 40. (For 15W, 20W, and SAE 40, the HTHS limit is 3.7 cSt instead of 2.9 cSt.)

Coconut oil belongs to a unique group of vegetable oils called lauric oils. The chemical composition of coconut oil is given in Table 2 with lauric acid shown with a bigger percentage of 47.9 % to 51.0 %. This percentage of lauric acid was obtained through a study conducted by N.H. Jayadas and K. Prabhakaran Nair in a study titled Coconut oil as a base oil for industrial lubricants evaluation and modification of thermal, oxidative, and low-temperature properties. By using thermo-gravimetric analysis (TGA) of coconut oil, sesame oil, sunflower oil, and commercial 2T oil to study thermal and oxidative degradation. Using molecular dynamics simulation software (Spartan 02, Wavefunction Inc.) the percentage values of different saturated and unsaturated fatty acid chains (lauric, oleic, linoleic) and pour point. The results of the study showed that coconut oil showed a lower weight gain, an indicator of oxidative stability, under an oxidative environment and the highest pour point among the vegetable oils tested. This can be attributed to the saturated nature of most of its fatty acid constituents (Jayadas & Nair, 2006).

Table 2. Fatty acid composition of crude coconut oil (Jayadas & Nair, 2006; Tangsathikulchai et al., 2004)

Component	Fraction A (wt%)	Fraction B (wt%)
Lauric	51.0	47.9
Myristic	18.5	19.7
Caprylic	9.5	6.4
Palmitic	7.5	9.7
Oleic	5.0	6.6
Capric	4.5	4.5
Stearic	3.0	2.7
Linoleic	1.0	1.6

Before that, in 2004, a study titled Temperature effect on the viscosities of palm oil and coconut oil blended with diesel oil was conducted by C. Tangsathikulchai et al., this study reported viscosity data determined through a bob-and-cup viscometer swirling, for crude palm oil and coconut oil blended with diesel oil at a temperature range of 20°C - 80°C and for different blend compositions. The output of this study is the reduction of viscosity with increasing liquid temperature. Table 3 shows the coconut oil properties as used in this study. (Tangsathikulchai et al., 2004).

In 2011, P. Nellamegam and S. Krishnaraj undergo an experiment on the viscosity of coconut oil in the temperature range of 30°C to 90°C by using the training pattern for associative neural networks (ASNN) and regression analysis (RA). The ASNN is a combination of memory-based and memory-less methods which offers an elegant approach to incorporating “on the fly” the user’s data (Igor & Tetko, 2002). It is an extension of the

committee of machines that goes beyond a simple or weighted average of different models. The viscosity of coconut oil is determined with a calibrated Cannon-Ubbelohde viscometer at an interval of 10°C. The measured value for the viscosity of coconut oil for different temperatures is given in Table 4 (Nellamegam & Krishnaraj, 2011).

Table 3. Coconut oil properties (Tangsathikulchai et al., 2004)

Oil Properties	ASTM Standard	Value
Density at 15.5°C	D 1298	0.915 g/cm ³
Flash point	D 93	200°C
Gross heating value	D 240	40,500 kJ/kg
Kinematic viscosity	D 445	
@ 40°C		27.4 mm ² /s
@ 100°C		6.91 mm ² /s
Reid vapor pressure @ 37.8°C	D 323	0.027 bar
Cetane index	D 976	35
Viscosity index	D 2270	230

Table 4. Viscosity of coconut oil against temperature (Nellamegam & Krishnaraj, 2011)

Temperature, °C	Viscosity, 10 ⁻¹ Pa.s
30	3.2937
40	2.7135
50	2.2217
60	1.4992
70	1.0740
80	0.8177
90	0.5500

In other words, coconut oil is consumable oil extracted from the kernel of mature coconuts gathered from the coconut palm. It has different applications due to its highly soaked fat substance; it is delayed to oxidize and, in this way, impervious to rancidification, enduring as long as a half year at 24°C without ruining. Fresh coconut oil has a high gelling temperature (22°C - 25°C), a high viscosity, and a pH of 7-8. In this study, the fresh coconut oil used is homemade.

Since mono-grade engine oil cannot be added with polymers for VII and the advantage of coconut oil with a constant alkali level, this research paper presents some findings on the blending of mono-grade engine oil with fresh coconut oil. The main objective of this study is to determine the effectiveness of fresh coconut oil being added to SAE 40 mono-grade engine oil by a different mixture composition. In this study, density, viscosity, kinematic viscosity, and viscosity index (VI) number is a measurement parameters. At this stage, focusing of these studies just only on the properties of blended mono-grade engine oil with coconut oil under fresh conditions in a laboratory experiment. To fulfill the main objective of this project, the secondary objectives need to be fulfilled. The secondary objectives include,

- a. Gain familiarity with a phenomenon or achieve new characteristics in the blend of SAE 40 engine oil with coconut oil.
- b. Portray the properties of the mixture of SAE 40 engine oil and coconut oil such as viscosity, kinematic viscosity, density against temperature, and different compositions of the mixture.
- c. Relationship between the composition of the mixture and viscosity index (VI).

Overall, contributions to knowledge in this study can be seen in the following aspects,

- a. Changes in the properties of mono-grade engine oil against the composition of coconut oil blended.
- b. Changes to the VI value of the composition percentage.
- c. Measurable ability at temperatures below 20°C.

Methodology

Specimen Materials

In this study, Petronas Mach 5 SAE 40 with API SF engine oil and fresh coconut oil were used as the specimen for testing. Petronas Mach 5 SAE 40 is a mono-grade crude oil-based engine oil. The product data sheet for Petronas Mach 5 SAE 40 API SF is shown in Table 5. For fresh coconut oil, the product data sheet is shown in

Table 2. However, the product data-sheet displayed in Tables 2 and 5 is only used as a reference because, in this study, the re-measurement of the properties of the two oils was carried out using the 2nd generation Stabinger Viscometer SVM 3000 (SVM 3000/G2) equipment.

Table 5. Petronas Mach 5 SAE 40 API SF product data sheet

Characteristic	Value
Density @ 15°C (kg/m ³)	897.1
Pour point (°C)	-6
Flashpoint (°C)	256
Kinematic viscosity (mm ² /s)	
@ 40°C	160.8
@ 100°C	15.2
Viscosity index	96

In the eyes view, the original non-blended mono-grade Petronas Mach 5 SAE 40 API SF engine oil showed darker brown compared to non-blended fresh coconut oil which is more yellowish. When more percentage composition of fresh coconut oil is blended with Petronas Mach 5 SAE 40 API SF, the color of the mixture changes slowly bright yellowish as shown in Figure 1.



Figure 1. View inspection (Change in engine oil color against the composition percentage)

Instrumentation

In this study, the 2nd generation Stabinger Viscometer 3000 (SVM 3000/G2) as shown in Figure 2 is used to measure the density, dynamic viscosity (viscosity), kinematic viscosity, and viscosity index of the blended Petronas Mach 5 SAE 40 API SF with fresh coconut oil. The SVM 3000/G2 is designed for measuring liquid substances such as lubricant oil, hydraulic oil, and petroleum oil and also includes food liquid based. The technical specification of SVM 3000/G2 is highlighted in Table 6.



Figure 2. The 2nd generation stabinger viscometer 3000 (SVM 3000/G2)

Table 6. Technical specification of SVM 3000/G2

Characteristics	
Test methods	ASTM D7042 - Dynamic viscosity and density ASTM D445 - Kinematic viscosity ASTM D4052 - Density ISO 23581 - Kinematic viscosity ISO 12185 - Density EN 16896 - Kinematic viscosity
Kinematic viscosity (mm ² /s)	
Minimum	0.2
Maximum	30,000
Density (g/cm ³)	
Minimum	0
Maximum	3
Temperature (°C)	
Minimum	-60
Maximum	135
Precision	
Viscosity repeatability (%)	0.1
Viscosity reproducibility (%)	0.35
Density repeatability (g/cm ³)	0.00005
Density reproducibility (g/cm ³)	0.0001
Cloud/freeze point repeatability (°C)	<0.5/<0.5
Cloud/freeze point reproducibility (°C)	<2.5/<1.3
Temperature repeatability (°C)	0.005
Temperature reproducibility (°C)	0.03 from +15 to +100 0.05 outside range
Performance	
Simple volume minimum/typical (mL)	1.5/1.5
Solvent volume minimum/typical (mL)	1.5/6.0
Maximum sample throughput (samples/hour)	33

Procedures

In this study, the mixture of the mono-grade Petronas Mach 5 SAE 40 API SF engine oil and fresh coconut oil specimen be bottled by the percentage of fresh coconut oil inside mono-grade Petronas Mach 5 SAE 40 API SF as tabled in Table 7.

Table 7. Composition of mono-grade Petronas Mach 5 SAE 40 API SF and fresh coconut oil

Mono-Grade Petronas Mach 5 SAE 40 API SF (%)	Fresh Coconut Oil (%)	Mono-Grade Petronas Mach 5 SAE 40 API SF (mL)	Fresh Coconut Oil (mL)
100	0	50	0
90	10	45	5
80	20	40	10
70	30	35	15
60	40	30	20
50	50	25	25
40	60	20	30
30	70	15	35
20	80	10	40
10	90	5	45
0	100	0	50

Each specimen needs to undergo 9 measurements due to temperature setting will be started from 20°C to 100°C with an interval of 10°C. The selection of the starting temperature of the measurement at a temperature of 20°C is due to the SVM 3000/G2 not being able to give a reading at 0°C when fresh coconut oil is 40% and above mixed with mono-grade Petronas Mach 5 SAE 40 API SF engine oil as shown in Table 8. This happen when the blended engine oil with coconut oil was frozen inside the test chamber which lead to the instrument being unable to generate output that was far from its standard range.

Table 8. Starting temperature for measuring properties of mono-grade Petronas Mach 5 SAE 40 API SF engine oil blended with fresh coconut oil.

Temperature (°C)	Density, ρ (g/cm ³)					
	Composition of Fresh Coconut Oil Blended in Mono-Grade Petronas Mach 5 SAE 40 API SF Engine Oil					
	0%	10%	20%	30%	40%	50%
0	0.9073	0.9096	0.9106	0.9146	x	x
6	0.9032	0.9055	0.9065	0.9105	0.9138	x
9	0.9012	0.9035	0.9045	0.9085	0.9118	0.9146
10	0.9005	0.9028	0.9038	0.9078	0.9111	0.9139
13	0.8985	0.9008	0.9018	0.9058	0.9091	0.9119
15	0.8971	0.8994	0.9004	0.9044	0.9077	0.9105
16	0.8964	0.8987	0.8997	0.9037	0.9070	0.9099

Temperature (°C)	Density, ρ (g/cm ³)				
	Composition of Fresh Coconut Oil Blended in Mono-Grade Petronas Mach 5 SAE 40 API SF Engine Oil				
	60%	70%	80%	90%	100%
0	x	x	x	x	x
6	x	x	x	x	x
9	x	x	x	x	x
10	x	x	x	x	x
13	0.9149	x	x	x	x
15	0.9136	0.9163	0.9188	0.9213	x
16	0.9129	0.9156	0.9181	0.9207	0.9238

Each measure required 40 mL of the specimen. For backup, the quantity of the specimen is set at 50 mL, this quantity is required for any re-measure or re-test if any error case. A magnetic stirrer lab stir mixer plate with 200 rpm was used for the blending process as shown in Figure 3.



Figure 3. Magnetic stirrer lab stir mixer plate

Results and Discussion

From the measurement of the mixture of mono-grade Petronas SAE 40 API SF with fresh coconut oil through SVM 3000/G2, readings of density, dynamic viscosity, and kinematic viscosity at each research temperature were obtained as shown in Tables 9, 10, and 11, respectively.

Table 9^(a). The density value (composition of fresh coconut oil from 0% to 50%)

Temperature (°C)	Density, ρ (g/cm ³)					
	Composition of Fresh Coconut Oil Blended in Mono-Grade Petronas SAE 40 API SF Engine Oil					
	0%	10%	20%	30%	40%	50%
20	0.8936	0.8960	0.8970	0.9010	0.9043	0.9072
30	0.8868	0.8891	0.8902	0.8942	0.8975	0.9004
40	0.8799	0.8822	0.8833	0.8873	0.8907	0.8936
50	0.8729	0.8753	0.8764	0.8805	0.8839	0.8868
60	0.8660	0.8684	0.8694	0.8736	0.8770	0.8799
70	0.8590	0.8614	0.8625	0.8666	0.8701	0.8730
80	0.8520	0.8544	0.8555	0.8597	0.8632	0.8661
90	0.8450	0.8474	0.8485	0.8527	0.8562	0.8592
100	0.8379	0.8404	0.8415	0.8457	0.8493	0.8523

Table 9^(b). The density value (composition of fresh coconut oil from 60% to 100%)

Temperature (°C)	Density, ρ (g/cm ³)				
	Composition of Fresh Coconut Oil Blended in Mono-Grade Petronas SAE 40 API SF Engine Oil				
	60%	70%	80%	90%	100%
20	0.9102	0.9129	0.9154	0.9180	0.9211
30	0.9035	0.9062	0.9087	0.9113	0.9145
40	0.8967	0.8994	0.9020	0.9046	0.9078
50	0.8899	0.8926	0.8952	0.8978	0.9011
60	0.8831	0.8858	0.8884	0.8911	0.8943
70	0.8762	0.8790	0.8816	0.8843	0.8875
80	0.8694	0.8721	0.8748	0.8775	0.8808
90	0.8625	0.8653	0.8679	0.8706	0.8739
100	0.8555	0.8584	0.8610	0.8638	0.8671

From Table 9^(a) and Table 9^(b), increasing the composition of fresh coconut oil, will increase the density at all set temperatures. Figure 4, shows more clearly the increase in the density of blended mono-grade Petronas Mach 5 SAE 40 API SF engine oil with fresh coconut oil at temperatures of 40°C and 100°C for each composition of fresh coconut oil. This proves that the mixture of fresh coconut oil in the engine oil can change the density value of the engine oil.

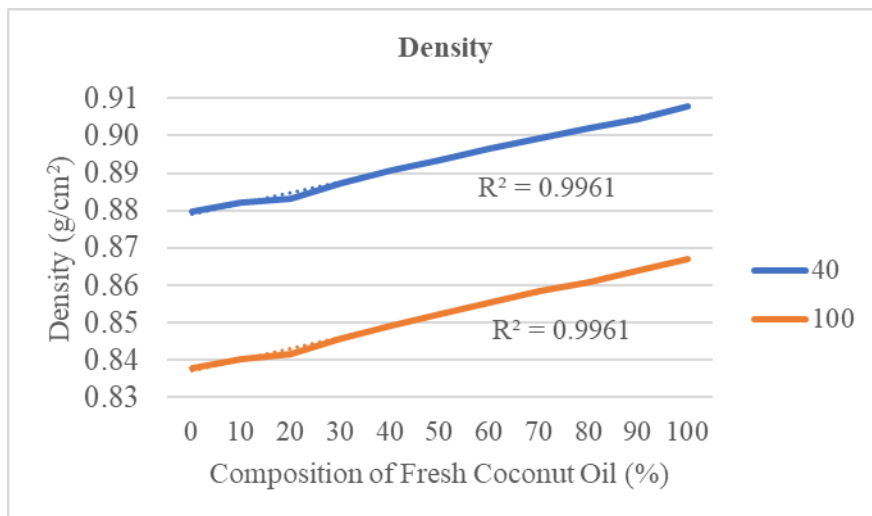


Figure 4. Increasing density of blended mono-grade Petronas Mach 5 SAE 40 API SF engine oil with fresh coconut oil at temperatures 40°C and 100°C.

This is due to fresh coconut oil is predominantly composed of saturated fatty acids (about 94%), with a good percentage (above 62%) of medium-chain fatty acids and it has been shown the density of fresh coconut oil is higher than mono-grade Petronas Mach 5 SAE 40 API SF engine oil. This is clearly shown in Table 9(a), where

0% of the composition is referred to as 100% of mono-grade Petronas Mach 5 SAE 40 API SF engine oil, and in Table 9(b), 100% of the composition is referred to 100% of fresh coconut oil as shown in Figure 5.

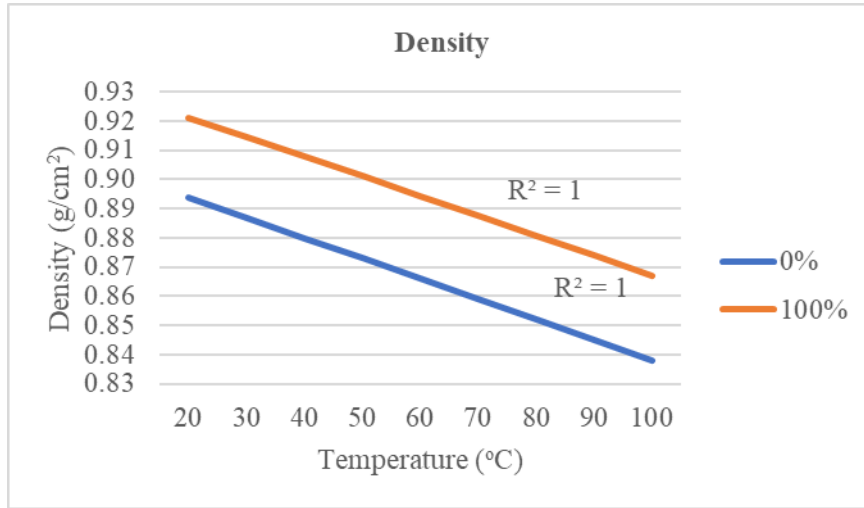


Figure 5. Density for 100% mono-grade Petronas Mach 5 SAE 40 API SF (0% composition) and 100% fresh coconut oil (100% composition)

Tables 10^(a) and 10^(b), display the results of dynamic viscosity measurements, also known as absolute viscosity. It is clearly shown increasing the composition of fresh coconut oil will reduce the dynamic viscosity of the blended mono-grade Petronas Mach 5 SAE 40 API SF engine oil as shown in Figure 6. Figure 6, also shows the range of differences in dynamic viscosity reading reduction against the percentage of fresh coconut oil composition narrows at high temperatures. The best comparison is the dynamic viscosity reading at 40°C and 100°C. It is the opposite of the output of density as shown in Tables 9^(a) and 9^(b).

Table 10^(a). The dynamic viscosity value (composition of fresh coconut oil from 0% to 50%)

Temperature (°C)	Dynamic Viscosity, μ (mPa.s)					
	Composition of Fresh Coconut Oil Blended in Mono-Grade Petronas SAE 40 API SF Engine Oil (%)					
	0	10	20	30	40	50
20	533.964	490.643	446.385	403.371	359.678	315.517
30	262.044	241.691	220.930	200.769	180.278	159.560
40	141.488	131.039	120.370	110.034	99.533	88.898
50	82.720	76.952	71.045	65.346	59.544	53.665
60	51.700	48.296	44.799	41.447	38.025	34.556
70	34.169	32.028	29.830	27.722	25.575	23.394
80	23.675	22.290	20.866	19.508	18.121	16.711
90	17.072	16.155	15.208	14.311	13.394	12.461
100	12.736	12.084	11.410	10.772	10.121	9.458

Table 10^(b). The dynamic viscosity value (composition of fresh coconut oil from 60% to 100%)

Temperature (°C)	Dynamic Viscosity, μ (mPa.s)				
	Composition of Fresh Coconut Oil Blended in Mono-Grade Petronas SAE 40 API SF Engine Oil (%)				
	60	70	80	90	100
20	271.096	226.301	181.197	135.857	90.307
30	138.736	117.713	96.541	75.259	53.889
40	78.210	67.416	56.549	45.618	34.647
50	47.756	41.787	35.777	29.731	23.667
60	31.074	27.550	24.002	20.434	16.854
70	21.205	18.990	16.758	14.513	12.262
80	15.298	13.864	12.421	10.969	9.514
90	11.526	10.577	9.619	8.656	7.693
100	8.791	8.116	7.434	6.749	6.064

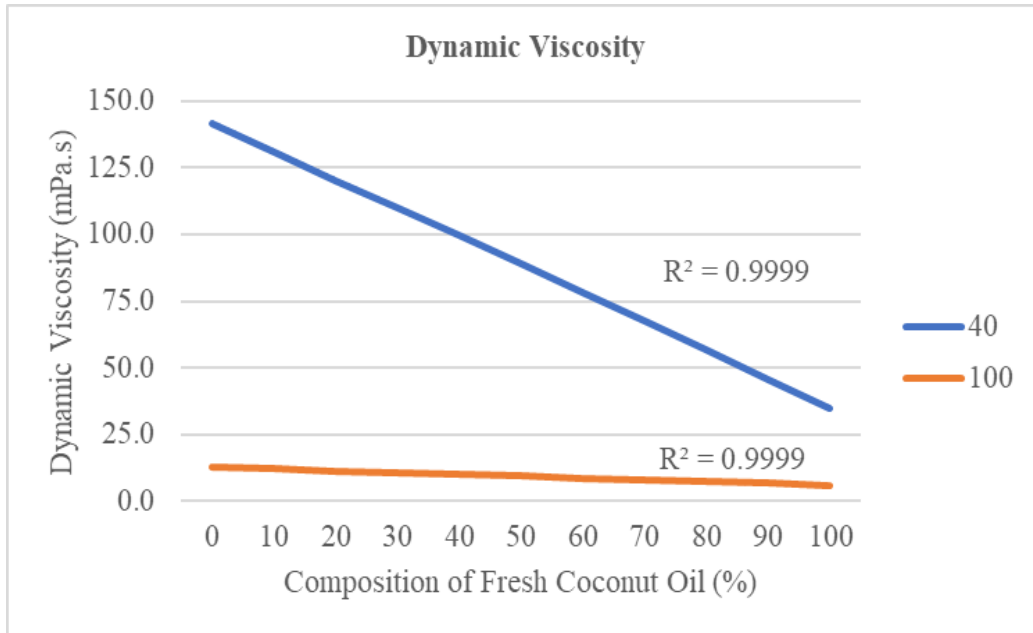


Figure 6. Decreasing dynamic viscosity of blended mono-grade Petronas Mach 5 SAE 40 API SF engine oil with fresh coconut oil at temperatures 40°C and 100°C.

The dynamic viscosity measurement results obtained in this study are on the right track, which is by referring to the results of the P. Nellamegam & S. Krishnaraj, 2011 study stated in Table 4. Even the results of the study also prove that the dynamic viscosity of Petronas mono-grade Mach 5 SAE 40 API SF is higher than the dynamic viscosity of fresh coconut oil as shown in Figure 7. That addition of fresh coconut oil into mono-grade Petronas Mach 5 SAE 40 API SF engine oil, will reduce the dynamic viscosity of that engine oil.

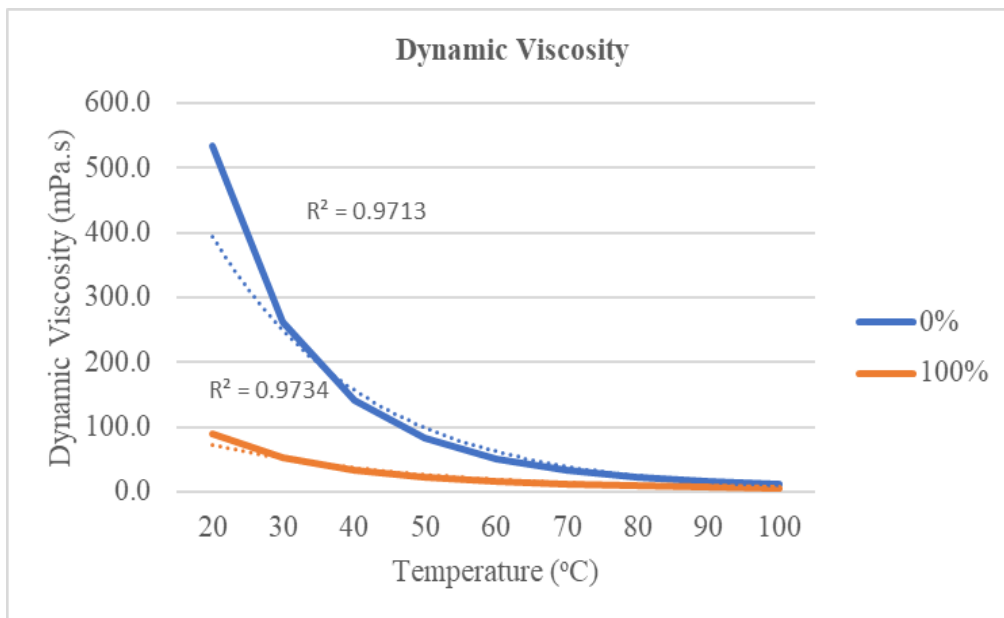


Figure 7. Dynamic viscosity for 100% mono-grade Petronas Mach 5 SAE 40 API SF (0% composition) and 100% fresh coconut oil (100% composition)

In the context of kinematic viscosity, typically the pattern of the SVM 3000/G2 output for this study, looks similar to dynamic viscosity. Tables 11^(a) and 11^(b) display the measurement results of kinematic viscosity and viscosity index. In general, the viscosity index is obtained from 2 kinematic viscosity readings at different temperatures. The first reading is at a temperature of 40°C and the second reading is at a temperature of 100°C. By using the VI calculator provided by Anton Paar who is the manufacturer of the SVM 3000/G2, it simplifies the calculation of the VI. The result of the VI value obtained from the Anton Paar calculator is a result based on the ASTM D2270 standard and ISO 2909.

Table 11^(a). The kinematic viscosity and viscosity index value (composition of fresh coconut oil from 0% to 50%)

Temperature (°C)	Kinematic Viscosity, ν (mm ² /s)					
	Composition of Fresh Coconut Oil Blended in Mono-Grade Petronas SAE 40 API SF Engine Oil (%)					
	0	10	20	30	40	50
20	597.542	547.592	497.642	447.692	397.742	347.793
30	295.494	271.837	248.181	224.524	200.867	177.211
40	160.800	148.537	136.273	124.010	111.746	99.483
50	94.765	87.915	81.065	74.215	67.365	60.515
60	59.700	55.615	51.529	47.444	43.358	39.273
70	39.778	37.182	34.586	31.989	29.393	26.797
80	27.787	26.089	24.390	22.692	20.993	19.295
90	20.204	19.064	17.924	16.784	15.644	14.504
100	15.200	14.379	13.559	12.738	11.917	11.097
Viscosity Index (VI)						
	94.6	94.2	94.1	94.2	94.8	96.2

Table 11^(b). The kinematic viscosity and viscosity index value (composition of fresh coconut oil from 60% to 100%)

Temperature (°C)	Kinematic Viscosity, ν (mm ² /s)				
	Composition of Fresh Coconut Oil Blended in Mono-Grade Petronas SAE 40 API SF Engine Oil (%)				
	60	70	80	90	100
20	297.843	247.893	197.943	147.993	98.043
30	153.554	129.897	106.240	82.584	58.927
40	87.220	74.956	62.693	50.429	38.166
50	53.665	46.815	39.965	33.115	26.265
60	35.188	31.102	27.017	22.931	18.846
70	24.201	21.605	19.008	16.412	13.816
80	17.596	15.898	14.199	12.501	10.802
90	13.363	12.223	11.083	9.943	8.803
100	10.276	9.455	8.634	7.814	6.993
Viscosity Index (VI)					
	98.5	102.7	110.0	122.0	146.1

Tables 11^(a) and 11^(b), display the results of kinematic viscosity and viscosity index (VI) measurements. It is clearly shown increasing the composition of fresh coconut oil will reduce the kinematic viscosity of the blended mono-grade Petronas Mach 5 SAE 40 API SF engine oil as shown in Figure 8. For kinematic viscosity, it is directly proportional to dynamic viscosity.

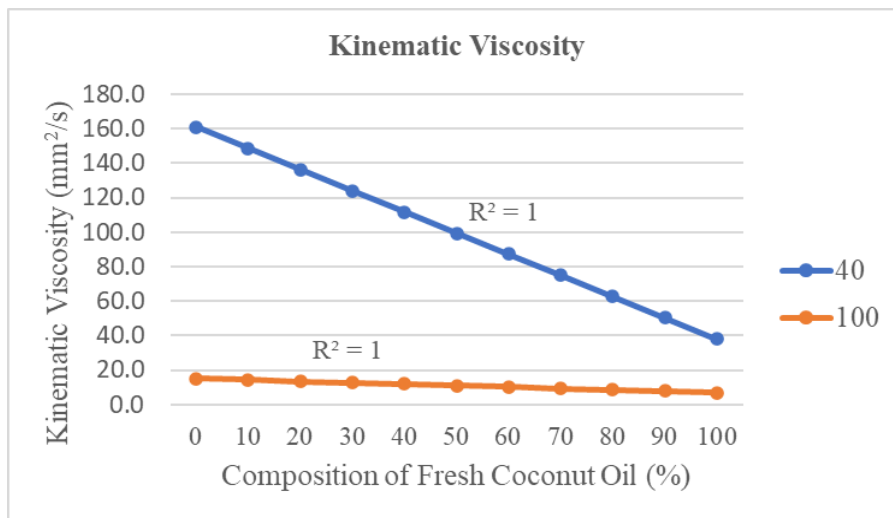


Figure 8. Decreasing kinematic viscosity of blended mono-grade Petronas Mach 5 SAE 40 API SF engine oil with fresh coconut oil at temperatures 40°C and 100°C

Figure 8, also shows the range of differences in kinematic viscosity reading reduction against the percentage of fresh coconut oil composition narrows at high temperatures. The best comparison is the kinematic viscosity reading at 40°C and 100°C. It is similar to the output of dynamics viscosity as shown in Tables 10(a) and 10(b). This similarity between dynamic viscosity and kinematic viscosity can refer to the value of R^2 . For dynamic viscosity, R^2 for 40°C is 0.9845 and for 100°C is 0.9893. For kinematic viscosity, R^2 for 40°C and 100°C is 1.0 and for dynamic viscosity for 40°C is 0.9713 and for 100°C is 0.9734.

The kinematic viscosity measurement results obtained in this study are on the right track, which is by referring back to Tables 3 and 5. Even the results of the study also prove that the kinematic viscosity of Petronas mono-grade Mach 5 SAE 40 API SF is higher than the kinematic viscosity of fresh coconut oil as shown in Figure 9. That addition of fresh coconut oil into mono-grade Petronas Mach 5 SAE 40 API SF engine oil, will reduce the kinematic viscosity of that engine oil.

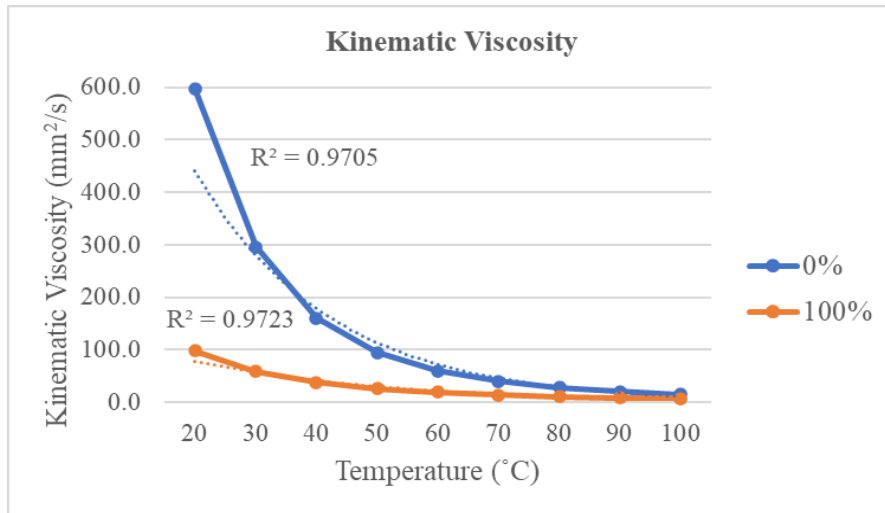


Figure 9. Kinematic viscosity for 100% mono-grade Petronas Mach 5 SAE 40 API SF (0% composition) and 100% fresh coconut oil (100% composition)

The last in this study is the discovery of the viscosity index. This viscosity index is important to classify lubricating oil, especially cooking oil. To the viscosity index data released by Anton Paar, mineral oil-based lubricating oil, its VI is between 95 to 105, multi-grade oil between 140 to 200, PAO oil between 135 to 160, and vegetable oil between 195 to 210. However, Petronas Mach 5 mono-grade mixture SAE 40 API SF engine oil with fresh coconut oil show composition of the fresh coconut oil from 0% to 70%, and blended SAE 40 engine oil is under mineral oil-based lubricating. Other than that, it is under multi-grade oil. This is as shown in Tables 11^(a) and 11^(b) with Figure 10.

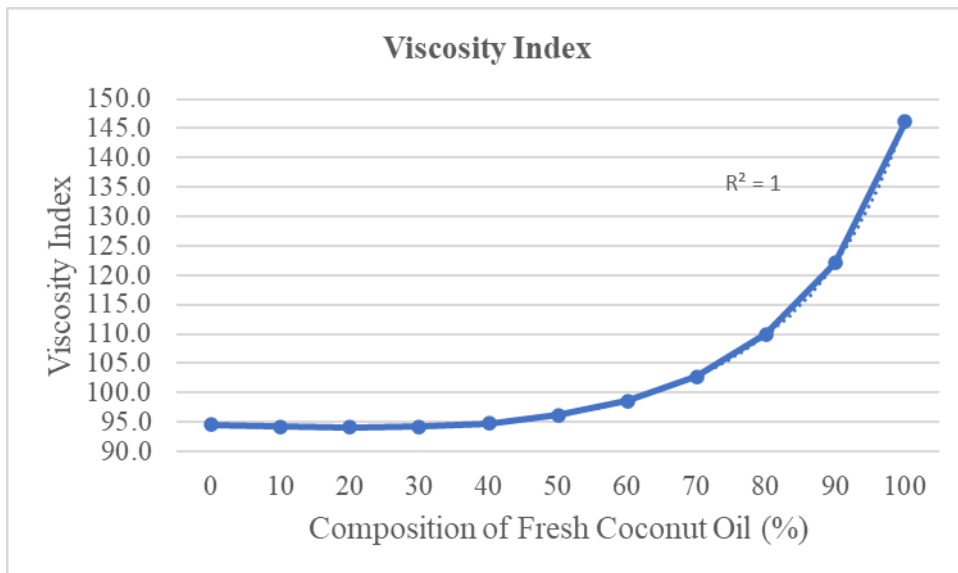


Figure 10. Viscosity index (VI) for each composition of fresh coconut oil

It can be said that at the composition of fresh coconut oil 0% to 70%, blended mono-grade Petronas Mach 5 SAE 40 API SF is still a mineral base lubricant. At a composition of 80% fresh coconut oil, this oil mixture seems to be fully influenced by fresh coconut oil and can be categorized as semi-synthetic base oil. However, this statement still requires continued research involving other vegetable oils such as palm oil and olive oil to see if the VI mixture of palm oil and olive oil is similar to the results of this study.

Conclusion

From this study, in general, the mixture of fresh coconut oil in mono-grade engine oil has changed the properties of the engine oil in terms of density, dynamic viscosity, kinematic viscosity, and viscosity index. By looking at the viscosity index, the properties of mono-grade engine oil have changed into the properties of multi-grade engine oil as a result of mixing mono-grade engine oil with fresh coconut oil. The viscosity index obtained from this study can be divided into 2 regions, namely the mono-grade engine oil region with a mixture of 0% to 70% coconut oil, the multi-grade region with a mixture of 80% to 100% coconut oil, and it looks as semi-synthetic oil. Even so, increasing the percentage of fresh coconut oil causes an increase in the melting temperature of the blend of mono-grade engine oil with fresh coconut oil. This is due to the fatty acids found in fresh coconut oil. This affects the usability of this oil mixture in the internal combustion engine.

Recommendations

This study can be used as a catalyst for further research proposals such as

- a. Study blends of mono-grade engine oil with other vegetable oils such as palm oil and olive oil.
- b. Further studies on the properties of engine oil that are not specified in this study such as temperature at the pour point, the temperature at the flash point, total base number, and total acid number.
- c. Conducting a study on the usability of a blend of mono-grade engine oil with vegetable oil in an internal combustion engine to see the real performance of the new blend of engine oil.

Scientific Ethics Declaration

The authors declare that the scientific ethical and legal responsibility of this article published in EPSTEM journal belongs to the authors.

Acknowledgements

* This article was presented as an oral presentation at the International Conference on Research in Engineering, Technology and Science (www.icrets.net) held in Budapest/Hungary on July 06-09, 2023.

*This study would not have been possible without the financial support of the University of Technology Sarawak under a research grant UTS/RESEARCH/4/2022/02.

References

- Guan, L., Feng, X. L., & Xiong, G. (2008). Engine lubricating oil classification by SAE grade and source based on dielectric spectroscopy data. *Analytica Chimica Acta*, 628, 117-120.
- Inayatullah, O., Jamaludin, N., Nor, M. J. M., Ali, Y., & Mat, F. (2010). Development of acoustic emission viscosity model for measuring engine oil viscosity relationship with engine oil in-service age. *Tribology Online*, 5(6), 255-261.
- Jamaludin, N., Inayatullah, O., Nor, M. J. M., & Mat, F. (2011). Relationship between engine oil viscosity with age and temperature. *Sains Malaysiana*, 40(5), 509-513.
- Jayadas, N. H., & Nair, K. P. (2006). Coconut oil as a base oil for industrial lubricants-evaluation and modification of thermal, oxidative, and low-temperature properties. *Tribology International*, 39, 873-878.

- Nellamegam, P., & Krishnaraj, S. (2011). Estimation of liquid viscosities of oils using associative neural networks. *Indian Journal of Chemical Technology*, 18, 463-468.
- Tangsathitkulchai, C., Sittichaitaweekul, Y., & Tangsathitkulchai, M. (2004). Temperature effect on the viscosities of palm oil and coconut oil blended with diesel oil. *Journal of the American Oil Chemists' Society*, 81, 401-405.
- Tetko, I. V. (2002) Neural network studies: Introduction to associative neural networks. *Journal of Chemical Information and Computer Science*, 42, 717-728.

Author Information

Othman Inayatullah

University of Technology Sarawak
No 1 Jalan Universiti 96000 Sibul Sarawak Malaysia
Contact e-mail: drothman@uts.edu.my

Mohamad Faizi ZAINULABIDIN

University of Technology Sarawak
No 1 Jalan Universiti 96000 Sibul Sarawak Malaysia

Nor Asrina Ramlee

University of Technology Sarawak
No 1 Jalan Universiti 96000 Sibul Sarawak Malaysia

To cite this article:

Inayatullah, O. Zainulabidin M.F. & Ramlee, N.A. (2023). Properties experimental analysis bio-monograde engine oil: part 1 - blended mono-grade engine oil sae 40 with fresh coconut oil. *The Eurasia Proceedings of Science, Technology, Engineering & Mathematics (EPSTEM)*, 23, 189-201.

The Eurasia Proceedings of Science, Technology, Engineering & Mathematics (EPSTEM), 2023

Volume 23, Pages 202-208

ICRETS 2023: International Conference on Research in Engineering, Technology and Science

Blockchain Security-Efficiency Analysis based on DEA-SBM Model

Thi Minh Nhut Vo

National Kaohsiung University of Science and Technology

Chia-Nan Wang

National Kaohsiung University of Science and Technology

Fu-Chiang Yang

National Kaohsiung University of Science and Technology

Van Thanh Tien Nguyen

Industrial University of Ho Chi Minh City

Abstract: It is estimated that by 2023 the security market will reach a value of \$1.4 billion. This growth is primarily driven by the increasing use of technology in sectors like finance, healthcare and logistics. As more companies adopt technology there is a growing need to protect their data from hacking and other malicious activities. The security of the network plays a role in ensuring the implementation and adoption of technology. Given the rise in cyberattacks and data breaches it is expected that the importance of security will continue to grow in the coming years. In this study we will explore some companies that specialize in providing security solutions. Our analysis will be based on three factors and two desired outcomes. The selected companies include Hacken, Quantstamp, OpenZeppelin, Trail of Bits, ConsenSys, Certik, LeastAuthority, PWC Switzerland, Slowmist and Runtime Verification. The purpose of this research paper is to assess the effectiveness of the security industry for decision makers, experts and government entities. By gaining insights into this sector and enhancing network security measures for implementations, across industries.

Keywords: Blockchain security, Efficiency analysis, DEA-SBM model, Cybersecurity companies, Network security.

Introduction

The market, for technology has seen growth in recent years and is projected to reach a value of \$1.4 billion by 2023. The widespread adoption of technology across industries like finance, healthcare and logistics has contributed to its rising popularity. However companies involved in blockchain face challenges in safeguarding their data against hacking and other criminal activities.

In this study, our focus lies on examining the ten firms in the market for their expertise in ensuring secure blockchain systems. These firms include Hacken, Quantstamp, OpenZeppelin, Trail of Bits, ConsenSys, Certik, LeastAuthority, PWC Switzerland, Slowmist and Runtime Verification. Through our research findings we aim to guide policymakers, experts and governments in enhancing security measures within the network.

To determine the firms within the blockchain security landscape our selection criteria consider factors such as market capitalization revenue generation and reputation through analyzing variables like employee count R&D expenditure and marketing costs as input metrics and revenue generation, profitability and market share, as output metrics we assess these companies effectiveness.

- This is an Open Access article distributed under the terms of the Creative Commons Attribution-Noncommercial 4.0 Unported License, permitting all non-commercial use, distribution, and reproduction in any medium, provided the original work is properly cited.

- Selection and peer-review under responsibility of the Organizing Committee of the Conference

© 2023 Published by ISRES Publishing: www.isres.org

The DEA SBM approach is used to assess the effectiveness of companies operating in the security sector. Through data analysis we gain insights, into the performance of the security industry highlighting both businesses and areas that require improvement. This information can be invaluable for decision makers, professionals and governments when making investment decisions implementing regulations and providing industry support. Furthermore by deepening our understanding of the security challenges faced by companies this research contributes to the adoption and implementation of technology across various industries. We strive to enhance network security and integrity within the blockchain ecosystem. The study identifies performing businesses in this field while employing DEA SBM techniques to evaluate their effectiveness. The findings from our research will drive industry growth. Facilitate utilization of blockchain technology, across multiple sectors.

Literature Review

Creating access control policies that can be customized to a degree along, with implementing a mechanism to prevent tampering or violation of rules, within the IoT platform will undoubtedly play a crucial role in the widespread adoption of IoT based solutions. A. Rizzardi et. AL. suggest incorporating a permissioned blockchain into a distributed middleware layer that's honest but not trusted (Rizzardi et al., 2022). The goal is to ensure resource access management, for all parties. In their study, Li et. Al. (2022) suggest an approach called PDGNN (Phishing Detection Graph Neural Network) to counteract phishing attacks. However the computational demands and storage needs associated with this framework also present an obstacle when it comes to spreading messages (Li, Xie, Xu, Zhou, & Xuan, 2022) . Vishwakarma et. al. (2022) have proposed the introduction of a security protocol called LBSV. This lightweight blockchain based solution aims to address the challenges related to secure communication and storage in the context of SDN enabled IoV (Vishwakarma, Nahar, & Das, 2022). In their study (Zur et. Al., 2022) researchers proposed a model that incorporates transaction fees as variable block rewards making it more realistic (Bar-Zur, Abu-Hanna, Eyal, & Tamar, 2022). They introduced "Proof of Work" (PoUW) based on the concept of Proof of Work (PoW) where the resources wasted in PoW are utilized for calculations. Another interesting approach called "Proof of Learning" (PoLe) was suggested by (Zhang et. al., 2022) which utilizes the wasted resources to train machine learning models (B. Zhang, Zhang, & Sun, 2022). With the advancements, in intelligence we now have automated tools that leverage learning and machine learning algorithms to make predictions about cancer. Nasir et. Al. Conducted a study where they introduced a model that combines the Internet of Medical Things (IoMT) transfer learning techniques and deep learning algorithms to identify early stage kidney cancer (Nasir et al., 2022). To ensure the security of patients data this model incorporates clouds based on technology and transfer learning trained models. In their study, Aljumaie et. al., 2022 propose a version of the LEACH PRO protocol that incorporates security techniques to safeguard Wireless Sensor Networks (WSNs) (Aljumaie & Alhakami, 2022).

Zhao et. al., 2022 conducted a study that combines the efficiency slack based measure (SBM) model and the window analysis model to assess the CEE (customer experience excellence) in the freight transport industry across 31 Chinese provinces from 2008, to 2019 (Zhao et al., 2022). Meanwhile Zhang et. al., 2022 aimed to understand the factors influencing residents participation in sports consumption and provide insights, for enterprises to develop marketing strategies. They developed an integrated framework that focuses on participation sports service products and takes into account the preferences and demands of participation sports consumers (T. Zhang, Wang, & neuroscience, 2022). In Huang's study conducted in 2022 a model based on factor analysis was employed to assess and rank the sports abilities of provinces, in China (Huang, 2022). This industry faces a challenge due, to the scarcity of workers to fill roles, which negatively impacts its potential for sustainable growth. Therefore the researchers chose a approach to examine the textual data provided by experts.

Methodology

The Research Frameworks

Selection of the Ten Most Successful Blockchain Security Companies

The process of selecting companies in the security industry involved considering important factors to ensure a well rounded and diverse representation of successful players, in the field. These factors included both quantitative aspects with the goal of identifying companies that have demonstrated their expertise built a reputation, in the market and have a history of innovation (C.-N. Wang, Yang, Vo, & Nguyen, 2023; C. N. Wang, Yang, Vo, & Nguyen, 2022).

In Table 1 you will find a list of Decision Making Units (DMUs) that consist of organizations operating in the blockchain security market. Each DMU is identified by a code. Accompanied by the name of the corresponding firm. The table encompasses companies, each, with its distinct role and impact, on the field of blockchain security.

Table 1. List of DMUs

DMU	Company Name
B1	Hacken
B2	Quantstamp
B3	OpenZeppelin
B4	Trail of Bits
B5	ConsenSys
B6	Certik
B7	LeastAuthority
B8	PWC Switzerland
B9	Slowmist
B10	Runtime Verification

Selection of Input and Output Variables

When evaluating companies, in the security industry it is crucial to select the input and output variables. These variables help us understand how efficient and successful these companies are. We have chosen variables for this assessment;

Input Variables:

- **Investment in Research and Development (R&D):** This reflects how much a company invests in innovation and technology development. Companies that allocate resources to R&D are likely to be focused on staying in blockchain security advancements and offering cutting edge solutions.
- **Employee Expertise:** The qualifications and expertise of a company's workforce play a role as an input variable. Skilled employees contribute to the company's efficiency and their ability to deliver top notch security services.
- **Security Partnerships:** Collaborations with organizations to enhance security capabilities demonstrate a company's efforts to leverage expertise and resources. Strategic partnerships can lead to improved efficiency and a wider range of security solutions.

Output Variables:

- **Market Share:** This refers to the portion of the market that a company has been able to capture. On the hand Customer Satisfaction is an indicator that measures the level of satisfaction among clients or customers.
- **Customer Satisfaction:** A company's competitiveness and ability to attract and retain clients can be gauged by its market share.

When it comes to measuring the level of satisfaction clients experience with a companys services customer satisfaction becomes a factor. High customer satisfaction indicates that the company meets client expectations delivers value and fosters customer loyalty and repeat business. The choice of input and output variables, in evaluating efficiency in the blockchain security industry aligns with goals. Input variables such as R&D expenditure and employee expertise reflect the companys commitment to innovation and expertise. On the hand market share and customer satisfaction as output variables provide insights into the companys performance in the market and levels of client satisfaction.

Considering these variables collectively an efficiency analysis will comprehensively evaluate how selected companies utilize their resources and efforts to achieve outcomes in the blockchain security sector. The findings will help identify companies uncover practices and highlight areas, for potential improvement. Ultimately this will contribute to a innovative blockchain ecosystem.

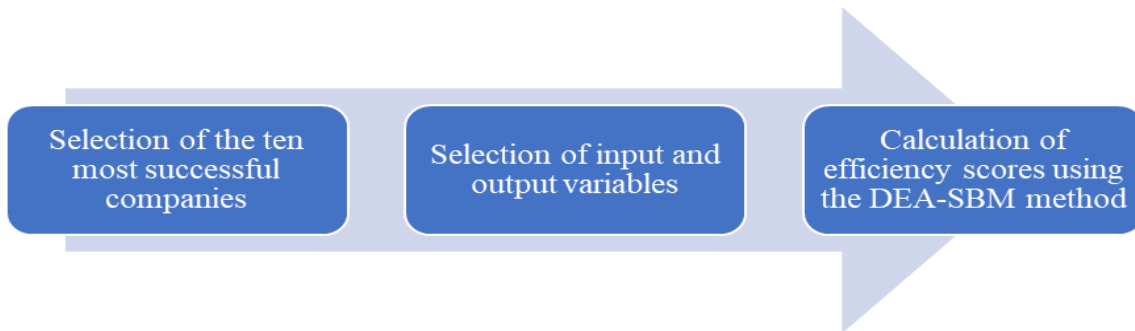


Figure 1. Calculation process of efficiency scores

Calculation of Efficiency Scores Using the DEA-SBM Method

In years the attention, towards technology has grown significantly due to its potential to enhance security across various industries. The initial step in evaluating security effectiveness involves identifying the 10 companies operating within this sector. Once these top 10 companies are determined the subsequent step entails selecting the input and output variables that will be used for analysis. The statistics in Table 2 provide insights into performance metrics. Serve as a basis for assessing and comparing the efficiency and effectiveness of the DMUs in terms of blockchain security. If theres a deviation it means there's more variability, among the DMUs regarding that specific variable. The Average column gives us an idea of what values we can expect to see across the DMUs helping us understand how they perform as a whole.

Table 2. Statistics on input/output data

	R&D Expenditure	Employee Expertise	Security Partnerships	Market Share	Customer Satisfaction
Max	9	9	9	9	9
Min	3	6	6	3	3
Average	7.4	8.1	7.5	6	7
SD	1.959591794	1.374773	1.5	2.569047	2.366432

Table 3. Correlation on input and output data.

	R&D Expenditure	Employee Expertise	Security Partnerships	Market Share	Customer Satisfaction
Research and Development (R&D) Expenditure	1	0.801784	0.51031	0.556187	0.603807
Employee Expertise	0.801783726	1	0.654654	0.764471	0.737711
Security Partnerships	0.510310363	0.654654	1	0.856349	0.676123
Market Share	0.55618651	0.764471	0.856349	1	0.789542
Customer Satisfaction	0.603807364	0.737711	0.676123	0.789542	1

When examining security efficiency potential input variables may include power, storage capacity, employee count and research and development expenditures. On the hand possible output variables could encompass metrics, like implementation of blockchain solutions instances of security breaches detected and cost savings experienced by consumers through utilizing blockchain technology (see Table 3).

The Average column gives us a perspective of the values we observe across the different DMUs. The findings reveal correlations between Research and Development (R&D) Expenditure and Employee Expertise (0.801) Security Partnerships (0.510) Market Share (0.556) as well, as Customer Satisfaction (0.604). By utilizing the DEA SBM model blockchain security companies can assess their efficiency and effectiveness compared to their peers. Moreover this approach helps identify areas for performance improvement by analyzing factors contributing to inefficiency or ineffectiveness.

Additionally the DEA SBM model serves as a benchmarking tool, for comparing security systems or companies. This analysis helps identify which companies are performing well. Armed with this information investors can make decisions, about where to invest their resources.

The SBM model evaluates a company's efficiency by measuring its slack resources that can be utilized for improvement. These slack resources represent potential that if properly leveraged can enhance a company's performance. Unlike the DEA model the SBM model provides a comprehensive and realistic assessment of performance by considering these untapped resources and their impact, on efficiency.

$$P = \{(x, y) | x \geq \sum_{j=1}^n \beta_j x_j, 0 \leq y \leq \sum_{j=1}^n \beta_j y_j, \beta \geq 0\} \quad (1)$$

$\beta_j = (\beta_1, \beta_2, \dots, \beta_n)^T$ Is called the intensity vector

To change the inequalities in equation (1) to equalities, we can introduce slacks for the J as follows:

$$\begin{aligned} x &= \sum_{j=1}^n \beta_j x_j + s^- \\ y &= \sum_{j=1}^n \beta_j y_j - s^+ \\ s^- &\geq 0, s^+ \geq 0, \end{aligned}$$

The slacks that are denoted as Where $s^- = (s^-_1, s^-_2, \dots, s^-_m) \in R^m$ and $s^+ = (s^+_1, s^+_2, \dots, s^+_m) \in R^S$ respectively are referred to as input and output slacks.

The SBM model is designed to tackle a programming problem. Its goal is to maximize the efficiency score (θ) while ensuring that the slack variables are non negative and the inputs and outputs of DMUs (Decision Making Units) are properly weighted. This approach provides an efficiency score, for each DMU indicating how effectively it utilizes its resources and produces outputs. To put it simply the SBM model is a tool for assessing the performance of DMUs across industries. By considering slack variables it offers a comprehensive evaluation of efficiency enabling us to pinpoint areas with potential for improvement.

Data Analysis and Discussion

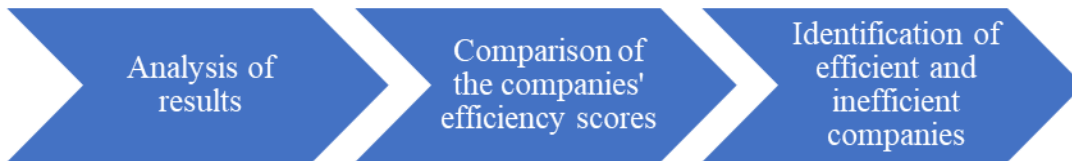
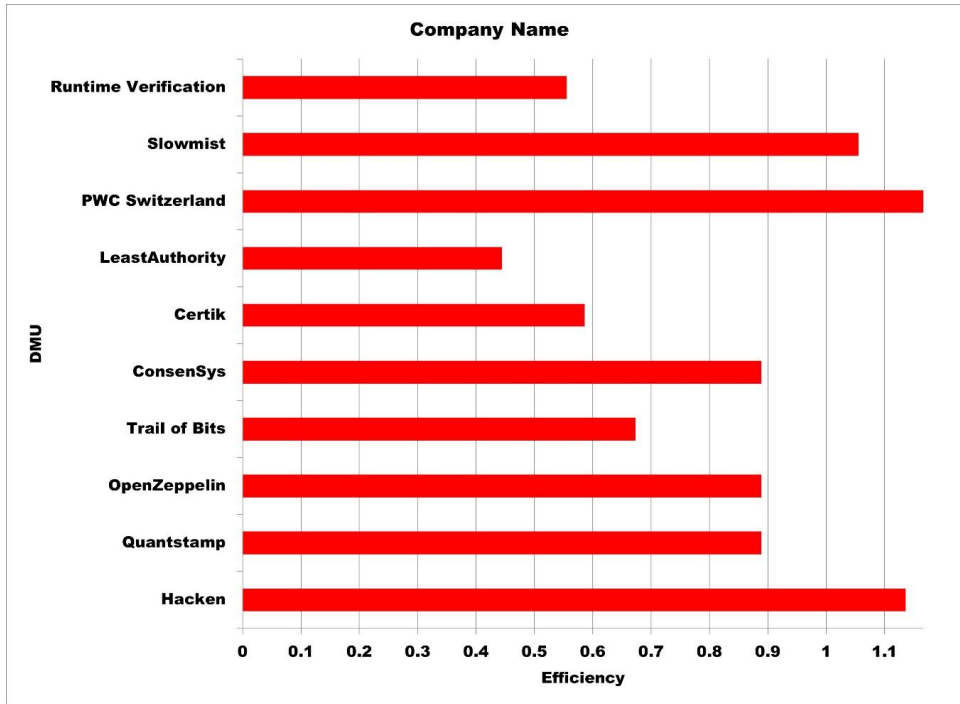


Figure 2. Data analysis process.

In figure 2, we can move forward with our analysis using DEA SBM approach involved calculating efficiency scores for each company under consideration. The outcomes revealed that certain companies were more effective than others, in utilizing resources to accomplish their objectives. Indeed the study revealed that PWC Switzerland and ConsenSys performed well in terms of efficiency whereas Slowmist and Certik showed levels of efficiency.

In Figure 3, you can see a list of the 10 blockchain security companies. This ranking is based on their performance metrics, which determine their positions. Each company has its position with the highest ranked company being recognized as the most effective and successful, in their blockchain security efforts. When we compared the efficiency scores of companies we noticed differences, in how they utilized their input and output variables. For example PWC Switzerland scored well in terms of power while ConsenSys excelled in the number of implementations. On the hand both Slowmist and Certik received scores in both categories. Based on this analysis we can conclude that inefficient companies were identified based on their resource utilization. Companies with high efficiency scores showed allocation of resources to achieve their objectives. In contrast those with scores were considered ineffective, in utilizing their resources. As a result PWC Switzerland and ConsenSys emerged as companies while Slowmist and Certik were categorized as performers.

Figure 3. Ranking of 10 blockchain security companies



Conclusion

The DEA SBM method is an essential tool, for evaluating the efficiency of companies across industries. Its impact becomes more significant in the field of security. The study reveals insights, into ten companies operating in this industry. Highlights the ability of the DEA SBM to identify the most efficient players based on their effective use of input and output variables. By differentiating between companies this research provides information for decision makers and investors showcasing the effectiveness of various blockchain security firms. In a changing security landscape maintaining efficiency and effectiveness is crucial. The DEA SBM model serves as a tool for companies in this industry guiding them towards success and innovation. It helps security firms refine their strategies and improve performance by identifying areas that need improvement. Moreover this model not benefits company operations. Also provides investors with well informed insights to channel investments towards the most promising and efficient players. Looking ahead future studies that utilize the DEA SBM approach will undoubtedly play a role in harnessing the potential of technology. As the emerging blockchain security industry continues to advance it is essential to understand and optimize its efficiency for adoption and transformative impact. Researchers and stakeholders can leverage the power of the DEA SBM model to unlock avenues of growth and innovation within this industry. In summary the DEA SBM model proves to be a methodology, for evaluating the efficiency and effectiveness of security systems and companies operating in this field. Its capacity to reveal discrepancies, in effectiveness and recognize chances for enhancement renders it a crucial tool for bolstering the performance and competitiveness of the security sector. Embracing this strategy is not optional; rather it is imperative for any participant seeking success, in the evolving domain of security.

Scientific Ethics Declaration

The authors declare that the scientific ethical and legal responsibility of this article published in EPSTEM journal belongs to the authors.

Acknowledgements or Notes

* This article was presented as an oral presentation at the International Conference on Research in Engineering, Technology and Science (www.icrets.net) held in Budapest/Hungary on July 06-09, 2023.

* The authors would like to thank the Ministry of Science and Technology, Taiwan. We also would like to thank the National Kaohsiung University of Science and Technology, Industrial University of Ho Chi Minh City, and Thu Dau Mot University for their assistance. Additionally, we would like to thank the reviewers and editors for their constructive comments and suggestions to improve our work.

References

- Aljumaie, G. S., & Alhakami, W. J. S. (2022). A secure LEACH-PRO protocol based on blockchain. *Sensors*, 22(21), 8431.
- Bar-Zur, R., Abu-Hanna, A., Eyal, I., & Tamar, A. (2022). WeRLman: to tackle whale (transactions), go deep (RL). *Proceedings of the 15th ACM International Conference on Systems and Storage*, 148-148.
- Huang, Y. (2022). The role of artificial intelligence technology in promoting the development of my country's sports industry. *The 2nd International Conference on Artificial Intelligence, Automation, and High-Performance Computing (AIAHPC 2022)*.
- Li, P., Xie, Y., Xu, X., Zhou, J., & Xuan, Q. (2022). Phishing fraud detection on ethereum using graph neural network. *Proceedings International Conference on Blockchain and Trustworthy System*, 362-375, Singapore: Springer Nature Singapore.
- Nasir, M. U., Zubair, M., Ghazal, T. M., Khan, M. F., Ahmad, M., Rahman, A.-u., . . . Mansoor, W. J. S. (2022). Kidney cancer prediction empowered with blockchain security using transfer learning. *Sensors*, 22(19), 7483.
- Rizzardi, A., Sicari, S., Miorandi, D., & Coen-Porisini, A. (2022). Securing the access control policies to the Internet of Things resources through permissioned blockchain. *Concurrency and Computation: Practice and Experience*, 34(15), e6934..
- Vishwakarma, L., Nahar, A., & Das, D. (2022). Lbsv: Lightweight blockchain security protocol for secure storage and communication in sdn-enabled iov. *IEEE Transactions on Vehicular Technology*, 71(6), 5983-5994.
- Wang, C.-N., Yang, F.-C., Vo, N. T., & Nguyen, V. T. T. J. B. (2023). Enhancing Lithium-Ion battery manufacturing efficiency: A comparative analysis using DEA malmquist and epsilon-based measures. *Batteries*, 9(6), 317.
- Wang, C. N., Yang, F. C., Vo, N. T. M., & Nguyen, V. T. T. (2022). Wireless communications for data security: efficiency assessment of cybersecurity industry-A promising application for UAVs. *Drones*, 6(11). <https://doi.org/10.3390/drones6110363>
- Zhang, B., Zhang, B., & Sun, J. (2022, August). Pole-2p: Improved consensus algorithm based on proof of learning. In *Second International Conference on Digital Signal and Computer Communications (DSCC 2022)* (Vol. 12306, pp. 209-214). SPIE.
- Zhang, T., & Wang, W. (2022). Consumer group identification algorithm for ice and snow sports. *Computational Intelligence and Neuroscience*, Article ID 2174910. <https://doi.org/10.1155/2022/2174910>
- Zhao, X., Wang, J., Fu, X., Zheng, W., Li, X., & Gao, C. (2022). Spatial-temporal characteristics and regional differences of the freight transport industry's carbon emission efficiency in China. *Environmental Science and Pollution Research*, 29(50), 75851-75869.

Author Information

Thi Minh Nhut Vo

National Kaohsiung University of Science and Technology,
415 Jiangong, Sanmin, Kaohsiung, Taiwan
Thu Dau Mot University, Vietnam

Chia-Nan Wang

National Kaohsiung University of Science and Technology,
415 Jiangong, Sanmin, Kaohsiung, Taiwan

Fu-Chiang Yang

National Kaohsiung University of Science and Technology,
415 Jiangong, Sanmin, Kaohsiung, Taiwan

Van Thanh Tien Nguyen

Industrial University of Ho Chi Minh City
12, Nguyen Van Bao, Go Vap, Ho Chi Minh City, Vietnam
Corresponding author contact e-mail: thanhtienck@ieee.org

To cite this article:

Vo, T.M.N., Wang, C.N., Yang, F.C. & Nguyen, V.T.T. (2023). Blockchain security- efficiency analysis based on DEA-SBM Model. *The Eurasia Proceedings of Science, Technology, Engineering & Mathematics (EPSTEM)*, 23, 202-208.

The Eurasia Proceedings of Science, Technology, Engineering & Mathematics (EPSTEM), 2023

Volume 23, Pages 209-219

ICRETS 2023: International Conference on Research in Engineering, Technology and Science

Bi-Directional LSTM-Based COVID-19 Detection Using Clinical Reports

Salah Bouktif

United Arab Emirates University

Akib Khanday

United Arab Emirates University

Ali Ouni

University of Quebec

Abstract: COVID-19 has affected the entire globe with its rapid spreading, causing a high transmission rate. A huge amount of people come in contact with this deadly virus, and early diagnosis of such kind of viruses may save many lives. This paper proposes an improved approach for detecting COVID-19 based on Long Short Term Memory (LSTM) and taking advantage of early clinical reports. To train the LSTM-based classifier for COVID-19 detection, various preprocessing techniques and word embeddings are employed. These techniques ensure the data is in a suitable format for the LSTM model. The proposed LSTM model is then compared against state-of-the-art ensemble models like Bagging and Random Forest, demonstrating its superior performance. The evaluation results showcase a testing accuracy of 87.15%, with a precision of 91% and a recall of 88%. These metrics indicate the effectiveness of the proposed LSTM model in accurately detecting COVID-19-positive cases. By leveraging early clinical reports and utilizing advanced deep learning techniques, our approach achieves significant improvements in COVID-19 detection compared to existing ensemble models.

Keywords: LSTM, COVID-19, Diagnosis, Detecting, Embeddings, Classifier

Introduction

The COVID-19 pandemic has emerged as a severe global health crisis, with far-reaching consequences for societies, economies, and the overall well-being of individuals on a worldwide scale (Mangal et al., 2020). Since its emergence in late 2019, this highly infectious disease has rapidly spread, leading to a significant number of infections and fatalities across the globe. The virus primarily targets the respiratory system, giving rise to a wide range of symptoms that span from mild flu-like manifestations to severe respiratory distress and organ failure (Ucar & Korkmaz, 2020). It is important to note that certain populations, particularly older adults and individuals with pre-existing health conditions, are at a heightened risk of experiencing severe outcomes. The impact of this pandemic has been profound, causing widespread disruptions and necessitating urgent measures to address its implications.

In response to the spread of COVID-19, governments and health organizations worldwide have implemented a range of measures aimed at curbing the transmission of the virus. These strategies include widespread testing, contact tracing, quarantine protocols, travel restrictions, and the development and distribution of vaccines (Horry et al., 2020). The pandemic has emphasized the critical importance of global cooperation and information sharing in effectively addressing and managing public health emergencies.

- This is an Open Access article distributed under the terms of the Creative Commons Attribution-Noncommercial 4.0 Unported License, permitting all non-commercial use, distribution, and reproduction in any medium, provided the original work is properly cited.

- Selection and peer-review under responsibility of the Organizing Committee of the Conference

© 2023 Published by ISRES Publishing: www.isres.org

Beyond its impact on health, COVID-19 has triggered significant disruptions to economies across the world. Lockdowns, restrictions, and social distancing measures have resulted in the closure of businesses, substantial job losses, and reduced economic activity. Sectors such as tourism, hospitality, and retail have been particularly hard-hit by these measures (Rabani et al., 2023). Governments have responded by implementing fiscal stimulus packages to alleviate the economic burden and provide support to affected individuals and businesses (Mathieu et al., 2021; Ndwandwe & Wiysonge, 2021).

The pandemic has also taken a toll on mental health, as the necessary measures to contain the virus, such as isolation, fear, and uncertainty, have contributed to heightened levels of stress, anxiety, and depression among individuals. Access to mental health services and support has become crucial in addressing the psychological consequences of the pandemic (Khanday et al., 2020).

As the long-term implications of COVID-19 continue to unfold, it becomes increasingly essential to promptly and accurately diagnose cases using various Artificial Intelligence (AI) techniques. AI has shown promising results across diverse fields, including healthcare, education, and defense. Early detection facilitated by AI-assisted diagnosis holds the potential to mitigate human losses (Moore & Offit, 2021; Yan et al., 2020). Ongoing research aims to comprehensively understand the long-term health effects, evaluate vaccine efficacy against emerging variants, and develop robust strategies to prevent future pandemics (Mathieu et al., 2021; Soleimanpour & Yaghoubi, 2021).

Machine learning, has been used in different domains ranging from engineering (Almarimi et al., 2019, Daagi et al., 2017, Daaji et al., 2021) to education (Bouktif and Manzoor, 2021) and healthcare (Gudigar et al., 2021). With its capability to analyze vast and intricate datasets, has played a pivotal role in enhancing COVID-19 detection, monitoring, and response efforts (Lazarus et al., 2021). By leveraging the power of machine learning, healthcare professionals, researchers, and policymakers can make data-driven decisions that significantly improve public health outcomes. This study proposes the development of a diagnostic system specifically designed to enhance the detection of COVID-19 cases by mining clinical reports. In particular, the research focuses on investigating the role of Natural Language Processing (NLP) in identifying COVID-19 using Long Short-Term Memory (LSTM). Given the extensive utilization of LSTM in various prediction tasks across different domains (Bouktif et al., 2020), we capitalize on its text mining capabilities (Bouktif & Awad, 2013) to effectively classify texts using word embeddings, thereby leveraging its advanced classification capabilities. a type of deep learning model known for its text mining capabilities and ability to leverage embeddings. Notably, this work deviates from previous approaches that primarily rely on image processing for patient case classification. By customizing LSTM to train on COVID-19-related word embeddings, the accuracy and methodology for detecting COVID-19 cases can be enhanced, offering a promising avenue for more effective diagnosis.

The rest of the paper is organized as follows. In Section 2, we present the background as well as the relevant literature of our work and contribution. Section 3 discusses the proposed our LSTM based Detecting approach. An empirical evaluation of our model and results of its comparison with benchmarks are discussed in Section 4. In Section 5, we draw conclusion and give insights into our future works.

Background and Related Work

Artificial intelligence (AI) has ushered in a transformative era across various domains, encompassing healthcare, defense, economics, and education. Within the realm of disease detection and diagnosis, researchers have been actively harnessing the power of machine learning and deep learning techniques to address the complex challenges posed by life-threatening conditions like cancer and tumors (Gudigar et al., 2021). Amid the ongoing efforts to diagnose COVID-19, a wealth of literature has been meticulously compiled from reputable databases, including SCOPUS and Web of Science. This comprehensive collection of research has been facilitated through a keyword-based mechanism, primarily centered around retrieving pertinent journal articles published by esteemed entities such as Elsevier, IEEE, Taylor Francis, Wiley, MDPI, and ACM.

In the context of COVID-19 diagnosis, machine learning and deep learning have emerged as indispensable tools. For instance, Alazab et al. (2020) achieved successful detection of the Coronavirus from CT scans through the utilization of Convolutional Brain organizations, attaining an impressive accuracy rate of 94.80% in Australia and 88.43% in Jordan. Roberts et al. (2021) delved into the realm of AI-based COVID-19 detection and prediction by employing chest radiographs and CT scans. However, their study revealed strategic flaws and inherent biases within existing models, indicating that none of the models were deemed suitable for clinical

implementation. Mangal et al. (2020) introduced an innovative deep neural network model named CovidAID: Coronavirus Artificial Intelligence Locator, specifically designed to prioritize patients for appropriate testing. Trained on a publicly available COVID-19 chest X-ray dataset, this model showcased an accuracy of 90.5% with 100% recall in detecting Coronavirus infections. Furthermore, Islam et al. (2020) proposed a deep learning approach that combined a Convolutional Neural Network (CNN) with Long Short-Term Memory (LSTM) to automate the diagnosis of Coronavirus based on X-ray images. Their system utilized an extensive dataset of 4,575 X-ray images, including 1,525 cases of COVID-19, and demonstrated exceptional performance metrics, boasting an accuracy of 99.4%, AUC of 99.9%, specificity of 99.2%, sensitivity of 99.3%, and F1-score of 98.9%.

Using audio analysis, Hassan et al. (2020) employed a Recurrent Neural Network (RNN), particularly LSTM, to scrutinize acoustic features such as coughing, breathing, and voice patterns for early screening and diagnosis of COVID-19. The results revealed relatively lower accuracy rates for voice samples in comparison to coughing and breathing sound samples. Furthermore, Kaya et al. (2022) proposed an innovative approach that utilized the Affine Transformation (AT) technique in conjunction with a hybrid deep learning model merging GoogleNet and LSTM for COVID-19 detection through X-ray images. Remarkably, their proposed method achieved a high classification accuracy rate of 98.97% employing a dataset from Mendeley. These examples serve as a glimpse into the recent advancements made in the field of COVID-19 detection using machine learning and deep learning methodologies. Table 1 provides a concise summary of some noteworthy works within this area, highlighting the progress achieved in combating the ongoing pandemic.

Table 1. Related work

Technique	Contribution	Results	Research Gap
Deep Learning	Proposed SqueezeNet based diagnostic of the coronavirus disease and classified it into 3 classes (COVID19/ Pneumonia /Normal)	The accuracy of the model achieved is 87%	Only Images are used.
Machine Learning	Used Traditional Approaches of Machine Learning for classifying the text into binary class.	The classification Accuracy achieved from this approach is 80%	Only 212 data records are used.
Deep Learning	Proposed a tailored deep neural network for classifying an x-ray image into three classes (COVID-19/ PNEUMONIA/ NORMAL)	An accuracy of 91.3% is achieved.	X-Ray images are used and there is scope for Hyperparameter tuning.
Deep Learning	Proposed nCOVnet for detecting COVID from X-ray images(Binary Classification).	The model achieved 87.3% accuracy.	Multi class classification can be performed.
Deep Learning	Deep learning approach for detecting COVID-19 into three classes (COVID-19/ PNEUMONIA /NORMAL)	The proposed approach achieves an accuracy of 97%.	Only worked on X-Ray images. CT Scan images may be used.
Deep Learning	Covid detection based on Generative Adversal Learning	Accuracy of 99% is achieved by the proposed approach.	Work can be explored to other multimodalities.

After studying the relevant work following conclusions are drawn:

- Most of the work is being performed on image datasets like X-Rays and CT Scan images using image processing techniques, with less focus on text mining.

- Also the data published by the World Health Organization (WHO) contains various metadata which need to be investigated to improve the model’s efficiency.
- Word Embeddings play a major role in text mining, and using word embeddings for detecting COVID-19 may be helpful.

Methodology

The field of Natural Language Processing (NLP), an emerging discipline within Artificial Intelligence, has demonstrated promising outcomes in tackling machine translation and classification challenges. This study focuses on utilizing text mining techniques to detect COVID-19 from early clinical textual reports, aiming to expedite the diagnosis process and enable early intervention. Additionally, humans possess the ability to observe various irregularities in individuals, and healthcare professionals often document their findings in written reports when examining patients. Consequently, this research endeavors to address a similar problem by developing a classification system to identify COVID-19 or Normal cases from clinical reports. The proposed approach leverages NLP and text mining methodologies to extract relevant information and classify the reports effectively. Figure 1 provides an overview of the comprehensive framework employed in this study, illustrating the interconnected components and their contribution to the overall approach. By harnessing the power of NLP and text mining, this research aims to contribute to the early detection and diagnosis of COVID-19, potentially saving time and facilitating timely medical intervention.

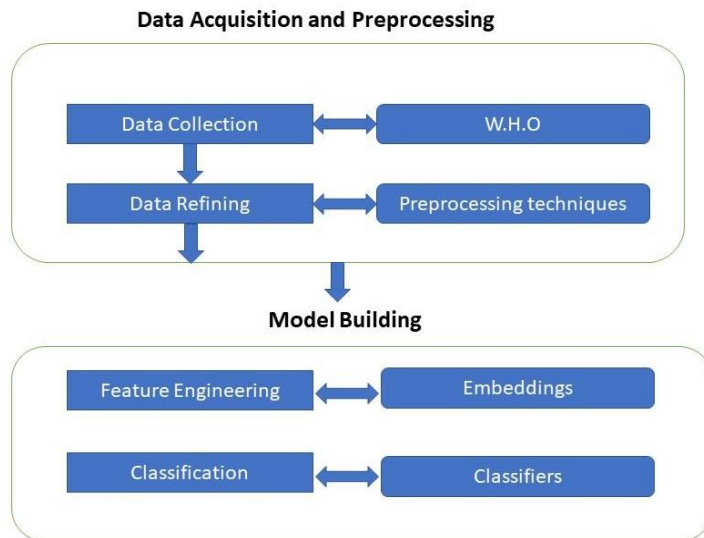


Figure 1. Overall framework for classification

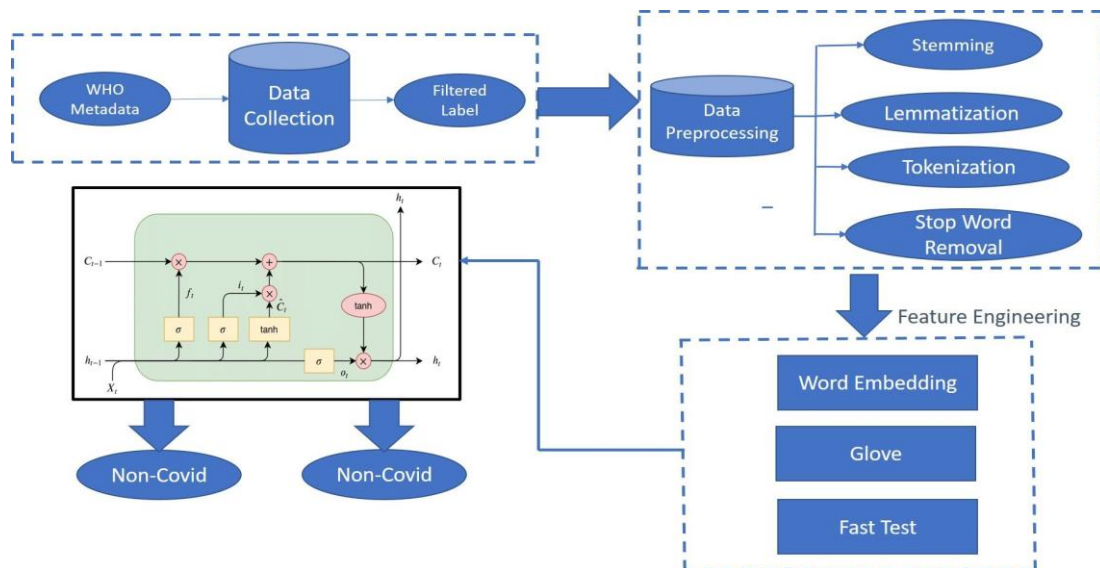


Figure 2. LSTM based COVID-19 detection.

Data Collection

A dataset on COVID-19 is sourced from a publicly available database published by the WHO. This dataset contains textual reports that encompass essential information pertaining to COVID-19, including symptoms, medical history, and laboratory test results. Each record within the collected dataset is carefully labeled to indicate whether the individual is COVID-19 positive or negative. Notably, the dataset consists of a substantial total of 915 records, offering a significant sample size that is valuable for the purposes of analysis and modeling.

Data Preprocessing

Data preprocessing is a crucial phase in the proposed methodology as it prepares the data to meet the input criteria of LSTM. Several techniques are applied during this phase, including converting the text to lowercase, removing punctuation marks, tokenizing the text into individual words, and excluding stop words. Moreover, it is recommended to consider additional methods like stemming or lemmatization to further standardize the words. In order to visualize the distribution of text lengths, Figure 3 presents a histogram that illustrates the frequency distribution of text lengths.

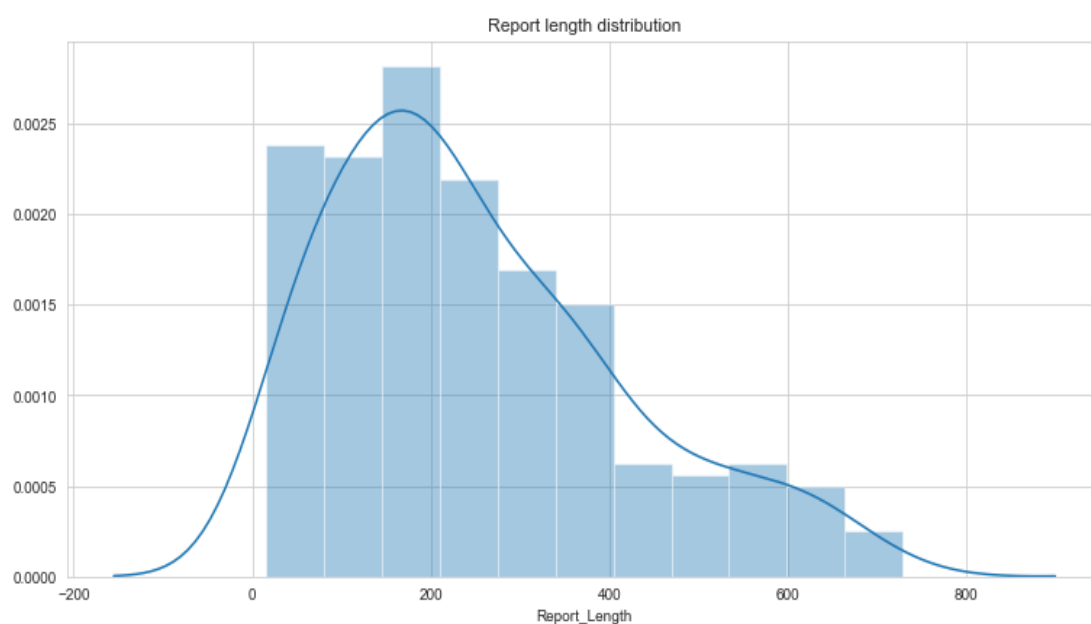


Figure 3. Clinical reports with their length

Feature Selection

In order to conduct the classification, the preprocessed text undergoes a transformation into word embeddings, which represent words as dense vectors. Pre-trained word embeddings, such as Word2Vec, GloVe, or FastText, can serve as suitable algorithms for this purpose. These embeddings capture the semantic relationships between words and enable the LSTM to comprehend the meaning of the text effectively. Furthermore, it is essential to ensure that all text sequences possess the same length by padding or truncating them as required. This step is crucial for creating fixed-length input sequences that can be processed by the LSTM. It is recommended to select an appropriate sequence length that captures sufficient contextual information from the text..

Classification

The LSTM architecture typically consists of an embedding layer to handle the input, one or more LSTM layers to capture sequential information, and one or more fully connected layers for classification. To enhance the performance of the model, one can explore different configurations of LSTM layers, such as stacked LSTMs or bidirectional LSTMs. Figure 2 provides a visual representation of the LSTM model's architecture employed in this study. To facilitate model training and evaluation, the dataset is divided into training, validation, and testing sets. The training set is used to train the LSTM model, while the validation set aids in fine-tuning

hyperparameters and monitoring the model's performance. Finally, the testing set is used to assess the model's performance on unseen data. During the training process, the LSTM model is optimized by minimizing a loss function, such as binary cross-entropy. This optimization is achieved using an optimizer such as Adam or RMSprop. Hyperparameters, such as learning rate and batch size, are adjusted to optimize the model's performance. In addition, Figure 4 illustrates the architecture of the bidirectional LSTM model, which can be an alternative configuration explored in this research work.

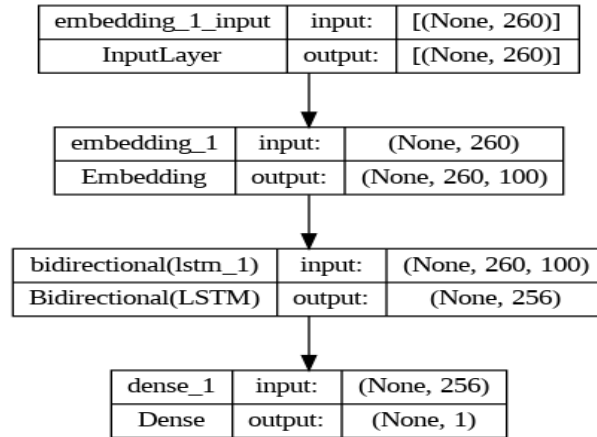


Figure 4. Bi-directional LSTM architecture

The LSTM model's effectiveness depends on the training data's quality and representativeness, the selection of word embeddings, and the design of the LSTM architecture. Regular model evaluation and validation on diverse datasets are crucial to ensure its robustness and generalizability. The Pseudo Code of the proposed framework is shown in Pseudo-Code 1.

Pseudo Code 1: Bi-Directional LSTM based COVID-19 Detection

```

Require: Reports, Label
Ensure: Covid or Normal
1 Start
2 For i from 1 to n do
3   P[i]= Report[i]+Label
4   Q[i]=Length(P[i])
5 End For
6 For i from 1 to n do
7   R[i]=Tokenise(P[i])
8   R[i]=Stopword Removal (Lemmatization(R[i]))
9 End For
10 For i from 1 to n do
11   F[i]=Embeddings(F[i])+Q[i]
12 End For
13 Classifier(Bi-Directional LSTM, Report[i], F[i])
14 End
  
```

Emperical Evaluation

In this section, we present the evaluation of the proposed LSTM model for COVID-19 case detection, building upon our previous work. The evaluation process consists of two main steps. Firstly, we evaluate the model using cross-validation to assess its performance across multiple folds of the dataset. Secondly, we compare our model with ensemble-based solutions, aiming to demonstrate the effectiveness of leveraging machine learning techniques in improving the performance of COVID-19 detection models. Indeed, One of the key contributions of this work is the utilization of machine learning techniques to enhance the accuracy of COVID-19 diagnosis based on early clinical symptoms. We achieve this by fine-tuning the hyperparameters of the LSTM model to optimize its performance. To validate the effectiveness of our customized LSTM model, we establish a set of benchmark models that serve as a basis for comparison. Specifically, we employ Bagging and Random Forest algorithms as benchmarks in our empirical evaluation.

By conducting this comprehensive evaluation, we aim to demonstrate the superiority of our proposed LSTM model in detecting COVID-19 cases compared to the benchmark models. This evaluation serves to validate the effectiveness of our approach and highlight its potential contribution to the field of COVID-19 diagnosis.

Evaluation Measures

Using the four metrics of the confusion Matrix, i.e. True Positive (TP), True Negative (TN), False Positive (FP), and False Negative (FN), we calculated the following evaluation measures of the our model performance.

Accuracy: It is one of the standard metrics used to evaluate the classifiers. It measures the ratio of the total number of corrected predicted instances over the total number of predictions.

$$Accuracy = \frac{TP + TN}{TP + TN + FP + FN} \quad (1)$$

Precision: It is a metric that determines the ratio of true positives over the total predicted positives.

$$Precision = \frac{TP}{TP + FP} \quad (2)$$

Recall: It is a metric that determines the ratio of true positives over total actual positives.

$$Recall = \frac{TP}{TP + FN} \quad (3)$$

F1-score: It is a metric used to measure the performance of the classifier/model when that model needs a balance between Precision and Recall.

$$F1 - score = \frac{2 * Precision * Recall}{Precision + Recall} \quad (4)$$

Experimental Settings

The sequential model is used with embeddings from the vocabulary. The sigmoid activation function is used with one dense layer. Binary Cross Entropy is utilized as a loss function and Adam as an optimization function. Ten epochs are run with a batch size of 32. The various metrics used to evaluate classification results are confusion matrix, Accuracy, Precision, Recall and F-Measure

The dataset used in this study is obtained from the public repository of [iee80231](#). To ensure the data is suitable for classification, various preprocessing techniques such as tokenization, lemmatization, stemming, punctuation removal, stopwords removal, and normalization are applied. The refined dataset is then utilized for training a fine-tuned LSTM classifier. The dataset is split into a training set and a testing set in an 80:20 ratio, with 80% of the data used for training the classifier and 20% for testing.

Model Performance

To evaluate the proposed model, several performance measures including Precision, Recall, and F1-score are computed. The model demonstrates an overall accuracy of 87.15%, with precision, recall, and F1-score of 89%, 87%, and 86% respectively. The results of the proposed approach are presented in Table II, providing a comprehensive summary of the model's performance. Figure 5 depicts the Confusion Matrix, providing visual insights into the classification outcomes.

The model is validated using k-fold cross-validation, in which the value of k equals 5. Five iterations are performed while validating the model; the results are shown in Figure 5. After performing the validation, the average validation score came near to the accuracy achieved on the testing dataset. Also, the results show no overfitting or underfitting of the model.

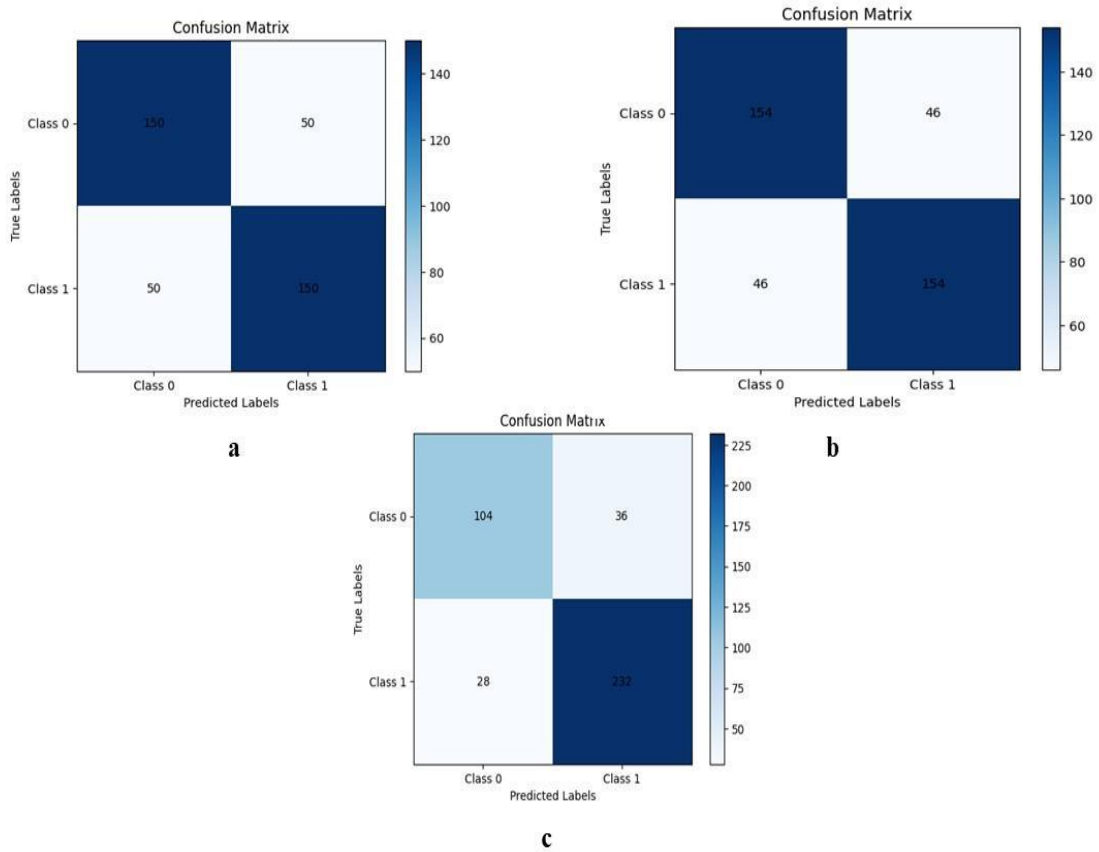


Figure 5. Confusion metrics a: Bagging, b: Random forest, c: LSTM

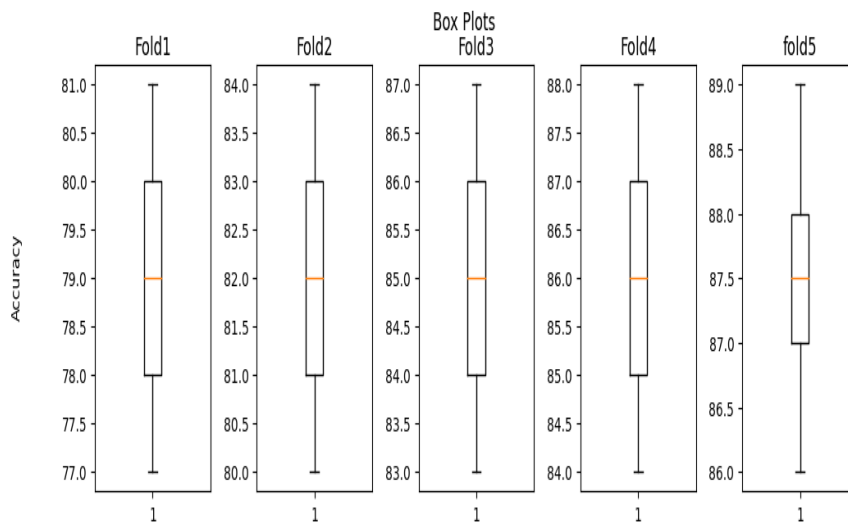


Figure 6. Cross validation

Comparison with Ensemble Model Benchmarks

The validity of the proposed approach is confirmed by conducting a comparative study with other benchmarks commonly used for COVID-19 detection. In this study, we employed 5-fold cross-validation as a model validation method. The results of the proposed approach using the 5-fold cross-validation showed impressive performance measures. The precision was determined to be 89%, indicating the accuracy of correctly identifying COVID-19 cases.

Table 2. Comparative analysis

Classifier	Class	Precision	Recall	F1-Score	Accuracy
Bagging	Normal	0.70	0.75	0.72	75%
	COVID	0.80	0.75	0.77	
Random Forest	Normal	0.77	0.76	0.76	77.5%
	COVID	0.78	0.79	0.79	
Bi-Directional LSTM	Normal	0.89	0.87	0.86	87.15%
	COVID	0.91	0.88	0.84	

The recall, representing the proportion of true COVID-19 cases detected, achieved a value of 87%. The F-measure, which combines precision and recall, was calculated at 86%. Furthermore, the overall accuracy of the proposed approach was measured at 87.15%. Random Forest, one of the benchmark algorithms used in the comparative study, also exhibited relatively good performance. It achieved a precision of 78%, recall of 77%, F-measure of 77.5%, and an accuracy of 77.5%. Table 2 presents the mean values of these different performance measures, providing a comprehensive overview of the comparative study between our proposed LSTM model and other ensemble machine learning algorithms, namely Bagging and Random Forest. These results showcase the superior performance of our LSTM model in COVID-19 detection compared to the benchmark algorithms.

Conclusion

This study presents the utilization of a deep learning algorithm, specifically the Bi-directional LSTM, for the classification of clinical textual reports into COVID-19 and Non-COVID-19 cases. Our approach diverges from previous methods that primarily rely on image processing for patient case classification. Instead, we leverage the potential of LSTM by customizing the Bi-directional LSTM variant to train on COVID-19-related word embeddings. Furthermore, we compare the performance of our model with state-of-the-art benchmarks in the field. The dataset used in this research is obtained from the World Health Organization (WHO) website, where we filter and extract the necessary textual attributes along with their corresponding labels. To facilitate the binary classification task, Word Embeddings are employed in conjunction with the LSTM model. The experimental results, obtained through 5-fold cross-validation, showcase a testing accuracy of 87%, demonstrating the model's effectiveness in accurately classifying clinical reports. As part of future directions, we propose the fusion of two models: one trained on Clinical Symptoms and the other on Clinical Reports. This fusion approach aims to enhance the efficiency of the classification process by leveraging information from both sources. A second avenue for future research is the development of COVID-19 explainable models, drawing inspiration from our previous work in promoting interpretability (Bouktif and Awad, 2013). These explainable models will provide insights into the decision-making process of the classification system, enhancing transparency and understanding in the context of COVID-19 diagnosis.

Scientific Ethics Declaration

The authors declare that the scientific ethical and legal responsibility of this article published in EPSTEM journal belongs to the authors.

Acknowledgements or Notes

* This article was presented as an oral presentation at the International Conference on Research in Engineering, Technology and Science (www.icrets.net) held in Budapest/Hungary on July 06-09, 2023.

*This work was supported by ASPIRE Award for Research Excellence (AARE-2020). (ASPIRE award number AARE20-100 grant #21T55) .

References

- Alazab, M., Awajan, A., Mesleh, A., Abraham, A., Jatana, V., & Alhyari, S. (2020). COVID-19 prediction and detection using deep learning. *International Journal of Computer Information Systems and Industrial Management Applications*, 12(June), 168–181.
- Almarimi, N., Ouni, A., Bouktif, S., Mkaouer, M. W., Kula, R. G., & Saied, M. A. (2019). Web service api recommendation for automated mashup creation using multi-objective evolutionary search. *Applied Soft Computing*, 85, 105830.
- Bouktif, S. & Awad, M. A. (2013). Ant colony based approach to predict stock market movement from mood collected on twitter. In *Proceedings of the 2013 IEEE/ACM International Conference on Advances in Social Networks Analysis and Mining*, 837–845.
- Bouktif, S., Fiaz, A., & Awad, M. (2020). Augmented textual features-based stock market prediction. *IEEE Access*, 8, 40269–40282.
- Bouktif, S. & Manzoor, A. (2021). Artificial intelligence as a gear to preserve effectiveness of learning and educational systems in pandemic time. In *2021 IEEE Global Engineering Education Conference (EDUCON)*, 1703–1711.
- Daagi, M., Ouniy, A., Kessentini, M., Gammoudi, M. M., & Bouktif, S. (2017). Web service interface decomposition using formal concept analysis. In *2017 IEEE International Conference on Web Services (ICWS)*, 172–179.
- Daaji, M., Ouni, A., Gammoudi, M. M., Bouktif, S., & Mkaouer, M. W. (2021). Multi-criteria web services selection: Balancing the quality of design and quality of service. *ACM Transactions on Internet Technology (TOIT)*, 22(1):1–31.13
- Ghoshal, B., & Tucker, A. (2020). Estimating uncertainty and interpretability in deep learning for coronavirus (COVID-19) detection. *ArXiv Preprint ArXiv:2003.10769*.
- Gudigar, A., Raghavendra, U., Nayak, S., Ooi, C. P., Chan, W. Y., Gangavarapu, M. R., Dharmik, C., Samanth, J., Kadri, N. A., Hasikin, K., & others. (2021). Role of artificial intelligence in COVID-19 detection. *Sensors*, 21(23), 8045.
- Hassan, A., Shahin, I., & Alsabek, M. B. (2020). COVID-19 detection system using recurrent neural networks. *2020 International Conference on Communications, Computing, Cybersecurity, and Informatics (CCCI)*, 1–5.
- Horry, M. J., Chakraborty, S., Paul, M., Ulhaq, A., Pradhan, B., Saha, M., & Shukla, N. (2020). COVID-19 detection through transfer learning using multimodal imaging data. *IEEE Access*, 8, 149808–149824.
- Islam, M. Z., Islam, M. M., & Asraf, A. (2020). A combined deep CNN-LSTM network for the detection of novel coronavirus (COVID-19) using X-ray images. *Informatics in Medicine Unlocked*, 20, 100412.
- Kaya, Y., Yiner, Z., Kaya, M., & Kuncan, F. (2022). A new approach to COVID-19 detection from X-ray images using angle transformation with GoogleNet and LSTM. *Measurement Science and Technology*, 33(12), 124011.
- Khanday, A. M. U. D., Rabani, S. T., Khan, Q. R., Rouf, N., & Mohi Ud Din, M. (2020). Machine learning based approaches for detecting COVID-19 using clinical text data. *International Journal of Information Technology*, 12, 731–739.
- Lazarus, J. V., Ratzan, S. C., Palayew, A., Gostin, L. O., Larson, H. J., Rabin, K., Kimball, S., & El-Mohandes, A. (2021). A global survey of potential acceptance of a COVID-19 vaccine. *Nature Medicine*, 27(2), 225–228.
- Mangal, A., Kalia, S., Rajgopal, H., Rangarajan, K., Namboodiri, V., Banerjee, S., & Arora, C. (2020). CovidAID: COVID-19 detection using chest X-ray. *ArXiv Preprint ArXiv:2004.09803*.
- Mathieu, E., Ritchie, H., Ortiz-Ospina, E., Roser, M., Hasell, J., Appel, C., Giattino, C., & Rodés-Guirao, L. (2021). A global database of COVID-19 vaccinations. *Nature Human Behaviour*, 5(7), 947–953.
- Moore, J. P., & Offit, P. A. (2021). SARS-CoV-2 Vaccines and the growing threat of viral variants. *JAMA*, 325(9), 821. <https://doi.org/10.1001/jama.2021.1114>
- Ndwandwe, D., & Wiysonge, C. S. (2021). COVID-19 vaccines. *Current Opinion in Immunology*, 71, 111–116.
- Rabani, S. T., Khanday, A. M. U. D., Khan, Q. R., Hajam, U. A., Imran, A. S., & Kastrati, Z. (2023). Detecting suicidality on social media: Machine learning at rescue. *Egyptian Informatics Journal*, 24(2), 291–302.
- Roberts, M., Driggs, D., Thorpe, M., Gilbey, J., Yeung, M., Ursprung, S., Aviles-Rivero, A. I., Etmann, C., McCague, C., Beer, L., & others. (2021). Common pitfalls and recommendations for using machine learning to detect and prognosticate for COVID-19 using chest radiographs and CT scans. *Nature Machine Intelligence*, 3(3), 199–217.
- Soleimanpour, S., & Yaghoubi, A. (2021). COVID-19 vaccine: where are we now and where should we go? *Expert Review of Vaccines*, 20(1), 23–44.
- Ucar, F., & Korkmaz, D. (2020). COVIDiagnosis-Net: Deep Bayes-SqueezeNet based diagnosis of the coronavirus disease 2019 (COVID-19) from X-ray images. *Medical Hypotheses*, 140, 109761.

Yan, L., Zhang, H.-T., Goncalves, J., Xiao, Y., Wang, M., Guo, Y., Sun, C., Tang, X., Jing, L., Zhang, M., & others. (2020). An interpretable mortality prediction model for COVID-19 patients. *Nature Machine Intelligence*, 2(5), 283-288.

Author Information

Salah Bouktif

College of Information Technology
United Arab Emirates University
Al Ain, UAE
Contact email : salahb@uaeu.ac.ae

Akib Mohi Ud Din Khanday

College of Information Technology
United Arab Emirates University
Al Ain, UAE

Ali Ouni

École de technologie supérieure,
ÉTS Montréal, University of Quebec,
Montreal, Canada.

To cite this article:

Bouktif, S., Khanday, A. & Ouni A. (2023). Bi-directional LSTM-based Covid-19 detection using clinical reports. *The Eurasia Proceedings of Science, Technology, Engineering & Mathematics (EPSTEM)*, 23, 209-219.

The Eurasia Proceedings of Science, Technology, Engineering & Mathematics (EPSTEM), 2023

Volume 23, Pages 220-224

ICRETS 2023: International Conference on Research in Engineering, Technology and Science

The Effectiveness of the Implementation of Speech Command Recognition Algorithms in Embedded Systems

Kamoliddin Shukurov

TUIT named after Mukhammad al-Khwarazmi

Umidjon Khasanov

TUIT named after Mukhammad al-Khwarazmi

Boburkhan Turaev

TUIT named after Mukhammad al-Khwarazmi

A'lokhan Kakhkharov

TUIT named after Mukhammad al-Khwarazmi

Abstract: Speech is the basis of human-computer interfaces, smart house, IoT and control systems. Implementing a real time voice control system through speech commands recognition in different environments requires simple algorithms and special purpose systems. The article analyzes the existing speech commands recognition algorithms in embedded systems. A simple and efficient algorithm for voice control systems through limited speech commands has been proposed.

Keywords Human-computer interface (HCI), Hardware-software platform, Embedded system

Introduction

Speech command control is widely used in various fields, speech control of devices and equipment, voice assistant in call centers, smart home and Internet of Things (IoT), speech identification, speech control interface for people with disabilities and can be applied other fields (Mazo et al., 1995). In this case, the processing of speech signals involves complex recognition algorithms.

Implementation of such human-computer interfaces requires special hardware and software platforms. However, with the increasing complexity of speech processing algorithms and the number of speech commands, the computing resource and memory size of the hardware-software platform increase dramatically. In addition, most human-computer interfaces work in real time. When recognizing speech commands in different environments, speech signals are affected by external noise and interference. Real-time mode, in turn, requires speed, compactness, and ease of use (Ngoset et al., 2011; Bahoura & Ezzaidi, 2013; Mosleh et al., 2010; Veitchet al., 2011; Melnikoff, et al., 2001; Vargas et al., 2001; Tamulevicius et al., 2010; Sujuan et al., 2008).

Literature Survey

The simplest view of a point signal for analysis is that of extracted words. Usually, speech words and their dictionaries will be limited. In modern complex speech recognition systems, the recognition of key words is carried out mainly. This is very useful in speech command system control systems.

- This is an Open Access article distributed under the terms of the Creative Commons Attribution-Noncommercial 4.0 Unported License, permitting all non-commercial use, distribution, and reproduction in any medium, provided the original work is properly cited.

- Selection and peer-review under responsibility of the Organizing Committee of the Conference

© 2023 Published by ISRES Publishing: www.isres.org

Speech recognition algorithms and models have been developed for the Romance-Germanic family and for some Asian languages. However, the models and algorithms developed for these languages are not appropriate for Uzbek. In addition, their implementation in hardware and software is still relevant today and requires special approaches (Мусаев, 2017; Мусаев, et al., 2019; Алимурадов & Чураков, 2015; Musaev, et al., 2020; Мусаев & Рахимов, 2018).

Methodology

A speech signal is a model of a complex dynamic process, the analysis of which relies on several indicators (features) that describe the signal and its fragment. These main features of speech signals are: formant frequency, basic tone frequency, spectral components. Automatic speech recognition systems are implemented in the following stages: Pre-processing, feature extraction, training, and recognition.

The pre-processing consists of signal reception, conversion from analog to digital, filtering. Feature extraction - removes areas of silence, passes through windows, calculates spectral values and MFCC parameters. Training and Recognition - where each speech word is taught and recognized by machine learning and artificial intelligence algorithms according to the parameters obtained. Because speech signals are complex signals, there are problems with processing these signals, storing them in memory, and transmitting them through communication channels. To solve these problems, scientists have proposed approaches such as signal compression in the processing of speech signals, extraction features from the signal, working with signal spectral values. All of this is aimed at simplifying the signal processing process (Musaev et al., 2014; Мусаев & Кардашев, 2014).

The method of finding cepstral coefficients (MFCC - Mel frequency cepstral coefficients) for extraction certain features in speech signals is widely used, and this method is very common in automatic speech recognition. The extraction of the MFCC characteristic properties is determined by calculating the power spectrum, Mel-Spectrum, and Mel-Cepstral (Figure 1). The main advantage of the algorithm is that it allows to recognize and implement speech with a high degree of accuracy (Мусаев & Кардашев, 2014).

In the first stage of the algorithm for calculating the MFCC features, the speech signal recorded from the microphone is divided into 25 msec frames. With the exception of the first frame, each frame includes the last 10 ms of the previous frame. This process is done until the end of the signal. Since in most cases the sampling frequency of the speech signal is 16 KHz, the frame length is $N = 256$ and the shift length is $M = 160$.

When splitting speech signals into frames, it is recommended that the optimal overlap typically cover 50-75% of the frame length. In the second and third stages, a weight window is applied to reduce distortions on the extraction frames and grind them, followed by a spectral replacement procedure. In practice, the use of Hemming window as a window is common.

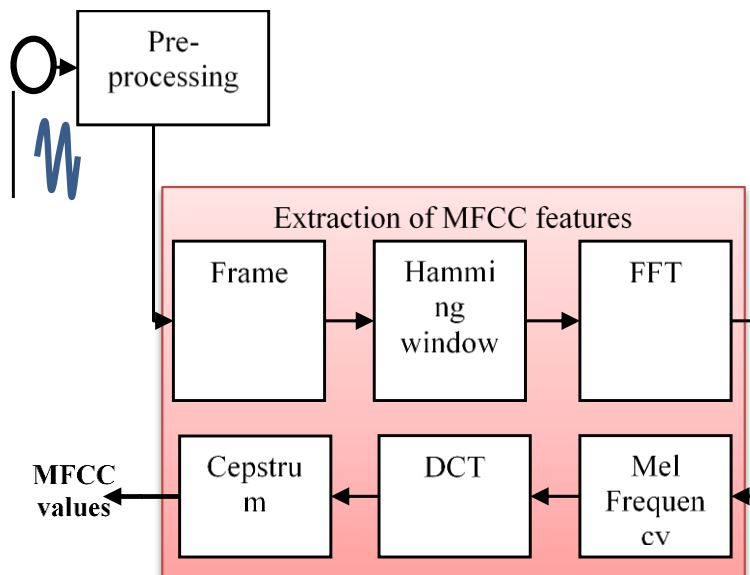


Figure 1. Modern methods of feature extraction of speech signals

Effective algorithms for compressing audio or low frequency signals are based on discrete orthogonal transforms. One of these transforms is the Singular value decomposition (SVD) [20]. The SVD algorithm for modifying a matrix by singular values is one of the most powerful instrumental tools of linear algebra.

There are many ways to reduce the size of data in machine learning with different efficiencies, including by modifying and displaying one-dimensional space to another dimensional space. These methods include PCA (Principal component analysis), ICA (Independent component analysis), NMF (Non-negative matrix factorization) and K-means.

The operations and algorithms used in all speech recognition require a certain complex number of methods and corresponding processing algorithms. Spectral analysis, wavelet transformation, filtering, scraping, cepstral analysis, etc. are performed on different bases of Fourier including. These algorithms and techniques are more difficult to implement in specialized software or hardware systems. This requires a special approach and the implementation of optimal algorithms.

The sequence of speech command interrupt algorithms, depended or in depended to the speaker in the proposed real-time mode, is shown in Figure 2. Recognition of speech commands by this method is performed in the following algorithmic steps.

1. An analog signal in the form of an incoming speech is converted to a digital signal in the form of a 16 kHz frequency.
2. Speech commands clear from external noise and interference.
3. Extraction areas of silence from speech signals.
4. Framing.
5. Henning window.
6. Short time Fourier transform (STFT).
7. Reduce dimensions. The singular value decomposition method was used to reduce the signal size.
8. Determination of formant frequencies.
9. Mel Frequency Cepstral Coefficients (MFCC).
10. Checking and recognizing the conformity of the features.

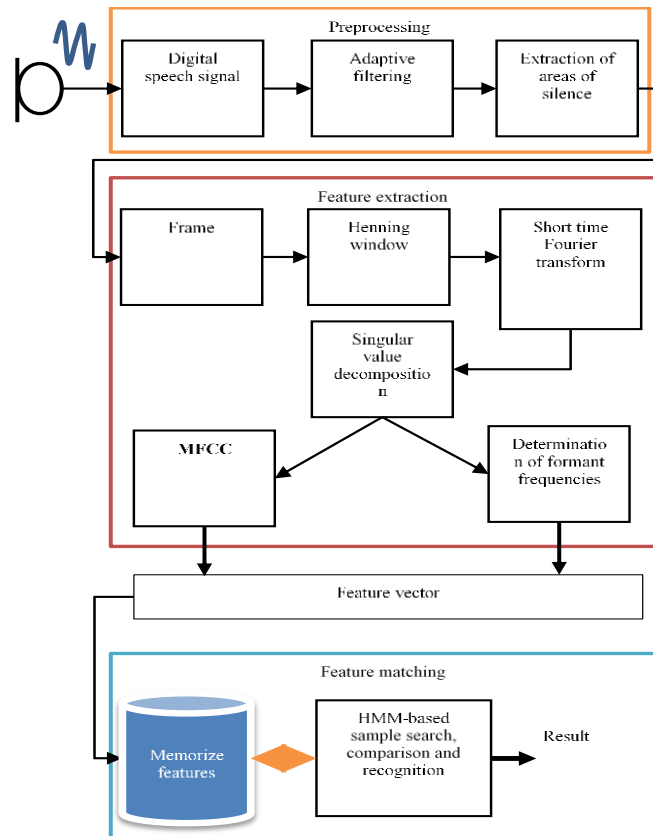


Figure 2. Stages of feature extractions and familiar algorithms from the proposed speech signals.

The process of recognizing speech signals is done through various intellectual processing steps and algorithms. According to the problem statement and speech command recognition requirements, DTW (Dynamic time warping), VQ (Vector quantization), SVM (Support vector machine), HMM (Hidden Markov model), ANN (Artificial neural network) algorithms are common.

The above speech signal processing algorithms can be implemented in the hardware and software part of the computer in different ways using a database of different elements. The elemental database includes a variety of non-programmable and programmable devices.

Experimental Results

The above-mentioned speech command recognition algorithms for recognizing Uzbek speech commands were implemented in the EM3288 module. These words are: “talaba, malika, samalyot, lola, bola, ona, masala, mamlakat, olti, oltin, lochin, lozar, kitob, maktab, archa, chelak, gul, yulduz, sayyora, viloyat, tegirmon, dala, vagon, bekobod, angren, yangiyo'l, yunusobod, umid”.

Recognition of Uzbek speech commands in the EM3288 module showed the following accuracy (Fig.4).

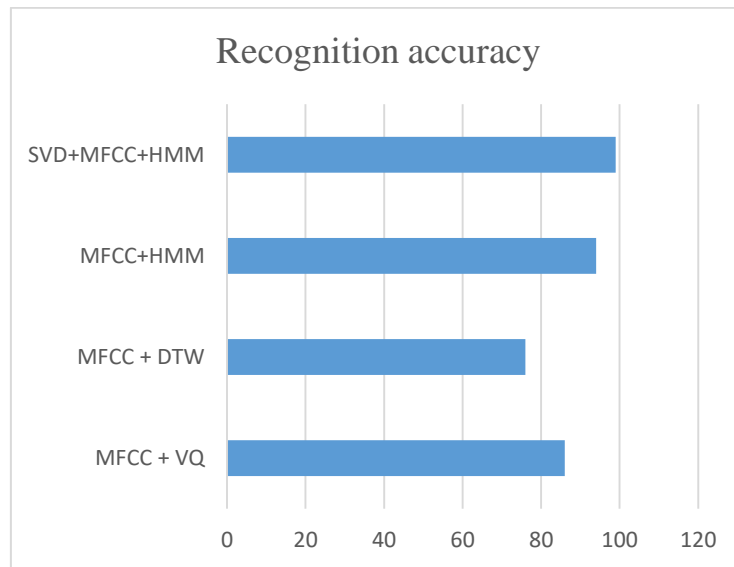


Figure 4. Accuracy of speech command recognition using various algorithms.

From the figure above, it can be seen that the spectral values of the speech signal and the MFCC parameters showed 86%, 76% and 94% accuracy, respectively, when obtained by VQ, DTW and HMM algorithms. The signal parameters obtained by the STFT + SVD algorithms proposed by us showed 98% accuracy when recognized by the HMM algorithm.

Conclusion and Future Work

The built-in EM3288 system comes in handy when implementing speech control systems through speech commands in different environments. Because through this device it is possible to combine algorithms and programs for processing complex speech signals under a single operating system. The HMM model has shown high results in recognizing limited speech commands in embedded systems. Recognition of speech commands in systems installed using the proposed STFT+SVD+HMM algorithm showed 98% accuracy.

References

Алимурадов А.К. & Чураков П.П. (2015). Обзор и классификация методов обработки речевых сигналов в системах распознавания речи. *Измерение.Мониторинг.Управление.Контроль*, 2,12 27-35. [In Russian].

- Bahoura M. & Ezzaidi H. (2013). Hardware implementation of MFCC feature extraction for respiratory sounds analysis. *8th Workshop on Systems, Signal Processing and their Applications (WoSSPA)*, 226-229.
- Mazo M., Rodriguez F.J., Lazaro J.L., Urena J., Garcia J.C., Santiso E., Revenga P. & Garcia J.J. (1995). Wheelchair for physically ultrasonic and infrared sensor control. *Autonomous Robots*, 2, 203-204.
- Melnikoff S.J., Quigley S.F. & Russell M.J. (2001). Implementing a hidden Markov Model speech recognition system in programmable logic. *11-th International Conference on Field Programmable Logic and Applications, Lecture Notes in Computer Scienc*, 2147, 81-90.
- Mosleh M., Setayeshi S., Mehdi Lotfinejad M. & Mirshekari A. (2010). FPGA implementation of a linear systolic array for speech recognition based on HMM. *The 2nd International Conference on Computer and Automation Engineering (ICCAE)*, 3, 75-78.
- Musaev M.M., Berdanov U.A. & Shukurov K.E. (2014). Hardware and software solution signal compression algorithms based on the Chebyshev polynomial. *International Journal of Information and Electronics Engineering*, 5, 380-383.
- Musaev M., Khujayorov I. & Ochilov M. (2020). The use of neural networks to improve the recognition accuracy of explosive and unvoiced phonemes in Uzbek language. *Information Communication Technologies Conference (ICTC)*, 231-234.
- Мусаев М.М. & Кардашев М.С. (2014). Спектральный анализ сигналов на многоядерных процессорах. *Цифровая обработка сигналов*, 3, 82-86. [In Russian].
- Мусаев М. М. (2017). Современные методы цифровой обработки речевых сигналов. *Вестник ТУИТ*, 42, 2-13. [In Russian].
- Мусаев М. М. & Рахимов М. Ф. (2018). Алгоритмы параллельной обработки речевых сигналов. *Вестник ТУИТ*, 46, 2-13. [In Russian].
- Мусаев М.М., Хужаяров И.Ш. & Очилов М.М. (2019). Машинали ўқитиш алгоритмлари асосида ўзбек тили фонемаларини таниб олиш. *Информатика ва энергетика муаммолари*. [In Uzbek].
- Ngos V.V., Whittington J. & Devlin J. (2011). Real-time hardware feature extraction with embedded signal enhancement for automatic speech recognition. *Speech Technologies, Intech*, 29-54.
- Sujuan K., Yibin H., Zhangqin H. & Hui L. (2008). A HMM speech recognition system based on FPGA. *International Congress on Image and Signal Processing (CISP 2008)*, 305-309.
- Tamulevicius G., Arminas V., Ivanovas E. & Navakauskas D. (2010). Hardware accelerated FPGA implementation of Lithuanian isolated word recognition system. *Electronics & Electrical Engineering*, 99, 57-62.
- Vargas F.L., Fagundes R.D.R., & Junior D.B. (2001). A FPGA-based Viterbi algorithm implementation for speech recognition systems. *2001 IEEE International Conference on Acoustics, Speech, and Signal Processing. Proceedings (Cat. No.01CH37221)*, 2, 1217-1220.
- Veitch R., Aubert L.M., Woods R. & Fischhaber S. (2011). FPGA Implementation of a pipelined Gaussian calculation for HMM-based large vocabulary speech recognition. *International Journal of Reconfigurable Computing*, 1-10.

Author Information

Kamoliddin Shukurov

TUIT named after Mukhammad al-Khwarazmi,
Artificial intelligence department, Uzbekistan
Contact e-mail: keshukurov@gmail.com

Umidjon Khasanov

TUIT named after Mukhammad al-Khwarazmi,
Artificial intelligence department, Uzbekistan

Boburkhan Turaev

TUIT named after Mukhammad al-Khwarazmi,
Artificial intelligence department, Uzbekistan

A'lokhan Kakhkharov

TUIT named after Mukhammad al-Khwarazmi,
Artificial intelligence department, Uzbekistan

To cite this article:

Shukurov, K., Khasanov, U., Turaev, B., & Kakhkharov, A. (2023). The effectiveness of the implementation of speech command recognition algorithms in embedded systems. *The Eurasia Proceedings of Science, Technology, Engineering & Mathematics (EPSTEM)*, 23, 220-224.

The Eurasia Proceedings of Science, Technology, Engineering & Mathematics (EPSTEM), 2023

Volume 23, Pages 225-231

ICRETS 2023: International Conference on Research in Engineering, Technology and Science

Improved Tailings Consolidation Using Dewatering Agents: A Step towards Safer and Sustainable Mining Waste Management

Ljupcho Dimitrov

University of Mining and Geology "St. Ivan Rilski"

Irena Grigorova

University of Mining and Geology "St. Ivan Rilski"

Abstract: Tailings consolidation is a critical step in mining waste management. Tailings are a byproduct of mining and mineral processing operations, and they are typically composed of finely ground rock particles, water, and reagents used in the mineral processing. The tailings disposal is a significant environmental and safety concern, as unconsolidated or unstable tailings can result in catastrophic failures and environmental damage. Therefore, it is crucial to use reagents for tailings consolidation to ensure the stability and safety of tailings storage facilities (TSFs). That is the reason to decide to test different dewatering aids to determine which one gives the best results in tailings dewatering. Many experiments were carried out using the reagents Aerodri 104, Aerodri 105, PEG – 400, and polyvinylpyrrolidone K30 and K90. Factors such as water release, consolidation speed, and consolidation time were considered and monitored. The best results are obtained with the Aerodri 104 using 300 g/t and 500 g/t reagents.

Keywords: Consolidation, Dewatering, Flocculants, Tailings disposal

Introduction

Efficient and safe disposal of the waste generated in the mining activity is one of the most important things in the mining industry. Plenty of authors (Tayebi-Khorami et al., 2019; Yankova, 2020; Yankova, 2021), emphasize the critical problems with mining and processing waste along with tailings storage, mining waste amount reduction, and safe storage. Effective waste management is the basis of sustainable development. The tailings from ore and coal processing are composed of fine material, water, and reagents from the process. The traditional tailings disposal in conventional tailings storage facilities (TSF) with high water content and unconsolidated tailings can lead to dam failure and high ecological casualties.

According to Grigorova & Koprev (2020), using an integrated mine waste facility (IMWF) minimizes the overall project footprint and avoids needing a conventional tailings dam because the facility can be progressively rehabilitated while the project is operational. During operations, the external faces of the completed portions of the IMWF can be covered with topsoil and vegetated. This means that the majority of the IMWF can be rehabilitated prior to the end of the mining operations. For this purpose, to ensure better consolidation and water drainage in the facility, reagents can be used. Wide use have the surfactants for dewatering sulfide, non-sulfide flotation concentrates, iron and coal concentrates, tailings and aluminum trihydrate etc. (Besra et al., 1998; Yan et al., 2003; Pears, 2003; Burat et al., 2015; Patra et al., 2016, Rezaei et al., 2020 etc.). The selection of an appropriate reagent depends on many factors, such as water content, particle size distribution (PSD), mineral and chemical composition, and pH of the material and used reagents for the beneficiation process. In the current research, many experiments are conducted so that the suitable reagent is found for dewatering and enhanced consolidation of the tailings. The laboratory tests were conducted using the reagents Aerodri 104, Aerodri 105, PEG 400, and the flocculants PVP K30 and PVP K90. The reagents

- This is an Open Access article distributed under the terms of the Creative Commons Attribution-NonCommercial 4.0 Unported License, permitting all non-commercial use, distribution, and reproduction in any medium, provided the original work is properly cited.

- Selection and peer-review under responsibility of the Organizing Committee of the Conference

© 2023 Published by ISRES Publishing: www.isres.org

consumption was 150, 300, and 500 g/t. They were added as 1 % water-reagent solution. First, the particle size distribution, mineral and chemical composition, pH, water content, suspension density, and dry material density were determined.

Methodology

A thickened tailings sample was collected for the research. The PSD, water content, pH, and chemical and mineral composition were determined. The particle size distribution is determined by wet sieving with sieve openings +75 μm , +45 μm , and +32 μm . The chemical analysis was conducted using the ICP OES analysis, and the mineral composition was studied using X-ray diffraction analysis. In the current experiment, to decrease the water content and enhance faster consolidation are used anionic surfactants from the series Aerodri 104 and 105, manufactured by Cytec, nonionic surfactant PEG-400, delivered by Parchem and the nonionic polymers PVP K30 and PVP K90 made by Roth, Germany. Indicators such as speed and time of consolidation and the volume of water released from the tailings were monitored. The material monitored was with different consumption for each reagent. The consumption was 150, 300, and 500 g/t. All the reagents used are water-soluble and biodegradable, with low toxicity and minimal negative impact on nature.

The first experiment was conducted without adding additional reagents. The test was carried out in a glass cylinder, and the sedimentation rate was monitored every 24 h. The volume of the cylinder was 3930 ml, and the mass of the solid was 3836 g (3.386 kg). Experiments with different reagent consumption were conducted after determining the sample consolidation rate without reagent. The impact of the different consumption on the consolidation rate was determined. The tailings used for the different experiments had the same characteristics. The solid content was 61%, tailings density 1.60 g/cm^3 , and dry solid density 2.60 g/cm^3 . All the experiments were conducted in cylinders with 4 l volume. The measurements were taken from the initial start to the top of the consolidated layer of solids. The consolidation rate is determined by calculating the sedimentation rate.

Results and Discussion

The particle size distribution is determined by wet sieve analysis with sieves sizes +75 μm , +45 μm , +32 μm . The results show that the tailings are composed mostly of (75.36 %) particles - 32 μm (Table 1). The results from the conducted ICP OES analyses (table 2) show that the main components in the tailings sample are mainly SiO_2 and less Al_2O_3 , Fe_2O_3 , and K_2O . Minor amounts (< 1%) of other oxides and sulfur are present.

Table 1. Particle size distribution

Size sieve	Yield		Oversize	Undersize
μm	g	%	%	%
75	3.57	3.44	3.44	96.56
45	6.89	6.7	10.14	89.86
32	17.9	14.49	24.63	75.36
-32+0	77.47	75.36	99.99	0
Total	102.8	99.99	-	-

Table 2. Chemical composition of the tailings

Components	Content (wt %)
SiO_2	70.69
Al_2O_3	9.07
Fe_2O_3	4.69
TiO_2	0.51
CaO	0.64
MgO	0.40
MnO	0.13
Na_2O	0.16
K_2O	3.75
P_2O_5	0.07
SO_3	0.50
Loss on ignition	4.97
Moisture	0.45
S	< 0.05

The data from the X-ray diffraction (XRD) study show that the tailings are composed chiefly of quartz (66%), feldspars – potassium feldspar, and plagioclase (3%). In small percent, there are also clay minerals – kaolinite (6%) and muscovite or hydromica–illite (6%). Also, carbonates - calcite (2%) and dolomite (2%) are present in the waste. The presence of sulfides is not found. The ore minerals are composed of minimal quantities of iron oxides - ilmenite or titanomagnetite (1%) and hematite (< 0.05%).

Tailings Consolidation Experiments

Sedimentation Rate Determination of the Solids in the Tailings, without Additional Reagents

A well-homogenized 3930 ml tailings sample was poured into a 4-liter cylinder. The consolidation process was monitored by measuring the height of the newly formed clear water volume and the height of the consolidated solids every 24 hours till the end of the consolidation process. The 24 h readings continued for eight days from the experiment's start till the consolidation process's end. The consolidation ended when the solids layer will not change its height. In this experiment, the height of the volume of water reached 10 cm. Both the volume of the solids and the sedimentation rate were calculated. The obtained results are given in Table 3 and Figure 1. The data shows that without any additional reagents, the consolidation of the tailings is slow, and it takes seven days till complete consolidation.

Table 3. Sedimentation rate of the sampled tailings

Consolidation time, h	24	48	72	96	120	144	168
Height of the volume of water, cm	3.2	5.3	7.3	8.8	9.5	9.7	10
Height of the solids layer, cm	39.8	37.7	35.7	34.2	33.5	33.3	33
The volume of the solids layer, ml	3577.0	3388.3	3208.5	3073.7	3010.8	2992.8	2965.9
Sedimentation rate, mm/min	0.0222	0.0184	0.0169	0.0153	0.0132	0.0112	0.0099

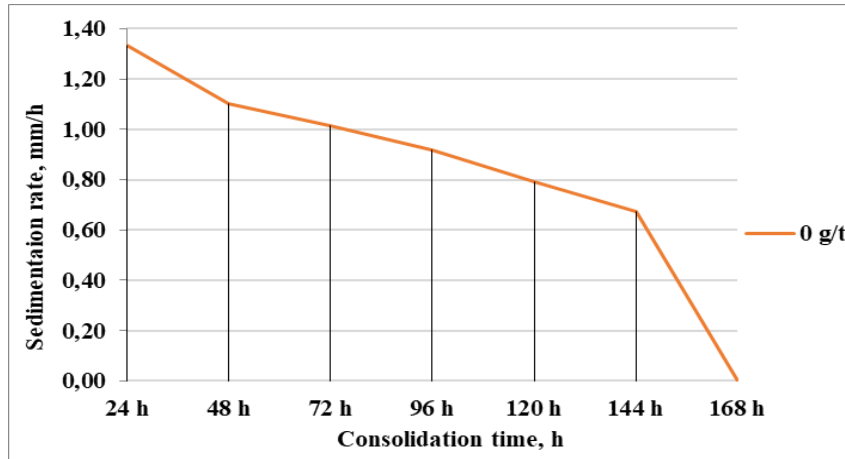


Figure 1. Sedimentation rate as a function of consolidation time

Consolidation Rate Determination of the Tailings Solids, with Added Additional Reagents

The impact of the Aerodri 104, Aerodri 105, PEG-400, PVP K30 and PVP K90 was studied with a series of laboratory experiments. The reagents were added as a 1% solution into the 3930 ml tailings, with a 1.6 g/cm³ density and solid content of 3836 g (3.386 kg). The laboratory tests were conducted in four separate tests for each one of the reagents. The tailings were placed in 4-liter cylinders and the reagent was added as 0, 150, 300 and 500 g/t for each cylinder. The height of the volume of water and the volume of solids was monitored every 24 hours and the sedimentation rate was calculated.

Determining the Impact of the Aerodri 104 over the Consolidation of the Tailings

The results show that the Aerodri 104 gives the best outcome with reagent consumption of 300 and 500 g/t, with which the consolidation time is shortened for two days compared to the results without adding additional reagents (Figure 2). With the 500 g/t reagent consumption the sedimentation rate is at its highest.

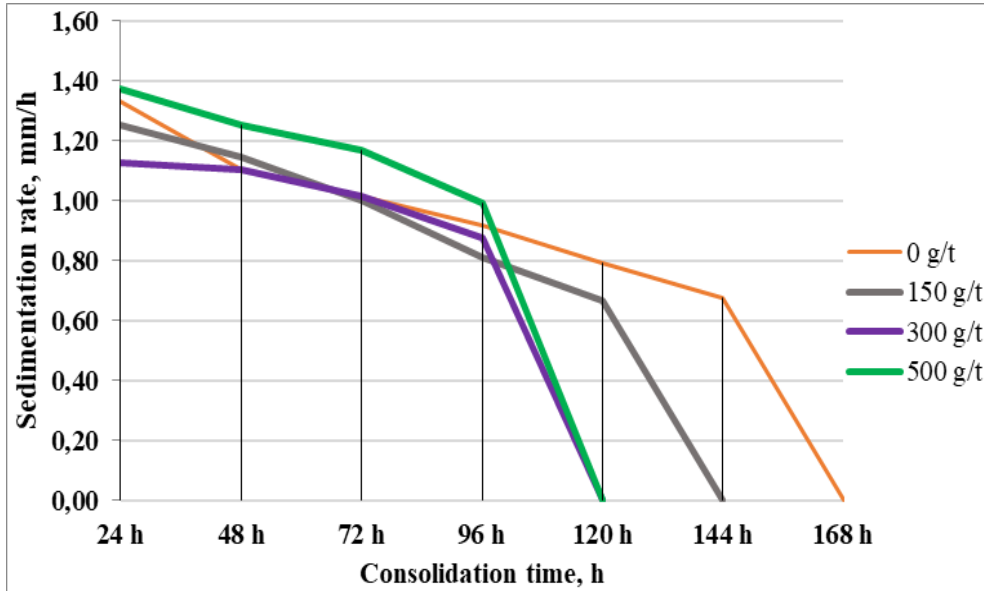


Figure 2. Sedimentation rate as a function of different Aerodri 104 dosage

Determining the Impact of the Reagent Aerodri 105 over the Consolidation Rate of the Tailings

The results from the experiments with adding Aerodri 105 with a consumption of 300 and 500 g/t show that the consolidation time reduces by one day compared to the sample without additionally added reagents (Figure 3). The dewatering surfactants from the series Aerodri 104 and 105 show different results, and it might be because of the difference in viscosity, which is higher in Aerodri 105.

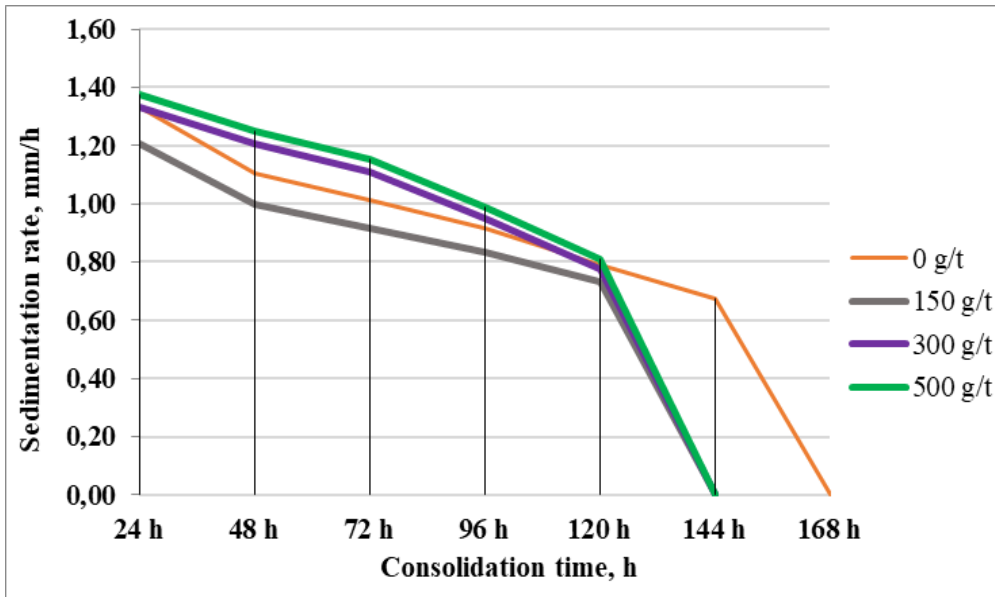


Figure 3. Sedimentation rate as a function of different Aerodri 105 dosage

Determining the Impact of the PEG-400 over the Consolidation Rate of the Tailings

The reagent PEG 400 is a low molecular weight polyethylene glycol (average about 400), biodegradable and low toxicity. Therefore, it has a variety of applications, including in the pharmaceutical industry. According to some authors, PEG-400 is an effective surfactant that can be used for dewatering different mineral raw materials, coal, tailings, etc. PEG-400 increases the hydrophobicity of solid mineral particles (Burat et al., 2015).

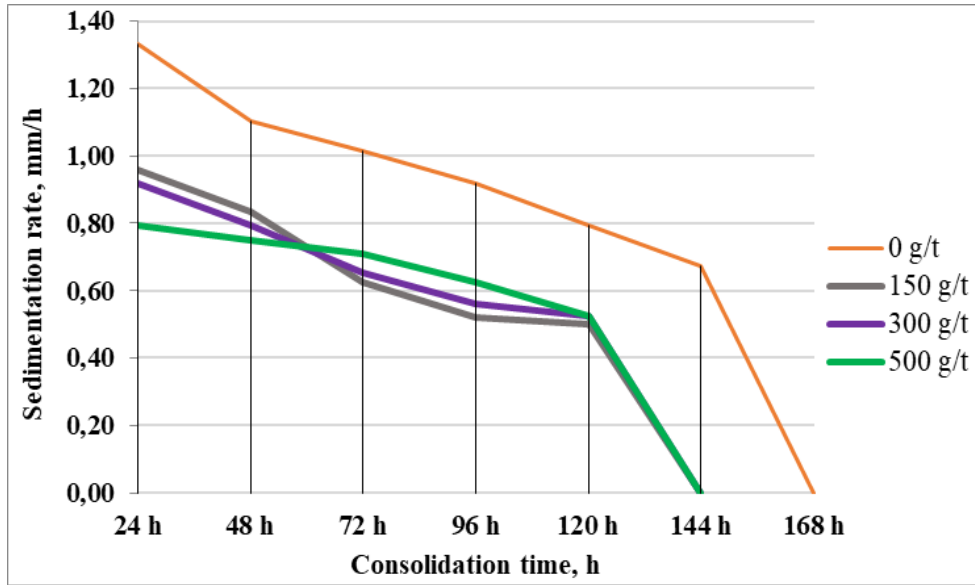


Figure 4. Sedimentation rate as a function of different PEG 400 dosage

The data from the laboratory experiments show that the different reagent dosage does not significantly affect tailings dewatering (Figure 4). At all different reagent dosages (150, 300, and 500 g/t), the sedimentation rate remained almost the same and lower than that without added reagents (Figure 4). It should be noted that the consolidation time decreases by one day, but the water content in the volume of the solid phase substance does not decrease significantly. It was found that this reagent was unsuitable for the tailings consolidation.

Determining the Impact of the Reagent PVP K30 over the Consolidation of Tailings

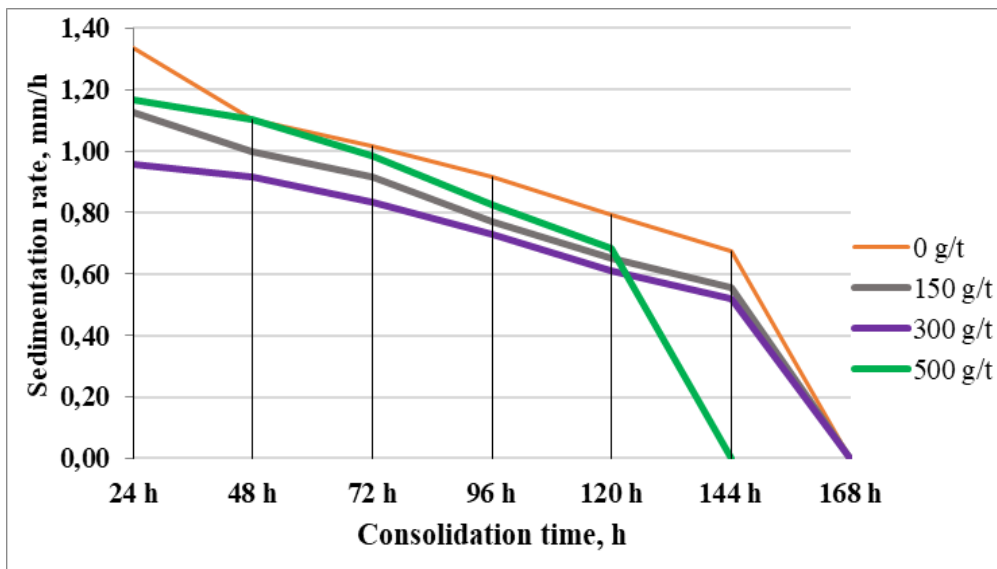


Figure 5. Sedimentation rate as a function of different PVP K30 dosage

The reagents from the series PVP (K25, K30, K60, K90 etc.) are flocculants and nonionic biopolymers. The value of K is related to the molecular weight of the polymer and characterizes its viscosity in a water solution. At larger coefficient K values, the polymer's viscosity in water solution is greater, and the adhesion properties are much stronger. According to Wang et al. (2021) polyvinylpyrrolidone (PVP) is a polymeric flocculant that adsorbs on the surface of quartz and kaolinite particles at low doses and eases their aggregation. The same authors consider that polyvinylpyrrolidone (PVP) can be successfully applied for the removal of quartz and clay impurities in coal flotation. Due to the high content of quartz (66%) and the presence of kaolinite in the flotation tailings, experiments were carried out to enhance the consolidation with the application of PVP K30 and PVP

K90. The data from the four laboratory tests showed that with the use of PVP K30, at a consumption of 500 g/t, the settling time of the solid phase is accelerated and compared to gravity settling and is shortened by one day (Figure 5).

Determining the Impact of the Reagent PVP K30 over the Consolidation of Tailings

Adding 300 and 500 g/t PVP K90 the highest sedimentation rate is reached. The consolidation stops on the second day after adding the PVP K90, but there is not enough dewatering as with the rest of the reagents. When 150 g/t is added, the sedimentation rate is even less than the sample without any additional reagents. The results show that the PVP K90 does not give a satisfactory result as it does not release enough volume of water (Figure 6).

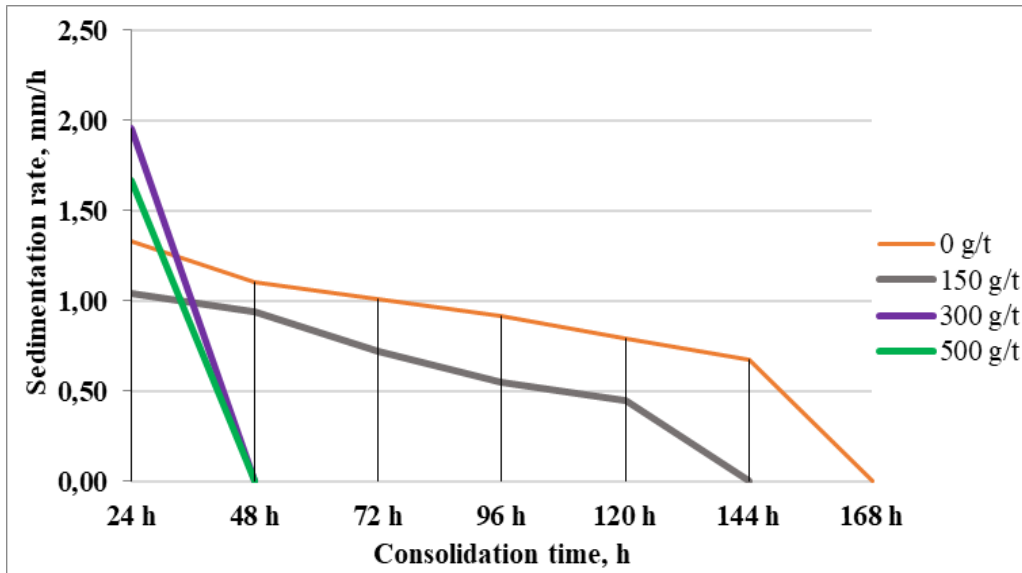


Figure 6. Sedimentation rate as a function of different PVP K90 dosage

The data from the experiments show that when the reagent consumption is lower, the settling rate is also low, and the settling rate increases with increasing reagent consumption. When PVP K90 is added, the tailings turn from slurry to paste in seconds, making mixing even more difficult. The best results are given by Aerodri 104, with the shortest consolidation time and high settling speed.

Conclusion

The results of the series of laboratory experiments for the determination of a suitable reagent to shorten the time of tailings consolidation showed that the most appropriate reagent is the surfactant Aerodri 104. With a consumption of 500 g/t Aerodri 104, the consolidation time shortens for two days compared to the sample without additional reagents. A shorter consolidation time will enhance the operational sequence and improve water drainage. That means that, the construction of the next bench can begin earlier hence a new cell will be available sooner than without additional reagent. Also, the water will be released faster and can be reused in the process. When adding the surfactant, the consolidated tailings do not have a lower moisture content than the one without additional reagent. The high content of fine mineral particles (75.36%) has an adverse effect. Some authors (Patra et al., 2016) note that the fine particles adsorb much moisture due to their extensive surface area, and that leads to higher water content hence it is difficult to significantly lower the moisture content in flotation tailings and concentrates.

Scientific Ethics Declaration

The authors declare that the scientific ethical and legal responsibility of this article published in EPSTEM journal belongs to the authors.

Acknowledgments

* This article was presented as an oral/poster presentation at the International Conference on Research in Engineering, Technology and Science (www.icrets.net) held in Budapest/Hungary on July 06-09, 2023.

* This research is supported by the Bulgarian Ministry of Education and Science under the National Program "Young Scientists and Postdoctoral Students – 2".

References

- Besra, L., Sengupta, D. K., & Roy, S. K. (1998). Flocculant and surfactant aided dewatering of fine particle suspensions: A review. *Mineral Processing and Extractive Metallurgy Review: An International Journal*, 18, 67-103.
- Burat, F., Sirkeci, A. A., & Onal, G. (2015). Improved fine coal dewatering by ultrasonic pretreatment and dewatering aids. *Mineral Processing and Extractive Metallurgy Review: An International Journal*, 36, 129-135.
- Grigorova, M. & Koprev, I. (2020). Mining and technical conditions in open pit "Khan Krum" gold mine in Southeastern Bulgaria. *XI International Scientific Conference Geobalcanica*. Republic of North Macedonia.
- Yan, D., Parker, T. & Ryan, S. (2003). Dewatering of fine slurries by the Kalgoorlie Filter Pipe. *Minerals Engineering*, 16, 283–289.
- Yankova, T. (2020). Mineral processing waste utilization. *XX International Multidisciplinary Scientific GeoConference SGEM 2020*. Albena, Bulgaria.
- Yankova, T. (2021). Mining damaged landscape reclamation study, *XXI International Multidisciplinary Scientific GeoConference SGEM 2021*.
- Patra, A. S., Makhija, D., Mukherjee, A. K., Tiwari, R., Sahoo, C. R., & Mohanty, B. D. (2016). Improved dewatering of iron ore fines by the use of surfactants. *Powder Technology*, 287, 43-50.
- Pearse, M. J. (2003). Historical use and future development of chemicals for solid–liquid separation in the mineral processing industry. *Minerals Engineering*, 16, 103–108.
- Rezaei, A., Abdollahi, H., Gharabaghi, M., & Mohammadzadeh, A. A. (2020). Effects of flocculant, surfactant, coagulant, and filter aid on efficiency of filtration processing of copper concentrate: Mechanism and optimization. *Journal of Mining and Environment (JME)*, 11, 1, 119-141.
- Tayebi Khorami, M., Edraki, M., Corder, G. & Golev, A. (2019). Re-thinking mining waste through an integrative approach led by circular economy aspirations, *Minerals*, 9 (286), 1–12.
- Wang, Y., Zhou, W., Li, Y., Liang, L., Xie, G. & Peng, Y. (2021). The role of polyvinylpyrrolidone in the selective separation of coal from quartz and kaolinite minerals. *Colloids and Surfaces A: Physicochemical and Engineering Aspects*, 626, 1-7.

Author Information

Ljupcho Dimitrov

University of Mining and Geology "St. Ivan Rilski"
Sofia, Bulgaria
Contact e-mail: ljupcho.dimitrov@mgu.bg

Irena Grigorova

University of Mining and Geology "St. Ivan Rilski"
Sofia, Bulgaria

To cite this article:

Dimitrov, L., & Grigorova, I. (2023). Improved tailings consolidation using dewatering agents: A step towards safer and sustainable mining waste management. *The Eurasia Proceedings of Science, Technology, Engineering & Mathematics (EPSTEM)*, 23, 225-231.

The Eurasia Proceedings of Science, Technology, Engineering & Mathematics (EPSTEM), 2023

Volume 23, Pages 232-240

ICRETS 2023: International Conference on Research in Engineering, Technology and Science

Evaluation of the Spread of Respiratory Diseases in the City of Batna Cover a Period of Five Years (2018-2023)

Sahraoui Nabil
University of Batna 2

Laidoune Abdelbaki
University of Batna 2

Abstract: Respiratory diseases pose a major public health concern in many cities worldwide, and the city of Batna is no exception. Over the past five years (2018-2023), respiratory diseases have likely been one of the primary health concerns for healthcare professionals and public health authorities in this region. This article provides an in-depth evaluation of the spread of these diseases in the city of Batna, focusing on trends, risk factors, high-risk seasons, and implications for public health and presents a comprehensive evaluation of the spread of respiratory diseases in the city of Batna over a five-year period, from 2018 to 2023. Respiratory diseases constitute a major public health issue in this urban region and have been a significant concern for healthcare professionals and authorities. The study methodology relies on extensive data collection from hospitals, health centers, and clinics in Batna, taking into account demographic, climatic, and environmental factors. Trend analysis reveals seasonal variations and significant increases in the spread of respiratory diseases. Risk factors such as air pollution, outbreaks of respiratory viruses, smoking, and housing conditions are also examined. The findings provide recommendations to improve prevention, early diagnosis, and management of respiratory diseases, with the goal of reducing their impact on the population of Batna. This study offers future perspectives to strengthen public health strategies and deepen the understanding of the mechanisms of disease propagation. By highlighting these crucial aspects, this article contributes to raising awareness among policymakers and healthcare professionals about the importance of combating respiratory diseases in this specific region.

Keywords: Respiratory diseases, Health, Disease propagation

Introduction

Respiratory diseases have long been a significant global health concern, affecting millions of people and imposing a substantial burden on healthcare systems (Jerrett et al., 2005). In urban areas, such as the city of Batna, these diseases can escalate due to various factors like pollution, population density, and lifestyle habits. Understanding the patterns and dynamics of respiratory disease propagation is vital for effective public health (planning and intervention strategies (Brunekreef & Holgate, 2002).

Atmospheric pollutants can have significant adverse effects on human health, impacting various organ systems and leading to a range of health problems. Some major effects of atmospheric pollutants on health include: Respiratory issues: Air pollutants, particularly fine particulate matter (PM_{2.5}), ozone (O₃), nitrogen dioxide (NO₂), sulfur dioxide (SO₂), and carbon monoxide (CO), can irritate the respiratory system (Hamra, G. et al., 2014). Prolonged exposure to these pollutants can lead to conditions such as asthma, chronic obstructive pulmonary disease (COPD), bronchitis, and respiratory infections (Eisner et al., 2010). Cardiovascular problems: Air pollution has been linked to an increased risk of cardiovascular diseases, including heart attacks, strokes, and hypertension. Particulate matter and gaseous pollutants can enter the bloodstream and cause i

- This is an Open Access article distributed under the terms of the Creative Commons Attribution-NonCommercial 4.0 Unported License, permitting all non-commercial use, distribution, and reproduction in any medium, provided the original work is properly cited.

- Selection and peer-review under responsibility of the Organizing Committee of the Conference

© 2023 Published by ISRES Publishing: www.isres.org

nflammation and oxidative stress, contributing to cardiovascular issues. Neurological effects: Some pollutants, such as lead and certain volatile organic compounds (VOCs), can negatively affect the nervous system (Dockery & Pope, C. A. (2020). Long-term exposure to these substances may impair cognitive function, cause developmental delays in children, and increase the risk of neurodegenerative diseases. Allergies and exacerbation of existing conditions: Air pollution can worsen allergy symptoms and trigger asthma attacks in susceptible individuals (Hoek, G., et al., 2013). Pollutants can irritate the airways and make people more sensitive to allergens. Cancer (Guarnieri, & Balmes, 2014) : Certain airborne pollutants, such as benzene, formaldehyde, and polycyclic aromatic hydrocarbons (PAHs), are considered carcinogenic. Prolonged exposure to these substances increases the risk of developing various types of cancer, including lung cancer. Reduced lung function: Children and adolescents exposed to high levels of air pollution may experience reduced lung growth and impaired lung function, leading to long-term health implications (Lozano et al., 2012)

This article delves into the evaluation of respiratory disease spread within the city of Batna over a comprehensive five-year period, spanning from 2018 to 2023. The study aims to shed light on the prevalence, trends, risk factors, and seasonal variations of these diseases, providing crucial insights for public health authorities and healthcare practitioners. By conducting a thorough analysis of data collected from hospitals, health centers, and clinics, along with relevant demographic, climatic, and environmental factors, this research offers an in-depth understanding of the challenges posed by respiratory diseases in the urban context of Batna.

Overview of Major Respiratory Diseases: Asthma, COPD, Lung Cancer.

Major respiratory diseases, such as asthma, chronic obstructive pulmonary disease (COPD), and lung cancer, are significant health issues that affect the airways and lungs. Here's an overview of each of these diseases:

Asthma: Asthma is a chronic disease of the airways that causes breathing difficulties. It is characterized by episodes of wheezing, coughing, shortness of breath, and a feeling of tightness in the chest. These symptoms are often triggered by allergens (such as dust, pollen, and animal dander) or irritants (such as cigarette smoke and air pollutants) (Balmes, 2019). Asthma can affect people of all ages and can be managed with medications, inhalers, and avoiding triggers.

Chronic Obstructive Pulmonary Disease (COPD): COPD is a chronic respiratory disease characterized by progressive obstruction of the airways (Lelieveld et al., 2015). The primary risk factors for COPD are smoking (both active and passive smoking) and exposure to air pollutants. Symptoms include persistent cough, excessive mucus production, difficulty breathing, and shortness of breath. COPD is a severe and progressive disease, but treatments can help slow its progression and relieve symptoms (Schikowski et al., 2015).

Lung Cancer: Lung cancer is a malignant tumor that forms in the lung tissues. It is often associated with smoking, but it can also affect individuals who have never smoked, although this is less common (Raghu et al., 2017). Symptoms may include persistent cough, coughing up blood, unexplained weight loss, and chest pain. Lung cancer is a serious disease and can spread to other parts of the body. Treatments vary based on the stage and type of cancer, including surgery, chemotherapy, radiation therapy, and immunotherapy (Di et al., 2017).

Pollution of Area of Batna:

Unfortunately, like many urban cities, Batna also faces issues of air pollution. The main sources of air pollution in this region are usually related to industrial activities, traffic emissions, power plant emissions, as well as agricultural practices and residential heating. (Cohen et al., 2017). The primary air pollutants that can be present at concerning levels in the city of Batna include:

Fine Particulate Matter (PM_{2.5} and PM₁₀): These are small solid or liquid particles suspended in the air, originating from fossil fuel combustion, road dust, agriculture, and industry (Qian et al., 2015). These particles can penetrate deep into the respiratory system and cause health problems, especially for individuals with pre-existing respiratory conditions.

Sulfur Dioxide (SO₂): This gas mainly comes from the combustion of sulfur-containing fossil fuels, such as coal and diesel. It can irritate the airways and worsen respiratory issues in sensitive individuals.

Tropospheric Ozone (O₃): Low-level ozone is a secondary pollutant formed by the chemical reaction between nitrogen oxides (NO_x) and volatile organic compounds (VOCs) in the presence of sunlight. It can cause respiratory irritation and worsen asthma and other respiratory problems. (Buist et al., 2007).

Nitrogen Oxides (NO_x): These gases primarily come from vehicle emissions and industrial facilities. They can contribute to the formation of tropospheric ozone and worsen air quality (Kelly & Fussell 2012).

Volatile Organic Compounds (VOCs): They are emitted by chemicals, solvents, paints, exhaust fumes, and other sources. In the presence of NO_x, they can contribute to the formation of tropospheric ozone and poor air quality (Pope & Dockery, 2006).

Air pollution in Batna can be more pronounced during periods of hot and dry weather, when meteorological conditions can contribute to the stagnation of pollutants. Air pollution can have a negative impact on the health of the population, especially on sensitive individuals such as children, the elderly, and those with chronic respiratory problems.

To address this issue, it is essential for local and national authorities to implement effective measures to reduce pollutant emissions and improve air quality in the city of Batna. This may include promoting cleaner transportation modes, controlling industrial emissions, raising public awareness, and adopting more sustainable environmental and energy policies.

Respiratory Diseases in the city of Batna: Causes and Consequences

Respiratory diseases in the city of Batna are influenced by various causes and have significant consequences on public health. Here is an overview of the main causes and consequences of these respiratory diseases.

Causes of Respiratory Diseases in Batna:

Air pollution: Air pollution caused by industrial emissions, dense traffic, agricultural practices, and residential heating is a major cause of respiratory diseases in Batna. Fine particulate matter, nitrogen oxides, sulfur dioxide, and volatile organic compounds present in polluted air can irritate the airways and worsen existing respiratory conditions (Guarnieri, M., & Balmes, 2014).

Smoking: Active and passive smoking remains a major concern in the city of Batna. Smokers and non-smokers exposed to secondhand smoke are at risk of developing respiratory problems, such as asthma, chronic bronchitis, and obstructive lung diseases. (Raaschou Nielsen et al., . 2013)

Environmental factors: Environmental conditions, such as dry and dusty climate or occupational exposures to toxic substances, can contribute to the development of respiratory diseases among the residents of Batna.

Social and economic factors: Poor living conditions, low-quality housing, and limited access to healthcare can also play a role in the prevalence of respiratory diseases (Adeloye, et al., 2015).

Consequences of Respiratory Diseases in Batna:

Increased hospitalizations: Respiratory diseases lead to an increase in hospital admissions in Batna, putting additional pressure on healthcare services and medical resources.

Impact on quality of life: Individuals suffering from respiratory diseases may experience breathing difficulties, frequent symptoms, and a significantly reduced quality of life.

School and work absenteeism: Respiratory diseases can result in high rates of school and work absenteeism, affecting productivity and education.

Increased risk of complications: Individuals with chronic respiratory diseases are more susceptible to developing severe complications during respiratory disease outbreaks such as influenza or viral respiratory infections. To address these challenges, it is crucial to implement preventive and public health measures to reduce the causes of respiratory diseases, such as promoting clean transportation, enforcing stricter industrial

emission standards, conducting anti-smoking campaigns, and improving environmental and living conditions for the residents of Batna. A multidisciplinary approach involving local authorities, healthcare professionals, and the community is necessary to protect the respiratory health of Batna's population and enhance overall quality of life in the city.

Method

Clinical examinations and syndromic surveillance systems in addition to laboratory surveillance are tools that allow reliable statistics on respiratory diseases. The data collected per year allowed us to have an idea of the state of spread of respiratory diseases in the city of Batna and to make an evaluative approach in terms of the impact of the factors which are at the origin of the genesis of these damages. The test of the evaluation of the degree of impact of the risk factors which are important in our city, namely: pollution due to vehicles, air pollution due to discharges from neighboring factories: ceramic factories and cement factories without forget the impact of cigarettes on the health of the population because the number of smokers continues to increase from year to year.

Presentation of Survey Results:

Table 1. Distribution of the main respiratory diseases cover the period 2018-2023

Respiratory diseases/years	Asthma	COPD	Lung Cancer
2018	1223	1226	191
2019	1492	1419	212
2020	641	888	201
2021	742	867	194
2022	1910	1146	246
2023	1416	1237	273

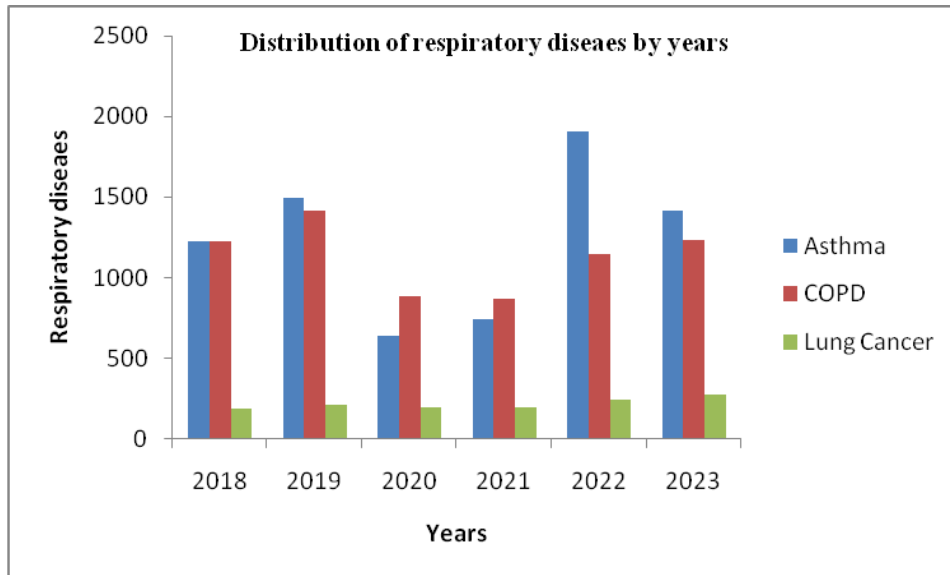


Figure 1. Graphical representation of the distribution of respiratory diseases during the period 2018-2023

Table 2. Spread of asthma by age group during the period 2018-2023

Respiratory disease(Asthma)	Asthma	Asthma	Asthma
Age group	13-30 ans	30-50 ans	Sup 50 ans
2018	523	425	275
2019	689	502	301
2020	315	222	104
2021	412	204	126
2022	735	699	476
2023	566	463	387

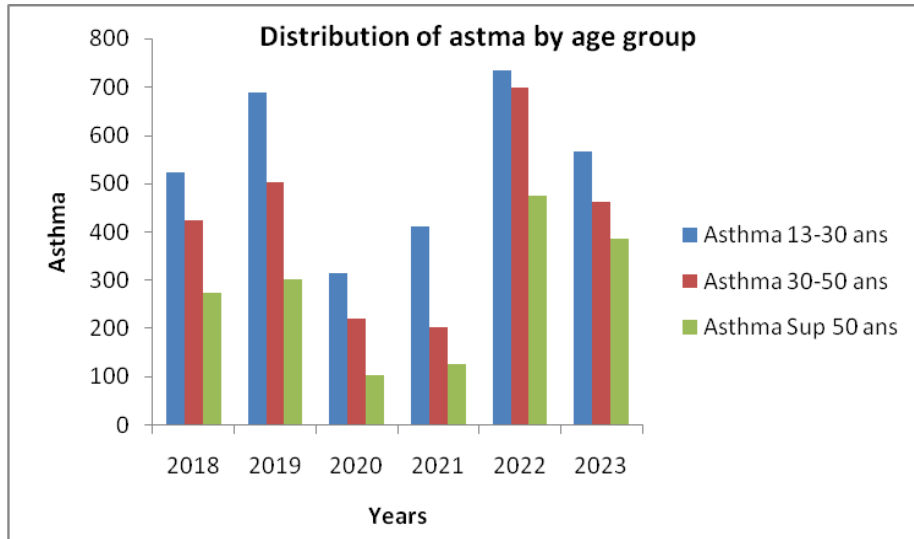


Figure 2. Graphic representation of the spread of asthma by age group during the period 2018-2023

Table 3. Spread of COPD by age group during the period 2018-2023

Respiratory disease (COPD)	COPD	COPD	COPD
Age group	13-30	30-50	Sup 50
2018	236	365	625
2019	256	412	751
2020	165	321	402
2021	145	266	456
2022	325	345	476
2023	312	356	569

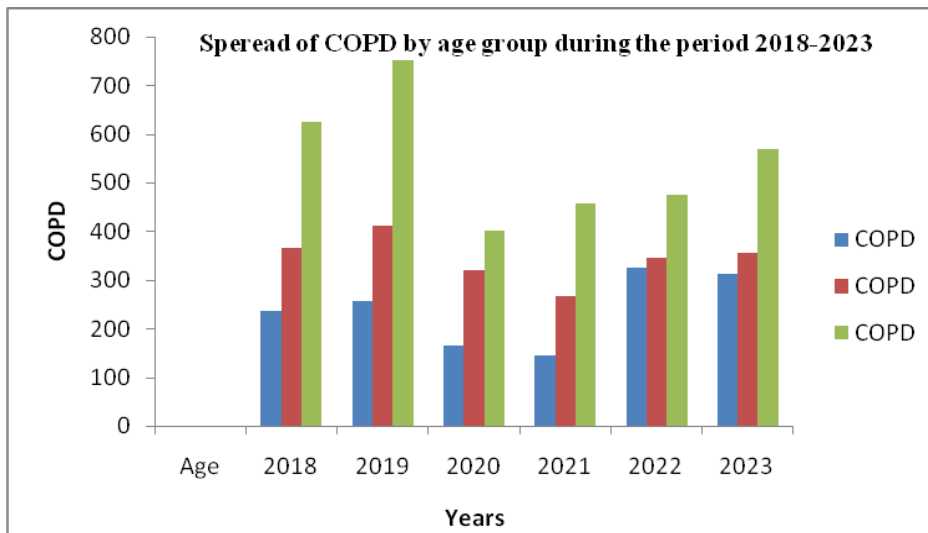


Figure 3. Graphic representation of the spread of COPD by age group during the period 2018-2023

Table 4. Spread of Lung cancer by age group during the period 2018-2023

Respiratory disease (Lung cancer)	Lung cancer	Lung cancer	Lung Cancer
Age group	13-30 years	30-50 years	Sup 50 years
2018	12	77	102
2019	13	67	132
2020	9	56	136
2021	6	45	141
2022	8	69	169
2023	8	88	177

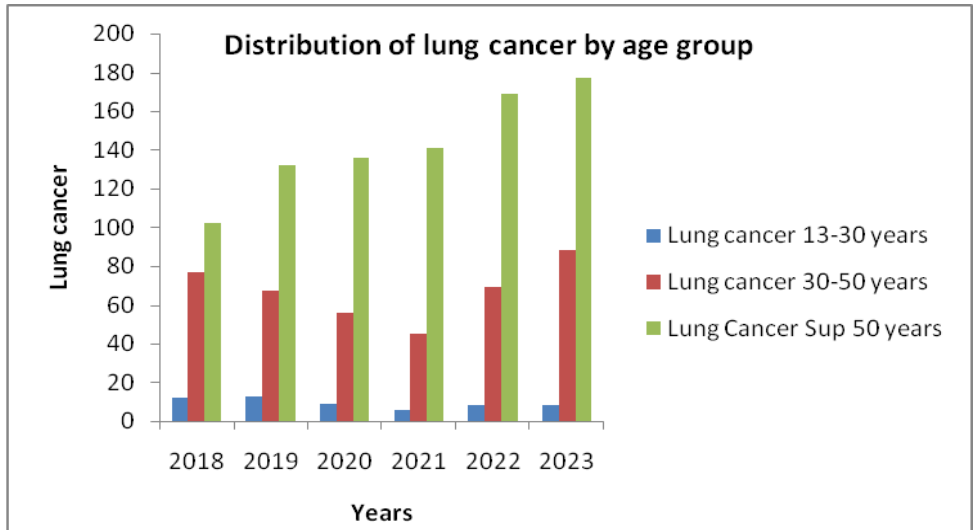


Figure 4. Graphic representation of the spread of lung cancer by age group during the period 2018-2023

Table 5. Spread of respiratory diseases by sex during the period 2018-2023

Respiratory diseases Sex	Asthma		BPCO		Lung Cancer	
	Male	Feminine	Male	Feminine	Male	Feminine
2018	864	359	1012	214	184	7
2019	1123	369	1236	183	208	4
2020	496	145	613	275	196	5
2021	587	155	625	242	188	6
2022	1645	265	1146	177	238	8
2023	1263	153	1123	114	269	4

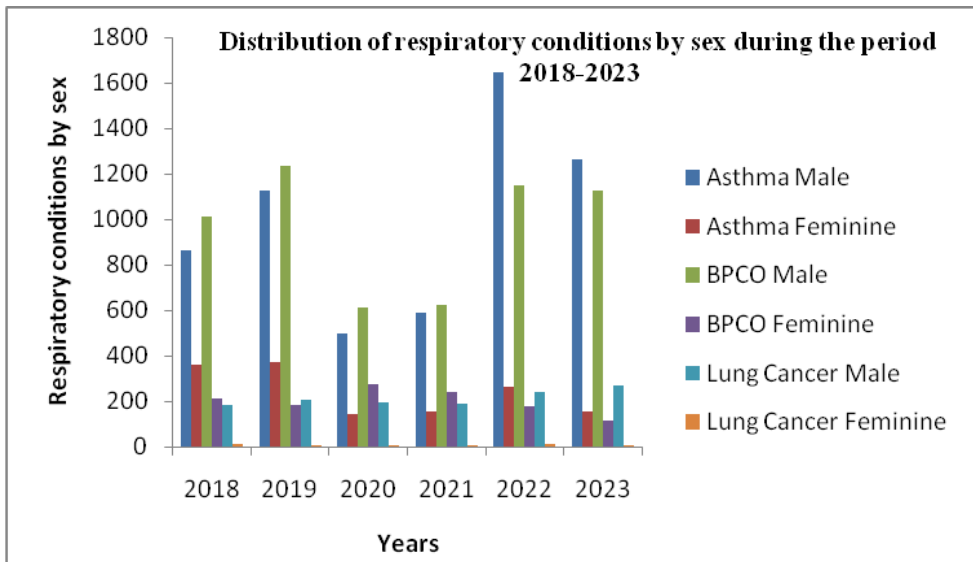


Figure 5. Graphic representation of the spread of respiratory diseases by sex during the period 2018-2023

Results and Discussion

According to the results obtained dealing with the spread of respiratory diseases during the period of 2018-2023, it is noted that the situation is alarming in view of the number of people affected and more particularly the age group 30-50 years and over. 50 years old, is this due to several risk factors which are:

The pollution rate is high since the city of Batna is surrounded by very polluting factories such as ceramics manufacturing factories and cement factories. in addition, according to statistics, the number of smokers in this age group is very high and exceeds 60%.

Confirmation illustrated by the results presented in Tables 1,2,3,4 and 5 consolidated by graphic representations, which indicate that the number of people affected by major respiratory diseases: Asthma, BPCO and Lung cancer are growing significantly while the fall in values during the years 2020-2021 are due to total containment and the closure of factories completely for two years due to COVID-19.

It should also be noted that according to the results of the spread of respiratory diseases during the period 2018-2023, we note that the female segment is very little affected by these respiratory diseases is this is mainly due to: the rate of women who smoke is negligible, exposure to pollutants is minimal, because according to our tradition the woman spends most of her time at home, something that is confirmed by the results see table and fig 5. Smoking is the main risk factor for the development of respiratory diseases, including asthma, chronic bronchitis and chronic obstructive pulmonary disease (COPD). Cigarette smoke irritates the airways and damages the lungs, which can lead to reduced breathing capacity and an increased risk of respiratory infections. Lung cancer: Smoking is the most common cause of lung cancer. Cigarette smoke contains carcinogenic substances that damage the DNA of lung cells, thus promoting the growth of cancer cells (Pope III, et al., 2011).

Conclusion

Through our study it appears that the city of Batna is exposed to a serious problem of the spread of respiratory diseases especially among men and more particularly among the category of 30-50 years and 50 years and over and this is mainly due to the high pollution rate caused by the fumes of exhaust gases from dilapidated vehicles as well as the smoke from factories bordering the towns: ceramic factories and cement factories in addition to the high rate of smokers in the city. This study will serve as a springboard and database for attempts to resolve this scourge which causes a health disaster and a huge loss in terms of therapeutic care for this type of complicated and often irreversible disease.

Recommendations

To overcome this problem, it is imperative to take the following decisions: Imposing a depollution system on neighboring factories or else closing them, renewing old vehicles that generate a high level of pollution, carrying out an intense awareness campaign on the health risks of cigarettes and applying the new regulations prohibiting smoking cigarettes in public spaces to dissuade people from quitting smoking, without forgetting treatment in public hospitals.

Scientific Ethics Declaration

The authors, Dr Sahraoui Nabil & Dr Laaidoue Abdelbaki, declare that the scientific ethical and legal responsibility of this article published in EPSTEM journal belongs to the authors.

Acknowledgements or Notes

* This article was presented as an oral presentation at the International Conference on Research in Engineering, Technology and Science (www.icrets.net) held in Budapest/Hungary on July 06-09, 2023.

* Our thanks go to the managers of the health structures for their collaboration.

References

- Adeloye, D., Chua, S., Lee, C., Basquill, C., Papan, A., Theodoratou, E., Nair, H., Gasevic, D., Sridharar, D., Campbell, H., Chan, K. Y. Sheikh, A., & Rudan, I. (2015). Global and regional estimates of COPD prevalence: Systematic review and meta-analysis. *Journal of Global Health*, 5(2), 020415.
- Balmes, J. R. (2019). Air pollution and lung disease in low- and middle-income countries. *Seminars in Respiratory and Critical Care Medicine*, 40(05), 568-575.

- Buist, A. S., McBurnie, M. A., Vollmer, W. M., Gillespie, S., Burney, P., Mannino, D. M., ... & Jensen, R. L. (2007). International variation in the prevalence of COPD (the bold study): A population-based prevalence study. *The Lancet*, 370(9589), 741-750.
- Brunekreef, B., & Holgate, S. T. (2002). Air pollution and health. *The Lancet*, 360(9341), 1233-1242.
- Cohen, A. J., Brauer, M., Burnett, R., Anderson, H. R., Frostad, J., Estep, K., ... & Forouzanfar, M. H. (2017). Estimates and 25-year trends of the global burden of disease attributable to ambient air pollution: an analysis of data from the global Burden of diseases study 2015. *The Lancet*, 389(10082), 1907-1918.
- Di, Q., Amini, H., Shi, L., Kloog, I., Silvern, R., Kelly, J., ... & Schwartz, J. D. (2017). An ensemble-based model of PM_{2.5} concentration across the contiguous United States with high spatiotemporal resolution." *Environmental Science & Technology*, 51(15), 8811-8820.
- Dockery, D. W., & Pope, C. A. (2020). Acute respiratory effects of particulate air pollution. *Annual Review of Public Health*, 41, 413-434.
- Eisner, M. D., Anthonisen, N., Coultas, D., Kuenzli, N., Perez Padilla, R., Postma, D., ... & Romieu, I. (2010). An official American Thoracic Society public policy statement: Novel risk factors and the global burden of chronic obstructive pulmonary disease. *American Journal of Respiratory and Critical Care Medicine*, 182(5), 693-718.
- Guarnieri, M., & Balmes, J. R. (2014). Outdoor air pollution and asthma. *The Lancet*, 383(9928), 1581-1592.
- Guarnieri, M., & Balmes, J. R. (2014). Air pollution and airway disease. *Clinical & Experimental Allergy*, 42(5), 705-714.
- Hamra, G. B., Guha, N., Cohen, A., Laden, F., Raaschou-Nielsen, O., Samet, J. M., ... & Vineis, P. (2014). Outdoor particulate matter exposure and lung cancer: A systematic review and meta-analysis. *Environmental Health Perspectives*, 122(9), 906-911.
- Han, L., Zhou, W., Li, W., Li, X., & Lin, L. (2018). Fine particulate matter air pollution and elderly hospital admissions for chronic obstructive pulmonary disease: A case-crossover study in the Pearl River Delta, China. *Environmental Pollution*, 236, 208-214.
- Hoek, G., Krishnan, R. M., Beelen, R., Peters, A., Ostro, B., Brunekreef, B., & Kaufman, J. D. (2013). Long-term air pollution exposure and cardio-respiratory mortality: A review. *Environmental Health*, 12(1), 1-15.
- Jerrett, M., Burnett, R. T., Ma, R., Pope III, C. A., Krewski, D., Newbold, K. B., ... & Thurston, G. (2005). "Spatial analysis of air pollution and mortality in Los Angeles." *Epidemiology*, 16(6), 727-736.
- Kelly, F. J., & Fussell, J. C. (2012). Air pollution and airway disease. *Clinical & Experimental Allergy*, 42(5), 705-714.
- Lelieveld, J., Evans, J. S., Fnais, M., Giannadaki, D., & Pozzer, A. (2015). The contribution of outdoor air pollution sources to premature mortality on a global scale. *Nature*, 525(7569), 367-371.
- Lozano, R., Naghavi, M., Forema, K., Lim, S., Shibuya, K., Aboyans, V.,... & Murray, C. J.L. (2012). Global and regional mortality from 235 causes of death for 20 age groups in 1990 and 2010: A systematic analysis for the global burden of disease study 2010. *The Lancet*, 380(9859), 2095-2128.
- Pope III, C. A., Burnett, R. T., Turner, M. C., Cohen, A., Krewski, D., Jerrett, M., ... & Thurston, G. D. (2011). Lung cancer and cardiovascular disease mortality associated with ambient air pollution and cigarette smoke: shape of the exposure-response relationships. *Environmental Health Perspectives*, 119(11), 1616-1621.
- Pope, C. A., & Dockery, D. W. (2006). "Health effects of fine particulate air pollution: Lines that connect. *Journal of the Air & Waste Management Association*, 56(6), 709-742.
- Qian, Z., He, Q., Lin, H. M., Kong, L., Liao, D., & Dan, J. (2015). Short-term effects of gaseous pollutants and particulate matter on daily hospital admissions for cardio-respiratory diseases in urban China. *Environmental Pollution*, 199, 91-98
- Raaschou-Nielsen, O., Andersen, Z. J., Beelen, R., Samoli, E., Stafoggia, M., Weinmayr, G., ... & Hoek, G. (2013). Air pollution and lung cancer incidence in 17 European cohorts: prospective analyses from the European study of cohorts for air pollution effects (escape). *The Lancet Oncology*, 14(9), 813-822
- Raghu, G., Chen, S. Y., Yeh, W. S., Maroni, B., Li, Q., & Lee, Y. C. (2017). Collagen content in lung parenchyma as a marker of disease and predictor of mortality in COPD. *Respiratory Research*, 18(1), 207.
- Schikowski, T., Adam, M., Marcon, A., Cai, Y., Vierkötter, A., Carsin, A. E., ... & Jacquemin, B. (2015). Association of ambient air pollution with the prevalence and incidence of COPD. *European Respiratory Journal*, 44(3), 614-626.

Author Information

Sahraoui Nabil

University of Batna 2

Batna, Algeria

Contact e-mail: n.sahraoui@univ-batna2.dz

Laidoune Abdelbaki

University of Batna 2

Batna, Algeria

To cite this article:

Nabil, S. & Abdelbaki, L. (2023). Evaluation of the spread of respiratory diseases in the city of Batna cover a period of five years (2018-2023). *The Eurasia Proceedings of Science, Technology, Engineering & Mathematics (EPSTEM)*, 23, 232-240.

The Eurasia Proceedings of Science, Technology, Engineering & Mathematics (EPSTEM), 2023

Volume 23, Pages 241-252

ICRETS 2023: International Conference on Research in Engineering, Technology and Science

From Human to Robot Interaction towards Human to Robot Communication in Assembly Systems

Ikrom Kambarov

Friedrich-Alexander-University (FAU),
Turin Polytechnic University in Tashkent

Jamshid Inoyatkhodjaev

Turin Polytechnic University

David Kunz

Friedrich-Alexander-University (FAU),

Matthias Brossog

Friedrich-Alexander-University (FAU),

Jörg Franke

Friedrich-Alexander-University (FAU),

Abstract: The interaction between humans and robots has been a rapidly developing technology and a frequently discussed research topic in the last decade because current robots ensure the physical safety of humans during close proximity assembly operations. This interaction promises capability flexibility due to human dexterity skills and capacity flexibility due to robot accuracy. Nevertheless, in these interactions, the humans are marginally outside of the system, while the robots are seen as a crucial component of the assembly activities, which causes the systems to lack flexibility and efficiency. Therefore, this paper presents a study on Human to Robot communication in assembly systems. We conducted a systematic review of related literature and industrial applications involving human and robot interaction modes over the last decade to identify research gaps in the integration of collaborative robots into assembly systems. We believe that we are in a transformation phase from physical interaction mode towards cognitive interaction mode between humans and robots, where humans and robots are able to interact with each other during mutual working conditions and humans are able to guide robots. The main contribution of this paper is to propose a future mode of human-robot interaction in which a skilled operator performs not only physical cooperative tasks with robots but also work aided by smart technologies that allow communication with robots. This interaction mode allows for an increase in the flexibility and productivity of the assembly operation as well as the wellbeing of the human operator in a human-centered manufacturing environment.

Keywords: Human robot communication, Human robot interaction, Industry 4.0, Industry 5.0.

Introduction

Manufacturing has evolved over time, and the future vision is for a more sustainable, resilient, and human-centered manufacturing sector (Xun et al., 2021). Simultaneously, the market is demanding more customized products with

- This is an Open Access article distributed under the terms of the Creative Commons Attribution-Noncommercial 4.0 Unported License, permitting all non-commercial use, distribution, and reproduction in any medium, provided the original work is properly cited.

- Selection and peer-review under responsibility of the Organizing Committee of the Conference

© 2023 Published by ISRES Publishing: www.isres.org

improved final product quality and continuously decreasing production times, which challenges the manufacturing sectors to manage flexibility requirements in the assembly operations. The authors of the paper (Carsten et al., 2016) argue that the efficiency of managing these assembly flexibilities in production might be achieved by integrating humans and robots in the same assembly operation. Because, according to (Romero et al., 2016), assembly operations can benefit from capacity flexibility due to robot accuracy and speed and capability flexibility due to human dexterity skills.

Human-robot interaction (HRI) is growing automation trend in which robots are integrated into manual assembly operations (Tsarouchi et al., 2016), can facilitate safe interaction between human and robot resources. By integrating robots into the same assembly cell with human, robot can deal with heavy lifting, repetitive tasks, and tasks that require high accuracy, while the human focuses on tasks that need the flexibility skills of the human (Müller & Vette, 2016).

As a result, HRI systems have been one of the most widely debated topics in the last decade; however, research to date indicates that interactions between humans and robots are associated with physical interaction between resources and are focused on the human experience (Carsten et al., 2016). Consequently, it is time to investigate a new interaction mode in human-robot interaction systems, in which humans are viewed as an essential part of the assembly operations. We argue that this new mode of human-robot interaction opens up new possibilities for the assembly operation, enhancing its efficiency and flexibility. Therefore, this paper investigates the future mode of human-robot interaction as a smart and skilled worker who performs not only "collaborative tasks" with robots but also "work aided" by using aided technologies to interact with robots. In this paper, we analyzed the current state of the art in human-robot interaction in the past decade. After giving some background research topics covered by human robot interaction systems in the last decade, we simply narrow our focus to define the future human-centered human robot communication assembly system framework.

The outlines of this paper are the following. Section 3 provides a review of human and robot interaction modes over the last decade, additionally research topics covered by academia and industry, industrial applications, the opportunities and challenges of existing interaction modes. Then Section 4 starts to define HRI research gaps in assembly operations and concludes with a visualization of the current state. Section 5 highlights the vision of a future human robot interaction mode under human-centered assembly operations and suggests the framework of the new human centered human robot communication mode. Finally, it concludes and highlights the future research directions.

Literature Review

An assembly workstation that combines human and robot resources is known as a human-robot interaction system. (Abdelfetah et al., 2019). The systematic literature analysis showed that humans have excellent cognitive ability and adaptability skills, whereas robots are more efficient at executing repetitive and non-ergonomic tasks more efficiently and with a consistent level of accuracy (Chryssolouris et al., 2017). The following Table 1 summarizes the most valuable characteristics of humans and robots' resources when they work in close proximity during assembly operations.

Table 1. Human and robot characteristics

Advantages skills of human	Advantages skills of robots
Special attention is paid to:	Special attention is paid to:
High availability	Integrated process control
Handling of complex components	Handling heavy, sharp-edged components
Reliable execution of complex joining processes	Exact playback of defined paths
Simple magazine loading of components	Reliable performance of repetitive activities

The proper integration of robots into manual assembly systems opens many new possibilities. By integrating robots into manual assembly systems, new applications are enabled, and assembly processes can be built up more

efficiently by integrating robots into manual assembly systems or by using assistive robots for repetitive and non-ergonomic tasks controlled by a human (Romero et al., 2016). Alternatively, the investment in automation equipment can be concentrated on the most important manufacturing steps, maintaining a high degree of flexibility with respect to reconfiguring of the production equipment and human dexterity, while still introducing a partial degree of automation. In assembly operations, combining the best abilities of humans and robots can improve productivity (Kuhlenkötte, 2016) and ergonomic factors (Chryssolouris et al., 2016).

Human and Robot Interaction Research Topics

The quantity of research studies has increased during the past decades on human-robot interaction in assembly operations, because current robots ensure the physical safety of humans during close proximity assembly operations. Nevertheless, a crucial question continues: how should a human-robot interaction system be designed in the assembly operations? The literature analysis showed that the recent human-robot interaction studies focus on the investigation of physical interaction between resources (Flacco et al., 2012). The goal of this research allows close proximity between human and robot during the assembly tasks that need the high characteristics of the robot in terms of accuracy, speed, and payload. Considered the above motivation of human and robot interactions in assembly processes, the following three main research categories in HRI can be divided, which are shown in Figure 1, can be identified an interaction mode related topic, safety interaction topics, and task distribution related topic.

Interaction related topics	Coexistence Cooperation mode Collaborative mode
Safety related topics	Safety monitored Speed and Separation Power and Force Limiting
Task distribution related topics	Task assignment Task allocation Resource planning

Figure1. HRI main research topics

Interaction Mode Related Research Topics

In recent years, the interaction between humans and robots has been divided into three main modes based on their shared workstation and tasks during assembly operations. These three classifications of human-robot interaction are explained as follows (Lihui et al., 2020):

- **Coexistence mode:** the task is performed by humans and robots independently of each other;
- **Cooperation mode:** the task performed by humans and robots after each other, also known as synchronous mode.
- **Collaborative mode:** the common task is performed by humans and robots at the same time.

Coexistence, cooperation, and collaboration are different types of interactions. The cooperation and collaboration modes are distinguished by the close proximity of resources. In coexistence mode, humans and robots work on different subtasks.

Safety-Related Research Topics

Today's robots can work closely with humans and perform assembly tasks in tandem with them (Waurzyniak, 2015). Furthermore, these developments result in violations of established safety standards and the removal of physical barriers between assembly workstations (Robla Gómez et al., 2017). The robots are able to move their bodies by force, very quickly, and always handle dangerous and sharp equipment. Therefore, the following safety and mode research topics are considered when designing human-robot interaction systems.

- **Safety monitored stop:** In this type of interaction, robots are defined by minimal interaction with humans. Usually, these types of robots are actually similar to industrial robots, with several sensors that stop robot execution when a human enters the work space. The coexistence mode is the best example of a safety monitored stop (Galín & Meshcheryakov, 2019; Maurice, 2014).
- **Speed and separation:** In this type of interaction, robots are embedded with more advanced vision technologies that slow their task execution when an operator approaches and decrease their speed when a worker is close to the robot. The cooperation mode can be an example of this type of interaction (Galín & Meshcheryakov, 2019; Murtua et al., 2017).
- **Power and force limiting:** these types of collaborative robots are embedded with collision sensors to rapidly recognize human touch and slow execution. The collaboration mode can be an example of this type of interaction.

We argue that future research on safety and mode in human–robot interaction should not only focus on optimizing the performance of the robot but also include human wellbeing and focus on human-centered perspectives (Galín & Meshcheryakov, 2019; Khalid et al., 2017).

Task Distribution Related Research Topics

Task distribution during human-robot interaction is based on combining the respective strengths of humans and robots in close proximity during the assembly operation. Humans, with their flexibility and decision-making skills, are able to react to defective components or changing parameters of parts and assembly processes. Robots' advantages include their accuracy, repeatability, ability to handle heavy loads, and endurance (Thomos, Bjoem, & Kuhlenkötter, 2016). Finally, the following Table 2 summarizes the respective strengths of humans and robots in industrial applications for task allocation between resources.

Table 2. Human and robot characteristics

Human Characteristics	Robot Characteristics
Special attention is paid to	Special attention is paid to
Flexibility	Speed
Cognitive	Power
Dexterity	Precision
Creativity	Repeatability
Decision making	Endurance

The research activities performed on task distribution between human and robots during the last decade performed on the following key words which is summarized in the following Table 3.

Table 3. Task distribution research topics

Mode of task distribution	Focus
Task assignment	Process oriented (Muller et al., 2016), Economic and work capability aspects (Blankemeyer, et al., 2020), technical, qualitative, economic, safety indexes (Gualtieri et al., 2019), weight, displacement, accuracy requirements, dexterity requirements (Bruno & Antonelli, 2018).
Task allocation	Task complexity, Ergonomics Payload Repeatability (Dianatfar et al., 2019), task characteristics and agent capabilities (Liau & Ryu, 2020), task complexity (Malik & Bilberg, 2019), capability based (Ranz et al., 2017)
Resource planning	Resource suitability, resource availability and process time (Tsarouchi et al., 2017)

In their research (Mateus et al., 2019), they subdivided the assembly tasks into the following a six-step hierarchy by using a CAD model. The first step is called operation, followed by subassembly, task, function, function stage, and motion levels. Then, in their research (Nikolakis et al., 2018), they distributed the collaborative tasks among resources into two step hierarchy models that collected data by task and operation. At that time, they applied a multi-criteria decision-making structure for offline task allocation and online rescheduling. Then, (Tsarouchi, et al., 2016) proposed the structure for task allocation using three cases; resource suitability, resource availability, and operation time.

Based on the above literature, we can conclude that the research highlighted above is mostly concentrated on task allocation based on criteria instead of the optimization of assembly performance. Nevertheless, (Bänziger et al., 2018) optimized queue time and moving distance within the hybrid workstation. Then (Dalle Mura & Dini, 2019) concentrated on cost reduction, the number of skilled operators, and energy load variance issues in an assembly system. In their investigations, both researchers used a genetic algorithm. Finally, the available studies concerning task assignment in a human-robot interaction system focused only on resource analysis-based task assignment or optimization of task assignment.

We believe that task allocation between humans and robots is one of the most important steps in the design of human-robot interaction systems. An efficient task allocation guarantees the safety and ergonomics of humans and the optimum performance in terms of cycle time and flexibility of the hybrid assembly system. Therefore, we think future task allocation between humans and robots needs more human-centered studies that explore the conditions under which human operators still feel responsible for the cognitive, decision-making, and supervision conditions of the overall assembly operation.

Method

A comprehensive review of the literature to synthesize the effects of HRI in assembly operations has been conducted. The review methodology is described in following subsections.

Search Criteria

We conducted a systematic review of the literature for papers published between 2010 and 2022 that used collaborative robots in assembly operations. Practical experiments and key words like "human and robot collaboration," "assembly, task allocation," "task assignment," and "resource planning" between humans and robots were included in the reviewed papers. An electronic search on databases to cover relevant publications in engineering from both academia and manufacturing (Scopus, Science Direct, IEEE Xplore, and Web of Science) was conducted. Data collection was preceded by deep learning of key research field input words between 2010 and 2023. We decided to look at research papers published after 2010, because HRI is a novel approach that emerged at the beginning of this decade. Both conference papers and journal articles were included. We finalized the search in April 2023. Keywords used for each criterion are presented in Table 4.

The search resulted in 739 papers: 178 papers from Scopus, 284 papers from IEEE Xplore, 155 papers from Science Direct and 122 papers from Web of Science.

Table 4. Keywords for each criteria

Criteria	Search phase
Involves human and robot	Collaborative, cooperation or coexistence
Studies about assembly and safety control	Safety monitored Speed and separation Power and force limiting
Refers to task distribution	Task assignment, allocation and resource planning

Study Selection

We filtered the studies using three main steps to eliminate papers that were not related to the focus of this review. The data collection methodology for this paper is depicted in Figure 2.

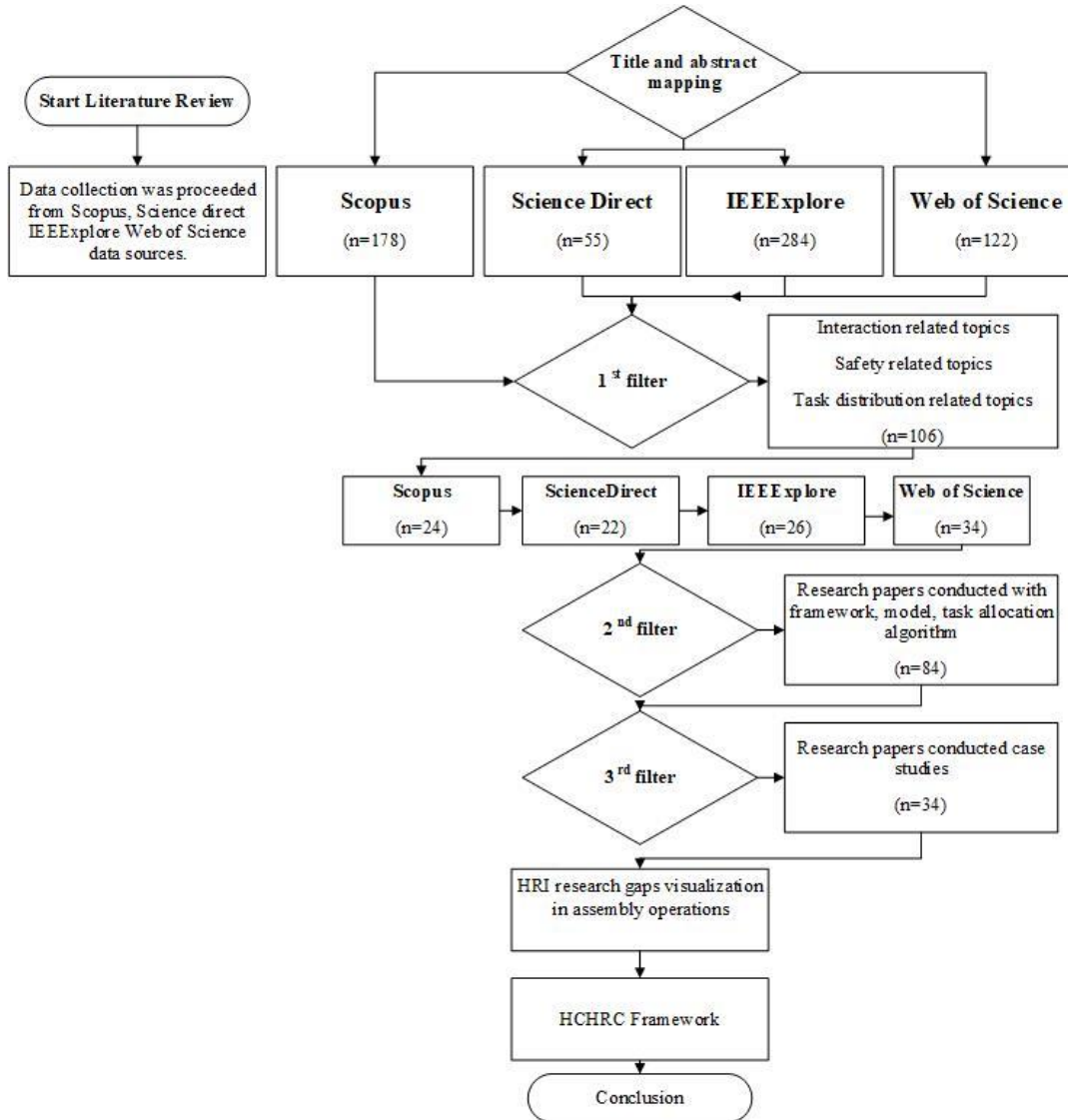


Figure 2. Methodology for data collection

Results and Discussion

Robots as a Central Part of the Interaction

The majority of HRI research topics to date has considered robots as the core of the assembly operations, while humans have been considered peripheral (Blankemeyer, et al., 2020). This interaction between human and robot was supposed to reduce the workload for the human operator through physical assistance by robots. When it comes to trust in robots, we defined that loss of trust happens over time in actual assembly operations. This led to the systems suffering from flexibility and efficiency. In addition to this, most studies are conducted in laboratory conditions and focus on short-term physical interaction between humans and robots, and there is little research on communication structures.

Lack of Larger Team Interaction

Another research gap is that recent human-robot interaction has been performed with a single operator and robots, and there has been no research on larger team structures with other factory workers or robot programming without the requirement of expert knowledge. Novel programming approaches, such as gestures or speech, and augmented reality must be introduced to avoid the bottleneck of traditional interaction modes.

HRI Design Methodology

Due to the fact that HRI assembly research is still in its initial stages, no mature integration methodology has been developed. HRI assembly systems involve much more human-related uncertainties than traditional assembly systems, where everything is pre-programmed and hence under strict control. Therefore, the integration of human operators and robots in the same environment remains a challenging research task. To achieve these goals, proper design methods must be addressed, which means control laws, sensors, task allocation, and planning approaches that allow the human operator to safely stand close to the robot, actively sharing the working area and tasks, and providing the interaction system with the required flexibility.

HRI Assembly System Efficiency

The current HRI assembly systems still suffer from low efficiency. Assembly efficiency may be lower than that of human assembly teams or robotic assembly teams. There is a critical capability missing from the current HRI assembly system. A very small number of sensors are installed, as well as intelligence algorithms. To improve current HRI assembly systems, we need to take full advantage of human cognitive skills. Therefore, we need to design a user-friendly interface so that human operators can easily communicate with the robot during assembly operations. In the following Figure 3 we summarized the visualization of identified research gaps in HRI in assembly operations.

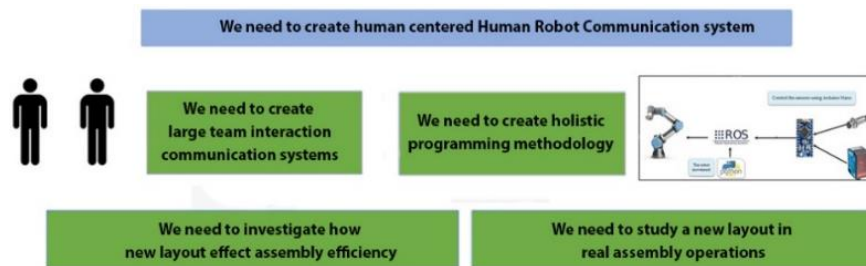


Figure 3. HRI research gaps visualization in assembly operations

Human Centered Human-Robot Communication (HCHRC) Framework

Designing a user-friendly interface that enables easy communication between human operators and the robot during assembly processes is essential to properly utilizing human cognitive capacities. On the one hand, providing inputs to the robot and programming it should be intuitive for the worker so that the operator is less concerned with how to communicate and can focus on the tasks and goals at hand. The information provided as feedback by the robot, on the other hand, should be sufficient to provide the user with the situational awareness required to comprehend the current system behavior and facilitate intervention in dynamic and unforeseen situations. To meet these objectives, actual design approaches must be taken, including control laws, sensors, task allocation, and planning strategies that permit the human operator able to works close with the robot in a safe manner while actively sharing the working place and tasks and giving the interaction system the necessary flexibility.

Generally speaking, future human and robot interaction in assembly systems should focus on how human operators supported by robots and advanced technologies in sociotechnical environment to satisfy human wellbeing in hybrid

human robot interaction teams. The following Figure 4 summarizes the future human centered human robot communication (HCHRC) framework during assembly operations.

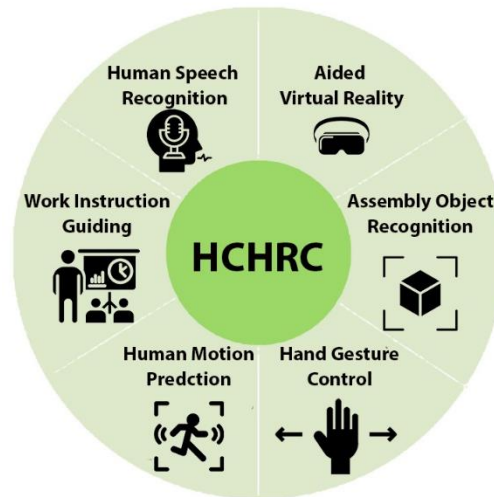


Figure 4. The future human and robot communication framework during assembly operation

The application of the Internet of Things (IoT) technology to assembly processes is the keystone of HCHRC systems. Every assembly workstation, storage location, piece of equipment, product, worker and robots embedded with sensors to communicate in real-time specific data. An assembly work instruction system leverages these data to implement proper models and methods to automatically manage and configure the assembly operations. This HCHRC framework eases the development of different applications which define the main characteristics of human centered assembly operation.

Aided Virtual Reality

Aided virtual reality training will be first step towards HCHRC, because VR technology can provide a combination of interactive virtual reality and advanced simulations of realistic scenarios for optimized decision-making and training for the smart operator during close proximity with collaborative robot. During assembly operation with collaborative robots, the worker is aided through augmented reality devices, as head-worn displays, which suggest the sequence of activities to complete an assembly task considering the customer personalization. Cobots automatically adjust their configuration in real-time to best fit with the worker physique and the assembly task features. Moreover, cobots provide to the worker an artificial force to perform hazardous activities reducing the ergonomic risk of strenuous tasks.

Aided virtual reality technology offer many significant benefits (e.g. decrease assembly cycle times, reliability, reduced failure rate and traceability of human) to support the smart operator in real-time during close proximity with robots by becoming a digital assistance system for reducing human errors and at the same time reducing the dependence on printed work instructions, computer screens and operator memory, which need to be interpreted first by a skilled worker (Romero et al., 2016).

Besides, aided virtual reality technology can comprise a new human-robot interface to manufacturing IT applications and assets, disposing real-time response about assembly processes and robots to the operator in order to improve decision-making (Gorecky et al., 2014). This can be applied at machine level using traditional Programmable Logic Controllers (PLCs) and Supervisory Control & Data Acquisition (SCADA) systems nonetheless also emerging Internet of Things (IoT) technologies for assets assembly sequences monitoring. In addition aided virtual reality technologies can be implemented also at mid-level operations like Manufacturing Execution Systems (MES), novel production line simulations and big data-driven quality controls and at higher levels such as the Enterprise Resource Planning (ERP) systems.

Assembly Object Recognition

Assembly operations involving both human operators and robots provide a unique co-working environment (Bjoen et al., 2016). As a result, object recognition is one of the building blocks of future HCHRC assembly systems. Within an operation, the object can include various physical information, such as assembly tools and assembly parts. A human operator can easily perceive all of the mentioned object recognition information in a communication assembly operation using cognitive skills, but robots can understand any of the mentioned context information using sensors and recognition algorithms. Furthermore, during close proximity with robots during assembly operations, a human operator can be guided by cyber physical systems (CPS), increasing the operator's productivity.

Hand Gesture and Haptic Control

Normally, human operators can use control codes to command an industrial robot with a programming-based user interface (Flacco et al., 2012). However, we believe future HCHRC workstations require a more flexible and intuitive way to control collaborative robots. A recent development in this direction is hand gesture control of the robots (Rafiqul & Noor, 2012). This control interface is designed for intuitive robot control. Hand gesture robot control can provide intuitive ways for human operators to control collaborative robots. Thus, the robot can dynamically adapt its task plan to collaborate with human operators in the same assembly operation. We believe that, it is important to identify and implement hand gesture and haptic control systems in order to jog/move the robot in different ways, covering all the movement types of a regular teaching pendant, and possibly adding more movement types and functionalities.

Human Motion Prediction

In order to address the human safety problems when it comes to close proximity with robots during assembly operations, we need design human motion prediction system that employs different cameras that tracks the human approach and gestures at different proximity of the user. This system allows improvement on safety of human operator and wellbeing during assembly operations.

Work Instruction Guiding

The human operator is crucial in assembly systems because they are in charge of the most flexible operations during the processes. Nevertheless, an operator faces some major problems during the assembly process. First, the management of hundreds of different product mixes, distinguished by different assembly cycles, as well as thousands of different parts, hundreds of tools, equipment, and several worker qualifications (Tsarouchi & Matthaiakis, 2017). Second, assembly tasks experience several challenges, such as the growing complexity of their processes and supply networks, cost pressures, and increasing customer expectations for quality, lead time, and customization (Bänziger et al., 2018).

The current problems may be solved by traditional assembly-aid methods such as paper, tables, and other drawings. However, these conventional paradigms have the drawback that employees have to look at different objects and search for the correct information by flicking through the work instructions, which is a time-consuming operation. Better suited technologies for displaying information would make manual assembly processes more efficient and less error-prone.

Thus, conventional operator support systems have to be substituted by digital and smart media systems to provide instructions in the most efficient way to the employees. The digital assistance system provides information about failures and information for the right execution of the process. However, displaying data and work instructions on a display is not the only suitable option for an assistance system. Furthermore, the second part is to check if an assembly process is executed properly or not. Consequently, assembly systems must be equipped with sensors and cameras to compare the target state and actual state of an assembly process.

Speech Recognition and Control

The quality of sensors for hand and voice control of robots still cannot satisfy industrial standards, and the recognition accuracy of the algorithms is also limited (Gustavsson et al., 2017). Hence, this communication between humans and robots is still at the laboratory stage and cannot be directly adapted in the manufacturing industry. Therefore, it is important to identify and implement appropriate speech recognition systems that can function in industrially noisy environments such as assembly manufacturing.

Conclusion and Future work

Human–robot communication is a new mode for assembly operations, and we believe that human centered human–robot synergy will constitute a relevant factor in industry for improving assembly operations in terms of performances and flexibility. However, we believe that, this will only be achieved with systems that are fundamentally safe and a user-friendly interface operator, intuitive to use, and easy to set up so that human operators can easily communicate with the robot during assembly operations. At glance, this paper has provided an overview of the current state of art research topics related to Human–Robot Collaboration, showing that it can be applied in a wide range of different modes. A literature analysis was carried out papers published between 2010 and 2022 that used collaborative robots in assembly operations. Within the context of assembly applications, we focused on the control systems, the collaboration methodologies, and the tasks assigned to the cobots in HRC studies. From our analysis, we identified that the majority of research is largely focused on robot centered applications and when it comes to trust in robots, we defined that loss of trust happens over time in actual assembly operations. This led to the systems suffering from flexibility and efficiency point of view.

We found that we are in a transformation phase from physical interaction mode towards cognitive interaction mode between humans and robots, where humans and robots are able to communicate with each other during mutual working conditions and humans are able to guide robots. Generally speaking, future human and robot interaction in assembly systems should focus on how human operators supported by robots and advanced technologies in sociotechnical environment to satisfy human wellbeing in hybrid human robot interaction teams. Therefore, we in this paper we proposed the future human centered human robot communication (HCHRC) framework during assembly operations. This HCHRC system boosted by assembly context recognition, hand gestures control, work instruction assistant and human activity prediction and other advanced technologies. We hope that by utilizing a human-centered human-robot communication mode, the flexibility and productivity of the assembly operation, as well as the human operator's well-being, will improve. Future work will identify and address the specific topics of the HCHRC framework types.

Scientific Ethics Declaration

The authors declare that the scientific ethical and legal responsibility of this article published in EPSTEM journal belongs to the authors.

Acknowledgements or Notes

This article was presented as an oral presentation at the International Conference on Research in Engineering, Technology and Science (www.icrets.net) held in Budapest/Hungary on July 06-09, 2023.

References

Abdelfetah, H., Aouache, M., Maoudj, A., & Akli, I. (2019). Human–robot interaction in industrial collaborative robotics: a literature review of the decade 2008–2017. *Advanced Robotics*, 1568-5535 .

- Bänziger, T., Kunz, A., & Wegener, K. (2018). Optimizing human–robot task allocation using a simulation tool based on standardized work descriptions. *Journal of Intelligent Manufacturing*, 1-14.
- Bjoen, M., Bern, K., & Carsten, T. (2016). Human-robot collaboration – new applications in industrial robotics. *International Conference on Competitive Manufacturing*. (pp. 293-299).
- Blankemeyer, S., Wiemann, R., Vett, U.-K., Recker, T., Pischke, D., & Raatz, A. (2020). Efficient use of human-robot collaboration in packaging through systematic task assignment. *Conference on Production Systems and Logistics*.
- Bruno, G., & Antonelli, D. (2018). Dynamic task classification and assignment for the management of human-robot collaborative teams in workcells. *The International Journal of Advanced Manufacturing Technology*, 9(12), 2415-2427.
- Dalle Mura, M., & Dini, G. (2019). Designing assembly lines with humans and collaborative robots: A genetic approach. *CIRP Annals*, 1-6.
- Dianatfar, M., Latokartano, J., & Lanz, M. (2019). Task balancing between human and robot in mid-heavy assembly tasks. *Procedia CIRP*, 81, 157-161.
- Flacco, F., Kroger, T., De Luca, A., & Khatib, O. (2012). A depth space approach to human-robot collision avoidance. *IEEE International Conference on Robotics and Automation*. Saint Paul, USA.
- Karagiannis, P., Makris, S., Tokcalar, O., & Chryssolouris, G. (2016). Augmented reality (AR) applications for supporting human-robot interactive cooperation. *Procedia CIRP*, 41(1), 370-375.
- Galim, R., & Meshcheryakov, R. (2019). Review on human–robot interaction during collaboration in a shared workspace. *International Conference on Interactive Collaborative Robotics*.
- Gualtieri, L., Rauch, E., Vidoni, R., & Matt, D. (2019). An evaluation methodology for the conversion of manual assembly systems into human-robot collaborative workcells. *Procedia Manufacturing*.
- Gustavsson, P., Syberfeldt, A., Brewster, R., & Wang, L. (2017). Human-robot collaboration demonstrator combining speech recognition and haptic control. *Procedia CIRP*, 63, 396-401.
- Khalid, A., Kirisci, P., Ghrairi, Z., Thoben, K., & Pannek, J. (2017). Towards implementing safety and security concepts for human-robot collaboration in the context of Industry 4.0. *International Conference on Advanced Manufacturing*.
- Liau, Y., & Ryu, K. (2020). Task allocation in human-robot collaboration (HRC) based on task characteristics and agent capability for mold assembly. *Procedia Manufacturing*, 51(1), 179-186.
- Lihui, W., Sichao, L., Hongyi, L., & Xi Vincent, W. (2020). Overview of human-robot collaboration in manufacturing. *5th International Conference on the Industry. 4.0 Model for Advanced*. Belgrad, Serbia.
- Malik, A., & Bilberg, A. (2019). Human centered Lean automation in assembly. *52nd CIRP Conference on Manufacturing Systems*, 81, 659-664.
- Mateus, J. C., Claeys, D., Limère, V., Cottyn, J., & Aghezzaf, E. (2019). A structured methodology for the design of a human-robot collaborative assembly workplace. *The International Journal of Advanced Manufacturing Technology*, 5(8), 2663-2681.
- Maurtua, I., Ibaruren, A., Kildal, J., Susperregi, L., & Sierra, B. (2017). Human–robot collaboration in industrial applications: Safety interaction and trust. *International Journal of Advanced Robotic Systems*, 1-10.
- Muller, R., Vette, M., & Mailahn, O. (2016). Process-oriented task assignment for assembly processes with human-robot interaction. *6th CIRP Conference on Assembly Technologies and Systems (CATS)*, 44, 210-215.
- Nikolakis, N., Kousi, N., Michalos, G., & Makris, S. (2018). Dynamic scheduling of shared human-robot manufacturing operations (pp.9-14). *Procedia CIRP*.
- Maurice, P. S. (2014). Automatic selection of ergonomic indicators for the design of collaborative robots: a virtual-human in the loop approach. *14th IEEE-RAS International Conference on Humanoid Robots*.
- Rafiqul, Z., & Noor, I. (2012). Hand gesture recognition: A literature review. *International Journal of Artificial Intelligence & Applications*, 3(4).
- Ranz, F., Hummel, V., & Sihn, W. (2017). Capability-based task allocation in human-robot collaboration. *Procedia Manufacturing*, 9, 182 – 189.
- Robla Gómez, S., Becerra, V. M., & Llata, J. R. (2017). Working together: a review on safe human-robot collaboration in industrial environments. *IEEE Access*, 1(99), 26754–26773.
- Romero, D., Wuest, T., Stahre, J., & Noran, O. (2016). Towards an operator 4.0 typology: A human-centric perspective on the fourth industrial revolution technologies. *International Conference on Computers & Industrial Engineering (CIE46)*, 1-11. Tianjin, China. .
- Thomas, C., B, M., & Kuhlenkötte, B. (2016). Human-robot-collaboration-New applications in industrial robotics. In *International Conference on Competitive Manufacturing (COMA 2016)*, 293-299.

- Tsarouchi, P., Matthaiakis, A., Makris, S., & Chryssolouris, G. (2017). On a human-robot collaboration in an assembly cell. *International Journal of Computer Integrated Manufacturing*, 30(6), 580-589.
- Tsarouchi, P., Spiliotopoulos, J., Michalos, G., Koukas, S., Athanasatos, A., Makris, S., & Chryssolouris, G. (2016). A decision making framework for human robot collaborative workplace generation. *Procedia CIRP*, 44, 228-232.
- Waurzyniak, P. (2015). Fast, lightweight robots help factories go faster. *Manufacturing Engineering*, 3, 55-64.
- Xun, X., Yuqian, L., Birgit, V.-H., & Lihui, W. (2021). Industry 4.0 and Industry 5.0 -inception, conseption and perception. *Journal of Manufacturing Systems*, 61, 530-535.

Author Information

Ikrom Kambarov

Friendrich – Alexander University
Erlangen, Germany
Turin Polytechnic University
Tashkent, Uzbekistan
Contact e-mail: ikrom.kambarov@faps.fau.de

Matthias Brossog

Friendrich – Alexander University
Erlangen, Germany

Jörg Franke

Friendrich – Alexander University
Erlangen, Germany

David Kunz

Friendrich – Alexander University
Erlangen, Germany

Jamshid Inoyatkhodjaev

Turin Polytechnic University
Tashkent, Uzbekistan

To cite this article:

Kambarov, I., Inoyatkhodjaev, J., Kunz, D., Brossog, M., & Franke, J. (2023). From human to robot interaction towards human to robot communication in assembly systems. *The Eurasia Proceedings of Science, Technology, Engineering & Mathematics (EPSTEM)*, 23, 241-252.

The Eurasia Proceedings of Science, Technology, Engineering & Mathematics (EPSTEM), 2023

Volume 23, Pages 253-261

ICRETS 2023: International Conference on Research in Engineering, Technology and Science

Embracing Green Choices: Sentiment Analysis of Sustainable Consumption

Ceren Cubukcu-Cerasi
Gebze Technical University

Yavuz Selim Balcioglu
Gebze Technical University

Ash Kilic
Gebze Technical University

Farid Huseynov
Gebze Technical University

Abstract: Currently, resource scarcity and climate change are among the main global problems. Governments are actively seeking regenerative solutions so that humans and nature can co-exist in harmony in the face of ecological destruction and resource limitations. One of these solutions is green consumption. Making greener consumption decisions is necessary for society to become sustainable. If sustainable consumption is to be promoted, public perception must shift, and achieving this shift will be simpler if society's shift toward green consumption is understood. This research aims to explore the sentiment and attitudes towards sustainable consumption on YouTube, a popular online platform with a vast pool of user-generated content. We employ a combination of data mining techniques and sentiment analysis to process and analyze a large dataset of YouTube videos and comments related to sustainable consumption topics. The data collection includes videos from various categories, such as reviews of eco-friendly products, vlogs of sustainable living, and informative content on environmentally responsible practices. The study focusses on understanding user engagement, sentiment polarity, and the factors influencing positive or negative attitudes toward sustainable consumption. In this way, the attitude of society toward green consumption and the role of social networks in public opinion can be understood. Overall, the study shows how data mining techniques and social networks have the potential to help with the shift to more sustainable growth paths.

Keywords: Sustainability, Green consumption, Sentiment analysis, Data mining, Social media

Introduction

Individuals and businesses are seeking ways to adopt eco-friendly practices and make greener choices with growing awareness about the impact of human activities on the planet. The shift towards sustainable consumption is driven by both ethical considerations and by the realization that our consumption patterns can directly contribute to environmental degradation or restoration. That is, the shift towards sustainable consumption is happening because we now understand more clearly how our actions affect the well-being of the planet. We humans can now see the harmful consequences of unsustainable practices like using too many resources, causing pollution, cutting down forests, and emitting greenhouse gases. As people become more aware of the impact of their daily choices on the environment, they are reconsidering their consumption habits and actively looking for more environmentally friendly options.

- This is an Open Access article distributed under the terms of the Creative Commons Attribution-Noncommercial 4.0 Unported License, permitting all non-commercial use, distribution, and reproduction in any medium, provided the original work is properly cited.

- Selection and peer-review under responsibility of the Organizing Committee of the Conference

© 2023 Published by ISRES Publishing: www.isres.org

Ethics are playing a crucial part in encouraging the transition towards sustainable consumption (Tomsa et al., 2021; Suphasomboon & Vassanadumrongdee, 2022). Increasingly, individuals are recognizing the moral responsibility to safeguard and maintain the environment for the well-being of future generations. We have come to understand that our current consumption patterns are causing significant harm. We are depleting finite resources, putting biodiversity at risk, and worsening climate change. This realization has sparked a strong sense of responsibility to act and minimize harm while promoting environmental stewardship. Additionally, we now recognize that our choices as consumers directly impact the environment, which has created a pressing need to adopt sustainable practices. We feel an urgent drive to embrace eco-friendly alternatives and contribute to the restoration of our planet. By choosing environmentally friendly products, minimizing waste, and endorsing sustainable production methods, both individuals and organizations can play an active role in promoting positive environmental outcomes. This understanding empowers consumers to make well-informed decisions that align with their values and actively engage in the collective endeavor to tackle urgent environmental issues.

The shift towards sustainable consumption goes beyond individual efforts and also encompasses organizations in different sectors (Kong et al., 2002; Hobson, 2004; Charter et al., 2017; Bocken, 2017). Businesses are recognizing the importance of sustainable practices in ensuring their long-term success and competitiveness. Consumers are increasingly showing a strong inclination towards environmentally responsible products and services, prompting companies to incorporate sustainability into their fundamental strategies. This acknowledgement of the business value of sustainability further propels the adoption of greener alternatives, as organizations grasp the advantages of aligning their operations with environmental and social considerations. In summary it can be said that the shift towards sustainable consumption is driven by both ethical concerns and the recognition that our consumption choices directly affect the environment. With the awareness of the interconnectedness between our actions and the planet's well-being, individuals and organizations should be encouraged to actively seek environmentally friendly alternatives and adopt greener choices. By encouraging sustainable consumption, we can work together towards a better connection between human actions and the Earth, creating a more sustainable and resilient future.

The purpose of this research is to examine the sentiments and attitudes surrounding sustainable consumption on YouTube, utilizing data mining techniques and sentiment analysis. By analyzing a vast dataset comprising YouTube videos and comments related to sustainable consumption, including various categories like eco-friendly product reviews, sustainable living vlogs, and informative content promoting responsible practices, the study aims to gain valuable insights into user engagement, sentiment polarity, and the factors influencing positive or negative perspectives towards sustainable consumption. Through understanding societal attitudes towards green consumption and recognizing the impact of social networks on shaping public opinion, this research contributes to our knowledge of how data mining techniques and social networks can facilitate the transition to more sustainable growth paths.

Literature Review

Most of the literature-based study on sustainability has used a group of participants and questionnaires on various aspects. Biswas (2016) conducted a study with the technology acceptance model theory to evaluate the effect of social media use on green consumption. In his study, data was collected through a questionnaire survey and for analysis binary logistic regression analysis, one-way MANOVA and factor analysis were used. As a result of the study, it has been observed that social media has a positive effect on consumer green choice behavior.

Hui and Khan (2021) while investigating the effect of social exclusion on green consumption intention, with data collected through online surveys, expanded the theory of planned behavior (TPB) by taking green self-identity into account. Structural equation modeling (SEM) technique was used to test the model presented in the study.

Wang (2021) collected data with a questionnaire survey consisting of 3 main parts, to investigate the effect of consumers' green cognition on green consumption behavior. Those 3 main parts consisted of the participant's green consumption behavior in everyday life, level of green cognition and personal information such as the age, gender, occupation and monthly disposable income. 110 valid questionnaires were collected from the surveys. The study's findings indicate that consumer understanding of green consumption and their perspectives on environmental issues are key to helping consumers become aware of green consumption and adopt green behaviors.

Sarac (2022) conducted a study on the sustainable consumption levels of gender and cultural tourists. In his study, he used data collected from questionnaires answered by 449 participants. As a result, it has been observed that the level of sustainable consumption varies according to gender. The results were also gathered under four dimensions as "environmental awareness, non-need purchasing, savings and reusability" according to the answers given by cultural tourists who have high sustainable consumption levels.

There are different market segmentation approaches such as demographic segmentation approach, which groups the market with demographic information including consumer's age, gender, race, religion, education and so on; psychographic segmentation, which groups the market with information like consumer's personal qualities, beliefs, behaviors, expectations and similar, and behavioral segmentation, which groups according to consumer's real behavior, reaction to the product and the use (Huseynov & Yıldırım, 2019).

Bedard and Tolmie (2018) found a positive correlation between social media and online interpersonal influence on green purchasing intentions in the millennial generation. In addition, it has been revealed that individuality has no effect on green purchasing, but masculinity weakens the relationship.

Although there are green consumption studies using machine learning with the development of technology, the numbers are not very high. Jain et al. (2020) developed a framework to describe the elements of green purchase intentions and social media usage, interpersonal influence and E-WOM used as exogenous variables in the research. As a result, it has been seen that the biggest factor on purchasing is social media.

Tang et al. (2020) developed a model to determine the green consumption behaviors and prominent features of college students. The estimation method is based on the one of the simplest classification approaches K-Nearest Neighbor (KNN) model with OBLFA_GWO, a swarm intelligence method. The data were collected through 2020 questionnaires distributed to 9 different universities.

Materials and Methods

This section outlines the integrated framework employed for data collection, data cleaning/preprocessing, and text mining approaches for analysis. The schematic framework shown in Figure 1 illustrates the methodological architecture. The first stage involved is data acquisition. For this study, YouTube was selected as the primary data source. Videos and associated comments related to sustainable consumption were collected using the YouTube Data API.

In the second stage, the text data (video comments and descriptions) obtained from YouTube were preprocessed for the final analysis. This step involved cleaning the data by removing non-essential elements such as URLs and non-alphanumeric characters and preparing the text for analysis through techniques such as tokenization and lemmatization. More detailed information on the data collection and preprocessing stages can be found in the section 'Data collection and preprocessing'.

The third stage involved is data analysis. A variety of text mining techniques were employed for this purpose, including:

1. Topic Modelling: This was used to identify latent topics in the text data.
2. Semantic Network Analysis: This method visualized the semantic relationships between words in the corpus.
3. Sentiment Analysis: This was used to identify emotions and feelings expressed in the comments, providing information on public opinion on sustainable consumption.

Through this three-stage methodology, the study aimed to achieve a comprehensive understanding of sentiments and attitudes toward sustainable consumption on YouTube.

Data Collection and Pre-Processing

In recent years, social networking sites (SNS) such as Facebook, Twitter, MySpace, FriendFeed, and GooglePlus have transformed global communication. These SNS platforms generate vast real-time data for researchers in fields such as linguistics, sociology, behavioral sciences, health, and psychology. YouTube is one of the most popular platforms today, hosting millions of videos and serving billions of users. Most conversations on YouTube, particularly comments on videos, are publicly available and easily accessible through YouTube's Application Programming Interface (API). Therefore, YouTube was chosen as the data source for this study.

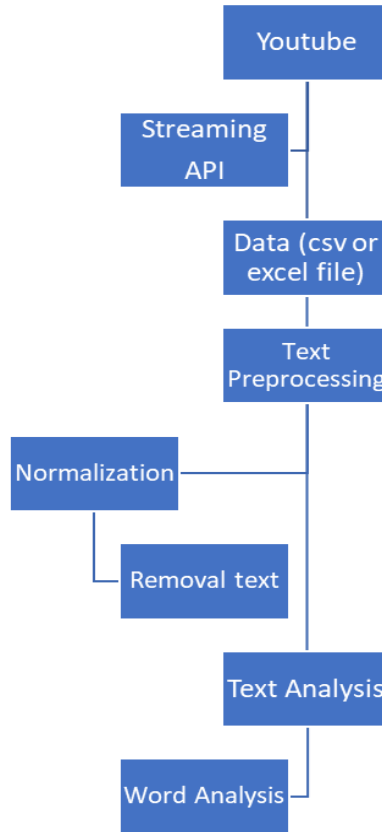


Figure 1. A proposed framework of the text data analysis method.

The Python programming language, particularly its libraries for data manipulation and analysis (Pandas, NumPy) and for web scraping and API interaction (Requests, BeautifulSoup), was used for data collection and preprocessing. The video metadata and comments related to "sustainable consumption" were extracted using the YouTube Data API. We collected data from videos posted between 1 December 2021 and 30 December 2022, resulting in a raw data set of 39,678 comments. After removing duplicates, 26,425 unique comments remained for analysis.

YouTube data, like most user-generated content, is often unstructured and noisy; therefore, it was pre-processed before the main analyses. The Python libraries NLTK (Natural Language Toolkit) and spaCy were used for this purpose. These libraries helped improve the quality of our corpus by removing irrelevant content that did not contribute to the meaning of the text, such as numbers, URLs, punctuation, stop words, and excessive whitespace. This text cleaning process facilitated more accurate subsequent analysis of the data.

Text Mining Approaches

Topic Modelling

For this study, we used Latent Dirichlet Allocation (LDA)-based topic modelling, a generative probabilistic model based on a three-level hierarchical Bayesian model. This method has been employed across various fields and has demonstrated superior performance among several topic modelling algorithms, offering proven reliability.

In Python, the LDA implementation was achieved using the 'gensim' library, which provides tools for topic modelling. LDA is an unsupervised learning algorithm that uncovers latent topics based on patterns of word co-occurrences within the corpus. The fundamental principle behind LDA modelling is that each document (in this case, each comment) from a set of D documents is a mixture of K latent topics. Moreover, each topic is a multinomial distribution of words from a vocabulary of W words.

Here, ϕ_k (for all $k = 1, \dots, K$) is the probabilistic distribution over words for each latent topic, and θ_d (for all $d = 1, \dots, M$) is the distribution per document topic. In this context, M represents the number of comments and N represents the number of words in the vocabulary.

α and β are Dirichlet parameters where α represents per-document topic distributions, and β represents per-topic word distribution. For each comment d in the corpus, the words are generated in a two-stage process. In the first stage, a distribution is randomly chosen. Based on this distribution, a topic is randomly selected for each word in the comment. This approach allows us to extract meaningful topics from the YouTube comments and to understand the main themes in the discussions about sustainable consumption.

Semantic Network Analysis

Semantic Network Analysis is a subfield of Natural Language Processing (NLP) and Machine Learning that constructs structures to approximate concepts within a large corpus. This analysis creates an interactive visual system that depicts the semantic networks of words in the corpus. Each word is represented by a node in the network structure, and the edges signify semantic connections between words.

For this study, we used the Python library network for creating and analyzing the semantic network, and community for community detection in the network. We implemented the Louvain Community Detection Algorithm (LCDA) to identify semantic clusters. This method aims to maximize a modularity score for each cluster, where the modularity quantifies the quality of the assignment to clusters. The algorithm evaluates how much more densely connected the nodes are within a cluster compared to connections in a random network.

The Louvain algorithm's primary inspiration is to optimize modularity, a scale that measures the relative density of edges within the network. This value can range from -0.5 to 1. The modularity function gauges the strength of division of a network into clusters. By applying this method to YouTube comments, we can better understand the semantic relationships between the words used in discussions about sustainable consumption.

Sentiment Analysis

Sentiment Analysis (SA) is a computational linguistics technique that is used to identify and extract sentiment associated with a piece of text data. It is a subset of Natural Language Processing (NLP) that analyses subjective information such as opinions and emotions expressed in text.

There are two primary methods for conducting SA: lexicon-based and corpus-based. For this study, we used the lexicon-based method. Numerous lexicons are available to perform sentiment analysis, such as SentiWordNet, General Inquirer, Q-WordNet, Lexicon of Subjectivity Clues, LIWC dictionary, and Sentiment-based Lexicon.

We chose to use the NRC Emotion Lexicon, also known as EmoLex, because of its ability to classify emotions into eight basic categories: anger, fear, sadness, anticipation, disgust, joy, surprise, and trust, in addition to identifying positive and negative sentiments in the data.

To implement sentiment analysis, we used Python's NLTK (Natural Language Toolkit) library, which has an interface to the NRC EmoLex. This allowed us to extract and analyse the sentiments expressed in YouTube comments on sustainable consumption, providing valuable insights into public opinion on the topic.

Results and Discussion

LDA Model

Prior to performing LDA topic modelling, we executed perplexity and coherence tests to evaluate our model's quality. Perplexity is a measure of the overall quality of the model. It gauges how well the model can describe a document based on a generative process learnt from the set of topics. However, topic coherence captures the optimal number of topics by measuring the degree of semantic similarity between high-scoring words within the topic, thereby yielding human-interpretable topics.

Table 1 presents perplexity scores for keywords ranging from 1 to 50. A lower perplexity score indicates that the probability distribution is more effective in predicting the document. The optimal keywords are determined based on perplexity validation, where the score reaches the lowest point before rising again. To compute perplexity and coherence scores in Python, we used the 'gensim' library's built-in functions. This provided us with a systematic and quantitative way to evaluate our keyword models and choose the best one for further analysis.

Table 1. Perplexity values for different keywords.

Key words	Validation Perplexity	Key words	Validation Perplexity	Key words	Validation Perplexity	Key words	Validation Perplexity	Key words	Validation Perplexity
1	290.4	2	285.7	3	281.3	4	276.9	5	272.5
6	268.1	7	263.7	8	259.3	9	254.9	10	250.5
11	246.1	12	241.7	13	237.3	14	232.9	15	228.5
16	279.5	17	282.3	18	280.4	19	278.7	20	277.6
21	275.9	22	273.5	23	271.7	24	269.4	25	267.8
26	265.2	27	263.5	28	261.9	29	260.3	30	258.6
31	256.9	32	255.3	33	253.6	34	251.9	35	250.3
36	248.6	37	246.9	38	245.3	39	243.6	40	241.9
41	240.3	42	238.6	43	236.9	44	235.3	45	233.6
46	231.9	47	230.3	48	228.6	49	226.9	50	225.3

It is observed that validation perplexity generally decreases as keyword numbers increase, which is an expected outcome in the topic modelling process. This trend indicates that the model's ability to predict or understand the text data improves as more keywords are considered. For example, the validation perplexity for Keyword 1 is highest at 290.4, indicating a relatively poor fit of the model. However, as we progress to Keyword 50, the perplexity value decreases to 225.3, indicating a better fitting model. However, there are some anomalies to this trend. For example, the perplexity value increases slightly between keywords 15 and 16, and again between keywords 16 and 17. These minor inconsistencies could be due to the specific content and context of the keywords and how they interact with the rest of the text data. Overall, these results suggest that increasing the number of keywords aids the model in capturing the semantic richness of the YouTube comments data, thus enhancing the overall topic modelling performance. However, it is also crucial to monitor for potential overfitting, where the model starts to capture noise instead of the underlying semantic structures as the keyword count increases. Therefore, the choice of the number of keywords should be carefully considered based on both the perplexity values and the interpretability of the resulting topics.

In Table 2, the terms are grouped into several categories, indicating the multifaceted nature of sustainable consumption. These categories include Environment, Consumerism, Lifestyle, Development, Energy, Production, Waste Management, and others. Terms such as "green consumption", "green product", "green industry", and "green development" reflect the prominence of the "green" branding in sustainable consumption. This could indicate a marketing trend towards promoting products and services as environmentally friendly. The terms "Consumer behavior", "Consumption behavior", and "Online consumer behavior" suggest that understanding consumer attitudes and behaviors is crucial for promoting sustainable consumption. This implies the importance of psychological and sociological approaches in studying sustainable consumption. The presence of terms such as "Gen y", "social media", and "Online consumer behavior" points to the role of younger generations and digital platforms in driving sustainable consumption. The terms "recycle", "recycling", "reusability", "virtual water", and "Water footprint" highlight the importance of waste management and water conservation in sustainable consumption. The presence of the terms "balance of trade", "energy consumption", "Energy efficiency", and "green infrastructure" show that sustainable consumption also intersects with broader economic and infrastructural concerns. The terms "Environmental Awareness", "Environmental concern", "Pro-environmental Behavior", and "Pro-environment" reflect the significance of public awareness and attitudes toward the environment in promoting sustainable consumption.

We used the TextBlob library for sentiment analysis within the Python environment. Initially, we loaded the text data (YouTube comments), tokenized each word to form a list, and applied the TextBlob sentiment polarity method. This method computes sentiment scores based on comparison with a built-in lexicon, returning a polarity score ranging from -1 (negative sentiment) to +1 (positive sentiment). According to our sentimental results (Figure 2), people exhibit mixed sentiments (i.e. positive and negative) toward sustainable consumption. However, positivity appears to be more prominent in our results, possibly due to the presence of high positive emotions (anticipation, joy, and trust).

Some phrases associated with positive sentiments include abundance, health, opportunity, mindful, delicious, confident, prefer, recovery, protection, etc. Conversely, phrases associated with negative sentiments include 'toxic', 'junk', 'waste', 'degradable', 'irresponsible', 'guilty', 'loss', etc. The sentiment polarity and subjectivity scores assigned by TextBlob provided a comprehensive understanding of the overall sentiment toward sustainable consumption on the YouTube platform

Table 2. Keywords with key terms.

Keyword ID	Term	Label
1	Balance of trade	Economy
2	Clean production	Production
3	Consumer behavior	Consumerism
4	Consumption	Lifestyle
5	Consumption behavior	Consumerism
6	Consumption environment	Environment
7	Ecological behavior	Environment
8	Ecological product	Production
9	Ecology	Environment
10	Ecotourism	Tourism
11	Energy consumption	Energy
12	Energy efficiency	Energy
13	Enviroment	Environment
14	Enviromental concern	Environment
15	Enviromental consensus	Environment
16	Enviromental ethics	Ethics
17	Enviromental management	Management
18	Environmental awareness	Environment
19	Environmental concern	Environment
20	Environmental problem	Environment
21	Environmentally friendly	Lifestyle
22	Gen y	Demographics
23	Go green	Lifestyle
24	Green attitude	Lifestyle
25	Green building	Construction
26	Green cognition	Psychology
27	Green consumerism	Consumerism
28	Green consumption	Lifestyle
29	Green consumption beh	Consumerism
30	Green development	Development
31	Green food products	Food
32	Green industry	Industry
33	Green infrastructure	Infrastructure
34	Green marketing	Marketing
35	Green product	Production
36	Green purchase	Consumerism
37	Green purchase intentions	Consumerism
38	Green self id	Identity
39	Online consumer behavior	Consumerism
40	Planned behavior theory	Psychology
41	Practice SDG	Development
42	Pro environmental behavior	Environment
43	Pro-enviroment	Environment
44	Purchase motives	Consumerism
45	Recycle	Waste Management
46	Recycling	Waste Management
47	Reusability	Waste Management
48	Social consumption	Sociology
49	Social media	Media
50	Sustainability	Environment

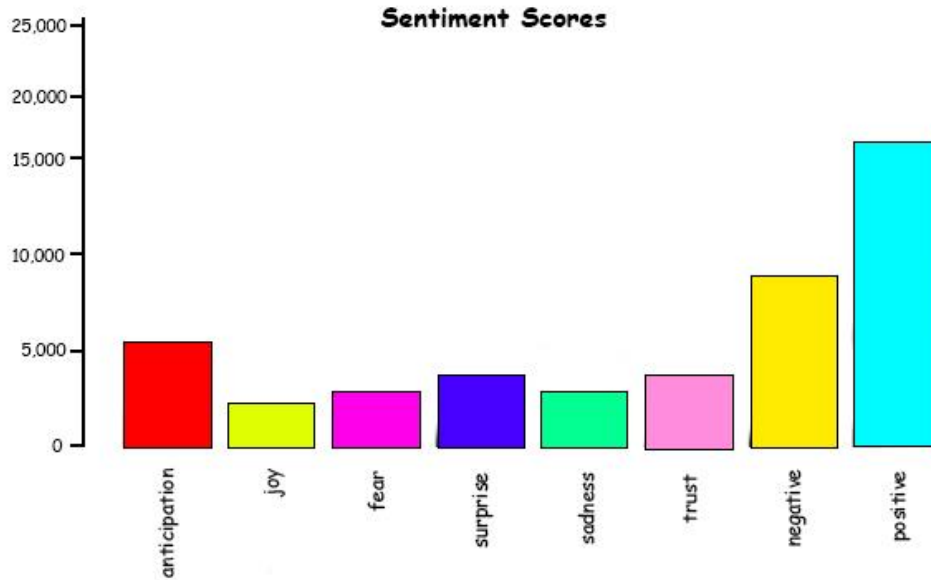


Figure 2. Sentiment towards sustainable consumption.

Conclusion

This article analyzed recent video comments on sustainable consumption posted on YouTube. The main strength of this study lies in its novel findings, obtained through advanced text mining approaches, such as Latent Dirichlet Allocation (LDA) for topic modelling and the Louvain Algorithm for semantic network analysis. One of the significant contributions of this work is the use of social media data, specifically from YouTube, as opposed to the conventional method of obtaining data from interviews and questionnaire-based surveys. Every day, millions of comments are posted on YouTube that contain unbiased and rich opinions. Therefore, YouTube is an excellent source of data for researchers to better understand public behaviors, opinions, and sentiments. Traditional methods such as interviews often introduce bias / subjectivity, as the interviewer's preconceived response, idea or opinion could affect the responses of interviewees. In contrast, people freely express their unbiased views on social media platforms such as YouTube. This study employed the Python programming language, known for its powerful libraries for data processing and analysis. The use of Python opened up a range of analytical possibilities, making it easier to handle large data sets, apply advanced text mining techniques, and present the findings in a visually appealing manner. In general, the application of these methods to YouTube data offers valuable insight into public sentiment about sustainable consumption, providing a more nuanced understanding of the topic than traditional survey methods could achieve. This study underscores the potential of using social media data in conjunction with robust data analysis tools like Python for research in various fields.

Scientific Ethics Declaration

The authors declare that the scientific ethical and legal responsibility of this article published in EPSTEM journal belongs to the authors.

Acknowledgements or Notes

* This article was presented as an oral presentation at the International Conference on Research in Engineering, Technology and Science (www.icrets.net) held in Budapest/Hungary on July 06-09, 2023.

* This study is one of the preliminary outputs of the project numbered 2022-A-113-07 funded by Research Fund of Gebze Technical University.

References

- Bedard, S. A. N., & Tolmie, C. R. (2018). Millennials' green consumption behaviour: Exploring the role of social media. *Corporate Social Responsibility and Environmental Management*, 25(6), 1388-1396.
- Biswas, A. (2016). Impact of social media usage factors on green consumption behavior based on technology acceptance model. *Journal of Advanced Management Science*, 4(2), 92-97..
- Bocken, N. (2017). Business-led sustainable consumption initiatives: Impacts and lessons learned. *Journal of Management Development*, 36(1), 81-96.
- Charter, M., Gray, C., Clark, T., & Woolman, T. (2017). The role of business in realising sustainable consumption and production. In *System Innovation for Sustainability 1* (pp. 56-79). Routledge.
- Hobson, K. (2004). Sustainable consumption in the United Kingdom: The “responsible” consumer and government at “arm’s length”. *The Journal of Environment & Development*, 13(2), 121-139.
- Hui, Z., & Khan, A. N. (2022). Beyond pro-environmental consumerism: role of social exclusion and green self-identity in green product consumption intentions. *Environmental Science and Pollution Research*, 29(50), 76339-76351.
- Huseynov, F., & Özkan Yıldırım, S. (2019). Online consumer typologies and their shopping behaviors in B2C e-commerce platforms. *Sage Open*, 9(2). <https://doi.org/10.1177/215824401985463>
- Jain, V. K., Gupta, A., Tyagi, V., & Verma, H. (2020). Social media and green consumption behavior of millennials. *Journal of Content, Community and Communication*, 10(6), 221-230.
- Kong, N., Salzmänn, O., Steger, U., & Ionescu-Somers, A. (2002). Moving Business/Industry towards sustainable consumption: The role of NGOs. *European Management Journal*, 20(2), 109-127.
- Sarac, O. (2022). Differences in sustainable consumption behaviours of cultural tourists according to gender: A *Journal of Humanities and Tourism Research*. 12(2), 265-283.
- Suphasomboon, T., & Vassanadumrongdee, S. (2022). Toward sustainable consumption of green cosmetics and personal care products: The role of perceived value and ethical concern. *Sustainable Production and Consumption*, 33, 230-243.
- Tang, H., Xu, Y., Lin, A., Heidari, A. A., Wang, M., Chen, H., ... & Li, C. (2020). Predicting green consumption behaviors of students using efficient firefly grey wolf-assisted K-nearest neighbor classifiers. *IEEE Access*, 8, 35546-35562.
- Tomşa, M. M., Romoñi-Maniu, A. I., & Scridon, M. A. (2021). Is sustainable consumption translated into ethical consumer behavior?. *Sustainability*, 13(6), 3466.
- Wang, Y. (2021). Research on the Influence Mechanism of Green Cognition Level on Consumers' Green Consumption Behavior: An Empirical Study Based on SPSS. In 2021 *International Conference on Management Science and Software Engineering (ICMSSE)* (pp. 175-178). IEEE.

Author Information

Ceren Cubukcu-Cerasi

Gebze Technical University
Kocaeli, Turkey
Contact e-mail: ceren.cubukcu@gmail.com

Yavuz Selim Balcioglu

Gebze Technical University
Kocaeli, Turkey

Ash Kilic

Gebze Technical University
Kocaeli, Turkey

Farid Huseynov

Gebze Technical University
Kocaeli, Turkey

To cite this article:

Cubukcu-Cerasi, C., Balcioglu, Y.S., Kilic, A. & Huseynov, F. (2023). Embracing green choices: Sentiment analysis of sustainable consumption. *The Eurasia Proceedings of Science, Technology, Engineering & Mathematics (EPSTEM)*, 23, 253-261.

The Eurasia Proceedings of Science, Technology, Engineering & Mathematics (EPSTEM), 2023

Volume 23, Pages 262-268

ICRETS 2023: International Conference on Research in Engineering, Technology and Science

Enhancing Cybersecurity with Trust-Based Machine Learning: A Defense against DDoS and Packet Suppression Attacks

Adnan Ahmed

Quaid-e-Awam University of Engineering, Science and Technology

Muhammad Awais

Quaid-e-Awam University of Engineering, Science and Technology

Mohammad Siraj

King Saud University

Muhammad Umar

Quaid-e-Awam University of Engineering, Science and Technology

Abstract: As technology becomes more intertwined with our daily lives, it is increasingly important to protect our data from attackers. Cyber security has become a top priority for individuals, businesses, and governments, as the threat of cybercrime is constantly evolving and becoming more sophisticated. With the rapid increase in cyberattacks, it has become tricky and cumbersome for cybersecurity experts to react to them all, predict new attacks and analyze the impact of damage being done to business. Traditional security measures such as firewalls, anti-virus software, and intrusion detections are no longer adequate in protecting against new vulnerabilities, especially insider and misbehavior attacks. Recently, Artificial Intelligence based techniques have brought tremendous improvements in cybersecurity with the integration of machine learning (ML) algorithms. ML methods have been built upon large volumes of real-time network data to deploy automated security and threat detection systems. Nonetheless, various cyber-attacks still circumvent traditional security mechanisms deployed to detect those attacks. To address the challenge, in this paper, we propose a machine learning-enabled trust-based routing protocol (TrustML-RP) that identifies the attacking nodes responsible for Distributed Denial of Service (DDoS) and packet suppression attacks. The proposed TrustML-RP scheme first adopts a distributed trust model for establishing trust factor among the participating nodes and later employs an effective combination of ML algorithms e.g., Artificial Neural Network (ANN) and Support Vector Machine (SVM) to find an optimal and secure route and identify attacker nodes. A comprehensive performance evaluation of the proposed scheme is carried out to demonstrate the efficiency on a reasonably sized network containing mixed nodes. The results demonstrate the effectiveness of the proposed scheme in building a trusted network environment and improving network security. The research findings suggest that the integration of a trust-based model and ML techniques can improve traditional cybersecurity methods thereby enabling cybersecurity professionals to design more effective cybersecurity systems.

Keywords: Cyber security, Machine learning, Trust-based routing, Cyber-attacks, DDoS, Packet suppression attack

Introduction

The advancement in the internet, information and communication technologies have demonstrated significant progress in various fields such as internet-of-things, cloud computing, e-government, e-commerce, e-banking, cloud computing and smart cities. Such advancement and improved networking technologies also facilitated the

- This is an Open Access article distributed under the terms of the Creative Commons Attribution-Noncommercial 4.0 Unported License, permitting all non-commercial use, distribution, and reproduction in any medium, provided the original work is properly cited.

- Selection and peer-review under responsibility of the Organizing Committee of the Conference

© 2023 Published by ISRES Publishing: www.isres.org

evolution of more sophisticated hacking techniques and tools, thereby allowing cyber-criminals to carry out more complex and advanced cyber-attacks (Awais Rajput et al., 2022; Malaivongs et al., 2022). Due to ever-increasing data breaches, it has become tricky and cumbersome for cybersecurity experts to react to them all, predict new attacks and analyze the impact of damage being done to business. Despite the effectiveness of traditional security methods, they often exhibit vulnerabilities to mitigate attacks such as Distributed Denial of Service (DDoS), flooding, insider threats, node misbehavior and packet suppression attacks, which can cripple an organization's network infrastructure (Cheema et al., 2022). Trust-based schemes have demonstrated significant advantages while mitigating such attacks by monitoring the traffic flows and developing the degree of trustworthiness between network devices (Shafi et al., 2023; Zeng et al., 2022). However, the existing trust-based schemes lack the ability to handle the volume and complexity of network traffic data generated by distributed devices. This has created a pressing need for AI and machine learning (ML) techniques to detect attacks and provide robust cybersecurity defense systems (Hasan et al., 2023). AI and ML techniques have been paramount in building automated security systems, automatically learning from the network traffic data, adapting to new attack patterns and threat detection by examining the huge amount of data in real-time (Zhang et al., 2022).

In this paper, we have proposed an enhanced cybersecurity scheme, TrustML-RP, that integrates the trust-based method with ML techniques in routing decisions to counter node misbehavior and Distributed Denial of Service (DDoS) cyber-attacks. The DDoS attack overwhelms a targeted network or computer by flooding a huge amount of traffic (might be fake traffic) from multiple sources. TrustML-RP aims to counter TCP SYN flooding, UDP flooding and ICMP flooding attacks. Moreover, the proposed scheme also mitigates the node misbehavior attack in which a normal participating node switches its behavior to a malicious node. A brief description of these attacks is provided below:

TCP SYN attack: An attacker sends a large number of TCP SYN packets to a target machine that doesn't allow a three-way handshake, leaving the target machine to wait for a response that never comes. Consequently, system resources are tied up and become unavailable to authorized users.

UDP flood attack: Unlike the TCP SYN attack, the UDP flood attack doesn't require a three-way handshake, and overwhelms the target machine with the massive amount of UDP traffic.

ICMP flood attack: An attacker sends a storm of ICMP packets, called *Pings*, to the victim machine, and causes the system to be overloaded with ICMP packets, which results in denial of service or degraded performance.

Packet Suppression attack: It's a type of routing attack in which an attacker node sends the fake route response packet to the source node and announces them as the most suitable candidate to forward packets to the destination device. However, after receiving the packets, either it drops selective packets or all received packets to create transmission disruption and denial of service (Grover et al., 2011).

To counter these attacks, the TrustML-RP scheme employs a trust-based machine learning methodology that can help in building trust in machine learning-based cybersecurity systems. This methodology involves identifying the types of DDoS and packet suppression attacks, defining trust-based metrics, collecting training data, training the machine learning model, integrating the model into the system, and evaluating the performance of the system.

The main contribution of this paper is twofold: (i) trust-based routing scheme to establish trustworthiness among the participating devices (nodes). The proposed TrustML-RP scheme incorporates the trust factor and route discovery mechanisms from our previous work (Ahmed et al., 2015). (ii) integration of ML techniques such as ANN and SVM to detect the attacker nodes. Based on the detection, attacker nodes are isolated from the active routes for packet transmission.

The rest of the paper is organized as follows: Section 2 provides a literature review of the existing research. Section 3 describes the methodology of the proposed TrustML-RP scheme. Section 4 presents the results and finally, Section 5 summarizes the research findings.

Related Work

The authors in (Zahra et al.2022) proposed a machine learning based schemes called, multiclass machine-learning-based model leveraging the light gradient boosting machines (MC-MLGBM), for detecting Rank and

wormhole attacks in the network. The dataset is generated using the Cooja network simulator which models the both static and mobile networks. The performance of proposed scheme is validated using multiclass-specific metrics such as cross-entropy, Cohn's kappa, and Matthews Correlation Coefficient (MCC). A distributed IDS scheme is presented (Ercan et al., 2022) for vehicular area networks to detect position falsification attack. The features used to detect position falsification attacks are estimated distance between sender and receiver, the difference between the declared and estimated distance between sender and receiver and estimated angle of arrival. The distance between sender and receiver is measured using Received Signal Strength (RSS) method. The proposed scheme is implemented using KNN, RF and ensemble learning based ML methods. The OMNET++ and SUMO simulators have been used for simulating the vehicular network and generating VeReMi dataset that consist of 5 different attacks and 3 attacker rates 10%, 20% and 30% for various traffic densities (van der Heijden et al., 2018). A machine learning based routing scheme is proposed by (Luong et al., 2019) to detect and prevent flooding attacks. The proposed scheme Flooding Attack Prevention Routing Protocol (FAPRP) scheme is based on kNN ML method which uses route discovery frequency vector for feature selection such as route discovery time and inter-route discovery time. The NS2 simulator has been used to build and train the dataset. The kNN classifier is used to organize the nodes into two class vector Normal Vector Class (NVC) and Malicious Vector Class (MVC).

Proposed Scheme

In this section, the working mechanism of the proposed TrustML-RP scheme is presented to counter DDoS and node misbehavior attacks. The methodology is comprised of two phases. The first phase is responsible for establishing trust among the nodes in an ad-hoc network using distributed trust model. TrustML-RP incorporates the trust model from our previous work (Ahmed et al., 2015), however, a brief description of trust estimation is provided in the subsequent subsection. Whereas, the second phase is responsible for using ML techniques ANN and SVM to find possible routes and detect attacker nodes in the network based on the provided dataset.

Trust Estimation

The trust estimation factor is based on the packet forwarding behavior of a node. To estimate the trustworthiness of nodes, a methodology can be followed that involves collecting evidence, calculating trust values, setting a threshold, identifying trusted and misbehaving nodes, taking appropriate action, and updating trust values. The evidence is collected based on observing the packet forwarding behavior of a node by monitoring the traffic patterns that indicate potential attacks. Based on the collected evidence, the trust level of a node is calculated. If a node correctly forwards the packets to the intended destination, its trust rating is increased. Conversely, if it behaves abnormally and drops the packets instead of forwarding them to the destination its trust rating is decreased. The trust values fall within the range of [0,1] and a threshold value of 0.5 is used to differentiate between the normal (trusted) and attacker (misbehaving) nodes. The nodes whose trust value fall below the threshold is considered malicious node while the nodes having trust values above the threshold are considered normal nodes. Appropriate action can then be taken against misbehaving nodes, such as isolating or blocking them, or deploying additional security measures to prevent further attacks. It is important to continue monitoring and updating trust values based on node behavior to maintain an accurate and up-to-date assessment of node trustworthiness.

Machine Learning Model

Following the trust estimation, the labelled data is prepared for training of the ML models. This involves checking and removing any null values, removing redundancy, and fixing structural errors. Relevant features from the dataset are selected based on the attack type. A feature mapping step then captures the input ranges in a suitable space for training purpose. The dataset is divided into train and test data by a ratio of 70:30 to get around overfitting. The workflow of proposed scheme is shown in Figure 1.

An artificial neural network (ANN) and a support vector machine (SVM) model are fit to the train data. The ML model's parameters are provided in Table 1. The trained models are exported and integrated into the system by deploying it at the network edge to process incoming traffic in real-time. The model should generate a trust score for each incoming packet and use it to make decisions about forwarding or dropping the packet. The

performance of the trust-based machine learning scheme is evaluated by measuring its accuracy, F1-score, and processing time.

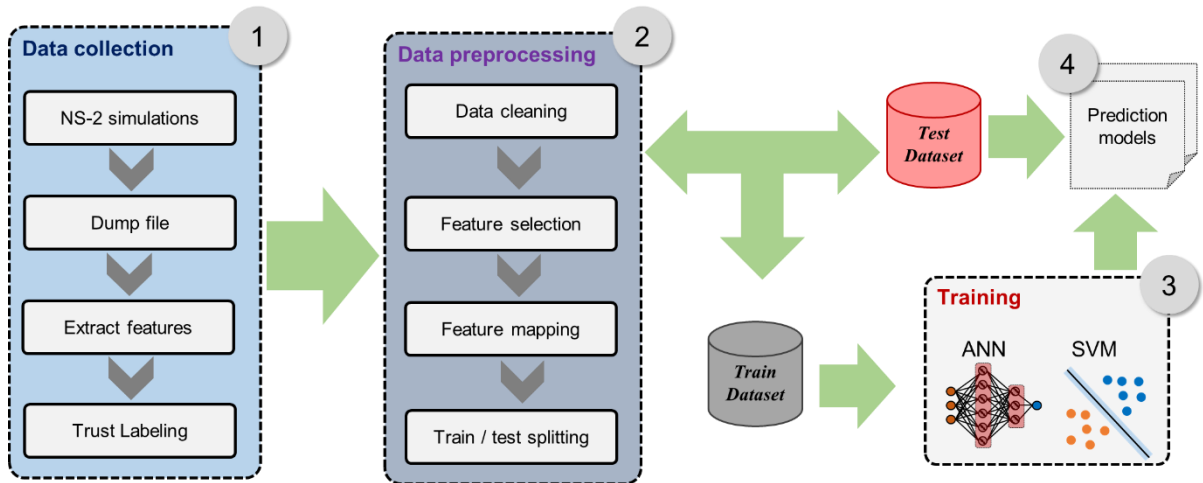


Figure 1. Trust-ML workflow

Table 1. Parameters of ML Models

Algorithm	Parameter configuration
ANN	epochs=100
	batch_size=64
	activation=relu
	optimizer=adam
SVM	Gamma=0.1
	C=1000

Results and Discussion

The proposed scheme is evaluated on the test dataset and the results are presented in this section mainly for accuracy and training time. The NS-2 simulator has been used to simulate the network of 300 nodes, where the nodes are randomly deployed in an area of 100m x 100m. The attacker nodes are also randomly deployed which model the behavior of packet suppression and DDoS attacks (TCP-SYN, UDP and ICMP flood).

Figure 2 visualizes the accuracy score of the trained models i.e., the SVM and ANN classifiers on the test data for the three attack types (TCP-SYN attack, UDP and ICMP flood attacks). Overall, the SVM classifier outperforms the ANN by reaching up to 91% accuracy (in case of UDP attack). ANN's maximum accuracy score remained 71% for TCP_SYN attack types. We believe that this might be caused by mainly two factors: size of the dataset and the architecture of the ANN which was kept simple for the sake of training complexity. However, when sufficient training data and time is available, ANN's performance could be greatly improved.

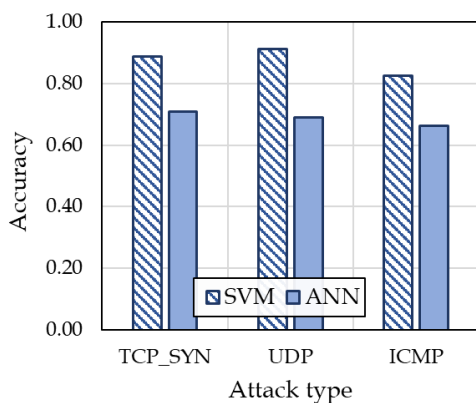


Figure 2. Accuracy of ML methods

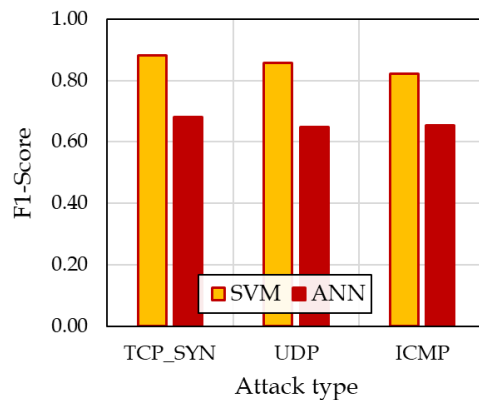


Figure 3. F1-score of ML methods

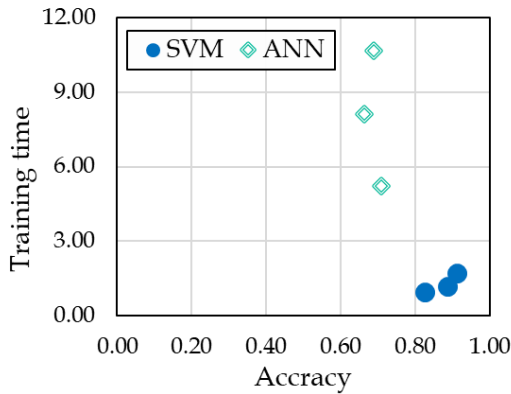


Figure 4. Accuracy vs. Training time for TCP_SYN attack

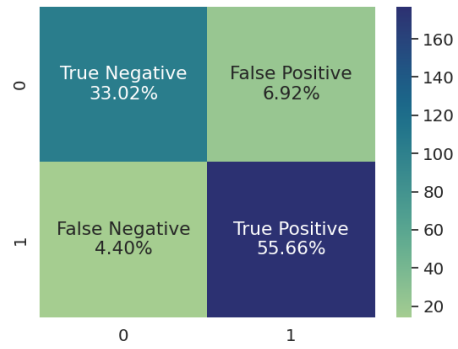


Figure 5. Confusion matrix for the SVM classifier for TCP_SYN attack

In Figure 3, we show the F1-score of the ML methods. Here, again a similar trend is to be observed and SVM classifier obtains way better F1-scores as compared to the ANN. In our case, we plot a tradeoff curve for training times and accuracy in Figure 4. In this case it is clearly seen that the ANN classifier tends to occupy the center part of the graph whereas the points on the lower right corner are more favorable points which represent higher accuracy and lower training times. The training times of both classifiers are detailed in Table 2. Finally, in Figure 5 a confusion matrix for the TCP_SYN attack is shown for the SVM classifier showing a distribution of predictions made by the classifier.

Table 2. Training time for ML algorithms

Algorithm	Training time (s)	
	SVM	ANN
TCP_SYN	1.19	5.21
UDP	1.72	10.64
ICMP	0.96	8.12

Overall, the experimental results demonstrated that the ML methods are greatly capable of capturing the behavior of the malicious nodes in a real-time network environment. Particularly, we evaluated SVM and ANN classifier to differentiate normal and malicious nodes. The SVM classifier in this case showed superior performance for the test dataset. This enables the proposed TrustML-RP scheme to make more informed decision regarding the trusted and malicious nodes and isolate them from the active routes thereby leads to the selection of trusted routes. Consequently, results in the improved network performance as compared to existing schemes, in terms of the throughput and end-to-end delay as shown in the Figures 6 and 7. The various number of malicious nodes are randomly deployed in the network of 300 nodes. The design of TrustML-RP centered upon integration of trust and AI methods, thereby significantly minimizes the impact of misbehaving nodes and outperform their counterpart schemes.

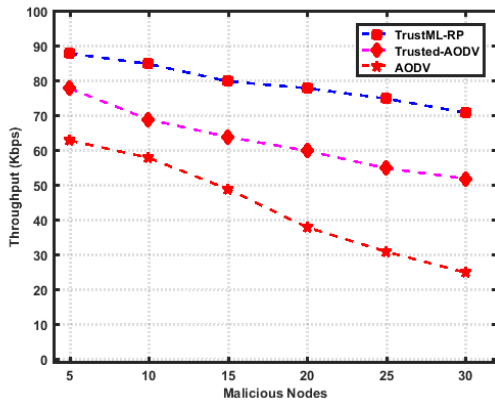


Figure 6. Throughput performance

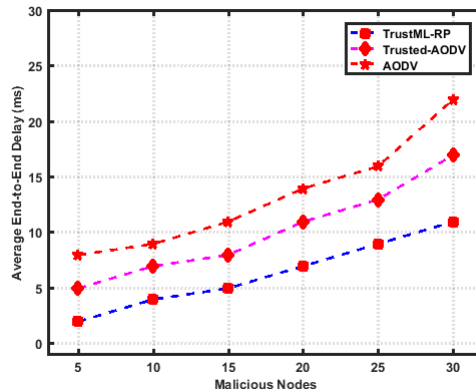


Figure 7. End-to-End delay performance

Conclusion

This paper presented a TrustML-RP scheme to counter packet suppression and DDoS attacks such as TCP-SYN attack, UDP and ICMP flooding attacks. The TrustML-RP scheme integrates the concept of trust and ML methods (ANN and SVM) to improve the attack resilience capability of cybersecurity scheme. The presented results depicted that the proposed TrustML-RP scheme efficiently detected the malicious nodes with better accuracy, isolated them from the active routes, paved the way for trusted network environment and improved the level of network security. Furthermore, the result finding also suggested that traditional cybersecurity mechanism can become more effective with the integration of AI-based machine learning techniques thereby enables cybersecurity professional to deploy automated security and threat detection system.

Scientific Ethics Declaration

The authors declare that the scientific ethical and legal responsibility of this article published in EPSTEM journal belongs to the authors

Acknowledgement

* This article was presented as an oral presentation at the International Conference on Research in Engineering, Technology and Science (www.icrets.net) held in Budapest/Hungary on July 06-09, 2023.

*This work was supported by Pakistan Science Foundation (PSF) via grant number PSF/P&D/TG-ND (882)/2023.

References

- Ahmed, A., Bakar, K. A., Channa, M. I., Haseeb, K., & Khan, A. W. (2015). TERP: A trust and energy aware routing protocol for wireless sensor network. *IEEE Sensors Journal*, 15(12), 6962–6972.
- Awais Rajput, M., Umar, M., Ahmed, A., Raza Bhangwar, A., Suhail Memon, K., & Misbah, A. (2022). Evaluation of machine learning based network attack detection. *Sukkur IBA Journal of Emerging Technologies*, 5(2), 58–66.
- Cheema, A., Tariq, M., Hafiz, A., Khan, M. M., Ahmad, F., & Anwar, M. (2022). Prevention techniques against distributed denial of service attacks in heterogeneous networks: A systematic review. *Hindawi Security and Communication Networks*.
- Ercan, S., Ayaida, M., & Messai, N. (2022). Misbehavior detection for position falsification attacks in VANETs using machine learning. *IEEE Access*, 10, 1893–1904.
- Grover, J., Prajapati, N. K., Laxmi, V., & Gaur, M. S. (2011). Machine learning approach for multiple misbehavior detection in VANET (pp.644-653). *International Conference on Advances in Computing and Communications*. Springer.
- Hasan, M. K., Habib, A. A., Shukur, Z., Ibrahim, F., Islam, S., & Razzaque, M. A. (2023). Review on cyber-physical and cyber-security system in smart grid: Standards, protocols, constraints, and recommendations. *Journal of Network and Computer Applications*, 209.
- Luong, N. T., Vo, T. T., & Hoang, D. (2019). FAPRP: A machine learning approach to flooding attacks prevention routing protocol in mobile ad hoc networks. *Wireless Communications and Mobile Computing*.
- Malaivongs, S., Kiattisin, S., & Chatjuthamard, P. (2022). Cyber trust index: A framework for rating and improving cybersecurity performance. *Applied Sciences*, 12(21).
- Shafi, S., Mounika, S., & Velliangiri, S. (2023). Machine learning and trust based AODV routing protocol to mitigate flooding and blackhole attacks in MANET. *Procedia Computer Science*, 218, 2309–2318.
- van der Heijden, R. W., Lukaseder, T., & Kargl, F. (2018). VeReMi: A dataset for comparable evaluation of misbehavior detection in VANETs. *Lecture Notes of the Institute for Computer Sciences, Social- Informatics and Telecommunications Engineering, LNICST*, 254, 318–337.
- Zahra, F., Jhanjhi, N. Z., Brohi, S. N., Khan, N. A., Masud, M., & AlZain, M. A. (2022). Rank and wormhole attack detection model for RPL-based internet of things using machine learning. *Sensors*, 22(18), 6765. <https://doi.org/10.3390/s22186765>

- Zeng, P., Liu, A., Zhu, C., Wang, T., & Zhang, S. (2022). Trust-based multi-agent imitation learning for green edge computing in smart cities. *IEEE Transactions on Green Communications and Networking*, 6(3), 1635–1648.
- Zhang, Z., Ning, H., Shi, F., Farha, F., Xu, Y., Xu, J., Zhang, F., & Choo, K. K. R. (2022). Artificial intelligence in cyber security: research advances, challenges, and opportunities. *Artificial Intelligence Review*, 55(2), 1029–1053.

Author Information

Adnan Ahmed

Quaid-e-Awam University of Engineering, Science and Technology,
Nawabshah, Pakistan.

Contact e-mail: adnan.ahmed03@quest.edu.pk

Muhammad Awais

Quaid-e-Awam University of Engineering, Science and Technology
Nawabshah,, Pakistan

Mohammad Siraj

King Saud University
Riyadh, Saudi Arabia

Muhammad Umar

Quaid-e-Awam University of Engineering, Science and Technology,
Nawabshah, Pakistan.

To cite this article:

Ahmed, A., Awais, M., Siraj, M., & Umar, M. (2023). Enhancing cybersecurity with trust-based machine learning: A defense against DDoS and packet suppression attacks. *The Eurasia Proceedings of Science, Technology, Engineering & Mathematics (EPSTEM)*, 23, 262-268.

The Eurasia Proceedings of Science, Technology, Engineering & Mathematics (EPSTEM), 2023

Volume 23, Pages 269-281

ICRETS 2023: International Conference on Research in Engineering, Technology and Science

Some Engineering Properties of Pineapple Fruit

Rosnah Shamsudin

Universiti Putra Malaysia

Hasfalina Che-Man

Universiti Putra Malaysia

Siti Hajar Ariffin

Universiti Putra Malaysia

Siti Nor Afiekah Mohd-Ghani

Universiti Putra Malaysia

Nazatul Shima Azmi

Universiti Putra Malaysia

Abstract: Pineapple is a tropical fruit that is highly relished for its unique aroma and sweet taste. In contrast to other tropical fruits, pineapples typically feature medium-sized fruits with yellow flesh. Based on the physical properties of pineapple fruit variety MD2 such as dimensions, geometric mean diameter (D_g), arithmetic mean diameter arithmetic mean diameter (D_a), surface area, volume, sphericity, aspect ratio, and projected area and the best-fit mass models have been determined. From the result obtained, the physical properties such as length, thickness, width, D_g , D_a and circumference were found to be 217.8mm, 132.7mm, 132.9mm, 156.5mm, 161.2mm, 394.3mm respectively. Meanwhile for the aspect ratio, mass, volume surface area, sphericity and projected area perpendicular to dimension namely PA_L , PA_T , AND PA_W were found to be 0.61, 1730.4g, 1420 cm^3 , 77107.4 mm^2 , 0.72, 22746.0 mm^2 , 13942.9 mm^2 , and 16866.3 mm^2 respectively. For all physical properties except volume, the best fit mass model to predict mass of pineapple fruits was the quadratic model. Additionally, the findings demonstrated that, in comparison to other attributes, the mass model based on actual volume was more appropriate, with the highest determination coefficient (R^2) for Quadratic and S-curve model. For developing and optimizing machinery for handling, maintenance, distribution, and storage, the mass model of pineapple fruits according to the actual volume in the outcomes is relatively important.

Keywords: Pineapple, MD2 variety, Physical properties, Mass model

Introduction

Pineapple or *Ananas comosus* is a tropical fruit that is highly relished for its unique aroma and sweet taste. It is originally from the American tropics and is a member of the botanical family Bromeliaceae (Izli et al., 2012). Typically, pineapple fruits have yellow flesh colour and are relatively medium in size compared to other tropical fruits. They are made up of many fruitlets and have a distinct maturation pattern from the top near the crown to the bottom of the fruit that determines the maturity level and the time of harvesting. The evaluation based on physical, physicochemical, and chemical attributes of fruit with acceptable flavour and morphological characteristics is used as maturity indicators (Nadzirah et al., 2012). Pineapples can be found all over the world with many regions of pineapple plantations. According to the Malaysian Pineapple Industry Board (MPIB), in 2019, Costa Rica is the biggest producer of pineapples with 3,328,100 MT of pineapples produced followed by Philippines and Brazil with 2,747,856 MT and 2,426,526 MT respectively, while Malaysia is in 22nd place in

- This is an Open Access article distributed under the terms of the Creative Commons Attribution-Noncommercial 4.0 Unported License, permitting all non-commercial use, distribution, and reproduction in any medium, provided the original work is properly cited.

- Selection and peer-review under responsibility of the Organizing Committee of the Conference

© 2023 Published by ISRES Publishing: www.isres.org

the world with 299,912 MT. There are more than 100 varieties of pineapple fruits available in the world but only 6 to 8 varieties are grown commercially (Steingass et al., 2020). In Malaysia, the most common cultivated varieties include Morris, Sarawak, Josaphine, Gandul, Yankee, Masphine, N36 and the most recent, MD2 (Lasekan et al., 2018).

Due to its great flavour, sweetness, golden flesh and skin colour, and ideal cylindrical shape, pineapple variety MD2 is currently the most widely traded variety in the world of international commerce (Shafawi et al., 2020). In addition, pineapple fruit variety MD2 has smaller fruits with an average weight of 1.5 kg, a constant bright gold colour, a sweeter flavour, four times as much vitamin C, less fibre, and less acidity. Its shelf life is also longer.

Before being marketed, pineapples were often classified according to a certain grade based on their mass or size. Due to this, it is essential to determine the relationship between the physical properties to design and optimise a grading machine. Furthermore, the design of other postharvest processing processes, including as handling, sorting, cleaning, transporting, and packaging, depends on the physical characteristics of fruits and their interactions. According to Shahbazi & Rahmati (2020), in comparison to electrical grading systems, which are more complicated and expensive, and mechanical systems, which operate slowly, weight-based grading may be more cost-effective. Therefore, creating a system of rating fruits according to their mass may be practical and applicable. Dimension, mass, volume, and estimated area are the factors that will have the biggest impact on how the grading system is designed. Grading operations based on mass can be achieved by using appropriate models based on the fruit's physical properties. The common regression relationships used in previous studies were Linear, Quadratic, S-curve, and Power models. Thus, this study was undertaken to determine the physical properties (dimensions, D_g , D_a , surface area, volume, sphericity, aspect ratio, and projected area) of pineapple fruit specifically 'MD2' variety and fit into the best mass model.

Material and Methods

Raw Materials

Five pineapple fruits variety MD2 were supplied and harvested from the local farm located in Sg. Merab, Kajang, Selangor, Malaysia on the same day. The fruits chosen were from indices 4 (ripe) which were free from damage and pests. Thus, only mature and healthy fruits were chosen for the conduct of this experiment. The fruits were then stored in room conditions until further used.

Determination of Dimension and Shape of Pineapple Fruit

The three principal dimensions namely length (L), width (W) and thickness (T) were measured as in Figure 1 for each pineapple fruit by using the thread and ruler (accuracy 1 mm). The measurements of the L, W and T of the whole fruit of the pineapple MD2 variety were done. The principal dimensions were measured for five whole fruits and the average value was calculated.

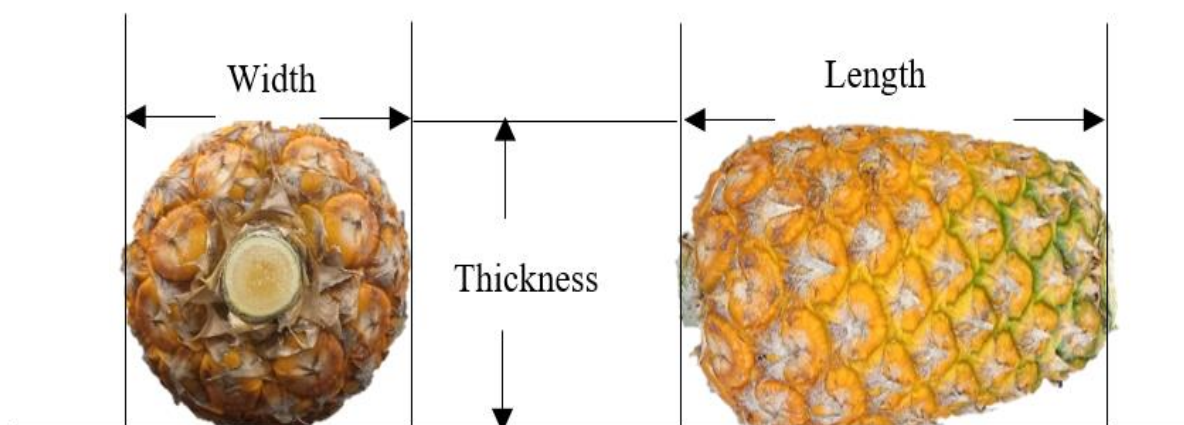


Figure 1. Dimensions of pineapple fruits variety MD2

Determination of Geometric Mean Diameter (D_g) and Arithmetic Mean Diameter (D_a)

D_g and D_a of 5 pineapple fruits were determined using the measured dimensions of L, W, and T. D_g and D_a were then calculated by the following relationships Equations (1) and (2) given by Lorestani (2012), and Zainal A'Bidin et al. (2020).

$$D_g = (LWT)^{\frac{1}{3}} \quad (1)$$

$$D_a = \frac{L+W+T}{3} \quad (2)$$

Where L is the length in mm, W is the width in mm, T is the thickness in mm, D_g is the geometric mean diameter in mm and D_a is the arithmetic mean diameter of pineapple fruit.

Determination of Surface Area

Surface area (SA) was theoretically calculated as apparent surface area using equations given by Lorestani (2012), Shahbazi.& Rahmati (2013) and Panda et al.(2020). The surface area of each pineapple fruit was calculated based on the geometric mean diameter (D_g) using the following Equation (3.3).

$$SA = \pi(D_g)^2 \quad (3)$$

Where SA is surface area in mm², and D_g is the geometric mean diameter in mm.

Determination of Mass

Five samples of whole pineapple fruits were weighed individually by using the analytical balance (TX3202L, Shimadzu, Kyoto, Japan) with an accuracy of 0.01g. The weight was measured in grams (g).

Determination of Volume

The water displacement method was used to measure the volume of the pineapple fruits (Abdul Halim, 2021). The container with a volume of 5 litres was filled with 4.4 litres of water and the initial volume was recorded. The displaced water when the fruit was placed in the container is recorded as the volume of the sample.

Determination of Sphericity

Sphericity (Ø) is defined as the ratio of the surface area of a sphere having the same volume as the fruit to the surface area of the fruit (Dhineshkumar & Siddharth, 2015). The shape of a food material is usually expressed in terms of its sphericity. The sphericity of each pineapple fruit was calculated based on Equation (4) given by Bhore et al. (2015), Azman et al. (2020), and Birania et al. (2022).

$$\emptyset = \frac{(LWT)^{\frac{1}{3}}}{L} \quad (4)$$

Where L is the length in mm, W is the width in mm (diameter), and T is the thickness in mm.

Determination of Aspect Ratio

The aspect ratio (R_a) was obtained using the following relationship Equation (5) as recommended by Azman et al. (2020) and Birania et al. (2022).

$$R_a = \frac{W}{L} \quad (5)$$

Where R_a is the aspect ratio, L is the length in mm, and W is the width in mm.

Determination of Projected Area

The following formulas equations (6), (7), (8), and (9) were used with perpendicular directions to determine the projected areas of pineapple fruits and the criteria projected area (CPA)), suggested by Azman et al. (2022) and Panda et al. (2020).

$$PA_L = \frac{\pi LW}{4} \quad (6)$$

$$PA_T = \frac{\pi TW}{4} \quad (7)$$

$$PA_W = \frac{\pi WW}{4} \quad (8)$$

$$CPA = \frac{PA_L + PA_T + PA_W}{3} \quad (9)$$

Mass Modelling

To estimate the mass, M of pineapple fruits Linear, Quadratic, S-curve, and Power were used and fitted with the data from the trials. These models are presented in Equations (10), (11), (12) and (13) respectively (Shahbazi & Rahmati, 2012; Azman et al., 2020):

$$M = a + bX \quad (10)$$

$$M = a + bX + cX^2 \quad (11)$$

$$M = a + \frac{b}{x} \quad (12)$$

$$M = aX^b \quad (13)$$

where X = the value of an independent parameter, in order to determine how it relates to mass; a , b , and c = curve fitting parameters which are different in each equation.

Statistical Analysis

Employing statistical tools SigmaPlot (Version 18.0), data analysis and mass modelling prediction were carried out. Standard error of the estimate (SEE) and coefficient of determination (R^2) were chosen as the conditions to assess the efficacy of regression models. The models that were appropriate were those with greater R^2 and lower SEE values. In general, for regression equations, the R^2 value near 1.00 shows a good fit with the model (Shahbazi & Rahmati, 2012).

Result and Discussion

Dimension and Shape

Table 1 shows that the average L of pineapple fruits was 217.8 mm, with a range of 193.0 to 240.0 mm. The average D and T of a pineapple fruit, however, were 132.7 mm and 132.9 mm, respectively. The numbers for maximum and minimum W were 143.0 mm and 114.0 mm, respectively, whereas the values for maximum and

minimum T were 142.0 mm and 116.0 mm, respectively. As can be seen, the pineapple fruits' mean L had the highest values when compared to thickness and width. The average thickness and width values were almost identical at the same time. The reason for this is that pineapple fruits resemble pinecones in shape. The measurements' relative standard deviations for L, T, and W were 16.1 mm, 8.8 mm, and 9.8 mm, with L having the highest standard deviation. Because there were only 5 samples of pineapple fruits utilised in the experiment, the standard deviation has a higher value. Circumference (D), which was also measured, had a mean value of 394.3±35 mm. The measurements of the circumference of pineapple fruits ranged from 307.0 mm to 432.0 mm. In a comparison of the 'MD2' variety with the other varieties of pineapple fruits, it can be said that the mean length of MD2 variety (217.8 mm) is larger than Josapine variety, which is 126.35mm (Shamsuddin et al., 2009). The same observation was also observed for the T and W, where the MD2 variety has a larger mean of T (132.7 mm) and W (132.9 mm) compared to the Giant Kew variety (95.6 mm) and (86.56 mm) respectively (Bhore et al., 2017).

Table 1. Physical properties of pineapple fruit variety MD2

Parameter	Mean	Standard deviation	Maximum Value	Minimum Value
L (mm)	217.8 ± 16.1	16.1	240.0	193.0
T (mm)	132.7 ± 8.8	8.8	142.0	116.0
W (mm)	132.9 ± 9.8	9.8	143.0	114.0
D _g (mm)	156.5 ± 8.7	8.7	169.5	138.1
D _a (mm)	161.2 ± 8.7	8.7	175.0	142.7
D (mm)	394.3 ± 35.0	35.0	432.0	307.0
AR	0.61 ± 0.06	0.06	0.72	0.51
m (g)	1730.4 ± 193.5	193.5	1996.1	1507.3
V (cm ³)	1420 ± 120.7	120.7	1600.0	1300.0
SA (mm ²)	77107.4 ± 8427.5	8427.5	90258.2	59927.3
Ø	0.72 ± 0.05	0.05	0.8	0.64
PA _L (mm ²)	22746.0 ± 2560.9	2560.9	26941.2	17540.04
PA _T (mm ²)	13910.0 ± 1849.2	1849.2	15940.2	10471.90
PA _W (mm ²)	13942.9 ± 1986.3	1986.3	16052.4	10201.86
CPA (mm ²)	16866.3 ± 1993.5	1993.5	19644.6	12767.24

Geometric Mean Diameter (D_g) and Arithmetic Mean Diameter (D_a)

Based on Table 1, D_g of pineapple fruits was recorded as 156.5±8.7 mm. The maximum and minimum values of D_g were 169.5 mm and 138.1 mm respectively. Compared to the other variety of pineapple fruits such as the Giant Kew variety, pineapple fruits variety MD2 had a larger mean value of D_g, which was 156.5 mm compared to 102.6 mm for the Giant Kew variety (Bhore et al., 2017). The mean value of D_a of pineapple fruits was 161.2±8.7 mm. D_a had values as high as 138.1 mm and as low as 169.6 mm, respectively. Designing sorting and packaging machinery can benefit from knowing the details of D_g and D_a, especially for goods having asymmetrical geometrical shapes.

Surface area is expressed as the total area over the outside of a fruit. Based on Table 1, the mean value of the surface area of pineapple fruits variety MD2 was 77107.4±8427.5 mm². The maximum and minimum values of pineapple fruits' surface area were 90258.2 mm² and 59927.3 mm² respectively. Clayton et al. (1996) claimed that surface area is important when expressing the transfer of heat into or out of fruits and vegetables. Comparing the surface area of pineapple fruits with other fruits such as papaya fruit, pineapple fruit has a smaller surface area (77107.4 mm²) than papaya fruit which has a surface area of 643.40 cm² or 164340 mm² (Khet et al., 2018). Thus, it can be concluded that the rate of energy transfer through the surface area of the pineapple fruit is much slower compared to the papaya fruit.

Mass

According to Table 4.1, the mean value of the mass of pineapple fruit was shown. The mean value for pineapple fruits' mass varied from 1507.3 g to 1996.1 g, with a mean value of 1730.4 g. The standard deviation for the mass of pineapple fruits was 8427.5 g. Siti Rashima et al. (2019) claimed that the mass of pineapple fruits of variety MD2 ranged from 1.5 kg to 3.0 kg, and that their discovery was consistent with the observed result.

However, nutritional aspects, crop load, water availability, as well as physiological aspects including seed weight, carbohydrate availability, and bloom quality, may affect the pineapple fruit's mass.

Table 4. Model validation for Quadratic model based on volume with a given volume.

Sample	Mass measured, m (g)	Volume measured, V (cm ³)	Estimated mass, m _e (g)	Error %
1	1996.03	1600.00	2011.32	0.77
2	1569.60	1300.00	1538.82	1.96
3	1893.07	1500.00	1873.82	1.02
4	1685.73	1400.00	1716.32	1.81
5	1507.30	1300.00	1538.82	2.09

Based on a study by Mohd Ali et al. (2020) that looked at the average weight of pineapple fruits for a number of different cultivars, including Smooth Cayenne, Sarawak, Hilo, Champaka, Kew, N36, Queen, Morris, Ripley, Mauritius, Alexandra, Yankee, Josapine, Mas Merah, Red Spanish, Gold, MD2, Perola, Pernambuco, Sugar Loaf, Perolera, and These kinds were divided into 7 categories, with the average mass of each group being 2-3kg, 0.8-1.5kg, 1-2kg, 1.5-3.0kg, 1-5kg, and 3-4kg, respectively. These groups were Cayenne, Queen, Spanish, Extra Sweet Cayenne Hybrids, Pernambuco, Modilonus, and Perolera. The MD2 variety's average mass ranges from 1.5 to 3.0kg because it is in Extra Sweet Cayenne Hybrids.

Volume

As tabulated in Table 1, the mean volume for pineapple fruits was recorded as 1420 cm³ with a standard deviation of 120.7 cm³. The volume varied from 1300 cm³ to 1600 cm³. Lapcharoensuk et al. (2017) studied the correlations of all physicochemical properties including volume and they found that weight correlated positively with volume. This showed that the weight and volume of pineapple fruit rose along with its size. Additionally, they claimed that depending on its ripeness, pineapple fruit volume fluctuates (Lapcharoensuk et al., 2017). When comparing the MD2 variety's volume (872 to 1200 cm³) to that of the Smooth Cayenne variety, the MD2 variety is greater (1420 cm³).

Sphericity

Sphericity is defined as the characteristic shape of a solid object relative to that of a sphere of the same volume. Sphericity is used to describe the shape of the pineapple where if the value of sphericity is close to 1, it can be considered an ideal sphere. Based on the result obtained, the mean value of the sphericity of pineapple fruits was 0.72±0.05. The maximum and minimum values of pineapple fruits were 0.64 to 0.80, respectively. Thus, from the mean value of sphericity, the pineapple fruits cannot be considered an ideal sphere because the sphericity value of pineapple fruits was smaller than one. A study conducted by Bhore et al. (2017) found that the sphericity of pineapple fruit was in the range between 0.65 and 0.85 with an average value of 0.77 at the standard deviation of ± 0.05. This finding was nearly the same as the result obtained.

Aspect Ratio

Aspect ratio, which compares the width to the length of the fruits in proportion, is one of the phrases used to describe the shape of a food material. The mean value of the aspect ratio of pineapple fruits is 0.61 with a standard deviation of 0.06. The minimum and maximum values of the aspect ratio of pineapple fruits were 0.72 and 0.51 respectively, as shown in Table 1. This high aspect ratio suggested that rather than rolling like gram, pineapple fruits will slide along their flat surface like oil bean seeds. The design of hoppers must take into account this propensity to roll or slide (Dash et al., 2008). However, there is no information from the previous research about the aspect ratio of pineapple fruit. From previous research, the aspect ratio for Ipoli fruits was found to be 0.7 (Burubai, 2014) while dabai fruits were found to be 0.56 (Abdul Halim, 2021).

Projected Areas

Based on Table 1, the mean value for other measured physical properties was projected area perpendicular to the length (PA_L), projected area perpendicular to the thickness (PA_T), projected area perpendicular directions to the width (PA_W), and criteria projected area (CPA) of pineapple fruits were $22746.0 \pm 2560.9 \text{ mm}^2$, $13910.0 \pm 1849.2 \text{ mm}^2$, $13942.9 \pm 1986.3 \text{ mm}^2$, $16866.3 \pm 1993.5 \text{ mm}^2$, respectively. The minimum and maximum values of PA_L were 17540.0 mm^2 and 26941.2 mm^2 , while for PA_T , the minimum and maximum values were 10471.9 mm^2 and 15940.2 mm^2 . Other than that, the minimum and maximum values of PA_W were 10201.9 mm^2 and 16052.5 mm^2 . The minimum and maximum values of CPA were 12767.2 mm^2 and 19644.6 mm^2 respectively. Projected area values play a significant role in machine vision-based grading system design and development. To predict the ideal time to harvest, the amount of water lost, and the amount of heat and mass transferred during drying and cooling, the projected area can be used to determine the respiration rate, maturity index, and gas permeability. Additionally, the natural diversity in fruit dimensional qualities may be the cause of the projected disparity in the physical properties (Azman et al., 2020).

Mass Modelling

In mass modelling, the dimensions, geometric mean diameter, arithmetic mean diameter, volumes, surface areas, and projected areas in three perpendicular directions of pineapple fruits were used. Table 2 showed the best models for predicting mass using the mean dimensions, weight, surface areas, projected area and volume of pineapple fruits along with their coefficients of determination, R^2 , and SEE. Using the coefficient of determination (R^2), the regression mass was assessed, and the best-fit model was identified by a higher R^2 value.

Table 2. Mass models of pineapple fruits based on physical properties L, T, W, D_g , D_a and D

Dependent parameter	Independent parameter	Model equation	Regression constant			Statistical parameter		The best fitted model
			a	b	c	R^2	SEE	
M (g)	L (mm)	Linear	-772.634	11.492	-	0.915	58.493	Quadratic
M (g)	L (mm)	Quadratic	5536.354	-46.936	0.135	0.937	52.550	
M (g)	L (mm)	S-curve	4174.550	-529603.009	-	0.894	65.294	
M (g)	L (mm)	Power	0.653	1.464	-	0.919	57.181	
M (g)	T (mm)	Linear	-863.930	19.727	-	0.831	86.936	Quadratic
M (g)	T (mm)	Quadratic	19874.523	-303.408	1.252	0.954	47.663	
M (g)	T (mm)	S-curve	4173.446	-319584.668	-	0.800	94.600	
M (g)	T (mm)	Power	0.908	1.548	-	0.839	84.876	
M (g)	W (mm)	Linear	-1476.855	23.956	-	0.806	88.422	Quadratic
M (g)	W (mm)	Quadratic	22153.119	-335.620	1.363	0.940	52.030	
M (g)	W (mm)	S-curve	4754.771	-403419.002	-	0.768	96.734	
M (g)	W (mm)	Power	0.125	1.946	-	0.822	84.694	
M (g)	D_g (mm)	Linear	-1999.495	23.739	-	0.835	80.495	Quadratic
M (g)	D_g (mm)	Quadratic	8750.875	-113.506	0.437	0.857	78.356	
M (g)	D_g (mm)	S-curve	5394.705	-574512.893	-	0.816	84.915	
M (g)	D_g (mm)	Power	0.141	1.863	-	0.804	88.866	
M (g)	D_a (mm)	Linear	-1529.034	423.379	-	0.821	85.053	Quadratic
M (g)	D_a (mm)	Quadratic	9333.968	-116.006	0.426	0.865	76.926	
M (g)	D_a (mm)	S-curve	4854.465	-502084.419	-	0.789	92.263	
M (g)	D_a (mm)	Power	0.090	1.940	-	0.832	82.328	
M (g)	D (mm)	Linear	-976.008	6.796	-	0.881	68.374	Quadratic
M (g)	D (mm)	Quadratic	15537.922	-77.207	0.106	0.935	48.706	
M (g)	D (mm)	S-curve	4350.654	-	1038940.164	0.859	74.387	
M (g)	D (mm)	Power	0.123	1.595	-	0.887	66.654	

Models Based on Dimensions

Table 2 shows the mass prediction results of the pineapple fruits based on the L, T, W, D_g and D_a . It shown that, for all features specified on dimensions, the Quadratic model was the best-fit model to determine and assess the mass of pineapple fruits (length, thickness, width, circumference, D_g , and D_a). For pineapple fruits, T had the

highest value of R^2 and the lowest value of SEE, which were 0.9539 and 47.663, respectively, as shown in Table 2. Highest value of coefficient determination (R^2) showed that a respectable percentage of the variability in the dependent variable is explained by the model (Azman et al., 2020), while lower standard error estimate (SEE) indicated that the approximate size of the prediction errors (Siegel & Wagner, 2022). The lower the SEE value, smaller the prediction error and more accurate the fitted model. Equation (41) displays the equation of the Quadratic model found based on physical properties thickness (T).

$$M = 19874.523 - 303.408 T + 1.252 T^2 \tag{14}$$

According to Table 2, the best fit model for mass prediction of pineapple fruits based on the length (L) was quadratic model with highest R^2 of 0.9368 and lowest SEE of 52.55, followed by Power model with R^2 of 0.9189, Linear model with R^2 of 0.9151 and lastly S-curve model with R^2 of 0.8942. The SEE values for Power model Linear model and S-curve model were 57.181, 58.493 and 65.294, respectively. The best model for mass determination based on L was a Quadratic model following Equations (15)

$$M = 5536.354 - 46.936L + 0.135 L^2 \tag{15}$$

A study conducted by Nur Salihah et al. (2015), suggested the best model for mass determination based on L for pomelo fruit was a Quadratic model which was similar to the findings. A similar model for onion and pepper berries in another study was suggested and reported by Ghabel et al. (2010) and Azman et al. (2020), where the best model for mass determination based on L was a Quadratic model.

Table 2. Mass models of pineapple fruits based on L, T, W, D_g , D_a and D

Dependent parameter	Independent parameter	Model equation	Regression constant			Statistical parameter		The best fitted model
			a	b	c	R^2	SEE	
M (g)	L (mm)	Linear	-772.634	11.492	-	0.915	58.493	Quadratic
M (g)	L (mm)	Quadratic	5536.354	-46.936	0.135	0.937	52.550	
M (g)	L (mm)	S-curve	4174.550	-529603.009	-	0.894	65.294	
M (g)	L (mm)	Power	0.653	1.464	-	0.919	57.181	
M (g)	T (mm)	Linear	-863.930	19.727	-	0.831	86.936	Quadratic
M (g)	T (mm)	Quadratic	19874.523	-303.408	1.252	0.954	47.663	
M (g)	T (mm)	S-curve	4173.446	-319584.668	-	0.800	94.600	
M (g)	T (mm)	Power	0.908	1.548	-	0.839	84.876	
M (g)	W (mm)	Linear	-1476.855	23.956	-	0.806	88.422	Quadratic
M (g)	W (mm)	Quadratic	22153.119	-335.620	1.363	0.940	52.030	
M (g)	W (mm)	S-curve	4754.771	-403419.002	-	0.768	96.734	
M (g)	W (mm)	Power	0.125	1.946	-	0.822	84.694	
M (g)	D_g (mm)	Linear	-1999.495	23.739	-	0.835	80.495	Quadratic
M (g)	D_g (mm)	Quadratic	8750.875	-113.506	0.437	0.857	78.356	
M (g)	D_g (mm)	S-curve	5394.705	-574512.893	-	0.816	84.915	
M (g)	D_g (mm)	Power	0.141	1.863	-	0.804	88.866	
M (g)	D_a (mm)	Linear	-1529.034	423.379	-	0.821	85.053	Quadratic
M (g)	D_a (mm)	Quadratic	9333.968	-116.006	0.426	0.865	76.926	
M (g)	D_a (mm)	S-curve	4854.465	-502084.419	-	0.789	92.263	
M (g)	D_a (mm)	Power	0.090	1.940	-	0.832	82.328	
M (g)	D (mm)	Linear	-976.008	6.796	-	0.881	68.374	Quadratic
M (g)	D (mm)	Quadratic	15537.922	-77.207	0.106	0.935	48.706	
M (g)	D (mm)	S-curve	4350.654	-	1038940.164	0.859	74.387	
M (g)	D (mm)	Power	0.123	1.595	-	0.887	66.654	

For mass prediction of pineapple fruits based on width (W), the quadratic model has the highest R^2 of 0.940 and the lowest SEE of 52.030 compared to the Linear ($R^2 = 0.806$), S-curve ($R^2 = 0.768$), Power ($R_2 = 0.822$) model. The equation of quadratic model obtained showed in Equation (16).

$$M = 22153.119 - 335.620 W + 1.363 W^2 \tag{16}$$

For mass prediction of pineapple fruits based on D_g and D_a , the quadratic model was the best fit model which had the highest R^2 of 0.857 and the lowest SEE of 78.356 for D_g , and highest R^2 of 0.865 and the lowest SEE of 76.926 for D_a compared to the other model as in Table 2. The equation of quadratic model obtained to predict the mass of pineapple fruits based on D_g and D_a showed in Equation (17) and (18) respectively.

$$M = 8750.875 - 113.506 D_g + 0.437 D_g^2 \tag{17}$$

$$M = 9333.968 - 116.06 D_a + 0.426 D_a^2 \tag{18}$$

According to Table 2, the pineapple fruits had circumference (D) values with the highest R^2 (0.935) and the lowest SEE (48.706). The model equation obtained for these parameters was Quadratic. Equations (19) were determined for the parameters D.

$$M = 15537.922 - 77.207 D + 0.106 D^2 \tag{19}$$

As for the entire dimensions, the S-curve model was reported to have lower R^2 values except for D_g parameter, which had lower R^2 value for Power model. The lower R^2 values might be caused by the pineapple fruits' non-uniform mass corresponding to their size. Therefore, it is recommended to size pineapple fruits according to their length as suggested by Nur Salihah et. al [25], Ghabel. [26] and Azman [14].

Models Based on Volume

Based on Table 3, it showed the mass prediction results of the pineapple fruits based on actual volume (V), the Quadratic model and S-curve model based on V was found to be the best fit when compared to the other models. They had the similar and highest R^2 which was 0.981 and the lowest SEE of 28.840 (Quadratic model) and 28.038 (S-curve model). S-curve model was chosen as the best fitted model because it had highest R^2 and lowest SEE compared to Quadratic model. This finding was differed from previous study conducted by Nur Salihah et al., (2015), who found the Quadratic model was the best model

Table 3. Mass models of pineapple fruits based on volume, surface area and projected area

Dependent parameter	Independent parameter	Model equation	Regression constant			Statistical parameter		The best fitted model
			a	b	c	R^2	SEE	
M (g)	V (cm ³)	Linear	-520.534	1.585	-	0.978	29.567	S-curve
M (g)	V (cm ³)	Quadratic	-2588.677	4.475	-0.001	0.981	28.840	
M (g)	V (cm ³)	S-curve	4039.966	-3258111.845	-	0.981	28.038	
M (g)	V (cm ³)	Power	0.144	1.294	-	0.977	30.178	
M (g)	SA (mm ²)	Linear	141.028	0.021	-	0.806	88.364	Quadratic
M (g)	SA (mm ²)	Quadratic	3206.432	-0.062	5.4E-07	0.861	77.803	
M (g)	SA (mm ²)	S-curve	3146.330	-107890514.3584	-	0.734	103.553	
M (g)	SA (mm ²)	Power	0.049	0.932	-	0.804	88.870	
M (g)	PA _L (mm ²)	Linear	168.048	0.069	-	0.827	83.571	Quadratic
M (g)	PA _L (mm ²)	Quadratic	2018.558	-0.097	3.66E-06	0.850	81.076	
M (g)	PA _L (mm ²)	S-curve	3171.832	-32388213.738	-	0.764	97.527	
M (g)	PA _L (mm ²)	Power	0.185	0.912	-	0.825	84.044	
M (g)	PA _T (mm ²)	Linear	-757.736	0.173	-	0.831	75.526	Quadratic
M (g)	PA _T (mm ²)	Quadratic	9810.755	-1.293	5.06E-05	0.866	70.759	
M (g)	PA _T (mm ²)	S-curve	4213.347	-35567762.670	-	0.812	79.601	
M (g)	PA _T (mm ²)	Power	0.003	1.393	-	0.833	74.996	
M (g)	PA _W (mm ²)	Linear	-490.851	0.154	-	0.845	72.388	Quadratic
M (g)	PA _W (mm ²)	Quadratic	11070.146	-1.456	5.57E-05	0.912	57.429	
M (g)	PA _W (mm ²)	S-curve	3911.703	-31279492.453	-	0.817	78.515	
M (g)	PA _W (mm ²)	Power	0.007	1.301	-	0.848	71.512	
M (g)	CPA (mm ²)	Linear	-347.108	0.121	-	0.852	74.091	Quadratic
M (g)	CPA (mm ²)	Quadratic	2692.564	-0.234	1.03E-05	0.868	73.488	
M (g)	CPA (mm ²)	S-curve	3759.205	-34558470.684	-	0.822	81.423	
M (g)	CPA (mm ²)	Power	0.013	1.212	-	0.855	73.537	

for Malaysian variety of pomelo fruit. The same result also reported by Azman et al. (2020). The Power model was found to have the lowest R^2 (0.977) compared to the other models.

$$M = -2588.677 + 4.475 V - 0.001 V^2 \quad (20)$$

$$M = 4039.966 - \frac{3258111.845}{V} \quad (21)$$

Models Based on Surface Area

Table 3 showed the results of mass prediction of pineapple fruits based on surface area (SA). The Quadratic model was the best fit based on the highest value of R^2 compared to the other models. The values of R^2 and SEE for Quadratic model were 0.861 and 77.803, respectively. The equation of Quadratic model obtained showed in Equation (22).

$$M = 3206.432 - 0.062 SA + 5.4E - 07 SA^2 \quad (22)$$

Linear model had the highest R^2 (0.806) after Quadratic model followed by Power model with R^2 of 0.804 and lastly S-curve model, which had the lowest R^2 (0.734) and highest SEE value of 103.553. Therefore, the Quadratic form was shown as the suggested mass model.

Models Based on Projected Area

Among the models based on the projected area were PA_L , PA_T , PA_W , and CPA. Table 3 showed the results of mass prediction of pineapple fruits based on projected area PA_L , PA_T , PA_W , and CPA. It was found that the best fit model for PA_L , PA_T , PA_W , and CPA were quadratic model based on the highest values of R^2 and lowest values of SEE. The Quadratic model comprising PA_L was the best fit with the highest R^2 of 0.85 and lowest SEE of 81.076. While the Quadratic model comprising, PA_T was the best fit with the highest R^2 0.866 and lowest SEE of 70.759 as shown in Table 4.3. The Quadratic model based on PA_W also achieved with the highest R^2 of 0.912 and lowest SEE of 57.429. While for criteria projected area (CPA), the Quadratic model was the best fit with the highest R^2 of 0.868 and lowest SEE of 73.488 compared to models. The equation of Quadratic model based on PA_L , PA_T , PA_W , and CPA obtained to predict mass of pineapple fruits were showed in Equation (23), (24), (25), (26) respectively.

$$M = 2018.558 - 0.097 PA_L + 3.66 \times 10^{-6} PA_L^2 \quad (23)$$

$$M = 9810.755 - 1.293 PA_T + 5.06 \times 10^{-5} PA_T^2 \quad (24)$$

$$M = 11070.146 - 1.456 + 5.57 PA_W \times 10^{-5} PA_W^2 \quad (25)$$

$$M = 2692.564 - 0.234 CPA + 1.03 \times 10^{-5} CPA^2 \quad (26)$$

In addition, the Quadratic model of projected area perpendicular to the width (PA_W) shown in Table 3 was preferred as the best model to calculate the mass of pineapple fruits. This was due to the high R^2 value of 0.912 compared to PA_L (0.85), PA_T (0.866) and CPA (0.868). All three projected areas are necessary to be specified and applied in grading the pineapple fruits by using this model.

Model Validation

From previous section, it was found that the recommended mass model is based on the volume which had the highest value of determination coefficient (R^2). The equation 4.7 and 4.8 showed the equation that can be used to predict the mass of pineapple fruits. Model validation is needed in order to determine the validation of the model. To determine the validation of the mass model based on the volume, the physical properties which is

volume is needed. The percentage of error is calculated to determine the validity of the model. Equation 27 is used to calculate the percentage of errors:

$$\text{Percentage of errors} = \frac{|\text{Estimated mass} - \text{Measured mass}|}{\text{Measured mass}} \times 100\% \quad (27)$$

Table 4 and 5 shows model validation for Quadratic model and S-curve model based on volume with given volume. Based on Table 4 and 5, can be observed that the percentage of error for both model when predict the mass of pineapple fruits is below 10 percent. According to Seyedpoor, S. (2014), the appropriate error percentage must be below 10%. Thus, it can be concluded that the mass model based on the volume is valid and can be used to predict the mass of pineapple fruits.

Table 4. Model validation for Quadratic model based on volume with a given volume.

Sample	Mass measured, m (g)	Volume measured, V (cm ³)	Estimated mass, m _e (g)	Error %
1	1996.03	1600.00	2011.32	0.77
2	1569.60	1300.00	1538.82	1.96
3	1893.07	1500.00	1873.82	1.02
4	1685.73	1400.00	1716.32	1.81
5	1507.30	1300.00	1538.82	2.09

Table 5. Model validation for S-curve model based on volume with a given volume.

Sample	Mass measured, m (g)	Volume measured, V (cm ³)	Estimated mass, m _e (g)	Error %
1	1996.03	1600.00	2003.65	0.38
2	1569.60	1300.00	1533.73	2.29
3	1893.07	1500.00	1867.89	1.33
4	1685.73	1400.00	1712.74	1.60
5	1507.30	1300.00	1533.73	1.75

Conclusion

The physical properties for dimension of pineapple fruits such as L, T, W, D_g, D_a and circumference were found to be 217.8mm, 132.7mm, 132.9mm, 156.5mm, 161.2mm, 394.3mm respectively. Meanwhile for aspect ratio, mass, volume, surface area, sphericity, PA_L, PA_T, and PA_W were found to be 0.61, 1730.4g, 1420 cm³, 77107.4 mm², 0.72, 22746.0 mm², 13942.9 mm², and 16866.3 mm² respectively. The Quadratic model is best fitted with all physical properties due to its economical viewpoint excluding for actual volume which best fit with Quadratic and S-curve model.

Recommendations

The mass model of pineapple fruits based on actual volume in the obtained results is recommended for designing and optimizing machines for handling, cleaning, conveying, and storing.

Acknowledgements or Notes

* This article was presented as an oral presentation at the International Conference on Research in Engineering, Technology and Science (www.icrets.net) conference held in Budapest, Hungary on July 06-09, 2023.

* The authors declare no conflict of interest.

* R.S. supervised the research and revised the manuscript. S.H.A. and H.C.H. supervised the experiments. N. S. A. wrote the manuscript. S.N.A.M.G. conducted the experiments, collected and analyzed the data of results. All authors have read and agreed to the published version of the manuscript.

* The authors express their gratitude to the Universiti Putra Malaysia for providing financial and technical support under grant GP-IPB/9687803 to conduct this research work.

* The datasets generated during and/or analysed during the current study are available from the corresponding author on reasonable request.

* All the data and images in the manuscript are approved to be published

References

- Abdul Halim, A. A. (2021). *Physical characteristics and effects of blanching treatment on the color and textural properties of dabai fruit (Canarium Odontophyllum Miq.) Variety "Ngemah"*. [Undergraduate Dissertation].
- Azman, P.N.M.A., Shamsudin, R., Che Man, H., & Ya'acob, M. E. (2020). Some physical properties and mass Modelling of pepper berries (*Piper nigrum* L.), variety Kuching, at different maturity levels. *PRO* 8(10), 1314.
- Bhore, N., Surwade, S., Swami, S., & Thakor, N. (2017). Studies on physico-chemical properties of pineapple fruit and development of pineapple peeler. *Indian Society of Agricultural Engineers*, 41(3), 8-15
- Birania, S., Attkan, A. K., Kumar, S., Kumar, N., & Singh, V. K. (2022). Mass modeling of strawberry (*Fragaria* × *Ananasa*) based on selected physical attributes. *Journal of Food Process Engineering*, 45(5). <https://doi.org/10.1111/jfpe.14023>
- Clayton, M., Amos, N. D., Banks, N. H., & Morton, R. H. (1995). Estimation of apple fruit surface area. *New Zealand Journal of Crop and Horticultural Science*, 23(3), 345–349. <https://doi.org/10.1080/01140671.1995.9513908>
- Dhineshkumar, V., & Siddharth, M. (2015). Studies on physical properties of orange fruit. *Journal of Food Research and Technology*, 3(4), 125–130. http://jakraya.com/Journal/pdf/10-jfirtArticle_2.pdf
- Ghabel, R., Rajabipour, A., Ghasemi-Varnamkhasti, M., & Oveisi, M. (2010). Modeling the mass of Iranian export onion (*Allium cepa* L.) varieties using some physical characteristics. *Research in Agricultural Engineering*, 5(1), 33–40. <https://doi.org/10.17221/23/2009-rae>
- Izli, N., Izli, G., & Taskin, O. (2018). Impact of different drying methods on the drying kinetics, color, total phenolic content and antioxidant capacity of pineapple. *CyTA - Journal of Food*, 16(1), 213–221. <https://doi.org/10.1080/19476337.2017.1381174>
- Kher, R. M., Sahu, F. M., Sigh, S. N., & Patel, V. B. (2018) Estimation of surface area of papaya fruits. *International Journal of Current Microbiology and Applied Sciences*, 7(11), 3601-3607.
- Lapcharoensuk, R., Phannote2, N., & Kasetyangyunsapa, D. (2017). Physicochemical properties of pineapple at difference maturity. The 10th TSAE International Conference, Thailand.
- Lasekan, O., & Hussein, F. K. (2018). Classification of different pineapple varieties grown in Malaysia based on volatile fingerprinting and sensory analysis. *Chemistry Central Journal*, 12(1). <https://doi.org/10.1186/s13065-018-0505-3>
- Lorestani, A. N. (2012). Some physical and mechanical properties of caper. *Journal of Agricultural Technology*, 8(4), 1199–1206.
- Mohd Ali, M., Hashim, N., Abd Aziz, S., & Lasekan, O. (2020). Pineapple (*Ananas comosus*): A comprehensive review of nutritional values, volatile compounds, health benefits, and potential food products. *Food Research International* 137, 109675. <https://doi.org/10.1016/j.foodres.2020.109675>
- Nadzirah, K. Z., Zainal, S., Noriham, A., Normah, I., & Roha, A. M. S. (2012). Physico-chemical properties of pineapple crown extract variety n36 and bromelain activity in different forms. *APCBEE Procedia* 4, 130–134. <https://doi.org/10.1016/j.apcbee.2012.11.022>
- Nur Salihah, B., Rosnah, S., & Norashikin, A. A. (2015). Mass modeling of malaysian varieties pomelo fruit (*Citrus grandis* L. osbeck) with some physical characteristics. *International Food Research Journal*, 22(2), 488–493.
- Panda, G., Vivek, K., & Mishra, S. (2020). Physical characterization and mass modeling of kendu (*Diospyros melanoxylon* roxb.) fruit. *International Journal of Fruit Science*, 20(sup3), S2005–S2017. <https://doi.org/10.1080/15538362.2020.1851339>
- Syedpoor, S.. (2014). Re: How much variation between experimental and numerical results is acceptable ?. <https://www.researchgate.net/post/How-much-variation-between-experimental-and-numerical-results-is-acceptable/545bc89fd4c1188e228b45ce/citation/download>.
- Shafawi, N., Azmi, A., Zain, Z.-I., Azid, S., Fareez, M., Syahira, N., Mustaffa, R., Cho, J., Ying, L., Isahak, N., & Khairulfuaad, R. (2020). Reducing sunburn incidence in md2 pineapple using chemical pre-harvest

treatment to overcome post-harvest losses in malaysia. sept) *International Journal of Agriculture, Forestry and Plantation*, 10.

- Shahbazi, F., & Rahmati, S. (2012). Mass modeling of fig (*Ficus carica* L.) fruit with some physical characteristics. *Food Science and Nutrition*, 1(2), 125–129. <https://doi.org/10.1002/fsn3.20>
- Shahbazi, F., & Rahmati, S. (2013). Mass modeling of sweet cherry (*prunus avium*) fruit with some physical characteristics. *Food and Nutrition Sciences*, 4(1), 1–5. <https://doi.org/10.4236/fns.2013.41001>
- Shamsudin, R., Wan Daud, W. R., Takrif, M. S., & Hassan, O. 2009. Physico-mechanical properties of josaphine pineapple fruits. *Pertanika Journal Science and Technology*, 17(1), 117-123.
- Siegel, A. F., & Wagner, M. R. (2022). Correlation and regression. In *Practical Business Statistics*, 313–370. Academic Press. <https://doi.org/10.1016/b978-0-12-820025-4.00011-7>
- Siti Rashima, R., Maizura, M., Wan Nur Hafzan, W. M., & Hazzeman, H. (2019). Physicochemical properties and sensory acceptability of pineapples of different varieties and stages of maturity. *Food Research*, 3(5), 491–500. [https://doi.org/10.26656/fr.2017.3\(5\).060](https://doi.org/10.26656/fr.2017.3(5).060)
- Steingass, C. B., Vollmer, K., Lux, P. E., Dell, C., Carle, R., & Schweiggert, R. M. (2020). HPLC-DAD-APCI-MS analysis of the genuine carotenoid pattern of pineapple (*Ananas comosus* [L.] Merr.) infructescence. *Food Research International*, 127, 108709. <https://doi.org/10.1016/j.foodres.2019.108709>
- Zainal A'Bidin, F. N., Shamsudin, R., Mohd Basri, M. S., & Mohd Dom, Z. (2020). Mass modelling and effects of fruit position on firmness and adhesiveness of banana variety nipah. *International Journal of Food Engineering*, 16(10), 20190199. <https://doi.org/10.1515/ijfe-2019-0199>

Author Information

Rosnah Shamsudin

Department of Process and Food Engineering, Faculty of Engineering, Universiti Putra Malaysia, 43400 UPM Serdang, Selangor, Malaysia
Contact e-mail: rosnahs@upm.edu.my

Hasfalina Che Man

Department of Biological and Agricultural, Faculty of Engineering, Universiti Putra Malaysia, 43400 UPM Serdang, Selangor, Malaysia

Siti Hajar Ariffin

Department of Process and Food Engineering, Faculty of Engineering, Universiti Putra Malaysia, 43400 UPM Serdang, Selangor, Malaysia

Siti Nor Afiekah Mohd Ghani

Department of Process and Food Engineering, Faculty of Engineering, Universiti Putra Malaysia, 43400 UPM Serdang, Selangor, Malaysia

Nazatul Shima Azmi

Department of Process and Food Engineering, Faculty of Engineering, Universiti Putra Malaysia, 43400 UPM Serdang, Selangor, Malaysia

To cite this article:

Shamsudin, R., Che-Man, H., Ariffin, S. H., Mohd-Ghani, S. N. A. & Azmi, N. S. (2023). Some engineering properties of pineapple fruit. *The Eurasia Proceedings of Science, Technology, Engineering & Mathematics (EPSTEM)*, 23, 269-281.

The Eurasia Proceedings of Science, Technology, Engineering & Mathematics (EPSTEM), 2023

Volume 23, Pages 282-291

ICRETS 2023: International Conference on Research in Engineering, Technology and Science

Synthesis, Biological Evaluation and Theoretical Studies of Hydrazone Derivatives

Noura Kichou

Mouloud Mammeri University of Tizi-Ouzou

Nabila Guechtouli

Mouloud Mammeri University of Tizi-Ouzou

Karima Ighilahriz

Mouloud Mammeri University of Tizi-Ouzou

Manal Teferghennit

Laboratory of Electrochemistry-Corrosion

Zakia Hank

Laboratory of Electrochemistry-Corrosion

Abstract: The aim of this work is to synthesize, characterize and evaluate the biological activity of a series of hydrazone derivatives. These compounds were characterized by elemental analysis, IR spectroscopy, mass spectrometry, UV-Vis Spectroscopy, ¹HNMR spectra. In vitro, their antibacterial and antifungal activities were screened against bacterial species (*Staphylococcus aureus*, *Pseudomonas aeruginosa* and *Escherichia coli*) and fungi (*Candida sp*). Amikacin was used as references for antibacterial and antifungal studies. The compounds were optimized at DFT/B3LYP/6-31G (d,p) level of theory. In silico, The Toxicity of the hydrazone derivatives were studied by ADMET(Absorption, distribution, metabolism, excretion, and toxicity) simulations using ADMET lab 2.0 server. The molecular docking studies are carried out to better comprehend the preferential mode of binding of these compounds against biomecular targets such as InhA enzyme characteristic of Mycobacterium Tuberculosis bacteria.

Keywords: Hydrazone derivative, Synthesis, Antibacterial activity, Theoretical study.

Introduction

The Hydrazones possesses some particular properties which make them a potential candidate for designing new moieties. They contain a C=N bond in conjugated form with a functional nitrogen electron pair. They are distinguished from other members of this class (imines, oximes) by the presence of two interlinked nitrogen atoms. These nitrogen atoms are nucleophilic, while the carbon has both an electrophilic and nucleophilic nature and further combining hydrazones with numerous functional groups leads to the formation of products with unique biological properties (Abdullah Shah & Hussain, 2022; Popiolek et al., 2016). Isoniazid is a first-line antitubercular drug and it acts by inhibiting enoyl reductase (InhA) in Mycobacterium Tuberculosis. This drug is a prodrug and needs to be activated by KatG catalase-peroxidase (Al-Khattaf, 2021). A number of hydrazone derivatives have been synthesized from isoniazid and were found to have potentiated activities against various bacterial and fungal strains (Maccari, 2005) including hydrazones with benzohydrazide and menthone (Al-Khattaf, 2021; Krátký, 2017). Furthermore, metal complexes of isonicotinic hydrazones including, copper, zinc, manganese, nickel showed enhanced activities against microbes, tumor and free radicals (Jabeen, 2018).

- This is an Open Access article distributed under the terms of the Creative Commons Attribution-Noncommercial 4.0 Unported License, permitting all non-commercial use, distribution, and reproduction in any medium, provided the original work is properly cited.

- Selection and peer-review under responsibility of the Organizing Committee of the Conference

© 2023 Published by ISRES Publishing: www.isres.org

During the past decades, the human population affected with life-threatening infectious diseases caused by multidrug-resistant Gram-positive and Gram-negative pathogenic bacteria increased at an alarming level around the world. Hence, the development of newer antimicrobial agents is essential to overcome the rapidly developing drug resistance and side effects. In this work, a series of nicotinic acid benzylidene hydrazide derivatives (A-G) was synthesized by condensation of isoniazid with derivatives of aldehydes and tested in vitro for biological evaluations.

Method

Experimental Method

All research chemicals were purchased from Across organics, Sigma-Aldrich and used as such for the reactions. Melting points (mp) were determined on a Veego melting point apparatus (VMP PM, 32/1104). Reactions were monitored by thin layer chromatography carried out using pre-coated silica gel plates. Microanalyses were performed on a Thermo Finnigan C, H, N analyser. The mass spectra were obtained on a Hewlett Packard Electron Impact mass spectrometer GCD-1800A (70 eV EI source) using a direct insertion probe and a Quadrupole TOF Mass spectrometer using electrospray ionisation (Positive mode). UV studies were carried out on a UV Visible spectrophotometer (Shimadzu 1700) in acetonitrile. The IR spectra (KBr) were recorded on a FTIR spectrophotometer with Diffuse Reflectance attachment (Shimadzu 8400S). The ^1H NMR spectra were obtained on an NMR Spectrophotometer (Bruker Avance II 400 NMR) using dimethyl sulphoxide- d_6 as the solvent. In vitro antimicrobial activities against Gram-positive (*Staphylococcus aureus* (ATCC 25923)), Gram-negative bacteria (*Escherichia coli* : (ATCC 25922) et *Pseudomonas aeruginosa* (ATCC 27853) and fungi (**Levure** : *Candida* sp) were evaluated.

Computational Method

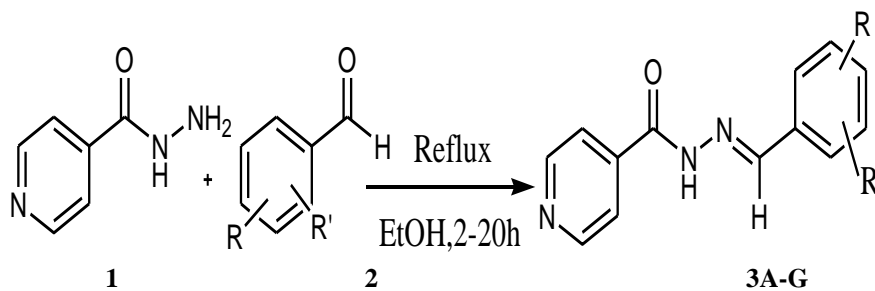
The compounds were optimized at DFT/B3LYP/6-31G (d,p) level of theory. The minimized structures of the investigated molecules were docked with the target protein using MOE 2015.10 software (Chemical Computing Group, 2015). The starting point of the docking simulation was the X-ray structure of ethenoylacyl carrier protein reductase "InhA" with PDB ID 4TZK obtained through the protein data bank (PDB) and imported to MOE interface. The structure of the protein was prepared with MOEQuikPreptool at default parameters, where the ligand and all water molecules that are farther than 4.5 Å from the protein were removed, except the co-factor NAD^+ (Angelova et al., 2017) all necessary hydrogen atoms were added to the structure, followed by its energy optimization.

The prepared InhA structure and the investigated molecules were subject to a number of docking runs. The best binding conformation was selected based by following to "standard" docking solutions considered as typical in docking analysis i.e., (1) the minimal binding energy (ΔG), that reflects the best docking pose, (2) the lowest with lowest root mean square deviation (RMSD) value that validate the docking process (Shawn, 2016) For each investigated molecule, a protein-ligand interactions diagram was constructed based on the best binding pose, using Ligand interactions entry in MOE software. The interactions were in the maximum distance of 4.5 Å; between heavy atoms of the ligand and the receptor residues, and their nature was identified according to the diagram legend given in Ligand interactions entry.

In silico predictive models are frequently applied to get an early estimation of the ADMET profile (Absorption, distribution, metabolism, excretion, and toxicity), this estimation has become a standard step nowadays in drug discovery. Thus, ADMETlab 2.0 server (Xiong et al., 2021) was used to predict the ADMET profile of the tested compounds.

Synthesis

In a 250 ml flask, an equimolar mixture of isoniazid (isonicotinic hydrazide acid, INH) and aldehyde was introduced in 10 ml of ethanol. The reaction mixture was refluxed with stirring for (2 to 20 hours), and after cooling, a solid formed. This solid was then recovered by filtration and purified by washing with ethanol.



A: R= H, R'=H, **B:** R= H, R'= 4-OH, **C:** R= H, R'= 4-Cl, **D:** R= H, R'=4-N(CH₃)₂, **E:**R= H, R'= 4-NO₂,
F: R= H, R'= 4-OCH₃, **H:** R= H, R'= 4-CH₃

Figure 1. Condensation of isoniazid with derivatives of aldehydes

Results and Discussion

Characterization

The compounds 3 A-G were prepared in excellent yields in a one-step reaction of isonicotinylhydrazone (1) with various substituted aryl aldehydes 2A-G in ethanol. yields of reactions are influenced by the nature of the electron-donating or electron-withdrawing substituents on the benzaldehydes (Table 1). The structures of the synthesised compounds were further confirmed by mass spectra and elemental analysis (Table 2). The UV-Visible spectra of compounds 3A-G reveal two absorptions, with the most intense one attributed to the $\pi \rightarrow \pi^*$ transition, and the weaker one characterizing the $n \rightarrow \pi^*$ electronic transition(Table 3).

The IR spectra of derivatives of compounds 3A-G show the appearance of characteristic bands at 3100-3500 cm^{-1} , 1712-1789 cm^{-1} and 1550-1650 cm^{-1} (Thomas, 2016) which correspond respectively to the elongation vibrations of the -NH group, of the C=O carbonyl group and of the C=N imine group. The Table 4 summarizes the main vibration bands corresponding to the different functional groups of compounds 3A-G. Another piece of evidence for condensation isoniazid with derivatives of aldehydes is the appearance of a singlet signal equivalent to 1 proton in¹HNMR spectrum between 7.4 and 8.4 ppm (signal of N=CH) and a equivalent to 1 proton between 8 and 8.35 ppm (signal of NH)(Table 5).

Table 1. Melting points Mp and yields of compounds A- G

Compound	Mp (°C)	y(%)	Colour
A	192-200	75	White
B	264-268	93	Yellow
C	218-221	85	White crystals
D	104-106	88	Yellow
E	225-257	75	Yellow
F	170-173	90	White
G	198-201	80	white

Table 2. Elemental analysis and mass spectrometry data

Compound	m/z (M+H) ⁺	Anal. Calcd			Found		
		C%	H%	N%	C%	H%	N%
B	242.5	C ₁₃ H ₁₁ N ₃ O ₂ (241.25)			C, 64.57; H, 4.52; N, 17.36 %.		
C	260.4	C ₁₃ H ₁₀ ClN ₃ O (259.69)			60.34, 3.76, 16.13		
D	269.5	C ₁₅ H ₁₆ N ₄ O (268.31)			67.58, 6.12, 21.13		
E	271.4	C ₁₃ H ₁₀ N ₄ O ₃ (270.24)			58.07, 3.68, N, 20.51		
F	256.5	C ₁₄ H ₁₃ N ₃ O ₂ (255.27)			65.43, 5.64, 16.80		
					65.87, 5.13, 16.46.		

Table 3. UV-vis spectral analysis

Compounds	λ (nm)	Transition
A	240	$\pi \rightarrow \pi^*$
B	242	$\pi \rightarrow \pi^*$
	322	$n \rightarrow \pi^*$
C	242	$\pi \rightarrow \pi^*$
	295	$n \rightarrow \pi^*$
D	358	$\pi \rightarrow \pi^*$
E	277	$\pi \rightarrow \pi^*$
	325	$n \rightarrow \pi^*$
F	277	$\pi \rightarrow \pi^*$
	325	$n \rightarrow \pi^*$
G	312	$\pi \rightarrow \pi^*$

Table 4. IR bands for the compounds A-G as KBr pellets

Fonction Compound	ν (NH)	ν C=O	ν C=N	ν C=C	ν C-H	ν OH	ν C-Cl	ν -NO ₂
A	3653	1691	1565	1538	3184-3194	/	/	/
B	3231	1657	1555	1647-1670	3018-3227	3340	/	/
C	3510	1667	1592	/	/	/	698	/
D	3415	1665	1592	1647	/	/	/	/
E	3510	1791	1693	1647	/	/	/	1512 1334
F	3510	1791	1611	1611-1619	3166-3228	/	/	/

Table 5. ¹H NMR data of hydrazone derivatives

Chemical shift δ (ppm)	B	C	D	E	F
(d, Pyridine 2H)	8.8-8.5	8.88-8.91	8.73 8.72	9.32 9.25	8.75 8.85
	8.4-8.3		7.82 7.84	8.51 8.55	7.63 7.70
(s, N=CH)	7.8	8.32	8.35	8.1	.4
(s, NH),	8	8.65	8.65	8.34	8.35
(d, Aromatic 2H),	7.0-6.8	7.0-7.5	7.62 7.6	7.89 7.93	7.63 7.70
	7.5-7.3		6.69 6.66	7.6 7.62	6.84 6.89
(s, OH)	11.5	/	/	/	/
(s, CH ₃ , - 6H)	/	/	3.07	/	/
(s, O-CH ₃ ,3H)	/	/	/	/	3.78

Biological Evaluation

Table 6. Antimicrobil activity via disc diffusion method

Compounds	E.coli	P.aeruginosa	S.aureus	Candida sp
	ATCC 25922	ATCC 27853	ATCC 25923	
Zone of Inhibition (mm) (mm)				
A	6	9	11	11
B	8	8	15	13
C	12	13	15	14
D	11	8	10,5	13
E	12	11	14	15
F	8	11	6	15
Amikacin	22	24	33	25

The antibacterial sensitivities of test compounds were assayed using the paper disc. Diffusion method using Amikacin for comparison, as shown in Table 6. From the screening, it was concluded that compounds show

varied responses against the bacteria. The presence of electron withdrawing NO_2 and Cl groups in the molecular structure leads to a steep increase in antibacterial activity. Regarding the antifungal activity, all the compounds exhibit moderate activity

Molecular Docking

Isonicotinohydrazide is one of the drugs routinely used against Mycobacterium Tuberculosis, a bacterium that causes Tuberculosis disease. This bacterium can affect all age groups (Carren, 2011) representing a global health problem that induced the death of two millions of people each year. With the resistance of Mycobacterium Tuberculosis to Isonicotinohydrazide, molecular docking studies were extensively conducted in the last years to propose derivatives that had better interaction with Mycobacterium tuberculosis enoyl-acyl carrier protein reductase (InhA) enzyme than isonicotinohydrazide (Abdullah Shah & Hussain, 2022; Dogan et al., 2020).

In this study, molecular docking study was performed in an effort to evaluate the binding interactions of the investigated N-benzoylisonicotinohydrazide derivatives with InhA, and predict the best InhA inhibitor among them. The molecules were docked in the active site of InhA and the results are summarized in table 7.

As seen from Table 7, all N-benzoylisonicotinohydrazide derivatives (**B-G**) fitted well in the active site of InhA and showed more negative binding energy values than N-benzoylisonicotinohydrazide molecule (M^1), which is indicating a better enzyme inhibition, with the molecule **D** ranking by the docking as the top score, and predicted as the best inhibitor.

The influence of the substituents in the p-position of the benzene ring on the binding with InhA is clearly demonstrated in here, the order based on the substituents was found to be: **D**(benzene- $\text{N}(\text{CH}_3)_2$) > **E**(benzene- NO_2) > **F**(benzene- OCH_3) > **C**(benzene-Cl) > **G**(benzene- CH_3) > **B**(benzene-OH) > **A**(benzene-H). The substitution with electron withdrawing groups (NO_2), and (Cl) seems to be favorable in enhancing the binding affinity between the substituted molecules and InhA enzyme, although (Cl) group is a weak electron withdrawing group (Sun, 2017) the binding still better than with M^1 . Meanwhile, molecules with electron donating substituents like (OH), (OCH_3) and (CH_3) showed moderate binding energy values. The OCH_3 and CH_3 groups, being weak electron donating groups (Sun, 2017), slightly improved the binding affinity compared with OH.

To sum, the substitution with powerful electron withdrawing groups was favored, particularly with (NO_2) group. In contrast, substitution with strong electron donating groups such as (OH) was disfavored. Besides, the substituents that are weak electron withdrawing group as (Cl) and weak electron donating such as (OCH_3), (CH_3) had almost the same influence, molecules containing those groups showed close binding energies values and hence near binding affinity with InhA.

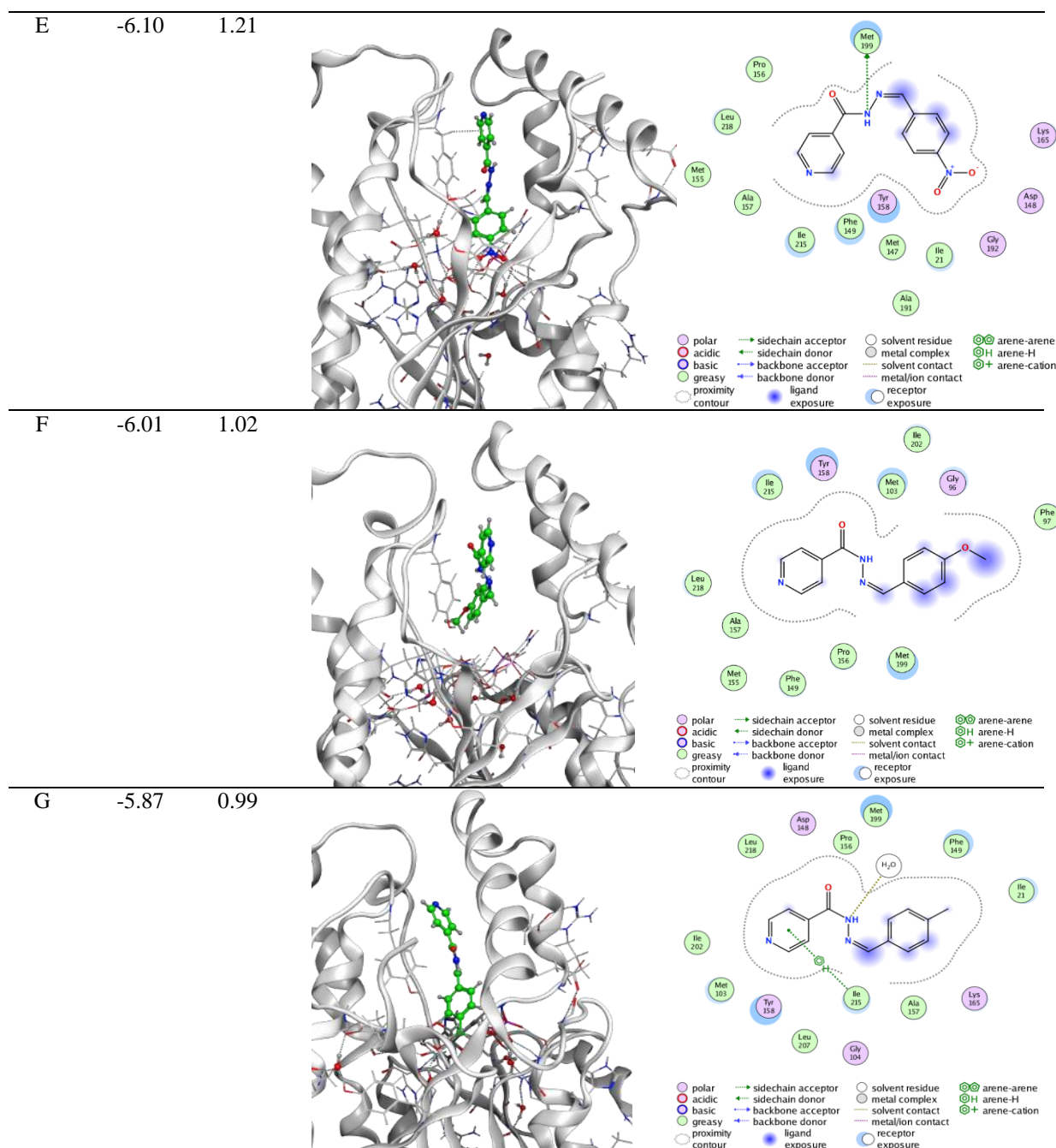
However, although **D** molecule have an electron donating substituent ($\text{N}(\text{CH}_3)_2$), it was ranked by the best docking score (-6.46 Kcal/mol). This is probably due to the nature of the interactions involved in the binding with amino-acids residue, which will be detailed in the following paragraph.

A protein-ligand interactions diagram of InhA amino-acids residues with all investigated molecules (**A-G**) was provided by molecular docking analysis, in the main to elucidate the nature and number of the interactions involved in the binding. The results are showing that residues Met 103, Tyr 158, Met 199 and Ile 215 demonstrated an exposure to all the molecules, these residues were explicitly mentioned as very important since they are located in the binding site of InhA enzyme. Molecule A did not demonstrate any interaction with amino-acids residues.

Whereas, almost all the derivatives molecules exhibited one or more interactions. Molecule M^4 displayed one hydrogen bond interaction with Tyr 158 (between OH group of tyrosine 158 and benzene ring), this type of interaction is known to play important roles in protein-ligand complex formation and stability (Andersson et al., 2020; Moreno Fuquen, 2022) which enhances the binding affinity, reflected in here by the highest binding score (-6.46 Kcal/mol). Molecule **G** exhibited also one hydrogen bond interaction via the benzene ring but with another amino-acid residue namely Isoleucine 215 (Ile 215), while Tyr 158 is in total exposure, the molecule showed a second hydrogen bond with H_2O solvent. The rest of the molecules showed VDW interactions with Methionine 199 (Met199) through the azote atom of the hydrazide part. Although, **F** molecule did not show any interactions, the docking ranking was quite good and the residues mentioned before as important residues were still close.

Table 7. Binding energy and RMSD values of N-benzoylisonicotinohydrazide and its derivatives best poses along with their corresponding 2D and 3D representations.

Mol	ΔG (Kcal/mol)	RMSD (Å)	3D representation of the best Binding conformations	2D diagram of ligand-protein interactions
A	-5.53	0.81		
B	-5.58	0.72		
C	-5.90	1.33		
D	-6.46	1.27		



ADMET Analysis

ADMET properties of the investigated molecules A-G were reported in Table 8. All the tested molecules were predicted as non-carcinogenic; don't induce cancer to humans, and non hERG channel blockers. It worth mentioning that hERG channel is known for its role in coordinate the heart's beating (Angelova et al., 2017) any blockage causes sudden death (Shawn, 2016). Additionally, almost all molecules demonstrated a non-AMES Toxicity, except for **D** and **E**, that were predicted to be AMES Toxic which means that they can induce changes and damages in DNA (Carren, 2011) However, all the investigated molecules were predicted to cause eye irritation and skin sensitization. Additionally, D presented a high probability of respiratory toxicity. Concerning the intestinal absorption, all the investigated molecules presented Caco-2 Permeability indices higher than -5, expressing their good permeability across the human carcinoma intestinal cells (Gabriela, 2022). In contrast, the same molecules showed a poor human intestinal absorption rate (HIA% < 30%). All the studied molecules are non-inhibitors and non-substrates of Permeability-GlycoProtein (Pgp) that is localized in the intestine, hepatocytes and renal tubules. Therefore, besides of its localisation, Pgp appears to be not involved in limiting the intestinal absorption or enhancing the excretion of the tested molecules from out of the human

body. After the intestinal absorption, molecules are distributed through the body's blood into tissues. To evaluate the distribution, protein plasma binding rate (PPB%), volume of distribution (VD) and blood-brain barrier (BBB) penetration were predicted. Interestingly, almost all the tested molecules were predicted to be permeable into the blood-brain barrier (BBB) except for **A**, **B**, **E**. It should be noted that penetrating the blood-brain barrier is critical for molecules targeting central nervous system, such as antidepressants, however for non-target molecules it can cause neurotoxicity. All molecules showed high rates (>90%) for binding to plasma proteins, including serum albumin, hemoglobin and α -acid glycoproteins. As only unbound molecule can be distributed into tissues, the distribution of the studied molecules may fail (Sun, 2017). It is well-known that molecules that are extensively bound to plasma proteins will have a low volume of distribution (VD), and have low clearance (CL) by both liver (hepatic) and kidney (Renal) routes. This was confirmed here by low values of volume of distribution (VD) ranging between 0.54 and 0.89 L/kg. It should be noted that the acceptable range is between 0.04-20 L/Kg. Moreover, the clearance index for almost all the tested molecules was low (CL < 5 mL/min/Kg) and quite moderate (CL > 5 mL/min/Kg) for **B**, **D** and **F** molecules. Remember that, for a better clearance, CL index should be higher than 15 mL/min/Kg. A part from direct elimination of a molecule by hepatic and Renal routes, a molecule can be inactivated through biotransformation to allow clearance from the body, this is facilitated by metabolizing enzymes i.e., CYP450 cytochromes such as CYP2D6 (Shoombutang et al., 2017). Among the tested molecules, **D** and **F** can be metabolized by CYP2D6. While, **C** and **F** are predicted to be significant inhibitors of CYP2D6, leading to a decrease in the metabolism of CYP2D6 substrates (Shoombutang et al., 2017).

Table 8. ADMET properties of the molecules A-G

Absorption	A	B	C	D	E	F	G
Caco-2 Permeability	-4.37	-4.55	-4.38	-4.39	-4.43	-4.44	-4.40
HIA (%)	< 30	< 30	< 30	< 30	< 30	< 30	< 30
Pgp-inhibitor	No						
Pgp-substrate	No						
Distribution PPB (%)	95.70	94.35	97.05	95.11	95.51	95.79	96.17
VD (L/Kg)	0.68	0.54	0.82	0.89	0.64	0.67	0.82
BBB Penetration Metabolism	No	No	Yes	Yes	No	Yes	Yes
CYP2D6 inhibitor	No	No	Yes	No	No	Yes	No
CYP2D6 substrat	No	No	No	Yes	No	Yes	No
Excretion CL (mL/min/Kg) Toxicity	4.26	6.98	3.07	6.23	2.42	5.65	3.86
AMES Toxicity	No	No	No	Yes	Yes	No	No
Carcinogenicity	No						
hERG Blockers	No						
Eye Irritation	Yes						
Skin Sensitization	Yes						
Respiratory Toxicity	No	No	No	Yes	No	No	No
Absorption	A	B	C	D	E	F	G
Caco-2 Permeability	-4.37	-4.55	-4.38	-4.39	-4.43	-4.44	-4.40
HIA (%)	< 30	< 30	< 30	< 30	< 30	< 30	< 30
Pgp-inhibitor Distribution	No						
PPB (%)	95.70	94.35	97.05	95.11	95.51	95.79	96.17
VD (L/Kg)	0.68	0.54	0.82	0.89	0.64	0.67	0.82
BBB Penetration Metabolism	No	No	Yes	Yes	No	Yes	Yes
CYP2D6 inhibitor	No	No	Yes	No	No	Yes	No
CYP2D6 substrat Excretion	No	No	No	Yes	No	Yes	No
CL (mL/min/Kg) Toxicity	4.26	6.98	3.07	6.23	2.42	5.65	3.86
AMES Toxicity	No	No	No	Yes	Yes	No	No
Carcinogenicity	No						
hERG Blockers	No						
Eye Irritation	Yes						
Skin Sensitization	Yes						
Respiratory Toxicity	No	No	No	Yes	No	No	No

Conclusion

In the present study, the synthesis and activity of benzylidene isonicotinohydrazide derivatives have been described. It was observed that the tested compounds containing electron withdrawing (nitro, halogen and dimethoxy) moiety on phenyl ring of the compounds were found to have significant in vivo. In silico, The molecule **E** : N-(4-methoxybenzylidene) isonicotinohydrazide is a better candidate for the treatment against Mycobacterium Tuberculosis, the molecule presented a better ADMET profile and a good binding energy with InhA enzyme of Mycobacterium Tuberculosis.

Scientific Ethics Declaration

The authors declare that the scientific ethical and legal responsibility of this article published in EPSTEM journal belongs to the authors.

Acknowledgements or Notes

* This article was presented as an oral presentation at the International Conference on Research in Engineering, Technology and Science (www.icrets.net) held in Budapest/Hungary on July 06-09, 2023.

References

- Abdullah Shah, M., & Hussain, H. (2022). Synthesis and characterization of novel hydrazone derivatives of isonicotinohydrazide and their evaluation for antibacterial and cytotoxic potential. *Molecules*, 27, 6770–6782.
- Andersson, B., Mishra, K., Forsgren, N., Ekstrom, F., & Linusson, A. (2020). Physical mechanisms governing substituent effects on arene–arene interactions in a protein milieu, *The Journal of Physical Chemistry B*, 124(30), 6529.
- Angelova, V. T., Valcheva, V., Pencheva, T., Voynikov, Y., Vassilev, N., Mihaylova, R., Momakov, G., & Shivachev, B. (2017). Synthesis, antimycobacterial activity and docking study of 2-aryl benzopyrano[4,3-c] pyrazol-4(1H)-one derivatives and related hydrazide-hydrazones, *Bioorganic & Medicinal Chemistry Letters*, 27(13), 2996–3002.
- Chemical Computing Group. (2015). *Molecular operating environment (MOE)*. <http://www.chemcomp.com>.
- Carren, P. (2011). An investigation into pharmaceutically relevant mutagenicity data and the influence on Ames predictive potential. *Journal of Cheminformatics*, 3, 51.
- Falcón Cano, G. (2022). Reliable prediction of caco-2 permeability by supervised recursive machine learning approaches. *Pharmaceutics*, 14(10).
- Jabeen, M., Mehmood, K., Ain Khan, M., Aslam, N., Zafar, A.M., Noreen, S., Aslam, S., & Ghafoor, A. (2018). Microwave and conventional synthesis of Co (II), Cu (II) and Ni (II) metal complexes of some acid hydrazones with their spectral characterization and biological evaluation. *Pakistan Journal of Pharmaceutical Sciences*, 31, 1003–1011.
- Khattaf, F.S., Mani, A., Hatamleh, A.A., & Akbar, I. (2021). Antimicrobial and cytotoxic activities of isoniazid connected menthone derivatives and their investigation of clinical pathogens causing infectious disease. *Journal of Infection and Public Health*, 14, 533–542.
- Krátký, M., Bosze, S., Baranyai, Z., Stolarikova, J., & Vinsova, J. (2017). Synthesis and biological evaluation of hydrazones derived from 4-(trifluoromethyl) benzohydrazide. *Bioorganic & Medicinal Chemistry Letters*, 27, 5185–5189.
- Maccari, R., Ottanà, R., & Vigorita, M.G. (2005). In vitro advanced antimycobacterial screening of isoniazid-related hydrazones, hydrazides and cyanoboranes: Part 14. *Bioorganic & Medicinal Chemistry Letters*, 15, 2509–2513.
- Moreno Fuquen, R., García-Torres, E., Arango Daraviña, K., & Ellena, J. (2022). Structural, theoretical analysis and molecular docking of two benzamide isomers. Halogen bonding and its role in the diverse ways of coupling with protein residues. *Chemical & Pharmaceutical Bulletin (Tokyo)*, 70(11), 782–790.
- Lamothe, S. M. (2016). The human ether-a-go-related gene (hERG) potassium channel represents an unusual target for protease-mediated damage. *The Journal of Biological Chemistry*, 291, 20387–20401.
- Popiolek, L., Stefanska, J., Kielczykowska, M., Musik, I., Biernasiuk, A., Malm, A., & Wujec, M. (2016). Alkylation, dissociation constants and antimicrobial activity of novel 2, 3-disubstituted-1, 3-thiazolidin-4-one derivatives. *Journal of Heterocyclic Chemistry*, 53, 393–402.

- Sun, L. (2017). in silico prediction of compounds binding to human plasma proteins by QSAR models. *ChemMedChem*, 13, 572-581
- Soombuatong, W., Prathipati, P., Prachayasittikul, V., Schaduangrat, N., Malik, A. A., Pratiwi, R., Wanwimolruk, S., Wikberg, J. E. S., Gleeson, M. P., Spjuth, O., & Nantasenamat, C. (2017). Towards predicting the cytochrome P450 modulation: from QSAR to proteochemometric modeling. *Current Drug Metabolism*, 18(6), 540–555.
- Thomas, A.S., & Hamane, S.C. (2016). Synthesis and biological evaluation of Schiff's bases and 2 azetidinones of isonocotinyl hydrazone as potential antidepressant and nootropic agents. *Arabian Journal of Chemistry*, 9, 79-90.
- Xiong, G., Wu, Z., Yi, J., Fu, L., Yang, Z., Hsieh, C., Yin, M., Zeng, X., Wu, C., Lu, A., Chen, X., Hou, T., & Cao, D. (2021). ADMETlab 2.0: an integrated online platform for accurate and comprehensive predictions of ADMET properties, *Nucleic Acids Research*, 5–14.

Author Information

Noura Kichou

Mouloud Mammeri University of Tizi-Ouzou,
Tizi-Ouzou, Algeria
Contact e- mail: noura.kichou@ummo.dz

Nabila Guechtouli

Mouloud Mammeri University of Tizi-Ouzou
Tizi-Ouzou, Algeria

Karima Ighilahriz

Mouloud Mammeri University of Tizi-Ouzou
Tizi-Ouzou, Algeria

Manal Tefergennit

Laboratory of Electrochemistry-Corrosion
El Alia, Algeria.

Zakia Hank

Laboratory of Electrochemistry-Corrosion
El Alia, Algeria.

To cite this article:

Kichou, N., Guechtouli, N., Ighilahriz, K., Tefergennit, M., & Hank, Z. (2023). Synthesis, biological evaluation and theoretical studies of hydrazone derivatives. *The Eurasia Proceedings of Science, Technology, Engineering & Mathematics (EPSTEM)*, 23, 282-291.

The Eurasia Proceedings of Science, Technology, Engineering & Mathematics (EPSTEM), 2023

Volume 23, Pages 292-299

ICRETS 2023: International Conference on Research in Engineering, Technology and Science

Applicability of a Gage R&R Study on a Home Blood Glucose Meter

Zoltan Varadi
Óbuda University

Gyozo Attila Szilagyi
Óbuda University

Abstract: Home glucose meters have become widely accessible and, in addition to self-monitoring applications, are now commonly used to support biohacking. Accu-Chek Instant is an easy-to-use and cheaply available device, and thus, it is recommended to use in a known lifestyle change program. Participants and users do not require special knowledge, though have due or undue concerns about changes in blood glucose levels. The study aims to find the minimal magnitude of change in blood glucose level, i.e. the effective resolution of the fore-mentioned device. In addition, we are seeking applicability of the standard Gage R&R study method which is well known in the automotive industry. As Gage R&R requires to incorporate several variance factors into the study, we reproduced typical home applications and daily routines of laymen. Our results on measurement uncertainty turned to be in range with the accuracy specified by the manufacturer, and the Gage R&R method helped us to formulate answer to home user concerns on a layman's language.

Keywords: Gage R&R, Measurement uncertainty, Blood glucose meter, Biohacking, Accu-Chek instant

Introduction

Modelling a human being with the analogy of a combustion engine provides a simplified energy balance calculation, with food and drinks being the fuel of such an engine. Like the operation of the combustion machine, biochemical processes in the human body can be characterized by numerous measurable parameters. Physiological parameters of human bodies are typically defined with a range considered to be healthy, and the same parameter having a value outside of that range may be an indication of an unhealthy condition; very similarly to the technical parameters of the engine or its components which are considered to function acceptable if they fall within the specified range; and are defective if they are outside the specification limits (Horváth, 2023). The fuel system of a human combustion engine contains complex and interrelated biochemical reactions, which transform food intake to usable energy to various parts of the body. The energy is then conveyed by blood circulation in various forms like ketone or glucose, and the energy balance is accompanied by several types of molecules of the hormone system take part in or control the use of energy. The energy is stored in various reserves in the body for immediate availability, short term storage, or long-term reserve (Lakatos, 2020). Long-term reserves are for example the subcutaneous or visceral fat deposits, which, above a certain percentage, turns to obesity. Excess fat reserves are only built up if there is excess energy in the body over a significant period, though it is an oversimplification to say that reducing energy intake will solve obesity problems.

Biohacking Program and Its Questions

By adjusting the ratio of macro- and micro-nutrients in the intake to the load of the human engine, biohacking targets to alter one's biological setup towards an optimum, often doing that without medical supervision. Those

- This is an Open Access article distributed under the terms of the Creative Commons Attribution-Noncommercial 4.0 Unported License, permitting all non-commercial use, distribution, and reproduction in any medium, provided the original work is properly cited.

- Selection and peer-review under responsibility of the Organizing Committee of the Conference

© 2023 Published by ISRES Publishing: www.isres.org

do-it-yourself programs use recent technology of smart tools such as smart armbands or body analyzer scales, and traditional tools like a measuring tape, to measure the activities of the people in study, and the body's reaction to the physical activity: e.g. with immediate feedback, adjust intensity to pulse rate during sports; monitor blood oxygen saturation; or count the number of steps taken during a day; or measure and monitor waist/hip ratio. The personalized programs are said to help prevent from elderly degradation of health, and are promoted with warnings of excessive healthcare costs and risks. The effect of biohacking is a concurrent topic widely studied in various forms. Biohacking has made biotechnology widely known, and the evolution of home use equipments made it financially accessible to those who would otherwise wouldn't need them for medical observations. Medical professionals are worried as users without proper knowledge and education are risking misusing the diagnostic tools and arrive at inadequate conclusions and undue concerns. On the other hand, many patients are overwhelmed and are keen on keeping their health in their own hand (Zheng, 2021). This study is not intending to take position on either side of the worries but takes a more technical approach on understanding the measurement uncertainty that might influence decisions of participant in DIY biohacking.

In his book, Lakatos (2020) introduces diverse approaches for maintaining and recovering healthy conditions. His portfolio includes considerations on food composition, on activities and muscle conditions, on breathing, and many others. Training programs and guided courses are set up to help people learn the basics and understand their body biology to adjust nutrition and activities. Participants are warned to understand their own physical conditions and set up some home measurement routines. Measured parameters are body dimensions and composition on a weekly basis; breathing, activity and sleep indicators daily; and blood glucose levels before-after every meal resulting in 5-15 or even more blood tests per day. The huge number of blood glucose values helps participants understand how certain foods influence their energy reserve. Closed groups on social media platforms are set up to facilitate communication with and between members of the training program, where participants raise their questions and share their experiences. Target audience of such a program is people over the hill who are or want to be active though, most of them live with obesity and its consequences.

The Spring 2023 training program has started with 1144 participants, most of them living in Hungary. When subscribing, they were provided with a list of recommended tools; one of them was a glucometer, the recommended type is Accu-Chek Instant due to its simplicity and convenience in frequent use. The meter is packed with test stripes and a lancing device in a carry case; its outfit and quick start guide made it an ideal starting kit at an affordable price below €20 at that time. The group communication has not thoroughly been analyzed, though it is frequently seen that participants are concerned about their blood glucose measurement results. A typical question looks like: "My morning fasting level was 5.0, I haven't eaten anything yet, though it went up to 5.2 by now. What happened?" – cited from one question in the group discussions.

Glucometer Accuracy

Understanding measurement results of blood glucose levels helps diet and body shaping programs as well as medical treatments of diabetes. It is known that blood glucose levels are influenced by many factors including stress or activities, in addition to nutrition, and measurement conditions have significant effect on the readings, despite, diabetes patients must rely on the measurement results. In their article, Erbach et al. (2016) suggest that patients with diabetes as well as medical professionals in the treatment teams shall be well-informed about limitations and interferences. This may even be more crucial in case of DIY biohacking programs as they are lacking regular medical supervision of the participants' health conditions.

Various methods have been used to determine accuracy and reliability of glucometers. In their comparative study, Moore et al. (2021) have chosen young athletes on a ketogenic diet as sample and compared two types of field meters. With regards to the glucose testing, they found relatively small bias, and good agreement at fasting glucose level of 80 mg/dl (that is, 4.4 mmol/l). Their plot however shows wide variance, that is partly due to repeatability and partly due to differences in sample. Weak point of the comparative analysis is that they used a commercial field meter as a reference, not a gold standard laboratory method. The study concludes that those commercial meters are appropriate to detect nutritional ketosis conditions.

Accu-Chek instant accuracy has been studied in various ways. Both FDA and ISO have formulated standards that blood glucose meters shall meet. The ISO expectation for home use is that readings are 95 percent accurate within 15 percent of blood glucose equal to or above 100 mg/dl and are 95 percent accurate within 15 mg/dl for readings under 100mg/dl. As 1mg/l equals 0.0555mmol/l, the above means that an average healthy person's fasting glucose level of 5.6mmol/l needs to have a 0.83 mmol/l confidence interval at 95% confidence level. After two hours of eating a plate equivalent to 75g of carbohydrate, the glucose levels on an average healthy

adult stands not above 7.8mmol/l, which is 2.2mmol/l higher than the fasting level. The expected confidence interval, which we consider as an upper bound for allowed measurement uncertainty, is consuming 37.5% of that change due to food, which is surprisingly far above the typically tolerated uncertainty budget of measurement systems used in automotive (VDA 5, 2021). The wider the range of uncertainty is, the more difficult it becomes for biohackers to fine-tune their diet with respect to effects of various food components. In addition to hygienic factors, i.e., washing hands before testing, testing conditions and tester conditions influence the reading. Typical sampling points are fingerprints, as the blood glucose level may change if sampled from other part of the body. The minimum amount of blood in the case of Accu-Chek Instant it is 0.6µl, according to its user manual. Environmental factors also contribute to the measurement reading, influencing its uncertainty (Smith, 2019), especially test strips are sensitive to handling related error sources.

Accuracy of the Accu-Chek Instant glucometer system is capable to measure blood glucose levels from 0.6mmol/l to 33.3mmol/l, with a readable resolution of 0.1mmol/l. The default target range is set to 3.9mmol/l to 8.9mmol/l (Roche, 2018). According to the documentation of test stripes (Roche, 2021), the system accuracy is within ±0.83mmol/l or 15% in the range of 2.2 to 26.7mmol/l, tested on 600 test stripes, which is in accordance with ISO inspection criteria (Freckmann et al., 2015). References of comparative analyses were gold standard laboratory methods. Detailed measurement uncertainties are given by the standard deviation of repeated measures (Table 1).

Table 1. Repeatability errors of Accu-Chek Instant (Roche, 2021)

Average level (mmol/l)	2.6	4.7	6.6	7.6	12.0
Standard deviation (mmol/l)	0.1	0.1	0.2	0.2	0.3

Manufacturers' criteria as well as ISO or FDA standard criteria are used for pre-market evaluation of self-monitoring devices, though these conditions may not be applicable on field evaluations as there is limited number of available batches of test stripes and references. Ziegler et al. (2014) raise importance of determining accuracy in practical field application, though application circumstances are hard to standardize. Questions raised are: How do we define goodness of measurement? Is the measurement biased? What is the precision of measurement, i.e., is the repeatability error small? Is error influenced by reproducibility components? As bad decisions coming from measurement errors may have consequences on health conditions of people, it is very important to establish a concise and easy to implement method to evaluate glucometer accuracy.

In automotive industry, Gage R&R is a frequently used, mandatory tool to demonstrate that measurement processes are good enough for the respective control or inspection activities, and despite its simplicity and frequent use, Gage R&R is hardly used in health industries. This study is aiming to test how well the Gage R&R method can determine measurement uncertainty and what suggestions it may give to users of Accu-Chek Instant glucometer.

Method

The Gage R&R method (AIAG MSA, 2010) is suitable to determine applicability of a variable gage, like the Accu-Chek Instant self-monitoring glucometer. Amongst the various applications, the AIAG handbook recommends the ANOVA approach as it measures interactions of sources of measurement error, i.e., the part to operator interaction, and is flexible to incorporate other factors of measurement error into the model. The amount of calculation required to perform the analysis of variances (ANOVA) suggests using a computerized solution. Minitab Statistical Software v.21.4 has been chosen to perform the analysis, and all the charts below are generated with Minitab's Gage R&R function available under the menu of Stat → Quality Tools → Gage Study → Gage R&R Study (Crossed). We assume to set up an experimental design where a given sample's glucose level is considered constant throughout the repeated measurements, so repeatability is measurable. Methods and formulae, as well as the interpretation of statistics and graphs displayed are well described in Minitab's support (Minitab, 2023).

Setting up the Gage R&R Study

A crucial part of proper Gage R&R study is obtaining a sample that represents the realistic range of variation. In this case, we understood the concerns and methods of typical participants of the fore-mentioned biohacking

program (Lakatos, 2020). The range of participants and measurement habits has been represented by 3 people aging between 45-61 years, a female and two males, with different but not unusual levels of obesity and some affectedness by IR. The typical range of measurable blood glucose level were simulated by multiple conditions of each people: morning fasting state; after a coffee; before meal and 90 minutes after meal. To keep the privacy of the medical conditions of sample, different people and conditions are not identified in the article below, every person and every condition of testing is identified as one sample, numbered from 1 to 10. Lancet sampling and testing was performed according to the user manual (Roche, 2018). Although the MSA manual (AIAG MSA, 2010) recommends using larger sample sizes for better confidence levels, automotive industry professionals used to stick with 10 samples as illustrated by the examples of the manual. So stayed we in our study at 10 samples.

Repeatability, in general, is understood as the same device is measuring the same workpiece, while circumstances are kept stable, however in this study it is practically impossible to repeat the same measurement on the same piece as test stripes are single use by design. Knowing that test stripes are well analyzed during manufacturing processes (Smith, 2019), we excluded the variance factor of test stripes by choosing to use the same batch of stripes throughout the whole experiment. Test stripe data are as follows: Lot id: 302037-04015630066810, Ref: 07819382053, best before date is May 15, 2024. In addition, we had to make sure that when a drop of blood is gained from fingerprint, it comes in sufficient volume to enable multiple tests within a short time. Knowing that measuring blood glucose level is very sensitive, we set up a little practice with the study participants to make sure we are able to do the 9 repeats within the shortest period of time. Processing one sample with 3 repeats in the 3 different testers is illustrated below (Figure 1.):

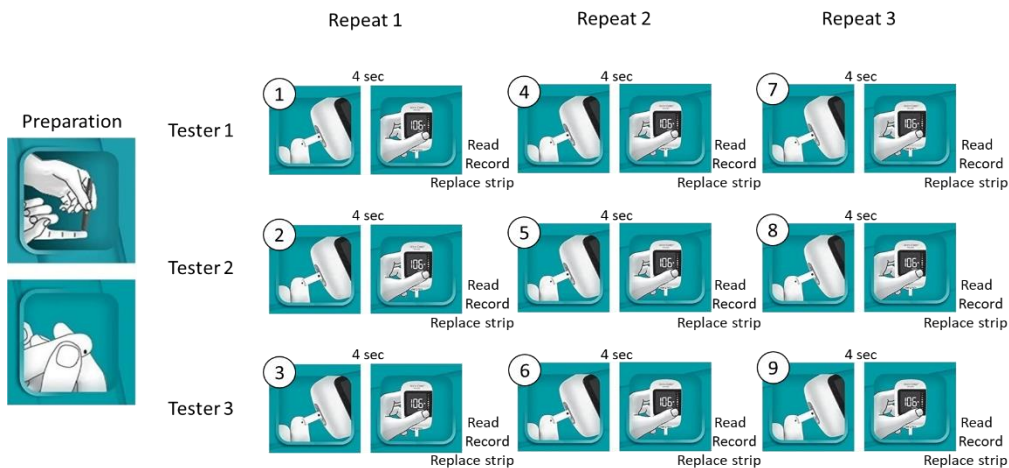


Figure 1. Illustration of how one sample was measured in 3 testers, with 3 repeats (Own figure, with illustrations from Accu-Check quick start guide)

As bias is not tested in the Gage R&R study, there is no need to for a golden standard laboratory method as a reference. Reproducibility is often interpreted as appraiser variation (AIAG MSA, 2010), though in our case there may be other sources of variation. In self glucose monitoring, the operator him- or herself is the sample, we cannot evaluate the effect of operators. However, thousands of biohackers use the same type of glucometer, they are not using the very same equipment, and comparative gold standard laboratory techniques are hardly available. In the study we are examining if the three glucometers of the same Accu-Chek Instant type are identical with regards to the measurement results and uncertainty, thus the equipment being the reproducibility factor in the study. The glucometers used in the study are from various batches and purchases, and are identified in the table below (Table 2).

Table 2. Glucometers used in the study

Tester	Symbol in study	Type	Serial Number	GTIN
Tester 1	G	Accu-Check Instant	97308838832	04015630086627
Tester 2	K		97308493063	04015630086627
Tester 3	Z		98008221952	04015630086580

The total analysis eventually consisted of 90 readings of having 10 samples tested 3 times in three testers, with the same batch of test stripes throughout the whole study. The coverage factor (VDA 5, 2021) estimating the

width of the uncertain range is chosen to be $k=2$, i.e., $\pm 2\sigma$ represents 95% confidence interval, and this rounding is typically used in automotive industry. The process specification limits are of dispute in the case of blood glucose testing. In the study, we have chosen the default target range of Accu-Chek Instant as specification limits, the lower limit is set to 3.9mmol/l and the upper limit is set to 8.9mmol/l (Roche, 2018).

Results and Discussion

The 90 observations are plotted on a Gage Run Chart (Figure 2.) to inspect the range and any unusual patterns on the data. Time sequence for each sample follows the sequence as illustrated on Figure 1. No clear indications of time dependent factors are seen on the graph. Sample ranges from 5.5 to 9.0 mmol/l, that is comparable to the default target range, so we can conclude that the sample is a good representation of the realistic expected range. In some cases, there are unusually large variations observed, e.g. with the results of sample 3 at tester Z, but those do not seem to follow a recognizable pattern, and double checking records of memories from tester devices did not help identifying any variations of special causes.

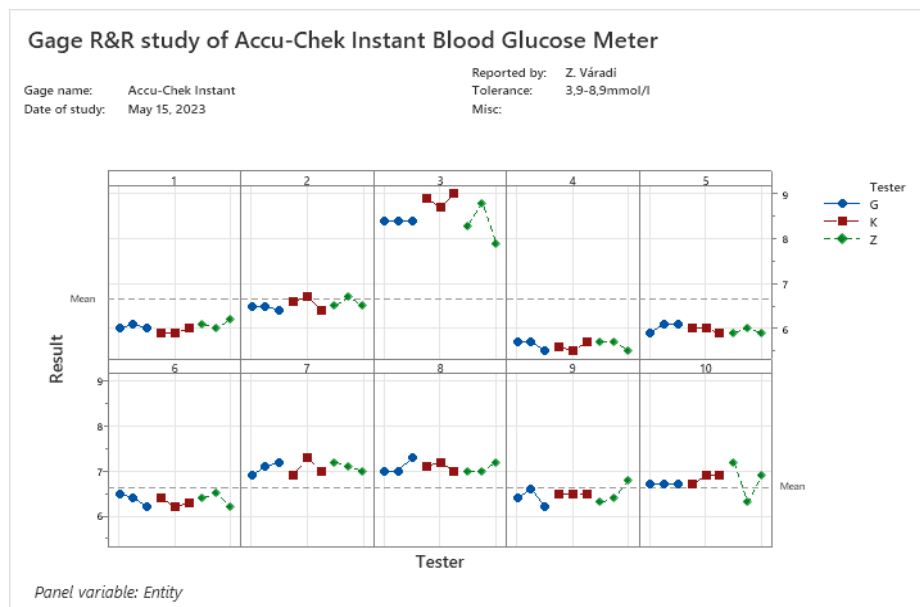


Figure 2. Gage run chart (own graph)

The ANOVA table (Tables 3.) indicate the significance of factors in the study. First check is at the significance of the interaction term: if the interaction is not significant, Minitab removes that term from the model and repeats the calculation again, as degrees of freedom (DF) and the sums of squares of deviations (SS) change. In our study, interaction term is removed from the model, and the ANOVA results with the main effects only is summarized in (Table 4.) below.

Table 3. ANOVA tabulated results with interactions

Source	DF	SS	MS	F	P
Sample	9	53.8333	5.98148	177.863	0.000
Tester	2	0.0436	0.02178	0.648	0.535
Sample * Tester	18	0.6053	0.03363	1.173	0.312
Repeatability	60	1.7200	0.02867		
Total	89	56.2022			

Looking at the significance of main effects, we can conclude that not all of the samples are identical at 95% confidence level, i.e., the measurement system is capable to differentiate between glucose levels on the examined range. Practically speaking, this is a positive outcome as it means the measurement uncertainty is not hiding detectable changes, thus, the measurement system is good, though its goodness is yet unquantified. The other main effect, the difference between the three testers does not turn significant, i.e., different production batches and wear conditions in this period did not have any detectable effect on the measurement result.

Table 4. ANOVA tabulated results without interactions, $\alpha=0,05$ to remove interactions

Source	DF	SS	MS	F	P
Sample	9	53.8333	5.98148	200.640	0.000
Tester	2	0.0436	0.02178	0.731	0.485
Repeatability	78	2.3253	0.02981		
Total	89	56.2022			

In addition to the statistical analysis, there needs to be an answer to the acceptability, i.e., the goodness of that measurement system, which consists of Accu-Chek Instant glucometers, lancets, test stripes, the sampled humans, and measurement conditions. We chose to use the automotive practices (AIAG MSA, 2010) saying if $GRR\% < 10\%$, the measurement system is generally considered acceptable; if $GRR\% > 30\%$ then the measurement system is generally considered unacceptable; and in-between there may be some conditions to consider when deciding about acceptability of the measurement system. GRR percentages study (Table 5.) of the indicate that the total gage variation represented by the $\pm 2\sigma$ range accounts for 13.81% of the target range of 3.9 to 8.9 mmol/l, and that percentage is considered conditionally acceptable.

Table 5. Gage R&R results

Source	StdDev (σ)	Study Var ($4*\sigma$)	%Study Var	GRR% of the spec range
Total Gage R&R	0.172661	0.69065	20.77	13.81
- Repeatability	0.172661	0.69065	20.77	13.81
- Reproducibility	0.000000	0.00000	0.00	0.00
- Tester	0.000000	0.00000	0.00	0.00
- Part-To-Part	0.813201	3.25281	97.82	65.06
Total Variation	0.831329	3.32532	100.00	66.51

An additional metric of acceptability of a measurement system is the number of distinct categories (NDC), of which values above 5 are in general considered acceptable. For the measurement system analysis performed, $NDC=6$, suggesting the system is acceptable.

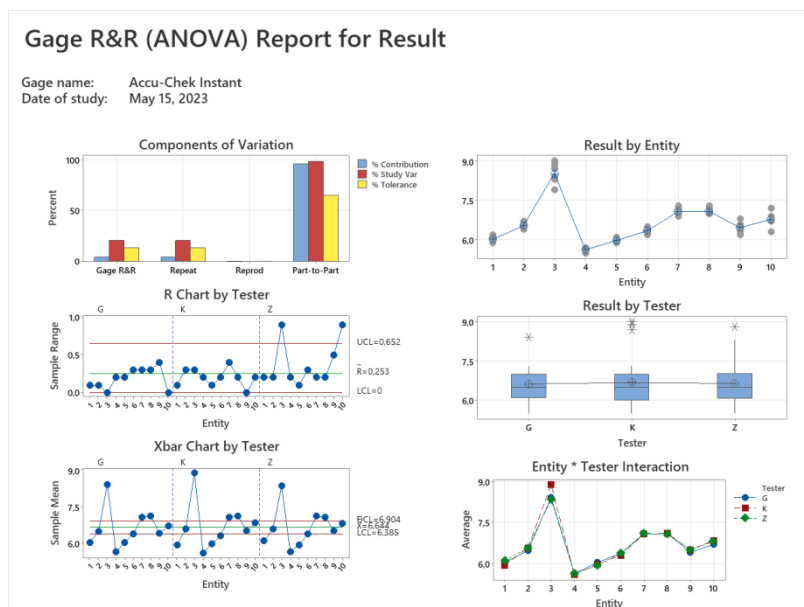


Figure 3. Gage R&R report details (own graph)

The standard deviation of the total gage turns $\sigma_{GageR\&R}=0.17$ mmol/l, and the average of our 90 measurements are 6.64mmol/l. If we compare that $\sigma_{GageR\&R}$ to those standard deviations given by the manufacturer in Table 1., we can conclude that the Gage R&R method provided very similar results.

Before finally judging the goodness of the measurement system, the assessors have to make sure that the system is stable during the measurement process, and during the experiment. Stability is understood in terms of statistical process control (SPC), meaning that no special cause variation shall influence the process in study.

Neither of the above metrics would by itself indicate stability or signs of special case variations; and so are they unable to identify details of improvement opportunities.

The SPC charts, the R and Xbar charts (Figure 3.) help us identify any unusual pattern or signs of instabilities. Firstly, we need to understand the R chart where any dot represents the range of values of the three repeated measurements on the same sampled blood with a respective glucometer. We see that samples 3 and 10 have extremely large ranges at tester “Z”, i.e., the minimum and the maximum of repeated measurements from the same drop of blood at sample 3 and 10 are atypically far from each other. Investigating the process and the data, no special reason of that unusual range was identified. Assessors suspect that the conditions of tester “Z” may be an unstudied factor: We know that the affected tester “Z” is the oldest equipment of the three, having more than a year of regular use, whereas the other two glucometers were fresh purchases and have been used only for a week or a month, respectively. It is suspected that by aging or wear the measurement uncertainty might change, and it needs to be examined in a further study.

Conclusion

In contrast to the manufacturer’s analysis methods of measurement errors, which are performed on hundreds of tests during and after the manufacturing process, and are difficult to apply on field practices, a routine Gage R&R study brings very similar results on the uncertainty expressed by the total Gage standard deviation. The calculated σ_{Gage} turned to be 0.17 mmol/l, which matches the standard deviation stated by the manufacturer, thus, our study with real field application “in the kitchen” was capable to reproduce the same level of accuracy.

The ANOVA method is very flexible on expanding the study with additional factors of measurement result, and there is no special restriction on samples and study apart from having a sample that represents the range in study. The MSA manual and automotive practices define acceptance criteria for measurement systems, which may serve as guidelines to establish similarly structured acceptance criteria for measurement processes with self-monitoring devices applied on the field.

The simple definition of a GRR% limit may help practitioners and biohackers to judge if their measurement process is good enough for their application. The weakest part of determining GRR% is the sample range: despite our efforts to cover the target range of the glucometer, very low levels of blood glucose are not represented in our sampling, despite, the default target range is well represented. Accu-Chek Instant, a cheap and simple to use self-monitoring device, is capable to perform well in biohacking programs where the main target is to check on a regular basis what effect a certain food brings to the user, or is the blood glucose level low enough to maintain nutritional ketosis.

Recommendations

Repeatedly occurring of questions from participants of biohacking course has motivated the author to perform a Gage R&R analysis on Accu-Chek Instant. A suggestion of the study for the course trainers is to emphasize measurement uncertainty better and support it with numbers. Based on the study, we can suggest setting a limit, e.g., the half width of the 95% confidence interval, that is $2\sigma = 0.34\text{mmol/l}$. However, an average biohacker is not necessarily familiar with those statistical terms, and preparation of participants shall more happen on the layman’s language. The instructor may, for example, warn not to worry if a single measurement is not more than 0.3mmol/l off the expected or baseline value.

Scientific Ethics Declaration

The authors declare that the scientific ethical and legal responsibility of this article published in EPSTEM journal belongs to the authors.

Acknowledgements or Notes

I would like to say thank you for my kind colleagues who dared to adjust their diet to the experiment and contributed with their own blood to the measurements.

* This article was presented as an oral presentation at the International Conference on Research in Engineering, Technology and Science (www.icrets.net) held in Budapest/Hungary on July 06-09, 2023.

References

- Automotive Industry Action Group. (2010). *Measurement systems analysis. Reference manual* (4th ed.). Chrysler Group LLC, Ford Motor Company, General Motors Corporation
- Erbach, M., Freckmann, G., Hinzmann, R., Kulzer, B., Ziegler, R., Heinemann, L., & Schnell, O. (2016). Interferences and limitations in blood glucose self-testing: An overview of the current knowledge. *Journal of Diabetes Science and Technology*, 10(5), 1161-1168.
- Freckmann, G., Schmid, C., Baumstark, A., Rutschmann, M., Haug, C., & Heinemann, L. (2015). Analytical performance requirements for systems for self-monitoring of blood glucose with focus on system accuracy. *Journal of Diabetes Science and Technology*, 9(4), 885-894.
- Horváth, G. (2023). Examination of the physiological effects of functional foods pilot study. *American Journal of Research, Education and Development*, 1, 58-69.
- Lakatos, P. (2020). *Kortalanul!* (1st ed.). Budapest, Hungary: Jaffa Kiadó és Kereskedelmi Kft.
- Minitab. (2023). *Minitab® 21 Support: Methods and formulas for method of analysis in Crossed Gage R&R Study*. State College, PA: Minitab. Retrieved from <https://support.minitab.com/en-us/minitab/21/help-and-how-to/quality-and-process-improvement/measurement-system-analysis/how-to/gage-study/crossed-gage-r-r-study/methods-and-formulas/method-of-analysis/>
- Roche. (2018). *Accu-chek instant: User's manual. Ref: 07947836003* Indianapolis, IN: Roche Diabetes Care
- Roche. (2021). *Accu-chek instant: Tests. Ref:07819382* Indianapolis, IN: Roche Diabetes Care
- Smith, T. (2019). How accurate are blood glucose meters? *Beyond Type 2*. Retrieved from <https://www.accu-chek.com/print/7961>
- Verband der Automobilindustrie. (2021). *Volume 5 measurement and inspection processes. Capability, planning and Mġmanagement* (3rd ed.). Verband der Automobilindustrie.
- Zheng, J. (2021). Ethical implications of biohacking as activism: Democratized health care, danger, or what? *Aresty Rutgers Undergraduate Research Journal*, 1(3).
- Ziegler, R., Freckmann, G., Heinemann, L. (2014). Genauigkeit von Blutzuckermessgeräten in der Praxis evaluieren: Ist das möglich?. *Diabetes, Stoffwechsel und Herz*, 23.

Author Information

Zoltán Váradi
Óbuda University,
Budapest, Hungary

Contact e-mail: varadi.zoltan@kgk.uni-obuda.hu

Győző Attila Szilágyi
Óbuda University,
Budapest, Hungary

To cite this article:

Varadi, Z., Szilágyi, G. A. (2023). Applicability of a gage R&R study on a home blood glucose meter. *The Eurasia Proceedings of Science, Technology, Engineering & Mathematics (EPSTEM)*, 23, 292-299.

The Eurasia Proceedings of Science, Technology, Engineering & Mathematics (EPSTEM), 2023

Volume 23, Pages 300-306

ICRETS 2023: International Conference on Research in Engineering, Technology and Science

A Comparative Study on Microwave Assisted Dyeing Properties of Conventional and Recycled Polyester Fabrics

Yasemin Dulek

SYK Textile Research and Development Center

Ipek Yildiran

SYK Textile Research and Development Center

Bugce Sevinc

SYK Textile Research and Development Center

Esra Mert

SYK Textile Research and Development Center

Burcu Yilmaz

Marmara University

Dilek Kut

Bursa Uludag University

Abstract: In the literature, microwave studies are predominantly on cellulosic based fabrics and there are limited studies in microwave assisted polyester dyeing. Today, due to the interest in recycled polyester, it was decided to study conventional and microwave heating in the exhaust dyeing methods of recycled polyester and conventional polyester fabrics. The aim of the study was to determine whether microwave heating could be used to shorten dyeing process times and to obtain dyeing with sufficient colour fastness. Accordingly, two samples, 100% polyester and 62% recycled polyester 38% polyester woven fabrics, are used. The samples were dyed with 1.5% Bemacron Smart Red EE disperse dye. The colorimetric properties, colour fastnesses and tear strength of the dyed fabrics were investigated and compared with each other. Spectrophotometer measurements were evaluated that 100% polyester fabric dyed with the microwave method had a darker colour compared to the conventional method, on the other hand, there was no significant colour difference between the conventional and microwave dyeing method of the 62% recycled polyester 38% polyester woven fabric. Colour fastness test results were evaluated that all the fastness results of the recycled and conventional polyester fabrics in the microwave tests were obtained 4 and 4-5. The advantages of microwave heating over the conventional method are that the dyebath heats up in a short time and gives good colour fastnesses without any deterioration in the properties of dyed materials.

Keywords: Polyester fabric, Recycle, Dyeing, Microwave

Introduction

In textile industry, conventional polyester fiber is the most used synthetic fiber and used in global textile clothing about 60%. Polyester fiber has excellent properties, like as spinnability, durability, dyeability, good abrasion resistance and wrinkle resistance but not an environmentally friendly fiber because of reduce fossil fuels which is non-renewable material. Recycled polyester fiber is made from plastic bottles. Recycled polyester

- This is an Open Access article distributed under the terms of the Creative Commons Attribution-Noncommercial 4.0 Unported License, permitting all non-commercial use, distribution, and reproduction in any medium, provided the original work is properly cited.

- Selection and peer-review under responsibility of the Organizing Committee of the Conference

© 2023 Published by ISRES Publishing: www.isres.org

fiber production is important as it releases less CO₂ into the environment than conventional polyester fiber production, reduces oil fuel waste and overall carbon footprint (Basit et al., 2023; Qian et al., 2021).

Polyester dyeing is hard because the polyester fiber has high crystalline fiber microstructure and absence of reactive sites. Polyester is generally dyed with disperse dyes and using high temperature dyeing method which require high energy and water consumption (Syed et al., 2014). In recent years, textile sector has been looking for equivalent production methods to conventional production methods for sustainable eco-friendly production. Since textile wet processes are the processes that most pollute the environment during textile production, alternative production methods are sought for these processes. Utilizing microwave energy in textile wet processes provides sustainable environmentally friendly production by reducing energy costs and processing time (Eyuboglu, 2020).

Microwaves are high-frequency, short-wavelength electromagnetic fields that lie between radio and infrared waves on the electromagnetic spectrum. Microwave length range is between 1 cm and 1 m, microwave frequency range is between 30 GHz and 300 MHz. Microwaves interact with materials in three ways: reflection, absorption and transmission. When the material absorbs the microwave energy, microwaves reach all the particles of the material at the same time uniformly and microwaves heat the material. For this reason, microwave heating provides faster, more effective and homogeneous heating than conventional heating (Öner et al., 2013; Eyupoglu, 2020). In the textile industry, microwave energy is used not only for drying but also for microwave dyeing, fixation of printed fabrics, and surface modification processes (Ozerdem et al., 2008; Kocak et al., 2015).

In the literature, there are many studies on developing different techniques, including microwave irradiation, to improve dyeing behavior of fibers. But there are limited studies in microwave assisted polyester dyeing to reduce high energy and water consumption and improve dyeing behavior. For example, Adeel et al. (2018) observed that the color strength of disperse dyed polyester fabrics improved in the microwave method application and there was no significant change on the polyester fabric properties. Elshemy et al. (2017) studied that the effects of microwave dyeing process parameters (dye concentration, temperature and time) on the color yield, fastness, strength and elongation properties of dyed fabrics for the microwave dyeing process applied to different polyester woven fabrics. As a result of the microwave dyeing process, uniform dyeing and good fastness properties were observed on the polyester woven fabrics. El Apasery et al. (2017) observed that polyester fabrics disperse dyed with ultrasound dyeing method and microwave dyeing method have good fastness properties and energy savings are achieved as the process takes place at lower temperature. Likewise, Syed et al. (2014); Oner et al. (2013); Al Mousawi et al. (2013); Kim et al. (2003) observed that polyester fabrics disperse dyed with microwave irradiation energy method showed good fastness, uniform dyeing, low energy, short time.

In this study, different from the literature, due to the interest in recycled polyester, dyeing properties of recycled polyester woven fabrics according to conventional exhaust dyeing method and microwave irradiation energy dyeing method were investigated. The aim of the study was to determine the usability of microwave energy to shorten dyeing process time and to obtain uniform dyeing with sufficient colour fastness for recycled polyester woven fabrics.

Method

For the study, two different samples, 100% polyester (100% PES) and 62% recycled polyester 38% polyester (62% r-PES 38% PES) woven fabrics, were used. Table 1 shows the structural properties of woven fabrics. Woven fabrics were produced by using polyester yarns in warp direction, polyester and recycled polyester yarns in weft direction.

Table 1. Woven fabrics properties

Fabric Name	PES	Recycled PES
Fabric Composition (%)	100% PES	62% r-PES 38% PES
Warp Yarn	75den/36f Polyester	75den/36f Polyester
Weft Yarn	150den/144f Polyester	150den/144f Recycled Polyester
Warp Density (yarn/cm)	40	40
Weft Density (yarn/cm)	32	32
Weave	Twill	Twill
Weight (g/m ²)	120	120

The samples were dyed with 1,5% Bemacron Smart Red EE disperse dye according to the conventional high temperature exhaust method (HT Dyeing) (130°C, 40 minute) (dyeing diagram is seen at Figure 1.)

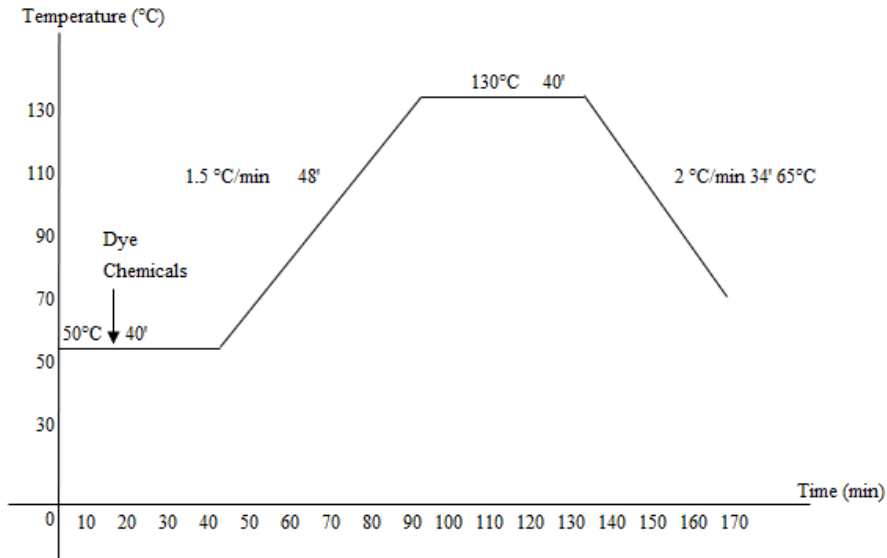


Figure 1. Conventional (HT dyeing) disperse dyeing diagram

It was inspired by the studies in the literature Kocak et al. (2015) and Oner et al. (2013) to improve the microwave assisted disperse dyeing process. Kocak et al. (2015) applied 460 W microwave energy for 3 minutes and then 120 W energy for 5 minutes in order to develop the microwave disperse dyeing process of polypropylene fibers. As a result of the pre-microwave processes, it was decided to use 480 W and 160 W microwave energy. Microwave assisted dyeings were carried out a liquor ratio of 50:1 and 480 W for 7.5 minutes and 160 W for 12.5 minutes in a microwave oven (Arcelik MD 820 model, maximum power 1200 W, 2450 MHz). Dyeing diagram is seen at Figure 2.

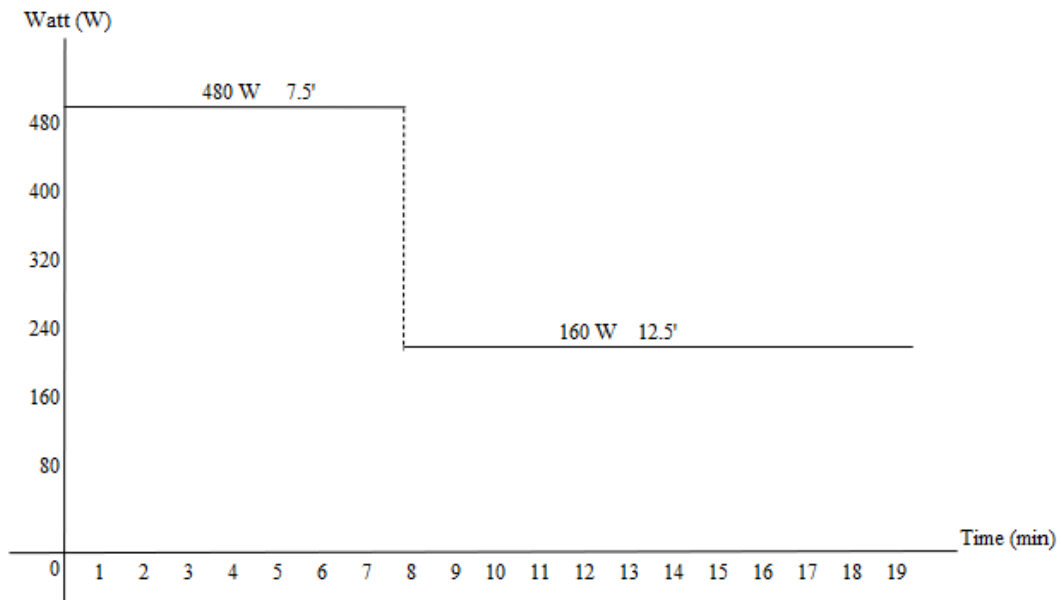


Figure 2. Microwave assisted disperse dyeing diagram

At the end of the dyeing processes, a reduction clearing process was carried out a liquor ratio of 10:1, 1 g/l sodium hydrosulfite and 2 g/l sodium hydroxide for 20 min at 80 °C. After reduction clearing process, neutralizing with 1 g/l acetic acid for 5 min and rinsing in cold water. Dyed samples were dried at ambient temperature.

The CIELab values of fabrics were measured using a Datacolor (USA) SF600 Plus-CT spectrophotometer (D65 and 10° standard observer values). TS EN ISO 13937-2 tear strength (single tear method), TS EN ISO 105 C06

colour fastness to washing, TS EN ISO 105 E01 colour fastness to water, TS EN ISO 105 E04 colour fastness to perspiration, TS EN ISO 105 X12 colour fastness to rubbing tests were determined according to ISO standards.

Results and Discussion

The colorimetric properties, fastness and tear strength (single tear method) of polyester and recycled polyester woven fabrics dyed according to conventional and microwave method were investigated comparatively. The colorimetric parameters obtained for conventional dyed and microwave dyed polyester and recycled polyester fabrics are given in Table 2. Table 2 show that the recycled polyester fabrics dyed with microwave method is slightly lighter ($\Delta L^* = 0.01$), less green ($\Delta a^* = -0.96$), more yellow ($\Delta b^* = 1.21$), slightly less saturated ($\Delta C^* = -0.9$) and the colour difference (ΔE^*) is 0.79 compared with the recycled polyester fabric dyed with conventional method. On the other hand, the conventional polyester fabrics dyed with microwave method is darker ($\Delta L^* = -1.61$), more green ($\Delta a^* = -2.55$), more yellow ($\Delta b^* = 1.23$), less saturated ($\Delta C^* = -2.5$) and the colour difference (ΔE^*) is 1.43 compared with the conventional polyester fabric dyed with conventional method. Commercially, ΔE^* value of less than 1 indicates that the color difference is acceptable.

Table 2. CIELab test results

Fabric Name	Dyeing Method	ΔL^*	Δa^*	Δb^*	ΔC^*	ΔH^*	CMC ΔE
Recycled PES	HT Dyeing (Referance)						
	Microwave Dyeing	0.01	-0.96	1.21	-0.9	1.23	0.79
PES	HT Dyeing (Referance)						
	Microwave Dyeing	-1.61	-2.55	1.23	-2.5	1.25	1.43

Table 3 presented colour fastness values to washing of conventional disperse dyed and microwave disperse dyed polyester and recycled polyester fabrics. Staining values for multifibres (acetate, cotton, polyamide, polyester, acrylic, wool) were between 4 and 4-5 and color change values were 3-4 and 4-5 (Table 3).

Table 3. Washing fastness test results

Fabric Name	Dyeing Method	Staining						Colour change
		Acetate	Cotton	Polyamide	Polyester	Acrylic	Wool	
PES	HT Dyeing	4-5	4-5	4	4-5	4-5	4-5	3-4
PES	Microwave Dyeing	4	4-5	4	4-5	4-5	4-5	4-5
Recycled PES	HT Dyeing	4-5	4-5	4	4-5	4-5	4-5	4
Recycled PES	Microwave Dyeing	4-5	4-5	4-5	4-5	4-5	4-5	4-5

Table 4 presented colour fastness values to water of conventional disperse dyed and microwave disperse dyed polyester and recycled polyester fabrics. Staining values for multifibres (acetate, cotton, polyamide, polyester, acrylic, wool) were between 4 and 4-5 and color change values were 3-4 and 4-5 (Table 4).

Table 4. Water fastness test results

Fabric Name	Dyeing Method	Staining						Colour change
		Acetate	Cotton	Polyamide	Polyester	Acrylic	Wool	
PES	HT Dyeing	4	4	4	4-5	4-5	4-5	3-4
PES	Microwave Dyeing	4-5	4-5	4-5	4-5	4-5	4-5	4
Recycled PES	HT Dyeing	4	4-5	4	4-5	4-5	4-5	4
Recycled PES	Microwave Dyeing	4-5	4-5	4-5	4-5	4-5	4-5	4-5

Table 5 and 6 presented colour fastness values to acidic and alkaline perspiration of conventional disperse dyed and microwave disperse dyed polyester and recycled polyester fabrics. Staining values for multifibres (acetate, cotton, polyamide, polyester, acrylic, wool) were between 4 and 4-5 and color change values were 4 and 4-5 (Table 5 and 6).

Table 5. Acidic perspiration fastness test results

Fabric Name	Dyeing Method	Staining					Wool	Colour change
		Acetate	Cotton	Polyamide	Polyester	Acrylic		
PES	HT Dyeing	4	4	4	4-5	4-5	4	4
PES	Microwave Dyeing	4-5	4-5	4-5	4-5	4-5	4-5	4
Recycled PES	HT Dyeing	4	4-5	4	4-5	4-5	4-5	4
Recycled PES	Microwave Dyeing	4-5	4-5	4-5	4-5	4-5	4-5	4-5

Table 6. Alkaline perspiration fastness test results

Fabric Name	Dyeing Method	Staining					Wool	Colour change
		Acetate	Cotton	Polyamide	Polyester	Acrylic		
PES	HT Dyeing	4	4	4	4-5	4-5	4	4
PES	Microwave Dyeing	4-5	4-5	4-5	4-5	4-5	4-5	4
Recycled PES	HT Dyeing	4	4-5	4	4-5	4-5	4	4
Recycled PES	Microwave Dyeing	4-5	4-5	4-5	4-5	4-5	4-5	4-5

Table 7 presented colour fastness values to rubbing (wet and dry) of conventional disperse dyed and microwave disperse dyed polyester and recycled polyester fabrics. Color change values were 4 and 4-5 (Table 7).

Table 7. Wet and dry rubbing fastness test results

Fabric Name	Dyeing Method	Wet	Dry
PES	HT Dyeing	4-5	4-5
PES	Microwave Dyeing	4	4
Recycled PES	HT Dyeing	4-5	4-5
Recycled PES	Microwave Dyeing	4-5	4-5

Table 8 presented tear strength (single tear method) values of conventional disperse dyed and microwave disperse dyed polyester and recycled polyester woven fabrics. There was no significantly difference in the tear strength values (Table 8). Accordingly, it can be said that microwave irradiation energy not had a negative effect on the tearing properties of polyester and recycled polyester fabrics.

Table 8. Tear strength (single tear method) test results

Fabric Name	Dyeing Method	Warp Tear Strength (N)
PES	HT Dyeing	37.07
PES	Microwave Dyeing	39.99
Recycled PES	HT Dyeing	28.35
Recycled PES	Microwave Dyeing	36.14

Conclusion

Advantages of microwave irradiation energy dyeing process according to high temperature conventional dyeing process in different aspects are given below:

- Uniform dyeing process is obtainable with good colouristic properties and adequate colour fastnesses without any loss tear strength. Spectrophotometer measurements were evaluated that conventional polyester fabric dyed with the microwave method had a darker colour compared to the conventional method. This indicates that the same colour can be obtained with less dyestuff concentration. On the other hand, there was no significant colour difference between the conventional and microwave dyeing method of the recycled polyester woven fabric. It is determined that microwave dyeing not have a negative effect on the colour yield.

– The dyebath heats up in a short time with microwave heating. The microwave assisted dyeing process was completed in approximately 20 minutes, while high temperature conventional dyeing process was completed in approximately 170 minutes. As a result, high level of energy and time savings were achieved.

Considering cost-effectiveness, energy-saving and time saving of the microwave assisted dyeing process method, microwave irradiation heating is promising in textile dyeing processes.

Recommendations

With this study, it has been indicated that the amount of dyestuff and the process time can be reduced in microwave dyeing. In this context, it can be studied on the reducing the amount of dyestuff in dyeing different fibers by microwave dyeing and the optimization of different textile processes such as washing, bleaching, mercerization in future studies.

Scientific Ethics Declaration

The authors declare that the scientific ethical and legal responsibility of this article published in EPSTEM journal belongs to the authors.

Acknowledgements or Notes

*This work is supported by the equity project number AG-02-22-SYK-00 of SYK Textile R&D Center supported by the Ministry of Industry and Technology, Republic of Turkey.

* This article was presented as an oral presentation at the International Conference on Research in Engineering, Technology and Science (www.icrets.net) held in Budapest/Hungary on July 06-09, 2023.

References

- Adeel, S., Khan, S.G., Shahid, S. Saeed, M., Kiran, S., Zuber, M., Suleman, M., & Akhtar, N. (2018). Sustainable dyeing of microwave treated polyester fabric using disperse yellow 211 dye. *Journal of Mexican Chemical Society*, 62(1), 1-9.
- Al Mousawi, S.M., El Apasery, M. A., & Elnagdi, M.H. (2013). Microwave assisted dyeing of polyester fabrics with Disperse Dyes. *Molecules*, 18, 11033-11043.
- Basit, A., Rehman, A., Iqbal, K. & Abid, H. A. (2023). Optimization of the tencel/cotton and polyester/recycled polyester blended knitted fabrics to replace cvc fabric. *Journal of Natural Fibers*, 20(1), 1-12.
- El Apasery, M. A., Abdelghaffar, R.A., Kamel, M.M., Kamel, M. M., Youssef, B.M., & Haggag, K.M. (2017). Microwave, ultrasound assisted dyeing- part I: Dyeing characteristics of C.I. disperse red 60 on polyester fabric. *Egypt. J. Chem. Special Issue, The 8th. International Conference Text. Res. Div., Nat. Res. Centre, Cairo*, 143-151.
- Elshemy, N.S., Elshakankery, M.H., Shahien, S.M., Haggag, K. & El Sayed, H. (2017). Kinetic investigations on dyeing of different polyester fabrics using microwave irradiation. *Egypt. J. Chem. Special Issue, The 8th. Int. Conf. Text. Res. Div., Nat. Res. Centre, Cairo*, 79 – 88.
- Eyupoglu, S. (2020). Investigation of dyeing properties of flax fabric according to different methods with natural dye obtained from wild crop flower. *Duzce University Journal of Science and Technology*, 8, 317- 325.
- Kocak, D., Akalın, M., Merdan, N., & Sahinbaskan, B.Y. (2015). Effect of microwave energy on disperse dyeability of polypropylene fibres. *Marmara Journal of Pure and Applied Sciences*, 1, 27-31.
- Kim, S.S., Leem S.G., Ghim, H.D., Kim, J.H., & Lyoo, W.S. (2003). Microwave heat dyeing of polyester fabric. *Fibers and Polymers*, 4(4), 204-209.
- Oner, E., Buyukakinci, Y., & Sokmen, N. (2013). Microwave-assisted dyeing of poly (butylene terephthalate) fabrics with disperse dyes. *Society of Dyers and Colourists, Coloration Technology*, 129, 125–130.
- Ozerdem, A., Tarakcioglu, I., & Ozguney, A. (2008). The use of microwave energy for the fixating of reactive printed cotton fabrics. *Textile & Apparel*, 4(2008), 289-296.

- Syed, U., Marri, H.B. & Majid, T. (2014). Dyeing of polyester woven fabric with disperse dye using conventional and microwave technique. *Mehran University Research Journal of Engineering & Technology*, 33(3), 359-364.
- Qian, W., Ji, X., Xu, P., & Wang, L. (2021). Carbon footprint and water footprint assessment of virgin and recycled polyester textiles. *Textile Research Journal*, 91(21-22), 2468-2475.

Author Information

Yasemin Dulek

SYK Textile Research & Development Center
Bursa, Turkey
Contact e-mail: yasemindulek@sykteks.com

Ipek Yildiran

SYK Textile Research & Development Center
Bursa, Turkey

Bugce Sevinc

SYK Textile Research & Development Center
Bursa, Turkey

Esra Mert

SYK Textile Research & Development Center
Bursa, Turkey

Burcu Yilmaz

Marmara University
Istanbul, Turkey

Dilek Kut

Bursa Uludag University
Bursa, Turkey

To cite this article:

Dulek, Y., Yildiran, I., Sevinc, B., Mert, E., Yilmaz, B., & Kut, D. (2023). A comparative study on microwave assisted dyeing properties of conventional and recycled polyester fabrics. *The Eurasia Proceedings of Science, Technology, Engineering & Mathematics (EPSTEM)*, 23, 300-306.

The Eurasia Proceedings of Science, Technology, Engineering & Mathematics (EPSTEM), 2023

Volume 23, Pages 307-315

ICRETS 2023: International Conference on Research in Engineering, Technology and Science

Benefits of Circular Design Adoption in the Nigerian Building Industry

Taofeek Suleman
Covenant University

Isidore Ezema
Covenant University

Peter Aderonmu
Redeemer's University

Abstract: Circular economy (CE) is hinged upon resource optimisation as a more viable and sustainable approach against the extractivist linear economic model that has resulted in resource scarcity, affordability issues, and environmental degradation. Design plays a critical role as the foundation of the circular approach, however, limited studies have examined the inherent benefits of circular design (CD) adoption from the building design firms' (BDFs) perspectives, more importantly, none exist in Nigeria to the best of the author's knowledge. This study assesses the benefits of CD adoption in the Nigerian building industry (NBI). Primary data were collected from 216 architectural and engineering design firms domiciled in Lagos using a questionnaire survey. The findings indicated the top five benefits which include reduction in energy use by efficient utilization through design, development of new skill sets in circularity by design teams, reduction in pollution through reduced burning of fossil fuel, reduction of construction/demolition waste generation, improvement of public health by preserving local biodiversity. While increasing competitiveness amongst BDFs and resource security through optimisation and dematerialisation were ranked the least. The outcome can be ascribed to the fact that Nigeria currently faces an energy crisis with efforts being made in developing energy-efficient buildings and the need to minimize the environmental impact of construction practices. It was suggested that BDFs need to invest in CD expertise development through training and education, voluntary stewardship, and providing the requisite technologies to aid CD implementation. This study provided the basis for the needed debates on the relative benefits of CD adoption in the NBI.

Keywords: Building design firms, Circular design, Circular economy, Lagos-Nigeria, Benefits

Introduction

The concept of circular economy (CE) is currently a topic of discussion across different sectors around the world regarding sustainability. Its benefits include reducing the impact of resource extraction and optimising efficiency (Ezema et al., 2023). CE aims to establish waste-free systems by utilising regenerative and restorative approaches through thoughtful design and implementation according to the Ellen MacArthur Foundation in 2017. The architecture, engineering, construction, and operations (AECO) sector is recognised for its high usage of resources, consuming around 40% of environmental resources, producing 40% of global carbon emissions (Naneva, 2022), utilising 43% of global energy, and producing 40% of global waste (Al-Hamrani et al., 2021; Hasheminasab et al., 2022). In addition, the AECO sector is recognised for its use of the linear economy (LE) model, where resources are taken, made into products, and disposed of at the end of their life cycle (Al-Hamrani et al., 2021). This type of economy is often referred to as an extractivist economy (Hentges et al., 2022). If we continue consuming resources at our current rate, global production will need to increase twofold by 2030 and triple by 2050 to keep up with the growing population's demands (Ezeudu et al., 2021; Okafor et al., 2021).

- This is an Open Access article distributed under the terms of the Creative Commons Attribution-Noncommercial 4.0 Unported License, permitting all non-commercial use, distribution, and reproduction in any medium, provided the original work is properly cited.

- Selection and peer-review under responsibility of the Organizing Committee of the Conference

© 2023 Published by ISRES Publishing: www.isres.org

However, this will also result in a substantial amount of waste generated from production processes and infrastructure development for human activities (Adewuyi & Adewuyi, 2020; Tongo et al., 2021). The concept of CE has been considered an expansion of sustainable practices due to its ability to achieve optimal utilization of resources.

The emergence of CE in the AECO industry has influenced various stages of the building procurement process (Çimen, 2021; Ellen MacArthur Foundation [EMF], 2017; Ezeudu & Ezeudu, 2019; Mbolli et al., 2020), particularly in the design stage (Al-Hamrani et al., 2021; Kayacetin et al., 2022). The design stage has been identified as the most efficient and effective phase of sustainable construction for implementing CE strategies (Dewagoda et al., 2022). Circular design strategies have made it feasible to integrate CE into the design stage, providing a range of advantages. Nonetheless, it has been observed that differences exist in the adoption of circular design (CD) between developed and developing economies due to variations in geographical location, sectoral, organisational, technological, and economic differences (Guerra & Leite, 2021; Hart et al., 2019). While CD benefits have been extensively researched in developed economies (Adams et al., 2017), there have been few studies investigating the potential benefits of CD adoption in the Global South (Bilal et al., 2020; Hossain & Khatun, 2021), specifically from the viewpoint of building design firms (BDFs). To the best of our knowledge, no such study has been conducted in Nigeria. Therefore, this research aims to evaluate the advantages of implementing CD in the Nigerian building industry (NBI).

Adoption of Circular Design Strategies: Salient Benefits

Circular design strategies (CDS) are a set of resource optimisation techniques employed during the building development's design stage. These methods aim to ensure that materials are continually used and reused at their highest value, thus slowing down the resource loop. CDS also involves designing out waste to narrow the resource loop and promote the regeneration of materials in both the technical and biological cycles, ultimately closing the resource loop. CE embraces a design philosophy that focuses on restoring and regenerating resources to promote maximum efficiency. This is accomplished by employing various strategies such as modular design, design for deconstruction and disassembly, design for flexibility and adaptation, design for excellence, whole systems design, design in layers, and design for reuse (Çimen, 2021; Ezeudu & Ezeudu, 2019) among other techniques. Most of the previous CE research conducted in the NBI has centered on life-cycle assessment, end-of-life, materials, and waste valorization, with little emphasis placed on the significance of the design stage (Osobajo et al., 2020), which has been identified as the most effective stage for implementing CE (Dewagoda et al., 2022). Nevertheless, there are significant benefits to be gained from adopting CD in building development, particularly in addressing environmental degradation, affordability challenges, and resource scarcity.

Table 1. Benefits of circular design adoption

Code	Benefits	References
BN1	Relieve on the global ecosystem/ resource consumption	Guerra and Leite (2021)
BN2	Circular design supports climate change mitigation	Cruz Rios et al. (2021)
BN3	Reduction of construction/demolition waste generation	Guerra and Leite (2021)
BN4	Reduces energy use by efficient utilization through design	Ghisellini et al. (2018)
BN5	Protecting underground/surface waterways from contamination	Purchase et al. (2021)
BN6	Increased use of recycled materials (Upcycling/downcycling)	Purchase et al. (2021)
BN7	Improving public health by preserving local biodiversity	Guerra and Leite (2021)
BN8	Reduce pollution through reduced burning of fossil fuel	Purchase et al. (2021)
BN9	Mitigate the demand-driven materials price volatility risks	Guerra and Leite (2021)
BN10	Building components reuse for reduced building cost and time	Minunno et al. (2020)
BN11	New market for reusable/reclaimed components and elements	Minunno et al. (2020)
BN12	Potential reduction in operating cost of building maintenance	Minunno et al. (2020)
BN13	Increases competitiveness amongst building design firms	Adams et al. (2017)
BN14	Resource security through optimization and dematerialization	Adams et al. (2017)
BN15	New horizon for eco-innovations in the building market/sector	Minunno et al. (2020)
BN16	Development of new skill sets in circularity by design teams	Purchase et al. (2021)
BN17	Scraping of dump sites for more quality land for developments	Laurea, (2020)
BN18	Government creating means of achieving sustainability goals	Purchase et al. (2021)
BN19	Regulations on the certification of reclaimed components	Minunno et al. (2020)
BN20	Corporate social responsibility practices by design firms	Laurea (2020)

Hartwell et al. (2021) have highlighted that promoting recycling and reusing resources at the end-of-life stage is crucial in achieving reduction in carbon emission and minimizing waste generation. Additionally, Ritzen et al. (2019) found that incorporating component reuse in new dwellings could potentially result in a 90% reduction in embodied carbon emissions. According to Ghisellini et al. (2018), CE revolutionizes the entire value chain process by transforming the linear end-of-life approach to a multi-cycle approach that enhances efficiency and optimisation in resource utilization. The environmental impact and economic value of salvaged materials are influenced by factors such as the availability of secondary-use material markets, shorter transportation distances, and the process and method of deconstruction. Ghisellini et al. (2018) have identified that refurbishing offers a more sustainable option than demolition or new construction, and it has a shorter payback period for achieving a return on investment. Purchase et al. (2021) conducted a review on the impact of CE on construction and demolition waste management, and the study found that circularity strategies in buildings offer several benefits. These benefits include meeting sustainability goals, improving public health, reducing pollutants and greenhouse gas emissions, providing quality land to meet the demand for housing, conserving and preserving biodiversity, and creating job opportunities. Minunno et al. (2020) conducted a comparative study between a circular modular building designed for disassembly and secondary-use steel structures and a conventional linear modular building. The aim was to assess the environmental benefits of incorporating secondary-use materials through a life cycle assessment method. According to the study conducted by Minunno et al. (2020), the circular modular building designed for disassembly and secondary-use steel structures showed significant environmental benefits. These included an 88% reduction in greenhouse gas emissions and eutrophication, and an 87% reduction in acidification potentials. Additionally, the study found that circular buildings offered other benefits, such as savings on land used for landfills, component reuse, and the establishment of a market for reusable building components. Hentges et al. (2022) identified the benefits of CD adoption in the Brazilian construction sector, including the creation of CD guidelines, the adoption of Green Building Information Modelling (GreenBIM), and the implementation of circularity stewardship programmes. Furthermore, Hartwell et al. (2021) highlighted the environmental opportunities available in Europe, America, and Asia, due to the implementation of CE regulations and economic incentives that encourage pro-environmental innovations. The adoption of circularity strategies could also foster innovation in the building sector. Table 1 presents the benefits identified from the reviewed literature.

Method

The study's participants were architectural, civil/structural engineering, and building services engineering firms registered with their respective national regulatory bodies and based in Lagos, Nigeria. Lagos was chosen as the study area because it accounts for two-thirds of the construction activities ongoing in Nigeria. Moreover, Lagos is home to over 70% of the BDFs and head offices of construction companies in Nigeria (Ogunmakinde, 2019). To account for the varying characteristics and attributes of the study population, the study employed a quota random sampling method. Primary data was collected through a questionnaire survey administered to the BDFs, which sought responses on the firms' demographics, awareness of CD, and benefits of CD adoption. The questionnaires were distributed through two means: hand-delivered and electronically, using Google Forms sent via email and WhatsApp. Before conducting the main study, a pilot study was conducted. The responses from the pilot study were subjected to a Cronbach's Alpha reliability test to ensure that the questionnaire survey design measured the constructs appropriately and achieved internal consistency, as recommended by Robson & McCartan (2017). The Cronbach's Alpha reliability test yielded a score of 0.975 for the 20 benefits, which was higher than the threshold of 0.70 (Ogunmakinde, 2019). A total of 307 questionnaires were distributed, and 216 of them were fully completed by the respondents. The respondents were asked to rate the level of importance on a five-point Likert scale, ranging from 1 (very low importance) to 5 (very high importance). Statistical Products and Service Solutions version 21 was used for data analysis, management, and coding. The Shapiro-Wilk test was conducted to test for normality in the data distribution, which revealed that the survey data was distribution-free. The analyses conducted on the data included mean score ranking, standard deviation, and the Kruskal-Wallis Test, which was used to determine if there was a statistically significant difference in the responses.

Results and Discussion

Firms' Demography

According to Figure 1, BDFs exist in different forms depending on the services they provide. The majority of the respondents (158, 73.1%) were BDFs that offer architectural design services, while civil/structural engineering design service (31, 14.4%), electrical engineering design service (15, 6.9%), and mechanical

engineering design service (12, 5.6%) were less common. The reason for this could be attributed to the fact that there are three times more registered architectural design firms than engineering design firms with their respective national regulatory bodies in the study area. When it comes to the age distribution of the firms, 59 (27.3%) of them have been in existence for one to five years, 52 (24.1%) for six to ten years, 41 (19.0%) for over 25 years, 37 (17.1%) for 11 to 15 years, and 11 (5.1%) of the firms have been around for 21 to 25 years. The majority of BDFs observed were relatively new start-up organisations that have been in operation for less than six years. This is likely due to the abundance of market opportunities in the building sector, as there are many building construction projects currently taking place in Lagos. This is second to none in the country, as mentioned by Ogunmakinde (2019), and is also due to the rate of urbanization in the state. Another factor to consider is the number of staff that BDFs have. The majority (71.8%) of these firms are small in size, with less than eleven staff members. This can be attributed to the ownership structure of these firms, with half (50.5%) being owned by sole proprietors, followed by partnership-owned (32.9%), and consortium-owned firms being the least common type among the respondents. The study found that the majority of BDFs (118, 54.6%) are aware of circular design. Meanwhile, 79 (36.6%) of respondents indicated that they have not heard of it, and 19 (8.8%) were unsure. It is noteworthy that more than half of the BDFs are familiar with CD. This finding is consistent with Bilal et al. (2020) research, which reported a 58% overall level of awareness of CE in the building sector of developing countries. Likewise, this discovery is in line with previous research conducted by Liu & Bai (2014) and Masi et al. (2018), albeit slightly lower. The disparity could be due to the limited number of studies on CD at the BDF level in the NBI. However, this study shed light on the significant benefits that laced the adoption of CD in the NBI as seen from the BDFs' perspective.

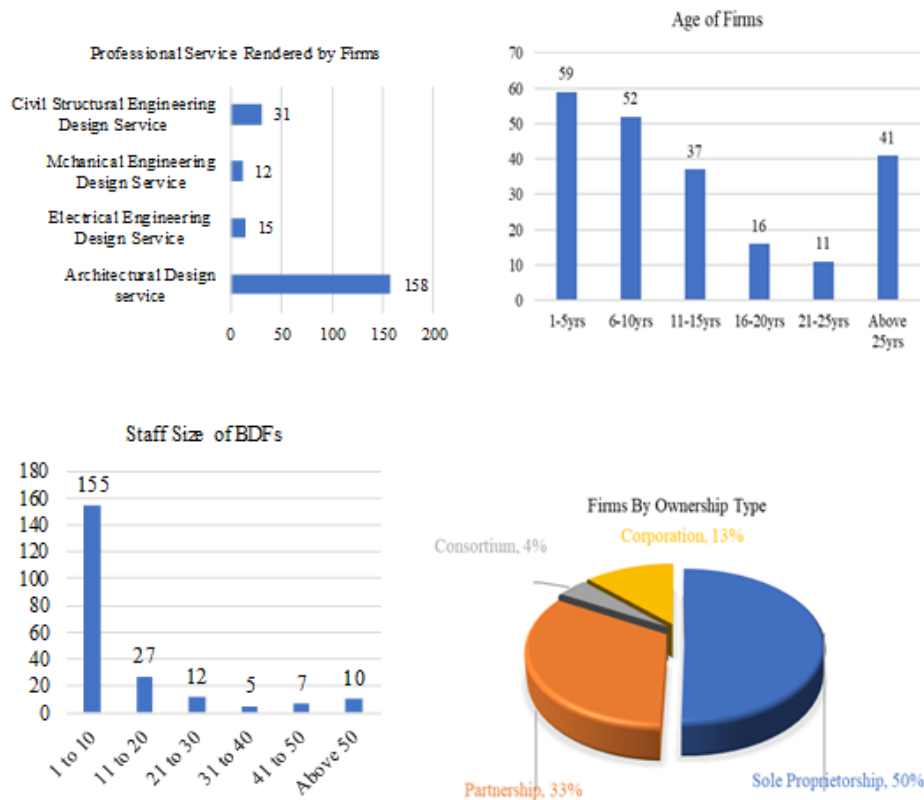


Figure 1. Distribution of firms by demographic characteristics

Benefits of CD Adoption in the NBI

The study evaluated the significance of the advantages of CD adoption in the NBI. Table 2 displays the mean scores and rankings of these benefits, with all of them above 3.50, as suggested by Wuni & Shen, (2022), indicating their importance. BN4, which is "reduction in energy use by efficient utilization through design," was ranked the most significant. Gupta (2019) reported that the implementation of CD could lead to a 64% reduction in energy operating costs in India. Nigeria is currently grappling with an energy crisis. In 2016, the Federal Ministry of Power, Works, and Housing in Nigeria conducted an analysis revealing the construction industry's high energy consumption and the necessity to create energy-efficient structures. Hence, the call for a need for energy-efficient building design strategies as argued by Sholanke et al. (2022). Minunno et al. (2020) pointed out that adopting CD can help achieve savings on operating costs and foster openness to innovative practices in

Australia. Gupta (2019) suggests that passive cooling and heating design approaches can help reduce operating costs and optimise energy consumption. While Akande et al. (2021) argued that the adoption of low-impact materials such as clay, hemp, and compressed stabilised bricks can significantly reduce the energy demand in housing delivery in the NBI. However, they strongly recommended the need for adequate public awareness and societal enlightenment. This would require the involvement of professionals with the necessary technical abilities in energy-efficient design as noted by Akhimien & Latif (2019). The second most significant benefit is the development of new skill sets in circularity by design teams (BN16). van Bueren et al. (2019) discovered that collaborations among design teams, both locally and internationally, can accelerate the development of new design capacities and skills while also contributing to knowledge acquisition, new technologies, and policy formulation. Given the limited CD knowledge among BDFs, they need to acquire new technical expertise in building design that incorporates CE principles. Professional training programmes such as workshops and seminars on circular building design can help BDFs equip their employees with the necessary knowledge for seamless implementation. According to Purchase et al. (2021), governments can play a significant role in organizing professional training in the form of educational workshops, seminars, and formal education in the NBI.

Table 2. Benefits of circular design adoption: Inter-group comparisons

Code	Archi. Firm		Electrical Eng. Firm		Mech. Eng. Firm		Civil/Struct. Eng. Firm		Overall			Kruskal-Wallis Test	
	Mean	Rk	Mean	Rk	Mean	Rk	Mean	Rk	Mean	StD	Rk	χ^2	Sig.
BN1	3.82	9 TH	3.93	16 TH	3.58	11 TH	3.71	12 TH	3.81	.997	9 TH	1.080	.782
BN2	3.77	12 TH	4.00	8 TH	3.67	6 TH	3.77	6 TH	3.76	.976	12 TH	1.597	.660
BN3	3.89	3 RD	4.13	5 TH	3.50	18 TH	3.58	19 TH	3.88	.997	4 TH	4.471	.215
BN4	3.96	1 ST	4.20	3 RD	3.58	12 TH	3.94	1 ST	3.93	.900	1 ST	6.455	.091
BN5	3.65	18 TH	4.00	9 TH	3.58	13 TH	3.74	8 TH	3.67	1.015	17 TH	1.938	.585
BN6	3.84	7 TH	3.87	18 TH	3.75	1 ST	3.71	13 TH	3.82	1.030	7 TH	.561	.905
BN7	3.85	5 TH	4.00	10 TH	3.50	19 TH	3.71	14 TH	3.84	1.013	5 TH	1.279	.734
BN8	3.90	2 ND	4.27	1 ST	3.58	14 TH	3.52	20 TH	3.89	1.017	3 RD	5.368	.147
BN9	3.65	19 TH	4.00	11 TH	3.58	15 TH	3.74	9 TH	3.67	1.002	18 TH	2.114	.549
BN10	3.77	13 TH	3.73	20 TH	3.58	16 TH	3.81	4 TH	3.74	1.006	14 TH	.953	.813
BN11	3.80	11 TH	3.80	19 TH	3.67	7 TH	3.68	15 TH	3.80	.928	11 TH	.252	.969
BN12	3.70	15 TH	4.27	2 ND	3.67	8 TH	3.68	16 TH	3.75	.967	13 TH	6.074	.108
BN13	3.66	17 TH	3.93	17 TH	3.58	17 TH	3.81	5 TH	3.67	1.012	19 TH	2.145	.543
BN14	3.62	20 TH	4.07	6 TH	3.67	9 TH	3.84	3 RD	3.65	.962	20 TH	3.096	.377
BN15	3.83	8 TH	4.07	7 TH	3.75	2 ND	3.74	10 TH	3.81	.974	10 TH	1.818	.611
BN16	3.81	10 TH	4.00	12 TH	3.67	10 TH	3.65	18 TH	3.90	.957	2 ND	1.371	.712
BN17	3.88	4 TH	4.20	4 TH	3.75	3 RD	3.77	7 TH	3.68	1.050	16 TH	2.371	.499
BN18	3.68	16 TH	4.00	13 TH	3.50	20 TH	3.87	2 ND	3.84	.937	6 TH	1.909	.592
BN19	3.85	6 TH	4.00	14 TH	3.75	4 TH	3.68	17 TH	3.74	.964	15 TH	.713	.870
BN20	3.72	14 TH	4.00	15 TH	3.75	5 TH	3.74	11 TH	3.82	.918	8 TH	1.222	.748

*Archi – Architectural; Eng. – Engineering; Struct. – Structural; Rk – Rank; StD – Standard Deviation; χ^2 - Chi Square Value; Sig. – p-value

The third most significant benefit, as ranked by BDFs, was the "reduction in pollution through reduced burning of fossil fuel" (BN8). Minunno et al. (2020) stated that designing structures for disassembly and component reuse can reduce the global warming potential, GHG by 88%, waste to landfill, and eutrophication and acidification potential of the environment. This approach can also save the potential depletion of the ozone layer and abiotic by 5% and 23%, respectively. The fourth most significant benefit, as identified by BDFs, is the "reduction of construction/demolition waste generation" (BN3). Aboginije et al. (2021) indicated that waste management approaches utilized in Nigerian construction projects, specifically at the design phase are still not sustainable. Akanbi et al. (2018) and Olanrewaju and Ogunmakinde (2020) emphasized that the implementation of CD can help minimize the generation of construction and demolition waste. Purchase et al. (2021) noted that reusing construction waste onsite and reducing the amount of waste transported to landfills can lower carbon emissions. This will assist the NBI to move towards decarbonisation and clean production processes. The fifth most significant benefit of CD adoption in the NBI, as ranked by BDFs, is "improving public health by preserving local biodiversity" (BN7). According to Gupta (2019), implementing CD in public infrastructure developed to provide waste services, sanitation, and water can support material cycles and active urban nutrients that enhance public health. According to Guerra & Leite (2021) and Purchase et al. (2021), the implementation of CD can provide protection against uncontrollable material price escalation risks in the supply chain, ensure resource sufficiency, improve public health and well-being, and create employment opportunities.

Other benefits identified in the study are also of advantage to the NBI. Even though Nigeria has not yet established regulations and financial incentives that specifically promote CE in the building sector, BDFs in the country are still conscious of the environment. They have shown interest in protecting the environment amid the ongoing global campaign for preserving and conserving natural resources, waste management, pollution control, and reduction of carbon emissions. Tirado et al. (2022) highlighted that the environmental opportunities associated with CE can lead to the creation of local jobs and boost the economy. Guerra & Leite (2021) added that the transition to the circular building sector can also bring various environmental benefits, such as stakeholder engagement through public-private partnerships on case projects, policy amendments in national building codes and regulations, and voluntary stewardship for building circularity. Tirado et al. (2022) stated that the environmental opportunities associated with CE can lead to the creation of local employment and economic growth. This will be favourable to the unemployment level estimated at above 40% at the same time creating stability in the local economy in Nigeria. Similarly, the implementation of CD can enhance the competitiveness of BDFs in the built environment (Adams et al., 2017) and promote risk management as a corporate social responsibility by reducing practices that lead to environmental pollution (Laurea & Rivato, 2020)

It can be deduced from the outcome of this study that environmental and technical benefits are the most significant to CD adoption in the NBI. This finding is consistent with previous research conducted by Guerra & Leite (2021) in the US, Gupta (2019) in India, Tirado et al. (2022) in France, among others. Gupta (2019) and Tirado et al. (2022) identified environmental opportunities as being the most significant in the building sector in France and India, respectively, due to the need to reduce the ecological footprint in the areas of sustainability and resilience. The consistency in findings could be as a result of the fact that the issues of climate change as a consequence of over exploitation of environmental resources has become top among the current global debates. Similarly, this may be because many BDFs view CD primarily from the perspective of efficient resource utilization, the 3R principle (reduce, reuse, and recycle), and sustainability. However, there is not much focus on environmental conservation in the design by BDFs in the NBI, as environmental impact assessments are rarely conducted for such designs. Architects and engineers should receive training that emphasizes environmental protection and awareness of climate change mitigation on a global scale (Ezema & Maha, 2022). However, the results of this study are not consistent with some previous research, such as Torgautov et al. (2021) in the construction sector in Kazakhstan. This study identified economic benefits as being the most significant due to the financial savings achieved through the reuse or recycling of construction materials, which serves as the primary motivation for stakeholders. The difference in findings could be attributed to the scope of the present study and previous studies. The current research focused on CD adoption at the level of BDFs, whose professional ethics prioritize resource security and responsibility toward delivering a healthy environment. Adopting CD can result in economic benefits, such as promoting eco-innovation in the building sector, creating a market for reused components, mitigating price volatility, reducing the cost of operation and maintenance, minimizing construction time, and addressing resource scarcity (Minunno et al., 2020). The NBI has been challenged with the investment cost in building development as well as the concerns bordering on foreign exchange rate associated with the importation market. Research has shown that there are significant opportunities for adopting CD (Minunno et al., 2020) in developing economies in Africa (Dabaieh et al., 2021), particularly in Nigeria (Ogunmakinde, 2019), as the innovation is relatively new in the region. The significance of circular industrial activities in bringing about sustainable development in Nigeria was stressed by Ogunsanwo & Ayo-Balogun (2020). The studies asserted that promoting the reuse and recycling of resources has become essential, specifically in the NBI. Onogwu (2014) acknowledged the significance of certain essential incentives, including robust institutions, government funding and interventions, and the adoption of circular programmes, in the implementation of CE in Nigeria. The practical implication of these findings is that BDFs must take on an effective leadership role in promoting CD awareness and its associated benefits among stakeholders throughout the value chain. To achieve the environmental goals of CD, BDFs should foster technical skills in CD via knowledge sharing and exchange, as well as invest in GreenBIM. To better respond to environmental challenges, design optimisation software should be integrated into design workflows and processes to enable the early assessment and evaluation of design options. These findings can help BDFs develop guidelines and tools for designing that facilitate the implementation of CD more easily.

Conclusion

CE has been a prevalent topic of discussion in the built environment globally, but the adoption of CE varies between countries due to their unique geographical and economic circumstances and the associated benefits. This study examined the benefits of CD adoption in the NBI, from the perspective of BDFs, using empirical

evidence. The results of this study suggest that environmental and technical benefits are more significant to CD adoption in the NBI, while organisational benefits are less significant. These findings highlight the importance of debating the relative benefits of CD adoption in the NBI. BDFs should incorporate circular design thinking into design workflows and processes to manage and allocate resources in building developments. To operate in the new circular building procurement system, BDFs should employ circular project management approaches and stages that differ from conventional project management systems, based on circular business models. Additionally, it was suggested that BDFs adopt new methods of design, materials, and components sourcing by implementing design for availability. To achieve this, a new technical and technological infrastructure needs to be established. BDFs should create an assessment mechanism to evaluate affordability and stakeholders' willingness to invest in circular building projects. Additionally, there is a need for increased awareness and adoption of BIM among BDFs because it can significantly contribute to CD output through material passport and digital tracking throughout the building lifecycle.

Recommendations

According to the results of this study, BDFs should invest in developing CD technical expertise through training, continuous professional development programmes, and workshops. Moreover, they should raise awareness by collaborating with other firms and stakeholders, government making concerted efforts in launching voluntary stewardships, and providing necessary technologies to facilitate CD implementation in building developments. The government should create CE policies to facilitate a top-down approach and provide incentives and awards to encourage bottom-up CD adoption. Additionally, the government should take the lead by investing in case/pilot projects for future developments. To promote resource optimisation and other environmentally-friendly solutions, sustainability and circularity should be included in the curricula of architecture and engineering courses at higher institutions of learning. additionally, if strategic actions are put in place, government policies and regulations could also drive the systemic shift.

Scientific Ethics Declaration

The authors declare that the scientific ethical and legal responsibility of this article published in EPSTEM journal belongs to the authors.

Acknowledgements or Notes

* This article was presented as oral presentation at the International Conference on Basic Sciences, Engineering and Technology (www.icrets.net) held in Budapest/Hungary on July 06-09, 2023.

*The authors express their gratitude towards Covenant University Centre for Research, Innovation, and Discovery CUCRID for the assistance provided in conducting the research that resulted in this publication.

References

- Aboginije, A., Aigbavboa, C., & Thwala, W. (2021). A holistic assessment of construction and demolition waste management in the Nigerian construction projects. *Sustainability*, 13(11), 1–14.
- Adams, K. T., Osmani, M., Thorpe, T., & Thornback, J. (2017). Circular economy in construction: Current awareness, challenges and enablers. *Waste and Resource Management*, 170(1), 15–24.
- Adewuyi, T. O., & Adewuyi, T. O. (2020). Reduction potentials of material waste control construction methods on building sites in South-South, Nigeria. *International Journal of Advances in Scientific Research and Engineering*, 6(8), 100–120.
- Akanbi, L. A., Oyedele, L. O. L. O., Akinade, O. O., Ajayi, A. O., Delgado, M. D., Bilal, M., & Bello, S. A. (2018). Salvaging building materials in a circular economy: A BIM-based whole-life performance estimator. *Resources, Conservation and Recycling*, 129, 175–186.
- Akande, O., Akoh, S., Francis, B., Odekina, S., Eyigege, E., & Abdulsalam, M. (2021). Assessing the potentials of low impact materials for low energy housing provision in Nigeria. *Journal of Sustainable Construction Materials and Technologies*, 6, 156–167.
- Akhimien, N., & Latif, E. (2019). Incorporating circular economy into passive design strategies in tropical

- Nigeria. *International Journal of Engineering Management and Economics*, 13(10), 1380–1385.
- Al Hamrani, A., Kim, D., Kucukvar, M., & Onat, N. C. (2021). Circular economy application for a green stadium construction towards sustainable FIFA world cup Qatar 2022TM. In *Environmental Impact Assessment Review*, 87
- Bilal, M., Khan, K. I. A., Thaheem, M. J., & Nasir, A. R. (2020). Current state and barriers to the circular economy in the building sector: Towards a mitigation framework. *Journal of Cleaner Production*, 276,
- Cimen, O. (2021). Construction and built environment in circular economy: A comprehensive literature review. *Journal of Cleaner Production*, 305, 127180.
- Cruz Rios, F., Grau, D., & Bilec, M. (2021). Barriers and enablers to circular building design in the US: An empirical study. *Journal of Construction Engineering and Management*, 147(10).
- Dabaieh, M., Maguid, D., & El-Mahdy, D. (2021). Circularity in the new gravity—re-thinking vernacular architecture and circularity. *Sustainability*, 14(1),
- Dewagoda, K. G., Thomas Ng, S., & Kumaraswamy, M. M. (2022). Design for Circularity: The case of the building construction industry. *IOP Conference Series: Earth and Environmental Science*, 1101(6).
- Di Laurea, T., & Rivato, M. (2020). *Circular economy: limits and benefits of its implementation*. (Master dissertation). [Universita Decli Study Di Padova].
- Ellen MacArthur Foundation [EMF]. (2017). *What is a circular economy?* Retrieved From <https://ellenmacarthurfoundation.org/topics/circular-economy-introduction/overview>
- Ezema, I. C., & Maha, S. A. (2022). Energy efficiency in high-rise office buildings: An appraisal of its adoption in Lagos, Nigeria. *IOP Conference Series: Earth and Environmental Science*, 1054(1), 12037.
- Ezema, I. C., Suleman, T. A., & Okorigba, R. K. (2023). Perspective chapter on promoting circular design strategies in housing delivery in Nigeria. In A. Battisti (Ed.). *Future housing* (pp. 1–24). IntechOpen Limited.
- Ezeudu, O. B., & Ezeudu, T. S. (2019). Implementation of circular economy principles in industrial solid waste management: Case studies from a developing economy (Nigeria). *Recycling*, 4(42).
- Ezeudu, O. B., Ezeudu, T. S., Ugochukwu, U. C., Agunwamba, J. C., & Oraelosi, T. C. (2021). Enablers and barriers to implementation of circular economy in solid waste valorization: The case of urban markets in Anambra, Southeast Nigeria. *Environmental and Sustainability Indicators*, 12(100150).
- Ghisellini, P., Ripa, M., & Ulgiati, S. (2018). Exploring environmental and economic costs and benefits of a circular economy approach to the construction and demolition dector. A literature review. *Journal of Cleaner Production*, 178, 618–643.
- Guerra, B. C., & Leite, F. (2021). Circular economy in the construction industry: An overview of United States stakeholders' awareness, major challenges, and enablers. *Resources, Conservation and Recycling*, 170, 105617.
- Gupta, S. (2019). Barriers and opportunities in circular economy in the construction industry in India. *Global Research and Development Journal for Engineering*, 4(7), 22–27.
- Hart, J., Adams, K., Giesekam, J., Tingley, D. D., & Pomponi, F. (2019). Barriers and drivers in a circular economy: The case of the built environment. In Z. F., S. S.J., & S. J.W. (Eds.). *26th CIRP Life Cycle Engineering (LCE) Conference*, 80, 619–624. Elsevier.
- Hartwell, R., Macmillan, S., & Overend, M. (2021). Circular economy of façades: Real-world challenges and opportunities. *Resources, Conservation and Recycling*, 175.
- Hasheminasab, H., Zolfani, S. H., Kharrazi, M., & Streimikiene, D. (2022). Combination of sustainability and circular economy to develop a cleaner building industry. *Energy & Buildings*, 258, 111838..
- Hentges, T. I., Motta, E. A. M., de Lima Fantin, T. V., Moraes, D., Fretta, M. A., Pinto, M. F., & Boes, J. S. (2022). Circular economy in Brazilian construction industry: Current scenario, challenges and opportunities. *Waste Management and Research*, 40(6), 642–653.
- Hentges, Tatiane Isabel, Machado da Motta, E. A., Valentin de Lima Fantin, T., Moraes, D., Fretta, M. A., Pinto, M. F., & Spiering Böes, J. (2022). Circular economy in Brazilian construction industry: Current scenario, challenges and opportunities. *Waste Management and Research*, 40(6), 642–653.
- Hossain, M. S., & Khatun, M. (2021). A qualitative-based study on barriers to change from linear business model to circular economy model in built environment—Evidence from Bangladesh. *Circular Economy and Sustainability*, 1(3), 1–15.
- Kayacetin, N. C., Verdoodt, S., Leferve, L., & Versele, A. (2022). Evaluation of circular construction works during design phase: An overview of valuation tools. *Smart Innovation, Systems and Technologies*, 263, 89–100.
- Liu, Y., & Bai, Y. (2014). An exploration of firms' awareness and behavior of developing circular economy: An empirical research in China. *Resources, Conservation and Recycling*, 87, 145–152.
- Masi, D., Kumar, V., Garza-Reyes, J. A., & Godsell, J. (2018). Towards a more circular economy: exploring the awareness, practices, and barriers from a focal firm perspective. *Production Planning and Control*, 29(6), 539–550.

- Mboli, J. S., Thakker, D. K., & Mishra, J. (2020). An IoT-enabled decision Support system for circular economy business model. *Softw. Pract. Exper.*, 1–16.
- Minunno, R., O’Grady, T., Morrison, G. M., & Gruner, R. L. (2020). Exploring environmental benefits of reuse and recycle practices: A circular economy case study of a modular building. *Resources, Conservation and Recycling*, 160.
- Naneva, A. (2022). GreenBIM, a BIM-based LCA integration using a circular approach based on the example of the Swiss sustainability standard Minergie-ECO. *E3S Web of Conferences*, 349.
- Ogunmakinde, O. E. (2019). *Developing a circular-economy-based construction waste minimisation framework for Nigeria*. The University of Newcastle.
- Ogunsanwo, A., & Ayo-Balogun, A. (2020). Circular economy: A prototype for sustainable development in Nigeria. *SSRN Electronic Journal*. <http://dx.doi.org/10.2139/ssrn.3687567>
- Okafor, C., Madu, C., Ajaero, C., Ibekwe, J., & Otunomo, F. (2021). Situating coupled circular economy and energy transition in an emerging economy. *AIMS Energy*, 9(4), 651–675.
- Olanrewaju, S. D., & Ogunmakinde, O. E. (2020). Waste minimisation strategies at the design phase: Architects’ response. *Waste Management*, 118, 323–330.
- Onogwu, D. J. (2014). An essay on the transition to circular economy in Nigeria. *Toward a Media History of Documents*.
- Osobajo, O. A., Oke, A., Omotayo, T., & Obi, L. I. (2020). A systematic review of circular economy research in the construction industry. *Smart and Sustainable Built Environment*.
- Purchase, C. K., Al Zulayq, D. M., O’Brien, B. T., Kowalewski, M. J., Berenjian, A., Tarighaleslami, A. H., & Seifan, M. (2021). Circular economy of construction and demolition waste: A literature review on lessons, challenges, and benefits. *Materials*, 15(1), 76.
- Ritzen, M., Oorschot, J., Cammans, M., Segers, M., Wieland, T., Scheer, P., Creugers, B., & Abujidi, N. (2019). Circular (de)construction in the superlocal project. *IOP Conference Series: Earth and Environmental Science*, 225, 12048.
- Robson, C., & McCartan, K. (2017). *Real world research* (4th ed.).
- Sholanke, A. B., Alugah, K. D. T., Ademo, J. A., & Adisa, O. S. (2022). Impact of energy efficient design strategies on users comfort in selected mixed-use buildings in Lagos State, Nigeria. *IOP Conference Series: Earth and Environmental Science*, 1054(1), 12025.
- Tirado, R., Aublet, A., Laurenceau, S., & Habert, G. (2022). Challenges and opportunities for circular economy promotion in the building sector. *Sustainability*, 14(3), 1–17.
- Tongo, S. O., Adeboye, A. B., & Oluwatayo, A. A. (2021). Life cycle assessment of material waste generation from building construction projects in Southwest Nigeria. *IOP Conference Series: Earth and Environmental Science*, 665(1).
- Torgautov, B., Zhanabayev, A., Tleuken, A., Turkyilmaz, A., Mustafa, M., & Karaca, F. (2021). Circular economy: Challenges and opportunities in the construction sector of Kazakhstan. *Buildings*, 11(11), 1–19.
- van Bueren, B., Leenders, M., & Nordling, T. (2019). Case study: Taiwan’s pathway into a circular future for buildings. *IOP Conference Series: Earth and Environmental Science*, 225, 12060, 1–7.
- Wuni, I. Y., & Shen, G. Q. (2022). Developing critical success factors for integrating circular economy into modular construction projects in Hong Kong. *Sustainable Production and Consumption*, 29, 574–587.

Author Information

Taofeek Suleman

Covenant University,
Ogun State, Nigeria
Contact e-mail: taofeek.sulemanpgs@stu.cu.edu.ng

Isidore Ezema

Covenant University,
Ogun State, Nigeria

Peter Aderonmu

Redemer’s University
Ogun State, Nigeria

To cite this article:

Suleman, T., Ezema, I., & Aderonmu, P. (2023). Benefits of circular design adoption in the Nigerian building industry. *The Eurasia Proceedings of Science, Technology, Engineering & Mathematics (EPSTEM)*, 23, 307-315.

The Eurasia Proceedings of Science, Technology, Engineering & Mathematics (EPSTEM), 2023

Volume 23, Pages 316-331

ICRETS 2023: International Conference on Research in Engineering, Technology and Science

Improvement of Solution Using Local Search Operators on the Multi-Trip Electric Vehicle Routing Problem Backhaul with Time Window

Zelania In Haryanto

Sepuluh Nopember Institute of Technology

Niniet Indah Arvitrida

Sepuluh Nopember Institute of Technology

Abstract: In order to reduce greenhouse gas emissions, logistics companies are strongly encouraged to make their operations more environmentally friendly through efficient solutions by implementing electric vehicles (EVs). However, the driving range is one of the aspects that restricts the introduction of EVs in logistics fleets as it poses new challenges in designing distribution routes. In this regard, this paper investigates the issue of the Electric Vehicle Routing Problem (EVRP) raised by logistics companies in real time. There are many models that extend the classic VRP model to consider electric vehicles, but VRP by combining the features of capacity VRP, VRP with time window, backhaul VRP, multi-trip VRP, and electric VRP (MT-EVRPBTW) has not been worked out yet. We present a mathematical model of the MT-EVRPBTW to explain the problem in detail with the objective function to minimize the total distance travelled, where each vehicle could be charged nightly at the depot and during the day at the rest time of the driver in the depot. A feasible initial solution is built using a constructive heuristic to solve this problem, namely, the sequential insertion heuristic, which will be done by improving the solution using Local Search operators. Several Local Search processes using inter-route and intra-route operators for improvement solutions are tested and compared to their performance in measuring the impact of Local Search operator usage on overall travelled distance. Computational experiments for five Local Search operators will be presented and analyzed based on data from one of Indonesia's post and parcel companies.

Keywords: Electric vehicle routing problem, Backhauls, Multiple trips, Time window, Local search operator

Introduction

Under the 2015 Paris Agreement, Indonesia must reduce 30% of GHG emissions by 2035 (Indonesian Minister of Industry Regulation Number 27, 2020). However, Indonesia ranks fourth as the highest carbon-emitting country in the world (World Bank, 2020). The transportation sector is responsible for emitting large amounts of CO₂. Emissions generated from the transportation sector are 157,326 Gg CO₂e, with an average increase in emissions of 7.17% per year (ESDM, 2019). In addition, freight vehicle contributes to most of this emission growth. The procurement of freight vehicles continues to increase by 4.7% per year, accompanied by an increase in post and logistics services.

Reducing emissions produced by the logistics sector is important to create an environmentally friendly logistics system. Furthermore, emissions reduction can enhance the overall effectiveness and efficiency of the logistics network (Indonesian Ministry of Energy and Mineral Resources, 2019). One strategy to reduce emissions produced by the logistics sector is implementing policies to use more energy-efficient vehicles such as, electric vehicles (Aziz and Abidin, 2021). EV vehicles are considered more environmentally friendly and to have a great potential to reduce GHG emissions from transportation (Tang et al., 2022; Pan et al., 2023). In light of the growing emphasis on environmental sustainability and improved quality of life, logistics service providers in various countries have initiated fuel-switching strategies for their freight vehicles (Muñoz et al., 2019). Several leading logistics service providers have switched to electric vehicles, including FedEx, UPS, and DHL (Ehrler et al., 2021).

- This is an Open Access article distributed under the terms of the Creative Commons Attribution-Noncommercial 4.0 Unported License, permitting all non-commercial use, distribution, and reproduction in any medium, provided the original work is properly cited.

- Selection and peer-review under responsibility of the Organizing Committee of the Conference

© 2023 Published by ISRES Publishing: www.isres.org

The transition to electric vehicles in Indonesia is supported by the transformation policy that regulates battery-powered electric motor vehicles used in road transportation, as stated in Presidential Regulation No. 55 of 2019. This policy is designed to stimulate the rapid advancement of battery-based electric motor vehicles in road transportation. Its primary objectives are to enhance energy efficiency, promote energy conservation within the transportation sector, and contribute to adopting clean energy sources. Moreover, this policy aligns with Indonesia's commitment to reduce greenhouse gas emissions and fosters cleaner and more environmentally friendly air quality. However, the EV implementation in logistics service providers is facing significant mileage and recharge time limitations. Given these challenges, companies need efficient route planning techniques by considering the characteristics of electric vehicles. The routing approaches for conventional vehicles do not apply to electric vehicles, which leads to a new optimization problem called the Electric Vehicle Routing Problem (EVRP).

A basic EVRP is usually a series of routes to reach a specific destination function that serves all customer demands while considering the fulfilment of mileage restrictions and electric vehicle recharging requirements. Therefore, a real-world EVRP study that considers the operating issues of postal and parcel delivery companies in Indonesia is presented in this paper. Driven by the challenges mentioned earlier, postal and parcel delivery companies decided to change their vehicle fleet from fuel-powered vehicles to electric vehicles. In this case, a homogeneous vehicle departs from the depot to deliver the customer's package first until the vehicle's load is empty and then picks up the package. The policy can be called backhauling: all delivery operations are restricted to being carried out before the pick-up operation. The vehicle can return to the depot more than once to unload the collected package and load the parcel to be delivered. A full recharge can be performed if the service tour cannot be completed due to insufficient vehicle energy levels. However, drivers spend rest time at the depot, so the company focuses on having vehicle recharging stations used during drivers' rest periods. The goal is to minimize the overall distance travelled by vehicle. So, the problem is addressed by combining the variant VRP capacity (Toth and Vigo, 2002), VRP with time window (Braysy and Gendreau, 2007), VRP multi-trip (Taillard et al., 1996), VRP backhaul (Goetschalckx and Jacobs, 1989) and EVRP with charging station (Nolz et al., 2022).

Many studies have discussed VRP variants using electric vehicles (EVRP) before. However, to the best of the researchers' knowledge, studies discussing the merging of route problems with backhaul variants and multi-trip with time windows using electric vehicles (MT-EVRPBTW) have never been conducted. As stated by Zhang and Zhang (2022) in their research review literature, there are still few studies that discuss the MT-EVRP problem. Kucukoglu et al. (2021), in conducting a comprehensive study in which there are 136 references to variants of the Electric Vehicle Routing Problem (EVRP), two researchers were found to discuss the Electric Vehicle Routing Problem Backhaul (EVRPB), namely Echeverri et al. (2020) and Cubides et al. (2019). The EVRPB research has not considered the existence of multi trips in the depot to carry out the unloading and loading process more than once.

Since the EVRP is classified as an NP-hard combinatorial optimization problem, finding an optimal solution within a reasonable time is challenging. There have been several methods in recent years that offer potential solutions. The exact algorithms, such as branch-and bound, are recognized as the most straightforward method for deriving the optimal solution. However, due to their high computational complexity, exact algorithms are only practical for small-scale problems (Garey and Johnson, 1979). To address this limitation, the heuristic algorithms that rely on thumb, intuition, and experience are proposed as an alternative for quickly finding good solutions (Tang et al., 2023). In the last decade, many successful heuristic algorithms have been developed to solve instances of several hundred customers to near-optimal solutions within minutes of computational time (Vidal et al., 2013). Most heuristics are based on metaheuristic designs. Many authors have shown that metaheuristics have high-quality results that can be achieved with different designs (However, one component that all good heuristics for EVRP may have in common is Local Search (Arnold and Sörensen, 2019).

Local Search (LS) has been established as a successful cornerstone for addressing EVRP and is included in many advanced heuristics. This paper aims to show that a well-implemented Local Search is enough to create heuristics that compute high-quality solutions quickly. To fill the gap of the EVRP variant, this paper first adapts MT-EVRPBTW drawn from real-world cases. Then, five commonly used LS operators, namely Shift (1,0), Swap (1,1), Swap (2,2), Relocation, and Reinsert, were used to solve the MT-EVRPBTW problem to investigate the influence of five LS operators in finding promising solutions for MT-EVRPBTW.

The rest of the study is structured as follows. Section 2 provides a brief review of the pertinent literature about the EVRP. Next, Section 3 establishes a mathematical model of the problem being studied. Section 4 describes

the Local Search operators we used in this study. We define these operators with illustrations and describe the initial solution (Sequential Insertion Heuristic) used. Section 5 presents the results of tests conducted with these operators. Finally, Section 6 concludes the study and discusses future work.

Related Works

VRP was first proposed by Dantzig and Ramser (1959). Many studies have developed VRP variants for several applications. MTPVRP is one variant that extends the classic VRP by adding some restrictions. It has a set of vehicles and drivers working on several routes or trips in a certain period. MTPVRP was first introduced by Fleischmann (1990). Furthermore, MT-VRP considering the time window, was addressed in Azi, Gendreau, and Potvin (2007). They formulated it as an integer programming model with a weighted sum of two conflicting objectives, i.e., maximization of total revenue and minimization of total distance, and solved it by using branch and price. Extending from MT-VRPTW, Neiraa (2020) learned Two-Integer Programings (IP) models for multi-trip vehicle routing problems with time windows, service-dependent loading times, and limited trip duration (MTPVRPTW-SDLT). Huang (2021) introduces a multi-trip vehicle routing problem variant with a time window on urban garbage collection, where vehicles must wait in queues after the unloading capacity is filled. To complete the model, they proposed a Branch-And-Price-And-Cut Algorithm (BPC). Recently, Chena et al. (2023) investigated route planning for cold supply chain distribution of fresh food companies. They address route issues considering time windows, multiple trips per vehicle, heterogeneous fleets, parking constraints, loading and unloading times at customer positions, and limited duration to minimize associated operational costs. They formulated this problem as a Mixed-Integer Programming mode.

The VRPB is also an extension of the classical VRP. Further constraints include vehicles delivering to all the linehaul customers before visiting any backhaul customers. Koc and Laporte (2018) conducted a comprehensive literature study on VRPB, including variants of VRPB, heuristic, and metaheuristic approaches to complete VRPB applications. For example, Chavez et al. (2016) proposed a Pareto Ant Colony Algorithm to solve a multi-objective variant of Multi-Depot VRPB where the goal is to minimize distance, travel time, and energy consumption. Bajegani et al. (2021) present a mathematical model for a single depot, time-dependent vehicle routing problem with backhaul considering the First In First Out (FIFO) assumption. Their proposed Variable Neighborhood Search (VNS) meta-heuristic and mat-heuristic algorithms have been designed that were applied to the real case study in the post office of Khomeini-Shahr town, Iran, and resulted in a reduction in vehicle travel time.

However, little literature is available on the MTPVRPB, and the company needs to visit the transfer stations on multiple rounds daily for package delivery and pickup, where each round is called a batch. Ong dan Suprayogi (2011) developed the new VRP variants: VRP with backhauls, multiple trips, and time window (VRPBMTTW), that solved Ant Colony Optimization (ACO) and Sequential Insertion as the initial solution algorithm, minimizing the number of vehicles, the total duration time and the range of duration times. Wassan et al. (2017) presented the MTPVRPB with a homogenous fleet by filing ILPs for small and medium-sized instances to minimize the total cost by reducing the total distance travelled and the suitable number of vehicles used. Meanwhile, a metaheuristic VNS two-level variable neighborhood search algorithm was employed for large instances. Sethanan and Jamrus (2020) examined MTPVRPB for beverage distribution with a heterogeneous fleet that uses glass bottles for soft drinks to deliver to all customers who need soft drinks in glass bottles before making any pickups of empty glass bottles from clients to return to the Depot. This study aimed at both an integer linear programming formulation and a novel hybrid differential evolution algorithm involving a genetic operator with a fuzzy logic controller whose objective function is to minimize total cost related to distance travelled.

In recent years, there have been more and more studies on EVRP due to increasing social concern over low carbon consumption and environmental sustainability. EVRP is an expansion of VRP where the vehicles use electric vehicles. EVRP was first introduced by Conrad and Figliozzi (2011), where electric vehicles can recharge at a fixed customer location to extend their trip. Then Schneider et al. (2014) introduced EVRP with full vehicle recharging based on a linear charging function.

Research on the expansion of VRPB using electric vehicles (EVRPB) was conducted by Cubides et al. (2019), which is formulated as a mixed-integer linear programming model that considers the operation of the DN in conditions of maximum power demand. This problem is formulated by adopting a multi-objective approach where transportation and the operation of power distribution networks are modelled. The study considered recharging electric vehicle batteries at the end of linehaul or during backhaul routes. Granada et al. (2020)

examined the Electric Vehicle Routing Problem with Backhauls (EVRPB) to minimize two operating costs. The first is the total cost of the travel route used for shipping and picking up goods, and the second is the cost of the travel route to the recharging station. The solution method uses the exact method of Mixed Integer Linear Programming (MILP), which can produce solutions quickly and effectively. Nolz et al. (2022) researched EVRPB by adding time window limits for each customer and consistency of customer visit time. The recharging point is based on the end of the linehaul service route within the depot during the break time. The settlement method uses the Adaptive Large Neighborhood Search (ALNS) method in a case study at an Austrian parcel delivery company.

Research on the expansion of MT-VRP using electric vehicles (MT-EVRP) was conducted by Zhang and Zhang (2022) regarding electric buses that pick up where vehicles have more than one route. The solution to these problems used genetic algorithms with an improved recombination strategy (GA-IR). Wang et al. (2023) combined multi-trip EVRP with a heterogeneous fleet with the objective function of this study, which is to minimize the total mileage time and total fixed costs of electric vehicles by using the Hybrid LNS method using benchmark data from previous studies. Zhao and Lu (2019) combined various variants by considering time windows, heterogeneous fleets, and multi-trip (MT-EVRPHFTW). The model is applied to logistics companies in Wuhan to minimize the total cost of total mileage and recharge costs completed using the Adaptive Large Neighborhood Search (ALNS) method.

Studies that examine VRP with Multi-trip, backhaul, and time window (MT-VRPBTW) are still limited. At the same time, MT-VRPBTW, which uses electric vehicles with recharging (MT-EVRPBTW), has yet to be worked out. Therefore, this study proposes an MT-EVRPBTW that integrates EVRP with multi-trip, backhaul and time window that considers mileage with energy consumption.

Proposed Model for the EVRPB

Problem Description

In MT-EVRPBTW, the central depot has two types of customers served, namely customers with linehaul requests and customers with pick-up requests. Linehaul customers must be served first before serving backhaul customers. Vehicles can return to the depot more than once to carry out the unloading of goods and also the loading process, which is the filling of the cargo of goods. The depot is also used by drivers as a place to rest until the next departure. In the VRP variant with electric vehicles (EVRP), the vehicle requires recharging to increase driving range. Many researchers assume that electric vehicle batteries are in full state and ready for use in vehicles departing from depots at the beginning of the time horizon. Electric vehicles can recharge if the range cannot perform services during the time horizon. The location of recharging vehicle batteries used in this study is a charging depot. The level of recharge power is assumed to be constant, and this assumption has been widely used by researchers such as Zhang and Zhang (2022), Hierman et al. (2016), Wang et al. (2023), and Nolz et al. (2022).

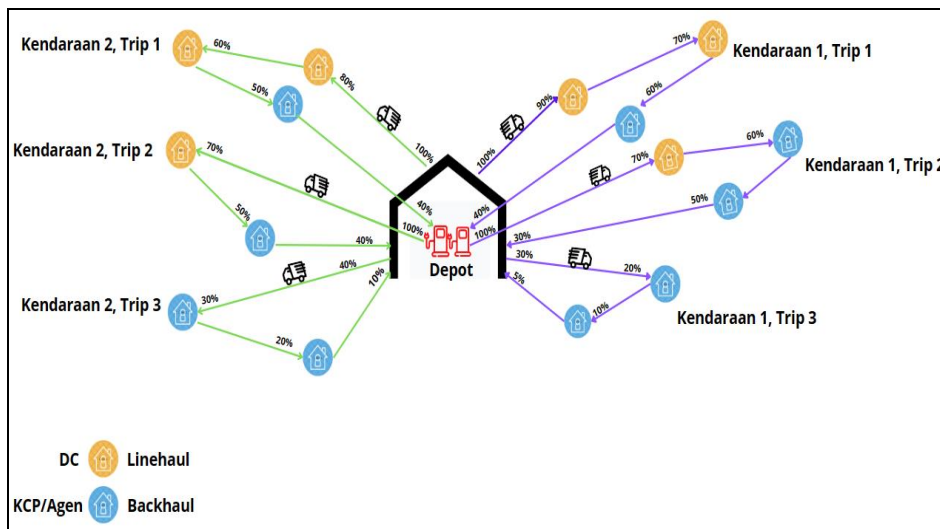


Figure 1. Illustration from MT-EVRPBTW

The strategy used in developing this research model uses a full charging strategy, with a long recharging time that is assumed to be constant. This assumption can be found in various studies such as Zhao and Lu (2019), Afroditi et al. (2014), and Erdogan and Miller (2012). The energy consumption used in this study is linear with the distance travelled. This assumption is widely used in EVRP problems by many researchers, such as Zhang and Zhang (2022), Nolz et al. (2022), Keskin and Çatay (2016), Schiffer and Walther (2017), Erdelić et al. (2019). Customers served have a time window, and vehicles are not allowed to arrive before the specified service time. An illustration of the system can be seen in Figure 1 above.

Table 1. Notation and decision variables

Notation	
I	The set of nodes, $I = V \cup C \cup \{0, n + 1\}$, V is the customer node, C the charging station, 0 the initial depot and $n + 1$ the final depot
A	Arc set $A = \{(i, j) i, j \in I, i \neq j\}$
V	The set of customers, $V = L \cup B$, where the linehaul customers $L = \{l_1, l_2, \dots, l_{n+1}\}$ and backhaul customers are $B = \{b_1, b_2, \dots, b_{n+1}\}$.
N'	The set of recharge points where refilling takes place at a depot, $N' = \{C, n + 1\}$
K	The set of electric vehiclee, $\{k_1, k_2, \dots, k_{n+1}\}$
U	The set of trips, $\{u_1, u_2, \dots, u_n\}$
a_i	The earliest time of receipt of service to customers i
b_i	The latest time of receipt of service to customers i
a_{rech}	Earliest start time of recharge
b_{rech}	The latest start time of recharge
c_{ij}	Travel time between nodes i and j
w_{ik}^u	Dwell time is the waiting time for the vehicle at the final depot on the trip u
T_{li}	Service time for customers L
T_{bi}	Service time for customers B
T_{ni}	Service time in the depot
T_{ck}^u	Electric vehicle recharging time
v_k	Time to start recharging the energy of vehicle k
w_k	The end time of recharging the energy of vehicle k
q_i	The number of requests for customers i , which i is based on the type of customer, namely L if the delivery request, and B if pick-up requests
E	Electric vehicle battery capacity
G	Recharging power level
d_{ij}	The distance between points on the arc (i, j)
pm_E	Energy consumption per kilometer
s	Vehicle speed
Q_i	Maximum capacity of vehicles for customers i
M	The value of the large constant
Decision Variables:	
x_{ijk}^u	A binary variable that has a value of 1 if the arc (i, j) is traversed by a vehicle during the trip u and a value of 0 otherwise
y_{ik}^u	A binary variable that has a value of 1 if the vehicle k visits a point i along the trip u and a value of 0 otherwise
t_{ik}^u	Time of the vehicle k when visiting points i along the trip u , $t_{ijk}^u \geq 1$
e_{ik}^u	Remaining energy of vehicle k when visiting points i on a trip u , $e_{ijk}^u \geq 1$
e_{ck}^u	Additional energy of vehicle k when recharging at a recharging station on a trip u , $e_{ijk}^u \geq 1$

In the formulation of the MT-EVRPBTW mathematical model, there is one depot and n customers that must be served. The problem can be described as a complete directed graph $G = (I, A)$, where $I = V \cup C \cup \{0, n + 1\}$. V is a node or customer point which $V = L \cup B$ consists of linehaul customers $L = \{l_1, l_2, \dots, l_{n+1}\}$ and backhaul

customers $B = \{b_1, b_2, \dots, b_{n+1}\}$. 0 is the initial depot as the departure of the vehicle to start a trip, and the final depot $n + 1$ is the place of return of the vehicle after a trip is completed. The set $N' = C \cup n + 1$ is a depot that can be used to make multi trips as well as for recharging vehicle C . The set $A = \{(i, j) | i, j \in I, i \neq j\}$ is the set of arcs.

Each customer V has a service request q_i that is not allowed to exceed the maximum capacity Q_i . Homogeneous vehicles $k \in K$ travel distances d_{ij} with as much travel time c_{ij} and have a constant speed s to make a trip $u \in U$. Service time in carrying out service activities such as loading or unloading is divided into three, namely, service time for linehaul customers amounting to T_{li} , service time for backhaul customers amounting to T_{bi} , and service time in the depot amounting to T_{ni} , assuming that the service time on each node is constant. Each customer must be served within their respective time window ranges with a start time a_i and an end time b_i . Vehicles that have finished the service in the depot but the initial time window for customers has not been opened, then the vehicle must wait inside the depot with a waiting time w_{n+1k}^u before departing again.

The vehicle has a battery capacity E with battery energy consumption per kilometer pm_E . Energy consumption is assumed to be linear with mileage. If the battery energy contained in the vehicle is insufficient to cover a route, then the vehicle needs to recharge the battery during the recharge time T_{ck}^u and with the recharge power level G . Recharging is done in the depot during rest periods that have a period $[a_{rech}, b_{rech}]$. Related notations are summarized in Table 1.

Mathematical Formulation

We propose a mathematical formulation for the MT-EVRPBTW inspired by Zhang and Zhang (2022) with their research MT-EVRPTW with the addition of the following constraints:

$$\text{Min} \sum_{(i,j) \in A} d_{ij} \sum_{k \in K} \sum_{u \in U} x_{ijk}^u \quad (1)$$

Subject to:

[Route selection constraints]

$$\sum_{j \in V \cup N'} x_{ijk}^u = \sum_{j \in 0 \cup V} x_{ijk}^u = y_{ik}^u \quad \forall i \in V, k \in K, u \in U \quad (2)$$

$$\sum_{j \in V \cup C} x_{0jk}^u = \sum_{j \in V} x_{jn+1k}^u \quad \forall k \in K, u \in U \quad (3)$$

$$\sum_{j \in V} x_{jn'}^u \leq 1 \quad \forall k \in K, u \in U \quad (4)$$

$$\sum_{k \in K} \sum_{u \in U} y_{ik}^u = 1 \quad \forall i \in V \quad (5)$$

$$\sum_{k \in K} \sum_{u \in U} y_{ik}^u \leq 1 \quad \forall i \in C \quad (6)$$

$$x_{ijk}^u = 0 \quad \forall i \in B, j \in L \quad (7)$$

$$x_{in'}^u = 0 \quad \forall i \in L \quad (8)$$

[Time constraints]

$$a_i y_{ik}^u \leq a_i y_{ik}^u \leq t_{ik}^u \leq b_i y_{ik}^u \quad \forall i \in V \cup E, k \in K, u \in U \quad (9)$$

$$t_{ik}^u + T_{li} + c_{ij} \leq t_{jk}^u + M(1 - x_{ijk}^u) \quad \forall i \in L, j \in V, k \in K, u \in U \quad (10)$$

$$t_{ik}^u + T_{bi} + c_{ij} \leq t_{jk}^u + M(1 - x_{ijk}^u) \quad \forall i \in B, j \in B, k \in K, u \in U \quad (11)$$

$$a_i y_{ik}^u \leq t_{ik}^u + T_{n0} + c_{ij} \leq t_{jk}^u + M(1 - x_{ijk}^u) \quad \forall i \in \{0\} \in V, k \in K, u \in U \quad (12)$$

$$a_i y_{ik}^u \leq t_{ik}^u + T_{bi} + c_{in+1} \leq t_{n+1k}^u + M(1 - x_{in+1k}^u) \quad \forall i \in B, k \in K, u \in U \quad (13)$$

$$t_{ik}^u \leq b_{rech} y_{ik}^u \quad \forall i \in C, k \in K, u \in U \quad (14)$$

$$a_{rech} y_{ik}^u \leq t_{ik}^{u+1} + T_{n0} \quad \forall i \in C \in K, u \in U \quad (15)$$

$$T_{ck}^u = \frac{E - e_{ik}^u}{G} \quad \forall k \in K \quad (16)$$

$$a_i y_{ik}^u \leq t_{ik}^u + T_0 + T_{cik}^u + c_{ij} \leq t_{jk}^u + M(1 - x_{ijk}^u) \quad \forall i \in C, j \in V, k \in K, u \in U \quad (17)$$

$$t_{0k}^{u+1} = t_{n+1k}^u + T_0 + w_{n+1k}^u \quad \forall k \in K, u \in U \quad (18)$$

$$t_{ck}^{u+1} = t_{ck}^u + T_0 + T_{ck}^u + w_{ck}^u \quad \forall k \in K, u \in U \quad (19)$$

$$c_{ij} = \frac{d_{ij}}{s} \quad \forall (i, j) \in A \quad (20)$$

[Remaining power and capacity constraints]

$$e_{ak}^u - d_{ij} pm_E \geq e_{jk}^u - M(1 - x_{ijk}^u) \quad \forall i \in C, j \in V, k \in K, u \in U \quad (21)$$

$$e_{ik}^u - d_{ij} pm_E \geq e_{jk}^u - M(1 - x_{ijk}^u) \quad \forall i \in V \cup \{0\}, j \in V, k \in K, u \in U \quad (22)$$

$$e_{ik}^u \geq \min\{d_{ij} pm_E + d_{jn+1} pm_E, d_{in+1} pm_E\} \quad \forall i \in V, j \in V, k \in K, u \in U \quad (23)$$

$$e_{0k}^{u+1} = e_{n+1k}^u + e_{ck}^u y_{ck}^u \quad \forall k \in K, u \in U \quad (24)$$

$$\sum_{i \in L} q_i y_{ik}^u \leq Q_i \quad \forall i \in L, k \in K, u \in U \quad (25)$$

$$\sum q_i y_{ik}^u \leq Q_i \quad \forall i \in B, k \in K, u \in U \quad (26)$$

$$x_{ijk}^u \in \{0,1\} \quad \forall i \in L, j \in L \cup B \cup C \cup \{0\}, k \in K, u \in U \quad (27)$$

$$x_{ijk}^u \in \{0,1\} \quad \forall i \in B, j \in B \cup C \cup \{0 \cup n + 1\}, k \in K, u \in U \quad (28)$$

$$y_{ik}^u \in \{0,1\} \quad \forall (i, j) \in A, k \in K, u \in U \quad (29)$$

$$e_{ck}^u \geq 0 \quad \forall i \in I, k \in K, u \in U \quad (30)$$

The objective function [1] is to minimize vehicle mileage. Constrain [2]-[3] represents flow conservation and ensures that vehicles departing from the depot are the same as vehicles arriving back at the depot. Constrain [4] This constraint indicates whether the vehicle will depart back from the final depot or not. The constraint indicates the existence of multi-trip where departure and return at the depot are possible more than once. Constrain [5] indicates that each customer must be visited exactly once by one vehicle on one trip. Constrain [6] limits recharging activities to no more than once. Constraint [7] that ensures that there is a prohibition on vehicles from visiting linehaul customers after visiting backhaul customers. Constrain [8] ensure the prohibition of vehicles from directly visiting the final depot after serving linehaul customers. Constrain [9] states the arrival time at the customer's point to be between the customer's time window intervals $[a_i, b_i]$. Constrain [10] and constrain [11] states the prohibition of the arrival of the vehicle at the customer j before the arrival time of the vehicle at the customer i has finished servicing and traveling from the customer i to the customer j . Where I for linehaul customers [10] and backhaul customers [11]. Constrain [12] states the prohibition of arrival at the customer j before a certain time $(t_{ik}^u + T_{n0} + c_{ij})$ if they travel from the depot to the customer j . Constrain [13] states the prohibition of arrival at the customer j before a certain time $(t_{ik}^u + T_{bi} + c_{in+1})$ if they travel from the

customer j backhaul to the final depot $n + 1$. The arrival of the vehicle at the recharging station must be less than the end time of recharge [14]. While the departure time of the vehicle from the recharging station must be more than the initial time of recharging plus the service time [15]. Constraint [16] calculates the recharging time assuming the battery recharging rate G is a constant. Constraint [17] states the prohibition of arrival at the customer j before a certain time $(t_{ik}^u + T_0 + T_{cik}^u + c_{ij})$ if they perform from the recharge station to the customer j . Constraint [18]-[19] states the time of route sequence, where the departure time of the next trip is equal to the arrival time of the previous trip plus the service time plus the waiting time of the vehicle [18]. While Constraint [19] states the order of route if the departure of the vehicle from the recharging station. Constraint [20] states the relationship between speed and travel time and distance traveled.

Constraint [21] ensures that the vehicle has enough battery energy to travel toward the customer after recharging at the depot recharging station. Constraint [22] ensures that the vehicle has sufficient battery energy to travel to the customer j if the vehicle departs from a depot or another customer i . Constraint [23] ensures that the remaining energy of the vehicle battery must be sufficient when visiting a customer and then directly traveling back to the depot, or the remaining energy must be sufficient when visiting other customers i before returning to the depot. Constraint [24] states that the remaining energy of the vehicle battery when departing from the depot for the next trip is the same as the remaining battery energy upon arrival at the depot on the previous trip plus the additional energy if the vehicle recharges in the depot. A value of y_{ik}^u is 1 if the vehicle recharges, and a value of 0 if the vehicle does not recharge. Constraint stating that the number of customer requests carried by a vehicle does not exceed its maximum capacity, constraint [25] for linehaul customers and [26] for backhaul customers. Constraints [27]-[30] specify the types and ranges of the decision variables.

Methodology

Local Search

Local Search (LS) is one of several common approaches to combinatorial optimization problems with empirical success (Johnson et al., 1988). Local Search is a good method for producing quality solutions in completing vehicle routing relatively quickly (Arnold and Sörensen, 2019). The basic idea underlying Local Search is to start with some feasible solution x of the problem; the neighborhood of a Local Search operator is the set of solutions $N(x)$ that can be reached from x by applying a single move of that type. To evaluate it (i.e., calculate the corresponding objective function $f(x)$ and then evaluate $f(y)$ for some feasible solution y , which is a neighborhood of x . If a neighborhood y provided that this solution is better than the current solution ($f(y) < f(x)$) is found, then select y and repeat the same procedure. If no improving solution is found in the neighborhood of the current solution, a local optimum has been reached. In some cases, Local Search provides a near-optimal or even optimal solution quickly (Smet et al., 2016). It is particularly suitable for large instances where the search space is too large to explore in a reasonable amount of time.

In the Local Search process, an operator defines the environment, which is the set of solutions that can be generated by applying the operator to a single solution. A move is a transition from one solution to another in its environment. The success of the Local Search is highly dependent on the surrounding environment and the operators used. In general, Local Search operators for VRP can be distinguished between operators for intra-route optimization and operators for inter-route optimization. These two operator types reflect the two tasks that one has to solve in a VRP: (1) the optimization is carried out on two or more than one different route (inter-route optimization), and (2) the optimization of each route in itself (intra-route optimization). In this paper, we mainly embed five common LS operators widely used for traditional VRP by taking the three intra-route operators found in the research of Subramanian et al. (2010), and two inter-route operators in the research of Silva et al. (2015). Here are some changes in the structure of the neighborhood inter-route and intra-route:

Shifts (1,0)

A node c is transferred from route 1 to route 2. In Figure 2b, node 7, which was originally on route 1, was moved to route 2. So, route 1, which originally had 5 nodes (1-2-8-9-10), had 6 nodes (1-2-7-8-9-10), and route 2, which originally had 6 nodes (6-7-11-3-4-5), had 5 nodes (6-11-3-4-5) because node 7 has been moved.

Swap (1,1)

Swap (1,1) was introduced by Boudia et al. (2007); it is a permutation between node c_1 from route 1 and node 2 from route 2. In Figure 2c, node c_2 from route 1 is swapped with node c_6 from route 2. This operation is also known as 1-1 Neighborhood Exchange.

Swap (2,2)

Swap (2,2) has almost the same move as swap (1,1) by moving 2 nodes instead of moving 1 node. The interchange between two adjacent nodes, c_1 , and c_2 , from a route 1 by another two adjacent nodes, c_3 , and c_4 , belonging to a route 2. The opposite arcs (c_2, c_1) and (c_4, c_3) are also considered, yielding 4 possible combinations (Fig 2d- Fig 2g).

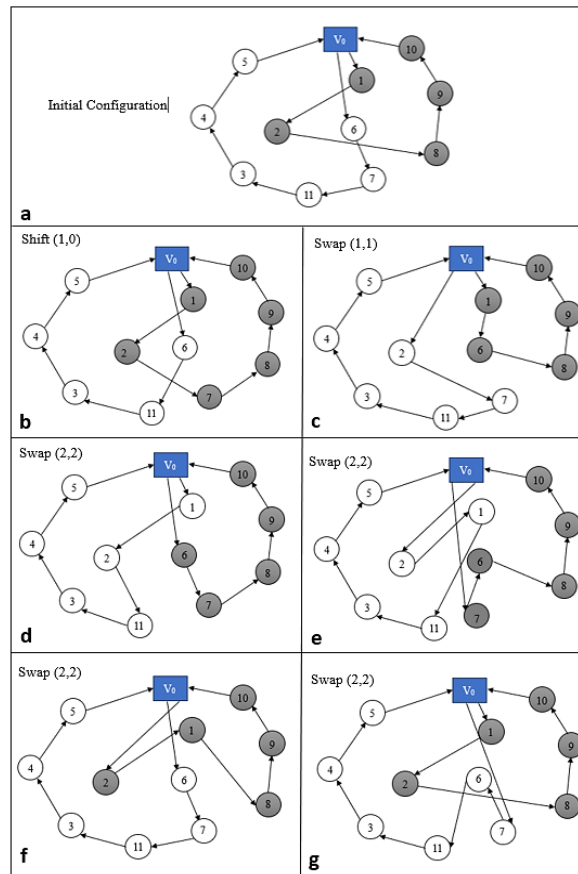


Figure 2. Inter-route neighborhoods.

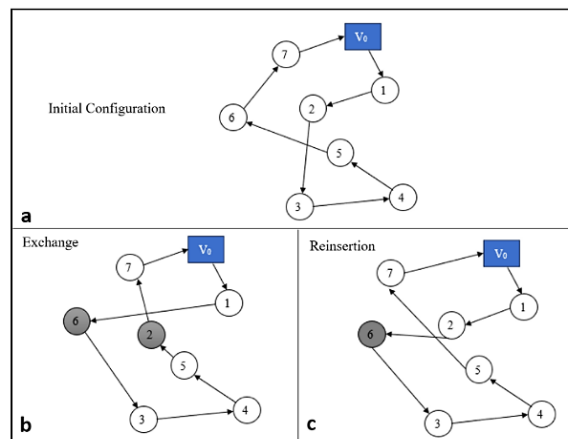


Figure 3. Intra-route neighborhoods.

In Fig. 2d, the adjacent node c6 and c7 were exchanged with the adjacent node c1 and c2. In Fig. 2e, the adjacent node c7 and c6 were exchanged with the adjacent node c2 and c1. In Fig. 2f, the adjacent node c6 and c7 were exchanged with the adjacent node c2 and c1. In Fig. 2g, the adjacent node c7 and c6 were exchanged with the adjacent node c2 and c1. In Fig. 2f, the adjacent node c7 and c6 were exchanged with the adjacent node c1 and c2. Two intra-route neighborhood structures were also implemented. Fig. 3 shows an example of each one of these neighborhood operators. The following two intra-route neighborhood structures were considered:

Exchange

Permutations between two nodes. This Exchange is shaped like Swap (1,1) but is in an intra-route version or occurs in the same route. An example of the Exchange move is shown in In Fig. 3b, that the nodes 2 and 6 were swapped. So that the sequence of nodes which was originally 1-2-3-4-5-6-7 becomes 1-6-3-4-5-2-7.

Reinsertion

One customer in the route is deleted, then the customer is reinserted into a different position on the same route. An example of the Exchange move is shown in In Fig. 3c that node 6 is deleted from the previous sequence and then moved to the sequence after node 2. So, the sequence of nodes which was originally 1-2-3-4-5-6-7 became 1-2-6-3-4-5-7.

All types of movement from the operators above must pay attention to the constraints that have been determined previously, and these constraints may not be violated for each movement. As an example of the capacity of each swap transfer (1,1), where the capacity of node 2 (q_2) from route 1 exchanged with node 6 from route 2 with capacity (q_1) cannot exceed the capacity of vehicle Q Time window limit for each customer $[a_i, b_i]$. may not be violated. The energy consumption (pm_E) at each node movement must not violate the electric vehicle battery capacity E . Rules for backhaul where nodes with shipping customers are always served first before nodes with pickup services.

Initial Solution

Based on Joubert and Claasen (2006), the heuristic algorithm is used as a problem-solving approach to obtain a feasible initial solution. It can reduce the computation time for finding a solution. In this study, the initial solution was built using the Sequential Insertion heuristic method, and then the solution was repaired using the LS operators described earlier. Solomon (1987) conducted a study by comparing several heuristic methods, concluding that the sequential insertion method provides a better output value than the other methods.

Based on Campbell and Saverbergh (2002), the basic principle of the insertion algorithm is to try to insert customers between all the arcs on the current route. The sequential insertion algorithm begins by selecting a customer point as the first customer in a route after the depot point. The first customer is called the "seed." The selection of the first customer that researchers most use is the customer with the earliest time window deadline or the customer who has the farthest distance from the depot. After the initial customer is identified and entered, the SIH algorithm considers the points not included in the route while still checking the eligibility in the route.

The sequential insertion algorithm consists of a number of work procedures to find the solution. Based on the SI algorithm used for the EVRPTW problem by Keskin and Çatay (2016), a new development is made of certain processing steps that are adapted to multi-trip conditions by recharging during breaks. Customers who will be inserted on a route will be checked for eligibility first. The eligibility in question includes the eligibility of the capacity load, the fulfilment of backhaul rules, the fulfilment of the customer's time window, and the energy charge of the battery.

The rules for determining seeds apply to all initial customer formation in each trip. After updating the information, then calculate all insertion costs that have the eligibility time window and capacity. Insertion costs are obtained from adding the distance d if insertion of customer d is carried out between customer i and customer k which can be calculated as $d_{ji} + d_{ik} - d_{jk}$. The best insertion to be included in the route is the one with the minimum additional distance. Table 2 is the sequential insertion pseudocode used for initial solution development.

Table 2. Sequential insertion heuristic pseudocode

Algorithm 1	Initial Solution construction
1	Start a new route with the customer who have the earliest time window deadline
2	<i>repeat</i>
3	Calculate insertion cost of all unserved customers to the current route
4	<i>If</i> no customer can be added because of violating the capacity of the vehicle <i>then</i>
5	Start a new trip with the unserved customer who have the earliest time window deadline
6	<i>else</i>
7	Select the customer which increases the distance least and make the insertion
8	<i>end if</i>
9	<i>If</i> no customer can be added because of violating the time window <i>then</i>
10	Start a new route with the unserved customer who have the earliest time window
11	deadline
12	<i>else</i>
13	Select the customer which increases the distance least and make the insertion
14	<i>end if</i>
15	<i>If</i> vehicle traverse lunch time <i>then</i>
16	Insert charging
17	<i>end if</i>
18	Select the customer which increases the distance least and make the insertion
19	<i>end if</i>
	<i>until</i> all customer are served

Experiments and Results

All numerical experiments were performed using a single-core Intel(R) Core(TM) i5-10500H CP machine with 2.50 GHz and 8.00 GB RAM, each running Windows 11 Home Single Language. All Local Search operators were solved using the Python 3.10 programming language, and programs are solved using PyCharm. Each run of the solution approach was carried out 10 times, and the best results were presented in the next section. The total time limit allowed for the proposed algorithm was set to 300 seconds, and the time limit allowed to complete QP and CP was set to 5 seconds.

We tested the proposed solution approach on 24 tests in attitudes derived from historical data of parcel delivery companies in Indonesia. The fleet consists of an unlimited number of identical electric vehicles with a battery capacity of 38.7kWh or a maximum range of 160 km and a cargo capacity of 750 kg for Linehaul customers and 300 for backhaul customers. The vehicle is always fully recharged with a fixed recharging time. Note that more advanced functions can be used to model the behaviour of the charging process (interested readers refer to Montoya et al. (2017) for more details on nonlinear charging functions). Travel times are given in minutes and are based on the actual road network of the focus area. Customer demand is determined by the percentage of delivery and collection, which determines the percentage of customer requests that require delivery or collection, namely 30% and 70%, respectively. The number of customers varies between 10,25,50,75,100 to 300 customers (2 in each instance) based on the recharge power (G). The recharging process relies on slow charging as it takes place at the depot, hence low-power home charging is implemented. Electricity companies in Indonesia have reported that home charging typically requires between 3 kW and 6 kW of power. Our research indicates that it takes approximately 6 hours to fully charge a vehicle from 0% to 100% using slow charging, as per data provided by car manufacturers.

Table 3 above presents an example column consisting of column "C", namely customers, and column "S", which states the charging power used, which is 3 kW and 6 kW for each number of customers. The Initial solution column is the initial feasible solution used to build routes using Sequential Insertion. Initial Solution column consists of column "Kv", which states the number of vehicles used, and the "Sol". column, which is a solution resulting from the development of the Initial solution. The number of vehicles used in the initial solution increases with the number of customers. Interestingly, vehicles that recharge with a 3 kW power source require more units compared to those that recharge with a 6 kW power source, even when the number of customers is the same. For example, if there are, If the vehicles are being charged at 3 kW power, it would require 10 vehicles to complete the charging process. However, it would take 10 vehicles to complete the charging process when recharging with 3 kW power. However, if the charging power is increased to 6 kW, only 7 vehicles would be required. This is due to the fact that the amount of energy put into the battery depends on the charging power used. If electric vehicle batteries take too long to recharge, it can cause service delays and

violate time windows for customers, which is especially crucial for parcel delivery. Similarly, the initial solution for the Sol. column indicates the completion value of the solution in terms of distance (kilometers). As more customers and vehicles are utilized, the distance increases. This is because more vehicles enable additional trips, resulting in an increase in the distance traveled to return and depart from the depot.

Table 3. Comparison among different Local Search operators

1	2			3	4			5			6			7			8		
Instance	Initial Solution			3S	Shift (1,0)			Swap (1,1)			Swap (2,2)			Relocation			Reinsert		
C	S	v	Sol.		Sol.	Gap	Sol.	Gap	Sol.	Gap	Sol.	Gap	Sol.	Gap	Sol.	Gap	Sol.	Gap	
10	3	1	51.45	40.23	42.24	41.28	40.28	0.05	41.77	1.54	47.04	6.8	40.23	0					
10	6	1	51.45	32.19	45.5	13.31	41.19	9	32.19	0	40.69	8.5	41.56	9.37					
25	3	1	116.31	95.63	111.35	15.72	102.57	6.94	95.63	0	109.28	13.65	106.89	11.26					
25	6	1	116.31	99.71	114.58	14.87	109.61	9.9	99.71	0	110.49	10.78	103.33	3.62					
50	3	2	180.55	164.76	174.76	10	166.59	1.83	167.92	3.17	170.28	5.52	164.76	0					
50	6	2	180.55	160.11	172.99	12.89	165.55	5.44	160.11	0	173.45	13.34	171.27	11.16					
75	3	3	242.34	221.87	239.34	17.47	231.06	9.19	221.87	0	230.89	9.01	231.73	9.86					
75	6	3	304.13	286.15	301.28	15.13	295.99	9.83	295.06	8.9	295.59	9.43	286.15	0					
100	3	5	592.74	576.64	585.13	8.49	577.09	0.45	583.87	7.23	589.29	12.65	576.64	0					
100	6	4	585.54	572.36	579.57	7.21	572.36	0	572.88	0.53	578.91	6.55	574.17	1.81					
125	3	5	646.35	629.04	640.22	11.18	640.9	11.86	635.25	6.21	637.47	8.44	629.04	0					
125	6	4	633.53	622.28	630.82	8.54	624.13	1.85	622.28	0	624.54	2.26	624.37	2.09					
150	3	6	770.63	755.08	766.63	11.55	756.45	0	755.08	0	758.28	3.2	759.19	4.11					
150	6	5	754.05	738.05	752.96	14.91	741.02	2.97	738.05	0	746.2	8.15	743.86	5.81					
175	3	7	921.21	906.44	915.29	8.85	906.51	0.07	912.55	6.11	915.97	9.52	906.44	0					
175	6	6	897.38	877.53	896.19	18.66	889.58	12.05	877.53	0	891.94	14.42	886.31	8.78					
200	3	9	1062.32	1048.07	1056.26	8.19	1048.07	0	1048.58	0.52	1051.62	3.56	1053.1	5.04					
200	6	7	1026.63	1008.9	1017.62	8.72	1022.35	13.45	1010.43	1.53	1021.15	12.26	1008.9	0					
225	3	9	1154.33	1138.08	1148.06	9.97	1149.44	11.36	1138.08	0	1146.07	7.99	1140.33	2.25					
225	6	7	1129.64	1115.64	1127.75	12.12	1120.28	4.65	1115.64	0	1119.52	3.88	1122.43	6.79					
250	3	10	1386.99	1371.61	1382.35	10.74	1371.61	0	1374.26	2.65	1378.5	6.9	1375.32	3.72					
250	6	8	1356.09	1344.43	1350.3	5.87	1344.43	0	1345.4	0.97	1345.59	1.16	1349.68	5.25					
300	3	11	1551.08	1534.91	1546.27	11.35	1542.46	7.54	1537.35	2.44	1544.36	9.45	1534.91	0					
300	6	8	1519.53	1507.7	1513.09	5.4	1508.39	0.69	1509.12	1.42	1511.78	4.08	1507.7	0					
Average			717.96		712.94	12.6	707	4.96	703.78	1.8	709.95	7.98	705.76	3.79					

Table 4. Run time of different Local Search operators

Instance			Run time				
C	S	Kv	Shift (1,0)	Swap (1,1)	Swap (2,2)	Relocation	Reinsert
10	3	1	10.4	39.75	28.18	26.67	35.88
10	6	1	21.06	31.08	40.33	52.9	18.53
25	3	1	45.35	47.02	70.33	82.49	80.34
25	6	1	45.59	22.3	39.64	37.35	45.1
50	3	2	50.33	36.1	53.64	30.08	29.09
50	6	2	36.99	60.66	56.36	40.01	49.78
75	3	3	159.09	145.34	164.22	162	147.76
75	6	3	190.12	171.44	186.38	189.18	171.49
100	3	5	288.16	319.77	307.303	305.19	305.43
100	6	4	309.06	153.83	176.51	190.18	182.69
125	3	5	592.46	417.33	464.8941	418.66	436.33
125	6	4	368.83	215.72	252.277	215.03	407.8
150	3	6	568.47	411.33	252.277	402.53	431.15
150	6	5	381.14	206.12	449.9006	201.93	426.37
175	3	7	642.64	485.42	564.028	470.6	606.39
175	6	6	528.5	352.4	440.4486	357.02	578.53
200	3	9	535.43	363.42	449.4251	362	732.62
200	6	7	415.44	263.95	339.6964	259.24	692.34
225	3	9	610.47	423.22	516.843	433.82	730.27
225	6	7	496.89	316.66	406.78	327.84	708.65
250	3	10	705.23	533.38	619.3081	535.31	970.73
250	6	8	510.08	350.96	430.5204	347.74	925.64
300	3	11	933.18	741.24	837.209	752.13	1126.69
300	6	8	741.37	588.52	664.9457	588.08	1093.34

The results of each operator can be found in columns 4 through 8, with column 3 designated as "BS," indicating the best result attained by any of the operators in each instance. Each operator is represented by two columns: "Sol" and "Gap." The "Sol" column displays the result produced by each operator in each instance, while the "Gap" column reveals the disparity between the "Sol" result and the value in the "BS" column. The average gap obtained can be seen in Table 5. Table 4 showcases the average duration spent looking for a solution in the run timetable. It is important to note that generating a solution takes longer when the instance size increases. For example, as seen in Table 2, it takes more time to generate a solution for 300 than 200 customers. Furthermore, the inter-route operator, which involves using the order Swap (2,2) - Swap (1,1) - Shift (1,0), takes longer than the intra-route operator that uses the Relocation-Reinsert order. Transferring neighbours between routes requires more complex combinatorial work than intra-route transfers.

Table 5 Comparison of average solutions

Component	Average Sol.	Average Gap
Initial Solution	717.96	15.99
Shift (1,0)	712.94	12.60
Swap (1,1)	707.00	4.96
Swap (2,2)	703.78	1.80
Relocation	709.95	7.98
Reinsert	705.76	3.79

Table 5 compares the results of various LS operators and shows that all of them outperformed the initial solution. This suggests that the resulting operator can enhance the obtained solution. The Swap (2,2) operator generated the most optimal solution, as indicated by the average gap in Table 5. This operator explores a larger solution space as the processing time increases. Reinsert follows Swap (2,2) and performs well because it systematically explores each node of the created environment. Swap (1,1) demonstrates a smaller gap than Reinsert and offers a better solution than Relocation, as it exchanges one node's space with another on a different route, rather than on the same route. Shift (1,0) produces a lower solution compared to other operators since moving a customer node to another route can potentially disrupt the vehicle capacity. To summarize, from the above extensive experiments, it is demonstrated that the inter-route Swap (2,2) operator is the most effective LS approach for solving MT-EVRPTW out of all five investigated LS methods.

Conclusions and Future Research

In this paper, we investigate the MT-EVRPBTW, a variation of the VRP that takes into account multiple trips, time windows, and backhaul using electric vehicles. We present a mathematical model that aims to minimize the total distance traveled. To solve the MT-EVRPBTW, we use the Sequential Insertion Heuristic to develop an initial feasible solution. We then introduce five widely used Local Search operators (LS) to further improve the solution: Inter route operators (Shift (1,0), Swap (1,1) and Swap (2,2)) and intra-route operators (Relocation and Reinsert). We compare the quality of the resulting solutions in real-world package delivery cases in Indonesia. All LS operators show good performance in generating solutions compared with the initial solution. Swap (2,2) is the most effective LS operator, followed by Reinsert and Swap (1,1), in achieving good performance in solving MT-EVRPBTW.

Based on the above investigations, we highly recommend using the above LS operator in developing new effective optimization methods for such difficult problems. Further work can be done by combining several local searches to explore the search space and obtain out of the optimum trap. Furthermore, since the MT-EVRPBTW is a new model, there is a need for extensive attention to design the addition of other VRP variants, such as heterogeneous and partial recharging schemes that consider the length of time for recharging vehicles to get closer to the real system.

Scientific Ethics Declaration

The authors declare that the scientific ethical and legal responsibility of this article published in EPSTEM journal belongs to the authors.

Acknowledgments

* This article was presented as an oral presentation at the International Conference on Research in Engineering, Technology and Science (www.icrets.net) held in Budapest/Hungary on July 06-09, 2023.

*The authors would like to thank the Center for Higher Education Fund (BPPT) and Indonesia Endowment Fund for Education (LPDP), for providing funding for this research.

References

- Aziz, A., & Abidin, M. Z. (2021). Reducing emissions and logistics cost in Indonesia: An Overview. *IOP Conference Series: Earth and Environmental Sciences*, Surakarta.
- A. Keyvanfar, A. Shafaghat, N. Z. Muhammad and M. S. Ferwati. (2018). Driving Behaviour and Sustainable Mobility-Policies and Approaches Revisited. *Sustainability*, vol. 10, no. 1152,
- Afroditi, A., Boile, M., Theofanis, S., Sdoukopoulos, E., & Margaritis, D. (2014). Electric vehicle routing problem with industry constraints: trends and insights for future research. *Transportation Research Procedia*, 3, 452-459.
- Arnold, F., & Sorensen, K. (2019). Knowledge-guided Local Search for the vehicle routing problem. *Computers & Operations Research*, 105, 32-46.
- Azi, N., Gendreau, M., & Potvin, J. Y. (2007). An exact algorithm for a single-vehicle routing problem with time windows and multiple routes. *European journal of operational research*, 178(3), 755-766.
- Bajegani, E., Mollaverdi, N., & Alinaghian, M. (2021). Time-dependent vehicle routing problem with backhaul with FIFO assumption: Variable neighborhood search and mat-heuristic variable neighborhood search algorithms. *International Journal of Industrial Engineering Computations*, 12(1), 15-36.
- Boudia, M., Louly, M. A. O., & Prins, C. (2007). A reactive GRASP and path relinking for a combined production–distribution problem. *Computers & Operations Research*, 34(11), 3402-3419.
- Bräysy, O., & Gendreau, M. (2005). Vehicle routing problem with time windows, Part I: Route construction and Local Search algorithms. *Transportation Science*, 39(1), 104-118.
- Campbell, A. M., & Savelsbergh, M. (2004). Efficient insertion heuristics for vehicle routing and scheduling problems. *Transportation science*, 38(3), 369-378.
- Chen, Y. Y., Chen, T. L., Chiu, C. C., & Wu, Y. J. (2023). A multi-trip vehicle routing problem considering time windows and limited duration under a heterogeneous fleet and parking constraints in cold supply chain logistics. *Transportation Planning and Technology*, 46(3), 335-358.
- Conrad, R. G., & Figliozzi, M. A. (2011, May). The recharging vehicle routing problem. In *Proceedings of the 2011 industrial engineering research conference*, 8. IISE Norcross, GA.
- Cubides, L. C., Arias Londoño, A., & Granada Echeverri, M. (2019). Electric vehicle routing problem with backhauls considering the location of charging stations and the operation of the electric power distribution system. *TecnoLógicas*, 22(44), 3-22.
- Dantzig, G. B., & Ramser, J. H. (1959). The truck dispatching problem. *Management Science*, 6(1), 80-91.
- Erdelic, T. & Caric, T. (2019). A survey on the electric vehicle routing problem: Variants and solution approaches. *Journal of Advanced Transportation*. Article ID 5075671 <https://doi.org/10.1155/2019/5075671>
- Ehrler, V. C., Schoder, D., & Seidel, S. (2021). Challenges and perspectives for the use of electric vehicles for last mile logistics of grocery e-commerce—findings from case studies in Germany. *Research in Transportation Economics*, 87, 100757.
- Erdoğan, S., & Miller Hooks, E. (2012). A green vehicle routing problem. *Transportation Research Part E: Logistics and Transportation Review*, 48(1), 100-114.
- Fleischmann, B. (1990). *The vehicle routing problem with multiple use of vehicles*. Fachbereich Wirtschaftswissenschaften, Universität Hamburg.
- Garey, M. R., & Johnson, D. S. (1990). A guide to the theory of np-completeness. *Computers and Intractability*, 37-79.
- Goetschalckx, M., & Jacobs Blecha, C. (1989). The vehicle routing problem with backhauls. *European Journal of Operational Research*, 42(1), 39-51.
- Granada-Echeverri, M., Cubides, L., & Bustamante, J. (2020). The electric vehicle routing problem with backhauls. *International Journal of Industrial Engineering Computations*, 11(1), 131-152.
- Hiermann, G., Puchinger, J., Ropke, S., & Hartl, R. F. (2016). The electric fleet size and mix vehicle routing problem with time windows and recharging stations. *European Journal of Operational Research*, 252(3), 995-1018.

- Huang, N., Li, J., Zhu, W., & Qin, H. (2021). The multi-trip vehicle routing problem with time windows and unloading queue at depot. *Transportation Research Part E: Logistics and Transportation Review*, 152, 102370.
- Indonesian Ministry of Energy and Mineral Resources. (2019). Inventarisasi emisi GRK bidang energi, pusat data dan teknologi *Informasi Energi dan Sumber Daya Mineral*, Jakarta Pusat,
- Johnson, D. S., Papadimitriou, C. H., & Yannakakis, M. (1988). How easy is local search?. *Journal of Computer and System Sciences*, 37(1), 79-100.
- Joubert, J. W., & Claasen, S. J. (2006). A sequential insertion heuristic for the initial solution to a constrained vehicle routing problem. *ORiON*, 22(1), 105-116.
- Keskin, M., & Çatay, B. (2016). Partial recharge strategies for the electric vehicle routing problem with time windows. *Transportation Research Part C: Emerging Technologies*, 65, 111-127.
- Koc C., & Laporte, G. (2018). Vehicle routing with backhauls: Review and research perspectives. *Computers & Operations Research*, 91, 79-91.
- Kucukoglu, I., Dewil, R., & Cattrysse, D. (2021). The electric vehicle routing problem and its variations: A literature review. *Computers & Industrial Engineering*, 161, 107650
- Muñoz-Villamizar, A., Quintero-Araújo, C. L., Montoya-Torres, J. R., & Faulin, J. (2019). Short-and mid-term evaluation of the use of electric vehicles in urban freight transport collaborative networks: a case study. *International Journal of Logistics Research and Applications*, 22(3), 229-252
- Neira, D. A., Aguayo, M. M., De la Fuente, R., & Klapp, M. A. (2020). New compact integer programming formulations for the multi-trip vehicle routing problem with time windows. *Computers & Industrial Engineering*, 144, 106399.
- Nolz, P. C., Absi, N., Feillet, D., & Seragiotto, C. (2022). The consistent electric-vehicle routing problem with backhauls and charging management. *European Journal of Operational Research*, 302(2), 700-716.
- Ong, J. O. (2011). Vehicle routing problem with backhaul, multiple trips and time window. *Jurnal Teknik Industri*, 13(1), 1-10.
- Pan, S., Yu, W., Fulton, L. M., Jung, J., Choi, Y., & Gao, H. O. (2023). Impacts of the large-scale use of passenger electric vehicles on public health in 30 US. metropolitan areas. *Renewable and Sustainable Energy Reviews*, 173, 113100.
- Pirabán-Ramírez, A., Guerrero-Rueda, W. J., & Labadie, N. (2022). The multi-trip vehicle routing problem with increasing profits for the blood transportation: An iterated local search metaheuristic. *Computers & Industrial Engineering*, 170, 108294.
- Presidential Regulation Number 55. (2019). Percepatan program kendaraan bermotor listrik berbasis baterai (battery electric vehicle) untuk transportasi jalan, Jakarta.
- Reynaud, L., Chavez, K. G., & de Cola, T. (2016, September). Quality of service for LTE public safety networks with satellite backhaul. In *2016 IEEE 27th Annual International Symposium on Personal, Indoor, and Mobile Radio Communications (PIMRC)* (pp. 1-6). IEEE.
- Schiffer, M., & Walther, G. (2017). The electric location routing problem with time windows and partial recharging. *European Journal of Operational Research*, 260(3), 995-1013.
- Schneider, M., Stenger, A., & Goeke, D. (2014). The electric vehicle-routing problem with time windows and recharging stations. *Transportation Science*, 48(4), 500-520.
- Silva, M. M., Subramanian, A., & Ochi, L. S. (2015). An iterated local search heuristic for the split delivery vehicle routing problem. *Computers & Operations Research*, 53, 234-249.
- Smet, L., Thomas, C., Deville, Y., Schaus, P., & Saint-Guillain, M. (2016). *Local search for the vehicle routing problem*. (Master thesis). Catholique de Louvain University.
- Solomon, M. M. (1987). Algorithms for the vehicle routing and scheduling problems with time window constraints. *Operations Research*, 35(2), 254-265.
- Subramanian, A., Drummond, L. M., Bentes, C., Ochi, L. S., & Farias, R. (2010). A parallel heuristic for the vehicle routing problem with simultaneous pickup and delivery. *Computers & Operations Research*, 37(11), 1899-1911.
- Sethanan, K., & Jamrus, T. (2020). Hybrid differential evolution algorithm and genetic operator for multi-trip vehicle routing problem with backhauls and heterogeneous fleet in the beverage logistics industry. *Computers & Industrial Engineering*, 146, 106571.
- Taillard, E. D., Laporte, G., & Gendreau, M. (1996). Vehicle routing with multiple use of vehicles. *Journal of the Operational Research Society*, 47(8), 1065-1070.
- Tang, M., Zhuang, W., Li, B., Liu, H., Song, Z., & Yin, G. (2023). Energy-optimal routing for electric vehicles using deep reinforcement learning with transformer. *Applied Energy*, 350, 121711.
- Tang, X., Zhou, H., Wang, F., Wang, W., & Lin, X. (2022). Longevity-conscious energy management strategy of fuel cell hybrid electric vehicle based on deep reinforcement learning. *Energy*, 238, 121593.
- Toth, P., & Vigo, D. (2002). Models, relaxations and exact approaches for the capacitated vehicle routing problem. *Discrete Applied Mathematics*, 123(1-3), 487-512.

- Vidal, T., Crainic, T. G., Gendreau, M., & Prins, C. (2013). Heuristics for multi-attribute vehicle routing problems: A survey and synthesis. *European Journal of Operational Research*, 231(1), 1-21.
- Wang, Y., Zhou, J., Sun, Y., Fan, J., Wang, Z., & Wang, H. (2023). Collaborative multidepot electric vehicle routing problem with time windows and shared charging stations. *Expert Systems with Applications*, 219, 119654.
- Wassan, N., Wassan, N., Nagy, G., & Salhi, S. (2017). The multiple trip vehicle routing problem with backhauls: Formulation and a two-level variable neighbourhood search. *Computers & Operations Research*, 78, 454-467.
- World Bank (2019). *World development indicators*. World Bank
- Zhang, J., & Zhang, X. (2022). A multi-trip electric bus routing model considering equity during short-notice evacuations. *Transportation Research Part D: Transport and Environment*, 110, 103397.
- Zhao, M., & Lu, Y. (2019). A heuristic approach for a real-world electric vehicle routing problem. *Algorithms*, 12(2), 45, <https://doi.org/10.3390/a12020045>

Author Information

Zelania In Haryanto

Institut Teknologi Sepuluh Nopember
Surabaya, 60264, Indonesia
Contact e-mail: zelainha96@gmail.com

Niniet Indah Arvitrida

Institut Teknologi Sepuluh Nopember
Surabaya, Indonesia

To cite this article:

Haryanto, Z.I. & Arvitrida, N.I. (2023). Improvement of solution using local search operators on the multi-trip electric vehicle routing problem backhaul with time window. *The Eurasia Proceedings of Science, Technology, Engineering & Mathematics (EPSTEM)*, 23, 316-331.

The Eurasia Proceedings of Science, Technology, Engineering & Mathematics (EPSTEM), 2023

Volume 23, Pages 332-337

ICRETS 2023: International Conference on Research in Engineering, Technology and Science

A Comparative Analysis of Uncertainty Assessment for Annual Yield Prediction of Citrus Growth Using FIS and ANFIS Models

Filiz Alshanableh
Near East University

Abstract: Accurate prediction of citrus fruit yield is essential for effective agricultural planning, resource allocation, and decision-making. This study aims to compare the uncertainty analysis of developed Fuzzy Inference System (FIS) and Adaptive Neuro-Fuzzy Inference System (ANFIS) models in the context of predicting the annual yield of citrus growth. To achieve this, a comprehensive dataset comprising relevant features such as climate variables, soil conditions, and historical yield records is collected. FIS and ANFIS models were constructed using average temperature, average rainfall, and average relative humidity as input parameters and annual citrus yield as output parameters for the 1980–2019 harvesting season. Out of 40 historical data sets, 35 of them were used to train the models. The last five years were utilized for testing the proposed models. The proposed FIS and ANFIS models were found to be in close agreement with their actual counterparts, i.e. R^2 values were 0.913 and 0.935 for FIS and ANFIS, respectively. To evaluate the uncertainty associated with the predictions of both models, a Monte Carlo simulation technique is employed. Preliminary results indicate that the FIS and ANFIS models exhibit promising performance in predicting the annual yield of citrus growth. However, a detailed comparison of uncertainty metrics suggests that the ANFIS model tends to provide more precise and reliable predictions, with narrower confidence intervals, than the FIS model. This could be attributed to the adaptive learning capabilities of ANFIS, allowing it to effectively capture complex nonlinear relationships between input variables and citrus yield.

Keywords: Uncertainty analysis, FIS, ANFIS, Citrus fruits yield

Introduction

The prediction of citrus fruit yield plays a crucial role in agricultural planning and decision-making processes in the Northern Cyprus economy. The citrus industry, including oranges, mandarins, clementine, grapefruit, and lemons, accounts for 40% of Northern Cyprus's total agricultural production of which Guzelyurt and Lefke districts in West Mesaria region produce almost 98 % of all citrus cultivation (TRNC, 2023). Agriculture is a significant sector of many economies, and accurate yield predictions help in economic planning. Governments and businesses can anticipate fluctuations in crop production and adjust their policies, investments, and trading strategies accordingly. Crop yield prediction allows for better management of agricultural resources. Farmers can make informed decisions about the amount of seeds, fertilizers, water, and other inputs to use, optimizing resource allocation and minimizing waste.

In recent years, fuzzy inference systems (FIS) and adaptive neuro-fuzzy inference systems (ANFIS) have emerged as powerful soft computing tools for yield prediction in various agricultural domains. In the work of Khoshnevisan et al. (2014), the ANFIS model yielded better than the artificial neural networks (ANN) model, because it implements fuzzy rules, to predict potato yield. ANFIS was also used earlier by Pankaj (2011) to predict wheat yields. Forecasting crop yields also frequently makes use of fuzzy time series. Narendra et al. (2012) forecasted wheat yield using the same methods as Sakin did in 2010, who generated fuzzy time series for the prediction of rice production. Al-Shanableh in 2022, as a part of the current study, used FIS to predict annual citrus yield grown in Northern Cyprus.

- This is an Open Access article distributed under the terms of the Creative Commons Attribution-Noncommercial 4.0 Unported License, permitting all non-commercial use, distribution, and reproduction in any medium, provided the original work is properly cited.

- Selection and peer-review under responsibility of the Organizing Committee of the Conference

© 2023 Published by ISRES Publishing: www.isres.org

This study aims to compare the uncertainty analysis associated with the annual yield prediction of citrus growth using FIS and ANFIS models. To achieve this, a comprehensive dataset comprising relevant features such as climate variables in terms of temperature, humidity, and precipitation, and historical yield records for the 1980–2019 harvesting season were collected. The FIS model is developed by defining linguistic rules based on expert knowledge and using fuzzy logic to approximate the relationships between input variables and citrus yield. On the other hand, the ANFIS model incorporates a learning algorithm to optimize fuzzy rules and adaptively adjust model parameters. By analyzing the variations in predictions across multiple Monte Carlo simulation runs, the uncertainties associated with each model were quantified.

Method

Data Collection

Historical data sets for the 1980–2019 harvesting season were gathered in order to anticipate citrus yield. The West Mesaria region's Guzelyurt area provided the majority of the data, which also included information on the overall amount of oranges collected and the weather during this time. Irrigation, weather, and soil types and conditions all have an impact on citrus tree productivity. In this study, weather conditions such as temperature, precipitation, and relative humidity were chosen as the input parameters. Table 1 lists the value range for input/output data sets within a 40-year time window.

Table 1. Input/output data sets for FIS and ANFIS modelling

	Data Description	Range
Inputs	Average temperature (°C)	17.0 - 25.0
	Average rainfall (mm)	140.0 - 600.0
	Average relative humidity (%)	55.0 – 80.0
Output	Citrus yield (kg/donum)	6,000 – 17,000

Fuzzy Logic Modelling

FIS is a soft computing technique that mimics human reasoning, allowing for the representation of uncertainty and ambiguity in the data. FIS has been used successfully to solve different nonlinear engineering problems creating a relationship between input and output parameters (Al-Shanableh et al., 2017; Al-Shanableh & Evcil, 2022). FIS modeling consists of three basic stages; fuzzification stage, fuzzy inference system (FIS), and defuzzification stage (Al-Shanableh et al., 2020).

A total of 40 historical data sets which were covering the 1980-2019 period were provided to train and test Mamdani type FIS model using MATLAB R2015a (8.5.0.197613., Mathworks Inc., Natick, USA) Fuzzy Logic Designer. Data sets consisted of average temperature, average rainfall, the average relative humidity for inputs, and actual citrus fruit yield for output. The numerical values for both input and output variables were transformed into various linguistic variables such as low, mid, and high through fuzzification. Several membership functions (MFs) such as triangular, trapezoidal, and bell-shaped were then identified along with their parameters, including the base width for each parameter. The second stage, FIS, is the core part of fuzzy logic that comprises fuzzy IF-THEN rules that link fuzzy input variables to fuzzy output variables (Mamdani, 1976). In this section 35 data sets were used to create if-then rules between the fuzzified inputs and output. The last stage called defuzzification converts fuzzy output sets back into crisp values to obtain the final prediction. Citrus yields were predicted by providing input data sets to the rule reviewer section of MATLAB Fuzzy Logic Designer (Al-Shanableh, 2022). The predicted values were compared with the actual yield values and relevant evaluation metrics, such as mean squared error (MSE) and R-squared were calculated.

ANFIS Modelling

The Adaptive Neuro-Fuzzy Inference System (ANFIS) is a powerful hybrid model that combines the strengths of fuzzy logic and neural networks to tackle complex prediction tasks (Al-Shanableh et.al., 2019). ANFIS comprises five interconnected layers as shown in Figure 1, each serving a specific purpose in the prediction process: fuzzification layer, fuzzy inference-rule layer, product layer, defuzzification layer, and overall output summation layer.

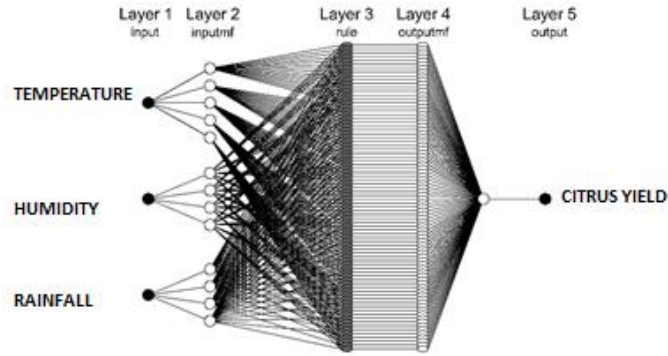


Figure 1. Structure of the ANFIS model used to predict the citrus yield

FIS model was extended by training an ANFIS model using the backpropagation algorithm with the same dataset. Prediction models for the ANFIS were generated using MATLAB R2015a (8.5.0.197613., Mathworks Inc., Natick, USA) Neuro-Fuzzy Designer. A significant number of simulations were conducted during the development of prediction models. In Neuro-Fuzzy Designer, the training and verification data sets are loaded into the workspace. Those crisp data sets were fuzzified into fuzzy linguistic variables using membership functions. Based on a predetermined number of MFs, a Sugeno-type FIS was generated using the grid partition method. The number of MF could be specified in association with each input. After FIS generated, the firing strength of each rule was divided by the sum of all rule firing strengths to obtain normalized values. The consequent parameters of the fuzzy rules were adjusted using a linear combination of the normalized firing strengths and multiplied with the function of Sugeno fuzzy rules. Next, defuzzification occurred by calculating the centroid area under MFs. A single node is used to compute the sum of all outputs in the last layer. In the end, the weighted average method results in a crisp result from the fuzzy result (Jang, 1993). The predicted values were compared with the actual yield values and relevant evaluation metrics, such as mean squared error (MSE) and R-squared were calculated.

Uncertainty Analysis of Predicted Models

The Monte Carlo simulation technique is a statistical method used to understand the uncertainty associated with a model's predictions. It involves creating a large number of random samples for each input variable, drawing from appropriate probability distributions. These random samples are then fed into the prediction model to generate a corresponding set of output values. By analyzing the variations in predictions Monte Carlo simulation were run and the uncertainties associated with each model were quantified by *d*-factor (Noori et.al., 2010). *d*-factor calculated as follow;

$$d - factor = \frac{\overline{d}_x}{\sigma_x}$$

where σ_x is the standard deviation of the measured variable X and \overline{d}_x is degree of uncertainty or the average distance between the upper and lower 95 percent prediction uncertainties. \overline{d}_x can be express as

$$\overline{d}_x = \frac{1}{k} \sum_{i=1}^k (X_U - X_L)$$

where *k* is the number of observed data points. Zero is the ideal *d*-factor value. The *d*-factor should have a value lower than 1 (Noori et.al., 2010). Larger uncertainty corresponds to a larger *d*-factor.

Results and Discussion

Proposed FIS Model

A fuzzy model was generated to predict the annual citrus fruit harvest in Northern Cyprus's Guzelyurt area. 35 historical data sets from the 1980–2014 time period were used to train the model, and 5 data sets from the 2015–

2019 time period were used to test it. The proposed FIS model was constructed by [6 4 5] trapezoidal MFs (trapmf) for input parameters which mean average temperature made up of 6 trapmf average rainfall had 4 and relative humidity had 5 trapmf. While the output layer that was citrus yield had 5 trapmf. The base width of each input/output parameter could be obtained from previous research by Al-Shanableh (2022). In FIS section 32 rules were created to train the fuzzy model and by using those rules lowest RMSE was obtained. Trained FIS was used to test for the data sets which were covered last 5 years. Citrus yields were predicted for the last 5 years and listed in Table 2. Because only training data sets were used to generate rules, the test phase results were impressive with a tighter prediction of real values.

Table 2. Predicted citrus yield for testing data sets

Year	Temp. (°C)	Rainfall (mm)	Relative Humidity (%)	Actual Citrus Yield (kg/donum)	Predicted Citrus Yield by FIS (kg/donum)	Predicted Citrus Yield by ANFIS (kg/donum)
2015	19.3	357.2	61.4	9,368	10,100	8,541
2016	19.9	282.9	58.5	7,819	8,060	6,160
2017	19.4	146.6	60.7	9,192	8,950	9,754
2018	20.1	405.8	57.2)	8,441	8,950	8,805
2019	19.7	465.4	62.6	10,736	11,000	11,876

Proposed ANFIS Model

Various input and output MF topologies with different types and numbers were used to simulate alternative models for annual citrus yield predictions. The goal was to achieve low RMSE values both in the training and verification phases. For each alternative model, the output was taken into account as constant MF, since linear MF produced high verification errors. The best conditions for both the training and verification phases were obtained for input MF using a generalized bell with grid partition FIS. Table 3 shows some alternative models generated during the trial stage. ANFIS-7 with the least error tolerance both in the training and verification phase was chosen as the predictive model. Citrus yields were predicted using generated ANFIS model for the last 5 years and listed in Table 2.

Table 3. Some simulation results for citrus yield prediction models

Model name	Type of input MF	Number of Input MF	Number of Rule	Epochs	RMSE	
					Training	Verification
ANFIS-1	gbellmf	[2 2 2]	28	610	1.9854	2.1047
ANFIS-2	gaussmf	[3 3 3]	32	410	2.9873	2.8074
ANFIS-3	gauss2mf	[3 3 3]	32	780	2.3489	2.4573
ANFIS-4	gbellmf	[3 3 3]	32	660	1.7641	2.0814
ANFIS-5	gbellmf	[4 4 4]	44	780	1.5524	1.8932
ANFIS-6	gbellmf	[5 4 4]	50	900	1.3381	2.1205
ANFIS-7 (*)	gbellmf	[5 5 4]	62	980	0.7524	1.3932
ANFIS-8	gbellmf	[5 5 5]	68	1100	0.2381	2.1205

(*) Ideal model for prediction

The prediction capabilities of the proposed FIS and ANFIS models

Figure 2 shows the prediction capabilities of the proposed FIS model together with the proposed ANFIS model. Prediction error was found to be highest for 1987 with 2273 kg/donum. Both 1993 and 2002 have relatively high prediction errors of 1216 and 2130, respectively. The reason largely depended on data sets with different input parameters but the same output value, which led to high prediction errors. On the other hand, for the ANFIS Model, the largest prediction error was obtained for 1984 with 1470 kg/donum.

R² and RMSE of the proposed FIS model for citrus yield prediction are tabulated at Table 4 along with the ANFIS model comparison. Overall R² for the ANFIS model with 0.935 showed better capability compared to the FIS model that had 0.913. When predicting unseen last five years, it was found that developed FIS predicted citrus yield with better accuracy. This can be explained, by expert knowledge that can be translated into linguistic rules effectively in FIS Modelling. If domain experts can articulate rules and membership functions to represent uncertainties and relationships between variables clearly, FIS can capture this knowledge and provide

interpretable results. ANFIS might not be able to provide similar transparency, as its structure involves neural network components, making it harder to extract explicit rules.

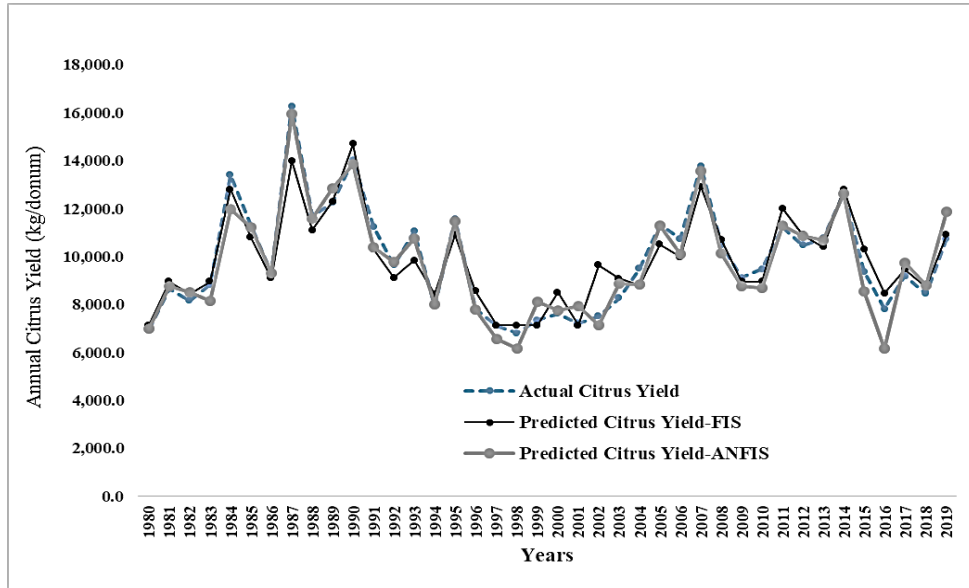


Figure 2. Comparison of citrus yield values of the proposed FIS and ANFIS models with actual counterparts

Table 4. Evaluation of statistical metrics for developed FIS and ANFIS models

Data Sets	FIS		ANFIS	
	RMSE	R ²	RMSE	R ²
Training	0.952	0.938	0.943	0.966
Verification	-	-	1.393	0.897
Testing	1.109	0.899	1.669	0.855
Overall	1.066	0.913	1.160	0.935

Uncertainty Analysis of Proposed Models

By measuring the confidence intervals of the simulation findings, uncertainty analysis of the expected annual citrus yield during the training and testing processes had been quantified. While the *d*-factor for the developed FIS Model was calculated as 0.72, for the ANFIS Model, it was found as 0.88. Both FIS and ANFIS can forecast the annual citrus yield with a *d*-factor lower than 1, which is acceptable. Uncertainty analysis revealed that the developed ANFIS Model forecasts yearly citrus yield more accurately than FIS Model.

Conclusion

This study investigates the prediction of citrus fruit yield using fuzzy inference system and adaptive neuro-fuzzy inference system. Input parameters used in FIS and ANFIS model construction were average temperature, average rainfall and average relative humidity for the 1980–2019 harvesting season. Out of 40 historical data set, 35 of them used to train FIS model. For ANFIS model construction, approximately one third of the training sets were used for verification of the model developed. The last five years were utilized for testing the proposed models and estimated citrus yield values by the proposed FIS and ANFIS models were found to be in close agreement with their actual counterparts, i.e. R² values were 0.913 and 0.935 for FIS and ANFIS, respectively. By employing the Monte Carlo simulation technique, the uncertainties associated with these models were compared. The findings shed light on the reliability, robustness, and predictive capabilities of each model in capturing the complexities and uncertainties present in citrus fruit production. This research contributes to the agricultural domain by providing insights into effective modeling techniques for yield prediction and aiding in decision-making processes for citrus growers and agricultural planners.

Further research may focus on incorporating additional environmental variables, exploring different membership functions and fuzzy rules, and applying advanced optimization techniques to improve the accuracy and reliability of yield predictions.

Scientific Ethics Declaration

The author declares that the scientific ethical and legal responsibility of this article published in EPSTEM journal belongs to the author.

Acknowledgements

* This article was presented as an oral presentation at the International Conference on Research in Engineering, Technology and Science (www.icrets.net) held in Budapest/Hungary on July 06-09, 2023.

References

- Al-Shanableh, F. (2022). Prediction of the annual yield of citrus growth in the Guzelyurt district using fuzzy inference systems. In: C. Kahraman, A.C. Tolga, S. Cevik Onar, S. Cebi, B. Oztaysi, & I.U. Sari (Eds.). *Intelligent and Fuzzy Systems*. Cham: Springer.
- Al-Shanableh, F., Bilin, M., Evcil, A., & Savas, M.A. (2023). Estimation of cold flow properties of biodiesel using ANFIS-based models, *Energy Sources, Part A: Recovery, Utilization, and Environmental Effects*, 45(2), 5440-5457.
- Al-Shanableh, F., Bilin, M., Evcil, A., Savas, M.A. (2020). a study of jojoba oil extraction based on a fuzzy logic Model. *4th International Symposium on Multidisciplinary Studies and Innovative Technologies. ISMSIT 2020 - IEEE Conferences Proceedings*.
- Al-Shanableh, F., Evcil, A., & Savas, M.A. (2017). Fuzzy logic model for prediction of cold filter plugging point of biodiesel from various feedstock. *Procedia Computer Sciences*, 120, 245–252.
- Al-Shanableh, F., & Evcil, A., (2022). Prediction of energy consumption of residential buildings in Northern Cyprus using fuzzy interference system. *Energy and Buildings*, 256, 111555.
- Jang, J.R. (1993). ANFIS: Adaptive-network-based fuzzy inference system. *IEEE Transactions on Systems, Man, and Cybernetics*, 23, 665-685.
- Khoshnevisan, B., Rafiee, S., Omid, M., & Mousazadeh, H. (2014). Prediction of potato yield based on energy inputs using multi-layer adaptive neuro-fuzzy inference system. *Measurement*, 47, 521–530.
- Mamdani, E.H. (1976). Advances in the linguistic synthesis of fuzzy controllers. *International Journal of Man-Machine Studies*, 8(6), 669–678.
- Narendra, K., Ahuja, S., Kumar, V., & Kumar, A. (2010). Fuzzy time series forecasting of wheat production. *International Journal of Computer Science and Engineering*, 2, 635–640.
- Noori, R., Hoshyaripour, G., Ashrafi, K., & Araabi, B.N. (2010). Uncertainty analysis of developed ANN and ANFIS models in prediction of carbon monoxide daily concentration. *Atmospheric Environment*, 44, 476-482.
- Pankaj, K. (2011). Crop yield forecasting by adaptive neuro fuzzy inference system. *Mathematical Theory and Modeling*, 11(1),1–7.
- Sakin, K., & Kumar, N. (2012). A novel method for rice production forecasting using fuzzy time series. *International Journal of Computer Science Issues*, 9, 455–459.
- TRNC. (n.d.). *Agriculture and natural resources ministry homepage*. <http://tarim.gov.ct.tr/tr-tr/istatistik.aspx>

Author Information

Filiz Al-Shanableh

Near East University

Nicosia, Cyprus

Contact e-mail: filiz.shanableh@neu.edu.tr

To cite this article:

Alshanableh, F. (2023). A comparative analysis of uncertainty assessment for annual yield prediction of citrus growth using FIS and ANFIS models. *The Eurasia Proceedings of Science, Technology, Engineering & Mathematics (EPSTEM)*, 23, 332-337

The Eurasia Proceedings of Science, Technology, Engineering & Mathematics (EPSTEM), 2023

Volume 23, Pages 338-348

ICRETS 2023: International Conference on Research in Engineering, Technology and Science

Single Objective Optimization of Cutting Parameters for Surface Roughness in Turning of Inconel 718 Using Taguchi Approach

Fatlume Zhujani
University of Pristina

Georgi Todorov
Technical University of Sofia

Konstantin Kamberov
Technical University of Sofia

Abstract: The majority of work in cutting machining processes is focused on choosing the parameters that will result in the greatest rate of material removal and the least amount of surface roughness, cutting temperatures, cutting pressures, vibrations, etc., which are the main quality responses. Surface roughness is one of the most precise quality criteria that affects how machined parts work. By choosing the appropriate cutting settings, it should be possible to get a greater surface finish and a longer service life for the machined parts. The link between changes in surface roughness caused by turning operations with respect to different machining settings is investigated in this study using the Taguchi method L9(3³). The orthogonal array, signal-to-noise ratio, and analysis of variance are utilized to examine the performance characteristics when turning Inconel 718 bars with CCMT09T308N-SU coated cemented carbide insert tools. The optimal setting of cutting parameters to lessen surface roughness is chosen using the Taguchi method. Speed, feed rate, and cut depth are the three cutting parameters. Experimental results are given to illustrate the effectiveness of this strategy.

Keywords: Taguchi, Turning, Inconel 718, S/N ratio.

Introduction

The aerospace and aeronautical engineering sectors predominantly use the heat-resistant nickel-based superalloy Inconel 718. Due to its peculiar mechanical and thermal properties, the material is referred to as being challenging to cut. From the past to the present, research has been done to improve the machinability of nickel-based alloys (Wassila Frifita, 2020).

The surface roughness of machined parts is a crucial product quality characteristic that pertains to the deviation from the nominal surface. The significance of surface roughness is evident in numerous applications, including but not limited to precision fits, fastener holes, aesthetic specifications, and components that are exposed to fatigue loads. The selection of cutting parameters and machine tools during the process development is significantly constrained by surface roughness, as noted in reference (Abhang & Hamedullah, 2010). The act of turning is a fundamental procedure utilized in the majority of industrial production activities. The surface finish of turned components holds significant sway over the overall quality of the final product. The surface finish during turning operations is subject to the influence of several factors, including but not limited to feed rate, work material properties, workpiece hardness, unstable built-up edge, cutting speed, depth of cut, cutting time, tool nose radius, tool cutting edge angles, machine tool and workpiece setup stability, chatter, and use of cutting fluids (Palanikumar, 2006).

- This is an Open Access article distributed under the terms of the Creative Commons Attribution-Noncommercial 4.0 Unported License, permitting all non-commercial use, distribution, and reproduction in any medium, provided the original work is properly cited.

- Selection and peer-review under responsibility of the Organizing Committee of the Conference

© 2023 Published by ISRES Publishing: www.isres.org

The evaluation of a machining operation's efficacy is often predicated on the surface finish of the machined parts, which is considered a crucial criterion. Furthermore, the surface finish is a crucial attribute that can potentially govern the functional specifications of numerous constituent parts. Components with good surface finish offer numerous advantages when compared to those with poor surface finish (Mallampati & Chittaranjan Das, 2012).

The degree of surface roughness plays a crucial role in the effectiveness and excellence of subsequent surface coatings for all materials, as stated in reference (Thomas, 2014). Among the various techniques available for preparing metal surfaces, machining is one of the most commonly employed methods due to its ability to achieve low levels of surface roughness (Benardos, 2003). For optical applications, machining can yield surface roughness values of approximately 50 nm (Guenther et al., 1984).

Optimizing machining parameters is imperative for enhancing cutting efficacy, minimizing expenses, and ensuring superior product quality. The primary focus of contemporary machining industries centers on attaining superior quality with regards to work piece dimensional accuracy and surface finish. The term "surface roughness" pertains to the minute irregularities present in the surface texture, which encompasses the feed marks produced during the machining operation (Kumar, 2013).

Typically, the selection of optimal parameters is based on the operator's expertise or design data books. However, this approach can result in decreased productivity due to suboptimal utilization of machining capabilities, leading to increased machining costs and reduced quality. Therefore, the implementation of statistical design of experiments and statistical/mathematical models is utilized to reduce both machining cost and time, as stated in reference (Raykar, 2014). The Taguchi experimental design method is a widely recognized and effective approach for enhancing the quality of products or processes. The application of this technique is prevalent in the analysis of experimental data and in the resolution of optimization problems. Taguchi has devised a factorial experimental design known as an orthogonal array, which encompasses the complete parametric space with a reduced number of experiments (Kanlayasiri & Boonmung, 2007).

Taking into account the information provided, this study may be summed up in three ways:

First, it was determined how the CNC turning of the Inconel 718 alloy with PVD AlTiSiN-coated carbide inserts affected the surface roughness and rate of material removal. For the studies, Taguchi's L9 (3³) orthogonal-array was utilized. To find the best cutting parameters (cutting speed, feed rate, and depth of cut) for the lowest surface roughness Taguchi's signal-to-noise ratio was applied. The significant cutting parameters impacting the Ra were then identified using an analysis of variance (ANOVA).

Second, using regression analysis, a linear first-order mathematical model was created to estimate the results of varying amounts of input parameters. Finally, validation experiments were carried out to confirm that the developed models were accurate.

Experimental Design and Procedure

Machining Conditions

Machine Tool

The study involved conducting experiments in a dry cutting environment using a CNC lathe machine of the GOODWAY brand, specifically the GLS-200 M model, which boasts a spindle power of 7.5 kW and a maximum spindle speed of 4000 rpm, as illustrated in (Figure 1).

Workpiece Material

The test specimen utilized for the cutting turning tests is a molded round bar of Inconel 718 alloy that has undergone hot treatment. The dimensions of the test specimen are 63.5mm in diameter and 500mm in length, with a post-treatment hardness of 411 HBW. The Inconel 718 alloy is of British origin and has been subjected to certification by Special Metals Wiggin Limited. The material has been issued a certificate of inspection bearing the number 433803 v 1, dated 28th August 2020, in accordance with the EN 10204-3.1/ISO 9001/EN/AS/JISQ

9100 standard. Table 1 displays the chemical composition of material and Table 2 displays the mechanical properties.



Figure 1. CNC Lathe Machine GLS-200 M

The specimen was partitioned into nine uniform segments, each measuring 15 mm in length and separated by a 4 mm wide and 2 mm deep slit. This was done to conduct a set of nine experiments using Taguchi's L9 orthogonal array design, with the objective of minimizing the impact of wear on the results. Prior to each test, a fresh cutting edge was employed.

Table 1. Chemical composition of Inconel 718

C	SI	MN	AL	CO	CR	FE	MO	NB	NI	TI	SE
0.03	0.06	0.07	0.49	0.25	19.3	17.3	3.3	5.28	52.9	0.96	≤3

Table 2. Mechanical properties of Inconel 718

Tensile Strength (MPa)	Yield Strength (MPa)	Young Modulus (MPa)	Density (KG/M ³)	Melting Point(°C)	Hardness (HBW)	Hardness After Heat Treated (HBW)	Thermal Conductivity (W/MK)
1197	1248	205×10 ³	819	1290	245	411	11.20

Cutting Inserts

The finish turning tests of the Inconel 718 alloy were conducted using carbide tool inserts that conform to the ISO specification CCMT09T308N-SU. These inserts were coated with the PVD ultra multi-layer thin layer AlTiSiN process, utilizing Sumitomo grade AC5005S. The tool inserts are affixed in a fixed manner to a toolholder with the designation SCLCR 2020 K89, as illustrated in Figure 2.



Figure 2. a) Toolholder SCLCR 2020 K89 – Techno Takim, b) Cutting insert CCMT 09T308N

Surface Roughness Measurement

The surface roughness of the machined surface was evaluated using the Mitutoyo 2D SJ-310 surface roughness tester in accordance with the EN-ISO 4287-1998 standards, and the arithmetic mean of the profile deviation (Ra) was determined. The experimental surface tester utilized in the study is illustrated in (Figure 3).



Figure 3. Surface roughness measurements with Mitutoyo SJ-310

Selection of Factors and Their Levels

Extensive preliminary tests were conducted on the work piece material and the inserts of the cutting tools utilized in this research. These tests established the limit values of the processing parameters, specifically the range of input variables. Table 3 displays the machining parameters that will be examined, including cutting speed, feed rate, and depth of cut, along with their respective levels.

Table 3. Machining parameters and their levels

Cutting parameters	Notation	Unit	Levels		
			1	2	3
Cutting speed	v	m/min	60	80	100
Feed rate	f	mm/rev	0.05	0.071	0.092
Depth of cut	d	mm	0.2	0.3	0.4

Experimental Design and Optimization

In the realm of experimental design, the Taguchi method is a widely recognized approach. The Taguchi design, alternatively referred to as an orthogonal array, is a method utilized for constructing experiments that generally necessitates a reduced number of total factorial combinations (C., 2021). Consequently, it is possible to assess each factor in isolation, without any impact on the evaluation of the other factors. Orthogonal arrays have the ability to reduce the number of tests considerably by minimizing the impact of uncontrollable variables. Furthermore, it provides a clear, efficient, and organized approach for determining the ideal machining parameters in the course of the production procedure. The Taguchi methodology ascertains the disparity between the actual values obtained from experiments and the target values by employing a loss function. The loss function is utilized to generate the signal-to-noise (S/N) ratio.

The signal data (S) is comprised of the intended impact on the test outcomes, while the noise data (N) encompasses the unintended impact on the test outcomes. Optimal performance is achieved when the signal-to-noise ratio is at its maximum. There exist three discrete methodologies for computing signal-to-noise ratios. The three approaches under consideration are the smaller-the-better, the nominal-is-best, and the larger-the-better.

The current investigation employed the smaller-the-better options of the signal-to-noise (S/N) quality characteristic to determine the optimal combination for achieving low surface roughness (Ra). The concept of the smaller-the-better is articulated as follows, as documented in reference (Saeheaw, 2022).

Smaller-the-better (minimize):

$$S/N_{Ra} = -10 \log \left(\frac{1}{n} \sum_{i=1}^n y_i^2 \right) \quad (1)$$

In the context of machining experiments, the variable "y_i" denotes the observed outcomes of a given machining characteristic under a specific trial condition repeated "n" times. The presence of a negative sign in Eq. (1) serve the purpose of indicating the quality characteristic of smaller-the-better.

Experimental Work

The experimental tests were conducted on the GOODWAY CNC lathe, utilizing the parameters and levels as presented in (Table 3). The workpiece model was designed in SolidWorks CAD software in 3D, and the cutting path for the tests was calculated using AZ-CAM software, employing Taguchi's experimental design. A total of nine trials were conducted using the standard orthogonal array L9 to machine the workpiece. The resulting surface finish parameter (Ra) were evaluated and recorded in Table 4.

Table 4. Coded experimental matrix layout using an L9 orthogonal array for Ra.

Exp.No.	Cutting speed (n/min)	Feed (mm/rev)	Depth of cut (mm)	Ra (μm)
1	1	1	1	0.18
2	1	2	2	0.24
3	1	3	3	0.25
4	2	1	2	0.17
5	2	2	3	0.22
6	2	3	1	0.24
7	3	1	3	0.15
8	3	2	1	0.16
9	3	3	2	0.22

Table 5. Experiment results and STN ratio for Ra

Exp. No.	Cutting speed (n/min)	Feed rate (mm/rev)	Depth of cut (mm)	Ra (μm)	S/N Ratio
1	60	0.050	0.2	0.14	17.077
2	60	0.071	0.3	0.18	14.895
3	60	0.092	0.4	0.22	13.152
4	80	0.050	0.3	0.14	17.077
5	80	0.071	0.4	0.17	15.391
6	80	0.092	0.2	0.18	14.895
7	100	0.050	0.4	0.13	17.721
8	100	0.071	0.2	0.14	17.077
9	100	0.092	0.3	0.17	15.391

The Taguchi methodology was employed to assess the surface roughness by utilizing an orthogonal array for every permutation of the experimental variables, and the signal-to-noise (S/N) ratios were utilized to optimize the process parameters. (Table 5) presents the signal-to-noise ratios that were calculated based on the experimental outcomes utilizing the equation denoted as Eq1. (1). Subsequently, the data underwent further examination to ascertain the impact of cutting parameters on surface roughness. The generation of main effect plots was carried out utilizing Minitab-18 software, as depicted in (Figure 5).

Analysis and Assessment of Experimental Results

Analysis of the Signal-to-Noise (S/N) Ratio

The analysis of process parameters, including cutting speed, feed rate, and depth of cut, was conducted using a S/N response table generated through the Taguchi technique. This can be observed in (Tables 6). The authors illustrate the signal-to-noise ratio (S/N) for every level of the control factors and its variation as the control factors settings are modified from one level to another (Basmacı, et al., 2023).

Figure 5 illustrates the relationship between surface roughness and diverse process parameters. A negative correlation was observed between cutting speeds and Ra. The observed phenomenon can be attributed to the thermal softening of the workpiece and the consequent reduction of spread materials on the machined surface, which are caused by elevated cutting temperatures in the machining zone that are directly proportional to the increase in cutting speed (Agari, 2022). Elevating the feed rate leads to an augmented Ra value. The impact of each control element's magnitude can be observed through the graphical representation of the S/N ratio effects, as illustrated in Figure 5. Specifically, the slope of the line connecting the levels provides insight into the extent of the effect.

Table 6. Response table for surface roughness (Ra)

	Control Factors					
	S/N ratio			Means		
	v	f	d	v	F	d
Level 1	15.04	17.29	16.35	0.1800	0.1367	0.1533
Level 2	15.79	15.79	15.79	0.1633	0.1633	0.1633
Level 3	16.73	14.48	15.42	0.1467	0.1900	0.1733
Delta	1.69	2.81	0.93	0.0333	0.0533	0.0200
Rank	2	1	3	2	1	3

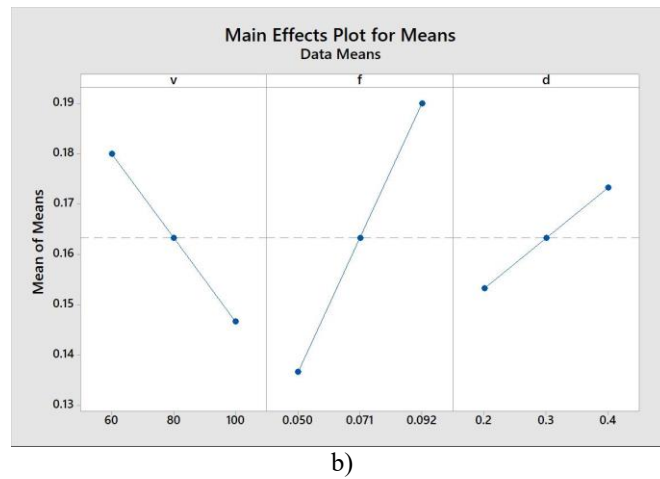
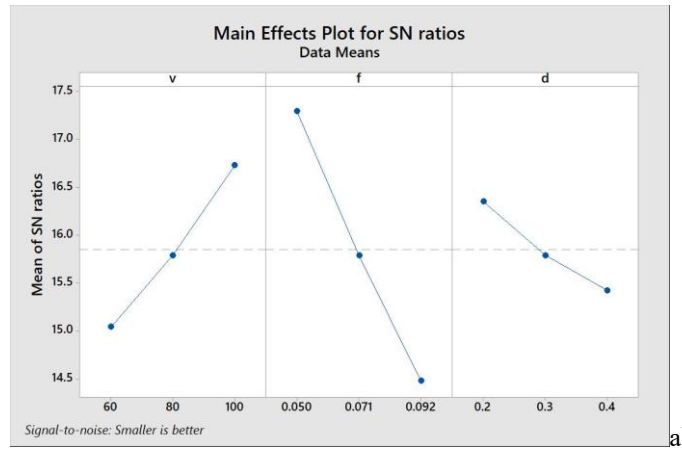


Figure 5. Main effects plot for Ra: a) for S/N ratio and b) for Means

Empirical evidence suggests that the feed rate is the most significant factor affecting surface roughness, as it holds the topmost (rank 1). In contrast, cutting speed holds a lower rank (rank 2) in terms of its impact on surface roughness. Additionally, the depth of cut holds the least influence (rank 3), as evidenced by the gentle slope of the lines.

Analysis of Variance (ANOVA)

The utilization of analysis of variance (ANOVA) is a computational technique employed to assess error variance and determine significant process parameters that have the greatest impact on performance characteristics, such as surface roughness. The ANOVA results were obtained and displayed in (Tables 7) using the statistical software Minitab 18. The Fisher's ratio, also known as the F-value, is employed in the analysis of variance (ANOVA) to ascertain the significant impact of a given parameter on the chosen surface roughness.

If the value of the calculated F-stat test is greater than the critical F- stat at $\alpha=0.05$, derived from the null hypothesis i.e. $F_{\alpha,1,2}=18.513$, a statistically significant relationship can be inferred between the factors and the

outcome variable. A probability value (P-value) below 0.05 indicates statistical significance of the parameters at a confidence level of 95%, as stated in reference (Neha Makwana, 2023).

Table 7. Analysis of variance for means of Ra

Source	DF	SS	MS	F	P	Contribution (%)
v	2	0.00167	0.00083	25.00	0.038	25.30
f	2	0.00427	0.0021	64.0	0.015	64.70
d	2	0.00060	0.0003	9.00	0.100	9.09
Error	2	0.00007	0.00035			1.06
Total	8	0.00660				100

Table 7 presents the ANOVA results, which reveal that the feed rate variable has the greatest impact on the total variance in surface roughness, explaining 64.7% of the variance. The variable of cutting speed accounts for 25.30% of the contribution, whereas the variable of depth of cut displays a comparatively lower level of significance, contributing only 9.09% to the overall variance. The calculated percentage of error for Ra was determined to be 1.06%, which suggests a noteworthy degree of precision. Upon analyzing (Table 7), it can be inferred that the P-values for the cutting speed (0.038) and feed rate (0.015) are both below the predetermined significance level of $\alpha = 0.05$, thereby indicating a confidence level of 95%.

Thus, it can be inferred that the aforementioned two factors exert a notable impact on the surface roughness. On the other hand, the statistical analysis indicates that the depth of cut is not significant, as its P-value of 0.1 exceeds the predetermined level of significance. The aforementioned discovery is consistent with the corresponding F-value of 9.0, which exhibits a lower value than the F-statistic obtained from the null hypothesis ($F_{\alpha,1,fer} = F_{0.05,1,2} = 18.513$). Based on the analysis conducted, it can be inferred that the F-critical value and P-value lead to a consistent outcome, which is the presence of a significant correlation between the dependent variables and at least two independent variables.

Development and Analysis of Regression Model

Regression analysis has been a frequently employed statistical technique in numerous scientific investigations to establish a correlation between independent variables and experimental outcomes. The Minitab 18.0 software tool was utilized to create mathematical predictive models for Ra and MRR based on cutting speed (v), feed (f), and depth of cut (d). The regression statistics for these models can be found in (Tables 8).

Table 8. Regression statistics and coefficients for linear regression of Ra

Regression statistics		Coefficients	
Multiple R	0.960373	Intercept	0.158333
R-sq	0.922316	Cutting speed	-0.00117
R-sq (adj)	0.875706	Feed rate	1.666667
Standard error	0.01354	Depth of cut	0.066667

The linear prediction equation indicated in Eq. (2) is obtained through regression statistic for Ra presented in (Table 8).

$$Ra = 0.158333 - 0.00117 * v + 1.66667 * f + 0.066667 * d \tag{2}$$

The correlation coefficient, as indicated by multiple R values, is approximately 0.96 for Ra. This indicates that the regression model that was fitted provided an explanation for over 96% of the variability observed in surface roughness.

The expected R-squared metric indicates the degree of precision with which a regression model predicts the response of new observations. Existing literature proposes that the coefficient of determination (R-squared) should fall within the range of 0.8 to 1 (Davide Chicco et al., 2021).

The coefficient of determination, denoted as R-sq, was found to be 0.92 for Ra in this study. This value indicates a strong level of significance for the proposed model.

A graphical method was employed to investigate the residual of the model. The adequacy of the models was assessed by scrutinizing the residuals. The statistical soundness of the models was evaluated through examination of specific diagnostic charts pertaining to the model.

The residuals in typical residual plots exhibit a linear pattern, indicating a uniform distribution of errors, as depicted in (Figure 6). This presents empirical support for the significance and precision of the developed model.

The coefficient of determination, denoted as R-sq, has been calculated to be 0.92 for Ra in this study. This value indicates a strong correlation and underscores the significance of the proposed model. A graphical method was employed to investigate the residual of the model. The adequacy of the models was assessed by scrutinizing the residuals. The statistical soundness of the models was evaluated through the examination of specific diagnostic charts pertaining to the model. The residuals in conventional residual plots exhibit a linear pattern, indicating that the errors are uniformly distributed, as depicted in (Figures 6). This indicates that the developed model holds significance and precision.

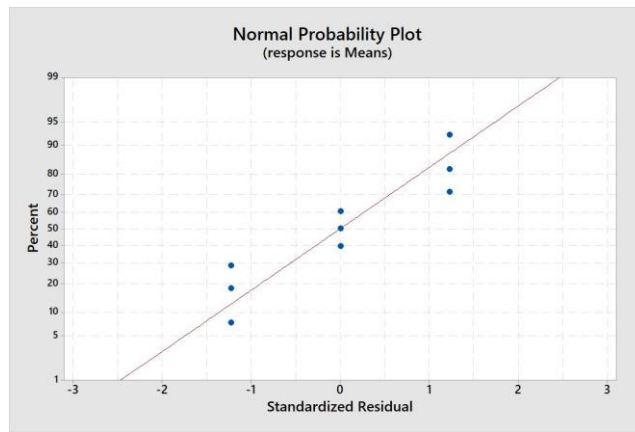


Figure 6. Normal probability charts for surface roughness

Selection of Optimum Cutting Conditions for Ra

The determination of optimal cutting conditions for improved surface quality involves the acquisition of a main effects plot for S/N ratios and mean data means through the utilization of Minitab-18 statistical software, as depicted in Figures 5a and 5b. Irrespective of the category of performance attributes being evaluated, a superior performance is always indicated by a higher signal-to-noise (S/N) ratio. Therefore, the optimal configuration for the process parameters is the configuration that produces the highest signal-to-noise ratio, as stated in reference (Qazi , 2020).

The presented graphs depict the impact of individual parameters on the signal-to-noise ratio and the slope of the line. Additionally, they illustrate the recommended cutoff parameter levels, which are identified as the highest points in Figure 5.a and the lowest points in Figure 5.b. Hence, the Taguchi method was employed to ascertain the most suitable anticipated process parameters that would result in minimal surface roughness. The determined optimal values for the parameters were $v = 100$ m/min, $f = 0.05$ mm/rev, and $d = 0.2$ mm, as highlighted in bold in response (Table 6).

The findings suggest that the most favorable amalgamation was distinguished by factor v at level 3 ($v=100$ m/min, S/N 16.73 dB, mean: 0.1467 μm), factor f at level 1 ($f=0.05$ mm/rev, S/N=17.29 dB, mean: 0.1367 μm), and factor d at level 1 ($d=0.2$ mm, S/N = 16.35 dB, and mean: 0.1533 μm). The optimal combination that has been predicted for surface roughness is denoted as ($v_3-f_1-d_1$), as illustrated in Table 9.

Table 9. Optimum conditions for surface roughness

Parameter	Notation	Ra (μm)	
		Best level	Value
Cutting speed (m/min)	V	3	100
Feed rate (mm/rev)	F	1	0.05
Depth of cut (mm)	D	1	0.2

Estimation of Optimum Surface Roughness

In the final stage of the Taguchi method, it is necessary to perform a verification experiment in order to validate the precision of the optimization. The experiment for verification was conducted using the optimal levels of the variables that were selected, as presented in Table 6. Consequently, based on the information presented in the (Table 6), the most favorable mean value for quality attributes, specifically surface roughness, is determined to be $(v_3-f_1-d_1)$, as seen in Eq.3.

$$Ra_{popt} = \overline{P_{Ra}} + (\overline{V_3} - \overline{P_{Ra}}) + (\overline{F_1} - \overline{P_{Ra}}) + (\overline{D_1} - \overline{P_{Ra}}) \quad (3)$$

where the variable P_{Ra} represents the mean value of performance attributes, specifically surface roughness, as indicated by all the L9 measurements in (Table 5). The acronym " Ra_{popt} " denotes the anticipated average of the surface roughness rate when subjected to ideal conditions. Meanwhile, the values denoted by " $(\overline{V_3}-\overline{F_1}-\overline{D_1})$ " represent the mean surface roughness values obtained when the process parameters are set to their optimal levels, as presented in Table 6.

The response averages have been computed and the resulting values are presented below. The surface roughness values for P, V3, F1, and D1 are 0.1634 μm , 0.1467 μm , 0.1367 μm , and 0.1533 μm , respectively. Upon incorporation of the aforementioned values into Equation (3), it is projected that the average optimal magnitude of surface roughness will manifest as $Ra_{popt}=0.1099 \mu\text{m}$.

The confidence interval (CI_{Ra}) was determined for the estimated surface roughness through the utilization of Eqs. (4) and (5) as stated by reference (Dvivedi & Kumar, 2007).

$$Cl = \sqrt{F_{\alpha,1,fer} \cdot V_{er} \cdot \left(\frac{1}{n_{eff}} + \frac{1}{R}\right)} \quad (4)$$

$$n_{eff} = \frac{N}{1+T_{dof}} \quad (5)$$

The equation denoted as (4) provides the F ratio at a confidence level of 95%, where the variables α , f_{er} , V_{er} , R , and n_{eff} represent the significance level, degree of freedom of the error, error variance, number of replications for the verification test, and effective number of replications, respectively. The equation denoted as (5) expresses T_{dof} as the aggregate primary factor of the degree of freedom, while N represents the overall quantity of tests conducted. The F-test table indicates that the value of $F_{\alpha,1,2}$ is 18.513. Moreover, as presented in (Table 7), the value of V_{erRa} is 0.00035, while the parameters R , N , and T_{dof} are 3, 9, and 6, respectively. Applying Equation (5), the resulting value of n_{eff} is 1.285. The confidence interval (CI_{Ra}) was computed as ± 0.08484987 using equations (4) and (5).

At a confidence level of 95%, the anticipated mean optimal surface roughness is as stated below:

$$[Ra_{popt} - CI_{Ra}] < [Ra_{opt} < [Ra_{popt} + CI_{Ra}], \text{ i.e.}; [0.1099- 0.08484987] < Ra_{exp} < [0.1099+ 0.08484987]= 0.025 < Ra_{exp} < 0.1947.$$

The Ra_{exp} value derived from the confirmatory trial, as presented in Table 10, falls within the confines of the confidence interval. The Taguchi method was effectively employed to optimize the system at a significance level of 0.05 during the turning of Inconel 718 alloy under varying cutting conditions.

Experimental Validation

Confirmation testing was conducted on the process parameters at optimal and random levels for the Taguchi technique and regression equations. (Table 10) displays the comparison between the test results and the anticipated values obtained through the Taguchi method and regression equation (Eq. 2). The observed outcomes and the anticipated values exhibit a high degree of similarity. According to reference (Columb, & Atkinson, 2016), statistical analysis can only be deemed reliable if the error values remain below 20%.

Hence, the success of this optimization can be deemed valid, as substantiated by the outcomes of the verification tests.

Table 10. Conformation results for Taguchi method and linear regression

Level	Taguchi method			Linear regression		
	EXp	Pred.	Error (%)	EXp	Pred.	Error (%)
$v_3f_1d_1$ (Optimum)	0.12	0.11	8.33	0.12	0.1383	15.25
$v_2f_2d_2$ (Random)	0.18	0.163	9.44		0,20	11.11
$v_1f_2d_3$	0.19	0.18	5.26		0.23	21

Conclusion

The current study utilized the Taguchi methodology to determine the most effective machining parameters for the turning process of Inconel 718 alloy, utilizing *CCMT09T308N-SU* PVD coated carbide inserts in the absence of any cutting fluid. ANOVA was utilized to perform statistical analysis on the experimental results. It is conceivable to deduce the ensuing inferences:

The investigation ascertained the most advantageous degrees of control variables with the aim of reducing surface roughness and enhancing material removal rate, employing signal-to-noise ratios. The study determined that the optimal conditions for achieving favorable surface roughness results were determined to be at $v_3f_1d_1$, which corresponds to a cutting speed of 100 mm/min, a feed rate of 0.05 mm/rev, and a depth of cut of 0.2 mm.

The statistical analysis indicated that the feed rate exhibited the most significant level of importance in terms of surface roughness, explaining 64.70% of the variability. The multiple R values obtained have an approximate value of 0.96. The aforementioned results suggest that the fitted regression model exhibited a high level of explanatory capability, with a percentage exceeding 96%, in relation to the surface roughness.

The results suggest that the Taguchi methodology is a reliable technique for reducing machining duration and manufacturing costs in the computer numerical control (CNC) turning procedure of Inconel 718 alloy.

Recommendations

In order to enhance the machinability of Inconel 718 alloy material in CNC turning machines and to place particular emphasis on the quality of the machined surface, the present investigation may be extended in the following manner:

- Additional research can be conducted by incorporating a greater quantity of process parameters and responses.
- The experimentation process can be enhanced by increasing the spindle speed and utilizing diverse cutting tool inserts and conditions.

Furthermore, it is recommended that future research endeavors focus on exploring alternative prediction models for mathematical optimization models of machinability characteristics' cutting parameters, such as second-order and higher-degree models.

Scientific Ethics Declaration

The authors declare that the scientific ethical and legal responsibility of this article published in EPSTEM journal belongs to the authors.

Acknowledgements or Notes

* This article was presented as an oral presentation at the International Conference on Research in Engineering, Technology and Science (www.icrets.net) held in Budapest/Hungary on July 06-09, 2023.

References

- Abhang L.B., & Hamedullah, M. (2010). Chip-tool interface temperature prediction model for turning process. *International Journal of Engineering Science and Technology*, 2(4), 382-393.
- Agari, S. R. (2022). Wear and surface characteristics on tool performance with CVD coating of Al₂O₃/TiCN inserts during machining of Inconel 718 alloys. *Archive of Mechanical Engineering*, 69(1), 59-75.
- Basmacı, G., Kayacan, M. Y., Ay, M., & Etyemez, A. (2023). Optimization of cutting forces and surface roughness via ANOVA and grey relational analysis in machining of In718. *Open Chemistry*, 21(1).
- Benardos, P., & Vosniakos, G. C. (2003). Predicting surface roughness in machining - review. *International Journal of Machine Tools and Manufacture*, 43(8), 833-844.
- Columb, M. O., & Atkinson, M. S. (2016). Statistical analysis: sample size and power estimations. *BJA Education*, 16(5), 159-161.
- Davide Chicco, M. J., Warrens, M. J., & Jurman, G. (2021). The coefficient of determination R-squared is more informative than SMAPE, MAE, MAPE, MSE and RMSE in regression analysis evaluation. *PeerJ Comput Science*, 7. e623.
- Dvivedi, A., & Kumar, P. (2007). Surface quality evolution in ultrasonic drilling through the Taguchi techniques. *The International Journal of Advanced Manufacturing Technology*, 34, 131-140.
- Guenther, K. H., Wierer, P. G., & Bennett, J. M. (1984). Surface roughness measurements of low-scatter mirrors and roughness standards. *Applied Optics*, 23(21).
- Hamzacebi, C. (2021). Taguchi method as a robust design tool . *Intelligent Manufacturing, Robust Design and Charts*, 1-19.
- Kanlayasiri, K & Boonmung, S. (2007). Effects of wire- EDM machining variables on surface roughness of newly developed DC 53 die steel: Design of experiments and regression model. *Journal of Materials Processing Technology*, 192, 459-464
- Kumar, U., & Narang, D. (2013). Optimization of cutting parameters in high speed turning by grey relational analysis. *Business, Materials Science*, 3(1), 832-839.
- Mallampati, M., & Chittaranjan Das, V. D. (2012). Optimization of cutting parameters as speed, feed & depth of cut based on surface roughness in turning process using genetic algorithm (Ga) and particle swarm Optimization (pso). *International Journal of Engineering Research & Technology (IJERT)*, 1(7). 1-11.
- Neha Makwana, A. K. (2023). Optimisation of cutting parameters by using Annova method. *Journal of Emerging Technologies and Innovative Research (JETIR)*, 10(5), d748-d760.
- Palanikumar, L. K. (2006). Assessment of factors influencing surface roughness on the machining of glass – reinforced polymer composites. *Materials & Design*, 27(10), 862-871.
- Qazi M., R. , Akhtar, R., Abas, M., Khalid, Q.S., Babar, A. R., & Pruncu, C. I. (2020). An integrated approach of GRA coupled with principal component analysis for multi-optimization of shielded metal arc welding (smaw) process. *Materials*, 13(16), 3457.
- Raykar, S., & D'Addona, D. M. (2014). Analysis of surface topology in dry machining of EN-8 steel. *Procedia Material Science*, 6, 931-938
- Saeheaw, T. (2022). Application of integrated CRITIC and GRA-based Taguchi method for multiple quality characteristics optimization in laser-welded blanks. *Heliyon*, 8(11). <https://doi.org/10.1016/j.heliyon.2022.e11349>
- Thomas, T. (2014). Roughness and function. *Surface Topography. Metrology and Properties*. 2(1), 014001
- Wassila Frifita, S. B. (2020). Optimization of machining parameters in turning of Inconel 718 Nickel-base super alloy. *Mechanics & Industry* 21(2), 203.

Author Information

Fatlume Zhujani

University of Pristina
Street Agim Ramadani, Kosovo
Contact e-mail: Fatlume.zhujani@uni-pr.edu

Georgi Todorov

Technical University of Sofia
Sofia 1000, 8 Kl. Ohridski Blvd, Bulgaria

Konstantin Kamberov

Technical University of Sofia
Sofia 1000, 8 Kl. Ohridski Blvd, Bulgaria

To cite this article:

Zhujani, F. & Todorov, G. & Kamberov, K. (2023) Single Objective Optimization of Cutting Parameters for Surface Roughness in Turning of Inconel 718 Using Taguchi Approach. *The Eurasia Proceedings of Science, Technology, Engineering & Mathematics (EPSTEM)*, 23, 338-348

The Eurasia Proceedings of Science, Technology, Engineering & Mathematics (EPSTEM), 2023

Volume 23, Pages 349-360

ICRETS 2023: International Conference on Research in Engineering, Technology and Science

Technological Trend Analysis for Surgical Operation Duration Estimation

Ziya Karakaya

Konya Food and Agriculture University,

Bahadır Tatar

ARD Group Information Technologies Inc.

Abstract: Surgical procedures are complex in nature and operative time is subject to variability influenced by many factors. Accurate estimation of the surgical operation duration not only helps to maximize Operation rooms' efficiency, but also helps to optimize hospital resources which are a crucial factor in planning surgical procedures. In this regard, AI techniques such as machine learning and deep learning promise to significantly improve the duration estimation by identifying hidden factors and make more accurate prediction. They achieve this success by identifying latent factors which are generally hard to be explored by human intelligence. Eventually, accuracy in time estimation added to a good scheduling optimization leads to make more efficient utilization of hospital resources by better aligning Operation Room, relevant equipment, and human resources. This study addresses the recent trends in research on surgical operations duration estimation, considering the relevant factors.

Keywords: Surgical procedure duration, Time estimation, Operating room scheduling, Operation room optimization, Scheduling

Introduction

The duration of a surgery is expressed in terms of the time a patient spends in the operating room, regardless of whether the operation has started or not (Wang et al., 2021). In the literature, studies on the prediction of surgery duration have shown that the target parameter, the surgery duration, depends on various factors such as the type of surgery, the performing surgeon's experience, and the surgical team's proficiency (Wang et al., 2021, Rath et al., 2021). These factors can either reduce the surgery duration compared to the predicted time or extend it further.

Although studies focusing on predicting surgery durations hold a significant and popular place in medical literature, this process is complex and challenging to implement. Surgery procedures inherently possess a multi-layered and variable structure, leading to different approaches in the literature regarding this subject. When studies and applied methods on operating room planning and scheduling in the medical literature are examined on a daily, weekly, and yearly basis, a continuous process of method improvement is observed. Hospitals' approaches to surgery-time management involve not only online and offline planning but also strategic and tactical planning.

Due to the performance of various types of surgeries in operating rooms, harmonious long-term planning can be established among different surgical groups on a yearly basis. Additionally, medium-term planning on a weekly level can also be applied. Another method is to plan the surgeries of non-urgent patients within a predetermined date range (Kroer et al., 2018). In this approach, the surgery dates of patients can be planned according to specific rules or based on surgical priorities. The aim is to optimize the utilization of available resources in the

- This is an Open Access article distributed under the terms of the Creative Commons Attribution-Noncommercial 4.0 Unported License, permitting all non-commercial use, distribution, and reproduction in any medium, provided the original work is properly cited.

- Selection and peer-review under responsibility of the Organizing Committee of the Conference

© 2023 Published by ISRES Publishing: www.isres.org

healthcare facility where the operation will take place, ensuring that the needs and productivity of healthcare professionals are not compromised by avoiding unfavorable conditions.

In addition to this method, there is an approach focusing on the analysis and control of a planned surgery during its operational process. At this level, the emphasis is on anticipating and providing responses to unforeseen circumstances that may arise during the planned procedure to ensure the smooth progression of subsequent operations. Controlling the pre-operative and post-operative needs of patients, preparing the equipment to be used during the surgery, managing the participation of healthcare workers in the surgery, and organizing the operating room for the surgical procedure are crucial at this level (Erwin et al., 2012).

Literature Review

Various studies in the literature focus on resource optimization in surgical processes. Researchers often concentrate on mathematical modeling at this point. Decisions that need to be made in accordance with varying needs, depending on the problem definition, are modeled to yield the outcome of the decision. The complexity imposed by operating room conditions has prompted researchers to develop different methods to achieve better results.

In the study conducted by Master et al. (2016) various prediction models for Surgical Duration Estimation were investigated, each offering different levels of automation and utilization of input from surgeons. Some models provided automated predictions, leveraging features available in electronic records without the need for additional input from surgeons. On the other hand, semi-automated models utilized electronic record features but also incorporated valuable insights from surgeons. Most particularly, tree-based prediction methods, such as decision tree regressor, adaptively boosted regression trees, and random forest regressor were employed in the analysis. The dataset encompassed 4475 distinct procedures, serving as a substantial foundation for the model training process. Post-training, it was evident that the random forest regressor and adaptively boosted regression trees exhibited superior accuracy among the evaluated methods.

Contrary to findings in the existing medical literature, the study's models showcased remarkable performance, outperforming currently used algorithms and, in certain instances, even rivaling human experts in Surgical Duration Estimation. These findings signify the potential of their proposed models to enhance surgical duration prediction practices, paving the way for more effective and informed decision-making in medical settings.

Surgery durations have been attempted to be predicted using statistical methods such as standard deviation and coefficient of variation, as well as machine learning-based approaches, which have also started to be preferred by researchers (Fairley et al., 2019). Predictions based on patients' past hospital records and the professional experience of the performing surgeon play a significant role in statistically estimating surgery duration. Data from all types of factors that are believed to influence surgery duration are collected and interpreted with a statistical distribution as part of the prediction approaches. In particular, the Log-Normal Distribution (Zhang et al., 2020) and Empirical Distribution (Cappanera et al., 2014) are among the most popular methods in the literature. Surgical operation durations, which have multi-factorial uncertainty, can be better comprehended, and more effectively channeled into real-life problems with the help of uncertainty sets.

Method

In this study, systematic mapping (Petersen et al., 2015) has been conducted by compiling the existing surgical duration estimation papers in the literature along with the methods used in these papers and their respective results. This section summarizes the systematic mapping study conducted in the field of Surgical Operation Duration Estimation. As a result of the publication searches carried out in the popular databases mentioned in Table 1, a total of 351 candidate articles were identified in the Surgical Operation Duration Estimation domain. These candidate articles were meticulously evaluated based on the inclusion and exclusion criteria provided in Table 2 and Table 3. Consequently, following the evaluation process, 24 final articles were selected, and the research continued with these articles.

During the systematic mapping study, the following search string was employed:

((“surgical duration” OR “surgery time”) AND (“estimation” OR “prediction” OR “forecasting”)).

This search string aimed to ensure the efficiency and comprehensiveness of the research. Focusing on studies related to the prediction of surgical durations, it facilitated the identification of potentially relevant articles. The results obtained in this study are intended to serve as an important resource for understanding the current state of research in the Surgical Operation Duration Estimation domain and identifying potential areas of opportunity for future research.

Table 1. Database sources

Literature Database	Direct Link
Science Direct	https://www.sciencedirect.com/
IEEE Xplore	https://ieeexplore.ieee.org/
Springer Link	https://link.springer.com/
Pubmed	https://www.ncbi.nlm.nih.gov/pmc/
Google Scholar	https://scholar.google.com/

Table 2. Inclusion criteria of the systematic mapping

Inclusion criteria
The publications directly related to surgical duration estimation are included.
The publications containing the utilized methods, evaluation metrics, and results are included.
The publications available as full text in the literature are included.

Table 3. Exclusion criteria of the systematic mapping

Exclusion criteria
Publications not directly related to surgical duration estimation have been excluded.
Publications that are not written in the English language have been excluded.
Publications that are not in the form of academic journals or conference papers in the literature have been excluded.

The following research questions are considered to shed light on significant topics related to Surgical Duration Estimation:

RQ1) How frequently are machine learning, deep learning, and statistics-based methods used in the studies conducted in the field of surgical duration estimation?

RQ2) What evaluation metrics are preferred by researchers in the literature to assess the reliability of the employed methods?

RQ3) After applying inclusion and exclusion criteria, in which years was an increasing trend observed in the number of studies conducted in the field of Surgical Duration Estimation?

Data Creation

After the systematic mapping process, a total of 24 final papers were selected and subjected to a detailed data extraction procedure. During the data extraction phase, comprehensive information was retrieved from each paper, encompassing the author's details, publication years, employed methodologies, descriptions of the utilized datasets, and, finally, the reported results. The extracted data from all the papers have been compiled and presented in Table 4.

The data extraction phase is a crucial step in the research process, as it allows for the synthesis and organization of relevant information from the selected papers. By meticulously extracting and collating key details, Table 4 provides a comprehensive overview of the literature on Surgical Duration Estimation. The extracted data serves as a valuable resource for gaining insights into the research landscape, identifying prevailing trends, and discerning the various methodologies employed by researchers in the field.

Moreover, the extracted results provide a clear representation of the findings reported in the literature, enabling further analysis and comparison among the studies. This compiled information will aid in shaping a comprehensive understanding of the advancements made in Surgical Duration Estimation research and contribute to the identification of potential research gaps and opportunities for further investigations in the domain.

Table 4. Extracted data of the 24 main papers from the systematic mapping results.

Study	Year	Method	Data Detail	Results
Hinterwimmer et al.	2023	Extreme Gradient Boosting (XGBoost) Algorithm	864 cases were collected at Klinikum rechts der Isar (Munich) from 2016 to 2019	Accuracy of 92.0%, Sensitivity of 34.8%, Specificity of 95.8%, and Area Under the ROC Curve (AUC) of 78.0%
Gabriel et al.	2023	Multivariable Linear Regression (MLP), Random Forest (RF), Bagging, and Extreme Gradient Boosting (XGBoost)	A total of 3189 surgeries were examined	XGBoost performed best scores with a variance score of 0.778, R-Square of 0.770, Root Mean Square Error (RMSE) of 92.95 minutes, and Mean Absolute Error (MAE) of 44.31 minutes
Jiao et al.	2022	Artificial Neural Network (ANN)	70,826 cases were collected from eight hospitals	Accuracy of 89%
Chu et al.	2022	Extreme Gradient Boosting (XGBoost), Random Forest, Artificial Neural Network (ANN), 1-dimensional Convolution neural network (1dCNN)	124,528 records from January 2015 to September 2019 from Shin Kong Wu Huo-Shih Memorial Hospital	XGBoost model with the values 31.6 min, 18.71 min, 0.71, and 28% for Root Mean Square Error (RMSE), Mean Absolute Error (MAE), Coefficient of Determination (R-Square), Mean Absolute Percentage Error (MAPE), respectively
Abbas et al.	2022	Mean Regressor, Linear Regression, SGD Regression, Elastic Net, Linear SVM, KNN, Decision Tree, Random Forest, AdaBoost, XGBoost, Scikit-learn Multilayer Perceptron (MLP), PyTorch MLP	A total of 302,300 patients were analyzed	Mean Squared Errors (MSEs) of PyTorch MLP for the duration of surgery and length of stay are 0.918 and 0.715, respectively.
Ito et al.	2022	Random Forest (RF)	9567 surgical cases from the National Cancer Center Hospital East, between April 2015 and March 2018 are collected.	Mean Absolute Error (MAE) of 39.94, R-Square value of 0.80, and adjusted R-Square value of 0.77
Martinez et al.	2021	Linear Regression (LR), Support Vector Machines (SVM), Regression Trees (RT), and Bagged Trees (BG)	The dataset is consisting of 206,587 records of the university hospital in Bogotá, Colombia between	Root Mean Squared Error (RMSE) value of 26 min. for BG

Ramos et al.	2021	Backward stepwise linear regression modeling	December 2004 to April 2019 Data were collected from 14 cases.	Mean Absolute Error (MAE) of 3.7 minutes (± 41.1)
Yuniartha et al.	2021	K-Nearest Neighbors (kNN), Decision Tree, Support Vector Machine (SVM), Stochastic Gradient Descent (SGD), Random Forest (RF), Linear Regression (LR), AdaBoost	Historical data of Hospital A and Hospital B	Hospital A: Linear Regression with a Mean Absolute Error (MAE) of 25.143 min. Hospital B: Random Forest with a Mean Absolute Error (MAE) of 23.038 min.
Jiao et al.	2020	Bayesian statistical method (Bayes), Decision Tree (DT), Gradient Boosted Decision Tree (GBT), Mixture Density Network (MDN), Random Forest (RF)	53,783 cases performed during 4 year-period at a tertiary-care pediatric hospital	Continuous Ranked Probability Score (CRPS) of 18.1 minutes for MDN
Soh et al.	2020	Linear Regression (LR)	First Synthetic Dataset, Second Synthetic Dataset, and Third Synthetic Dataset	Root Mean Squared Error (RMSE) values of First Synthetic Dataset, Second Synthetic Dataset, and Third Synthetic Dataset are 6.72 mins., 13.46 mins, and 4.91 mins., respectively.
Zhao et al.	2019	Multivariable Linear Regression (MLR), Ridge Regression (RG), Lasso Regression (LR), Random Forest (RF), Boosted Regression Tree (BRT), and Neural Network (NN)	500 cases from January 1, 2014 to June 30, 2017, are examined.	Root Mean Squared Error (RMSE) of 86.8 min for MLR, RMSE of 82.4 min for RG, RMSE of 81.3 min for LR, RMSE of 81.9 min for RF, RMSE of 80.2 min for BRT, RMSE of 89.6 min for (NN)
Bartek et al.	2019	Linear Regression (LR) and Extreme Gradient Boosting (XGBoost)	46,986 scheduled operations performed between January 2014 to December 2017	Mean Absolute Percentage Error (MAPE) of 26 min for Surgeon-specific XGBoost and 74% Accuracy for Surgeon-specific XGBoost
Twinanda et al.	2019	Convolutional Neural Network (CNN) and Long-Short Term Memory (LSTM)	Cholec120 Dataset and BYPASS170 Dataset	Mean Absolute Error (MAE) of 7.7 ± 5.2 min for TimeLSTM Model and MAE of 15.6 ± 7.9 min for RSDNet Model
Bodenstedt et al.	2019	Convolutional Neural Networks (CNN)	Publicly available Cholec80 dataset is used	Mean Absolute Error (MAE) of 2093 \pm 1787 seconds Baseline Type Model.

Shahabikargar et al.	2017	Generalized Linear Model (GLM), Multivariate Adaptive Regression Splines (MARS) and Random Forests (RF) algorithms	60362 data collected between 01/07/2008 to 30/06/2012 from HBCIS and ORMIS	Mean Absolute Percentage Error (MAPE) of 0.38 for RF
Spangenberg et al.	2017	Linear Regression (LR), Decision Tree (DT), Random Forest (RF), Multilayer perceptron (MP)	Data consists of 15 surgeries of two different surgery types.	Mean Absolute Error (MAE) of 17.52±15.17 for LR, Root Mean Squared Error (RMSE) of 23.14 for LR, Mean Squared Error (MAE) of 535.34 for LR, and R-Square value of 0.88 for LR
Master et al.	2017	Decision Tree Regressor (DTR), Random Forest Regressor (RFR), Gradient Boosted Regression (GBR)	Electronic medical records from hospital information systems	Overall R-Square values of DTR, RFR, and GBR are 0.28, 0.38, and 0.44, respectively.
Edelman et al.	2017	Linear Regression	Data was collected from a Dutch benchmarking database that encompassed all surgeries conducted in six academic hospitals in The Netherlands between 2012 and 2016.	Mean Absolute Error (MAE) of 29.2 minutes and a Mean Squared Error (MSE) of 2,320.7 minutes for the predictions made between 2012 and 2015. For the predictions made in 2016, the MAE was 31.3 minutes with a MSE of 2,366.9 minutes.
Shahabikargar et al.	2014	Linear Regression (LR), Multivariate Adaptive Regression Splines (MARS), and random forests (RF)	The research utilized administrative and perioperative data spanning four years (from 1st July 2008 to 30th June 2012) obtained from a prominent teaching hospital in Queensland, Australia.	Root Mean Square Error (RMSE) of 28.12 for LR, Mean Absolute Percentage Error (MAPE) of 0.68 for RF, and R-squared value of 0.65 for RF
Kays et al.	2014	Bootstrap-enhanced least absolute shrinkage operator	The cases within two years (2010-2011) in the seven main operating rooms at a large children's hospital in the US is analyzed. 10292 surgery data is collected.	R-Square of 0.64 and Mean Absolute Deviation (MAD) of 39.98 ± 0.58.
Devi et al.	2012	Adaptive Neuro Fuzzy Inference Systems (ANFIS),	Data from 100 surgeries each of	ANFIS: Root Mean square Error (RMSE)

		Artificial Neural Networks (ANN) and Multiple Linear Regression Analysis (MLRA)	corneal transplant surgery, cataract surgery, and oculoplastic surgery (total of 300 data), performed by the same surgeons and anesthetists.	of 0.0697 for cataract surgery. ANN: Root Mean square Error (RMSE) of 0.1427 for cataract surgery. Regression: Root Mean square Error (RMSE) of 0.1768 for cataract surgery.
Schneider et al.	2011	Log-Linear Mixed Regression Model (LLMRM) and Univariable Random Effect Model (UREM)	Historical data of 312 patients	Prediction Error: 17.5 min for LLMRM and 21.6 min for UREM
Eijkemans et al.	2010	Linear Mixed Modeling	17,000 operation cases are analyzed.	Overestimation: 2.8 min Underestimation: 6.6 min

Results and Discussion

As a response to the first research question, in the context of studies related to Surgical Duration Estimation in the literature, researchers exhibit varying preferences for the methodologies employed. According to the Figure 1, analysis of the data reveals that Machine Learning stands out as the most favored approach, accounting for 45.8% of the studies. It appears to be a popular choice due to its ability to process and learn from large datasets, enabling the development of predictive models for surgical duration. Machine Learning methods used in papers can be seen in Figure 2. Statistics, constituting 16.7% of the studies, also retain their significance, offering traditional and well-established methods for data analysis and inference. Statistical methods used in papers can be found in Table 5. Surprisingly, Deep Learning, with a preference rate of 12.5%, emerges as a relatively less frequently utilized method, despite its widespread application in various fields. Overall Deep Learning methods used in papers can be seen in Figure 3. Interestingly, a subset of studies (4.2%) adopts a comprehensive approach, combining Machine Learning, Deep Learning, and Statistics, likely to harness the complementary strengths of these methodologies.

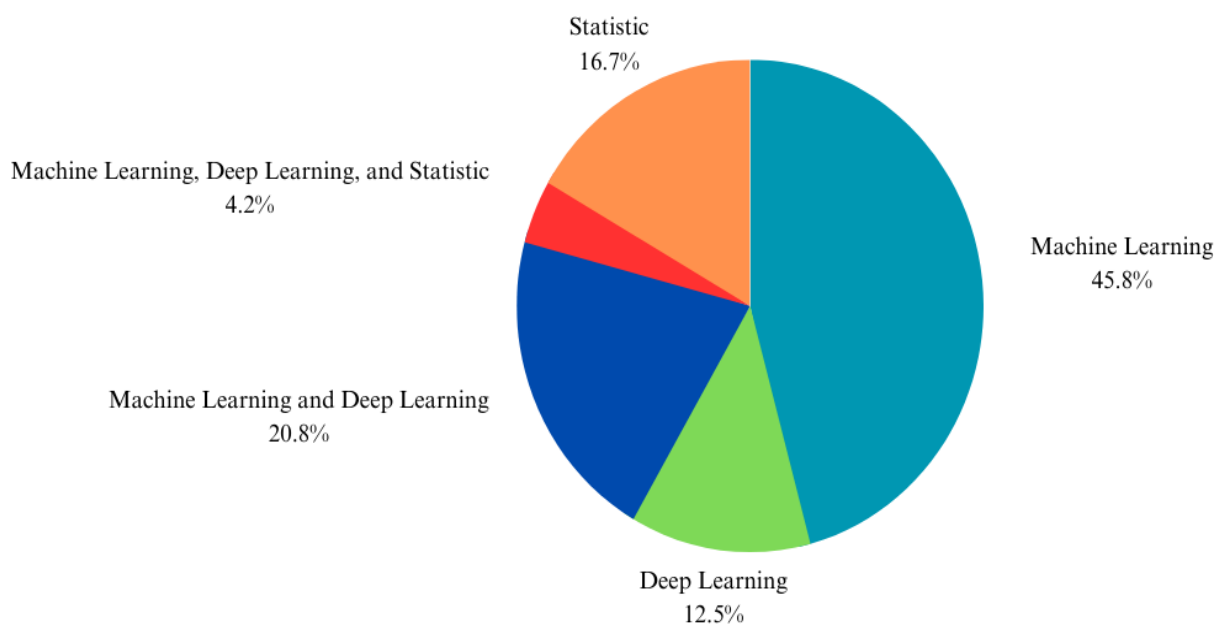
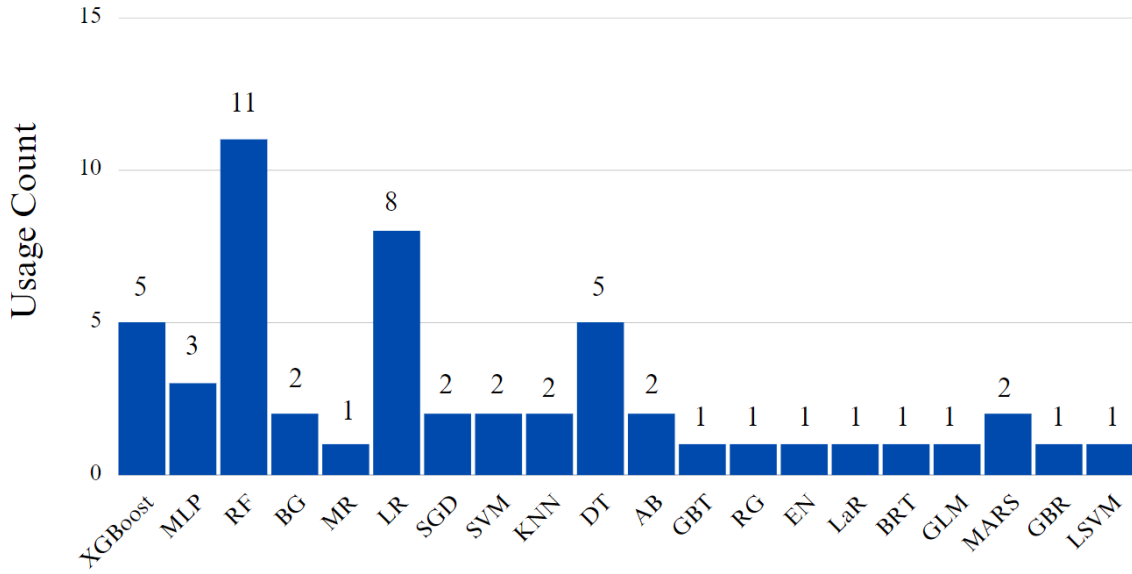


Figure 1. Chart showing the distribution of the methods used in the studies.



Machine Learning Methods

Figure 2. Usage numbers of machine learning methods used in papers.

(XGBoost: Extreme Gradient Boosting, MLP: Multivariable Linear Regression, RF: Random Forest, BG: Bagged Trees, MR: Mean Regressor, LR: Linear Regression, SGD: Stochastic Gradient Descent Regression, SVM: Support Vector Machine, KNN: K-Nearest Neighbors, DT: Decision Tree, AB: AdaBoost, GBT: Gradient Boosted Decision Tree, RG: Ridge Regression, EN: Elastic Net, LaR: Lasso Regression, BRT: Boosted Regression Tree, GLM: Generalized Linear Model, MARS: Multivariate Adaptive Regression Splines, GBR: Gradient Boosted Regression, LSVM: Linear Support Vector Machine)

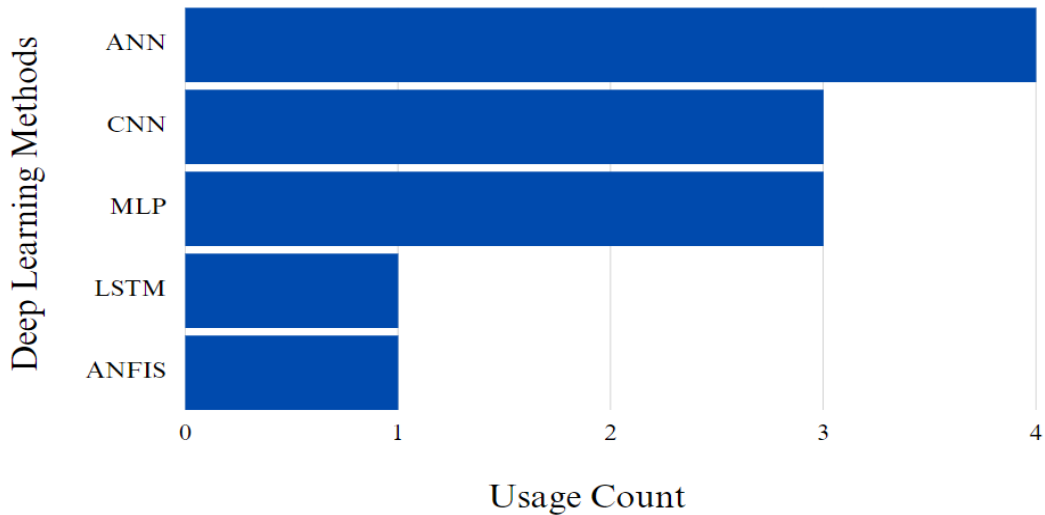


Figure 3. Usage numbers of deep learning methods used in papers.

(ANN: Artificial Neural Networks, CNN: Convolution Neural Networks, MLP: Multilayer Perceptron, LSTM: Long-Short Term Memory, ANFIS: Adaptive Neuro Fuzzy Inference Systems)

Table 5. Usage numbers of Statistical Methods used in papers.

Statistical Methods	Usage Count
Backward stepwise linear regression modeling	1
Bayesian statistical method	1
Bootstrap-enhanced least absolute shrinkage operator	1
Log-Linear Mixed Regression Model	1
Univariable Random Effect Model	1
Linear Mixed Modeling	1

For the second research question, in the realm of Surgical Duration Estimation research, researchers utilize various evaluation metrics, Table 6, to assess the accuracy and performance of the employed methods. The analysis of the literature reveals a discernible preference for certain metrics over others. Specifically, Mean Absolute Error (MAE) emerges as the most favored evaluation metric, with 9 instances of usage, highlighting its significance in quantifying the average absolute difference between predicted and actual surgical durations. Following closely is Root Mean Square Error (RMSE), which yields 8 instances, serving as an essential indicator of the model's predictive accuracy by measuring the square root of the average squared differences between predictions and actual values. R-Square (R2) is another frequently employed metric, observed in 7 instances, acting as a valuable measure of the model's performance of fit and its ability to explain the variance in surgical duration data. While Mean Absolute Percentage Error (MAPE) and Accuracy were conducted as 4 and 3 instances, respectively, they also exhibit a significant presence in the literature, reflecting their relevance in evaluating the relative percentage error and overall predictive correctness. In contrast, evaluation metrics such as Mean Squared Error (MSE), Adjusted R-Square, Continuous Ranked Probability Score (CRPS), Sensitivity, Specificity, and Area Under the ROC Curve (AUC) demonstrate limited prevalence, each with only one instance of usage, indicating their less frequent adoption in assessing the accuracy of the employed methods.

Table 6. Evaluation metrics used in the papers and their frequencies of usage.

Evaluation Metrics	Usage Count
Mean Absolute Error (MAE)	9
Root Mean Square Error (RMSE)	8
R-Square (R2)	7
Mean Absolute Percentage Error (MAPE)	4
Accuracy	3
Mean Squared Error (MSE)	2
Adjusted R-Square	1
Continuous Ranked Probability Score (CRPS)	1
Sensitivity	1
Specificity	1
Area Under the ROC Curve (AUC)	1

The third research question refers that the analysis of the literature on Surgical Duration Estimation, following the application of inclusion and exclusion criteria, revealing significant years, Figure 4A, showcasing an increasing trend in the number of conducted studies. Specifically, the years 2017, 2019, and 2022 stand out, each featuring four studies in the field. This surge in research activity during these periods indicates a growing interest and recognition of the significance of Surgical Duration Estimation as a subject of investigation. The observed trend suggests an expanding body of knowledge and a potential emphasis on exploring novel methodologies and technologies to enhance the accuracy and efficiency of surgical duration predictions. The consistent rise in the number of studies during these years underscores the field's dynamic nature, encouraging further exploration and advancement in this critical domain of medical research.

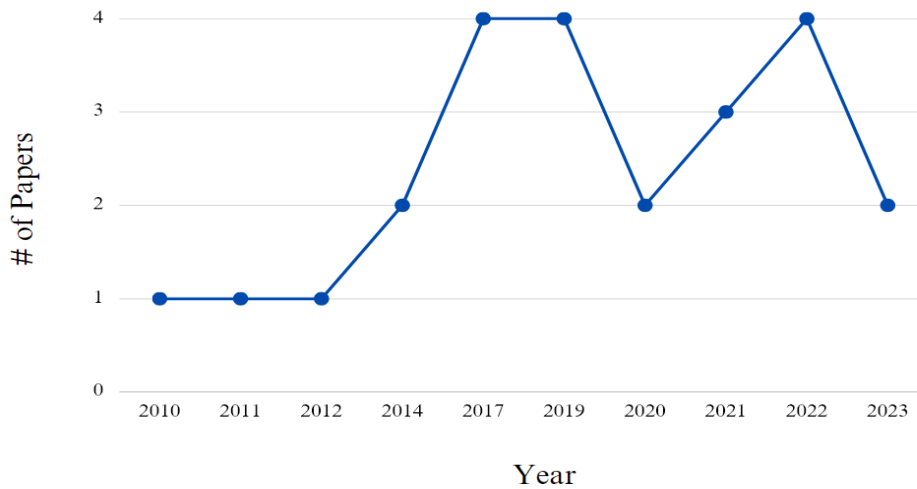


Figure 4. The number of articles changing over the years.

Conclusion

This study has provided an analysis of the methodologies, evaluation metrics, and temporal trends in the field of Surgical Operation Duration Estimation. The comprehensive analysis of 24 selected papers has shed light on the prevailing trend methodologies in the field. The insights derived from this study can inform future research endeavors, inspire the development of novel methodologies, and aid in improving the accuracy and efficiency of surgical duration prediction models.

The first research question highlighted the varying preferences of researchers regarding the employed methodologies. Machine Learning emerged as the most favored approach, accounting for 45.8% of the studies, owing to its capacity to handle large datasets and develop predictive models for surgical duration. Statistics also retained significance, constituting 16.7% of the studies, while Deep Learning, with a preference rate of 12.5%, appeared less frequently utilized despite its widespread applications.

The second research question delved into the evaluation metrics used to assess the accuracy of the employed methods. Mean Absolute Error (MAE) emerged as the most favored metric, followed by Root Mean Square Error (RMSE) and R-Square (R²). While MAPE and Accuracy were also prevalent in the literature, other metrics such as MSE, Adjusted R-Square, CRPS, Sensitivity, Specificity, and AUC were less frequently adopted.

Lastly, the third research question addressed the temporal trends in Surgical Duration Estimation research. The years 2017, 2019, and 2022 exhibited a notable increase in research activity, indicating a growing interest and recognition of the importance of this domain. This trend signifies the dynamic nature of the field and suggests ongoing efforts to explore novel methodologies and technologies for more accurate surgical duration predictions.

All in all, this systematic mapping study has provided valuable insights for researchers, practitioners, and decision-makers in the medical field. The findings contribute to a comprehensive understanding of the current state of research, prevailing methodologies, and preferred evaluation metrics in Surgical Duration Estimation. The observed trends can serve as a guide for future research endeavors, encouraging the development of innovative approaches to enhance surgical planning and resource allocation, and ultimately improve patient outcomes in the domain of surgical care.

Scientific Ethics Declaration

The authors declare that the scientific ethical and legal responsibility of this article published in EPSTEM journal belongs to the authors.

Acknowledgements or Notes

* This article was presented as an oral presentation at the International Conference on Research in Engineering, Technology and Science (www.icrets.net) held in Budapest/Hungary on July 06-09, 2023.

References

- Abbas, A., Mosseri, J., Lex, J. R., Toor, J., Ravi, B., Khalil, E. B., & Whyne, C. (2022). Machine learning using preoperative patient factors can predict duration of surgery and length of stay for total knee arthroplasty. *International Journal of Medical Informatics*, 158, 104670.
- Bartek, M. A., Saxena, R. C., Solomon, S., Fong, C. T., Behara, L. D., Venigandla, R., Velagapudi, K., Lang, J. D., & Nair, B. G. (2019). Improving operating room efficiency: Machine learning approach to predict case-time duration. *Journal of the American College of Surgeons*, 229(4), 346–354.
- Bodenstedt, S., Wagner, M., Mündermann, L., Kennigott, H., Müller-Stich, B., Breucha, M., Mees, S. T., Weitz, J., & Speidel, S. (2019). Prediction of laparoscopic procedure duration using unlabeled, multimodal sensor data. *International Journal of Computer Assisted Radiology and Surgery*, 14, 1089-1095.

- Cappanera, P., Visintin, F., & Banditori, C. (2014). Comparing resource balancing criteria in master surgical scheduling: A combined optimisation-simulation approach. *International Journal of Production Economics*, 158, 179-196.
- Chu, J., Hsieh, C.H., Shih, Y.N., Wu, C.C., Singaravelan, A., Hung, L.P., & Hsu, J. L. (2022). Operating room usage time estimation with machine learning models. *Healthcare*, 10(8), 1518.
- Devi, S. P., Rao, K. S., & Sangeetha, S. S. (2012). Prediction of surgery times and scheduling of operation theaters in ophthalmology department. *Journal of Medical Systems*, 36, 415-430, 2012.
- Edelman, E. R., van Kuijk, S. M. J., Hamaekers, A. E. W., de Korte, M. J. M., van Merode, G. G., & Buhre, W. F. F. A. (2017). Improving the prediction of total surgical procedure time using linear regression modeling. *Frontiers in Medicine*, 4, 85.
- Eijkemans, M. J. C., van Houdenhoven, M., Nguyen, T., Boersma, E., Steyerberg, E. W., & Kazemier, G. (2010). Predicting the unpredictable: A new prediction model for operating room. *Times Using Individual Characteristics and the Surgeon's Estimate, Anesthesiology*, 112(1), 41-49.
- Erwin, W. H., & Vanberkel, P. T. (2012). *Operating theatre planning and scheduling hand book of healthcare system scheduling* (pp. 105-130). Springer.
- Fairley, M., Scheinker, D., and Brandeau, M. L. (2019). Improving the efficiency of the operating room environment with an optimization and machine learning model. *Health Care Management Science*, 22, 756-767.
- Gabriel, R. A., Harjai, B., Simpson, S., Du, A. L., Tully, J. L., George, O., & Waterman, R. (2023). An ensemble learning approach to improving prediction of case duration for spine surgery: Algorithm development and validation. *JMIR Perioperative Medicine*, 6, e39650.
- Hinterwimmer, F., Lasic, I., Langer, S., Suren, C., Charitou, F., Hirschmann, M. T., Matziolis, G., Seidl, F., Pohlig, F., Rueckert, D., Burgkart, R., & von Eisenhart-Rothe, R. (2023). Prediction of complications and surgery duration in primary TKA with high accuracy using machine learning with arthroplasty-specific data. *Knee Surgery, Sports Traumatology, Arthroscopy*, 31, 1323-1333.
- Ito, M., Hoshino, K., Takashima, R., Suzuki, M., Hashimoto, M., & Fujii, H. (2022). Does case-mix classification affect predictions? A machine learning algorithm for surgical duration estimation, *Healthcare Analytics*, 2, 100119.
- Jiao, Y., Sharma, A., Abdallah, A. B., Maddox, T. M., & Kannampallil, T. (2020). Probabilistic forecasting of surgical case duration using machine learning: model development and validation, *Journal of the American Medical Informatics Association, JAMIA*, 27(12), 1885-1893.
- Jiao, Y., Xue, B., Lu, C., Avidan, M. S., & Kannampallil, T. (2022). Continuous real-time prediction of surgical case duration using a modular artificial neural network, *British Journal of Anaesthesia*, 128, 829-837.
- Kayis, E., Khaniyev, T. T., Suermondt, J., & Sylvester, K. (2014). A robust estimation model for surgery durations with temporal, operational, and surgery team effects. *Health Care Management Science*, vol. 18, 222-233.
- Kroer, L. R., Foverskov, K., Vilhelmsen, C., Hansen, A. S., & Larsen, J. (2018). Planning and scheduling operating rooms for elective and emergency surgeries with uncertain duration. *Operations Research for Health Care*, 19, 107-119.
- Martinez, O., Martinez, C., Parra, C. A., Rugeles, S., & Suarez, D. R. (2021). Machine learning for surgical time prediction, *Computer Methods and Programs in Biomedicine*, 208.
- Master, N., Scheinker, D. & Bambos, N. (2016). *Predicting pediatric surgical durations*. (Master dissertation). Department of Electrical Engineering, Stanford University, Stanford, CA.
- Master, N., Zhou, Z., Miller, D., Scheinker, D., Bambos, N., & Glynn, P. (2017). Improving predictions of pediatric surgical durations with supervised learning, *International Journal of Data Science and Analytics*, 4, 35-52.
- Petersen, K., Vakkalanka, S., & Kuzniarz, L. (2015). Guidelines for conducting systematic mapping studies in software engineering: An update, *Information and Software Technology*, 64, 1-18, 2015.
- Ramos, O., Mierke, A., Chung, J. H., Cheng, W. K., & Danisa, O. (2021). Estimation of the duration of three common spine procedures as a tool for operating room utilization, *Perioperative Care and Operating Room Management*, 24, 100195.
- Rath, S., Rajaram, K., & Mahajan, A. (2017). Integrated anesthesiologist and room scheduling for surgeries: Methodology and application. *Operations Research*, 1460-1478.
- Schneider, A., Wilhelm, D., Schneider, M., Schuster, T., Kriner, M., Leuxner, C., Can, S., Fiolka, A., Spanfellner, B., Sitou, W., & Feussner, H. (2011). Laparoscopic cholecystectomy – a standardized routine laparoscopic procedure: Is it possible to predict the duration of an operation?, *Journal of Healthcare Engineering*, 2, 259-269.
- Shahabikargar, Z., Khanna, S., Good, N., Sattar, A., Lind, J., & O'Dwyer, J. (2014). Predicting procedure duration to improve scheduling of elective surgery (pp.998-1009). *Pacific Rim International Conference on Artificial Intelligence*. Springer.

- Shahabikargar, Z., Khanna, S., Sattar, A., & Lind, J. (2017). Improved prediction of procedure duration for elective surgery. *Studies in Health Technology and Informatics*, 239, 133-138.
- Soh, K. W., Walker, C., O'Sullivan, M., & Wallace, J. (2020). An evaluation of the hybrid model for predicting surgery duration. *Journal of Medical Systems*, 44, 42.
- Spangenberg, N., Wilke, M., & Franczyk, B. (2017). A big data architecture for intra-surgical remaining time predictions. *Procedia Computer Science*, 113, 310-317.
- Twinanda, A. P., Yengera, G., Mutter, D., Marescaux, J., & Padoy, N. (2019). RSDNet: Learning to predict remaining surgery duration from laparoscopic videos without manual annotations. *IEEE Transactions on Medical Imaging*, 38(4), 1069-1078.
- Wang, L., Demeulemeester, E., Vansteenkiste, N., & Rademakers, F. (2021). Operating room planning and scheduling for outpatients and inpatients: A review and future research. *Operations Research for Health Care*, 31.
- Yuniartha, D. R., Masruroh, N. A., & Herliansyah, M. K. (2021). An evaluation of a simple model for predicting surgery duration using a set of surgical procedure parameters. *Informatics in Medicine Unlocked*, 25.
- Zhang, J., Dridi, M., and El Moudni, A. (2020). Column-generation-based heuristic approaches to stochastic surgery scheduling with downstream capacity constraints. *International Journal of Production Economics*, 229.
- Zhao, B., Waterman, R. S., Urman, R. D., & Gabriel, R. A. (2019). A machine learning approach to predicting case duration for robot-assisted surgery. *Journal of Medical Systems*, 43, 32.

Author Information

Ziya Karakaya

Konya Food and Agriculture University,
Konya, Turkey

Contact e-mail: ziya.karakaya@gidatarim.edu.tr

Bahadır Tatar

ARD Group Information Technologies Inc.
Ankara, Turkey

To cite this article:

Karakaya, Z., & Tatar, B. (2023). Technological trend analysis for surgical operation duration estimation. *The Eurasia Proceedings of Science, Technology, Engineering & Mathematics (EPSTEM)*, 23, 349-360.

The Eurasia Proceedings of Science, Technology, Engineering & Mathematics (EPSTEM), 2023

Volume 23, Pages 361-371

ICRETS 2023: International Conference on Research in Engineering, Technology and Science

Determination of the Shear Force in RC Interior Beam-Column Connections

Albena Doicheva

University of Architecture, Civil Engineering and Geodesy (UACEG)

Abstract: The calculation of frame structures requires special attention when modeling the beam-column connection. Often the joint is assumed to be rigid, but this does not correspond to the real behavior of the beam-column connection, as well as the real response of frame structures. The leading countries in seismic research (USA, New Zealand, Japan) have uniform procedures introduced in their seismic codes for studying the moment resisting frame. However, regarding the determination of the shear force in the beam-column connection, there is still a discrepancy in how it is determined. In the present work, a mathematical model is proposed for the analytical determination of the shear force. The emerging large deformations in the beam, which could be realized during earthquake, have been taken into account. The material is elastic. The obtained values are compared with results determined by mathematical procedures proposed in other literature sources.

Keywords: Beam-column connection, Shear force, Reinforced concrete, Elastic material, Large deformations

Introduction

The beam-column connection is a basic element of frame structures. Its task is to transfer the loads between the connected elements. The preservation of the integrity of the joint in moment resisting reinforced concrete frames is guaranteed in static load calculations by the recommendations in the current codes. However, failures in many frame structures during cyclic loading (such as earthquakes) indicate abrupt destruction due to joint shear. Detailed studies of the beam-column connection date back to the last 5 to 6 decades.

The first quantitative definition of the shear force was given by Hanson and Connor (1967). In their report of the test results of RC interior beam-column connections they define joint shear as a horizontal force transferred at the midheight of a horizontal section of a beam-column connection. They suggested that joint shear failure may be precluded by limiting the joint shear stress to the level at which joint shear failure occurs. This definition has been adopted worldwide and subsequent studies lead to the adoption of design provisions providing a limiting value of joint shear stress. The distribution of forces and the response of beam-column connection has occupied scientists for the past few decades (Park & Paulay, 1975; Park & Keong, 1979; Paulay, 1989; Paulay & Priestley, 1992; Park, 2002; Lowes & Altoontash, 2003; Altoontash, 2004; Celik & Ellingwood, 2008; Sharma et al., 2009; Shafaei et al., 2014). However, research in different countries has led to different proposals for the modeling and detailing of frame joints in terms of shear force. Detailed review of interior and exterior joints of special moment resisting reinforced concrete frames, with reference to three codes of practices: American Concrete Institute (ACI 318M-02), New Zealand Standards (NZS 3101, 1995) and Eurocode 8 (EN 1998-1, 2003) was performed by Uma & Jain (2006). Tran et al. (2014) propose a new empirical model to estimate the joint shear strength of both exterior and interior beam-column. A parametric study was carried out to evaluate the dependence of the predicted to tested joint shear strength ratio on the four influence parameters.

Contrary to the general acceptance, Shiohara (2001) proposed a new model for the calculation and detailing of the beam-column connection. The study shows an irrationality in the joint shear failure model, which is adopted in the most current design codes of reinforced concrete beam-to-column joint. It is based on the data of tests of

- This is an Open Access article distributed under the terms of the Creative Commons Attribution-NonCommercial 4.0 Unported License, permitting all non-commercial use, distribution, and reproduction in any medium, provided the original work is properly cited.

- Selection and peer-review under responsibility of the Organizing Committee of the Conference

© 2023 Published by ISRES Publishing: www.isres.org

twenty reinforced concrete interior beam-to-column-joint failed in joint shear. The analysis indicated that joint shear stress had increased in the most specimens, even after apparent joint shear failure starts.

Problem

Hanson and Connor (1967) defined the joint shear V_j in an interior beam-column connection from Figure 1 as given in (1). The joint shear V_j in (1) is an internal force acting on the free body along the horizontal plane at the midheight of the beam-column connection.

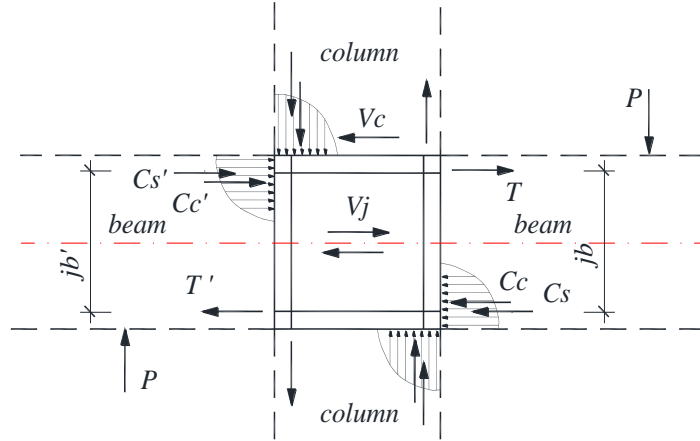


Figure 1. Definition of joint shear in interior RC beam-column connection

$$V_j = T + C_s' + C_c' - V_c = T + T' - V_c \tag{1}$$

where: C_s and C_s' - compressive force in bottom and top longitudinal reinforcing bars in beam passing through the connection;
 C_c and C_c' - compressive force in concrete on the bottom and top edge of beam;
 T and T' - tensile forces in top and bottom reinforcing bars in beam passing through the connection;
 V_c - column shear force

This definition is clear and has been used in the design of beam-column connections. The contribution of steel and concrete is taken into account separately. The difficulty encountered in determining the forces from (1) leads to the adoption of another way of writing the expression for the shear force in the literature. Usually T and T' are defined by (2).

$$T = \frac{M_b}{j_b} \text{ and } T' = \frac{M_b'}{j_b'} \tag{2}$$

where: M_b and M_b' - moment at column face;
 j_b and j_b' - the length of bending moment arm at the column face. It is assumed to be constant and unchanging in the process of deformation.

Then (1) is rewritten from moment in the beam section at column faces into (3).

$$V_j = \frac{M_b}{j_b} + \frac{M_b'}{j_b'} - V_c \tag{3}$$

The assumption (2) obliges us to assume equal forces in the bottom and top reinforcement of the beam at the face of the column. In the author's previous publications, these values were shown to differ substantially. In this article, the following tasks are set: 1. to determine expressions for the forces from Figure 1, at the column face, 2. to perform comparisons of the obtained results with the results of (2) and (3).

Method

Mathematical Model of Beams

Case I - Cantilever Beam

A cantilever beam is considered. It is supported on one side by column as is the case in the specimens in beam-to-column joint subassemblages for tests. The beam is statically indeterminate, prismatic and symmetric. The beam is under the conditions of special bending with tension/compression and Bernoulli-Euler hypothesis is considered.

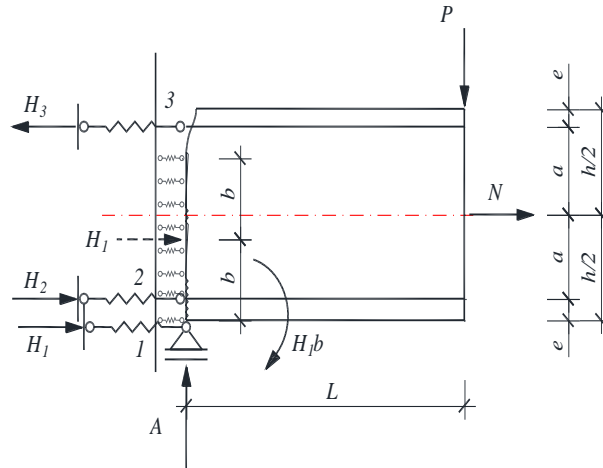


Figure 2. Supports of cantilever beam to column

The beam is loaded with a vertical force $P [kN]$. The support takes place in vertical support 1, where a vertical support reaction $A [kN]$ occurs. At the level of the reinforcing bars, elastic supports 2 and 3, with linear spring coefficients k_2 and k_3 , are introduced. They are set as the reduced tension/compression stiffness of the reinforcing bar.

$$k_2 = \frac{E_2 A_2}{L} \quad \text{and} \quad k_3 = \frac{E_3 A_3}{L} \quad (4)$$

where: $L [cm]$ - the length of the beam;

$A_2 [cm^2]$ and $A_3 [cm^2]$ - the area of the cross-section of bottom and top longitudinal reinforcing bars in beam passing through the connection;

$E_2 [kN/cm^2]$ and $E_3 [kN/cm^2]$ - the modulus of elasticity of the bottom and top longitudinal reinforcing bars in beam passing through the connection

The supporting reactions that occur here are $H_2 [kN]$ and $H_3 [kN]$.

Linear spring supports act along the vertical wall of the beam. They account for the connection of the concrete of the beam to that of the column. The forces in all the springs are reduced to one force $H_1 [kN]$. In case of large deformations, part of the vertical edge is destroyed. The unbroken edge has length $2b [cm]$. The reaction $H_1 [kN]$, which is symmetrically located with respect to the intact lateral edge, moves along the height of the beam as the crack length increases. For convenience, it has been transferred $H_1 [kN]$ to the support along the lower edge (support one), after applying Poinot's theorem concerning the transfer of forces in parallel to their directrix. This necessitated the introduction of compensating moments $H_1 b [kN.cm]$. The coefficient of the linear spring is k_1 . It is set as the reduced tensile/compressive stiffness of the concrete section.

$$k_1 = \frac{E_1 A_1}{L} \quad (5)$$

where: $L [cm]$ - the length of the beam;

$A_1 [cm^2]$ - the area of the cross-section of the concrete

$E_1 [kN/cm^2]$ - the modulus of elasticity of the concrete

As a consequence of the linear deformations in the cantilever beam, a normal axial force occurs $N [kN]$, which is introduced at the free end of the beam.

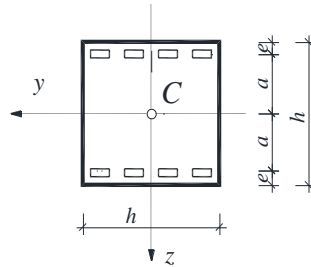


Figure 3. Cross-section of the beam

The following notations have also been introduced:

$h [cm]$ - the length of the beam;

$e [cm]$ and $a [cm]$ - offset of the reinforcing bars from the bottom and top edges of the beam and from the axis of the beam, respectively;

$E_2 A_2$ and $E_3 A_3$ - tensile (compressive) stiffness of the reinforcing bars;

$E_1 A_1$ - tensile (compressive) stiffness of the concrete cross-section;

$E_2 I_2$ and $E_3 I_3$ - bending stiffness of the reinforcing bars;

$E_1 I_1$ - bending stiffness of the concrete cross-section;

$I_1 (I_{y1})$, $I_2 (I_{y2})$ and $I_3 (I_{y3})$ are the moment of inertia of the concrete cross section and the moment of inertia of the bottom and top reinforcing bars relative to the principal axis of inertia y , respectively;

$EA = E_1 A_1 + E_2 A_2 + E_3 A_3$ - tensile (compressive) stiffness of the composite section;

$EI = E_1 I_1 + E_2 I_2 + E_3 I_3$ - bending stiffness of the composite section.

Support Reactions

The solution is based on Menabria's theorem about statically indeterminate systems in first-order theory. The potential energy of deformation in special bending, combined with tension (compression) and with the effect of linear springs taken into account, will be:

$$\Pi = \frac{1}{2} \int_0^L \frac{M^2(x)}{EI} dx + \frac{1}{2} \int_0^L \frac{N^2(x)}{EA} dx + \frac{H_1^2}{2k_1} + \frac{H_2^2}{2k_2} + \frac{H_3^2}{2k_3}. \quad (6)$$

It is a well-known fact that, according to Menabria's theorem, the desired hyperstatic unknown is determined by the minimum potential energy condition with respect to it or will be:

$$\frac{\partial \Pi}{\partial H_1} = 0; \quad \frac{\partial \Pi}{\partial H_2} = 0; \quad \frac{\partial \Pi}{\partial H_3} = 0. \quad (7)$$

The three equilibrium conditions of statics give us respectively:

$$1. \sum V = 0 \rightarrow A_v = P \quad (8)$$

$$2. \sum H = 0 \rightarrow N = H_3 - H_1 - H_2 \quad (9)$$

$$3. \sum M_1 = 0 \rightarrow -PL - H_1 b + H_3(h - e) - H_2 e - N \frac{h}{2} = 0 \quad (10)$$

Substitute (9) in (10) and after simplifying for H_2 we get:

$$H_2 = \frac{PL - H_1 \left(\frac{h}{2} - b \right)}{a} - H_3 \quad (11)$$

The bending moment for the beam is:

$$M(x) = Ax + H_1 b - H_1 \frac{h}{2} - H_2 a - H_3 a, \quad (12)$$

Substitute (8) in (12) and substitute the resulting expression in (6) together with (9). Expressions (7) apply. A system of three linear equations with respect to the three unknowns is obtained. The solutions give the formulas for the horizontal support reactions shown below:

$$H_1 = \frac{-PLk_1 \{EAh_1 N_1 + 2EIL[k_2 n_1 - k_3 n_2] + 2L^2 a^2 K_{23} n_2\}}{EI \{EAD_1 + D_2\}} \quad (13)$$

$$H_2 = \frac{PLk_2 \{EAa N_2 + 4EIL[k_1 n_1 + k_3 4a] + L^2 a K_{13} n_2\}}{2EI \{EAD_1 + D_2\}} \quad (14)$$

$$H_3 = \frac{PLk_3 \{4EAa N_1 + 4EIL[k_1 n_2 + k_2 4a] - L^2 a K_{12} n_1 n_2\}}{2EI \{EAD_1 + D_2\}} \quad (15)$$

where

$$\begin{aligned} h_1 &= 2b + h; & n_1 &= 2a + h_1; & n_2 &= 2a - h_1 \\ K &= k_1 + k_2 + k_3; & K_{12} &= k_1 k_2; & K_{13} &= k_1 k_3; & K_{23} &= k_2 k_3. \\ N_1 &= 2EI - k_2 L a^2; & N_2 &= 8EI + L(k_1 h_1^2 + k_3 4a^2) \\ D_1 &= (k_2 + k_3) 4a^2 + k_1 h_1^2 \\ D_2 &= L \left[k_1 k_2 (2a + h_1)^2 + k_1 k_3 (2a - h_1)^2 + k_2 k_3 16a^2 \right] \end{aligned} \quad (16)$$

The solution was performed in the symbolic environment of the MATLAB R2017b program.

Case II - Simple Beam

A beam from a frame structure is considered. The supporting is analogous to that of a cantilever beam.

Due to the symmetry of the beam, with respect to the mid-section, the horizontal forces on the left side are equal to those on the right side. The beam is three times statically indeterminate. All geometric and material characteristics introduced up to this point are preserved.

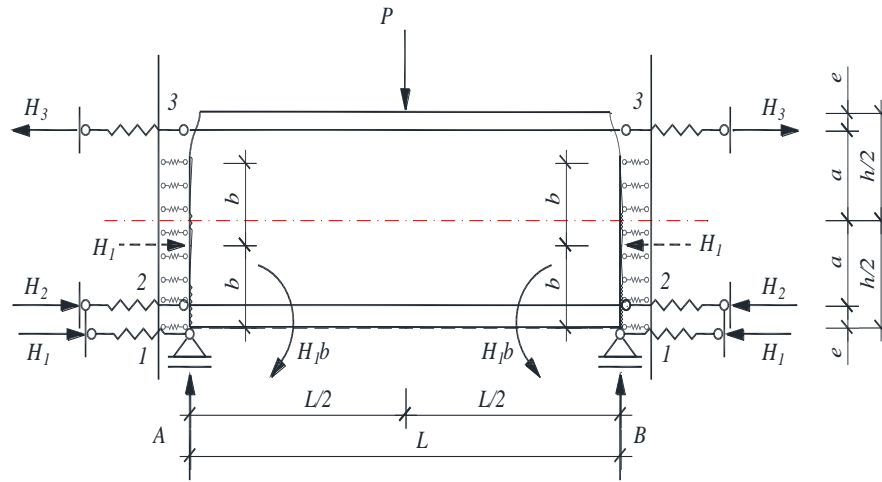


Figure 4. Supports of simple beam to columns

The vertical support reactions are:

$$A = \frac{P}{2} \quad \text{and} \quad B = \frac{P}{2}. \quad (17)$$

The bending moments for both part of the beam will be:

$$M_1 = \frac{P}{2}x - H_3a - H_2a - H_1\left(\frac{h}{2} - b\right); \quad (18)$$

$$M_2 = \frac{P}{2}\left(\frac{L}{2} - x\right) - H_3a - H_2a - H_1\left(\frac{h}{2} - b\right); \quad (19)$$

and the normal force respectively:

$$N = H_3 - H_1 - H_2. \quad (20)$$

Substitute (18), (19) and (20) in (21)

$$\Pi = \frac{1}{2} \int_0^{L/2} \frac{M_1^2(x)}{EI} dx + \frac{1}{2} \int_0^{L/2} \frac{M_2^2(x)}{EI} dx + \frac{1}{2} \int_0^{L/2} \frac{N^2(x)}{EA} dx + \frac{H_1^2}{k_1} + \frac{H_2^2}{k_2} + \frac{H_3^2}{k_3} \quad (21)$$

and it is made a solution proceeds in a similar way like a Case I. Derived the formulas of the horizontal support reactions are:

$$H_1 = \frac{-PL^2k_1 \{2EAh_1 + Lk_2n_1 - Lk_3n_2\}}{4\{2EA[8EI + LD_1] + 8EILK + LD_2\}} \quad (22)$$

$$H_2 = \frac{PL^2k_2 \{4EAa + Lk_1n_1 + Lk_34a\}}{4\{2EA[8EI + LD_1] + 8EILK + LD_2\}} \quad (23)$$

$$H_3 = \frac{PL^2k_3 \{4EAa + Lk_1n_2 + Lk_24a\}}{4\{2EA[8EI + LD_1] + 8EILK + LD_2\}} \quad (24)$$

The expressions show good agreement with the expressions reported in Doicheva (2021) and Doicheva (2022), taking into account the relevant geometrical and force conditions embedded in them.

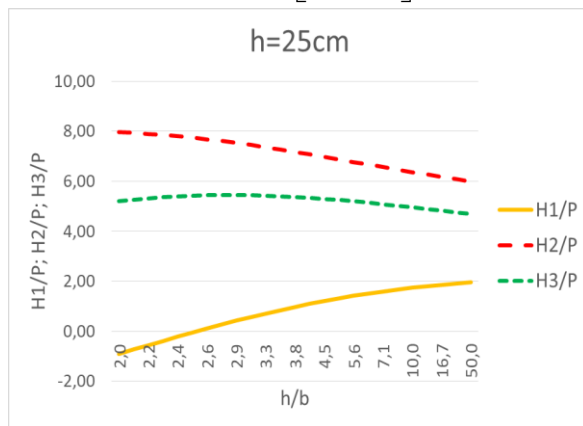
Results and Discussion

For the numerical results, a beam with a cross-section of $25/25\text{ cm}$ was introduced. For all examples considered $P = const$, the distances $e = 3\text{ [cm]}$ and $a = 9,5\text{ [cm]}$. And more $A_2 = A_3 = 12,5\text{ [cm}^2\text{]}$ and $E_2 = E_3 = 21000\text{ [kN/cm}^2\text{]}$. The distance $b\text{ [cm]}$ varies in the interval $[12,5; 0)$ and is monitored by the ratio h/b .

Case I - Cantilever Beam

The beam is with a length of $L = 125\text{ cm}$. Two examples with a difference only in the modulus of elasticity of concrete are considered. The modules used are $E_1 = 1700\text{ [kN/cm}^2\text{]}$ for normal concrete and $E_1 = 3700\text{ [kN/cm}^2\text{]}$ for High-strength concrete.

Example I- the modulus of elasticity of the concrete is $E_1 = 1700\text{ [kN/cm}^2\text{]}$



Example II- the modulus of elasticity of the concrete is $E_1 = 3700\text{ [kN/cm}^2\text{]}$

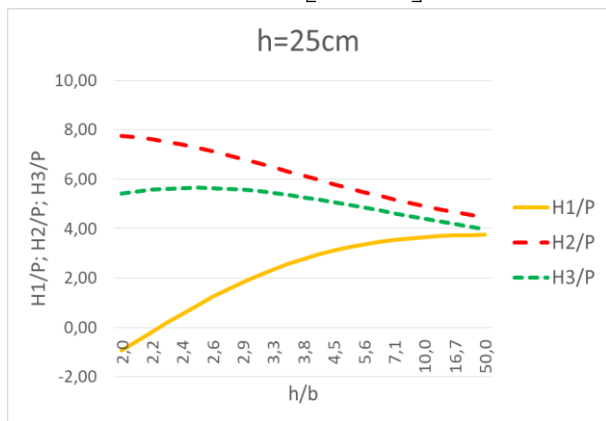
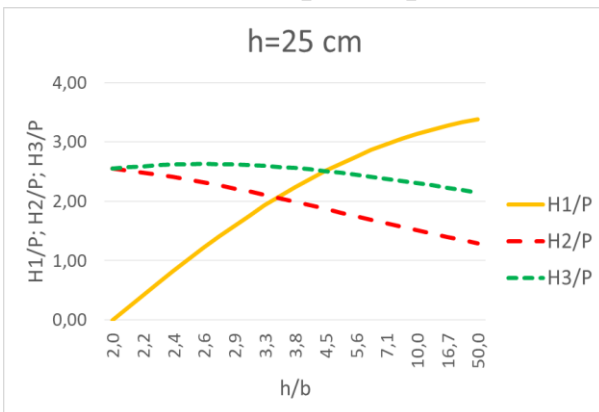


Figure 5. The parameters of the three support reactions - cantilever beam

Case II - Simple Beam

The beam is with a length of $L = 1000\text{ cm}$.

Example I- the modulus of elasticity of the concrete is $E_1 = 1700\text{ [kN/cm}^2\text{]}$



Example II- the modulus of elasticity of the concrete is $E_1 = 3700\text{ [kN/cm}^2\text{]}$



Figure 6. The parameters of the three support reactions - simple beam

The graphs in Figure 5 and Figure 6 clearly show the discrepancy between the magnitudes of the forces in the top and bottom reinforcement, i.e. $H_2 \neq H_3$, as well as the significant increase in the force absorbed by the concrete in its intact part (H_1). Also is visible the significant quantitative change of the forces with the change of only one of the material characteristics - the modulus of elasticity of the concrete $E_1 [kN/cm^2]$. These inferences call into question the acceptance in (2) and (3). A new method for the analytical determination of the shear force is proposed.

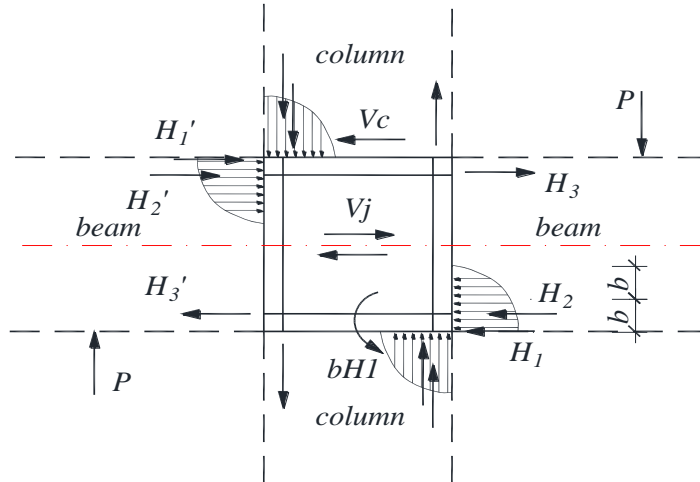


Figure 7. New definition of joint shear in interior RC beam-column connection

A new model to Determination of the Shear Force in RC Interior Beam-Column Connections is proposed.

$$V_j = H_3 + H_2' + H_1' - V_c \quad (25)$$

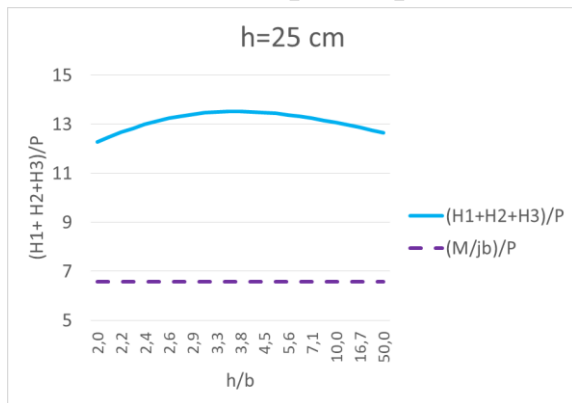
If the frame is symmetric and other conditions being equal, we will have the equality of $H_1 = H_1'$, $H_2 = H_2'$ and $H_3 = H_3'$. Then (25) becomes

$$V_j = H_3 + H_2 + H_1 - V_c \quad (26)$$

Comparison of the Results of (3) and (26)

Case I - Cantilever Beam

Example I- the modulus of elasticity of the concrete is $E_1 = 1700 [kN/cm^2]$



Example II- the modulus of elasticity of the concrete is $E_1 = 3700 [kN/cm^2]$

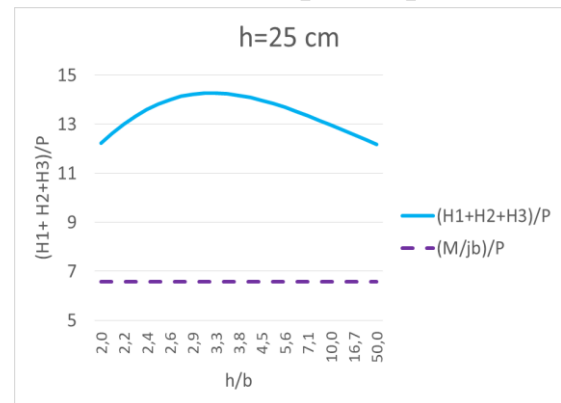


Figure 8. Comparison of the results of (3) and (26) - cantilever beam

The result comparison of the new model and the one known from the literature show the following:

A large discrepancy is observed in the results of (3) and (26), with certainty in favor of (26). The difference determined for the extreme values of (26) with these in (3) is respectively:

- Example I – 105% at $h/b = 3,8$
- Example II – 112% at $h/b = 4,5$

There is a serious underestimation of the contribution of the beam forces to the value of the joint shear force, from the expressions known in the literature. The new model shows, that the contribution of the beam forces is greater.

Case II - Simple Beam

Example I- the modulus of elasticity of the concrete is

$$E_1 = 1700 \text{ [kN / cm}^2 \text{]}$$

Example II- the modulus of elasticity of the concrete is

$$E_1 = 3700 \text{ [kN / cm}^2 \text{]}$$

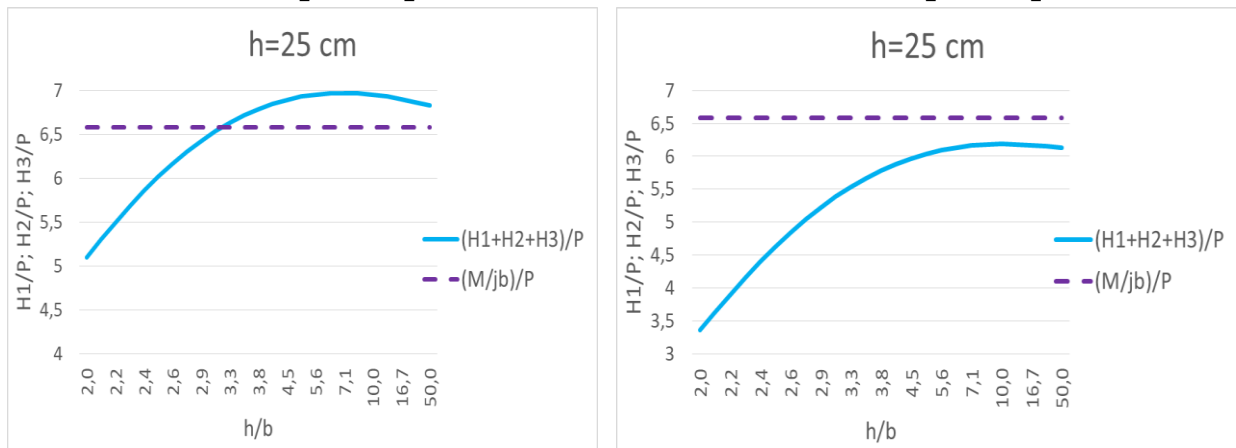


Figure 9. Comparison of the results of (3) and (26) - simple beam

For the simple beam, the results of the old and the new solution are almost similar.

The difference determined for the extreme values of (26) with these in (3) is respectively:

- Example I – 6% at $h/b = 7,1$, the certainty is in the direction of (26)
- Example II – 6% at $h/b = 10$, the certainty is in the direction of (3)

Conclusion

A solution of a cantilever beam with a special arrangement of the support devices was carried out. The real height of the beam was taken into account.

The derived expressions for the horizontal supports reactions, although not very short, give results which clearly show the distribution of the forces along the height of the beam, into corresponding support.

The derived expressions for the support reactions take into account the influence of both the geometry of the beam and the material properties of its components.

A comparison is made for the contribution to the value of the shear force from the forces in the beam determined with the obtained expressions and the formulas known from the literature.

A new model is proposed for determining the contribution of the beam forces to the value of the Shear Force in RC Interior Beam-Column Connections.

The obtained results can be of interest to both researchers and practicing engineers. The research from this article can help in the interpretation of the results obtained from structural analyzes and experimental tests.

Recommendations

This article will focus attention on how forces are distributed along the height of the beam and the subsequent load from the beam, on the beam-column connection, with an emphasis on determining the shear force at the joint.

Scientific Ethics Declaration

The author declares that the scientific ethical and legal responsibility of this article published in EPSTEM journal belongs to the author.

Acknowledgements or Notes

* This article was presented as an oral presentation at the International Conference on Research in Engineering, Technology and Science (www.icrets.net) held in Budapest/Hungary on July 06-09, 2023.

References

- Altoontash, A. (2004) *Simulation and damage models for performance assessment of reinforced concrete beam-column joints*. (Doctoral dissertation). Department of Civil and Environment Engineering, Stanford University, Stanford, California.
- Celik, O.C., & Ellingwood, E.R. (2008) Modelling beam-column joints in fragility assessment of gravity load designed reinforced concrete frames. *Journal of Earthquake Engineering*, 12, 357–381.
- Doicheva A., (2021) Off-center supported beam with additional elastic supports located at the height of the beam. *X-th International Scientific Conference on Architecture and Civil Engineering ArCivE*, Varna, Bulgaria (in Bulgarian), 370-379.
- Doicheva, A. (2022). Off-center supported beam with additional elastic supports located at the height of the beam and asymmetrical cross section. *International Conference on Basic Sciences, Engineering and Technology (ICBASET)*, 120-129.
- Hanson, N W., & Conner, H. W. (1967) Seismic resistance of reinforced concrete beam-column joint. *Journal of the Structural Division*, 93, 533-560.
- Lowes, L., & Altoontash, A. (2003) Modeling reinforced-concrete beam-column joints subjected to cyclic loading. *Journal Structural Engineering*, 129, 1686–1697.
- MathWorks. (2017). *MATLABR2017b*. Natick, USA.
- Park, R. (2002). A summary of results of simulated seismic load tests on reinforced concrete beam-column joints, beams and columns with substandard reinforcing details. *Journal of Earthquake Engineering*, 6 (2), 1-27.
- Park, R., & Keong, Y. S. (1979), Test on structural concrete beam-column joints with intermediate column bars. *Bulletin of the New Zealand National Society for Earthquake Engineering*, 12(3), 189-203.
- Park, R., & Paulay, T.(1975). *Reinforced concrete structures*. John Wiley & Sons.
- Paulay, T. (1989) Equilibrium criteria for reinforced-concrete beam-column joints. *ACI Struct Journal*, 86, 635–643.
- Paulay, T., M. J. N. Priestley, (1992), *Seismic design of reinforced concrete and masonry buildings*. John Wiley&Sons, Inc.
- Shafaei, J., Zareian M. S., Hosseini A., & Marefat M. S. (2014). Effects of joint flexibility on lateral response of reinforced concrete frames. *Engineering Structures*, 81, 412-413.
- Sharma, A., Reddy G.R., Vaze K.K., Ghosh A.K., Kushwaha H.S., Eligehausen R. (2009). *Joint model to simulate inelastic shear behavior of poorly detailed exterior and interior beam-column connections reinforced with deformed bars under seismic excitations*. Bhabha Atomic Research Centre. https://inis.iaea.org/search/search.aspx?orig_q=RN:41076014
- Shiohara, H. (2001) New model for shear failure of RC interior beam-column connection. *Journal of Structural Engineering*, 127(2), 152-160.

- Tran, T. M., Hadi, M. N. S., & Pham, T. M. (2014). A new empirical model for shear strength of reinforced concrete beam – column connections. *Magazine of Concrete Research*, 66(10), 514-530.
- Uma, S. R., & Jain, S.K. (2006), Seismic design of beam-column joints in RC moment resisting frames - review of codes. *Structural Engineering and Mechanics*, 23(5), 579-597.

Author Information

Albena Doicheva

University of Architecture, Civil Engineering and Geodesy (UACEG)

Sofia, Bulgaria

Contact e-mail: *doicheva_fhe@uacg.bg*

To cite this article:

Doicheva, A. (2023). Determination of the shear force in RC interior beam-column connections. *The Eurasia Proceedings of Science, Technology, Engineering & Mathematics (EPSTEM)*, 23, 361-371.

The Eurasia Proceedings of Science, Technology, Engineering & Mathematics (EPSTEM), 2023

Volume 23, Pages 372-380

ICRETS 2023: International Conference on Research in Engineering, Technology and Science

Development of Inventory Model for Perishable Product with Dynamic Pricing

Teodosius Raditya Ananto

Sepuluh Nopember Institute of Technology

Nurhadi Siswanto

Sepuluh Nopember Institute of Technology

Abstract: Perishable products are products whose value decreases over time. Inventory management for perishable products is a challenge experienced by retailers. Problems arise when inventory costs increase due to a large amount of wasted or waste products. This research aims to maximize profit by providing policy recommendations for inventory procurement under dynamic pricing. This research optimization focuses on determining the optimal order size and reorder level. To solve this problem, a simulation model is created by considering changes in product prices as product quality decreases. The simulation method in this study is a discrete event simulation using simulation software. Events in this inventory simulation include the arrival of customers and the addition or reduction of inventory levels. The replenishment policy in this study is continuous reviews. Simulation scenarios were generated to obtain an optimum order size and reorder level. The best scenario is obtained from a combination of optimum order size and reorder level. An inventory simulation model was generated based on fruit inventory data at one of the major retailers in Indonesia.

Keywords: Perishable product, Inventory model, Dynamic pricing, Discrete event simulation

Introduction

Inventory is one factor determining the level of costs retailers incur in their business activities. In this paper, we focus on perishable product inventory management. Perishable products have a useful life, such as food, vegetables, human blood, etc (Goyal and Giri, 2001). Challenges that can be experienced by retailers in managing the inventory of perishable products are food loss, food waste, and food surplus (Papargyropoulou et al., 2014). Food waste is wholesome edible material intended for human consumption, arising at any point in the food supply chain that is instead discarded, lost, degraded, or consumed by pests (FAO, 2011). Food waste at retailers of a food supply chain imposes a high cost since the operating cost is high while the overall margins on food products are lower (Teller, et al., 2018).

Various problems can be experienced by retailers in managing the inventory of perishable products. An example of a problem is the decreased quality of food products in the warehouse (Fauza, 2013). This decrease in quality will cause food waste because food products are considered unfit for sale. Factors causing the decline in food quality include food, including products that are dynamic or change over time (Heldman, 2011). Feng (2017) researched maximizing inventory profit with perishable product demand as a multivariate function of unit price, freshness condition, and inventory level simultaneously.

In this paper, we focus on maximizing the profit of perishable product inventory under dynamic pricing. Perishable product inventory management has many factors. Chaudary et. al (2018) divide these factors into demand type, shelf life, replenishment policy, and modeling techniques. Dynamic pricing based on quality is often used on perishable products such as apples Kayicki et al. (2022) and meat Buisman et al. (2019). This

- This is an Open Access article distributed under the terms of the Creative Commons Attribution-Noncommercial 4.0 Unported License, permitting all non-commercial use, distribution, and reproduction in any medium, provided the original work is properly cited.

- Selection and peer-review under responsibility of the Organizing Committee of the Conference

© 2023 Published by ISRES Publishing: www.isres.org

study will focus on stochastic demand and random shelf life. Simulation-based on dynamic pricing is used to decide the optimal reorder point and order size as the replenishment policy.

Method

Dynamic Pricing Based on Quality for Perishable Products

This research will refer to the model of Kayicki et al., (2022) in dividing the freshness level percentage into multiple stages, namely 100% -80%; 80%-60%; 60%-20%; and <20%. Our research object is avocado fruit so in determining the quality or freshness score, we refer to the research of Sierra et al., (2019). This study used life expectancy units based on fruit firmness according to storage temperature. The relationship between avocado fruit firmness and life span was analyzed by linear regression using the Arrhenius formula. The study stated that the best quality fruit had a firmness level of $143.4 \pm 7.9N$, while the lowest firmness was 9.8N. We combined these two research as the basis of quality decrease and selling price. Avocado quality and selling price have 3 levels. Optimum quality has the highest selling price, while the lowest quality will be disposed of. Premium, medium, and poor-quality limits are 120 N, 80 N, and 40 N, respectively. After passing these 3 quality levels, the fruit is considered unfit for sale and becomes waste.

Conceptual and Simulation Model

The conceptual and simulation model of the perishable product inventory was made before optimization. The model's Variables consisted of state, parameter, decision, response, and binary. The decision variables were reorder level (kg) and order size (kg). The main response variables are profit (Rp) and loss from expired (kg). Table 1 provides further details on all variables used in the simulation.

Table 1. List of variables in simulation

Variable Type	Variable Name	Explanation	Initial Value
State	Inventory	Amount of inventory per time	50
	Firmness	Firmness value per unit time	143,3
	SellPrice	Selling price per kg (Rp/kg)	17000
	ArrTime	Arrival time of fruit supply	-
Parameter	DiscountRate	Discount rate per quality	5%
	InitialSellPrice	Best quality product selling price (Rp/kg)	17000
	MaxStock	Maximum inventory capacity (kg)	50
	Demand	Demand rate from customer	-
Decision	PriceExpectations	Price expectations each customer	NORM (17000;400)
	ReorderLevel	Inventory level to reorder	-
	OrderSize	Quantity of fruit to buy from supplier	-
Response	Profit	Profit in Rupiah	-
	FruitExpired	Number of expired fruit (kg)	-
	AmountLost	Number of lost sales fruit (kg)	-
	LostCustomer	Number of lost customer (person)	-
Binary	DemandMet	Number of demands met (kg)	-
	OrderOn?	Binary decision for fruit supply	0

Initial values on variables were based on the company's data and policy. Limitations of this simulation are maximum order size should not exceed the maximum inventory capacity, which is 50 kg. There is also an assumption that the initial conditions and quality degradation of each fruit in one batch are homogeneous or the same. Fruit quality in the model applies to one batch (kg).

There are two data inputs needed for simulation, which are customer arrival rate and demand per customer rate. Data fit distribution from the company's record is done to obtain the probability distribution expression of these two inputs. The expression for customer arrival rate and demand per customer rate is $3,5 + WEIB(8,41; 1,86)$ and $LOGN(0,571; 0,809)$, respectively. We make a conceptual model before building a simulation model. Figure 1 provides a conceptual model of perishable product inventory.

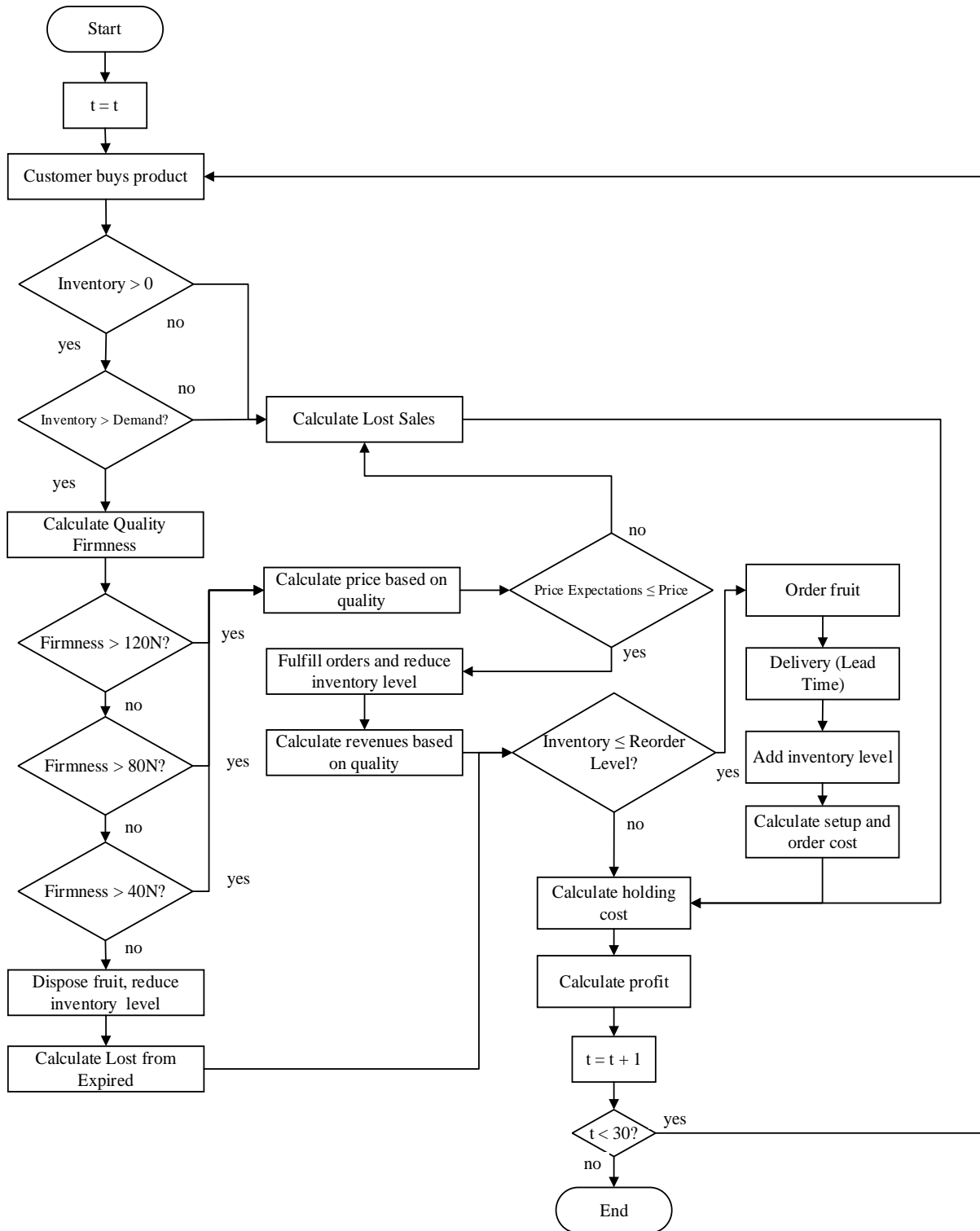


Figure 1. Conceptual model for perishable product inventory

The simulation model runs once every day. The time unit t in the conceptual model represents days 1 to n . The stopping criterion in this simulation model is when the simulation has been running for 30 days. The simulation begins with the arrival of customers per time. Consumers who come have a number of orders for avocados with a certain probability distribution. Customer requests will be met if inventory is available, and vice versa becomes lost sales if inventory is not available. If the inventory level has touched the reorder point, the retailer will order products from the supplier in the amount of order size. The price of the product will decrease as the quality decreases. Profit will be calculated from revenue based on quality minus lost sales costs, ordering costs, and lost expired costs. Another measured performance is the number of expired fruits based on the number of fruits discarded during the simulation.

Experimental Design and Optimization using Simulation

The experimental design and optimization of scenarios of the perishable product inventory were investigated by using the simulation method. Scenarios are generated using OptQuest ARENA tools. The input needed to use this tool is objective, constraints, and the range value of each decision variable. The best scenario is the combination of optimum reorder level and order size. Table 2 provides the experimental design used in the optimization process.

Table 2. Experimental Design for Optimization

Decision Variable	Variable Value Range (kg)		
	Minimum	Maximum	Increment
Order Size	5	50	5
Reorder Level	5	50	5

The model’s objective is to maximize profit with a limitation of maximum order size (50 kg). All decision variables have the same minimum, maximum, and increment values. Every possible scenario combination based on the decision variable value range will be run until the optimum solution or scenarios are found.

Results and Discussion

Optimum Solution

After all possible scenarios have been generated, the optimization is continued with OptQuest. Table 3 shows the 3 best scenarios resulting in maximum profit. Mark * in #NewBest indicates the best-case scenario as optimization progresses. The best scenario results are in the ninth iteration: the combination of the decision variables Order Size 15 kg and Reorder Level 5 kg.

Table 3. Optimum Scenarios for Profit Maximization

#NewBest	Iteration	Objective Value (Profit)	Constraint Order (≤ 50)	Order Size (kg)	Reorder Level (kg)
*	7	431102,01	30	30	5
*	8	454768,38	20	20	5
*	9	477299,70	15	15	5

This scenario generates a maximum profit of approximately IDR 477299.70 / month. The summary of maximum profit results from each iteration can be seen in Figure 2.

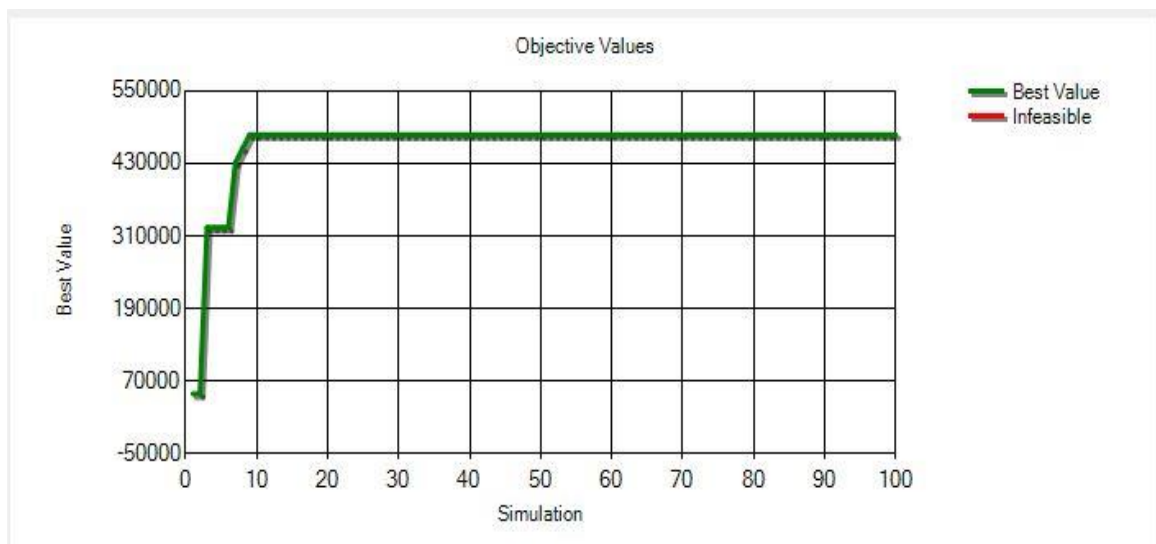


Figure 2. Maximum profit of simulation

The graph above shows the maximum profit from all scenarios as the optimization progresses. The graph shows no change in the maximum profit after the 9th scenario until the end of the optimization.

Sensitivity Analysis

Sensitivity analysis is performed by changing the price, discount rate, and order size to profit. An important variable used for sensitivity analysis is *PriceExpectations* or price expectations from customers. This variable represents the customer's shopping interest which is influenced by price expectations and the selling price itself. The analysis was carried out with the Process Analyzer and displayed in graphs.

Effect of Selling Price to Profit

The initial selling price of the simulation model is IDR 17,000. This value will be changed with a certain range to see the effect on profit. Other variables have fixed values, namely order size (15kg), reorder level (5kg), and discount (10%). Figure 3 shows a comparison of the selling price and profit.

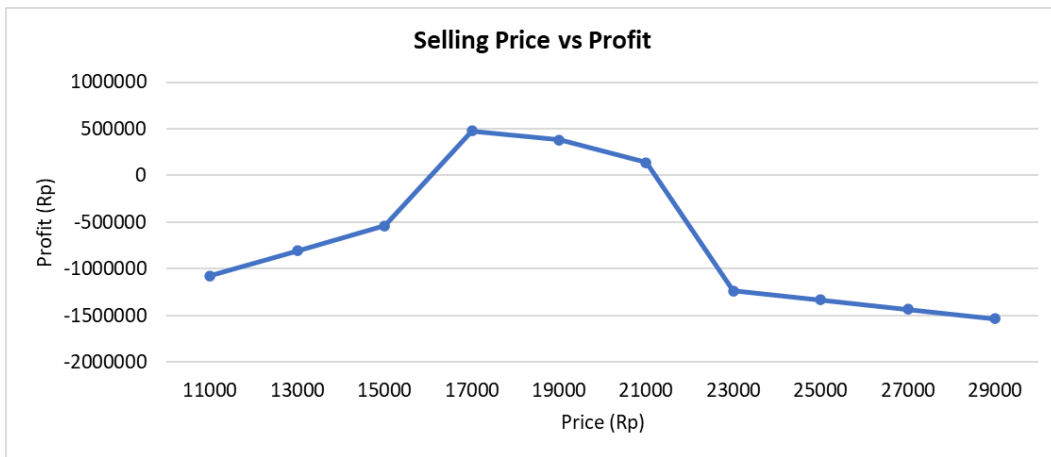


Figure 3. Sensitivity analysis selling price vs profit.

The graph above shows that the profit will increase as the selling price increases to IDR 17,000/kg. The 17,000-intersection point represents the maximum profit and minimum lost fruit. After that, the profit will decrease significantly. This is because prices that are too high will reduce customer interest in fruit shopping. Figure 4 shows the number of fruits sold for each price.

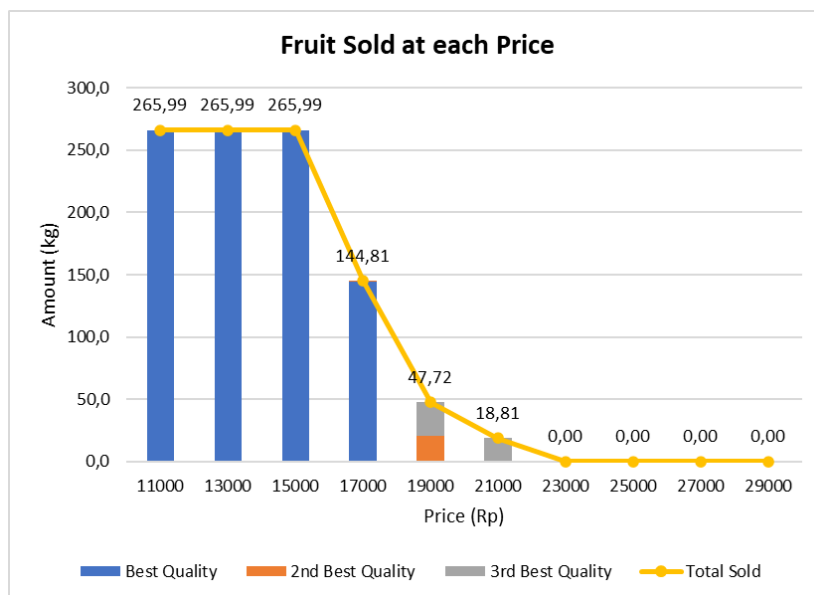


Figure 4. Fruit sold at each price.

Lost sales and expired fruit will increase as the price rises to IDR 23,000. Figure 5 shows the graphic of the number of lost on each price. This sensitivity analysis suggested that retail does not increase the selling price by more than IDR 17,000 to maintain the maximum profit value of IDR 477,299.70.



Figure 5. Fruit lost on each price

Effect of Discount Rate on Profit

The initial discount rate on the model is 10%. This value will be changed with a certain range to see the effect on profit. Other variables have fixed values: order size (15kg), reorder level (5kg), and a selling price of IDR 17,000/kg. Figure 6 shows a comparison of the discount rate and profit.



Figure 6. Sensitivity analysis discount rate vs profit

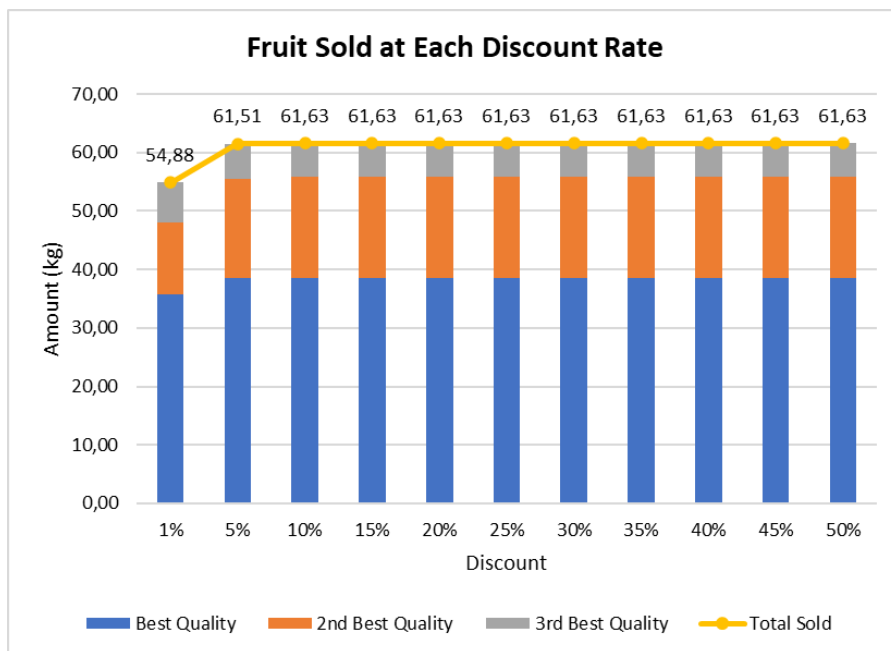


Figure 7. Fruit sold at each discount rate

The graph above shows that the profit will increase as the discount percentage increases to 5%. The 5% discount intersection point represents the maximum profit and minimum lost fruit. After that, the profit will decrease significantly. Initially, the profit value will increase as the discount given increases. A large discount value will increase customer shopping interest, increasing profit value. Furthermore, the profit value decreases at a discount rate of 5% and above. A discount that is too large causes total revenue to decrease, so it cannot cover revenue costs even though shopping interest remains high. Figure 7 shows the number of fruits sold for each discount rate.

After touching the discount rate of 5% and above, the number of fruits sold for each quality has the same value. This is because price expectations from customers have been fulfilled since the 5% discount was given. The profit value still has a difference caused by the difference in the selling price of each discount. The greater the discount given, the effect on the decrease in income received. Figure 8 shows the number of lost on each discount rate.



Figure 8. Fruit lost on each discount rate

The total lost value has the same result from 10% off and above. This is also related to the total value of the number of fruits sold, which is stable after a certain discount. So, this sensitivity analysis suggests that retail does not increase the discount percentage by more than 5% to maintain the maximum profit value, which is approximately IDR 376,182.4.

Effect of Order Size on Profit

The order size value on the model is 15kg. This value will be changed with a certain range to see the effect on profit. Other variables have a fixed value: the reorder level (5kg), a 10% discount, and a selling price of IDR 17,000/kg. Figure 9 shows a comparison of the order size and profit.

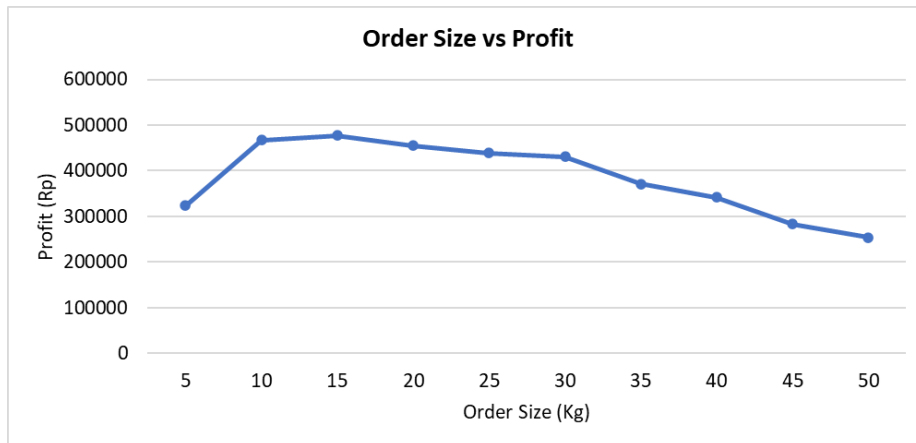


Figure 9. Sensitivity analysis order size vs profit

The graph above shows that profit will increase as the order size value increases to 15 kg. The intersection point of the 15 kg batch size represents the maximum profit and the minimum number of fruits lost. After passing this point, profits will decrease significantly. The profit value will initially increase as the batch size value used increases. A high batch size value will increase the amount of inventory, thereby reducing the possibility of lost sales. Furthermore, the profit value begins to decrease in the order size value of 15 kg and above. An order size value that is too large makes the inventory too high to exceed the customer's shopping interest. As a result, there will be an increase in expired or expired fruit. Figure 10 shows the number of fruits sold for each order size.

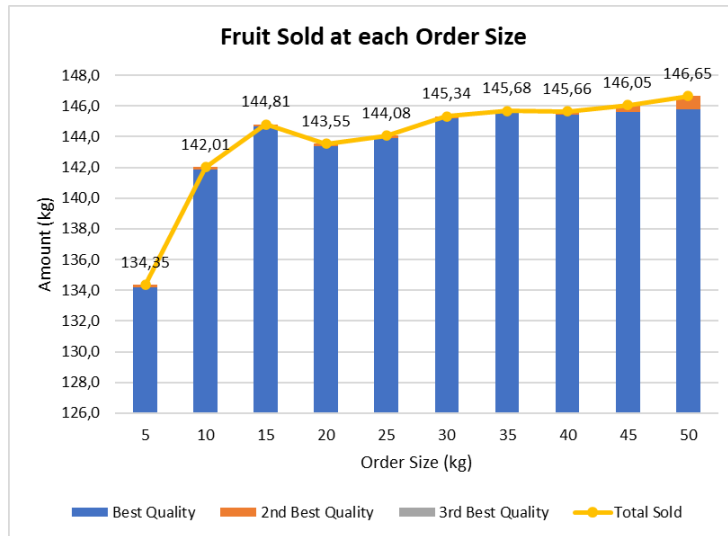


Figure 10. Fruit sold at each order size

The total number of fruits sold has an increasing trend as the batch size value increases. Most of the fruit sold is premium quality. This means that the demand for fruit is high, so the fruit sold has not experienced a decline in quality. Figure 11 shows the number of lost on each order size.



Figure 11. Fruit lost on each order size

Most of the lost are lost sales due to unfulfilled customer requests. The expired amount value in each order size has a value of 0. This means that customer demand is high, so the supply has run out before the fruit expires. So, in this sensitivity analysis, it is suggested that retail does not use an order size value of more than 15 kg to maintain the maximum profit value of approximately IDR 477,299.70.

Conclusion

This research uses simulation to optimize the order size and reorder level of perishable product inventory on retailers. The quality type of fruit firmness is used to determine the dynamic pricing of the product. The inventory simulation model obtains a maximum profit of IDR 477,299.7 with a scenario combination of order size and reorder level. The optimum order size value is 15 kg, and the reorder level value is 5 kg. Sensitivity analysis shows that the value of order size, discount rate, and selling price impact the profit value. Research

suggests that the order size value is no more than 15 kg, the discount is no more than 5%, and the selling price is no more than IDR 17,000/kg so that profits do not decrease.

Scientific Ethics Declaration

The authors declare that the scientific ethical and legal responsibility of this article published in EPSTEM journal belongs to the authors.

Acknowledgements or Notes

This article was presented as an oral presentation at the International Conference on Research in Engineering, Technology and Science (www.icrets.net) held in Budapest/Hungary on July 06-09, 2023.

References

- Buisman, M. E., Haijema, R., & Bloemhof-Ruwaard, J. M. (2019). Discounting and dynamic shelf life to reduce fresh food waste at retailers. *International Journal of Production Economics*, 209, 274-284.
- Chaudhary, V., Kulshrestha, R., & Routroy, S. (2018). State-of-the-art literature review on inventory models for perishable products. *Journal of Advances in Management Research*, 15(3), 306-346.
- Fauza, G., Amer, Y., & Lee, S. H. (2013). *Model of an integrated procurement-production system for food products incorporating quality loss during storage time*. Volume 75 IACSIT-Internal Association of Computer Science.
- Feng, L. (2019). Dynamic pricing, quality investment, and replenishment model for perishable items. *International Transactions in Operational Research*, 26(4), 1558-1575.
- Goyal, S. K., Giri, B.C. (2001). Recent trends in modelling of deteriorating inventory. *European Journal of Operational Research*, 134, 1 – 16.
- Heldman, D., R. (2011). "2 – kinetic models for food systems," in *food preservation process design* (pp. 19-48). San Diego: Academic Press.
- Kayikci, Y., Demir, S., Mangla, S. K., Subramanian, N., & Koc, B. (2022). Data-driven optimal dynamic pricing strategy for reducing perishable food waste at retailers. *Journal of Cleaner Production*, 344, 131068.
- Papargyropoulou, E., Lozano, R., Steinberger, J. K., Wright, N., & bin Ujang, Z. (2014). The food waste hierarchy as a framework for the management of food surplus and food waste. *Journal of Cleaner Production*, 76, 106-115.
- Sierra, N. M., Londoño, A., Gómez, J. M., Herrera, A. O., & Castellanos, D. A. (2019). Evaluation and modeling of changes in shelf life, firmness, and color of 'Hass' avocado depending on storage temperature. *Food Science and Technology International*, 25(5), 370-384.
- Teller, C., Holweg, C., Reiner, G., & Kotzab, H. (2018). Retail store operations and food waste. *Journal of Cleaner Production*, 185, 981-997.

Author Information

Teodosius Raditya Ananto

Sepuluh Nopember Institute of Technology
Surabaya, Indonesia
Contact e-mail: anantoteo@gmail.com

Nurhadi Siswanto

Sepuluh Nopember Institute of Technology
Surabaya, Indonesia

To cite this article:

Ananto, T. R. & Siswanto, N. (2023). Development of inventory model for perishable product with dynamic pricing. *The Eurasia Proceedings of Science, Technology, Engineering & Mathematics (EPSTEM)*, 23, 372-380.

The Eurasia Proceedings of Science, Technology, Engineering & Mathematics (EPSTEM), 2023

Volume 23, Pages 381-387

ICRETS 2023: International Conference on Research in Engineering, Technology and Science

Investigation of Magnetorheological Shock Absorber Used in Semi-Active Suspension

Ramazan Ferik
Maysan Mando A.Ş.

Murat Yazici
Bursa Uludag University

Orhan Kurtulus
Maysan Mando A.Ş.

Abstract: The automotive industry is rapidly moving towards autonomous vehicles. In this case, the answers of the vehicles can be change in different scenarios. At this point, the suspension system must be semi-active or fully active. Magnetorheological shock absorbers can be used in semi-active suspension systems. In this study, studies were carried out on the examination and testing of magnetorheological shock absorbers. These systems can change the stiffness of the shock absorber with the effect of magnetic field depending on the data coming from the road and the condition of the vehicle. It does this by changing the viscosity with the nano powders affected by the magnetic field. Ferromagnetic nanoparticle additives are used in the shock absorber. However, one of the biggest risks in these shock absorbers is the precipitation of nano powders in the oil. If this happens, it starts to fail to fulfill its shock absorber feature. To prevent this, oil density and nano powder density should be close. In this study, low density polystyrene coated with magnetic material and these particles was added to the oil in the shock absorber. As a result, particles with a density of 0.877 gr/cm³ were obtained and oil with a density of 0.971 gr/cm³. As a result of the observation, no significant precipitation was observed in the liquid formed. A prototype MR damper was produced using this mixture. In the next step, the effects of the electromagnetic field on the shock absorber were investigated and the shock absorber is controlled by electromagnetic field. As a result, the piston velocities of the damper in response to the force were measured under 3 different forces, without magnetic particles and at different current values after the magnetic particle was added. Damper hardening with current was observed.

Keywords: Shock absorber, MR damper, Semi-active suspension system, Nanocomposite

Introduction

The suspension system is located between the vehicle body and the wheel carrying the vehicle, and usually includes shock absorbers, springs, arms, bushing connections, etc. These are systems that provide comfort, safety and performance for the vehicle. As the automotive industry develops, suspension systems also constantly evolve. The main reason for better optimizing these systems in the development of the suspension system is to ensure safe driving by keeping the communication between the vehicle and the driver at a high level. The automotive suspension on a vehicle typically has the following basic tasks (Rajamani, 2012; Isermann, 2005):

- 1) To isolate a car body from road disturbances in order to provide good ride quality.

Ride quality in general can be quantified by the vertical acceleration of the passenger locations. The presence of a well-designed suspension provides isolation by reducing the vibratory forces transmitted from the axle to the vehicle body. This in turn reduces vehicle body acceleration.

2) To keep good road holding

The road holding performance of a vehicle can be characterized in terms of its cornering, braking and traction abilities. Improved cornering, braking and traction are obtained if the variations in normal tire loads are minimized. This is because the lateral and longitudinal forces generated by a tire depend directly on the normal tire load. The road holding performance of a suspension can therefore be quantified in terms of the tire deflection performance.

3) To provide good handling

The roll and pitch accelerations of a vehicle during cornering, Braking and traction are measures of good handling. Half-car and full-car models can be used to study the pitch and roll performance of a vehicle. A good suspension system should ensure that roll and pitch motion are minimized.

4) To support the vehicle static weight

This task is performed well if the rattle space requirements in the vehicle are kept small. The short working range of the suspension can play an important role in ensuring the weight balance of the vehicle.

As the automotive industry progresses, customer demands have also increased proportionally. Among these requests, there are issues that will take the safety and comfort of the vehicle to the next level. In addition to these requests, raising and lowering options that will improve visuals or hardness settings that will increase performance have also been added. Although all these adjustment parameters reveal weaknesses in strength, this weakness can be overcome with the development of technology and production methods.

Vehicles are exposed to impact and vibration due to the vertical movement of the wheel due to irregularities on the road. The first suspension system elements that absorb these vibrations are the springs, and preventing the vibrations from being transmitted to the chassis is possible by compressing the springs. After this compression, the aim is for the springs to relax slowly and slightly so that they do not continue the movement. Shock absorbers perform this task in the suspension system (Dixon, 2007).

Considering these and other functions of shock absorbers, their structural integrity must be preserved under operating conditions in order to continue their function. For this reason, the physical behavior of the lower parts of the shock absorber under different conditions should be examined and necessary precautions should be taken during the design phase. (Güney & Tüfekçi, 2016).

Suspension systems used in automobiles continue to become more complex as autonomous vehicle technology advances. The main reason for this situation is that different responses are expected from the vehicle under different conditions. In this case, the suspension must be activated. This need can be met with fully active or semi-active suspension. Fully active suspensions can change the operating parameters of the suspension system automatically or at the user's discretion. However, semi-active suspensions affect the operation of the suspension by changing the operating parameters of a component on the system, not all the parameters of the system. In this case, fully active suspensions have more variability, but are more expensive and can fail more often due to the more complex parts. Semi-active suspensions are relatively less complex, more reliable and less costly. Examples of fully active suspension systems include air suspension and electromechanical suspension. Examples of semi-active suspensions are active valve technology and magnetorheological shock absorbers.

Objective

Magnetorheological shock absorbers are becoming common in semi-active suspension systems in automobiles. In mr shock absorbers, magnetic particles added to the oil can change the viscosity of the oil with the effect of a magnetic field. Electromagnets are used to create a magnetic field. Accordingly, a magnetic field of a magnitude directly proportional to the magnitude of the electric current in the system will be generated. In this case, the magnetic particles will start to fulfill their task. Also, one of the biggest advantages of mr shock absorbers is that even if it loses its active feature, it can continue to work like a passive shock absorber. This increases the structural reliability of the shock absorber.

Method

This study was conducted in collaboration between Maysan Mando Turkey R&D Center and Uludağ University Automotive Engineering. In this study, the structure, working principle and usage areas of the MR shock absorber were examined in order to complete the deficiencies of passive shock absorbers. After this, an experimental investigation of the mr shock absorber was carried out with the prototype shock absorber produced. Experimental conditions are shown in Table 1.

Table 1. Force and magnetic field combination table

MAGNETIC FIELD EFFECT				
FORCE VALUES	0.72 N. Force without	0.72 N. Force with	0.72 N. Force with	0.72 N. Force with
	Magnetic Field	0.2 Ampere Current	0.3 Ampere Current	0.4 Ampere Current
	4 N. Force without	4 N. Force with	4 N. Force with	4 N. Force with
	Magnetic Field	0.2 Ampere Current	0.3 Ampere Current	0.4 Ampere Current
	7.1 N. Force without	7.1 N. Force with	7.1 N. Force with	7.1 N. Force with
	Magnetic Field	0.2 Ampere Current	0.3 Ampere Current	0.4 Ampere Current

An electromagnet was used in the experiment. It is aimed to observe the change in the magnetic field according to the current given on the electromagnet. Some of the prototype shock absorber parts were produced with a 3D printer. This gave the work an advantage in rapid prototyping. Polystyrene foam with low density was used to prepare magnetic particles. In this way, the density of the composition using metal powder could be controlled.

Material

Silicone oil was used as the carrier phase and polystyrene foam and iron powder were used for magnetic particles.

Carrier Phase (Oil)

Silicone oil was used as the carrier phase. It is colorless and odorless. Usually easy to find on the market. They have different properties according to their varying viscosity values and chemical structures. It can protect its physical properties between -700 °C and 2500 °C. For these reasons, silicone oil would be ideal for the experiment. The specific properties of silicone oil are shown in Table 2.

Table 2. Specific properties of silicone oil

Silicone Oil	DM1000
Viscosity (cst)	1000
Flash Point (°c)	> 300
Freeze Point (°c)	-50
Density at 25 °C(gr/cm^3)	0,971
Surface Tension (mN/m)	21,2
Refractive Index (25 °C)	1,403

Magnetic Particles

Polystyrene grain with relatively low density was used in the experimental shock absorber. Contrary to common usage, polystyrene was coated with metal powder in this study. In this way, the density of the mixture could be controlled. This is important to prevent the particles from settling or floating in the oil.

Table 3. Specific properties of polystyrene

Specific properties of polystyrene	Value
Density (gr/cm^3)	0,02814
Thermal Conductivity (W/m.K)	0,037-0,039
Water Absorption (%; 24 hours)	0,03-0,1
Particle Diameter (mm)	1,5-2
Bending Strength (kPa)	75-125
Compression Stress at 10% Deformation (kPa)	1,403

Polystyrene

It is a synthetic and aromatic polymer obtained using styrene monomer, a liquid petrochemical. It can be hard or foamy. It is a polymer with low unit cost. While transparent in its natural state, color can be added using colorants. Specific properties of polystyrene are shown in Table 3.

Carbonyl Iron

Its grain structure is very small. This will make it easier to coat the polystyrene. It is mixed with the adhesive to form a resin, which is then applied to the polystyrene and magnetizes the polystyrene. polystyrene material will be more in volume, the density will remain low. Specific properties of carbonyl iron are shown in Table 4.

Table 4. Specific properties of polystyrene

Specific properties of polystyrene	Value
Density (gr/cm^3)	7,86
Particle Diameter (μm)	5
Iron percentage (m/m, %)	> 97

Magnetic Particle Production

When polystyrene material interacts with some liquids, it dissolves on its surface and becomes sticky. Acetone ($\text{C}_3\text{H}_6\text{O}$) is one of these liquids. The surface of the polystyrene material in contact with a small amount of acetone erodes and becomes sticky. This allows iron dust to adhere to the surface of the polystyrene. In this way, the magnetic particles are ready. Figure 1 shows these coating stages.



Figure 1. Stages of coating polystyrene with iron powder

Magnetic Particle Addition

In order to observe whether these magnetic particles would decompose in silicon, the particles were kept in silicon liquid for 3 days. In this mixture, 70% oil and 30% magnetic particles were used by volume. No significant segregation of the particles or precipitation in the liquid was observed at the end of the expected time. The magnetic particles obtained were examined under a microscope. Diameter values are between 1.7 and 2.7 mm.

Electromagnet

Electromagnets are made by coiling insulated thin wires around matter. When current is applied to this coiled cable, a magnetic field is created. The gravitational force of the electromagnet will increase or decrease in direct proportion to this current. The operating voltage of the electromagnet gives us information about the ranges in

which we can work. In this study, a 20 mm. high, 25 mm. diameter electromagnet was used. This magnet works with DC current. Specific properties of electromagnet are shown in Table 5.

Table 5. Specific properties of electromagnet

Specific Properties of Electromagnet	Value
Work Voltage (V)	12
Work Area (A)	0,3
Power (W)	4
Retention Force (N)	50
Magnet Diameter (mm)	10

Prototype Mr Shock Absorber

Some parts of the prototype shock absorber were produced using a 3D printer. This technology was utilized in the rapid prototyping part. The requested design was also achieved in this way. Figure 2 shows the visuals of these parts.



Figure 2. Shock absorber parts produced with 3D printer

The produced parts were then assembled and the experimental setup was prepared. The fluid used in the prototype shock absorber contains 65% silicone oil and 35% magnetic particles by volume. Figure 3 shows the experimental setup prepared. The quantity of magnetic particles used is about 16 ml. In return, around 30 ml. of silicone oil was used.

During the test, a force of 0.72 N, 4 N and 7.1 N was applied to the shock absorber. The speed of the piston in response to these forces will give information about the stiffness of the shock absorber. The lower velocity at high force can be considered as an increase in hardness.



Figure 3. Test setup

Results and Discussion

In the experiments for comparison, the velocity, was first measured without the addition of magnetic particles for reference. Afterwards, particles were added and experiments were carried out under a current of 0.2 A, 0.3 A and 0.4 A. The achieved test results are shown in Table 6.

Table 6. Test results

	No magnetic field No particles	0.2 Amper	0.3 Amper	0.4 Amper
0.72 N.	0.179 cm/sn	0.047 cm/sn	0.054 cm/sn	0.062 cm/sn
4 N.	1.101 cm/sn	0.406 cm/sn	0.531 cm/sn	0.772 cm/sn
7.1 N.	2.083 cm/sn	0.550 cm/sn	0.954 cm/sn	0.973 cm/sn

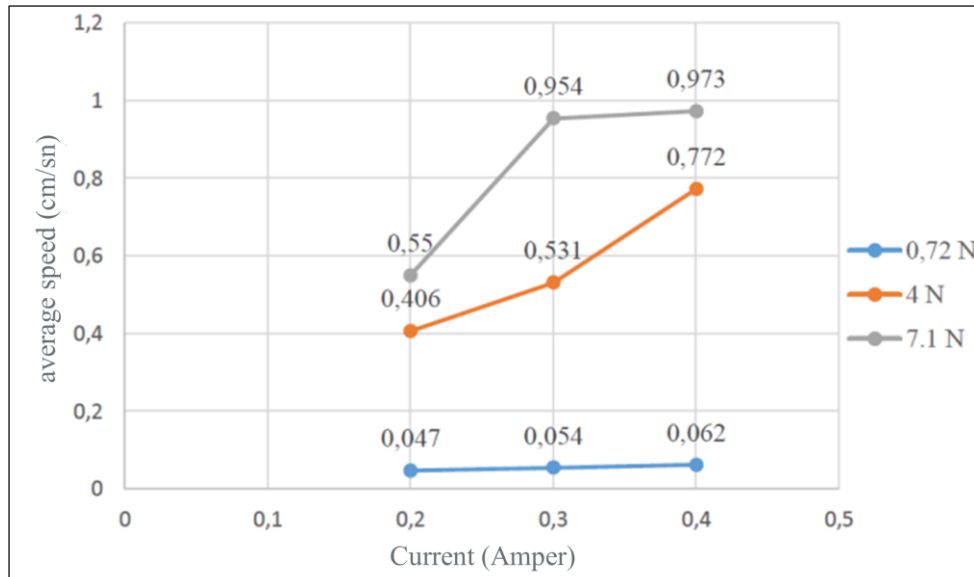


Figure 4. Graph of velocities obtained in test results

As seen in the results, the velocity values obtained after the addition of magnetic particles decreased significantly compared to the previous situation. The increase in velocity as the current increases is also due to some wear and tear in the setup due to the experimental conditions. In the next stages of the study, this situation will be prevented and more accurate control will be ensured depending on the current.

Another important issue, the problem of precipitation in mr shock absorbers, has also been prevented. The oil has a density of 0.971 gr/cm^3 , On the other hand, the average density of the particles produced from polystyrene and iron powder was 0.877 gr/cm^3 . In this case, due to the close densities, problems such as sedimentation or floating are not encountered.

As seen in the study, mr dampers provide an increase in force. However, the control of this increase is not always as planned. This may be due to inadequate test conditions or particle size. After this study, the test shock absorber will be prepared with more accurate materials in the following stages. In this way, more stable operation can be achieved. By reducing the particle structure, the test can be repeated with a piston with a better groove structure.

The magnetic particles have a density close to the carrier liquid, preventing precipitation or floating. This is important for the shock absorber to give the correct performance after a longer period. These characteristics are also mentioned in different scientific publications. Sedimentation stability is also mentioned in the scientific publication by Ergin & Altıparmak (2013). In the study, experiments were conducted with particles with different settling rates. As a result, it was decided to use the least settling particle.

In the scientific publication by Söylemez (2018), another study on this subject, the effect of different temperature values on the magnetic field was examined. the related study, experiments were carried out with different temperatures under the same conditions. Different evaluation criteria such as temperature can be added to our study. This allows more comprehensive correlations to be made and the correct operating position for the shock absorber to be found by controlling temperature and current.

Conclusion

In conclusion, there is still room for improvement in the field of Mr shock absorbers. With advancing technology, different manufacturing methods and composite materials can be used to increase both the structural strength and operational stability of shock absorbers. We will continue our efforts to take important steps by working to make developments even faster.

Scientific Ethics Declaration

The scientific ethical and legal responsibility of this article published in EPSTEM journal belongs to Ramazan FERİK as the main author.

Acknowledgements

*I would like to thank Prof. Dr. Murat YAZICI and Orhan KURTULUŞ for their support and continuous help in my master's thesis.

* This article was presented as an oral presentation at the International Conference on Research in Engineering, Technology and Science (www.icrets.net) held in Budapest/Hungary on July 06-09, 2023.

References

- Dixon, J. C. (1999). *The shock absorber handbook*. SAE International.
- Ergin T., & Altıparmak D. (2013). Karbonil demir ve manyetit esaslı manyetoreolojik sıvıların sönümleme performansı ve katkı maddesi olarak silika dumanı kullanımı. *Gazi Üniv. Müh. Mim. Fak. Der. Cilt 28*, No 4, 695-703.
- Güney S., Tüfekçi M. (2016). Hafif ticari araç amortisörünün çalışma koşulları altındaki yapısal analizi, testleri ve sonuçların korelasyonu, *IMSEC*; 4224-4232
- Isermann, R. (2005). *Mechatronic systems fundamentals*. Springer, New York.
- Rajamani R. (2012). *Vehicle dynamics and control, mechanical engineering series*, 2nd edition. Springer, New York.
- Söylemez M. E., (2018). *Farklı sıcaklık şartları altında manyetoreolojik sıvılı bir sönüm elemanının dinamik karakterizasyonunun elde edilmesi* (Master's thesis, Sakarya Üniversitesi).

Author Information

Ramazan Ferik
Maysan Mando A.Ş.
Bursa/TURKEY
rferik@maysanmando.com

Murat Yazici
Bursa Uludağ University
Bursa/TURKEY

Orhan Kurtuluş
Maysan Mando A.Ş.
Bursa/TURKEY

To cite this article:

Ferik R., Yazici, M. & Kurtulus O. (2023). Investigation of magnetorheological shock absorber used in semi-active suspension. *The Eurasia Proceedings of Science, Technology, Engineering & Mathematics (EPSTEM)*, 23, 381-387.

The Eurasia Proceedings of Science, Technology, Engineering & Mathematics (EPSTEM), 2023

Volume 23, Pages 388-399

ICRETS 2023: International Conference on Research in Engineering, Technology and Science

Internet of Things (IoT): Wireless Communications for Unmanned Aircraft System

Thi Minh Nhut Vo

National Kaohsiung University of Science and Technology

Chia-Nan Wang

National Kaohsiung University of Science and Technology

Fu-Chiang Yang

National Kaohsiung University of Science and Technology

Van Thanh Tien Nguyen

Industrial University of Ho Chi Minh City

Mandeep Singh

University of Technology Sydney,
The University of New South Wales

Abstract: In times of technological advancements, the use of aerial vehicles (UAVs), commonly known as drones, has become increasingly prevalent across various commercial and industrial sectors. UAVs find applications in agriculture, filmmaking, law enforcement, package delivery, aerial photography, videography, etc. There are benefits associated with utilizing UAVs. One key advantage is their ability to cover areas quickly and efficiently while accessing locations that may be challenging or hazardous for humans. Wireless communication technologies play a role in ensuring the functioning of Unmanned Aircraft Systems (UAS). Without these technologies, the United States of America would face difficulties communicating with ground control stations or relaying information to operators. This would significantly impede the country's mission execution and overall responsibilities. Wireless communication technologies (WCT) enable the United States to maintain awareness—essential for achieving successful and secure operations. Additionally, wireless technologies allow for Unmanned Aerial Systems (UAS) control, which is crucial for missions carried out in hostile or dangerous environments. The increasing usage of drones has highlighted the need to improve networks in the United States focusing on their ability to work together effectively handle volumes of data and provide reliable broadband connectivity. This research delves into communication technologies, in this domain emphasizing their advantages, limitations, industry standards and potential areas for future investigation to address the challenges revealed by this study.

Keywords: Wireless communications, Drones, A.I. security, Internet of things-IoT, Internet of drones.

Introduction

The Internet of Things (IoT) and innovative technology enhance control, automation, and domain efficiency. IoT is being utilized in many sectors such as healthcare, agriculture, smart cities, military, and other sectors to improve services and operations. As technology advances, it will create opportunities for streamlining processes, enhancing customer experiences and boosting efficiency. The up-to-date total number of IoT devices is expected to triple from about 9.7 billion in 2020 to about 29 billion by 2030. Both consumer markets and business verticals adopt devices extensively. By 2020 it is projected that the consumer market will account for

- This is an Open Access article distributed under the terms of the Creative Commons Attribution-Noncommercial 4.0 Unported License, permitting all non-commercial use, distribution, and reproduction in any medium, provided the original work is properly cited.

- Selection and peer-review under responsibility of the Organizing Committee of the Conference

© 2023 Published by ISRES Publishing: www.isres.org

than 60% of all connected devices a trend that is anticipated to remain consistent over Drones are among the devices utilized in both public and private sectors. In settings drones have applications including search and rescue missions, mapping land areas, conducting surveys and delivering medical supplies to remote locations. Drones have found applications in the sector including photography delivering goods and agricultural purposes. Looking ahead drones are anticipated to have a substantial impact on our daily lives. Their usage is expected to expand into areas such as search and rescue operations, traffic monitoring and weather observation. Unmanned Aircraft Systems (UAS) have diverse applications, including search and rescue, mapping, photography, and agricultural activities. With increasing internet-based technologies, drones are expected to revolutionize tasks in various fields. Wireless communications are crucial for safe and efficient UAS operations, providing real-time data to enhance decision-making and minimize risks. This article serves as an encompassing introduction to Wireless Communication Technologies for the UAS, exploring their potential applications and future implications in the rapidly expanding IoT landscape.

As unmanned aircraft system (UAS) technology is becoming particularly widespread in the present day, it should not be surprising that this study's objectives are aspirational. As a result, because this article is about Wireless Communication Technologies for the UAS, it ought to perform the function of an all-encompassing introduction to the subject matter.

Wireless Communications Technology History

James C. Maxwell proposed and verified the existence of electromagnetic waves in the 1860s (Kong, 1975; Sengupta, Sarkar, & Magazine, 2003), while Heinrich R. Hertz experimentally validated their presence in 1888 (Vainshtein, 1988). Marconi received Morse code from a spark-gap transmitter 2.4 kilometers away in 1895 (Smith & Pol., 2007). This experiment established wireless communication's essential structure. In wireless communication, the transmitter superimposes target information on a carrier wave, and the receiver extracts it (Lee, Shen, Lee, & Weng, 2016). After that, wireless technologies were created and upgraded for military usage. Broadcasting, one of the primary wireless uses, also increased commercially. Radio and T.V. began in the early half of the 20th century (Sarkar, Mailloux, Oliner, Salazar-Palma, & Sengupta, 2006). Since the late 1980s, wireless communication has been widely used in mobile phones and other mobile terminals as semiconductor and software technologies developed along with the internet's new infrastructure (Seymour & Shaheen, 2011). These change corporate and social models (Seymour & Shaheen, 2011).

Wireless communication technologies are developing and spreading. Wireless sensor network research and development is accelerating (Abdalkafor & Aliesawi, 2022). New systems are being created that can operate for several years on batteries while configuring their networks. Wireless digital technologies have advanced, and their practical utility for tackling security difficulties like radio interception or interference has progressed. Wireless communication technologies are spreading to fields such as disaster prevention, disaster response, crime prevention, security checks, environmental protection, health and welfare, transport, and logistics, and building monitoring and control (Parikh, Kanabar, & Sidhu, 2010; Ramli & Ahmad, 2011; Yang et al., 2015; Zeng, Zhang, & Lim, 2016; Zheng, You, Mei, Zhang, & Tutorials, 2022). Figure 1 provides an overview of recent wireless communication protocols applied for drones.

Wireless Communication Technologies

Wireless technologies are transforming the operation of unmanned aerial vehicles. With the capacity to communicate data wirelessly, UAVs may now be remotely controlled, allowing for greater operational flexibility and efficiency (Khandal, Jain, & Technology, 2014; H. Kim & Choi, 2016). In addition, wireless technology enables real-time monitoring of UAVs, enabling operators to make decisions and take swift action (Alsemmeiri, Bakhsh, & Alsemmeiri, 2016; Arya, Bhadoria, & Chaudhari, 2018; Molisch, 2012; Zheng et al., 2022). This strength is crucial in missions where time is of the essence, such as search and rescue missions. At the data link layer, several wireless technologies are now accessible to application developers. Each technology has distinctive qualities that make it attractive and acceptable for use (Beke et al., 2018; C. Chen et al., 2022; J. Chen, Wang, Zhou, Ahmed, & Wei, 2021; Custers, 2016; Nouacer et al., 2020; Savkin, Verma, & Anstee, 2022). Dependability, security, safety, and the absence of guiding cables are just a few of the critical advantages of WCT. The many technologies used for wireless communication in IoT devices have been covered by when selecting the most suitable IoT communication-based applications, authors considered the following 7 WCTs (Haider et al., 2022; Kamruzzaman, 2022; Nguyen, Masaracchia, Sharma, Poor, & Duong, 2022; Oberascher, Rauch, Sitzenfrei, & Society, 2022; C. Pu & Zhu, 2022; Shilpa, Radha, & Movva, 2022; Tlili, Mnasri, & Val,

2022; Yu, Das, Park, & Lorenz, 2022). In Table 1, we show the most recently applied WCT technologies for UAS and the related parameters.

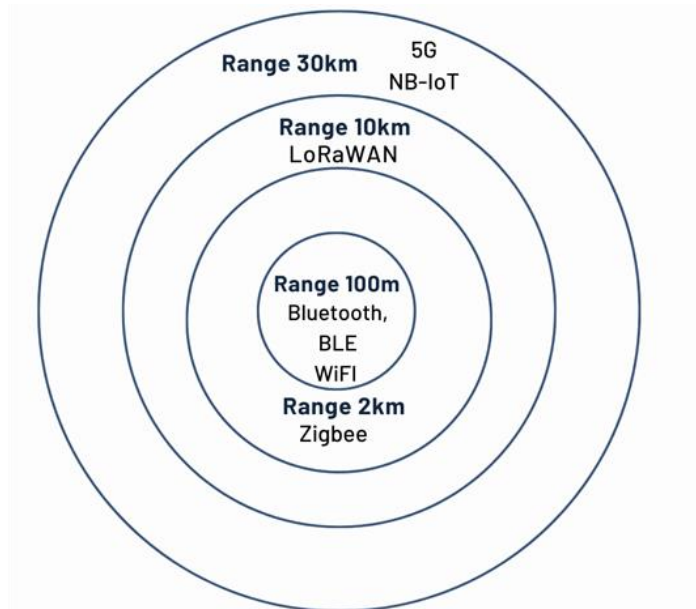


Figure 1. Recent wireless communication protocols for UAVs

Table 1: Popular wireless communication technologies applied for UAS

WCT Tech	Range	Power Use	Frequency/Bandwidth
Bluetooth	10m	Low	2.4 Ghz
Bluetooth Low Energy	8-10m	Very low	2.4 Ghz
Wi-fi	100m	Medium	2.4 Ghz, 5 Ghz
Zigbee	100-1500 m	Low	868 Mhz, 915 Mhz, 2.4 Ghz
LoRaWAN	30km	Low	500 Mhz, 868Mhz, 900 Mhz
Narrow Band-IoT	10km	Low	450 Mhz, 3.5 Ghz,
5G Network	30km	Low-High	200 Khz, 900 Khz

Bluetooth

Bluetooth wireless technology will replace the interconnect wires between several personal gadgets, such as notebook computers, cell phones, personal digital assistants (P.D.A.s), digital cameras, etc (Bluetooth, 2006). Bluetooth wireless technology intends to act as a ubiquitous, low-cost, user-friendly air interface that will replace the multitude of proprietary cords that individuals must carry and utilize to connect their gadgets (Jianfan Chen et al., 2021; Cho & Shin, 2021). While most personal devices communicate via the RS-232 serial port protocol, proprietary connectors and pin configurations prevent using the same cables to connect devices from various manufacturers and occasionally even the same manufacturer (Christoe, Yuan, Michael, & Kalantar-Zadeh, 2021; Claverie & Esteves, 2021). The primary objective of Bluetooth wireless technology is to provide a flexible cable connector with customizable pin configurations that enable several portable devices to communicate with one another.

This system relies on the IEEE 802.15.1 standard. In addition to other technologies, Bluetooth has four alternative data rate settings to accommodate a variety of transmission distances: 2 Mbps, 1 Mbps, 500 kbps, and 125 kbps (Pierleoni et al., 2021; Z. Pu, Cui, Tang, Wang, & Wang, 2021; Sollie, Gryte, Bryne, & Johansen, 2022).

Bluetooth drones offer several advantages to users. As they use the same technology with many consumer electronics, drones applied Bluetooth technology are more user-friendly. Bluetooth drones are much more affordable than other types of drones, making them a great option for those on a budget (Aguilar, Soria, Arrue, & Ollero, 2017; Kitchen, Chase, Sauter, & Bixler, 2020; Li et al., 2021b; Vucic & Axell, 2022). Bluetooth drones are equipped with advanced sensors, which allow them to navigate in a variety of terrain and environments.

With the smaller and lighter size, Bluetooth drones are extremely portable, allowing them to be taken virtually anywhere (Boccardo, Santorsola, & Grieco, 2020; Ezuma, 2022; H. Kim & Choi, 2016; J. Kim et al., 2013).

While Bluetooth UAS offer a great deal of flexibility and convenience, they do have some drawbacks which must be considered (Li et al., 2021b; Liu, Noguchi, Liang, & Agriculture, 2019; Mandal et al., 2016). UAS rely on Bluetooth technology can be prone to interference from other electronic devices. This could lead to a loss of communication with the aircraft and a decrease in safety. Due to their reliance on Bluetooth, Bluetooth UAS are not suitable for long distance applications as the signal strength weakens over long distances (Medaiyese, Ezuma, Lauf, & Adeniran, 2022; Medaiyese, Ezuma, Lauf, Guvenc, & Computing, 2022). Bluetooth drones are also limited in their payload capacity, meaning they may not be suitable for heavier applications (Oh, Lim, & Kang, 2022; Soria, Palomino, Arrue, & Ollero, 2017; Swinney & Woods, 2021). Finally, due to their small size, Bluetooth drones as can be easily damaged in windy conditions, making them unsuitable for certain applications (Vucic & Axell, 2022; M. Zhou, Lin, Liang, Du, & Cheng, 2017).

Bluetooth Low Energy (BLE)

The most significant data rate that BLE can accomplish is 1Mbps, which may not always be sufficient for devices like wireless headphones that demand continuous data streaming (Avilés-Viñas et al., 2022; Barsocchi, Girolami, & La Rosa, 2021; Belwafi, Alkadi, Alameri, Al Hamadi, & Shoufan, 2022; Cantizani-Esteva et al., 2022). On the other hand, another internet of thing application requires periodic small data transmissions. BLE can be used to provide wireless control of a UAV, as well as to stream data from the UAV to a ground control station (Cayre et al., 2021; Guruge, Kocer, & Kayacan, 2015; Hashmi & Research, 2021).

Bluetooth Low Energy has a much lower latency than other types of wireless connections, which is vital for a drone to respond quickly to commands (Li et al., 2021a; Li et al., 2021b; Lodeiro-Santiago, Santos-González, & Caballero-Gil, 2016; Lodeiro-Santiago, Santos-Gonzalez, Caballero-Gil, Caballero-Gil, & Computing, 2020; Loke, Alwateer, & Abeysinghe Achchige Don, 2016). By utilizing BLE technology, these drones are more energy efficient, meaning they can fly for longer periods of time. Additionally, BLE UAVs/drones can communicate with other devices, allowing for more efficient data transfer and remote management (Loke et al., 2016; Long, 2021; Nishiura & Yamamoto, 2021; Nyholm, 2020). BLE drones are also able to transmit data faster and with greater accuracy. This strength makes them ideal for surveillance, mapping, aerial reconnaissance, and asset monitoring applications (Long, 2021; Rajakaruna et al., 2019; Singh & Swaminathan, 2022). BLE UAS can be easily integrated with other enterprise systems, allowing for seamless data exchange and faster decision-making (Rajakaruna et al., 2018; Stute, Heinrich, Lorenz, & Hollick, 2021; Vucic & Axell, 2022). BLE drones are more secure and can be easily tracked, providing greater peace of mind for users. UAV BLE offer a wide range of benefits and can be utilized to greater flexibility in flight paths and can be used in applications where traditional drones may not be as effective.

BLE technology for drones can provide many advantages, but there are also some potential disadvantages. The range of Bluetooth Low Energy UAS is typically limited to around 30 meters, which can be an issue if the drone needs to travel farther than that (Singh & Swaminathan, 2022; Vucic & Axell, 2022; Xu & Systems, 2022). Furthermore, the battery life of Bluetooth Low Energy UAS can be considerably shorter than other technologies, which can be a concern for applications with long flight times. Besides that, the cost of Bluetooth Low Energy UAS is typically much more expensive than other solutions, which can be a challenge for those with limited budgets (Rajakaruna et al., 2018; Singh & Swaminathan, 2022; Xu & Systems, 2022). Overcoming these disadvantages of BLE includes using a reliable and robust communication protocol and ensuring that the design accounts for potential interference. Finally, it's important to ensure the system is thoroughly tested, maintained correctly, and meets the necessary performance requirements to operate reliably in real-world conditions (Tan et al., 2020). These steps allow BLE UAS systems to overcome their disadvantages and provide reliable, cost-effective solutions.

Wi-Fi

The term "Wi-Fi Wireless Fidelity," commonly known as Wi-Fi, is widely utilized as a wireless technology to connect various electronic devices through wireless area networks (WAN). This facilitates data transmission, including images and videos, over the network, making Wi-Fi drones ideal for live streaming and real-time data collection applications. W.N.I.C. can be either internal expansion cards or external USB or PCI devices, enabling computers to communicate wirelessly with one another through Wi-Fi or Bluetooth technology.

W.N.I.C.s play a crucial role in controlling drones, allowing remote control or formation flying.(de Carvalho Bertoli, Pereira, & Saotome, 2021).

Wi-Fi drones can also be susceptible to interference, leading to potential difficulties in control. Technological advancements in radar, GPS, and tracking technologies can aid in detecting and avoiding other aircraft in proximity (Khan, Hamila, Kiranyaz, & Gabbouj, 2019; Meesriyong, Wongwirat, & Namuduri, 2020; Nožica, Blažević, & Keser, 2021; Rubbestad & Söderqvist, 2021). Taking a proactive approach to safety and security will contribute to the reliable and responsible operation of Wi-Fi UAS.

Zigbee

Zigbee has gained popularity as a wireless technology option due, to its power consumption. This makes it a great choice for applications like UAS, where energy efficiency's crucial in the design process. While Zigbee UAS offers advantages for applications it's important to address some drawbacks. One concern is its nature, which means devices from manufacturers may not work together seamlessly. Zigbee can also be susceptible to interference from devices affecting its performance (Jia & Song, 2022; Katende, 2022; Krishna & engineering, 2017).

Table 2. Notable studies used Zigbee to conduct unmanned aircraft systems.

Authors	Title	Experiment	Empirical results
Zhou et al.(Q. Zhou, Wang, Yu, Huang, & Zhou, 2019)	"Unmanned patrol system based on Kalman filter and ZigBee positioning technology"	Estimate each UAV's location and exchange telemetry data between the aircraft and ground base.	Following use of a Kalman filter, the estimation is reliable.
Sineglazov and Daskal(Sineglazov & Daskal, 2017)	"Unmanned aerial vehicle navigation system based on IEEE 802.15.4 standard radiounits"	UAV navigation system based on IEEE 802.15.4 radio equipment.	A wireless network can be used to make a prediction as to where a UAV is.
Bacco et al.(Bacco, Berton, Gotta, & Caviglione, 2018)	"IEEE 802.15.4 air-ground UAV communications in smart farming scenarios"	This study creates a test to assess the performance of IEEE 802.15.4 while considering a sensor network made up of fixed ground sensors and a UAV.	The transmission range between the ground nodes and the UAV is only around one third of its nominal value due to aerial mobility.
Ueyama et al.(Ueyama et al., 2014)	"Exploiting the use of unmanned aerial vehicles to provide resilience in wireless sensor networks"	A UAV system to increase wire-free sensor network resilience and lessen the impact of malfunctioning nodes or nodes damaged by natural disasters	Transporting UAVs to the disaster region and utilizing them as a router or data mule can help to reduce fault-related issues.
Mushtaq et al.(Mushtaq et al., 2015)	"Innovative conceptualization of Fly-By-Sensors (F.B.S.) flight control systems using ZigBee wireless sensors networks"	This research uses a fly-by-sensors (F.B.S.) control system, which is frequently employed for the main associated observation of in-flight operations.	The advantages of using ZigBee technology for regulating and monitoring the controlling function are highlighted by the authors: affordable price, low power consumption, dependable operation.
Nasution et al.(Nasution, Siregar, & Yasir, 2017)	"UAV telemetry communications using ZigBee protocol"	This study is a development of a UAV test system using the ZigBee protocol	Information can be successfully transferred from a UAV to a ground base where messages can contain up

To overcome these challenges organizations, need to prioritize the development of technologies that can minimize latency and interference problems. At the time efforts should focus on improving the range and accuracy of data transmission. Establishing cybersecurity protocols is critical to safeguarding UAS data and networks from threats posed by malicious actors. By investing in these areas, we can effectively minimize any impacts. Enhance the overall capabilities of Zigbee technology, for U.A.S applications. Table 2 shows some notable studies used Zigbee to conduct unmanned aircraft systems, their experiment design, and empirical results.

LoRaWAN

Long Range Wide Area Network (LoRaWAN) was developed to cater to the needs of Internet of Things (IoT) applications ensuring they meet requirements such as power efficiency, affordability, dynamics, dependability, and duplex communication. Many drones lack communication technologies that can cover areas while conserving power. Hence the focus of this investigation is to create a communication system with a range that consumes energy. Considering its power consumption LoRa emerges as one of the wireless physical layer technologies. Leveraging LoRaWAN in Unmanned Aerial Systems (UAS) enables the establishment of a range and low power wireless network. However, it should be noted that a limitation of LoRaWAN UAS Is their range— 10 kilometers before requiring proximity to a LoRaWAN gateway(Bianco, Mejia-Aguilar, & Marrocco, 2022; bin Edi, Abd Rashid, Ismail, & Cengiz, 2022; Calabrò & Giuliano, 2021; Cardoso et al., 2022). This constraint limits their applicability in long distance scenarios. Additionally, they have speeds with a maximum capability of around 20 kilometers, per hour¹. Nonetheless there are measures to mitigate these drawbacks and ensure efficient utilization of LoRaWAN UAS systems.

Narrow Band-IoT

The "band" aspect of NB IoT refers to a radiofrequency used to communicate with these devices. NB IoT is primarily intended for areas with coverage such as basements or rural regions and for devices that don't require significant data usage like heart monitors or security sensors. Developed by 3GPP to cater to a range of devices and services, NB IoT is specifically designed for Internet of Things (IoT) applications that demand low bandwidth and long battery life. It operates on a spectrum ensuring quality of service (QoS) and security(Elijah et al., 2018; Kavuri, Moltchanov, Ometov, Andreev, & Koucheryavy, 2020; Malik, Bilandi, Gupta, & Engineering, 2022; Popli, Jha, & Jain, 2021).

NB IoT finds application in scenarios, including smart meters, asset tracking systems, security setups, environmental monitoring solutions and much more. Its low power consumption and extended battery life make it ideal for applications that involve periodic data transmissions. It caters to use cases requiring data rates and/or long-lasting battery performance, like smart meters, asset tracking systems and industrial monitoring setups.

NB IoT is a next generation version of the LTE standard that has been developed specifically for use, in spectrum. One of the advantages of NB IoT is its ability to greatly improve power consumption and spectral efficiency while still offering the coverage and capacity benefits as LTE. This makes it an ideal technology for applications that require lasting battery life and operate in difficult to access areas(Song, Zhang, Ji, Jiang, & Li, 2020; Wang, Chang, Fan, & Sun, 2020). However, it's worth noting that NB IoT does have some drawbacks, such as data rates, limited range and shorter battery life compared to types of UAS. To address these limitations one possible solution is to utilize a wider bandwidth. By doing more data can be. Received, leading to an overall enhancement, in data quality.

5G Network

The 5G network is seen as an advancement in technology offering speed and reliability. It achieves this by utilizing radio waves, which allows for data capacity and faster speeds. However, it's important to note that due to its susceptibility to interference and limited signal range additional technologies like beamforming and MIMO are needed to optimize signal direction and transmission. Unmanned aerial vehicles (UAVs) can benefit from 5G by enabling high speed communication with latency resulting in coordination for swarm operations and safer missions. Time video streaming and fast data transmission play a role in applications such as search and rescue missions, delivery services, surveillance operations and mapping.

While there are advantages to using 5G for UAVs we must also acknowledge the associated costs of deployment and infrastructure challenges as drawbacks. Nevertheless these challenges can be mitigated by leveraging existing infrastructure resources utilizing spectrum bands effectively and collaborating with service providers specializing in 5G for UAVs. By planning and executing strategies effectively we can overcome these obstacles. Unlock the full potential of 5G for UAV technology while reducing deployment costs. Another approach to address the disadvantages of 5G is, by using spectrum allocation methods.(Damodaram, Reddy, Giri, Manikandan, & Engineering, 2022; Fu, Zhao, Su, & Jian, 2018; Ghazal & Engineering, 2021). Utilizing a 5G solution can greatly enhance network performance. To ensure implementation of 5G technology it is crucial to invest in cutting edge 5G UAS Technology and collaborate with 5G UAS Service providers. These measures will not make the technology more accessible. Also overcome any deployment challenges that may arise(Ning et al., 2021; Popli et al., 2021)⁻¹⁰⁵.

Conclusions

Remarkable Findings

In this paper, we presented the history of wireless communications and seven wireless communications technologies which have been applied for UAS surveillance, wildlife surveys, military training, weather monitoring, and local law enforcement. Wireless communication technologies are essential for enabling the UAS to do their jobs more effectively, safely, and efficiently. They serve as a link for facilitating communication between components of the UAS including ground stations, payloads, and sensors. This enables the collection and transmission of data. Additionally, the utilization of communication technologies on UAS Platforms has numerous advantages. These technologies eliminate the need for wiring, making the UAS Lighter and more efficient. As wireless communication technologies advance and become more advanced it is highly probable that UAS Operations will continue to reap their benefits in the years.

Wireless communication technologies for the UAS have been widely adopted in the past few years due to their potential to provide reliable, low-cost communications for various applications. Additionally, more research is needed to develop techniques to ensure secure data transmission and communication links resilient to various forms of interference. Finally, research is required to establish energy-efficient communication protocols that can operate with the limited power sources of the UASs. Filling these research gaps will ensure that UASs can provide reliable and secure communication services.

Future Research and Future Trends

Research trends focus on developing reliable and robust wireless communication systems for UAS operations. Research is being conducted in signal processing and communications protocols for UAS communication links. In addition, scientists are currently conducting studies to enhance the effectiveness and dependability of communication connections for systems (UAS). They are exploring technologies, like software defined radio input multiple output (M.I.M.O.) and cognitive radio to achieve this goal. The main research areas include signal processing algorithms, communication protocols, and network optimization. Additionally, researchers are exploring the potential of wireless communications for UAS operations in reconnaissance, surveillance, and search and rescue operations.

The advancements in communications for aerial systems (UAS) have been remarkable in recent years and it's just the start. Ongoing research in this field involves enhancing flight control algorithms, expanding transmission range, and ensuring data transfer. This progress aims to enable secure transmission of data volumes facilitating more intricate missions and operations. Wireless communications technologies are rapidly advancing, and with that, the options for UAS are increasing. These technologies will also help to ensure the safe operation of these vehicles in airspace that is heavily populated by other aircraft.

Scientific Ethics Declaration

The authors declare that the scientific ethical and legal responsibility of this article published in EPSTEM journal belongs to the authors.

Acknowledgements or Notes

* The authors would like to thank the Ministry of Science and Technology, Taiwan. We also would like to thank the National Kaohsiung University of Science and Technology, Industrial University of Ho Chi Minh City, and Thu Dau Mot University for their assistance. Additionally, we would like to thank the reviewers and editors for their constructive comments and suggestions to improve our work.

* This article was presented as an oral presentation at the International Conference on Research in Engineering, Technology and Science (www.icrets.net) held in Budapest/Hungary on July 06-09, 2023.

References

- Abdalkafor, A. S., & Aliesawi, S. A. (2022). Data aggregation techniques in wireless sensors networks (WSNs): taxonomy and an accurate literature survey. *Paper presented at the AIP Conference Proceedings*.
- Aguilar, J., Soria, P. R., Arrue, B. C., & Ollero, A. (2017). Cooperative perimeter surveillance using bluetooth framework under communication constraints. *Paper presented at the Iberian Robotics conference*.
- Alsemmeiri, R. A., Bakhsh, S. T., & Alsemmeiri, H. (2016). Free space optics vs radio frequency wireless communication. *Int. J. Inf. Technol. Comput. Sci*, 8(9), 1-8.
- Arya, K. V., Bhadoria, R. S., & Chaudhari, N. S. (2018). Emerging wireless communication and network technologies: *Springer*.
- Avilés-Viñas, J., Carrasco-Alvarez, R., Vázquez-Castillo, J., Ortigón-Aguilar, J., Estrada-López, J. J., Jensen, D. D., & Castillo-Atoche, A. (2022). An accurate UAV ground landing station system based on BLE-RSSI and maximum likelihood target position estimation. *Applied Sciences*, 12(13), 6618.
- Bacco, M., Berton, A., Gotta, A., & Caviglione, L. (2018). IEEE 802.15. 4 air-ground UAV communications in smart farming scenarios. *IEEE Communications Letters*, 22(9), 1910-1913
- Barsocchi, P., Girolami, M., & La Rosa, D. J. S. (2021). Detecting proximity with bluetooth low energy beacons for cultural heritage. *Sensors*, 21(21), 7089.
- Beke, É., Bódi, A., Katalin, T. G., Kovács, T., Maros, D., & Gáspár, L. (2018). The role of drones in linking industry 4.0 and ITS Ecosystems. *Paper presented at the 2018 IEEE 18th International Symposium on Computational Intelligence and Informatics (CINTI)*.
- Belwafí, K., Alkadi, R., Alameri, S. A., Al Hamadi, H., & Shoufan, A. (2022). Unmanned Aerial Vehicles' Remote Identification: A Tutorial and Survey. *IEEE Access*, 10, 87577-87601.
- Bianco, G. M., Mejia-Aguilar, A., & Marrocco, G. (2022). Numerical and experimental characterization of LoRa-based helmet-to-unmanned aerial vehicle links on flat lands: A numerical-statistical approach to link modeling. *IEEE Antennas and Propagation Magazine*, 65(1), 79-92.
- bin Edi, M. E. I., Abd Rashid, N. E., Ismail, N. N., & Cengiz, K. (2022, August). Low-Cost, Long-Range Unmanned Aerial Vehicle (UAV) Data Logger Using Long Range (LoRa) Module. In *2022 IEEE Symposium on Wireless Technology & Applications (ISWTA)* (pp. 1-7). IEEE.
- Bluetooth, S. I. G. (2006). *Bluetooth. Go faster. Go further white paper*. Available online: https://www.bluetooth.com/wp-content/uploads/2019/03/Bluetooth_5-FINAL.pdf (accessed on 11 September 2021).
- Boccadoro, P., Santorsola, A., & Grieco, L. A. (2020). A dual-stack communication system for the internet of drones. *Paper presented at the International Conference on Ad-Hoc Networks and Wireless*.
- Calabrò, A., & Giuliano, R. (2021). Integrated Wi-Fi and LoRa network on UAVs for localizing people during SAR operations. *Paper presented at the 2021 AEIT International Conference on Electrical and Electronic Technologies for Automotive (AEIT AUTOMOTIVE)*.
- Cantizani-Esteba, J., Bravo-Arrabal, J., Fernández-Lozano, J., Fortes, S., Barco, R., García-Cerezo, A., & Mandow, A. J. I. A. (2022). Bluetooth low energy for close detection in search and rescue missions with robotic platforms: An experimental evaluation. *IEEE Access*, 10, 106169-106179.
- Cardoso, C. M., Barros, F. J., Carvalho, J. A., Machado, A. A., Cruz, H. A., de Alcântara Neto, M. C., & Araújo, J. P. (2022). SNR prediction with ANN for UAV applications in IoT networks based on measurements. *Sensors*, 22(14), 5233.
- Cayre, R., Galtier, F., Auriol, G., Nicomette, V., Kaâniche, M., & Marconato, G. (2021). WazaBee: attacking Zigbee networks by diverting Bluetooth Low Energy chips. *Paper presented at the 2021 51st Annual IEEE/IFIP International Conference on Dependable Systems and Networks (DSN)*.
- Chen, C., Xiang, J., Ye, Z., Yan, W., Wang, S., Wang, Z., & Xiao, M. J. D. (2022). Deep learning-based energy optimization for edge device in UAV-aided communications. *Drones*, 6(6), 139.
- Chen, J., Wang, W., Zhou, Y., Ahmed, S. H., & Wei, W. J. I. N. (2021). Exploiting 5G and blockchain for medical applications of drones. *IEEE Network*, 35(1), 30-36.

- Chen, J., Zhou, B., Bao, S., Liu, X., Gu, Z., Li, L., Li, Q. (2021). A data-driven inertial navigation/Bluetooth fusion algorithm for indoor localization. *IEEE Sensors Journal*, 22(6), 5288-5301.
- Cho, H.-W., & Shin, K. G. (2021). BlueFi: bluetooth over WiFi. *Paper presented at the Proceedings of the 2021 ACM SIGCOMM 2021 Conference*.
- Christoe, M. J., Yuan, J., Michael, A., & Kalantar-Zadeh, K. J. I. A. (2021). Bluetooth signal attenuation analysis in human body tissue analogues. *IEEE Access*, 9, 85144-85150
- Claverie, T., & Esteves, J. L. (2021). Bluemirror: reflections on bluetooth pairing and provisioning protocols. *Paper presented at the 2021 IEEE Security and Privacy Workshops (SPW)*.
- Custers, B. (2016). Drones here, there and everywhere introduction and overview. In *The future of drone use* (pp. 3-20): Springer.
- Damodaram, A., Reddy, L. V., Giri, M., Manikandan, N. (2022). A study on 'LPWAN' technologies for a drone assisted smart energy meter system in 5g-smart city Iot-cloud environment. *Journal of Applied Science and Engineering*, 26(8), 1195-1203.
- de Carvalho Bertoli, G., Pereira, L. A., & Saotome, O. (2021). Classification of denial of service attacks on Wi-Fi-based unmanned aerial vehicle. *Paper presented at the 2021 10th Latin-American Symposium on Dependable Computing (LADC)*.
- Elijah, O., Rahman, T., Yeen, H., Leow, C., Sarijari, M., Aris, A., & Han, C. (2018). Application of UAV and low power wide area communication technology for monitoring of river water quality. *Paper presented at the 2018 2nd International Conference on Smart Sensors and Application (ICSSA)*.
- Ezuma, M. C. (2022). *UAV detection and classification using radar, radio frequency and machine learning techniques*. North Carolina State University.
- Fu, S., Zhao, L., Su, Z., & Jian, X. J. S. (2018). UAV based relay for wireless sensor networks in 5G systems. *Sensors*, 18(8), 2413
- Ghazal, T. M. (2021). *Positioning of UAV base stations using 5G and beyond networks for IOMT applications*. <https://repositoriobibliotecas.uv.cl/handle/uvsc1/3128>
- Guruge, P., Kocer, B. B., & Kayacan, E. (2015). A novel automatic UAV launcher design by using bluetooth low energy integrated electromagnetic releasing system. *Paper presented at the 2015 IEEE Region 10 Humanitarian Technology Conference (R10-HTC)*.
- Haider, S. K., Nauman, A., Jamshed, M. A., Jiang, A., Batool, S., & Kim, S. W. (2022). Internet of drones: Routing algorithms, techniques and challenges. *Mathematics*, 10(9), 1488.
- Hashmi, A. (2021). A novel drone-based search and rescue system using bluetooth low energy technology. *Engineering, Technology & Applied Science Research*, 11(2), 7018-7022.
- Jia, F., & Song, Y. (2022). UAV automation control system based on an intelligent sensor network. *Journal of Sensors*, Article ID 7143194, <https://doi.org/10.1155/2022/7143194>
- Kamruzzaman, M. M. (2023). 6G wireless communication assisted security management using cloud edge computing. *Expert Systems*, 40(4), e13061.
- Katende, M. (2022). Design of a communication module based on zigbee mesh topology for unmanned aerial vehicles (Doctoral dissertation).
- Kavuri, S., Moltchanov, D., Ometov, A., Andreev, S., & Koucheryavy, Y. (2020). Performance analysis of onshore NB-IoT for container tracking during near-the-shore vessel navigation. *IEEE Internet of Things Journal*, 7(4), 2928-2943.
- Khan, M. A., Hamila, R., Kiranyaz, M. S., & Gabbouj, M. (2019). A novel UAV-aided network architecture using Wi-Fi direct. *IEEE Access*, 7, 67305-67318.
- Khandal, D., & Jain, S. (2014). Li-Fi (Light Fidelity): The future technology in wireless communication. *International Journal of Information & Computation Technology*, 4(16), 1687-1694.
- Kim, H., & Choi, K. (2016). A modular wireless sensor network for architecture of autonomous UAV using dual platform for assisting rescue operation. *Paper presented at the 2016 IEEE SENSORS*.
- Kim, J., Lee, S., Ahn, H., Seo, D., Park, S., & Choi, C. (2013). Feasibility of employing a smartphone as the payload in a photogrammetric UAV system. *ISPRS Journal of Photogrammetry and Remote Sensing*, 79, 1-18.
- Kitchen, S., Chase, R., Sauter, J., & Bixler, K. (2020). Simulated RF environments for UAV-mounted Bluetooth 5.0 receivers. *Paper presented at the Unmanned Systems Technology XXII*.
- Kong, J. A. (1975). *Theory of electromagnetic waves*. EMW Publishing Cambridge, Massachusetts, USA
- Krishna, B. R. (2017). Agriculture drone model with zigbee network. *International Journal of Advanced Research in Electrical, Electronics and Instrumentation Engineering*, 6(10), 7445-7450.
- Lee, C.-T., Shen, T.-C., Lee, W.-D., & Weng, K.-W. (2016). A novel electronic lock using optical Morse code based on the Internet of Things. *Paper presented at the 2016 International Conference on Advanced Materials for Science and Engineering (ICAMSE)*.
- Li, K., Lu, N., Zheng, J., Zhang, P., Ni, W., & Tovar, E. (2021a). A practical secret key management for multihop drone relay systems based on bluetooth low energy. *Paper presented at the 2021 18th Annual*

IEEE International Conference on Sensing, Communication, and Networking (SECON).

- Li, K., Lu, N., Zheng, J., Zhang, P., Ni, W., & Tovar, E. (2021). Bluetooth: A secure aerial relay system using bluetooth connected autonomous drones. *ACM Transactions on Cyber-Physical Systems*, 5(3), 1-22.
- Liu, Y., Noguchi, N., & Liang, L. (2019). Development of a positioning system using UAV-based computer vision for an airboat navigation in paddy field. *Computers and Electronics in Agriculture*, 162, 126-133.
- Lodeiro-Santiago, M., Santos-González, I., & Caballero-Gil, P. (2016). UAV-based rescue system for emergency situations. In *Ubiquitous Computing and Ambient Intelligence* (pp. 163-173): Springer.
- Lodeiro-Santiago, M., Santos-Gonzalez, I., Caballero-Gil, P., & Caballero-Gil, C. (2020). Secure system based on UAV and BLE for improving SAR missions. *Journal of Ambient Intelligence and Humanized Computing*, 11, 3109-3120.
- Loke, S. W., Alwateer, M., & Abeysinghe Achchige Don, V. S. (2016). Virtual space boxes and drone-as-reference-station localisation for drone services: An approach based on signal strengths. *Paper presented at the Proceedings of the 2nd Workshop on Micro Aerial Vehicle Networks, Systems, and Applications for Civilian Use*.
- Long, S. L. (2021). Long distance bluetooth low energy exploitation on a wireless attack platform. <https://scholar.afit.edu/etd/5035/>
- Malik, P. K., Bilandi, N., & Gupta, A. (2022). Narrow band-IoT and long-range technology of IoT smart communication: Designs and challenges. *Computers & Industrial Engineering*, 172, 108572.
- Mandal, S., Saw, S., Shaw, K., Thakur, A. K., Seth, V., & Singh, P. (2016). Low-cost bluetooth-arduino hover control design of a quad copter. *IOSR Journal of Electronics and Communication Engineering (IOSR-JECE)*, 11(4), 11.
- Medaiyese, O. O., Ezuma, M., Lauf, A. P., & Adeniran, A. A. (2022). Hierarchical learning framework for UAV detection and identification. *IEEE Journal of Radio Frequency Identification*, 6, 176-188.
- Medaiyese, O. O., Ezuma, M., Lauf, A. P., & Guvenc, I. (2022). Wavelet transform analytics for RF-based UAV detection and identification system using machine learning. *Pervasive and Mobile Computing*, 82, 101569.
- Meesriyong, K., Wongwirat, O., & Namuduri, K. (2020). An experimental study of Wi-Fi access service using drones in container yard. *Paper presented at the 2020 20th International Conference on Control, Automation and Systems (ICCAS)*.
- Molisch, A. F. (2012). *Wireless communications*, John Wiley & Sons.
- Mushtaq, Z., Shairani, L., Sani, S. S., Mazhar, A., Saeed, M. A., & Aftab, N. (2015). Innovative conceptualization of Fly-By-Sensors (FBS) flight control systems using ZigBee wireless sensors networks. *Paper presented at the 2015 IEEE International Conference on Wireless for Space and Extreme Environments (WiSEE)*.
- Nasution, T., Siregar, I., & Yasir, M. (2017). UAV telemetry communications using ZigBee protocol. *Paper presented at the Journal of Physics: Conference Series*.
- Nguyen, K. K., Masaracchia, A., Sharma, V., Poor, H. V., & Duong, T. Q. (2022). RIS-assisted UAV communications for IoT with wireless power transfer using deep reinforcement learning. *IEEE Journal of Selected Topics in Signal Processing*, 16(5), 1086-1096.
- Ning, Z., Dong, P., Wen, M., Wang, X., Guo, L., Kwok, R. Y., & Poor, H. V. (2021). 5G-enabled UAV-to-community offloading: Joint trajectory design and task scheduling. *IEEE Journal on Selected Areas in Communications*, 39(11), 3306-3320.
- Nishiura, S., & Yamamoto, H. (2021). Large-term sensing system for agriculture utilizing UAV and wireless power transfer. *Paper presented at the 2021 International Conference on Information Networking (ICOIN)*.
- Nouacer, R., Hussein, M., Espinoza, H., Ouhammou, Y., Ladeira, M., & Castiñeira, R. (2020). Towards a framework of key technologies for drones. *Microprocessors and Microsystems*, 77, 103142.
- Nožica, D., Blažević, D., & Keser, T. (2021). Unmanned aerial vehicle swarm uses Wi-Fi to search for stranded people in remote areas embedded devices as active scanners in search for Wi-Fi-enabled mobile phones. *Paper presented at the 2021 10th Mediterranean Conference on Embedded Computing (MECO)*.
- Nyholm, H. (2020). Localizing sheep using a bluetooth low energy enabled unmanned aerial vehicle for round-trip time of arrival-based multilateration (Master's thesis, NTNU).
- Oberascher, M., Rauch, W., & Sitzenfrei, R. (2022). Towards a smart water city: A comprehensive review of applications, data requirements, and communication technologies for integrated management. *Sustainable Cities and Society*, 76, 103442.
- Oh, J., Lim, D.-w., & Kang, K.-m. (2022). Energy efficiency improvement rate for low power UAV identification environment. *Paper presented at the 2022 13th International Conference on Information and Communication Technology Convergence (ICTC)*.

- Parikh, P. P., Kanabar, M. G., & Sidhu, T. S. (2010). Opportunities and challenges of wireless communication technologies for smart grid applications. *Paper Presented at the IEEE PES General Meeting*.
- Pierleoni, P., Gentili, A., Mercuri, M., Belli, A., Garello, R., & Palma, L. (2021). Performance improvement on reception confirmation messages in Bluetooth mesh networks. *IEEE Internet of Things Journal*, 9(3), 2056-2070.
- Popli, S., Jha, R. K., & Jain, S. (2021). A comprehensive survey on Green ICT with 5G-NB-IoT: Towards sustainable planet. *Computer Networks*, 199, 108433.
- Pu, C., & Zhu, P. (2022). Mitigating Routing Misbehavior in the Internet of Drones Environment. *Paper presented at the 2022 IEEE 95th Vehicular Technology Conference:(VTC2022-Spring)*.
- Pu, Z., Cui, Z., Tang, J., Wang, S., & Wang, Y. (2021). Multimodal traffic speed monitoring: A real-time system based on passive Wi-Fi and Bluetooth sensing technology. *IEEE Internet of Things Journal*, 9(14), 12413-12424.
- Rajakaruna, A., Manzoor, A., Porambage, P., Liyanage, M., Ylianttila, M., & Gurtov, A. (2019). Enabling end-to-end secure connectivity for low-power IoT devices with UAVs. *Paper presented at the 2019 IEEE Wireless Communications and Networking Conference Workshop (WCNCW)*.
- Rajakaruna, A., Manzoor, A., Porambage, P., Liyanage, M., Ylianttila, M., & Gurtov, A. (2018). Lightweight dew computing paradigm to manage heterogeneous wireless sensor networks with uavs. *arXiv preprint arXiv:1811.04283*.
- Ramli, S. N., & Ahmad, R. (2011). Surveying the wireless body area network in the realm of wireless communication. *Paper presented at the 2011 7th International Conference on Information Assurance and Security (IAS)*.
- Rubbestad, G., & Söderqvist, W. (2021). *Hacking a Wi-Fi based drone*. <https://www.diva-portal.org/smash/record.jsf?pid=diva2%3A1586253&dsid=-6362>
- Sarkar, T. K., Mailloux, R., Oliner, A. A., Salazar-Palma, M., & Sengupta, D. L. (2006). *History of wireless*: John Wiley & Sons.
- Savkin, A. V., Verma, S. C., & Anstee, S. (2022). Optimal navigation of an unmanned surface vehicle and an autonomous underwater vehicle collaborating for reliable acoustic communication with collision avoidance. *Drones*, 6(01), 27.
- Sengupta, D. L., & Sarkar, T. K. (2003). Maxwell, Hertz, the Maxwellians, and the early history of electromagnetic waves. *IEEE Antennas and Propagation Magazine*, 45(2), 13-19.
- Seymour, T., & Shaheen, A. (2011). History of Wireless Communication. *Review of Business Information Systems (RBIS)*, 15(2), 37-42. <https://doi.org/10.19030/rbis.v15i2.4202>.
- Shilpa, B., Radha, R., & Movva, P. (2022). Comparative analysis of wireless communication technologies for IoT applications. In *Artificial Intelligence and Technologies* (pp. 383-394): Springer.
- Sineglazov, V., & Daskal, E. (2017). Unmanned aerial vehicle navigation system based on IEEE 802.15. 4 standard radiounits. *Paper presented at the 2017 IEEE 4th International Conference Actual Problems of Unmanned Aerial Vehicles Developments (APUAVD)*.
- Singh, D., & Swaminathan, R. (2022). Comprehensive performance analysis of hovering UAV-based FSO communication system. *IEEE Photonics Journal*, 14(5), 1-13.
- Smith, J. M. (2007). Morse code, Da Vinci code, tax code and... churches: An historical and constitutional analysis of why section 501 (c)(3) Does not apply to churches. *JL & Pol.*, 23, 41.
- Sollie, M. L. M., Gryte, K., Bryne, T. H., & Johansen, T. A. (2022). Outdoor Navigation Using Bluetooth Angle-of-Arrival Measurements. *IEEE Access*, 10, 88012-88033.
- Song, K., Zhang, J., Ji, Z., Jiang, J., & Li, C. (2020). Energy-efficiency for IoT system with cache-enabled fixed-wing UAV relay. *IEEE Access*, 8, 117503-117512.
- Soria, P. R., Palomino, A. F., Arrue, B., & Ollero, A. (2017). Bluetooth network for micro-uavs for communication network and embedded range only localization. *Paper presented at the 2017 International Conference on Unmanned Aircraft Systems (ICUAS)*.
- Stute, M., Heinrich, A., Lorenz, J., & Hollick, M. (2021). Disrupting continuity of apple's wireless ecosystem security: New tracking, {DoS}, and {MitM} attacks on {iOS} and {macOS} through bluetooth low energy, {AWDL}, and {Wi-Fi}. *Paper presented at the 30th USENIX Security Symposium (USENIX Security 21)*.
- Swinney, C. J., & Woods, J. C. (2021). RF detection and classification of unmanned aerial vehicles in environments with wireless interference. *Paper presented at the 2021 International Conference on Unmanned Aircraft Systems (ICUAS)*.
- Tan, Z., Yang, X., Pang, M., Gao, S., Li, M., & Chen, P. (2020). UAV-assisted low-consumption time synchronization utilizing cross-technology communication. *Sensors*, 20(18), 5134.
- Tlili, S., Mnasri, S., & Val, T. (2022). The internet of things enabling communication technologies, applications and challenges: a survey. *International Journal of Wireless and Mobile Computing*, 23(1), 9-21.
- Ueyama, J., Freitas, H., Faical, B. S., Geraldo Filho, P. R., Fini, P., Pessin, G., ... & Villas, L. A. (2014).

- Exploiting the use of unmanned aerial vehicles to provide resilience in wireless sensor networks. *IEEE Communications Magazine*, 52(12), 81-87.
- Vucic, T., & Axell, C. (2022). *Tracking sheep by radio tags and UAV: A field study of Bluetooth round-trip time ranging and multilateration* (Master's thesis, NTNU).
- Wang, S.-Y., Chang, J.-E., Fan, H., & Sun, Y.-H. (2020). Performance comparisons of NB-IoT, LTE Cat-M1, Sigfox, and LoRa moving at high speeds in the air. *Paper presented at the 2020 IEEE Symposium on Computers and Communications (ISCC)*.
- Xu, Z. (2022). UAV surveying and mapping information collection method based on Internet of Things. *Internet of Things and Cyber-Physical Systems*, 2, 138-144.
- Yang, N., Wang, L., Geraci, G., Elkashlan, M., Yuan, J., & Di Renzo, M. (2015). Safeguarding 5G wireless communication networks using physical layer security. *IEEE Communications Magazine*, 53(4), 20-27.
- Yu, S., Das, A. K., Park, Y., & Lorenz, P. (2022). SLAP-IoD: Secure and lightweight authentication protocol using physical unclonable functions for internet of drones in smart city environments. *IEEE Transactions on Vehicular Technology*, 71(10), 10374-10388.
- Zeng, Y., Zhang, R., & Lim, T. J. (2016). Wireless communications with unmanned aerial vehicles: Opportunities and challenges. *IEEE Communications Magazine*, 54(5), 36-42.
- Zheng, B., You, C., Mei, W., & Zhang, R. (2022). A survey on channel estimation and practical passive beamforming design for intelligent reflecting surface aided wireless communications. *IEEE Communications Surveys & Tutorials*, 24(2), 1035-1071.
- Zhou, M., Lin, J., Liang, S., Du, W., & Cheng, L. (2017). A UAV patrol system based on Bluetooth localization. *Paper presented at the 2017 2nd Asia-Pacific Conference on Intelligent Robot Systems (ACIRS)*.
- Zhou, Q., Wang, L., Yu, P., Huang, T., & Zhou, M. (2019). Unmanned patrol system based on Kalman filter and Zigbee positioning technology. *Paper presented at the Journal of Physics: Conference Series*.

Author Information

Thi Minh Nhut Vo

National Kaohsiung University of Science and Technology,
415 Jiangong, Sanmin, Kaohsiung, Taiwan
Thu Dau Mot University, Vietnam

Chia-Nan Wang

National Kaohsiung University of Science and Technology,
415 Jiangong, Sanmin, Kaohsiung, Taiwan

Fu-Chiang Yang

National Kaohsiung University of Science and Technology,
415 Jiangong, Sanmin, Kaohsiung, Taiwan

Van Thanh Tien Nguyen

Industrial University of Ho Chi Minh City
12, Nguyen Van Bao, Go Vap, Ho Chi Minh City, Vietnam
Corresponding author Contact e-mail: thanhtienck@ieee.org

Mandeep Singh

School of Mechanical and Manufacturing Engineering,
Faculty of Engineering, The University of New South
Wales, Sydney, NSW 2052, Australia

To cite this article:

Vo, T.M.N., Wang, C.N., Yang, F.C., Nguyen, V.T.T. & Singh, M. (2023). Internet of things (IoT): Wireless communications for unmanned aircraft system. *The Eurasia Proceedings of Science, Technology, Engineering & Mathematics (EPSTEM)*, 23, 388-399.

The Eurasia Proceedings of Science, Technology, Engineering & Mathematics (EPSTEM), 2023

Volume 23, Pages 400-405

ICRETS 2023: International Conference on Research in Engineering, Technology and Science

Comprehensive Modeling Study of the Electrical Performance of a Sono-Electrolyzer under a Voltage and Current Sources Supply: From Grey to Green Hydrogen

Nour Hane Merabet

Karlsruhe University of Applied Sciences

Kaouther Kerboua

National Higher School of Technology and Engineering

Abstract: Hydrogen production from water electrolysis is seen as a promising technology to produce hydrogen with high purity of 99.99%. However, the increase of the ohmic resistance in the electrolyte remains a challenge for the electrolytic technique. In the present work, we study the transition from grey hydrogen to green hydrogen using alkaline electrolysis (25% w/w KOH solution electrolysis). We compare hydrogen production efficiency using a voltage source simulating the conventional DC generator, and a current source simulating the PV power supply. Water electrolysis was coupled to an indirect ultrasound source in order to investigate its effect on hydrogen production process in both cases of power supply. The question was tackled experimentally using an H-cell electrolyzer and an ultrasonic bath, and numerically using a MatLab code. Energy conversion efficiency and hydrogen production rate were determined both experimentally and through simulation. It was demonstrated that the integration of sonication reduces the ohmic resistance within the electrolyzer and thus decreases the cell voltage for the same current, which enhances the energy efficiency in the case of current source for the same hydrogen production rate. For instance, an enhancement of 1% was recorded in the energy efficiency using a current source of energy, while it equals 2.68% in the case of voltage source. Therefore, the coupled of sono-electrolysis process to solar PV seems to be a promising pathway for an environmentally friendly hydrogen production technique from an energetic perspective.

Keywords: Conventional electricity, Hybrid, Water electrolysis, PV, Matlab modeling, Ultrasounds.

Introduction

Global energy consumption has increased as a result of population growth and rising living standards. Therefore, the production of green energy sources has become more urgent due to global warming and environmental emissions (Gielen et al., 2019). The possibility of using hydrogen as a sustainable fuel is a highly attractive topic in the literature. Although most of the technologies that could make a significant contribution are still at an early stage, the introduction of hydrogen as a clean fuel is a key pillar of the decarbonization strategy for industry and transport (Global Hydrogen Review, 2021). Water electrolysis is a clean and sustainable technology that provides the high-purity hydrogen that fuel cells need in particular, to produce clean and sustainable electricity (Boudries, 2013). However, because it is much more expensive than producing H₂ by steam methane reforming (SMR), only a small percentage of the world's H₂ is produced by water electrolysis (Esposito, 2017). This interesting method of hydrogen production accounts for only 4% of worldwide hydrogen production today, however it is estimated to grow significantly in the coming years, to reach 22% by 2050 (Maggio et al., 2022). Besides, the operating expenditure associated with the electricity used to supply electrolysis reaction is currently the largest single cost of water electrolysis (Esposito, 2017; Shaner et al., 2016). However, the cost of green electricity produced by solar PV and wind continues to fall (Esposito, 2017).

- This is an Open Access article distributed under the terms of the Creative Commons Attribution-NonCommercial 4.0 Unported License, permitting all non-commercial use, distribution, and reproduction in any medium, provided the original work is properly cited.

- Selection and peer-review under responsibility of the Organizing Committee of the Conference

© 2023 Published by ISRES Publishing: www.isres.org

Photovoltaic electrolysis (PV-EL) has a comparatively high level of technical maturity (Nour Hane Merabet, Kaouther Kerboua, 2023). However, the overall efficiency of the PV electrolysis system barely attain 10%, as commercial electrolyzers achieve efficiencies ranging from 60% to 85%, while PV cells reach 18% (Song et al., 2022). Several studies have focused on the optimization of these key parameters, as the system efficiency mainly depends on the efficiency of both the PV generator system and the electrolyzer (Nguyen et al., 2019).

Industrial electrolyzers operate at around 70% efficiency when producing hydrogen. However, significant power losses due to the Joule effect and parasitic reactions in the solution are a major problem with these systems (Sellami & Loudiyi, 2017). Research has shown the potential for increasing the efficiency of water electrolysis by applying magnetic fields, light energy fields, ultrasonic fields and pulsed electric fields, while only few studies have been conducted on the application of such fields (Burton et al., 2021). The integration of ultrasounds to electrolysis process has been reported to be efficient by several authors (Merabet & Kerboua, 2022). by improving mass transport and electrode cleaning through a combined effect of micro-jetting and micro-flow, and lowering the overall potential through degasification effects or electrode surface modification (Kerboua & Merabet, 2023).

The aim of the present study is to compare the efficiency of sono-electrolysis hydrogen production using a voltage source as a conventional source of electrical energy, i.e., conventional DC generator, and a current source by consisting of a PV power supply, acting as a green energy source for the production of green hydrogen.

Material and Methods

An H-cell electrolyzer composed of anodic and cathodic chambers was used. The volume of the used electrolyte is 300 mL filled with KOH electrolyte at 25% w/w. The adopted parameters are reported in Table.1.

Table 1. Characteristics of the adopted configurations

Parameters		DC generator supplied sono-electrolysis	Pv supplied sono-electrolysis
Power supply	Voltage	5.95 V	According to solar radiation
Electrolyte	Type	KOH	KOH
	Concentration	25% w/w, 4.46 M	25% w/w, 4.46 M
Sonication	Type	indirect	indirect
	Frequency	40 kHz	40 kHz
	Power	60 W _e	60W _e
Electrode's material	Mode	Continuous	Continuous
	Nickel plates	Nickel plates	Nickel plates

The experiments performed using PV supply have been set in order to lead to a cell potential of 5.95 V, this has been met under 827 W/m² with silent conditions, and 938.5 W/m² with US conditions.

Numerical Modeling

MatLab Modeling

The matlab programm is based on the combination of the PV model and the electrolyzer model according to the list of equations below. The PV current, submitted to a maximum power point tracking, is deuced from Eq.1, based on Eqs. 2 to 4. The resulting polarization curve, linking to current to the potential of the PV panel allows the determination of the feeding current, corresponding to the maximum deliverable power, provided by the MPPT tracker. I_{pv} is the light-generated current of the PV cell is directly dependent on the solar irradiation G. The current feeding the electrolysis cell governs the values of the overpotentials created in the cell, i.e., the activation overpotential indicated in Eq.7, the Ohmic overpotential as shown in Eq.8, and the concentration overpotential given in Eq.9 (E_{rev} is the reversible voltage, U_{act} is the activation voltage, U_{ohm} is the ohmic voltage and U_{conc} is the concentration voltage). All these overpotentials, added to the reversible potential, determine the cell potential value, according to Eq.5. We pay a particular attention to the ohmic resistance, including the electrolyte resistance, with both bubble free and bubble components, shown in Eqs. 10 to 12, respectively.

Table 2. Mathematical equations of the numerical model

Equations	Number	Reference
$I = I_{pv} - I_d - I_{sh}$	(1)	(Villalva et al., 2009)
$I_{pv} = \frac{(I_{pv0} + K\Delta T)G}{G_0}$	(2)	(Villalva et al., 2009)
$I_d = I_0 \left(e^{\left(\frac{R_s I + V}{V_t a} \right)} - 1 \right)$	(3)	(Rahim et al., 2015; Villalva et al., 2009)
$I_{sh} = \frac{V + R_s I}{R_p}$	(4)	(Rahim et al., 2015; Villalva et al., 2009)
$U_{cell} = E_{rev} + U_{act} + U_{ohm} + U_{conc}$	(5)	(Mohamed et al., 2016)
$E_{rev}(T, P) = E_{rev}(T) + \frac{RT}{ZF} \ln \left(\frac{P_v^* (P - P_v)^{1.5}}{P_v} \right)$	(6)	(LeRoy et al., 1980)
$U_{act} = \frac{2.3026 RT}{ZF a_a} \log \left(\frac{I_a}{I_{0a}} \right) + \frac{2.3026 RT}{ZF a_c} \log \left(\frac{I_c}{I_{0c}} \right)$	(7)	(Allen J. Bard, Larry R. Faulkner, 2022)
$U_{ohm} = I(R_{cell} + R_{electrodes} + R_{electrolyte} + R_{electrical})$	(8)	(Abul Kalam Azad & Khan, n.d.)
$U_{conc} = \frac{RT}{ZF} \left(\ln \left(1 - \left(\frac{I}{I_{lim}} \right) \right) \right)$	(9)	(Mohamed et al., 2016)
$R_{electrolyte} = R_{bf} + R_b$	(10)	(Gambou et al., 2022)
$R_{bf} = \frac{1}{\sigma_{bf}} \left(\frac{d_a}{S_a} + \frac{d_c}{S_c} \right)$	(11)	(Gambou et al., 2022)
$R_b = R_{bf} \left(\frac{1}{\left(1 - \frac{2}{3} e \right)^{1.5}} - 1 \right)$	(12)	(Gambou et al., 2022)

The influence of the ultrasound power was evaluated according to the electrode coverage by bubbles e that influences the ohmic resistance as shown in Eq.8-10 in which R_b Bubble resistance, R_{bf} is the bubble free electrolyte resistance, S_a and S_c are anode and cathode cross sections respectively, d_a and d_c are distances from anode and cathode to membrane, σ_{bf} is the bubble-free electrolyte conductivity and finally, the energy conversion efficiency is assessed experimentally according to the Eq.11

$$E_{H_2} = \frac{\dot{m}_{H_2} H_{H_2}}{U_{cell} \times I} \quad (13)$$

Where $H_{H_2} = 142 \text{ MJ/Kg}$ and \dot{m}_{H_2} is the flow of produced hydrogen

Results and Discussion

The average values of the mass flow rates of hydrogen produced and energy efficiency, obtained from the respective series of repeated tests (3 trials each), are considered below. In Fig.1, the effects of ultrasound integration on the mass flow rate of H_2 during electrolysis are presented using voltage source (a) and PV solar panel (b). It can be seen that the improvement in the flow rate of hydrogen produced by the integration of continuous ultrasound is higher when a voltage source is used.

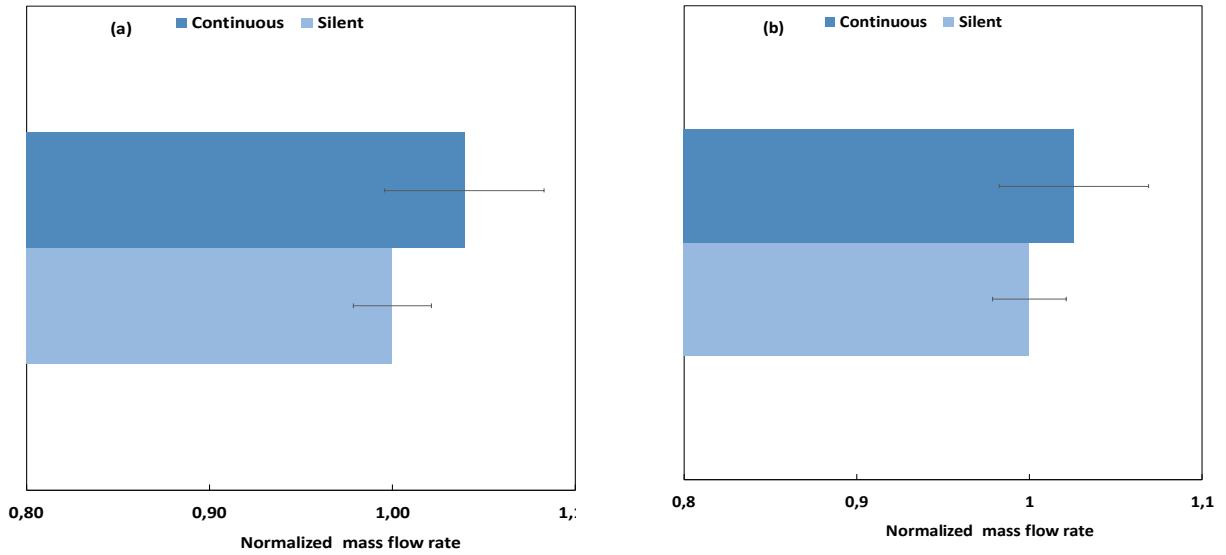


Figure 1. Normalized mass flow rates of hydrogen produced by electrolysis and continuous sono-electrolysis supplied by a voltage source (a) and a PV panel (b)

In Fig.2, the energy efficiency is presented for both power supply (a) voltage source and (b) for PV sources under silent and continuous ultrasound conditions. It can be seen as well that the improvement in the energy efficiency of the process due to the integration of continuous ultrasound is higher when a voltage source is used. For example, a 0.98% improvement in energy efficiency was recorded using a current source, while it equals 2.68% in the case of a voltage source.

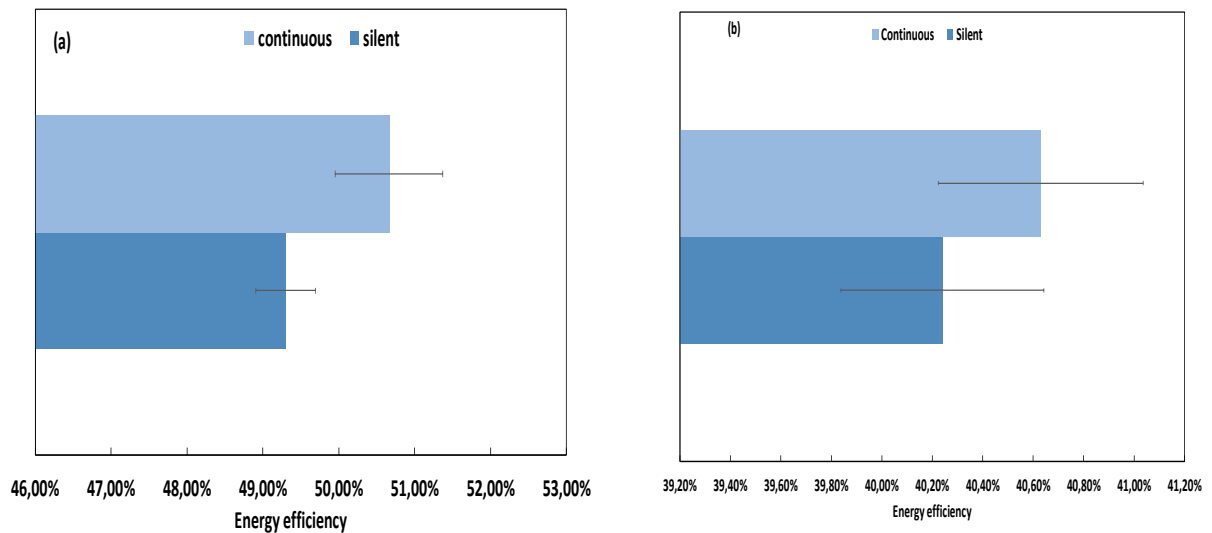


Figure 2. Energy efficiency of hydrogen produced by electrolysis and continuous sono-electrolysis supplied by a voltage source (a) and a PV panel (b).

The improvement obtained with the use of a voltage source is explained by the increase in the current at constant potential due to the drop in the ohmic resistance, which accelerates the kinetics, together with an improved recovery of the gas due to a greater and faster desorption. Hence, in the case of a voltage source, the improvement in H₂ flow rate is due to both effects (increase in current and improved desorption). Whereas in the case of a current source such as the PV supply, for a given delivered current under a given value of global incident solar radiation, the observed improvement in H₂ flow rate can only be explained by the improvement in desorption.

Fig.3 shows the polarization curves under silent and sonicated conditions in continuous mode in order to study the effect of ultrasonic irradiation on the evolution of the current as a function of the electrolysis voltage.

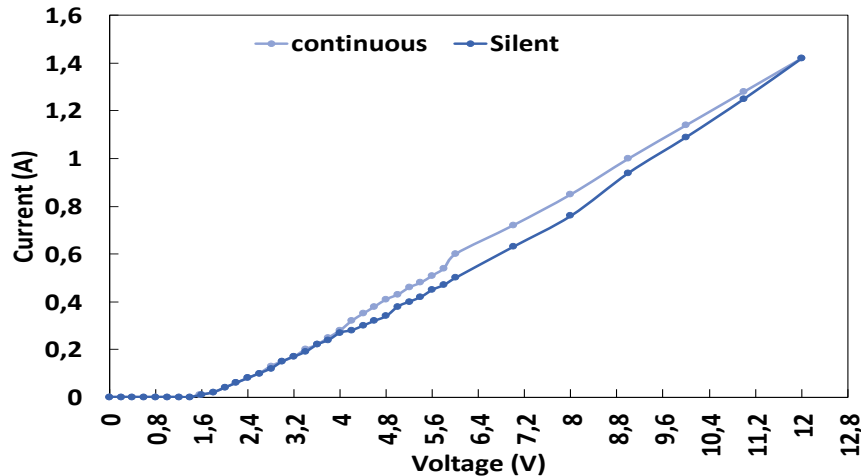


Figure 3. Comparison of I-V curves during water electrolysis and water sono-electrolysis for hydrogen production

Comparing the two curves obtained under silent and ultrasonic conditions shows that sonication increases the value of the current flowing through the electrolyzers for a given voltage. The improvement rate in this case is 1.78%, which can be attributed to the efficient enhancement of mass transport due to the propagation of the ultrasound power in the electrolyte solution, which in turn increases electron transport and thus improves the cell current.

Conclusion

A comparative study of the efficiency of grey and green hydrogen production using a voltage source and a solar PV power supply was carried out. It was observed that, the improvement in the flow rate of produced hydrogen due to the integration of continuous ultrasound is higher when a voltage source is used due to the improvement in both current and desorption. In terms of energy efficiency, 1 % improvement has been observed using a current source, compared to 2.68 % using a voltage source. Therefore, a promising avenue for an environmentally friendly hydrogen production technique seems to be the coupling of the sono-electrolysis process with solar PV, particularly from an energetic perspective.

Scientific Ethics Declaration

The authors declare that the scientific ethical and legal responsibility of this article published in EPSTEM journal belongs to the authors.

Acknowledgements or Notes

* This article was presented as an oral presentation at the International Conference on Research, Engineering and Technology (www.icrets.net) conference held in Budapest/Hungary on July 06-09 2023.

References

- Azad, A.K. & Khan, M. M. K. (2021). *Bioenergy resources and technologies*. Elsevier.
- Bard, A. J., Faulkner, L. R., & White, H. S. (2022). *Electrochemical methods: fundamentals and applications*. John Wiley & Sons.
- Boudries, R. (2013). Analysis of solar hydrogen production in Algeria: Case of an electrolyzer-concentrating photovoltaic system. *International Journal of Hydrogen Energy*, 38(26), 11507–11518.
- Burton, N. A., Padilla, R. V., Rose, A., & Habibullah, H. (2021). Increasing the efficiency of hydrogen production from solar powered water electrolysis. *Renewable and Sustainable Energy Reviews*, 135(July 2020), 110255.

- Esposito, D. V. (2017). Membraneless electrolyzers for low-cost hydrogen production in a renewable energy future. *Joule*, 1(4), 651–658.
- Gambou, F., Guilbert, D., Zasadzinski, M., Rafaralahy, H., Gambou, F., Guilbert, D., Zasadzinski, M., Rafaralahy, H., Gambou, F., Guilbert, D., Zasadzinski, M., & Rafaralahy, H. (2022). A comprehensive survey of alkaline electrolyzer modeling: electrical domain and specific electrolyte conductivity To cite this version: HAL Id: hal-03663132 A comprehensive survey of alkaline electrolyzer modeling: electrical domain and specific elect. *Energies*, 15(9).
- Gielen, D., Boshell, F., Saygin, D., Bazilian, M. D., Wagner, N., & Gorini, R. (2019). The role of renewable energy in the global energy transformation. *Energy Strategy Reviews*, 24(01), 38–50.
- Kerboua, K., & Merabet, N. H. (2023). Sono-electrolysis performance based on indirect continuous sonication and membraneless alkaline electrolysis: Experiment, modelling and analysis. *Ultrasonics Sonochemistry*, 96(February), 106429.
- LeRoy, R. L., Bowen, C. T., & LeRoy, D. J. (1980). The thermodynamics of aqueous water electrolysis. *Journal of the Electrochemical Society*, 127(9), 1954–1962.
- Maggio, G., Squadrito, G., & Nicita, A. (2022). Hydrogen and medical oxygen by renewable energy based electrolysis: A green and economically viable route. *Applied Energy*, 306, 117993.
- Merabet, N., & Kerboua, K. (2022). Sonolytic and ultrasound-assisted techniques for hydrogen production: A review based on the role of ultrasound. *International Journal of Hydrogen Energy*, 47(41), 17879–17893.
- Mohamed, B., Ali, B., Ahmed, B., Ahmed, B., Salah, L., & Rachid, D. (2016). Study of hydrogen production by solar energy as tool of storing and utilization renewable energy for the desert areas. *International Journal of Hydrogen Energy*, 41(45), 20788–20806.
- Nguyen, T., Goshome, K., & Endo, N. (2019). Optimization strategy for high efficiency 20 kW- class direct coupled photovoltaic-electrolyzer system based on experiment data. *International Journal of Hydrogen Energy*, 44(09), 26741–26752.
- Nour Hane Merabet, Kaouther Kerboua, O. H. (2023). Converting PV solar energy to green hydrogen. In *Reference Module in Earth Systems and Environmental Sciences* (pp. 1–10). Elsevier. <https://doi.org/10.1016/B978-0-323-93940-9.00043-8>
- Rahim, A. H. A., Salami, A., Fadhlullah, M., Hanapi, S., & Sainan, K. I. (2015). Optimization of direct coupling solar PV panel and advanced alkaline electrolyzer system. *Energy Procedia*, 79, 204–211.
- Sellami, M. H., & Loudiyi, K. (2017). Electrolytes behavior during hydrogen production by solar energy. *Renewable and Sustainable Energy Reviews*, 70(November 2015), 1331–1335.
- Shaner, M. R., Atwater, H. A., Lewis, S., & Mcfarland, E. W. (2016). A comparative technoeconomic analysis of energy. *Energy & Environmental Science*, 9(5), 2354–2371.
- Song, H., Luo, S., Huang, H., Deng, B., & Ye, J. (2022). Solar-driven hydrogen production: Recent. *ACS Energy Letters*, 7, 1043–1065.
- Villalva, M. G., Gazoli, J. R., & Filho, E. R. (2009). Comprehensive approach to modeling and simulation of photovoltaic arrays. *IEEE Transactions On Power Electronics*, 24(5), 1198–1208.

Author Information

Nour Hane Merabet

Center of Applied Research, Karlsruhe University of Applied Sciences, Moltkestr, 30, 76133 Karlsruhe, Germany

National Higher School of Technology and Engineering, 23005 Annaba, Algeria
Laboratory of Technologies of Energetic Systems
E3360100, 23005 Annaba, Algeria

Contact Email: n.merabet@esti-annaba.dz

Kaouther Kerboua

National Higher School of Technology and Engineering, 23005 Annaba, Algeria

To cite this article:

Merabet N. H. & Kerboua K. (2023). Comprehensive modeling study of the electrical performance of a sono-electrolyzer under a voltage and current sources supply: from grey to green hydrogen. *The Eurasia Proceedings of Science, Technology, Engineering & Mathematics (EPSTEM)*, 23, 400-405.

The Eurasia Proceedings of Science, Technology, Engineering & Mathematics (EPSTEM), 2023

Volume 23, Pages 406-412

ICRETS 2023: International Conference on Research in Engineering, Technology and Science

Analysis of Temperature Change Effect on Dissipation of Energy in Functionally Graded Beams

Victor Rizov

University of Architecture, Civil Engineering and Geodesy

Abstract: In this paper, an analysis of the energy dissipation in functionally graded beam structures of viscoelastic behaviour under bending is presented with considering the effects of temperature change. There is an obvious need of carrying-out of such analyses because very often various load-bearing beam structures made of functionally graded viscoelastic materials are exposed to temperature changes simultaneously with external mechanical loading during their lifetime. Rheological model with one spring and two viscous components is used for treating the beam viscoelastic behaviour. The energy dissipation analysis accounts for the temperature change by correcting the time-dependent modulus of elasticity. A parametric study is performed. The general trend of the results obtained is that the dissipated energy decreases when the temperature increases.

Keywords: Dissipation of energy, Temperature change, Functionally graded beam structure

Introduction

Excellent properties of the functionally graded materials (these materials pertain to the category of continuously inhomogeneous engineering materials) make them potential substitute of the conventional engineering structural materials like metals and classical fiber reinforced composites (Fanani et al., 2021; Gururaja Udupa et al., 2014; Gandra et al., 2011). Therefore, functionally graded materials have been widely used for manufacturing of various load-bearing structural members applied in different spheres of modern engineering in the recent decades (Mahamood & Akinlabi, 2017; Nagaral et al., 2019). Ensuring of safety, stability and durability of functionally graded load-bearing structural applications in the process of their engineering design represents an important condition for guaranteeing of the reliable work of these structures (this necessitates development of methods for analyzing the mechanical behaviour of functionally graded structural members under various external loadings) (Radhika et al., 2020; Rizov, 2020; Toudhdehghan et al., 2017).

The present paper addresses the problem of energy dissipation analysis in functionally graded viscoelastic beam structures subjected to bending simultaneously with temperature change. The necessity of performing of such analysis is aroused by the fact that previous publications devoted to this topic consider mainly the effect of external mechanical loading applied on the beam structures (Narisawa, 1987; Rizov, 2021). However, in many situations the load-bearing engineering structures are under external mechanical loading simultaneously with temperature change. Therefore, the innovation in the present paper is that the strain energy dissipation in a functionally graded beam of viscoelastic behaviour under both external mechanical loading and temperature change is analyzed.

Analysis of Energy Dissipation

The length, thickness and width of the cantilever beam structure displayed in Fig. 1 are marked with l , h and b , respectively. The material is functionally graded along the beam thickness. Besides, the material has

- This is an Open Access article distributed under the terms of the Creative Commons Attribution-Noncommercial 4.0 Unported License, permitting all non-commercial use, distribution, and reproduction in any medium, provided the original work is properly cited.

- Selection and peer-review under responsibility of the Organizing Committee of the Conference

© 2023 Published by ISRES Publishing: www.isres.org

viscoelastic behaviour. The beam is under bending so that the change of the angle of rotation, φ , of the beam free end with time, t , is given by logarithmic law, i.e.

$$\varphi = \ln(1 + \beta_\varphi t), \quad (1)$$

where β_φ is a parameter governing the change of φ .

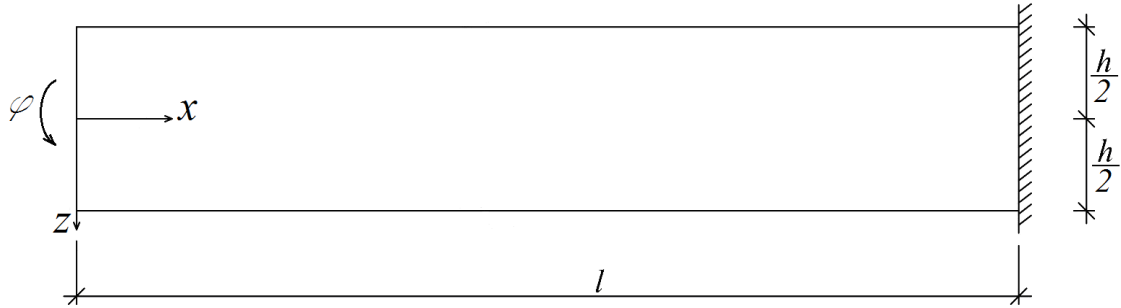


Figure 1. Functionally graded viscoelastic cantilever beam structure.

The viscoelastic behaviour of the beam structure is analyzed with the help of the rheological model displayed in Fig. 2. The model has two viscous components with coefficients of viscosity, η_{up} and η_{lw} , and a linear-elastic component (a spring) with modulus of elasticity, E .

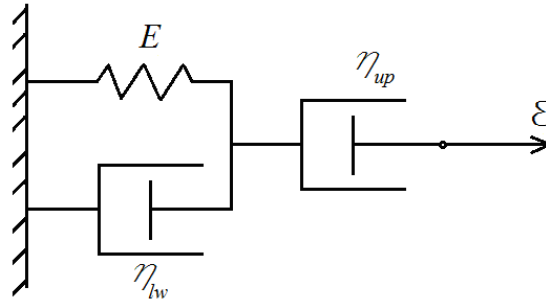


Figure 2. Rheological model.

The model is under strain, ε . The change of the strain with time is written as

$$\varepsilon = \ln(1 + \beta_\varepsilon t), \quad (2)$$

where β_ε is a parameter governing the change of ε .

In order to determine the strain, ε_{lw} , in the viscous component with coefficient of viscosity, η_{lw} , the following differential equation is worked-out:

$$\dot{\varepsilon}_{lw} = \frac{\rho_1}{1 + \beta_\varepsilon t} + \rho_2 \varepsilon_{lw}, \quad (3)$$

Where

$$\rho_1 = \frac{\eta_{up} \beta_\varepsilon}{\eta_{up} + \eta_{lw}}, \quad \rho_2 = -\frac{E}{\eta_{up} + \eta_{lw}}. \quad (4)$$

In Eq. (3) $\dot{\varepsilon}_{lw}$ is the first derivative of ε_{lw} with respect to time. By solving Eq. (3), the following expression for ε_{lw} is found:

$$\varepsilon_{lw} = \frac{\rho_1(e^{\rho_2 t} - 1)}{\rho_2(1 + \beta_\varepsilon t)}. \quad (5)$$

By applying the Hook's law and Eq. (5), one derives the following expression for the stress, σ_{lw} , in the viscous component with coefficient of viscosity, η_{lw} :

$$\sigma_{lw} = \eta_{lw} \frac{e^{\rho_2 t} \rho_1 \rho_2 (1 + \beta_\varepsilon t) - \rho_1 \beta_\varepsilon (e^{\rho_2 t} - 1)}{\rho_2 (1 + \beta_\varepsilon t)^2}. \quad (6)$$

By summing up the stresses in the spring and in the viscous component with coefficient of viscosity, η_{lw} , one obtains the following expression for the stress, σ , in the rheological model:

$$\sigma = E \frac{\rho_1(e^{\rho_2 t} - 1)}{\rho_2(1 + \beta_\varepsilon t)} + \eta_{lw} \frac{e^{\rho_2 t} \rho_1 \rho_2 (1 + \beta_\varepsilon t) - \rho_1 \beta_\varepsilon (e^{\rho_2 t} - 1)}{\rho_2 (1 + \beta_\varepsilon t)^2}. \quad (7)$$

Equation (7) holds also for the stress, σ_{up} , in viscous component with coefficient of viscosity, η_{lw} . The strain, ε_{up} , in viscous component with coefficient of viscosity, η_{lw} , is determined as

$$\varepsilon_{up} = \varepsilon - \varepsilon_{lw}, \quad (8)$$

where ε and ε_{lw} are obtained by Eq. (2) and Eq. (5), respectively.

Combination of Eq. (2) and Eq. (7) yields the following expression for the time-dependent modulus of elasticity, E_* , of the rheological model:

$$E_* = E \frac{\rho_1(e^{\rho_2 t} - 1)}{\rho_2(1 + \beta_\varepsilon t) \ln(1 + \beta_\varepsilon t)} + \eta_{lw} \frac{e^{\rho_2 t} \rho_1 \rho_2 (1 + \beta_\varepsilon t) - \rho_1 \beta_\varepsilon (e^{\rho_2 t} - 1)}{\rho_2 (1 + \beta_\varepsilon t)^2 \ln(1 + \beta_\varepsilon t)}. \quad (9)$$

The change of η_{up} , η_{lw} and E along the beam thickness is given by exponential laws

$$\eta_{up} = \eta_{up0} e^{q_1 \frac{\frac{h}{2} + z}{h}}, \quad (10)$$

$$\eta_{lw} = \eta_{lw0} e^{q_2 \frac{\frac{h}{2} + z}{h}}, \quad (11)$$

$$E = E_0 e^{q_3 \frac{\frac{h}{2} + z}{h}}, \quad (12)$$

where η_{up0} , η_{lw0} and E_0 are the values of η_{up} , η_{lw} and E at the upper surface of the beam structure, q_1 , q_2 and q_3 are material properties, z is the vertical centric axis of the beam ($-h/2 \leq z \leq h/2$). Beams of high aspect ratio are under consideration in the present paper. Therefore, the hypothesis for conservation of plane cross-section can be applied. Hence, the change of the strain along the beam thickness is given as

$$\varepsilon = \kappa(z - z_n), \tag{13}$$

where κ is the beam curvature, z_n is the neutral axis coordinate. In order to determine κ the angle of rotation of the beam free end is expressed as a function of κ by applying the integrals of Maxwell-Mohr. The expression obtained is treated as equation with unknown κ . The solution of this equation is found as

$$\kappa = \frac{\ln(1 + \beta_\varphi t)}{l}. \tag{14}$$

The neutral axis coordinate is determined by using the following equation of equilibrium:

$$N = b \int_{-\frac{h}{2}}^{\frac{h}{2}} \sigma dz, \tag{15}$$

where σ is given by Eq. (7), N is the axial force (for the beam under consideration $N = 0$). Eq. (15) is solved with respect to z_n by the MatLab computer program at various values of time. The beam structure under consideration is subjected also to change of the temperature, T . This causes variation of the time-dependent modulus of elasticity, E_* . Therefore, E_* is corrected by applying the following relations (Narisawa, 1987):

$$E_{*T_0} \left(\frac{t}{\alpha_T} \right) = \frac{T_0 r_0}{T r_1} E_*, \lg \alpha_T = - \frac{C_p (T - T_p)}{C_R + (T - T_p)}, \tag{16}$$

where the value of E_* at room temperature is marked with E_{*T_0} , the ratio, $T_0 r_0 / (T r_1)$, is unit, T_p is a material property, $C_p = 8.86$ and $C_R = 101.6$ (Narisawa, 1987). The unit dissipated energy, u_0 , is found as

$$u_0 = \int_0^t (\sigma_{lw} \varepsilon_{lw} + \sigma_{up} \varepsilon_{up}) dt, \tag{17}$$

where ε_{lw} , σ_{lw} , σ_{up} and ε_{up} are given by Eqs. (5), (6), (7) and (8), respectively. The dissipated energy, U , in the beam structure under consideration (Fig. 1) is expressed as

$$U = bl \int_{-\frac{h}{2}}^{\frac{h}{2}} u_0 dz. \tag{18}$$

The integral in Eq. (18) is solved by the MatLab computer program at various values of time.

Numerical Results

Numerical results are presented hereafter. The influence of the temperature change and the material gradient on the dissipated energy in the functionally graded viscoelastic beam structure is studied by performing calculations of U .

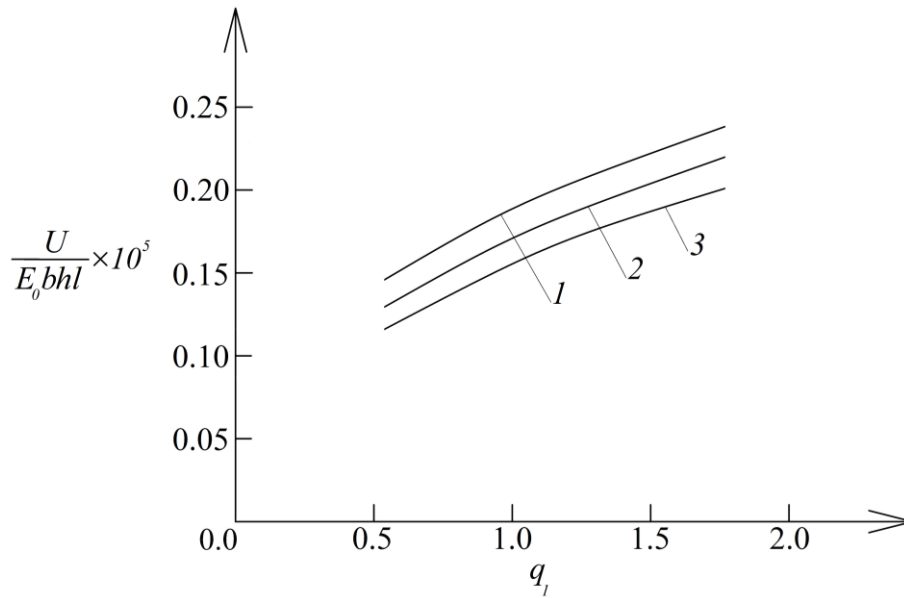


Figure 3. Variation of the dissipated energy with respect to q_1 (curve 1 - at $T/T_p = 1.1$, curve 2 - at $T/T_p = 1.3$ and curve 3 - at $T/T_p = 1.5$).

The following data are used: $l = 0.300$ m, $b = 0.015$ m, $h = 0.020$ m and $\beta_\varphi = 0.3 \times 10^{-7}$ 1/s.

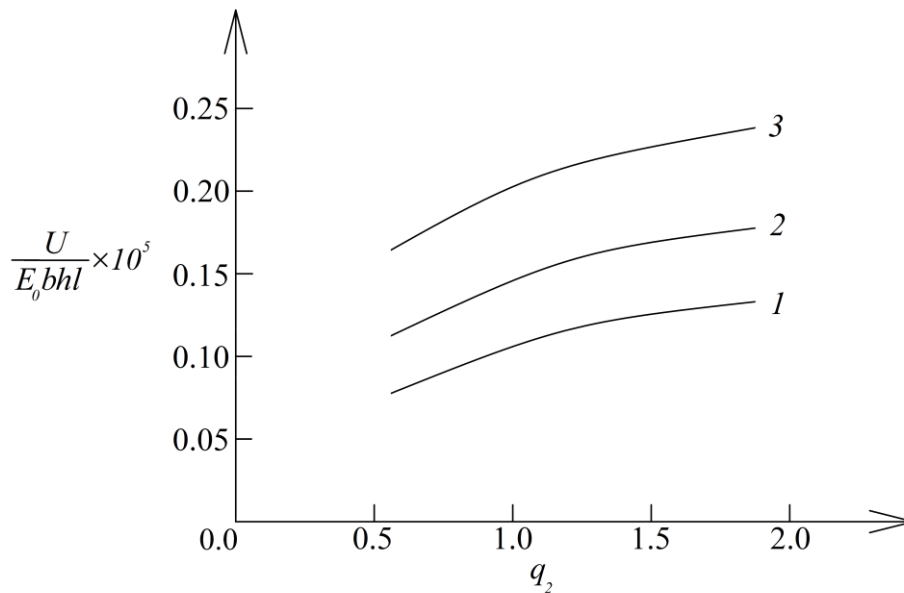


Figure 4. Variation of the dissipated energy with respect to q_2 (curve 1 - at $q_3 = 0.5$, curve 2 - at $q_3 = 1.0$ and curve 3 - at $q_3 = 2.0$).

The dissipated energy is calculated for a range of values of q_1 for three T/T_p ratios. The curves obtained are plotted on the graph presented in Fig. 3. One can observe in Fig. 3 that the shape of each curve is similar for every T/T_p ratio. One can notice also the increase of dissipated energy with increase of q_1 (Fig. 3). Since η_{up} depends on q_1 through the exponential relationship (10), one can draw a general conclusion from the graph in Fig. 3 that a higher coefficient of viscosity, η_{up} , results in higher values of the dissipated energy in the beam structure under consideration. Concerning the influence of the temperature on U , one can see in Fig. 3

that as the T/T_p ratio increases, the dissipated energy decreases (this observation agrees with results of previous studies dealing with homogeneous engineering structures (Kishkilov & Apostolov, 1994).

In order to investigate the effects of the change of the coefficient of viscosity, η_{lw} , and the modulus of elasticity, E , along the beam thickness, the dissipated energy is evaluated for various values of q_2 and q_3 . A graph of the dissipated energy in non-dimensional form against q_2 for three values of q_3 is given in Fig. 4. It can be seen from Fig. 4 that the higher the values of q_2 and q_3 , the higher the value of the dissipated energy (these observations agree with results of previous papers (Narisawa, 1987; Rizov, 2021).

Conclusion

A theoretical study of the effects of temperature change on the energy dissipation in functionally graded beam structures which exhibit viscoelastic behaviour under bending is conducted. A rheological model constructed by one spring and two viscous components is applied in the analysis. The unit dissipation energy is obtained and then integrated in order to derive the dissipated energy in the beam. The time-dependent modulus of elasticity is corrected to take into account the effect of the temperature change on the dissipated energy. The study leads to several main observations. Firstly, the dissipated energy decreases when the temperature increases. In other words, the energy dissipation capacity of the two viscous components of the rheological model is reduced with increasing the temperature. Also, it is observed that increase of q_1 , q_2 and q_3 generates an increase of the dissipated energy. Having in mind that q_1 , q_2 and q_3 are exponents in the functions describing the change of η_{up} , η_{lw} and E along the beam thickness, one can draw the conclusion that when the coefficients of viscosity and the modulus of elasticity increase, the dissipated energy increases too.

Recommendations

Analyzing energy dissipation in functionally graded beam structures exhibiting non-linear viscoelastic behavior can be recommended as a future task.

Scientific Ethics Declaration

The author declares that the scientific ethical and legal responsibility of this article published in EPSTEM journal belongs to the author.

Acknowledgements or Notes

* This article was presented as a poster presentation at the International Conference on Research in Engineering, Technology and Science (www.icrets.net) held in Budapest/Hungary on July 06-09, 2023.

References

- Fanani, E.W.A., Surojo, E., Prabowo, A. R., & Akbar, H. I. (2021). Recent progress in hybrid aluminum composite: Manufacturing and application. *Metals*, *11*, 1919-1929.
- Gandra, J., Miranda, R., Vilaça, P., Velhinho, A., & Teixeira, J.P. (2011). Functionally graded materials produced by friction stir processing. *Journal of Materials Processing Technology*, *211*, 1659-1668.
- Gururaja Udupa, Shrikantha Rao, S., & Rao Gangadharan, K. (2014). Functionally graded composite materials: An overview. *Procedia Materials Science*, *5*, 1291-1299.
- Kishkilov, M., & Apostolov, R. (1994). *Introduction to theory of plasticity*. HIACE.
- Mahamood, R. C., & Akinlabi, E. T. (2017). *Functionally graded materials*. Springer.

- Nagaral, M., Nayak, P. H., Srinivas, H. K., & Auradi V. (2019). Characterization and tensile fractography of Nano ZrO₂ reinforced copper-zinc alloy composites. *Frattura ed Integrità Strutturale*, 13, 370-376.
- Narisawa, I. (1987). *Strength of polymer materials*. Chemistry.
- Radhika, N., Sasikumar, J., Sylesh, J. L., & Kishore, R. (2020). Dry reciprocating wear and frictional behaviour of B4C reinforced functionally graded and homogenous aluminium matrix composites. *Journal of Materials Research and Technology*, 9, 1578-1592.
- Rizov, V. I. (2020). Longitudinal vertical crack analysis in beam with relaxation stresses. *World Journal of Engineering*, 18, 452-457.
- Rizov, V. I. (2021). Energy dissipation in viscoelastic multilayered inhomogeneous beam structures: An analytical study. *Materials Science Forum*, 1046, 39-44.
- Toudehdeghan, J., Lim, W., Foo1, K. E., Ma'arof, M. I. N., & Mathews J. (2017). A brief review of functionally graded materials. *MATEC Web of Conferences*, 131.

Author Information

Victor Rizov

University of Architecture, Civil Engineering and Geodesy

Sofia, Bulgaria

Contact e-mail: v.rizov_fhe@uacg.bg

To cite this article:

Rizov, V. (2023). Analysis of temperature change effect on dissipation of energy in functionally graded beams. *The Eurasia Proceedings of Science, Technology, Engineering & Mathematics (EPSTEM)*, 23, 406-412.

The Eurasia Proceedings of Science, Technology, Engineering & Mathematics (EPSTEM), 2023

Volume 23, Pages 413-419

ICRETS 2023: International Conference on Research in Engineering, Technology and Science

Stochastic Longitudinal Autopilot Tuning for Best Autonomous Flight Performance of a Morphing VTOL Drone

Tugrul Oktay

Erciyes University

Firat Sal

Iskenderun Technical University

Oguz Kose

Erzincan Binali Yıldırım University

Abdullah Kocamer

Erciyes University

Iskenderun Technical University

Abstract: In this conference paper autonomous flight performance maximization of a morphing vertical take-off and landing (i.e., VTOL) drone is considered by using stochastic optimization approach. For flight control system a PID based hierarchical control system is applied. In this paper PID controller which is used for pitch angle is considered. In this research only longitudinal flight and longitudinal control system is evaluated during aircraft mode where the pitch motion is in primary interest and the used control surface is the elevator of VTOL drone. For optimization approach simultaneous perturbation stochastic approximation (i.e., SPSA) is chosen. It is fast and safe in stochastic optimization problems when it is not possible to evaluate gradient analytically. At the end of this paper a cost function consisting terms such that settling time, rise time and overshoot is minimized. A detailed graphical analysis is made in order to better evaluate effect of morphing on longitudinal flight of a morphing vertical take-off and landing drone flight. Moreover, the cost function consists of rise time, settling time, and overshoot during trajectory tracking.

Keywords: VTOL drone, Stochastic optimization, Morphing, Autonomous performance

Introduction

In recent years, Unmanned Aerial Vehicles (UAV) have been widely used for various purposes such as image acquisition, target determination, search and rescue. UAVs are also used in situations such as pesticides that may be dangerous for humans, working in chemical or radioactive areas, and working under enemy fire (Husain et al., 2022).

UAVs can be basically divided into fixed-wing and rotary-wing vehicles (Coban et al., 2020). Rotary wing vehicles have high manoeuvrability and do not need a runway during take-off and landing, but due to their aerodynamic structure, power efficiency is low (Alanezi et al., 2022). Fixed-wing vehicles, on the other hand, have a lower airtime due to their lower power consumption, and a longer range due to their higher speed (Falanga et al., 2019). However, the negative aspects of fixed-wing vehicles are that they need a runway or launch pad during take-off and landing, and they do not have the ability to hover. In such cases, while the available space for fixed-wing vehicles to take off and land is limited, rotary-wing vehicles do not have sufficient range and transport. Autonomous landings of fixed-wing vehicles are also relatively more difficult.

- This is an Open Access article distributed under the terms of the Creative Commons Attribution-Noncommercial 4.0 Unported License, permitting all non-commercial use, distribution, and reproduction in any medium, provided the original work is properly cited.

- Selection and peer-review under responsibility of the Organizing Committee of the Conference

© 2023 Published by ISRES Publishing: www.isres.org

Combining the superior features of fixed-wing and rotary-wing vehicles, vertical take-off and landing (VTOL) hybrid aircraft, UAVs, are created. Fixed-wing VTOL vehicles have the ability to take off and land vertically, hang in the air at a certain point, and fly horizontally, quickly and efficiently. In this way, they can reach the target point quickly, land and take off without the need for a runway, or perform their mission by hanging (Uzun et al., 2023).

VTOL vehicles have two different flight modes that have the characteristics of fixed-wing and rotary-wing vehicles. Fixed-wing VTOL vehicles can generally be divided into two categories: systems that have the ability to tilt partially or completely (tilt) and that do not lose the horizon plane during mode transitions and the mechanical equipment remains fixed (no-tilt) (Kocamer et al., 2022).

In this study, four rotary wing and fixed wing VTOLs were given a backward variable angle control to the fixed wings to improve roll control in horizontal flight. In this way, it has gained the ability to provide its lateral balance against atmospheric noise in different speed profiles. The best value will be obtained by using the backward angle value of the wings using the SPSA algorithm (Kose et al., 2021, 2022). SPSA, which is the algorithm where the angle of the wings can change the moment of inertia of the aircraft and the controller can respond to this situation the fastest, was preferred in this study (Kose et al., 2023).

Material and Method

Because the planes move around three axes, they have a wide range of motion. Airplanes can make horizontal and vertical turns, as well as movements that are a combination of both. A turning airplane (as opposed to automobiles) is in stable flight. This means that there is no lateral force pushing the pilot out of the turn, as in an automobile, in the aircraft making the turn. In some turns, the resultant of the forces acting on the banked plane acts towards the center of the turn. This type of rotation is called a balanced and coordinated rotation. Sometimes planes make a so-called horizon turn. This means turning at a fixed altitude.

Turning is not done using the rudder on the airplane. Because of as a result of such an application, lateral forces may occur and the aircraft may be thrown out of the control. For this reason, turning is done by using the aileron and elevator in coordination in high-speed aircraft. When making a turn in an airplane flying to the horizon, first of all, the plane is controlled by ailerons (winglets). After the plane has banked to a certain degree, the elevator is controlled to turn the plane.

The control surface that makes a turn to a banked aircraft is the elevator. The force that turns the plane is the lift force. The lift force of an airplane at rest is divided into two component vectors, vertical and horizontal. The horizontal component vector gives the aircraft acceleration towards the center of rotation. When the airplanes are moving at a fixed altitude, the wings are parallel to each other and the lift force is equal to the weight (lift = weight) (Fig.1).

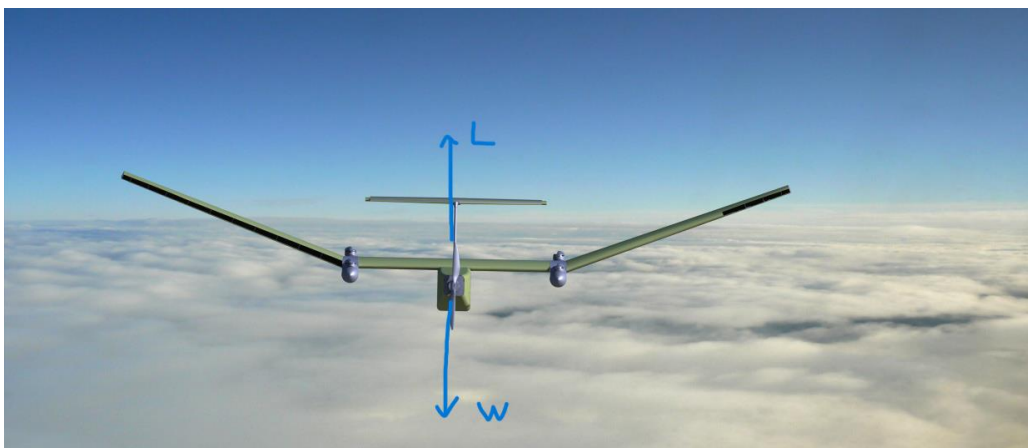


Figure 1. Fixed Altitude Flight

When the turn starts, the balance is disturbed. Sufficient acceleration must be gained in order to ensure the rotation. This creates a new force that helps to make a balanced and coordinated turn. This force on the horizontal axis is the centrifugal force. Fig.2 shows this force.

As with quadrotor, hexarotor and octorotor type UAVs, a mathematical model must be obtained for the decacopter type UAV. Newton's laws of motion and Euler's laws are used for the mathematical model of such UAVs (Mustapa, 2015). Accordingly, the mathematical position vectors (x, y and z) of the decacopter are shown in equations 1, 2 and 3 and the Euler angles (θ) are shown in equations 4, 5 and 6.

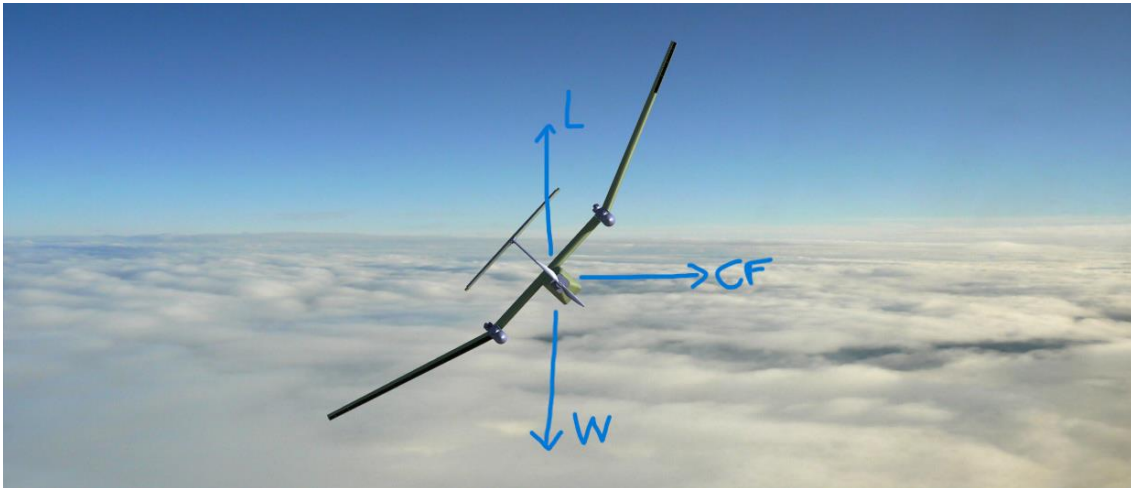


Figure 2. Formation of centrifugal force

In order to maintain the altitude during the turn, the lifting force during the turn must be equal to the resultant force (resultant force) created by the centrifugal force and the weight.

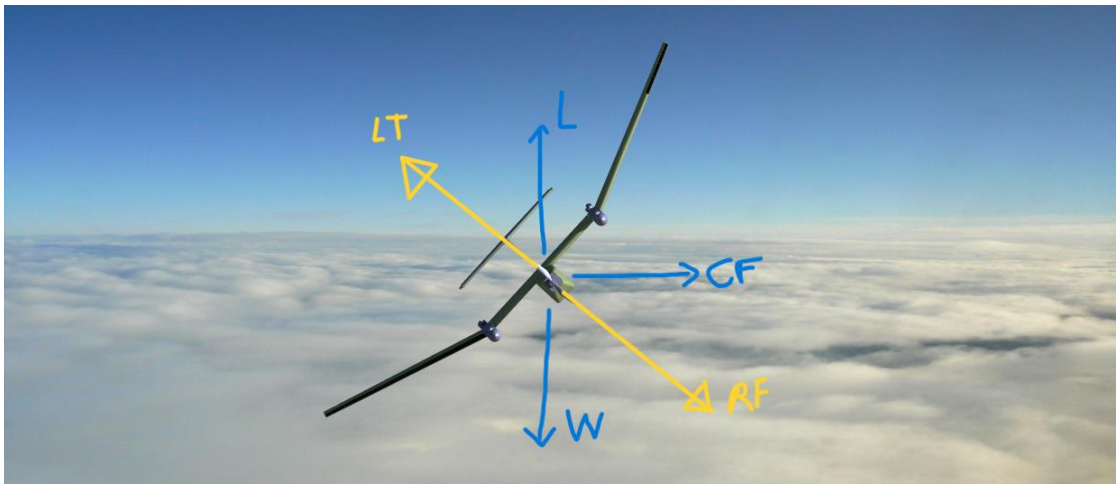


Figure 3. Formation of the resultant force and Lift in Turn.

As can be seen from the equation, either the lift coefficient (C_L) or the velocity (V) must be increased in order to increase the lift force. If the aircraft is in cruise flight, the lift coefficient is increased. If it is flying at low speeds, the C_L value is not changed because it is close to its maximum value, and the turn is made by increasing the speed.

$$L = \frac{1}{2} \rho V^2 C_L S \quad (1)$$

Smaller angles can be turned at low speeds, and larger angles can be turned at higher speeds. While all these calculations are being made, it is necessary that the airplane does not enter a stall. The following formula can be used for this:

$$\frac{V_{turn}}{V_{level}} = \sqrt{n} \quad (2)$$

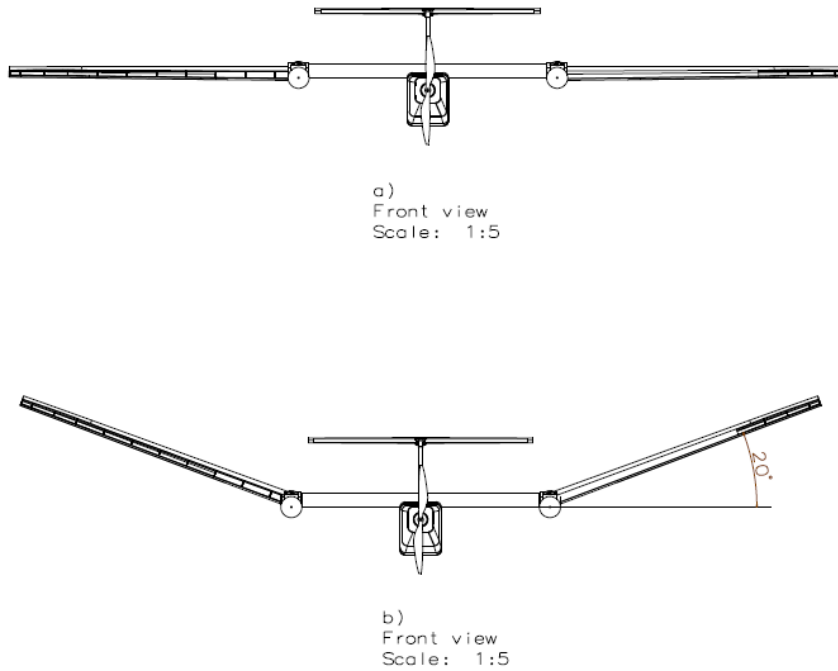


Figure 4. a) Non-morphing, b) morphing

Vturn: Stall speed during turn, Vlevel: Stall speed in level flight, n: Load factor.

VTOL aircraft can change shape during flight. It does this by changing the dihedral angle. The dihedral angle affects the lateral stability of the aircraft. Bank motion command or atmospheric disturbance can affect aircraft attitude. The measure of the aircraft's wing dihedral angle will affect stability and enable the aircraft to return to its course and continue flying. The condition before and after the shape change is shown in Fig. 4.

Conclusion

In order for an airplane to fly, not only lift equal to weight is required, sometimes more and sometimes less lift than weight is needed. If an airplane is turning at a fixed altitude, it creates a centrifugal force in addition to the weight if it comes out of the dive. The moment the aircraft exits the dive and moves into full straight (horizontal) flight, the lift force becomes equal to the vectorial sum of the lift force and the centrifugal force. Therefore, the buoyant force required is greater than the weight. The ratio of the resultant force to weight generated by the center force and weight generated by the aircraft rotating at an angle of 20° to 40° is called the load factor, denoted by 'n'. It is also called the g(ci) charge (gload). As the rotation angle increases, the value of the load factor also increases. During lateral movement, the wing in the direction of lying down will produce more lifting force depending on the amount of lateral angle. Aerodynamic force; allows the control surfaces of the aircraft to land without moving. In this study, the variable dihedral amount, PID coefficients and optimum values were obtained by using innovative approach methods. The SPSA algorithm was added to the controller design and the dihedral angle, PID coefficients were calculated. These values; fig. 5,6,7,8,9,10 and 11 were also given. These values were obtained from the simulation study.

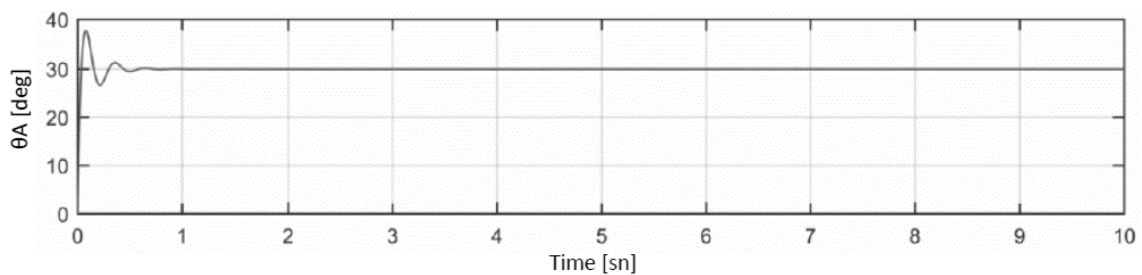


Figure 5. Longitudinal closed-loop responses (pure turbulence is ready) of the UAV with morphing wingtip

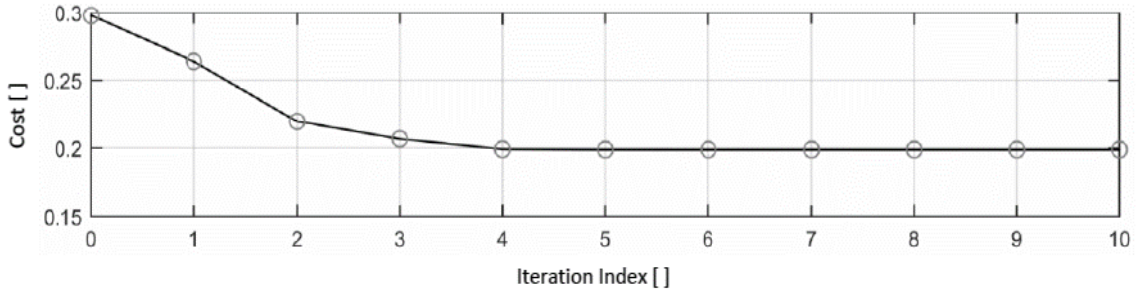


Figure 6. Cost improvement at each iteration

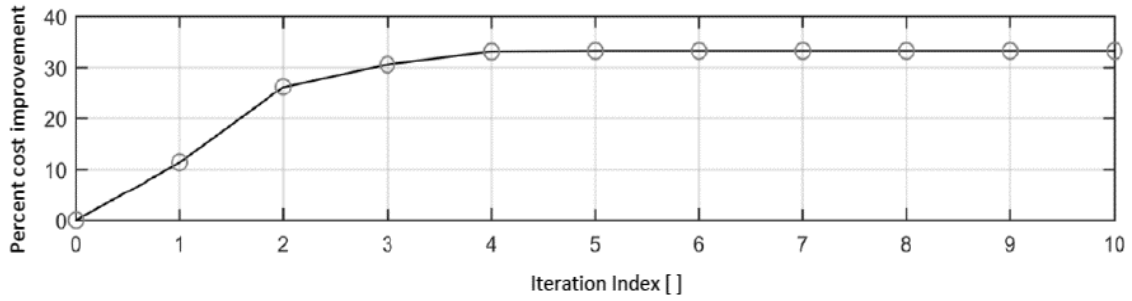


Figure 7. Optimization results of cost-index with varying number of iteration

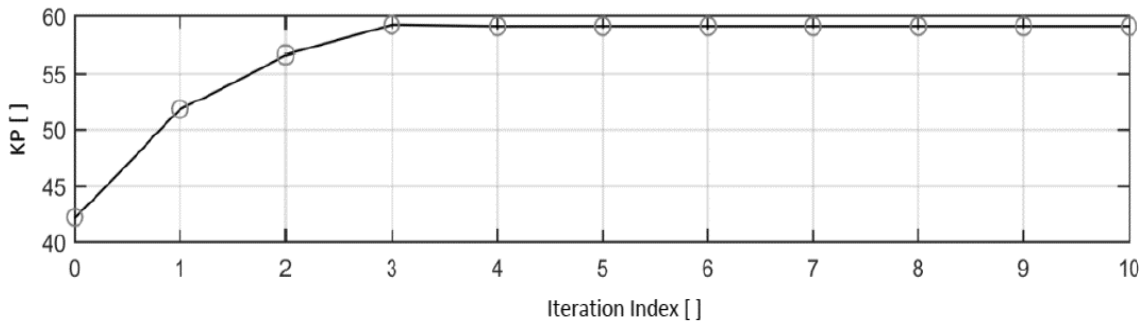


Figure 8. Optimization results of P coefficients with varying number of iteration

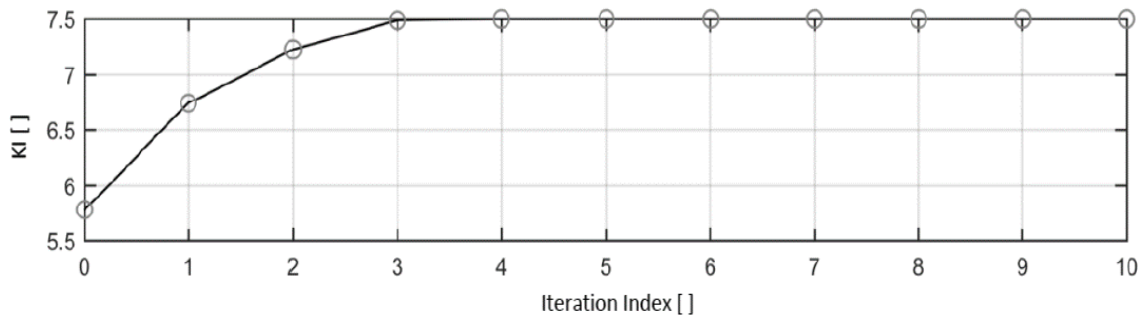


Figure 9. Optimization results of I coefficients with varying number of iteration

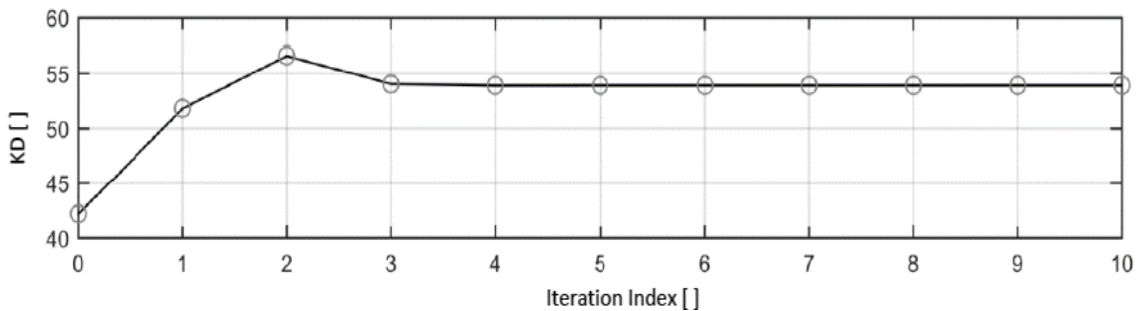


Figure 10. Optimization results of D coefficients with varying number of iteration

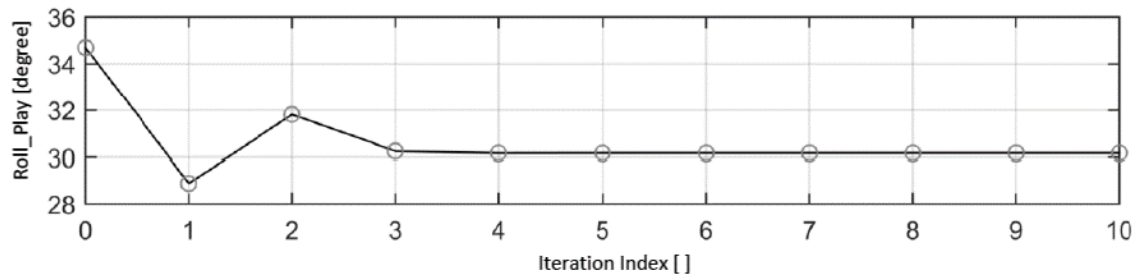


Figure 11. Roll play value of each iteration index

In this study, a UAV is redesigned using an innovative conversion approach to improve the autonomous flight performance of VTOL. The wing tip can change the dihedral angle from 20 to 40 degrees. Simultaneously, movable wing tip design and control system design are considered together. The control system is implemented in a traditional hierarchical structure consisting of six PID controllers, these for 3 longitudinal and 3 lateral movements, and autonomous flight performance is defined as the sum of longitudinal trajectory tracking parameters. Longitudinal PID coefficients and wingtip dihedral angle are optimized within the constraints to improve performance using SPSA.

The concurrent design idea combined with SPSA optimization resulted in a significant 33.5% improvement in longitudinal cost to the initial state. The PID coefficients of the initial condition were developed and the basic wing design resulted in a design with a 30 degree wing tip dihedral angle. Satisfactory closed-loop responses were obtained without any catastrophic release.

Scientific Ethics Declaration

The authors declare that the scientific ethical and legal responsibility of this article published in EPSTEM journal belongs to the authors.

Acknowledgements or Notes

* This article was presented as a poster presentation at the International Conference on Research in Engineering, Technology and Science (www.icrets.net) held in Budapest/Hungary on July 06-09, 2023.

*This work has been supported by Erciyes University Scientific Research Projects Coordination Unit under grant number FDK-2023-12554.

References

- Alanezi, M. A., Haruna, Z., Sha'aban, Y. A., Boucekara, H. R. E. H., Nahas, M., & Shahriar, M. S. (2022). Obstacle avoidance-based autonomous navigation of a quadrotor system. *Drones*, 6(10), 1–19. <https://doi.org/10.3390/drones6100288>
- Coban, S., Bilgic, H. H., & Akan, E. (2020). Improving autonomous performance of a passive morphing fixed wing UAV. *Information Technology and Control*, 49(1), 28–35. <https://doi.org/10.5755/j01.itc.49.1.23275>
- Falanga, D., Kleber, K., Mintchev, S., Floreano, D., & Scaramuzza, D. (2019). The Foldable Drone: A Morphing Quadrotor That Can Squeeze and Fly. *IEEE Robotics and Automation Letters*, 4(2), 209–216. <https://doi.org/10.1109/LRA.2018.2885575>
- Husain, Z., Al Zaabi, A., Hildmann, H., Saffre, F., Ruta, D., & Isakovic, A. F. (2022). Search and Rescue in a Maze-like Environment with Ant and Dijkstra Algorithms. *Drones*, 6(10), 1–30. <https://doi.org/10.3390/drones6100273>
- Kocamer, A., & Oktay, T. (2022). A Novel Morphing Approach Tilt-Rotor VTOL UAV. In *In Research & Reviews in Engineering* (pp. 213–224).
- Kose, O., & Oktay, T. (2021). Quadrotor Flight System Design using Collective and Differential Morphing with SPSA and ANN. *Nternational Journal of Intelligent Systems and Applications in Engineering (IJISAE)*, 9(4), 159–164.
- Kose, O., & Oktay, T. (2022). Hexarotor Yaw Flight Control with SPSA , PID Algorithm and Morphing.

International Journal of INTELLIGENT SYSTEMS AND APPLICATIONS IN ENGINEERING, 10(2), 216–221. <https://doi.org/10.1039/b000000x>

Kose, O., & Oktay, T. (2023). Simultaneous design of morphing hexarotor and autopilot system by using deep neural network and SPSA. *Aircraft Engineering and Aerospace Technology*, 95(6), 939–949. <https://doi.org/10.1108/AEAT-07-2022-0178>

Mustapa, M. Z. (2015). Altitude controller design for quadcopter UAV. *Jurnal Teknologi*, 74(1), 187–194. <https://doi.org/10.11113/jt.v74.3993>

Uzun, M., & Oktay, T. (2023). Simultaneous UAV having actively sweep angle morphing wing and flight control system design. *Aircraft Engineering and Aerospace Technology*, 95(7), 1062–1068. <https://doi.org/10.1108/AEAT-09-2022-0259>

Author Information

Tugrul Oktay

Erciyes University
Kayseri, Turkey
Contact e-mail: tugruloktay52@gmail.com

Firat Sal

Iskenderun Technical University
Iskenderun, Turkey

Oguz Kose

Erzincan Binali Yıldırım University
Merkez / Erzincan, Turkey

Abdullah Kocamer

Erciyes University
Kayseri, Turkey
Iskenderun Technical University
Iskenderun, Turkey

To cite this article:

Oktay, T., Sal, F., Kose, O., & Kocamer, A. (2023). Stochastic longitudinal autopilot tuning for best autonomous flight performance of a morphing VTOL drone. *The Eurasia Proceedings of Science, Technology, Engineering & Mathematics (EPSTEM)*, 23, 413-419.

The Eurasia Proceedings of Science, Technology, Engineering & Mathematics (EPSTEM), 2023

Volume 23, Pages 420-428

ICRETS 2023: International Conference on Research in Engineering, Technology and Science

Route Choice Preferences of Public Transport Passengers in Different Cities

Agoston Winkler

Szechenyi Istvan University

Abstract: In public transport network planning, it is essential to know the demands as well as the decision-making aspects of the passengers. A special timetable information and journey planning application has been developed and applied in 17 cities with different sizes and structures in North West Hungary since 2016 which is also able to collect and utilize the decisions of the users. Based on the collected real-life decision data, different logit models have been built for the different cities as well as for different age groups of the passengers. The examined variables are basically the time equivalents for transfers, walking and waiting phases of the journeys. This paper presents the main experiences of this project and the comparison of the decision models constructed so far. Results show clearly the differences between passenger layers of different cities and different ages in many cases, especially in larger cities where a higher amount of data is already available.

Keywords: Public transport, Passenger preferences, Urbanization, Route choice

Introduction

For the planning and development of sustainable public transport systems, it is important to have a deep understanding of the passengers' requirements and decision criteria system (Esztergár-Kiss & Caesar, 2017). To facilitate this, an online local transport timetable and journey planning system called "MenetRendes" was developed. This was used from June 2016 until October 2019 (and partly after that) by the former ÉNYKK Északnyugat-magyarországi Közlekedési Központ (North West Hungarian Transportation Center) Zrt. (reorganized in 2019) in 17 cities of various sizes and types (Ajka, Balatonfüred, Balatonfűzfő, Győr, Keszthely, Körmend, Lenti, Mosonmagyaróvár, Nagykanizsa, Pápa, Sopron, Szombathely, Tapolca, Várpalota, Veszprém, Zalaegerszeg, Zirc, their location is shown in Figure 1.) This created an opportunity to examine passenger preferences by city types (Winkler, 2017). This paper summarizes more than 3 years of operational experience and the scientific conclusions drawn from it, structured as follows. The next section takes a look at the functionalities of the "MenetRendes" software and the types of data the program logged. It will be followed by discussing how the logit decision-making models can be built from the data regarding the decision-making habits of the passengers, and how the models' coefficients can be determined. The section after this will show the usage statistics logged by ÉNYKK since June 2016 and also the decision-making models by cities based on the logged decision data. This will be followed by the preferences of the 6 passenger types (students, workers, pensioners at the start of their travel and during their travel) which are distinguished by the system, based on previous research (Winkler, 2010, 2011, 2013). Finally, the paper will be concluded.

The "MenetRendes" program

The main goal of the "MenetRendes" system (<http://menetrendes.hu/>) is to display the local (urban) public transport timetables in a unified format, including journey planning options (Winkler, 2010). The program's main functions are:

- This is an Open Access article distributed under the terms of the Creative Commons Attribution-Noncommercial 4.0 Unported License, permitting all non-commercial use, distribution, and reproduction in any medium, provided the original work is properly cited.

- Selection and peer-review under responsibility of the Organizing Committee of the Conference

© 2023 Published by ISRES Publishing: www.isres.org

- then, they have to choose a pass type (single line or for all lines) and travel discount (e.g., travel for free) that is used to determine the price of the journey
- if they do not have a pass or ID valid for all lines, they can set the default ticket type for the system to calculate with
- it is enough to set these once for each city: if cookies are allowed in the browser, these setting will be stored
- next, they have to choose the start and end point (based on the closest stop or on the map)
- then, they can set (it's not mandatory) the date and time of the journey, the default is the actual date and time, and other parameters can be set
- lastly, they have to click on the "Planning" button.



Which group do you belong to?

What travel certificate do you have?

Which ticket do you prefer?

Where will you start from? Filter:

Where is your destination? Filter:

When will you start?
 Year: Month: Day: Time: :
 Or: at the time of the request (recommended for creating a bookmark)

Other settings: without using tickets backbone lines only recommended transfers only

transfers maximum minutes safety for boardings (except for guaranteed connections)

minutes waiting maximum metres walking maximum

Recommended journey plans:

<p>(I) Arrival: 15:33 (28 July 2023)</p> <p>Journey time: 33 min</p> <p>Number of transfers: 1</p> <p>Waiting time: 10 min</p> <p>In-vehicle time: 19 min</p> <p>Walking distance: 318 m</p> <p>Price: 500.00 Ft</p> <p>Used line(s): 6, 7</p>	<p>I CHOOSE THIS!</p> <p>Please click here for details.</p>
<p>(II) Arrival: 15:59 (28 July 2023)</p> <p>Journey time: 59 min</p> <p>Number of transfers: 0</p> <p>Waiting time: 12 min</p> <p>In-vehicle time: 29 min</p> <p>Walking distance: 1161 m</p> <p>Price: 250.00 Ft</p> <p>Used line(s): 17B</p>	<p>I CHOOSE THIS!</p> <p>Please click here for details.</p>

Figure 2. User interface of "MenetRendes" with two alternative journey plans

The software will offer 2 alternative plans as shown on the bottom part of Figure 2 with its main parameters (time of arrival, journey time, number of transfers, waiting time, in-vehicle journey time, walking distance, price of journey) appearing on the bottom of the page. Blue marks the more suitable version, while red marks the less ideal option to aid the choice. For those familiar with the city, there is also a list of bus lines to be used. To display the details of the chosen plan, one has to click on "I CHOOSE THIS!" next to the plan. If, after reviewing the details, the user still prefers the other plan, it is possible to change by clicking on the "I RATHER CHOOSE THIS!" button.

For each choice, the software logs the following data (of course anonymously, it does not identify a specific user):

- query identifier (to manage modified decisions)
- city
- passenger layer
- type of day
- for both alternative journey plans:
 - generalized journey time (other features of the travel plan converted to in-vehicle time equivalent)
 - number of transfers (number)
 - in-vehicle journey time (minute)
 - total walking time (minute)
 - total waiting time (minute)
 - extra costs (HUF)
- the user's choice.

Building the Decision Models

One of the most commonly used model families for transport decision modelling, logit, was used for model building (Ortúzar & Willumsen, 1990). In case of logit models, the probability of choosing a particular option can be calculated with the following formula:

$$P_{jq} = \frac{e^{V_{j,q}}}{\sum_i e^{V_{i,q}}} \quad (1)$$

where P_{jq} is the probability that q individual chooses option j , and V_{iq} is the observed utility (or cost) of q individual for option i . The five explanatory variables in the current analysis are, in accordance with the system logs explained at the end of the previous section, the following:

- number of transfers
- in-vehicle journey time (minutes)
- total walking time (minutes)
- total waiting time (minutes)
- extra costs (forint).

Based on the above, the utility (or cost) function can be defined as:

$$V_{jq} = TRANSF_q transf_j + \sum VTIME_q vtime_j + \sum WALK_q walk_j + \sum WAIT_q wait_j + PAY_q pay_j \quad (2)$$

where

- $TRANSF_q$ is the coefficient of the number of transfers in case of q passenger (layer)
- $transf_j$ is the number of transfers in case of j journey
- $VTIME_q$ is the coefficient of in-vehicle journey time in case of q passenger (layer)
- $vtime_j$ is the in-vehicle journey time in case of j journey
- $WALK_q$ is the coefficient of total walking time in case of q passenger (layer)
- $walk_j$ is the total walking time in case of j journey
- $WAIT_q$ is the coefficient of total waiting time in case of q passenger (layer)
- $wait_j$ is the total waiting time in case of j journey
- PAY_q is the coefficient of extra costs in case of q passenger (layer)
- pay_j means the extra costs in case of j journey.

The model above as well as data logged by "MenetRendes" (the parameters of alternative journey plans and user decisions) were used to estimate the values of the above coefficients using the BIOGEME software (Bierlaire, 2009), grouping the decisions by city and passenger layer.

Estimating the Coefficients of Decision-Making Models by City

In the examined period, thousands of people used the services of “MenetRendes”, that includes 73,227 journey plans that involved stating their preferences indirectly. However, as seen on Figure 3, the users’ distribution by city was not uniform.

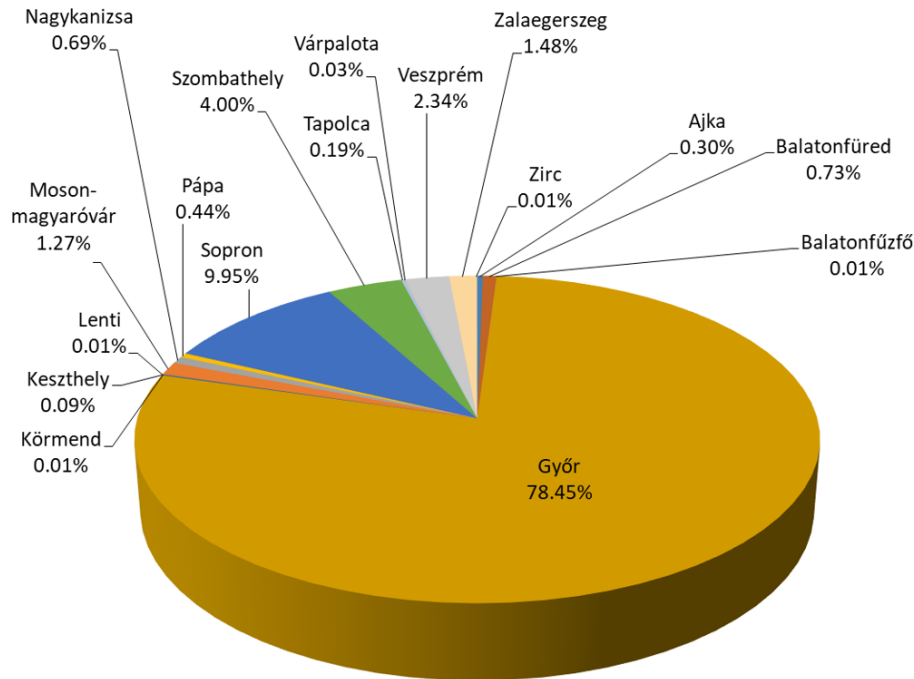


Figure 3. Share of journey planning usage per city

The software was used to plan journeys in Győr with a surprisingly high ratio of 78%. Even though among the examined cities, Győr’s population is the biggest (Table 1), this ratio is still too high, in relation to the population. An explanation could be that the trial version of “MenetRendes” has been available for Győr’s local bus service since 2013, so passengers in Győr have had more opportunities to use the software regularly. For the other newly added cities, the usage rate is already more or less proportional to the population of the cities.

Table 1. Results for different cities

City	Number of decisions processed	Choice rate of primarily recommended journey plan	In-vehicle time equivalent of a transfer (minutes)	In-vehicle time equivalent of 1 minute walking (min)	In-vehicle time equivalent of 1 minute waiting (min)
Ajka	219	76%	not significant	0.69	0.31
Balatonfüred	531	73%	58.89	2.06	0.91
Balatonfüzfő	5	80%	not significant	not significant	not significant
Győr	57,446	78%	20.03	2.46	1.09
Keszthely	69	88%	not significant	not significant	not significant
Körmend	8	63%	not significant	not significant	not significant
Lenti	9	78%	not significant	not significant	not significant
Mosonmagyaróvár	930	82%	not significant	not significant	not significant
Nagykanizsa	507	78%	not significant	not significant	not significant
Pápa	319	83%	not significant	not significant	not significant
Sopron	7,285	80%	24.35	2.66	1.20
Szombathely	2,929	75%	27.19	3.15	1.27
Tapolca	140	72%	not significant	not significant	not significant
Várpalota	23	70%	not significant	not significant	not significant
Veszprém	1,713	77%	14.77	2.37	0.85
Zalaegerszeg	1,082	77%	31.09	3.31	1.26
Zirc	10	18%	not significant	not significant	not significant
All together	73,225	78%	22.37	2.58	1.10

The method introduced above was used to calculate the coefficients of the utility (or cost) function in formula (2) for the corresponding logit model for all 17 cities. Table 1 does not show directly these, but more illustrative values converted to in-vehicle travel time equivalents for transfers, walking and waiting. The "not significant" marking in the table means that BIOGEME could not find statistically significant correlation. This usually occurs with cities for one or more coefficients where few people used the journey planner of "MenetRendes", so there were few decision-making data logged and analyzed. The analysis of monetary value only produced a significant result in Győr, where the value of 1 hour of travel was 4,544 HUF (~12 EUR), that correlates with previous results (Imam & Chryssanthopoulos, 2012). In the case of other cities, this matter may be the subject of further research.

When analyzing the results, it is useful to check the proportion of users who chose the primary or secondary recommended journey plans. Previous research (Winkler, 2013) concluded that if the discovered passenger preferences were neglected (meaning the only aspect that was regarded was the journey time), 73% of users chose the primary recommended option. With the use of the preference coefficients based on the research on previous decisions of users from Győr, this value reaches 78% in the 17 cities together, as shown in Table 1 and Figure 4. In the future, even better accuracy can be expected using the latest coefficients.

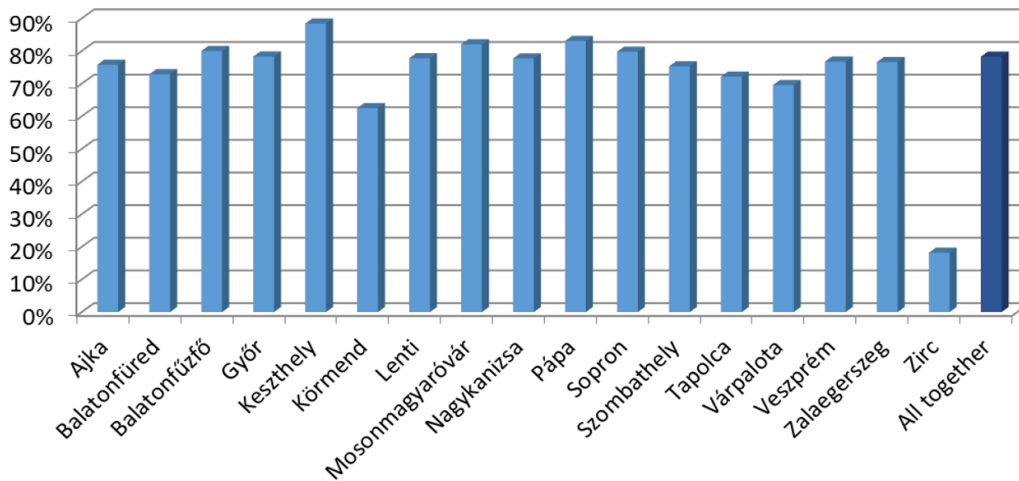


Figure 4. Choice rate of primarily recommended journey plan

The in-vehicle time equivalents which are statistically significant are shown by city in Table 1 and visually illustrated in Figures 5, 6, 7.

Figure 5 shows the in-vehicle time equivalent of transfers: in line with previous research (Sjöstrand, 2001; Winkler, 2013, 2017), the data show that the transfer "penalty" in various cities ranges from 14 to 32 minutes (however, slightly elevated, compared to the earlier results). The only outstanding data was found in Balatonfüred with 59 minutes. However, there is no visible correlation between the size of the cities and the time equivalent of transfers.

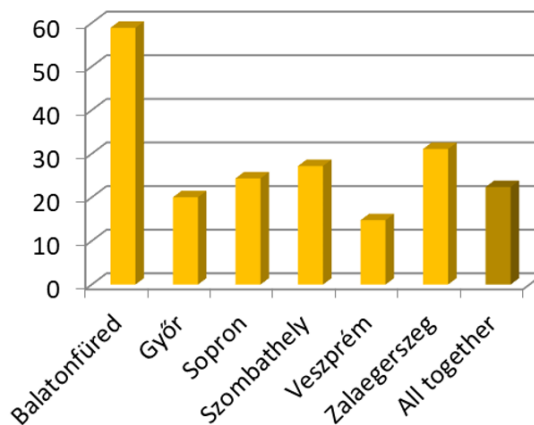


Figure 5. In-vehicle time equivalent of a transfer (minutes)

Figure 6 shows the time equivalent of walking (compared to the time equivalent of in-vehicle journey). Except for Ajka (where presumably the relatively small amount of data, and thus insufficiently representative sample, led to unexpected results) we can conclude, that in each city, time spent walking is a bigger burden for passengers than in-vehicle journey time. The degree of discomfort is described by multipliers ranging from 2.37 (Veszprém) to 3.15 (Szombathely).

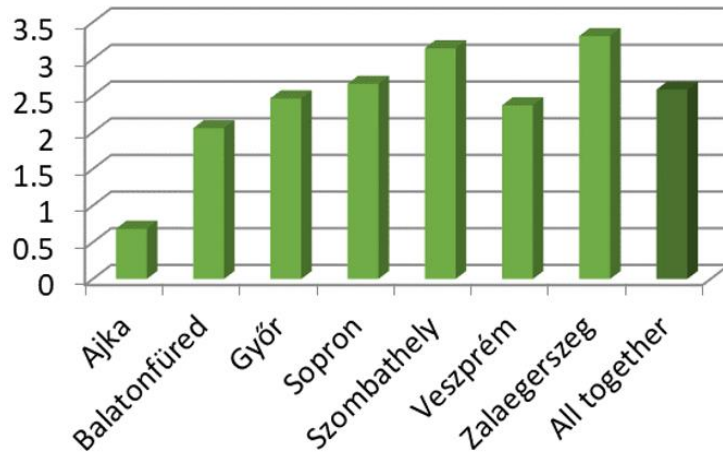


Figure 6. In-vehicle time equivalent of 1 minute walking (minutes)

Figure 7 shows the in-vehicle time equivalent of total waiting time. A particular feature of journey planning programs is that passengers usually do their planning in the comfort of their own homes or workplaces, often before the actual trip starts. As a result, they tend to perceive waiting as less of a disadvantage than if they were already at the bus stop, as they can spend their time in a useful and comfortable way until they actually have to leave for the bus stop. As a result, the calculated time equivalents are less than 1 in several cities, so the result was more favorable than the in-vehicle time. (This is of course truer before the journey starts, less so during the journey, as it will be shown in Table 2.) Due to this anomaly, no correlation was found between the values per city and the characteristics of the cities, and further research could be conducted to eliminate this deviation.

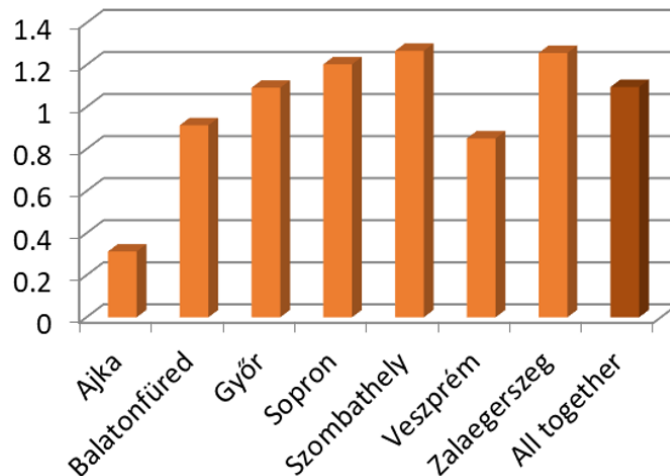


Figure 7. In-vehicle time equivalent of 1 minute waiting (minutes)

Estimating the Coefficients of Decision-Making Models by Passenger Layer

Although the primary focus of this paper is to examine the variation in passenger preferences by city, it was worthwhile to re-examine the coefficients (Winkler, 2013) for the 6 previous passenger layers (all cities combined), to take advantage of the relatively large sample size. The distribution of the logged decisions by passenger layer is shown in Figure 8, while the results of the model estimation with BIOGEME are shown in Table 2.

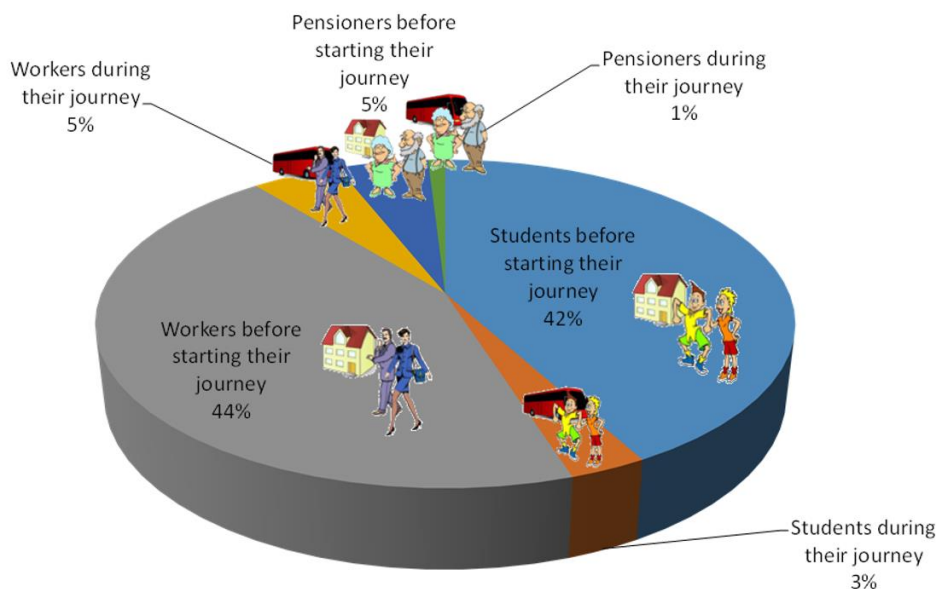


Figure 8. Share of users by passenger layers

Table 2. Results for different passenger layers

Passenger layer	Number of decisions processed	Choice rate of primarily recommended journey plan	In-vehicle time equiv. of a transfer (minutes)	In-vehicle time equiv. of 1 min walking (minutes)	In-vehicle time equiv. of 1 min waiting (min)
 Students before starting their journey	30,782	77%	18.10	2.73	1.10
 Students during their journey	2,225	76%	20.57	2.79	1.17
 Workers before starting their journey	32,269	79%	26.21	2.50	1.08
 Workers during their journey	3,563	79%	21.77	2.16	1.00
 Pensioners before starting their journey	3,698	80%	16.64	1.68	0.90
 Pensioners during their journey	690	76%	24.28	2.23	1.17

As previously mentioned, in case of preferences taken up during the journey, the coefficient of waiting time is typically higher compared to the in-vehicle time. This is understandable as the waiting time that comes with transfers cannot be used for any other purposes, and the circumstances would be less comfortable as waiting at the starting point (home, workplace). Similar results have been received for transfers and walking, apart from a few anomalies that would be expected to disappear if an even larger sample size could be used.

Conclusion

The paper introduced “MenetRendes”, an online system containing urban public transport timetable information and journey planning, and discussed operational experiences from 17 cities that were served by the former ÉNYKK Északnyugat-magyarországi Közlekedési Központ (North West Hungarian Transportation Center) Zrt. Based on 3+ years of experience, logit decision-making models were built that describe the criteria system of passengers in different cities and users from different passenger layers. The studies have shown certain correlations, confirming previous research results, although for several cities the amount of data recorded was

not sufficient to achieve statistically significant results, and in some cases (typically also in the small sample size cities) the results were different from those expected and less realistic. For these reasons, a more detailed analysis with different passenger layers inside the cities is not actual as this would lead to even smaller sample sizes and thus even less significant results. However, the results discussed above already show that the system can be used to discover the preferences of public transport users with the goal of designing increasingly high-quality public transport services and information systems.

Scientific Ethics Declaration

The author declares that the scientific ethical and legal responsibility of this article published in EPSTEM journal belongs to the author.

Acknowledgements and Notes

*The author would like to thank the former ÉNYKK Északnyugat-magyarországi Közlekedési Központ (North West Hungarian Transportation Center) Zrt. for the permission to use the data collected on their website for research purposes.

*This article was presented as an oral presentation at the International Conference on Research in Engineering, Technology and Science (www.icrets.net) held in Budapest/Hungary on July 06-09, 2023.

References

- Bierlaire, M. (2009). *Estimation of discrete choice models with BIOGEME 1.8*. <https://transport.epfl.ch/pythonbiogeme/archives/v18/tutorialv18.pdf>
- Esztergár Kiss, D. & Caesar, B. (2017). Definition of user groups applying Ward's method. *Transportation Research Procedia*, 22, 25-34.
- Imam, B. M., & Chryssanthopoulos, M. K. (2012). Causes and consequences of metallic bridge failures. *Structuring Engineering International: Journal of the International Association for Bridge and Structural Engineering (IABSE)*, 22(1), 93-98.
- Ortúzar, J. D. & Willumsen, L. G. (1990). *Modelling transport*. Chichester, United Kingdom: John Wiley & Sons.
- Sjöstrand, H. (2001). *Passenger assessments of quality in local public transport – measurement, variability and planning implications*. (Doctoral dissertation). <https://lup.lub.lu.se/search/publication/42015>
- Winkler, Á. (2010). Collecting public transport passenger preference data online. *Pollack Periodica*, 5(2), 119-126.
- Winkler, Á. (2011). Experiments to discover passenger preferences in public transport. *International Scientific Conference Mobilita'11: Sustainable Mobility, Slovak University of Technology in Bratislava, Bratislava, Slovak Republic*.
- Winkler, Á. (2013). *Utazói döntések modellezése a városi közforgalmú közlekedésben*. (Doctoral dissertation). <https://mmtti.sze.hu/winkler-agoston-2013->
- Winkler, Á. (2017). Utazói preferenciák vizsgálata eltérő méretű és típusú hazai városok helyi közforgalmú közlekedésében. *Közlekedéstudományi konferencia Győr 2017*, Széchenyi István University, Győr, Hungary.

Author Information

Ágoston Winkler
Széchenyi István University
Győr, Hungary
Contact e-mail: awinkler@sze.hu

To cite this article:

Winkler, A. (2023). Route choice preferences of public transport passengers in different cities. *The Eurasia Proceedings of Science, Technology, Engineering & Mathematics (EPSTEM)*, 23, 420-428.

The Eurasia Proceedings of Science, Technology, Engineering & Mathematics (EPSTEM), 2023

Volume 23, Pages 429-441

ICRETS 2023: International Conference on Research in Engineering, Technology and Science

Impact of Deepfake Technology on Social Media: Detection, Misinformation and Societal Implications

Samer Hussain Al-Khazraji
University of Diyala

Hassan Hadi Saleh
University of Diyala

Adil Ibrahim Khalid
University of Diyala

Israa Adnan Mishkhal
University of Diyala

Abstract: Deepfake technology, which allows the manipulation and fabrication of audio, video, and images, has gained significant attention due to its potential to deceive and manipulate. As deepfakes proliferate on social media platforms, understanding their impact becomes crucial. This research investigates the detection, misinformation, and societal implications of deepfake technology on social media. Through a comprehensive literature review, the study examines the development and capabilities of deepfakes, existing detection techniques, and challenges in identifying them. The role of deepfakes in spreading misinformation and disinformation is explored, highlighting their potential consequences on public trust and social cohesion. The societal implications and ethical considerations surrounding deepfakes are examined, along with legal and policy responses. Mitigation strategies, including technological advancements and platform policies, are discussed. By shedding light on these critical aspects, this research aims to contribute to a better understanding of the impact of deepfake technology on social media and to inform future efforts in detection, prevention, and policy development.

Keywords: Deepfake, Social media, Artificial intelligence, Generative adversarial networks, Deep neural networks.

Introduction

Deepfake technology refers to the use of artificial intelligence (AI) techniques, particularly machine learning (ML) algorithms, to manipulate and fabricate audio, video, and images in a way that convincingly deceives viewers. It leverages Deep Neural Networks (DNN), generative adversarial networks (GANs), and other advanced algorithms to create highly realistic synthetic media (Kietzmann, et al., 2020; Jones, 2020; Veerasamy & Pieterse., 2022). Deepfakes have gained attention due to their ability to generate convincing forgeries that can be indistinguishable from authentic recordings. This technology employs a two-step process: training a DNN on a large dataset of real media to learn patterns and then using that knowledge to generate new content by altering or replacing elements within the media (Nowroozi et al ., 2022).

In terms of audio manipulation, deepfake algorithms can imitate voices with remarkable accuracy by analyzing speech patterns, tone, and intonation from a source recording (Gao, 2022). This enables the creation of entirely new audio clips that resemble the voice of a specific individual. For video and image manipulation, deepfake

- This is an Open Access article distributed under the terms of the Creative Commons Attribution-Noncommercial 4.0 Unported License, permitting all non-commercial use, distribution, and reproduction in any medium, provided the original work is properly cited.

- Selection and peer-review under responsibility of the Organizing Committee of the Conference

© 2023 Published by ISRES Publishing: www.isres.org

algorithms can seamlessly swap faces or superimpose one person's face onto another's, creating the illusion that the target individual is saying or doing something they never actually did (Khichi et al., 2021). This can be achieved by training a deep neural network to learn facial features, expressions, and movements from numerous source videos and then applying that knowledge to manipulate the target video or image (Haliassos et al., 2021). The advancements in deepfake technology have raised concerns about their potential misuse (Yu et al., 2021). Deepfakes can be exploited to spread false information, manipulate public perception, damage reputations, and facilitate various forms of fraud and identity theft (de Rancourt-Raymond & Smaili, 2023). They pose significant challenges for media authenticity and trust, potentially undermining the credibility of visual and auditory evidence (Haney, 2003). Deepfake technology is a significant and disturbing innovation in media manipulation that necessitates ongoing research, technological countermeasures, and ethical considerations in order to address the possible hazards and implications it brings. As a result, numerous researchers worldwide are actively engaged in studying various aspects of deepfakes and striving to make significant discoveries in the field (Zachary, 2020). One crucial area of research focuses on developing robust and efficient detection techniques to identify deepfake media. Researchers are exploring approaches such as DNN, computer vision algorithms, and forensic analysis to differentiate between real and manipulated content. The aim is to create automated tools that can accurately and reliably detect deepfakes, enabling individuals, organizations, and social media platforms to identify and mitigate their spread (Nguyen et al., 2022). Another important avenue of research involves understanding the impact of deepfakes on society, particularly in areas such as journalism, politics, and public trust. Researchers are investigating the psychological and sociological effects of deepfake dissemination, exploring how it can alter perceptions, influence public opinion, and erode trust in visual and auditory evidence. Such studies help in formulating effective countermeasures and policies to mitigate the potential harm caused by deepfakes (Hall et al., 2022). Moreover, ethical considerations are a key focus for researchers studying deepfake technology. They are examining the ethical implications of creating and sharing deepfakes, as well as the responsibilities of individuals, content creators, and technology platforms in combating their misuse. Research efforts are directed towards establishing guidelines and frameworks that promote responsible use of AI and prevent the malicious application of deepfake technology (Dilrukshi et al., 2022). Thus, researchers are committed to expanding our understanding of deepfake technology and its societal consequences. They hope to achieve these goals through developing effective detection technologies, raising awareness, encouraging responsible use, and facilitating the formulation of ethical principles and legislation. Researchers, policymakers, and experts may collaborate to reduce the risks connected with deepfakes and build a safer and more trustworthy media environment.

Detection Techniques for Deepfake Content

Detecting deepfake content is a challenging task due to the increasing sophistication of deepfake algorithms and the ability to create highly realistic and deceptive media (Ali et al., 2021). However, researchers and experts have been developing various techniques to identify and differentiate between genuine and manipulated content (Masood et al., 2021). In this section, we discuss some of the key detection techniques for deepfake content:

Forensic Analysis: It involves examining the visual and audio characteristics of media to identify signs of manipulation. Techniques such as analyzing noise patterns, inconsistencies in lighting and shadows, and discrepancies in facial movements can help detect potential deepfake content. Digital forensics experts use specialized tools to scrutinize the metadata, compression artifacts, and digital footprints left behind during the creation or modification of deepfake media (Zhang et al., 2023).

AI-based Algorithms: AI-based algorithms play a significant role in deepfake detection, leveraging the advancements in ML and computer vision. Supervised learning algorithms, such as DNNs, can be trained on large datasets of both real and deepfake media to learn patterns and characteristics that differentiate between them. These algorithms extract features from the media, such as facial landmarks, motion patterns, or audio spectrograms, and use them as inputs to make predictions about the authenticity of the content (Masood et al., 2023).

Facial and Body Movements Analysis: Deepfake often struggle to precisely replicate natural facial and body movements, leading to potential inconsistencies that can be exploited for detection. Analysis of facial landmarks, eye movements, blinking, can help identify subtle abnormalities in deepfake videos. Advanced techniques, such as facial action coding systems, can be utilized to scrutinize the authenticity of facial expressions and detect signs of manipulation (Borji, 2023).

Multi-Modal Approaches: Deepfake detection can benefit from combining multiple modalities, such as analyzing both visual and audio aspects of the media. Integrating facial and voice recognition technologies can provide a more comprehensive assessment of the authenticity of the content. Fusion of information from different modalities can enhance accuracy and reliability of deepfake detection systems (Malik et al., 2022).

Dataset and Model Analysis: Deepfake detection can involve analyzing the characteristics of the datasets used to train deepfake algorithms or scrutinizing the models themselves. Researchers examine the distribution and quality of training datasets, as deepfake algorithms often have limitations in capturing the full complexity and variability of real-world data. Additionally, reverse-engineering deepfake models can aid in identifying specific artifacts or signatures that indicate the presence of manipulated content (Giudice et al., 2021).

It is worth noting that deepfake detection is an ongoing research area, and the development of robust and reliable detection techniques is a constant race against evolving deepfake technology (Yang et al., 2023). Combining these detection techniques enhances the overall effectiveness in identifying deepfake content. AI-based algorithms provide automated and scalable solutions, while forensic analysis adds a layer of technical scrutiny. User-reported mechanisms leverage the collective intelligence of users to identify and report suspicious content (Stroebel et al., 2023). The synergy among these approaches enables a multi-faceted and comprehensive deepfake detection framework. Table 1 present strengths and limitation of some Deepfake techniques.

Spread of Misinformation and Disinformation

This section explores the role of deepfakes in the dissemination of false information. It delves into the techniques employed by malicious actors to leverage deepfakes for their agenda, examines case studies illustrating deepfake-driven false narratives, and analyzes the potential consequences on public trust and societal implications. By understanding the impact of deepfakes on the spread of misinformation and disinformation, we can begin to develop effective strategies to combat this growing challenge and safeguard the integrity of information in the digital era.

Deepfakes have emerged as a powerful tool for spreading misinformation and disinformation, posing significant challenges to society (Choraś et al., 2021). The following analysis explores how deepfakes contribute to the dissemination of false information (Godulla et al., 2022).

Authenticity and Trust (Godulla et al., 2021): Deepfakes blur the line between reality and fabrication by creating highly convincing fake media. This erodes trust in visual evidence and challenges the authenticity of digital content. Misinformation can easily gain credibility when it is disguised as a genuine video or image, making it more likely to be shared and believed by unsuspecting individuals.

Amplification of False Narratives (Chesney & Citron, 2019): Deepfakes enable the creation of compelling narratives that manipulate public opinion. Malicious actors can use deepfakes to portray individuals saying or doing things they never actually did. These false narratives are designed to provoke emotional responses, reinforce existing biases, or exploit societal divisions, thereby amplifying the spread of misinformation.

Virality and Speed (Hobbs, 2020): Deepfakes can quickly go viral due to their sensational nature, captivating audiences and generating significant attention. In the fast-paced world of social media, the speed at which deepfakes can spread makes it challenging to contain the dissemination of false information. Even after debunking, the deepfake may have already reached a wide audience, making it difficult to rectify the damage done.

Targeted Manipulation (Hartmann & Giles, 2020): Deepfakes can be specifically targeted to exploit vulnerabilities in individuals or organizations. By creating tailored deepfakes, malicious actors can manipulate public figures, politicians, or key influencers to disseminate false information or create chaos. This targeted manipulation aims to sow doubt, confuse public discourse, and undermine trust in institutions and leaders.

Difficulty in Detection (Gosse & Burkell, 2020): The increasing sophistication of deepfake technology poses challenges for detection and debunking. As deepfakes become more realistic, distinguishing between genuine and manipulated content becomes harder. This allows deepfakes to circulate undetected for extended periods, further fueling the spread of misinformation.

Table 1. Strengths & Limitation of Some Deepfake Techniques

Strengths	Limitations
AI-based algorithms can leverage the power of ML to automatically analyze and classify large volumes of media (Choraś et al., 2021).	AI-based algorithms heavily rely on the availability of diverse and well-curated training datasets that represent the full range of deepfake variations (Kayes & Iamnitchi, 2017).
They can learn complex patterns and features that distinguish between real and manipulated content (Choraś et al., 2021).	The arms race between deepfake creators and detection algorithms means that new and more sophisticated deepfake techniques may outpace the detection capabilities (Kayes & Iamnitchi, 2017).
These algorithms can adapt and improve over time as they are exposed to more data (Choraś et al., 2021).	Adversarial attacks, where deepfake generators are designed to specifically evade detection algorithms, can pose challenges to AI-based detection systems (Kayes & Iamnitchi, 2017).
AI-based detection systems can be deployed in real-time or automated settings, making them efficient for large-scale content analysis (Wu et al., 2019).	
Forensic analysis can provide valuable insights into the technical aspects of deepfake content, such as metadata, compression artifacts, and inconsistencies (Paraskevoudis et al., 2020).	Forensic analysis may require technical expertise and specialized tools, making it less accessible to non-experts (Kayes et al., 2022).
It can detect specific anomalies or artifacts that may indicate manipulation (Cao et al., 2020).	Deepfake creators can employ sophisticated techniques to minimize or disguise forensic traces, making it challenging to detect manipulations (Tahir et al., 2021).
Forensic techniques can be applied to various types of media, including images, videos, and audio (Cao et al., 2020).	False positives and false negatives are possible, as legitimate media may exhibit some artifacts or inconsistencies that can be mistaken for manipulation (Hansen et al., 2008).
Deepfake creators can employ sophisticated techniques to minimize or disguise forensic traces, making it challenging to detect manipulations (Zhou et al., 2018).	
User-reported mechanisms leverage the collective intelligence of social media users, allowing for a broader network of detection (Zhou et al., 2018).	
Users can identify and report suspicious or potentially deepfake content based on their intuition or awareness (Zhou et al., 2018).	
User-reported mechanisms can serve as an early warning system for emerging deepfake trends or new manipulation techniques (Dang Nguyen et al., 2015).	Reliance on user reports can introduce delays in detection and may not be scalable for large volumes of content (Orben & Przybylski, 2019).
Reliance on user reports can introduce delays in detection and may not be scalable for large volumes of content (Dang Nguyen et al., 2015).	User reporting can be subjective, leading to potential false positives or false negatives (Iacobucci et al., 2021).
User reporting can be subjective, leading to potential false positives or false negatives. (Zhou et al., 2018).	Some users may lack the necessary awareness or understanding to identify deepfake content accurately (Lyu, 2022).
Users may lack the necessary awareness or understanding to identify deepfake content accurately (Lyu, 2022).	

Psychological Impact (Vasist, Pramukh Nanjundaswamy, and Satish Krishnan, 2022): Deepfakes can have profound psychological effects on individuals. When people encounter deepfakes that target their personal or collective identities, it can lead to confusion, anxiety, and a sense of distrust. The emotional impact of encountering convincing deepfakes can significantly influence individuals' perceptions and beliefs, perpetuating the spread of misinformation.

To combat the spread of misinformation and disinformation through deepfakes, it is crucial to develop robust detection techniques, promote media literacy, raise awareness about the existence and implications of deepfakes, and establish policies that hold creators and disseminators of malicious deepfakes accountable (Godulla et al., 2021). By addressing the underlying issues and understanding the mechanisms through which deepfakes contribute to the spread of misinformation, we can work towards mitigating their impact and fostering a more informed and resilient society. Investigating case studies and examples of deepfake-driven false narratives sheds light on the real-world impact and implications of this technology. Here are a few notable instances (Rini et al., 2022):

- 1) **Political Manipulation:** In 2019, a deepfake video of Belgian politician Koen Geens went viral. The video, created by a political party, portrayed Geens giving a speech in which he appeared to support climate change denial. The deepfake aimed to damage Geens' reputation and influence public opinion on environmental policies.
- 2) **Fake News and Election Interference:** During the 2019 Indian elections, deepfake videos featuring political candidates were circulated on social media platforms. These videos showed candidates making controversial statements or engaging in unethical activities, which were entirely fabricated. The intent was to spread disinformation, manipulate public perception, and sway voter opinions.
- 3) **Revenge Porn and Non-consensual Content:** Deepfakes have been used to create explicit videos or images by superimposing someone's face onto adult content without their consent. This non-consensual use of deepfakes not only violates personal privacy but also has severe emotional and psychological consequences for the individuals targeted.
- 4) **Celebrity Impersonations:** Deepfakes have been utilized to create convincing impersonations of celebrities. These videos show celebrities engaging in activities they never participated in, such as controversial interviews or endorsing products. Such deepfake-driven false narratives can damage the reputations of celebrities and mislead their fan base.
- 5) **Fake Corporate Communications:** Deepfake technology has also been used to mimic the voices of high-level executives or company representatives. Fraudsters have employed deepfakes to create audio messages or phone calls that mimic the voices of CEOs, deceiving employees or shareholders into performing unauthorized actions, such as transferring funds or sharing sensitive information.

These case studies illustrate the wide-ranging implications of deepfake-driven false narratives. They highlight the potential for malicious actors to manipulate public opinion, spread misinformation, and harm individuals or organizations. Understanding the real-world consequences of deepfake-driven false narratives is essential for developing effective countermeasures, strengthening legal frameworks, and raising awareness about the risks associated with this technology. The potential consequences of deepfake technology on public trust and societal implications are significant and far-reaching. Here is a discussion of some of these consequences (Karnouskos, 2020):

- A. **Erosion of Public Trust** (Karnouskos, 2020): Deepfakes have the power to undermine public trust in media, institutions, and even personal relationships. When people can no longer discern real from fake, it becomes challenging to trust the authenticity of any information or visual evidence. This erosion of trust can have profound societal implications, including increased skepticism, polarization, and a breakdown of consensus on shared realities.
- B. **Spread of Disinformation and Manipulation** (Lorenzo, 2022): Deepfakes enable the creation and dissemination of highly realistic false narratives. Malicious actors can exploit this technology to propagate disinformation, manipulate public opinion, and influence societal discourse. Deepfakes can be used to fuel conspiracy theories, defame individuals, sway elections, or exacerbate social divisions. The consequences include a distorted public discourse, compromised democratic processes, and the amplification of harmful narratives.
- C. **Impact on Journalism and Media Credibility** (Geddes, 2020): Deepfakes pose significant challenges for journalists and media organizations. As deepfakes become more convincing, verifying the authenticity of visual evidence becomes more complex. This can undermine the credibility of journalists and news outlets,

as false information presented as genuine can be inadvertently disseminated. The public's trust in journalism may diminish, making it harder to differentiate reliable sources from manipulated content.

- D. **Psychological and Emotional Impact** (Yazdinejad et al., 2021): Deepfakes can have a profound psychological and emotional impact on individuals who are targeted or exposed to manipulated content. Victims of non-consensual deepfake pornography, for example, may suffer from trauma, humiliation, and damage to their personal and professional lives. Moreover, encountering convincing deepfakes can lead to anxiety, confusion, and a general sense of mistrust, affecting individuals' overall well-being.
- E. **Legal and Ethical Challenges** (Yazdinejad et al., 2021): The rise of deepfakes raises complex legal and ethical questions. Laws and regulations are struggling to keep up with the rapid advancement of technology, leaving legal systems ill-equipped to address the harmful consequences of deepfakes adequately. Determining accountability, establishing guidelines for content creation and dissemination, and protecting individual rights in the face of deepfake threats present ongoing challenges.
- F. **Need for Technological and Policy Solutions** (Yazdinejad et al., 2021): Addressing the societal implications of deepfakes requires a multifaceted approach. Technological advancements in deepfake detection, authentication, and content attribution are essential. Collaborative efforts between researchers, industry, and policymakers are necessary to develop robust solutions. Additionally, the implementation of policies and regulations that discourage the malicious use of deepfakes and provide legal frameworks for addressing deepfake-related issues is crucial.

By recognizing the potential consequences of deepfakes on public trust and understanding their societal implications, we can work towards mitigating their negative impact. Combating deepfakes requires a combination of technological innovation, media literacy initiatives, legal measures, and public awareness campaigns to foster a more informed and resilient society (Rini et al., 2020).

Societal Implications of Deepfake Technology

The emergence of deepfake technology has profound societal implications across various domains. Here are some key societal implications of deepfake technology (Yazdinejad et al., 2020):

- i. **Misinformation and Trust Crisis** (Yazdinejad et al., 2021): Deepfakes contribute to the spread of misinformation, eroding public trust in media, institutions, and public figures. The ability to create convincing fake content undermines the authenticity of information, making it difficult for individuals to discern truth from falsehood. This trust crisis has implications for democratic processes, public discourse, and the functioning of society as a whole.
- ii. **Political Manipulation and Election Integrity** (Yazdinejad et al., 2021): Deepfakes pose a significant threat to political integrity. Malicious actors can leverage deepfakes to manipulate public opinion, create false narratives, and influence elections. By spreading fake videos or audio clips of political figures, deepfakes can undermine trust in candidates, distort public debates, and disrupt the democratic process.
- iii. **Damage to Reputation and Personal Harm** (Yazdinejad et al., 2020): Individuals can be targeted by deepfakes, resulting in severe personal harm and reputational damage. Non-consensual deepfake pornography, for instance, violates privacy, subjects victims to emotional distress, and impacts their personal and professional lives. Deepfakes can also be used to defame public figures, tarnish their reputations, and disrupt their careers.
- iv. **Legal and Ethical Concerns** (Traboulsi, 2020): Deepfakes raise complex legal and ethical questions. Existing laws often struggle to keep pace with the rapidly evolving technology, making it challenging to hold individuals accountable for the creation and dissemination of deepfakes. Balancing free speech rights with the need to prevent harm and protect individuals' rights poses ongoing challenges for policymakers and legal frameworks.
- v. **Impact on Journalism and Media Landscape** (Yazdinejad et al., 2021): Deepfakes have implications for journalism and the media landscape. Journalists face the challenge of verifying the authenticity of media content in an era of sophisticated deepfakes. The proliferation of deepfakes undermines the credibility of news sources and creates a fertile ground for the spread of misinformation, making it more challenging for the public to differentiate between reliable information and manipulated content.
- vi. **Privacy and Consent** (Yazdinejad et al., 2020): Deepfakes raise concerns about privacy and consent. The ability to manipulate and fabricate audio, video, and images poses threats to individuals' privacy and control over their personal data. Deepfakes can be created without consent, leading to violations of personal boundaries and potential harm to individuals' well-being.
- vii. **Cultural and Social Impacts** (Yazdinejad et al., 2020): Deepfakes can have broader cultural and social impacts. They can perpetuate stereotypes, reinforce biases, and deepen societal divisions. The ease of

manipulating audio, video, and images challenges the notion of objective truth, potentially leading to a society where subjective realities and subjective truths become more prevalent.

Addressing the societal implications of deepfake technology requires collaboration between technology developers, policymakers, legal experts, and society as a whole (Traboulsi, 2020). Efforts should focus on developing robust detection and authentication mechanisms (Yazdinejad et al., 2020). Only through comprehensive approaches can we effectively navigate the challenges posed by deepfake technology and minimize its negative societal impacts (Rini et al., 2022).

Strategies and Countermeasures

Strategies and countermeasures play a vital role in mitigating the negative impact of deepfake technology (Yazdinejad et al., 2020). Here are some key strategies and countermeasures that can be employed:

- a) **Advancing Deepfake Detection Technology** (Yazdinejad et al., 2021): Continued research and development of deepfake detection algorithms and technologies are crucial. By investing in advanced machine learning techniques, deepfake detection models can be trained to identify patterns, inconsistencies, and artifacts specific to manipulated media. Collaboration between researchers, industry experts, and technology companies is essential for developing robust detection tools.
- b) **Building Robust Authentication Systems** (Yazdinejad et al., 2021): Developing secure and tamper-proof authentication systems can help verify the authenticity of media content. Techniques such as digital watermarking, cryptographic hashing, and blockchain technology can be employed to ensure the integrity and provenance of media files. Incorporating these authentication mechanisms into social media platforms and content distribution networks can enhance trust and discourage the proliferation of deepfake content.
- c) **Strengthening Platform Policies** (Yazdinejad et al., 2021): Social media platforms need to implement and enforce strict policies against the creation, distribution, and amplification of deepfake content. Clear guidelines should be established to govern the use of artificial intelligence and media manipulation technologies on these platforms. This includes setting up reporting mechanisms for users to flag potential deepfakes and implementing appropriate consequences for those who violate the policies.
- d) **Promoting Media Literacy and Education** (Yazdinejad et al., 2021): Enhancing media literacy and digital literacy among users is critical to combat the spread of deepfake content. Educational initiatives can focus on teaching individuals how to critically evaluate media, identify signs of manipulation, and verify the authenticity of content. By empowering users with the knowledge and skills to navigate the digital landscape, they can become more resilient to deepfake-driven misinformation.
- e) **Collaboration between Technology Companies and Researchers** (Yazdinejad et al., 2021): Collaboration between technology companies and researchers is essential for staying ahead of deepfake advancements. Companies can provide data and resources to researchers, enabling them to improve detection methods and develop more effective countermeasures. Open dialogue and information sharing can help identify emerging threats and develop proactive strategies to combat deepfakes.
- f) **Legal and Policy Frameworks** (Traboulsi, 2020): Governments and policymakers should develop comprehensive legal and policy frameworks to address the challenges posed by deepfakes. These frameworks should outline the legal consequences for creating and disseminating malicious deepfake content, provide guidelines for content removal, and establish mechanisms for victims to seek legal recourse. International cooperation is vital to address the global nature of deepfake-related issues.
- g) **Raising Public Awareness** (Traboulsi, 2020): Public awareness campaigns can play a crucial role in educating individuals about the existence and potential risks of deepfakes. These campaigns can highlight the implications of deepfakes on various aspects of society, such as politics, journalism, and personal privacy. By raising awareness, individuals can become more vigilant consumers of media and more proactive in reporting and combating deepfake content.

Implementing these strategies and countermeasures requires a collaborative effort involving technology companies, researchers, policymakers, educators, and users (Traboulsi, 2020). By combining technological advancements, policy interventions, and user empowerment, society can better protect against the negative impacts of deepfakes and maintain trust in media and information sources (Kozyreva et al., 2020).

Mitigating the negative impact of deepfakes requires a multi-faceted approach that involves technological advancements, policy interventions, and user empowerment. Here are some strategies and techniques proposed to address the challenges posed by deepfakes presented in table (Sahu, et al., 2023; Paterson, & Hanley, 2020; Mustak, et al., 2023; Hobbs, 2020; Langa, 2021; Rothstein et al., 2021; Bateman, 2020):

Table 2. Techniques for addressing deepfake challenges

Ref.	Technique	Strategy
[58]	Deepfake Detection and Authentication	This includes leveraging ML, computer vision, and audio analysis to identify inconsistencies and artifacts indicative of manipulation. Additionally, explore the use of watermarking, digital signatures, and blockchain technology to verify the authenticity of media content.
[59]	Collaboration and Information Sharing	Foster collaboration between technology companies, researchers, and government agencies to share knowledge, datasets, and expertise in combating deepfakes.
[60]	Platform Policies and Content Moderation	Enforce robust policies on social media platforms to prevent the creation, distribution, and amplification of deepfake content. Establish clear guidelines that prohibit the malicious use of deepfakes and provide reporting mechanisms for users to flag potentially fake content
[61]	Media Literacy and Education	Promote media literacy and digital literacy initiatives to educate users about the existence and risks of deepfakes. Teach individuals how to critically analyze media content, identify signs of manipulation, and verify the authenticity of sources.
[62]	Legal Frameworks and Consequences	Develop comprehensive legal frameworks that address the creation, distribution, and malicious use of deepfake technology. Establish laws and regulations that hold individuals accountable for creating and disseminating harmful deepfake content.
[63]	Ethical Guidelines for AI and Deepfake Technologies	Promote the development and adoption of ethical guidelines for the responsible use of AI and deepfake technologies. Encourage technology companies and developers to prioritize ethical considerations, such as obtaining proper consent, respecting privacy rights.
[64]	Public Awareness Campaigns	Launch public awareness campaigns to educate the general public about the existence and potential risks of deepfakes. These campaigns can raise awareness about the implications of deepfakes on various aspects of society, including politics, journalism, and personal privacy.
[65]	Technological Innovation	Foster ongoing technological innovation to stay ahead of evolving deepfake techniques. Continuously invest in research and development to improve <u>detection algorithms, authentication methods, and countermeasures.</u>

Table 3. Technological advancements in deepfake detection and prevention

Ref.	Technique	Strategy
[68]	ML Algorithms	Researchers are continually refining ML algorithms to improve the accuracy and efficiency of deepfake detection. Techniques such as CNNs, RNNs, and GANs are used to train models on large datasets of both real and manipulated media.
[69]	Face and Voice	This methods leverage advancements in face and voice biometrics to identify
[70]	Deepfake-specific Forensics	Researchers are developing specialized forensics tools and techniques to analyze digital media for signs of manipulation. These tools utilize deepfake-specific artifacts, such as inconsistencies in lighting, shadows, reflections, to detect and attribute deepfake content
[71]	Multi-Modal Analysis	This methods are incorporating multi-modal analysis, combining information from multiple sources such as audio, video, and text, to improve accuracy. By examining inconsistencies across different modalities, these techniques can identify subtle discrepancies that may be harder to detect using single-modal analysis alone.
[72]	Synthetic Media Generation Techniques	Researchers are exploring the use of synthetic media generation techniques to create large-scale datasets for training deepfake detection models. This approach helps in staying ahead of evolving deepfake creation techniques.

[73]	Real-Time Detection	Real-time deepfake detection systems are being developed to identify and flag manipulated media in near real-time. These systems leverage optimized algorithms and hardware acceleration to analyze media streams in live settings, such as video conferences or social media platforms.
[74]	Collaboration with Industry	Collaboration between researchers, technology companies, and social media platforms is crucial for developing effective deepfake detection and prevention methods. Technology companies can provide access to data and resources for training and testing detection models, while social media platforms can integrate detection algorithms into their content moderation systems
[75]	Technological Innovation	Foster ongoing technological innovation to stay ahead of evolving deepfake techniques. Continuously invest in research and development to improve detection algorithms, authentication methods, and countermeasures.

By implementing these strategies and techniques, it is possible to mitigate the negative impact of deepfakes and foster a more trustworthy and resilient digital ecosystem (Sahu et al., 2020). However, it requires a collaborative effort involving stakeholders from technology, policy, education, and society at large to effectively address the challenges posed by deepfakes (Mustak et al., 2023; Hobbs, 2020; Langa, 2021; Rothstein et al., 2020; Diakopoulos & Johnson, 2021; Bateman, 2020; Pavis, 2021). Technological advancements in deepfake detection and prevention are crucial for mitigating the negative impact of deepfake technology (Mustak et al., 2023). Table 3 includes some of key areas of technological development in this field: Technological advancements in deepfake detection and prevention are essential for staying ahead of the evolving nature of deepfakes. Continuous research, innovation, and collaboration are key to developing robust and effective solutions that can detect and mitigate the negative impact of deepfakes on social media and beyond.

Conclusion

The research has yielded several key findings and insights. Here is a summary of the significant findings:

1. Deepfake technology poses a significant threat: Deepfakes have the ability to manipulate and fabricate audio, video, and images with high accuracy, making it difficult for users to discern between real and fake content.
2. Prevalence of deepfakes on social media: Deepfakes are increasingly prevalent on social media platforms, leading to the spread of misinformation and disinformation. They can be used to create false narratives, deceive the public, and manipulate public opinion.
3. Detection techniques are advancing: Various detection techniques, including AI-based algorithms, forensic analysis, and user-reported mechanisms, are being developed to identify deepfake content. However, these techniques have limitations and are constantly evolving to keep up with the evolving sophistication of deepfakes.
4. Consequences on public trust: The spread of deepfakes undermines public trust in media and information sources. Deepfakes can be used to create fake news, impersonate individuals, and manipulate public discourse, leading to a erosion of trust in digital content.
5. Societal implications: Deepfake technology has far-reaching societal implications. It can impact journalism, politics, privacy, and social dynamics. The ability to fabricate audio, video, and images can have serious consequences for individuals, organizations, and society as a whole.
6. Strategies and countermeasures: To mitigate the negative impact of deepfakes, various strategies and countermeasures have been proposed. These include advancements in deepfake detection and authentication, collaboration between stakeholders, user education, platform policies, legal frameworks, and technological innovation.

Deepfake technology presents significant implications and challenges that require careful reflection. Here are some key points to consider:

1. Threat to trust and credibility: Deepfakes pose a serious threat to trust and credibility in media and information sources. As the technology advances, it becomes increasingly difficult for users to distinguish between real and fake content. This erosion of trust can have far-reaching consequences, including the spread of misinformation, damage to reputations, and the manipulation of public opinion.

2. **Impact on society and democracy:** Deepfakes have the potential to disrupt societal norms and democratic processes. They can be used to manipulate elections, create false narratives, and incite social unrest. The rapid spread of deepfakes on social media platforms amplifies their impact, making it challenging to control the dissemination of false information and ensuring the integrity of public discourse.
3. **Privacy concerns:** Deepfake technology raises significant privacy concerns. The ability to manipulate someone's appearance or voice without their consent can infringe upon their privacy rights. Deepfakes can be used for malicious purposes such as revenge porn, harassment, or identity theft, leading to serious personal and psychological harm.
4. **Importance of collaborative efforts:** Addressing the challenges posed by deepfakes requires collaborative efforts between researchers, technology companies, policymakers, and users.
5. **Need for ongoing research and innovation:** Deepfake technology is constantly evolving, necessitating ongoing research and innovation. It is essential to stay at the forefront of technological advancements in both deepfake creation and detection to effectively address the challenges. Continued research will help develop new techniques, algorithms, and tools to combat deepfakes and protect individuals and society from their harmful effects.

Recommendations

Reflecting on the implications and challenges posed by deepfake technology highlights the urgency of addressing this issue. It calls for a multi-faceted approach that encompasses technological advancements, legal frameworks, ethical considerations, user education, and collaborative efforts to ensure the responsible use of deepfake technology and protect the integrity of digital media. Based on the findings, the following recommendations can be made for future research, policy development, and technological advancements:

- A. **Enhance deepfake detection techniques:** Continued research and development are needed to improve the accuracy and efficiency of deepfake detection methods. This includes exploring new ML algorithms, leveraging advanced computer vision techniques, and incorporating multi-modal analysis to detect deepfakes across different media types.
- B. **Develop robust and standardized evaluation metrics:** Establishing standardized evaluation metrics is crucial to compare and benchmark the performance of deepfake detection algorithms. This will facilitate the assessment of detection techniques, foster collaboration between researchers, and drive advancements in the field.
- C. **Foster interdisciplinary research collaborations:** Encourage collaborations between researchers from various disciplines, such as computer science, psychology, media studies, and law. This interdisciplinary approach will facilitate a deeper understanding of the psychological, societal, and legal implications of deepfake technology, leading to more comprehensive solutions.
- D. **Increase investment in deepfake research and development:** Governments, funding agencies, and industry stakeholders should allocate resources to support research and development efforts specifically focused on deepfake technology. Increased investment will drive innovation, accelerate the development of detection techniques, and facilitate the creation of effective countermeasures.
- E. **Develop comprehensive legal frameworks:** Policymakers need to establish comprehensive legal frameworks that address the creation, distribution, and malicious use of deepfakes. This includes considering legislation around consent, privacy rights, intellectual property, and the responsible use of deepfake technology. Clear and enforceable laws will serve as a deterrent and provide a legal recourse for individuals impacted by deepfakes.
- F. **Strengthen platform policies and accountability:** Social media platforms should adopt and enforce stricter policies to combat the spread of deepfakes. They should implement mechanisms for reporting and removing deepfake content, promote transparency in content moderation practices, and hold users accountable for malicious activities. Regular audits and transparency reports can help assess the effectiveness of platform policies.
- G. **Promote media literacy and digital literacy:** Education initiatives should be developed to enhance media literacy and digital literacy skills among users. This includes teaching individuals how to critically evaluate information, identify signs of manipulation, and verify the authenticity of media content. By empowering users with the necessary skills, they can better navigate the digital landscape and make informed decisions.
- H. **Foster international collaboration and information sharing:** Encourage international collaboration among governments, technology companies, and researchers to address the global nature of deepfake challenges. Sharing information, best practices, and lessons learned will foster a collective effort to combat deepfakes and protect global digital ecosystems.

1. Encourage responsible use of deepfake technology: Promote ethical guidelines and responsible practices among creators and users of deepfake technology. Emphasize the importance of obtaining consent, respecting privacy rights, and using deepfake technology for legitimate and non-malicious purposes. Public awareness campaigns can play a significant role in highlighting the ethical considerations and responsible use of deepfake technology.

By implementing these recommendations, future research, policy development, and technological advancements can contribute to mitigating the negative impact of deepfake technology, safeguarding public trust, and ensuring the responsible development and use of deepfake detection tools and countermeasures.

Scientific Ethics Declaration

The authors declare that the scientific ethical and legal responsibility of this article published in EPSTEM journal belongs to the authors.

Acknowledgements or Notes

* This article was presented as an oral presentation at the International Conference on Research in Engineering, Technology and Science (www.icrets.net) held in Budapest/Hungary on July 06-09, 2023.

References

- Ali, S., DiPaola, D., & Breazeal, C. (2021). What are GANs?: Introducing generative adversarial networks to middle school students. *Proceedings of the AAAI Conference on Artificial Intelligence*, 35(17), 15472-15479).
- Bateman, J. (2020). *Carnegie endowment for international peace*. <https://carnegieendowment.org/2020/07/08/deepfakes-and-synthetic-media-in-financial-system-assessing-threat-scenarios-pub-82237>
- Borji, A. (2023). Qualitative failures of image generation models and their application in detecting deepfakes. *arXiv*, 1.
- Cao, J., Qi, P., Sheng, Q., Yang, T., Guo, J., & Li, J. (2020). Exploring the role of visual content in fake news detection. *Disinformation, Misinformation, and Fake News in Social Media*, 141-161.
- Chesney, B., & Citron, D. (2019). Deep fakes: a looming challenge for privacy, democracy, and national security. *California Law Review*, 107, 1753.
- Chintha, A., Thai, B., Sohrawardi, S.J., Bhatt, K., Hickerson, A., Wright, M., & Ptucha, R. (2020). Recurrent convolutional structures for audio spoof and video deepfake detection. *IEEE Journal of Selected Topics in Signal Processing*, 14(5), 1024-1037.
- Choraś, M., Demestichas, K., Gielczyk, A., Herrero, Á., Ksieniewicz, P., Remoundou, K., Urda, D., & Woźniak, M. (2021). Advanced machine learning techniques for fake news (online disinformation) detection: A systematic mapping study. *Applied Soft Computing*, 101.
- Dang Nguyen, D.T., Pasquini, C., Conotter, V., & Boato, G. (2015). Raise: a raw images dataset for digital image forensics. In *Proceedings of the 6th ACM multimedia systems conference*, 219-224.
- de Rancourt-Raymond, A., & Smali, N. (2023). The unethical use of deepfakes. *Journal of Financial Crime*, 30(4), 1066-1077.
- Diakopoulos, N., & Johnson, D. (2021). Anticipating and addressing the ethical implications of deepfakes in the context of elections. *New Media & Society*, 23(7), 2072-2098.
- Gamage, D., Ghasiya, P., Bonagiri, V., Whiting, M. E., & Sasahara, K. (2022). Are deepfakes concerning? analyzing conversations of deepfakes on reddit and exploring societal implications. *Proceedings of the 2022 CHI Conference on Human Factors in Computing Systems (CHI '22)*. Association for Computing Machinery, 1, 1-19.
- Gao, Y. (2022). *Audio deepfake detection based on differences in human and machine generated speech*. (Doctoral dissertation). Carnegie Mellon University.
- Geddes, K. (2020). Ocularcentrism and deepfakes: Should seeing be believing? *Fordham Intellectual Property, Media & Entertainment Law Journal*, 31, 1042.
- Giudice, O., Guarnera, L., & Battiato, S. (2021). Fighting deepfakes by detecting gan dct anomalies. *Journal of Imaging*, 7(8), 128.

- Godulla, A., Hoffmann, C.P., & Seibert, D. (2021). Dealing with deepfakes—an interdisciplinary examination of the state of research and implications for communication studies. *SCM Studies in Communication and Media*, 10(1), 72-96.
- Gosse, C., & Burkell, J. (2020). Politics and porn: How news media characterizes problems presented by deepfakes. *Critical Studies in Media Communication*, 37(5), 497-511.
- Haliassos, A., Vougioukas, K., Petridis, S., & Pantic, M. (2021). Lips don't lie: a generalisable and robust approach to face forgery detection. *Proceedings of the IEEE/CVF Conference on Computer Vision and Pattern Recognition*, 5039-5049.
- Hall, M., Hearn, J. & Lewis, R.. (2022). *Digital gender-sexual violations, violence, technologies, motivations*. London: Taylor & Francis.
- Haney, C. (2003). The psychological impact of incarceration: Implications for postprison adjustment. *Prisoners once Removed* (p. 33). Urban Institute Press 2003.
- Hansen, A. (2022). *Relationships, Religion and Robotics: The Soul and the Ethical Implications of AI*. (Doctoral dissertation) .
- Hartmann, K., & Giles, K. (2020). The next generation of cyber-enabled information warfare. *12th International Conference on Cyber Conflict (CyCon)*, 1300, 233-250. IEEE.
- Hobbs, R. (2020). *Mind over media: Propaganda education for a digital age*. WW Norton & Company.
- Iacobucci, S., De Cicco, R., Michetti, F., Palumbo, R., & Pagliaro, S. (2021). Deepfakes unmasked: the effects of information priming and bullshit receptivity on deepfake recognition and sharing intention. *Cyberpsychology, Behavior, and Social Networking*, 24(3), 194-202.
- Jones, V. (2020). *Artificial intelligence enabled deepfake technology: The emergence of a new threat*. (Doctoral dissertation). Utica College.
- Karnouskos, S. (2020). Artificial intelligence in digital media: The era of deepfakes. *IEEE Transactions on Technology and Society*, 1(3), 138-147.
- Kayes, I., & Iamnitich, A. (2017). Privacy and security in online social networks: A survey. *Online Social Networks and Media*, 3, 1-21.
- Khichi, M., & Yadav, R.K. (2021). Analyzing the methods for detecting deepfakes. *3rd International Conference on Advances in Computing, Communication Control and Networking (ICAC3N)*, 340-345. IEEE.
- Kietzmann, J., Lee, L.W., McCarthy, I. P., & Kietzmann, T. C. (2020). Deepfakes: Trick or treat? *Business Horizons*, 63(2), 135-146.
- Kozyreva, A., Lewandowsky, S., & Hertwig, R. (2020). Citizens versus the internet: Confronting digital challenges with cognitive tools. *Psychological Science in the Public Interest*, 21(3), 103-156.
- Langa, J. (2021). Deepfakes, real consequences: Crafting legislation to combat threats posed by deepfakes. *BUL Rev.*, 101, 761.
- Liu, K., Li, M., Liu, Y., Li, M., Guo, Z., & Hong, F. (2008). Passive diagnosis for wireless sensor networks. *Proceedings of the 6th ACM conference on Embedded network sensor systems*, 113-126.
- Lorenzo, D. (2022). *Analysis and conceptualization of deepfake technology as cyber threat*. Universita Degli Studi Firenze.
- Lyu, S. (2022). Deepfake detection. *Multimedia Forensics*, 313-331.
- Malik, A., Kuribayashi, M., Abdullahi, S.M., & Khan, A.N. (2022). DeepFake detection for human face images and videos: A survey. *IEEE Access*, 10, 18757-18775.
- Masood, M., Nawaz, M., Malik, K.M., Javed, A., Irtaza, A., & Malik, H. (2023). Deepfakes generation and detection: State-of-the-art, open challenges, countermeasures, and way forward. *Applied Intelligence*, 53(4), 3974-4026.
- Mills, A.M., Gammelgaard, A.Ø., Bek, A.S., Thomsen, M.R., & Fabricius, A.H. (2021). Voice data, power structures and technological enframing: a critical examination of Spotify as irrational regress.
- Moshayedi, A.J., Roy, A.S., Kolahdooz, A., & Shuxin, Y. (2022). Deep learning application pros and cons over algorithm. *EAI Endorsed Transactions on AI and Robotics*, 1(1).
- Mustak, M., Salminen, J., Mäntymäki, M., Rahman, A., & Dwivedi, Y.K. (2023). Deepfakes: Deceptions, mitigations, and opportunities. *Journal of Business Research*, 154, 113368.
- Nguyen, T.T., Nguyen, Q.V.H., Nguyen, D.T., Nguyen, D.T., Huynh-The, T., Nahavandi, S., Nguyen, T.T., Pham, Q.V., & Nguyen, C.M. (2022). Deep learning for deepfakes creation and detection: A survey. *Computer Vision and Image Understanding*, 223.
- Nowroozi, E., Seyedshoari, S., Mohammadi, M., & Jolfaei, A. (2022). Impact of media forensics and deepfake, In Society. *Breakthroughs in Digital Biometrics and Forensics*, Springer, 387-410.
- Orben, A., & Przybylski, A.K. (2019). The association between adolescent well-being and digital technology use. *Nature Human Behaviour*, 3(2), 173-182.
- Paraskevoudis, K., Panagiotis, K., & Elias P. K. (2020). Real-time 3d printing remote defect detection (stringing) with computer vision and artificial intelligence. *Processes*, 8(11), 1464.

- Paterson, T., & Hanley, L. (2020). Political warfare in the digital age: cyber subversion, information operations and 'deep fakes'. *Australian Journal of International Affairs*, 74(4), 439-454.
- Pavis, M. (2021). Rebalancing our regulatory response to Deepfakes with performers' rights. *Convergence*, 27(4), 974-998.
- Rini, R., & Cohen, L. (2022). Deepfakes, deep harms. *Ethics & Social Philosophy*, 22(1), 143.
- Rothstein, M.A., Wilbanks, J.T., Beskow, L.M., Brelsford, K.M., Brothers, K.B., Doerr, M., Evans, B.J., Hammack-Aviran, C.M., McGowan, M.L., & Tovino, S.A. (2020). Unregulated health research using mobile devices: Ethical considerations and policy recommendations. *Journal of Law, Medicine & Ethics*, 48(51), 196-226.
- Sahu, A.K., Umachandran, K., Biradar, V.D., Comfort, O., Sri Vigna Hema, V., Odimegwu, F., & Saifullah, M.A. (2023). A study on content tampering in multimedia watermarking. *SN Computer Science*, 4(3), 222.
- Stroebel, L., Llewellyn, M., Hartley, T., Ip, T.S., & Ahmed, M. (2023). A systematic literature review on the effectiveness of deepfake detection techniques. *Journal of Cyber Security Technology*, 7(2), 83-113.
- Tahir, R., Batool, B., Jamshed, H., Jameel, M., Anwar, M., Ahmed, F., Zaffar, M.A., & Zaffar, M.F. (2021). Seeing is believing: Exploring perceptual differences in deepfake videos. In *Proceedings of the 2021 CHI Conference on Human Factors in Computing Systems*.
- Tolosana, R., Vera-Rodriguez, R., Fierrez, J., Morales, A. and Ortega-Garcia, J. (2020). Deepfakes and beyond: A survey of face manipulation and fake detection. *Information Fusion*, 64, 131-148.
- Traboulsi, N. (2020). *Deepfakes: Analysis of threats and countermeasures*. (Doctoral dissertation). California State University, Fullerton.
- Vasist, P. N., & Satish Krishnan. (2022). Deepfakes: An integrative review of the literature and an agenda for future research. *Communications of the Association for Information Systems*, 51(1), 14.
- Veerasamy, N., & Pieterse, H. (2022). Rising above misinformation and deepfakes. *International Conference on Cyber Warfare and Security*.
- Wu, L., Morstatter, F., Carley, K.M., & Liu, H. (2019). Misinformation in social media: definition, manipulation, and detection. *ACM SIGKDD Explorations Newsletter*, 21(2), 80-90.
- Yang, W., Zhou, X., Chen, Z., Guo, B., Ba, Z., Xia, Z., Cao, X. and Ren, K. (2023). AVoid-DF: Audio-visual joint learning for detecting deepfake. *IEEE Transactions on Information Forensics and Security*, 18, 2015-2029.
- Yazdinejad, A., Zolfaghari, B., Azmoodeh, A., Dehghantanha, A., Karimipour, H., Fraser, E., Green, A.G., Russell, C., & Duncan, E. (2021). A review on security of smart farming and precision agriculture: Security aspects, attacks, threats and countermeasures. *Applied Sciences*, 11(16), 7518.
- Yu, N., Skripniuk, V., Abdelnabi, S., & Fritz, M. (2021). Artificial fingerprinting for generative models: Rooting deepfake attribution in training data. *Proceedings of the IEEE/CVF International Conference on Computer Vision*, 14448-14457.
- Zachary, G. (2020). Digital manipulation and the future of electoral democracy in the US. *Digital Manipulation and the Future of Electoral Democracy in the US*, 1(2), 104-112.
- Zhou, P., Han, X., Morariu, V.I., & Davis, L.S. (2018). Learning rich features for image manipulation detection. *Proceedings of the IEEE Conference on Computer Vision and Pattern Recognition*, 1053-1061.

Author Information

Samer Hussain Al-Khazraji
University of Diyala,
Diyala, Iraq
Contact e mail: samerbaq@yahoo.com

Hassan Hadi Saleh
University of Diyala,
Diyala , Iraq

Adil Ibrahim Khalil
University of Diyala,
Diyala , Iraq

Israa Mishkal
University of Diyala
Diyala, Iraq

To cite this article:

Al-Khazraji, S.H., Saleh H.H., Khalil, A.I., & Mishkal, I. A. (2023). Impact of deepfake technology on social media: Detection, misinformation, and societal implications. *The Eurasia Proceedings of Science, Technology, Engineering & Mathematics (EPSTEM)*, 23, 429-441.

The Eurasia Proceedings of Science, Technology, Engineering & Mathematics (EPSTEM), 2023

Volume 23, Pages 442-451

ICRETS 2023: International Conference on Research in Engineering, Technology and Science

Probabilistic Piecewise-Objective Optimization Model for Integrated Supplier Selection and Production Planning Problems Involving Discounts and Probabilistic Parameters: Single Period Case

Sutrisino Sutrisno
Diponegoro University

Widowati Widowati
Diponegoro University

Robertus Heri Soelistyo Utomo
Diponegoro University

Abstract: In manufacturing and retail industries, supplier selection problems deal with allocating the optimal raw material amount that should be purchased to each supplier such that the procurement cost is minimal. Meanwhile, production planning problems deal with maximizing the product amount to be produced. Decision-makers need to take optimal decisions for those problem to gain the maximal revenue. In this paper, a novel mathematical model in the class of probabilistic piecewise programming is proposed as a decision-making support that can be used to find the optimal decision in solving both integrated supplier selection and production planning problems involving discounts and probabilistic parameters. The objective is to gain the optimal performance of the supply chain, i.e., maximizing the profit from the production activity. The model covers multi-raw material, multi-supplier, multi-product, and multi-buyer situations. Numerical experiments were conducted to evaluate the proposed model and to illustrate how the optimal decision is taken. Results showed that the proposed decision-making support successfully solved the problem and provided the optimal decision for the given problem. Therefore, the proposed model can be implemented by decision-makers/managers in industries.

Keywords: Decision-making support, Discounts, Order-allocation, Piecewise-objective, Probabilistic optimization, Production planning, Supplier selection

Introduction

Manufacturing and retail companies keep trying to make optimal decisions in their activities to maximize their profit. The fundamental activities that are crucial to be optimized include supplier selection, or also called order allocation planning, and production planning. For the supplier selection, the decision-maker needs to decide to which suppliers the raw materials or parts has to be purchased and how much it is. The purchased raw materials have to satisfy the number that is needed for the production. Meanwhile, in production planning, the decision-maker needs to decide the number of each product type or brand to produce such that the demand from buyers or customers is fulfilled. Those decisions should be made in such a way that the profit is expected to be maximal. Furthermore, there are some constraints or conditions that should be met by the action taken by the decision-maker, such as suppliers' maximum capacities, production capacities, etc.

Those two topics have been widely studied by researchers and practitioners, and various approaches have been proposed to deal with those problems. The most common approach is building mathematical models of the form

- This is an Open Access article distributed under the terms of the Creative Commons Attribution-Noncommercial 4.0 Unported License, permitting all non-commercial use, distribution, and reproduction in any medium, provided the original work is properly cited.

- Selection and peer-review under responsibility of the Organizing Committee of the Conference

© 2023 Published by ISRES Publishing: www.isres.org

optimization models or programming. However, each model commonly deals with those problems with its own specifications. A simple linear programming model was built in (Ware et al., 2014), which can be used to solve supplier selection problems. However, it did not consider production planning in the model, and all parameters were certainly known. A slightly more complex model was built in (Sharma et al., 2019) for dealing with deteriorating products. Some other existing models consider various specific situations such as rapid service demand (Alegoz & Yapıcıoğlu, 2019) analytical hierarchy process (Manik, 2023) and machine learning (Ali et al., 2023), among others. Those models were built theoretically and simulated with randomly generated data. Meanwhile, some other reports showed practical applications in many fields such as logistics management (Ghorbani & Ramezani, 2020; Olanrewaju et al., 2020), food companies (Hajiaghayi Keshteli et al., 2023), glove industries (Joy et al., 2023), defense industries (Guner & Deveci, 2023), etc.

Note that studies that are mentioned above solved the supplier selection problem independently. Regarding the production planning problem, various mathematical models have also been formulated. Again, the models are based on the specifications of the problem. For example, a production planning problem in an uncertain environment has been solved via a linear optimization model in (Singh & Biswal, 2021) or nonlinear optimization in (Li et al., 2021). Some other approaches used single/multi-objective programming in solving production planning problems under sustainability requirements (Lahmar et al., 2022; Wu et al., 2020; Yazdani et al., 2021; Zarte et al., 2022) a mixed integer linear programming under nonconstant consumptions (Adrio et al., 2023) model predictive control approach as a sustainable aggregate approach (May et al., 2023) and many more. In particular, some practical reports are also available from multiple sectors such as food and agriculture (Angizeh et al., 2020) mining (Zhang et al., 2022) and chemical & pharmaceutical companies (Adrio et al., 2023; Lindahl et al., 2023) among others, showing the implementation of the theoretical results in practice.

Even though numerous models have been built and available to use, each model is suitable for problems with the specified conditions or specifications. When the situation is different, a modification or even a new model is often needed to formulate. In this paper, the supplier selection and production planning problems are considered with probabilistic parameters, and are solved in an integrated manner, meaning that the model can handle the flow of the raw materials and products between those two activities in one model. Furthermore, those problems are considered with discounted price features in which price functions such as for raw material prices, transportation costs, and product selling prices may contain discounts. No existing models is available in literature for this situation; this is the main contribution provided in this paper. The problem is modeled in a probabilistic programming with a piecewise objective function. Moreover, in the end of the paper, the proposed model will be demonstrated via numerical experiments.

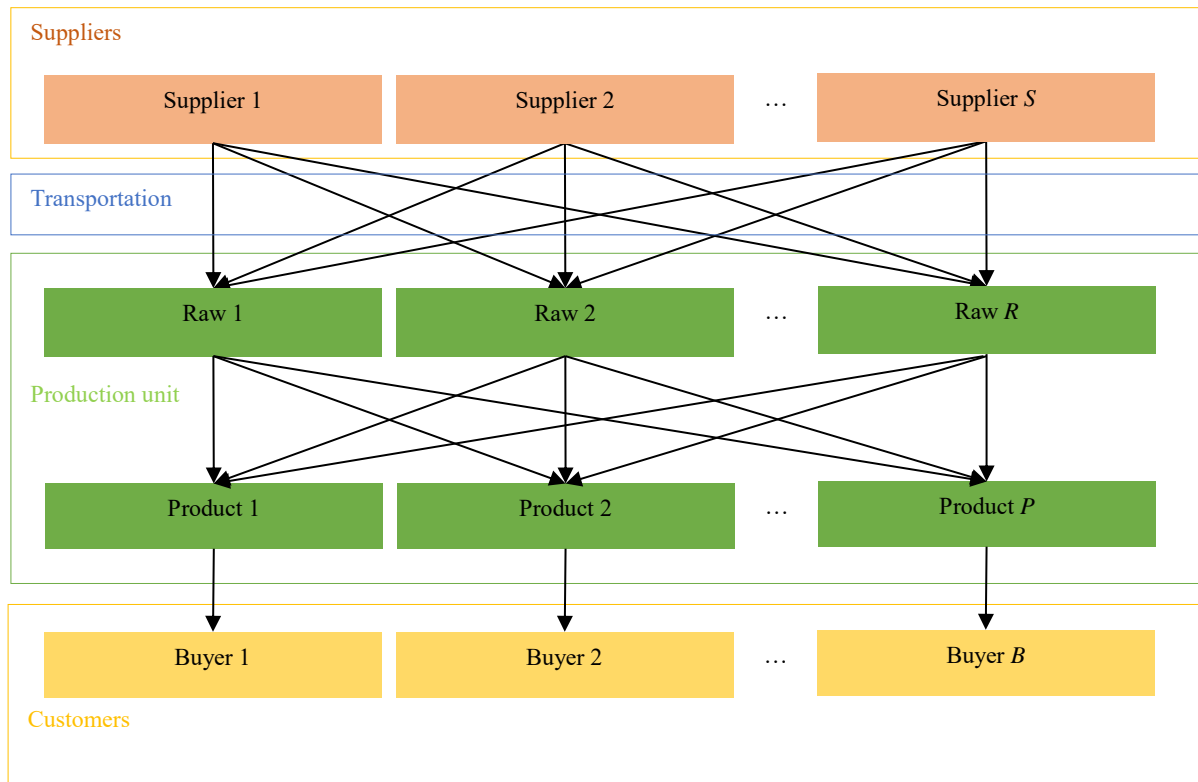


Figure 1. The flow of raw materials and products between suppliers, production units, and buyers

Method

Problem Setup

Suppose that a manufacturing company is planning to produce P product brands from R raw material types. Those raw materials will be purchased to S suppliers or vendors. Produced products will be sold to buyers. The flow of the raw materials and the products are shown in Fig. 1. The objective is to maximize the profit from this production activity subject to some limitations and specific conditions. Those limitations or constraints are explained in the following explanations. The performances of suppliers are varied. This includes the variation of the maximum capacity limit in supplying raw materials, prices, defect rates, transportation costs, and the punctuality. This makes the decision-making process in the raw material procurement is not obvious. Furthermore, the problem contains discounts on prices or cost. This includes discounted prices of raw materials from suppliers, transportation costs from carriers, and prices of products sold to buyers. In this study, the discounted price functions are assumed to follow piecewise constant functions in which prices for more raw materials or products are cheaper with some price break levels or points, for further technical details, see the mathematical modelling section. On the other hand, suppliers have some limitations on supplying raw materials. It includes maximum number of raw materials that can be ordered, some number of raw materials might be rejected when arrived at the manufacturer due to damaged or low quality, and some number of raw materials might be not delivered on time (in this case, those cannot be used in the production). The maximum capacities are known, however, the rate of rejected raw materials and the rate of late delivered raw materials are not known and are uncertain. Nevertheless, historical data are assumed to be available, and thus those uncertain values can be treated as probabilistic parameters with some suitable probability distribution functions such as normal or Gaussian distribution. All decision variables were assumed to have integer measurements in this study; this needs to be taken into account in the model.

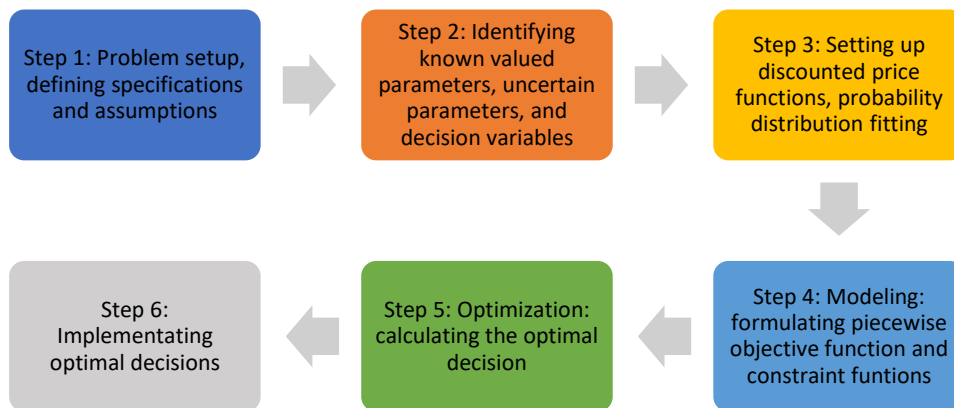


Figure 2. Problem solving steps

Methodology

The methodology is summarized as problem solving steps depicted in Figure 2. The first step has been explained above. In the second step, four uncertain parameters have been considered, i.e., rates of rejected and late delivered raw materials from suppliers, rejected product rate in the production, and product demand from buyers. Meanwhile, the decision variables are the number of each raw material type to be ordered to each supplier, the number of each product brand planned to be produced from the available raw materials, the number of trucks used in the raw material transportation, and artificial decision variables indicating whether a supplier is selected or not in supplying raw materials. The next step is formulating the discounted price/cost functions and probability distribution functions for the uncertain parameters. Piecewise constant functions were utilized in this study, see the mathematical modeling section for further technical details, and normal or Gaussian distribution functions were used, see the numerical experiment results for further explanations. After that, the problem is modeled into a mathematical programming. The objective function is formulated as the profit from the raw material procurement, production, and product selling activities, which was maximized. Constraint functions were formulated based on the problem's specifications described in the previous section, see the mathematical modeling section for more detailed descriptions. Next, the optimal decision is calculated from the derived mathematical programming. The interior point algorithm combined with branch-and-bound to find integer solutions were utilized. Finally, the derived optimal decision is implemented by the decision-maker.

Mathematical Model

The supplier selection and production planning problems defined in the previous section are modeled as follows. First, define the following symbols:

indices

r	:	type raw material;
s	:	index of supplier;
p	:	type of product brand;
B	:	index of buyer;
i, j, k	:	index of discount level;

decision variables:

X_{rs}	:	amount of raw material of type r purchased to supplier s ;
Y_p	:	amount of product type p produced by the manufacturer;
T_s	:	Delivery number to transport raw materials from supplier s to the manufacturer;
Z_s	:	indicator variable for supplier s whether some raw materials are purchased to the supplier or not; 1 if yes, 0 if not;

prices or costs with discounts:

$UP_{rs}^{(i)}$:	discounted price on discount level i for one unit of raw material r at supplier s ;
$PP_{pb}^{(j)}$:	discounted selling price on discount level j for one unit of product brand p sold to buyer b ;
$TC_s^{(k)}$:	discounted transportation cost on discount level k for one time of delivery in transporting raw materials from supplier s to the manufacturer;

probabilistic parameters:

DR_{rs}	:	rates of raw material type r 's defect amount that was ordered to supplier s ;
LR_{rs}	:	rates of raw material type r 's late delivered amount that was ordered to supplier s ;
DP_p	:	rates of product brand p 's defect amount.
DE_{pb}	:	amount of product brand p 's demand from buyer b .

deterministic parameters:

O_s	:	cost to order raw materials to supplier s ;
PC_p	:	cost to produce one unit of product brand p ;
SC_{rs}	:	supplier s 's maximum capacity limit in supplying raw material type r ;
TRC	:	maximum capacity of the truck used in transporting raw materials from suppliers to the manufacturer;
PL_{rs}	:	cost to penalize one unit of late delivered raw material type r that was ordered to supplier s ;
PD_{rs}	:	cost to penalize one unit of defected raw material type r that was ordered to supplier s ;
RR_{rp}	:	amount of raw material type r that is needed to produced one unit product brand p .

Now, we present the scheme of the discounted prices and costs. It is modeled as piecewise constant functions as follows. The discounted prices for raw materials are formulated as

$$UP_{rs} = \begin{cases} UP_{rs}^{(1)} & \text{if } 0 = X_{rs}^{(0)} < X_{rs} \leq X_{rs}^{(1)}, \\ UP_{rs}^{(2)} & \text{if } X_{rs}^{(1)} < X_{rs} \leq X_{rs}^{(2)}, \\ \vdots & \\ UP_{rs}^{(I)} & \text{if } X_{rs}^{(I-1)} < X_{rs} \leq X_{rs}^{(I)}. \end{cases} \quad (1)$$

Similarly, the discounted transport costs are formulated as

$$TC_s = \begin{cases} TC_s^{(1)} & \text{if } 0 = T_s^{(0)} < T_s \leq T_s^{(1)}, \\ TC_s^{(2)} & \text{if } T_s^{(1)} < T_s \leq T_s^{(2)}, \\ \vdots & \\ TC_s^{(K)} & \text{if } T_s^{(K-1)} < T_s \leq T_s^{(K)}. \end{cases} \quad (2)$$

Using the same scheme, the discounted product selling prices are formulated as

$$PP_{pb} = \begin{cases} PP_{pb}^{(1)} & \text{if } 0 = DE_{pb}^{(0)} < DE_{pb} \leq P_{pb}^{(1)}, \\ PP_{pb}^{(2)} & \text{if } DE_{pb}^{(1)} < DE_{pb} \leq DE_{pb}^{(2)}, \\ \vdots & \\ PP_{pb}^{(J)} & \text{if } DE_{pb}^{(J-1)} < DE_{pb} \leq DE_{pb}^{(J)}. \end{cases} \quad (3)$$

As the consequence of the discounted product selling prices defined above, the income (F_{0b}) has also the form of the piecewise function. This is formulated as

$$F_{0b} = \begin{cases} \sum_{p=1}^P [PP_p^{(1)} \cdot DE_{pb}] & \text{if } 0 = DE_{pb}^{(0)} < DE_{pb} \leq DE_{pb}^{(1)}, \\ \sum_{p=1}^P [PP_p^{(2)} \cdot DE_{pb}] & \text{if } DE_{pb}^{(1)} < DE_{pb} \leq DE_{pb}^{(2)}, \\ \vdots & \\ \sum_{p=1}^P [PP_p^{(J)} \cdot DE_{pb}] & \text{if } DE_{pb}^{(J-1)} < DE_{pb} \leq DE_{pb}^{(J)}. \end{cases}$$

Total of seven operational cost components was taken into account. This includes order cost, purchasing cost, delivery cost, penalty cost of late deliveries, penalty cost of defect raw materials, production cost, and penalty cost for defect products. Based on the discounted prices and costs defined above, those cost components are modeled as

$$\begin{aligned} F_1 &= \sum_{s=1}^S [OC_s \times Z_s] \\ F_2 &= \begin{cases} \sum_{r=1}^R \sum_{s=1}^S [UP_{rs}^{(1)} \times X_{rs}] & \text{if } X_{rs}^{(0)} < X_{rs} \leq X_{rs}^{(1)} \\ \sum_{r=1}^R \sum_{s=1}^S [UP_{rs}^{(2)} \times X_{rs}] & \text{if } X_{rs}^{(1)} < X_{rs} \leq X_{rs}^{(2)} \\ \vdots & \\ \sum_{r=1}^R \sum_{s=1}^S [UP_{rs}^{(d_u)} \times X_{rs}] & \text{if } X_{rs}^{(I-1)} < X_{rs} \leq X_{rs}^{(I)} \end{cases} \\ F_3 &= \begin{cases} \sum_{s=1}^S [TC_s^{(1)} \times T_s] & \text{if } T_s^{(0)} \leq T_s \leq T_s^{(1)} \\ \sum_{s=1}^S [TC_s^{(2)} \times T_s] & \text{if } T_s^{(1)} < T_s \leq T_s^{(2)} \\ \vdots & \\ \sum_{s=1}^S [TC_s^{(J)} \times T_s] & \text{if } T_s^{(J-1)} < T_s \leq T_s^{(J)} \end{cases} \\ F_4 &= \sum_{r=1}^R \sum_{s=1}^S [PL_{rs} \times LR_{rs} \times X_{rs}] \\ F_5 &= \sum_{r=1}^R \sum_{s=1}^S [PD_{rs} \times DR_{rs} \times X_{rs}] \\ F_6 &= \sum_{p=1}^P [PC_p \times Y_p] \\ F_7 &= \sum_{p=1}^P [PDY_p \times DY_p \times Y_p]. \end{aligned} \quad (4)$$

respectively. Based on the formulated income and costs, the expected profit, which needs to be maximized, can now be formulated, this is modeled as the following maximization problem:

$$\max Z = E \left[\sum_{b=1}^B [F_{0b}] - [F_1 + F_2 + F_3 + F_4 + F_5 + F_6 + F_7] \right] \quad (5)$$

where $E[\cdot]$ denotes the expectation value. We now present the mathematical modeling parts for the constraint functions based on the problem's specifications and conditions that should be met. First, the available raw materials should be sufficient to satisfy those that are needed to produce products. This is modeled as

$$\sum_{s=1}^S [X_{rs} - LR_{rs} \times X_{rs} - DR_{rs} \times X_{rs}] \geq \sum_{p=1}^P [RR_{rp} \times Y_p] \quad (6)$$

Second, the available product amount is expected to be sufficient to satisfy the demand, i.e., the amount of the produced products minus defect ones is expected to be larger or at least equal to the demand; this is modeled as

$$Y_p - DP_p \times Y_p \geq \sum_{b=1}^B [DE_{pb}] \quad (7)$$

Third, the total amount of raw materials ordered to supplier s should be not exceeding the total capacity of the trucks used in the delivery; this is modeled as

$$\sum_{r=1}^R X_{rs} \leq TRC \times T_s \quad (8)$$

Fourth, the amount of each raw material type ordered to supplier s should be not exceeding the supplier's maximum capacity in supplying the corresponding raw material type. This is modeled as

$$X_{rs} \leq SC_{rs} \quad (9)$$

The fifth constraint function is the indicator variables calculation to assign when supplier s is selected to supply raw materials. The indicator is set to be one if the corresponding supplier is selected, otherwise it is set to be zero. This is modeled as

$$Z_s = \begin{cases} 1 & \text{if } \sum_{r=1}^R X_{rs} > 0, \\ 0 & \text{otherwise;} \end{cases} \quad (10)$$

The last constraint function is the nonnegativity and integer assignments for the decision variables. This is simply modeled as

$$X_{rs}, T_s, Y_p \geq 0 \text{ and integer.} \quad (11)$$

The optimization problem (5) subject to constraint functions (6)-(11) belongs to probabilistic piecewise linear integer programming since the objective function is a piecewise function and it contains probabilistic parameters. However, the existence of an optimal solution is always guaranteed since the feasible set, as long as not empty, is closed and bounded.

Numerical Experiment Results and Discussion

Numerical experiments in a laboratory were conducted to verify the proposed decision-making support model with randomly generated data. All experiments were carried out with personal computers with standard specifications.

Problem's Specifications

Consider the supplier selection and production planning problems specified in the previous section where the number of raw material types is three (R1, R2, and R3), the number of suppliers is three (S1, S2, and S3), and the number of product types is also three (P1, P2, and P3). Meanwhile, the number of price break points or discount levels is also three (DL1, DL2 and DL3). The price/cost functions for each discounted price/cost are as follows:

The unit price for raw materials ordered to supplier is equal to $UP_{rs}^{(1)}$ if the number of raw materials is less or equal to 50 units, $UP_{rs}^{(2)}$ if the number of raw materials is larger than 50 units but not larger than 100 units, and $UP_{rs}^{(3)}$ if it is larger than 100 units. Meanwhile, the unit price for products sell to buyers is equal to $PP_{pb}^{(1)}$ if the number of products is less or equal to 100 units, $PP_{pb}^{(2)}$ if the number of products is larger than 100 units but not larger than 200 units, and $PP_{pb}^{(3)}$ if it is larger than 200 units. And, the one time transportation cost from suppliers to the manufacturer is equal to $TC_s^{(1)}$ if the number of deliveries is only one time, $TC_s^{(2)}$ if the number of deliveries is more than one time but less than 6 times, and $TC_s^{(3)}$ if it is more than 5 times. The values for those discounted prices or costs $UP_{rs}^{(i)}$, $PP_{pb}^{(j)}$ and $TC_s^{(k)}$ with $i, j, k = 1, 2, 3$ are shown in Tables 1 to 3.

Table 1. Discounted prices for raw materials ($UP_{rs}^{(i)}$)

Supplier	Raw material								
	R1			R2			R3		
	DL1	DL2	DL3	DL1	DL2	DL3	DL1	DL2	DL3
S1	20	20	18	10	10	10	15	14	13
S2	20	19	18	10	9	9.5	14	14	13
S3	19	19	18	45	9	9	15	14	14

Table 2. Discounted prices for products ($PP_{pb}^{(j)}$)

Product	Buyer								
	B1			B2			B3		
	DL1	DL2	DL3	DL1	DL2	DL3	DL1	DL2	DL3
P1	100	90	90	100	90	90	100	90	90
P2	120	115	110	120	115	110	120	115	110
P3	100	95	90	100	95	90	100	95	90

Table 3 Discounted costst of deliveries ($TC_s^{(j)}$)

Supplier	Discount level		
	DL1	DL2	DL3
S1	80	80	75
S2	75	75	75
S3	75	70	70

Table 4. Other parameters

Parameter	Supplier/raw/product type		
	S1/R1/P1	S2/R2/P2	S3/R3/P3
Order cost	100	120	140
Penalty cost for rejected raw materials	1	2	2
Penalty cost for late delivered raw materials	2	2	1
Penalty cost for defected products	1	0.5	0.5
Production cost	10	15	25
Rates of rejected raw materials (DR_{rs})	$N(0.02, 0.005)$		
Rates of late delivered raw materials (LR_{rs})	$N(0.01, 0.005)$		
Demands of products from buyers (DE_{pb})	$N(20, 5)$		

$N(\mu, \sigma)$: normal distribution with mean μ and variance σ

Table 5. Supplier’s Capacity

Supplier	Raw material type		
	R1	R2	R3
S1	400	250	120
S2	300	180	210
S3	210	150	200

Results and Discussion

All optimization processes were carried out in LINGO 20.0 software with primal simplex algorithm as the solver. The algorithm was combined with the branch-and-bound scheme to calculate integer solutions. The optimal solution regarding the amount of each raw material type that needs to be ordered to each supplier is shown in Figure 3. Note that this optimal solution provides the maximal expectation of the profit and was calculated under the uncertainty of the probabilistic parameters.

It can be seen that all suppliers S1, S2, and S3 were selected to supply raw materials. However, supplier S1 was less likely to be selected with only four units or raw material type R1. The number of raw materials ordered to suppliers S2 and S3 was always in the third discount level with more than 100 units for each type. This shows that ordering with lower numbers in the first or second discount level significantly increases the cost and thus was avoided. Meanwhile, the optimal number of products that should be produced in the production unit is 69 units of brand P1, 75 units of brand P2, and 72 units of brand P3. The maximal profit was expected to be 3499.851 with income 19065.73 and cost 15565.88.

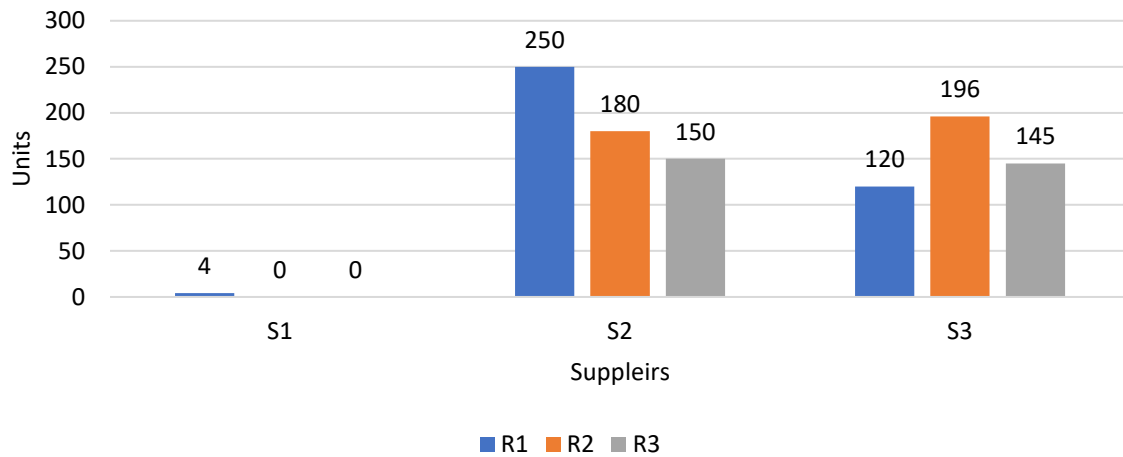


Figure 3. The optimal decision for the amount of raw materials to be ordered from suppliers

The results indicated that the proposed model successfully solved the problem and provided the optimal solution such that the expectation of the profit was maximized. In particular, based on the mathematical model derived in the modeling and the results of the numerical experiments, some managerial insights can be drawn, which can be considered by decision makers in implementing the proposed model. These are discussed as follows: first, the proposed model did not specify the kind of raw materials and products that can be handled. In principle, any kind of raw materials and products can be handled as long as it meets the specifications of the problem. Nevertheless, the specifications can be slightly modified without significant changes. For example, all raw material types and all product brands were measured as integer numbers. In practice, if the measurement follows real numbers, then the integer constraints can be removed, and in this case, the branch-and-bound scheme is not needed.

Further modifications and additions on the model can also be made. For example, some other operational costs such as maintenance costs on the production machines may be added to the objective function. Some other constraint functions can also be added, for example, limitations on the working hour of the production machines, budget limitations, and maximum number of deliveries, among others.

The numerical experiments were considered with small scale numbers of suppliers, raw materials types, and product brands. The computer used in the experiments completed the optimization process in minutes. Decision-

makers need to be aware of large-scale problems. Longer computational time might occur, and this should be taken into account especially for problems in which a decision should be made in a short period of time. One may use high-performance computers to solve large scale problems.

Finally, note that all decisions were calculated and executed before the uncertain parameters were known, and the profit provided by the mathematical optimization model was only an expectation. After all uncertain parameters are known, the actual profit can then be calculated, and the actual profit might be different from the value provided by the decision-making support. However, mathematically, this is the best thing the decision-makers can do in dealing with uncertainties.

Conclusion

A newly developed decision-making support has been proposed in this study, which can be utilized by decision-makers in manufacturing and retail industries in dealing with supplier selection and production planning problems under probabilistic uncertainties and discounted prices/costs. The problem was modeled as a probabilistic linear programming with a piecewise objective function. Numerical experiments with randomly generated data were performed to illustrate and evaluate the proposed model. Results showed that the proposed decision-making support successfully solved the problem and provided the maximal expectation of the profit.

Recommendations

The model can be further developed such that it can also handle more complex problems. One may consider other discounted price/cost functions. Moreover, the proposed model can be considered as a foundation in building further models for more complex supply chain schemes such as ones that also cover distributors and carriers. For large-scale problems, one may develop metaheuristic-based optimization algorithms such as customized genetic algorithm and ant colony optimization scheme to solve the corresponding programming models.

Scientific Ethics Declaration

The authors declare that the scientific ethical and legal responsibility of this article published in EPSTEM journal belongs to the authors.

Acknowledgements or Notes

*This article was presented as an oral presentation at the International Conference on Research in Engineering, Technology and Science (www.icrets.net) held in Budapest/Hungary on July 06-09, 2023.

*This work was financially supported by RPI UNDIP 2023 project under contract no. 569-112/UN7.D.2/PP/VII/2023

References

- Adrio, G., García-Villoria, A., Juanpera, M., & Pastor, R. (2023). MILP model for the mid-term production planning in a chemical company with non-constant consumption of raw materials. an industrial application. *Computers & Chemical Engineering*, *177*, 108361.
- Alegoz, M., & Yapicioglu, H. (2019). Supplier selection and order allocation decisions under quantity discount and fast service options. *Sustainable Production and Consumption*, *18*, 179–189.
- Ali, Md. R., Nipu, S. Md. A., & Khan, S. A. (2023). A decision support system for classifying supplier selection criteria using machine learning and random forest approach. *Decision Analytics Journal*, *7*, 100238.
- Angizeh, F., Montero, H., Vedpathak, A., & Parvania, M. (2020). Optimal production scheduling for smart manufacturers with application to food production planning. *Computers & Electrical Engineering*, *84*, 106609.

- Ghorbani, M., & Ramezani, R. (2020). Integration of carrier selection and supplier selection problem in humanitarian logistics. *Computers & Industrial Engineering*, 144, 106473.
- Guneri, B., & Deveci, M. (2023). Evaluation of supplier selection in the defense industry using q-rung orthopair fuzzy set based EDAS approach. *Expert Systems with Applications*, 222, 119846.
- Hajiaghayi Keshteli, M., Cenk, Z., Erdebilli, B., Selim Özdemir, Y., & Gholian Jouybari, F. (2023). Pythagorean fuzzy TOPSIS method for green supplier selection in the food industry. *Expert Systems with Applications*, 224, 120036.
- Joy, T. M., Aneesh, K. S., & Sreekumar, V. (2023). Analysis of a decision support system for supplier selection in glove industry. *Materials Today: Proceedings*, 72, 3186–3192.
- Lahmar, H., Dahane, M., Mouss, N. K., & Haoues, M. (2022). Production planning optimisation in a sustainable hybrid manufacturing remanufacturing production system. *Procedia Computer Science*, 200, 1244–1253.
- Li, F., Qian, F., Du, W., Yang, M., Long, J., & Mahalec, V. (2021). Refinery production planning optimization under crude oil quality uncertainty. *Computers & Chemical Engineering*, 151, 107361.
- Lindahl, S. B., Babi, D. K., Gernaey, K. V., & Sin, G. (2023). Integrated capacity and production planning in the pharmaceutical supply chain: Framework and models. *Computers & Chemical Engineering*, 171, 108163.
- Manik, M. H. (2023). Addressing the supplier selection problem by using the analytical hierarchy process. *Heliyon*, 9(7), e17997
- May, M. C., Kiefer, L., Frey, A., Duffie, N. A., & Lanza, G. (2023). Solving sustainable aggregate production planning with model predictive control. *CIRP Annals*, 72(1), 421–424.
- Olanrewaju, O. G., Dong, Z. S., & Hu, S. (2020). Supplier selection decision making in disaster response. *Computers and Industrial Engineering*, 143.
- Sharma, P., Sharma, A., & Jain, S. (2019). Inventory model for deteriorating items with price and time-dependent seasonal demand. *International Journal of Procurement Management*, 12(4), 363–375.
- Singh, S., & Biswal, M. P. (2021). A robust optimization model under uncertain environment: An application in production planning. *Computers & Industrial Engineering*, 155, 107169.
- Ware, N. R., Singh, S. P., & Banwet, D. K. (2014). A mixed-integer non-linear program to model dynamic supplier selection problem. *Expert Systems with Applications*, 41(2), 671–678.
- Wu, C. B., Guan, P. B., Zhong, L. N., Lv, J., Hu, X. F., Huang, G. H., & Li, C. C. (2020). An optimized low-carbon production planning model for power industry in coal-dependent regions - a case study of Shandong, China. *Energy*, 192, 116636.
- Yazdani, M. A., Khezri, A., & Benyoucef, L. (2021). A linear multi-objective optimization model for process and production planning generation in a sustainable reconfigurable environment. *IFAC-PapersOnLine*, 54(1), 689–695.
- Zarte, M., Pechmann, A., & Nunes, I. L. (2022). Knowledge framework for production planning and controlling considering sustainability aspects in smart factories. *Journal of Cleaner Production*, 363, 132283.
- Zhang, H., Zhao, J., Leung, H., & Wang, W. (2022). Multi-stage dynamic optimization method for long-term planning of the concentrate ingredient in copper industry. *Information Sciences*, 605, 333–350.

Author Information

Sutrisno Sutrisno

Diponegoro University
Semarang, Indonesia
Contact e-mail: s.sutrisno@live.undip.ac.id

Widowati Widowati

Diponegoro University
Semarang, Indonesia

Robertus Heri Soelistyo Utomo

Diponegoro University
Semarang, Indonesia

To cite this article:

Sutrisno, S., Widowati, W. & Utomo, R.H.S. (2023). Probabilistic piecewise-objective optimization model for integrated supplier selection and production planning problems involving discounts and probabilistic parameters: Single period case. *The Eurasia Proceedings of Science, Technology, Engineering & Mathematics (EPSTEM)*, 23, 442-451.

The Eurasia Proceedings of Science, Technology, Engineering & Mathematics (EPSTEM), 2023

Volume 23, Pages 452-463

ICRETS 2023: International Conference on Research in Engineering, Technology, and Science

Integrated Model of Lean and Risk Mitigation for Sustainability Performance Measurement in the Lubricants Manufacturing Industry

Fara Kamila Hudy

Institute Technology of Sepuluh Nopember

Nidaru Ainul Fikri

Institute Technology of Sepuluh Nopember

Udisubakti Ciptomulyono

Institute Technology of Sepuluh Nopember

Abstract: Green companies are needed for manufacturing related to maintaining the business. Evaluating sustainability performance in manufacturing processes and proposing strategies for sustainable growth is important. This study measures the performance of manufacturing sustainability in the lubricating oil industry sector. Several previous studies on measuring sustainable manufacturing performance only considered lean and green aspects. This study fills the existing gap by adding a risk perspective in measurement. Several suggestions for improvement analyzed from measurements of sustainability performance and risk mitigation, are validated using the BORDA. The lean and green philosophy is applied with the Sustainable Value Stream Mapping approach. Meanwhile, risk mitigation is analyzed using the House of Risk approach. The results of the assessment of sustainability performance measurements are analyzed using the efficiency approach and BORDA for weighting. This research is expected to be able to provide suggestions for improvements for manufacturing that are efficient and feasible to implement. So that high sustainability performance can be achieved with low risk.

Keywords: Sustainable value stream mapping, House of risk, BORDA, Manufacturing sustainability performance

Introduction

Green company is currently a business requirement because it is related to business continuity. It involves managing environmental factors to prevent pollution and damage to the environment during production, product or service usage by customers, and disposal. These demands and challenges have led to the emergence of the concept of sustainable development in manufacturing, aiming to improve people's quality of life through an environmentally friendly approach (Bogue, 2014). Therefore, it is important to evaluate sustainability performance in a manufacturing company's production process and propose strategies for sustainable growth (Swarnakar et al., 2021).

Lean manufacturing can be defined as the elimination of waste in production systems, including human effort, time, and inventory at each stage of production (Rahman et al., 2013). Lean and green can be implemented together and synergize with each other (Hartini et al., 2020). Companies that simultaneously apply lean and green practices have been proven to have better performance compared to those implementing only one of them (Bergmiller & McCright, 2009; Wiengarten et al., 2013). The application of lean manufacturing supports the achievement of green practices and vice versa. Sustainable manufacturing is a process that minimizes adverse

- This is an Open Access article distributed under the terms of the Creative Commons Attribution-Noncommercial 4.0 Unported License, permitting all non-commercial use, distribution, and reproduction in any medium, provided the original work is properly cited.

- Selection and peer-review under responsibility of the Organizing Committee of the Conference

© 2023 Published by ISRES Publishing: www.isres.org

environmental impacts, ensures worker safety, and has a positive long-term impact on the economy during the production process (Mubin et al., 2022). Sustainable manufacturing not only focuses on environmentally friendly production systems but also involves social responsibility with a wider scope, considering lean practices as part of sustainable manufacturing (Joung et al., 2013).

Several studies have been conducted to measure sustainability in manufacturing. Lee et al. (2014) developed concepts and methods to assess manufacturing sustainability performance at the factory level using a single index. Huang & Badurdeen (2018) introduced a framework for measuring sustainability performance at the production level. However, most manufacturing industries lack detailed sustainability data that aligns with the proposed models. Therefore, each manufacturer requires a specific methodology to help measure indicators and improve environmental, economic, and social aspects at the factory level (Hartini et al., 2020).

Operationally, sustainability performance cannot be simply calculated as a percentage. Mapping is also necessary to facilitate production operators' visual understanding of sustainability performance. Furthermore, mapping the production line at each workstation assists decision-makers in making sustainable decisions. Thus, the industry requires a comprehensive methodology to map and measure manufacturing sustainability performance at the production level (Mubin et al., 2022).

According to Hartini et al. (2021), value stream mapping, which evaluates sustainability indicators, was initially introduced by Simon & Mason (2003). Sustainable value stream mapping incorporates the triple bottom line concept into the production line, as first introduced by Brown et al. (2014). Sustainable value stream mapping (SVSM) is a visual representation of the energy flow and waste generated in the manufacturing process (Ikatinasari et al., 2018). Previous studies have utilized SVSM to measure and map manufacturing sustainability performance, such as Hartini et al. (2020), who proposed an MSA assessment framework based on SVSM and Delphi-AHP for the furniture industry. Similarly, Mubin et al. (2022) suggested using SVSM and weighting it with AHP, while also incorporating indicators of mental and physical workload in the plastics industry.

However, there are still limitations in mapping and measuring sustainability performance using SVSM. These measurements have not considered failure or risk factors and the interdependencies between production processes. Every production process entails risk, yet these risk factors are often overlooked or evaluated independently (Shah et al., 2012). Failure to effectively mitigate risks can leave companies behind in the ever-changing business landscape, as a company's future depends on its ability and responsiveness to external environmental changes (Soosay et al., 2016).

Inadequate management of risks can negatively impact company performance, whereas active and systematic control of risk variables can support business success (Oduoza, 2020). Therefore, risk factors should be incorporated into the evaluation of the MSA score and recommendations for improvement. Additionally, no research has been conducted on measuring the MSA score in the lubricating oil manufacturing industry. To reduce risk, the House of Risk (HOR) approach can be used. BORDA is used to weigh each variable in order to identify the cause factor order. As a result, the proposed improvements are considered worthy of implementation as they take into account all aspects, including waste, sustainability, and potential future risks.

Lubricants are substances utilized to minimize friction and wear between interacting surfaces, enabling relative motion in solids. Aside from their primary role in reducing wear and friction, lubricating fluids serve various other functions. They act as coolants in metalworking, prevent corrosion, facilitate power transfer, act as liquid seals in suspensions and moving contacts, and remove worn particles. Practical lubricating oils need to remain in liquid form across a wide temperature range. They must possess a low pour point to ensure pumpability during equipment startup at very low temperatures. Simultaneously, they should have a high flash point for safe operation and exhibit minimal volatility at maximum operating temperature.

The viscosity of lubricating oil needs to be adjusted based on the engine's compression. If the viscosity is too high for a given load and speed, it can lead to wasted engine power as it processes a thick layer of lubricant. Lubricating oil plays a crucial role in maintaining the machinery and equipment's operational continuity, despite its relatively small usage volume. Its application extends beyond the automotive industry and is also essential in various industrial and mining settings, ensuring the proper functioning of engine systems.

The measuring MSA scores using SVSM while considering sustainable risks in the lubricant manufacturing industry is required. The selected indicators are displayed using SVSM, waste analysis is done, and the

efficiency of each indicator is measured. In addition, sustainable risks in the economic, social, and environmental aspects of each process are identified using the House of Risk approach (HOR).

Considerations are assigned to indicators in SVSM and sustainable risk to determine the level of importance of each. Furthermore, the results of mapping and indicator assessment, through SVSM and identification of sustainable risk using HOR, are used to measure manufacturing sustainability scores. The research also uses the Borda Method for any proposed improvements based on SVSM indicators and sustainability risks. This research has made a significant contribution to this field by filling a gap in research into the lubricant industry. It provides a new reference for operations managers to assess sustainability performance in the company, considering its sustainability risk factors in various aspects. The study helps identify waste and risk areas, revealing the level of sustainability that the company achieves. In addition, the proposed improvements are efficient, feasible, and do not pose implementation risks.

Lean, Green and Sustainable Manufacturing

There are two main meanings associated with the term lean in the manufacturing context. First, lean refers to the goal of minimizing waste and maximizing value in the production process (Nawanir et al., 2018). This concept was first introduced by Toyota in the 1950s and since then has been widely adopted in manufacturing industries around the world. The goal of Lean Manufacturing (LM) is to eliminate activities that do not add value to the final product, including overproduction, excess inventory, defects, waiting time, unnecessary movements, and excessive processing. By eliminating waste and increasing efficiency, LM can reduce costs, improve quality, and enhance customer satisfaction.

The term lean is also used broadly to refer to a philosophy of continuous improvement and waste reduction in all aspects of business operations, not just in the manufacturing context. This wider application of lean principles is sometimes referred to as lean management (Leong et al., 2019). The LM approach focuses on increasing the productivity of the production process through adding value and reducing the 7 wastes or seven wastes in operations, namely over production, waiting, inventory, motion, transportation, over processing, defects.

Green manufacturing is focused on reducing the environmental impact of the manufacturing process while maximizing efficiency and value for customers (Abdul-Rashid et al., 2017). This theory is based on the integration of environmental sustainability into the LM principle, which emphasizes identifying and reducing waste, optimizing energy and resource consumption, and continuously improving production processes (Leong et al., 2019). The theory of sustainability focuses on assessing and improving the sustainability performance of manufacturing processes. Sustainability emphasizes the importance of considering social, economic, and environmental factors when evaluating the sustainability of manufacturing processes.

The main goals of sustainability are to reduce environmental impact, increase social and economic outcomes, and promote long-term sustainability. By considering these factors, organizations can improve their sustainability performance and contribute to a more sustainable future (Swarnakar et al., 2021). Overall, the manufacturing process has a large impact on the environment due to high energy consumption and unwanted waste disposal (Duflo et al., 2012). Manufacturing processes must be designed and operated in such a way as to reduce waste, eliminate hazardous substances, save material and energy, and minimize physical hazards (Jovane & Westkämper, 2008).

Many initiatives have been developed to reduce the impact of manufacturing on the environment, such as reducing energy consumption and CO₂ emissions, minimizing waste, and making material use more efficient. Effective energy management can significantly reduce manufacturing operating costs and increase production flexibility and quality (Christoffersen et al., 2006; Despeisse et al., 2012; Fang et al., 2011; Jayal et al., 2010; Pajunen et al., 2012).

Measurement of Manufacturing Sustainability Performance in SVSM

The efficiency measurement of each indicator described in Table 1 is visualized in the Sustainable-VSM map. In Hartini et al. (2020) the value of the efficiency of the performance indicators obtained. If a value below 65 is critical it will be represented by red between 60 and 90 is moderate and represented by yellow, more than 90 is very good and represented by green.

Table 1. Efficiency formula for sustainability indicators

No.	Indicator	Input	Formula	References
1	Time (minute)	TE = time efficiency VAT = time in value-added activities TT = total time NVAT = time in non-value-added activities n = process to n	$TE = \frac{VAT}{TT}$ $VAT = \sum_{i=1}^n (VAT_i)$ $NVAT = \sum_{i=1}^n (NVAT_i)$ $TT = VAT + NVAT$	Hartini et al. (2020)
2	Quality	QE = quality efficiency ND = number of defects TM = total material	$QE = 1 - (ND/TM)$	Hartini et al. (2020)
3	Material (kg)	ME = material efficiency MC = number of material consumed PR = number of product released	$MC = \sum MC_n$ $PR = \sum PR_n$ $ME = MC/PR$	Hartini et al. (2020); Helleno et al. (2017); Vinodh et al. (2014)
4	Energy (kWh)	EE = energy efficiency EP = Amount of energy used for production ED = amount of energy used for domestic TE = Total energy	$EP = \sum EP_n$ $ED = \sum ED_n$ $TE = EP + ED$ $EE = EP/TE$	Hartini et al. (2020); Helleno et al. (2017); Vinodh et al. (2014)
5	Water Consumption	WE = Water efficiency WP = amount of water used for production WD = amount of water used for domestic TW = total water	$WP = \sum WP_n$ $WD = \sum WD_n$ $TW = WP + WD$ $WE = AW/TW$	Faulkner and Badurdeen (2014)
6	Satisfaction level	SE = Satisfaction Efficiency TO = number of employee turnover NE = number of employees	$SE = 1 - (TO/NE)$	Hollmann et al. (Hollmann et al. 1998); Mubin et al. (Mubin et al. 2022)
7	Health Level	HE = Health Efficiency NA = number of employees absent NE = number of employees	$HE = 1 - (NA/NE)$	Hart and Staveland (1988); Mubin et al. (Mubin et al. 2022)
8	Employee training level	E_HRD = Human Resources & Development Efficiency NT = Number of employee training NE = Number of employee	$E_{HRD} = NT/NE$	Hartini et al. (2020)

House of Risk (HOR)

House of Risk is a new method of analyzing risk. Its application uses the principles of FMEA (Failure Mode and Error Analysis) to measure risk quantitatively combined with the House of Quality (HOQ) model to prioritize risk agents that must be prioritized first and then choose the most effective actions to reduce potential risks posed by agents. risk. The HOR model underlies risk management on a prevention focus, namely reducing the possibility of risk agents occurring. So the earliest stage is to identify risk events and risk agents. Usually one agent can cause more than one risk event. Adapting from the FMEA method, the risk assessment that is applied is the Risk Priority Number (RPN) which consists of 3 factors, namely the probability of occurrence, the severity of the impact that appears, and detection. The HOR method only assigns probabilities to risk agents and the severity of risk events. Because there is a possibility that one risk agent causes more than one risk event, it is necessary to have an aggregate potential risk quantity of the risk agent. Adapting the House of Quality (HOQ) model to define risk agents should be given priority as a precautionary measure. A rating is given to each risk

agent based on the magnitude of the ARP_j value for each j risk agent. Therefore, if there are many risk agents, the company can first select the agent with the greatest potential to cause risk events. The model with these two distributions is called the House of Risk (HOR) which is a modification of the HOQ model (Pujawan & Geraldin, 2009).

Borda

Borda is a method of voting used in a group decision support system for selecting a single winner or multiple winners, where voters give a rating to the selected alternative. The Borda method determines the winner by giving a certain number of points to each alternative according to the rating given by each voter. The winner is determined by the final number of points each alternative collects from each voter, with the voter with the highest number of points selected to be the winner. (Sidiq & Wardhana, 2018).

The Borda method operates on the principle of ranking and rating various choices. It assigns higher scores to options with higher rankings, gradually reducing the scores for lower-ranked options until they reach a minimum of 0 or 1. In essence, the Borda method mandates voters to both rank and assign a numerical value to each candidate. For example, the top-ranked choice receives a score of 3, the second-ranked choice gets a score of 2, and so on for each ranking. The third is given a value of 0. A board is a method of voting used in the decision-making of a group for the selection of a single winner or multiple winners. The board determines the winner by assigning a certain number of values to each alternative. Then the winner will be determined by the number of values collected alternately. In a group decision-support system, one of the problems we often face is how to aggregate the opinions of decision-makers to produce the right decision (Syaputra, 2020).

Method

The lean concept is intended to reduce costs and improve product quality by eliminating waste, while sustainable manufacturing focuses on efforts to protect the environment and achieve sustainability. In research, value stream mapping (VSM) is used as an approach to measuring company performance. VSM can identify inefficient activities and measure their efficiency level quantitatively. In addition, this research also utilizes the advantages of green and sustainable manufacturing to consider efforts to save the environment and achieve sustainability, things that have not been considered in previous lean manufacturing approaches. The integration of lean, green and sustainable manufacturing will be used as a basis for developing a comprehensive sustainability performance measurement model for manufacturing companies.

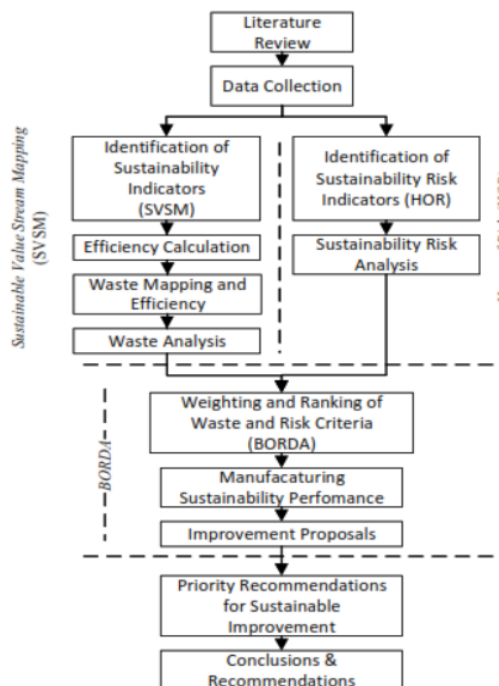


Figure 1. Research framework

The measurement model development process begins with selecting relevant indicators for the manufacturing company concerned. These indicators come from the concepts of lean and sustainable manufacturing so that they include economic, environmental, and social dimensions. Furthermore, a value stream mapping (VSM) is developed which is integrated with the selected indicators. VSM initially only paid attention to economic indicators, then developed into a sustainable-VSM involving environmental and social indicators. Indicators in sustainable-VSM are measured using an efficient approach. The resulting indicator score then becomes the basis for measuring the sustainability performance of manufacturing companies in the form of a manufacturing sustainability index.

In addition to utilizing SVSM, this study also uses sustainability risk to complete the perspective in research. Sustainability risk is considered important because it can affect future manufacturing performance. Risk mitigation in this study was carried out using the house of risk (HOR). HOR was developed by Pujawan & Geraldin (2009) by integrating the House of Quality (HOQ) with FMEA. HOR is a method for identifying and calculating risks that arise in the production process to find the right priority for corrective actions to be implemented based on the company's capabilities (Suryanti et al., 2020).

The proposed improvements are then analyzed using the Benefit, Cost, Opportunities, and Risk (BCOR) criteria. Improvement proposals are assessed from various aspects, starting from the advantages that are translated as benefits, unwanted proposals as costs, events that may occur and can be detrimental or profitable as criteria for opportunities, and risks as criteria for risk (Fitria Sari et al., 2020). It is hoped that the proposed improvements will be feasible to implement because they have considered all aspects, both in terms of waste, sustainability and possible risks that may arise in the future. The research framework is arranged schematically to make it easier to understand the direction of the research Figure 2.

Results and Discussion

Operational Aspect of Sustainability Indicator Efficiency

Time Indicators

The process of receiving base oil and additives is carried out by ship. The times calculated in the efficiency calculation are the dipping time and the pumping time. At the time of measurement, the time required for base oil pumping was 2 hours, 24 minutes. With a flow rate of 196.3 Kl/hour. Activities carried out in production consist of receiving and unloading materials, moving materials from the unloading shelter to the warehouse, activities in the warehouse, blending, filling lithos, and transferring finished goods to the finished goods warehouse. Some activities are included in value-added activities, and others are included in non-value-added activities. The calculation of time efficiency, the amount of Value Added time, and Non-Value Added Time during the lithos production process is described in Table 2.

Table 2. Calculation of lubricant lead time efficiency

	Formula	Result
VAT Lithos	\sum Value Added Time	91,128 minutes
NVAT Lithos	\sum Non-Value Added Time	24,96 minutes
Total Time lithos	\sum VAT + \sum NVAT	116,088 minutes
Time Efficiency (TE)	$(\sum$ VAT) / TT	0,78499
Percent efficiency	(TE) x 100 %	78,499 %

During the production process of Lihtos packaged lubricants, the amount of time needed for value-added activities (value-added time) is 91.128 minutes. While the time required for activities that are not value-added (Non-value-added activities) is 24.96 minutes, The total time required in the lithos packaging lubricant production process is 116.088 minutes. The time efficiency (TE) of the Lihtos packaged lubricant production process is 78.499%.

Quality Indicators

From the data collection process, the efficiency calculation results are as follows: The calculation of quality efficiency is based on a comparison between the amount of material that has defects and the total material. The number of product defects, total material, and quality efficiency calculations are described in Table 3.

Table 3. Calculation of quality efficiency

	Formula	Result
Number of Defect (ND)	\sum Number of Defect	212591 pcs
Total Material TM	\sum TM	36434357 pcs
Quality Efficiency (QE)	$1 - (\sum ND / TM)$	0,9942
Percent efficiency	$(TE) \times 100 \%$	99,42 %

During the lubricant production process, the number of materials that experience defects during the period June 2022 to.d. May 2023 of 212591 pcs. While the total material received during the period June 2022 to. May 2023 of 36434357 minutes. The quality efficiency (QE) of the Lihtos packaged lubricant production process is 99.42%.

Material Indicators

From the data collection process, the material efficiency calculation results are obtained as follows: The calculation of material efficiency is based on a comparison between the amount of hydrocarbon material consumed and the actual amount of lubricant production. Total hydrocarbon material consumed, total lubricant production realization, and material efficiency calculations are described in Table 4.

Table 4. Calculation of quality efficiency

	Formula	Result
Number of Material Consumed (MC)	\sum Number of Material Consumed	114.110.299 liters
Number of Product Realesed (PR)	\sum Number of Product Realesed	112.858.482 liter
Material Efficiency (ME)	PR / MC	0,9890
Percent efficiency	$(ME) \times 100 \%$	98,90 %

During the lubricant production process, the amount of material consumed during the period June 2022 to May 2023 was 114,110,299 liters. Meanwhile, the number of products released in the same period was 112,858,482 liters. The material efficiency (ME) of the lubricant production process is 98.90%.

Efficiency of Environmental Aspect Sustainability Indicators

Energy Consumption

From the data collection process, the energy consumption efficiency calculation results are obtained as follows: The calculation of energy consumption is based on a comparison between the amount of energy consumed for production and total energy. Total electrical energy consumed, total energy, and energy consumption calculations are described in Table 5.

Table 5. Calculation of energy consumption efficiency

	Formula	Result
Amount of Energy used for Production each month (EP)	\sum Amount of Energy Used for Production each month	1.412.018,27 kWh
Amount of Energy used for domestic each month (ED)	\sum Amount of Energy used for domestic each month	546.778,68 kWh
Total Energy (TE)	$\sum EP + \sum ED$	1.958.796,95 kWh
Energy Efficiency (EE)	EP / TE	0,72086
Percent Efficiency	$(EE) \times 100 \%$	72,086%

During the lubricant production process, the amount of energy consumed for production during the period June 2022 to.d. May 2023 of 1,412,018.27 kWh. Meanwhile, the amount of energy used domestically is 546,778.68 kWh. The total energy consumed is 1,958,796.95 kWh. The energy efficiency (EE) of the lubricant production process is 72.086%.

Water Consumption

From the data collection process, the water consumption efficiency calculation results are obtained as follows: The calculation of water consumption is based on the ratio between the amount of water used for production and the total water use. Total water used for production, total domestic water use, total water use, and calculated water consumption are presented in Table 6. During the lubricant production process, the amount of water consumed for production during the period June 2022 to May 2023 was 11607.155 m³. While the amount of water used for domestic use is 5169.164 m³. The total amount of water consumed is 16776.32 m³. The water efficiency (WE) of the lubricant production process is 69.187%.

Table 6. Calculation of water consumption

	Formula	Result
Amount of Water used for Production each month (WP)	\sum Amount of Water Used for Production each month	11607,155 m ³
Amount of Water used for domestic each month (WD)	\sum Amount of Water used for domestic each month	5169,164 m ³
Total Water (TW)	\sum WP + \sum WD	16776,32 m ³
Water Efficiency (WE)	WP / TW	0,69187
Percent efficiency	(WE) x 100 %	69,187%

The Efficiency of Social Aspect Sustainability Indicators

Satisfaction Level

From the data collection process, the efficiency calculation results are as follows: The calculation of the satisfaction level is based on a comparison between the number of employee turnovers, or the number of employees who resign, and the total number of employees. The number of employees who resigned, the total number of employees, and the calculation of the satisfaction level are described in Table 7. The number of workers who resigned during the period June 2022 to May 2023 is 10 people. The total number of workers involved in the company is 300. Satisfaction Level (SL) from lubricant manufacturing is 96.667%.

Table 7. Calculation of satisfaction level

	Formula	Result
Number of Employee Turnover (TO)	\sum Number of Employee Turnover (TO)	10 people
Number of Employee (NE)	\sum NE	300 people
Satisfaction Level (SL)	$1 - (\sum TO / NE)$	0,96667
Percent efficiency	(SL) x 100 %	96,667 %

Health Level

From the data collection process, the efficiency calculation results are as follows: The calculation of health level is based on a comparison between the number of employee absentees or the number of workers who are sick and the total number of employees during the period June 2022 to May 2023. The number of sick workers, total workers, and health level calculations are described in Table 8. The number of workers who received sick leave during the period June 2022–May 2023 was 23. The total number of workers involved in the company is 300. The health level (HL) in lubricant manufacturing is 92.33%.

Table 8. Calculation health level

	Formula	Result
Number of Employee Absent (NA)	\sum Number of Employee Absent (NA)	23 people
Number of Total Employee (NE)	\sum NE	300 people
Health Level (HL)	$1 - (\sum NA / NE)$	0,92333
Percent efficiency	(HL) x 100 %	92,33 %

Employee Training Level

From the data collection process, the results of calculating the efficiency of the training level are as follows: The calculation of the employee training level is based on a comparison between the number of employee training sessions or the number of employees who conduct training and the total number of employees during the period June 2022 to May 2023. The number of workers who attended training, the total number of employees, and the calculation of the employee training level are presented in Table 9. The number of workers who attended training during the period June 2022 to May 2023 was 161 people. The total number of workers involved in the company is 300 people. Employee Training Level (E_HRD) in lubricant manufacturing is 53.667% (Table 9).

Table 9. Calculation of employee training level

	Formula	Result
Number of Employee Training (NT)	\sum Number of Employee Training (NA)	161 orang
Number of Total Employee (NE)	\sum NE	300 orang
Employee Training Level (E_HRD)	$1 - (\sum NA / NE)$	0,53667
Percent efficiency	$(E_HRD) \times 100 \%$	53,667 %

Table 10. Efficiency result obtained from data calculations based on the formula previously mentioned.

Weight of Lean & Green Perspective	Weight of Risk Perspectives	Aspect	Weight of Sustainability Aspect	Indicators	Weight of Indicators	Global Weight	
0,5	0,5	Operational Aspect	0,5	Time	0,1667	0,0208375	
				Quality	0,1488	0,0186	
				Material	0,1845	0,0230625	
		Environmental Aspect	0,22		Energy Consumption	0,0952	0,005236
					Water Consumption	0,0833	0,0045815
					Satisfaction Level	0,1130	0,00791
					Health Level	0,1130	0,00791
		Social Aspect	0,28		Employee Training Level	0,0952	0,006664

This weighting is calculated with BORDA method using scoring the questioner that filled by supervisor and jr. supervisor in each section such as Human Resources, Operational, Warehouse, Quality Inspector, receiving and hoarding, and Techniq (Table 10).

Table 11. The results of calculating the efficiency of all indicators of sustainability

Sustainability Aspect	Indicators	Efficiency Score (a)	Global Weight (b)	Manufacturing Sustainability Performance ($\sum a \times b$)
Operational Aspect	Time	78,50%	0,0208375	83,128 %
	Quality	99,42%	0,0186	
	Material	98,90%	0,0230625	
Environmental Aspect	Energy Consumption	72,086%	0,005236	
	Water Consumption	69,187%	0,0045815	
Social Aspect	Satisfaction Level	96,667%	0,00791	
	Health Level	92,33%	0,00791	
	Employee Training Level	53,667%	0,006664	

The best efficiency level is the quality indicator of 99,42% and the lowest is the employee training level of 53,667% from the social aspect, and from the operational aspect is Time about 78,50%. Total Manufacturing Sustainability Score is 83,128% (Table 11).

The quality indicator is the third most crucial weight. Quality is the most critical indicator of sustainability. Manufacturing to ensure customer satisfaction. The findings of this study are consistent with those of Hartini et al. (Hartini et al. 2020). According to the findings of Lakatos et al. (Lakatos et al. 2021), product quality can influence customer satisfaction and purchase intent. As a result, businesses must devise strategies emphasizing product quality as a competitive advantage (Tyagi et al. 2015).

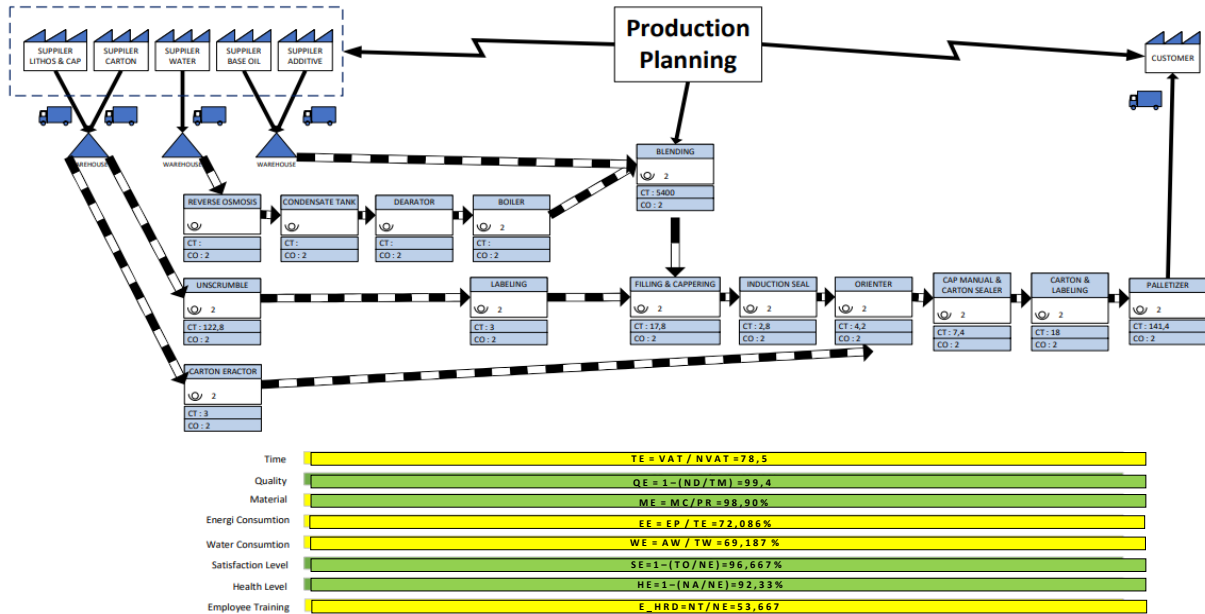


Figure 2. Mapping of SVSM

Conclusion

The primary goal of this research is to propose a new framework based on Risk mitigation and Lean methods for assessing sustainable manufacturing performance in a production line. This new framework has been successfully proposed to assess the performance of manufacturing sustainability in the production line. The proposed framework begins by selecting indicators, weighing indicators with BORDA, evaluating the efficiency of each indicator, and mapping SVSM. Then, each indicator's weight and performance determine the manufacturing sustainability score. This framework is used in Indonesian lubricant manufacturing. The case study findings indicate that the manufacturing performance of the lubricant industry could be improved, especially in terms of time production, material consumption, and employee training level.

Recommendations

Several recommendations are given to manufacturers including the following: employee training enhancement, Improve the level of employee training through structured and comprehensive programs to enhance technical skills and process understanding; visualizing work procedures, Implement visual aids such as icons, signs, or guidelines for easy comprehension; process standardization, Create clear and easily-followed standard work procedures for each production stage; implementation of quality control tools, apply simple quality control tools like Pareto charts, cause-and-effect diagrams, and process flowcharts. These tools help identify root causes, focus on relevant improvements, and monitor progress.; and Set Key Performance Indicators (KPIs) and monitor them regularly

Scientific Ethics Declaration

The authors declare that the scientific ethical and legal responsibility of this article published in EPSTEM journal belongs to the authors.

Acknowledgements or Notes

This article was presented as an oral presentation at the International Conference on Research in Engineering, Technology and Science (www.icrets.net) held in Budapest/Hungary on July 06-09, 2023.

References

- Abdul-Rashid, S. H., Sakundarini, N., Raja Ghazilla, R. A., & Thurasamy, R. (2017). The impact of sustainable manufacturing practices on sustainability performance: Empirical evidence from Malaysia. *International Journal of Operations and Production Management*, 37(2), 182–204.
- Arliana, A. G., & Soebroto, A. A. (2018). Group decision support systems for corporate unit performance assessment using the TOPSIS and Borda methods. *Journal of Information Technology Development and Computer Science*, 2 (12), 7348-7356.
- Arifin, S., Soetjipto, W. J., & Qudsy, H. N. (2021). Analisis risiko keterlambatan proyek Menggunakan metode house of risk. *Journal of Applied Civil Engineering and Infrastructure Technology*, 2(1), 19-26.
- Bergmiller, G. G., & Mccright, P. R. (2009). Parallel models for lean and green operations. *Proceeding of the 2009 Industrial Engineering Research Conference, (Volume 1, No: 1, pp. 22-26)*. Tampa, FL, USA: University of South Florida and Zero Waste Operations Research and Consulting.
- Bogue, R. (2014). Sustainable manufacturing: A critical discipline for the twenty-first century. *Assembly Automation*, 34(2), 117–122.
- Christoffersen, L. B., Larsen, A., & Togeby, M. (2006). Empirical analysis of energy management in Danish industry. *Journal of Cleaner Production*, 14(5), 516–526.
- Dufloy, J. R., Sutherland, J. W., Dornfeld, D., Herrmann, C., Jeswiet, J., Kara, S., Hauschild, M., & Kellens, K. (2012). Towards energy and resource efficient manufacturing: A processes and systems approach. *CIRP Annals - Manufacturing Technology*, 61(2), 587–609.
- Faulkner, W., Badurdeen, F., Templeton, W., & Gullett, D. (2012). Visualizing sustainability performance of manufacturing systems using sustainable value stream mapping (Sus-VSM) STEM education view project system level production modelling in coal mining industry view project. *Proceedings of the 2012 International Conference on Industrial Engineering and Operations Management*, 1–11.
- Hartini, S., Ciptomulyono, U., Anityasari, M., & Sriyanto, M. (2020). Manufacturing sustainability assessment using a lean manufacturing tool: A case study in the Indonesian wooden furniture industry. *International Journal of Lean Six Sigma*, 11(5), 957–985.
- Huang, A., & Badurdeen, F. (2018). Metrics-based approach to evaluate sustainable manufacturing performance at the production line and plant levels. *Journal of Cleaner Production*, 192, 462–476.
- Ikatinasari, Z. F., Hasibuan, S., & Kosasih, K. (2018). The Implementation Lean and Green Manufacturing through Sustainable Value Stream Mapping. *IOP Conference Series: Materials Science and Engineering*, 453(1).
- Joung, C. B., Carrell, J., Sarkar, P., & Feng, S. C. (2013). Categorization of indicators for sustainable manufacturing. *Ecological Indicators*, 24, 148–157.
- Jovane, F., & Westkämper, E. (2008). Towards competitive sustainable manufacturing. In *Springer*. Springer, Berlin, Heidelberg.
- Lee, J. Y., Kang, H. S., & Noh, S. do. (2014). MAS2: An integrated modeling and simulation-based life cycle evaluation approach for sustainable manufacturing. *Journal of Cleaner Production*, 66, 146–163.
- Leong, W. D., Lam, H. L., Ng, W. P. Q., Lim, C. H., Tan, C. P., & Ponnambalam, S. G. (2019). Lean and green manufacturing—a review on its applications and impacts. *Process Integration and Optimization for Sustainability*, 3(1), 5–23.
- Mubin, A., Utama, D. M., & Nusantara, R. C. (2022). Manufacturing sustainability assessment comprising physical and mental workload: An integrated modified SVSM and AHP approach. *Process Integration and Optimization for Sustainability*.
- Nawanir, G., Fernando, Y., & Teong, L. K. (2018). A second-order model of lean manufacturing implementation to leverage production line productivity with the importance-performance map analysis. *Global Business Review*, 19(3), 114–129.
- Oduoza, C. F. (2020). Framework for sustainable risk management in the manufacturing sector. *Procedia Manufacturing*, 51, 1290–1297.
- Pajunen, N., Watkins, G., Wierink, M., & Heiskanen, K. (2012). Drivers and barriers of effective industrial material use. *Minerals Engineering*, 29, 39–46.
- Pujawan, I. N., & Geraldin, L. H. (2009). House of risk: A model for proactive supply chain risk management. *Business Process Management Journal*, 15(6), 953–967.

- Rahman, N. A. A., Sharif, S. M., & Esa, M. M. (2013). Lean manufacturing case study with Kanban system implementation. *Procedia Economics and Finance*, 7, 174–180.
- Shah, L., Etienne, A., Siadat, A., & Vernadat, F. B. (2012). (Value, Risk)-based performance evaluation of manufacturing processes. *IFAC Proceedings Volumes (IFAC-PapersOnline)*, 45(6), 1586–1591.
- Soosay, C., Nunes, B., Bennett, D. J., Sohal, A., Jabar, J., & Winroth, M. (2016). Strategies for sustaining manufacturing competitiveness: Comparative case studies in Australia and Sweden. *Journal of Manufacturing Technology Management*, 27(1), 6–37.
- Suryanti, F., Sudiarno, A., & Sudarni, A. A. C. (2020). Combination of value stream mapping and house of risk methods to eliminate waste in productivity enhancement in production area of fertilizer company. *IOP Conference Series: Materials Science and Engineering*, 847(1).
- Swarnakar, V., Singh, A. R., Antony, J., Tiwari, A. K., & Cudney, E. (2021). Development of a conceptual method for sustainability assessment in manufacturing. *Computers and Industrial Engineering*, 158, 107403.
- Swarnakar, V., Singh, A. R., Antony, J., Kr Tiwari, A., Cudney, E., & Furterer, S. (2020). A multiple integrated approach for modelling critical success factors in sustainable LSS implementation. *Computers and Industrial Engineering*, 150, 106865.
- Vinodh, S., ben Ruben, R., & Asokan, P. (2016). Life cycle assessment integrated value stream mapping framework to ensure sustainable manufacturing: A case study. *Clean Technologies and Environmental Policy*, 18(1), 279–295.
- Wiengarten, F., Fynes, B., & Onofrei, G. (2013). Exploring synergetic effects between investments in environmental and quality/lean practices in supply chains. *Supply Chain Management*, 18(2), 148–160.

Author Information

Fara Kamila Hudy

Institute Technology of Sepuluh Nopember
Surabaya, Indonesia
Contact e-mail: farakamilahudy@gmail.com

Nidaru Ainul Fikri

Institute Technology of Sepuluh Nopember
Surabaya, Indonesia

Udisubakti Ciptomulyono

Institute Technology of Sepuluh Nopember
Surabaya, Indonesia

To cite this article:

Hudy, F.K., Fikri, N.A. & Ciptomulyono, U. (2023). Integrated model of lean and risk mitigation for sustainability performance measurement in the lubricants manufacturing industry. *The Eurasia Proceedings of Science, Technology, Engineering & Mathematics (EPSTEM)*, 23, 452–463.

The Eurasia Proceedings of Science, Technology, Engineering & Mathematics (EPSTEM), 2023

Volume 23, Pages 464-470

ICRETS 2023: International Conference on Research in Engineering, Technology and Science

User Evaluation of Innovative Megaprojects Induced by Environmental Change Using Primary Data

Janos Varga
Obuda University

Agnes Csiszarik-Kocsir
Obuda University

Abstract: The modern age and the associated rise in living standards have been achieved at the cost of enormous environmental damage. The environmental degradation of today, the environmental devastation of previous years, and global warming have presented the world with new and novel challenges that were not experienced in previous decades. Rising sea levels, increasing energy demand and the explosion in energy prices have created new focal points in the thinking of all spheres of economic life. All these environmental factors require a new and fresh approach to future sustainability. New solutions to energy supply are needed and solutions to sea-level rise must be sought. In this article, we undertake to examine in detail the Maldives floating city and the European energy island project from a user's perspective, specifically in terms of its progress and exemplary value. In this paper, we will examine the two flagship projects through the results of a primary research conducted in 2022 and 2023, formulating the main messages for the design of future projects.

Keywords: Change, Environment, Project, Energy, Sea level rise

Introduction

We experience significant changes every day. It is a well-known fact that the impacts of environmental and climate change are extremely wide-ranging. Not only our quality of life, but also our health and our future are determined by global processes that can be linked to changes in the natural environment (WHO, 2015; Costello et al., 2009). We can hardly be independent of environmental change. There are very few economic actors that are not directly or indirectly affected by some external environmental change. The environment in which economic actors operate has undergone significant changes in recent decades. Whereas in the past the pace of change was slower and the economic systems were not so extensive, these actors could operate in a much simpler, so-called static environment. In such an environment, the pace and speed of change was not so rapid that it would have placed a significant strain on the day-to-day functioning of economic agents. However, recent decades have changed this situation. After the Second World War, the world economy started to grow intensively, if we only look at GDP or world trade. Population growth has also been unprecedented in our history. It is practically impossible to list all the factors that have made the economic system of our time so complex and changeable. Yet the effects of globalisation, the development of telecommunications and the spread of the internet (digitalisation), the emergence of new consumer awareness, the easier availability of resources, the proximity of distant markets, etc., are very often highlighted, as are new trends such as sustainability (Garai-Fodor, et al., 2023; Garai-Fodor 2022; 2023). The reasons for the slow shift from a static environment to a turbulent global environment are almost endless. Of course, this does not mean that all areas of life have the same environmental conditions. But we can say that most economic actors are experiencing an acceleration of events and that these changes require us to respond in some way. We can relate climate variability in the natural environment to sudden and irreversible changes in ecosystems (Malhi et al., 2019).

- This is an Open Access article distributed under the terms of the Creative Commons Attribution-Noncommercial 4.0 Unported License, permitting all non-commercial use, distribution, and reproduction in any medium, provided the original work is properly cited.

- Selection and peer-review under responsibility of the Organizing Committee of the Conference

© 2023 Published by ISRES Publishing: www.isres.org

This study tries to direct attention to what significant influences we are exposed to today and what response the economic actors can make to the current challenges.

Literature Review

It was mentioned in the introduction that for most economic actors the world has accelerated and events are becoming more intense and varied, impacting on our daily lives (Russell-Jones, 2005). The complexity of economic globalisation and the increased dynamism of business have also led to a surge in unexpected events and changes. These come from our immediate environment and have an impact on our daily lives. Among the most significant environmental changes of our time are digitalisation, sustainability and the green transition, technological advances, the COVID-19 crisis, the Russian-Ukrainian conflict, the energy crisis and, last but not least, the environmental degradation that has been observed for decades, or the impact of global warming. There are common points and differences. The common point is that they all affect a large number of economic actors, while there is also a fundamental difference. Part of the environmental change is taking place in the natural environment, which we can only influence indirectly, while the other part is taking place in the social environment. Global environmental change is a topic that is increasingly discussed in the literature (Pyhälä et al., 2016). Changes in the natural environment include global warming, the green transition or resource scarcity. Changes in these areas could be caused or triggered by human activity, but it is essentially the natural environment itself that is driving the change process. In the social environment, on the other hand, it is humanity, the economic actors, who cause the change and who carry out the change. Digitalisation or the conflict between Russia and Ukraine are clearly changes caused by humanity and are also being carried out by people themselves. Human activity, which is mostly a feature of the social environment, is changing many of the world's natural systems, including the climate system (McMichael et al., 2008).

Global environmental change is challenging both natural and social scientists to better understand. Global climate change refers to the long-term alteration of Earth's climate patterns on a global scale. It encompasses shifts in temperature, precipitation, wind patterns, and other atmospheric conditions over extended periods, typically decades to centuries. The primary driver of contemporary global climate change is the increase in greenhouse gas concentrations in the atmosphere, primarily resulting from human activities such as the burning of fossil fuels, deforestation, and industrial processes. The consequences of global climate change are far-reaching, including rising global temperatures, melting polar ice caps and glaciers, sea-level rise, changes in weather patterns, and more frequent and severe extreme weather events. Global environmental change offers a strategy for combining the efforts of natural and social scientists to better understand how our actions affect global changes and how these changes affect us (NRC, 1992). Whatever the environment in which the change takes place, it will affect a narrow or broad range of actors. Each of the processes identified above has affected economic actors and people more broadly, so that none of the events has not been an epoch-shaping factor in recent years (Shi, 2018). Of the environmental changes, changes in the natural environment are the main focus. Among the changes in the natural environment, climate change is one of the most significant challenges (Lenton et al, 2019). It is a proven fact that climate change has negative impacts on people's lives (Stern, 2006) and is mostly the consequence of human related carbon emissions (Csutora & Harangozo, 2017; Csutora & Harangozo, 2019). In terms of concrete economic impacts, this is reflected in the deterioration of access to adequate drinking water, the negative impact on food production, and the deterioration of people's health and the quality and condition of the environment. Environmental change can only be considered in a complex, even global, way (Norgaard-Bode, 1998). This is because ecological change cannot be limited to a narrow geographical context. Global warming or resource scarcity does not stop at national borders and does not discriminate between people and people. What is more, the effects of changes in the natural environment spill over into the social environment, where they have their real impact. Changes in the natural environment can all affect the lives of societies more widely, but this is not always the case in the social environment, where, for example, the closure of an economic organisation that did not have a large market share anyway may not affect the lives of many people. In the natural environment, there are fewer changes that are concentrated in a narrow segment of society, if only because, for example, natural disasters do not happen every day, but in the economy, new products may be released on a daily basis, causing changes in some consumers. The social environment is more likely to generate a number of changes, but not all of them are comprehensive. In the natural environment, we see fewer changes, but most of them have a knock-on effect on several people or economic actors.

The drive for sustainability, which has also become a dominant trend today in many areas (Blaskovics, 2016; 2018; Blaskovics et al., 2023; Borzán & Szekeres, 2019; Borzán & Szekeres, 2021; Borzán et al., 2022; Györi et al., 2021) and is linked to the natural environment, can also be seen as a response to changes in the natural environment. The concept of sustainability dates back to the 1960s, although its roots go back even further

(McKenzie, 2004; Györi, 2012; Engelman, 2013, Györi & Csillag, 2019). The underlying causes of sustainability can be highlighted as societal environmental changes, such as globalisation, market liberalisation, international factor mobility or the emergence of economic integration. These have been created by the social environment and have had an impact on the natural environment. This has led to adverse processes in the natural environment, and nature has reacted in its own way. Climate change is now an alteration of the natural environment, the effects of which feed back into the environment that actually caused it, which was none other than our social environment. The consequences can be unforeseeable. Rising sea levels, rising average annual temperatures, water scarcity, drought, energy shortages, while our continuing population growth will only place greater demands on the planet's resources, which are in turn becoming increasingly scarce and scarce. Fossil fuels are extremely polluting, and we must take significant steps to keep our air and water clean. Climate change is a threat to vulnerable societies.

It can cause heat waves, floods, tornadoes, hurricanes, droughts, fires and the disappearance of glaciers (Cianconi et al., 2020; Church et al., 2013). We need new thinking and new awareness to protect the values of the natural environment. We need to implement projects and investments that are sufficiently innovative and green to mitigate or possibly prevent negative impacts on the natural environment and adverse changes in the natural environment. Understand the ecological dynamics of climate impacts, identify vulnerabilities and points of resilience. Identify intervention steps that can help build resilience of the biosphere to climate change. At the same time, ecosystems can also help mitigate and adapt to climate change. The mechanisms, opportunities and constraints of climate change solutions need to be explored and quantified as clearly as possible. Environmental problems are more common in developing countries and less developed countries need more money and investment to become more sustainable. Developing countries need to invest more in promoting environmentally friendly activities and responding to the risks of climate change (Ahmed et al., 2018). The compatibility of environmental and socio-economic development is a key area of sustainability research (Szigeti et al., 2017). However, there is no question that responding to environmental challenges requires funding and targeted investments, projects and development (Varga - Csiszárík-Kocsir, 2019; Dobos et al., 2022). Some people need to spend more and others less, but we are talking about something that is a common concern for all. We have talked about global environmental change, which includes the word global.

Material and Methods

The megaprojects presented in this study are included in the list of the top 50 projects published by the Project Management Institute (PMI, 2021). The study presents two projects that address contemporary environmental problems, meet the requirements of environmental protection and conservation, and are considered to be important and interesting from a user perspective. The two selected projects (Energy Island, Maldives Floating City) were evaluated from the perspective of ordinary people as users, i.e. there was no educational background or previous project management experience as a prerequisite for inclusion in the sample, so the questionnaire on which the evaluation was based could be completed by anyone. Respondents were asked to rate the selected projects according to some factors of project scope. Respondents rated the factors on a scale of 1 to 4, with a value of 1 indicating a very weak factor and a value of 4 indicating a very strong factor. We then examined how respondents rated the project overall on a scale of 1 to 5, where 1 was the weakest and 5 the best, and then used significance analysis to see if there was a correlation between the specific scope characteristic and the overall rating of the project. There were 172 evaluable responses to the questions. Of the sample respondents, 39.5% had a tertiary education and 60.5% had a secondary education. 12.2% of the respondents are Generation Y, 23.3% are Generation X and 64.5% are Generation Z. The survey was conducted in April and May 2022.

Results and Discussion

Opinions on the Energy Island Project

The project ranked 9th in the PMI Top 50. Thirty years after Denmark built its first offshore wind farm, it is now embarking on another gigantic project to secure the country's entire energy supply from renewable sources. To do this, they want to create an artificial offshore island capable of collecting, storing and delivering the energy generated by the surrounding wind farms to where it is needed. The surplus energy that they plan to produce will be sold to other parts of Europe, providing part of their electricity supply from renewable energy sources. The project is scheduled to come on stream in 2023, and will be defined as one of the largest construction projects in the country's history in terms of budget. The gigantic scale of the project could once

again serve as a model for other coastal countries, offering an alternative to renewable energy projects that take up land (PMI, 2021).

For some characteristics of the project coverage, it can be seen that, in contrast to the Maldives Floating City, there was a much higher proportion of characteristics above 3.5. The future focus of the project was ranked first, practically the highest on the scale, but utility, environmental awareness, public interest, sustainability and usability of the project were also highly rated (in descending order). The lowest score for each of the scope characteristics was for the profit orientation of the project, which was the only characteristic below 3 for the factors studied. At the very end of the list, in addition to profitability, were feasibility and cost-effectiveness. Overall, it can be said that the purpose of the project was clearly appreciated by the respondents.



Figure 1. Assessment of the scope of the Energy Island project

Source: own research, 2022, N = 172

On the project management side, we wanted to examine which stage of the project lifecycle was considered the most important by respondents. In order for project sponsors to come up with a breakthrough, innovative project, the idea is crucial and must be sufficiently innovative. We also know that a good project needs a good plan to prepare for unexpected events and challenges. Without a good plan, a project cannot be managed effectively, which also affects its implementation. With all these principles in mind, we asked users to rate each stage of the project, as shown in the figure below. Notwithstanding the above, users did not rate the initial phase of the project highly, preferring to give the highest score to the execution, and putting the idea itself almost at the bottom of the list. This shows that a preventive awareness campaign is very important from the users' point of view for similar projects, because of the recognition of the role of the project phases.

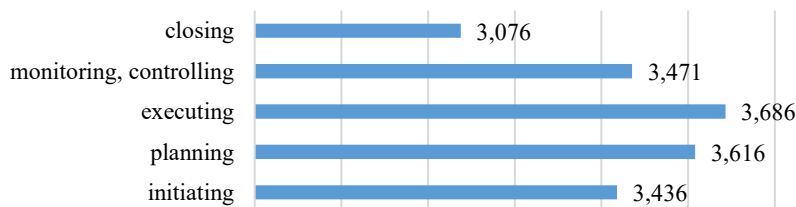


Figure 2. Assessment of the project phases of the Energy Island project

Source: own research, 2022, N = 172

Opinions on the Maldives Floating City project

The 24th ranked Maldivian floating city project looks like a utopia at first glance. But the problem it seeks to solve is very real. The island nation will be one of the biggest victims of global warming in the near future. It is estimated that sea levels could rise by as much as half a metre by 2100, which means that 77% of the island group will be covered by water. That is why decision-makers have tried to run ahead and find a solution to the looming problem. The project itself would be built in a warm-water lagoon not far from the Maldivian capital.

The project would provide homes for thousands of families, in addition to hospital and school facilities and commercial property. The floating city would rely entirely on renewable energy to protect the environment. The floating city would be both flexible and stable, following the geometric pattern of the local coral. If successful, the project could be a model for all countries involved, as it would be the world's first and largest floating structure, with 5,000 floating houses. Construction was scheduled to start in 2022, which is estimated to take 5 years (PMI, 2021).

Respondents gave the project the highest average rating of interest and a very high rating of novelty, above 3.5. The uniqueness of the project and its future focus also received a high rating, with an average of over 3.4. In addition, the project design presented was considered by many to be useful, usable, of public interest and feasible. However, the respondents felt that the environmental, profit orientation, and cost saving aspects of the project were less dominant. Thus, many fear that the project will be implemented with a very high budget, which will be a problem in terms of usability and utilisation, i.e. poorer people, who are more in need, will not be able to benefit from this solution.



Figure 3. Assessment of the scope of the Maldivian Floating City project

Source: own research, 2022, N = 172

In the case of this project, the most important aspect for the evaluation of the project phases is the design. The idea itself was also ranked better, coming in third place. In the case of the present project, users also gave a higher rating to the innovation itself, which the project itself conveys. Implementation was again rated as important by users, as it came second in the evaluation.



Source: own research, 2022, N = 172 Figure 4. Assessment of the project phases of the Maldivian Floating City project

Conclusion

Today's increasingly serious environmental problems call for new and innovative solutions. The challenges that have arisen from the environmental degradation of previous years cannot be tackled by traditional means because our existing knowledge is finite. That is why only innovation can provide solutions. The two projects presented in this study are highly regarded for their innovation. Both projects aim to address acute problems that could become serious in the decades ahead. Rising sea levels, the increasing depletion of conventional energy sources and the environmental damage they are causing are problems that must be addressed. The project plans presented in this study can only be described as pilot programmes for the time being, but their success will

provide solutions to the problems described above. The positive nature of the projects has been demonstrated by the present non-representative research and can be used as a model for future similar projects in order to provide more workable solutions to the challenges of environmental degradation. We intend to continue this research in the future, especially during the implementation phase of the projects, in order to provide a starting point for future projects with similar objectives.

Scientific Ethics Declaration

The authors declare that the scientific ethical and legal responsibility of this article published in EPSTEM journal belongs to the authors.

Acknowledgements or Notes

This article was presented as a poster presentation at the International Conference on Research in Engineering, Technology and Science (www.icrets.net) held in Budapest/Hungary on July 06-09, 2023.

References

- Ahmed, N., Islam Khan, T., & Augustine, A. (2018). Climate change and environmental degradation: a serious threat to global security. *European Journal of Social Sciences Studies*, 3(3), 161-172.
- Blaskovics, B. (2016). Differences between managing projects in an SME and in a large company. In *4th International Conference on Management and Organization Brdo* (pp. 159-176).
- Blaskovics, B. (2018). Aspects of digital project management. *Dynamic Relationship Management Journal*, 7(2), 25-37.
- Blaskovics, B., Maró, Z.M., Klimkó, G., Papp-Horváth, V., & Csiszárík-Kocsir, Á. (2023): Differences between public-sector and private-sector project management practices in Hungary from a competency point of view. *Sustainability*, 15(14), 11236.
- Borzán, A., & Szekeres, B. (2019). Accounting tourism development grants in Hungary. *Polgári Szemle*, 15, Special Issue, (pp. 334-349).
- Borzán, A., & Szekeres, B. (2021). A hazai turizmus támogatási formái. *Polgári Szemle*, 17. évf. 1-3. sz. pp. 78-94.
- Borzán, A., Szekeres, B., & Szigeti, C. (2022). Digitalizáció és fenntarthatóság a számvitel és a gazdasági szakismeretek tárgyak oktatásában. A számvitel és a controlling elmélete és gyakorlata: *Tanulmányok Bíró Tibor és Sztánó Imre tiszteletére. Budapesti Gazdasági Egyetem* (pp.175-188).
- Church, J.A., Clark, P.U., Cazenave, A., Gregory, J.M., Jevrejeva, S., & Levermann, A. (2013). *Sea level change*. Cambridge University Press Cambridge, United Kingdom
- Cianconi, P., Betró, S., & Janiri, L. (2020). The impact of climate change on mental health: A systematic descriptive review. *Frontiers in Psychiatry*, 11, 74.
- Costello, A., Abbas, M., Allen, A., Ball, S., Bell, S., Bellamy, R., & Lee, M. (2009). Managing the health effects of climate change. *Lancet*, 373:1693–733.
- Csutora, M., & Harangozó, G. (2017). Twenty years of carbon accounting and auditing—a review and outlook. *Society and Economy*, 39(4), 459-480.
- Csutora, M., & Harangozó, G. (2019). Széndioxid-elszámolás a hálózati gazdaságban/Carbon accounting in the network economy. *Vezetéstudomány-Budapest Management Review*, 50(9), 26-39.
- Dobos, O., Tóth, I.M., Csiszárík-Kocsir, Á., Garai-Fodor, M., & Kremmer, L. (2022). How generation Z managers think about the agility in a world of digitalization. In: Szakál, Anikó (ed.) *IEEE 20th Jubilee World Symposium on Applied Machine Intelligence and Informatics SAMI (2022)* : Proceedings, Poprad, Slovakia, (pp. 207-212).
- Engelman, R. (2013). *Beyond sustainable instate of the World: Is sustainability still possible?* Washington DC: Island Press.
- Garai-Fodor, M., Vasa, L., & Jäckel, K. (2023). Characteristics of segments according to the preference system for job selection, opportunities for effective incentives in each employee group. *Decision Making: Applications in Management and Engineering*, 6(2), 557-580.
- Garai-Fodor, M. (2022). The impact of the coronavirus on competence from a generation-specific perspective. *Acta Polytechnica Hungarica*, 19(8), pp. 111-125.

- Garai-Fodor, M. (2023). Digitalisation trends based on consumer research. *IEEE 17th International Symposium on Applied Computational Intelligence and Informatics SACI 2023*. Proceedings, IEEE Hungary Section, (pp.349-352).
- Györi, Z. (2012). *Corporate social responsibility and beyond: The history and future of CSR*. Lambert Academic Publishing (LAP), Saarbrücken, Németország
- Györi, Z., & Csillag, S. (2019). Vállalati felelősségvállalás és fogyasztóssággal élő személyek foglalkoztatása: külön múlt – közös jövő? - 2. rész: A fogyasztóssággal élő személyek foglalkoztatása a CSR-szakirodalomban és a gyakorlatban. *Vezetéstudomány*, 50(7-8), 16-30.
- Györi, Z., Kahn, Y., & Szegedi, K. (2021). Business model and principles of a values-based bank—Case study of MagNet Hungarian Community Bank. *Sustainability*, 13(16), 9239.
- Lenton, T.M., Rockström, J., Gaffney, O., Rahmstorf, S., Richardson, K., Steffen, W., & Schellnhuber, H.J. (2019). Climate tipping points - too risky to bet against. *Nature*, 575, 592-595.
- Malhi, Y., Franklin, J., Seddon, N., Solan, M., Turner, M.G., Field, C.B., & Knowton, N. (2020). Climate change and ecosystems: threats, opportunities and solutions. *Philosophical Transactions of the Royal Society B*, 375(1794), 20190104.
- McKenzie, S. (2004.) *Social sustainability: towards some definitions*. Hawke Research Institute. Working Paper Series. No. 27. University of South Australia. 2004.
- McMichael, A.J., Friel, S., Nyong, A., & Corvalan, C. (2008). Global environmental change and health: impacts, inequalities, and the health sector. *BMJ*. 26, 336(7637):191-4.
- Russell-Jones, N (2005). *Change management*. Manager Ltd. Budapest
- Norgaard, R. B., & Bode, C. (1998). Next, the value of God, and other reactions. *Ecological Economics*, 25, 1, 37-39.
- Pyhälä, A., Fernández-Llamazares, A., Lehvävirta, H., Byg, A., Ruiz-Mallén, I., Salpeteur, M., & Thornton, T.F. (2016). Global environmental change: local perceptions, understandings, and explanations. *Ecology and Society* 21(3), 25.
- Shi, Z. (2018). Impact of climate change on the global environment and associated human health. *Open Access Library Journal*, 5, 1-6.
- Stern, N. (2006). *Stern review on the economics of climate change*. Cambridge University Press, New York. (Internet: <http://www.hm-treasury.gov.uk>)
- Szigeti C., Tóth, G., & Szabó D.R. (2017). Decoupling – shifts in ecological footprint intensity of nations in the last decade. *Ecological Indicators*.72, 111-117.
- Varga, J., & Csiszárík-Kocsir, Á. (2019.) *redefining the role of project leader for achieving a better project result*. *PM World Journal*.8(8), 1-18.
- World Health Organization (2015). WHO calls for urgent action to protect health from climate change-sign the call. <http://www.who.int/globalchange/global-campaign/cop21/en/>

Author Information

János Varga

Óbuda University, Keleti Károly Faculty of Business and Management
1084 Budapest, Tavaszmező 15-17., Hungary

Ágnes Csiszárík-Kocsir

Óbuda University, Keleti Károly Faculty of Business and Management
1084 Budapest, Tavaszmező 15-17, Hungary
Contact e-mail: kocsir.agnes@uni-obuda.hu

To cite this article:

Varga, J. & Csiszárík-Kocsir, A. (2023). User evaluation of innovative megaprojects induced by environmental change using primary data. *The Eurasia Proceedings of Science, Technology, Engineering & Mathematics (EPSTEM)*, 23, 464-470.

The Eurasia Proceedings of Science, Technology, Engineering & Mathematics (EPSTEM), 2023

Volume 23, Pages 471-484

ICRETS 2023: International Conference on Research in Engineering, Technology and Science

Improving the Supply Chain - Marketing Interface, Translating the Voice of the Customer into Processes

Simone Franceschetto

Polytechnic University of Milan

Roberto Cigolini

Polytechnic University of Milan

Lucio Lamberti

Polytechnic University of Milan

Abstract: The aim of this paper is to develop and test a framework for leveraging the supply chain-marketing interface to deliver customer value through a standardized closed-loop customer feedback strategy. The manuscript begins with a literature review in the fields of both marketing and supply chain, resulting in a framework that defines a systematic process to deliver customer value by creating synergy between the two fields. This framework is then validated through empirical activities at Company Beta. Regarding the findings, it appears that the application of the conceptual framework, endorsing the importance of closed-loop customer feedback, highlights the role that a supply chain-marketing interface plays in delivering customer value. Nonetheless, there are some necessary prerequisites and contextual variables that must be taken into consideration to ensure a successful implementation of the framework. Since the framework validation is based on a single case study, results cannot be generalized. The preliminary results suggest that a contingent approach is necessary to adapt the framework to different company contexts, paving the way for future research. Existing studies address ways in which companies should restructure to support the integration of marketing and supply chains, and researchers are in harmony that the integration can contribute to company success. As of yet, there is no comprehensive guide for the inter-functional activities needed to leverage the supply chain-marketing interface towards customer-centricity and customer value creation.

Keywords: Supply chain-marketing interface, Voice of the customer, Customer centricity, Marketing automation, Customer journey

Introduction

Following a rise in globalisation, consumer preferences have strongly changed, favouring deeper customisation, higher quality, and shorter delivery times (Lamberti, 2013). This has made it necessary for companies to adopt customer-centric business strategies. Companies must revolutionise customer interactions and explore new marketing possibilities to remain competitive and offer a customer experience that matches its' time (López-Cabarcos et al., 2020). In this context, the effectiveness of delivering superior customer value is fundamental and, to achieve this, full coordination between marketing and supply chain functions is crucial.

As customers demand more personalised service offerings, companies can exploit advanced technologies, including Big Data and intelligent algorithms, to extract new insights from customers and identify business opportunities or areas of improvement in their supply chains (Noci, 2019). By integrating marketing and supply chain processes, a company can successfully deliver superior customer value through the development of customer-based product specifications and individualised customer journeys (De Haan et al., 2015).

- This is an Open Access article distributed under the terms of the Creative Commons Attribution-NonCommercial 4.0 Unported License, permitting all non-commercial use, distribution, and reproduction in any medium, provided the original work is properly cited.

- Selection and peer-review under responsibility of the Organizing Committee of the Conference

© 2023 Published by ISRES Publishing: www.isres.org

The objective of this manuscript is to define a process-driven methodology to leverage the synergy between marketing and supply chain activities to collect and translate new customer insights into operational processes, leading to the delivery of customer value.

This paper explores the possibility of integrating marketing and supply chain activities to achieve customer-centricity and leverages empirical activities in Company Beta, a company that delivers intelligent products and tailored solutions to its customers. In order to become more customer-centric, the company must define a systematic process to collect insightful feedback from customers at various critical touchpoints at the front end to drive operational improvements in the back end.

The most relevant touchpoints are highlighted by reviewing the company's vast range of customer journeys. A strategy is then deployed to collect the right information from customers at each critical touchpoint, evaluate the given feedback, and channel new insight to the right stakeholders in order to improve supply chains accordingly. The objective of empirical activities is to provide base material when developing a standardised strategy to enhance customer value by linking customer experience to operational improvements.

The paper is structured as follows: section 2 is devoted to the description of the research background to define the SC of the construction industry and the related risks as well as the main characteristics of blockchain technology. Section 3 describes the methodology adopted while section 4 illustrates the model. Section 5 shows the main findings. Finally, section 6 draws some conclusions and suggests future research paths.

Background

Customers are becoming more sophisticated and empowered to demand exactly what they want from companies, which accelerates the importance of understanding exact customer needs, and using those insights to drive supply chains and deliver superior customer value (Piercy, 2007).

Several factors contribute to today's modern marketing environment: globalisation, customer sophistication, shifting organizational structures, and increased dependence on information technology (Day, 2011). On the one hand, digital technologies and social networks are the reason behind customers' increasing expectations of personalised services, adding pressure on companies to adapt their offerings (Pero & Lamberti, 2013). However, those technologies may also help companies become more in touch with customers to identify their exact volatile needs and adopt responsive operational processes to deliver the appropriate offerings (Ardito et al., 2018).

As customers now interact with firms through a vast range of touchpoints in online and offline channels, customer journeys are becoming increasingly complex (Lemon & Verhoef, 2016). One way to keep up with the evolving consumer behaviour is to leverage the power of technology to collect both solicited and unsolicited feedback to listen to the voice of the customer (VoC) (Stegemyr & Thell, 2021). This way, customer needs, wants, and pain points can be captured in order to refine and develop an optimal product or service offering (Lee et al., 2014).

Digital marketing operations involve the application of technologies to scale and effectively enhance customer interactivity (Juttner et al., 2010). By incorporating digital technologies in the marketing process, companies can become more in touch with customers at different touchpoints throughout the customer lifecycle. This allows a company to build a complete picture of the experience they are delivering to every customer that they have at each step of the journey (Giménez & Ventura, 2003). Once this complete picture is formed, information can be extracted and fed back into the organisation.

As firms begin to focus their marketing processes on revealing exact customer needs, they must ensure that those insights drive productive and efficient actions in supply chains to achieve excellent business results (López Cabarcos et al., 2020). This highlights the need to create a common interface between a company's marketing and operational activities to achieve synergy (Zokaei & Hines, 2007).

If a company's marketing department is strongly focused on customer interactions and feedback, without directly communicating its results with the rest of the organisation, the company may fail to achieve efficiency in operational activities, leading to unfulfilled demand (Ardito et al., 2018). On the other hand, a company that

exclusively focuses on delivering optimal products from a cost-optimisation point of view would then struggle to deliver customer value (Jüttner et al., 2010). It is therefore important to create interdepartmental relationships between organisational units to introduce a joint decision-making process between front-end marketing and supply chains. The following research questions and scheme presented in Figure 1 will be addressed in this paper to gain the required knowledge and reach the final objective:

RQ1: what are the necessary conditions for a company to shift towards a customer-centric organisational structure?

RQ2: how can the marketing-supply chain interface contribute to the overall delivery of customer value?

RQ3: how do contextual factors influence the adoption of the supply chain-marketing interface?

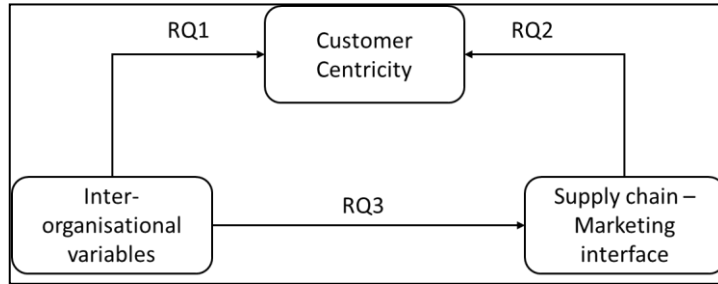


Figure 1. The research scheme used to steer the research paper

Literature Review

The literature review aims to explore literature addressing the ways in which an organisation can become more customer-centric by adopting strategic marketing activities and creating an interface between marketing and supply chain to remain competitive in dynamic markets. There are five pillars an organisation should consider in order to effectively bridge the gap between what customers expect and what they get (Todor, 2016). These attributes will serve as a guide to the structure of this literature review as depicted in Figure 2.

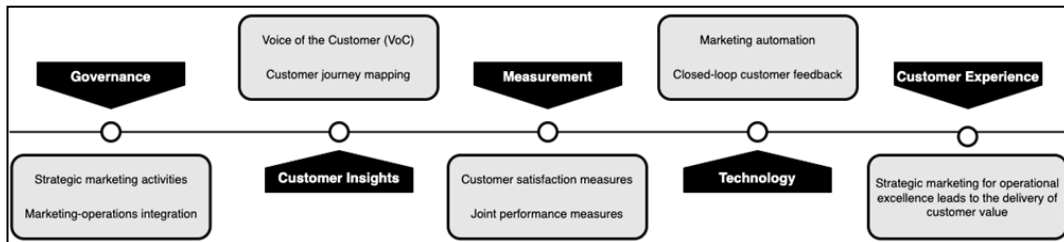


Figure 2. The five attributes of marketing operations required to keep up with evolving consumer behaviour

Strategic Marketing

Technology has turned some customer journeys fully digital, which allows companies to serve a global customer base (Ardito et al., 2018). However, to ensure that the customer experience delivers superior value, Tang (2009) highlights that people, processes, and governance must be structured to deliver efficient marketing activities. In line with this, literature has begun to acknowledge that marketing needs to be strategic rather than tactical to drive efficient changes in a company's strategy (Amico et al., 2022a). To do so, organisations must reform organisational structures and establish new guidelines in order to allow marketing to gain more relevance in an organisation (Zokaei & Hines, 2007).

According to Muralidharan and Raval (2018) while companies are adopting structured process improvement methods such as Lean Manufacturing and Six Sigma in their supply chains, the marketing field remains characterised by its unstructured work environment. Furthermore, although marketers are undertaking a wide

range of digital transformations to keep up with dynamic market demands, they are unable to deliver aspirations due to the non-scientific decision-making processes (De Haan et al., 2015).

As more firms attempt to increase their customer centricity and thereby improve their operational performance, Lee et al. (2014) examine the impact of an organisation's structural design on its marketing outcomes. They highlight how logical, standardised marketing processes serve to effectively link employees to customers, creating an organisational structure that prioritises being customer-focused rather than product-focused, which in turn maximises customers' overall experience (Day, 2011).

Supply Chain - Marketing Interface

The evolution of marketing and its integration with other organisational functional areas is a topic widely discussed in the literature (Giménez, & Ventura, 2003). Specifically, there is increasing focus on ways in which marketing should cooperate with supply chain to develop successful innovation and enhance competitiveness (Franceschetto et al., 2022). Several functions are critical to the customer journey, including marketing, sales, customer service, and technical support. However, back-end functions are usually overlooked by marketers although they are critical to the creation and delivery of customer value (Amico et al., 2022b). This is why the joint role of supply chain and marketing is imperative to success (Mollenkopf et al., 2010).

Several studies highlight the importance of the integration of a company's marketing and supply chain to achieve superior performance for the firm. Those studies provide a range model to interface between marketing and back-end organisational units. There are several integration archetypes, each having different goals and contingent factors that impact their adoption (Tang, 2009). According to Pero and Lamberti (2013), the integration can vary from mutual isolation, characterized by an absence of information exchange and an avoidance of considering the counterpart's objectives, to full collaboration; when two organisational functions come together to work towards a common objective.

In practice, marketing and supply chain often experience conflicts due to their respective roles and responsibilities (Mollenkopf et al., 2010). Marketing is an externally focused unit whose main responsibility is meeting customer expectations quickly, while the supply chain is a functional area that focuses on developing an operational plan in order to meet the demand imposed by the marketers in a cost and time-efficient manner (Tang, 2009).

Customer Centricity

A customer journey is the series of actions and experiences that customers go through when interacting with a company and its brand (Sawhney & Piper, 2002). Prior research has conceptualised a customer journey in three overall stages: pre-purchase, purchase, and post-purchase (Lemon & Verhoef, 2016). It is important to note that customer experience does not only occur within the sales and marketing units of an organisation; many of the activities that occur along the customer journey concern other functional units within an organisation (Franceschetto et al., 2023).

A customer journey map (CJM) is a diagram that presents every stage of the customer experience by outlining the steps a customer takes to engage with a brand (Moon et al., 2016). The diagram, usually presented in the form of a timeline, gives an overall view of the entire customer journey, from initial awareness to post-purchase. Previous research has defined several methodologies to design a CJM that depicts all the different interactions that a customer has with a company (Moon et al., 2016; Cigolini et al., 2022). However, in order to really understand the customer experience, it is important to take a close look into what happens within each stage of the customer journey, since the journey is often not linear (Payaro and Papa, 2014).

During each stage, customers interact with the company at various points of customer contact, known as customer touch points. As the number of touchpoints increases, journey mapping becomes increasingly important to better deliver customer value (Zokaei & Hines, 2007). According to Found and Harrison (2012), in order to understand exact customer value and therefore tackle the first element of measuring the VoC, the first step is to map the different touch points in order to identify the gap between customer experience and expectation at each point. Identifying customer touchpoints starts with making a list of all the instances and

channels that a customer is in contact with the organisation before, during, and after a transaction is made (Amico & Cigolini, 2023).

Customer input is crucial in this process as it is important to understand the customer journey from the customer’s perspective. These insights can be collected through qualitative customer research and allow a company to understand which touchpoints are critical to customer experience (Rosenbaum et al., 2017). Once an organisation can understand the VoC throughout the various touch points, it may begin improving value creation at each step, resulting in an enhancement of the customer journey and overall customer experience.

Marketing Automation

Marketing has a strong responsibility to lead with innovation and deliver superior customer value. To do so, it must leverage the application of technologies to improve customer knowledge and match their needs with operational activities (Sawhney & Piper, 2002). This way, customer insights captured by marketing can be used to drive operational changes and achieve growth by meeting exact customer expectations.

The previous sections outline the importance of structuring marketing activities in order to effectively capture the VoC and quantify customer satisfaction through relevant metrics. In line with this, marketing automation involves adopting technologies to help marketers manage their activities in a structured way (Xu et al., 2002). It leverages real-time data from multiple data sources to understand customer behaviour and respond accordingly to deliver customer value (Heimbach et al., 2015; Cigolini et al., 2021).

In addition, marketing automation is often associated with Customer Relationship Management (CRM), whose primary purpose is to use software to track customer behaviour and manage customer relationships in an organised manner (Xu et al., 2022). As the number of customer touch points increases in response to the continuous increase in supply and demand, it becomes more complex to collect insights from a wide range of customers (Lemon & Verhoef, 2016), This introduces the need for automation and CRM to facilitate feedback collection and efficiently process relevant insights.

Marketing automation also facilitates the integration of marketing and supply chain, as the actionable insights and metrics processed by the front-end can then be centralised on a common platform and shared across the organisation. This creates an efficient supply chain-marketing interface that continuously feeds new customer insights into back-end units and drives behind the scenes supply chains to improve customer experience (Todor, 2016).

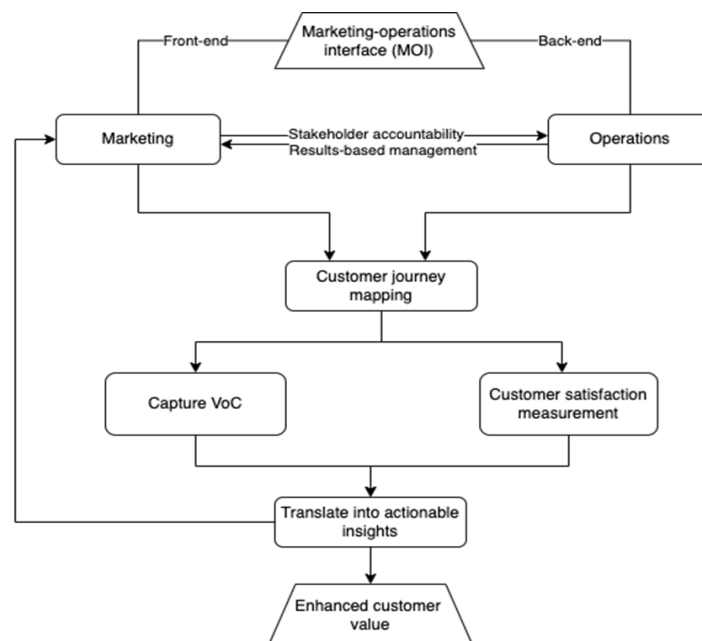


Figure 3. Marketing-supply chain integration framework for customer value creation

Conceptual Framework

This section supports the notion that a common supply chain-marketing interface contributes to the effectiveness of customer value creation. A conceptual framework is proposed, that defines a systematic process to deliver customer value by creating synergy through the integration of marketing and supply chain activities. The development of the conceptual framework involved two main phases. The first phase began by developing an initial framework using insights from existing literature. The second phase then involved testing and progressively refining it as a result of insights uncovered during the empirical activities conducted at Company Beta.

The conceptual framework aims to provide managers with guidelines for a joint marketing and supply chain planning process when they are struggling to deliver optimal customer value. However, before this interface can be implemented, a manager must first ensure that the organisation has a customer-centric organisational structure, meaning that its strategy and culture focus on fostering a positive customer experience at every stage of the customer journey (Lamberti & Pero, 2019). If this is not the case, structural changes must first be made to the organisation to accommodate the supply chain-marketing interface (Figure 3).

Methodology

The purpose of the empirical activities conducted in this research project is to test the conceptual framework developed as a result of a literature review on the integration of marketing and supply chain to deliver optimal customer value. This research is crucial since academia still lacks a definitive framework for the full integration of marketing and supply chain for customer-centricity and has not particularly investigated the organisational issues and dynamics required for this interface. An empirical investigation has been pursued because inter-organisational dynamics and emotional variables such as customer value measurement are hardly observable through explanatory studies. The research project is centred on capturing the VoC and delivering customer value by leveraging a supply chain-marketing interface. Two major sub-parts of the new VoC strategy have been launched.

The first part of the VoC strategy is deployed on a small scale, solely focusing on delivering value to Company Beta users, i.e., the developers. Currently, Company Beta has over 130.000 software downloads each month, which in turn has a strong impact on customer value. This has driven the division to completely transform their product development approach from a ‘product-out’ strategy, to directly working with developers to provide exactly what their customers need. In order to do so, they must put the developers at the centre of their activity, which is in line with the VoC strategy to be deployed.

The second part of the VoC strategy captures the VoC on a wider scale throughout Company Beta’s entire online ecosystem. Due to the competitive nature of the industry, Company Beta needs a good online presence in order to remain a key player. Currently, the Company beta’s online ecosystem offers a variety of online customer journeys and touchpoints. The VoC strategy involves highlighting Company Beta’s most relevant online touchpoints and collecting insights from users at different stages throughout the various customer journeys. This allows us to calculate customer satisfaction metrics across Company Beta’s offerings, which can then be compared in order to identify areas which require improvements, driving actionable insights to supply chains, who can then work to deliver customer value.

Table 1. The two main steps required to deploy the VoC strategy

Step 1: feedback collection	a. Customer journey mapping and critical touch point identification
	b. Developing a feedback collection strategy for each touch point
	c. Feedback collection at the derived touch points
Step 2: feedback handling	a. Feedback processing: calculation of metrics and translation into actionable insights
	b. Feedback reporting: channelling insights to the right stakeholders
	c. Closing the customer feedback loop

This way, information can be easily and quickly exchanged between marketing and technical experts, creating a strategic supply chain-marketing interface. Once this is achieved, we may begin to deploy the VoC strategy, which is divided into two main sub-parts, as described in Table 1.

VoC – Company Beta Software Users

Before the wide-scale launch of the VoC strategy across Company Beta’s range of customer journeys, it was first deployed for the customer journey of one of Company Beta’s most popular online offerings; embedded and development software. When exploring the stages, a developer goes through for a new embedded product design (see Figure 4), 50% of the total time spent occurs during the ‘detailed design’ and ‘testing & debugging’ stages, according to surveys conducted by Company Beta with lead developers. In those two time-consuming stages, software is a crucial tool required to successfully create a scalable prototype. This justifies the importance of prioritising Company Beta software for the VoC project, as it is a strong contributor to customer value.

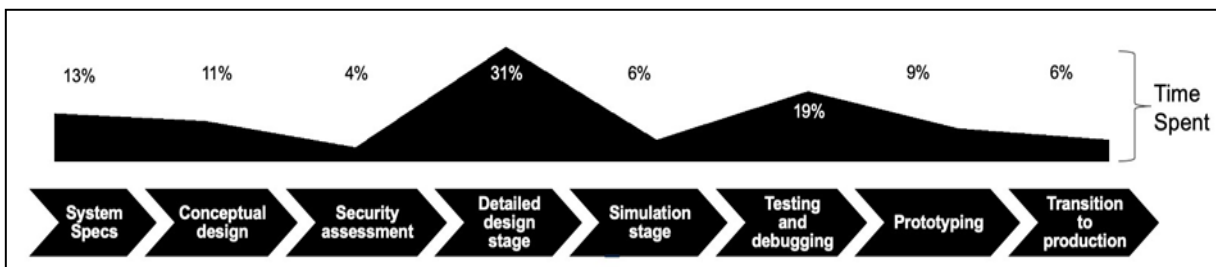


Figure 4. Stages of a new embedded product design process

In order to gain a holistic understanding of the software users’ experiences and identify areas that require improvement, it is important to understand users’ cumulative experience across the entire customer journey, considering both online and offline touch points. We first begin by mapping the users’ broad customer journey; from the moment the need for a specific software is realised, until the developed prototype is ready for production. This was then followed by an in-depth analysis of each stage of the customer journey in a detailed customer journey map (CJM), which was divided into three macro-phases; search, download, and use of the software.

There is a range of interaction points throughout the journey where the VoC can be captured. To identify those critical touch points from which customer feedback would be most constructive, they have been prioritised through an analysis of existing feedback from software users to identify touch points with a strong impact on customer value, along with analytics data to identify high-traffic touch points. Finally, the following touch points have been prioritised:

1. Software pages: the various pages on Company Beta’s online ecosystem where developers can access software information and download the software
2. Emails: feedback surveys sent by email to users after they have used the software for a period of time

For each of those touch points, a customer journey map is constructed to identify pain points a customer may face during the journey, along with possible strategic actions to overcome the barriers. Finally, specific metrics are assigned to each touch point to monitor the performance of the corrective actions taken and ensure they have had a positive impact on customer value delivery. Later, once feedback is collected from users through surveys, it’s possible to understand individual experiences and gather more in-depth insight into the different barriers they may face.

In order to begin the customer feedback collection process, a collaborative plan must be constructed involving all stakeholders who have an impact on customer experience throughout the software users’ customer journey. This plan is to be implemented across all critical touch points along the journey in order to ensure successful closed-loop customer feedback collection. The collaborative plan is presented in Table 2. Once the VoC plan has been defined, the two main steps of the VoC strategy must be adapted and deployed (Table 1). The next two sections will outline the activities required for step 1, adapted to each of the two explored touch points. Once this is done, the following section will introduce step 2 of the VoC strategy, which has been generalised for the entire software customer journey.

Table 2. The defined collaborative plan for the feedback collection strategy on Company Beta’s software

	Digital marketers: CJM + feedback collection & reporting Technical marketers: software presentation on Company Beta’s website
Stakeholder responsibilities	Software developers: software package quality & availability Web developers: technical implications on Company Beta’s website Technical support: provide technical assistance to software users
Joint performance measures	Customer satisfaction score (CSAT) Customer effort score (CES) Net promoter score (NPS) % of users encountering issues
Cross-functional team	Front-end: digital and technical marketers, and technical support Back-end: web and software developers
Periodic review reporting	Bi-weekly review sessions between involved stakeholders Monthly reporting sessions involving external stakeholders

Model

Touch Point: Online Software Pages

Currently, the Company beta’s online ecosystem offers a variety of online customer journeys and touchpoints. Software pages are a considerably high traffic touch point, with around half a million page visits and over 130 thousand software downloads each month. Users access software pages to get information about the software, and if it meets their needs, they download the software directly from the page. Therefore, it is crucial to optimise software pages, as it’s one of the most important touch points that can drive higher conversion rates.

Step 1: Customer Journey Mapping

Considering the entire customer journey map, the software ‘download’ phase corresponds to the stage in which a ‘visitor’ converts into a ‘customer’, making Company Beta’s software pages a critical final touch point where visitors make a decision to become users of Company Beta’s software. Going more in depth, the customer journey in Figure 4 outlines the steps a visitor undertakes on Company Beta’s website up to the point of ‘conversion’, once the software download begins.

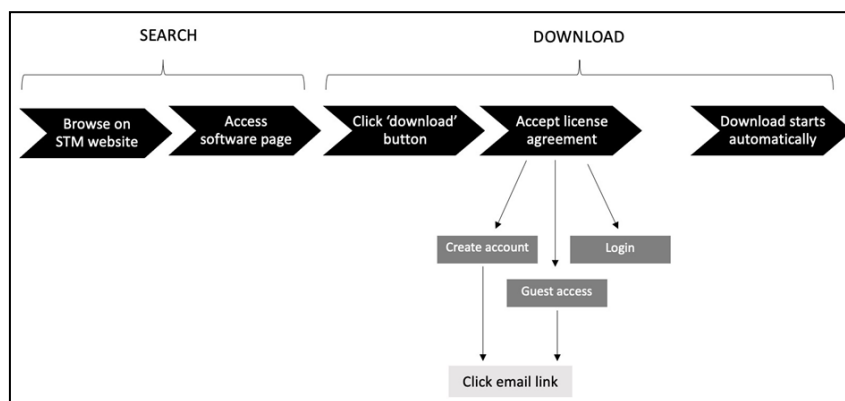


Figure 5. The journey an online visitor undergoes up to the point of conversion.

In order to collect real-time active feedback from users, the survey will appear in the form of a pop-up on the users’ screen once the software download begins. This interceptive survey method allows to capture the users’ attention and collects a large number of immediate responses while the users are waiting for their software to

finish downloading. In addition, since Company Beta has over 100 thousand software downloads each month, a sample size of 25% has been set, for which the survey will appear to a random selection of people, irrespective of the software they downloaded. This randomisation is done to ensure the results are representative of all software download journeys on Company Beta’s online ecosystem.

Finally, to ensure that the survey is not intrusive, specifically for users who download multiple Company Beta software, quarantine rules are applied. If a user has been exposed to the survey in the past X (predefined) days, they do not see the survey again until that time has elapsed.

Step 2: Develop a Feedback Collection Strategy

Once the survey has been defined, the following feedback collection strategy is developed, where decisions on the type of survey and the target segment exposed to the survey are made.

Table 3. Survey information

Survey type	Pop-up survey on Company Beta website
Survey trigger	Start of software download
Survey sampling	25% of all users downloading Company Beta software
Quarantine periods	Declined survey: 7 days
	Submitted feedback: 21 days

In order to collect real-time active feedback from users, the survey will appear in the form of a pop-up on the users’ screen once the software download begins.

Step 3: Feedback Collection

Once the survey and feedback collection strategy has been defined, the technical implementation required to launch the survey begins with collecting feedback. For this interceptive pop-up survey, the software’s automation rules can automatically trigger the survey upon the users’ software download.

Results

The conceptual framework defined as a result of the literature review has served as a guide throughout the entire VoC strategy deployment (see Figure 3). In turn, the results of the empirical activities reflect many benefits of the marketing-supply chain interface in customer value creation for Company Beta.

Following the deployment of both parts of the VoC strategy outlined in the Methodology and Model section, it’s possible to generate comparable customer satisfaction metrics for the explored touch point. In doing so, customer journeys which require corrective actions were identified, and the supply chain-marketing interface was leveraged to create a closed-loop customer feedback cycle, delivering enhanced customer value.

Overall, through joint performance measures comparable across touch points, along with full visibility between the stakeholders involved in the supply chain-marketing interface, accountable divisions were incentivised to reach and surpass their set targets. This has led to an overall improvement in customer satisfaction metrics across Company Beta’s entire online ecosystem. To provide an example of customer value improvement through the supply chain-marketing framework, the process to improve the customer effort score (CES) metric for Company Beta software is presented below.

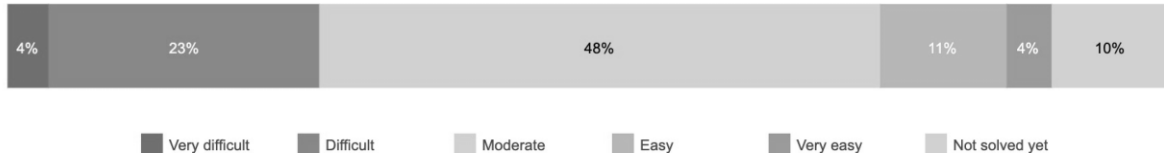
Firstly, proactive customer feedback was collected from software users through email surveys as outlined in the Methodology section. One insight captured through these surveys is the level of ease of resolving issues encountered with the software. Users who have indicated that they encountered an issue with the software are asked to rate how easy it was for them to solve their issues, through the question displayed in Figure 6.

How easy was it to resolve the issue(s) you experienced with the software?



Figure 6. Customer effort score (CES) questions

Once the responses were collected, the corresponding CES metric is calculated, at a considerably low value of 2,9 out of 5. Initially, 27% of users found it difficult (or very difficult) to solve their issues, only 15% of the users found it easy, and 10% have not yet managed to solve their issue (see Figure 7). This indicates that Company Beta needs to improve the software support services provided to increase the CES score.



(a) CES: distribution of user responses



(b) CES score

Figure 7. Initial customer effort score (CES): ease of resolving software issues

Company Beta provides a range of software support services to its users, meaning that in order to improve the CES score, there are many possible stakeholders to involve in a vast range of improvement activities. It is therefore important to identify and prioritise the services requiring immediate attention. To do so, the survey includes a question which asks users to select the support channels they have used (see Figure 8).

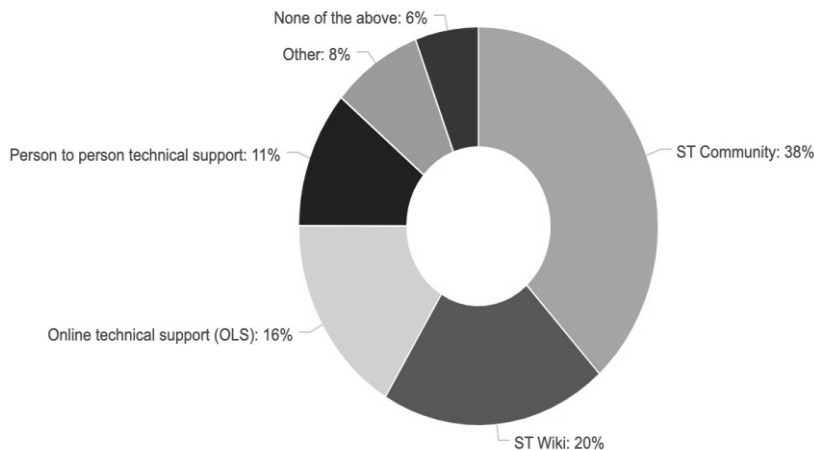


Figure 8. Distribution of Company Beta support channels used by software users

During the feedback processing step, the responses to the CES question were filtered by each support channel in order to rank the channels by performance and prioritise corrective actions for the support channels with lower CES values.

This aggregation of customer feedback by type of support channel allowed for actionable insights to be shared along the supply chain-marketing interface and routed to the divisions directly responsible for the three

aforementioned channels with a low CES score. The divisions must then dig further into the responses in order to allocate responsibilities to the accountable stakeholders. For example, the division responsible for 'Online technical support' has filtered the negative feedback responses by region, which allowed them to identify that the stakeholders responsible for support in China and Germany required the most improvement activities. Next, corrective actions are taken by the various stakeholders to attempt to improve the CES score and then documented on the platform. This way, all back-end activities are logged in a common platform to trace back improvements and avoid duplicated actions.

Finally, to close the customer feedback loop, the performance of software support is reassessed post-changes to identify whether the improvement activities taken by various divisions have led to an overall improvement in the CES metric. Overall, the CES increased by an increment of 0,5 (16,7% improvement), and looking closely, the percentage of users finding it difficult to solve their issues, or who were not able to solve them has reduced by 4% and 3% respectively.

This indicates that the corrective actions taken have led to an overall improvement in customer value delivery. Fortunately, the resources were invested in the right direction thanks to the result-based management strategy, which drives strategic data-driven decisions to be made in the back-end based on the voice of the customer. Furthermore, the supply chain-marketing interface has also contributed to Company Beta's overall business performance, as resources were prioritised and allocated to the touch points with relatively lower customer satisfaction ratings.

Thanks to the results-based management strategy, stakeholders are able to identify exactly which areas needed improvement, leading to an optimisation of both cost and time resources. Through the adoption of a closed-loop customer feedback cycle in the supply chain-marketing interface, which follows the structure of the Six Sigma DMAIC cycle (see Table 4), the following lean wastes were reduced:

Table 4. The lean wastes reduced by supply chain-marketing interface for value creation

Lean waste	Description
Defects	Customer pain points and issues were captured in real-time, allowing quick fixes to be made accordingly
Over-processing	The VoC uncovers exact customer preferences, leading to reduction in unnecessary value creation activities, and prioritisation of operational activities
Waiting	The supply chain-marketing allows for integration between divisions, reducing waiting times due to slow communication
Motion	Using an online platform to manage the supply chain-marketing leads to the reduction of unnecessary movements or overlapping activities between divisions
Talent and creativity	The integration of stakeholders across different divisions creates synergy between knowledge and skills

Overall, the variation of the customer satisfaction metrics when parameters in the feedback collection strategy are changed has introduced a constraint in the VoC strategy, since the performance of the different touch points on Company Beta's online ecosystem can only be compared as long as the same feedback collection strategy is used. This is because changing parameters within the strategy, such as the survey type or the time at which feedback is collected, strongly influences the users' psychology, leading to a variation in responses. Another implication uncovered by the empirical activities is the requirement of different degrees of integration between stakeholders in the supply chain-marketing interface. Due to the various roles and responsibilities, along with the complex nature of some touch points, full integration and transparency have caused some conflicts and a lack of teamwork between stakeholders due to different backgrounds, expertise, and cultures. As a result, the level of integration within the supply chain and marketing should be determined by contextual factors, depending on contingent variables specific to each explored customer journey.

Conclusions and Future Research Paths

The purpose of this paper is to provide a contribution to existing research on the integration of front-end marketing and supply chain activities. Specifically, it aims to outline the ways in which a strategic interface

between marketing and supply chain has a crucial role in the delivery of customer value, leading to overall business performance. To do so, the manuscript begins with an extensive literature review to develop an overview of the existing knowledge in the fields related to strategic marketing-supply chain integration and customer-centricity. From this, we infer that for a company to adopt a customer centric business model, some organisational changes must be made. Along with structural requirements such as modularity and decentralisation of activities, the application of systematic methodologies such as lean and six sigma to marketing activities is necessary to adopt a methodological rather than unstructured approach to marketing, leading to the overall efficiency of front-end activities. Once this is done, an organisation may begin to integrate its marketing and supply chain activities to put a continuous closed customer feedback loop in place. Existing research also addresses the requirements for a successful marketing-supply chain interface, along with the set of activities required to successfully capture the voice of the customer and ensure insights are processed strategically to drive operational improvements that deliver enhanced customer value.

Considering the contextual complexities outlined above, the marketing-supply chain interface requires added coordination costs and planning time, which may influence overall business performance. However, this drawback appears to be outweighed by the added benefits accrued to greater customer value delivery as well as the reduction of lean waste. To validate this, the research scope can be extended beyond the delivery of customer value to examine the impact of the proposed supply chain-marketing interface framework and the application of Lean Six Sigma tools in marketing on overall business performance. As with most studies, this research has some limitations that should be acknowledged. Firstly, although the conceptual framework has been successfully applied in a business context to create value for customers, the conclusions are limited in their generalisability, since one company does not represent a broader population of companies across different industries. The results of the study can be strengthened by further examination of the impact of the Supply chain-Marketing interface framework in various companies from the same industry as well in different industries. However, the results of this study are based on a VoC strategy which was deployed across a range of Company Beta's online offerings. This tested the supply chain-marketing interface framework in multiple customer journeys, involving a wide range of stakeholders within different divisions. This means that the results can be predicted to have more generality than those from a study focused on a single customer journey with a limited number of stakeholders.

Overall, the results of this study can be used as the base material for customer-centric organisations looking to involve their marketing and supply chain divisions in the customer value delivery process. The results of the empirical research are aligned with the literature review outcomes, and substantially confirm that the conceptual framework, endorsing the importance of closed-loop customer feedback, provides a starting point for understanding the role that a marketing-supply chain interface plays in delivering customer value. Nonetheless, to become a powerful tool applied to companies in different contexts, the framework and general insights uncovered from existing literature must be adapted according to specific contingencies.

Scientific Ethics Declaration

The authors declare that the scientific ethical and legal responsibility of this article published in EPSTEM journal belongs to the authors.

Acknowledgements

This article was presented as an oral presentation at the International Conference on Research in Engineering, Technology and Science (www.icrets.net) held in Budapest/Hungary on July 06-09, 2023.

References

- Amico, C., Cigolini, R., & Frances *XXVI Summer School Proceedings of the Summer School Francesco Turco Industrial Systems Engineering*. Bergamo, Italy.
- Amico, C., Cigolini, R., & Franceschetto, S. (2022a). Using blockchain to mitigate supply chain risks in the construction industry. *XXVI Summer School Proceedings of the Summer School Francesco Turco Industrial Systems Engineering*. Bergamo, Italy.

- Amico, C., Cigolini R., Franceschetto, S. (2022b). Supply chain resilience in the European football industry: the impact of Covid-19. *XXVI Summer School Proceedings of the Summer School Francesco Turco Industrial Systems Engineering*. Bergamo, Italy.
- Amico, C., Cigolini, R. (2023). Improving port supply chain through blockchain-based bills of lading: a quantitative approach and a case study. *Maritime Economics and Logistics*, 1-31.
- Ardito, L., Petruzzelli, A. M., Panniello, U., & Garavelli, A. C. (2018). Towards industry 4.0: Mapping digital technologies for supply chain management-marketing integration. *Business Process Management Journal*, 25(2), 323–346.
- Cigolini, R., Franceschetto S., & Sianesi A. (2021). Mitigating the bullwhip effect in the electric power industry: a simulation model and a case study. *Proceedings of the Summer School Francesco Turco Industrial Systems Engineering*. Bergamo, Italy.
- Cigolini, R., Franceschetto, S., & Sianesi, A. (2022). Shop floor control in the VLSI circuit manufacturing: a simulation approach and a case study. *International Journal of Production Research*, 60(18), 5450–5467.
- Day, G. S. (2011). Closing the marketing capabilities gap, *Journal of Marketing*, 75(4), 183–195.
- De Haan, E., Verhoef, P. C. and Wiesel, T. (2015). The predictive ability of different customer feedback metrics for retention, *International Journal of Research in Marketing*, 32(2), 195–206.
- Found, P., & Harrison, R. (2012). Understanding the lean voice of the customer, *International Journal of Lean Six Sigma*, 3(3), 251–267.
- Franceschetto, S., Amico C., Brambilla M., & Cigolini, R. (2023). Improving supply chain in the automotive industry with the right bill of material configuration. *IEEE Engineering Management Review*, 51(1), 214-237.
- Franceschetto S., Amico C., Cigolini R. (2022). The ‘new normal’ in the automotive supply chain after Covid. *XXVI Summer School Proceedings of the Summer School Francesco Turco Industrial Systems Engineering*. Bergamo, Italy.
- Giménez, C., & Ventura, E. (2003). Logistics-production, logistics-marketing and external integration: Their impact on performance. *International Journal of Operations & Production Management*, 25(1), 20-38.
- Heimbach, I., Kostyra, D. S., & Hinz, O. (2015). Marketing automation, *Business Information Systems Engineering*, 57(2), 129–133.
- Jüttner, U., Christopher, M., & Godsell, J. (2010). A strategic framework for integrating marketing and supply chain strategies, *The International Journal of Logistics Management*, 21(1), 104–126.
- Lamberti, L. (2013). Customer centricity: the construct and the operational antecedents. *Journal of Strategic Marketing*, 21(7), 588-612.
- Lamberti, L., & Pero, M. (2019). Special issue editorial: Managing the supply chain management–marketing interface. *Business Process Management Journal*, 25(2), 246-249.
- Lee, J.-Y., Kozlenkova, I. V., & Palmatier, R. W. (2014). Structural marketing: Using organizational structure to achieve marketing objectives, *Journal of the Academy of Marketing Science*, 43(1), 73–99.
- Lemon, K. N., & Verhoef, P. C. (2016). Understanding customer experience throughout the customer journey, *Journal of Marketing*, 80(6), 69–96.
- López Cabarcos, M. Á., Srinivasan, S., Vázquez-Rodríguez, P., (2020). The role of product innovation and customer centricity in transforming tacit and explicit knowledge into profitability. *Journal of Knowledge Management*, 24(5), 1037-1057.
- Mollenkopf, D. A., Frankel, R. and Russo, I. (2010). Creating value through returns management: Exploring the marketing-operations interface. *Journal of Operations Management*, 29(5), 391–403
- Moon, H., Han, S. H., Chun, J., & Hong, S. W. (2016). A design process for a customer journey map: A case study on mobile services, *Human Factors and Ergonomics in Manufacturing and Service Industries*, 26(4), 501–514.
- Muralidharan, K., & Raval, N. (2018). Scientific outlook of lean in six sigma marketing, *Seventh International Conference on Lean Six Sigma*. Dubai.
- Noci, G., (2019). The evolving nature of the marketing–supply chain management interface in contemporary markets. *Business Process Management Journal*, 25(2), 379-383.
- Payaro, A. & Papa, A. R. (2014). The wastes in lean marketing. a proposed taxonomy and an exploratory study on Italian smes, *Management and Marketing*, In *Proceedings of the 9th International Conference on Business Excellence*
- Pero, M., Lamberti, L. (2013). The supply chain management-marketing interface in product development: An exploratory study. *Business Process Management Journal*, 19(2), 217-244.
- Piercy, N. (2007). Framing the problematic relationship between the marketing and operations functions, *Journal of Strategic Marketing*, 15(2-3), 185–207.

- Rosenbaum, M. S., Otalora, M. L., & Ramírez, G. C. (2017). How to create a realistic customer journey map. *Business Horizons*, 60(1), 143–150.
- Sawhney, R., & Piper, C. (2002). Value creation through enriched marketing-operations interfaces: An empirical study in the printed circuit board industry. *Journal of Operations Management*, 20(3), 259–272.
- Stegemyr, J., Thell, L., (2021). Kano model deployment and its relation to customer centricity. *Chalmers University of Technology*, 1(1).
- Tang, C. S. (2009). A review of marketing-operations interface models: From co-existence to coordination and collaboration. *SSRN Electronic Journal*. https://papers.ssrn.com/sol3/papers.cfm?abstract_id=1568947
- Todor, R. D. (2016). Marketing automation. *Transilvania University of Brasov. Economic Sciences, Series V*, 9(2), 87-94.
- Xu, Y., Yen, D. C., Lin, B., & Chou, D. C. (2002). Adopting customer relationship management technology, *Industrial Management: Data Systems*, 102(8), 442–452.
- Zokaei, K. & Hines, P. (2007). Achieving consumer focus in supply chains, *International Journal of Physical Distribution; Logistics Management*. 37(3), 223–247.

Author Information

Simone Franceschetto

Polytechnic University of Milan
Milano, Italy
Contact e-mail: simone.franceschetto@polimi.it

Roberto Cigolini

Polytechnic University of Milan
Milano, Italy

Lucio Lamberti

Polytechnic University of Milan
Milano, Italy

To cite this article:

Franceschetto, S., Cigolini, R., & Lamberti, L. (2023). Improving the supply chain - marketing interface, translating the voice of the customer into operational processes. *The Eurasia Proceedings of Science, Technology, Engineering & Mathematics (EPSTEM)*, 23, 471-484

The Eurasia Proceedings of Science, Technology, Engineering & Mathematics (EPSTEM), 2023

Volume 23, Pages 485-494

ICRETS 2023: International Conference on Research in Engineering, Technology and Science

ETF Markets' Prediction & Assets Management Platform Using Probabilistic Autoregressive Recurrent Networks

Waleed Mahmoud Soliman

University of Nottingham Malaysia

Zhiyuan Chen

University of Nottingham Malaysia

Colin Johnson

University of Nottingham UK

Hy-Alpha Sdn Bhd

Sabrina Wong

University of Nottingham Malaysia

Abstract: The significance of macroeconomic policy changes on ETF markets and financial markets cannot be disregarded. This study endeavors to predict the future trend of these markets by incorporating a group of selected economic indicators sourced from various ETF markets and utilizing probabilistic autoregressive recurrent networks (DeepAR). The choice of economic indicators was made based on the advice of a domain expert and the results of correlation estimation. These indicators were then divided into two categories: "US" indicators, which depict the impact of US policies such as the federal reserve fund rate and quantitative easing on the global markets, and "region-specific" indicators. The findings of the study indicate that the inclusion of "US" indicators enhances the prediction accuracy and that the DeepAR model outperforms the LSTM and GRU models. Furthermore, a web platform has been developed to apply the DeepAR models, which enables the user to predict the trend of an ETF ticker for the next 15 time-steps using the most recent data. The platform also possesses the capability to automatically generate fresh datasets from corresponding RESTful API sources in case the current data becomes outdated.

Keywords: Macroeconomic policy, ETF markets, Financial markets, DeepAR, Economic indicators, Machine learning

Introduction

An ETF, or exchange-traded fund, is a type of investment security that functions similarly to a mutual fund. It usually follows a specific index, industry, commodity, or set of assets (JAMES CHEN, 2022). For the standard retail or institutional investor, the process of buying and selling ETF shares is straightforward. The guidelines and procedures for trading ETFs are similar to those of the stock market. The shares are traded on the secondary market, just like stocks or closed-end funds, and not directly bought from the fund or resold to it. As they are traded like stocks, ETFs can be bought or sold at any point during the trading hours (Gastineau, 2001).

An ETF comprises several underlying assets, as opposed to a stock which holds only one. Due to the presence of multiple assets in an ETF, it is often favored for the purpose of diversification (JAMES CHEN, 2022). Conversely, changes in macroeconomic policies and announcements play a significant role in impacting the daily trading volumes of ETFs (Daniel Nadler & Anatoly Schmidt, 2015).

- This is an Open Access article distributed under the terms of the Creative Commons Attribution-Noncommercial 4.0 Unported License, permitting all non-commercial use, distribution, and reproduction in any medium, provided the original work is properly cited.

- Selection and peer-review under responsibility of the Organizing Committee of the Conference

© 2023 Published by ISRES Publishing: www.isres.org

In particular, macroeconomic policies of the United States, such as changes in the federal funds rate and market volatility, not only affect the ETF markets within the country but also have a ripple effect on other markets globally. For instance, fluctuations in the US market can lead to changes in other markets such as India, Russia, Mexico, and Turkey, and similar spillover effects are observed with European market volatility impacting markets in Mexico and South Korea (Yavas & Rezayat, 2016). This research aims to explore the influence of incorporating a distinct macroeconomic indicator on a selected group of ETF markets.

Related Work

In the realm of stock and ETF market prediction, multiple approaches have been explored, utilizing a variety of techniques (Z. Chen et al., 2021). One study (Liew & Mayster, 2018) assessed the performance of three commonly used machine learning algorithms (DNNs, RFs, and SVM) in predicting ETF returns. The authors introduced a gain measure to evaluate the efficacy of each algorithm and horizon, while segmenting the input feature variables into different information sets. Their results indicate that the most important predictive features vary depending on the ETF being predicted.

Another approach (Matsunaga et al., 2019) utilized a graph neural network structure, connecting companies through various relations such as supplier-customer, shareholder, and industry affiliations. This technique leverages the network structure to incorporate the interconnectivity of the market for more accurate stock price predictions, rather than relying solely on historical stock prices or hand-crafted features. The authors used a rolling window analysis method on 225 markets in Japan over roughly 20 years and found that the combination of knowledge graph data and graph neural networks holds strong potential for creating a more generalizable and practical stock market prediction mechanism compared to a baseline LSTM model.

A study (Nelson et al., 2017) utilized a large number of technical indicators to feed an LSTM neural network, along with data from different stocks from the Brazilian stock exchange. The authors employed a rolling window approach, generating a new neural network at the end of each trading day and using the most recent model to make predictions on the following day. The results were promising, with up to 55.9% accuracy in predicting if a particular stock price would increase in the near future.

Another LSTM-based method for stock returns prediction (K. Chen et al., 2015) was applied to the China stock market, transforming historical data into 30-day sequences with 10 learning features and 3-day earning rate labeling. Based on the earning rate, the sequences were categorized into seven ranges, with the aim of ensuring a comparable number of training sequences in each category. The study found that normalization improved accuracy and suggested that different stock sets may impact prediction accuracy, warranting separate predictions for different stock types.

A comparison between ARIMA, LSTM, and GRU for time series forecasting (Yamak et al., 2019) was conducted using one-day interval Bitcoin exchange rate data in American dollars from November 28th, 2014 to June 5th, 2019. The authors applied normalization, log transformation, and dealt with stationarity and seasonality in the dataset. The results showed that the ARIMA model had the best accuracy and time, though this outcome may be due to several factors such as the chosen parameters and the amount of data, which was relatively small for this study. The results also revealed that GRU performed better than LSTM, although RNN is typically more effective on larger datasets.

Dataset

The dataset in question pertains to 18 different ETF tickers, as listed in Table 1. These tickers are differentiated into different regions, including but not limited to "US", "EU", and "China". A comprehensive analysis of the dataset reveals that there are three distinct sets of features, each of which is assigned to the tickers based on their respective regions. These sets of features are:

Base Features: This category of features is present across all regions and encompasses common ticker attributes, such as "Open", "Close", "High", "Low", "Volume", and "Adjusted Price". The data for these features is obtained from the "Yahoo Finance" API.

US Features: This category encompasses a set of selected USA macroeconomic and monetary indicators, including but not limited to the Federal Reserve Fund Rate, Consumer Price Index, and Federal Reserve Total Assets.

These indicators have been selected on the basis of recommendations from domain experts and are included in all regions. This approach is based on the assumption that the US economy and its policies have a significant impact on all regions. The primary source of data for these features is the "Federal Reserve Economic Data" API.

Region-Specific Features: As the name implies, this category of features comprises region-specific macroeconomic and monetary indicators that have a potentially significant impact on the respective regions. To maintain consistency, the data for this category of features is obtained from the same source as that for the US Features, that is, the "Federal Reserve Economic Data" API.

A complete summary of the different features and the corresponding regions is provided in Appendix 1 terms "Base", "US", and "RS" represent the Base Features, US Features, and Region-Specific Features, respectively.

Given that the timeseries starting date for each feature varies between different features within the same ticker, it was deemed appropriate to utilize the most recent starting date among these features in order to avoid any data gaps within the features of a single ticker. Additionally, a standard scaling technique has been applied to each ticker individually, in order to maintain the data shape for that particular ticker.

Table 1. Summary of ETF tickers and associated features in the platform.

No.	Code	Name	Region
1	BND	Vanguard Total Bond Market Index Fund	US
2	CEMB	iShares J.P. Morgan EM Corporate Bond	Emerging Markets
3	EMXC	iShares MSCI Emerging Markets ex China	Emerging Markets ex. China
4	EWG	iShares MSCI Germany	Germany
5	EWH	iShares MSCI Hong Kong	Hong Kong
6	EWQ	iShares MSCI France	France
7	EWU	iShares MSCI United Kingdom	UK
8	FXI	Shares China Large-Cap	China
9	GLD	SPDR Gold Shares	US
10	GOVT	iShares U.S. Treasury Bond	US
11	IGOV	iShares International Treasury Bond	US
12	IVOO	Vanguard S&P Mid-Cap 400 Index Fund	US
13	JNK	SPDR Bloomberg High Yield Bond	US
14	VGK	Vanguard European Stock Index Fund	EU
15	VIOO	Vanguard S&P Small-Cap 600 Index Fund	US
16	SPY	SPDR S&P 500 ETF Trust	US
17	VOO	S&P 500 ETF	US
18	VWOB	Vanguard Emerging Markets Government Bond Index Fund	Emerging Markets

Methodology

During the implementation phase, three distinct models were evaluated with respect to the various tickers: Long Short-Term Memory (LSTM) networks, Gated Recurrent Unit (GRU) networks, and Probabilistic Autoregressive Recurrent Networks (DeepAR).

The Long Short-Term Memory (LSTM) network is a specialized type of Recurrent Neural Network (RNN) that was first introduced in 1997 by Hochreiter and Schmidhuber. LSTMs were specifically designed to overcome the problem of long-term dependencies that can occur in traditional RNNs. The ability to retain information over extended periods of time is a defining characteristic of LSTMs (Christopher Olah, 2015; Hochreiter & Schmidhuber, 1997).

The LSTM cell contains additional gates, specifically the input, forget, and output gates, which are utilized to determine which signals will be transmitted to the subsequent node. The current connection between the previous hidden layer and the current hidden layer is represented by the weight matrix W . Meanwhile, the weight matrix U connects the inputs to the hidden layer. The candidate hidden state, denoted as \tilde{C} , is computed based on the current input and the previous hidden state. The internal memory of the unit, referred to as C , is a combination of the previous memory, multiplied by the forget gate, and the newly calculated hidden state, multiplied

by the input gate. The behavior of all gates in the LSTM cell is described by the equations depicted in Figure 1 (Varsamopoulos et al., 2018). The activation of the forget gate enables the LSTM to determine, at each time step, which information should not be forgotten and to accordingly modify the model's parameters. Consequently, this addresses the vanishing gradients problem (Nir Arbel, 2018).

GRU was introduced in 2014 by Cho et al. as a streamlined alternative to the Long Short-Term Memory (LSTM) cell. Despite achieving comparable performance to LSTMs, GRUs are computationally more efficient and often faster to compute (Cho et al., 2014).

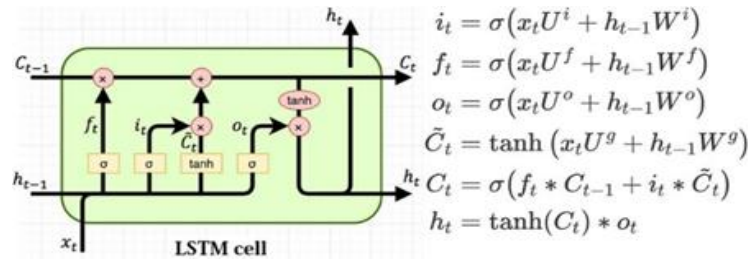


Figure 1. Diagram of the Structure and Mathematical Representation of an LSTM Cell

The GRU architecture consists of two gates, the reset gate and the update gate, which are used to control the flow of information from the previous hidden state to the current hidden state. The reset gate determines the extent to which the previous state should be remembered, while the update gate controls the proportion of the new state that is derived from the old state. These two gates are implemented as fully connected layers with a sigmoid activation function and their inputs are the current time step and the previous hidden state (Zhang Aston et al., 2022). Figure 2 provides a visual representation of the inputs and outputs of the reset and update gates in a GRU cell.

Finally, the DeepAR model differs from the previous two models LSTM and GRU, as they are deterministic models, while DeepAR is a probabilistic model. The latter may be more appropriate in the context of financial data, given its inherently uncertain nature. DeepAR proposes an RNN architecture for probabilistic forecasting, incorporating Gaussian likelihood for real-valued data and negative-binomial likelihood for positive count data, with special considerations for time series with widely varying magnitudes (Salinas et al., 2017).

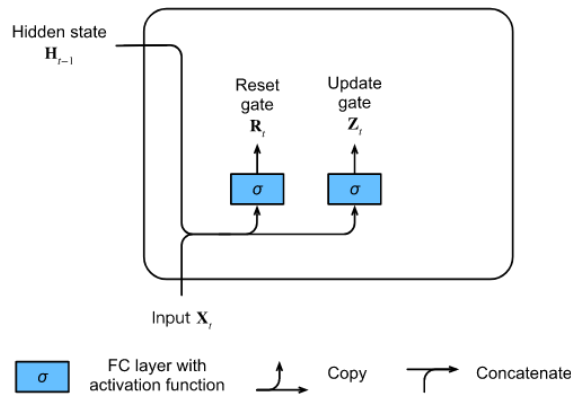


Figure 2. Structure and computation of the reset and update gates in a gated recurrent unit (GRU) model.

During the training process of DeepAR, as depicted in Figure 3, the network inputs at each time step t , include the covariates $x_{i,t}$, the target value at the previous time step $z_{i,t-1}$, and the previous network output $h_{i,t-1}$.

The network output:

$$h_{i,t} = h(h_{i,t-1}, z_{i,t-1}, x_{i,t}, \theta)$$

is then utilized to calculate the parameters $\theta_{i,t} = \theta(h_{i,t}, \theta)$ of the likelihood $\ell(z|\theta)$, which is used for training the model parameters. As for prediction, the history of the time series $z_{i,t}$ is fed in for $t < t_0$, then in

the prediction range for $t \geq t_0$ a sample $\hat{z}_{i,t} \sim \ell(\cdot | \theta_{i,t})$ is drawn and fed back for the next point until the end

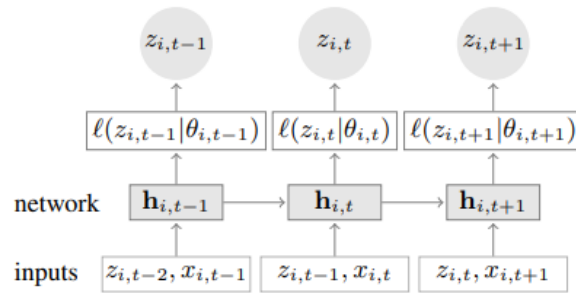


Figure 3. Mathematical operations in DeepAR during training.

of the prediction range $t = t_0 + T$ generating one sample trace. Repeating this prediction process yields many traces representing the joint predicted distribution (Salinas et al., 2017).

System Architecture

The platform functions predominantly through the utilization of Django, a highly regarded Python framework that offers robust authentication and authorization features. With access to the platform limited to registered users only, the framework ensures that all data is effectively stored and secured within a PostgreSQL database. The platform also incorporates an additional set of tables that are designed to allocate each Ticker with a specific set of features and to locate it within a designated country and region. It should be noted that these features can be assigned to multiple regions.

Users are provided with the ability to effortlessly update Ticker data and conduct predictions. Upon updating the Ticker data, a RESTful API call is automatically triggered to both the Yahoo and FRED APIs, thus facilitating the real-time compilation of the updated dataset. To guarantee the platform operates with optimal efficiency and reliability, a reverse proxy approach has been implemented through the utilization of the NGINX server. This approach ensures that user requests are first effectively handled by the NGINX server, and then passed efficiently to Django through Gunicorn as necessary, as demonstrated in **Hata! Başvuru kaynağı bulunamadı..**

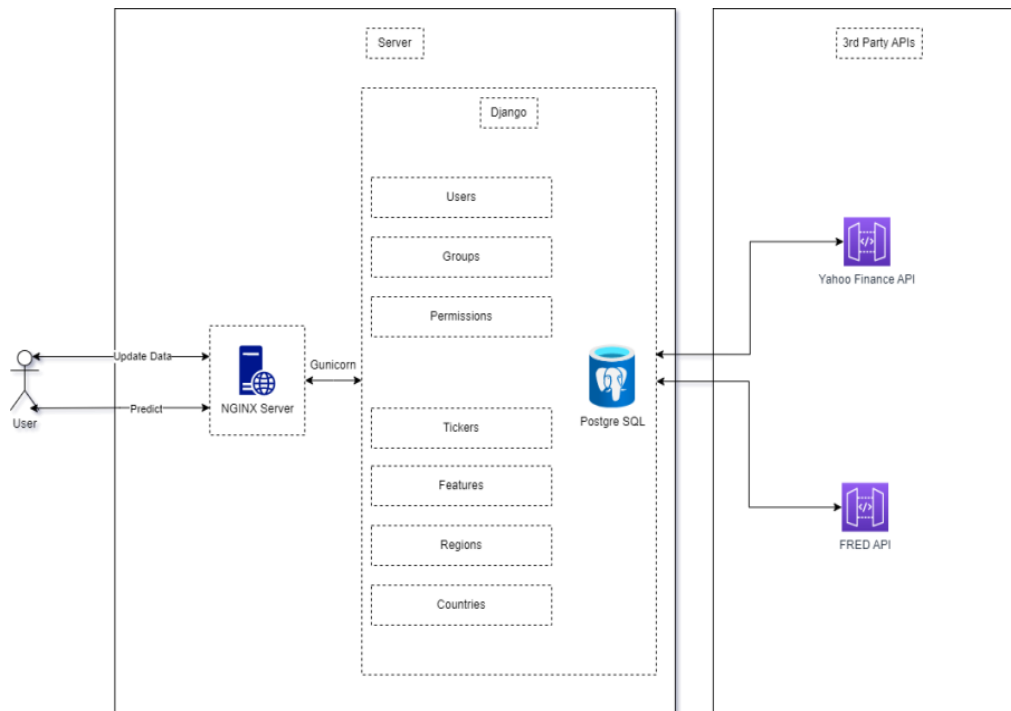


Figure 4. The architecture of the platform

Experiment

Prior to conducting experiments on the three models, several data preprocessing steps were undertaken. These included data standardization through the utilization of Standard Scaler and Min-Max Scaler and the calculation of a correlation matrix to identify and eliminate correlated features. Additionally, calculated features were added to the dataset, such as "3-Day Moving Average", "10-Day Moving Average", "Buy-Sell on Close", "Buy-Sell on Open", "Day of the Year", and "Month of the Year", with the aim of capturing additional trends in the data. Once the dataset was prepared, 20% was reserved for testing purposes and 80% was utilized for training. During the training phase, the sliding window technique was employed, with the model utilizing 30 time-steps for training and predicting the next 15 time-steps, as depicted in Figure 5.

The structure of the models utilized in this study comprised of a fully connected Recurrent Neural Network (RNN) structure with seven hidden layers and a ReLU activation function. During the training phase, the Adam optimization algorithm was utilized with a learning rate of 0.001 and a total of 700 epochs.

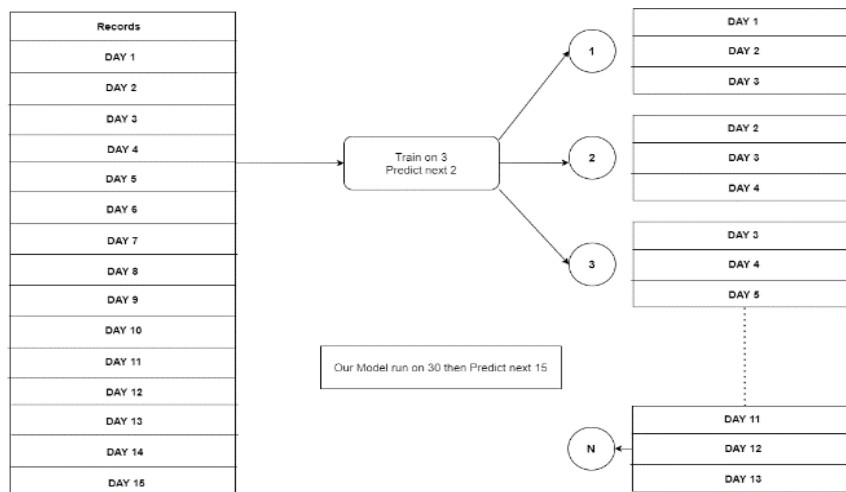


Figure 5. Sliding window training methodology for time-series predictions

Results

To ensure that the models could effectively predict future values without any data contamination, the predictions produced by the models were compared with a separate test dataset. The LSTM and GRU models are deterministic in nature, and as a result, they generated a single prediction for the predetermined time span. This is visually depicted in **Hata! Başvuru kaynağı bulunamadı.**, where the predicted values are represented in orange, and the actual values are shown in blue. Conversely, the DeepAR model is probabilistic, and therefore, it generated predictions with a 50% and 90% confidence interval, which are represented by light green and dark green in Figure 4, are compared against the actual values depicted in blue.

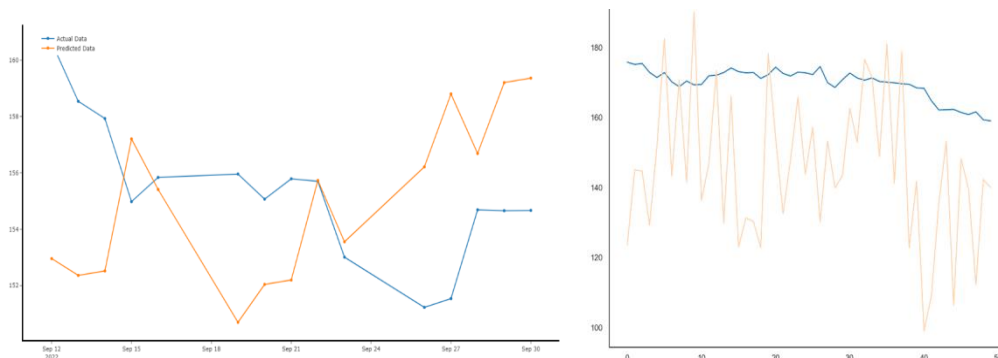


Figure 6. Comparative performance of LSTM (Left) and GRU (Right) models for ETF price prediction on GLD ticker.

In the present study, the Mean Absolute Percentage Error (MAPE) was utilized to assess the accuracy of the time-series models in comparison to actual values. MAPE is defined as the average absolute percent error of

each time period, calculated as the ratio of the absolute difference between actual and predicted values and the actual values(scikit-learn.org, n.d.). The mathematical expression for MAPE can be represented as follows:

$$MAPE(y, \hat{y}) = \frac{1}{n_{\text{samples}}} \sum_{i=0}^{n_{\text{samples}}-1} \frac{|y_i - \hat{y}_i|}{\max(\epsilon, |y_i|)}$$

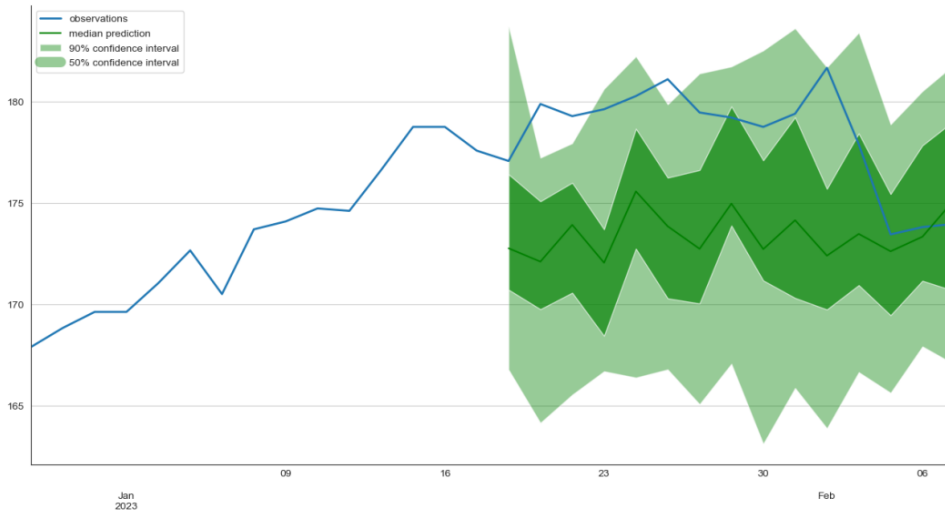


Figure 4. Assessment of DeepAR model for ETF price prediction on GLD ticker.

Additionally, the Root Mean Square Error (RMSE) was employed to evaluate the quality of the predictions. RMSE provides information on the deviation of the predictions from the true values, as determined through the Euclidean distance(C3 AI, 2022). The calculation of RMSE involves finding the square root of the mean square error, as described by the following equation(scikit-learn.org, 2022):

$$MSE(y, \hat{y}) = \frac{1}{n_{\text{samples}}} \sum_{i=0}^{n_{\text{samples}}-1} (y_i - \hat{y}_i)^2$$

Table 2 presents a comparison of the performance of the models: Long Short-Term LSTM, GRU, and DeepAR. The performance is measured by the above two metrics, MAPE and RMSE.

Table 2. Comparison of performance metrics for long short-term LSTM, GRU, and DeepAR models in ETF markets prediction.

Code	MAPE			RMSE		
	LSTM	GRU	DeepAR	LSTM	GRU	DeepAR
BND	0.063	0.054	0.044	6.43	5.10	3.45
CEMB	0.065	0.082	0.026	7.77	10.39	3.01
EMXC	0.046	0.092	0.034	8.19	12.17	4.78
EWG	0.075	0.099	0.069	5.86	9.63	5.09
EWH	0.055	0.066	0.011	9.51	11.24	6.12
EWQ	0.070	0.053	0.051	6.06	5.04	4.97
EWU	0.069	0.077	0.071	6.74	7.06	6.89
FXI	0.044	0.073	0.013	7.10	8.32	3.21
GLD	0.031	0.074	0.024	8.96	13.11	7.38
GOVT	0.088	0.087	0.036	9.14	8.97	5.64
IGOV	0.039	0.045	0.034	7.75	9.20	7.12
IVOO	0.084	0.087	0.075	4.87	5.83	4.29
JNK	0.056	0.064	0.058	5.02	6.41	5.81
VGK	0.057	0.100	0.030	8.23	12.58	6.04
VIOO	0.069	0.091	0.068	5.03	8.71	4.90
SPY	0.089	0.100	0.024	7.30	13.66	5.16
VOO	0.079	0.059	0.049	4.47	4.10	3.95
VWOB	0.040	0.099	0.039	8.87	11.84	7.65

The results indicate that, in general, the incorporation of macroeconomic features in time-series models leads to low MAPE values. The data demonstrates that DeepAR outperforms LSTM and GRU models, as it yields smaller MAPE values in almost all markets. For instance, in the BND market, DeepAR had a MAPE value of 0.044, while LSTM and GRU models recorded MAPE values of 0.063 and 0.054, respectively. In addition, the RMSE value of DeepAR in the BND market was 3.45, while LSTM and GRU models recorded RMSE values of 6.43 and 5.10, respectively.

Despite the superior performance of DeepAR compared to the other models, there is still room for improvement. In some markets, such as VWOB, the range of predicted values can be enhanced even further. To summarize, this comparison highlights the importance of including macroeconomic factors in time-series models and shows that the DeepAR model outperforms the LSTM and GRU models in terms of forecasting accuracy.

Conclusion

This study aimed to investigate the influence of macroeconomic policy changes on ETF markets and financial markets and predict their future trends. The study utilized a group of selected economic indicators sourced from various ETF markets and utilized probabilistic autoregressive recurrent networks (DeepAR) for prediction. The findings indicate that the inclusion of US indicators enhances the prediction accuracy and that the DeepAR model outperforms the LSTM and GRU models. Furthermore, the study developed a web platform, utilizing the Django framework and a PostgreSQL database, to apply the DeepAR models and predict the trend of an ETF ticker for the next 15 time-steps using the most recent data. The platform also possesses the capability to automatically generate fresh datasets from corresponding RESTful API sources. The results of this study contribute to a deeper understanding of the relationship between macroeconomic policy changes and ETF market trends and offer practical applications for financial forecasting.

Scientific Ethics Declaration

The authors declare that the scientific ethical and legal responsibility of this article published in EPSTEM journal belongs to the authors.

Acknowledgement

*This article was presented as a poster presentation at the International Conference on Research in Engineering, Technology and Science (www.icrets.net) held in Budapest/Hungary on July 06-09, 2023.

*The research presented in this paper was made possible through the support of a collaborative research program between Hy-Alpha Sdn Bhd and the University of Nottingham Malaysia Campus (Project NVHT0006).

References

- Arbel, N. (2018, December 21). *How LSTM networks solve the problem of vanishing gradients*. <https://medium.datadriveninvestor.com/how-do-lstm-networks-solve-the-problem-of-vanishing-gradients-a6784971a577>
- C3 AI. (2022). *Root Mean Square Error (RMSE)*. <https://c3.ai/glossary/data-science/root-mean-square-error-rmse/>
- Chen, J. (2022, October 22). *What is an exchange-traded fund (ETF)?* Investopedia. <https://www.investopedia.com/terms/e/etf.asp>
- Chen, K., Zhou, Y., & Dai, F. (2015). A LSTM-based method for stock returns prediction: A case study of China stock market. *Proceedings - 2015 IEEE International Conference on Big Data, IEEE Big Data 2015*, 2823–2824. <https://doi.org/10.1109/BigData.2015.7364089>
- Chen, Z., Soliman, W. M., Nazir, A., & Shorfuzzaman, M. (2021). Variational autoencoders and wasserstein generative adversarial networks for improving the anti-money laundering process. *IEEE Access*, 9, 83762–83785. <https://doi.org/10.1109/ACCESS.2021.3086359>
- Cho, K., van Merriënboer, B., Bahdanau, D., & Bengio, Y. (2014). *On the properties of neural machine translation: encoder-decoder approaches*. <http://arxiv.org/abs/1409.1259>

- Christopher, O. (2015, August 27). *Understanding LSTM networks*. <http://colah.github.io/posts/2015-08-Understanding-LSTMs/>
- Gastineau, G. (2001). *Exchange-traded funds: An introduction*. www.ijournals.com
- Hochreiter, S., & Schmidhuber, J. (1997). Long short-term memory. *Neural Computation*, 9(8), 1735–1780. <https://doi.org/10.1162/neco.1997.9.8.1735>
- Liew, J. K. S., & Mayster, B. (2018). Forecasting ETFs with machine learning algorithms. *Journal of Alternative Investments*, 20(3), 58–78. <https://doi.org/10.3905/jai.2018.20.3.058>
- Matsunaga, D., Suzumura, T., & Takahashi, T. (2019). *Exploring graph neural networks for stock market predictions with rolling window analysis*. <http://arxiv.org/abs/1909.10660>
- Nadler, D., & Schmidt, A. A. (2015). Impact of macroeconomic announcements on ETF trading volumes. *The Journal of Trading*, 10(3), 31-35.
- Nelson, D. M. Q., Pereira, A. C. M., & de Oliveira, R. A. (2017). Stock market's price movement prediction with LSTM neural networks. *Proceedings of the International Joint Conference on Neural Networks, 2017-May*, 1419–1426. <https://doi.org/10.1109/IJCNN.2017.7966019>
- Salinas, D., Flunkert, V., & Gasthaus, J. (2017). *DeepAR: Probabilistic forecasting with autoregressive recurrent networks*. <http://arxiv.org/abs/1704.04110>
- scikit-learn.org. (n.d.). *MAPE (Mean Absolute Percentage Error)*. Retrieved January 10, 2023, from https://scikit-learn.org/stable/modules/model_evaluation.html#mean-absolute-percentage-error
- scikit-learn.org. (2022). *Mean squared error*. https://scikit-learn.org/stable/modules/model_evaluation.html#mean-squared-error
- Varsamopoulos, S., Bertels, K., & Almudever, C. G. (2018). *Designing neural network based decoders for surface codes*. <https://www.researchgate.net/publication/329362532>
- Yamak, P. T., Yujian, L., & Gadosey, P. K. (2019). A comparison between ARIMA, LSTM, and GRU for time series forecasting. *ACM International Conference Proceeding Series*, 49–55. <https://doi.org/10.1145/3377713.3377722>
- Yavas, B. F., & Rezayat, F. (2016). Country ETF returns and volatility spillovers in emerging stock markets, Europe and USA. *International Journal of Emerging Markets*, 11(3), 419–437. <https://doi.org/10.1108/IJOEM-10-2014-0150>
- Zhang, A, Lipton, Z., Li, M., & Smola, A. (2022). *Dive into deep learning*. <https://d2l.ai/>

Appendix 1. Summary of macroeconomic indicators and their groups in the dataset

Code	Name	Group
Open	Open Price	Base
Close	Close Price	Base
High	High Price	Base
Low	Low Price	Base
Volume	ETF Volume	Base
Adj Close	Adjusted Close Price	Base
FEDFUNDS	Federal Reserve Fund Rate	US
CPALTT01USM661S	Consumer Price Index	US
DTWEXBGS	Nominal Broad U.S. Dollar Index	US
WALCL	Federal Reserve Total Assets (QE)	US
GDPIC1	Real Gross Domestic Product	US
DGS3MO	Market Yield on U.S. Treasury Securities at 3-Month Constant Maturity	US
EMVOVERALLEMV	Overall Equity Market Volatility Tracker	US
RBUSBIS	Real Broad Effective Exchange Rate	US
PAYEMS	Employment Level	US
IRLTLT01USM156N	Long-Term Government Bond Yields: 10-year	US
DGS2	Market Yield on U.S. Treasury Securities at 2-Year Constant Maturity	US
DGS10	Market Yield on Treasury Securities at 10-Year	US
DFII10	Market Yield on Treasury Securities at 10-Year - inflation	US
VIXCLS	CBOE Volatility Index	US

Code	Name	Group
EMVMACROINTEREST	Interest Rates Equity Market Volatility Tracker	US
EMVMACROBUS	Investment Sentiment Equity Market Volatility Tracker	US
NYGDPPCAPKDDEU	Germany Constant GDP per capita	RS
FPCPITOTLZGDEU	Germany Inflation, consumer prices	RS
RBDEBIS	Germany Real Broad Effective Exchange Rate	RS
IRLTLT01DEM156N	Germany Interest Rates: Long-Term Government Bond Yields: 10-Year	RS
LMUNRRTTDEM156S	Germany Registered Unemployment Rate	RS
NYGDPPCAPKDFRA	France Constant GDP per capita	RS
FPCPITOTLZGFRA	France Inflation, consumer prices	RS
RBFRBIS	France Real Broad Effective Exchange Rate	RS
IRLTLT01FRM156N	France Long-Term Government Bond Yields: 10-year	RS
LRHUTTTTFRM156S	France Harmonized Unemployment Rate: Total	RS
NYGDPPCAPKDGBR	UK Constant GDP per capita	RS
FPCPITOTLZGGBR	UK Inflation, consumer prices	RS
RBGBBIS	UK Real Broad Effective Exchange Rate	RS
IRLTLT01GBM156N	UK Long-Term Government Bond Yields: 10-year	RS
LMUNRRTTGBM156S	UK Registered Unemployment Rate	RS
NYGDPPCAPKDCHN	China Constant GDP per capita	RS
FPCPITOTLZGCHN	China Inflation, consumer prices	RS
RBCNBIS	China Real Broad Effective Exchange Rate	RS
SLEMPOTLSPZSCHN	China Employment to Population Ratio	RS
INTDSRCNM193N	China Interest Rates, Discount Rate	RS
NYGDPPCAPKDHKG	Hong Kong Constant GDP per capita	RS
FPCPITOTLZGHKG	Hong Kong Inflation, consumer prices	RS
RBHKBIS	Hong Kong Real Broad Effective Exchange Rate	RS
TDSAMRIAOGGHK	Hong Kong Amount Outstanding of Total Debt Securities in General Government Sector	RS
SLUEM1524ZSHKG	Hong Kong Youth Unemployment Rate	RS
CLVMEURSCAB1GQEU272020	EU Real Gross Domestic Product	RS
FPCPITOTLZGEUU	EU Inflation, consumer prices	RS
DEXUSEU	U.S. Dollars to Euro Spot Exchange Rate	RS

Author Information

Waleed Mahmoud Soliman

School of Computer Science, University of Nottingham Malaysia

Zhiyuan Chen

School of Computer Science, University of Nottingham Malaysia,
Contact e-mail: Zhiyuan.Chen@nottingham.edu.my

Colin Johnson

School of Computer Science, University of Nottingham UK

Sabrina Wong

School of Computer Science, University of Nottingham Malaysia

To cite this article:

Soliman, W.M., Chen, Z., Johnson, C. & Wong, S. (2023). ETF markets' prediction & assets management platform using probabilistic autoregressive recurrent networks. *The Eurasia Proceedings of Science, Technology, Engineering & Mathematics (EPSTEM)*, 23, 485-494.

The Eurasia Proceedings of Science, Technology, Engineering & Mathematics (EPSTEM), 2023

Volume 23, Pages 495-504

ICRETS 2023: International Conference on Research in Engineering, Technology and Science

Direct Labor Market Effects of Artificial Intelligence Assisted Applications Based on the Opinions of Illustrators and Company Managers: Hungarian Case Study

Szilard Berke
Óbuda University

Abstract: In the creative industry, the last six months have seen a remarkable and rapid change with the widespread availability of certain AI-based applications for the average user, such as the various Stable Diffusion image generators, the ControlNet that goes with them, and ChatGPT. In particular, the world of illustration, corporate design/design planning, translation, film production, copywriting, virtual education is all undergoing significant and irreversible change. In this article, we summarize what can be known about the impact of AI-assisted digital applications on the labour market for the illustration professionals. Based on exploratory research used in-depth interviews, opinions are markedly divided. Some see AI-assisted applications as a new opportunity, a rapid development of a hybrid toolkit to gain a competitive advantage. Others argue that they represent a threat to daily livelihoods and devalue hand-made creative work. According to business leaders, they can deliver significant cost savings without compromising on the level of quality expected, and on the contrary, they can enhance the user experience.

Keywords: Artificial intelligence, Ai painting, Digital illustration, Labour market, Competitiveness

Introduction

This year, programs such as DALL-E, Midjourney, Craiyon and other web solutions based on the Stable Diffusion model have become widely available worldwide (Goring et al., 2023). These programs are causing a major headache for illustrators and significantly changing the outlook for the industry. The digital revolution is still ongoing in the SME sector in Hungary (Tick et al, 2022; Saáry et al, 2022), and one of its aspects is the rapid spread of artificial intelligence-based applications. The vast majority of graphic designers work in the SME sector, and their income depends to a large extent on the needs of the client side. Graphic designers have a weak bargaining position in terms of wages. This could make them particularly vulnerable to the emergence of AI-based programs, which could further weaken their competitiveness. This sector is highlighted in our research because the rate of technological adoption is astonishingly fast.

The changes that have rippled through the industry have mainly been brought about by the dramatic shift in the way that AI assistive software has been made available to a wider audience in a web-based environment at the end of 2022. Such (not in all cases anymore) free or paid-based solutions include Midjourney, Playgroundai, Mage.space, Lexica.art, etc. There are significant differences between the tools in terms of the hardware background they require and the level of user skills needed to produce valuable results. The best known and clearly the market leader is Midjourney, which operates on Discord and has the largest number of registered users. Currently running version 5.1. which produces professional paintings using explicitly simple text commands. It requires no expert knowledge and can be run quickly and easily from an android smartphone as well. Its potential drawbacks are that it is not well suited to creating more complex compositions, and that it works with a specific, instantly recognisable colour style (mixing and overemphasis of ocean blue and yellow). Its advantage is that it has a high level of human anatomy, specifically in terms of hands and fingers. There is no

- This is an Open Access article distributed under the terms of the Creative Commons Attribution-Noncommercial 4.0 Unported License, permitting all non-commercial use, distribution, and reproduction in any medium, provided the original work is properly cited.

- Selection and peer-review under responsibility of the Organizing Committee of the Conference

© 2023 Published by ISRES Publishing: www.isres.org

official information about exactly what source code and AI architecture Midjourney uses (as it is private, with its own secured source code), but it is likely that it uses a different version of the latent diffusion model that powers Stable Diffusion, and adopts some elements of Stable Diffusion v2 (Ajaay, 2023).

The other groups of competing programs are those that are clearly based on Stable Diffusion versions 1.5 and/or 2.1, i.e. open source. Of course, these “brands” are also trying to develop their own modified source code (e.g. Playground V1), but mostly they try to differentiate their marketing by including different styles from CivitAi in their offerings (e.g. Duchaiten, RealisticVision v2, Deliberate, DreamShaper, LoRa). Probably the largest group of users running Midjourney, another larger group prefers the various web interfaces, while a third (presumably smallest) group uses the free SD versions available from GITHUB and installable on the computer. All styles are free to install from GITHUB, but web apps offer them as a part of a paid service.

The above ranking also shows the level of user intervention and the strong hardware background required to create a piece of art: Midjourney requires the lowest level of intervention and has low/average hardware requirements. Web-based services are more complex, more customisable and capable of creating more complex material, but require more user expertise and stronger hardware support. The installed version has the highest requirements in both respects (user skills and hardware environment).

Interestingly, the Web of Science database has about 6970 results (in 2023 at the end of July) for “AI + drawing”, 3600 publications available by searching for the keyword “AI + HR”, 538 for “AI + painting”, 81 for “AI + Stable Diffusion”, and 11 for “Midjourney”. In contrast, for example, 1,035,801 results are found for the term marketing. I believe that our research is completely novel, because there are very few studies on this topic, and they focus mainly on the creative process and the end result, rather than on the market impact (Sun et al., 2022; Koziol, 2023; Lyu et al., 2022; Goring et al., 2023; Ragot et al., 2020; Gu & Li, 2022). The available scientific articles on AI mainly analyse the marketing, HR or generic managerial aspect (Palos-Sánchez et al., 2022; Jia et al., 2018), especially logistics, education, knowledge transfer, financial markets, otherwise such as the workplace environment adoption, policy, recruiting, employer resilience, and industry examples such as military, law, geopolitics, cyber security and technological solutions in healthcare (Bencsik, 2021, 2022; Hwang et al., 2020; Lari et al., 2023; Aydin & Turan, 2023; Chen et al., 2020; Machová & Zsigmond, 2019, Dobos, & Csiszárík-Kocsir, 2022). The revolution in the creative industries is an extremely fresh and vibrant field, where, without exaggeration, there is an innovation almost every week.

Method

We used two internationally recognised methods of marketing research, the secondary and the primary methods. Secondary market research is the systematic collection, processing and analysis of existing social and economic statistical data according to the specific objectives and criteria of the researcher. Its importance lies in the fact that it provides a suitable starting point for the delineation of the area to be investigated and the definition of the decision problem. Primary market research is "original" data collection, as it collects information directly, through primary research, on the behaviour and opinions of market participants (Hair et al., 2009). Our ecoscopic studies have focused on understanding user behaviour in relation to the use of AI, and on mapping the domains in which it is used, focusing exclusively on creative industry applications. For the analyses, data were extracted from source works through targeted keyword searches on WOS, Scopus, Researchgate and Google Scholar. In the Hungarian context, we searched the results of mtmt.hu database and the Budapest Business Review for the last 5 years.

Primary market research can be divided into two broad categories, quantitative and qualitative qualitative research, according to the modern understanding of marketing. The basic aim of quantitative research is to be able to provide quantified answers to research questions with the highest possible reliability. Qualitative research, on the other hand, is “exploratory” in nature, seeking to understand the “whys” behind the actions of the user/user (Hair et al., 2009). Among the qualitative market research methods, the so-called semi-structured in-depth expert interview was used as the basis for this research. It was essential to get the views of stakeholders and industry decision-makers on the state of the domestic market.

The essence of in-depth interviews with experts via an online interface (combined with a semi-structured questionnaire and Facebook Messenger call) is that the researcher, based on his/her own experience and knowledge of the research objectives, determines the points and topics of the dialogue with the respondent that he/she wants to explore in more depth or that he/she wants to ignore. The interviews were conducted to get the opinion of recognised experts on the market conditions experienced in the industry.

We focused on the following issues and asked questions about them:

Which A.I.-based graphics software/tools do participants use in their graphics/illustration work?

How their work is influenced by the emergence of AI-based “text-to-image” applications?

What are the positive and negative impacts of these programs on the workplace?

A separate block of questions covered topics that target entrepreneurial competitiveness, such as:

- the impact on service quality,
- changes in the frequency of orders,
- the amount paid for illustration,
- copyrights,
- the workflow design phase,
- the role of product development,
- the issue of time savings,
- the area of comparison with traditional techniques.

The questions for company managers differed from the questions for illustrators, but the topics were the same, with the addition of the following two topics: cost efficiency and possibility to broaden the product range. In the pilot research, we asked illustrators and creative industry executives what they think about AI-assisted programs. The research was conducted via an online interface using semi-structured interviews with Google Forms and Messenger calls. 11 illustrators and 5 business leaders responded. The interview questions were composed after reviewing relevant literatures and also based on the author's own experience.

Three quarters of the respondents have been working as illustrators for more than 15 years (Figure 1). Half of the illustrators are full-time professional artists, a third are hobby artists, and two are part-time freelancers who supplement their income with drawing. Three quarters of respondents make digital paintings. They were the authors who contributed to the publication of their names: Gabor Szikszai, Gyula Pozsgay, Gergely Buttinger, Péter Tikos, Gergely Nagy, Norbert Birgány, Norbert Vakulya.

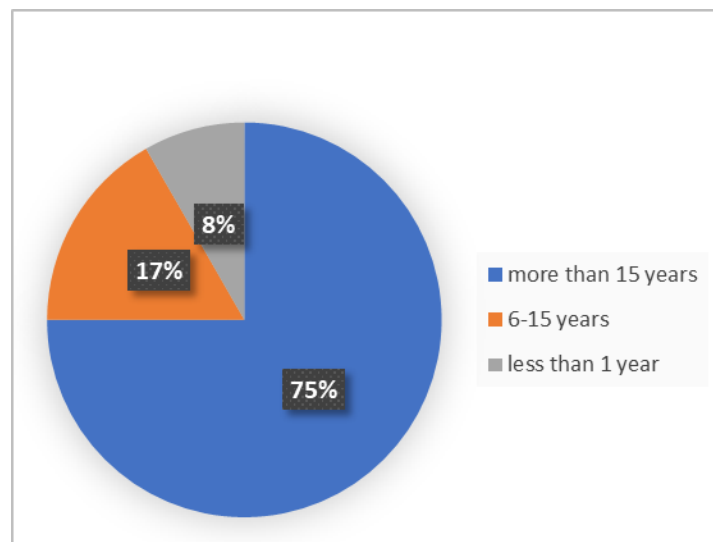


Figure 1. Working time in the industry in years (n=11)

Results and Discussion

Analysis of Illustrators' Opinions

The first question was “Which A.I.-based graphics software/tools do participants use in their illustration work?” Those who use these solutions mentioned SD installed from Github, PS Firefly, Ps Neural Filters, PS Upscaler (Lightroom), Devaiart Dreamup, PS Beta AI, other web interfaces. Users mentioned that, e.g.:

- Midjourney never generated what the designer wanted to see as the end result

- one said, “At the moment, I only do illustrations for US clients who have asked me not to use AI-generated images, bases or references.”
- and another said, “I don't use it, on the one hand I think it takes away the joy of the creative process to get something so ready-made (it's like cooking a bag of soup or heating a pizza), and on the other hand it's stealing and exploiting artists.”

To “What extent does the emergence of AI-based “text-to-image” applications (e.g. Midjourney, Stable Diffusion - installed or web app) influence your personal work as an illustrator?” we received these answers, summarized in Figure 2.

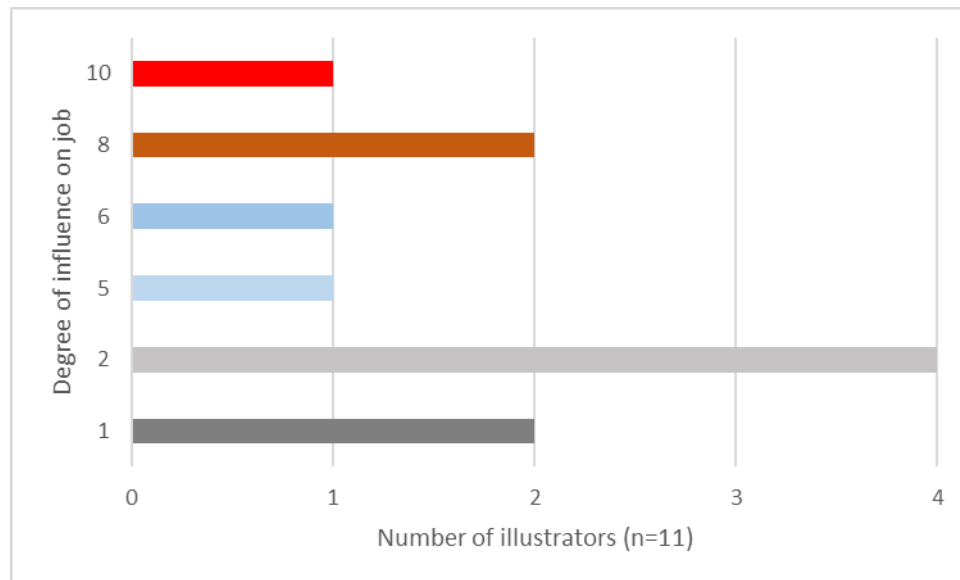


Figure 2. What extent does the emergence of AI-based "text-to-image" applications influence your personal work as an illustrator? (n=11)

More than half of the respondents do not use any of the programs, but they are also following changes in the industry. The same proportion say that their work is minimally or not at all influenced by the revolution in the creative industry - they are all senior illustrators. Among the younger generation, there is a palpable fear and resistance, a rejection of AI-based text-to-image solutions. One of them said, “I don't use it because I think it's the death of art”. There is a lot of misunderstanding and miscommunication, as some of the participants involved point out (VerevolfGD, 2023; Rajnerowicz, 2022).

In the following we ask, what are the positive and negative impacts of these programs on the workplace? Six or seven out of 11 artists said that using these solutions is a good idea at the initial stage: in the design, in pre-concepts, in sketches, or just as inspiration, to test the use of colour, or to develop different versions. Opponents say that it has no positive impact, that it is a “thieving technology”, market-distorting, harmful, and that it is killing the industry.

These were mentioned among the positive impacts in details:

- in retouching
- in idea-generation
- “Helps with reference, sketching, brainstorming, experimenting with variations. Can be useful for generating background behind certain content where precise details are not important. E.g. for a presentation.” Or as another of them put it:
- “They greatly help the workflow and can be used to create creative works of art by people who have only dreamed about it before.” And one who also works as an editor:
- “I've used it to complete 1-1 pictures when there wasn't enough runway for the picture.”

To pick out a few typical negative comments and dilemmas arose at the mention of negative impacts:

- “A lot of graphic design work can be outsourced to AI-based programs by clients, so many illustrators could lose orders.” Or:

- “It kills the joy of playing with compositions and sketching, the end result is soulless.”
- “It is unsuitable for individual illustrations and its legal background is questionable.”
- “It is easy for lay people to believe - as many did before the rise of AI - that the computer will produce the graphics on its own and therefore undervalue the work of the graphic designer.”
- “It’s a net thief technology. It institutionalises it and allows it and even relies on it.”
- “It has only negative effects, and anyone who is even tangentially informed on the subject can list them all. It has taken me 10 years in this profession (illustrator) to get to this point, and I can already feel that this is as far as it has come. In 2-3, maybe 5 years at the most, there will be maybe a dozen illustrators working in Hungary, those who have already managed to “break into” the industry (game development, film studios, matte painting, etc.), the rest will disappear into the background, along with me. For me, it is inconceivable that there are people in the industry who are happy with these tools.”
- “It is unsuitable for individual illustrations, in my opinion, and its legal basis is questionable.”
- “It can be frustrating, it can make you more inclined to build on AI foundations instead of your own solutions.”
- “Copyright infringement. Competing the AI generated image as a full-fledged work with other hand-made digital works.”
- “A lot of graphic design work can be replaced by AI-based programs by clients, so many illustrators could lose orders.”
- “It kills the joy of playing with compositions and sketching, the end result is soulless. These programs take away the work of illustrators because there is less and less demand for “expensive artists” when there is “cheap AI”. Which is understandable, obviously, but “paints” a very sad picture of the future.”
- “It’s already clear that publishers have taken the plunge, they will save money on artists, they don’t need to hire as many if they’re going to have AI doing a lot of the work. But in the same way, individuals will also use the services of artists less, which is typical in role-playing circles, for example, where people who might have had their character drawn by a graphic artist might now be happy with a machine solution.”
- There were also some less strident comments: “Copyright needs to be clarified as soon as possible. Nevertheless, I think such programs are similar to, for example, the SPSS statistical program. Without the human factor, they cannot create independent works.”
- “My fear is that it will take away a lot of work from the skilled artists who have been making a living from it. I can reconcile myself to this if graphic designers can use them as a supplement and their work is made easier, rather than the AI working for the graphic designer.”

Looking deeper into the industry and self-competitiveness, the following main findings can be made: overall, there is no deep fear of receiving fewer orders because of the emergence of low-cost “competitors” trying to use AI in the market. Only three people agree with the statement “Since Midjourney and SD, clients want to pay less for my work”.

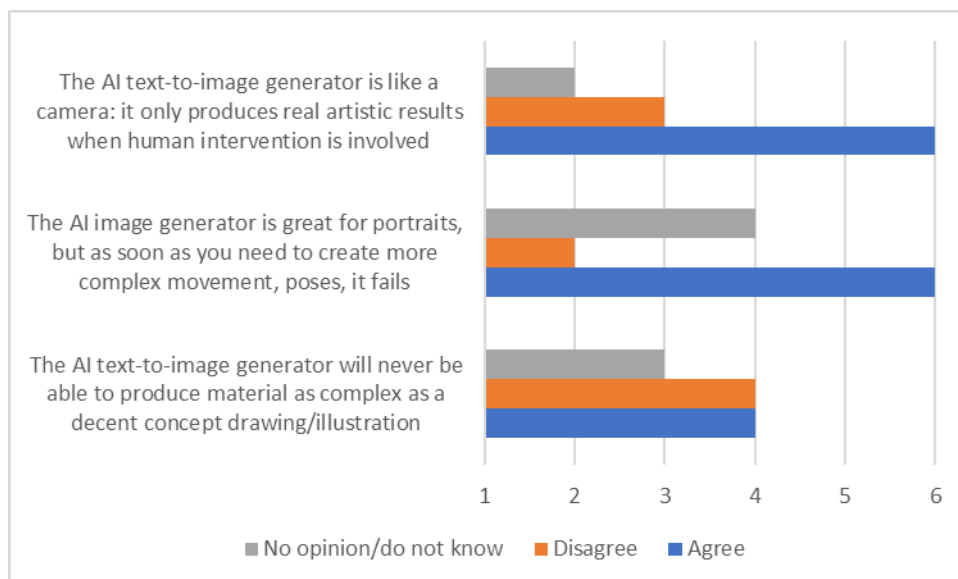


Figure 3. Capabilities and quality of AI-based "text-to-image" applications as judged by the illustrators (n=11)

One half of the respondents to the survey said that the AI text-to-image generator will never be able to produce complex material such as a good concept drawing/illustration. The other half of the group is not sure about this at the same time, because they see a potential in AI. This is reinforced by the fact that AI is great for portraits, but as soon as you need to do more complex movement and poses, it fails, said the vast majority. Many shared the view that “AI text-to-image generator is like a camera: it only produces real artistic results when human intervention is involved.” On the negative side, it has been mentioned that such work is often soulless, in the category of visual kitsch. The Figure 3 summarizes the main findings about the capabilities.

The use of the AI text-to-image generator is a violation of copyright, according to the overwhelming majority of illustrators involved (Figure 4). It's not a very creative idea to exclude traditional (hand-drawn) and digital illustrations from the learning phase of AI. Some people would think that if we ban them, they should no longer be thought of as a competitor, because their capabilities are dramatically reduced. This is not the case according to illustrators, the situation is more complex, the “genie is out of the bottle”. Illustrators uniformly feel that it is a bad idea to feed their work into the learning phase of AI, as they did in the first phase of development (see the case of Greg Rutkowski, Mayor, 2023). They do not believe that they can get royalties for their work because it is used by the image generator. They believe that this situation is unresolved, and that there is a violation of the rights of creators whose work is unauthorizedly exploited by deep learning systems.

On the question of whether the author of illustrations created with an AI text-to-image generator should also be entitled to copyright, there was no consensus: some said yes, he/she should, others said no, he/she should not. What will happen is similar to what happened with music or movie sharing sites: they will find a way to make illustrators get royalties if someone uses their work in such applications, some say, but just as many believe the opposite, that is, the situation will escalate.

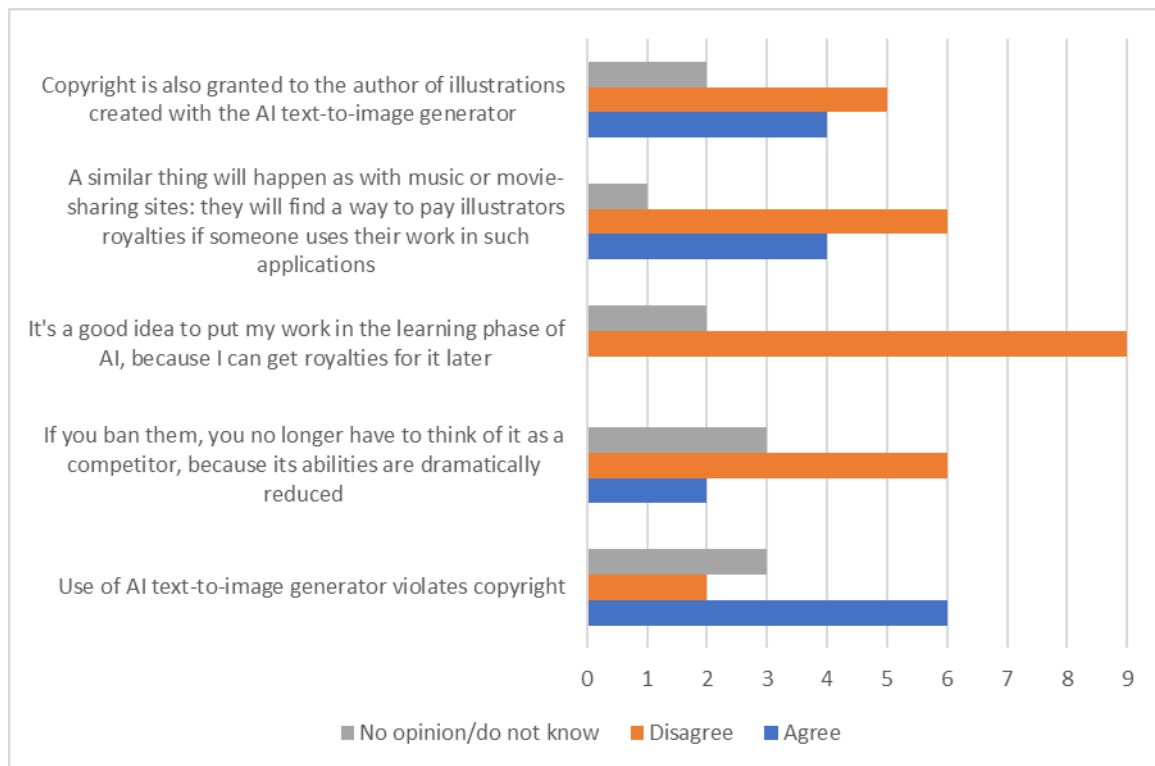


Figure 4. The treatment of copyright as perceived by illustrators (n=11)

On the positive side, the use of AI-based graphics solutions can increase the competitiveness of illustrators, mainly by saving them time. “My job is easier because AI helps me with certain parts of the process,” we asked, and the responses showed that the vast majority agreed with this statement. Turning to the potential benefits respondents were divided on the question “my work has become more valuable because hand-drawn illustrations are now considered more unique” (Figure 5). Some agreed, just as many disagreed. Surprisingly, it seems that professionals are still open to the future of using such applications. They said that although they see value in traditional things, and many people only paint traditionally, by hand, they may still give technology a chance in time. Everyone agreed without exception that the launch of the AI text-to-image generator is a milestone for the industry.

Analysis of CEOs`, decision makers' opinions

Turning to the views of the other target group, most of the senior managers and CEOs` (80%) surveyed have been working in the creative industry for more than 15 years, typically in publishing, game development and games publishing (with board games, card games, role-playing games, internet games portfolio). Some of them hire freelancers and are self-employed, others are senior managers in companies employing 2-25 people. The company managers replied that their company has the following A.I.-based programs: graphics programs, translator, educational program, marketing decision support analysis program.

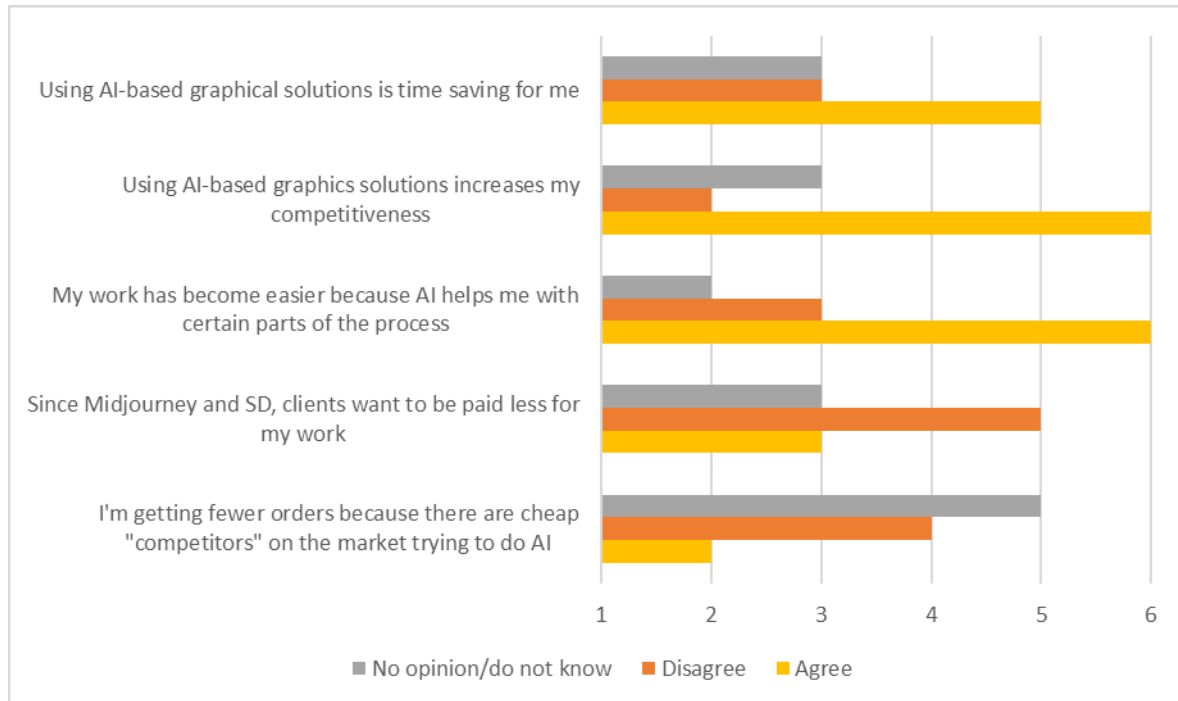


Figure 5. What extent does the emergence of AI-based "text-to-image" applications influence your personal work as an illustrator? (n=11)

When we asked about the positive benefits of A.I. based programs, the following answers were given by them:

- “Cheaper than using a human graphic designer, generates versions faster”,
- “Much faster in time”,
- “Illustrations are much more detailed and grants more variability”,
- “The advantage is that it is faster and cheaper to draw good or at least acceptable images”,
- “It expands creativity, it makes art accessible to everyone”,
- “It is affordable”.

In the context of negative effects, it has been claimed that:

- “There are ethical concerns about AI sourcing, unclear copyright, potential for fraud, visual kitsch”,
- “I think that the only negative impact is on graphic designers, but even there it is more likely to be on those with poorer abilities in drawing”,
- “Personally I like AI images less because they lack uniqueness”,
- “Human creativity is not 100% stimulated”,
- “Soulless”.

Their comments suggest that the emergence and diffusion of AI-based text-to-image generators save money because they will pay less for products made using this process. Overall, they believe that the final quality of the illustration paid for will be improved by such programs. There are significant time savings in choosing this solution because orders are completed more quickly. It also helps them to get a more varied content because they can choose from a wider range of pro-versions.

For many, their openness to these solutions is due to necessity: they need somewhere to save money in today's difficult market situation. Most executives believe that AI-based solutions could eventually drive some creative professions out of the market altogether. They said that it is a good thing that such a program exists, because it allows them to support more people, to commission more work.

However, they were divided on how impressive these programs are. Some think they are a must if you want to keep up with the times, others disagree. There was a statement that “this process will not be sustainable: the copyright problems will drive this phenomenon out of the market”. However, the vast majority of the business leaders interviewed believed that they would be a persistent feature among users.

To the question “To what extent does the emergence of AI-based "text-to-image" applications (Midjourney, Stable Diffusion) influence the performance of your business?" The answers were very different, a typical attitude was:

- “It doesn't make us more successful primarily in a financial sense, it just saves a lot of time and energy and avoids a lot of annoyance and compromise.”
- “We don't have many graphic designers working with them at the moment, and we don't want to go all the way, because the images lose their uniqueness.”
- “Graphic designers are not reliable, so it can be easier to work with them”.

In the Table 1 below, we have summarised which factors are the positive benefits of AI-based technology and which are the concerns about its use, based on the opinions of illustrators and business decision-makers.

Positive benefits of the AI-based "text-to-image" technology	Negative benefits of the AI-based "text-to-image" technology
Illustrators` opinions	
accelerates processes	killing art and the profession
supports brainstorming, planning and the development of different variations	takes the joy out of the creative process and the end result is soulless
allows you to quickly generate backgrounds, whether for presentations or illustrations	it's all about theft and exploitation of artists - thieving technology
excellent for inspiration	thieving technology and infringes copyright
useful for developing pre-concepts and sketches	has a market distorting effect
base-mesh (3D) modelling	no positive impact at all
non-artists can create with it	undervalues graphic design work (the computer does everything)
enhancing bad photos	unsuitable for creating a unique illustration
retouching	its legal background is unclear
colour grading	cheap, takes work away from graphic designers
Senior managers` opinions	
cheap, more work can be offered to more creators	raises ethical concerns about AI sourcing
get results much faster	copyright is unclear
more variability, more customisation	its use also opens the door to fraud
art becomes accessible to all	visual kitsch
saves a lot of time and energy	the end result is soulless
avoids a lot of frustration and compromise	human creativity is not fully exploited
	there is no uniqueness in such illustrations

It confirmed that the creative industry, and in particular the world of illustrators, is undergoing major, revolutionary changes. The perception of such programs is very divided, with stakeholders seeing them as both a source of danger and a new opportunity. The perception is varied among different generations, with young people more critical and fearful. For businesses, they provide significant cost savings. They are very useful at the design phase and can also achieve a higher level of customization, which is the basis and main objective of marketing orientation. The drawback is that these illustrations are basically soulless and not so unique, which may be due to the rudimentary level of facial mimicry or to the obstacles to the realisation of a unique drawing style (lack of clarity of copyright or difficulty in creating a good prototype).

In sum, all company managers agreed that using an AI-assisted program is cheaper than using only a “human graphic designer”, generates versions faster and provides more variability, thus allowing for more customisation.

It is likely that the situation will not be resolved soon, especially as uniform legislation will be a long time coming. An interesting market observation is that in Hungary, some clients request that the final illustration should differ by at least 15% from what the program generates based on the prompt. If this is met, the illustration is considered to be legally the product of the graphic designer. It is likely that the situation will not be resolved soon, especially as uniform legislation will be a long time coming. An interesting market observation is that in Hungary, some clients request that the final illustration should differ by at least 15% from what the program generates based on the prompt. If this is met, the illustration is considered to be legally the product of the graphic designer. Our expectation is that this technology will quickly spread among graphic designers, with initial pushback based on the theory of innovation adoption. And there will be other creators on the market who are not professional artists but who could be serious competitors. They will be a kind of “hybrid” of prompt engineer and digital illustrator. Overall, opinions suggest that some graphic designers may indeed be squeezed out of the labour market, as the customer side is clearly positive about the technology because of its low cost and diverse capabilities. At the same time, the technology offers an opportunity for a new group of “aintrepreneurs” to generate revenue and compete with professional artists. However, it is a fact that brush-drawing artist robots are already being developed, perhaps as a next step in the innovation process (Karimov et al, 2023). Following the pilot research, the next step will be to launch a large-scale national survey to explore attitudes and the potential advantages and disadvantages of the application through a quantitative process.

Scientific Ethics Declaration

The author declares that the scientific ethical and legal responsibility of this article published in EPSTEM journal belongs to the author.

Acknowledgements or Notes

This article was presented as an oral/poster presentation at the International Conference on Research in Engineering, Technology and Science (www.icrets.net) held in Budapest/Hungary on July 06-09, 2023.

References

- Ajaay (2023). Does midjourney use stable diffusion? <https://nerdschalk.com/author/ajaay/>
- Aydin, E., & Turan, M. (2023). An AI-based shortlisting model for sustainability of human resource management. *Sustainability*, 15, 2737. <https://doi.org/10.3390/su15032737>
- Bencsik A. (2021). The sixth generation of knowledge management – the headway of artificial intelligence. *Journal of International Studies*, 14 (2), 84-101. <https://doi.org/10.14254/2071-8330.2021/14-2/6>
- Bencsik A. (2022.) Artificial intelligence in the middle east European countries, in: Munoz, J. Mark; Maurya, Alka (szerk.) *International Perspectives on Artificial Intelligence*. London, Anthem Press, 138 p. pp. 52-62., <https://doi.org/10.2307/j.ctv270kv9x>
- Chen L., Chen P., & Lin Z. (2020). Artificial intelligence in education: A review. *IEEE Access*, 2020(8),75264-75278, <https://doi.org/10.1109/ACCESS.2020.2988510>
- Dobos, O.,& Csiszárík-Kocsir, A. (2022). The role of project management in cyber warfare with the support of artificial intelligence. *The Eurasia Proceedings of Science Technology Engineering and Mathematics*, 17, pp. 26-37., <https://doi.org/10.55549/epstem.1175898>
- Goring, S., Rao, RRR., Merten, R., & Raake, A. (2023). Analysis of appeal for realistic AI-generated photos. *IEEE Access*, 11, 38999-39012, <https://doi.org/10.1109/ACCESS.2023.3267968>
- Gu, L.,& Li, Y. (2022) Who made the paintings: Artists or artificial intelligence? The effects of identity on liking and purchase intention. *Frontiers in Psychology*, 13: 941163, <https://doi.org/10.3389/fpsyg.2022.941163>
- Hair, J.F., Bush, R.P. & Ortinau, D.J. (2009). *Marketing research: In a digital information environment*. 4th Edition, McGraw-Hill Higher Education, Cape Town, 690.
- Hwang, G-J., Xie, H., Wah, B.W., & Gašević, D. (2020). Vision, challenges, roles and research issues of artificial intelligence in education. *Computers and Education: Artificial Intelligence*, 1, 100001, <https://doi.org/10.1016/j.caeai.2020.100001>
- Jia Q., Guo Y., Li R., Li Y.R., & Chen Y.W. (2018). A conceptual artificial intelligence application framework in human resource management. In Proceedings of *The 18th International Conference on Electronic Business* (pp. 106-114). ICEB, Guilin, China, December 2-6.

- Karimov, A., Kopets, E., Leonov, S., Scalera, L., & Butusov, D. (2023). A robot for artistic painting in authentic colors. *Journal of Intelligent & Robotic Systems*, 107(3), 34, <https://doi.org/10.1007/s10846-023-01831-4>
- Koziol, M. (2023). 5 questions for Anton Troynikov: His company's creation identifies the art behind AI-generated images. *IEEE Spectrum*, 60(5), 23, <https://doi.org/10.1109/MSPEC.2023.10120687>
- Lari, H.A., Vaishnav, K., Manu K.S., (2022). Artificial intelligence in E-commerce: Applications, implications and challenges. *Asian Journal of Management*, 13(3), <https://doi.org/10.52711/2321-5763.2022.00041>
- Lyu, YR., Wang, XX., Lin, RT., & Wu, J. (2022). Communication in human-AI co-creation: Perceptual analysis of paintings generated by text-to-image system. *Applied Sciences*, 12(22), 11312, <https://doi.org/10.3390/app122211312>
- Machová, R., & Zsigmond, T. (2019). The connection between knowledge organization and artificial intelligence. In: *Helena, Majdúchová Aktuálne problémy podnikovej sféry: Zborník vedeckých prác z medzinárodnej vedeckej konferencie*, Bratislava, Ekonóm, 452 p. pp. 297-303.
- Mayor, L. (2023) AI: *Digital artist's work copied more times than Picasso*. BBC News, 2023.07.20., <https://www.bbc.com/news/uk-wales-66099850>
- Palos-Sánchez, P. R., Baena-Luna, P., Badicu, A., & Infante-Moro, J. C. (2022). Artificial intelligence and human resources management: A bibliometric analysis. *Applied Artificial Intelligence*, 36(1), 2145631.
- Ragot, M., Martin, N., Cojean, S. (2020). AI-generated vs. human artworks. *A Perception Bias Towards Artificial Intelligence? CHI 2020*, April 25–30, 2020, Honolulu, HI, USA, pp 1-10., <https://doi.org/10.1145/3334480.3382892>
- Rajnerowicz K. (2022). Will AI Take Your Job? *Fear of AI and AI Trends for 2023*. <https://www.tidio.com/blog/ai-trends/>
- Saáry, R., Tick, A., Judit, Kárpáti-Daróczi, J. (2022). Digitalisation in hungarian SMEs technology or culture? In: Milan, Trumić (szerk.) *Possibilities and barriers for Industry 4.0 implementation in SMEs in V4 countries and Serbia*. Bor, Serbia: University of Belgrade, Technical Faculty in Bor (2022), 510 p. pp. 207-230.
- Sun Y., Yang, C-H., Lyu, Y., Lin, R. (2022). From Pigments to Pixels: A Comparison of Human and AI Painting. *Applied Sciences*, 12, 3724. <https://doi.org/10.3390/app12083724>
- Tick, A., Saáry, R., & Kárpáti-Daróczi, J. (2022). Conscious or indifferent - concerns on digitalisation and sustainability among SMEs in Industry 4.0. *Serbian Journal of Management* 17(1), 145-160.
- VerevolfgD (2023). *The misunderstanding of AI art*. <https://www.deviantart.com/verevolfgd/journal/The-Misunderstanding-of-AI-Art-948728694>

Author Information

Szilárd Berke

Óbuda University
1084 Budapest, Tavaszmező str. 17.
Hungary
Contact e-mail: berke.szilard@uni-obuda.hu

To cite this article:

Berke, S. (2023). Direct labor market effects of artificial intelligence assisted applications based on the opinions of illustrators and company managers - Hungarian case study. *The Eurasia Proceedings of Science, Technology, Engineering & Mathematics (EPSTEM)*, 23, 495-504.

The Eurasia Proceedings of Science, Technology, Engineering & Mathematics (EPSTEM), 2023

Volume 23, Pages 505-512

ICRETS 2023: International Conference on Research in Engineering, Technology and Science

The Role of Public Transport in Transport Safety and Public Safety

Diana Henezi

Széchenyi István University

Agoston Winkler

Széchenyi István University

Abstract: Public transport has a significant role in sustainable urban transport including the reduction of congestion, noise and air pollution. The main purpose of this paper is to present other important impacts of public transport i.e., the improvement of transport safety and public safety, too. Public transport is one of the safest transport modes according to the indication numbers in traffic accident and injuries. This phenomenon is illustrated through literature research as well as statistical data. Further opportunities are presented with a case study based on the transport system of the city of Győr, especially the positive impacts of the possible expansion of night public transport services. The severity of traffic accidents at nights is significant, and the enhancement of public safety is outstanding. Marketing is one of the most important tools for attitude formation, the paper contains some suggestions in this regard as well as in order to promote the goals above.

Keywords: Public safety, Public transport, Traffic safety, Sustainable mobility

Introduction

Transport as a process does not create value, the user (may it be the driver, the person passing by or the passenger) realizes their goal through transport. This is what we call derived trait. Travel happens when the end result creates a higher value than the costs (including monetary and time spent). It is evident, that commuting to work and school is an everyday activity that carries this value (Kharola et al., 2010). Despite that, traffic-related accidents are one of the top leading causes of death in the EU and in Hungary. As transport is an integral part of everyday life, road safety is an important interest of society.

Each year in Hungary more than 20 000 people get injured in traffic accidents and out of that around 500-600 people lose their lives. The number of severe injuries is around 5000, and more than 14 000 people suffer less-serious injuries. These numbers are not just part of the statistics as these accidents have a direct effect on society as an accident or injury can change a family's life, it affects the healthcare sector, and has an effect on other transport participants when it comes to congestion and lost time caused by the accidents. Around 90% of traffic accidents are caused by human error, but we should not overlook the fact that infrastructure (road and its surroundings), and mechanical issues can also contribute to their occurrence.

If we examine indicators and mileage, it can be concluded, that in most cases the vehicle is at fault. If we consider the severity of injuries, unprotected participants such as motorcyclists, cyclists and pedestrians are highly endangered. The severity of injuries depends on various factors including age, physical fitness, and condition. A directive from the EU states that road accident fatalities and serious injuries should be reduced by 50% until 2030. Moreover, there is a „Zero Vision” goal for 2050 meaning that no one should lose their lives in a traffic accident. In order to reduce the number of accidents we can utilize and introduce a range of tools and activities. We can approach this goal from various perspectives:

- This is an Open Access article distributed under the terms of the Creative Commons Attribution-Noncommercial 4.0 Unported License, permitting all non-commercial use, distribution, and reproduction in any medium, provided the original work is properly cited.

- Selection and peer-review under responsibility of the Organizing Committee of the Conference

- infrastructure: building self-explanatory roads, inspecting existing roads, creating forgiving roads
- authorities: increasing the number of police inspections = higher probability of in flagrante delicto
- people: improving education
- other instruments: promoting public transport (with continuous marketing activity), campaigns (European Mobility Week, The Day of Transport Culture, raising awareness in kindergartens, schools, and workplaces).

The Role and Advantages of Public Transport

The main function of public transport is to offer transport possibilities to people who are not able to use other transport modes (personal vehicle, bicycle, etc.). Reasons could be:

- their age limits their driving capabilities
- they are not able to afford a personal vehicle
- they are not able to drive due to medical reasons.

Apart from this, public transport should offer such possibilities where individuals who do have personal vehicles choose public transport instead. This can be achieved with push & pull (stick & carrot) methods (e.g., creating bus lanes, dynamic timetables, wide network connections). However, we should not forget, that there will always be social groups who will choose their personal vehicle regardless (Nævestad et al., 2022). Compared to individual transport, public transport has several advantages.

Even with 50% occupancy, buses use approximately five times less energy per passenger kilometer than cars. With public transport modes, urban air pollution could be four to eight times less per passenger compared to personal vehicles. The most significant advantage of public transport is connected to space occupancy: buses take up only 5% of space per passenger compared to personal vehicles (Koren et al., 2007). As a result, it is not surprising that both Hungary and the EU set goals to improve and promote public transport.

Connection between Public Transport and Road Safety

Changing the model split, specifically improving and promoting public transport (one of the safest modes) could be a great solution to reduce traffic accidents: this is supported by several studies. Table 1 shows accident data in Hungary between 2018 and 2022 broken down by cause.

Table 1. Accidents in Hungary (2018-2022)

Year	Passenger vehicle	Of this:				Cargo vehicle	Pedestrians	Other accidents	Total
		Motor-bike	Passenger car	Bicycle	Scooter				
2018	14 193	668	10 920	1 742	631	1 501	988	269	16 951
2019	14 042	766	10 865	1 607	604	1 467	848	270	16 627
2020	11 692	599	8 839	1 600	512	1 224	601	261	13 778
2021	12 047	623	9 484	1 289	483	1 362	557	267	14 233
2022	12 486	549	9 926	1 326	501	1 222	680	360	14 748
Total	64 460	3 205	50 034	7 564	2 731	6 776	3 674	1 427	76 337
%	84.44	4.20	65.54	9.91	3.58	8.88	4.81	1.87	

It is apparent that personal vehicles are responsible for more than 65% of accidents. Based on the table collected from the central database, the number of road accidents between 2018 and 2022 involving public transport vehicles is indicated in Table 2.

The Table 2 contains accident data for buses, suburban railway lines, trams, and trollies. If we compare this with the total number of accidents, we can see that they cause far less accidents than personal vehicles (note: the most accurate ratio would be based on data per mileage, but we do not have the sufficient information). As a first step, promoting public transport, and increasing the number of passengers would reduce congestion as if people choose public transport instead of their personal vehicles, the number of cars on the road would decrease.

Table 2. Road accidents involving public transport vehicles (2018-2022)

Accident type	2018	2019	2020	2021	2022
Collision between oncoming vehicles	52	50	28	50	33
Collision between vehicles travelling in the same direction	108	97	74	101	94
Collision between vehicles travelling in opposite directions	144	144	112	122	131
Collision between a railway vehicle and a road vehicle	3	4	3	1	3
Collision between vehicles travelling straight ahead and turning	121	129	90	96	105
Collision with a stationary vehicle	19	15	10	11	15
Collision with a solid object on the road	1	4	1	1	2
Slip, swerve, overturn on the road	17	8	4	10	10
Leaving the track without hitting a solid object	11	10	8	7	9
Leaving the road, hitting a solid object outside the road	8	5	4	6	4
Hitting a pedestrian	116	131	77	71	111
Passenger accidents	112	114	72	78	88
Collision with a wild animal	0	5	3	3	3
Other	1	1	2	0	0
Total	713	717	488	557	608

The Example of Győr-Moson-Sopron County

We illustrate through the example of a county's public transport its safety, and effect that the introduction of night services would have. Due to the continuous structural changes of the bus service provider, we only have detailed data from 2015 to 2019, but our hypothesis is that trends and ratios have not changed; however, this sets new research goals. In this period, 804 accidents occurred in the county altogether that involved buses. This number includes all incidents involving personal injury or damages in property (Table 3).

Table 3. Accidents in Győr-Moson-Sopron county involving buses (2015-2019)

Only damages in property	Personal injury	Injury caused by scattering
732	64	8

It's apparent that only 8.1% of all accidents involved personal injury. In this period 100 people suffered injuries, with 72 people suffering minor, 25 people severe, and 3 people fatal injuries. In Győr-Moson-Sopron County the accident data in Table 4 was observed in this period.

Table 4. Accidents in Győr-Moson-Sopron County (2015-2019)

Accident	Death	Severe injuries	Minor injuries	All injuries
3,759	211	1472	3602	5285

In terms of bus accidents resulting in minor injuries, in 33% of cases the bus driver was at fault. This shows that personal vehicles cause most of the accidents. For accidents resulting in major injuries, this rate is only 16%. The most common causes of accidents are:

- reckless driving
- neglecting turning rules.

Even though we do not have data about mileage, the absolute numbers show that public transport is significantly safer than individual transport. We did not receive data from the transport service company for 2020. For 2021 and 2022 the company provided the data about accidents resulting in personal injuries in Győr's local public transport as seen in Table 5.

Table 5. Personal injuries in Győr's local public transport

Year	Number of accidents
2021	9
2022	5

Unfortunately, we did not receive detailed statistics about the ratio of injuries (fatal, severe, minor). However, the decrease in the number of accidents in 2022 compared to 2021 is still apparent which is due to several factors. One of them is the reduction of mileage as reduced mileage means lower accident risk. Also, the

frequency and standard of education can also make a difference in public transport safety. It is a question if this tendency continues in the coming years.

Passenger Injury

Passenger injuries are considered separately in this context as it is possible that the driver avoids an accident with an emergency brake, so financial damages do not occur (Amadori & Bonino, 2012). However, the emergency brake causes passengers to fall down and sustain injuries. These are what we call passenger injuries. We divide these into three main categories:

- during boarding and disembarking
- on the move
- in case of emergency braking.

In its public service report for the years 2021 and 2022, the company provided data on passenger accidents in this breakdown, which were as shown in Table 6.

Table 6. Passenger accidents in Győr’s local public transport

Type of accident	2021	2022
During boarding and disembarking	6	4
On the move	4	5
In case of emergency braking	4	9
Total	14	18

There is a significant increase in passenger accidents during emergency braking in 2022 compared to 2021. Unfortunately, the causes and details of the accidents were not provided. The best way to avoid passenger accidents is to provide seating areas and proper handrails. Here we should consider increasing the capacity of buses during peak hours as well as optimizing vehicle design (Wang et al., 2020).

Despite this, public transport still has many advantages (especially safety) over individual transport. If we look at the statistics it is evident, that bus transport is considerably safer than using personal vehicles. It is important to use various methods to encourage more people to use this safe transport mode, e.g., safe design of buses as well as the use of the aforementioned push & pull tools (e.g., convenient timetables and routes, preference techniques).

Introducing and Promoting Night Bus Services

A highlighted category of traffic accidents are the so-called disco-accidents that often involve drunk driving and a specifically high rate of major injuries. The severity of accidents is worsened by the higher speed, and the risk of accident is increased due to driving under influence.

The severity of night accidents is twice as significant as day accidents, and as the data from Győr-Moson-Sopron County shows (Table 7), drunk driving is a major contributor. Győr is one of the most dynamic cities in Hungary and the center of the Western Transdanubia region with a population of 130,000 and with its own university. Consequently, the city has a number of various services and transport infrastructure as well as a high demand for them. This is true for public transport, too, however most of the services are scheduled around factory working hours (4 am to 11 pm).

It has to be noted that the local government has organized several events that go on longer than the regular service time for public transport. People attending summer opening and closing concerts as well as New Year’s Eve festivities have expressed the need for public transport services to be able to get home after these late-night events. An even bigger problem was that on 31 December, the bus services ended at 7 pm, so people were not able to get home even at 8 pm, let alone after midnight.

This problem was finally solved in 2009, when the local government organized a bus service on 6 specifically designed lines from 7 pm to 2 am. This compact service that reaches all parts of the city (but not every stop) is now running with 7 lines (Figure 1) after night events (Winkler & Szabó, 2019).

Table 7. Accidents in Győr-Moson-Sopron county (2015-2019)

Hour	Number of accidents	With alcohol consumption	Without alcohol consumption	With alcohol consumption (%)	Without alcohol consumption (%)
0	39	14	25	35.9	64.1
1	23	13	10	56.5	43.5
2	12	3	9	25.0	75.0
3	20	4	16	20.0	80.0
4	33	7	26	21.2	78.8
5	98	5	93	5.1	94.9
6	126	8	118	6.3	93.7
7	149	2	147	1.3	98.7
8	139	2	137	1.4	98.6
9	158	4	154	2.5	97.5
10	159	5	154	3.1	96.9
11	171	13	158	7.6	92.4
12	136	8	128	5.9	94.1
13	159	6	153	3.8	96.2
14	185	5	180	2.7	97.3
15	189	12	177	6.3	93.7
16	188	11	177	5.9	94.1
17	227	21	206	9.3	90.7
18	185	22	163	11.9	88.1
19	136	12	124	8.8	91.2
20	73	10	63	13.7	86.3
21	69	11	58	15.9	84.1
22	59	16	43	27.1	72.9
23	37	6	31	16.2	83.8

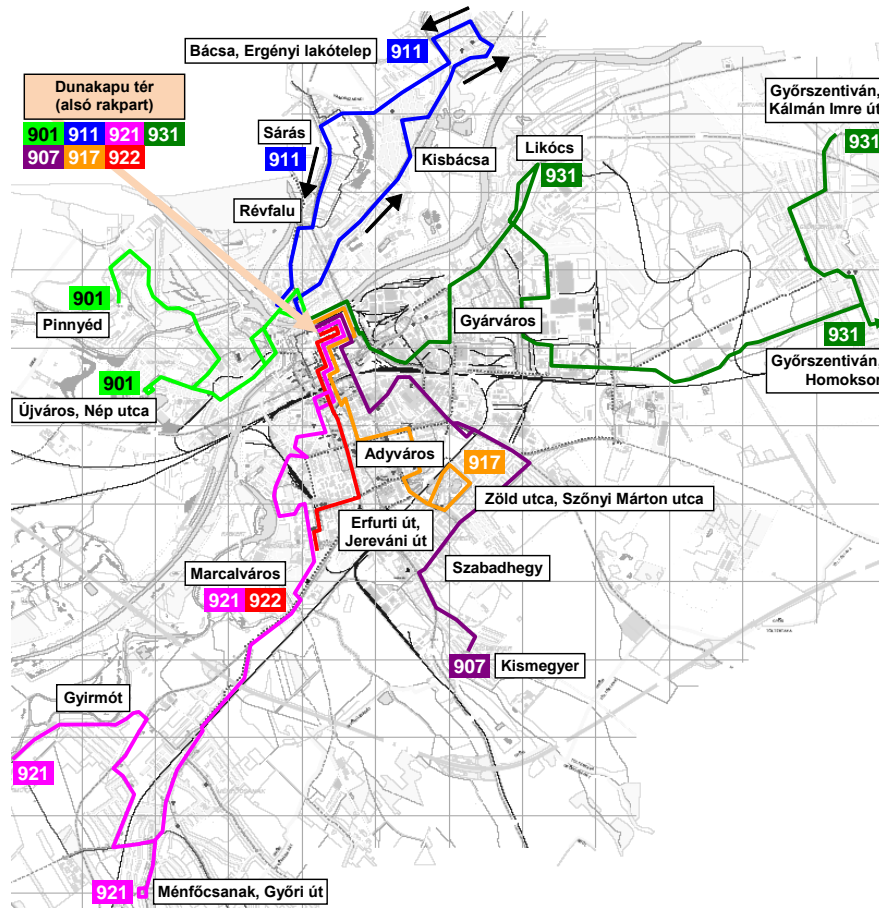


Figure 1. The route of special night buses in Győr

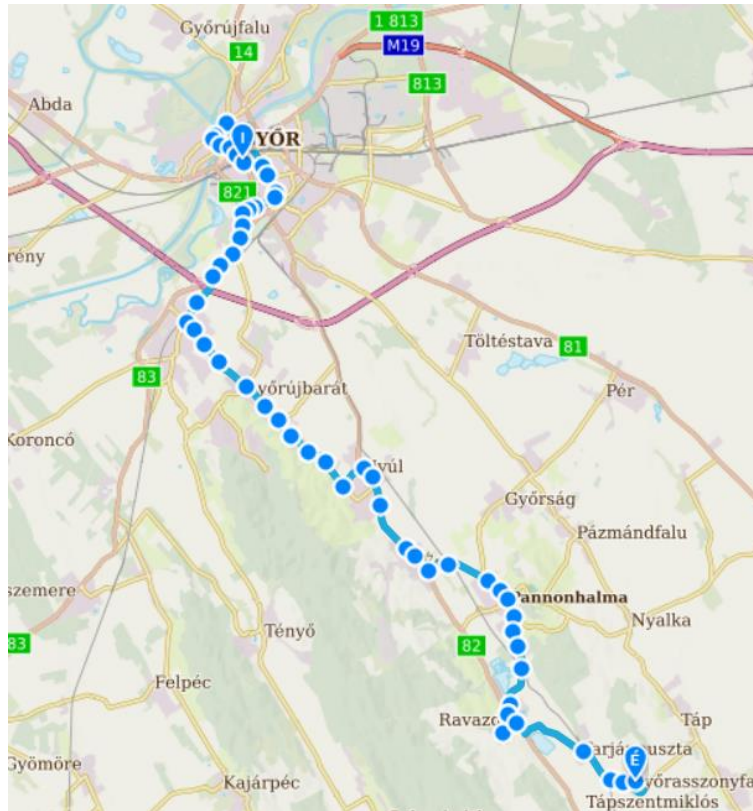


Figure 2. The route of night bus line 7044

This provides a solution for public transport on the most important nights, but this service is still not available most of the year. Even though during European Mobility Week several tests were successfully completed regarding running night services every weekend, it was only in 2018 when the next significant milestone was achieved.

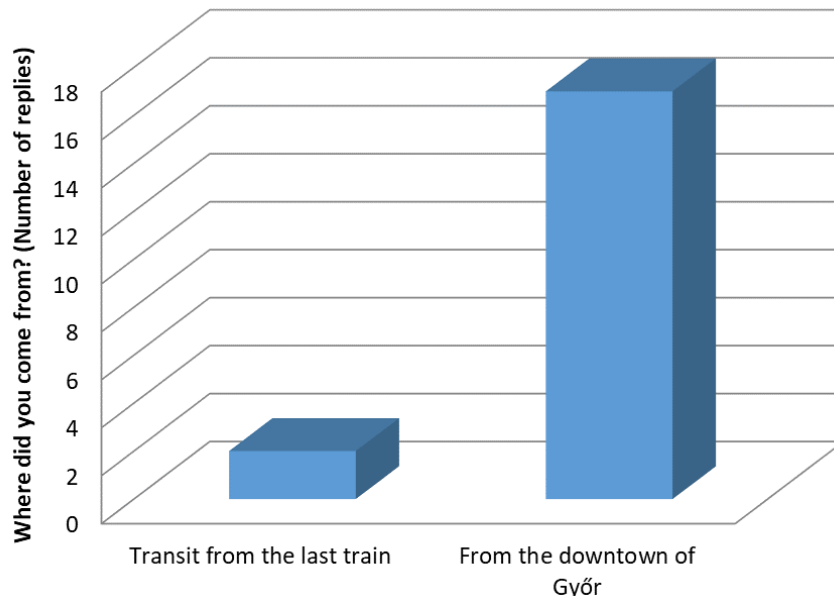


Figure 3. The reasons for using night bus line 7044

The S10 train leaving Budapest at 11:20 pm was extended from Komárom to Győr (based on civil requests) on 9 December 2018, and connected to this train there is regional bus line 7044 (city line number 900) that runs on the weekends and it passes through the major residential areas (Adyváros, Marcalváros) and has various stops in the agglomeration between 1 and 2 pm (Winkler & Szabó, 2019).

The service was initially on a demand-driven basis (departing only when there were passengers at the stop), but the number of passengers constantly grew, so from 16 May 2020, the service runs every weekend and covers a much bigger area (Szeghalmi, 2020): inside the city it stops at the university and at the city center, and in the southern agglomeration it has stops in Győrújbarát, Nyúl, Pannonhalma, Ravazd, Tarjánpuszta and Győrasszonyfa (Figure 2).

This night bus usually has around 15 to 30 passengers every time, but this number would increase with marketing activity. Although it is not possible to exactly show how many accidents and other incidents were avoided with the help of the bus service, but it is evident that it effectively improved road safety and public safety. However, a survey result from 2019 (Figure 3) indicates its relevancy as it shows that most passengers who take the night bus are using it to get home from a nightclub in the downtown of Győr (Winkler & Szabó, 2019).

Based on the data above the expansion of the night bus service both in terms of route (northern parts of the city and agglomeration) and time (frequency and service even during the weekdays, especially in the summer) would be beneficial. Győr's recently accepted Sustainable Urban Mobility Plan (SUMP) also indicated: these developments are some of the most efficient transport measures (Makó et al., 2023).

Conclusion

In this paper we discussed the benefits of public transport in terms of traffic and public safety, as well as its potential for development and promotion. In case of night accidents, the ratio of intoxication is significant, so we highlighted the importance of night public transport, illustrated by a case study from Győr. In order to achieve positive changes, it would be essential to raise awareness (from an early age), promote existing public transport services and advertise new services through targeted marketing activities.

Scientific Ethics Declaration

The authors declare that the scientific ethical and legal responsibility of this article published in EPSTEM journal belongs to the authors.

Notes

This article was presented as an oral presentation at the International Conference on Research in Engineering, Technology and Science (www.icrets.net) held in Budapest/Hungary on July 06-09, 2023.

References

- Amadori, M., & Bonino, T. (2012). A methodology to define the level of safety of public transport bus stops, based on the concept of risk. *Procedia - Social and Behavioral Sciences*, 48, 653-662.
- Kharola, P. S., Tiwari, G., & Mohan, D. (2010). Traffic safety and city public transport system: Case study of Bengaluru, India. *Journal of Public Transportation*, 13(4), 63-91.
- Koren, Cs., Prileszky, I., Horváth, B., Makó, E., Tóth-Szabó, Zs., Hausel, I., Horváth, G., Horváth, R., Szabó, L., Borsos, A., & Farkas, I. (2007). *Győr tömegközlekedési koncepció*. Győr: Széchenyi István University.
- Makó, E., Szakonyi, P., Honvári, P., Winkler, Á., Koren, Cs., Juhász, M. & Fendt, T. (2023). *Győr megyei jogú város fenntartható városi mobilitási terve (SUMP)*. Győr, Hungary: Universitas Arrabona Kft.
- Nævestad, T-O., Elvik, R., Milch, V., Karlsen, K. & Phillips, R. (2022). Traffic safety in bus transport: An analysis of Norway's largest transit authority's contract requirements to bus companies. *Transportation Research Part F: Psychology and Behaviour*, 89, 317-333.
- Szeghalmi, B. (2020, May 15). Napi 7000 utast érint az új menetrend a 82-es főút mentén. Retrieved from <https://www.kisalfold.hu/helyi-kozelet/2020/05/napi-7000-utast-erint-az-uj-menetrend-a-82-es-fout-menten-mutatjuk-a-legfontosabb-valtozasokat>
- Wang, X., Yuen, K. F., Shi, W., & Ma, F. (2020). The determinants of passengers' safety behaviour on public transport. *Journal of Transport & Health*. 18, 100905.

Winkler, Á. & Szabó, R. (2019). Igényvezérelt megoldások a győri éjszakai közforgalmú közlekedés kialakítása céljából. *Közlekedéstudományi konferencia Győr 2019*. Győr, Hungary: Széchenyi István University.

Author Information

Diána Henézi

Széchenyi István University

Győr, Hungary

Contact e-mail: kdiana@sze.hu

Ágoston Winkler

Széchenyi István University

Győr, Hungary

To cite this article:

Winkler, A., & Henezi, D. (2023). The role of public transport in transport safety and public safe. *The Eurasia Proceedings of Science, Technology, Engineering & Mathematics (EPSTEM)*, 23, 505-512.

The Eurasia Proceedings of Science, Technology, Engineering & Mathematics (EPSTEM), 2023

Volume 23, Pages 513-520

ICRETS 2023: International Conference on Research in Engineering, Technology and Science

Investigating the Effect of Information Systems and Decision Quality on Organizational Performance in Business Firms

Ahmad Nabot
Zarqa University

Abstract: The development of information systems raised the quality of decision-making, significantly impacting businesses' organizational performance. To evaluate this impact, the current research aimed to investigate the relationship between information systems (IS) success factors, decision-making quality (DMQ), and organizational performance (OP). A quantitative research approach was adopted, and a survey was sent to 163 decision-makers who use information systems in business firms. The study model was evaluated using PLS-SEM. The study's empirical results indicated that information quality (IQ) significantly positively impacted decision-making quality (DMQ). However, system quality (SQ) did not affect decision-making quality (DMQ). Furthermore, information quality (IQ) was found to mediate the relationship between system quality (SQ) and organizational performance (OP). Finally, the decision-making quality (DMQ) was found to moderate the relationship between information quality (IQ), system quality (SQ), and organizational performance (OP). This study provided field practitioners with important recommendations and future work to evaluate the impact of information systems (ISs) impact on organizational performance (OP).

Keywords: Information system, Information quality, Decision-making quality, Organizational performance.

Introduction

Regardless of profitability, every business entity requires an information system within its department to function effectively. Decisions made within even non-profit organizations are based on various reports (Kapoor & Goel, 2017). Over the past few decades, as technology has swept across the globe, it was inevitable that it would permeate everyday professional life. These technological advancements have revolutionized how tasks are performed through information systems (IS), leading to a continuous and growing revolution (Smith, 2015). Initially, digitalization reduced the workload by employing technology for repetitive tasks, allowing organizations to focus on more advanced situations. This shift significantly improved organizational performance and productivity (Irfan et al., 2008). However, the key to efficiency is strategically utilizing information systems and tools (Schmitz & Leoni, 2019). Traditionally, an information system (IS) is as a system that enables data collection and processing, facilitating its use by decision-makers to improve organizational performance (OP) (Dagilene & Šutiene, 2019).

To ensure the success of IS, organizations must not only excel in creating the technological aspects but also foster a positive environment for information utilization, particularly in decision-making processes (Sun et al., 2018;) (Popovič et al., 2012). Many studies Ahmed (2021); Jasim and Raewf (2020); Puspitawati (2021). The topic of information system success has only recently gained attention in the literature, and few attempts have been made to examine the impact of these systems on the organizational performance. A significant gap remains, particularly regarding the decision-making quality that contributes to the success of these systems. This study introduces the dimension of Decision-Making Quality (DMQ) to the existing model and explores its effect on the relationship between information quality, information system on organizational performance (OP), aiming to address this unanswered question in the literature. However, earlier studies have not conducted an in-depth analysis of information system success, mainly due to its dependence on various factors, including

- This is an Open Access article distributed under the terms of the Creative Commons Attribution-Noncommercial 4.0 Unported License, permitting all non-commercial use, distribution, and reproduction in any medium, provided the original work is properly cited.

- Selection and peer-review under responsibility of the Organizing Committee of the Conference

information and system quality, as highlighted by numerous studies in different fields Al-Okaily (2022) and Ouiddad et al. (2020) and Popovič et al. (2012). This research seeks to investigate whether current information systems have succeeded in enhancing the quality of organizational decision-making in improving organizational performance. This study contributes to the body of knowledge by proposing a model that measures the impact of information systems on organizational performance through decision-making quality, utilizing DeLone and McLean (D&M) success model.

The organization of this study is as follows: Section 2 offers a background, while Section 3 presents the main concepts, research hypotheses, and study model. The study methodology is outlined in Section 4, followed by the presentation of the study results in Section 5. Lastly, Section 6 encompasses the study discussion, limitations, and future work.

Background

The rapid technological revolutions of recent times have tremendously impacted the business world, leading to significant changes and advancements. Entities have been compelled to adapt to emerging trends and effectively keep up with technological growth. Automation has become a prevalent concept in various business sectors, with four key components—cloud accounting, Internet of Things (IoT), blockchain, and big data—recognized as crucial elements in this process, as indicated by Qasim and Kharbat (2020). These approaches have gained prominence within firms, with researchers acknowledging their potential to drive automation.

By effectively integrating these four concepts, there is a significant opportunity to reduce individuals' reliance on manual record-keeping. Instead, a single individual can solely rely on technology to generate all the necessary reports. For instance, blockchain technology has proven beneficial in various aspects of firms. Firstly, as most documents are automated, they can easily be directed to numerous other applications. Secondly, all participants have access to the transaction history on the blockchain, which enhances system efficiency and reliability. Lastly, it reduces the occurrence of fraud due to the inherent difficulty in altering blockchain data, providing transparency to all participants.

Additionally, blockchain facilitates faster, paperless invoice exchanges between parties involved in a transaction, eliminating potential misuse (Fanning & Centers, 2016). However, it is essential to acknowledge that the application of this technology, like any other new technology, comes with its challenges, weaknesses, and potential adverse effects. One ongoing debate revolves around insufficient tools to ensure the system functions as intended, reducing system reliability (Qasim & Kharbat, 2020).

Main Concepts, Research Hypothesis, and Model

D&M success model is widely utilized by various studies examining the ISs success as indicated by Al-Okaily et al. (2021); Popovič et al. (2012). The model was initially introduced by DeLone and McLean (1992), who set several categories as standard dimensions of information system success. These dimensions include system quality (SQ), and information quality (IQ).

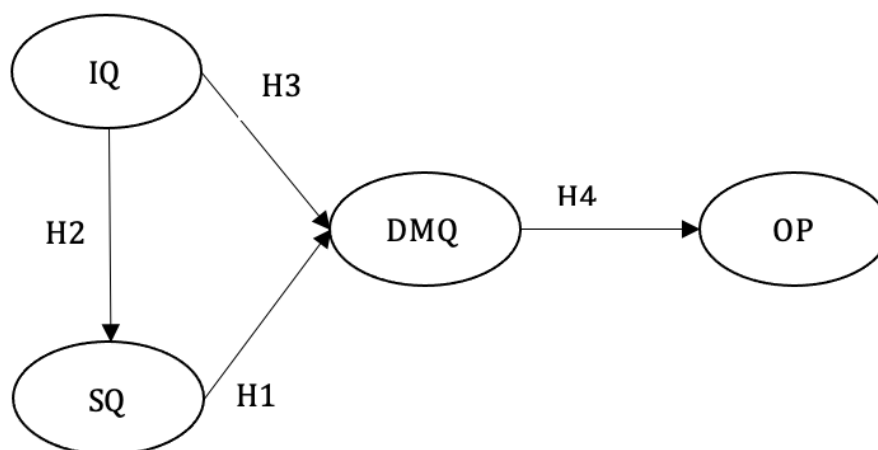


Figure 1. Study first model

The model, along with its subsequent modifications, assures the perception of the interconnections between these dimensions of information system success, ultimately leading to the final success variable referred to as "net benefits" in the original model Add ref. In the present study, the Decision-Making Quality (DMQ) dimension has been incorporated as a critical factor in assessing the contribution of information systems to organizational performance, as depicted in Figure 1.

System Quality (SQ)

System quality refers to essential factors within a system that enables it to fulfill the desired tasks. These factors encompass flexibility, accuracy, reliability, ease-of-use, and availability (DeLone & McLean, 2016). Prior studies have indicated a positive association between system quality and decision-making quality, as an effective system reduces the effort required in the decision-making process, thereby enhancing its overall quality (Arnott & Pervan, 2016). However, some studies reported conflicting results (Al Fraihat et al., 2020; Motaghian et al., 2013), prompting this study to contribute to this field of studies. Consequently, the following hypothesis is formulated:

H1. System quality (SQ) directly affects decision-making quality (DMQ).

Information Quality (IQ)

High quality information is acknowledged as an important factor for firms to make successful decisions and succeed in the current dynamic and fast business advancements (Elezaj et al., 2023; Pirttimäki et al., 2006). IQ reduces uncertainty based on the available alternatives for decision making by understanding the potential consequences associated with selecting one option over another. Based on this understanding, the following hypotheses were proposed as follows:

H2. Information quality (IQ) positively affects system quality (SQ)

H3. Information quality (IQ) positively affects decision-making quality (DMQ)

Decision-Making Quality (DMQ)

Decision-making is identified as the process of identifying and selecting the most suitable action from various alternatives to achieve organizational goals. This process is considered critical aspect for firm's management at all levels REF. The quality of decisions made significantly impacts organizational performance, with high-quality decisions yielding positive outcomes, while low-quality decisions can adversely affect the organization. Moreover, the availability and quality of resources, such as systems and information, can influence the quality of decision-making either positively or negatively. In this context, system quality and information quality play crucial roles as facilitators, providing decision-makers with the necessary tools and information to make effective decisions and enhance the overall quality of the decision-making process. Based on these considerations, the following hypothesis has been formulated:

H4. Decision-making quality (DMQ) positively affects organizational performance (OP).

Organizational Performance (OP)

Organizational performance (OP) is recognized as the achievement of the business processes after realizing firm goals (Cahyono et al., 2023). In information technology, the software system has many factors that affect organizational performance. These factors lie in the software quality attributes, information quality, and decision-making quality. Each factor has measures that affect OP based on how these factors are used to improve the firm's competencies (Ravichandran & Lertwongsatien, 2014). In addition to the available resources and capabilities to improve the quality of decision-making process and then enhance OP (Santhanam & Hartono, 2003).

Methodology

Measurement Instrument

The survey employed in this study utilized constructs and measures previously supported in the existing literature to ensure the validity and reliability of the study survey. For instance, to assess SQ, four items were derived from the works of Cahyono et al. (2023) and Guy et al. (2008), which focused on the technical aspects of the IS. Similarly, three measures were adopted from previous literature to evaluate IQ, specifically examining the characteristics of information generated by IS Lin (2010) and Guy et al. (2008). DMQ evaluated using three items adapted from the studies conducted by Alalwan et al. (2014) and Ouiddad et al. (2020). Finally, to gauge organizational performance, three items were employed, adapted from a recent study conducted by Cahyono et al. (2023).

Data Collection

The research data was gathered from various firms in Jordan involving different users, including managers, supervisors, and employees. A total of 250 survey were distributed to decision-makers within these organizations. After data collection, 177 questionnaires were collected before conducting a thorough screening process. Of these collected responses, 163 valid responses were deemed suitable for further analysis. Table 1 presents a detailed description of the respondents' Demographic information.

Table 1. Respondents' demographic information.

Measure	Option	Frequency
Gender	Male	93
	Female	70
Age	Less than 30	46
	30-40	58
	41-50	37
	Above 50	22
Education	Diploma	5
	BSc.	81
	MSc.	66
	Ph.D.	11
Job title	Employee	104
	Supervisor	41
	Manager	18
Experience	Less than 5	32
	5-10	54
	11-20	36
	Above 20	41

Results

Assessing the measurement model is a fundamental stage in evaluating the reliability and validity of the PLS-SEM. The measurement model evaluation involves several criteria. First, survey items' reliability was assessed using factor loading (FL) test of 0.7. Furthermore, Cronbach's alpha (α) test was utilized to evaluate the internal consistency of the survey items and composite reliability (CR) of 0.7 and above. Finally, average variance extracted (AVE) of 0.5 and above was utilized to assess the convergent validity.

Table 2 and Figure 2 present the results, indicating that all items' factor loadings are within the suggested range. Additionally, all research factors' CR and AVE values surpass the cutoff values of 0.7 and 0.5, respectively. These results confirm the measurement model's reliability.

Discriminant validity measures how the measurement items differentiate their respective factors from other items in the proposed model. Three methods to assess discriminant validity exist the heterotrait-monotrait (HTMT) ratio, Fornell and Larcker correlation, and cross-loadings. The HTMT ratio, proposed by (Henseler et al., 2015), is an alternative method in PLS-SEM. Values close to 1 indicate insufficient discriminant validity. Table 3 displays the HTMT criterion values, satisfying the recommended threshold and indicating adequate discriminant validity.

Table 2. Results summary for the outer model measurements

Value	Indicators	Reliability and Validity				Discriminant validity
		Convergent validity	Internal consistency validity	FL	AVE	
		FL	AVE	α	CR	HTMT
		>0.7	≥ 0.5	≥ 0.7	≥ 0.7	<0.9
System quality	SQ1	0.905	0.779	0.910	0.934	Yes
	SQ2	0.917				
	SQ3	0.900				
	SQ4	0.803				
Information quality	IQ1	0.962	0.835	0.902	0.938	Yes
	IQ2	0.846				
	IQ3	0.930				
Decision-making quality	DMQ1	0.925	0.863	0.921	0.950	Yes
	DMQ2	0.928				
	DMQ3	0.934				
Organizational performance	OP1	0.973	0.841	0.922	0.941	Yes
	OP2	0.898				
	OP3	0.877				

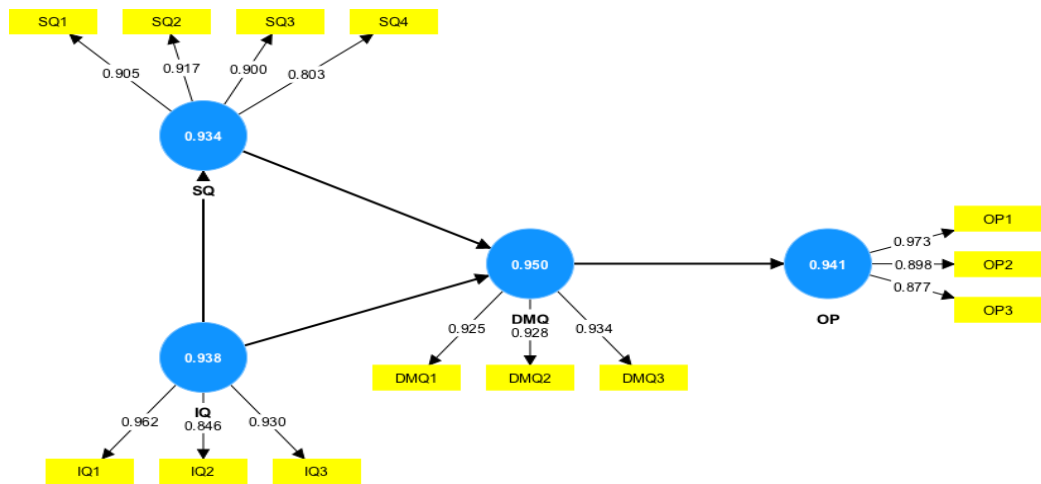


Figure 2. Measurement model

Table 3. Heterotrait-monotrait (HTMT) test

Indicator	DMQ	IQ	OP	SQ
DMQ				
IQ	0.128			
OP	0.050	0.247		
SQ	0.217	0.737	0.217	

Table 4. Fornell-Larcker correlation matrix

Indicator	DMQ	IQ	OP	SQ
DMQ	0.929			
IQ	0.131	0.914		
OP	0.041	0.275	0.917	
SQ	0.209	0.748	0.234	0.882

One approach to assess discriminant validity is through the utilization of the Fornell-Larcker correlation matrix. Fornell and Larcker (1981) propose this method, wherein discriminant validity is deemed to be established if the average variance extracted (AVE) of a factor surpasses the squared multiple correlations between that factor and other factors. Table 4 presents the square root of AVE values for latent factors. These values, highlighted in bold font, are more significant than the correlations with other factors, affirming discriminant validity according to the Fornell-Larcker principle.

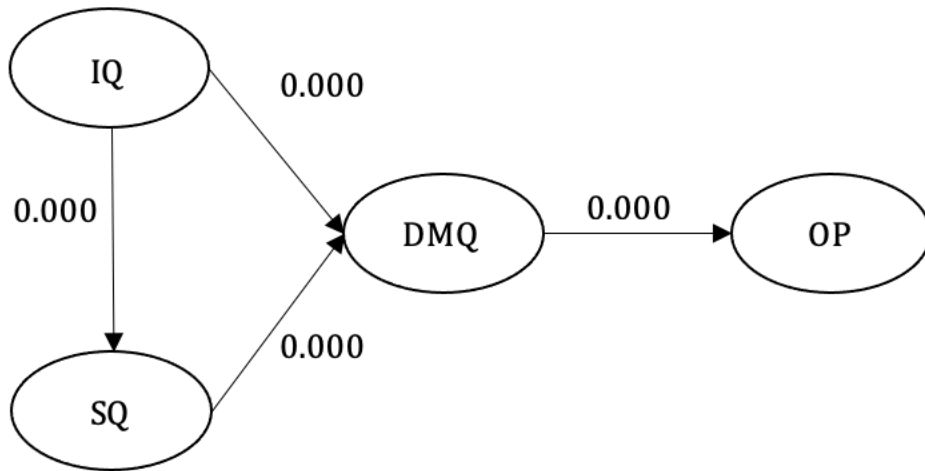


Figure 3. Study second model test results

Table 5. Hypothesis test results

-Hypothesis	Path	Beta (β)	P-value	Decision
H1	SQ \rightarrow DMQ	0.290	0.000	Accepted
H2	IQ \rightarrow SQ	0.786	0.000	Accepted
H3	IQ \rightarrow DMQ	0.890	0.000	Accepted
H4	DMQ \rightarrow OP	0.330	0.000	Accepted

Table 5 presents the test results for the four hypotheses examined in the study. The findings indicate that the beta (β) value falls within the acceptable range, and the P-value associated with the hypothesis demonstrates its level of significance.

Discussion and Conclusion

The present study makes a valuable contribution to the existing literature by examining critical factors in the IS success model and explaining their impact on organizational performance. This study focuses on SQ, IQ, and DMQ effect on OP. The empirical findings provide strong evidence supporting the positive influence of system quality and information quality on decision-making quality, thereby accepting hypotheses H1 and H2. These findings are in-line with the studies conducted by Kulkarni et al. (2017) and Yeoh and Popovič (2016), which indicate that IQ as a crucial factor for the success of ISs leading to high quality information for decision making and organizational performance improvement. Furthermore, IQ positively impacted DMQ and OP in Jordanian firms, resulting in the acceptance of hypotheses H3 and H4. These findings are in-line with study conducted by DeLone and McLean (2016) confirming the crucial role of IQ in improving OP. Similarly, Pirttimäki et al. (2006) indicates the importance of IQ in decision making for firms. In addition, the study findings are consistent with the study conducted by Wieder and Ossimitz (2015), which identifies a significant relationship between both IQ and DMQ.

Limitations and Recommendations

The limitations of this study are acknowledged and should be taken into account when interpreting the results. one of these limitations lies in the generalizability of the results due to the limited sample scope of Jordanian firms. The study was conducted on a limited sample of firms in Jordan. Thus, the findings may not be applicable in other fields. Moreover, the data collection was limited to firms in the capital city of Jordan, and it is recommended for future research to extend the scope of the study to include other cities. These limitations present opportunities for further research to understand how information systems contribute to the organizational performance. Thus, future research needs to consider more industries, which also utilize information systems in their daily business processes.

Scientific Ethics Declaration

The author declares that the scientific ethical and legal responsibility of this article published in EPSTEM journal belongs to the author.

Acknowledgements or Notes

* This article was presented as an oral presentation at the International Conference on Research in Engineering, Technology and Science (www.icrets.net) held in Budapest/Hungary on July 06-09, 2023.

References

- Ahmed, A. A. A. (2021). Corporate attributes and disclosure of accounting information: Evidence from the big five banks of China. *Journal of Public Affairs*, 21(3), e2244.
- Alalwan, J. A., Thomas, M. A., & Weistroffer, H. R. (2014). Decision support capabilities of enterprise content management systems: An empirical investigation. *Decision Support Systems*, 68, 39–48.
- Al Fraihat, D., Joy, M., Masa'deh, R., & Sinclair, J. (2020). Evaluating e-learning systems success: An empirical study. *Computers in Human Behavior*, 102, 67–86
- Al Okaily, A., Al Okaily, M., & Teoh, A. P. (2021). Evaluating ERP systems success: evidence from Jordanian firms in the age of the digital business. *VINE Journal of Information and Knowledge Management Systems*, (ahead-of-print).
- Al Okaily, M., & Al Okaily, A. (2022). An empirical assessment of enterprise information systems success in a developing country: the Jordanian experience. *TQM Journal*, 34(6), 1958–1975.
- Arnott, D., & Pervan, G. (2016). A critical analysis of decision support systems research. *Formulating Research Methods for Information Systems*, 2, 127–168
- Cahyono, Y., Purwoko, D., Koho, I. R., Setiani, A., Supendi, Setyoko, P. I., Sosiady, M., & Wijoyo, H. (2023). The role of supply chain management practices on competitive advantage and performance of halal agroindustry SMEs. *Uncertain Supply Chain Management*, 11(1), 153–160.
- Dagilene, L., & Štitiene, K. (2019). Corporate sustainability accounting information systems: A contingency-based approach. *Sustainability Accounting, Management and Policy Journal*, 10(2), 260–289.
- DeLone, W. H., & McLean, E. R. (2016). Information systems success measurement. *Foundations and Trends® in Information Systems*, 2(1), 1–116.
- Fanning, K., & Centers, D. P. (2016). Blockchain and its coming impact on financial services. *Journal of Corporate Accounting & Finance*, 27(5), 53–57.
- Guy, G., Sedera, D. ;, & Chan, T. (2008). Re-conceptualizing information system success: The is-impact measurement model. *Journal of the Association for Information Systems*, 9(7), 377–408.
- Henseler, J., Ringle, C. M., & Sarstedt, M. (2015). A new criterion for assessing discriminant validity in variance-based structural equation modeling. *Journal of the Academy of Marketing Science*, 43(1), 115–135.
- Irfan, D., Xiaofei, X., & Chun, D. S. (2008). Developing approaches of supply chain management systems of enterprises in Pakistan. *International Arab Journal of Information Technology (IAJIT)*, 5(3).
- Jasim, Y. A., & Raewf, M. B. (2020). Information technology's impact on the accounting system. *Cihan University-Erbil Journal of Humanities and Social Sciences*, 4(1), 50–57.
- Kapoor, N., & Goel, S. (2017). Board characteristics, firm profitability and earnings management: Evidence from India. *Australian Accounting Review*, 27(2), 180–194.
- Kulkarni, U., Robles-Flores, J. A., Popovič, A., Kulkarni, U. R., & Antonio Robles-Flores, J. (2017). Business intelligence capability: The effect of top management and the mediating roles of user participation and analytical decision making orientation. *Journal of the Association for Information Systems*, 18(7), 1.
- Lin, H. F. (2010). An investigation into the effects of IS quality and top management support on ERP system usage. *21(3)*, 335–349.
- Motaghian, H., Hassanzadeh, A., & Moghadam, D. K. (2013). Factors affecting university instructors' adoption of web-based learning systems: Case study of Iran. *Computers & Education*, 61(1), 158–167.
- Ouiddad, A., Okar, C., Chroqui, R., & Beqqali Hassani, I. (2020). Assessing the impact of enterprise resource planning on decision-making quality: An empirical study. *Kybernetes*, 50(5), 1144–1162.
- Pirttimäki, V., Länqvist, A., & Karjalainen, A. (2006). Measurement of business intelligence in a Finnish telecom-munications company. *Electronic Journal of Knowledge Management*, 4(1), pp83-90-pp83-90.

- Popovič, A., Hackney, R., Simões Coelho, P., & Jaklič, J. (2012). Towards business intelligence systems success: Effects of maturity and culture on analytical decision making. *Decision Support Systems*, 54, 729–739.
- Puspitawati, L. (2021). Strategic information moderated by effectiveness management accounting information systems: Business strategy approach. *Jurnal Akuntansi*, 25(1), 101–119.
- Qasim, A., & Kharbat, F. F. (2020). Blockchain technology, business data analytics, and artificial intelligence: Use in the accounting profession and ideas for inclusion into the accounting curriculum. *Journal of Emerging Technologies in Accounting*, 17(1), 107–117.
- Ravichandran, T., & Lertwongsatien, C. (2014). Effect of information systems resources and capabilities on firm performance: A resource-based perspective. *Journal of Management* 21(4), 237–276.
- Santhanam, R., & Hartono, E. (2003). Issues in linking information technology capability to firm performance. *MIS Quarterly : Management Information Systems*, 27(1), 125–153.
- Schmitz, J., & Leoni, G. (2019). Accounting and auditing at the time of blockchain technology: A research agenda. *Australian Accounting Review*, 29(2), 331–342.
- Smith, S. S. (2015). Accounting: Evolving for an integrated future. *Finance & Management Strategy*, 10(1), 1–12.
- Wieder, B., & Ossimitz, M. L. (2015). The impact of business intelligence on the quality of decision Making – a mediation model. *Procedia Computer Science*, 64, 1163–1171.
- Yeoh, W., & Popovič, A. (2016). Extending the understanding of critical success factors for implementing business intelligence systems. *Journal of the Association for Information Science and Technology*, 67(1), 134–147.

Author Information

Ahmad Nabot

Zarqa University

Zarqa, Jordan

Contact e-mail: anabotl@zu.edu.jo

To cite this article:

Nabot, A. (2023). Investigating the effect of information systems and decision quality on organizational performance in business firms. *The Eurasia Proceedings of Science, Technology, Engineering & Mathematics (EPSTEM)*, 23, 513-520.

The Eurasia Proceedings of Science, Technology, Engineering & Mathematics (EPSTEM), 2023

Volume 23, Pages 521-530

ICRETS 2023: International Conference on Research in Engineering, Technology and Science

Desk Analysis of Crisis Communication by Public Authorities During Health Crises

Stjepan Petricevic

Alma Mater Europaea ECM

Abstract: Communication by public authorities during a crisis is an important and essential part of responding to situations that can endanger lives and property. Social media platforms, identified as the main source of news according to research, provide a significant opportunity for communication. Media outlets played a crucial role during the COVID-19 pandemic, with Facebook continuing to lead as a news source compared to other social media platforms. This study analyzes the posts from the official Facebook profile "Koronavirus.hr," which serves as the government's official page for COVID-19 information in the Republic of Croatia. Using a desk analysis method, the study examines the content of the posts across four pandemic waves, considering the number of cases, post size, type of visual/video content, and social reactions. The analysis reveals that the average post size is approximately 37 words, with the most common length being 51 words. The posts predominantly feature general visual/video materials, with an average video duration of around 50.40 minutes. Social reactions to posts about the number of new cases have an average count of 38.18 per post, with an average of 5.61 comments and 1.55 shares. The correlation analysis shows a statistically significant positive correlation between the number of new cases reported in a post and the total number of comments and shares. Additionally, there are statistically significant positive correlations between post size (word count) and the total number of reactions, comments, and shares. However, further analysis reveals a lack of a statistically significant relationship between post size (word count) and the total number of reactions. This study provides guidelines for the future creation of posts by public authorities on social media during crisis situations and opens the way for further research in the field of communication strategies.

Keywords: Crisis communication, Health crises, Communication strategies, Social media, COVID 19

Introduction

In the modern age, fast and effective communication during crisis situations is a crucial factor in preserving safety and public trust. Crisis communication is a scientific and practical discipline that deals with strategies and tactics for managing communication during life-threatening situations (Plenković, 2015). It pertains to the strategies and tactics that public authorities employ to manage communication during situations that endanger lives and property. With the development of mass communication, particularly electronic media, social and individual identities have become more interconnected than ever before, influencing the organization of society and individuals (Bošnjak, 1998). This revolution in science and technology deeply transforms our way of life, affecting our knowledge, needs, and cultural creation in new ways (Božilović & Petković, 2015). New technologies facilitate the mass exchange of information and change the way materials and knowledge are shared. However, despite the progress, the communication and media industries still dominate public and private spaces, raising new questions about ethics and quality decision-making (Eid, 2014). In the context of technological development, interactive health communication applications have great potential for improving health, but they can also cause harm. Physicians and other healthcare professionals should promote and participate in the evidence-based development of interactive health communication applications, supporting efforts to assess their safety, quality, and usefulness (Robinson et al., 1998; Henderson et al., 1999). Alongside technological advancements, social media has become ubiquitous and has a significant impact on our daily

- This is an Open Access article distributed under the terms of the Creative Commons Attribution-NonCommercial 4.0 Unported License, permitting all non-commercial use, distribution, and reproduction in any medium, provided the original work is properly cited.

- Selection and peer-review under responsibility of the Organizing Committee of the Conference

© 2023 Published by ISRES Publishing: www.isres.org

lives. However, when it comes to healthcare, there is a particular challenge to using social media for professional communication among healthcare professionals. Stevanović and Pristaš emphasize that professional communication among healthcare professionals through social networking is less applicable due to the protection of personal identity and data (Stevanović & Pristaš, 2011.).

Social media has shown usefulness for communication about crisis situations and risks at the individual, organizational, and official levels (Day et al., 2019). They have various advantages, such as reaching a wide audience, low costs, fast communication, and easy updating, but there are risks related to misinformation and maintaining patient privacy (Mayer et al., 2018). We are increasingly recognizing the importance of communication for healing and the impact it can have on the course of illness. Empirical research confirms that the mind and body are closely connected, and the social context has important implications for health (Thomas, 2006). Therefore, health communication becomes a key research topic as anyone facing a serious illness or having a loved one struggling with a life-threatening or terminal illness comes into contact with healthcare professionals or encounters health messages in the media (Ellingson, 2002). Social media, like other forms of mass media, have a significant influence on public awareness and knowledge. Public health campaigns often rely on mass media to convey information and increase awareness, although behavior change is often achieved to a lesser extent (Catalán-Matamoros, 2011). A well-designed public approach, which includes competence, security, anticipation, knowledge, creativity, and personal strength, is crucial for successful public opinion action (Marković, 2008, p. 75). Ganis and Kohirkar emphasize that social media has become a two-way street that allows users to express their opinions and communicate at speeds unimaginable with traditional media. The popularity of social media continues to grow exponentially (Ganis & Kohirkar, 2015).

Effective media communication is a crucial element in managing emergencies and crises. Communication by public authorities during a crisis is essential in responding to situations that can endanger lives and property, and social media provide a unique opportunity for communication (Tabbaa, 2010; Quinn, 2018). Timely and accurate communication can reduce panic, improve risk perception, and foster trust in institutions. The COVID-19 pandemic has further emphasized the importance of media communication in crisis situations, and social media have proven to be effective in risk management and public mobilization through the dissemination of relevant information (Sezgin et al., 2020).

Based on previous research that has demonstrated the role and importance of social media in health crisis situations, as well as examples of research conducted in Croatia to provide context and significance, the aim of this study is to analyze the effectiveness of crisis communication by public authorities through the use of a social media platform, specifically the official Facebook profile, during the COVID-19 pandemic. The main focus is on the connection between the news posts published on the official Government profile and social reactions. This research seeks to provide a foundation for future creation of posts by public authorities on social media in similar crisis scenarios.

Crisis Communication in Croatian Healthcare

The importance of monitoring the trend in communication technology development from a healthcare perspective has been supported by scientific research. In addition to global technological and communication changes, it is necessary to note that Croatia has also experienced significant social changes after the dissolution of Yugoslavia in the 1990s. In a study on the impact of propaganda on journalism in crisis situations, Laiho states that electronic media and the press were strictly controlled by the ruling structures in all socialist Yugoslav countries (Laiho, 2008). The influence of media control in recent history can negatively affect public trust in the media, media literacy, and understanding the role of the media in crisis situations.

Further literature reviews and research focus on examples of communication in Croatian healthcare. Within the healthcare system in Croatia, there are various challenges associated with contemporary social development, such as transitional difficulties and the impact of modern information technologies (Zrinščak, 2007). Changes in the healthcare system require the active participation of healthcare personnel, the acquisition of new knowledge, and the application of information and communication technologies (Kern, 2014). The results of research conducted among healthcare professionals and non-healthcare staff indicate differences in the use of health-related knowledge sources, with healthcare professionals more inclined to rely on professional sources, while non-healthcare staff more commonly use informal sources of information (Grčić et al., 2014). The Baxter affair in October 2011, in which dialyzers caused the deaths of 24 people, highlighted the lack of communication in healthcare, both horizontally (between healthcare institutions) and vertically (between institutions and ministries). Vuletić states, "Given that the Baxter affair was a typical example of a crisis situation, which clearly

demonstrated the realization that healthcare professionals do not know enough, in fact, they know very little about crisis communication (both internal and external), ..." (Vuletić, 2014, p. 23). Interestingly, considering the widespread use of social media over the years, Vujević notes in his work that "No scientific study has been conducted in Croatia describing the impact of social media on the professionalism of physicians, possible dangers they may encounter, or any guidelines to guide them in the use of these highly popular platforms to help them maintain their professional reputation, which is essential for their future work with patients" (Vujević, 2018). The lack of strategic and effective communication by healthcare institutions with the public is also emphasized, as concluded in a 2019 study on public relations in healthcare institutions in Croatia by Duljaj, who states, "The public relations profession is well-developed and known in Croatia, yet many organizations fail to recognize the benefits of its use. Some of these organizations are healthcare institutions that struggle or refuse to recognize the importance of good public relations" (Duljaj, 2019, p. 39).

Method

For this research, a desk analysis of the official Facebook profile "Koronavirus.hr" was conducted as an example of communication by public authorities in Croatia. Facebook's social media platform was chosen because "Facebook continues to lead as a news source compared to other social media platforms," and in the Croatian context, Facebook also holds a high position as a news source (Vozab & Peruško, 2021). A retrospective analysis was performed on all posts from the "Koronavirus.hr" Facebook profile across four COVID-19 pandemic waves. For further analysis, all posts providing information about the number of new cases were selected using an analytical matrix. Posts related to the number of new cases were chosen because they represented a constant factor across the four pandemic waves. Within each wave, posts from the week at the beginning of the wave, the week at the peak with the highest number of new cases, and the week towards the end of the wave were analyzed. Data on the number of new cases was retrieved from the Koronavirus.hr website, updated daily, and sourced from Our World in Data (ourworldindata.org) as of February 12, 2022, which is considered relevant data on the official government website Koronavirus.hr (Koronavirus.hr, 2022). The unit of analysis includes individual media posts. The analytical matrix is based on sentiment analysis research and consists of a total of 12 segments. The content analysis method was used to determine the representation and connections between categories within the unit of analysis, including the date of news posts, the number of new cases, the size of the post (number of words), the duration of videos (in minutes), the content of visual/video materials, the total number of rapid reactions, the total number of comments, the total number of shares, and the author's response to comments.

Microsoft Excel was used for the statistical analysis of the collected data. Various statistical methods were applied to obtain a detailed analysis of the collected data. Descriptive methods such as mean, standard deviation, and percentage were first used to describe the basic characteristics of the data set. These methods allow for the identification of the central tendency, the dispersion of values, and the proportion of individual categories in the data. To investigate relationships between different variables, correlation methods were applied. Due to the non-normal distribution of the data, Spearman's rank correlation test was chosen for further analysis of relationships and correlations with other variables. Significance tests were also conducted to verify the statistical significance of differences or relationships in the data. For this purpose, Mann-Whitney U tests were used to compare independent samples. All statistical analyses were performed using the functions and tools available in Microsoft Excel. These methods enable obtaining quantitative results and statistical conclusions based on the collected data.

Limitation

It is important to note that this methodology is based on the content analysis of a single Facebook profile, which may have its limitations. Data obtained from a single source may not necessarily represent the entire picture of public authorities' communication, and further research is needed to obtain a comprehensive understanding of their communication. The research is based on the analysis of content on Facebook, the primary social media platform. However, it should be noted that there are many other social media platforms and channels that also play a role in public authorities' communication. Similarly, the research focuses on analyzing posts during the four pandemic waves. As the situation may evolve over time, the research findings may be relevant only for that specific time period. Although desk analysis and statistical data processing were utilized, depending on the selected categories and analytical methods, it is possible that some important aspects or relationships between variables were not thoroughly explored. The limitations of the research may stem from the specific conditions and context of Croatia, and the results may not necessarily be generalizable to other countries or situations.

Results and Discussion

In this chapter, we present the results of research conducted on the official Facebook profile "Koronavirus.hr". The retrospective analysis included four pandemic waves, with a focus on posts providing information about the number of new cases. During the observed period, a total of 300 posts on the Facebook profile "Koronavirus.hr" were analyzed (n=300). It was found that posts about the number of cases or new cases were present in all four pandemic waves (n=91), indicating their consistency and importance in the communication of public authorities, thus being selected for further analysis. However, in the first observed period, out of the total number of observed posts (n=8), the majority of posts (n=7) were about the total number of cases (with an average total number of cases of 261.25 individuals), without information about the number of new cases, while all subsequent posts addressed the number of new cases. For the purpose of further analysis and data accuracy, only one post addressing the number of new cases was analyzed in the first observed period, resulting in a total of 84 posts related to the number of new cases, which constitutes 28% of the total number of posts (n=300).

For the analysis of the results, an analytical matrix was applied to a total of 84 posts, on which the results of this study were based. The analyzed sample of 84 posts is relatively large. A larger sample can provide more reliable results as it encompasses a greater number of posts and reduces the likelihood of random variations. A confidence level of 95% suggests that the obtained results can generally be applied to the population from which the samples were drawn with 95% confidence. This means that there is a high probability that the results are representative of the entire population of posts on the topic of the number of new cases on the social media platform. It is important to have a sufficiently representative sample in order to draw conclusions about the overall population. Considering the sample size and a confidence level of 95%, it can be considered that the obtained results are reliable and generalizable to the population of posts on the topic of the number of new cases on the social media platform.

Table 1. Analyzed posts in observed periods

Period	Total Number of Posts	Number of Posts about New Cases	Percentage of Posts about New Cases	Average Number of New Cases
17.03.2020. – 24.03.2020.	69	1	1,45%	21
30.03.2020. – 05.04.2020.	72	5	6,94%	73,2
01.06.2020. – 07.06.2020.	28	7	25,00%	0,14
08.06.2020. – 14.06.2020.	21	7	33,33%	0,71
07.12.2020. – 13.12.2020.	9	7	77,78%	3647,57
22.02.2021. – 28.02.2021.	13	8	61,54%	464,5
01.03.2021. – 07.03.2021.	16	10	62,50%	496,9
05.04.2021. – 11.04.2021.	13	8	61,54%	1886,1
21.06.2021. – 27.06.2021.	19	8	42,11%	74,6
28.06.2021. – 04.07.2021.	23	8	34,78%	84,6
08.11.2021. – 14.11.2021.	10	8	80,00%	5484,2
20.12.2021. – 26.12.2021.	7	7	100,00%	2555,7

Table 1 presents the results of the study regarding the number of posts about new cases on the observed Facebook profile during the defined time periods. The table includes data on the total number of posts, the number of posts about new cases, the percentage of those posts in the total number of posts, and the average number of new cases mentioned in those posts for each period. The data in the table provides statistics on the number of posts related to new cases during specific time periods. It can be observed that the percentage of posts about new cases varied across different periods. For example, in some periods, the percentage was very

low (e.g., 1.45%), while in others, it was significantly higher or even the only type of post (e.g., 100%). The average number of new cases mentioned in the posts also varies from period to period.

The results of the analysis of the total number of posts on the "Koronavirus.hr" Facebook profile, regardless of their topic, are presented in Table 1. In the 12 observed time periods, the total number of posts was 300, with a range of values from 7 to 72. The mean value indicates an average of 25 posts, which means that, on average, the "Koronavirus.hr" profile posted 25 times during each observed period, providing insights into the overall rhythm and activity of the profile. The variability in the number of posts is quite high, as reflected by the standard deviation of 22.12, suggesting that the profile's activity varied throughout different periods. Some periods had a higher number of posts (e.g., March 30, 2020, to April 5, 2020), while others had a lower number of posts (e.g., December 20, 2021, to December 26, 2021).

Out of the total number of posts, 84 were related to the number of new cases, with a range of values from 1 to 10. The mean number of posts about the number of new cases was 7, indicating regularity and frequency in addressing this specific topic. The standard deviation was 2.22, suggesting lower variability in the number of posts related to this topic and indicating consistent reporting of the number of new cases throughout different periods. Some periods had a high proportion of posts about the number of new cases compared to the total number of posts, such as December 7, 2020, to December 13, 2020, with a proportion of 77.78%. On the other hand, some periods had a lower proportion of posts about the number of new cases, such as June 1, 2020, to June 7, 2020, with a proportion of 25.00%. The average number of new cases also varied across different time periods. In some periods, like November 8, 2021, to November 14, 2021, the average number of new cases was very high (5484.2), while in others, like June 1, 2020, to June 7, 2020, it was very low (0.14). A graphic representation of the total number of posts and the number of posts about the number of new cases during the observed periods is illustrated in Figure 1.

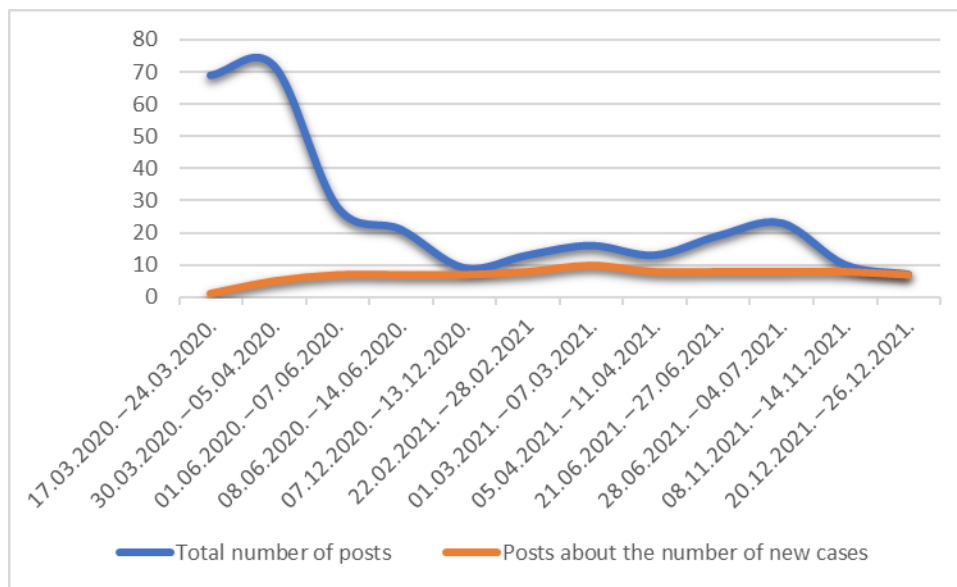


Figure 1. Posts in observed periods

The data for the total number of posts ($D = 0.288$) and the number of posts about the number of new cases ($D = 0.333$), based on the Kolmogorov-Smirnov (K-S) test, indicated a normal distribution of the data. The results of the correlation analysis showed that there is a statistically significant negative correlation between the total number of publications and the number of publications on the number of new cases ($r = -.801$, $p < .001$). The negative correlation indicates that as the total number of posts increases, the number of posts about the number of new cases tends to decrease, and vice versa. In other words, when the total number of posts is higher, the number of posts about the number of new cases is lower, and vice versa. This may indicate that the "Koronavirus.hr" profile focused on other topics or aspects of the pandemic during certain periods rather than solely on the number of new cases. The conceptual analysis of posts about the number of new cases provides insights into the characteristics of textual posts, types of visual/video materials, and video duration on the topic of the number of new cases on the social network.

First, the textual characteristics of the posts were examined. The average post size is approximately 37 words, with a standard deviation of 21, indicating variability in post length. The range of post values is from 0 to 69,

meaning that there are posts without text as well as several longer posts. The mode and median post length is 51 words, which suggests that this length is the most common and occurs 22 times in the analyzed posts.

The visual/video materials in the posts were also analyzed. Visual/video materials were present in every post, but they varied in content. The content of visual/video materials was divided into four categories. The results of the analysis of visual content show the frequency of using specific types of visual/video materials in published articles. For example, the most commonly used type of material is "General visual/video material," with a total of 51 posts, while the least used type is "Face (person) of one of the participants in the feature," with only 2 posts. The results of the analysis are presented in Figure 2.

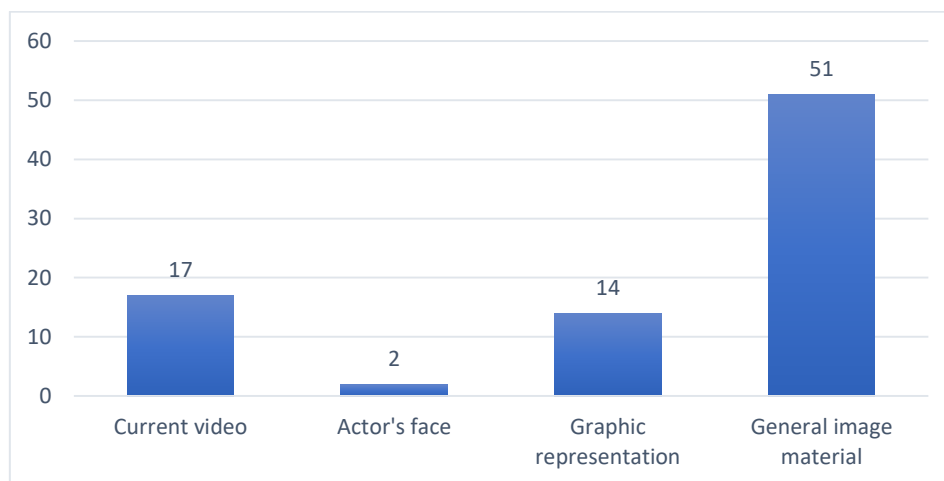


Figure 2. Types of visual/video content in posts

Additionally, an analysis of video durations was conducted. The research found that the average video duration based on the analyzed data is approximately 50.40 minutes. To obtain the average duration, each video was converted to minutes by adding the seconds divided by 60. A total of 17 videos were analyzed, and their durations were summed to obtain the overall duration of all videos, which amounted to 856.82 minutes. The average video duration is obtained by dividing the total duration by the total number of videos. Therefore, if we divide 856.82 minutes into 17 videos, the average duration is 50.40 minutes.

Table 2. Statistical measures for social reactions, comments, and shares

	<i>Social reactions</i>	<i>Comments</i>	<i>Shares</i>
M	38.18	5.61	1.55
SE	3.53	0.63	0.16
Md	27	5	1
Mo	6	5	1
SD	32.36	5.81	1.51
S ²	1047.45	33.78	2.27
K	3.23	2.83	2.93
Sk	1.73	1.77	1.37
R	151	25	8
Min	4	0	0
Max	155	25	8
Σ	3207	471	130
N	84	84	84
Largest (1)	155	25	8
Smallest (1)	4	0	0
CL (95,0%)	7.02	1.26	0.33

The analysis also examined the social reactions, comments, and shares in posts about the number of new cases (Table 2). In the analyzed posts, the total number of reactions is 3,207, with an average value of 38.18 reactions per post. The median is 27, and the mode is 6, indicating variability and the presence of several extremely high values. The range of reactions ranges from 4 to 155. Regarding comments, the total number is 471, with an average value of 5.61 comments per post. The median is 5, and the mode is also 5. In terms of shares, the total

number is 130, with an average value of 1.55 shares per post. The median is 1, and the mode is also 1. The accuracy of the estimated average values of reactions, comments, and shares is confirmed by 95% confidence intervals. The data indicate variability and asymmetry in the distribution, with several extremely high values.

Two distribution tests were conducted to analyze the data on the total number of new cases and the size of posts on the Facebook social network. The results of the Kolmogorov-Smirnov (K-S) tests confirmed that the data is not normally distributed for both variables (see Table 3). The distribution test for the total number of new cases yielded a test statistic value (D) of 0.31016 with a p-value less than 0.00001, while the distribution test for the size of posts had a test statistic value (D) of 0.31462 with a p-value less than 0.00001. Based on these results, it can be concluded that the data on the total number of new cases and the size of posts are not normally distributed. Therefore, for further analysis of relationships and correlations with other variables, the Spearman's Rho correlation test was chosen.

Table 3. Kolmogorov-Smirnov Test: New cases and post size

Variable	N	M	Md	Sd	Sk	Kt	K-S Test Statistic (D)	p-value
Total number of new cases	84	1342.12	349.5	1965.12	1.55	1.37	0.31	< 0.00001
Size of posts	84	37.06	51	21.11	-0.46	-1.52	0.31	< 0.00001

Table 4 displays the results of the Spearman's Rho correlation test between the variable "Number of new cases published in the post" and other variables (Total number of reactions, Total number of comments, Number of post shares).

Table 4. Spearman's rho correlation test for new cases posts

	X Ranks [Number of new cases published in the post]	Y Ranks [Total number of reactions]	Y Ranks [Total number of comments]	Y Ranks [Number of post shares]
Mean	42.5	42.5	42.5	42.5
SD	24.37	24.38	24.26	23.66
Combined	Combined	Combined	Combined	Combined
Covariance	-	114.73	261.42	250.17
R	-	0.193	0.442	0.434
rs	-	0.19307	0.4422	0.43382
p (2-tailed)	-	0.07847	3.00E-05	4.00E-05

The Table 4 presents the correlation coefficients (Rho) between the variable "Number of new cases published in the post" and the other two variables (Total number of reactions, Total number of comments, Number of post shares), along with the p-values. Based on the p-values, the correlation between the number of new cases published in the post and the total number of reactions is statistically insignificant, indicating that there is not enough evidence to support a significant relationship between the number of new cases published in the post and the number of reactions received. However, there are statistically significant positive correlations between the number of new cases and the total number of comments and post shares, indicating higher new case numbers tend to generate more engagement in terms of comments and shares.

Similarly, the correlation between the size of the post (expressed in the number of words) and other variables, including the total number of reactions, total number of comments, and number of post shares, was analyzed. The Spearman's Rho correlation test was applied to determine the statistical significance of these relationships. Table 5 presents the results of the Spearman's Rho correlation test for each combination of variables.

The Table 5 displays the correlation coefficients (Rho) between the variable Size of the post (number of words) and the other two variables (Total number of reactions, Total number of comments, and Post shares), along with the p-values. Based on the p-values, all three correlations between the size of the post (number of words) and the

other variables are statistically significant. The high value of the correlation coefficient (0.37028) between the size of the post (number of words) and the total number of reactions, as well as the high value of the correlation coefficient (0.39882) between the size of the post (number of words) and the total number of comments, indicate a positive correlation. This means that a larger post (number of words) often accompanies a higher number of reactions and comments. Additionally, there is a statistically significant but weaker correlation between the size of the post (number of words) and the number of post shares (Rho = 0.24516), suggesting that a larger size of the post (number of words) often corresponds to a higher number of shares. It is important to note that statistical significance does not necessarily imply a strong or clinically relevant relationship. Further research and analysis are needed to better understand the nature and intensity of these relationships.

Table 5. Spearman's rho correlation test for post size

	X Ranks [Size of the post]	Y Ranks [Total number of reactions]	Y Ranks [Total number of comments]	Y Ranks [Post shares (Total number of shares)]
Mean	42.5	42.5	42.5	42.5
SD	24.1	24.38	24.26	23.66
Combined	-	Combined	Combined	Combined
Covariance	-	217.6	233.17	139.81
R	-	0.37	0.399	0.245
rs	-	0.37028	0.39882	0.24516
p (2-tailed)	-	0.00053	0.00017	0.0246

To further investigate the presence or absence of relationships between variables, we conducted additional research and analyzed the data. The non-parametric Mann-Whitney U test was applied to compare independent samples, as the data for the total number of reactions did not follow a normal distribution according to the results of the Kolmogorov-Smirnov (K-S) test (D = .1952, p-value = .00279) presented in Table 6. The results of the Mann-Whitney U test are presented in Table 7.

Table 6. The Kolmogorov-Smirnov Test: Total reactions data

Variable	N	M	Md	Sd	Sk	Kt	K-S Test Statistic (D)	p-value
Total number of reactions	84	38.18	27	32.36	1.73	3.23	0.1952	0.00279

Table 7. Mann-Whitney U test related to quick reactions

Variables	U-value	Z-score	p-value
Post Size (number of words) vs. Total number of reactions	3334.5	0.61225	0.54186
Number of newly reported cases vs. Total number of reactions	1585.5	616.052	< 0.00001

The results of the Mann-Whitney U test did not show a statistically significant difference between the post size (number of words) and the total number of reactions (Sample 1 U-value = 3334.5, Sample 2 U-value = 3721.5, expected U-values = 3528), suggesting a lack of a statistically significant relationship between these variables. Additionally, the combined results for both samples show an average rank of 84.5. Although there is a tendency for larger post sizes to have a higher number of reactions based on the U-values, the Z-value for the combined results is 0.61225, with a p-value of 0.54186. Given the significance level of $p < .05$, the result is not statistically significant, indicating a lack of evidence for a statistically significant relationship between post size and the total number of reactions. In contrast, a statistically significant positive relationship exists between the Number of newly reported cases published in posts and the Total number of reactions, as indicated by higher ranks in Sample 1 and lower ranks in Sample 2 (U-value = 1585.5, Z-value = 6.16052, $p < .00001$).

Conclusion

Based on the research conducted on posts on the official Facebook profile "Koronavirus.hr" related to the number of new cases during the four pandemic waves, the following conclusions can be drawn: The research results demonstrate a consistent presence of posts about the number of cases throughout all waves, indicating their importance in government communication. The analysis was conducted solely on posts about the number of new cases, which constitute 28% of the total number of posts. The share of posts about the number of new cases varied during different periods. The research findings are generalizable to the population of posts concerning the number of new cases on the social media platform with a 95% level of confidence.

The obtained findings provide valuable insights into the significance of posts about the number of new cases on the Facebook profile "Koronavirus.hr" during pandemic waves and highlight the need for adjusting the communication strategies of public authorities in pandemic situations. The analysis of textual posts reveals an average post size of approximately 37 words, with variability in length. The most common post length is 51 words. General visual/video content is frequently used in the posts, and the average duration of videos related to the number of new cases is approximately 50.40 minutes.

Social reactions to posts about the number of new cases have an average count of 38.18 per post; the average number of comments per post is 5.61; while the average number of shares per post is 1.55, with variability and several extremely high values. The correlation analysis between the number of new cases posted and the total number of comments and shares reveals a statistically significant positive correlation. This implies that a higher number of new cases posted is often accompanied by a higher number of comments and shares. The correlation analysis between the size of the post (expressed in the number of words) and the total number of reactions, comments, and shares also shows statistically significant positive correlations. This means that a larger post size (more words) is often associated with a higher number of reactions, comments, and shares. It is important to note that correlation does not imply a causal relationship but only an association between variables.

Further research results indicate a lack of a statistically significant relationship between the size of the post (number of words) and the total number of reactions. Although there is a correlation between the size of the post and the total number of reactions, this difference may not be sufficiently large or consistent to be considered statistically significant according to the Mann-Whitney U test.

Recommendations

These results provide guidelines for understanding audience engagement and developing communication strategies related to the number of new cases on social media platforms, thereby achieving the goal of this research, which is to provide a foundation for future creation of posts by public authorities on social media in similar crisis situations.

Scientific Ethics Declaration

The author declares that the scientific ethical and legal responsibility of this article published in EPSTEM journal belongs to the author.

Acknowledgements or Notes

This article was presented as an oral presentation at the International Conference on Research in Engineering, Technology and Science (www.icrets.net) held in Budapest/Hungary on July 06-09, 2023.

References

- Bošnjak, Z. (1998). Postmoderna i internet. *Revija za Sociologiju*, 29(1-2), 59-74.
- Božilović, N., & Petković, J. (2015). Masovna kultura, komunikacija i medijska manipulacija. In N. Božilović & J. Petković (Eds.), *Državnost, demokratizacija i kultura mira: Tematski zbornik radova sa četvrtog međunarodnog naučnog skupa Nauka i savremeni univerzitet* (pp. 181-197). Niš: Izdavački centar Niš.
- Catalán-Matamoros, D. (2011). The role of mass media - communication in public health. *Health Management – Different Approaches and Solutions*, 5, 399-414.
- Day, A. M., O'Shay-Wallace, S., Seeger, M. W., & McElmurr, S. P. (2019). Informational sources, social media use, and race in the Flint, Michigan water crisis. *Communication Studies*, 70(3), 352-376.
- Duljaj, E. (2019). *Odnosi s javnošću zdravstvenih ustanova u Hrvatskoj*. Zagreb: Sveučilište u Zagrebu, Fakultet političkih znanosti.
- Eid, M. (2014). Ethics, media, and reasoning: systems and applications. In B. van den Berg, D. C. Howe, & R. W. Mittelman (Eds.), *Evolving Issues Surrounding Technoethics and Society in the Digital Age* (pp. 188-197). Hershey, PA: IGI Global.

- Ellingson, L. L. (2002). Communication, collaboration, and teamwork among health care professionals. *Communication Research Trends*, 21(1), 1-44.
- Ganis, M., & Kohirkar, A. (2015). Preface: Mining for gold (or Digging in the mud). In *Social Media Analytics* (p. XXI). New Jersey, USA: International Business Machines Corporation.
- Grčić, M., Zoranić, S., & Sindik, J. (2014). Stavovi zdravstvenog i nezdravstvenog osoblja o medijima i zdravlju. *SG/NJ*, 3, 211-219.
- Henderson, J., Noell, J., Reeves, T., Robinson, T., & Strecher, V. (1999). Developers and evaluation of interactive health communication applications. *American Journal of Preventive Medicine*, 16(1), 30-34.
- Kern, J. (2014). Informacijske i komunikacijske tehnologije u sestrinstvu. *Acta Med Croatica*, 68, 3-5.
- Koronavirus.hr. (2022). *Koronavirus – statistički pokazatelji za Hrvatsku i EU*. Retrieved from <https://www.koronavirus.hr/koronavirus-statisticki-pokazatelji-za-hrvatsku-i-eu/901> (Accessed 12.02.2022).
- Laiho, H.-P. (2008). Krizno komuniciranje. *MediAnali*, 15(2), 49-68.
- Marković, M. (2008). *Poslovna komunikacija sa poslovnim bontonom*. Beograd: Clio.
- Mayer, M. A., Leis, A., Mayer, A., & González, A. (2018). How medical doctors and students should use social media: A review of the main guidelines for proposing practical recommendations. *Studies in Health Technology and Informatics*, 247, 853-857. doi:10.3233/978-1-61499-101-4-853
- Plenković, M. (2015). Krizno komuniciranje. *Media, Culture and Public Relations*, 6(2), 113-118.
- Quinn, P. (2018). Crisis communication in public health emergencies: The limits of 'legal control' and the risks for harmful outcomes in a digital age. *Life Sciences, Society and Policy*, 14(1), 1-20.
- Robinson, T. N., Patrick, K., Eng, T. R., & Gustafson, D. (1998). An evidence-based approach to interactive health communication - A challenge to medicine in the information age. *JAMA*, 280(14), 1264-1269.
- Sezgin, D., Karaaslan, Y. S., & Ersoy, İ. (2020). The pandemic infodemic: The role of risk communication and media in a pandemic. *Gazi Medical Journal*, 31(Supplement 1), 325-327.
- Stevanović, R., & Pristaš, I. (2011). Nove informacijsko-komunikacijske tehnologije i komunikacija u medicini i zdravstvu. *MEDIX*, 92, 32-37.
- Tabbaa, D. (2010). Emerging zoonoses: responsible communication with the media—lessons learned and future perspectives. *International Journal of Antimicrobial Agents: Supplement 1*, 36, S80-S83.
- Thomas, R. K. (2006). The history of health communication. In R. L. Heath & R. E. O'Hair (Eds.), *Health Communication: A Handbook for Health Professionals* (pp. 40-60). New York: Lawrence Erlbaum Associates.
- Vozab, D., & Peruško, Z. (2021). *Digitalne publike vijesti u Hrvatskoj 2017.-2021*. Zagreb: CIM - Centar za istraživanje medija i komunikacije, Fakultet političkih znanosti, Sveučilište u Zagrebu.
- Vujević, F. (2018). *Utjecaj društvenih mreža na profesionalizam liječnika - diplomski rad*. Zagreb: Sveučilište u Zagrebu, Medicinski fakultet.
- Vuletić, S. (2014). *Javni diskurs – izazovi suvremenog zdravstva*. Zagreb: Sveučilište u Zagrebu Medicinski fakultet; Škola narodnog zdravlja "Andrija Štampar".
- Zrinščak, S. (2007). Zdravstvena politika Hrvatske. *U vrtlogu reformi i suvremenih društvenih izazova. Revija za socijalnu politiku*, 14(1-2), 193-220.

Author Information

Stjepan Petričević

Alma Mater Europaea ECM
Slovenska 17, 2000 Maribor, Slovenia
Contact e-mail: stjepan.petricevic@almamater.si

To cite this article:

Petricevic, S. (2023). Desk analysis of crisis communication by public authorities during health crises. *The Eurasia Proceedings of Science, Technology, Engineering & Mathematics (EPSTEM)*, 23, 521-530.

The Eurasia Proceedings of Science, Technology, Engineering & Mathematics (EPSTEM), 2023

Volume 23, Pages 531-538

ICRETS 2023: International Conference on Research in Engineering, Technology and Science

Estimation of Poultry Meat Production in Turkey Using GM (1,1) with Second Parameter Fitting-Markov Model

Halil Sen

Burdur Mehmet Akif Ersoy University

Abstract: Considering that poultry meat is an economical and stable food source and its place in a balanced diet, it is an indispensable food item for today as well as tomorrow. It is the most produced poultry meat in the world among other meat types since 2015. Turkey ranks 10th in the world in chicken meat production. Chicken farming and backyard poultry farming, which was mostly family-run until the 1980s, has left its place to giant facilities today. There are over 15,000 broiler breeding farms in Turkey and the annual turnover of the sector, which provides a livelihood for approximately 3 million people with all its stakeholders, has reached 5.5 billion USD. It is currently the biggest alternative to red meat. Today, white meat is preferred all over the world in terms of protein source and the per capita consumption of poultry meat is increasing every year in the world. Our per capita consumption of poultry meat has reached 21 kg/year. Accurate estimation of poultry meat production in Turkey is important for establishing short, medium and long-term policies that will balance supply and demand. In this study, GM (1, 1) with second parameter fitting-Markov model, which is a combination of the Markov chain method and the GM (1, 1) model with the second parameter fitting, which can be used to predict future data with very limited data and information, was used in the estimation of poultry meat production. The obtained results show that GM (1, 1) with second parameter fitting-Markov model used has high predictive precision and applicability.

Keywords: Grey estimation model, Markov chain, Poultry meat production

Introduction

Poultry meat has a remarkable position in meeting the need for animal protein, which is one of the cornerstones of a healthy diet, because it is economical. In other words, poultry meat is an important and strategic food source in proper and healthy nutrition because it is not only "beneficial for health" but also "low cost" compared to some other protein sources. In Turkey, the animal protein deficit resulting from the gradual decline in red meat production due to cost problems and crises has been balanced by the increase in chicken and turkey meat production. The world consumption of chicken meat shows an increasing trend due to its low fat, high protein value, rich in vitamins and minerals, and low price compared to red meat (Hekimoglu & Altindoger, 2009).

In Turkey, industrialization efforts in the white meat sector started after 1960, and integrated institutions related to broiler production and egg production were put into operation in the 1970s. After 1980, with the increase in exports to the sector and the implementation of Resource Utilization Support Fund in 1985, a large number of poultry farms with projects and modern structures were established and the sector developed rapidly (Kenanoglu et al., 1999).

Today, this sector has reached the desired level in terms of production amount and technology; however, the most important problem in the sector today is that the products have to be sold below the cost in the country due to the narrowing of export opportunities. This situation brings about an intense competition with the red meat sector.

- This is an Open Access article distributed under the terms of the Creative Commons Attribution-Noncommercial 4.0 Unported License, permitting all non-commercial use, distribution, and reproduction in any medium, provided the original work is properly cited.

- Selection and peer-review under responsibility of the Organizing Committee of the Conference

© 2023 Published by ISRES Publishing: www.isres.org

The fact that the poultry meat sector in Turkey has been identified as one of the few sub-sectors in the food sector that can compete with the EU; the fact that the sector creates a large workforce employment and is one of the best organized food sub-sectors reveals the importance of the poultry meat sector for Turkey (Hekimoglu & Altindeger, 2009). Since chicken and turkey meat constitute almost all of Turkey's poultry meat production, only chicken and turkey meat were included in the scope of this study.

Method

In this study, the situation of Turkey's poultry meat production in the following years was tried to be estimated by using the GM(1,1) with Second Parameter Fitting-Markov Model.

GM(1,1) with Second Parameter Fitting-Markov Model

The grey system theory developed Ju Long (1982). In research in the field of condition analysis, forecasting and decision making, it focuses on uncertainty and lack of information to analyse and understand systems (Ju Long, 1982). Grey system theory, which is an interdisciplinary approach, is an alternative method for quantifying uncertainty. The basic idea in its emergence is to predict the behaviour of uncertain systems, which cannot be overcome by stochastic or fuzzy methods, with the help of a limited number of data.

The main feature that distinguishes the grey prediction method, which is one of the main fields of work of grey system theory, from traditional prediction methods is that it needs a limited number of data to predict the behaviour of uncertain systems. Unlike traditional prediction methods, the main feature of the grey prediction method is that it does not need strict assumptions about the data set and can be successfully applied in the analysis of systems with limited data. The grey prediction method has been developed to make predictions about the future with the help of the grey model GM(1,1) using the available data. GM(1,1) is a time series forecasting model that contains a set of differentiable equations. The GM(1,1) notation is used to express the grey model with first-order differentiable equations with a single variable. Wang et al. (2018), put forward a grey Markov forecasting model to predict mine gas emissions by combining grey system theory and Markov chain theory. In order to eliminate the error and improve the prediction accuracy of the model, secondary parameter fitting was performed based on the GM (1, 1) model. GM(1,1) with second parameter fitting-Markov model consists of the basic steps described in detail below.

Step-1: Let $X^{(0)}$ be the raw time series sequence with a single variable valence n magnitude that forms the time series.

$$X^{(0)} = (x^{(0)}(1), x^{(0)}(2), x^{(0)}(3), \dots, x^{(0)}(n)); n \geq 4 \quad (1)$$

$X^{(1)}$ is constructed using the first-order aggregate production operator.

$$x^{(1)}(k) = \sum_{i=1}^k x^{(0)}(i), \quad (i = 1, 2, 3, \dots, n) \quad (2)$$

$$X^{(1)} = (x^{(1)}(1), x^{(1)}(2), x^{(1)}(3), \dots, x^{(1)}(n)); n \geq 4 \quad (3)$$

Step-2: Determination of Coefficients: $x^{(0)}(k) + ax^{(1)}(k) = b$ represents the original form of the model G(1,1). k is the time points; a is the coefficient of improvement; b represents the driver coefficient. $Z^{(1)}$ is generated using the first-order mean value generation operator.

$$z^{(1)}(k) = 0.5x^{(1)}(k) + 0.5x^{(1)}(k-1) \quad (4)$$

$$Z^{(1)} = (z^{(1)}(1), z^{(1)}(2), z^{(1)}(3), \dots, z^{(1)}(n)) \quad (5)$$

The basic form of the G(1,1) model is written as $x^{(0)}(k) + az^{(1)}(k) = b$ in which the $Z^{(1)}$ series is used. The least squares method is used in estimating the a and b parameters. If the equation is written in matrix form, $Y = B\tilde{a}$ equality can be obtained. Here, Y , B and \tilde{a} represent the matrices.

$$B = \begin{bmatrix} -z^{(1)}(2) & \dots & 1 \\ \vdots & \ddots & \vdots \\ -z^{(1)}(n) & \dots & 1 \end{bmatrix} \quad (6)$$

$$Y = \begin{bmatrix} x^{(0)}(2) \\ \vdots \\ x^{(0)}(n) \end{bmatrix} \tag{7}$$

$$\tilde{a} = \begin{bmatrix} a \\ b \end{bmatrix} \tag{8}$$

In order to obtain the vector \tilde{a} , the following operations must be performed in order.

$$Y = B\tilde{a} \tag{9}$$

$$B^T Y = B^T B \tilde{a} \tag{10}$$

$$\tilde{a} = (B^T B)^{-1} B^T Y \tag{11}$$

Step-3: Obtaining the GE equation. The prediction model is obtained by solving the differential equation 12.

$$\frac{dx^{(1)}(k)}{dk} + ax^{(1)}(k) = b \tag{12}$$

$$\hat{x}^{(1)}(k + 1) = \left[x^{(1)}(0) - \frac{b}{a} \right] e^{-ak} + \frac{b}{a} \tag{13}$$

Since the original data is made into a cumulative series for the GM (1,1) model to work, in order to obtain the forecast results, a backward cumulative series should be created using equation 14.

$$\hat{x}^{(0)}(k + 1) = \hat{x}^{(1)}(k + 1) - \hat{x}^{(1)}(k) \tag{14}$$

Step-4: Second Parameter Fitting Method of GM (1, 1) Model. Equation (13) is the time response of GM (1, 1) model equation. There are large amount of data proved that original data will produce error if we use Equation (13) to fit. To improve the fitting precision and prediction precision, we do secondary parameter fitting to Equation (13) and change it into,

$$\hat{x}^{(1)}(k + 1) = \alpha e^{-ak} + \beta \tag{15}$$

According to the first estimate of a value a and estimation of original series $X^{(1)}$ to α and β

$$\begin{aligned} x^{(1)}(0 + 1) &= \alpha e^{-a0} + \beta \\ x^{(1)}(1 + 1) &= \alpha e^{-a1} + \beta \\ x^{(1)}(2 + 1) &= \alpha e^{-a2} + \beta \\ &\vdots \\ &\vdots \\ x^{(1)}((n - 1) + 1) &= \alpha e^{-a(n-1)} + \beta \end{aligned}$$

written in matrix form is

$$X^{(1)} = G \begin{pmatrix} \alpha \\ \beta \end{pmatrix} \tag{16}$$

In which,

$$X^{(1)} = [x^{(1)}(1), x^{(1)}(2), x^{(1)}(3), \dots, x^{(1)}(n)]^T$$

$$G = \begin{bmatrix} e^{-a(1-1)} & \dots & 1 \\ \vdots & \ddots & \vdots \\ e^{-a(n-1)} & \dots & 1 \end{bmatrix}$$

According to the least square method,

$$\begin{pmatrix} \alpha \\ \beta \end{pmatrix} = (G^T G)^{-1} G^T X^{(1)} \tag{17}$$

At last, second parameter fitting of GM (1, 1) model was got, combined Equation (17) with Equation (15) (Wang et al., 2018).

Step-5: In forecasting time series, the high volatility of the series usually reduces the forecasting performance. This can be overcome by modifying the results or combining different techniques. In this study, the GM (1,1) model is combined with a Markov chain (He & Huang, 2005).

$$\mathcal{E}^{(0)}(k) = (x^{(0)}(k) - \hat{x}^{(0)}(k))/x^{(0)}(k), k=1,2,3,4,\dots,n ;$$

obtained from the GM (1,1) model. Let the sequence of errors be expressed as $(\mathcal{E}^{(0)} = (\mathcal{E}^{(0)}(1), \mathcal{E}^{(0)}(2), \mathcal{E}^{(0)}(3), \dots, \dots, \mathcal{E}^{(0)}(k))$. In this case, we can divide the errors from the prediction model into S different states, and this new process is a Markov process. The intervals for the states are determined by considering the relative error values.

$$S_{i-} = A_i, S_{i+} = B_i, \tag{18}$$

Here, when it is expressed as S_{1i} and S_{2i} , any s state within these states can be expressed as $S_i = [S_{1i}, S_{2i}]$. In obtaining the transition probabilities matrix $P_{ij}(a)$, a indicates the number of steps, G_{ij} is probability of transition from state S_i to state S_j ; and G_i is the number of observations in the S_i state.

$$p_{ij}(a) = \frac{G_{ij}(a)}{G_i} \quad (i, j = 1, \dots, s) \tag{19}$$

a-step transition probability matrix is;

$$P_{ij}(a) = \begin{pmatrix} p_{11}(a) & \cdots & p_{1j}(a) \\ \vdots & \ddots & \vdots \\ p_{i1}(a) & \cdots & p_{ij}(a) \end{pmatrix} \quad (i, j = 1, \dots, s) \quad \sum_{i=1}^s p_{ij}(a) = 1 \tag{20}$$

The transition probabilities matrix is used to predict the state of the next observation. Suppose that the Markov chain under consideration is currently in state S_i . Then when the line i elements in matrix $P_{ij}(1)$ are examined, $\max_j (p_{ij}(1)) = p_{i3}(1)$ the equality is satisfied, the Markov chain is predicted to transition to state S_3 in the next step. Finally, the modified forecasting data can be calculated:

$$\tilde{x}^{(0)}(k) = \hat{x}^{(0)}(k)[1 + 0.5(A_i + B_i)] \tag{21}$$

It is seen that other grey-Markov chain models are frequently used in all fields in the literature. The grey Markov chain model has been used to forecast annual maximum water levels at hydrological stations (Dong et al., 2012), to forecast fire accidents (Mao & Sun, 2011), to forecast financial crises for an enterprise (Chen & Guo, 2011) and to forecast the need for electrical energy in China (He & Huang, 2005). Duan et al. (2017), used a grey Markov chain model enhanced with Taylor approximation for forecasting urban medical services demand in China. In their study, Hu et al. (2017), presented a novel grey prediction model combining Markov chain with functional-link net and applied it to foreign tourist forecasting.

Ye et al. (2018), presented a grey-Markov prediction model based on background value optimization and a central point triangular whitenization weight function. Yu et al. (2015) and Zhang & Chen (2021) used the grey Markov chain model in tax forecasting. Jia et al. (2020), presented a study based on the grey-Markov chain model for forecasting coal consumption in Gansu Province. Song et al. (2020), used grey model theory to perform load forecasting of medium and long term power system and the accuracy of the model in load forecasting is tested using the posterior difference method. Liu (2022), conducted an empirical analysis of the relationship between renewable energy consumption and economic growth based on the grey Markov model.

Results and Discussion

In this study, Grey-Markov chain model is used to predict the poultry meat production in Turkey in the coming years. The annual data from TURKSTAT in Table 1 below constituted the data set of the study. Data on chicken

and turkey meat were evaluated. In the grey Markov chain model, the forecast data obtained by using the second parameter fitting method of the GM (1, 1) Model were used.

Table 1. Annual meat production of poultry

Year	Chicken (Ton)	Turkey (Ton)
2011	1 613 309	36 331
2012	1 723 919	41 931
2013	1 758 363	39 627
2014	1 894 669	48 662
2015	1 909 276	52 722
2016	1 879 018	46 501
2017	2 136 734	52 363
2018	2 156 671	69 536
2019	2 138 451	59 640
2020	2 136 263	58 212

Source: TURKSTAT, Poultry Production Statistics

In this study, data on chicken meat production are analysed first. First, the second parameter fitting method of the GM (1, 1) model is used to forecast future production levels. Then, the Grey-Markov chain model is used to improve the forecasting performance. Table 2 shows the results obtained for chicken meat production. Compared to real data, the Grey-Markov chain model produced more realistic results. As can be seen in the graph in Figure 1, it can be seen visually that the forecasting performance improves with the Grey-Markov model.

Table 2. Chicken meat production in Turkey actual and estimated values

Year	Actual Values (Tons)	Second Parameter Fitting Method of GM (1,1) Model	Estimated Values (Tons) with the Grey-Markov Chain Model
2011	1613309,282	1613309,28	1.622.804,1554
2012	1723918,629	1693498,10	1.731.424,0670
2013	1758362,830	1808451,09	1.759.380,4582
2014	1894668,634	1862827,97	1.904.546,0862
2015	1909276,471	1918839,87	1.898.453,4162
2016	1879017,521	1976535,94	1.890.272,4605
2017	2136734,369	2035966,83	2.115.175,6080
2018	2156671,119	2097184,70	2.144.151,2471
2019	2138450,721	2160243,29	2.137.292,0769
2020	2136262,909	2225197,93	2.128.081,9000
2021		2292105,64	2.267.753,4755
2022		2361025,15	2.452.880,2313
2023		2432016,94	2.526.633,9406
2024		2505143,32	2.602.605,2918
2025		2580468,49	2.680.860,9652
2026		2658058,55	2.717.585,8875

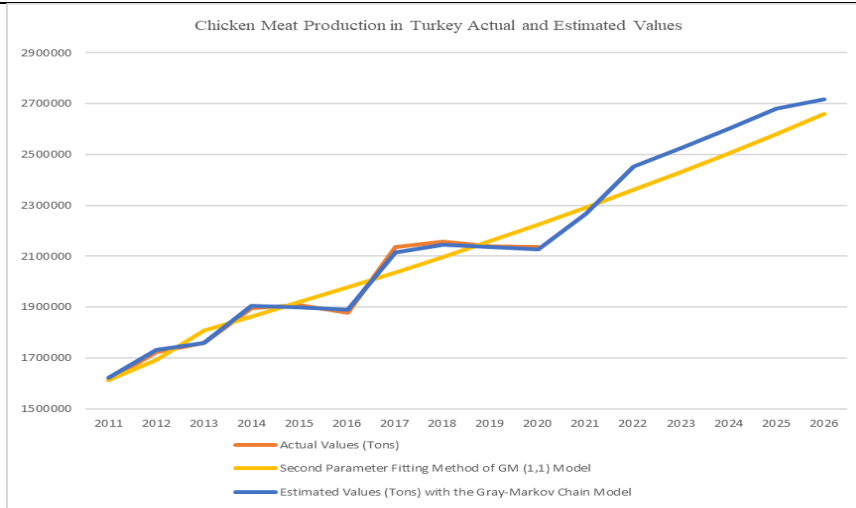


Figure 1. Chicken meat production actual and estimated value graph

Secondly, data on turkey meat production were analysed. First of all, the production levels of the next years were tried to be estimated by using the second parameter fitting method of the GM (1, 1) Model. Then, the Grey-Markov chain model is used to improve the prediction performance. Table 3 shows the results obtained for turkey meat production. Compared with real data, the Grey-Markov chain model gave more realistic results. As seen in the graph in Figure 2, it can be visually seen that the estimation performance has increased with the Grey-Markov model for turkey meat production estimations.

Table 3. Turkey meat production in Turkey actual and estimated values

Year	Actual Values (Tons)	Second Parameter Fitting Method of GM (1,1) Model	Estimated Values (Tons) with the Grey-Markov Chain Model
2011	36331,341	36331,34	36.080,9317
2012	41930,989	38893,17	42.442,1862
2013	39627,346	44761,90	40.060,3223
2014	48662,486	47154,19	49.143,1086
2015	52722,416	49674,34	51.769,5555
2016	46500,727	52329,18	46.832,7728
2017	52362,560	55125,90	52.040,8499
2018	69535,564	58072,10	66.220,8856
2019	59639,544	61175,76	60.754,1101
2020	58212,444	64445,29	57.676,2633
2021		67889,56	77.415,9446
2022		71517,90	64.006,0074
2023		75340,17	74.820,8965
2024		79366,71	71.030,4162
2025		83608,46	74.826,6273
2026		88076,90	91.791,8994

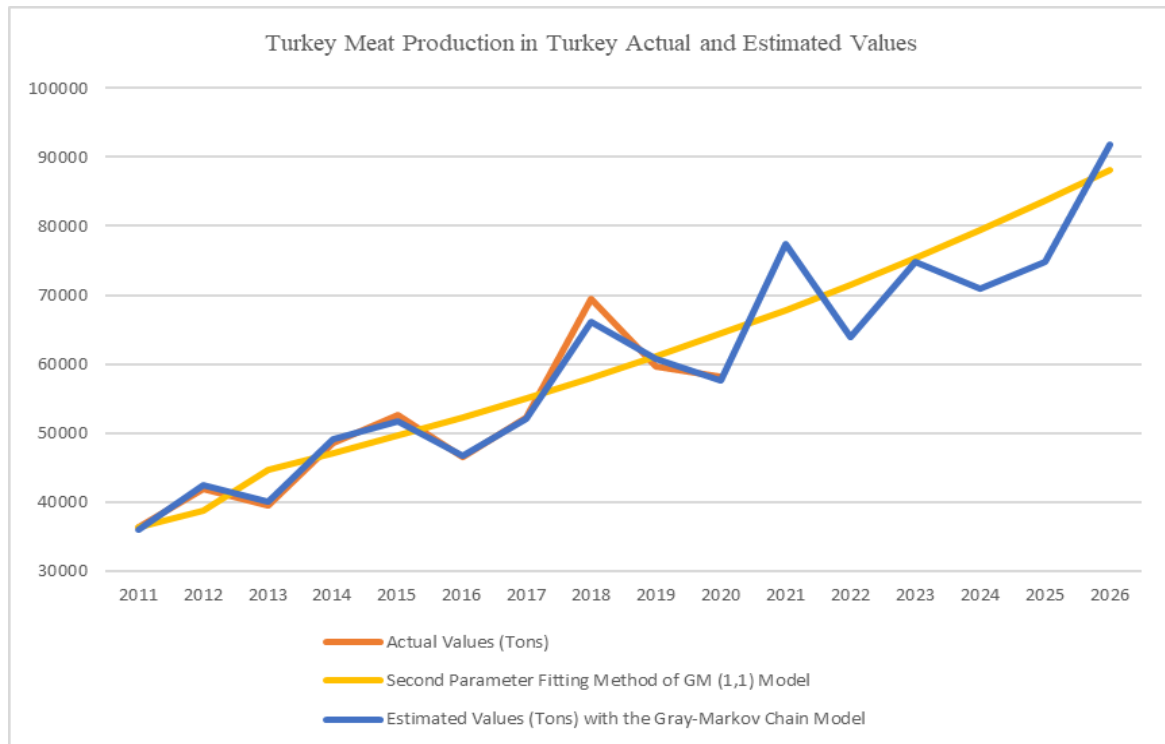


Figure 2. Turkey meat production actual and estimated value graph

Conclusion

Today, poultry meat sector has reached the desired level in terms of production amount and technology; however, the most important problem in the sector today is that the products have to be sold below their cost in

the country due to the narrowing of export opportunities. This situation brings with it intense competition with the red meat sector.

In this study, the production amounts of chicken and turkey meat production until 2026 were estimated. When we look at the production estimations, it is seen that chicken meat production, which was 2.136.263 tons in 2020, will reach 2.717.585 tons in 2026, and turkey meat production will increase from 58.212 tons to 91.791 tons. The rise in red meat prices has led consumers to poultry meat, but it is important that the fluctuations in this trend are tolerable. Accurate estimation of red meat production, one of the dynamics affecting the sector, will be important in the policies to be implemented for the development of the sector in the coming years. It is important that the performance of our forecast data is high when policies are being implemented to develop the sector both in the domestic and foreign markets. In this study, it has been studied to increase the performance of this forecast data.

Scientific Ethics Declaration

The author declares that the scientific ethical and legal responsibility of this article published in EPSTEM journal belongs to the author.

Acknowledgements or Notes

* This article was presented as an oral presentation at the International Conference on Research in Engineering, Technology and Science (www.icrets.net) held in Budapest/Hungary on July 06-09, 2023.

References

- Chen, L. H., & Guo, T. Y. (2011). Forecasting financial crises for an enterprise by using the Grey Markov forecasting model. *Quality and Quantity*, 45(4), 911–922.
- Dong, S., Chi, K., Zhang, Q., & Zhang, X. (2012). The application of a Grey Markov model to forecasting annual maximum water levels at hydrological stations. *Journal of Ocean University of China*, 11(1), 13–17.
- Duan, J., Jiao, F., Zhang, Q., & Lin, Z. (2017). Predicting urban medical services demand in China: An improved Grey Markov Chain model by Taylor approximation. *International Journal of Environmental Research and Public Health*, 14(8), 883.
- He, Y., & Huang, M. (2005). A Grey-Markov forecasting model for the electric power requirement in China. *Lecture Notes in Computer Science (Including Subseries Lecture Notes in Artificial Intelligence and Lecture Notes in Bioinformatics)*, 574–582.
- Hekimoglu, B., & Altindoger, M. (2009). Poultry meat industry report problems and solutions. *Samsun Tarım İl Müdürlüğü, Strateji Geliştirme Birimi; Samsun*.
- Hu, Y. C., Jiang, P., Chiu, Y. J., & Tsai, J. F. (2017). A novel grey prediction model combining Markov Chain with functional-link net and its application to foreign tourist forecasting. *Information*, 8, 8(4), 126.
- Jia, Z. Q., Zhou, Z. F., Zhang, H. J, Li, B., & Zhang, Y. X. (2020). Forecast of coal consumption in Gansu Province based on Grey-Markov chain model. *Energy*, 199, 117444..
- Ju-Long, D. (1982). Control problems of grey systems. *Systems and Control Letters*, 1(5), 288–294.
- Kenanoğlu, Z., Saner, G., & Kaya, F. (1999). Türkiye’de ve Ege bölgesinde hayvancılık sektörüne yönelik teşvik belgeli yatırımlar kapsamında tavukculuğun yeri ve önemi üzerine bir inceleme. *Uluslar Arası Hayvancılık*, 99, 21–24.
- Liu, C. (2022). Empirical Analysis of the Relationship between renewable energy consumption and economic growth based on the Grey Markov Model. *Journal of Mathematics*, Article ID 5679696 <https://doi.org/10.1155/2022/5679696>
- Mao, Z.L., & Sun, J. H. (2011). Application of Grey-Markov Model in forecasting fire accidents. *Procedia Engineering*, 11, 314–318.
- Song, F., Liu, J., Zhang, T., Guo, J., Tian, S., & Xiong, D. (2020). The Grey Forecasting Model for the medium- and Long-Term Load Forecasting. *Journal of Physics: Conference Series*, 1654(1).
- TURKSTAT. (n.d.). *Poultry production statistics*. Retrieved July 29, 2023, from <https://biruni.tuik.gov.tr/medas/?kn=80&locale=tr>
- Wang, Y., Yao, D., Lu, H., Wang, Y., Yao, D., & Lu, H. (2018). Mine gas emission prediction based on Grey Markov prediction model. *Open Journal of Geology*, 8(10), 939–946.

- Ye, J., Dang, Y., & Li, B. (2018). Grey-Markov prediction model based on background value optimization and central-point triangular whitenization weight function. *Communications in Nonlinear Science and Numerical Simulation*, 54, 320–330.
- Yu, Z., Yang, C., Zhang, Z., & Jiao, J. (2015). Error correction method based on data transformational GM(1,1) and application on tax forecasting. *Applied Soft Computing Journal*, 37, 554–560.
- Zhang, H., & Chen, Y. (2021). Analysis and application of Grey-Markov chain model in tax forecasting. *Journal of Mathematics*, Article ID 9918411, <https://doi.org/10.1155/2021/9918411>

Author Information

Halil Sen

Burdur Mehmet Akif Ersoy University,

Burdur, Turkiye

Contact e-mail: halilsen@mehmetakif.edu.tr

To cite this article:

Sen, H. (2023). Estimation of poultry meat production in Turkey using GM (1,1) with second parameter Fitting-Markov Model. *The Eurasia Proceedings of Science, Technology, Engineering & Mathematics (EPSTEM)*, 23, 531-538.

The Eurasia Proceedings of Science, Technology, Engineering & Mathematics (EPSTEM), 2023

Volume 23, Pages 539-547

ICRETS 2023: International Conference on Research in Engineering, Technology and Science

The Effect of Clay Type, Fineness and Methylene Blue Value on Mini-Slump Performance of Cementitious Systems

Fatmanur Sahin

Bursa Uludag University

Oznur Biricik

Bursa Uludag University

Ali Mardani

Bursa Uludag University

Abstract: It is known that the fresh and hardened properties of cementitious systems are adversely affected by the increase in aggregate clay content. It was emphasized that the fresh state properties of cementitious systems are affected by the clay type. In this study, the effects of clay type, fineness and methylene blue value on the mini-slump performance of cement paste mixtures were investigated. For this purpose, 3% of the cement weight, bentonite, kaolin and limestone powder passed through a 0.125 mm sieve were used. It was determined that bentonite clay used within the scope of the study had a 5 times higher methylene blue value compared to kaolin. It was determined that the mini-slump value of the mixtures increased with the increase of the water/cement ratio, independent of the clay type, and the said values decreased with the addition of clay. In terms of mini-slump performance, the clay fineness parameter was found to be more dominant than the methylene blue value.

Keywords: Bentonite, Kaolin, Water requirement, Mini slump, Methylene blue value

Introduction

As a result of facilities such as dams built on rivers where the aggregate used in concrete mixtures is supplied, the supply of aggregate has become difficult (Güneşli et al., 2010; Deşik et al., 2019). For this reason, the use of crushed aggregate, which has a lower cost, has become widespread in concrete (Güneşli et al., 2010). The main usage area of limestone in the world is the construction and building sector with a rate of 40-70% (Bozkurt et al., 2008). Limestone provides a certain skeleton and strength to the concrete mix, especially thanks to its use as aggregate. Limestone deposits are formed in the form of travertine in groundwater, and as a result of chemical, organic or mechanical precipitation in sea or fresh waters (Turan, 2010). Limestone theoretically contains 56% CaO (hydrated Lime) and 44% CO₂, but it is never found in pure form in nature (Turan, 2010, Özbek et al., 2016). Limestone contains at least 90% CaCO₃ (Calcium Carbonate) in its chemical composition, as well as compounds such as MgCO₃ (magnesium carbonate), clay minerals, iron silicate-oxide and SiO₂ (Turan, 2010). As the clay bands that may be between the sedimentary rock layers are fed directly to the crushers without separating from the broken rocks, harmful substances such as clay and silt in the soiled material can mix with the crushed sand (Ozbebek et al., 2011; Güneşli et al., 2010). In addition, in rainy periods, clay and silt take the form of mud and adhere to the rocks (Desik et al., 2019). If production is not carried out in accordance with the technique in the crusher plant, harmful materials deteriorate the quality of crushed sand (Ozbebek et al., 2011; Güneşli et al., 2010). As a result of the use of the uncleaned aggregate in the concrete, the clay penetrates into the concrete (Muslu, 2019). The clay ratio in the aggregate is determined by the methylene blue and sand equivalence test (Muslu, 2019).

- This is an Open Access article distributed under the terms of the Creative Commons Attribution-Noncommercial 4.0 Unported License, permitting all non-commercial use, distribution, and reproduction in any medium, provided the original work is properly cited.

- Selection and peer-review under responsibility of the Organizing Committee of the Conference

© 2023 Published by ISRES Publishing: www.isres.org

The presence of clays in cementitious systems leads to various negative situations (Kirthika, et al., 2019). The presence of clay in the concrete aggregate reduces the adherence between cement paste and aggregate (Ozbebek et al., 2011). Due to the high water absorption ability of the clay mineral, it causes volume expansion and as a result, cracks in the concrete and tensile stresses caused by shrinkage (Desik et al., 2019). In addition, clay minerals increase the specific surface area value of the aggregate (Muslu, 2019). As a result, as the amount of mixing water and w/c ratio required for concrete increases, hydration is delayed, setting time increases, and durability and strength values decrease (Ozbebek et al., 2011; Desik et al., 2019). Since extra cement and chemical admixtures will be used to keep the w/c ratio constant in mixtures with higher clay content, the cost of 1m^3 concrete increases accordingly. Since clay contaminates the aggregate, the consistency losses that occur depending on time in concrete made with dirty aggregate make it difficult to pump (Ozbebek et al., 2011; Desik et al., 2019). In addition, it was declared that due to the layered structure of clays, chemical admixtures are intercalated between these layers (Muslu, 2019). It was emphasized by various researchers that this situation leads to more admixture use (Ozbebek et al., 2011; Desik et al., 2019; Ma et al., 2022). Clay is a layered or fibrous hydrated aluminum or magnesium silicate with a size of less than 0.02 mm (Ozbebek et al., 2011). Depending on the bonding of tetrahedral and octahedral layers, which are the basic structural units in clay minerals, various clay minerals can be formed (Kalpaklı et al., 2022). The quality of the clays and the areas in which they can be used are related to the type of clay minerals, their composition and the amount of these minerals. Clays have properties such as color, particle size, specific surface area, adsorption, cation exchange capacity, cohesion, plasticity. Clay minerals have very small particle sizes and have inner and outer crystal surfaces due to trioctahedral (tetrahedral-octahedral-tetrahedral) or dioctahedral (tetrahedral-octahedral) molecular structures, while increasing the porous structure and surface area of the clays, while increasing the area to be adsorbed (Kalpaklı et al., 2022). The fact that clays have a very large and complex mineral array, the presence of impurities in them, the place of formation and the variation in their properties cause them to be classified in many ways. Clays can be classified as Kaolin group, Illite group, Chlorite group, Smectite group, Mica group.

Bentonite is the most common of the smectite group clays and is found in nature as rocks composed of mineral mixtures (Al-Hammood et al., 2021). In addition to the predominant montmorillonite mineral, bentonite rocks contain clay minerals such as kaolinite, illite, and palygorskite, as well as non-clay minerals such as gypsum, quartz, calcite (Al-Hammood et al., 2021). Since bentonite clay is formed as a result of bonding an octahedral aluminum layer between two tetrahedral silicon layers, the expression (2:1) is used to describe this lattice number (Kalpaklı et al., 2022; Al-Hammood et al., 2021). When bentonite meets water, it swells 20-30 times (Kalpaklı et al., 2022). It was declared that bentonite has higher methylene blue adsorbing capacity due to the higher specific surface area than kaolin group clays (Mesboua et al., 2018). Bentonite, which is rich in magnesium, is used in the construction industry for impermeable layer and soil stabilization (Mesboua et al., 2018). Raw bentonite is characterized by its relatively low specific gravity and relatively high surface area compared to Portland cement (Al-Hammood et al., 2021). Substitution of cement with raw bentonite has two opposing effects on the consistency of the cement paste. It was reported that bentonite particles cause an increase in the fluidity of paste mixtures with the dispersion effect, while at the same time, it causes a decrease in fluidity due to its high absorption capacity (Al-Hammood et al., 2021). It was observed that sodium bentonite (Na-RB) has high water absorption, while calcium bentonite (Ca-RB) has relatively low absorption (Al-Hammood et al., 2021). In the study conducted by Mesboua et al. (2018), it was reported that the mini-slump diameter values of cementitious mixtures decreased, while the viscosity and shear stress values increased with the increase in the bentonite substitution ratio. The fine bentonite particles provide additional nucleation sites that promote the hydration process and subsequently accelerate the setting time. In addition, it was reported that the high absorption of bentonite accelerates cement paste setting. On the other hand, it was reported that the substitution of Portland cement with raw bentonite causes an increase in the setting time because it reduces the cement components C_3A and C_3S that accelerate the setting (Al-Hammood et al., 2021). It was declared that the compressive strength of concrete decreases due to the substitution of raw bentonite for cement, and high replacement rates (35-50%) cause decreases in the compressive strength of approximately (45-60%) (Al-Hammood et al., 2021). However, Karthikeyan et al. (2015) emphasized that there was a 30% increase in compressive strength with 20% bentonite substitution.

Kaolin clay is a two-layered phyllosilicate group clay (1:1) formed by the combination of tetrahedron and octahedron (Kalpaklı et al., 2022). Since the surfaces of kaolinites with tetrahedrons are covered with an oxygen octahedron and a hydroxide layer, there is a strong attraction force between the two layers and this prevents them from absorbing water and swelling (Kalpaklı et al., 2022). Naganathan et al. (2010), it was reported that the setting time of mixtures without kaolin was 5-7.5 hours, while the setting time of mixtures containing kaolin was 12-32 hours. It was reported that the presence of SiO_2 and Al_2O_3 in kaolin delays hydration and therefore prolongs the initial setting time. In the same study, it was observed that while bleeding was between 1% and

11% in mixtures without kaolin addition, it was 1% or less in all mixtures with kaolin. This was interpreted as the addition of kaolin and the increase in the water-absorbing powder content of the mixture, resulting in decreased bleeding. In addition, it was concluded that the compressive strength values of mixtures with kaolin were lower than the compressive strength values of mixtures without kaolin addition. The decrease in strength was attributed to the reduction of Van der Waals forces due to kaolin. It was reported that water absorption, sorption and initial surface absorption values increase due to the increase in the amount of kaolin added to cements (Naganathan et al., 2010).

As a result, it was emphasized by many researchers that aggregates with a methylene blue value greater than 1.50 g/kg are not suitable for use in concrete production (Kirthika et al., 2019). It was also understood from the literature that the type, fineness and amount of clay affect the fresh and hardened state properties of cementitious systems. In this study, the effect of bentonite, kaolin and limestone powder passing through a 0.125 mm sieve on the mini-slump performance of the cement paste mixture was investigated.

Material and Method

Material

Within the scope of the study, Bursa Cement, Kaolin Company and Technical Mineral Mining Company, CEM I 42.5R type cement, kaolin and bentonite clay were used, respectively. Some chemical, physical and mechanical properties of cement, bentonite, kaolin and sand powder supplied by the manufacturers are presented in Table 1 and Table 2. It was reported by the manufacturer that bentonite clay is composed of a minimum of 85% montmorillonite and a maximum of 15% cristobalite-opal.

Table 1. Chemical properties of cement, kaolin, bentonite and limestone sand powder

Oxide (%)	Cement	Kaolin	Bentonite	Limestone Sand Powder
SiO ₂	18.74	46.5	71.00 (± 0.50)	4.60
Al ₂ O ₃	5.37	37.0	12.50 (±0.50)	2.32
Fe ₂ O ₃	3.04	0.5	0.75 (±0.10)	1.33
CaO	64.11	0.15	1.12 (±0.10)	90.50
MgO	1.21	0.15	1.25 (±0.10)	0.782
SO ₃	2.68	-	0.02 (±0.01)	0.0562
Na ₂ O	0.34	0.05	0.04 (±0.01)	-
K ₂ O	0.62	0.60	0.25 (±0.02)	0.284
Cl ⁻	0.038	-	-	-
Free CaO	2.12	-	-	-
P ₂ O ₅	-	-	-	0.137
SrO	-	-	-	0.0444
Loss on ignition	3.6	-	-	13.00 (±0.50)
PH	-	6.5-8.5	8.5(±0.5)	-
Maximum moisture (%)	-	1	12	-

Table 2. Physical properties of cement, kaolin, bentonite and limestone sand powder

Properties	Cement	Kaolin	Bentonite	Limestone Sand Powder
Specific gravity	3.15	2.782	2.71	2.73
Swelling (ml/2g)	-	-	30.00 (±2,00)	-
Cation exchange capacity (mg/100g)	-	-	86.00 (5.00)	-
Specific surface area (Blaine, cm ² /g)	3600	10491	1100	1000
Residue in 0.045 mm sieve (%)	7.4	0.60	D ₉₇ < 20μ D ₁₀₀ < 30μ	-
Residue in 0.090 mm sieve (%)	0.4	0.15	-	-

Preparation of Mixtures

The w/b ratio was kept constant as 0.35 in all mixtures prepared to examine the mini-slump performance of cement paste mixtures. However, in the mixtures produced, the w/b ratio was chosen as 0.39, since spreading

did not occur. In addition to the control mixture, which does not contain clay and limestone sand powder, 3% of the weight of the cement, kaolin, bentonite clays and limestone sand powder were added and a total of 4 different series of paste mixtures were prepared. In the preparation of the mixtures, firstly, 800 g of cement and 3% of the cement weight of fine material were mixed homogeneously. 312 g of water was added to the prepared homogeneous dry material and mixed at 20 rpm (slow) for 30 seconds. At the end of 30 seconds, the walls of the container were cleaned with the help of a spatula. It was then mixed at 40 rpm (fast) for 2 minutes. Mini-slump test was performed on the prepared mixtures. The amount of material contained in the paste mixtures produced for the mini-slump test is given in Table 3. The denotation of the mixtures is made according to the w/b ratio and the type of fine material it contains. For example, the mixture containing kaolin clay with a w/b ratio of 0.39 was named Kaolin_0.39.

Table 3. The amount of material contained in the paste mixes produced for the mini-slump test

Mixture	Cement (g)	Kaolin (g)	Bentoni te (g)	Limestone sand powder (g)	Water (g)	Water/Binder
Control_0.35	800	-	-	-		
Kaolin_0.35	800	24	-	-	280	0.35
Bentonite_0.35	800	-	24	-		
Limestone_0.35	800	-	-	24		
Control_0.39	800	-	-	-		
Kaolin_0.39	800	24	-	-	312	0.39
Bentonite_0.39	800	-	24	-		
Limestone_0.39	800	-	-	24		

Method

Methylene Blue Value

The methylene blue test was carried out in accordance with the TS 706, EN 12620 Standard. Limestone aggregate sieved through a 2 mm mesh sieve was added to a beaker filled with 500±5 ml distilled water. After stirring at 0 rpm for 5 minutes, 5 ml of methylene blue solution was added to the beaker. The material in the beaker was mixed at 400 rpm for 1 minute and the stain test was carried out on the filter paper with a dropper. Solution addition and staining experiments were continued until the halo appeared.

The aggregate passing through a 2 mm sieve was sieved under water in a 0.064 mm sieve and washed sand was obtained. In order to determine the effect of clays on methylene blue value, the experiment was carried out by substituting 5 g of montmorillonite/kaolin clay for sand. The methylene blue value was calculated with the help of equation 1:

$$MB = (V1/M1) \times 10 \quad (1)$$

In this equation, MB is the methylene blue value, M1 is the mass of the test sample (g), V1 is the total volume of the added dye solution (ml).

Mini-Slump

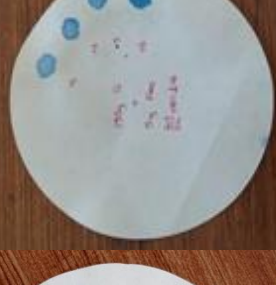
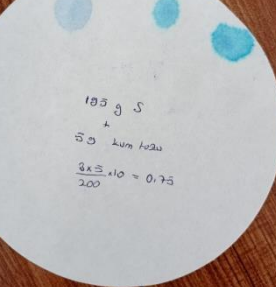
The mini-slump experiment was carried out in accordance with the method proposed by Kantro (1980). The paste mixture prepared in the mini-slump test was filled into a truncated conical apparatus with a lower inner diameter of 38.1 mm, an upper inner diameter of 19 mm and a height of 57.2 mm, placed in the center of a smooth surface. The mini-slump funnel was slowly lifted vertically. Then, with the help of a ruler, the spreading diameter in two perpendicular directions was measured and the average was recorded.

Discussion and Conclusion

Methylene Blue Value

The methylene blue test results are shown in Table 4. As seen in Table 4, the methylene blue value of the sand before washing was 4.25 g/kg, while this value was measured as 0 g/kg after washing under a 0.063 mm sieve. By substituting 5% of bentonite, kaolin and limestone powder for washed sand, the methylene blue value was determined to be 5, 1 and 0.75 g/kg, respectively. Thus, it was understood that bentonite clay is 5 times more aggressive than kaolin. The methylene blue value of the sand powder, on the other hand, took the minimum value with 0.75 g/kg.

Table 4. Methylene blue value test results

Sample	Methylene blue value experiment filter paper	Methylene blue value (g/kg)
Sand		4.25
Washed sand		0
195 g sand+5 g bentonite		5
195 g sand+5 g kaolin		1
195 g sand+5 g limestone sand powder		0.75

Mini-Slump

Mini-slump test results of paste mixes are given in Figure 1. In addition, the images of the mini-slump test of mixtures with 0.35 w/b ratio without any spreading are shown in Table 5. Regardless of the clay type, the mini-slump values of the mixtures increased with the increase of the w/b ratio. With the increase of the w/b ratio from 0.35 to 0.39, the slump values of the mixtures containing control, bentonite, kaolin and limestone powder increased by 56%, 22%, 11% and 33%, respectively. It was determined that the mini-slump values decreased with the addition of fine material to the mixture, regardless of the fine material type. It was understood that the lowest and highest mini-slump values were measured in the mixture containing control and Kaolin, respectively.

As it is known, with the increase in the methylene blue value of the aggregate, its negative effect on cementitious systems increases. In the study conducted by Beixing et al. (2011) it was reported that the workability and compressive-flexural strength of cementitious mixtures decreased with the increase in the methylene blue value of the aggregate (0.35-2 g/kg). On the other hand, Chen et al. (2020) declared that the combined effect of fine material content and methylene blue value has a significant effect on the workability of concrete. It was stated that when the methylene blue value is less than 7 g/kg, sand produced with a high micro-fine content (15 to 20%) can effectively improve the workability of concrete. In this study, it was observed that although bentonite clay had the highest methylene blue value, the mixture containing bentonite was not the mixture with the lowest performance in terms of mini-slump. It was understood that kaolin clay affected the flow performance of the mixture more negatively than bentonite clay. This is thought to be due to the fact that kaolin clay is 10 times thinner than bentonite clay (Table 2). In this context, it was understood that the fineness parameter is more dominant than the methylene blue value in terms of the flow performance of the mixtures. As is known, the binder fineness parameter seriously affects the flow performance of cementitious systems (Mardani Aghabaglou et al., 2016). It was reported by various researchers that the hydration rate increases with the increase of binder fineness, and accordingly, the flow performance of the mixture is adversely affected (Mardani-Aghabaglou et al. 2016, Aydın et al., 2009). Hammat et al. (2021), it was emphasized that the flow performance of the mixture decreased with the increase of the natural pozzolan substitution ratio. It was reported that this is due to the fact that natural pozzolana is thinner and more porous than cement. In the study conducted by Benjeddou et al., (2021), it was stated that the Marsh funnel flow time values increased with the increase of limestone powder fineness. It was emphasized that the cohesion of cementitious mixes increased with the increase of limestone powder fineness (Diederich et al., 2012). Biricik et al. (2022), it was reported that the mixture containing the marble powder with the highest Blaine fineness value had the lowest setting time. However, it was also reported that the flow performance of cementitious mixtures is positively affected by the increase in fly ash fineness, which is another supplementary material (Jamkar et al., 2013; Sahin et al., 2022). Jamkar et al. (2013) concluded that fly ash fineness increases both workability and compressive strength of geopolymer concrete. Şahin et al. (2022) stated that the mini-slump values increase with the increase of fly ash fineness.

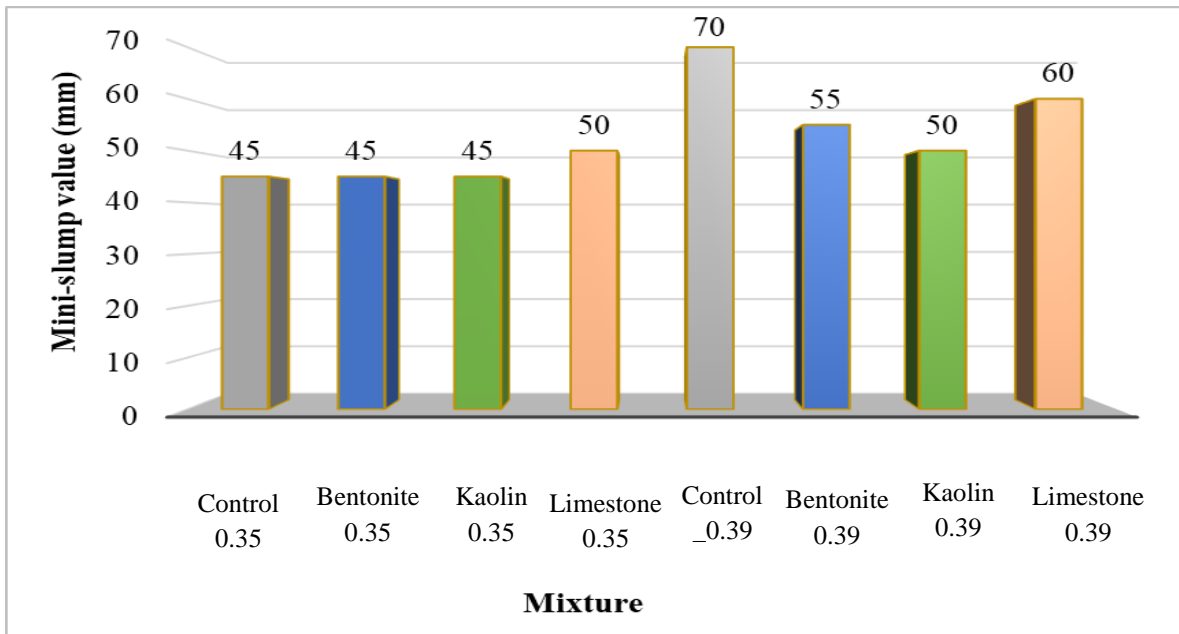
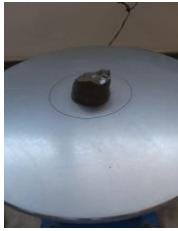
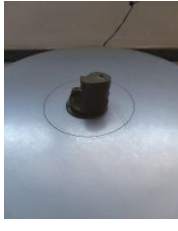


Figure 1. Mini-slump value of mixtures

Table 5. Mini-slump test images of paste mixes with 0.35 w/b ratio

Control_0.35		
Bentonite_0.35		
Kaolin_0.35		
Limestone_0.35		

Conclusion

The results summarized below were obtained in line with the materials used in the study and the experiments applied:

- Bentonite clay has been determined to have 5 times higher methylene blue value compared to kaolin.
- It was observed that the mini-slump values of the mixtures increased with the increase of the w/b ratio, independent of the clay type, and decreased with the addition of clay.
- Mixtures containing control and kaolin without fine material exhibited the highest and lowest performance in terms of mini-slump behavior.
- In terms of flow performance, it was understood that the fineness parameter was more dominant than the methylene blue parameter.

Data Availability Statement

All data, models, and code generated or used during the study appear in the submitted article.

Funding

This research did not receive any specific grant from funding agencies in the public, commercial, or not-for-profit sectors.

Conflicts of Interest/Competing Interests

The authors declare that they have no known competing financial interests or personal relationships that could have appeared to influence the work reported in this paper.

Scientific Ethics Declaration

The authors declare that the scientific ethical and legal responsibility of this article published in EPSTEM journal belongs to the authors.

Acknowledgements or Notes

*The authors would like to acknowledge Bursa Cement Factory, Technical Mineral Mining Company, Kaolin Company for their assistance in supplying cement, bentonite clay and kaolin clay, respectively, and determining the technical specifications of these products.

*This article was presented as a poster presentation at the International Conference on Research in Engineering, Technology and Science (www.icrets.net) held in Budapest/Hungary on July 06-09, 2023.

References

- Al-Hammood, A. A., Frayyeh, Q. J., & Abbas, W. A. (2021). Raw bentonite as supplementary cementitious material—a review. *Journal of Physics: Conference Series*, 1795(1), IOP Publishing.
- Altun, M. G. (2021). *Yüksek oranda su azaltıcı katkı kimyasal yapısının ucucu kul içeren cimentolu sistemlerin özelliklerine etkisi* (Doctoral dissertation). Bursa Uludag University, Bursa, Turkey.
- Aydın, S., Aytac, A. H., & Ramyar, K. (2009). Effects of fineness of cement on polynaphthalene sulfonate based superplasticizer–cement interaction. *Construction and Building Materials*, 23(6), 2402-2408.
- Beixing, L., Mingkai, Z., & Jiliang, W. (2011). Effect of the methylene blue value of manufactured sand on performances of concrete. *Journal of Advanced Concrete Technology*, 9(2), 127-132.
- Benjeddou, O., Alwetaishi, M., Tounsi, M., Alyousef, R., & Alabduljabbar, H. (2021). Effects of limestone filler fineness on the rheological behavior of cement–limestone filler grouts. *Ain Shams Engineering Journal*, 12(4), 3569-3578.
- Biricik, O., Aytekin, B., & Mardani, A. (2022). Farklı tur atık toz malzeme kullanımının cimentolu sistemlerin priz suresi ve akış özelliklerine etkisi. *The 14th International Scientific Research Congress*. Ankara, Turkey
- Bozkurt, A., & Kurtuluş, C. (2008). Yukarı Hereke bölgesinde yer alan killi kirettaşlarının fiziksel özelliklerinin belirlenmesi. *Uygulamalı Yerbilimleri Dergisi*, 7(1), 1-15.
- Chen, X., Yuguang, G., Li, B., Zhou, M., Li, B., Liu, Z., & Zhou, J. (2020). Coupled effects of the content and methylene blue value (MBV) of microfines on the performance of manufactured sand concrete. *Construction and Building Materials*, 240. 117953.
- Desik, F., & Ustabaş, İ. (2019). Kiret taşı kokenli kırma kumdaki ince madde oranının beton kıvamına ve dayanımına etkisi. *Gümüşhane Üniversitesi Fen Bilimleri Dergisi*, 9(2), 262-271.
- Diederich P., Mouret M., de Ryck A., Ponchon F., & Escadeillas G. (2012) The nature of limestone filler and self-consolidating feasibility—Relationships between physical, chemical and mineralogical properties of fillers and the flow at different states, from powder to cement-based suspension, *Powder Technology*, 218, 90–101.
- Guneyli, A. (2010). *Adana ve çevresinde üretilen agregaların beton üretiminde kullanılabilirlikleri*. (Master's thesis). Science Institute.
- Hammat, S., Menadi, B., Kenai, S., Thomas, C., Kirgiz, M. S., & de Sousa Galdino, A. G. (2021). The effect of content and fineness of natural pozzolana on the rheological, mechanical, and durability properties of self-compacting mortar. *Journal of Building Engineering*, 44. 103276
- Jamkar, S. S., Ghugal, Y. M., & Patankar, S. V. (2013). Effect of fly ash fineness on workability and compressive strength of geopolymer concrete. *The Indian Concrete Journal*, 87(4), 57-61.
- Kalpıklı, Y., Aşın, T., & Balkan, A. (2022) *Killer, modifikasyon yöntemleri ve asit aktivasyonu*. İksad.
- Kantro, D. L. (1980). Influence of water-reducing admixtures on properties of cement paste—a miniature slump test. *Cement, Concrete and Aggregates*, 2(2), 95-102.

- Karthikeyan, M., Ramachandran, P. R., Nandhini, A., & Vinodha, R. (2015). Application on partial substitute of cement by bentonite in concrete. *International Journal ChemTech Research*, 8(11), 384-88.
- Kaya, T., & Yazıcioglu, S. (2015). Kalsine bentonit katkılı harcların fiziksel ve mekanik ozelliklerine yüksek sıcaklık etkisi. *BEU Journal of Science*, 4(2), 150-160.
- Kirthika, S. K., Surya, M., & Singh, S. K. (2019). Effect of clay in alternative fine aggregates on performance of concrete. *Construction and Building Materials*, 228. 116811
- Mardani Aghabaglou, A. (2016). *Portland cimentosu ve super akiskanlastırıcı katkı uyumunun incelenmesi* (Doctoral dissertation). Ege University, Graduate School of Natural and Applied Sciences, İzmir, Turkey.
- Mardani Aghabaglou, A., Son, A. E., & Ramyar, K.(2016) Cimento inceliginin süperakışkanlastırıcı katkı iceren cimento hamurunun marsh hunisi akıs suresi ve yayılmasına etkisi. *International Mediterranean Science and Engineering Congress*.
- Melo, K. A., & Carneiro, A. M. (2010). Effect of metakaolin's finesses and content in self-consolidating concrete. *Construction and Building Materials*, 24(8), 1529-1535.
- Mesboua, N., Benyounes, K., & Benmounah, A. (2018). Study of the impact of bentonite on the physico-mechanical and flow properties of cement grout. *Cogent Engineering*, 5(1), 1446252.
- Muslu, A. (2019) *Berdiga formasyonuna ait kirectaslarının (Duzkoy-Trabzon) agrega olarak kullanılabilirliğinin araştırılması* (Master's thesis). Karadeniz Technical University, Graduate School of Natural and Applied Sciences, Trabzon, Turkey.
- Naganathan, S., Razak, H. A., & Hamid, S. N. A. (2010). Effect of kaolin addition on the performance of controlled low-strength material using industrial waste incineration bottom ash. *Waste Management & Research*, 28(9), 848-860.
- Ozbebek, H., & Acık, H. (2011). İnce agregalarda yapılan metilen mavisi ve kum eşdeğerliği deney sonuclarının beton ozelliklerine ve maliyetine etkisi. *THBB Beton*.
- Ozbek, A. (2016). Kahramanmaraş ve çevresindeki kirectaslarının fiziksel ve mekanik ozellikleri. *Kahramanmaraş Sutcu İmam Universitesi Mühendislik Bilimleri Dergisi*, 19(3), 146-156.
- Senbil, U. E., Bagdatlı, O., Koseoglu, K., & Andic, O. (2014). Farklı metilen mavisi degerlerine sahip kırma kumların karakterizasyonu ve beton üzerindeki etkileri. *Engineer & the Machinery Magazine*, (649).
- Turan, C. (2010). *Akarca koyu (Hatay) kirectaslarının hammadde elliklerinin belirlenmesi ve kalsinasyon davranışının incelenmesi*. (Master's thesis). Cukurova University, Graduate School of Natural and Applied Sciences, Adana, Turkey.

Author Information

Fatmanur Sahin
Bursa Uludag University
Bursa, Turkiye

Oznur Biricik
Bursa Uludag University
Bursa, Turkiye

Ali Mardani
Bursa Uludag University
Bursa, Turkiye
Contact e-mail: alimardani@uludag.edu.tr

To cite this article:

Sahin, F., Biricik, O.& Mardani, A. (2023). The effect of clay type, fineness and methylene blue value on mini-slump performance of cementitious systems. *The Eurasia Proceedings of Science, Technology, Engineering & Mathematics (EPSTEM)*, 23, 539-547.

The Eurasia Proceedings of Science, Technology, Engineering & Mathematics (EPSTEM), 2023

Volume 23, Pages 548-555

ICRETS 2023: International Conference on Research in Engineering, Technology and Science

DFT Study of a Schiff Base Ligand and Its Nickel and Copper Complexes: Structure, Vibration, Chemical Reactivity and in Silico Biological

Nabila Guechtouli

Mouloud Mammeri University of Tizi-Ouzou (UMMTO)

Noura Kichou

Mouloud Mammeri University of Tizi-Ouzou (UMMTO)

Amal Bouzaheur

University of Sciences and Technology Houari Boumediene

Celia Adjal

University of Sciences and Technology Houari Boumediene

Abstract: Schiff base complexes are extensively studied because of their affinity, selectivity, and sensitivity to a wide variety of metals. They have been found to be very useful in catalysis, medicine as antibiotics, anti-inflammatory agents and also in industry as compounds with anti-corrosive properties. In this work, we will focus on the study of some Schiff base ligands and their complexes based on nickel and copper. An energetic, structural, spectral (IR, UV) and electronic study was carried out, using the density functional theory method. All the calculations have been made with density functional theory (DFT) using Becke's three parameters hybrid method and the Lee-Yang-Parr correlation functional (B3LYP) with LANL2DZ basis set for heavy metals and 6-31G** for all others atoms in gas phase using Gaussian 03 program package. We used the GaussView program to draw the optimized geometries and to visualize the the normal modes vibrations. The stability of the considered complexes has been studied in the basis of the binding energies. A study of reactivity indices will be highlighted in order to predict attack sites. The in-silico biological properties of compounds studied have been calculated and discussed. The theoretical results will be compared with the available experimental ones.

Keywords: Schiff base, Complexes, Reactivity, ADMET properties, Drug likeness properties.

Introduction

Schiff's base derivatives are excellent chelating ligands (Munde, 2010). They present very varied potential interests for a large number of interdisciplinary fields (Ramana, 2009). This is due to the simplicity of their preparation, the diversity of their application through the relative stability of their complexes with the majority of transition metals. They have been found to be very useful in medicine as antibiotics, anti-inflammatory, antibacterial, and anticarcinogenic agents (Brodowska, 2014). The condensation of substituted o-phenylenediamine with various diketones is used in the preparation of a variety of pharmaceuticals (Carvalho, 2014). And also in industry as compounds with anti-corrosive properties. Indeed, Schiff's bases (o-PDA) are involved in the synthesis of insecticides, corrosion inhibitors and pigments (Verma, 2014). In coordination chemistry, phenylenediamine (o-PDA) is an important ligand precursor. Oxidation of metal-phenylenediamine complexes yields the imine derivatives, which are intensely colored and often exist in multiple stable oxidation states (Abu Dief, 2015). The resistance of bacteria to antibiotics poses serious problems in therapy. This has caused a growing need to develop new antibacterial agents (Massai, 2013).

- This is an Open Access article distributed under the terms of the Creative Commons Attribution-Noncommercial 4.0 Unported License, permitting all non-commercial use, distribution, and reproduction in any medium, provided the original work is properly cited.

- Selection and peer-review under responsibility of the Organizing Committee of the Conference

© 2023 Published by ISRES Publishing: www.isres.org

In this work, we are interested in the study of a Schiff-based ligand and its complexes based on nickel and copper (Figure 1). An energetic, structural, spectral and electronic study was carried out using the density functional theory method. A study of reactivity indices will be highlighted in order to predict attack sites. A biological study was also carried out in order to study the pharmacokinetic profile and to determine the interactions of the ligand and its complexes with DNA.

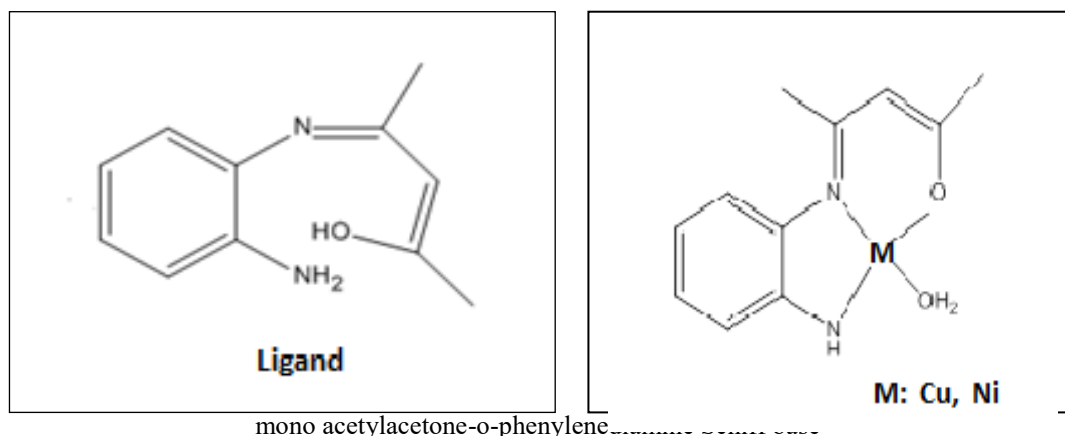


Figure 1. Ligand and complexes structures

Computational Method

Quantum Mechanical Analysis

Full geometry optimization have been made with density functional theory (DFT) using Kohn–Sham’s Density Functional Theory subjected to the gradient-corrected hybrid density functional B3LYP [36-38]. This functional is the combination of Becke’s three parameters hybrid method and the Lee–Yang–Parr correlation functional (B3LYP) (Lee, 1988) with LANL2DZ basis set for heavy metals (Ni and Cu atoms), and 6-31G (d,p), for all others atoms (H, N, C, O) (Pearson, 1985) in gas phase, as implemented by Gaussian 09 program (Frisch, 2009). Without any constraint of symmetry, followed by a calculation of the normal modes of vibration, to make sure that the stationary points were minima. Our complexes are all minima in their potential energy surface. Indeed, the analysis of the frequencies of the normal modes of vibration gives no imaginary frequency. We used the GaussView program to draw the optimized geometries and to visualize the the normal modes vibrations (Fresch, 2009).

We have determined the structure, the electronic parameters, the energies and the gaps $E_{\text{HOMO}}/E_{\text{LUMO}}$. Natural bond orbitals (NBO) atomic charges were also reported. The theoretical results obtained are compared with the available experimental data. In order to study the chemical reactivity of the ligand and its optimized complexes, we calculated the following parameters of several global reactivity descriptors by means of DFT, such as: the ionization potential (I), the electron affinity (A), electronic chemical potential (μ), the absolute hardness (η), the global softness (S) and the global electrophilicity (ω) (Azquez, 2008). The electronic chemical potential (μ) is defined by Parr and Pearson (Parr, 1983):

$$\mu = -\frac{1}{2}(I + A) = -\chi \quad (1)$$

Where χ is the electronegativity given by Mulliken.

The global hardness is defined by (Parr, 1991):

$$\eta = \frac{1}{2}(I - A) \quad (2)$$

The global softness S is obtained from:

$$S = \frac{1}{2\eta} \quad (3)$$

The global electrophilicity (ω) measures the affinity of compounds given by Parr (Parr, 1999) is calculated by:

$$\omega = \frac{\mu^2}{2\eta} \quad (4)$$

The nucleophilicity index equal to the negative of the ionization potential:

$$\text{Nu} = -I \quad (5)$$

A high value of the nucleophilicity index Nu characterizes a good nucleophile, while a low value indicates a good electrophile.

ADMET and Drug-Likeness Analysis

ADMET in silico analysis is performed to predict which the mono acetylacetonate-o-phenylenediamine Schiff base ligand and its corresponding Ni(II) and Cu(II) complexes produce toxicity after administration into the body or exhibit a pharmacokinetic profile. For this, the servers admetSAR (Cheng, 2012) and SwissADME (Daina, 2017) were used. Drug-likeness is a qualitative concept that evaluates the bioavailability of a compound in accordance with its physicochemical properties. Thus, compounds with good bioavailability can be considered as oral drug candidates (Pires, 2015). Thus, blood brain barrier (BBB) penetration, human intestinal absorption (HIA), Caco-2 permeability, AMES toxicity and carcinogenicity were calculated. Drug similarity properties of compounds with acceptable physicochemical properties were determined using several filter rules, namely Lipinski's rule (Lipinski, 2001), Veber's rule (Veber, 2002).

Results and Discussion

Geometry

Figure 2 shows the optimized structures of complexes and all geometric parameters are depicted in Table 1.

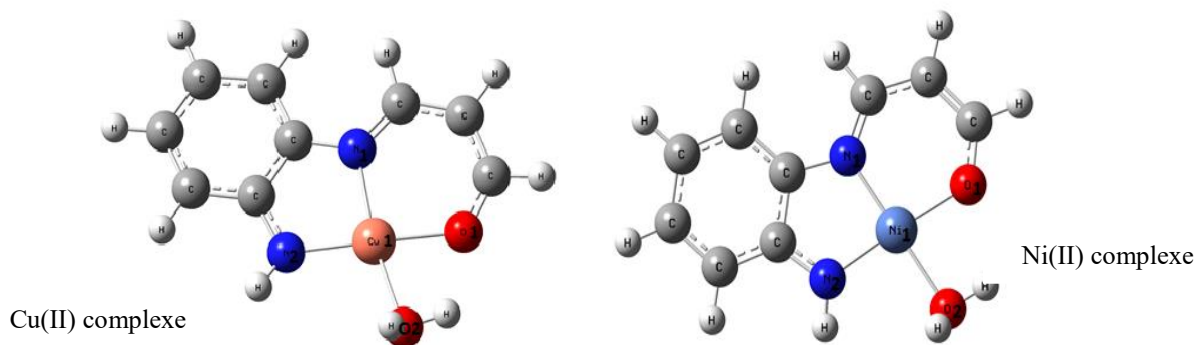


Figure 2. Optimized structures at DFT level

Table 1. Optimized structural parameters at DFT

Parameters	Ni(II) Complex	Cu(II)
Bond length (Å)		
M-N1	1.847	1.914
M-N2	1.873	2.010
M-O1	1.861	1.94
M-O2	1.988	2.168
Bond angles(°)		
N1-M-N2	97.4	84.1
N1-M-O1	93.6	94.6
N2-M-O2	97.4	104.1
O1-M-O2	78.4	82.8

Hydrogen Bonds

The complexes under consideration exhibit multiple hydrogen bonds, which contribute to their stability. Table 2 illustrates the hydrogen bonds involved in intramolecular interactions.

Table 2. Theoretical hydrogen bonds at DFT

Hydrogen bonds (Å)	Ni(II) Complex	Cu(II) Complex
O2...HO	2.096	2.041
N2...HO	2.874	2.981
O1...HN	2.744	2.885

Infrared Spectra

To facilitate the assignment of observed experimental peaks for the copper(II) and nickel (II) complexes, we conducted a theoretical analysis of the IR spectrum (Table 3) and compared it with the experimentally obtained results (SOAYED, 2013). Based on this analysis, we assigned the normal modes of vibration for both the ligand and its complexes. This allowed us to deduce the new vibrational modes that arise after complexation and to observe the influence of the metal change on the vibrational behavior.

Table 3. Selected theoretical and experimental IR frequencies (cm⁻¹).

Compound	ν O-H cm ⁻¹	ν C=N cm ⁻¹	ν C-O cm ⁻¹	ν N-H bending cm ⁻¹	ν M-O or M-N
Ligand	3451	1529	1300	1499	-
	3449 ^a	1523 ^a	1298 ^a	1504 ^a	-
Cu Complex	3396	1630	1322	1512	356 -440
	3460 ^a	1634 ^a	1298 ^a	1518 ^a	364 ^a , 393 ^a
Ni Complex	3457	1660	1259	1520	368, 397
	3448 ^a	1654 ^a	1256 ^a	1518 ^a	364 ^a , 393 ^a

a: experimental data

Theoretical spectra of the Cu(II) and Ni(II) complexes displayed broad bands at 3396 cm⁻¹ and 3457 cm⁻¹, respectively. These bands were experimentally appear at 3460 cm⁻¹ and 3448 cm⁻¹ and they have been assigned to the coordination of water molecules (Table 3). The displacement of the ν N-H bending band from 1504 cm⁻¹ in the ligand to 1512 cm⁻¹ and 1520 cm⁻¹, during complexation indicates the participation of the NH group in the formation of the complex. In the Cu and Ni complexes, new bands ranging from 356 to 440 cm⁻¹ were detected, and these bands were attributed to the vibrations of ν M-N and ν M-O.

Binding Energy Calculation

To conduct a comparative analysis of the complexes' stability, we calculated the Binding Energy (BE) using the following formula:

$$E_{\text{binding}} = E_{\text{complex}} - (E_{\text{metal}} + E_{\text{Ligand}}) \quad (6)$$

Here, E_{complex} represents the energy of the optimized complex, while E_{Ligand} and E_{metal} denote the single point energies of the ligand and metal in their respective optimized states. The complex with the highest BE corresponds to the most stable complex. The calculated BE values for the complexes are presented in Table 4.

The order found is as follows:

Cu(II) < Ni(II). The nickel complex is the most stable

Table 4. Binding energies (Kcal/mol) obtained at DFT.

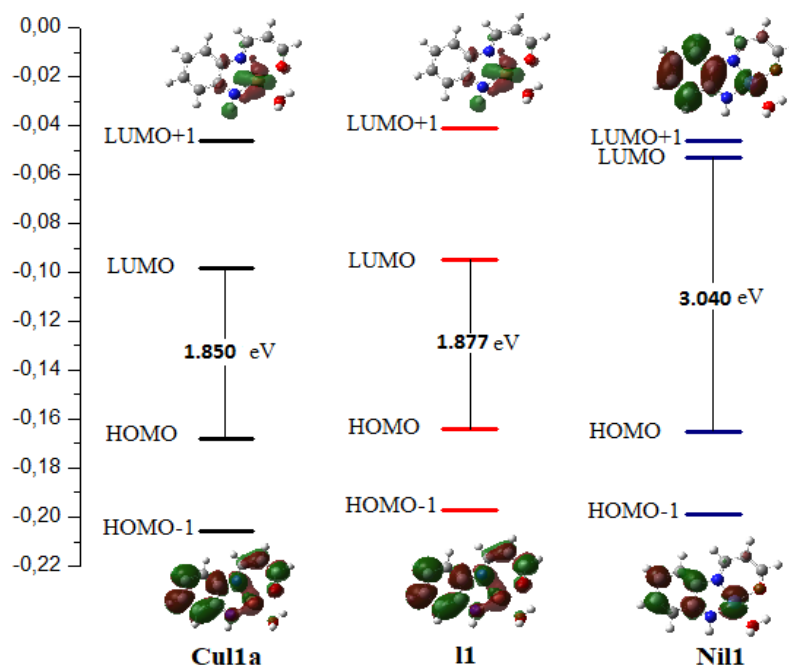
Parameters	Ni(II) Complex	Cu(II) Complex
Binding Energy (Kcal/mol)	-823.775	-776.920

Energetic Properties

The calculated dipole moment, NBO charge, HOMO, LUMO and gap energy are listed in Table 5.

Table 5. Energetic properties of the synthesized complexes at DFT.

Parameters	Ni(II) Complex	Cu(II) Complex
Energy (a.u.)	-778.3008	-
HOMO (eV)	-6.748	805.1151
LUMO (eV)	-2.608	-6.646
ΔE (eV)	4.140	-3.499
Dipole moment (Debye)	3.25	3.147
Charges NBO (e)		3.47
M	0.706	0.916
N ₁	-0.425	-0.503
N ₂	-0.560	-0.592
O ₁	-0.585	-0.751

Figure 3. FMO and gap $|HOMO-LUMO|$ for the studied structures

NBO charges are good predictors of electrophilic and nucleophilic attack sites (Chen, 2012). The values obtained for the metal atoms show a Ligand Metal Charge Transfer (LMCT). We find that the covalent character of the metal-ligand bonds decreases as follows:

Ni(II) > Cu(II).

The oxygen atoms possess a greater negative charge compared to the nitrogen atoms. Our results validate that oxygen exhibits higher reactivity when forming bonds with metals than nitrogen atoms.

Frontier Molecular Orbital (FMO)

For the ligand, the HOMO is located practically on all the atoms constituting it. In the case of Cu(II), the HOMO is fully localized on all the complex. While, it covers metal, and phenyl rings in nickel complex. The LUMO is mainly localized on nitrogen and oxygen atoms in ligand and copper complex the LUMO is located on the metal and phenyl ring in nickel complex (Figure 3).

Reactivity

The parameters μ , η , S , ω and Nu were calculated using the equations 1-5. The results are summarized in the Table 6.

Table 6. The reactivity parameters of two molecules.

Molecules	E_H	E_L	μ	η	ω
CuIa	-4.510	-2.660	-3.585	0.462	13.9
L1	-4.460	-2.584	-3.522	0.938	6.60
NiI1	-4.489	-1.442	-2.965	1.523	2.88

The values of ω and μ indicate that the copper complex is the most electrophilic and Ni(II) complex is the most nucleophilic. The decrease in energy gap explains the charge transfer (CT) taking place in the molecule, which can be responsible for their biological reactivity (Chen, 2012). As can be seen from Figure 3, Cu(II) complex has the lowest energy gap and appear the most reactive.

ADMET and Drug-Likeness

The predicted pharmacokinetic profiles of the Schiff base ligand and its Ni(II) and Cu(II) complexes are listed in Table 7. The obtained results show that all the compounds present high values of intestinal absorption and human adenocarcinoma cells (Caco-2) permeability ($\log P_{app} > 0.9$). These results suggest that the compounds would easily reach their target in the body. Moreover, the negative values of $\log BB$ indicate that the studied compounds are poorly distributed to the brain, which suggests their safety for the central nervous system. In addition, the ligand and its nickel (II) and copper (II) complexes are non-inhibitors of the isoenzymes CYP2C9 and CYP3A4. On the other hand, the compounds were tested for their compliance with Lipinski's rule (Lipinski, 2001), and Veber's rule (Veber, 2002). These rules evaluate the bioavailability and the oral administration efficacy of drugs according to their physicochemical properties. The ligand and its complexes are compliant with Lipinski's rule (molecular weight ≤ 500 g/mol, number of hydrogen bond donors and acceptors ≤ 5 and ≤ 10 , respectively, and octanol-water partition coefficient $\log P \leq 5$) and Veber's rule (polar surface area (PSA) < 140 Å² and a number of rotatable bonds < 10) (Table 8). Which indicates that the compounds show favorable drug-like properties.

Table 7. Predicted pharmacokinetic properties of the ligand complexes

Compounds	Caco-2 permeability (cm/s)	HIA (%)	BBB (LogBB)	CYP450		
				CYP2C9 Inhibitor	CYP3A4 inhibitor	Total clearance
L1	1.192	83.91	-0.353	No	No	0.716
NiL1	1.185	97.38	-0.217	No	No	1.076
CuL1	1.185	97.38	-0.21	No	No	1.095

Table 8. Prediction of the physicochemical properties of the studied compounds.

Compounds	Molecular Weight (g/mol)	PSA (Å ²)	HBD	HBA	Rotatable bonds	LogP	Lipinski rule	Veber rule
L1	162.11	58.61	2	2	2	2.05	Yes	Yes
NiL1	236.79	42.85	2	2	2	1.24	Yes	Yes
CuL1	241.64	42.85	2	2	0	1.24	Yes	Yes

Table 9. Toxicity prediction of the studied compounds.

Compounds	Skin sensitization	AMES toxicity (mutagenicity)	hERG inhibitor	Oral Rat Acute Toxicity (LD50) (mol/kg)	Maximum tolerated dose (mg/kg/day)	Hepatotoxicity
L1	No	No	No	2.045	1.452	No
niL1	No	Yes	No	2.837	-0.412	No
CuL1	No	No	No	2.837	0.439	No

Furthermore, the prediction of toxicity revealed that the ligand and the complexes are not inhibitors of the hERG (human Ether-a-go-go-Related Gene) potassium channels. The inhibition of the hERG potassium channels may cause arrhythmia (Garrido, 2020). Additionally, according to Table 9, all the compounds don't show skin sensitization and hepatotoxicity. Additionally, the acute oral toxicity of the complexes shows a lethal dosage

value (LD50) of 2.837 mol/kg. Consequently, the complexes show less toxicity than the ligand. The prediction of the pharmacokinetic properties and toxicity (ADMET), along with drug-likeness of the studied ligand and its corresponding nickel (II) and copper (II) complexes reveals that the compounds could be interesting oral drug candidates.

Conclusion

In this work, structural and energy parameters, spectroscopic analysis, electronic properties and reactivity descriptors and *in silico*-biological activities of the mono acetylaceton-o-phenylenediamine Schiff base ligand and its corresponding Ni(II) and Cu(II) complexes were calculated using the DFT methods. The aim is to investigate if these compounds could be interesting oral drug candidates. The results revealed that:

- The nickel complex is the most stable one, While, Cu(II) complex has the lowest gap energy and it's the most reactive one, which is in good consistent with the results of the OMF study.
- Our complexes exhibit multiple hydrogen bonds, which contribute to their stability.
- All the compounds studied present good absorption in the intestine which could help them to reach their target.
- Toxicity prediction shows that, in general, the compounds are not hERG inhibitors and don't show skin sensitization and hepatotoxicity.

The ligand and its complexes respect the rules of Lipinski and Viber. Thus, they present favorable drug-like properties.

Scientific Ethics Declaration

The authors declare that the scientific ethical and legal responsibility of this article published in EPSTEM journal belongs to the authors.

Acknowledgements or Notes

* This article was presented as an oral presentation at the International Conference on Research in Engineering, Technology and Science (www.icrets.net) held in Budapest/Hungary on July 06-09, 2023.

References

- Abu Dief, A. M., & Mohamed, I. M. A. (2015). A review on versatile applications of transition metal complexes incorporating schiff bases. *Journal of Basic and Applied Science*, 4, 119–133.
- Brodowska, K. M., & Lodyga Chruscinka, N. (2014). Schiff bases – interesting range of applications in various fields of science. *Chemik*, 68, 129-134.
- Carvalho, M. A., Shishido, S. M., Souza, B. C., de Paiva, R. E., Gomes, A. F., Gozzo, F. C., Formiga, A.L.B., & Corbi, P.P. (2014). A new platinum complex with tryptophan: Synthesis, structural characterization, DFT studies and biological assays in vitro over human tumorigenic cells. *Spectrochim. Acta Part A: Molecular and Biomolecular Spectroscopy*, 122, 209-215.
- Chen, S. L., Liu, Z., Liu, J., Han, G. C., & Li, Y. G. (2012). Synthesis, characterization, crystal structure, hirshfeld surface analysis and spectroscopic properties of bis (5-aminoisophthalato) bispicolinecopper (II). *Journal of Molecular Structure*, 1206.
- Cheng, F., Li, W., Zhou, Y., Shen, J., Wu, Z., Liu, G., Lee, P. W., & Tang, Y. (2012). admetSAR: a comprehensive source and free tool for assessment of chemical ADMET properties. *Journal of Chemical Information and Modeling*, 52(11), 3099-3105.
- Daina, A., Michielin, O., Zoete, V. (2017). SwissADME: a freeweb tool to evaluate pharmacokinetics, drug-likeness and medicinal chemistry friendliness of small molecules. *Scientific Reports*, 7.
- Fresch, A., Nielson, A. B., & Holder, A. J. (2009), *Gaussview user manual*. Pittsburg: Gaussian.Inc.
- Frisch, M. J., Trucks, G., Schlegel, W., Scuseria, H. B. & Al, G. E. (2009). Gaussian 03, revision a1. Pittsburgh, PA: Gaussian, Inc.

- Garrido, A., Lepailleur, A., Mignani, S.M., Dallemagne, P., Rochais, C. (2020) hERG toxicity assessment: useful guidelines for drug design. *European Journal of Medicinal Chemistry*, 195.
- Gazquez, J. L. (2008). Perspectives on density functional theory of chemical reactivity. *Journal of the Mexican Chemical Society*, 52(1), 3.
- Lee, C., Yang, W., & Parr, R.G. (1988). Development of the Colle-Salvati correlation- energy formula. *Physical Review B. Condens Matter*, 37(2), 785-789.
- Lipinski, C. A., Lombardo, F., Dominy, B.W., & Feeney, P.J. (2001). Experimental and computational approaches to estimate solubility and permeability in drug discovery and development settings. *Advanced Drug Delivery. Reviews*, 23(1-3), 3-25.
- Massai, L., Fernández Gallardo, J., Guerri, A., Arcangeli, A., Pillozzi, S., Contel, M., & Messori, L. (2015). Dalton trans. *Pub Med*, 44, 1-3.
- Munde, A.S., Jagdale, A., Jadhav, S.M., & Chondhekar, T.K. (2010). Synthesis, characterization and thermal study of some transition metal complexes of an asymmetrical tetradentate Schiff base ligand. *Journal of Serbian Chemical Society*, 75(3), 349-359.
- Parr, R. G., & Chattaraj, P. K. (1991). Principle of maximum hardness. *Journal of the American Chemical Society*, 113, 1854-1855.
- Parr, R. G., & Pearson, R. G. (1983). Absolute hardness companion parameter to absolute electronegativity. *Journal of the American Chemical Society*, 105(26), 7512-7516.
- Parr, R. G., Szentpaly, L., & Liu, S. (1999). Electrophilicity index. *Journal of the American Chemical Society*, 121, 1922-1924.
- Pearson, R. G. (1985). Absolute electronegativity and absolute hardness of Lewis acids and bases. *Journal of the American Chemical Society*, 107(24), 6801.
- Pires, D.E.V., Blundell, T.L., & Ascher, D.B. (2015), pkCSM. Predicting small-molecule pharmacokinetic and toxicity properties using graph-based signatures, *Journal of Medical Chemical Society*, 58, 4066–4072.
- Ramana, N., Mitub, L., Sakthivela, A., & Pandia, M.S.S. (2009). *Journal of the Iranian Chemistry Soc.*, 6(4), 738.
- Science.(n.d.). *Science Thechnique*, 2 (68), 129–134.
- Soayed, A., & Refaat, H. M. (2013). *Journal of the Chilean Chemical Society*, 58
- Verber, D. F. , Johnson, S. R. , Cheng, H. Y., Smith, B. R., Ward, K. W., & Kopple, K. D. (2002). Molecular properties that influence the oral bioavailability of drug candidates. *Journal of Medical Chemistry*, 45(12), 2615-2623.
- Verma, C. B., & Quarishi, M. A. (2014). Schiff's bases of glutamic acid and aldehydes as green Corrosion inhibitor for mild steel: Weight- loss, electrochemical and surface analysis. *International Journal of Innovative Research in Science Engineering and Technology*, 3(7), 14601–14613.
- Verma, C. B., Quraishi, M. A.(2014). Schiff ' s bases of glutamic acid and aldehydes as green corrosion inhibitor for mild steel: Weight-loss,

Author Information

Nabila Guechtouli

Mouloud Mammeri University of Tizi-Ouzou
Tizi Ouzou, Algeria
Contact e- mail: nabila.gue@ummo.dz

Noura Kichou

Mouloud Mammeri University of Tizi-Ouzou
Tizi Ouzou, Algeria

Amal Bouzaheur

University of Sciences and Technology Houari Boumediene
Bab Ezzouar, Algeria

Celia Adjal

University of Sciences and Technology Houari Boumediene
Bab Ezzouar, Algeria

To cite this article:

Guechtouli, N., Kichou N., Bouzaheur, A., & Adjal, C. (2023). DFT study of a Schiff base ligand and its nickel and copper complexes: Structure, vibration, chemical reactivity and in silico biological. *The Eurasia Proceedings of Science, Technology, Engineering & Mathematics (EPSTEM)*, 23, 548-555.

The Eurasia Proceedings of Science, Technology, Engineering & Mathematics (EPSTEM), 2023

Volume 23, Pages 556-563

ICRETS 2023: International Conference on Research in Engineering, Technology and Science

Renewal Energy Efficiency Assessment

Thi Minh Nhut Vo

National Kaohsiung University of Science and Technology

Chia-Nan Wang

National Kaohsiung University of Science and Technology

Fu-Chiang Yang

National Kaohsiung University of Science and Technology

Van Thanh Tien Nguyen

Industrial University of Science and Technology

Abstract: Over the years the significance of energy has greatly increased due to the pressing need to tackle climate change and reduce our dependence on fuels. Solar power, wind energy and hydroelectric power are considered as alternatives that can meet our energy requirements. By incorporating these energy sources into our mix, we can reap benefits such as job creation and economic growth particularly in rural and remote areas. To evaluate the potential of energy production in 11 countries a study was conducted using Data Envelopment Analysis (DEA) EBM analysis. The study considered three factors; the number of patents related to renewable energy, the capacity of energy installations and the gross domestic product (GDP). The output that was analyzed focused on energy production. The countries included in this study were Australia, Brazil, China, France, Germany, Japan, Netherlands, South Korea, Spain United Kingdom, and United States. This study's findings provide policymakers and investors with a framework for assessing each country's capability to generate energy. This methodology offers insights that can guide policy decisions concerning energy production across different nations.

Keywords: Renewable energy, Energy efficiency assessment, Data envelopment analysis, EBM analysis, Energy production

Introduction

In years there has been a global movement towards renewable energy sources to address concerns about climate change and achieve sustainable development. This movement brings benefits for the environment, economy, and society. However, to fully unlock the potential of energy sources we need to do more than just accept them; we must continuously strive to improve their efficiency and effectiveness.

Evaluating the efficiency of energy systems is crucial in this endeavor. By examining their performance, we can identify areas for optimization. Ensure utilization of available resources. Over time various strategies have been developed to assess the effectiveness of energy technologies. These range from approaches to advanced statistical models. However, many of these methodologies have limitations, such as oversimplifying dynamics or lacking assessment criteria.

In our paper we introduce an approach called Slack based Measurement (SBM) that analyzes the efficiency of energy systems. SBM offers a framework that considers inputs and outputs for a thorough assessment of

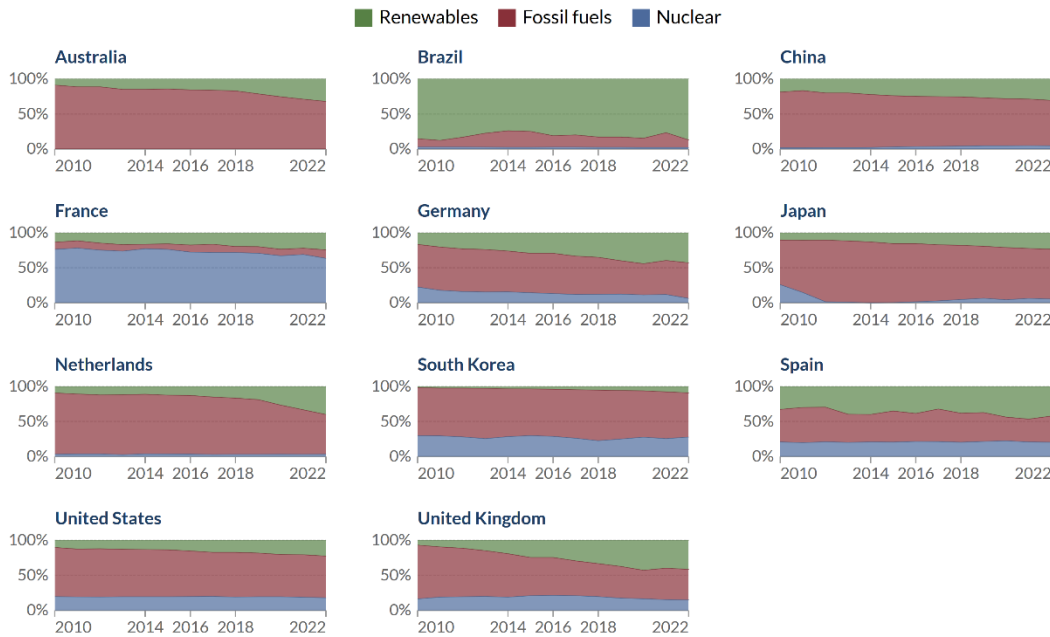
- This is an Open Access article distributed under the terms of the Creative Commons Attribution-Noncommercial 4.0 Unported License, permitting all non-commercial use, distribution, and reproduction in any medium, provided the original work is properly cited.

- Selection and peer-review under responsibility of the Organizing Committee of the Conference

© 2023 Published by ISRES Publishing: www.isres.org

renewable energy generation, distribution and consumption. Unlike approaches that solely focus on energy production, SBM considers critical factors, like resource utilization, waste generation and environmental implications. SBM takes an approach to assessing the efficiency of renewable energy systems leaving no aspect untouched.

Electricity production from fossil fuels, nuclear and renewables



Source: Our World in Data based on BP Statistical Review of World Energy (2022); Ember (2023)

OurWorldInData.org/energy • CC BY

Figure 1. Comparison of electricity production from fuels, nuclear power, and renewables.

The main objective of this study is to use the SBM approach to evaluate and compare the efficiency of energy systems in ten countries. We have selected these nations based on their locations, energy landscapes and stages of development. Our aim is to gain insights into how their renewable energy systems perform and identify areas that can be improved by conducting a thorough examination using the SBM approach. This comparative research serves as a foundation for making decisions and shaping policies by identifying best practices factors contributing to success and areas that need more attention.

This research offers two contributions. Firstly, we present a framework for analyzing energy efficiency using the SBM technique, which addresses the limitations of existing methods and provides a comprehensive evaluation of renewable energy systems. This framework can enhance decision making processes, guide policy formulation and assist in creating long term energy strategies. Secondly, we provide an analysis of energy efficiency, across the selected countries. Our findings offer insights that can influence collaborations, information sharing, technology transfer ultimately leading to improved global renewable energy efficiency.

This research holds importance in the context of accelerating the global shift towards renewable energy sources. Policymakers, energy planners and other stakeholders can make informed decisions. Develop effective strategies to promote renewable energy technologies by identifying areas for improvement and emphasizing best practices. Moreover, the findings of this study can be utilized to enhance collaboration, facilitate information sharing and support technology transfer thus contributing to the pursuit of a sustainable and low carbon future.

In the sections of this paper, we will delve into the methodology employed, outline the framework devised, conduct an analysis, and provide a comprehensive explanation of our findings. The aim of this project is to offer insights into assessing energy efficiency while shedding light on its implications for policy making and practical implementation. Through these explorations we also establish a foundation for research on this subject matter.

Literature Review

Existing Approaches of DEA SBM

The proposed model known as DEA SBM presents an opportunity to examine how efficiently Municipal Solid Waste (MSW) recycling systems promote learning (Chang et. al., 2013) (Chang, Liu, & Yeh, 2013). The research community is particularly interested in identifying the activities that have contributed to advancing this field. In their study Liu et. Al. (2016) aimed to uncover these research activities, also known as research fronts within the domain of DEA (Liu, Lu, & Lu, 2016). Yang et. al. (2017) focused on assessing the efficiency of water and energy resource utilization across provinces, in China (Yang & Li, 2017). To address challenges Mousavi et al. proposed a framework based on efficiency DEA that is not constrained by specific orientations (Mousavi & Ouenniche, 2018). Hu et.al.(2019) employed a slack based DEA model called SBM DEA with five input variables and four output variables to evaluate the eco efficiency of 281 CWWTPs located in 126 level parks (NIPs) (Hu, Guo, Tian, Chen, & Recycling, 2019). Evaluating waste and total energy consumption serves as the focus when assessing Chinas regional sustainable innovation according to Xu et.al.(2019) (Xu, Bossink, & Chen, 2019). The authors of a study in 2020 investigated how Koreas local governments are investing in research and development (R&D) using a data analysis method called slack based model data analysis (SBM DEA) (Lee, Choi, Seo, & Change, 2020). They proposed an efficiency model called data envelopment analysis and slacks-based measure considering undesirable outputs (S DEA SBM UO) which builds upon the traditional DEA model, for unexpected output. Another research paper by Li et. al. (2021) examined the spatiotemporal evolution characteristics and influencing factors related to this topic (Li, Sarwar, & Jin, 2021). Lastly Wang et al.s (2022) main contribution is providing ideas for promoting quality agricultural development during Chinas transition period by studying green biased technical changes, in Chinese agriculture (Wang, Zuo, Qian, & Health, 2022).

Methodology

The Slack-based Measurement (SBM) Method

The non-negative data input is a compulsory requirement in the application of DEA models. Tone 2001 and Tone 2002 (Tone & Sahoo, 2004) developed the Slacks-based measure of efficiency (SBM) to evaluate the efficiency of the DMUK by Equation:

$$P \setminus (x_0, y_0) = \left\{ (\bar{x}, \bar{y}) \mid x \geq \sum_{j=1, \neq 0}^n \lambda_j x_j, \bar{y} \leq \sum_{j=1, \neq 0}^n \lambda_j y_j, \bar{y} \geq 0, \lambda \geq 0 \right\}$$

Please keep in mind that the functions optimal value should be greater, than or equal to ρ_2 , which in turn should be greater than or equal, to 1.

Selection of Ten Countries and Input-Output Variables

Table 1. List of 11 selected countries.

No	DMUs	Countries
1	Coun1	Australia
2	Coun2	Brazil
3	Coun3	China
4	Coun4	France
5	Coun5	Germany
6	Coun6	Japan
7	Coun7	Netherlands
8	Coun8	South Korea
9	Coun9	Spain
10	Coun10	United Kingdom
11	Coun11	United States

Table 1 illustrates the studies employing Data Envelopment Analysis (DEA) to assess the efficiency performance of Decision-Making Units (DMUs) spanning various sectors. Moreover, it displays the utilization of distinct variables. Emphasis is placed on the prioritization of commonly utilized variables found in previous

studies. Specifically, this study focuses on eleven countries serving as DMUs, considering three inputs and one output. The performance efficiency evaluation for these eleven countries considers three variables: Total Number of Renewable Energy Innovation Patents (TNREIP), Total Renewable Energy Capacity (TREC), Gross Domestic Product (GDP), with Total Renewable Energy Production (TREP) being the designated output variable.

Results and Discussion

In this study, the focus lies on addressing the slack issues prevalent in conventional DEA models, such as CCR and BCC. To effectively tackle this challenge, we recognize the noteworthy merits of utilizing the SBM-I-C methodology in Data Envelopment Analysis (DEA). This choice is made with the intent of evaluating the efficiency units and rankings of individual countries under scrutiny (C. N. Wang, Yang, Vo, & Nguyen, 2022). By employing the SBM-I-C approach, we aim to overcome the limitations inherent in traditional DEA models and present a more comprehensive and accurate assessment of country efficiency. Table 2 shows the statistics on input and output data of 11 countries in 2020.

Table 2. Statistics on Input/Output Data for the Year 2020

2020	TNEIPs	TREC (MW)	GDP (Billion US)	TREP (GWH)
Max	128,933	899,625	21,060	2,149,534
Min	13	18,477	910	32,998
Average	13,989	165,052	5,144	403,528
SD	36,596	244,463	6,265	598,516

Table 3 displays the persuasive results of the Pearson correlation test performed on the inputs and outputs for the year 2020. The presence of significant positive connections validates the "homogeneity" and "isotonicity" statistics, so meeting two critical conditions for the successful application of the DEA model. Furthermore, the significant correlations identified among the variables provide major grounds for reasonable input and output selection. The extraordinary correlation coefficient of 0.9935 between TREC and TREP in relation to RE, for example, highlights the extraordinarily high level of reliability in the data collection method. This study shows that nations with a significant Total Renewable Energy Capacity (TREC) are more likely than their counterparts to attain a correspondingly larger Total Renewable Energy Production (TREP).

Table 3. Calculated Pearson correlation matrix of inputs and output

	TNEIPs	TREC (MW)	GDP (Bill. US)	TREP (GWH)
TNEIPs	1	0.9738	0.5776	0.9512
TREC (MW)	0.9738	1	0.6976	0.9935
GDP (Bill. US)	0.5776	0.6976	1	0.7243
TREP (GWH)	0.9512	0.9935	0.7243	1

Table 4 displays the Diversity Matrix, created using the DEA SBM I-C model to compare 11 nations' performance. The matrix shows how these countries differ in efficiency. The DEA SBM I-C model, which measures efficiency using input and output parameters, is a strong analytical framework. The diversity matrix reveals efficiency differences across the 11 countries. The diversity value in each matrix cell demonstrates how efficient two countries are. A smaller diversity number indicates similar efficiency levels, while a greater value indicates distinct ones.

Table 4. Diversity matrix

	TNEIPs	TREC (MW)	GDP (Bill. US)
TNEIPs	0	0.2650	0.2076
TREC (MW)	0.2650	0	0.2617
GDP (Bill. US)	0.2076	0.2617	0

Table 5 illustrates the DEA SBM I-C model's Affinity Matrix comparing 11 countries' efficiency. The Data Envelopment Analysis Slack-Based Measure Input-Oriented Slack Based model (DEA SBM I-C) is a powerful analytical tool that measures efficiency by considering input and output parameters (Kler et al., 2022). The affinity matrix links countries by efficiency. The affinity value between two countries reveals how efficient they are. Higher affinity values indicate greater similarity, whereas lower values indicate less.

Table 5. Affinity matrix

	TNEIPs	TREC (MW)	GDP (Bil US)
TNEIPs	1	0.4699	0.5849
TREC (MW)	0.4699	1	0.4767
GDP (Bil US)	0.5849	0.4767	1

In 2020 we can see the performance ranking of 11 countries, in Table 6. This ranking is based on the adjusted Slack Based Measure (SBM) model, which is derived from the CCR model. It shows us how efficient and effective each country is in using their resources to achieve their desired outcomes (Peng, Wang, Xuan, Nguyen, & Management, 2022). Policymakers and researchers can find this information valuable as it helps them identify which countries are performing well and where improvements can be made (C. N. Wang, Yang, Nguyen, & Vo, 2022).

Table 6. Performance ranking of 11 countries in 2020.

No.	DMU	Score	Rank
1	Australia	0.300436	11
2	Brazil	1	1
3	China	0.524808	4
4	France	0.482037	5
5	Germany	0.395533	8
6	Japan	0.373996	9
7	Netherlands	0.421178	7
8	South Korea	0.325747	10
9	Spain	0.438937	6
10	United Kingdom	0.574795	2
11	United States	0.559242	3

Figure 2 depicts the energy consumption rankings of 11 countries. Thanks to this visual representation, we can gain a feel of how different countries use renewable energy. The ranking assists us in identifying the countries that have successfully adopted and integrated renewable energy technologies. A rating is often presented from highest to lowest or lowest to highest.

Discussion of Findings

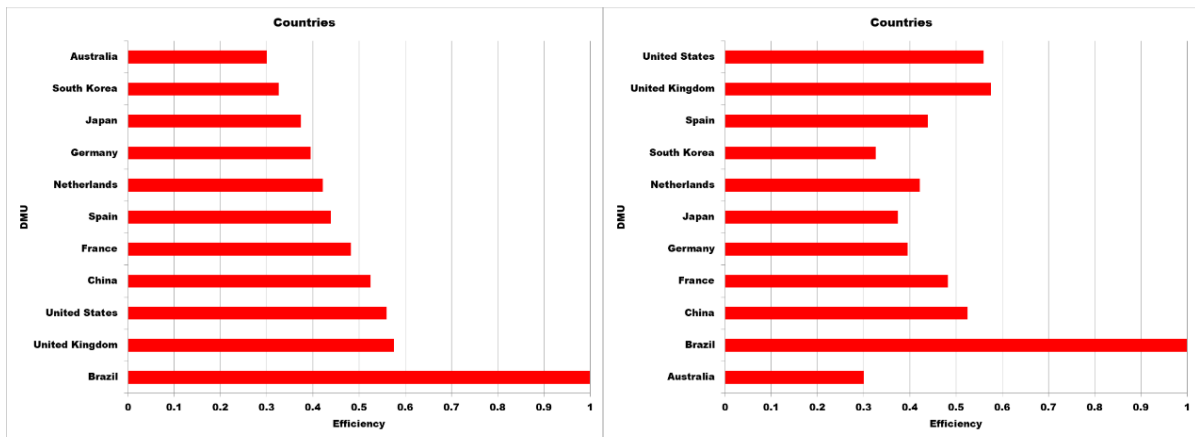


Figure 2. Ranking of 11 countries' renewable energy

Based on the data presented in Figure 2, which showcases the performance ranking of 11 countries in 2020 regarding renewable energy utilization, several noteworthy observations and insights can be gleaned. The findings offer a valuable basis for a comparative analysis of countries' renewable energy efficiency and highlight the varying levels of success in harnessing renewable energy sources.

The discussion of findings reveals Brazil as the top-ranked country, achieving the highest score of 1, signifying its exceptional performance in renewable energy utilization. Conversely, Australia secured the lowest rank with a score of 0.300436, indicating potential room for improvement in its renewable energy practices. Meanwhile,

the United Kingdom and the United States secured the second and third positions, respectively, showcasing commendable efficiency in their renewable energy initiatives.

Insights into renewable energy efficiency can be derived from the rankings, enabling a better understanding of how each country optimally utilizes its renewable energy resources. Such insights can contribute to the identification of best practices and success factors adopted by top-performing countries. These exemplary practices can serve as models for other nations aspiring to enhance their renewable energy efforts. Conversely, countries with lower rankings can benefit from this assessment by identifying potential areas for improvement. Analyzing the strategies and policies employed by higher-ranked countries can provide valuable guidance for addressing challenges and optimizing renewable energy utilization.

The data also holds crucial policy implications and recommendations for governments and policymakers worldwide. Countries with higher rankings can reinforce their policies and initiatives to sustain their renewable energy leadership, while lower-ranked countries can develop tailored strategies to elevate their renewable energy performance. The performance ranking of 11 countries in renewable energy offers valuable insights for comparison and evaluation. By leveraging these findings, countries can work towards a sustainable and greener future, ensuring optimal utilization of renewable energy sources and contributing to global efforts in combating climate change.

The analysis of the performance ranking of 11 countries in renewable energy utilization provides significant insights and implications for policymakers, researchers, and energy analysts. The discussion of findings encompasses a comprehensive examination of various aspects, including:

The ranking of the 11 countries reveals distinct variations in renewable energy efficiency. Brazil stands out as the top-performing country, attaining a perfect score of 1, showcasing exemplary practices in renewable energy utilization. On the other hand, Australia lags, securing the lowest rank with a score of 0.300436, indicating potential areas for improvement. The rankings offer a clear comparison of countries' performance, providing a baseline for evaluating their renewable energy efforts.

The data-driven ranking sheds light on the level of success achieved by each country in harnessing renewable energy sources. Countries like China, France, Germany, and the United Kingdom demonstrate notable efficiency in their renewable energy initiatives, obtaining competitive scores within the top five rankings. These insights provide valuable benchmarks for understanding the varying degrees of renewable energy utilization across nations.

The high-ranking countries offer valuable insights into the best practices and success factors that contribute to their renewable energy efficiency. Analyzing the strategies and policies implemented by top-performing countries can provide valuable lessons for other nations seeking to optimize their renewable energy utilization. Sharing and adopting these best practices can lead to significant improvements and advancements in renewable energy deployment.

For countries ranking lower in the performance assessment, the findings illuminate potential areas for improvement in their renewable energy endeavors. Identifying specific weaknesses and challenges can guide policymakers in formulating targeted policies and strategies to enhance renewable energy adoption. Addressing these areas can contribute to overall national progress in transitioning towards sustainable energy sources.

The performance ranking data carries crucial policy implications and recommendations. High-ranking countries can build on their achievements by reinforcing existing policies and exploring further opportunities for renewable energy expansion. Meanwhile, lower-ranked countries can utilize the insights gained to develop tailored policies and initiatives aimed at boosting renewable energy utilization. Policymakers can collaborate and learn from each other to accelerate global renewable energy deployment and combat climate change effectively.

The discussion of findings stemming from the performance ranking of 11 countries in renewable energy presents a valuable resource for understanding the landscape of renewable energy utilization. The insights garnered can inform strategic decision-making, foster international collaboration, and drive a collective effort towards a sustainable and greener future.

Conclusion

Limitations and Future Research

The study's conclusion must acknowledge certain limitations that may impact the interpretation and generalizability of the findings. Methodological limitations, such as the specific assumptions and simplifications inherent in the Data Envelopment Analysis (DEA) approach, should be recognized. Additionally, data availability and quality can pose challenges, as incomplete or unreliable data may affect the accuracy of the analysis. Addressing these limitations in future research endeavors can enhance the robustness and reliability of performance assessments in the renewable energy domain.

Furthermore, potential enhancements to the framework used for renewable energy efficiency evaluation should be explored. Refining the DEA approach and incorporating advanced analytical techniques can yield more nuanced insights into countries' renewable energy performance. Integrating qualitative data and conducting case studies could provide a deeper understanding of the contextual factors influencing renewable energy adoption and identify best practices.

Summary of Findings

The findings of this study make substantial contributions to the field of renewable energy assessment. The performance ranking of 11 countries offers a valuable benchmark for comparing renewable energy efficiency across nations, enabling policymakers and researchers to identify high-performing countries and areas for improvement. The insights into renewable energy efficiency shed light on successful strategies and best practices employed by leading countries, offering valuable lessons for others to emulate.

Implications for policy and practice are evident from the ranking results. High-ranking countries can bolster their efforts by reinforcing successful policies and scaling up renewable energy initiatives. Conversely, lower-ranked countries can utilize the findings to devise targeted policies aimed at accelerating renewable energy deployment.

Future directions for research in the renewable energy domain should consider addressing the identified limitations and expanding the scope of investigation. Comparative studies encompassing a broader range of countries and renewable energy sources can provide a more comprehensive understanding of the global renewable energy landscape. Exploring the potential impact of external factors, such as economic, political, and environmental conditions, can further enrich the analysis.

The study's findings offer valuable insights into renewable energy efficiency across countries and present opportunities for fostering sustainability. By recognizing the limitations and refining the methodology, future research can contribute to an evidence-based approach in promoting renewable energy adoption and facilitating the transition to a more sustainable energy future. The study's implications for policy and practice serve as a call to action for policymakers and stakeholders to collaborate in advancing renewable energy agendas for the benefit of future generations and the planet.

Scientific Ethics Declaration

The authors declare that the scientific ethical and legal responsibility of this article published in EPSTEM journal belongs to the authors.

Acknowledgements or Notes

*The authors would like to thank Ministry of Science and Technology, Taiwan. We also would like to thank the National Kaohsiung University of Science and Technology, Industrial University of Ho Chi Minh City, and Thu Dau Mot University for their assistance. Additionally, we would like to thank the reviewers and editors for their constructive comments and suggestions to improve our work.

* This article was presented as an oral presentation at the International Conference on Research in Engineering, Technology and Science (www.icrets.net) held in Budapest/Hungary on July 06-09, 2023.

References:

- Chang, D. S., Liu, W., & Yeh, L. T. (2013). Incorporating the learning effect into data envelopment analysis to measure MSW recycling performance. *European Journal of Operational Research*, 229(2), 496-504.
- Hu, W., Guo, Y., Tian, J., Chen, L. J. R. (2019). Eco-efficiency of centralized wastewater treatment plants in industrial parks: A slack-based data envelopment analysis. *Conservation, & Recycling*, 141, 176-186.
- Kler, R., Gangurde, R., Elmirzaev, S., Hossain, M. S., Vo, N. V. T., Nguyen, T. V. T., & Kumar, P. N. (2022). Optimization of meat and poultry farm inventory stock using data analytics for green supply chain network. *Discrete Dynamics in Nature and Society*, 1-8.
- Lee, H., Choi, Y., Seo, H. J. T. F. (2020). Comparative analysis of the R&D investment performance of Korean local governments. *157*, 120073.
- Li, Z., Sarwar, S., & Jin, T. (2021). Spatiotemporal evolution and improvement potential of agricultural eco-efficiency in Jiangsu Province. *Frontiers in Energy Research*, 9, 746405..
- Liu, J. S., Lu, L. Y., & Lu, W.-M. (2016). Research fronts in data envelopment analysis. *Omega*, 58, 33-45.
- Mousavi, M. M., & Ouenniche, J. (2018). Multi-criteria ranking of corporate distress prediction models: empirical evaluation and methodological contributions. *Annals of Operations Research*, 271, 853-886.
- Peng, F., Wang, Y., Xuan, H., Nguyen, T. V. T (2022). Efficient road traffic anti-collision warning system based on fuzzy nonlinear programming. *International Journal of System Assurance Engineering and Management*, 13(1), 456-461.
- Tone, K., & Sahoo, B. K. J. E. (2004). Degree of scale economies and congestion: A unified DEA approach. *European journal of operational research*, 158(3), 755-772.
- Wang, C. N., Yang, F. C., Nguyen, V. T. T., & Vo, N. T. M. (2022). CFD analysis and optimum design for a centrifugal pump using an effectively artificial intelligent algorithm. *Micromachines*, 13(8), 1208
- Wang, C. N., Yang, F. C., Vo, N. T. M., & Nguyen, V. T. T. (2022). Wireless communications for data security: efficiency assessment of cybersecurity industry-a promising application for UAVs. *Drones*, 6(11), 363.
- Wang, Y., Zuo, L., & Qian, S. (2022). Green-biased technical change and its influencing factors of agriculture industry: Empirical evidence at the provincial level in China. *19(23)*, 16369.
- Xu, K., Bossink, B., & Chen, Q. (2019). Efficiency evaluation of regional sustainable innovation in China: A slack-based measure (SBM) model with undesirable outputs, *12(1)*, 31.
- Yang, W., & Li, L. (2017). Analysis of total factor efficiency of water resource and energy in China: A study based on DEA-SBM model. *9(8)*, 1316.

Author Information

Thi Minh Nhut Vo

National Kaohsiung University of Science and Technology, 415 Jiangong, Sanmin, Kaohsiung, Taiwan
Thu Dau Mot University, Vietnam

Chia-Nan Wang

National Kaohsiung University of Science and Technology, 415 Jiangong, Sanmin, Kaohsiung, Taiwan

Fu-Chiang Yang

National Kaohsiung University of Science and Technology, 415 Jiangong, Sanmin, Kaohsiung, Taiwan

Van Thanh Tien Nguyen

Industrial University of Ho Chi Minh City
12, Nguyen Van Bao, Go Vap, Ho Chi Minh City, Vietnam
Contact e-mail: thanhtienck@ieee.org

To cite this article:

Vo, T.M.N., Wang, C.N., Yang, F.C. & Nguyen, V.T.T. (2023). Renewal energy efficiency assessment. *The Eurasia Proceedings of Science, Technology, Engineering & Mathematics (EPSTEM)*, 23, 556-563.

The Eurasia Proceedings of Science, Technology, Engineering & Mathematics (EPSTEM), 2023

Volume 23, Pages 564-572

ICRETS 2023: International Conference on Research in Engineering, Technology and Science

Activation Condition of a Fan that Cools a PV Panel by Blowing Ambient Air on Its Rear Face

Djamila Zembri-Nebbali

Mouloud Mammeri University of Tizi-Ouzou

Idir Kecili

Mouloud Mammeri University of Tizi-Ouzou.

Sonia Ait-Saada

Mouloud Mammeri University of Tizi-Ouzou

Rezki Nebbali

Mouloud Mammeri University of Tizi-Ouzou

Abstract: Under particular climatic conditions, the equilibrium temperature of a PV panel can increase excessively. This can significantly affect its electrical efficiency. The use of a cooling system, minimizing the negative effect of this temperature increase, can improve the efficiency of the cooled PV panel. In this work, we are interested in the cooling by a fan which blows ambient air on the rear face of a PV panel. This fan was activated by the PV panel itself. Thus, for an efficient use of this cooling system, it was necessary to define the activation conditions of this fan. To do this, a thermal model was used to determine the equilibrium temperature of the uncooled PV panel. Then, numerical simulations were performed by CFD code to evaluate the new equilibrium temperature of the cooled PV panel. This allowed to determine, by a one-diode electrical model, the improvement of electrical efficiency. The fan will then be activated from 5% improvement. This difference is then associated to the minimum temperature difference between the uncooled PV panel and the ambient air. For different values of solar radiation and air temperature, a correlation was established with this minimum difference.

Keywords: Air cooling, Activation condition, CFD, Fan, Photovoltaic panel

Introduction

The efficiency of photovoltaic (PV) panel is strongly linked to climatic conditions (Cuce et Cuce, 2014; Skoplaki et Playvos, 2009). The combined effect of high intensities of solar radiation and ambient air temperature can contribute significantly to the temperature rise of the PV panel whose efficiency is then affected.

To overcome this negative effect, several technical cooling are used. We distinguish the hybrid systems PV/T (Amori et al., 2012 ; Sarhaddi et al., 2010 ; Tiwari & Sodha, 2006). Moreover, Armstrong and Hurley (2010) propose to produce electricity by the action of wind which first drives a turbine and then cools a PV panel. Thus, they improve the electricity production by 36%. Rahimi et al. (2014) optimized a water jet design on a PV panel under high solar concentrations. This design allowed to cool the PV panel with low water pump power consumption.

However, due to the difficulties of implementation, this method limits the practical implementation of this cooling system. Other complex systems include evaporative cooling (Royne & Dey, 2007) or water spray cooling (Bahaidarah, 2016). To overcome these implementation difficulties, the natural circulation of air through the PV panel is used. This process is easy to perform but offers a low cooling effect (Alami, 2014).

Nebbali et al. (2020) propose an autonomous air-cooling system, composed by a fan that blow the ambient air on the rear face of a PV panel. The fan was supplied by the PV panel itself. They showed that for the case of a small size PV panel, the optimum operating point of this cooling system corresponds to an air flow of 8 g/s. The objective of this work is precisely to determine the activation condition of the fan that cools this PV panel. Fan cooling must ensure an efficiency improvement of the cooled PV panel of at least 5%

Problem Position

It is proposed here to cool a PV panel using a fan which blows ambient air on its rear face with an air mass flow rate of 8g/s. The fan is activated by the PV panel itself. The fan is centered on a plywood mounted on the backside of the PV panel (Nebbali et al., 2020) (Figure 1).

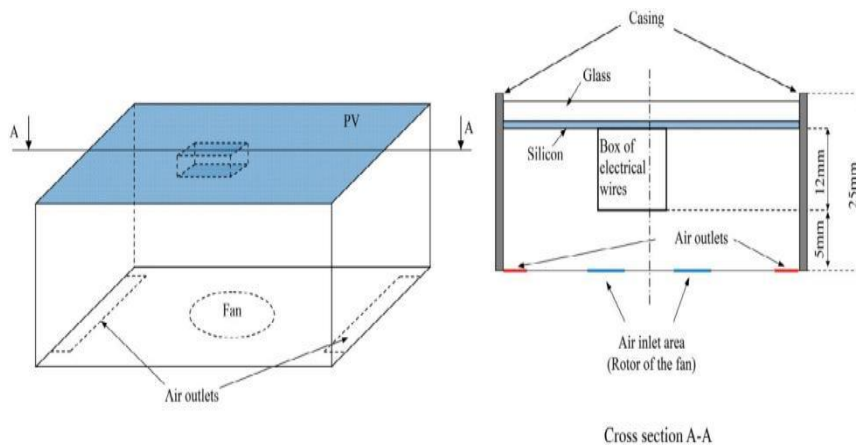


Figure 1. Sketch of the domain calculation (Nebbali et al., 2020).

This cooling system has already been modeled (Nebbali et al., 2020) and it has been established that the optimal operation is obtained for an airflow of 8g/s. With this air flow, we propose to determine from which temperature of the uncooled PV panel this fan must be activated to ensure a satisfactory efficiency improvement of the cooled PV panel. To do this, we need to determine the equilibrium temperature of the PV panel and the power it deliver at different climatic conditions.

The equilibrium temperature results from coupled equations of motion and energy. The complexity of these equations requires the use of the CFD tool for their resolutions. The electrical power delivered by the PV panel is then calculated using the one-diode electrical model. By taking into account the power consumed by the fan, we deduced the net power of the cooled PV panel. The efficiency improvement is then obtained by compared the efficiency of the cooled PV panel to that of the uncooled one.

Associated Equations

Fluid Media

The temperature distribution is determined by solving the equations of continuity, momentum, turbulent kinetic energy, dissipation rate and energy which are expressed by the following relationship, the variables of which are defined in the Table 1:

$$\frac{\partial}{\partial x_k} (\overline{u_k} \cdot \varphi) = -\frac{\gamma}{\rho} \frac{\partial P}{\partial x_i} + \frac{\partial}{\partial x_i} \left(\Gamma \cdot \frac{\partial \varphi}{\partial x_i} \right) + S_\varphi \quad (1)$$

Table 1. Governing equations in fluid medium (Nebbali et al., 2020)

Symboles	ϕ	γ	Γ	S_ϕ
Equation de Continuité	1	0	0	0
Momentum equation	u_i	1	0	$\nu \frac{\partial}{\partial x_j} \left(\frac{\partial \bar{u}_i}{\partial x_j} + \frac{\partial \bar{u}_j}{\partial x_i} \right) + \frac{\rho}{\rho_0} g_i - \frac{\partial}{\partial x_j} (\overline{u_i' u_j'})$
Turbulente kinetic energy	k	0	$\nu + \frac{V_t}{\sigma_k}$	$\nu_t S^2 - \varepsilon - 2\varepsilon M_t^2$
Dissipation rate	ε	0	$\nu + \frac{V_t}{\sigma_\varepsilon}$	$C_{1\varepsilon} \frac{\varepsilon}{k} (\nu_t S^2) - C_{2\varepsilon} \frac{\varepsilon^2}{k}$
Energy equation	T	0	δ	0

Solid Media

The temperature fields in the glass and silicon layers were determined by carrying out steady-state heat balances, which led to the following expression

$$\Delta T = \frac{\Omega}{\lambda} \tag{2}$$

Where Δ is the Laplace operator, and Ω is a source term that correspond to the net radiative heat flux of the short and long wavelengths, expressed as follows:

$$\Omega = \frac{\alpha_g R_G - \varepsilon_g \sigma (T_g^4 - T_{wall}^4)}{e_g}, \text{ for the glass layer.} \tag{3}$$

$$\Omega = \frac{\alpha_{PV} T_g R_g}{e_g}, \text{ for the silicon layer.} \tag{4}$$

A One-Diode Electrical Model

This model is expressed by the following equation (Nebbali et al, 2020) :

$$I = I_L - I_L \left[\exp \left(\frac{V + I R_s}{a} \right) - 1 \right] \tag{5}$$

Where :

$I_L=0.311$ A, $I_s=3.662 \cdot 10^{-6}$ A , $a=1.681$ and $R_s=0.473 \Omega$ are the constant of the one-diode model at reference conditions.

The electrical power delivred by the PV panel is the product of the voltage and the current it generates :

$$P = V \cdot I \tag{6}$$

The optimal value I_{opt} is determined from the following relation:

$$\frac{dP}{dI} \Big|_{I=I_{opt}} = 0 \tag{7}$$

And then V_{opt} is obtained by the equation (5)

Moreover, the current-voltage characteristics of a PV panel highlight an operating point of maximum power which corresponds to :

$$P_m = V_{opt} I_{opt} \quad (8)$$

The efficiency of the uncooled PV panel is expressed by the ratio between the maximum power delivered by the PV panel and the intensity of the incident solar radiation.

$$\eta_{uncooled} = \frac{P_m}{R_G S} \quad (9)$$

While the efficiency of the cooled PV panel, which considered the part of the energy consumed by the fan, is defined by this equation:

$$\eta_{cooled} = 100(P_m^{cooled} - P_{fan}) / (R_G S) \quad (10)$$

and:

$$P_{fan} = 1.88 \cdot 10^{-4} \left(\frac{T_{air}}{T_{air}^0} \right)^2 \left(\frac{q}{\rho_{air}^0} \right)^3 \quad (11)$$

and

$$\rho_{air} = 1.185 \text{ kg/m}^3 \text{ and } q = 8 \text{ gs}^{-1} \text{ (Nebbali et al. 2020)}$$

In addition, in order to quantify the improvement in the efficiency of the performance of the PV panel, the efficiency improvement is evaluated by:

$$\eta_r = 100 (\eta_{cooled} - \eta_{uncooled}) / \eta_{uncooled} \quad (12)$$

Results and Discussion

Equilibrium Temperature

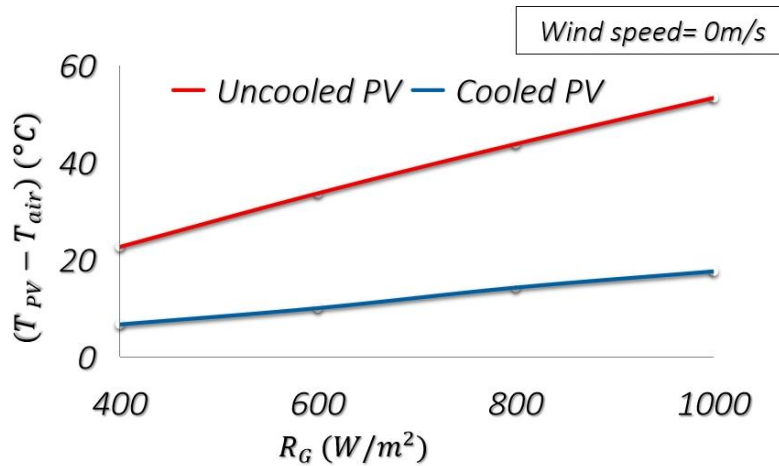


Figure 2. Temperature difference of the PV panel in absence of wind.

Figure (2) illustrates, in the absence of wind, the effect of the intensity of solar radiation on the temperature difference between the ambient air and the uncooled or cooled PV panel. We observe that in both uncooled and cooled PV panel situations, their equilibrium temperatures increases when the solar radiation increases. However, the temperature of the uncooled PV panel rises more than that of the cooled PV. Thus, the fan contributes to the cooling of the PV panel by about 30°C at $R_G=1000 \text{ W/m}^2$ and 15°C for $R_G= 400 \text{ W/m}^2$ (Table.2). Indeed, the ambient air blown by the fan improves the convective heat exchanges with the PV panel.

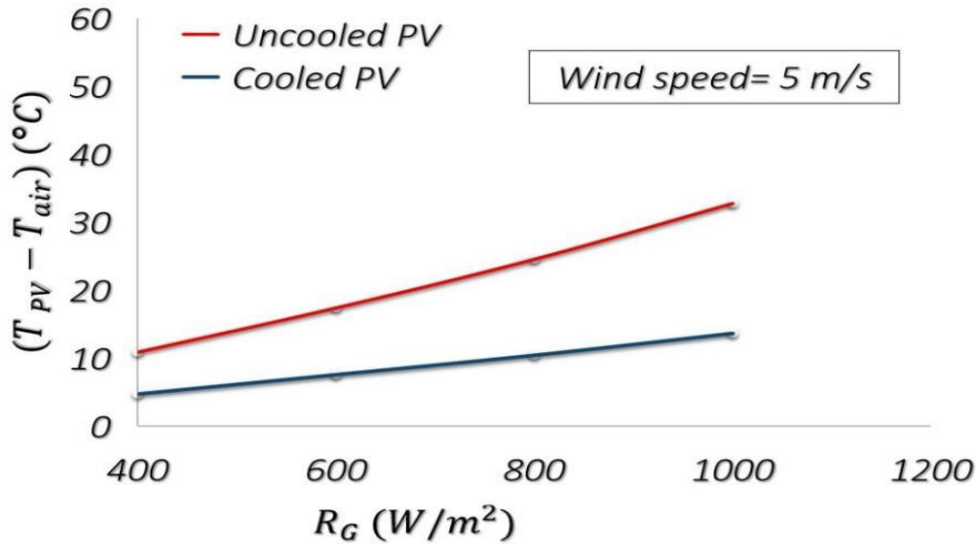


Figure 3. Temperature difference of the PV panel for a wind speed equal to 5m/s

In the presence of the wind speed of 5m/s (Figure 3, table.2), the temperature difference decreases to about 20°C at 1000W/m² and 5°C at 400 W/m². With 10 m/s of wind speed, the cooling occurred by the fan is less important (Figure.4, table.2). The temperature difference between the uncooled and cooled PV panel reaches 10°C at 1000W/m² and only 2°C at 400 W/m². It appears that for appreciable wind speed, the cooling by the fan could be useless, consequently it is important to determine the activating conditions of this fan.

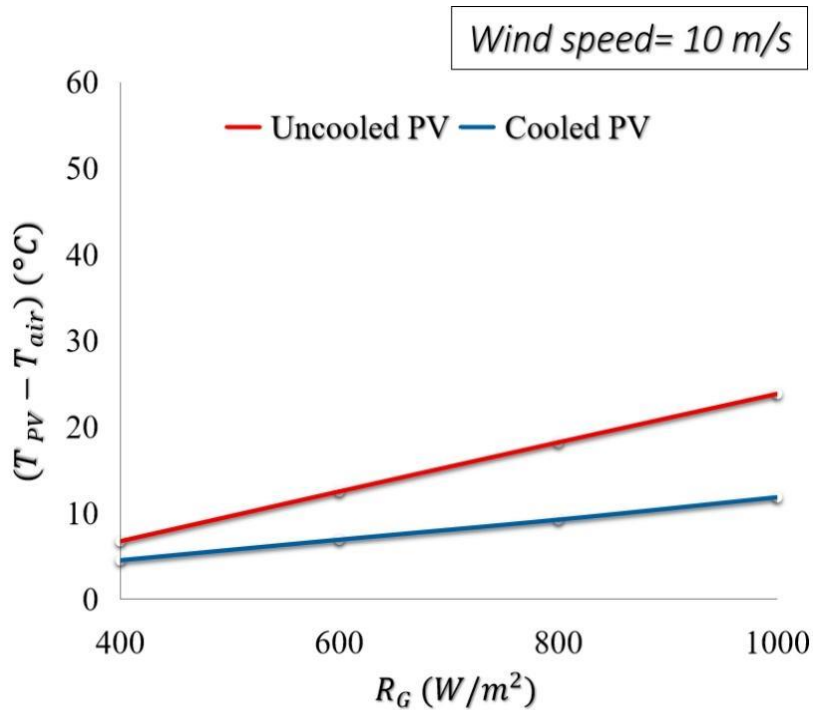


Figure 4. Temperature difference of the PV panel for a wind speed equal to 10 m/s

Table 2. Temperature difference between uncooled PV and cooled PV

Wind speed ($m s^{-1}$)	R_G (W/m^2)	Temperature difference ($^{\circ}C$)
0	400	15
	1000	30
5	400	5
	1000	20
10	400	2
	1000	10

Efficiency of the PV Panel

Through the figure (5) which highlights the evolution of the efficiency of the uncooled PV panel with the solar radiation intensity at different wind speeds, it is observed that this efficiency decreases when the solar radiation increases. However, this efficiency improves significantly, with a wind speed of 5 m/s, compared to that obtained in the absence of wind. Whereas from 10m/s of wind speed, the effect of the wind becomes less important.

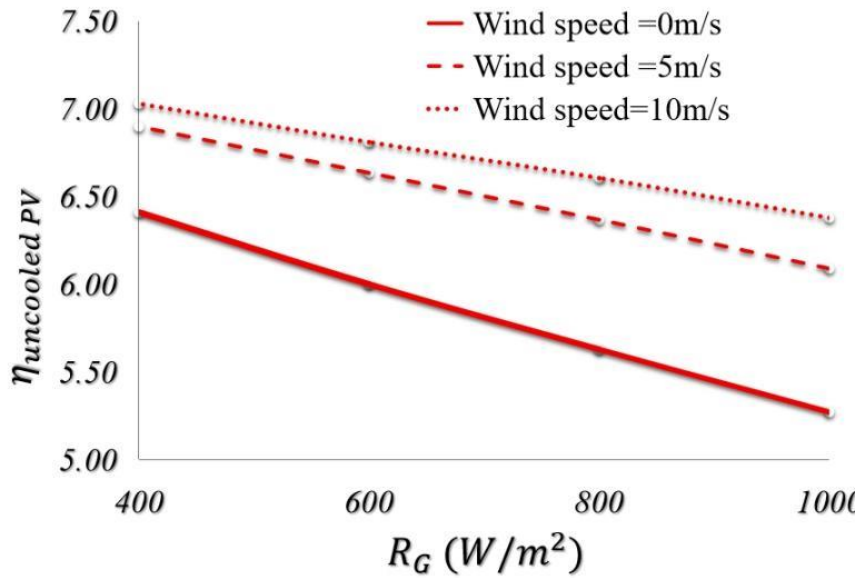


Figure 5. Efficiency evolution of the uncooled PV panel at different wind speed.

For the cooled PV panel (Figure.6), the same observation is made but with efficiencies more important of those of the uncooled PV panel. However, The presence of wind with an intensity of 5 m/s compared to the situation of the absence of wind, improves the efficiency of the PV panel. Moreover, increasing the wind speed does not further improve the efficiency.

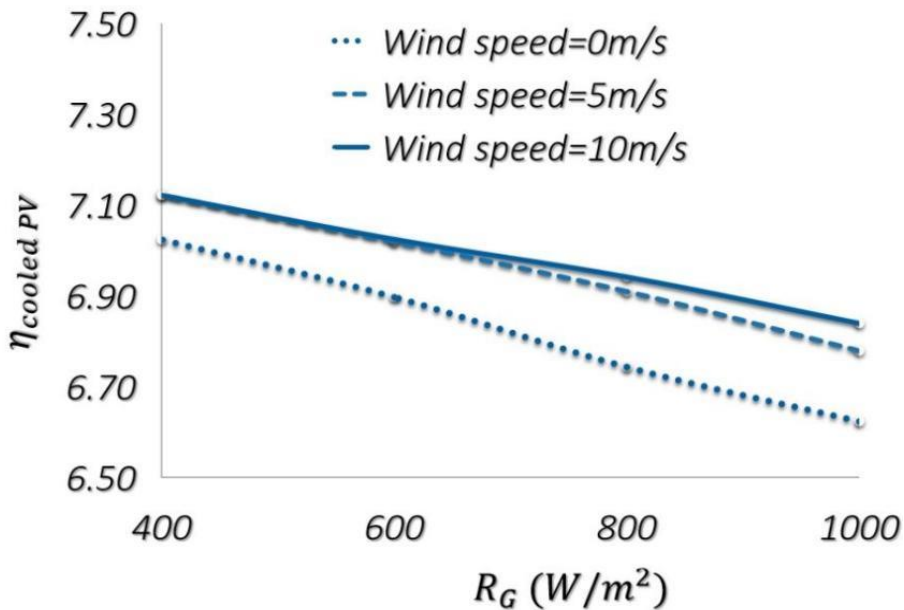


Figure 6. Efficiency evolution of the cooled PV panel at different wind speed.

As shown in figure (7), the efficiency improvement, in the absence of wind, is greater than that obtained in the presence of wind (Figure 7). We can observe the the presence of wind generates low or even negative efficiency improvements. Thus, the improvement provided by the PV panel is totally consumed by the fan.

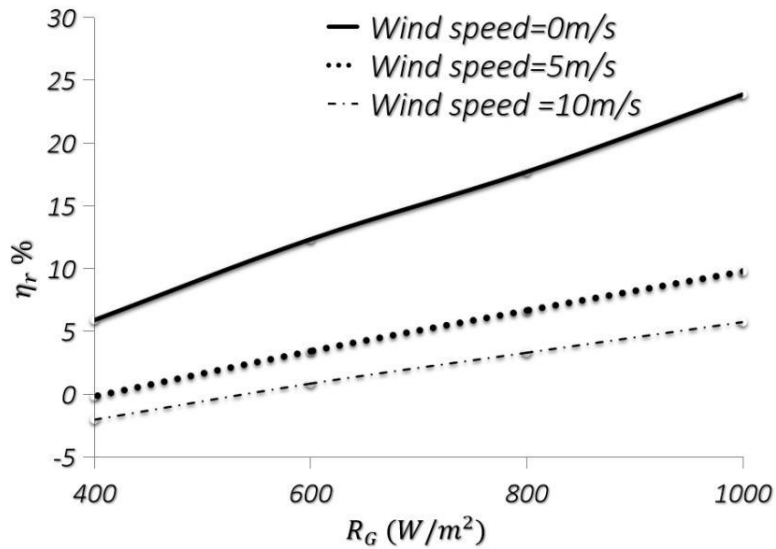


Figure 7. Efficiency improvement of the cooled PV for different wind speed.

Table 3. Efficiencies of the PV panel for various solar radiation intensities and wind speeds

Wind speed($m s^{-1}$)	R_G (W/m^2)	$\eta_{uncooled}$ (%)	η_{cooled} (%)	η_r (%)
0	400	6.50	7.00	5
	1000	5.25	6.70	22.5
5	400	6.95	7.10	5
	1000	6.75	6.88	8
10	400	7.25	7.10	-1
	1000	6.75	6.92	4

It can be seen from the table 3, that there are situations where the activation of the fan is not recommended. Indeed with a wind speed of 10m/s , the efficiency improvement of the cooled PV panel is negative. Thus, the excess electrical power delivered by the cooled PV panel may be totally consumed or insufficient to supply the fan. To overcome this, it is necessary to determine the activation conditions of the fan. To do this, we represent in Fig. 8 the evolution of the efficiency improvement of the cooled PV panel according to the temperature difference between the uncooled PV panel and the ambient air at different wind speeds. It appears that the efficiency improvement still greater than 5% from a temperature difference of 20°C. Therefore, the fan can be activated as soon as the temperature of the uncooled PV panel exceeds that of the ambient air by 20°C.

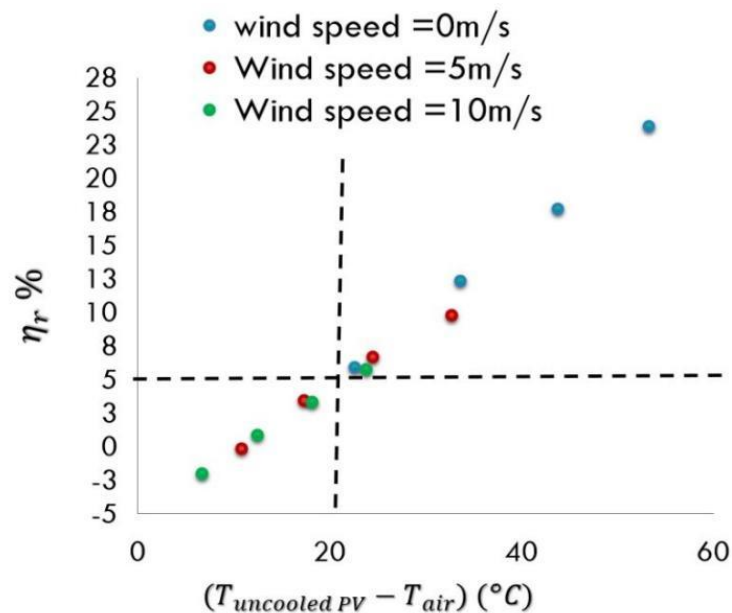


Figure 8. Efficiency improvement of PV panel as a function of temperature difference

Conclusion

Through this study we have shown that the use of a fan to cool a PV panel, allows significant efficiency improvement. It can be high in the absence of wind and low when the wind speed increases. Moreover, in the presence of wind, the efficiency improvement of the cooled PV panel can reach negative values. In order to overcome this negative effect, the fan must be activated as soon as the temperature difference between the uncooled PV panel and the ambient air exceeds 20°C. This ensures a minimum efficiency improvement of 5%.

Scientific Ethics Declaration

The authors declare that the scientific ethical and legal responsibility of this article published in EPSTEM journal belongs to the authors.

Acknowledgements or Notes

* This article was presented as an oral presentation at the International Conference on Research in Engineering, Technology and Science (www.icrets.net) held in Budapest/Hungary on July 06-09, 2023.

References

- Alami, A. H. (2014). Effects of evaporative cooling on efficiency of photovoltaic modules. *Energy Conversion and Management*, 77, 668–679.
- Amori, K., & Al-Najjar E. H. M. T. (2012). Analysis of thermal and electrical performance of a hybrid 11 (PV/T) air based solar collector for Iraq. *Applied Energy*, 98(12), 384–395.
- Armstrong, S., & Hurley, W.G. (2010). a thermal model for photovoltaic panels under varying 18 atmospheric conditions. *Applied Thermal Engineering*, 30(19), 1488–1495.
- Bahaidarah Haitham, M.S. (2016). Experimental performance evaluation and modeling of jet impingement cooling for thermal management of photovoltaics. *Solar Energy*, 135, 605–617.
- Bandou F., Hadj Arab A., Belkaid M.S., Logerais P. O., Riou O., & Charki, A. (2015). Evaluation and performance of photovoltaic modules after a long time operation in Saharan environment. 9, *International Journal of Hydrogen Energy*, 40, 13839–13848.
- Cuce, E., & Cuce, P. M. (2014). Improving thermodynamic performance parameters of silicon photovoltaic cells via air cooling. *International Journal of Ambient Energy*, 35, 193–199.
- Lu Z. H., & Yao, Q. (2007). Energy analysis of silicon solar cell modules based on an optical model for arbitrary layers. *Solar Energy*, 81, 636–647.
- Nebballi, D., Nebballi, R., & Ouibrahim, A. (2020). Improving photovoltaic panel performance via an autonomous air cooling system – experimental and numerical simulations. *International Journal of Ambient Energy* 41, 1387–1403.
- Nebballi, D. (2019). *Caractérisation d'une cellule solaire et optimisation de sa capacité de conversion énergétique*. (Master thesis). Mouloud Mammeri University of Tizi-Ouzou, Algeria.
- Odeh, S., & Behnia, M. (2009). Improving photovoltaic module efficiency using water cooling, *Heat Transfer Engineering*, 30(6), 499-505.
- Rahimi, M., Valeh-e-Sheyda, P., Parsamoghadam, M.A., Masahi, M.M., & Alsairafi, A.A. (2014). Design of a self-adjusted jet impingement system for cooling of photovoltaic cells. *Energy Conversion Management*, 83, 48–57.
- Royne, A., & Dey, C.J. (2007). Design of a jet impingement cooling device for densely packed PV 1 cells under high concentration. *Solar Energy*, 81, 1014–1024.
- Sarhaddi, F., Farahat, S., Ajam, H., Behzadmehr, A., & Mahdavi Adeli, M. (2010). An improved thermal and electrical model for a solar photovoltaic thermal (PV/T) air collector. *Applied Energy*, 87, 2328–2339.
- Skoplaki, E., & Playvos J. A. (2009). On the temperature dependence of photovoltaic module 3 electrical performance. Review of efficiency/power correlations. *Solar Energy*, 83, 614–624.
- Teo, H. G., Lee P. S., & Hawlader M. N. A. (2012). An active cooling system for photovoltaic Modules. *Applied Energy*, 90(1), 309–315.
- Tiwari, A., & Sodha, M.S. (2006). Performance evaluation of solar PV/T system: A 16 experimental validation. *Solar Energy*, 80, 751–759.

Author Information

Djamila Zembri-Nebbali

Mouloud Mammeri University of Tizi-Ouzou
Tizi-Ouzou, Algeria
Contact e-mail: djamila.nebbali@ummto.dz

Idir Kecili

Mouloud Mammeri University of Tizi-Ouzou
Tizi-Ouzou, Algeria

Sonia Ait Saada

Mouloud Mammeri University of Tizi-Ouzou.
Tizi-Ouzou, Algeria

Rezki Nebbali

Mouloud Mammeri University of Tizi-Ouzou.
Tizi-Ouzou, Algeria

To cite this article:

Zembri-Nebbali, D., Kecili, I., Ait Saada, S., & Nebbali, R. (2023). Activation condition of a fan that cools a PV panel by blowing ambient air on its rear face. *The Eurasia Proceedings of Science, Technology, Engineering & Mathematics (EPSTEM)*, 23, 564-572.